ISSN 0386-5878
Technical Memorandum
of PWRI No.3524

PROCEEDINGS OF THE 29TH JOINT MEETING OF U.S.-JAPAN PANEL ON WIND AND SEISMIC EFFECTS, UJNR

May 13 - 16, 1997
Tsukuba, Japan

Public Works Research Institute
Ministry of Construction

Copyright©(1997) by P.W.R.I.

All rights reserved. No part of this book may be reproduced by any means, nor transmitted, nor translated into a machine language without the written permission of the Director General of P.W.R.I.

この報告書は、土木研究所長の承認を得て刊行したものである。したがって、本報告書の全部又は一部の転載、複製は、土木研究所長の文書による承認を得ずしてこれを行ってはならない。

永久保存

Technical Memorandum
of PWRI No.3524

PROCEEDINGS OF THE 29TH JOINT MEETING OF U.S.-JAPAN PANEL ON WIND AND SEISMIC EFFECTS, UJNR

Edited by

Michio Okahara, Secretary-General
Japan-side Panel on Wind and Seismic Effects

Synopsis :
This publication contains the Proceedings of the 29th Joint Meeting of the U.S.-Japan Panel on Wind and Seismic Effects, UJNR, which was held at the Public Works Research Institute, Tsukuba, during 13-16 May 1997. Forty-seven papers were written, 23 by U.S. members and 24 by Japanese members. Thirty-Five papers were presented orally; 17 by the U.S. -side and 18 by the Japan-side. The papers were organized into five themes: Wind Engineering; Earthquake Engineering; Storm Surge and Tsunamis; Summary of Joint Cooperative Research Programs; and Seismic Information Systems.

Key words : Wind Engineering, Earthquake Engineering, Joint Coopertive Research, UJNR



CONTENTS

PREFACE 1
AGENDA OF JOINT TECHNICAL MEETING AND SITE VISITS 5
LIST OF PANEL MEMBERS 17
LISTS OF TASK COMMITTEE MEMBERS 39
RESOLUTIONS 47
PAPERS 53

THEME 1. Wind Engineering

Wind Engineering Research and Development in the United States
Ahsan KAREEM and Tracy KIJEWSKI 57

On the Wind Resistant Design Methods for Super Long-Span Bridges
Hiroshi SATO, Katsuya OGIHARA, Haruki AKIYAMA and Ryuichi TORIUMI 71

Improved Analysis of Extreme Wind Loads on Low-rise Structures
Muhammad R. HAJJ, H. W. TIELEMAN and D. A. JORDAN, ... 85

Active Mitigation of Wind-induced Response – Progress, Issues and Prospects
Bogusz BIENKIEWICZ and P. M. YOUNG 93

The Shimodate Downbursts on Jury 15, 1996
Hajime NAKAMURA 123

An Investigation of Tuned Liquid Dampers for Structural Control
Dorothy A. REED, H. YEH, J. YU and S. GARDARSSON 131

THEME 2. Earthquake Engineering

Preparation of Active Fault Maps in Urban Area
Hiroshi MASAHARU, Hidetoshi NAKAJIMA, Masuo TAGUCHI, Tatsuo SEKIGUCHI
and Satoko ODAGIRI 143

Simplified Design Provisions for Hybrid Precast Connections
H. S. LEW and G. CHEOK 149

Seismic Retrofit of Existing Highway Bridges in Japan
Shigeki UNJOH, Toru TERAYAMA, Yukio ADACHI and Jun-ichi HOSHIKUMA 161

Shake - Table Testing of U.S. and Japanese Bridge Column Design
W. Philip YEN, James D. COOPER, Toru TERAYAMA and Hisanori OTSUKA 179

Deformation of Kobe Ohashi Bridge Foundation Caused by 1995 Great Hanshin Earthquake, Japan
Hanlong LIU, Koji ICHII, Toshikazu MORITA and Susumu IAI 189

New Strong Motion Array Observation System of the Public Works Research Institute
Koichi YOKOYAMA , Keiichi TAMURA, Hideki SUGITA, Riki HONDA and Akira CHIBA 203

Site Amplifications for Generic Rock Sites
David M. BOORE and William B. JOYNER 219

The K-NET - a year after -
Shigeo KINOSHITA, Keiichi OHTANI and Tsuneo KATAYAMA 239

Seismic Design of Non-Structural Building Components in the United States
Andrew W. TAYLOR and Long T. PHAN(Presented by H. S. LEW) 245

Micro – Distribution of Peak Ground Acceleration in Hanshin Area Estimated by Seismograph Data
and Seismic Intensity obtained by Questionnaires for the 1995 Great Hanshin Earthquake
Shiro TAKADA and Ryuzo OZAKI 261

The 1996 Seismic Design Specifications of Highway Bridges
Kazuhiko KAWASHIMA , Masanori NAKANO, Kazuhiro NISHIKAWA, Jiro FUKUI,
Keiichi TAMURA and Shigeki UNJOH 275

Earthquake Strong Ground – Motion Measurement for Public Safety
Roger D. BORCHERDT and T. FUMAL, (Presented by William B. JOYNER) 301

IDNDR Activities of the World Road Association (WRA/PIARC)
Toshio IWASAKI, Kyohei ITO and Michio OKAHARA 311

Planning and Implementation of a Soil-structure interaction Experiment
Mehmet K. CELEBI 325

Deformation Properties of Coarse-grained Materials from Cyclic and Monotonic Loading Triaxial Tests
Tsuneo UESAKA, Hitoshi YOSHIDA and Tomoya IWASHITA 337

Modeling Dynamic Field Phenomena with the Army Centrifuge
R. H. LEDBETTER, R. S. STEEDMAN and W. F. MARCUSON, III
(Presented by A. G. FRANKLIN) 349

Long Term Health Consequences of the Great Hanshin-Awaji Earthquake and Strategies for Mitigating Them
Naotaka SHINFUKU 367

Rapid Needs Assessment and Loss Estimation from Natural Hazards: Lessons Learned from
Hurricane Marilyn, U.S. Virgin Islands
Joel D. SELANIKIO, Josephine MALILAY, and W. Dana FLANDERS 373

THEME 3. Storm Surge and Tsunamis

Offshore Tsunami Profiles Observed at the Coastal Wave Stations
Toshihiko NAGAI, Noriaki HASHIMOTO, Kazuyoshi SHIMIZU and Fujio KITAMURA 383

Hurricane Fran Storm Surge Assessment
William E. ROPER 393

Numerical Modeling of Recent Trans-Pacific Tsunami Recorded at Tide Gauges in Japan
Yuichiro TANIOKA and Masami OKADA 409

Use of Relationships Between Moment Magnitude and Water Level Measurement Station Amplitudes
by the Tsunami Warning System to Forecast Tsunamis in the Far Field
Michael E. BLACKFORD 419

THEME 4. Seismic Information Systems

Development of Real-time Seismic Information System for MOC
Shun-etsu ODAGIRI, Hideki SUGITA, Masahiro KANEKO, Tomohumi NOZAKI
and Tadashi HAMADA 425

Accessing Natural Hazards Data from CD-ROM and on the Web
A. M. HITTELMAN and P. K. DUNBAR 437

Development of the Disaster Information System (DIS/Earthquakes)
Kazuo OKAYAMA 449

The Use of GIS in Loss Estimation and Risk Assessment
Gil JAMIESON and Jeff MILHEIZLER (Presented by Richard N. WRIGHT) 463

THEME 5. Summary of Joint Cooperative Research Programs

U. S.-Japan Cooperative Earthquake Engineering Research Program on Composite and Hybrid Structures - Japan side Progress-
Isao NISHIYAMA and Hiroyuki YAMANOUCHI 473

U.S.-Japan Cooperative Earthquake Research Program on Composite and Hybrid Structures -- U.S.-side Progress
Subhash C. GOEL 479

Research and Development of Performance-Based Design and Engineering System in Japan
Hiroyuki YAMANOUCHI, Hisashi OKADA and Masaomi TESHIGAWARA 483

MANUSCRIPTS AUTHORED FOR THE PANEL MEETING BUT NOT PRESENTED ORALLY 497

Wind-Induced Response of a Roof Purlin,
J. Yin, D.A. Smith and K.C. Mehta 499

Design of Light – Gauge Steel Shearwalls for Residential Construction in High Wind and Seismic Conditions,
Jay H. Crandell, Shawn McKee and William F. Freeborne 513

Corps of Engineer Earthquake Engineering Research Program for Dams,
William E. Roper 523

National Strong-Motion Program of the U.S. Geological Survey,
Mehmet Celebi 535

Seismic Hazard Criteria for the U.S. Department of Energy Reservation in Oak Ridge, TN, Harish Chander, Karen E. Shaffer, R. Joe Hunt and J. K. Kimball 547

National Earthquake Loss Reduction Program – a New Approach for the United States,
Robert H. Volland 557

The Effects of Open Passage on Reducing Wind Response of Tall Buildings
Hisashi OKADA and Linze KONG 561

Strength and ductility Characteristics of Highway Bridge Foundations
Jiro FUKUI, Yoshitomi KIMURA, Masahiro ISHIDA and Toshiaki NANAZAWA 567

Experimental Study on Tensile Strength of Concrete for Dams
Isao NAGAYAMA, Kazuo WATANABE, Takashi SASAKI and Masahiro HATANO 583

Multidisciplinary Cooperative Research to Mitigate Medical Consequences after the Earthquake
Keiko OGAWA, Ichiro TSUJI and Sigeru HISAMICHI 591

Large-Scale Physical Model Test on Tsunami Overtopping and Bed Scour around Coastal Revetment
Kenji NOGUCHI and Shinji SATO 597

Correlation between Damage to Buildings and Landform in the 1995 Hyogo-ken Nanbu Earthquake
- An analysis by the application of GIS -
Naohisa OKADA, Satoru KAWASHIMA and Yoko YAMADA 605

APPENCIX

TASK COMMITTEE REPORTS 619
TECHNICAL SITE VISITS 645

PREFACE

This publication is the proceedings of the 29th Joint Meeting of the U.S.-Japan Panel on Wind and Seismic Effects. The meeting was held at the Public Works Research Institute, Tsukuba, Japan, during May 13-16, 1997. The proceedings include the program, list of members, panel resolutions, task committee reports and technical papers submitted to the Joint Panel Meeting, and summary of the technical site visits.

BACKGROUND

Responding to the need for improving engineering and scientific practices through exchange of technical data and information, research personnel, and research equipment, the United States and Japan in 1961 created the U.S.-Japan Cooperative Science Program. Three collateral programs comprise the Cooperative Science Program. The U.S.-Japan Cooperative Program in Natural Resources (UJNR), one of the three, was created in January 1964. The objective of UJNR is to exchange information on research results and exchange scientists and engineers in the area of natural resources for the benefit of both countries. UJNR is composed of 18 Panels each responsible for specific technical subjects.

The Panel on Wind and Seismic Effects was established in 1969. Seventeen U.S. and seven Japanese agencies participated with representatives of private sector organizations to develop and exchange technologies aimed at reducing damage from high winds, earthquakes, storm surge, and tsunamis. This work is produced through collaboration between U.S. and Japanese member researchers working in eleven task committees. Each task committee focuses on specific technical issues, e.g., earthquake strong motion data. The Panel provides the vehicle to exchange technical data and information on design and construction of civil engineering lifelines, buildings and waterfront structures, and to exchange high wind and seismic measurement records. Annual meetings alternate between Japan and United States (odd numbered years in Japan; even numbered years in U.S.). These one-week technical meetings provide the forum to discuss ongoing research and research results; they are followed by a one-week series of technical site visits.

The National Institute of Standards and Technology (NIST) provides the U.S.-side chairman and secretary-general. The Public Works Research Institute (PWRI), Japan, provides the Japan-side chairman and secretary-general.

Annual meetings provide the mechanism for interaction with the U.S. and Japanese researchers in wind and seismic engineering which provides opportunities to gain valuable information and to engage in cooperative research. Through these opportunities, the Panel member organizations have realized important advances in building and structures technology. The Panel's activities have resulted in improved building and structures codes and standards in both countries, for example:

- created and exchanged digitized earthquake records used as the basis of design and research for Japan and the United States;
- transferred earthquake engineering information and strong-motion measurement techniques for use by seismically active countries, e.g., Australia, Canada, Italy, Mexico, Peru, Taiwan, Turkey, and North Africa;
- produced data that advanced design and construction of bridge structures;
- produced large-scale testing data that advanced the seismic design standards for buildings;
- improved in-situ measurement methods for soil liquefaction and stability under seismic loads;
- created a database on storm surge and tsunamis and verified mathematical models of tsunami and storm surge warning systems;
- established a library resource of current research on wind and earthquake engineering and on storm surge and tsunamis;
- published proceedings of Panel meeting, Task Committee Workshops, and special publications such as List of Panel Publications and translated two-volume series on earthquake resistant construction using base isolation systems;
- provided earthquake science and technology expertise to the U.S.-Japan Natural Disaster Reduction Initiative of the U.S.-Japan Framework for New Economic Partnership (Common Agenda);
- created a Web Site for promoting the Panel's activities widely.

The Panel's efforts are exemplary of effective joint research and of technology delivery between researchers from the U.S. and Japan. Since its creation, more than 1800 papers were presented in 29 Joint Meetings and more than 55 Task Committee Workshops and over 200 guest researchers were exchanged. The Panel provides important information about the U.S. and Japan's civil engineering thrusts which influence both countries' research and provide the basis for improvements in building and structures codes and standards.

HIGHLIGHTS OF THE 29TH JOINT PANEL MEETING

Thirty-five papers were presented orally. The papers were organized into five themes: Wind Engineering; Earthquake Engineering; Storm Surge and Tsunamis; Summary of Joint Cooperative Research Programs; and Seismic Information Systems.

Highlights include:

- Technical presentations:
  - Important knowledge was exchanged for research and practice, e.g., analytical and experimental research results on wind engineering; seismic design of bridges, dams and buildings; disaster prevention information systems and risk assessment using GIS; and research in public health following natural disasters.
  - Information was exchanged about extensive U.S. / Japanese public works projects, civil

engineering research, and their applications into practice.

- Excellent projects are being performed by both sides in intelligent and smart materials and systems technologies.

- Task Committee activities grow in strength. The T/C structure is an extremely effective vehicle to explore in depth the technologies and methods being used by both countries.
  - Five Task Committee Workshops were held in the past year and seven Workshops/Committee Meetings are planed for the coming year.
  - Desirability to create a new T/C on Seismic Information Systems was recognized.

- Cooperative Research Programs continue to be productive.
  - Composite and hybrid structures,
  - Soil liquefaction and countermeasures, and
  - Smart materials.

Michio Okahara, Secretary – General
Japan- side Panel on Wind and Seismic Effects



U.S. Side and Japan Side Attendance

29th Joint Meeting of the U.S. –Japan Panel on Wind and Seismic Effects

Agenda of Joint Meeting and Technical Site Visits

AGENDA OF JOINT TECHNICAL MEETING AND TECHNICAL SITE VISITS

TECHNICAL MEETING

May 13 (Tue)

10:30 Opening Ceremonies [8F Conference Room]

11:45 Group Photograph

12:00 Lunch hosted by PHRI and MRI [1F Conference Room]

13:00 Session 1 (Wind Engineering 1) Chairman - R. N. WRIGHT

13:00 Wind Engineering Research and Development in the United States
Ahsan KAREEM and Tracy KIJEWSKI, University of Notre Dame

13:20 On the Wind Resistant Design Methods for Super Long-Span Bridges
Hiroshi SATO, Katsuya OGIHARA, PWRI, Haruki AKIYAMA
and Ryuichi TORIUMI, Honshu-Shikoku Bridge Authority

13:40 Improved Analysis of Extreme Wind Loads on Low-rise Structures
Muhammad R. HAJJ, H. W. TIELEMAN, Virginia Tech and D. A. JORDAN,
University of Virginia

14:00 Active Mitigation of Wind-induced Response – Progress, Issues and Prospects
Bogusz BIENKIEWICZ and P. M. YOUNG, Colorado State University

14:20 Discussion

14:40 Break

15:00 Task Committee Meetings

A: Strong-Motion Data and Applications	[5F Room 524]
C: Evaluation and Improvement of Structures*	[6F Room 617]
G: Structural Control and Intelligent Material Systems*	[6F Room 617]
D: Earthquake Engineering for Dams	[6F Room 627]
E: Design for Wind and Wind Hazard Mitigation	[5F Room 526]
I: Storm Surge and Tsunami	[5F Room 526]

16:30 Adjourn

18:30 Reception hosted by the Vice-Minister of Construction for Engineering Affairs
(Hotel Tsukuba Sun-Route, Tel. 0298-52-1151)

*Task Committee C 15:00～15:45; Task Committee G 15:45～16:30

May 14 (Wed)

9 : 0 0 Session 2 (Wind Engineering 2) Chairman - Seizo TSUJI

9 : 0 0 The Shimodate Downbursts on Jury 15, 1996
Hajime NAKAMURA, MRI

9 : 2 0 An Investigation of Tuned Liquid Dampers for Structural Control
Dorothy A. REED, H. YEH, J. YU and S. GARDARSSON, University of Washington

9 : 4 0 Discussion

9 : 5 0 Break

10 : 1 0 Session 3 (Earthquake Engineering 1) Chairman - Seizo TSUJI

10 : 1 0 Preparation of Active Fault Maps in Urban Area
Hiroshi MASAHARU, Hidetoshi NAKAJIMA, Masuo TAGUCHI, Tatsuo SEKIGUCHI and Satoko ODAGIRI, GSI

10 : 3 0 Simplified Design Provisions for Hybrid Precast Connections
H. S. LEW and G. CHEOK, NIST

10 : 5 0 Seismic Retrofit of Existing Highway Bridges in Japan
Shigeki UNJOH, Toru TERAYAMA, Yukio ADACHI and Jun-ichi HOSHIKUMA, PWRI

11 : 1 0 Shake - Table Testing of U.S. and Japanese Bridge Column Design
W. Philip YEN, James D. COOPER, FHWA, Toru TERAYAMA and Hisanori OTSUKA, PWRI

11 : 3 0 Deformation of Kobe Ohashi Bridge Foundation Caused by 1995 Great Hanshin Earthquake, Japan
Hanlong LIU, Koji ICHII, Toshikazu MORITA and Susumu IAI, PHRI

11 : 5 0 Discussion

12 : 2 0 Lunch hosted by NIED [1F Conference Room]

13 : 2 0 Session 4 (Earthquake Engineering 2) Chairman - Seizo TSUJI

13 : 2 0 New Strong Motion Array Observation System of the Public Works Research Institute
Koichi YOKOYAMA , Keiichi TAMURA, Hideki SUGITA, Riki HONDA and Akira CHIBA, PWRI

13 : 4 0 Site Amplifications for Generic Rock Sites
David M. BOORE and William B. JOYNER, USGS

14 : 00 The K-NET : - a year after -
Shigeo KINOSHITA, Keiichi OHTANI and Tsuneo KATAYAMA, NIED

14 : 20 Seismic Design of Non-Structural Building Components in the United States
Andrew W. TAYLOR and Long T. PHAN, NIST(Presented by H. S. LEW)

14 : 40 Micro – Distribution of Peak Ground Acceleration in Hanshin Area Estimated by Seismograph Data and Seismic Intensity obtained by Questionnaires for the 1995 Great Hanshin Earthquake
Shiro TAKADA and Ryuzo OZAKI, Kobe University

15 : 00 Discussion

15 : 30 Break

15 : 50 Task Committee Meetings
B: Design, Testing and Evaluation Procedures for Building Systems [5F Room 526]
F: Disaster Prevention Methods for Lifelines Systems [6F Room 617]
H: Soil Behavior and Stability During Earthquakes [5F Room531A]
J: Wind and Earthquake Engineering for Transportation Systems [5F Room 524]
K: Wind and Earthquake Engineering for offshore and Coastal Facilities [6F Room 627]

17 : 20 Adjourn

18 : 30 Dinner Hosted by Director-General of Public Works Research Institute (Ushiku-Chateau, Tel. 0298-73-3151)

May 15 (Thu)

9 : 0 0 Session 5 (Earthquake Engineering 3) Chairman - R. N. WRIGHT

9 : 0 0 The 1996 Seismic Design Specifications of Highway Bridges
Kazuhiko KAWASHIMA, Tokyo Institute Technology, Masahiro NAKANO, Economic Affairs Bureau, MOC, Kazuhiro NISHIKAWA, Jiro FUKUI, Keiichi TAMURA and Shigeki UNJOH, PWRI

9 : 2 0 Earthquake Strong Ground – Motion Measurement for Public Safety
Roger D. BORCHERDT and T. FUMAL, USGS(Presented by William B. JOYNER)

9 : 4 0 IDNDR Activities of the World Road Association (WRA/PIARC)
Toshio IWASAKI, Kyohei ITO, Civil Engineering Research Laboratory and Michio OKAHARA, PWRI

1 0 : 0 0 Discussion

1 0 : 2 0 Break

1 0 : 4 0 Session 6 (Earthquake Engineering 4) Chairman - R. N. WRIGHT

1 0 : 4 0 Planning and Implementation of a Soil-structure-interaction Experiment
Mehmet K. CELEBI, USGS

1 1 : 0 0 Deformation Properties of Coarse-grained Materials from Cyclic and Monotonic Loading Triaxial Tests
Tuneo UESAKA, Hitoshi YOSHIDA and Tomoya IWASHITA, PWRI

1 1 : 2 0 Modeling Dynamic Field Phenomena with Army Centrifuge
R. H. LEDBETTER, S. STEEDMAN and W. F. MARCUSON, Ⅲ, WES (Presented by A. G. FRANKLIN, WES)

1 1 : 4 0 Discussion

1 2 : 0 0 Lunch hosted by BRI [1F Conference Room]

1 3 : 0 0 Session 7 (Earthquake Engineering 5) Chairman - R. N. WRIGHT

1 3 : 0 0 Long Term Health Consequences of the Great Hanshin-Awaji Earthquake and Strategies for Mitigating Them
Naotaka SHINFUKU, Kobe University

1 3 : 2 0 Rapid Needs Assessment and Loss Estimation from Natural Hazards: Lessons Learned from Hurricane Marilyn, U.S. Virgin Islands
Joel SELANIKIO, Josephine MALILAY, CDC and W. Dana FLANDERS, Emory University

13：40 Discussion

13：50 Break

14：10 Session 8 (Storm Surge and Tsunamis) Chairman - R. N. WRIGHT

14：10 Offshore Tsunami Profiles Observed at the Coastal Wave Stations
Toshihiko NAGAI, Noriaki HASHIMOTO, PHRI, Katsuyoshi SHIMIZU, MOT and Fujio KITAMURA, Miyazaki Prefecture

14：30 Hurricane Fran Storm Surge Assessment
William E. ROPER, Corps

14：50 Numerical Modeling of Recent Trans-Pacific Tsunami Recorded at Tide Gauges in Japan
Yuichirou TANIOKA and Masami OKADA, MRI

15：10 Use of Relationships Between Moment Magnitude and Water Level Measurement Station Amplitude by the Tsunami Warning System to Forecast Tsunamis in the Far Field
Mike BLACKFORD, NOAA

15：30 Discussion

15：50 Break

16：10 Workshop Reports

17：20 Adjourn

18：30 Individually Hosted Dinner

May 16 (Fri)

9 : 0 0 Session 9 (Seismic Information Systems) Chairman - Seizo TSUJI

9 : 0 0 Development of Real-time Seismic Information Systems for MOC
Syun-etsu ODAGIRI, Hideki SUGITA, Masahiro KANEKO,
Tomohumi NOZAKI and Tadashi HAMADA, PWRI

9 : 2 0 Accessing Natural Hazards Data from CD-ROM and on the Web
A. HITTLEMAN and P. DUNBAR, NOAA

9 : 4 0 Development of the Disaster Information System (DIS/Earthquakes)
Kazuo OKAYAMA, NLA

1 0 : 0 0 The Use of GIS in Loss Estimation and Risk Assessment
Gil JAMIESON and Jeff MILHEIZLER, FEMA
(Presented by Richard N. WRIGHT, NIST)

1 0 : 2 0 Discussion

1 0 : 4 0 Break

1 1 : 0 0 Session 10 (Summary of Joint Cooperative Research Programs)
Chairman - Seizo TSUJI

1 1 : 0 0 U. S.-Japan Cooperative Earthquake Engineering Research Program on Composite and Hybrid Structures - Japan side Progress-
Isao NISHIYAMA and Hiroyuki YAMANOUCHI, BRI

1 1 : 2 0 U.S.-Japan Cooperative Earthquake Research Program on Composite and Hybrid Structures -- U.S.-side Progress
Subhash GOEL, University of Michigan

1 1 : 4 0 Research and Development of Performance-Based Design and Engineering System in Japan
Hiroyuki YAMANOUCHI, Hisashi OKADA and Masaomi TESHIGAWARA, BRI

1 2 : 0 0 Discussion

1 2 : 2 0 Lunch hosted by GSI [1F Conference Room]

1 3 : 2 0 Report of Task Committees
A: Strong-Motion Data and Applications
B: Testing and Evaluation Procedures for Building Systems
C: Design, Evaluation and Improvement of Structures
D: Earthquake Engineering for Dams
E: Design for Wind and Wind Hazard Mitigation

F: Disaster Prevention Methods for Lifelines Systems
G: Structural Control and Intelligent Material Systems
H: Soil Behavior and Stability During Earthquakes
I: Storm Surge and Tsunami
J: Wind and Earthquake Engineering for Transportation Systems
K: Wind and Earthquake Engineering for offshore and Coastal Facilities

15:20	Break
15:40	Adoption of Final Resolutions
16:30	Break
16:40	Closing Ceremonies
17:00	Conclusion of 29th Joint Panel Technical Sessions
18:00	Reception Hosted by U.S. Members (Hotel Grand Shinonome, Tel. 0298-56-2211)

OPENING CEREMONIES

May 16(Tue) 10:30～12:00

１０：３０ OPENING CEREMONIES

Call to order by Michio OKAHARA, Secretary-General, Japan Side

Opening remarks by Kotaro HASHIMOTO, Vice-Minister of Construction for Engineering Affairs

Remarks by Gerald J. WHITMAN, Minister-Counselor, Embassy of the United States of America

Remarks by Shin AOYAMA, Director, International Affairs Division, Science and Technology Promotion Bureau, Science and Technology Agency

Remarks by Seizo TSUJI, Chairman JAPAN-Side, Panel on Wind and Seismic Effects, Director-General, Public Works Research Institute, Ministry of Construction

Remarks by Richard N. WRIGHT, Chairman U.S.-Side, Panel on Wind and Seismic Effects, Director, Building and Fire Research Laboratory, National Institute of Standards and Technology, Department of Commerce

Introduction of JAPAN Members by Japan Panel Chairman

Introduction of U.S. Members by U.S. Panel Chairman

Elect Joint Meeting Chairman

Adopt Agenda

Adjourn

１１：４５ Group Photograph

CLOSING CEREMONIES

May 19(Fri) 16:40～17:00

１６：４０　CLOSING CEREMONIES

Call to Order by Michio Okahara, Secretary - General, JAPAN - side Panel

Closing Remarks by Richard N. WRIGHT, Chairman U.S. - side Panel

Closing Remarks by Seizo TSUJI, Chairman JAPAN - Side Panel

TECHNICAL SITE VISITS

May 12 (Mon.)

Visit Trans-Tokyo Bay Highway (under construction)
Visit Futtsu work yard laboratory of Nippon Steel Company

May 17 (Sat.)

Visit Shinjuku Park Tower Building with wind-induced vibration control devices
Visit Kajima technical research laboratory.

May 18 (Sun.)

Visit Edo (Tokyo) museum
Visit Kanto earthquake memorial park and building
Visit Tokyo Fire Dept.: Education (PR) works for disaster prevention

May 19 (Mon.)

Visit earthquake phenomena observation system at JMA.
Visit Land Mark Tower in Yokohama

May 20 (Tues.)

Visit Nukui dam (under construction)
Visit Miyajima
Visit Hiroshima castle

May 21 (Wed.)

Visit Tatara cable stayed bridge
Visit Kurushima suspension bridge (under construction)

May 22 (Thurs.)

Visit earthquake restoration site in Kobe
Visit Akashi straight bridge

May 24 (Fri.)

Visit Hanshin expressway, seismic retrofit construction site
Visit Kongobuji temple and Okunoin temple

May 24 (Sat.)

Visit Kiyomizu temple
Visit Yasaka shrine
Visit Chionin temple
Move to Kansai airport
U.S. members leave Japan

List of Panel Members

UNITED STATES-SIDE PANEL ON WIND AND SEISMIC EFFECTS MEMBERSHIP LIST

Dr. Richard N. Wright
Chairman, U.S. Side Panel on Wind and Seismic Effects
Director, Building and Fire Research Laboratory
National Institute of Standards and Technology
U.S. Department of Commerce
Gaithersburg, MD 20899
Tel: 301-975-5900 Fax: 301-975-4032
E-mail: richard.wright@nist.gov

Mr. Noel J. Raufaste
Secretary-General, U.S. Side Panel on Wind and Seismic Effects
Head, Cooperative Research Programs
Building and Fire Research Laboratory
National Institute of Standards and Technology
U.S. Department of Commerce
Gaithersburg, MD 20899
Tel: 301-975-5905 Fax: 301-975-4737
E-mail: noel.raufaste@nist.gov

Dr. Kharaiti L. Abrol
Principal Structural Engineering Consultant, Consulting Support Office (188)
Room 475
Department of Veterans Affairs
810 Vermont Avenue, N.W.
Washington, D.C. 20420
Tel: 202-565-5579 Fax: 202-565-5478
E-mail: abrkha@hq.med.va.gov

Dr. Jon P. Ake
Geophysicist, Seismotectonics and Geophysics Section
Code D-8330
P.O. Box 25007
Bureau of Reclamation
U.S. Department of the Interior
Denver, CO 80225
Tel: 303-236-4195 Ext. 276
Fax: 303-236-9127
E-mail: jake@seismo.usbr.gov

Mr. John R. Baals
Seismic Safety Coordinator
Bureau of Reclamation
U.S. Department of the Interior
Denver, CO 80225
Tel: 303-236-9129 Ext. 304
Fax: 303-236-9099
E-mail: jbaals@do.usbr.gov

Dr. Celso S. Barrientos
Supervisory Physical Scientist
National Environmental Satellite Data Information Service
National Oceanic and Atmospheric Administration
U.S. Department of Commerce
5200 Auth Road
Camp Springs, MD 20746
Tel: 301-763-8102 Fax: 301-763-8020
E-mail: cbarrientos@nesdis.noaa.gov

Dr. Eddie N. Bernard
Director, Pacific Marine Environmental Laboratory
Environmental Research Laboratories
National Oceanic and Atmospheric Administration
U.S. Department of Commerce
7600 Sand Point Way, NE
BIN C15700/Building 3
Seattle, WA 98115-0070
Tel: 206-526-6800 Fax: 206-526-6815
E-mail: bernard@pmel.noaa.gov

Mr. Michael E. Blackford
Director, Pacific Tsunami
Warning Center
National Weather Service, Pacific Region
National Oceanic and Atmospheric
Administration
U.S. Department of Commerce
91270 Fort Weaver Road
Ewa Beach, HI 96706-2928
Tel: 808-689-8207 Ext. 301
Fax: 808-689-4543
E-mail: mike@ptwc.noaa.gov

Dr. David M. Boore
Geophysicist, Branch of Seismology
U.S. Geological Survey
U.S. Department of the Interior
345 Middlefield Road MS 977
Menlo Park, CA 94025
Tel: 415-329-5616 Fax: 415-329-5163
E-mail: boore@samoa.wr.usgs.gov

Dr. Roger D. Borcherdt
Research Engineering Seismologist, Branch of Seismology
U.S. Geological Survey
U.S. Department of the Interior
345 Middlefield Road, MS 977
Menlo Park, CA 94025
Tel: 415-329-5619 Fax: 415-329-5163
E-mail: borcherdt@samoa.wr.usgs.gov

Dr. Harish Chander
Civil/Structural Engineer, Office of Nuclear
Safety Policy and Standards
U.S. Department of Energy (EH-31)
CXXI, Room 2016 (GTN)
19901 Germantown Road
Germantown, MD 20874-1290
Tel: 301-903-6681 Fax: 301-903-8693
E-mail: harish.chander@hq.doe.gov

Dr. Ken P. Chong
Director, Structural Systems and Construction
Processes
Engineering Directorate
National Science Foundation
4201 Wilson Boulevard, Room 545
Arlington, VA 22230
Tel: 703-306-1361 Fax: 703-306-0291
E-mail: KChong@NSF.gov

Dr. Riley M. Chung
Leader, Earthquake Engineering Group
Building and Fire Research Laboratory
National Institute of Standards and Technology
U.S. Department of Commerce
Gaithersburg, MD 20899
Tel: 301-975-6056 Fax: 301-869-6275
E-mail: riley.chung@.nist.gov

Mr. James D. Cooper
Deputy Chief, Structures Division, HNR-10
Turner-Fairbank Highway Research Center
Federal Highway Administration
6300 Georgetown Pike
McLean, VA 22101
Tel: 703-285-2060 Fax: 703-285-2766
E-mail: jcooper@cais.com

Dr. A. G. Franklin
Chief, Earthquake Engineering and
Geosciences Division
Geotechnical Laboratory
U.S. Army Engineer Waterways
Experiment Station
3909 Halls Ferry Road
Vicksburg, MS 39180-6199
Tel: 601-634-2658 Fax: 601-634-3453
E-mail: FRANKLA@mail.wes.army.mil

Mr. William E. Freeborne
Mechanical Engineer, Policy Development and Research
Department of Housing and Urban Development
Room 8132
451 Seventh Street, S.W.
Washington, D.C. 20410
Tel: 202-708-4370 Fax: 202-619-8360
E-mail: William_E._Freeborne@hud.gov

Mr. James H. Gates
Chief, Office of Earthquake Engineering
Division of Structures
Department of Transportation
State of California
P.O. Box 942874, MS9
Sacramento, CA 94274
Tel: 916-227-8773 Fax: 916-227-8898
E-mail: jhgates@IBM.NET

Mr. Peter E. Gurvin
Director, Building Design and Engineering Division
Foreign Building Operations
Building SA-6, Room 335
U.S. Department of State
Washington, D.C. 20520
Tel: 703-875-6117 Fax: 703-875-6204

Dr. Walter W. Hays
Chief Scientist, Research Applications
955 National Center
U.S. Geological Survey
U.S. Department of the Interior
12201 Sunrise Valley Drive
Reston, VA 22192
Tel: 703-648-6711 Fax: 703-648-6591
E-mail: whays@usgs.gov

Mr. Allen M. Hittleman
Chief, Solid Earth Geophysics Division
National Geophysical Data Center
National Oceanic and Atmospheric Administration
U.S. Department of Commerce
325 Broadway, Boulder, CO 80303-3328
Tel: 303-497-6591 Fax: 303-497-6513
E-mail: allen.m.hittelman@noaa.gov

Mr. Larry C. Hultengren
Senior Structural Engineer, Office of Civil/Structural Engineering
Foreign Building Operations
U.S. Department of State
Building SA-6, Room 346
Washington, D.C. 20520
Tel: 703-875-6194 Fax: 703-875-6204

Dr. William B. Joyner
Geophysicist, Branch of Seismology
U.S. Geological Survey
U.S. Department of the Interior
345 Middlefield Road, MS 977
Menlo Park, CA 94025
Tel: 415-329-5640 Fax: 415-329-5163
E-mail: joyner@samoa.wr.usgs.gov

Mr. Roger M. Kenneally
Senior Structural Engineer, Structural and Seismic Engineering Branch
Mail stop T10-L1
U.S. Nuclear Regulatory Commission
Washington, D.C. 20555
Tel: 301-415-6303 Fax: 301-415-5074
E-mail: rmk@nrc.gov

Dr. George C. Lee
Director, National Center for Earthquake Engineering Research
State University of New York at Buffalo
Red Jacket Quadrangle
Buffalo, NY 14261
Tel: 716-645-3391 Fax: 716-645-3399
E-mail: gclee@ubvm.cc.buffalo.edu

Dr. H. S. Lew
Chief, Structures Division
Building and Fire Research Laboratory
National Institute of Standards and Technology
U.S. Department of Commerce
Gaithersburg, MD 20899
Tel: 301-975-6061 Fax: 301-869-6275
E-mail: hai.lew@nist.gov

Dr. Shih-Chi Liu
Program Director, Structural Systems
Division of Biological and Critical Systems
National Science Foundation
Room 545
4201 Wilson Boulevard
Arlington, VA 22230
Tel: 703-306-1362 Fax: 703-306-0291
E-mail: cliv@nst.gov

Dr. Josephine Malilay
Epidemiologist, Disaster Assessment and Epidemiology Section
National Center for Environmental Health
Centers for Disease Control and Prevention
Mailstop F-46
4770 Buford Highway, NE
Atlanta, GA 30341
Tel: 770-488-7350 Fax: 770-488-7335
E-mail: jym7@cchdehl.em.cdc.gov

Dr. Francis G. McLean
Value Program Manager
Code D-8170
P.O. Box 25007
Bureau of Reclamation
U.S. Department of the Interior
Denver, CO 80225
Tel: 303-236-9120 Ext.236
Fax: 303-236-6737
E-mail: fmclean@do.usbr.gov

Dr. Raymond E. Meyer
Senior Program Manager, Office of Foreign Disaster Assistance
SA14/ Room 1705
USAID
Washington, D.C. 20523-1443
Tel: 703-875-1522 Fax: 703-875-1708

Dr. Martin C. Miller
Chief, Coastal Oceanography Branch
USAE, Waterways Experiment Station
Coastal Hydraulics Laboratory
(CEWES-CR-O)
3909 Halls Ferry Road
Vicksburg, MS 39180
Tel: 601-634-3999 Fax: 601-634-4314
E-mail: m.miller@cerc.wes.army.mil

Mr. Ugo Morelli
Policy Manager for Seismology
Federal Emergency Management Agency
500 C Street, S.W.
Washington, D.C. 20472
Tel: 202-646-2810 Fax: 202-646-2577
E-mail: umorell@fema.gov

Mr. Howard D. Nickerson
Earthquake Engineering and Weapons Specialist, Naval Facilities Engineering Command
Hoffman Building #2, Room 12S63,
Code 04B2
200 Stovall Street
Alexandria, VA 22332
Tel: 202-433-8599 Fax: 202-433-8777
E-mail:
howard d nickerson@esc61@navfac nfesc

Dr. William E. Roper
Director, Civil Works
Research and Development (Civil Works)
U.S. Army Corps of Engineers
20 Massachusetts Avenue, N.W.
Washington, D.C. 20314-1000
Tel: 202-761-0257 Fax: 202-761-0907
E-mail: Bill.Roper@inet.hq.USACE.army.mil

Dr. J. Eleonora Sabadell
Director, Natural and Technological
Hazards Mitigation Program
Directorate of Engineering
National Science Foundation
Room 545-03
4201 Wilson Boulevard
Arlington, VA 22230
Tel: 703-306-1361 Fax: 703-306-0291
E-mail: esabadel@nsf.gov

Dr. Charles E. Smith
Research Program Manager, Technology
Assessment and Research Program
Engineering Research Branch
Minerals Management Service
U.S. Department of the Interior
381 Elden Street, MS 4800
Herndon, VA 20170-4817
Tel: 703-787-1559 Fax: 703-787-1555
E-mail: smithc@smtp.mms.gov

Mr. Stan Strickland
Chief, Air Base Systems Branch
Stop 37, WL/FIVC/OL, Building 1120
139 Barnes Drive, STE 2
Tyndall AFB, FL 32403-6001
Tel: 904-283-3709 Fax: 904-283-3722
E-mail: stan@mail.intero2.com

Dr. Andrew W. Taylor
Research Structural Engineer, Structures
Division
Building and Fire Research Laboratory
National Institute of Standards and
Technology
Gaithersburg, MD 20899-1000
Tel: 301-975-6078 Fax: 301-869-6275
E-mail: andrew.taylor@ nist.gov

ALTERNATE MEMBERS

Dr. Clifford J. Astill
Program Director, Division of Biological and
Critical Systems
National Science Foundation
4201 Wilson Boulevard, Room 545
Arlington, VA 22230
Tel: 703-306-1361 Fax: 703-306-0291

Dr. Mehmet K. Celebi
Research Civil Engineer, Branch of
Earthquake and Geomagnetic Information
U.S. Geological Survey
U.S. Department of the Interior
345 Middlefield Road, MS 977
Menlo Park, CA 94025
Tel: 415-329-5623 Fax: 415-329-5163
E-mail: celebi@samoa.wr.usgs.gov

Mr. Michael Changery
Chief, Global Analysis Branch
National Climatic Data Center
National Oceanic and Atmospheric
Administration
U.S. Department of Commerce
Federal Building
Ashville, NC 28801
Tel: 704-271-4765 Fax: 704-271-4246

Dr. C.Y. Chen
Senior Civil/Geotechnical Engineer
Office of Foreign Buildings
Department of State
Code SA-6, Room 347
Washington, D.C. 20520
Tel: 703-875-6207 Fax: 703-875-6204

Mr. Vincent P. Chiarito
Research Structural Engineer, Structural Mechanics Division
Structures Laboratory
U.S. Army Engineer Waterways Experiment Station
3909 Halls Ferry Road
Vicksburg, MS 39180-6199
Tel: 601-634-2714 Fax: 601-634-3412

Dr. James F. Costello
Senior Structural Engineer, Structural and Geological Engineering Branch
Office of Nuclear Regulatory Research
U.S. Nuclear Regulatory Commission
Mail Stop T10-L1
Washington, D.C. 20555
Tel: 301-415-6009 Fax: 301-415-5074

Mr. Lucian G. Guthrie, P.E.
Structures Branch, Engineering Division
U.S. Army Corps of Engineerings
UQUSACE(CECW-ED)
Washington, D.C. 20314-1000
Tel: 202-761-8673 Fax: 202-761-4716
E-mail: civil_works.eng1_postguthrie

Dr. Robert L. Hall
Chief, Structural Analysis Group
U.S. Army Engineer Waterways Experiment Station
3909 Halls Ferry Road
Vicksburg, MS 39180-6199
Tel: 601-634-2567 Fax: 601-634-3412
E-mail: hallr3@mail.wes.army.mil

Dr. James R. Houston
Director, Coastal Engineering Research Center
U.S. Army Engineer Waterways Experiment Station/WESCV-Z
3909 Halls Ferry Road
Vicksburg, MS 39180-6199
Tel: 601-634-2000 Fax: 601-634-2055
E-mail:houston@coafs1.wes.army.mil

Mr. James Lander
Geophysicist, Cooperative Institute for Research in Environmental Sciences
University of Colorado
Campus Box 449, Room 152 RL3
3100 Marine Street
Boulder, CO 80309
Tel: 303-497-6446 Fax: 303-497-6513

Mr. Tingley K. Lew
Research Structural Engineer, Structures Division
Naval Facilities Engineering Service Center, Code C62
1110 23rd Ave.
Port Hueneme, CA 93043-4370
Tel: 805-982-1234 Fax: 805-982-1418

Mr. Michael Mahoney
Physical Scientist, Federal Emergency Management Agency
500 C Street, S.W.
Washington, D.C. 20472
Tel: 202-646-2794 Fax: 202-646-4387
E-mail: mmahoney@fema.gov

Dr. Erdal Safak
Research Structural Engineer
U. S. Geological Survey
Box 25046, MS 966
Denver Federal Center
Denver, CO 80225
Tel: 303-273-8593 Fax: 303-273-8600

Dr. John B. Scalzi
Program Director, Structures and Building Systems
National Science Foundation
4201 Wilson Blvd., Room 545
Arlington VA 22230
Tel: 703-306-1361 Fax: 703-306-0291
E-mail: jscalzi@nsf.gov

Dr. W. Phillip Yen
Research Structural Engineer
Structures Division, HNR-10
Turner-Fairbank Highway Research Center
Federal Highway Administration
6300 Georgetown Pike
McLean, VA 22101
Tel: 703-285-2315 Fax: 703-285-2766
E-mail: pyen@cais.com

JAPAN-SIDE PANEL ON WIND AND SEISMIC EFFECTS MEMBERSHIP LIST

STEERING COMMITTEE MEMBERS

Mr. Seizo Tsuji
Chairman, Japan-side Panel on Wind and Seismic Effects
Director-General, Public Works Research Institute
Ministry of Construction
1, Asahi, Tsukuba-shi, Ibaraki-ken 305
Tel: 0298-64-2821
Fax: 0298-64-2148

Dr. Michio Okahara
Secretary-General, Japan-side Panel on Wind and Seismic Effects
Director, Structure and Bridge Department
Public Works Research Institute
Ministry of Construction
1, Asahi, Tsukuba-shi, Ibaraki-ken 305
Tel: 0298-64-2211
Fax: 0298-64-0565
E-mail: okahara@pwri.go.jp

Dr. Hisahiro Hiraishi
Director, Department of Structural Engineering
Building Research Institute
Ministry of Construction
1, Tatehara, Tsukuba-shi, Ibaraki-ken 305
Tel: 0298-64-6633
Fax: 0298-64-6773
E-mail: hiraishi@kenken.go.jp

Dr. Susumu Iai
Chief, Geotechnical Earthquake Engineering Laboratory
Port and Harbour Research Institute
Ministry of Transport
Nagase, 3-1-1, Yokosuka-shi
Kanagawa-ken 239
Tel: 0468-44-5028
Fax: 0468-44-4095
E-mail: iai@cc.phri.go.jp

Dr. Takamasa Inatomi
Director, Structural Engineering Division
Port and Harbour Research Institute
Ministry of Transport
3-1-1, Nagase, Yokosuka-shi
Kanagawa-ken 239
Tel: 0468-44-5027
Fax: 0468-44-0839
E-mail: inatomi@cc.phri.go.jp

Mr. Akihiro Iseki
Senior Assistant for Disaster Prevention
Planning Division
Administration Department
Japan Meteorological Agency
1-3-4, Ohtemachi, Chiyoda-ku, Tokyo 100
Tel: 03-3212-8341 Ext. 2225
Fax: 03-3211-2032

Dr. Toshio Iwasaki
President, Civil Engineering Research Laboratory
1-18, Kanda Suda-cho, Chiyoda-ku, Tokyo 101
Tel: 03-3254-9481
Fax: 03-3254-9448

Mr. Takashi Kaminosono
Head, Construction Techniques Division
Department of Production Engineering
Building Research Institute
Ministry of Construction
1, Tatehara, Tsukuba-shi, Ibaraki-ken 305
Tel: 0298-64-6665
Fax: 0298-64-6774
E-mail: kamino@kenken.go.jp

Prof. Kazuhiko Kawashima
Professor, Department of Civil Engineering
Tokyo Institute of Technology
2-12-1, O-okayama, Meguro-ku, Tokyo 152
Tel: 03-5734-2922
Fax: 03-3729-0728
E-mail: kawasima@cv.titech.ac.jp

Mr. Takahide Kouchi
Director, Disaster Countermeasure Office
Coast Administration and Disaster Prevention Division
Ports and Harbours Bureau
Ministry of Transport
2-1-3, Kasumigaseki, Chiyoda-ku, Tokyo 100
Tel: 03-3580-7028
Fax: 03-5511-8280

Mr. Osamu Matsuo
Head, Soil Dynamics Division
Earthquake Disaster Prevention Research Center
Public Works Research Institute
Ministry of Construction
1, Asahi, Tsukuba-shi, Ibaraki-ken 305
Tel: 0298-64-2211
Fax: 0298-64-0598
E-mail: matsuo@pwri.go.jp

Mr. Chikahiro Minowa
Cooperative Research Officer
National Research Institute for Earth Science and Disaster Prevention
3-1, Tennodai, Tsukuba-shi, Ibaraki-ken 305
Tel: 0298-51-1611
Fax: 0298-51-5658
E-mail: minowa@geo.bosai.gov.jp

Mr. Yasuyuki Miyamoto
Director, Road Disaster Prevention Section
Road Bureau
Ministry of Construction
2-1-3, Kasumigaseki, Chiyoda-ku, Tokyo 100
Tel: 03-5251-1896
Fax: 03-5251-1949

Mr. Toshitaka Miyata
Director, International Affairs Division
Economic Affairs Bureau
Ministry of Construction
2-1-3, Kasumigaseki, Chiyoda-ku, Tokyo 100
Tel: 03-3580-4311
Fax: 03-3502-3955

Mr. Eishi Mochizuki
Head, Seismology and Volcanology Research Division
Meteorological Research Institute
Japan Meteorological Agency
1-1, Nagamine, Tsukuba-shi, Ibaraki-ken 305
Tel: 0298-53-8675
Fax: 0298-51-3730

Mr. Nobuo Nagai
Director, Geographic Department
Geographical Survey Institute
Ministry of Construction
1, Kitasato, Tsukuba-shi, Ibaraki-ken 305
Tel:0298-64-2667
Fax:0298-64-1804
E-mail: nagai@graph.gsi-mc.go.jp

Dr. Nobuyuki Narita
Professor, Civil Engineering Department
Tokyo Metropolitan University
1-1, Minamiosawa, Hachioji-shi, Tokyo 192-03
Tel: 0426-77-2782
Fax: 0426-77-2772

Dr. Isao Nishiyama
Head, Housing Construction Division
Department of Production Engineering
Building Research Institute
Ministry of Construction
1, Tatehara, Tsukuba-shi, Ibaraki-ken 305
Tel: 0298-64-2151
Fax: 0298-64-6774
E-mail: isao@kenken.go.jp

Dr. Shigeyuki Noto
Director, Structures Division
Civil Engineering Research Institute
Hokkaido Development Agency
1-3, Hiragishi, Toyohira-ku, Sapporo,
Hokkaido 062
Tel: 011-841-1111
Fax: 011-820-2714
E-mail: noto@ceri.go.jp

Mr. Roshi Ojima
Director, Hydraulic Engineering Division
Port and Harbour Research Institute
Ministry of Transport
3-1-1, Nagase, Yokosuka-shi, Kanagawa-ken 239
Tel: 0468-44-5009
Fax: 0468-41-3888
E-mail: ojima@cc.phri.go.jp

Dr. Hisashi Okada
Associate Director for Composite Structures
Department of Structural Engineering
Building Research Institute
Ministry of Construction
1, Tatehara, Tsukuba-shi, Ibaraki-ken 305
Tel: 0298-64-6641
Fax: 0298-64-6773
E-mail: okada@kenken.go.jp

Prof. Tsuneo Okada
Professor, Dipertment of Architecture and
Building Engineering
Shibaura Institute of Technology
3-9-14 Shibaura, Minato-ku, Tokyo 108
Tel: 03-5476-2452
Fax: 03-5476-2446

Mr. Kazuo Okayama
Director, Earthquake Disaster Countermeasure
Division
Disaster Prevention Bureau
National Land Agency
1-2-2, Kasumigaseki, Chiyoda-ku, Tokyo 100
Tel: 03-3501-5693
Fax: 03-3501-5199

Dr. Izuru Okawa
Head, Building Engineering Division
International Institute of Seismology and
Earthquake Engineering
Building Research Institute
Ministry of Construction
1, Tatehara, Tsukuba-shi, Ibaraki-ken 305
Tel: 0298-64-6758
Fax: 0298-64-6777
E-mail: okawa@kenken.go.jp

Mr. Keiichi Ohtani
Director, Disaster Prevention Research
Division
National Research Institute for Earth Science
and Disaster Prevention
Science and Technology Agency
3-1, Tennodai, Tsukuba-shi, Ibaraki-ken 305
Tel: 0298-51-1611 ex.321
Fax: 0298-52-8512
E-mail: ohtani@knetgk.k-net.bosai.go.jp

Mr. Hiroshi Sasaki
Director, Building Disaster Prevention Section
Housing Bureau
Ministry of Construction
2-1-3, Kasumigaseki, Chiyoda-ku, Tokyo 100
Tel: 03-3580-4311
Fax: 03-3580-7050

Dr. Hiroshi Sato
Head, Structure Division
Structure and Bridge Department
Public Works Research Institute
Ministry of Construction
1, Asahi, Tsukuba-shi, Ibaraki-ken 305
Tel: 0298-64-2874
Fax: 0298-64-0565
E-mail: hsato@pwri.go.jp

Dr. Shinji Sato
Head, Coast Division
River Department
Public Works Research Institute
Ministry of Construction
1, Asahi, Tsukuba-shi, Ibaraki-ken 305
Tel: 0298-64-2327
Fax: 0298-64-1168
E-mail: sato@pwri.go.jp

Mr. Tatsuyuki Shimazu
International Cooperation Coordinator
International Affairs Division
Science and Technology Agency
2-2-1, Kasumigaseki, Chiyoda-ku, Tokyo 100
Tel: 03-3593-0362
Fax: 03-3581-5909

Dr. Takahiro Sugano
Chief, Structural Dynamics Laboratory
Structural Engineering Division
Port and Harbour Research Institute
Ministry of Transport
3-1-1, Nagase, Yokosuka-shi
Kanagawa-ken 239
Tel: 0468-44-5029
Fax: 0468-44-0839
E-mail: macsuga@ipc.phri.go.jp

Dr. Keiichi Tamura
Head, Ground Vibration Division
Earthquake Disaster Prevention Research Center
Public Works Research Institute
Ministry of Construction
1, Asahi, Tsukuba-shi, Ibaraki-ken 305
Tel: 0298-64-2926
Fax: 0298-64-0598
E-mail: tamura@pwri.go.jp

Dr. Masaomi Teshigawara
Head, Structure Division
Department of Structural Engineering
Building Research Institute
Ministry of Construction
1, Tatehara, Tsukuba-shi, Ibataki-ken 305
Tel: 0298-64-6753
Fax: 0298-64-6773
E-mail: teshi@kenken.go.jp

Dr. Takaaki Uda
Director, River Department
Public Works Research Institute
Ministry of Construction
1, Asahi, Tsukuba-shi, Ibaraki-ken 305
Tel: 0298-64-2211
E-mail: uda@pwri.go.jp

Mr. Tetsushi Uehara
Director, Office of Disaster Prevention
Research Planning Division
Research and Development Bureau
Science and Technology Agency
2-2-1, Kasumigaseki Chiyoda-ku, Tokyo 100
Tel: 03-3581-5271
Fax: 03-3503-8169

Mr. Tsuneo Uesaka
Director, Dam Department
Public Works Research Institute
Ministry of Construction
1, Asahi, Tsukuba-shi, Ibaraki-ken 305
Tel: 0298-64-2211
Fax: 0298-64-2688

Dr. Shigeki Unjoh
Head, Earthquake Engineering Division
Earthquake Disaster Prevention Research Center
Public Works Research Institute
Ministry of Construction
1, Asahi, Tsukuba-shi, Ibaraki-ken 305
Tel: 0298-64-2932
Fax: 0298-64-0598
E-mail: unjoh@pwri.go.jp

Dr. Tatsuo Uwabe
Chief, Earthquake Disaster Prevention Laboratory
Structural Engineering Division
Port and Harbour Research Institute
Ministry of Transport
3-1-1, Nagase, Yokosuka-shi
Kanagawa-ken 239
Tel: 0468-44-5030
Fax: 0468-44-0839
E-mail: uwabe@cc.phri.go.jp

Prof. Makoto Watabe
Professor, Faculty of Environmental Information
Keio University
5322, Endou, Fujisawa-shi
Kanagawa-ken 252
Tel: 0466-47-5111

Mr. Joji Yanagawa
Director, Disaster Management Division
River Bureau
Ministry of Construction
2-1-3, Kasumigaseki, Chiyoda-ku, Tokyo 100
Tel: 03-3580-4311 Ext. 3431
Fax: 03-5251-1946

Dr. Hiroyuki Yamanouchi
Director, Department of Research
Administration and Management
Building Research Institute
Ministry of Construction
1, Takehara, Tsukuba-shi, Ibaraki-ken 305
Tel: 0298-64-2151 Ext. 6633
Fax: 0298-64-2989
E-mail: yamanoch@kenken.go.jp

Dr. Koichi Yokoyama
Director, Earthquake Disaster Prevention
Research Center
Public Works Research Institute
Ministry of Construction
1, Asahi, Tsukuba-shi, Ibaraki-ken 305
Tel: 0298-64-2829
Fax: 0298-64-0598
E-mail: yokoyama@pwri.go.jp

Mr. Shoin Yagi
Director, Typhoon Research Department
Meteorological Research Institute
Japan Meteorological Agency
1-1, Nagamine, Tsukuba-shi, Ibaraki-ken 305
Tel: 0298-53-8663
Fax: 0298-53-8735

Mr. Hitoshi Yoshida
Head, Fill-type Dam Division
Dam Department
Public Works Research Institute
Ministry of Construction
1, Asahi, Tsukuba-shi, Ibaraki-ken 305
Tel: 0298-64-2413
Fax: 0298-64-0164
E-mail: h-yshida@pwri.go.jp

SECRETARIES COMMITTEE MEMBERS

Dr. Michio Okahara
Secretary-General, Japan-side Panel on Wind and Seismic Effects
Director, Structure and Bridge Department
Public Works Research Institute
Ministry of Construction
1, Asahi, Tsukuba-shi, Ibaraki-ken 305
Tel: 0298-64-2211
Fax: 0298-64-0565
E-mail: okahara@pwri.go.jp

Mr. Jiro Fukui
Head, Foundation Engineering Division
Structure and Bridge Department
Public Works Research Institute
Ministry of Construction
1, Asahi, Tsukuba-shi, Ibaraki-ken 305
Tel: 0298-64-2211
Fax: 0298-64-0565
E-mail: @pwri.go.jp

Dr. Hisahiro Hiraishi
Director, Department of Structural Engineering
Building Research Institute
Ministry of Construction
1, Tatehara, Tsukuba-shi, Ibaraki-ken 305
Tel: 0298-64-6633
Fax: 0298-64-6773
E-mail: hiraishi@kenken.go.jp

Mr. Masakatsu Horino
Head, Planning Division
Geographic Department
Geographical Survey Institute
Ministry of Construction
1, Kitasato, Tsukuba-shi, Ibaraki-ken 305
Tel: 0298-64-5917
Fax: 0298-64-1804
E-mail: horino@graph.gsi-mc.go.jp

Dr. Susumu Iai
Chief, Geotechnical Earthquake Engineering Laboratory
Port and Harbour Research Institute
Ministry of Transport
3-1-1, Nagase, Yokosuka-shi
Kanagawa-ken 239
Tel: 0468-44-5028
Fax: 0468-44-4095
E-mail: iai@cc.phri.go.jp

Prof. Kazuhiko Kawashima
Professor, Department of Civil Engineering
Tokyo Institute of Technology
2-12-1 O-okayama, Meguro-ku Tokyo 152
Tel: 03-5734-2922
Fax: 03-3729-0728

Mr. Osamu Matsuo
Head, Soil Dynamics Division
Earthquake Disaster Prevention Research Center
Public Works Research Institute
Ministry of Construction
1, Asahi, Tsukuba-shi, Ibaraki-ken 305
Tel: 0298-64-2211
Fax: 0298-64-0598
E-mail: matsuo@pwri.go.jp

Mr. Chikahiro Minowa
Cooperative Research Officer
National Research Institute for Earth Science and Disaster Prevention
3-1, Tennodai, Tsukuba-shi, Ibaraki-ken 305
Tel: 0298-51-1611
Fax: 0298-51-5658
E-mail: minowa@geo.bosai.gov.jp

Mr. Akiyoshi Mukai
Head, Aerodynamics Division
Department of Structural Engineering
Building Research Institute
Ministry of Construction
1, Tatehara, Tsukuba-shi, Ibaraki-ken 305
Tel: 0298-64-6643
Fax: 0298-64-6773
E-mail: mukai@kenken.go.jp

Mr. Kazuhiro Nishikawa
Head, Bridge Division
Structure and Bridge Department
Public Works Research Institute
Ministry of Construction
1, Asahi, Tsukuba-shi, Ibaraki-ken 305
Tel: 0298-64-2905
Fax: 0298-64-0565
E-mail: knishika@pwri.go.jp

Dr. Nobuyuki Ogawa
Head, Earthquake Engineering Laboratory
National Research Institute for Earth Science
and Disaster Prevention
Science and Technology Agency
3-1, Tennodai, Tsukuba-shi, Ibaraki-ken 305
Tel: 0298-51-1611
Fax: 0298-51-5658
E-mail: ogawa@geo.bosai.go.jp

Dr. Hisashi Okada
Associate Director for Composite Structures
Department of Structural Engineering
Building Research Institute
Ministry of Construction
1, Tatehara, Tsukuba-shi, Ibataki-ken 305
Tel: 0298-64-6641
Fax: 0298-64-6773
E-mail: okada@kenken.go.jp

Mr. Masami Okada
Head, The First Research Laboratory
Seismology and Volcanology Research
Department
Meteorological Research Institute
Japan Meteorological Agency
Ministry of Transport
1-1, Nagamine, Tsukuba-shi, Ibaraki-ken 305
Tel: 0298-53-8677
Fax: 0298-51-3730

Mr. Hidetsugu Onuma
Director, Research Planning and Coordination
Section
Administration Division
Civil Engineering Research Institute
Hokkaido Development Agency
1-3, Hiragisi, Toyohira-ku, Sapporo-shi
Hokkaido 062
Tel: 011-824-1111
Fax: 011-824-1226
E-mail: h.onuma@ceri.go.jp

Mr. Keiichi Ohtani
Director, Disaster Prevention Research
Division
National Research Institute for Earth Science
and Disaster Prevention
Science and Technology Agency
3-1, Tennodai, Tsukuba-shi, Ibaraki-ken, 305
Tel: 0298-51-1611 Ext. 321
Fax: 0298-52-8512
E-mail: ohtani@knetgk,k-net,bosai.go.jp

Dr. Hiroshi Sato
Head, Structure Division
Structure and Bridge Department
Public Works Research Institute
Ministry of Construction
1, Asahi, Tsukuba-shi, Ibaraki-ken 305
Tel: 0298-64-2874
Fax: 0298-64-0565
E-mail: hsato@pwri.go.jp

Dr. Shinji Sato
Head, Coast Division
River Department
Public Works Research Institute
Ministry of Construction
1, Asahi, Tsukuba-shi, Ibaraki-ken 305
Tel: 0298-64-2327
Fax: 0298-64-1168
E-mail: sato@pwri.go.jp

Dr. Hideki Sugita
Head, Earthquake Disaster Prevention
Technology Division
Earthquake Disaster Prevention Research
Center
Public Works Research Institute
Ministry of Construction
1, Asahi, Tsukuba-shi, Ibaraki-ken 305
Tel: 0298-64-3244
Fax: 0298-64-0598
E-mail: sugita@pwri.go.jp

Dr. Keiichi Tamura
Head, Ground Vibration Division
Earthquake Disaster Prevention Research
Center
Public Works Research Institute
Ministry of Construction
1, Asahi, Tsukuba-shi, Ibaraki-ken 305
Tel: 0298-64-2926
Fax: 0298-64-0598
E-mail: tamura@pwri.go.jp

Mr. Nobuyuki Tsuneoka
Head, International Cooperation Division
Planning and Research Administration
Department
Public Works Research Institute
Ministry of Construction
1, Asahi, Tsukuba-shi, Ibaraki-ken 305
Tel: 0298-64-4412
Fax: 0298-64-4322
E-mail: tsuneoka@pwri.go.jp

Dr. Shigeki Unjoh
Head, Earthquake Engineering Division
Earthquake Disaster Prevention Research
Center
Public Works Research Institute
Ministry of Construction
1, Asahi, Tsukuba-shi, Ibaraki-ken 305
Tel: 0298-64-2932
Fax: 0298-64-4424
E-mail: unjoh@pwri.go.jp

Dr. Tatsuo Uwabe
Chief, Disaster Prevention Laboratory
Structural Engineering Division
Port and Harbour Research Institute
Ministry of Transport
3-1-1, Nagase, Yokosuka-shi
Kanagawa-ken 239
Tel: 0468-44-5030
Fax: 0468-44-0839
E-mail: uwabe@cc.phri.go.jp

Dr. Koichi Yokoyama
Director, Earthquake Disaster Prevention
Research Center
Public Works Research Institute
Ministry of Construction
1, Asahi, Tsukuba-shi, Ibaraki-ken 305
Tel: 0298-64-2829
Fax: 0298-64-0598
E-mail: yokoyama@pwri.go.jp

Mr. Hitoshi Yoshida
Head, Fill-type Dam Division
Dam Department
Public Works Research Institute
Ministry of Construction
1, Asahi, Tsukuba-shi, Ibaraki-ken 305
Tel: 0298-64-2413
Fax: 0298-64-0164
E-mail: h-yshida@pwri.go.jp

TEMPORARY MEMBERS

Mr. Koji Ichii
Research Engineer
Geotechnical Earthquake Engineering
Laboratory
Port and Harbour Research Institute
Ministry of Transport
3-1-1, Nagase, Yokosuka-shi
Kanagawa-ken 239
Tel: 0468-44-5028
Fax: 0468-44-4095

Mr. Nobuyuki Kinoshita
Senior Researcher, Physical Meteorology
Research Department
Meteorological Research Institute
Japan Meteorological Agency
1-1, Nagamine, Tsukuba-shi, Ibaraki-ken 305
Tel: 0298-53-8707
Fax: 0298-55-6936

Dr. Shigeo Kinoshita
Head, Earthquake and Volcanic Disaster
Prevention Laboratory
National Research Institute for Earth Science
and Disaster Prevention
Science and Technology Agency
3-1, Tennodai, Tsukuba-shi, Ibaraki-ken 305
Tel: 0298-54-4940
Fax: 0298-54-4941
E-mail: kinosita@geo.bosai.go.jp

Mr. Hiroshi Masaharu
Head, Third Geographic Division
Geographic Department
Geographical Survey Institute
Ministry of Construction
1, Kitasato, Tsukuba-shi, Ibaraki-ken 305
Tel: 0298-64-6920
Fax: 0298-64-1804

Dr. Hanlong Liu
STA Fellow, Geotechnical Earthquake
Engineering Laboratory
Port and Harbour Research Institute
Ministry of Transport
3-1-1, Nagase, Yokosuka-shi
Kanagawa-ken 239
Tel: 0468-44-5028
Fax: 0468-44-4095

Dr. Toshihiko Nagai
Chief, Marine Observation Laboratory
Hydraulic Engineering Division
Port and Harbour Research Institute
Ministry of Transport
3-1-1, Nagase, Yokosuka-shi
Kanagawa-ken 239
Tel: 0468-44-5017
Fax: 0468-42-5246

Mr. Isao Nagayama
Head, Dam Structure Division
Dam Department
Public Works Research Institute
Ministry of Construction
1, Asahi, Tsukuba-shi, Ibaraki-ken 305
Tel: 0298-64-2211
Fax: 0298-64-2688

Dr. Hajime Nakamura
Head, The Second Laboratory
Forecast Research Department
Meteorological Research Institute
Japan Meteorological Agency
1-1, Nagamine, Tsukuba-shi, Ibaraki-ken 305
Tel: 0298-53-8638
Fax: 0298-53-8649
E-mail: hnakamur@mri-jma.go.jp

Mr. Syunetsu Odagiri
Research Coordinator for Information Technology
Planning and Administration Department
Public Works Research Institute
Ministry of Construction
1, Asahi, Tsukuba-shi, Ibaraki-ken 305
Tel: 0298-64-2211
Fax: 0298-64-3146

Dr. Keiko Ogawa
Division of Public Health
Postgraduate School of Medicine
Tohoku University
2-1, Seiryo-machi, Aoba-ku, Sendai 980-77
Tel: 022-717-8122
Fax: 022-717-8125
E-mail: keikoo@mail.cc.tohoku.ac.jp

Prof. Naotaka Shinfuku
Professor, School of Medicine
Kobe University
7-5-1, Kusunoki, Chuo-ku, Kobe-shi
Hyogo-ken 657
Tel: 078-341-7451
Fax: 078-361-1241

Prof. Shiro Takada
Professor, Department of Architecture and Civil Engineering
Kobe University
Rokkodai, Nada-ku, Kobe-shi, Hyogo-ken 657
Tel: 078-803-1031
Fax: 078-803-1040
E-mail: takada@kobe-u.ac.jp

Dr. Yuichiro Tanioka
Researcher, Seismology and Volcanology Department
Meteorological Researcher Institute
Japan Meteorological Agency
1-1, Nagamine, Tsukuba-shi, Ibaraki-ken 305
Tel: 0298-52-9206
Fax: 0298-51-3730

ASSOCIATE MEMBERS

Dr. Minoru Fujiwara
Formerly, Professor, Department of Civil Engineering
Tohoku University
Aoba, Aoba-ku, Sendai-shi, Miyagi-ken 980-77

Dr. Masami Fukuoka
Formerly, Professor, Department of Civil Engineering
Science University of Tokyo
2641, Yamazaki, Noda-shi, Chiba-ken 278

Dr. Masaya Hirosawa
Professor, Kogakuin University
1-24-2-91, Nishishinjuku, Shinjuku-ku
Tokyo 163
Tel: 03-3342-1211

Dr. Shiro Ibukiyama
President, Kogyokusha College of Technology
5-14-2, Nishigotanda, Shinagawa-ku
Tokyo 141
Tel: 03-3493-5671

Dr. Kaoru Ichihara
President, Public Works Research Center
1-6-4, Taito, Taito-ku, Tokyo 110
Tel: 03-3835-3609

Dr. Ryuichi Iida
President, Japan Dam Engineering Center
2-4-5, Azabudai, Minato-ku, Tokyo 110
Tel: 03-3433-7811

Dr. Takashi Iijima
President, Sekisui-jushi Co., Ltd.
1-11-1, Kaigan, Minato-ku, Tokyo 106
Tel: 03-5400-1850

Dr. Toshio Iwasaki
President, Civil Engineering Research Laboratory
1-18, Kandasuda-cho,Chiyoda-ku, Tokyo 101
Tel: 03-3254-9481
Fax: 03-3254-9448

Mr. Shunichiro Kamijo
Mitsui Construction Co., Ltd.
3-10-1, Iwamoto-cho, Chiyoda-ku, Tokyo 106
Tel: 03-5223-3921

Mr. Kenji Kawakami
Adviser, Kubota Corporation
3-1-3, Nihonbashi-muromachi
Cyuoh-ku, Tokyo 103
Tel: 03-3245-3660

Dr. Eiichi Kuribayashi
Professor, Toyohashi University of Technology
1-1, Hibarigaoka, Tenpaku-cho
Toyohashi-shi 440
Tel: 0532-44-6967

Mr. Mitsuru Nagao
President, Japan Construction Mechanization Association
3-5-8, Shibakoen, Minato-ku, Tokyo 105
Tel: 03-3433-1501

Dr. Seiji Nakano
Professor, Tokyo Denki University
2-2, Kandanishiki-cho, Chiyoda-ku, Tokyo 101
Tel: 03-5280-3501

Dr. Kazuto Nakazawa
President, Regional Development Consultants Inc.
1-18, Kandasuda-cho, Chiyoda-ku, Tokyo 101
Tel: 03-3831-2916
Fax: 03-3836-4048

Dr. Nobuyuki Narita
Professor, Civil Engineering Department
Tokyo Metropolitan University
1-1, Minamiosawa, Hachiohji-shi
Tokyo 192-03
Tel: 0426-77-2782
Fax: 0426-77-2772

Dr. Shin Okamoto
Director-General
Building Technology Research Institute
The Building Center of Japan
3-2-2, Toranomon, Minato-ku, Tokyo 105
Tel: 03-3458-1011

Mr. Yoshijiro Sakagami
President, Rinkai Construction Co., Ltd.
2-3-8, Shiba, Minato-ku, Tokyo 105
Tel: 03-3453-4111

Mr. Tadahiko Sakamoto
President, Japan Dam Engineering Center
2-4-5, Azabudai, Minato-ku, Tokyo 110
Tel: 03-3433-7811

Prof. Yasushi Sasaki
Professor, Department of Civil and
Environmental Engineering
Hiroshima University
1-4-1, Kagamiyama, Higashihiroshima-shi
Hiroshima-ken 739
Tel: 0824-24-7783
Fax: 0824-24-7783
E-mail: ysasaki@ue.ipc.hiroshima-u.ac.jp

Dr. Yukihiko Sumiyoshi
Executive Counselor, Nippon Steel Co., Ltd.
2-6-3, Ohte-machi, Chiyoda-ku, Tokyo 100-71
Tel: 03-3275-5868

Mr. Jiro Taguchi
Managing Director, Trans-Tokyo Bay
Highway Co., Ltd.
15-5, Ichiban-cho, Chiyoda-ku, Tokyo 102
Tel: 03-3239-6582

Dr. Hiroshi Takahashi
Adviser, Engineering Department
Sato Kogyo Co., Ltd.
4-12-20, Nihonbashihon-cho, Cyuo-ku
Tokyo 103
Tel: 03-3661-2296

Dr. Masateru Tominaga
President, Public Works Research Center
1-6-4, Taito, Taito-ku, Tokyo 110
Tel: 03-3835-3609

Dr. Hajime Tsuchida
Executive Counselor, Nippon Steel Co., Ltd.
2-6-3, Ohte-machi, Chiyoda-ku, Tokyo 100-71
Tel: 03-3275-5894

Prof. Makoto Watabe
Professor, Faculty of Environmental
Information
Keio University
5322, Endou, Fujisawa-shi, Kanagawa-ken 252
Tel: 0466-47-5111

List of Task Committee Members

TASK COMMITTEE MEMBERSHIP LIST

Task Committee	U. S. Side	Japan Side
A: Strong-Motion Data and Applications	R. D. Borcherdt*	S. Iai*
	C. J. Astill	R. Honda
	M. K. Celebi	Y. Ichii
	A.G. Franklin	K. Mimura
	W. B. Joyner#	M. Miyata
	F. G. Mclean	E. Mochizuki
	C. S. Barrientos	I. Okawa
	T. K. Lew	K. Ohtani
	E. Safak	M. Sato
	+ J. Kimball	K. Tamura
	+ J. Hunt	H. Yamanouchi
	W. Freeborn	
	J. Ake	
	H. Meyers	
B: Testing and Evaluation Procedures for Building Systems	H. S. Lew*	K. Ohtani*
	V. P. Chiarito	T. Fukuta
	J. E. Sabadell	T. Kaminosono
	C. E. Smith	T. Morino
	K. Abrol	S. Nakata
	+ S. Sweeney	I. Nishiyama
	+ A. Bieniawski	H. Noguchi
	W. Freedorn	A. Tanaka
		A. Wada
C: Design, Evaluation and Improvement of Structures	K. P. Chong*	H. Hiraishi*
	N. Raufauste#	H. Fukuyama
	+ J. O. Jirsa	T. Kaminosono
	H. S. Lew	S. Otani
	T. K. Lew	A. Mukai
	H. D. Nickerson	M. Nakashima
	+ D. H. Oh	I. Nishiyama
	+ M. A. Phipps	M. Okahara
	J. B. Scalzi	H. Shiobara
	+ S. Woodson	M. Teshigawara
	R. L. Hall	A. Wada
	+ S. A. Asar	
	M. K. Celebi	
	K. L. Abrol	
	+ A. Bieniawski	
	+ K. Mutreja	

	P. Brady	
	D. Ellsworth	
	W. Freeborn	
D: Earthquake Engineering for Dams	W. E. Roper*	H. Yoshida*
	R. L. Hall	T. Fujino
	L. G. Guthrie	Y. Iida
	+ R. Davidson	J. Inomata
	+ M. E. Hynes	T. Iwashita
	A. G. Franklin	J. Kasui
	+ R. Navidi	I. Nagayama
	+ L. Von Thun	S. Nakamura
	+ W. Allerton	T. Ohmachi
	F. G. Mclean	Y. Ohne
		T. Sasaki
		S. Takasu
		J. Tamura
		M. Toyota
		T. Uesaka
		Y. Wakisaka
		K. Watanabe
		A. Yamagichi
		Y. Yamaguchi
E: Design for Wind and Wind Hazard Mitigation	A. Taylor*	T. Okada*
	E. Sabadell*	H. Sato*
	H. S. Lew#	H. Akiyama
		N. Kinoshita
		Y. Kimura
		G. Naito
		T. Mabuchi
		T. Tamura
		Y. Tamura
		Y. Uematsu
		S. Yagi
		H. Yamada
F: Disaster Prevention Methods for Lifelines Systems	R. M. Chung*	K. Yokoyama*
	N. Raufauste#	M. Hamada
	C. J. Astill	K. Honda
	M. K. Celebi	J. Hoshikuma
	J. D. Cooper	Y. Kajiya
	G. Al-Chaar	H. Kameda
	T. K. Lew	M. Kaneko
	J.B. Scalzi	T. Katayama
	J. S. Spencer	O. Matsuo

	S. Wu	K. Nakajo
	S. Sommer	N. Ogawa
		K. Sasabe
		K. Shimamura
		H. Suzuki
		Y. Taguchi
		S. Takada
		K. Tamura
		J. Toma
		T. Uwabe
		S. Unjoh
G: Structural Control and Intelligent Material Systems	S. C. Liu*	S. Unjoh*
	N. Raufauste#	Y.Adachi
	V. P. Chiarito	K. Asano
	K. P. Chong	Y. Fujino
	J. R. Hayes	H. Fujitani
	L. C. Hultengren	H. Fukuyama
	G. Lee	Y. Goto
		H. Iemura
		N.Inoue
		Y. Inoue
		T. Ishimaru
		K. Kawashima
		M. Kitazawa
		H. Kosaka
		Y. Makiguchi
		C. Minowa
		T. Moriya
		A. Nishitani
		H. Okada
		S. Okamoto
		A. Ogawa
		M. Sato
H: Soil Behavior and Stability During Earthquakes	A. G. Franklin*	O. Matsuo
	C. J. Astill	J. Fukui
	R. D. Borcherdt	S. Iai
	C. Y. Chen	M. Iiba i
	F. G. Mclean	H. Kobayash
	C. E. Smith	J. Koseki
	R. M. Chung	C. Minowa
		J. Nishikawa
		T. Sugano
		H. Suzuki
		K. Tamura

		I.Tohata
		J. Tohma
		Y. Yamaguchi
		S. Yasuda
		K. Yoshi
		H. Yoshida
I: Storm Surge and Tsunami	M. Blackford*	S. Sato*
	C. J Astill	T. Goto
	C. S. Barrientos	S. Iwasaki
	E. N. Bernard	K. Kawata
	H. L. Butler	T. Konishi
	J. Lander	T. Nagai
	W. E. Roper	T. Nakayama
	A. M. Hittelman	R. Ojima
		M. Okada
		T. Sasajima
		K. Satake
		N. Shuto
		T. Yamashita
J: Wind and Earthquake Engineering for Transportation Systems	J. D. Cooper*	M. Okahara*
	A. G. Franklin	H. Akiyama
	J. H. Gates	Y. Fujino
	J. B. Scalzi	R. Honda
	H. S. Lew	J. Fukui
	W. P. Yen#	T. Inatomi
	H. R. Bosch	M. Ishida
		K. Kawashima
		Y. Kimura
		M. Kitazawa
		H. Osaka
		T. Moriya
		J. Murakoshi
		K. Nishikawa
		A. Ogawa
		K. Ogiwara
		H. Sato
		M. Sato
		Y. Tanaka
		T. Terayama
		K. Tamura
		S. Unjoh
		K. Yokoyama

K: Wind and Earthquake Engineering for offshore and Coastal Facilities	C. E. Smith*	T. Uwabe*
	C. S. Barrientos	J. Fukui
	W. E. Roper#	S. Iai
	J. E. Sabadell	T. Inatomi
	+ M. C. Miller	M. Kazama
	M. K. Celebi	S. Noda
		A. Notsu
		M. Okada
		H. Shiojiri
		T. Sugano
		H. Tsuchida
		Y. Yoshida

* Chairman

\# Acting Task Committee Chairman for the 29th Joint Meeting

\+ TC Members not Panel Members

Resolutions

RESOLUTIONS OF THE TWENTY-NINTH JOINT MEETING
U.S.-JAPAN PANEL ON WIND AND SEISMIC EFFECTS (UJNR)
Public Works Research Institute, Tsukuba, Japan
May 13-16, 1997

The following resolutions are hereby adopted:

1. The Twenty-Ninth Joint Panel Meeting provided the forum to exchange valuable technical information that is beneficial to both countries. In view of the importance of cooperative programs on the subject of wind and seismic effects, the continuation of Joint Panel Meetings is considered essential.

2. The following activities have been conducted since the Twenty-Eighth Joint Meeting:

   a. Technology Exchanges. Technical experts, technical documents, and applications of the electronic media have been exchanged. These exchanges have contributed to the development of new research programs and enhanced ongoing research in both countries.

   b. Task Committee Workshops. The Panel held five workshops and technical site visits; Over 250 specialists from both countries participated in these activities:
      1. Task Committees (C&G), 2nd Workshop on Smart Structures Technology: Application to Large Civil Structures, 13-15 November 1996, University of Maryland, College Park, MD, USA.
      2. Task Committee (D), 1st Workshop on State-of-the-Art Review of U.S.-Japan Research on Earthquake Engineering for Dams, 12-14 November 1996, WES, Vicksburg, MS, USA.
      3. Task Committee (J), 12th Bridge Engineering Workshop, 29-30 October 1996, Buffalo, NY, USA.
      4. Task Committees (G&J), 4th Workshop on Earthquake Protective Systems for Bridges, 9-10 December 1996, Osaka, Japan.
      5. Task Committee (J), 3rd Workshop on Seismic Retrofit of Bridges, 10-11 December 1996, Osaka, Japan.

   c. Common Agenda. The Panel recognizes the importance of providing earthquake science and technology expertise to the 17 April 1996 U.S.-Japan Natural Disaster Reduction Initiative of the U.S.-Japan Framework for New Economic Partnership (Common Agenda). Panel members organized and participated in the First Earthquake Policy Symposium, 16-18 September 1996, Washington, D.C. and reviewed 35-proposals for the Earthquake Disaster Mitigation Partnership. The Panel is contributing to planning the 2nd Earthquake Policy Symposium, 17-19 September 1997, Kobe. The Panel will continue to provide technical

leadership and participation in appropriate research projects aimed at realizing the objectives of the Common Agenda. Appropriate Task Committees will respond to the Common Agenda in planning their work.

3. The Panel addressed a new theme on Seismic Information Systems. Important data and information were presented about disaster prevention information systems and risk assessment using Geographic Information System (GIS). The Panel recognizes the importance of this work and the desirability to create a new Task Committee on Seismic Information Systems.

4. The Panel will continue to seek methods to contribute to the International Decade for Natural Disaster Reduction (IDNDR) such as exchanging Proceedings of Joint Panel Meetings and of Task Committee Workshops with their respective country's National Committees for the IDNDR.

5. The Panel approved the Task Committee reports presented during the 29th Joint Panel Meeting. Each report included objectives, scope of work, accomplishments, future plans, and other information. The Panel will continue to review the Task Committees' progress toward meeting their objectives; consolidating, eliminating, and/or creating Task Committees as desirable.

6. The Panel endorsed the following seven proposed Task Committee Workshops/Committee Meetings during the coming year:
   a. Task Committee (A), Workshop on Soil-Structure Interaction, spring 1998 in USA.
   b. Task Committee (B), 1st Workshop on Test Procedure, Documentation, and Retrieval of Test Data will be conducted before the 30th Joint Panel Meeting.
   c. Task Committees (B&C), 4th U. S. -Japan Technical Coordinating Committee Meeting on Composite and Hybrid Structural Systems, October 1997, USA.
   d. Task Committee (E), 1st Workshop on Design for Wind and Wind Hazard Mitigation, 7-8 October 1997, East-West Center, University of Hawaii, HI, USA.
   e. Task Committee (F), 7th Workshop on Earthquake Disaster Prevention for Lifeline Systems, November 1997, Seattle, WA, USA.
   f. Task Committee (I), 5th Storm Surge and Tsunami Workshop, winter 1998, Tokyo.
   g. Task Committee (J), 13th Bridge Engineering Workshop, fall 1997 in Tsukuba, Japan.

   Scheduling for the Workshops will be done by the U.S. and Japan Chairmen of the respective Task Committees with concurrence of the Joint Panel Chairmen. Both sides' Secretaries- General will be kept informed of the planning. Results of each activity conducted before the 30th Joint Meeting will be presented at the 30th Joint Panel Meeting.

7. The Panel recognizes the importance of continuing its joint research programs on Composite and Hybrid Structures and on Soil Liquefaction and Countermeasures and expanding joint research in Smart Materials.

8. The Panel recognizes the importance of conducting research in the area of public health following natural disasters and recommends the subject be featured in the 30th Joint Panel Meeting.

9. The Panel published its fourth issue, Wind and Seismic Effects Newsletter, Winter 1997. The newsletter featured the Eleventh World Conference on Earthquake Engineering, the 28th Joint Panel Meeting, Task Committee D, Workshop on Earthquake Engineering for Dams, an article on Japan's Building Research Institute and on the U. S. 's Insurance Institute for Property Loss Reduction. The Panel endorses continuing the publication of the Panel's newsletter. The Japan-side will publish the fifth newsletter during the winter of 1997-98.

10. The Panel has created a Web Site. NIST will maintain the Site during the near term. Information from the Web Site was abstracted for Japan's Science and Technology Agency's development of a UJNR Program Web Site. The four Panel newsletters were added to the Web Site. The Panel encourages all members from both sides to use electronic media, as much as possible, in communicating Panel findings and summaries of its activities. The Web Site URL address is: http://www.bfrl.nist.gov/info/ujnr/ujnr1.html.

11. The Panel recognizes the importance of continued exchange of personnel, technical information, research results, and recorded data that lead to mitigating losses from strong winds and earthquakes. The Panel also recognizes the importance of using available large-scale testing facilities and other complementary capabilities in both countries. Thus, these activities should be continued, strengthened, and expanded. The Panel will provide official endorsement to facilitate these exchanges.

12. The Thirtieth Joint Panel Meeting of the UJNR Panel on Wind and Seismic Effects will be held at the National Institute of Standards and Technology, Gaithersburg, MD in June 1998. Specific dates, program, and itinerary will be proposed by the U.S.-side with concurrence of the Japan-side Panel.

Papers

Theme 1

Wind Engineering

Wind Engineering Research and Development in the United States

Ahsan Kareem[1]
Tracy Kijewski[2]

ABSTRACT

This paper provides an overview of the current direction in wind engineering research in the United States. While various projects in hazard mitigation and risk assessment have been prompted by recent hurricanes, other efforts have been devoted to improving current technologies. A wide host of active topics in wind engineering research, undertaken on the governmental, private, and university level, are addressed, ranging from bluff body aerodynamics to computational wind engineering.

KEYWORDS: turbulence, vibrations, hurricanes, tornadoes, reliability, hazard mitigation, low-rise building testing, computational wind engineering, bridge aerodynamics, building envelope

1. INTRODUCTION

Current research interests in wind engineering span a wide spectrum of topics from improvements in models of wind-structure interactions to the development of risk assessment models. Particularly, with the unprecedented destruction observed in recent hurricanes like Andrew, new awareness has been raised to deficiencies in current design strategies, prompting a host of studies. While it is impossible to fully address all the recent developments in the area of wind engineering, a concise summary is provided herein, discussing the activities at various institutions in the United States. Most of the information has been derived from the papers presented at the Seventh U.S. National Conference (USCWE) held in 1993 in Los Angeles, the Ninth International Conference on Wind Engineering held in 1995 at New Delhi and Hurricanes 92 in Miami, and abstracts of the 8th USCWE to be held in Baltimore in June. For convenience, the areas highlighted have been categorized by the following topics:

1. Hurricane Wind Speeds, Regionalization of Extreme Winds and Tornadoes
2. Performance of Building Envelope
3. Damage Control and Mitigation
4. Risk Assessment and Management
5. Bluff Body Aerodynamics and Unsteady Load Effects
6. Random Data Analysis, Modeling and System Identification
7. Tall Buildings and Engineering Structures
8. Mitigation and Control of Structural Response
9. Bridge Aerodynamics and Aeroelasticity
10. Knowledge-Based Expert Systems and Computational Wind Engineering
11. Wind Loading Test Concepts
12. Wind Engineering Research Applications

2. HURRICANE WIND SPEEDS, REGIONALIZATION OF EXTREME WINDS, AND TORNADOES

Hurricane wind speeds may be quantified by measurement of the footprints of its wind field near shore and after landfall. Based on these measurements, recent studies have shown that the gust factors in hurricane wind fields are higher than those presently used for extratropical storms. This is in part attributed to the movement of convective cell that introduces both nonstationarity as well as non-Gaussianity, thus precluding use of conventional analysis. On the simulation front, Monte Carlo-based simulations of hurricanes, applying phenomenological models, along with historical data on the wind field and filling of the hurricane, provide very useful information for design. Alternative simulations based on empirical schemes are also being studied which do not strictly account for the assumption of independence among the modeling parameters. In essence, the empirical simulation technique avoids, in a nonparametric way, the whole issue of joint probabilities among parameters by utilizing information based on actual historical data. Studies have also been conducted to compare Shapiro's model, featuring a new gust factor curve and radial profile exponent, with the ASCE 7-88 model for hurricanes into each model by feeding statistical information from previous hurricanes and seeing how well it simulates the winds experienced during the actual event, concluding that the Shapiro model, in most instances, appears to be superior to the more conservative ASCE 7-88 model. The applied Research Associates, National Institute of Standards and Technology, Hurricane Research Laboratory, American Association of Wind Engineers (AAWE), University of Notre Dame, University of Wyoming and University of Hawaii are involved in research concerning this topic.

In order to provide a better estimate of extreme

1. Professor, Dept. of Civil Engineering & Geological Sciences, University of Notre Dame, Notre Dame, IN 46556
2. Student, Dept. of Civil Engineering & Geological Sciences, University of Notre Dame, Notre Dame, IN 46556

winds at an ungauged site, regional zoning for extreme wind data collected at various weather stations in a large area is being developed. The applications are focussing on both regional zones and the entire U.S. Colorado State University, Texas Tech University, University of Hawaii and National Institute of Standards and Technology are working toward development of such regional zoning throughout the U.S. Reexamination of wind data and use of mega stations resulting from augmenting data from nearby stations has resulted in refinement of the ASCE7-95 wind speed map.

While hurricane damage has captured the attention of the wind engineering community, there is always concern for tornado-type winds. Studies of tornado wind forces have been conducted in low-speed, open-circuit wind tunnels coupled with an attachment to provide circulation of the flow, as angular momentum is introduced by the rotating of a wire screen. Such studies have proven the necessity of introducing surface roughness, via sandpaper, to wind tunnel simulations to accurately reproduce the vortex flow, delaying the transition to multiple vortices at low swirl ratios. A program has also been active at Texas Tech University and Colorado State University (TTU/CSU) in this area, attempting to identify major parameters and examine scaling relations and techniques for simulation of high-wind phenomena. These efforts have produced parameters for meaningful wind tunnel simulations and developed a tornado or microbust generator. Even through such efforts, it is still difficult to study tornado effects in wind tunnels because of the frequent changes in wind speed and direction. Consequently, efforts are now being devoted to exploring the use of computational fluid dynamics to study tornado effects. Such CFD models apply the 3D, incompressible, unsteady Navier Stokes equations, integrated by the control volume procedure, with convective terms approximated using hybrid upwinding, solved on a rectangular grid system. There is, however, the need for future study of turbulence models like the k-epsilon model or the Reynolds stress model, focusing on their lack of proper information on the turbulence statistics of tornado close to the boundary layer.

Besides research related to the effects of severe weather on infastructure pursued at universities, efforts by the federal government to better detect and define events during these storms are conducted at NOAA's Hurricane Research Division in Miami and Severe Storm Laboratory in Norman, Oklahoma. The thrust of work at these laboratories focuses more on the meteorological aspects which are useful for wind engineering applications.

3. PERFORMANCE OF THE BUILDING ENVELOPE

Several institutions in the U.S. are actively involved in researching the structural resistance to wind hazards. These institutions include: Texas Tech University, Texas A&M University, Clemson University, the University of Florida, Florida International University, Universities of Missouri at Columbia and Rolla, University of Notre Dame, University of Washington, Colorado State University, State University of New York at Buffalo, University of Hawaii, American Association for Wind Engineering, Applied Research Associates, Roofing Industry Research Institute, Lawrence Livermore Laboratory, Glass Industry, Underwriters Laboratory, and Model Building Codes. The research effort spans areas concerning documentation of damage from past disaster studies to performance of building envelopes, i.e. cladding, roofing and glazing, and quantification. A detailed discussion of these topics follows.

Efforts to better design and improve the performance of structural glazing, cladding and curtain walls are taking place at several academic institutions, within the glass industry, and among curtain wall consultants. Problems with performance of such systems are associated with the special nature of hurricane winds, being turbulent, sustained, varying in direction, and are often containing wind-borne debris. Measures to improve the performance of glazing in these respects are being investigated to ensure integrity of the building envelope following impact from wind-borne debris and the subsequent repetitive action of wind gusts. Coupled with studies to improve building envelope strength, are those dedicated to addressing this problem at its source by minimizing some of the air-borne debris, particularly roof aggregates. For the application of repetitive wind pressure with desired intensity and temporal characteristics on a portion of cladding, pneumatic chambers are being utilized. The University of Missouri at Rolla and Texas Tech are involved in glass studies, whereas Clemson University is pursuing both envelope and roofing studies. Applied Research Associates, Inc. have also developed a risk analysis model which predicts the failure due to wind borne debris. This is discussed in more complete detail in the section on risk assessment and management.

Some attention in research has also been devoted to sealant performance. While previous studies had indicated that sealants are capable of resisting cyclic loadings, current studies have been considering their performance under the joint effects of cyclic loading and environmental factors. A research project at Texas Tech University has investigated the failure strength of sealants under random wind loading. Still, while improvements in glazing and cladding quality are emphasized, researchers insist that integration of the designs of glass, mullions, frames, and frame anchorage would improve overall cladding performance.

Most of the studies concerning structural roofing have been initiated following major U.S. hurricanes in which it was observed that the primary failure of roofs during such extreme events occurred near roof corners and ridges. Wind tunnel studies, coupled with post-disaster investigation and full-scale measurements, have proven to be vital tools in developing better roof designs. In one study, an analysis of hurricane damage was used to determine the best roof design under hurricane conditions and the impact of slope on roof performance. Work has also been dedicated to the destruction of roof tiles under the impact of windborne debris, determining impact damage as a function of missile mass and velocity. Some work has also been done in the area of fatigue characteristics of roof pressures, using the rainflow count method as opposed to the upcrossing method to observe the characteristics of these fatigue characteristics.

Post-disaster studies have also been useful in determining the negative aspects of roofing structures, pointing out the need to fasten metal edge flashing, copings, gutters, aggregate, and rooftop air conditioners and equipment which may be ripped from the roof damaging it or becoming wind-borne missiles themselves. In one instance, a local filtering technique using the Haar function was applied to investigate the relationship between the approach flow and the dislodging of loose-laid roof pavers. Future roofing studies at Clemson will focus on measurements of flow over the roofs of scale models in a boundary layer wind tunnel using a three component fiberoptic laser Doppler anemometer system.

Most of the interest in low-rise building testing and codes has been spawned by the destructive path of the recent U.S. hurricanes, e.g. Andrew, Hugo. Based on the observations of engineers during the aftermath, suggestions have been made on the improvements to low-rise buildings, which were neglected in most engineering study until now. Many wind tunnel simulations are underway to develop improvements in building design to be incorporated into building codes. One study at Clemson utilized a device, BRERWOLF, to apply fluctuating pressures to cladding panels to study its effects under loading. Current research at the University of Notre Dame will also turn toward the development of a dynamic wind load simulator to investigate the performance of building components and systems under dynamic space-time variation of loads. Such tools were used to develop retrofit roofs to withstand severe winds and improve cladding so it may better function as a structural resistance and load path. Recent studies stress the improvement of the building envelope, consideration of increased internal pressures due to envelope rupture, and the need for retrofit measures to improve the connections on existing structures.

While some research projects have devoted themselves entirely to roofing, low-rise building tests, or cladding tests, one joint project has undertaken investigations of all three topics and others, thus warranting appropriate attention. A joint research effort Texas Tech University (TTU) and Colorado State University (CSU), CPWE, under the sponsorship of the National Science Foundation (NSF) to investigate various topics in wind engineering, of which include areas of cladding, roofing, and low-rise structure testing. TTU possesses a field laboratory, WERFL (Wind Engineering Research Field Laboratory), established in 1987, ideally suited for the study of low-slope roofing systems and the measurement of wind speeds and the associated wind-induced structural response of a one story test building. Not only has WERFL proven to be a source of data for the study of single-ply membrane roofs, but it has also proven to be a vital tool in determining the average wind pressure acting on a roof purlin and the wind pressures above and below loose-laid concrete pavers over an adhered single-ply membrane roof covering. WERFL has also been used to measure wind-induced pressure coefficients across the building centerline and the internal pressure coefficients for no opening, static openings of 1%, 2%, and 5% and sudden openings of 2%, providing insight into the increased internal pressures following the rupture of the building envelope. All this data has gone on to provide a basis for the development of analytical models for the stochastic modeling of wind speeds and the determination of wind-induced pressures

and admittance functions of the modified quasi-steady theory. Other work has also been devoted to structural sealants, the details of which were mentioned earlier, as well as information on other topics which will be alluded to in the appropriate sections.

Colorado State University's contributions to this joint effort are mainly in the investigation of fundamental and applied topics of wind engineering using physical modeling, performed in their long-test section boundary layer wind tunnel, analytical solutions, and more recently, numerical simulations. The data collected from wind tunnel simulations at CSU may then be compared to the full-scale measurements from WERFUL at Texas Tech. The good agreement between these two data sets verifies the accuracy of wind tunnel studies, which will enable researchers to study the effects of parameters affecting internal building pressures not easily replicated through full-scale investigations.

4. DAMAGE CONTROL AND MITIGATION

Several studies are focussing on efforts to control or mitigate damage by eliminating poor design or construction practices, which emphasize neither the provision of redundancies nor the elimination of weak links in structural systems that can lead to failure at wind speeds well below design values. Some of key items of interest include improved wind code specifications, better code enforcement, changes in practice from facts cited post disaster investigations, incorporation of redundancy and ductility in manufactured homes, improved standards for building envelope systems, utilization of expert systems and computer graphics technology, and negotiation of self-help retrofit activities.

One area receiving attention is the application of reliability theory to develop models of structural performance under extreme loads. One study undertaken at Texas A&M uses the theory to estimate damage to components. The model is capable of generating damage functions for structures along the Gulf and Atlantic coastlines by considering the time of construction, quality of construction, quality of building codes, building contents, regional construction practices, and quality building materials.

Aside from the concentrated efforts of individuals at several institutions devoted to damage control and mitigation, there are focussed group efforts to improve performance of structures under extreme wind events. The two leading examples are CSU/TTU Cooperative Program, mentioned earlier, and a program at Clemson University. A brief description of the program at Clemson is given here. Funded through the State of South Carolina and the Federal Emergency Management Agency (FEMA) the focus of this program is to mitigate wind hazards to low rise buildings. The major tasks include: evaluation of loads resulting from strong winds; evaluation of the resistance of enclosures; stability of low rise wood and masonry buildings; and improvement of codes, standards, and inspection practices. In addition, FEMA is also an active sponsor of extensive post-disaster analysis through their Building Performance Assessment Teams (BPSTs), deploying these teams over thirty times since 1979.

On a larger scale, the American Association of Wind Engineering (AAWE), formerly known as the Wind Engineering Research Council, Inc. (WERC), established in 1970, has also taken an active role in promoting wind hazard mitigation. AAWE hopes to implement a plan for legislative action that would foster the initiation of a National Wind Hazards Reduction Program. Such a program would provide support for wind engineering in the U.S. through improvement of understanding and codes, providing advanced methods for predicting wind loading, and encouraging the development of new technologies. AAWE also hopes to accomplish numerous tasks, among which include initiation of an active sharing of technology within the field primarily through their publication, "Wind Engineer," promotion and prioritization of wind engineering research, and leadership in learning from wind storms through post-storm data collection and analysis. Currently, AAWE is involved in establishing a post-storm data base containing a detailed description of the building, damage, and extreme event. The data was collected following the Hurricanes of Marilyn and Opal, various groups ranging from the Insurance Institute for Property Loss Reduction (IIPLR) to FEMA to the National Oceanic and Atmospheric Administration. The data base relies on wind speeds generated by the wind field models of the National Oceanic and Atmospheric Agency.

5. RISK ASSESSMENT AND MANAGEMENT

The area of risk assessment has some basic focus on gathering data after a disaster and using such

findings to develop or validate a model to assess the risk of failure of constructed facilities and provide a quantitative measure to estimate the extent of damage under a particular intensity of wind storm. This includes damage to the structure as well as building contents as a result of storm winds and wave action. To this effect there are various groups, academic, private, and governmental, who are actively researching risk assessment schemes, among these are Risk Management Solutions, Inc., IIPLR, State Farm Insurance Company, FEMA, and the National Oceanic and Atmospheric Administration. Various subcommittees in the U.S., including the U.S. Subcommittee on Natural Disasters Reduction (SNDR), have made it their goal to reduce human fatalities and suffering, environmental damage, and economic loss caused by natural disasters.

Computational schemes, through this effort, are being developed to forecast the probability and severity of hazardous events, namely hurricanes, over varying temporal and spatial scales. These schemes are based on a synergistic combination of essential ingredients of risk assessment, with the damage potential is being assessed through damage probability matrix, neural networks and fuzzy logic, as well as the use of probability trees. Artificial neural networks have been also developed to predict the damage of individual buildings. Work has been devoted to developing ways of expressing frequency, probability or level of confidence, and probability of the likelihood of an event. For hurricane models, features would include relations of the geophysical environment, including global warming, and features of the hurricane itself. Methods considered in such an analysis include the Monte Carlo simulation and the extended bootstrap simulation, as well as numerical models which predict the sea surface elevations and currents due to mesoscale processes like tides and storm surge. The overall risk assessment is also being considered in the light of projected consequences of global climate change. Studies in this area are being done at the University of Notre Dame, Clemson, Texas Tech, Texas A&M, University of Washington, Stanford, National Institute of Standards and Technology, and Applied Research Associates. The results of risk prediction models may then be displayed by geographic region by the Geographic Information Systems (GIS).

In addition to university involvement, risk assessment has been approached by other organizations and private firms. The INEL Advanced Combined Environments Test Station (ACETS) Program hopes to develop a sound, scientific, engineering and economic basis for evaluating the ability of a building to resist wind loads and wind effects which will lead to reduced losses in wind storms. Its first goal is to establish realistic test methods for evaluating the performance of the building components, connections, and systems in severe wind storms. Then, INEL will focus on the development and improvement of assessment tools which will be used to identify key areas of building deficiency as well as identify appropriate levels of economic expenditure to upgrade construction practices or for expenditures for retrofitting. Thus a cost/benefit assessment scheme will be developed. Other groups involved in risk assessment include the Texas Department of Insurance, funding a program for Texas A&M University. The Texas Department of Insurance has produced a new building code to provide adequate wind resistance for one and two family homes along the Texas coastline and a corresponding study by Texas A&M has evaluated the cost-effectiveness of retrofitting existing structures.

Applied Research Associates has recently developed a first-principle quantitative methodology for evaluating building envelope vulnerability to windborne debris to determine what level of protection, i.e. strength of building envelope, is required to protect homes in residential suburban settings under strong hurricane winds. The initial model performed such evaluations based on peak gust wind speed, spacing of the houses, and other factors; however, improvements now allow the model to consider failure based on specific missile types and/or degrees of damage by explicitly modeling the interaction between the missile damage and the increasing damage caused by internal pressures for a variety of building geometries under the impact of various missile types. The group has also established an integrated model considering the chain reaction initiated by envelope rupture, by coupling the missile damage probability with the increase in internal pressure, which increases the probability of roof failure. Another study undertaken by the group uses decision analysis formalism to illustrate how risk management decisions can be evaluated under conditions of uncertainty ranging from uncertainty in the modeling of loads to the age and condition of the facility. The model treats uncertainties in repair and replacement costs so to evaluate risk transfer, through insurance.

Another risk assessment group mentioned previously, Risk Management Solutions, Inc., comprised of researchers from universities and the risk assessment industry, insurance actuaries, and systems analysts, has developed models to assess monetary loss to individual and groups of properties due to hurricanes, analyzing the losses in a financial framework used by the insurance industry. Wind speeds in these models are derived from a wind field model based upon a historical storm data base.

While previous discussion of risk assessment has focused on the property damage and its relationship to the hazard, a society must view this topic from a holistic point of view and extend it to ascertain the impact of disasters on the socio-economics of the region. A principle which considers all changes in the system that occurred with the disaster and all changes that would have occurred had the disaster not taken place also needs to be considered. Meanwhile, the calculation of economic damages considers both the interruptions of production processes and the damages to assets. Such damages are direct damages. Secondary damages must also be assessed, which include the effects of the disaster which trigger a sudden reduction in demands for outputs within the effected region. Other considerations include those of cultural asset loss, i.e. the loss of historic sites or other sides which would be desirably passed on to future generations. While market values derived through appraisals are often used to estimate such losses, typically these losses are evaluated at a variety of different levels depending on the "significance" of the site. Work in this area is being done at several institutions, with Colorado State University and Texas A&M focusing specifically on wind.

6. BLUFF BODY AERODYNAMICS AND UNSTEADY LOAD EFFECTS

Over the past several decades, much attention has been focussed on the aerodynamics of streamline bodies; however, our knowledge of the aerodynamics of sharp-edged bluff bodies in turbulent boundary layers is far from complete. Efforts in this direction are in progress at several institutions, e.g., University of Notre Dame, Colorado State University, Clemson University, University of Minnesota, Virginia Polytechnic Institute, Johns Hopkins University and Florida Atlantic.

The various research topics undertaken in the area of bluff body aerodynamics involve extensive measurements of the pressure field around prisms, cylinders and bridge deck sections. These studies have examined the influence of scale and intensity of turbulence on pressure fluctuations. In addition, measurements and analyses of the space-time structure of random pressure fields and the area-averaged loads acting on the surface of prismatic and cylindrical bodies of different aspect ratios, exposed to simulated turbulent or turbulent boundary layer flows in various configurations, has vastly improved our understanding of the complex fluid-structure interactions. While most of the efforts have been focused on determining the mean forces and pressure distributions on these bodies, some interaction studies on groups of cylinders have also provided a measure of the fluctuating components of drag and lift forces and their corresponding spectra in the alongwind and acrosswind directions, yielding some vital insight into the dynamic response of a cylinder. Studies have also been concerned with the correlation structure of wind pressure fields on prismatic bodies of finite height immersed in a turbulent boundary layer flows, recognizing its importance to the characterization of wind pressure fields in that it determines the resulting aerodynamic effects on the body.

Several wind tunnel facilities in the U.S. have been involved in the development of measurement schemes to monitor unsteady load effects on such bluff bodies. These include both measuring fluctuating integral or local loads on buildings and bridge models and similar measurements on the full-scale structure. The measurement schemes include area-averaged pneumatic manifolding schemes, ultra-sensitive high frequency force balances, and second generation force balance to account for multiple level force measurements. The use of high speed scanning systems to monitor a large number of pressure taps are being developed that have the potential of replacing high sensitivity force balances. The senior writer has, in addition to the preceding schemes, utilized piezoelectric films to monitor area averaged loads, but the complexity of installation and the film's sensitivity to temperature, in addition to pressure, has limited its applications.

7. RANDOM DATA ANALYSIS MODELLING AND SYSTEM IDENTIFICATION

The analysis, modeling and system identification of random data are very important aspects in wind engineering studies. Recent advances in stochastic analysis and modeling provide useful tools towards

improved representation and interpretation of data. The studies in this area focus on time series modeling of random data, e.g., auto regressive and moving averages modeling (ARMA), estimation of frequency response of structures, identification of load effects on structures, simulation of stationary, nonstationary and non-Gaussian signals, conditional simulation and wavelet transforms. Activities under this topic are being pursued at different levels of concentration at various institutions involved in wind engineering research, e.g., Cornell University, University of Notre Dame, Johns Hopkins, Colorado State University, University of Southern California, Cal Tech, Princeton and Rice Universities.

Computer simulations have been developed for multiple wind pressure time series which are strongly non-Gaussian due to skewed spikiness in fluctuations and have strong cross-correlations of fluctuating features. Such simulations produce the exact sample cross-spectra as well as the auto-spectra of the target signals and have great flexibility in controlling non-Gaussian fluctuating features and some statistical properties of simulated signals, while preserving the target auto- and cross-spectral characteristics. Simulations of non-Gaussian features of wind pressure fluctuations under separated flow regions using higher-order spectral transformations and transient events by wavelet transforms have been performed. This approach leads to stochastic processes which represent non-Gaussian and non-stationary features, respectively. This is one of the current focuses of wind-related research at the University of Notre Dame. The resulting studies address the analysis, modeling, and simulation of measured full-scale wind pressure and velocity data sets which exhibit both non-Gaussian and nonstationary features. The PDF of the non-Gaussian pressure and pressure data are simulated in these studies, the latter by new static transformation techniques. The non-stationary portion of pressure data is isolated and decomposed into a set of localized basis functions using wavelet transformation techniques. Furthermore, studies at Colorado State have applied a mean multifractal plane to investigate nonstationarity and intermittency of the time series representing wind flow and wind-induced effects. Other probabilistic studies of the overall area-averaged pressures on the Texas Tech University building, as measured in a wind tunnel, have found that the skewed, non-Gaussian parent PDF may be approximated by a Gamma Distribution, while the peak PDF is best fit by a Fisher-Tippet Type I distribution. In the area of stationary processes, ARMA techniques have also been used in the simulation of the fluctuating component of wind and wind-induced pressures.

8. TALL BUILDINGS AND ENGINEERING STRUCTURES

In the area of tall buildings most of the innovations in structural system development come from industry, whereas, system response analysis, based on analytical considerations and wind tunnel studies, is generally conducted in universities (Colorado State University, CPP, Clemson, University of Notre Dame). Some of the work is focussed on research while other work is development related. In the research area, some work is still being done to refine the gust factor approach and to package it in a closed form expressions rather than the ASCE7-93 version that utilizes plots. One such approach has been adopted in ASCE7-95, ASCE Standard Minimum Design Loads for Buildings and Other Structures. Along these lines, a modified gust factor that accounts for non-Gaussian features resulting from the often ignored square of wind velocity term has been developed. This is particularly important for relatively stiff structures in high turbulence regions. The quantification of along-wind, acrosswind, and torsional loads for a wide range of buildings of different cross-sections and aspect ratios is essential for developing coupled lateral-torsional analysis of buildings. The analysis is being simplified for code application at the University of Notre Dame.

The torsional response of tall buildings has also been considered, since it has been observed that the torsional response can have a great effect on the total response of the eccentric building. There may also be some contribution to the response of an eccentric building, in the way of interference effects, by adjacent buildings. Such interactions have been studied through wind tunnel simulations, observing that, while an isolated building experiences inherent turbulence, the same building with interference from surrounding structures was found to manifest wake excitation. Special concern has also been given to situations in which the frequency of vortex shedding from the interfering building coincided with the natural frequency of the eccentric principle building, causing torsional resonant buffeting to the principle building.

The research in the area of engineering structures includes towers, transmission lines, chimneys,

which has been actively pursued in both academia and industry. For example, in the study of powerlines, researchers have attempted to estimate the electric drag coefficients used in determining wind forces on transmission line structures via numerical methods based on 2D Navier Stokes equations for viscous, incompressible, steady flow. Many studies have also devoted their efforts to improvement of instrumentation on power lines and towers for data collection and often utilize free-air wind tunnels to compare the drag coefficients estimated in wind tunnel studies with actual open air results. Furthermore, efforts are also being devoted to improved design of sign, signal, and luminare structures, which, in recent years, have failed under high winds injuring pedestrians and commuters below. Studies have utilized the data from wind tunnel studies to establish the static drag coefficients and root mean square estimates of the lift-coefficients of tapered cylinders in order to develop alternative, more aerodynamic cross-sectional shapes (e.g. octagonal) and designs capable of resisting cyclic loads in order to avoid future failures.

More recently, offshore platforms are receiving increased attention due to structural damage to deck structures and appurtenances in the Gulf of Mexico in the aftermath of Hurricane Andrew. As a result of the new breed of deepwater platforms, which are very sensitive to the gusting action of wind, focussed activity on the behavior of such platforms under the combined action of wind, waves and currents has developed. For such behavior to be studied, the wind fields surrounding such structures must be accurately modeled. The wind field, however, is not so much influenced by the form of the sea surface, but rather is sensitive to the energy loss and rate of momentum transfer due to surface friction. However, if a relationship between on-land wind characteristics and over-water wind characteristics is developed, existing on-land models may be somehow extended over the water to predict the wind fields. There are some difficulties with these attempts for spatial separations which may exceed the turbulence length scales, since the correlation function typically used by land-based structures inadequately describes the spatial structure of the wind field over the ocean. Further development and clarification of this approach is one topic for current study. The senior author is also involved in modeling the stochastic response of tension leg platforms to random wind and wave fields. In these studies, both the time and frequency domain procedures have been developed utilizing the Cray Y-MP to predict the nonlinear platform motion.

Under an Office of Naval Research (ONR) initiative entitled "Reliability of Nonlinear Ocean Structures Under Stochastic Excitation," several investigators are studying the response of ocean systems to extreme wind and other loadings. The senior author has a project concerning response statistics of ocean structures under wind, wave, and current loads. The major focus of this study rests upon the advancement of techniques for the determination of extreme response of moored floating ocean structures to wind, wave, and current loads. These improved techniques are then to be implemented in predicting the performance of such structures in different ocean environments and, hence, in predicting loading patterns. Particularly, the present effort will serve to quantify structural survivability and serviceability as well as prescribed motion control strategies for improved structural reliability. Other universities and institutions that are addressing wind related topics include Rutgers, Florida Atlantic, Stanford, NIST, and several Naval Laboratories.

Proposed future off-shore structure investigations include improving quantification of windfield models, better modeling of shielding effects, investigation of overturning caused by uplift forces, understanding of overall wave profiles, better design for gust loading factors, and investigation of the vortex shedding-induced vibration on cranes and flare booms. Most research of this nature is being conducted by the R&D groups of oil companies. At the university level, work is being done at the University of Notre Dame and Texas A&M University.

Dynamic load effects, structural reliability and risk assessment are receiving an increased attention from researchers while the need for practical application of these concepts to design is increasing. Dynamic effects are treated in codes primarily through gust factor approach, which has been the focus of concentrated effort particularly to improve our understanding of hurricane wind fields. The dynamic loads introduced by the acrosswind and torsion effects are being studied for developing simplified procedures for code applications, primarily with a reliability based format. Studies focussing on this aspect for both the low and high-rise construction are helping to provide a basis for preliminary discussions on reliability-based design.

9. MITIGATION AND CONTROL OF STRUCTURAL RESPONSE

The current trend toward buildings of ever increasing heights and lighter facades has led to the construction of relatively flexible structures possessing quite low damping. As a result, the serviceability of these buildings is affected by the excessive accelerations experienced at the higher levels in wind storms which may cause considerable discomfort to the building occupants. Ever since the evolution of high-rise construction, efforts, both in industry and academia, to improve the performance of buildings have developed. Such efforts are devoted to a wide range of topics from considering alternative structural systems to aerodynamic modifications with particular emphasis on damping systems. Research in active and passive systems, which includes active mass dampers, tuned mass dampers, tuned liquid dampers and hybrid tuned liquid dampers in single and/or multiple damper configuration, is currently being undertaken. While passive damper study has investigated multiple damper configurations, the area of active dampers has considered frequency domain based on H_2 control strategies for wind excited structures. Further research in the areas of tuned sloshing dampers is exploring the use of screens, nets, floating styrofoam beads, and baffles to increase the damping ability. Semi-active systems are also being considered in which the building motion is monitored and fed into a filter designed to represent the features of the optimally tuned damper. For example, semi-active tuned sloshing dampers may be incorporated with a feedback system, which adjusts a moveable sliding screen over a fixed screen or regulates opening vanes to achieve optimal damping. Research in both active and passive systems for wind applications is being carried out at the University of Notre Dame. Currently 3M Corporation and Colorado State University are jointly analyzing the effectiveness of viscoelastic dampers through wind tunnel studies. Other institutions involved in active/passive systems studies include, for example, CPP, University of Washington, SUNY at Buffalo, USC, UC Irvine and UC Berkley.

The American Society of Civil Engineers (ASCE) has two special task committees; one has just completed a study concerning motion perception criteria and motion mitigation, another is related to damping systems. The senior writer is chairing the task committee and it includes membership from Japan. The primary focus of this task committee is to address three important aspects of structural damping systems: a survey of inherent damping in buildings and bridges, the various methods of assessing damping levels from ambient data, and investigation of the different active and passive damping systems and their performance (Japanese building industry's experience). This would also require technology transfer through documentation of design procedures for various damping devices, including passive, active, or semi-active systems, utilizing fluid and viscoelastic dampers, as well as inertial systems like mass dampers.

A joint research program in structural control between several institutions from the U.S. and China concerns the full-scale implementation of passive and active control devices in the Nanjing Tower, a free-standing tower approximately 1000 ft tall with two levels of observation decks, to minimize the effects of wind and earthquake loads. This project pools the knowledge of experts in structural, wind, earthquake, and control engineering to design, install, and evaluate performance of the passive/active devices. The field testing and performance analysis will provide useful insight into the validity of modeling procedures involving wind-induced response of both the tower alone and with the addition of control devices, as well as, assess the adequacy of the passive tuned liquid dampers and the need for future developments.

In 1992, the National Science Foundation (NSF) initiated a five-year research program on structural control for safety, performance, and hazard mitigation. The objective of this initiative was to address a number of important technological, as well as, practical issues of cross-disciplinary nature in order to forge close ties between industry, research and practice and to accelerate the process of implementation. The scope of this initiative includes the areas of earthquakes, natural and man-made hazard mitigation, controls, and structural and building systems. Typical areas of research funded by the program range from sensor technology, actuator dynamics, control concepts, damage control, uncertain and nonlinear systems, and the actions of wind and earthquakes. Several wind related projects are funded under this initiative which include sloshing dampers, the next generation of liquid dampers, and general topics in the control of wind excited structures.

Base isolation systems are also being explored in which passive energy absorption mechanisms are installed that significantly reduce the base shears

felt by the building during a major event. Through such measures, the natural frequency of the structural system is shifted below those of the dominant excitation source, such as an earthquake or wind loads. Such isolators feature elastometric rubber bearings, with or without lead cores, which support the building superstructure, allowing deflection and sustaining the shear that would result if the building were fixed during an earthquake and may be used in conjunction with viscous dampers at the top of the building. The development of such systems has relied upon investigations of building response in both wind tunnels and on shaking tables.

10. BRIDGE AERODYNAMICS AND AEROELASTICITY

Both theoretical and experimental studies are being conducted to improve our understanding of the interaction of turbulent winds with the cable stayed and suspension bridges. While theoretical analysis is focussing on the effect of turbulence on flutter speed of long span bridges, experimental work has turned toward improved modeling and quantification of aerodynamic forces, considering their sensitivity to turbulence characteristics and the geometric form of the bridge section. A thorough understanding of these effects is essential for improvements in both design and theory. Some recent studies have raised questions about the validity of some assumptions made in modeling. For example, the existing quasi-static formulation of buffeting forces has been confirmed to give reasonable estimates of aerodynamic forces for streamlined bridge sections; however, its representation of these forces for bluff sections, where body-initiated or signature turbulence is prominent, has been deemed inaccurate. New approaches for modeling buffeting forces and aerodynamic admittance functions and incorporating signature turbulence, applicable to streamlined and bluff bridge sections, is currently being pursued. Another challenged assumption, the assumption that the correlation time of excitation is short compared with the relaxation time of the dynamic system, which allows the use of the Markov property, may not be appropriate when noise is modeled properly. Proper modeling of noise requires that when fluctuations are introduced, they cannot be modeled as white noise, but instead as colored. This is an essential consideration since colored noise does indeed influence the system stability quite differently than colored noise. Section model studies are also underway which investigate the effect of modifications of the deck cross-section, including the addition of plates, streamlined deflectors, and railings, to enhance aerodynamic performance as well as insure aeroelastic stability.

A variety of theoretical studies have been initiated in hopes of developing mathematical simulations of the pressure forces acting on and excitation of bridge decks. Recent studies have focused on aerodynamic stability of bridges in buffeting and self-excited loads using flutter derivatives, vortex-induced vibration modeling of bridge decks, and the modification of linear analysis to nonlinear cases. One study has attempted to develop theoretical relations for bridge deck excitation by utilizing modifications of airfoil theory and exploiting the analogy of a streamlined bridge deck to a airfoil. In addition, the use of the Ibrahim Time Domain Method, the force oscillation method, and the system-identification technique in a single study confirm that good consistency in determining flutter derivatives may be achieved by using any of these three approaches. Researchers have now also found ways of utilizing computational wind engineering to determine the wind flow around and the forces acting on a bridge deck. Such techniques, one of which uses the 2D unsteady, incompressible, laminar, Navier-Stokes equations in a body-fitted, curvilinear coordinate system, may, in the future, allow designers to weed out bad bride deck designs before wind tunnel tests are applied. Furthermore, some time has been devoted to exploring the validity of the Discrete Vortex Method, finding it to be effective in simulating flow around a suspension bridge for modest angles and a Reynolds Number of 200. Full-scale studies are also underway to validate the theoretical and wind tunnel findings. Johns Hopkins University, the Department of Transportation, and the University of Notre Dame are engaged in topics under this area. Some of the work in this field has also been conducted at Princeton and Colorado State University.

Recently, accompanying the seismic retrofit of the Golden Gate Bridge, a aerodynamic stability study was initiated and the findings used as a basis for modifications to the bridge. After finding the critical flutter velocity for the torsional mode of vibration of the bridge to be extremely low, modifications of the bridge section were proposed to reduce aerodynamic instability. The group found that by rounding the sharp leading edges, through the introduction of fairings, and by replacing the very solid railing with a open one, the bridge's

leading edge would become extremely airfoil-like, producing a stabilizing downward lift and increasing the critical flutter velocity to 105 m.p.h. In addition, another study analyzed the effect of viscous dampers, installed to dissipate energy during a seismic event, on the buffeting response of the bridge. By assuming that the supplemental damping manifested itself as additional modal damping, the study was able to conclude that the external dampers will increase flutter stability and reduce the buffeting response. This implies that external dampers may be employed to overcome problems of low flutter speeds or excessive buffeting deflections in long-span bridges.

Future studies should be devoted to investigating length scale, turbulence, and intensity effects and the dynamics of the vortex formation near separation. Furthermore, a multi-disciplinary research project to investigate the effects of turbulence length scale and intensity on the aerodynamics of bridge deck sections utilizing actively generated turbulence flow fields is currently being initiated at the University of Notre Dame. The study utilizes active turbulence generation devices, consisting of controlled air jets and oscillating screens in a large cross-section wind tunnel to identify the effects of properly scaled turbulence on the aerodynamics of a variety of generic deck sections. The use of active systems in this research allows for the simulation of turbulent length scales that cannot be produced with passive turbulence-generation techniques, while the jets add energy throughout the spectrum to supply energy that the grids are incapable of supplying and to ensure that the flows contain the appropriate fine-scale turbulence. Thus, this technique, by allowing for large models, permits the inclusion of additional deck geometric details that are often omitted due to scaling requirements. In order to determine unsteady buffeting and self-excited aerodynamic loads on the deck sections, synchronous pressure, pneumatically averaged pressure, and force measurements are collected.

11. KNOWLEDGE BASED EXPERT SYSTEMS (KBES) AND COMPUTATIONAL WIND ENGINEERING (CWE)

Knowledge based expert-systems can offer intelligent assistance to designers and planners in performing a vast array of tasks. Though KBES are not without their limitations, the potential applications of KBESs in wind engineering are many. They may include analysis and prediction of extreme winds, risk and damage assessment, design and synthesis, monitoring and control, urban and coastal community planning, and decision making for hurricane response. Currently, most of the effort in expert system development is focussed on damage and risk assessment utilizing expert system shells. The University of Washington, Stanford, Texas Tech, National Institute of Standards and Technology, Clemson University, and several consulting firms are active in this area.

An interactive computer program addressing the wind loading provisions of the ASCE standard7-95 has been developed at NIST. The software and the instructions for the user were developed by an expert system consultant with assistance from NIST staff in the interpretation of the standard wind loading provisions. Another knowledge-based program has been developed to overcome the problems of prescriptive of "Deemed-to-Comply" (DTC) standards. By creating the program in a user-friendly style, both the designer and builder of the structure may easily insure that the dwelling satisfies the wind code.

Recent advances in computational fluid dynamics are noteworthy, but major challenges remain in simulating flows common to wind engineering where both the structural geometry and the flow field are complex. Initial work in CWE has been focussed on a model which has succeeded in reproducing some of the integral features of flow field, but some discrepancies between numerical results and experimental data still remain. The flow field is modeled by the Navier-Stokes equations with appropriate boundary conditions. Turbulence models have been developed to simulate high Reynolds number flows that are not achievable with direct numerical simulation (DNS) due to computer limitations or to simulate a flow with a Reynolds number similar to DNS but with less computational effort. Currently the most widely used turbulence model is the k-epsilon method, which has the advantage of lower computational effort, but with a lower level of accuracy. The large eddy simulation (LES) approach has emerged as a more attractive scheme which has the promise of providing improved results with reasonable computational effort. In LES, fluid motion scales larger than the filter size are resolved and solved directly, while the scales smaller than the filter size are modeled by a subgrid scale model. The most commonly used LES simulation relies on the Smagorinsky model for subgrid scale viscosity. Coherent flow structures are responsible for the large scale pressure field rather than the eddies

associated with the transport of momentum and energy, therefore, a scheme that models essentially coherent structures is appropriate for wind engineering applications. It is referred to as coherent structure capturing (CSC) to distinguish it from LES. One should not expect CSC to simulate flow field characteristics that are associated with small scales. The LES for capturing of coherent structures has shown improved accuracy, upon comparison of predictions and experimental data, but not without high penalty in computational effort.

A new method, using computational fluid dynamics, for numerical simulation of the turbulent flow field around a structure with oblique wind angles based on a composite grid, has been proposed in a recent study. The method consists of a composite grid technique which connects two or more grids supported by a fortified solution algorithm to simulate 3D flow fields for various wind angles. Another numerical model of air flows created by the TTU/CSU joint research effort has produced a model capable of predicting the detailed flow field surrounding a building or other structure. The technique adopts a version of the CSU Regional Atmospheric Modeling System (CSU-RAMS) which is a nonhydrostatic compressible model designed for large eddy simulation. Other studies have applied techniques like discrete vortex methods which seem to show promise over grid based techniques.

The development of different approaches are underway at various institutions to improve our modeling capability of wind engineering related problems (e.g., Colorado State University, University of Notre Dame, Texas Tech, University of Washington, University of Arkansas, Stanford, and Johns Hopkins University). Recent developments in CWE were reported at the 2nd International Symposium on Computational Wind Engineering held at Colorado State University in August, 1996.

12. WIND LOADING TEST CONCEPTS

Much of our understanding of wind events and their impact on structures has arisen from studies of small-scale models; however, for a complete understanding of how wind loads are transmitted through structural systems and the performance of building components under extreme winds, many feel that full-scale and large-scale testing is a necessity. To address these issues, NSF and NIST have sponsored a Workshop on Large-scale Wind Testing Concepts for Structures to be hosted by AAWE in Washington D.C. in May of 1997.

Several full-scale and large-scale testing concepts will be presented at the workshop including the wall of wind which calls upon 8-10 fans to generated artificial wind forces capable of testing complete and partial full-scale and large-scale structures and full medium-scale structures. Another artificial wind simulator, applying up to two fans, the mock up test, is valid for the testing of partial full-scale structures. Traditional modeled wind in the form of the Boundary Layer Wind Tunnel in a large size is valid for full and partial testing of full to medium-scale structures and even full small-scale structures, as opposed to its conventional form, applicable to only medium-scale, partial large-scale, and full small-scale testing. However, such a facility becomes quite prohibitive cost-wise. A final synthetic wind concept applies actuators in mechanical or electromechanic form to enable full and partial testing on medium to full-scale structures. A similar pneumatic technique referred to earlier, BRERWOLF, is also capable of partial testing for both full-scale and large-scale structures. It is hoped that these proposed testing schemes will lead to a new generation of full-scale and large-scale testing facilities.

13. WIND ENGINEERING RESEARCH APPLICATIONS

One of the major objectives of research in wind engineering is to improve our understanding of the wind load effects on structures for subsequent implementation in codes and standards. So in this context the major application of research is for the development of codes. Building codes in each locality are responsible for the design and construction of buildings. Most communities across the United States adopt, in large part, one of the three model building codes: the National Building Code of the Building Officials and Code Administrators International (BOCA), the Standard Building Code, or the Uniform Building Code. The provisions for wind loads in these model building codes are patterned after the ASCE standard on Minimum Design Loads for Buildings and Other Structures, ANSI/ASCE7-95. Recently, a major effort has been completed toward the next revision of ASCE7. A number of university researchers, practicing engineers and code officials have been working together to draw information from recent research findings for inclusion in the revised version of ASCE standard (ASCE7-97). A vital addition to the ASCE standard would be the

inclusion of expressions for the acrosswind and torsional responses, which tend to have the greatest impact on occupant comfort. Internationally, few standards provide estimates of response in these two critical directions, despite the fact that their inclusion in standards would save time and money lost in unnecessary wind tunnel studies. Since response in these directions result from complex phenomena that is impossible to describe by the same quasi-steady or strip theory used in the along-wind direction, wind tunnel data must be collected to develop empirical expressions for the response in these directions, for various building aspect ratios and geometries, an area being addressed in current research efforts. This same set of wind tunnel data is also being used in a study both discussing various international standards and then evaluating their accuracy in predicting the along-wind and acrosswind response, where applicable, of a given structure.

In addition, since many of the expressions developed in ASCE7 are derived from wind tunnel tests, there is some concern for the standards by which the modeling is performed to insure valid results. Several criteria have been suggested to so that the high frequency turbulence, which is believed to affect the shear layer formation at points of flow separation, is sufficiently produced and to insure the overall accuracy of wind tunnel simulations on low-rise structures. These criteria address a variety of parameters from the mean velocity profile to the longitudinal integral length scale.

While one of the major objectives of research in wind engineering is to improve our understanding of the wind load effects on structures for subsequent implementation in codes and standards, the community also must insure that the knowledge acquired is disseminated throughout the scientific community. One example of such initiative is taking place at Texas Tech University. One strategy, sponsored by NSF, transfers wind engineering research results through CD-ROM packages for classrooms covering four topics: Thunderstorms, Tornadoes and Hurricanes -- A General Overview, Damage Caused by Hurricanes and Tornadoes, Impact of Windborne Debris, and Wind Loading on Low-Rise Buildings.

14. CONCLUDING REMARKS

In this article, an attempt has been made to summarize the wind engineering related activities in the U.S. Understandably, only general comments were made regarding the various areas of research interest; therefore, additional details should be obtained by contacting individuals at the institutions/organizations mentioned in this paper.

The author sincerely regrets an inadvertent omission of any institution from the different wind related activities listed in this paper. Most of the information has been drawn from the bibliography and through personal contacts.

15. ACKNOWLEDGEMENTS

The authors were supported in part by an NSF Grant # CMS95-22145.

16. BIBLIOGRAPHY

1. Hurricane of 1992, "Andrew and Iniki One Year Later," Proceedings of a Symposium Organized by The American Society of Civil Engineers (Preprints).

2. Hurricane Alicia: One Year Later, Proceedings of the Specialty Conference, ASCE, 1985 (A. Kareem, editor).

3. Proceedings of the Sixth U.S. National Conference on Wind Engineering, Vol. I & II, 1989 (A. Kareem, editor).

4. Proceedings of the Seventh U.S. National Conference on Wind Engineering, Vol. I & II, 1993 (G. C. Hart, editor).

5. "Wind and the Built Environment," U.S. Needs in Wind Engineering and Hazard Mitigation, Panel on the Assessment of Wind Engineering Issues in the U.S., National Academy Press, Washington, D.C., 1993.

6. Kareem, A., "Recent Advances in Wind Engineering: Part I," Journal of Wind Engineering and Industrial Aerodynamics, Vol. 36, 1990.

7. Cermak, J.E., "Recent Advances in Wind Engineering: Part II," Journal of Wind Engineering and Industrial Aerodynamics, Vol. 36, 1990.

8. Howe and Cochrane, "Natural Hazard Damage Handbook," Colorado State University, 1991.

9. "Cooperative Program in Wind Engineering," Inaugural Meeting of the International Wind Engineering Forum, Tokyo, 1994.

10. "Building an International Community if Structural Engineers," Proceedings of Structures Congress XIV, vol.2, ASCE (S.K. Ghosh & J. Mohammodi, editors).

11. "Engineering for Wind Hazard Mitigation," Project Summary by the American Association for Wind Engineering.

12."Wind Loading and Capacities of Components, Connections and Systems" ACETS INEL URC Project Description, Clemson University.

13. Summary Papers for the Ninth International Conference on Wind Engineering, 1995 (Krishna, Chairman).

14. Schechter, M.M., Schechter, E. and Simiu, E., "Developmental Computer-Based Version of ASCE 7-95 Standard Provisions for Wind Loads," NIST Technical Note 1415, 1996.

15. Abstracts for the Eighth U.S. National Conference on Wind Engineering, Conference Web Site, 1997. (Jones, Chairman)

16. Kareem, Ahsan, "Correlation Structure of Random Pressure Fields," to appear in the Journal of Wind Engineering and Industrial Aerodynamics, 1997.

17. "Natural Disaster Reduction," Proceedings of the 1996 International Conference and Exposition on Natural Disaster Reduction, ASCE (Housner & Chung, editors).

18. Gurley, K.,and A. Kareem, "Analysis and Interpretation Modeling and Simulation of Unsteady Wind and Pressure Data," to appear in the Journal of Wind Engineering and Industrial Aerodynamics, 1997.

ON THE WIND RESISTANT DESIGN METHODS FOR SUPER LONG-SPAN BRIDGES

by

Hiroshi SATO[1], Katsuya OGIHARA[2], Haruki AKIYAMA[3] and Ryuichi TORIUMI[4]

ABSTRACT

In Japan and in the world, there are several plans or ideas to construct bridges longer than the Akashi Kaikyo (strait) Bridge. In the design of such super long-span bridges, aerodynamic stability is one of the most important themes. By reviewing the wind tunnel studies for the Akashi Kaikyo Bridge and the Tatara Bridge conducted at the Large Boundary Layer Wind Tunnel, wind resistant design methods for super long-span bridges are discussed and proposed.

KEYWORDS

Wind resistant design method, Super long-span bridge, Flutter, Gust response, Analysis, Full aeroelastic model, Wind tunnel study

1. INTRODUCTION

The Akashi Kaikyo Bridge, which is now under construction in Japan, will have the main span length of 1990m. In Japan and in the world, there are several plans or ideas to construct bridges longer than the Akashi Kaikyo Bridge. In the design of such super long-span bridges, aerodynamic stability is one of the most important themes. Aerodynamic characteristics of slotted box girders were studied and proposed as one of the possible girders for super long-span bridges [1].

In Japan, the safety of proposed design of long-span bridges to wind-induced instabilities has been confirmed mainly by spring-mounted rigid sectional model test in smooth flow. Since the span length of the Akashi Kaikyo Bridge is much longer than the existent longest bridge in the world, it was thought that the wind-induced instabilities should be confirmed by more accurate wind tunnel study, namely full aeroelastic model study.

The Tatara Bridge, which is also under construction in Japan, will have the main span length of 890m. The bridge will be the world's longest cable-stayed bridge. In addition, the Tatara bridge will be surrounded by islands. Some of the islands have high mountains up to 400m above the sea level. Therefore, it was thought that the aerodynamic behavior should be confirmed through full aeroelastic model test with topographical model.

The wind tunnel studies for these bridges were conducted at the Large Boundary Layer Wind Tunnel, whose test section is 41m wide, 4m high and 30m long. Through the wind tunnel studies, the safety of these bridges were confirmed. In addition, some unexpected insights into flutter and gust response of super long-span bridges were found [2].

Considering the findings from the wind tunnel studies for the Akashi Kaikyo Bridge and the Tatara Bridge, wind resistant design methods for super long-span bridges are discussed and proposed in this paper.

2. EXISTING WIND RESISTANT DESIGN METHODS FOR LONG-SPAN BRIDGES IN JAPAN [3]

The wind resistant design of long-span bridges in Japan has been mostly based on the Wind Resistant Design Criteria for Honshu- Shikoku Bridges (hereinafter referred as to 'the Criteria'). The Criteria was originally formulated in 1967 and revised in 1976 by the ad hoc committee in the Japan Society of Civil Engineers. The Criteria prescribes the design wind load including the effect of gust and the evaluation method of wind-induced vibrations based on wind tunnel testing.

In the Criteria, the wind-induced vibrations of the bridge deck shall be estimated through spring-

---

1) Head, Structure Division, Structure and Bridge Department, Public Works Research Institute, Ministry of Construction
2) Senior Research Engineer, Structure Division, ditto
3) Manager, First Design Division, Design Department, Honshu-Shikoku Bridge Authority
4) Deputy Manager, First Design Division, ditto

mounted rigid model test in smooth flow. The critical wind speed Vcr for flutter and galloping at attack angles from -3 deg. to 3 deg. shall be higher than the following reference wind speed Vr.

$Vcr > Vr = 1.2V_D$

The standard method for wind tunnel testing is described in the Guideline of Wind Tunnel Testing for Honshu-Shikoku Bridges.

3. FINDINGS FROM THE WIND TUNNEL STUDY FOR THE AKASHI KAIKYO BRIDGE [4]

The 1/100 full aeroelastic model of the Akashi Kaikyo Bridge was designed so that the similarity of shape, mass distribution and stiffness distribution might be satisfied (Photo 1). The stiffening truss was modeled without stiffening spine at the center of cross section. The bending stiffness in the plane of tower was simulated as well as the bending stiffness in the plane of bridge and torsional stiffness about the axis of tower. In modeling of the cables, mass, drag force and axial stiffness were simulated, and aerodynamic interaction with stiffening truss was considered.

3.1 EXPERIMENTS IN SMOOTH FLOW

In the smooth flow test, remarkable static torsional displacement was observed (Fig.1). It was caused mainly by aerodynamic drag force acting to the stiffening truss. In case of ordinary suspension bridges, which have center span of about 1,000 m, static torsional displacement is negligibly small. It was found in the full aeroelastic model test of the Akashi Kaikyo Bridge, however, that relative angle of attack cased by the static displacement was not negligibly small, and that it varied along the bridge axis. Since angle of attack affects flutter characteristics, the effects of torsional displacement on the aerodynamic stability must be considered in case of super long-span bridges, which have center span of 2,000 m or over.

Coupled flutter was observed at the wind speed of 8.5m/s (85m/s for real bridge) (Fig.2). The rotation center lay on the windward side at the midspan, on the leeward side at quarter point of center span, and on the windward side again at the middle of side spans (Fig.3). During the flutter, its vertical bending vibrational mode was not similar to any of natural mode, while its torsional vibrational mode was similar to the first symmetric natural mode (Fig.4). Therefore it does not seem that aerodynamic stability of super long-span suspension bridges can be predicted directly from spring-mounted rigid model test.

In order to predict flutter of super long-span bridges analytically, the effect of the static torsional displacement should be considered, and higher natural modes as well as the first natural mode should be included. Besides, aerodynamic derivatives such as Drag due to Heaving motion, Drag due to Torsional motion, Lift due to Along-wind motion, and Pitching moment due to Along-wind motion should be included in addition to the following conventional aerodynamic derivatives.

Drag due to Along-wind motion
Lift due to Heaving motion
Lift due to Torsional motion
Pitching moment due to Heaving motion
Pitching moment due to Torsional motion

3.2 EXPERIMENTS IN TURBULENT FLOW

In the turbulent flow test, gust responses were observed in horizontal bending, vertical bending and torsional mode. As wind speed increased, the vibration of torsional 1st mode became dominant, and apparent damping became smaller. This seems to be the effect of flutter. Apparent damping in the turbulent flow was compared with that in the smooth flow. It was found that the effect of turbulence on flutter was small for this bridge model.

The observed gust responses were compared with the calculated ones. In the calculation, the following aerodynamic admittance and spatial correlation were applied.

i) aerodynamic admittance for drag [5]

$$Xu^2(fd)=2[kfd-1+\exp(-kfd)]/(kfd)^2$$

ii) aerodynamic admittance for lift and moment [6]

$$Xw^2(fb)=(a+\pi\, fb)/[a+(\pi\, a+1)\,\pi\, fb+2\pi\,(\pi\, fb)^2]$$

iii) spatial correlation [7]

$$R(fb)=\exp(-kfb\,|\,x1-x2\,|\,/B)$$

where,

a : constant (=0.1811)
B : width of stiffening truss
D : depth of stiffening truss
f : frequency
fb=fB/U
fd=fD/U

k : decay factor (assumed to be 8)
U : mean wind speed
x1, x2 : coordinate along bridge axis

As for vertical bending and torsional responses, the agreement was fairly good, however, the observed horizontal bending responses were much smaller than calculated ones (Table 1).

One of the causes of this discrepancy was thought to be the spatial correlation which was assumed as the exponential function of fb | x1-x2 | /B. Since the measured spatial correlation of wind speed (root co-coherence function, Fig.5) did not tend to unity as frequency became 0 when separation of measurement points were large, the calculation might lead to an overestimation as was pointed out in ref.[8] and [9].

Using the measured aerodynamic admittance and the spatial correlation based on the turbulent flow of the wind tunnel, gust responses were calculated again. The result is shown in Table 1. Although there still remains some discrepancy, accuracy of the calculation has been improved.

4. FINDINGS FROM THE STUDY FOR THE TATARA BRIDGE

4.1 EXPERIMENT IN SMOOTH FLOW [10]

The aerodynamic stability of the Tatara bridge was investigated in smooth flow. No divergent vibration such as flutter was observed. This means the Tatara bridge is aerodynamically stable. The only wind induced vibration observed was vortex-induced vibration with small amplitude.

4.2 EXPERIMENT WITH ISLAND MODEL [11]

Wind characteristics at the site are very complicated (Fig.6). For example, in the case of wind direction of NNW and SSE, a topographical effect is hardly recognizable. In other words, wind speed and turbulence intensity were scarcely changed by the topography. On the contrary, in the case of wind direction such as NE and W, wind characteristics were changed significantly by the topography. Particularly, in the case of NE direction, the turbulence intensity was considerably increased by the topography, but the wind speed was not remarkably decreased. In the design of the long-span bridge, these wind characteristics were thought to be critical.

Wind tunnel experiments were carried out for three cases of wind direction, namely 18, 36 and 180 degrees (Photo 2, Fig.7). Wind direction was defined clockwise from the north direction normal to bridge axis. When wind direction was 18 and 180 degrees, the topographical effect was hardly recognizable. On the other hand, in the case of 36 degrees, the topography increased the gust response significantly.

According to the quasi-steady theory, aerodynamic force due to approaching turbulence increases with square of mean wind speed and turbulence intensity. Fig. 8 shows the wind characteristics along the bridge axis in the three wind directions. In the case of 36 degrees, a significant increase in turbulence intensity along the bridge axis was recognized. However, the increase in turbulence intensity was associated with decrease in mean wind speed.

Another factor that influences the gust response of long-span bridges is correlation of fluctuating wind speed at different places. Table 2 shows turbulence intensity and integral scale of turbulence at the mid-point of the center span in case of 36 degree. It can be seen that the integral scale as well as intensity was increased very much by the topographical model. Fig.9 shows co-coherence of fluctuating wind speed at two places on the bridge axis. It can be seen that the correlation was much higher in case of 36 degree than in case of 180 degree.

From these measurements, it seems that the large gust response in case of wind direction 36 degree was caused by high turbulence intensity and high space-wise correlation of the turbulent flow generated by the topographical model.

5. WIND RESISTANT DESIGN METHODS FOR SUPER LONG-SPAN BRIDGES

5.1 DESIGN TOOLS

In general, there are three kinds of tools for wind resistant design. They are:

a) Section model test (spring mounted rigid model test, measurement of aerodynamic forces, and so on),
b) Analysis based on aerodynamic forces measured from section model tests, and
c) Full aeroelastic model test.

Section model test is the simplest method. If aerodynamic instability of interest can be assumed as one-degree of freedom (eg. Vortex-induced vibration, galloping, and torsional flutter) or two-degree of freedom, and if torsional deformation of the bridge deck due to steady aerodynamic forces is negligibly small, we can predict critical wind speed of the instability directly from the section model test. As was shown in the experiment for the Akashi Kaikyo Bridge, however, we could not predict the critical wind speed of flutter directly from the section model test, because the torsional deformation was not negligibly small, and because flutter mode consisted of higher vibrational modes as well as fundamental modes. For the wind resistant design of super long-span bridges, therefore, we may well regard the section model test as a tool for eliminating aerodynamically unfavorable cross section of bridge deck or a tool for obtaining aerodynamic data that will be used in the detailed analysis.

As was demonstrated in the wind tunnel studies for the Akashi Kaikyo Bridge and the Tatara Bridge, and as was pointed out by Irwin [12], full aeroelastic models give important and unexpected insights into the bridge response. In the full aeroelastic model test, turbulence effects can be well simulated; three-dimensional and local topographical effects can be studied; and influences of various modes and mode shape can be included. Disadvantages of full aeroelastic models are greater cost and time for building and testing them.

If the accuracy of an analytical method is verified by comparing with a full aeroelastic model test, we can use the analytical method instead of the full aeroelastic model test. When we apply an analytical method, we have to consider the limitation of the method. To predict flutter of the Akashi Kaikyo Bridge, for instance, the effect of the static torsional displacement and higher natural modes had to be considered, and several aerodynamic derivatives had to be included in addition to the conventional ones. To predict gust responses of the Akashi Kaikyo Bridge, more accurate spatial correlation model was required. Although the present analytical method has been improved by comparing with the full aeroelastic model tests of the Akashi Kaikyo Bridge, the verification of the method is necessary if the method is applied to the super long-span bridges that have longer span, inexperienced bridge deck configuration or inexperienced cable system.

5.2 DESIGN PROCEDURE

The procedure of wind resistant design for super long-span bridges can be proposed as follows:

a) Selection of bridge deck cross section by section model tests
b) Prediction and evaluation of wind-induced deformation and vibration by the analytical method that is the most reliable at that time
c) Verification and improvement of the analytical method by comparing with a full aeroelastic model test
d) (in case of slight change of bridge design) Prediction and evaluation of wind-induced deformation and vibration by the verified analytical method
e) (if the accuracy of the analytical model is not enough) Verification of the finalized bridge design by a full aeroelastic model test

6. CONCLUDING REMARKS

Full aeroelastic model tests give important and unexpected insights into the bridge response. This advantage was demonstrated in the wind tunnel studies for the Akashi Kaikyo Bridge and the Tatara Bridge. Since super long-span bridges will have inexperienced span length, inexperienced bridge deck cross section or cable systems, full aeroelastic model tests will play an important roll in wind resistant design of super long-span bridges. To overcome its disadvantage, namely greater cost and time, section model tests can be used to select aerodynamically favorable cross section, and analytical methods verified by the full aeroelastic model tests can be applied to predict and evaluate wind-induced response

REFERENCES

[1] Sato H. and Ogihara K., Aerodynamic characteristics of slotted box girders, Proc. of 28th Joint Panel Meeting on Wind and Seismic Effects, UJNR, 1996
[2] Sato H., Wind tunnel studies on long-span bridges conducted at the Large Boundary Layer Wind Tunnel in Tsukuba, Proc. of 28th Joint Panel Meeting on Wind and Seismic Effects, UJNR, 1996
[3] Honshu-Shikoku Bridge Authority, Wind Resistant Design Criteria for Honshu-Shikoku Bridges, 1976 (in Japanese)
[4] Sumiyoshi Y., Endo T., Miyata T., Sato H. and Kitagawa M., Experiments for the Akashi Kaikyo Bridge in a Large Boundary Layer Wind Tunnel,

Proc. of International Seminar on Utilization of Large Boundary Layer Wind Tunnel, Tsukuba, Japan, 1993
[5] Davenport A.G., Buffeting of a suspension bridge by storm winds, Proc. ASCE, Vol. 88, ST3, 1962
[6] Fung, Y.C., An Introduction to the Theory of Aeroelasticity, John Wiley & Sons, 1955
[7] Davenport A.G., The spectrum of horizontal gustiness near the ground in high winds, Q.J. Roy. Met. Soc., Vol. 87, 1961
[8] ESDU, Characteristics of atmospheric turbulence near the ground, Part Ⅲ: variations in space and time for strong winds (neutral atmosphere), 1975
[9] Irwin H.P.A.H., Wind tunnel and analytical investigations of the response of Lions' Gate Bridge to a turbulent wind, Laboratory Technical Report LTR-LA-210, National Research Council Canada, 1977
[10] Sato H., Toriumi R., Kitagawa M. and Katsuchi H., Wind tunnel experiment for a super long-span cable-stayed bridge in smooth flow, Proc. of 26th Joint Panel Meeting on Wind and Seismic Effects, UJNR, 1994
[11] Sato H., Kitagawa M. Toriumi R., and Katsuchi H., Wind-induced vibrations of a super long-span cable-stayed bridge in turbulent flow generated by surrounding islands, Proc. of 27th Joint Panel Meeting on Wind and Seismic Effects, UJNR, 1995
[12] Irwin P. A., Full aeroelastic tests, Aerodynamics of Large Bridges, A. A. Balkema, Rotterdam, Brookfield, 1992

Table 1 Gust Responses

	Horizontal (mm)	Vertical (mm)	Torsional (deg)
Measured	20	12	1.4
Calculated (Conventional calculation)	83	13	2.9
Calculated (Improved calculation)	38	11	1.5

Table 2 Turbulence Intensity and Integral Scale of Turbulence

Wind Characteristics (Center of center span)	with topographical model $\beta = 36°$	without topographical model $\beta = 36°$
Turbulence Intensity		
Iu (%)	15.6	9.3
Iw (%)	8.7	5.8
Integral Scale of Turbulence		
Lxu (m)	1.21(242)	0.58(116)
Lxw (m)	0.25(50)	0.31(62)
( ):converted real scale		

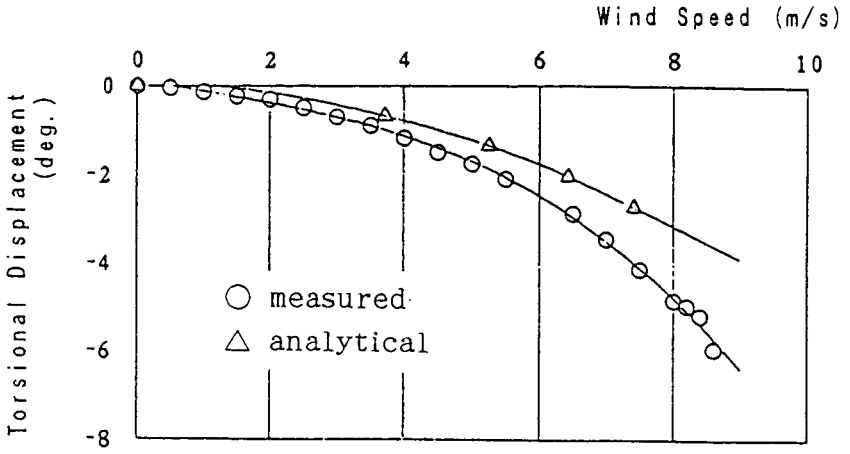


Fig.1 Torsional dispalcement by wind (midspan)

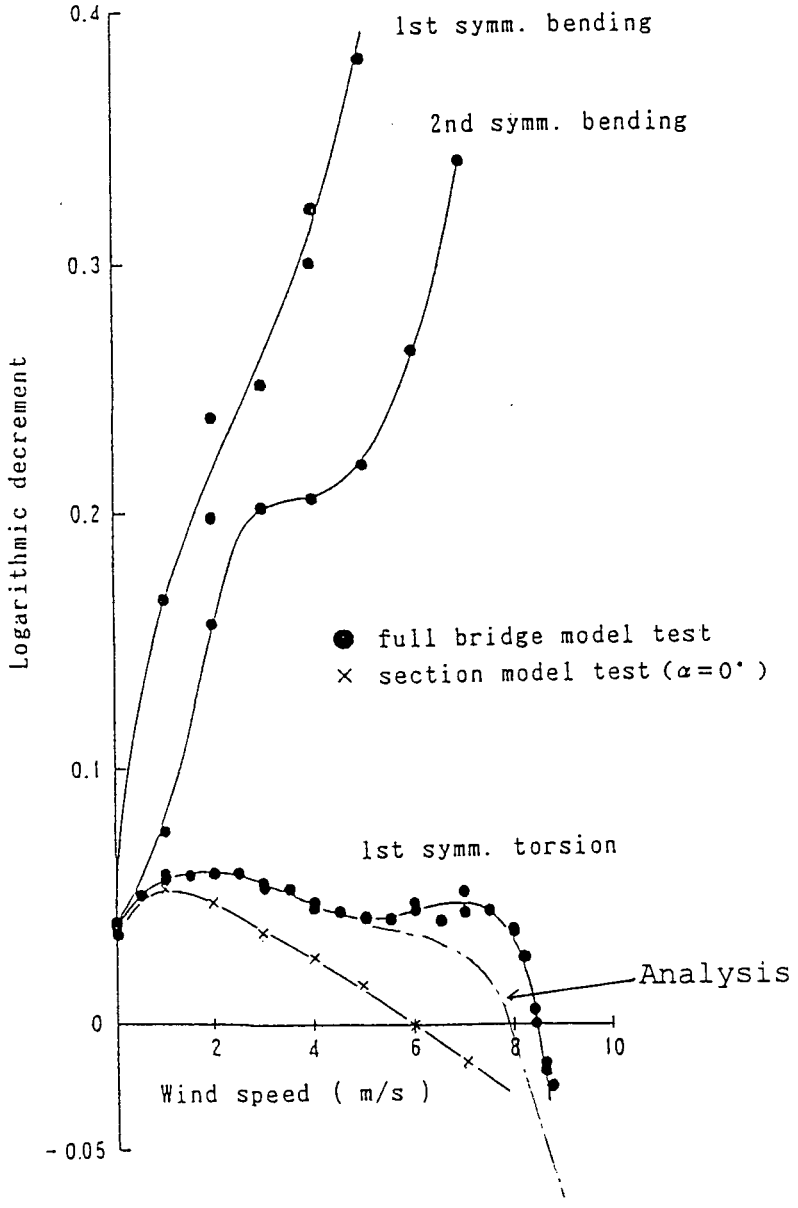


Fig.2 Change of aerodynamic damping

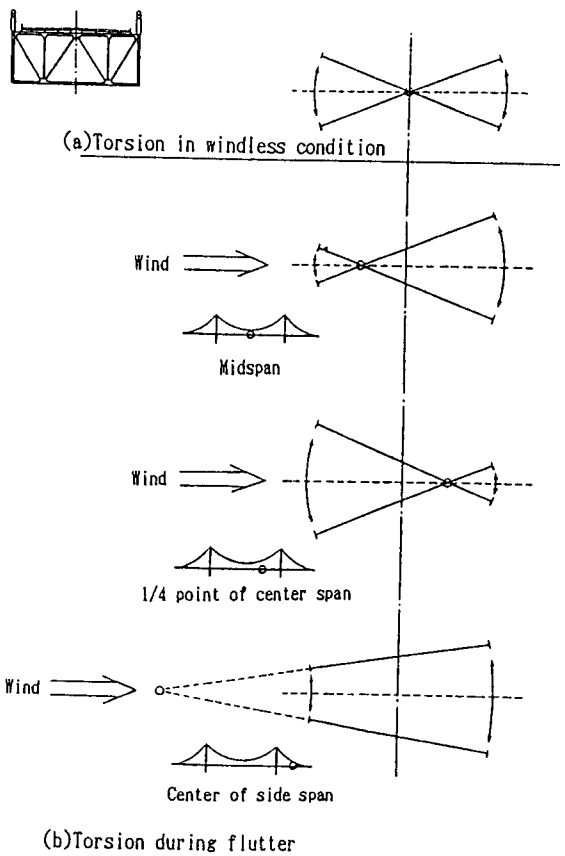


Fig.3 Movement of rotation center

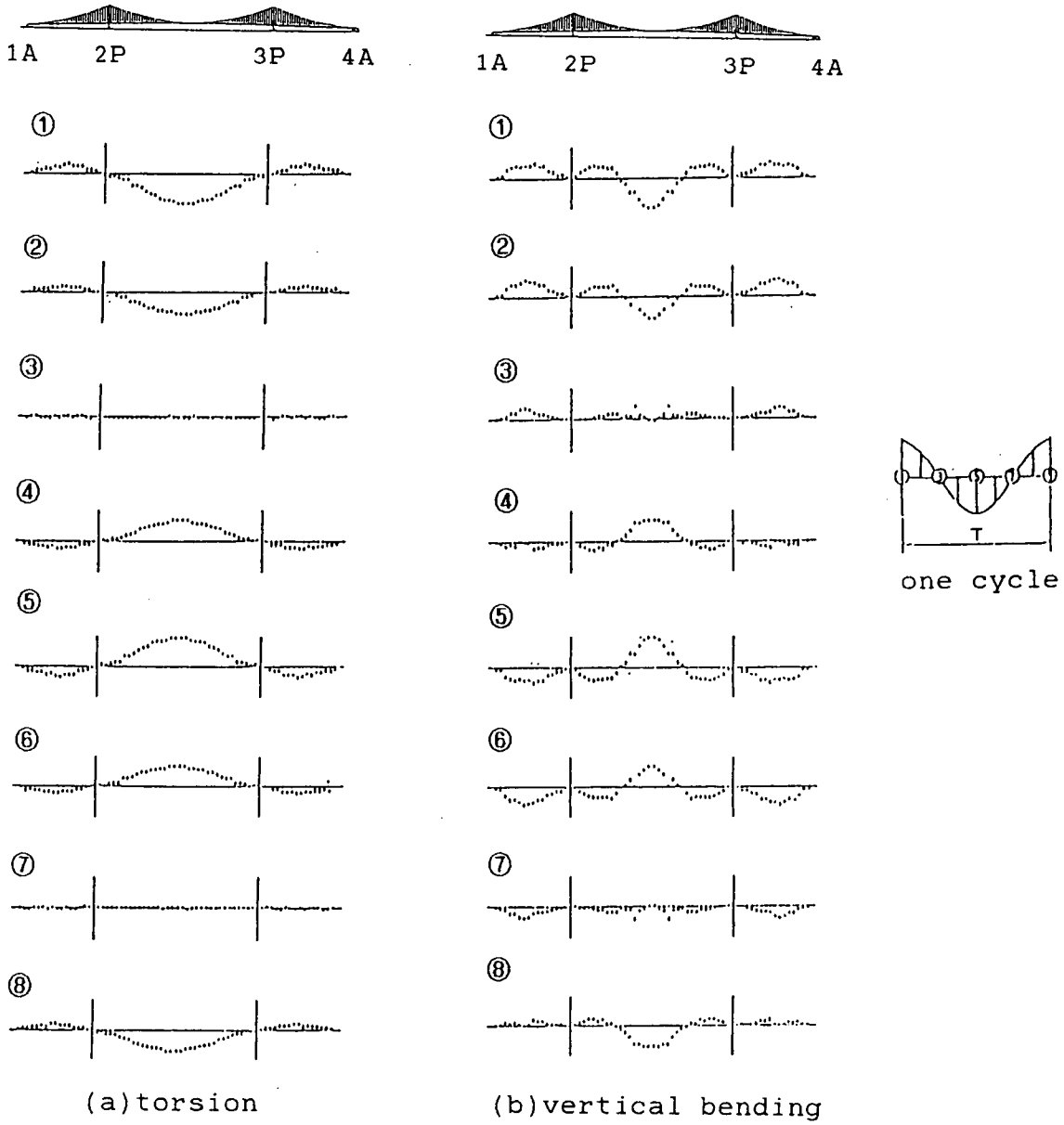


Fig.4 Response of girder cycle during flutter

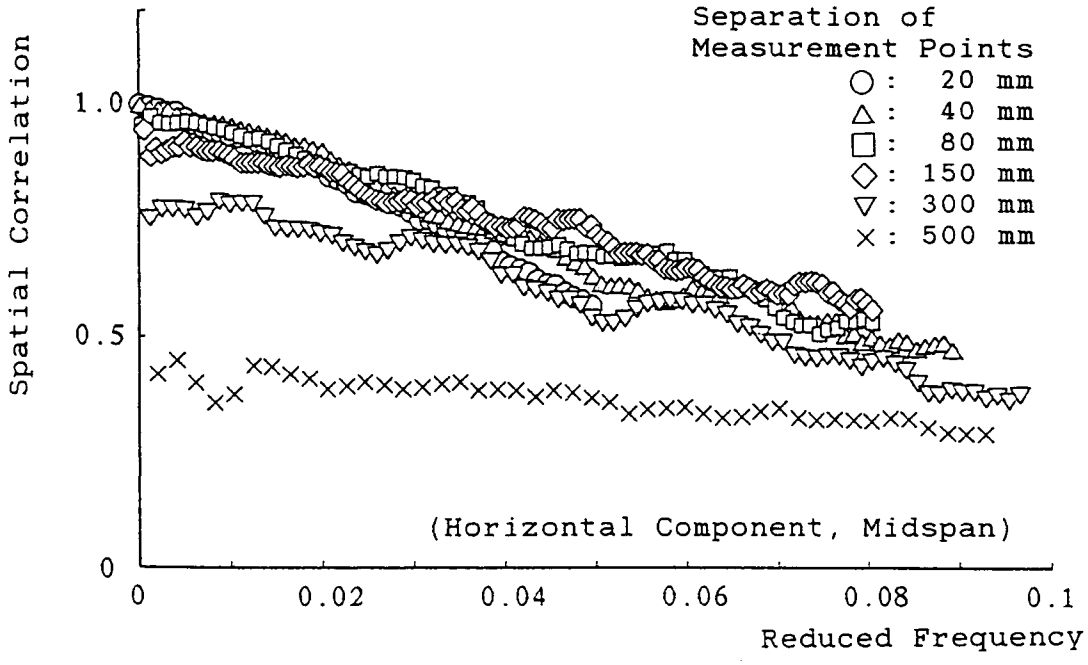


Fig.5 Spectral correlation of wind speed

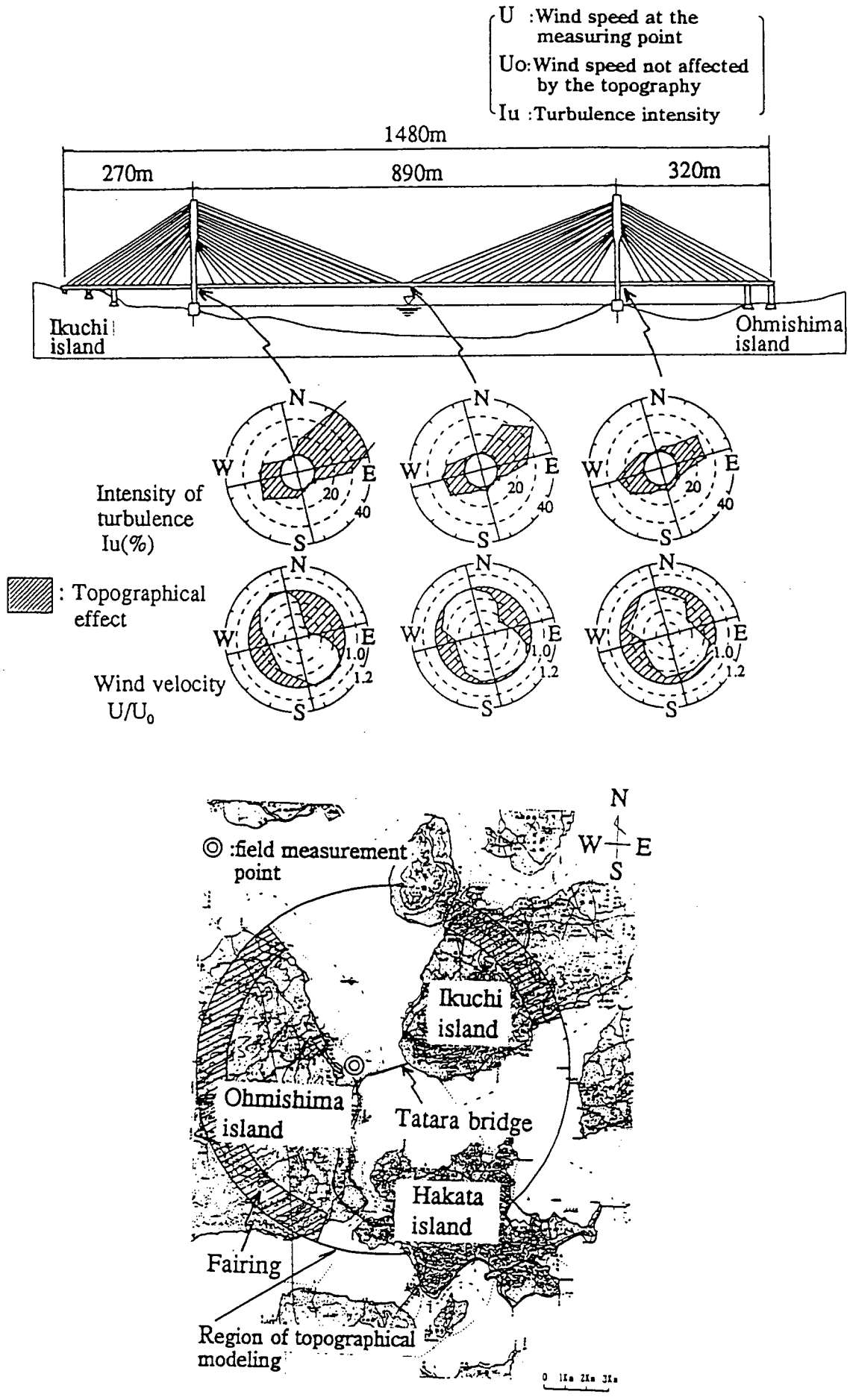


Fig.6 Wind flow pattern at the Tatara Bridge construction site

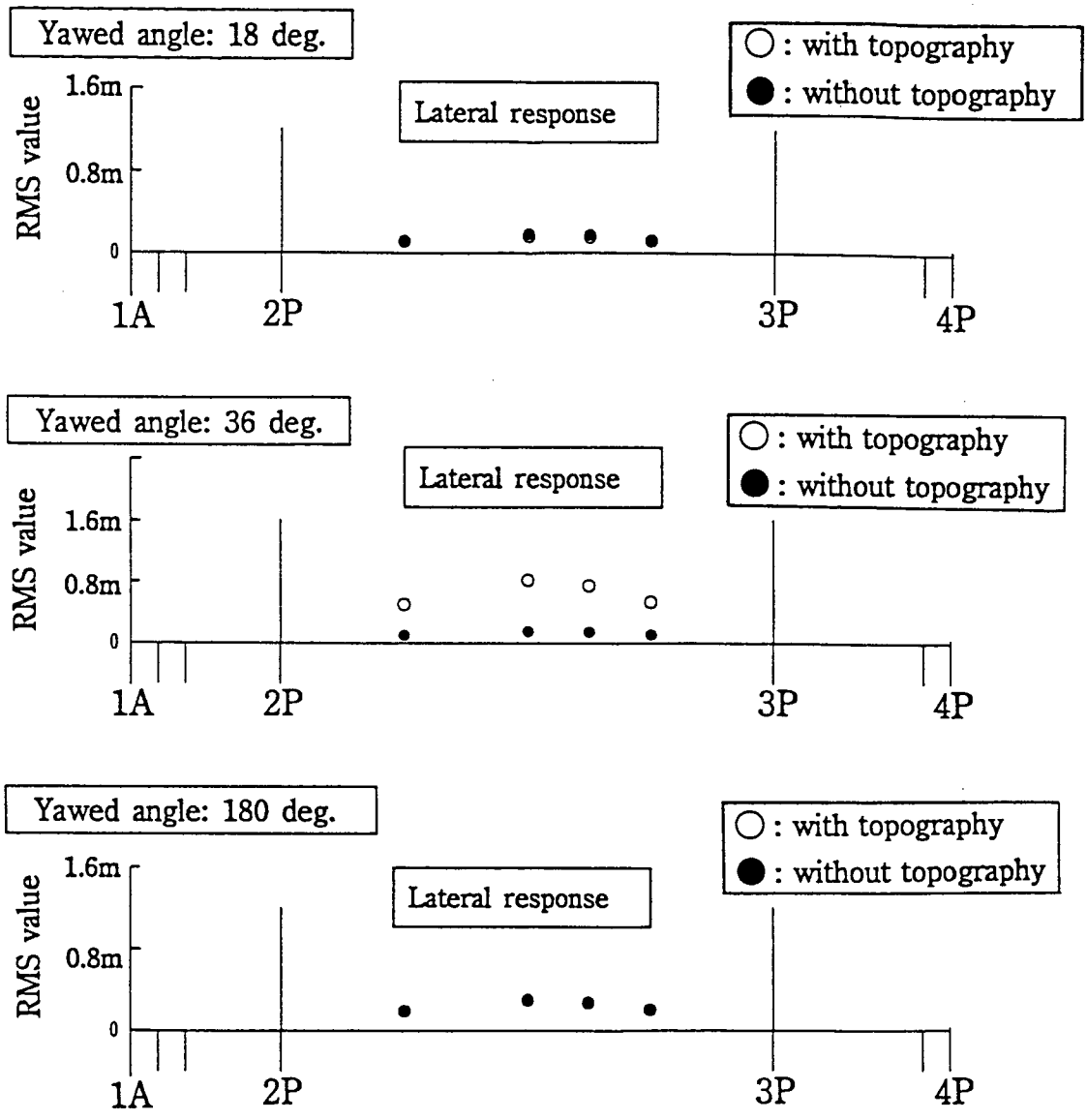


Fig.7 RMS value of girder's gust response

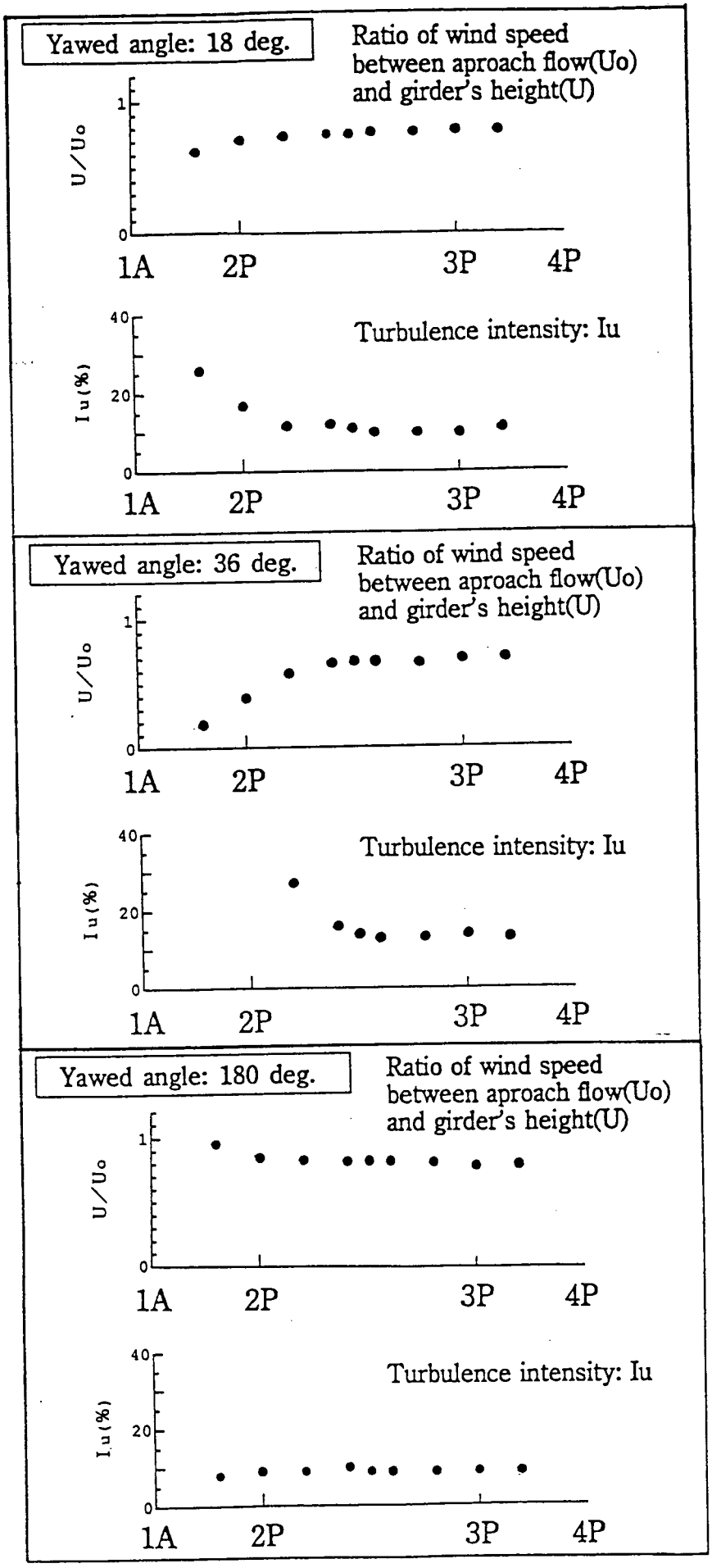
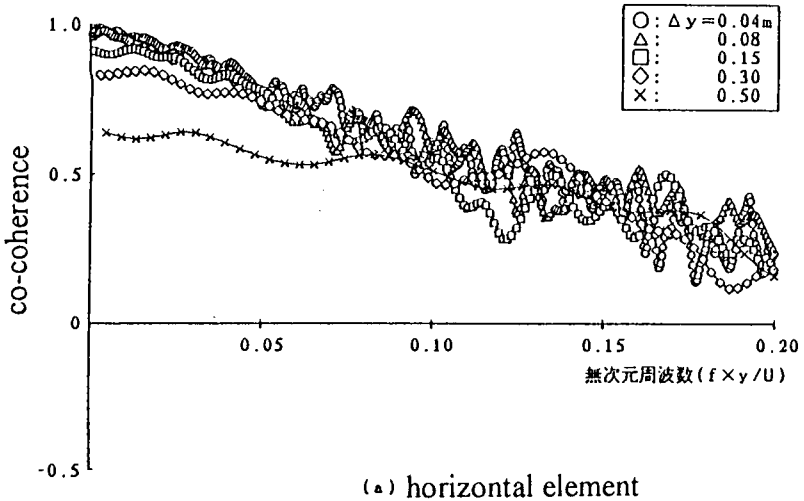
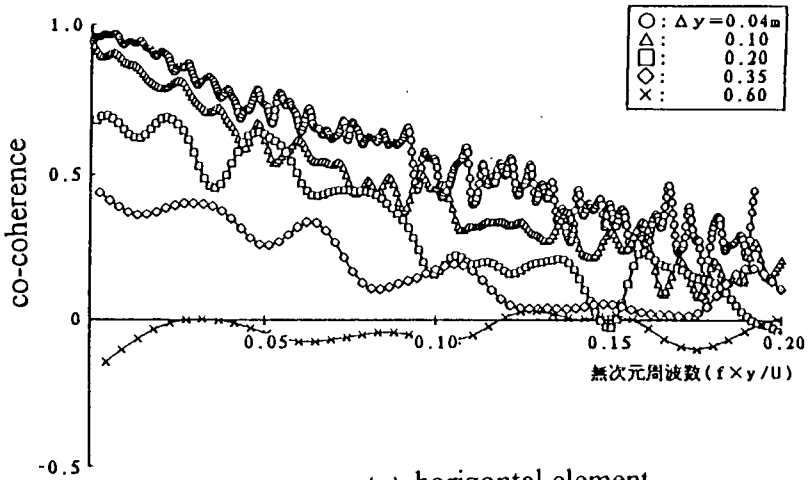


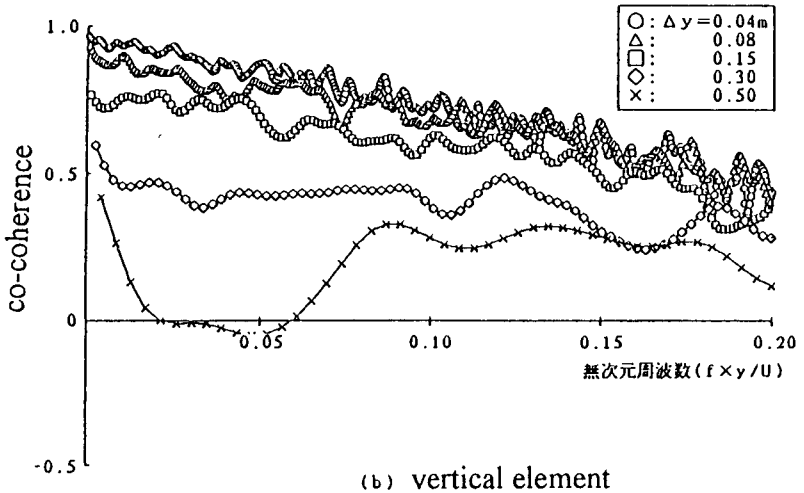
Fig.8 Wind characteristics along bridge axis



(a) horizontal element

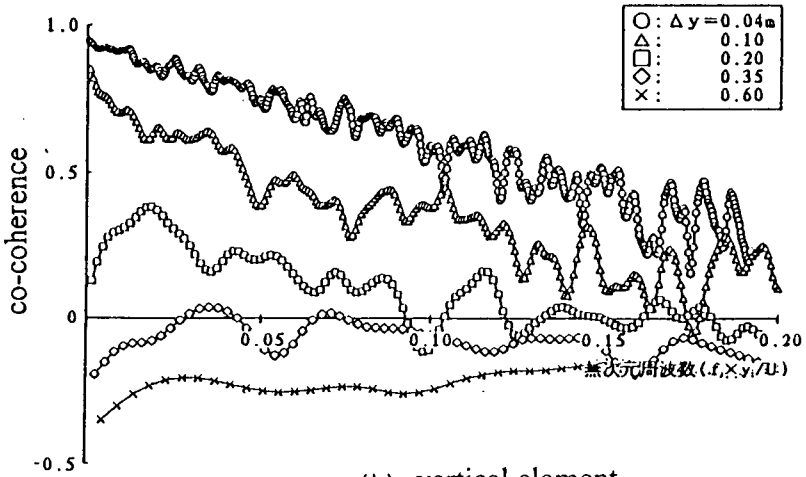


(a) horizontal element



(b) vertical element

(1) $\beta = 36^\circ$



(b) vertical element

(2) $\beta = 180^\circ$

△ y:distanse from the center of center span,direction is from the center of center span to 2P tower

Fig.9 Co-coherence of fluctuating wind speed at two places

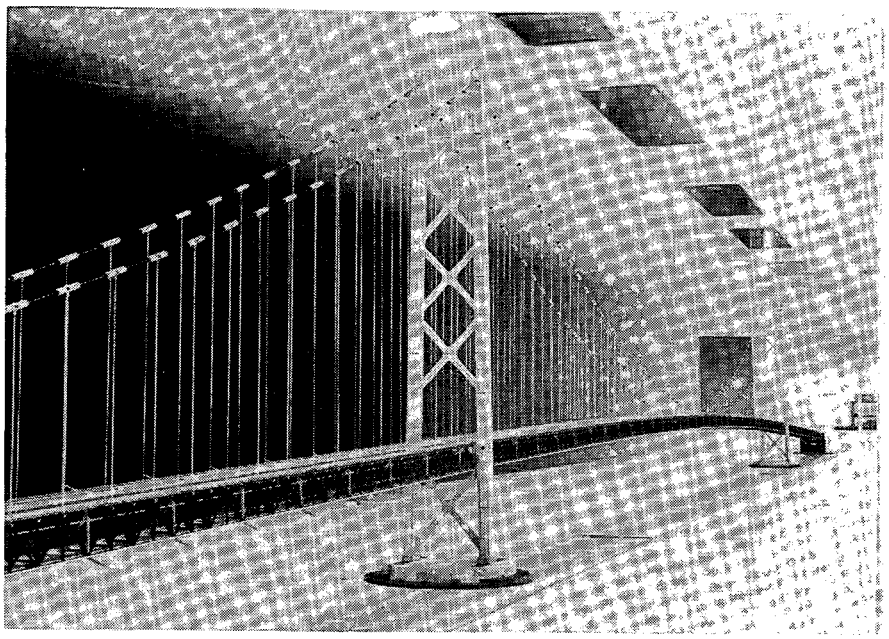


Photo 1 Full model test of the Akashi-Kaikyo Bridge

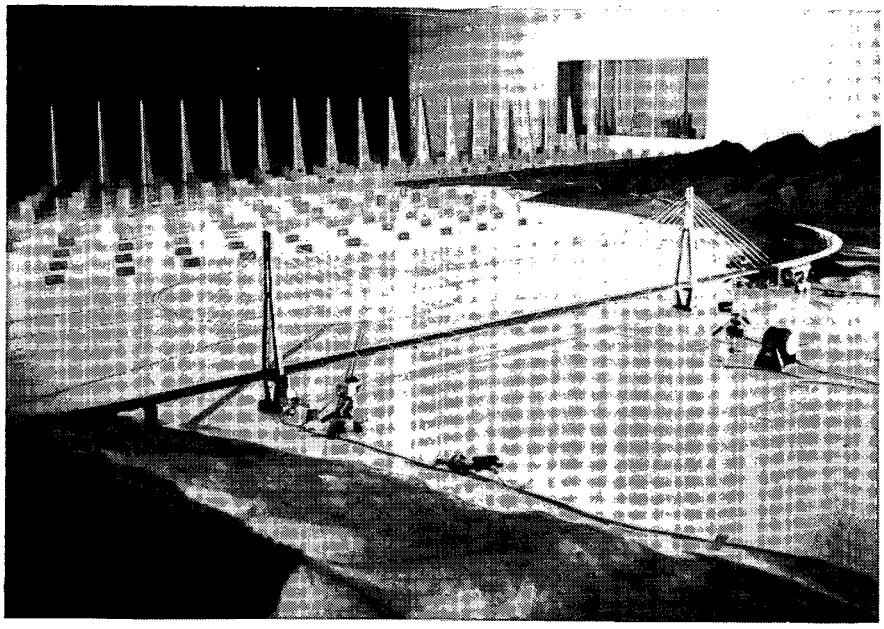


Photo 2 Model of the Tatara Bridge for the wind tunnel study in turbulent flow

Improved Analysis of Extreme Wind Loads on Low-Rise Structures

by

M. R. Hajj[1], D. A. Jordan[2], and H. W. Tieleman[1]

ABSTRACT

Characterizing atmospheric turbulence and determining the far-field velocity-pressure relation are important for simulation and prediction of extreme wind loads on structures. In this work, we show some shortcomings of Fourier decomposition and present wavelet analysis as a better suited technique for characterizing turbulence and modeling velocity-pressure relation. Examples from full and model scale experiments are presented. The results show that, with wavelet analysis, one could establish an intermittency character for atmospheric turbulence and relate low-pressure peaks to highly turbulent events in the atmospheric wind.

KEYWORDS: wind engineering, low-rise structures, turbulence, sepctral analysis, wavelet analysis.

1. INTRODUCTION

Over the past thirty years, there has been extensive research studies to mitigate against wind damage on structures. The results of many of these studies have found their way into building codes and have played an important role in reducing the extent of damage. Yet, it is fair to state that more improvements are needed in order to reduce losses. A simple comparison of wind tunnel experiments, code requirements, and full-scale measurements of pressure coefficients show a large scatter of data even for the simplest cases. These discrepancies are mainly due to the lack of consensus which has been hard to obtain because of the many variables and methods of analysis involved in determining wind loads. In particular, the atmospheric boundary layer is turbulent and consequently simulating turbulence characteristics is as important as simulating the mean flow. Moreover, the velocity-pressure relation is governed by Poissons equation which predicts that surface pressure is a function of the entire velocity field. Such equation has linear and nonlinear terms whereby the mean shear and turbulence contribute to the pressure. Consequently, two important questions would be: Is it possible to establish a model that predicts pressure from mean and turbulence parameters of the atmospheric wind? If so, which turbulence parameters should be considered? In this work, we present wavelet analysis as a suitable technique that could provide answers to these questions.

To date, Fourier decomposition has been the main tool used in the analysis and modeling of atmospheric turbulence and the velocity-pressure relation. The underlying process in Fourier decomposition is the representation of a time series, such as wind velocity or surface pressure, by a set of complex sinusoids. There are several advantages for such a representation. First, turbulence scales in the atmosphere can be represented by frequency components and their energy is obtained from the power spectrum. Second, estimates of spectral energy in particular frequency bands are statistically independent of the energy estimates in other bands. Third, for large sets of data, frequency decomposition can be obtained rapidly with FFT techniques. Fourth, higher-order moments can be used to determine nonlinear couplings among spectral components in one signal or between two signals, such as velocity and pressure. Finally, the velocity-pressure relation can be modeled by an input-output system that accounts for contributions from linear and nonlinear sources in the velocity fluctuations to the pressure.

The above mentioned advantages made the use of frequency domain analysis for the simulation and modeling of atmospheric turbulence and wind loads on structures very attractive. Yet, this analysis domain has many shortcomings which makes it of limited importance in characterizing wind flows for the purpose of predicting or simulating extreme wind loads on structures. The objectives of this paper are three-fold. The first is to discuss some shortcomings of frequency domain analysis when used to characterize the wind events that are of important value in prediction and simulation of wind loads on structures. The second is to present wavelet, i.e. time-scale, domain analysis as an alternative to the traditional frequency decomposition. In particular, we will show how quantita-

[1] Department of Engineering Science and Mechanics, Virginia Tech, Blacksburg, VA, 24061

[2] School of Engineering and Applied Science, University of Virginia, Charlottesville, VA 22903

tive information regarding extreme wind loads from the wavelet analysis can be derived. The third is to show how such information can be used to experimentally and numerically simulate or predict wind loads on structures. Examples from full and model scale experiments are presented.

2. SHORTCOMINGS OF FREQUENCY DOMAIN MODELS OF ATMOSPHERIC TURBULENCE

Models of normalized spectra of the velocity components of atmospheric wind have been developed to characterize energy content of turbulence scales which are represented by frequency components. The majority of these models are interpolation expressions between low-frequency and high-frequency asymptotes. Figures 1-a and 1-b show the time series of fifteen minutes records of the u- and v-velocity components obtained from the Wind Engineering Research Field Laboratory (WERFL) at Texas Tech. The sampling rate for these records is 10 Hz and the measurements were taken at an elevation, H, of about 4.0 m. The corresponding time record of the pressure coefficients at $x/H = 0.6$ and $y/H = 0.403$ is shown in figure 1-c. More information about the terrain and experimental set-up is given in Levitan and Mehta (1991). Those records were classified stationary by Smith and Mehta. A comparison of the power spectral density functions of these records and their respective analytical models (Tieleman (1994)) is given in figures 2-a and 2-b. The results clearly show that the observed spectra do not match the analytical models. This mismatch is due to the fact that, in our estimates of the spectra, no segment averaging was performed. Because only one segment was used, the variances of the spectra are equal to the estimated values. It should be noted here that when segment averaging was performed over a period of two hours, the estimated spectra became smooth and approached the analytical models. Yet, such an averaged spectra cannot be of any significant use in simulating or modeling low pressure peaks that take place over time periods of one to three seconds (see figure 1-c). These peaks cannot be related to average spectra estimated over a two-hour period. These peaks can only be related to time variations of the energy of turbulent fluctuations.

3. SHORTCOMINGS OF FREQUENCY-DOMAIN MODELING OF THE VELOCITY-PRESSURE RELATION

Several frequency-domain models have been proposed to establish a relation between incident velocity fluctuations and surface pressure fluctuations. These models are based on strip or quasi-steady approaches. In strip theory, the wind pressure is directly-related to the wind velocity at the same elevation Kawai (1983). In the linearized quasi-steady theory, the surface pressure fluctuations are considered to be directly proportional to instantaneous velocity and flow direction Kawai (1983). The modified (nonlinear version of) quasi-steady theory assumes that the flow is directly proportional to the squares of the fluctuating velocity components. Studies conducted to examine these theories show that, in general, they fail to predict many of the characteristics of the surface pressure fluctuations. This is especially true in the important regions of separation, vortex shedding and/or vortex formation. These results have lead to the idea of introducing frequency-dependent empirical aerodynamic admittance functions. Yet, measurements of these functions show large discrepancies. Often, it is assumed that these discrepancies arise from nonlinear effects that were not taken into consideration. In order to determine these effects, we performed analysis of nonlinear relations between velocity and pressure spectral components using higher-order statistical moments (Hajj et al. (1997)).

The extent to which spectral components in two signals are linearly correlated can be obtained from measurements of the linear coherence. For zero-mean stationary fluctuations $u(t)$ and $p(t)$, that represent random velocity and pressure waveforms, the linear coherence function, γ^2_{up}, is defined as

$$\gamma^2_{up} = \frac{| < P(f)U^*(f) > |^2}{\{< |U(f)|^2 >< |P(f)|^2 >\}} \qquad (1)$$

where $< ... >$ denotes time averaging and $U(f)$ and $P(f)$ are the complex Fourier amplitudes of $u(t)$ and $p(t)$ respectively. As explained by Hajj et al. (1997), the next higher-order spectral moments to the cross-power spectrum, namely the cross-bispectrum, can be used to investigate the nonlinear coupling among spectral components, with different frequencies, in two signals. For the velocity and pressure waveforms, the cross-bispectrum is defined as

$$S_{uup}(f_i, f_j) =< P(f_k)U^*(f_i)U^*(f_j) > \qquad (2)$$

where f_k is the algebraic sum of f_i and f_j. As defined here, the cross-bispectrum is a function of two frequency components and measures the degree of coherence among modes with frequencies f_k in the pressure spectrum and f_i and f_j in the velocity spectrum. If the

three modes are independent, their phases are statistically independent and subsequently, the phase of the cross-bispectrum is randomly distributed. The averaging, indicated in equation (2) by $< ... >$, yields a zero value for the cross-bispectrum. On the other hand, if the three modes are nonlinearly related, a phase coherence will exist among them and the averaging will result in a nonzero value for the cross-bispectrum. The normalized value of the cross-bispectrum is termed the cross-bicoherence and is given by

$$b^2_{uup}(f_i, f_j) = \frac{|S_{uup}(f_i, f_j)^2}{< |U(f_i)U(f_j)|^2 >< |P(f_k)|^2 >} \quad (3)$$

and, by Schwartz inequality, varies between zero and one.

In order to assess the extent of the nonlinear relation between spectral components of the velocity and pressure fluctuations, simultaneously measured velocity and pressure fluctuations were obtained from the Clemson wind-tunnel. The experimental model is a 1/50 scale of the experimental building at WERFL. Details of the experimental setup are given in Hajj et al. (1996). The wind tunnel data was chosen because higher-order statistical analysis require long data records that are stationary. Such data could not be obtained from full scale measurements. Spectra of the u-velocity component of the incident flow and of the pressure fluctuations at the corresponding point on the roof surface and the linear coherence between the two signals are shown in figures 3 and 4, respectively. The resulting pressure spectra show two broadband peaks around $fH/U = 0.02$ and 0.5. The linear coherence measurements reveal that only the very low-frequency band ($fH/U < 0.01$) in the velocity and pressure are linearly correlated. Beyond this band there is no indication of any linear coherence. By comparison of figures 3 and 4, the range of frequencies where relatively high velocity-pressure coherence occurs contains only a small portion of the spectral energy. Figure 5 shows contour plots of the cross-bicoherence between the velocity and pressure fluctuations. The results show that a low level of bicoherence is measured among all pairs of frequency components for the velocity and the pressure fluctuations. Such a low level (<0.1) shows that there is no direct nonlinear coupling between the frequency components in the pressure and the far-field velocity fluctuations.

The above results show that, while low-frequency components ($fH/U < 0.01$) in the incident turbulence and pressure fluctuations are linearly coupled, the relatively higher frequency components, which contain energy, are not coupled. These results are true for different angles of incidence and different flow configurations. Measurements of the cross-bicoherence show that the nonlinear effects are not the major cause for the low linear coherence in the high frequency range. These results show that the relation between frequency components of the incident velocity and pressure fluctuations is not direct and cannot be quantified. This is mainly due to segment averaging and elmination of temporal information.

4. DEFINITIONS AND IMPLEMENTATION PROCEDURES AND WAVELET DOMAIN ANALYSIS

As discussed in the previous section, one major shortcoming of frequency domain analysis is that it does not provide temporal information. Such information can be obtained from short-time Fourier transform or the Gabor transform. However, it is proposed to use wavelets for two reasons. First, the wavelet analysis has the advantage of providing a better time-scale resolution. A short-time Fourier transform uses a single analysis window. Consequently, the time-frequency resolution is fixed over the entire time-frequency plane. In contrast, the wavelet transform uses short windows at high frequencies and long windows at low frequencies. Because wind velocity components can contain low-frequency components over long durations and relatively high-frequency components of short duration, wavelet analysis is a more suitable technique than Fourier analysis. Second, while frequency analysis is performed by projecting a signal onto a number of sinsoids which are infinite in extent, wavelet analysis is performed by projecting the signal onto a set of highly localized basis functions. These basis functions are called wavelets and are obtained from a single "mother" wavelet by dilations and translations. Thus, in wavelet analysis, the notion of a scale replaces that of frequency which leads to the so-called time-scale representation. Because it is localized in time, a scale representation is more suitable than a frequency representation for examining temporal characteristics of turbulence.

Given a time signal, $f(t)$, its continuous wavelet transform is defined as

$$\mathcal{W}(a, \tau) =< f(t), \psi_{a,\tau} >= \int_{-\infty}^{\infty} f(t)\psi^*_{a,\tau}(t)dt, \quad (4)$$

with

$$\psi_{a,\tau} = a^{-\frac{1}{2}}\psi\left(\frac{t-\tau}{a}\right), \quad (5)$$

where $\psi_{a,\tau}$ is a function called a wavelet, a is a dilation parameter, τ is a translation or shift parameter and the $*$ denotes complex conjugate, when the wavelet is complex. The wavelet transform coefficients, $\mathcal{W}(a,\tau)$, represent the contribution of scales a to the signal at time, τ. Wavelet energy is defined from the wavelet coefficients as $\mathcal{W}\mathcal{W}^*$. From Farge (1992), a wavelet energy density (energy per scale size) can be defined as $\mathcal{W}\mathcal{W}^*/a$. When integrated over time, the wavelet energy density yields the global wavelet energy spectrum which gives the energy content at that scale.

In the following, we use a complex Morlet mother function which is given by

$$\psi(t) = exp(i\omega_\psi t)exp(-|t|^2/2), \qquad (6)$$

where ω_ψ is a constant that forces the wavelet to be admissible, i.e., it possess an inverse transform, the complex Morlet wavelet has been shown to have several advantages over real wavelet functions. The digital implementation of the continuous wavelet transform is a discrete convolution between the sampled time series and sampled versions of the analyzing wavelet at all scales. All scaled versions of the complex Morlet wavelet were sampled with enough samples to avoid aliasing and the convolutions were performed in the frequency domain using the FFT. A relationship can be established between the wavelet scale and the peak frequency, f_p, of the scaled wavelet bandpass filter. In our implementation procedure, this relationship is given by

$$f_p = \frac{2.90}{a}. \qquad (7)$$

Forty-seven values of a were spaced logarithmically to cover a frequency range from 2.9 Hz to about 0.022 Hz. The large scale cut-off was determined by the number of points in the sampled time series. More information about the application of wavelet analysis to the study of turbulence is given in (Farge, 1992).

5. CHARACTERIZATION OF ATMOSPHERIC TURBULENCE WITH WAVELETS

Contour plots of the wavelet energy density of the u- and v- velocity components in figures 1-a and 1-b are shown in figures 6-a and 6-b. The axes are time in seconds and the natural log of the scale, a. The plots show that scales corresponding to frequencies below 0.15 Hz contribute significantly but intermittently to the signal. Such contribution is seen in the high peaks at various times. The plots also show the presence of smaller scales indicated by the streaks. These scales correspond to the frequency range between .25 and 1.0 Hz. By examining time records of the velocity components in the atmospheric wind it can be noticed that the fluctuations are intermittent. By intermittency, we mean that the energy is not evenly distributed in time or space, Farge (1992); Following Townsend (1956), we define an intermittency factor as the percentage of time a measuring device sees the variable in its higher amplitude state.

Because turbulence fluctuations contain different time scales, we have opted to examine the intermittency of the whole time record. In order to estimate the percentage of time where these scales are in their higher amplitude state, it is necessary to define a threshold value and time of integration of energy. Here, the threshold is defined as twice the average energy content of that scale. The time of integration of a scale is taken to be equal to the inverse of the peak frequency of the magnitude of the Fourier transform of the wavelet. It must be recognized that the measured intermittency factor is dependent on the choice of threshold. However, varying the threshold value between 1.5 and 2.5 times the average did not cause significant variations in the measured intermittency factor. Once intermittent peaks in the wavelet transform energy were located, the total energy in these peaks were calculated. Figures 7-a and 7-b show the intermittency factor and percentage of energy content in the peaks of wavelet transform energy of the u- and v-velocity components shown in figures 1-a and 1-b. The results show that all scales are intermittent, i.e. energy is not distributed evenly in time. The measured intermittency factor, for both u- and v-components, varies around 0.12 for the smaller scales ($\ln a \leq 3.9$) and is slightly higher, up to 0.2, for the larger scales. Another feature is the percent of energy contained in these intermittent peaks. For the larger scales, the amount is 40 to 50%. These results imply that up to 50% of the total energy of these scales appears over less than 20% of the time.

6. WAVELET ANALYSIS THE VELOCITY-PRESSURE RELATION

In order to better assess the velocity-pressure relation, the wavelet cross scalogram of the continuous wavelet coefficients, $\mathcal{W}_u\mathcal{W}_p^*$ is used. The cross scalogram gives peaks where fluctuations from two time series fluctuate at the same time and same scale. If fluctuations do not appear at the same time and same scale, the magnitude of the cross-scalogram is very low. Figures 8-a and 8-b show the $u-p$ and $v-p$ cross-scalograms

for the records shown in figures 1-a, 1-b, and 1-c. The large peak in the $u-p$ and $v-p$ cross scalograms appears at times between 450 and 550 seconds By comparison of the $u-p$ and $v-p$ cross scalograms with the pressure time series, figure 1-c, it is noticed that the pressure peaks at t near 480 and 520 have their origin most probably in turbulent events in $u-$ and $v-$ velocity components. These results suggest the v- component of the velocity is important to the occurrence of peak pressures and should not be disregarded. Furthermore, the cross scalogram results suggest that there is a clear relation between the time-localized fluctuations of u- and v-velocity components and the pressure peaks. In particular, peaks in pressure are associated with fluctuations at the *same* scale and time as the velocity fluctuations from which they originate.

7. CONCLUSIONS

The above results show that wavelet analysis is better suited than Fourier decomposition for the characterization of atmospheric turbulence events and modeling the velocity-pressure relation. With wavelet analysis, we are able to show that:

Atmospheric turbulence is highly intermittent. Up to 60% of the energy of large and intermediate scales appears over less than 20/time.

The peaks in the energy distribution of the velocity fluctuations are related to low pressure peaks observed in the pressure coefficients.

Simulation of these events, along with Reynolds number, mean flow parameter, geometry and turbulence intensity, in wind tunnel experiments or in numerical analysis will improve the prediction of peak pressure coefficients.

Both u- and v- turbulence characteristics should be considered in the simulation.

While the wavelet analysis has been applied for the purpose of improving the analysis and simulation of wind loads on low-rise structures, such analysis can be used to characterize the response of bridges and tall buildings to wind forces. Using wavelet analysis, higher-order statistical analysis, perturbation techniques or a combination of them should improve significantly the undestanding of the dynamical behavior of structures subject to wind forces. One example on the modeling and identification of damping and nonlinear parameters of a three-beam structure with the use of the above techniques is given by Hajj et al (1995).

8. ACKNOWLEDGEMENTS

The financial support of the National Science Foundation under Grant # CMS-9412905 is greatly acknowledged. The authors would like to thank Drs. T. Reinhold and K. Mehta for providing the data. The authors would like to also thank Mr. C. Lusk for his help in preparing some of the figures.

9. REFERENCES

Farge M., "Wavelet transforms and their applications to turbulence," Ann. Rev. Fluid Mech., 24, 1992, 395-457.

M. R. Hajj, I. M. Janajreh, H. W. Tieleman and T. A. Reinhold, "On the frequency domain analysis of the linear and nonlinear relations between incident turbulence and fluctuating pressures on surface-mounted prisms," Journal of Wind Engineering and Industrial Applications, (in press).

M. R. Hajj, R. W. Miksad, and E. J. Powers, "Measurements and analyses of nonlinear wave interactions with higher-order spectral moments," Journal of Fluids Engineering, ASME. Vol. 119, 1997, 3-14.

M. R. Hajj, A. H. Nayfeh, and P. Popovic, "Identification of nonlinear systems parameters using polyspectral measurements and analyses," Proceedings of the 15th ASME Biennial Conference on Mechanical Vibration and Noise, Boston, MA, 17-21 September 1995, 651-661.

Kawai, H., "Pressure fluctuations on square prisms - applications of strip and quasi-steady theories," J. Wind Eng. Ind. Aerodyn., 13, 1983, 197-208.

Levitan, M. L. and Mehta, K. C., "Texas Tech field experiments for wind loads: building and pressure measuring systems," 8th International Conference on wind engineering, London, Ontario, Canada, 1991.

Smith, D. A., and Mehat, K. C., "Stochastic models for stationary and nonstationary wind data," 7th US National Conference on Wind Engineering, Los Angeles, CA, 1993.

Tieleman, H. W., "Universality of velocity spectra," J. Wind Eng. Ind. Aerodyn., 56, 1995, 55-69.

Townsend, A. A., "The structure of turbulent shear flows," Cambridge University Press, 1956.

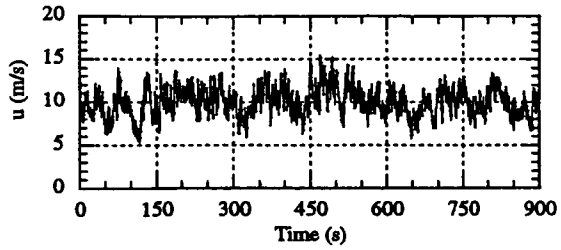


Figure 1-a: Time trace of the u-component of atmospheric wind.

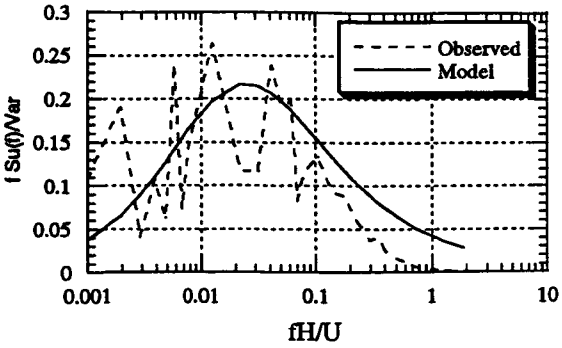


Figure 2-a: Observed and model spectra of the u-component of atmospheric wind

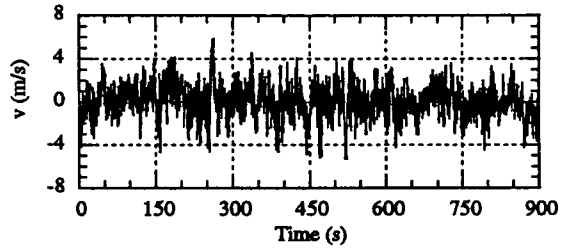


Figure 1-b: Time trace of the v-component of atmospheric wind.

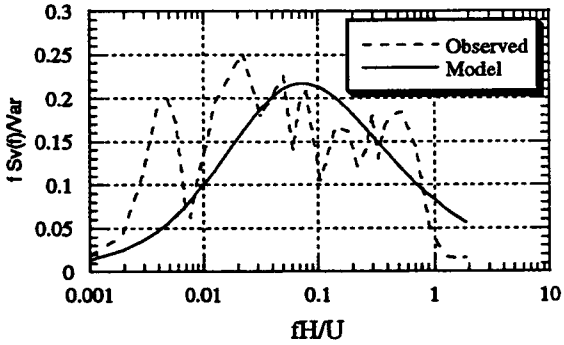


Figure 2-b: Observed and model spectra of the v-component of atmospheric wind

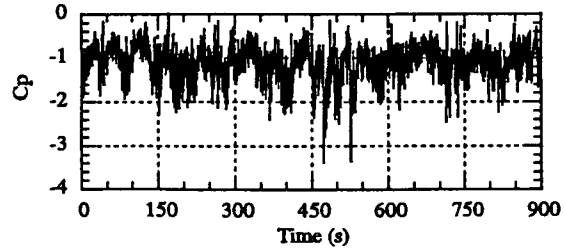


Figure 1-c: Time trace of the corresponding pressure coefficient at y/H = 0.318. (normal incidence)

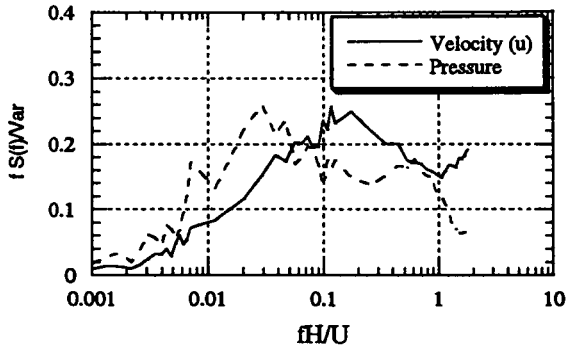


Figure 3: Spectra of the u-component and pressure from the Clemson tunnel.

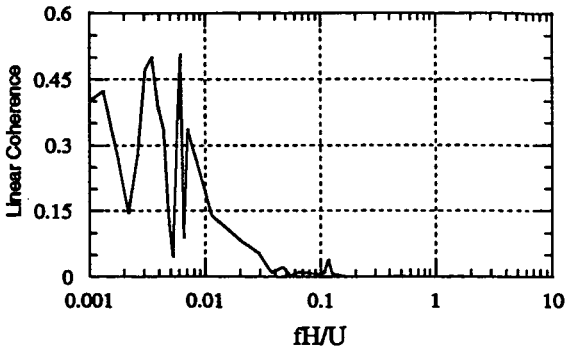


Figure 4: Linear coherence between spectral components of the u-component of the velocity and pressure fluctuations.

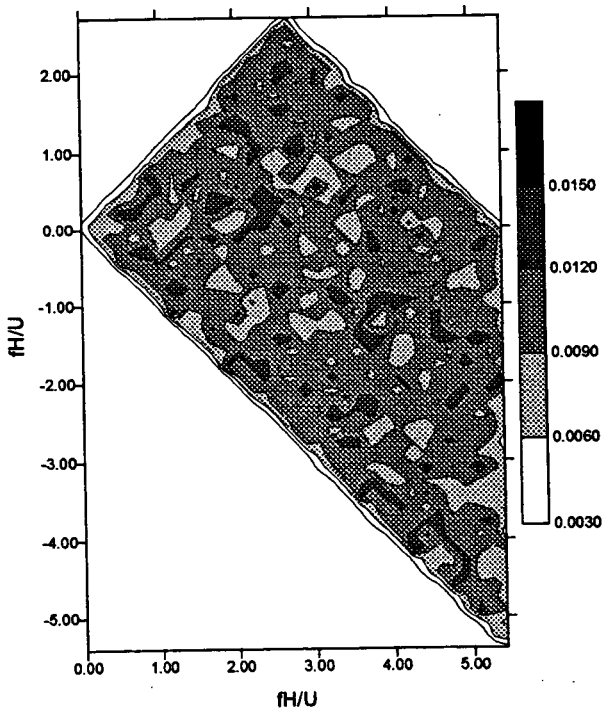


Figure 5: Cross-bicoherence between spectral components of the u- component of the velocity and pressure fluctuations

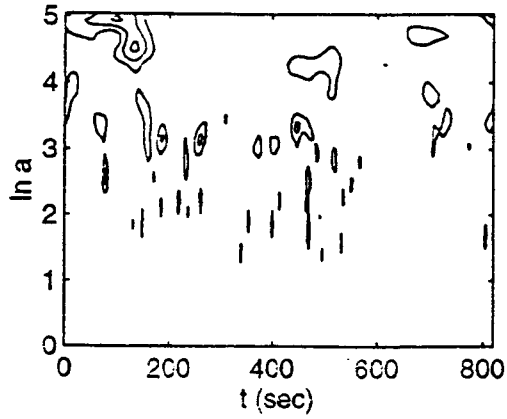


Figure 6-a: Wavelet energy density of the u-component of atmospheric wind (figure 1-a).

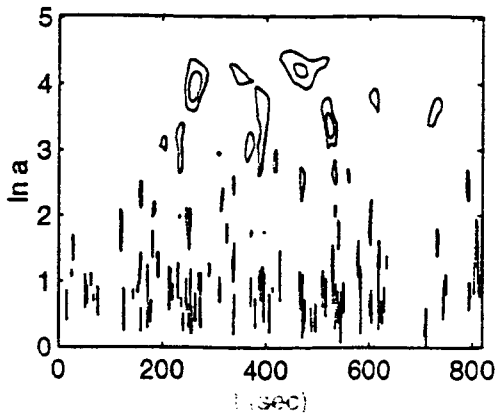


Figure 6-b: Wavelet energy density of the v-component of atmospheric wind (figure 1-b).

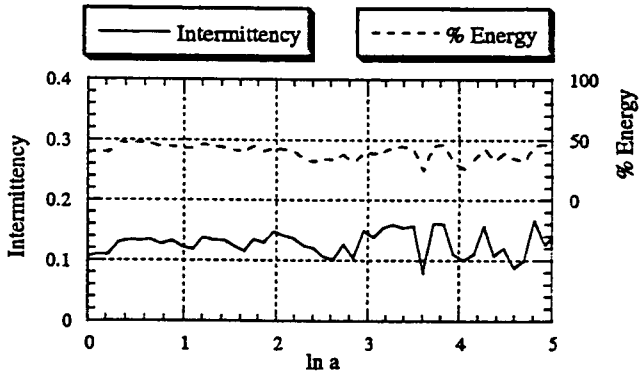


Figure 7-a: Intermittency factor and percent energy content of the u-component of atmospheric wind.

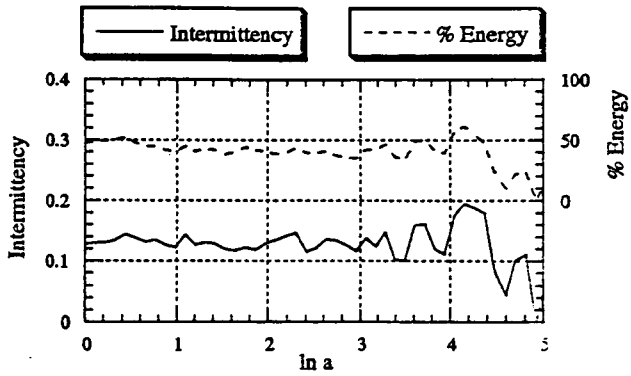


Figure 7-b: Intermittency factor and percent energy content of the v-component of atmospheric wind.

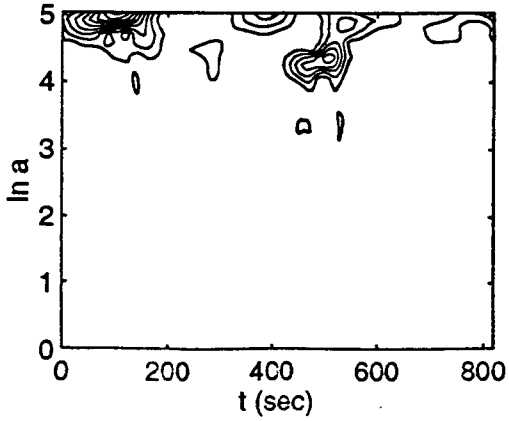


Figure 8-a: Cross scalogram of the wavelet coefficients of the u-component and pressure (figures 1-a and 1-c).

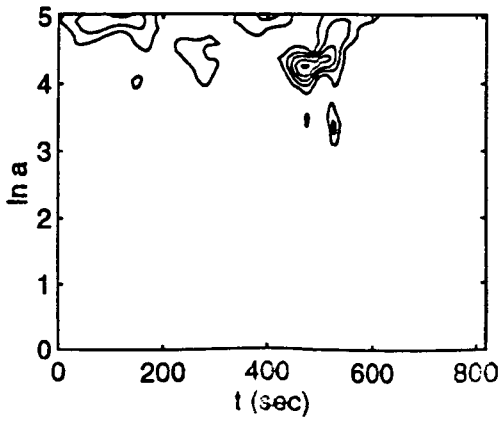


Figure 8-b: Cross scalogram of the wavelet coefficients of the v-component and pressure (figures 1-b and 1-c).

Active Mitigation of Wind-Induced Response-Progress, Issues and Prospects

by

Bogusz Bienkiewicz[1] and Peter M. Young[2]

ABSTRACT

The paper presents a brief overview of recent developments in the area of structural response control, with focus on active mitigation of wind-induced effects. Addressed are outstanding issues of response control and aspects specific to active control of wind-induced vibrations. Discussed are also control strategies, successfully implemented in non-civil engineering applications, which appear to be of tremendous, yet currently underutilized, potential for control of the response of buildings, bridges and other structures. A brief tutorial on optimal and robust response control is presented and application of robust control techniques is illustrated by considering a simple example. Optimal and robust control strategies are considered in analysis and design of an ideal model of a structure and a model subject to unmodeled dynamics and real parametric uncertainty. Reference is made to the existing analysis and simulation tools (Matlab/Simulink/μ-Tools) available to aid in robust controller design and validation. Potential impact of these techniques on the expected performance and reliability of practical active control systems for civil engineering applications is assessed. Finally, an initiation of a collaborative research, focused on application of robust active control for mitigation of wind-induced response is proposed.

KEYWORDS: active control; buildings; bridges; international collaboration; mitigation; μ-synthesis; response control; robust control; wind effects

1. INTRODUCTION

Focus on efficient utilization of land, space, and on more functional infrastructure is expected to sustain, and perhaps accelerate, the design and construction of buildings of increasing height, bridges of longer spans and other large-size structures. Material and labor cost considerations are expected to lead to buildings and structures of lower weight and to construction practices modeled on those developed and optimized in manufacturing industry.

Current designs of many light/flexible buildings and structures are often governed by serviceability considerations due to wind effects. The level of inherent structural damping of such structures is typically low and at times insufficient to bring the wind-induced response within the limits imposed by human comfort considerations. This situation has been recognized in design of tall buildings, long-span bridges and other wind-sensitive structures.

A number of schemes have been developed to mitigate structural response induced by natural phenomena (wind, earthquake, and wave loading) as well as man-generated effects, such as traffic induced vibrations and noise. This lead to emergence of the area of structural control, which has been recently attracting a growing interest worldwide, in the structural engineering community. Effort in this and related disciplines, in U.S., Japan and other countries, resulted in the development of innovative schemes for structural response mitigation. They include passive, semi-active, active and hybrid devices. A growing number of successful applications of passive systems, such as viscoelastic and tuned/liquid dampers, have been reported. Progress in this area

Department of Civil Engineering, Colorado State University, Fort Collins, Colorado, USA, 80523

Department of Electrical Engineering, Colorado State University, Fort Collins, Colorado, USA, 80523

has led to an intensified effort focused on systems incorporating active components and geared towards mitigation of earthquake and wind-induced response of civil engineering structures.

In the paper, we present a brief overview of recent developments in the area of structural control, with focus on active mitigation of wind-induced effects. Addressed are outstanding issues of response control and aspects specific to active control of wind-induced vibrations. Discussed are also control strategies, successfully implemented in non-civil engineering applications, which appear to be of tremendous, yet currently underutilized, potential for control of the response of buildings, bridges and other structures. A brief tutorial on optimal and robust response control is presented and application of robust control techniques is illustrated by considering a simple example. Optimal and robust control strategies are considered in analysis and design of an ideal model of a structure and a model subject to unmodeled dynamics and real parametric uncertainty. Reference is made to the existing analysis and simulation tools (Matlab/Simulink/μ-Tools) available to aid in robust controller design and validation. Potential impact of these techniques on the expected performance and reliability of practical active control systems for civil engineering applications is assessed. Finally, an initiation of a collaborative research, focused on application of robust active control for mitigation of wind-induced response is proposed.

2. RECENT DEVELOPMENTS IN STRUCTURAL CONTROL

It has been recognized that issues associated with response control of civil engineering structures (imprecise modeling, parameter changes due to aging, etc.) and stochastic variability of their loading require development of active control technologies (design/implementation) which may differ from those already established and validated in other disciplines. These issues have been the focal point of presentations and discussions documented in proceedings of meetings devoted to structural control, e.g. Leipholz (1980), Housner and Masri (1990), and Housner et al. (1994a), as well as recent workshops organized by the International Association of Structural Control (IASC), e.g. Joint US-Japan Workshop on Mitigation of Urban Disasters (1996), held in Kyoto, and Second International Workshop on Structural Control (1996), held in Hong Kong. They are also referred to in recent books on structural control, Meirovitch (1990), Soong (1990), and Gawronski (1996).

An increasing level of activities, recently observed in the area of structural control, may be partially due to a growing recognition of successful integration of control systems in other disciplines of engineering, including robotics and manufacturing, automotive and aerospace engineering, as well as computer and aircraft industry. One should also recognize a catalytic role in this area played by IASC (established in 1994) and impact in the U.S. of the National Science Foundation's Research Initiative on Structural Control. A large attendance (337 participants from 15 countries), and the number and scope (235 technical papers in 4 parallel sessions) of presentations during the First World Conference on Structural Control (WCSC), organized by IASC, Housner et al. (1994a), clearly indicate a growing interest of the civil engineering community in the area of structural control. One should also point out an increasing number of sessions on structural control, held during meetings of professional societies in the U.S., such as the ASCE Structures Congresses, e.g. Cheng (1996), as well as meetings in Japan, e.g. Yoshida and Nonami (1994).

The status of recent research and development in active control in the U.S. and Japan was summarized by Housner et al. (1994b) and Kobori (1994), respectively. Further updates on this topic were recently provided by Soong (1996) and Fujino et al. (1996). As pointed out by Housner et al. (1994b), significant progress has been achieved over the past 20 years in the area of active response control, both in the U.S. and Japan. However, the true potential of application of this technology in civil engineering has not

been fully recognized yet, especially in the U.S. Progress has been noted in a number of areas, including: control algorithms and modeling, sensing and actuation, innovative control modes (hybrid and semi-active), implementation issues, and other related disciplines, such as system identification, structural damage detection and health monitoring. This effort has been carried out keeping in mind distinguishing features of civil engineering structural control, listed in Table 1, after Housner et al. (1994b). It follows that most of full-scale implementations of active control technology took place in Japan.

3. PROGRESS IN ACTIVE MITIGATION OF WIND-INDUCED RESPONSE

The status of research and development in the area of systems employing active components to mitigate wind-induced structural response can be assessed from papers presented during WCSC, Housner et al (1994a). We note that, with respect to mitigation of wind-induced response, effort was carried out along two paths: (1) systems designed to counteract wind effects only, and (2) systems capable of mitigating both wind and earthquake-induced response.

The examples of recent work from the first group include: active fin system for a building structure, Mukai et al. (1994), active appendaches for a deck of a long-span bridge, Wilde et al. (1994), counteracting time-dependent torque for a deck of a long-span bridge, Miyata et al. (1994), a boundary layer control method for a tall building, Kubo et al. (1994), tuned liquid dampers for tall buildings, Kareem (1994), tendon control for cable stayed bridges, Kobayashi et al.(1994), use of active vibration control for a bridge tower under erection, Sakai et al. (1994), application of hybrid mass damper system, Tamura et al. (1994), and others. Recent papers from the second group are primarily focused on practical aspects. They include reports on preliminary testing of systems under development and on effectiveness of the installed devices, monitored during strong winds and moderate earthquakes, Ohyama et al. (1994), Nakamura et al. (1994), Yamamoto and Aizawa (1994), Ohrui et al. (1994), Fujita et al. (1994), Petti et al. (1994), and Sakamoto et al. (1994). Current work and references published elsewhere and related to mitigation of wind-induced response, using auxiliary devices with active components, are discussed by Kareem and Tamura (1996), and by Soong (1990).

It follows from the reported studies that a significant progress has been achieved in the development and application of systems, employing active components, and designed to mitigate wind-induced response. Innovative concepts are being tested, while the developed systems have been installed at a number of sites, mostly in Japan. Some of the operational systems have already experienced strong winds (and moderate earthquakes) and they were found to be very effective in attenuating the structural response.

Active control was also employed in Japan to mitigate the response during construction of towers of suspension bridges, and to stabilize cranes during erection of tall buildings, Fujino et al. (1996). The resulting response attenuation lead to significant reduction in construction time and improved working conditions. As a result, application of active control was recommended for other construction sites. According to Fujino et al. (1996), active systems in Japan are currently installed in 20 commercial buildings and they were employed during erection of 14 bridge towers.

4. OUTSTANDING ISSUES OF ACTIVE MITIGATION OF WIND EFFECTS

As we mentioned earlier, critical issues of active mitigation of wind effects on structures and structural control in general, are directly related to the distinguishing features listed in Table 1. Most of the related topics have been addressed in published references and during conference presentations and discussions. In fact a number of workshops on structural control was held in recent years, with ample time allocated for discussion of these problems by working groups. Reports of

these groups are included in workshop proceedings. Herein, we address some of the identified critical issues. Our discussion is largely based on a review paper by Housner et al. (1994b) and on reports of working groups of two workshops, Housner and Masri (1990), and Second International Workshop on Structural Control (1996).

As stated by Housner et al. (1994b), full-scale control installed systems "performed well for the purposes intended". Progress in active control technology for civil engineering structures has been made, but true potential of this approach for mitigation of wind (and earthquake) induced structural response has not been explored yet. Most of the developed systems are not capable of enhancing life safety against large environmental loads. Dominant control design practice is based on linear quadratic regulator formulation, which is not well suited for mitigation of response of civil engineering structures. This approach has been typically coupled with a linear model of a structure, which may be severely violated for the response levels associated with strong winds and earthquakes. Closer attention should be paid to issue of control robustness, in presence of imprecise modeling of structures, limitations of sensors and actuating mechanism, variability of the applied wind and other environmental loading, and effects of inherent noise. Optimal placement of sensors and actuators still remains an open question. New sensor and actuation technologies are desired. There is a need for more realistic model and full-scale experimental effort to assess effectiveness and practical aspects of control systems proposed for civil engineering applications. In addition, implementional issues require further attention. They include: system (software/hardware) integration, redundancy and fail-safe operation, system reliability and maintenance in context of intermittent operation and long dormant periods, system self-identification, diagnostic and corrective action. Strengthening of cross-disciplinary research and development is desired. Further effort should be also devoted to formulation of standardized benchmark problems and establishment of testbeds for experimental validation of control systems for specific civil engineering structures. A more rapid exchange of technical information and a closer cross-disciplinary and international collaboration are desired.

The above items have been originally identified in context of development and application of control systems for mitigation of structural response caused by earthquakes. However, most of these issues are equally relevant to systems designed primarily for mitigation of wind-induced structural response. The dominant difference between the two groups is the magnitude of the loading/response associated with severe wind/earthquake events and, in most cases, a relatively long prearrival time and duration of strong wind events.

We conclude that one of the most critical issues of active control for mitigation of wind-induced effects is imprecise modeling of a system (structure, sensors, actuators, presence of noise) and variability in wind loading. As we discuss this later, methods of optimal and robust control, advanced to address related problems in other disciplines, appear to be well suited to address this issue. They have been proven to be very effective in accounting for uncertainties in design of control systems in aerospace and aircraft industry. Application of this methodology has been also reported in civil engineering applications. However, it appears that the full potential of this approach has not been yet explored in structural control, including design of systems to mitigate wind-induced response. In this context, a brief tutorial on robust and optimal control is presented in the next section.

5. OPTIMAL AND ROBUST CONTROL

5.1 Introduction

The basic premise for optimal control design is to rearrange the problem into a canonical form, with a known plant model subject to unknown disturbances, and then to pose the controller design as an optimization problem for the

unknown controller subject to desired closed-loop performance objectives. Note that this assumes that one has an accurate model of the plant to be controlled, although it may be subject to disturbance signals which are not well known.

The situation is illustrated in Figure 1. Here the exogenous disturbances to the generalized plant P are collected together in the (vector) signal w, and the signals to be controlled are in z. A feedback controller K takes measurements y from the system sensors and generates control signals u which are used to drive actuators. The disturbance signal w represents uncontrolled variables which are unknown a-priori, such as wind loading and/or sensor noise. The variable z represents signals we wish to keep small, such as structural response (displacement/acceleration) and/or weighted control effort. Note that in this setting P represents a model of the structure (e.g. building, bridge, tower, etc.) , i.e. physical system, together with models of the sensors and actuators. Any desired weighting functions may be included in P. Hence the term *generalized* plant. In this context each control problem is rearranged to a disturbance rejection problem where we wish to design controller K to minimize the (closed-loop) gain from w to z, see Figure 1.

5.2 H_2 Optimal Control

Note that different optimal control problems can now be considered by specifying exactly what one means by "the closed-loop gain from w to z". If we denote T_{zw} as the system (transfer) from w to z in Figure 1, then we need some measure of the "size" of T_{zw}. This is provided in a precise mathematical sense by the notion of a norm. The classical H_2 optimal control problem measures the gain from w to z via the H_2 norm of the closed-loop system, which is given as

$$\| T_{zw} \|_2 \triangleq \sqrt{\frac{1}{2\pi}\int_{-\infty}^{\infty} Tr[T_{zw}^*(j\omega) T_{zw}(j\omega)]\, d\omega}$$

where $T_{zw}(j\omega)$ = the (complex) transfer matrix of the system, and $(\,)^*$ denotes complex conjugate. One can give this mathematical description some physical meaning, by a number of equivalent definitions: H_2 optimal control minimizes the power of the output signal z, assuming the disturbance signal w is zero-mean white noise. Thus H_2 optimal control assumes that the disturbance signals are a-priori known stochastic signals , see Zhou (1996) or Anderson and Moore (1990) for an in-depth treatment of H_2 optimal control. Note that the assumption of uncolored noise is not restrictive, since one may easily weight these signals, and absorb the weights into P, to better represent energy (power spectrum) of disturbance (e.g. wind loading). There are also equivalent characterizations of the problem in terms of impulse disturbance signals and non-zero initial conditions. In addition, there are a number of equivalent formulations for this control problem. For instance the Linear Quadratic Gaussian (LQG) problem is posed in terms of a penalty function involving the integral of a weighted quadratic combination of the outputs (structural response, accelerations) and control signals (due to actuators), but this procedure is readily shown to be equivalent to the above.

The solution to the H_2 optimal control problem satisfies a well-known separation structure, in that the optimal control for the above output feedback problem is composed of two parts. (This is also referred to as the certainty equivalence principle, see Zhou (1996) for detail.) One may first solve the corresponding Linear Quadratic Regulator (LQR) or state feedback problem, which assumes that all the states of the system can be measured. This solution is referred to as the optimal state feedback *gain*, since it involves no dynamics. One may then solve an estimation problem to optimally estimate the system state from the outputs. This requires a dynamic estimator referred to as a Kalman filter. The composition of these two stages generates the optimal H_2 or LQG output feedback controller.

Note that each of these two stages requires one to generate and solve the appropriate Riccati equation, so that the overall H_2 problem requires

the solution of two Riccati equations. This can be accomplished invoking commands of readily available software, such as Matlab. There are standard Matlab toolbox commands to do this. For instance the Control toolbox includes the commands *lqr* (solves the LQR problem for the optimal state feedback gain), *lqe* (solves the Kalman filter problem), and *reg* (combines the state feedback gain and Kalman filter to provide a controller solving the LQG problem). The μ-Tools toolbox includes the command *h2syn* which combines these stages into one command solving the H_2 output feedback problem directly as posed in Figure 1.

This design procedure is capable of producing high performance controllers (optimal in the above sense) for *known plants*. However, it is important to note that this procedure does not include any robustness requirements, since it is based on the setup in Figure 1, which does not include any unmodeled dynamics. Indeed for H_2 optimal control even the disturbance signals are in some sense assumed to be known (with characterizations either as white noise, or an impulse signal, or a non-zero initial condition). However, one might hope that the resulting controller has some desirable robustness properties, and in fact this turns out to be true for the optimal LQR controller. (This design can be guaranteed a-priori to have a gain margin of at least 6dB, and a phase margin of at least 60 degrees.) These results generated a good deal of excitement when they first appeared, since they seemed to indicate the inherent robustness of H_2 optimal control. Note, however, that the LQR problem requires that all the states are available for feedback, which is not usually the case in practice. One might further hope that these results carry over to the more practical output feedback or LQG case, where the states are estimated from the measured outputs. Unfortunately it turns out that this is not the case. It is shown in Doyle (1978) that the above robustness properties disappear for the output feedback case, and in fact H_2 optimal control designs provide no a-priori robustness guarantees whatsoever.

5.3 H_∞ Optimal Control

An alternative to H_2 optimal control is provided by H_∞ optimal control. This control philosophy is based on the exact same setup as before (see Figure 1), but with a different choice of norm, namely the H_∞ norm

$$\|T_{zw}\|_\infty \doteq \sup_\omega \bar{\sigma}[T_{zw}(j\omega)]$$

where $\bar{\sigma}$ denotes the largest singular value. Note that mathematically the H_∞ norm is simply defined as the peak value of the frequency response of the system. It turns out that this is equivalent to minimizing the energy of the output signal z, assuming that the disturbance signal w can be any signal of no more than unit energy. Thus the disturbance signals are not assumed known a-priori, but rather can take worst-case values from this allowed set. The interpretation of the H_∞ norm as the maximum energy-to-energy gain of the system is very appealing (and it provides many interesting connections to minimax and game-theoretic problems).

The H_∞ optimal control problem turns out to be more mathematically involved than the H_2 problem, and the solution was recently obtained in Doyle et al. (1989). Once again it requires solving two Riccati equations, although their solution is not so (numerically) straightforward as in the H_2 case. There is also a form of the separation principle for the solution, but it is more subtle than in the H_2 case. Once again powerful Matlab based tools exist for H_∞ optimal control design, and the μ-Tools toolbox command *hinfsyn* solves the output feedback H_∞ optimal control problem.

Note that for H_∞ optimal control the disturbance signals are unknown a-priori and may take worst-case values. Thus the controller is in some sense playing a game. It seeks to minimize the energy of the output signal z via the control signal u. At the same time Nature takes the role of the opposing player and attempts to maximize the energy of the output signal z via the disturbance signal w. This interpretation has led people to

believe that H_∞ optimal control is a robust design procedure. However, it is important to note that, although the disturbance signals are unknown, the plant is completely known in this formulation. Once again the design process does not account for unmodeled dynamics at all, and so in fact H_∞ optimal control is not a robust controller design procedure. Indeed there is nothing to show that an H_∞ optimal control design will be any more robust than an H_2 optimal control design. However, the inclusion of worst-case disturbances can be used to combine H_∞ optimal controller design with other techniques, so as to yield a design process for robust controllers, and this is outlined in the next section.

5.4 Robust Control - μ Synthesis and *D-K* Iteration

The optimal control techniques described in the preceding sections were developed to provide high performance controllers for systems where a high fidelity mathematical model is available. In particular, they have been used extensively in the aerospace industry. In many situations, and in particular for civil engineering structures, such high fidelity models are not available. In this case it may happen that a control design (possibly an optimal one) performs well in simulation on the available nominal model of the system, and performs poorly (may not even be stable) when implemented on the real physical system. The problem arises from the fact that the model is not sufficiently accurate in some aspect, and the high performance controller design is attempting to exploit knowledge of the system that is incorrect! The theory of robust control attempts to take into account these inherent inaccuracies in the model, and to provide systematic analysis and design techniques in the face of this "uncertainty."

In order to deal with this phenomenon we consider the canonical framework illustrated in Figure 2. Once again it is easy to rearrange many problems into this framework and we will present a simple example to illustrate the approach. Note that now the system is augmented with a perturbation or uncertainty block Δ. This uncertainty block captures any knowledge we have about the size and placement of model perturbations entering the system. Note, however, that we will not assume specific knowledge about the dynamics of Δ, but merely bounds of the size of its components. It is important to note that the inclusion of model perturbations or unmodeled dynamics in our analysis and design framework is a significant departure from merely allowing unknown disturbances. The effects of unmodeled dynamics on a system cannot be captured as simply another form of disturbance signal. For instance, while disturbance signals can degrade the performance of a nominally closed-loop stable system, they can never destabilize it. On the other hand model perturbations can not only degrade performance, but they can even drive the closed-loop system unstable.

Once again we need a characterization of size for the blocks of Δ, and it turns out that a convenient one is the H_∞ norm. Since this norm captures the maximum energy-to-energy gain of a system, it can capture the maximum signal amplification that a perturbation can inject into a system. One can use this information to develop analysis tools for the following questions:

Robust Stability: How large a perturbation can the system tolerate and still maintain closed-loop stability?

Robust Performance: How large a perturbation can the system tolerate and still maintain the desired closed-loop performance level? Here performance is measured via $\|\tilde{T}_{zw}\|_\infty$, where $\tilde{T}_{zw}$ is the *perturbed* closed-loop map from w to z.

The answers to these questions require some fairly involved mathematics, and the required computation is referred to as μ-analysis (also structured singular value analysis). A survey of these techniques is provided in Packard and Doyle (1993) for unmodeled dynamics and Young (1993) for parametric uncertainty. It turns out that μ is not amenable to exact computation, but there are readily computable upper and lower bounds, which usually provide an approximation sufficient

for engineering purposes. Once again the practitioner need not be familiar with the details of the solution and the Matlab μ-Tools toolbox command *mu* readily facilitates robust stability and performance analysis.

Once μ-analysis methods were established, it became natural to consider the μ-synthesis question, namely that of designing a controller K so as to optimize robust performance. Note that this amounts to an H_∞ optimal control problem, but now for the perturbed closed loop map $\tilde{T}_{zw}$. In this setting both the disturbance signal w and the model perturbation Δ are unknowns which may assume worst-case values. Mathematically speaking the μ-synthesis problem is much harder than H_2 or H_∞ optimal control, both of which are convex optimization problems for which the global optimum is readily found. The μ-synthesis problem is not convex, and we are forced to resort to approximate methods. A commonly used approach is the *D-K* iteration procedure. This process first approximates μ with its upper bound, which takes the form of an H_∞ norm, scaled by a certain *D*-operator. The synthesis problem thus becomes a scaled H_∞ optimal control problem and the *D-K* iteration attempts to solve this by alternately computing the D scaling from μ-analysis and the controller K from an H_∞ optimal control problem. The procedure is detailed in Stein and Doyle (1991). This iteration is implemented in the μ-Tools command *dkit*, which can be run in batch mode, or allow the user to interactively specify the iteration parameters.

It should be noted that this design process is not as straightforward as H_2 or H_∞ optimal control. Although software is available to implement the mechanics of the method, there are certain subtleties to the procedure, and typically the user must have some familiarity with these to produce an acceptable design. However, the payoff for this is a true robust controller, with a certain level of guaranteed robust performance. This means that the controller will guarantee closed-loop stability, and it will keep the energy of the output signal z below a specified level, despite any disturbance signal w, and any unmodeled dynamics Δ (both of the appropriate size). This guaranteed insensitivity of the design (in both stability and performance) to both disturbance signals and modeling errors is crucial to being able to provide high performance designs in a practical setting. The goal is to provide a controller which works well, not only in simulation, but also on the actual system, despite fairly crude models for the system (and unknown disturbance signals).

5.5 Illustrative Examples

In this section we offer some examples of applying the above techniques to structural control problems. A simple tutorial problem is considered first. Next we review two more realistic examples from the literature.

5.5.1 Tutorial Problem

In this section we consider a simple vibration suppression problem. We assume a one-mode representation of wind-induced vibrations of a slender structure (e.g. tall building, bridge tower, etc.). Let us suppose that the fundamental natural frequency of the structure is equal to 0.2 Hz and that its (viscous) damping ratio is 2%. It is further assumed that the considered mode of vibrations is linear and that the structure can be represented by a rigid body elastically supported at its base. Moreover, we assume that acceleration at the rooftop and a torque actuator (at the structure base) are available for feedback control. In order to keep the example as simple as possible, no dynamics are assumed for the sensor and actuator, although the measurement signal (acceleration) is subject to additive white noise. The wind-induced overturning moment is represented by white noise. A block diagram for this setup is shown in Figure 3. Of course this setup is very simple, and does not capture all the features required for a realistic design (e.g., computation delay, complex dynamics), but it will serve here to illustrate the application of optimal and robust control techniques.

In order to apply optimal control we first need to state our design criterion in the framework of

Figure 1. The Simulink model in Figure 4 shows our design model, with assumed numerical values and weighting and penalty functions. The generalized plant P can be extracted from this via the Simulink command *linmod*. Note that this plant includes weighting functions on the disturbance signals, and penalty functions for the outputs we wish to control. Again a fairly simple set of the (weighting/penalty) functions were selected. The same setup was used for both the H_2 and H_∞ optimal control designs. In practice one would probably choose different weights for each case, but we used the same weights for ease of comparison. We designed an H_2 and H_∞ optimal controller for this problem setup using the Matlab commands outlined earlier. Both controllers were of 4th order and stable, and they both stabilized the nominal closed-loop system, as was verified by eigenvalue analysis.

Robust controller design via μ-synthesis requires developing a design model in the framework illustrated in Figure 2, where an uncertainty structure is now included. The Simulink model in Figure 5 represents our design model. Note that again, for ease of comparison, we have selected the exact same weighting/penalty functions to specify the desired performance. However the design model now also includes a robustness requirement via the weighted uncertainty structure. This model was used to implement a μ-synthesis design via D-K iteration, as described earlier. The resulting controller was of 6th order and stable, and it stabilized the nominal closed-loop system.

The Simulink simulation model in Figure 6 was run for the open and closed loop configurations. Note the presence of "On/Off" blocks, which are set to 1/0 as required to switch in/out certain components: the controller (Feedback Compensator) and the perturbation block (High Frequency Unmodeled Dynamics). Note also that scaling blocks are included to convert the normalized units of the model into physical units for a considered hypothetical large structure.

The results for the case with the perturbation block turned-off are shown in Figures 7 through 10. They include an open-loop run, Figure 7, and three closed-loop simulations. Two of the closed-loop cases resulted from invoking H_2 and H_∞ controllers, Figures 8 and 9. The third case, Figure 10, corresponded to the robust (μ-synthesis) design. The resulting 2-norms of each signal are collected in Table 2 (the 2-norm corresponds to the energy of the signal). It is seen that the H_2 and H_∞ optimal controllers achieve high levels of performance for the nominal closed-loop system, with the H_∞ controller being slightly more aggressive in terms of control effort, and consequently achieving slightly higher performance. The μ-synthesis controller is less aggressive than the optimal control designs, and it achieves a lower level of performance for the nominal system, though it is still fairly high.

In order to illustrate the robustness properties of these controllers, a perturbed system was considered. (The μ-analysis techniques were used to determine a suitable problem perturbation.) The frequency response plots for the open-loop plant and the plant perturbation are shown in Figure 11. Note that the perturbation is much smaller than the original plant (H_∞ norm of plant is 25, versus 1.43 for the perturbation), and its effect is only significant at high frequency. The perturbation is of 4th order and it is stable.

The performance of the perturbed plant was simulated using the Simulink model in Figure 6, with the perturbation block (High Frequency Unmodeled Dynamics) switched on. The results for open-loop, and all three controllers, are contained in Figures 12-15, and the signal energies are tabulated in Table 3. It can be seen from the open-loop response, Figure 12, that the plant response contains now more energy at high frequency. The effect of this on the H_2 and H_∞ optimal controllers is devastating, as shown in Figures 13 and 14. It can be seen that the H_2 controller is barely stable, Figure 13, and is not able to deliver any performance (actually it is worse than open-loop), and the H_∞ controller is unstable for the perturbed closed-loop system,

Figure 14. In contrast, the μ-synthesis controller maintains stability, and is still able to deliver a reasonable level of performance, Figure 15 and Table 3.

The above example illustrates some of the methodologies of optimal and robust control design and the performance/stability properties of the resulting control systems. However, one should bear in mind that it is only a simple tutorial example and one should refrain from generalizing conclusions from this example to real, more complex systems. In the next section we briefly discuss (with references) two examples where the ideas of optimal and robust control have been applied in a practical setting.

5.5.2 Application Examples

The control of a large flexible structure, the Langley NASA Minimast was considered by Balas and Young (1995). It is a 18-bay truss structure equipped with accelerometers, displacement sensors, and torque wheel actuators. Feedback control can be implemented via a data-acquisition and control setup capable of operating at a sample rate of 80 Hz. A 28-mode model of the structure is available for analysis and simulation. The authors developed robust controllers for this structure based on a simplified 5-mode model, with deliberately introduced inaccuracies in the damping ratios and natural frequencies of these modes. No information about the higher-order modes was included in this representation. Despite the crude design model, the authors were able to use μ-synthesis to design controllers which used only a reduced set of the accelerometer measurements, no displacement measurements, and yet delivered very high performance levels. These designs were then verified, both in simulation, and experimentally on the structure. In contrast, H_∞ control designs for this model proved unstable on the more accurate model, and consequently were not experimentally implemented for the actual structure.

An example of application of μ-synthesis techniques to a civil engineering structure, a model of a three -story metal frame, Spencer et al (1997), may be found in Young and Bienkiewicz (1997). Here these techniques are applied to a benchmark problem in earthquake engineering. They were combined with a model reduction to yield a low-order robust controller for a fairly complex problem. In this case the experimental data is not currently available, but the resulting 4th order controller performs well in simulation, and satisfies the appropriate robustness analysis tests.

6. PROSPECTS

Recent developments in structural control and successful implementations of control systems for mitigation of response of civil engineering structures suggest wider application of this technology in the near future. From perspective of wind engineering, especially encouraging and valuable are reports on performance of installed (active/hybrid) systems. As mentioned before, many designs of tall/long-span structures are governed by serviceability (occupant comfort) criteria. It appears that improvement in comfort of occupants of buildings and other wind-sensitive structures will remain for the near future the primary function of active systems designed to mitigate wind effects. Experience gained from technology developed for this purpose will be very useful in the design of the next generation of control systems, namely those targeting limit state/safety issues related to extreme winds and other natural and man-made phenomena.

Application of active control technology continues to receive a high level of attention in the earthquake engineering community. Actually, experience with control systems to mitigate earthquake effects has been applied in design of active devices to suppress wind-induced structural response. We anticipate that, as interest in response control among wind engineers increases, stronger ties will be established between earthquake and wind engineering researchers and practitioners involved in structural control. This may lead to an accelerated progress in structural control technology, with benefits to both groups. One of immediate steps in this direction could

involve benchmark problems.

Wide response to a call for papers addressing two benchmark problems, Spencer et al. (1997), for active mitigation of earthquake effects is very encouraging. The issue of benchmark problems for structural control has been also identified by working groups of a recent workshop, Second International Workshop on Structural Control (1996). Two types of problems could be considered for control systems to mitigate wind effects: (1) Problems involving structural models selected also for studies of control of response due to earthquakes, and (2) Problems identified for testing structural control designs for wind effects. The second group might involve computer simulations coupled with wind tunnel studies of models of varied degree of fidelity. This leads to an issue of establishment of testbed facilities for laboratory (wind-tunnel) as well as full-scale testing.

The concept of testbed facility developed for the NASA Minimast facility might be used as a "blue print" for a full-scale testbed facility for active mitigation of wind effects. In fact, perhaps it would be possible to initially designate (on a temporary/trial basis) one of the exiting full-scale structural control research facilities, as a possible full-scale testbed site. Practical aspects and organizational issues could be identified and prioritized through a feasibility study and possibly a workshop initiated /organized by this panel and involving interested groups and individuals.

Implementation of the idea of testbed facilities, both for laboratory as well as field testing, is one of issues which are well suited for international collaboration. In particular, combination of practical experience resulting from development and operation of the installed control systems, expertise and perspective offered by wind engineering researchers and practitioners, and involvement of experts from control community in US, Japan, and possibly other countries, seems to be of great potential. The resulting synergy is expected to lead to major breakthroughs in a number of areas, including those identified earlier as critical issues.

Application and adaptation of techniques of robust control appear to offer unique opportunity for improving reliability, robustness, and performance of practical control systems for mitigation of wind effects on buildings and structures. The proposed activities might focus on control devices permanently integrated with a given structural system as well as temporary mechanisms, e.g. installed/used during construction, tentative retrofit, and under other circumstances.

7. CONCLUDING REMARKS

The outlook for wider application of control systems employing active components to mitigate wind-induced effects appears encouraging. Despite impressive progress in this area, more effort is needed to address a number of issues. Experience with practical and installed systems (in Japan) is very valuable. It seems clear that modern techniques and tools of robust optimal control have tremendous potential for the complex problems that arise in practice, in particular for civil engineering structures. Work is needed to evaluate which strategies perform best for a given class of structures and how to implement them in the most optimal manner.

It has been recognized that cross-disciplinary and international collaboration is the prerequisite for an accelerated progress in the area of structural control. It is proposed that the UJNR Panel on Wind and Seismic Effects considers research and development activities addressing systems with active control components to mitigate wind-induced response as one of high-priority topics.

Focus on devices targeting serviceability issues due to moderate winds seems to be timely and relevant. This case is very important, since such conditions occur quite frequently. An uncomfortable environment (e.g., in an office/hotel/residential skyscraper or other wind-sensitive structure) can adversely affect occupants and work productivity, and it may ultimately result in disruption in business cycle, and possible

financial losses.

8. ACKNOWLEDGMENTS

Work presented in the paper has been partially supported by Colorado State University, through a Research Initiation Grant and by Federal Highway Administration, through a contract managed by Engineering Incorporated.

9. REFERENCES

Anderson, B. D. O. and More, J. B. (1990) Optimal Control: Linear Quadratic Methods, Prentice Hall, New Jersey.

Balas, G. J. and Young, P. M. (1995) " Control Design for Variations in Structural Natural Frequencies,"" AIAA Journal of Guidance, Dynamics and Control, Vol. 18, pp. 325-332.

Cheng, F.Y. (Ed.) (1996) Analysis and Computation, Proc. of the twelfth Conference held in conjunction with ASCE Structures Congress XIV, Chicago, Ill, April 15-18, 1996, 522 pp.

Doyle, J. C. (1978) "Guaranteed Margins for LQG Regulators Control Problems," IEEE Transactions on Automatic Control, Vol. 23, pp. 756-757.

Doyle, J. C., Glover, K., Khargonekar, P, and Francis, B. A. (1989) "State Space Solutions to H_2 and H_∞ Control Problems," IEEE Transactions on Automatic Control, Vol. 34, pp. 831-847.

Fujino, Y., Song, T. T. and Spencer, B.F., Jr., (1996), "Structural Control: Basic Concepts and Applications," in Ghosh, S. K. and Mohammadi, J. (Eds.), Building and International Community of Structural Engineers, Proc. of ASCE Structures Congress XIV, Chicago, Ill, April 15-18, 1996, pp. 1277-1287, Vol. 2.

Fujita, T., Kamada, T., Teramoto, T., Kitamura, H., Suizu, Y., Masaki, N., Kanno, T., and Kawachi, H. (1994a), "Application of Hybrid Mass Damper Using Hydraulic Actuator and Multistage Rubber Bearing to High-Rise Building," in Housner G. W. et al. (1994), Vol. 3, FA4-53--FA4-62.

Fujita, T., Shimazaki, M., Tanaka, K., Ohyama, H., Nakamura, Y., Murakoshi, K., Hora, H., and Miyano, H. (1994b), "Development of Hybrid Mass Damper with Convertible Active and Passive Modes Using AC-Servomotors for Vibration Control of Tall Buildings," in Housner G. W. et al. (1994), Vol. 3, FA4-63--FA4-72.

Gawronski, W., (1996), Balanced Control of Flexible Structures, Springer-Verlag, 262 pp.

Housner, G. W. and Masri, S. F. (Eds.) (1990), Proceedings of the U.S. National Workshop on Structural Control Research, University of Southern California, October 25-26, 1990, USC Publication No. CE-9013, pp. 251.

Housner, G.W., Masri, S. F. and Chassiakos, A.G. (Eds.) (1994a), Proc. of the First World Conference on Structural Control, Pasadena, CA, August 3-5.

Housner, H. W., Soong, T. T. and Masri, S. F. (1994b), "Second Generation of Active Structural Control in Civil Engineering," Proc. of the First World Conf. on Struc. Control, 1994, Pasadena, CA, August 3-5, pp. Panel 3-18, Vol. 1.

"Joint US-Japan Workshop on Mitigation of Urban Disasters: Cooperative Research on Structural Control", Kyoto, Japan, March 14-15, 1996, Internet Proceedings, IASC Homepage, March 1997. 11 pp.

Kareem, A. (1994), "The Next Generation of Tunned Liquid Dampers," in Housner G. W. et al. (1994a), Vol. 3, pp. FP5-19--FP5-28.

Kareem, A. and Tamura, Y. (1996), "Mitigation of Wind-Induced Motions of Tall Buildings," Tall Building Structures - A World View, Proc. of 67th Regional Conference, in conjunction with ASCE Structures Congress XIV, Chicago, Ill, April 15-18, 1996, pp. 413-423.

Kobayashi, H., Hosomi, M., and Koba, K. (1994), "Tendon Control for Cable Stayed Bridge Vibration," in Housner G. W. et al. (1994a), Vol. 3, pp. FA1-23--FA1-29.

Kobori, T. (1994), "Future Direction on Research and Development of Seismic-Response-Controlled Structure," in Housner, G. W. et al. (1994a), Vol. 1, pp. Panel 19-31.

Kubo, Y., Hayashida, K., Kotsubo, C., and Kato, K. (1994a), "On the Suppression of Aerodynamic Vibrations of a Square Prism in High Angle of Attack by Boundary-Layer Control Method," in Housner, G. W. et al. (1994), Vol. 2, pp. TP1-13--TP1-20.

Leipholz, H. H. E. (Ed.) (1980), Structural Control, Proc. of the International IUTAM Symposium on Structural Control, University of Waterloo, Ontario, Canada, June 4-7, 1979, North-Holland Publishing Company, 810 pp.

Meirovitch, L. (1990) Dynamics and Control of Structures, John Wiley & Sons, Inc., 425 pp.

Miyata, T., Yamada, H., Dung, N. N., and Kazama, K. (1994a), "On Active Control and Structural Response Control of the Coupled Flutter Problem for Long Span Bridges," in Housner G. W. et al. (1994), Vol. 1, pp. WA4-40--WA4-49.

Mukai, Y., Tachibana, E., and Inoue, Y., (1994), "Experimental Study of Active Fin System for Wind-Induced Structural Vibrations", in Housner G. W. et al. (1994a), Vol. 1, pp. WP2-52--WP2-61.

Nakamura, Y., Tanaka, K., Ishii, M., Hirasawa, M., Nakayama, M., Ohyama, H., and Fujita, T. (1994), "Fault Diagnosis Method Using Energy Absorbing Performance for Hybrid Mass Damper for Vibration Control of Tall Buildings," in Housner G. W. et al. (1994a), Vol. 3, pp. FA2-33--FA2-42.

Ohrui, S., Kobori, T., Sakamoto, M., Koshika, N., Nishimura, I., Sasaki, K., Kondo, A., and Fukushima, I. (1994), "Development of Active-Passive Composite Tunned Mass Damper and Application to the High Rise Building," in Housner G. W. et al. (1994a), Vol. 2, pp. TP1-100--TP1-109.

Ohyama, H., Tanaka, K., Arai, N., Ishiguro, Y., Ishii, M., Murakoshi, K., Nakamura, Y., Miyano, H., Hora, H., Fujita, T. (1994), "Practical Application of Hybrid Mass Damper Using AC-Servomotor for Vibration Control of a Slender Tall Building," in Housner G. W. et al. (1994a), Vol. 1, pp. WP2-62--WP2-71.

Packard, A. K., and Doyle, J. C. (1993) "The Complex Structured Singular Value," Automatica, Vol. 29, pp. 71-109.

Petti, L., Soong, T. T., and Palazzo, B. (1994), "Hybrid Mass Dampers for Structural Control Against Wind and Earthquakes," in Housner G. W. et al. (1994a), Vol. 2, pp. TP1-110--TP1-118.

Sakai, F., Tamaki, T., Nishi, Y., Murai, K., and Katagaya, H. (1994), "Active Vibration Control of Bridge Tower under Erection," in Housner G. W. et al. (1994a), Vol. 2, pp. TP4-23--TP-432.

Sakamoto, M., Kobori, T., Yamada, T., and Takahashi, M. (1994), "Practical Applications of Active and Hybrid Response Control Systems and their Verifications by Earthquake and Strong Wind Observations," in Housner G. W. et al. (1994a), Vol. 1, WP2-90--WP2-99.

"Second International Workshop on Structural Control", Hong Kong, December 18-21, 1996, Internet Proceedings, IASC Homepage, March 1997, 40 pp.

Soong, T. T. (1996), "Basic Concepts and Applications of Structural Control," in Lin, Y. K. and Su, T.C. (Eds.), Proc. of the 11th Engineering Specialty Mechanics Conference, pp. 16-29, Vol. 1.

Soong, T. T. (1990), Active Structural Control, Longman Scientific & Technical, 194 pp.

Spencer Jr., B. F., Dyke, S. J., and Deoskar, H. S. (1997) "Benchmark Problems in Structural Control - Part I: Active Mass Driver, Proc. of the 1997 Structures Congress, Portland, Oregon.

Stein, G., and Doyle, J. C. (1991) "Beyond Singular Values and Loop Shapes," Journal of Guidance, Control and Dynamics, Vol. 14, No. 1, pp. 5-16.

Tamura, K. , Shiba, K., Inada, Y., and Wada, A. (1994), "Control Gain Scheduling of a Hybrid Mass Damper System against Wind Response of a Tall Building," in Housner G. W. et al. (1994a), Vol. 3, pp. FA2-13--FA2-22.

Yamamoto, M. and Aizawa, S. (1994), "Control Effects of Active Mass Damper System Installed on Actual Buildings," in Housner G. W. et al. (1994a), Vol. 3, pp. FP1-13--FP1-22.

Yoshida, K. and Nonami, K. (Eds.) (1994), Proceedings the Second International Conference on Motion and Vibration Control, Movic, Yokohama, Japan, August 30 - September 3, 1994.

Young, P. M. (1993) "Robustness with Parametric and Dynamic Uncertainty," Ph.D. Thesis, California Institute of Technology.

Young, P. M. and Bienkiewicz, B. (1997) "Robust Controller Design for the Active Mass Driver Benchmark Problem," submitted to special issue of Earthquake Engineering and Structural Dynamics.

Wilde, K., Masukawa, J., Fujino, Y., and Bhartia, B. (1994), "Active Control of Flutter Instability of Bridge Deck," in Housner G. W. et al. (1994a), Vol. 1, pp. WA4-50--WA4-59.

Zhou, K.(1996) Robust and Optimal Control, Prentice Hall, 596 pp.

Table 1. Some Distinguishing Features of Structural Control of Civil Engineering Structures, Housner et al. (1994a)

	FEATURES
STRUCTURE	* Complex system with few critical modes * Exhibit nonlinear behavior
SENSING & ACTUATION	* Few sensors & actuators * Limited response variables for sensing * Large control forces with high speed
CONTROL OBJECTIVES	* Reduction of selected maximum response * Imprecision in control objectives
CONTROL STRATEGIES	* Simple but robust and fault tolerant control * Suboptimal control * Implementable control laws

Table 2. Signal Energies for Unperturbed Response

Unperturbed Response	$\frac{\|u\|_2}{\|w\|_2}$ ($\frac{\text{Control Effort Energy}}{\text{Disturbance Energy}}$)	$\frac{\|z\|_2}{\|w\|_2}$ ($\frac{\text{Output Acceleration Energy}}{\text{Disturbance Energy}}$)
Open-Loop	0	1.564×10^{-12}
$\mathcal{H}_2$	0.631	7.34×10^{-13}
$\mathcal{H}_\infty$	0.646	7.08×10^{-13}
μ-Synthesis	0.480	9.92×10^{-13}

Table 3. Signal Energies for Perturbed Response

Perturbed Response	$\frac{\|u\|_2}{\|w\|_2}$ ($\frac{\text{Control Effort Energy}}{\text{Disturbance Energy}}$)	$\frac{\|z\|_2}{\|w\|_2}$ ($\frac{\text{Output Acceleration Energy}}{\text{Disturbance Energy}}$)
Open-Loop	0	1.41×10^{-12}
$\mathcal{H}_2$	2.79	2.02×10^{-12}
$\mathcal{H}_\infty$	14.1	9.02×10^{-12}
μ-Synthesis	0.545	1.18×10^{-12}

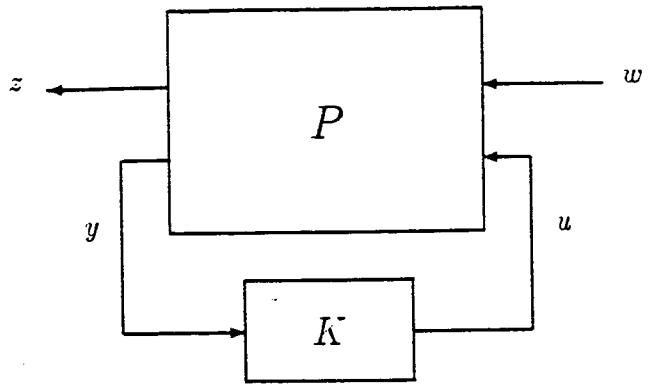


Figure 1. Canonical Form for Optimal Control

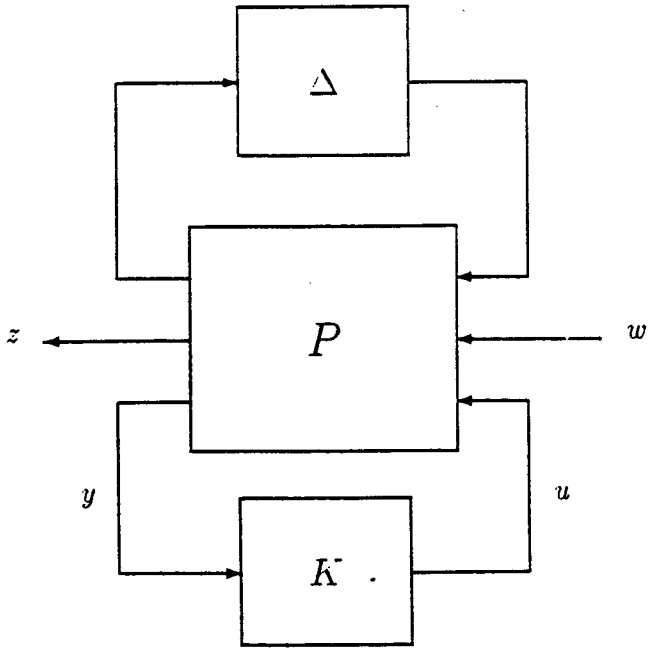


Figure 2. Canonical Form for Robust Control

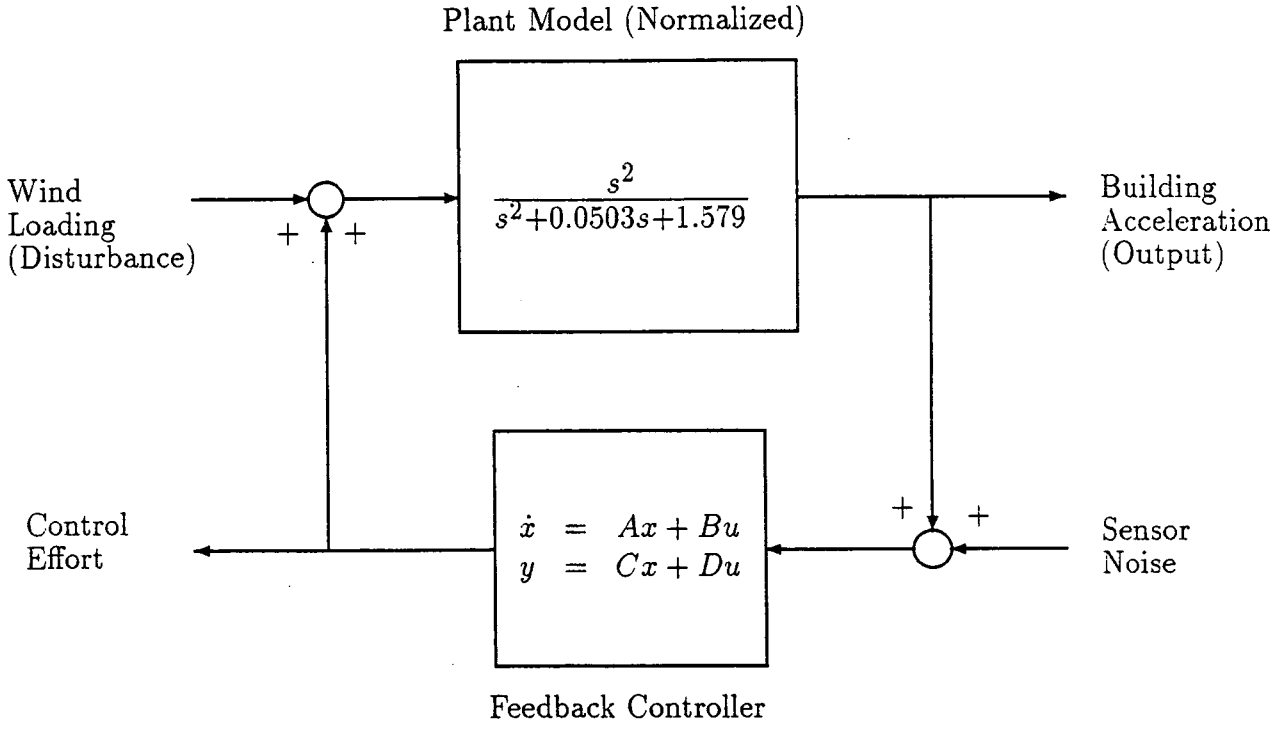


Figure 3. Structural Feedback Control

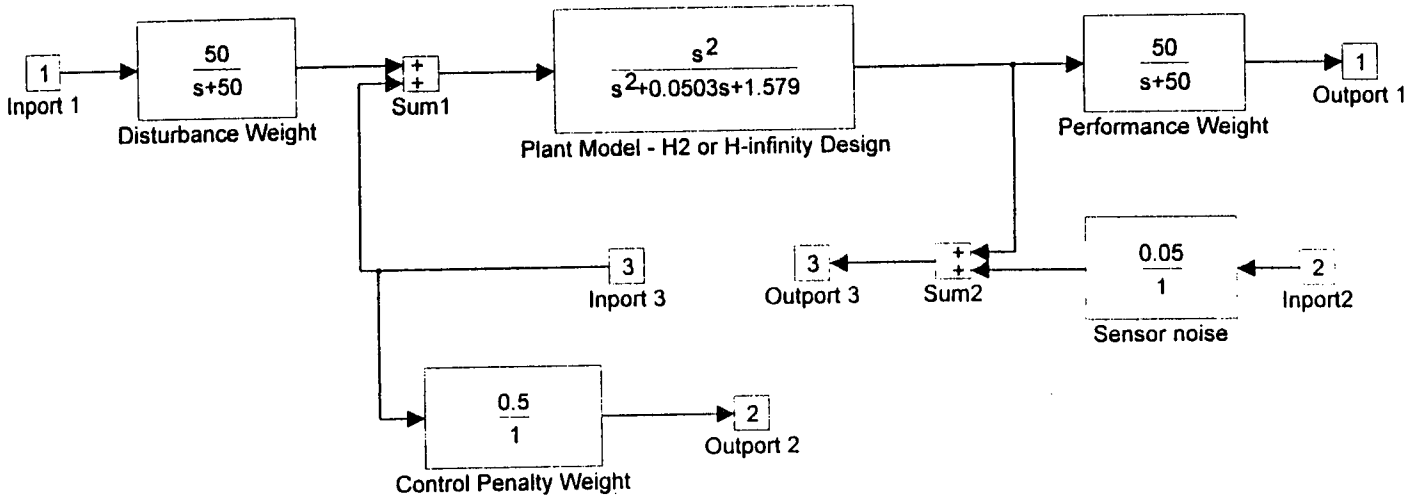


Figure 4. Optimal Control Design Model

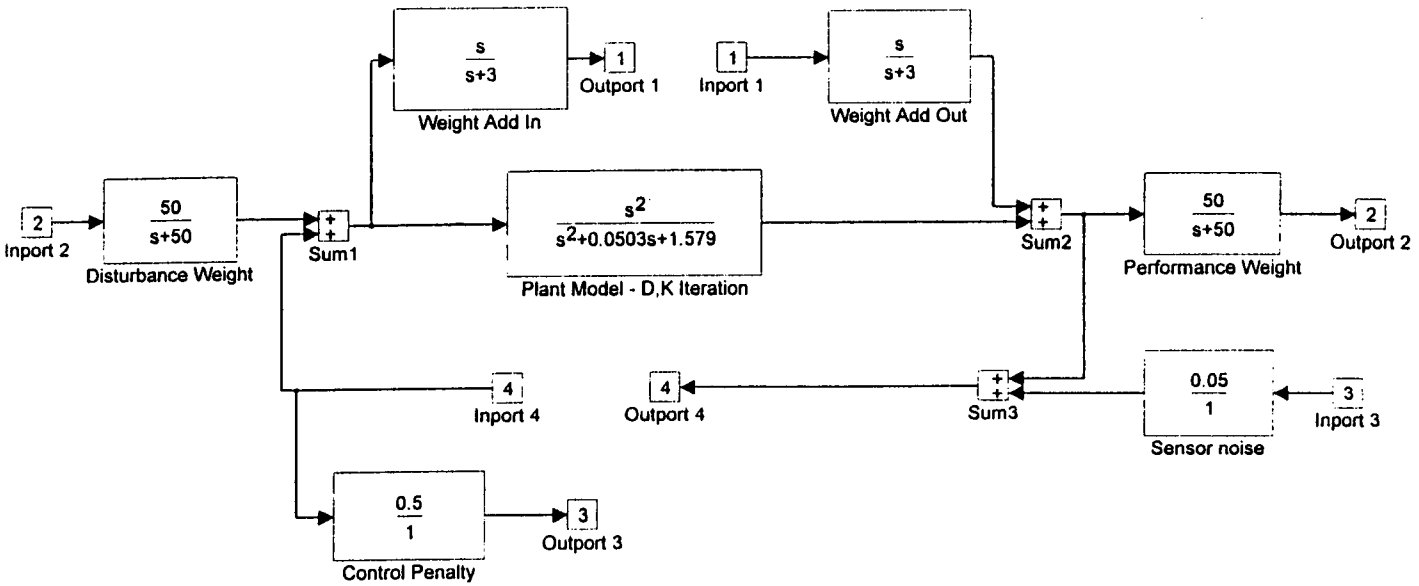


Figure 5. Robust Control Design Model

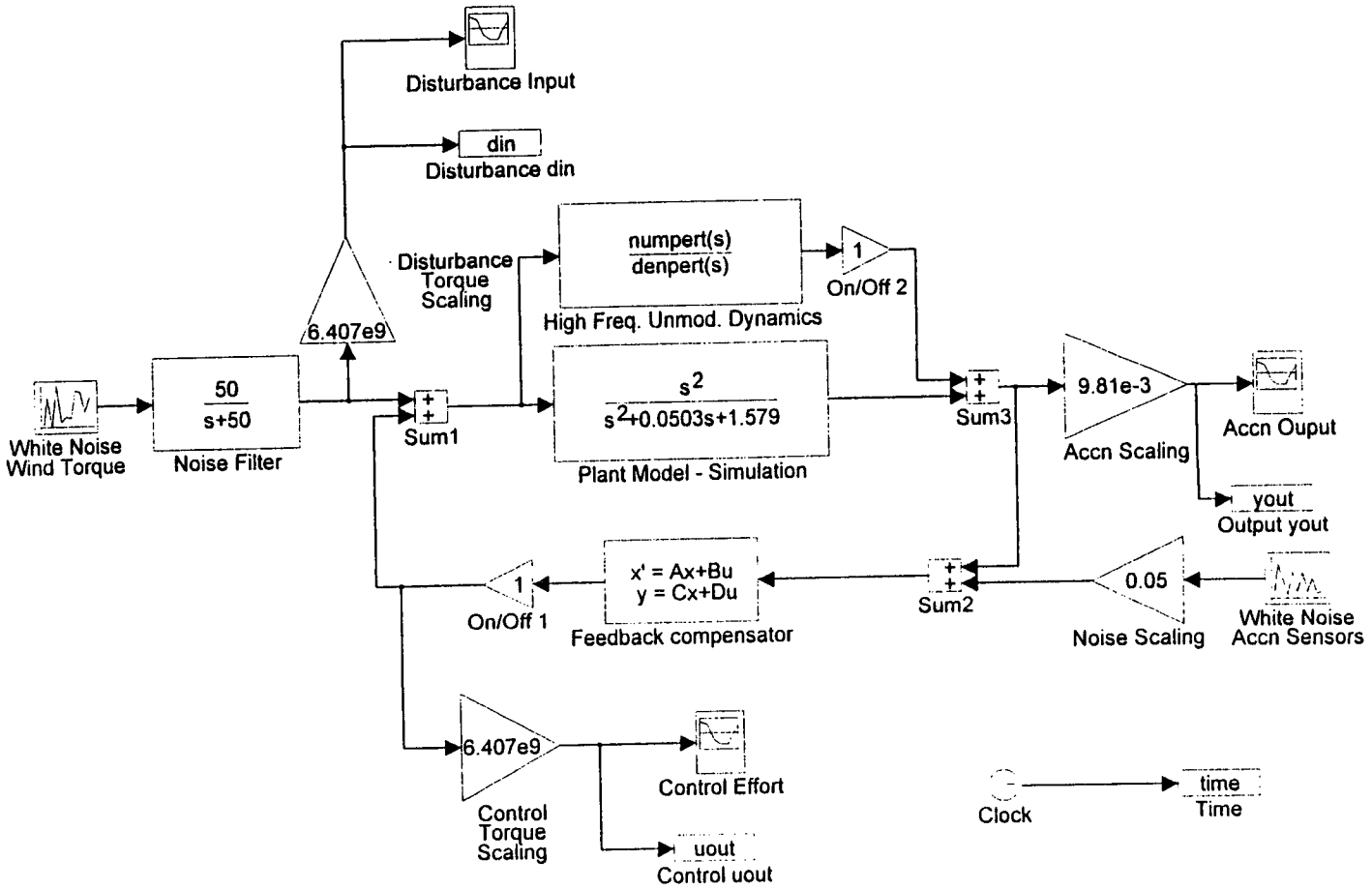


Figure 6. Simulation Model

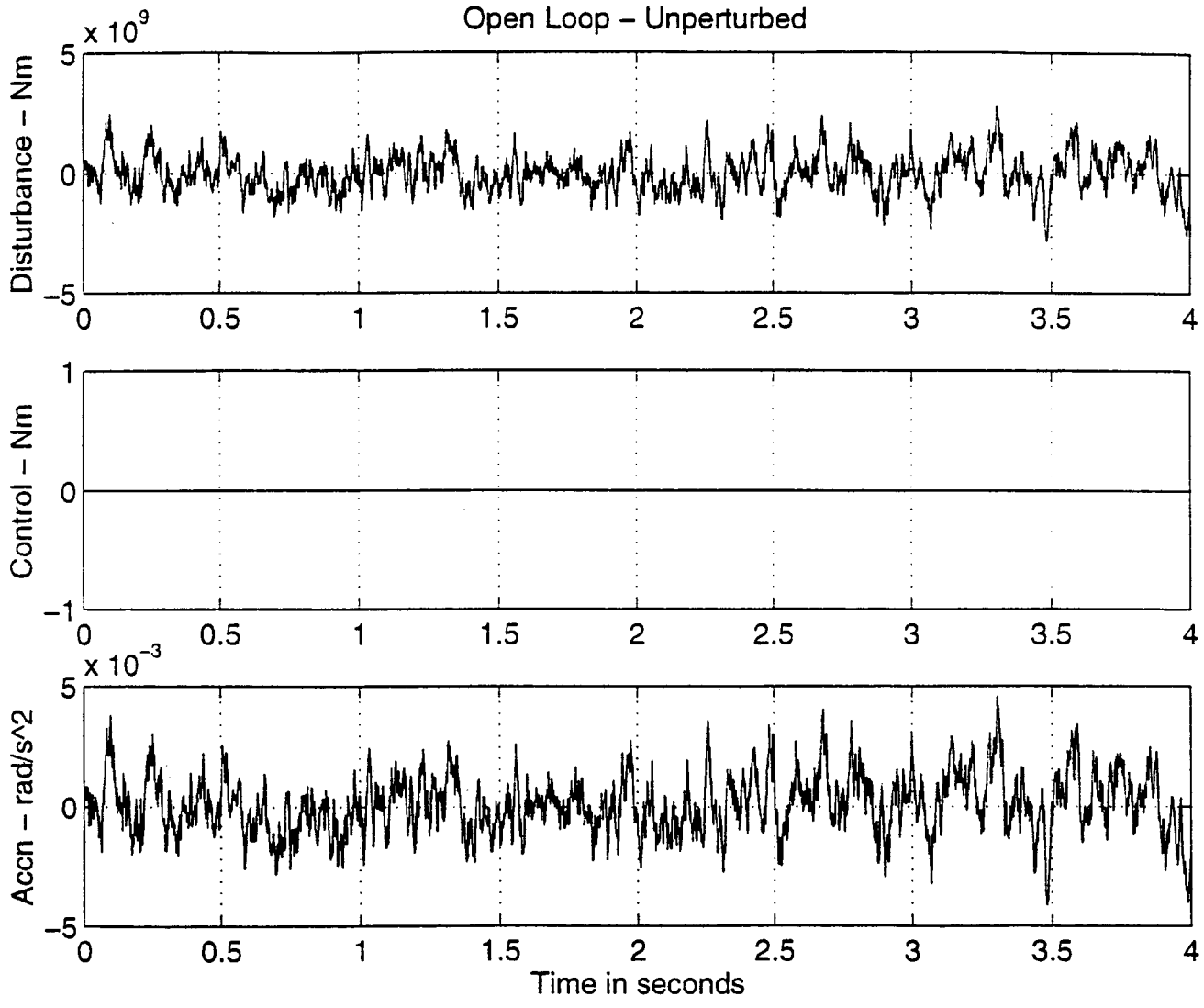


Figure 7. Unperturbed Open-Loop Response

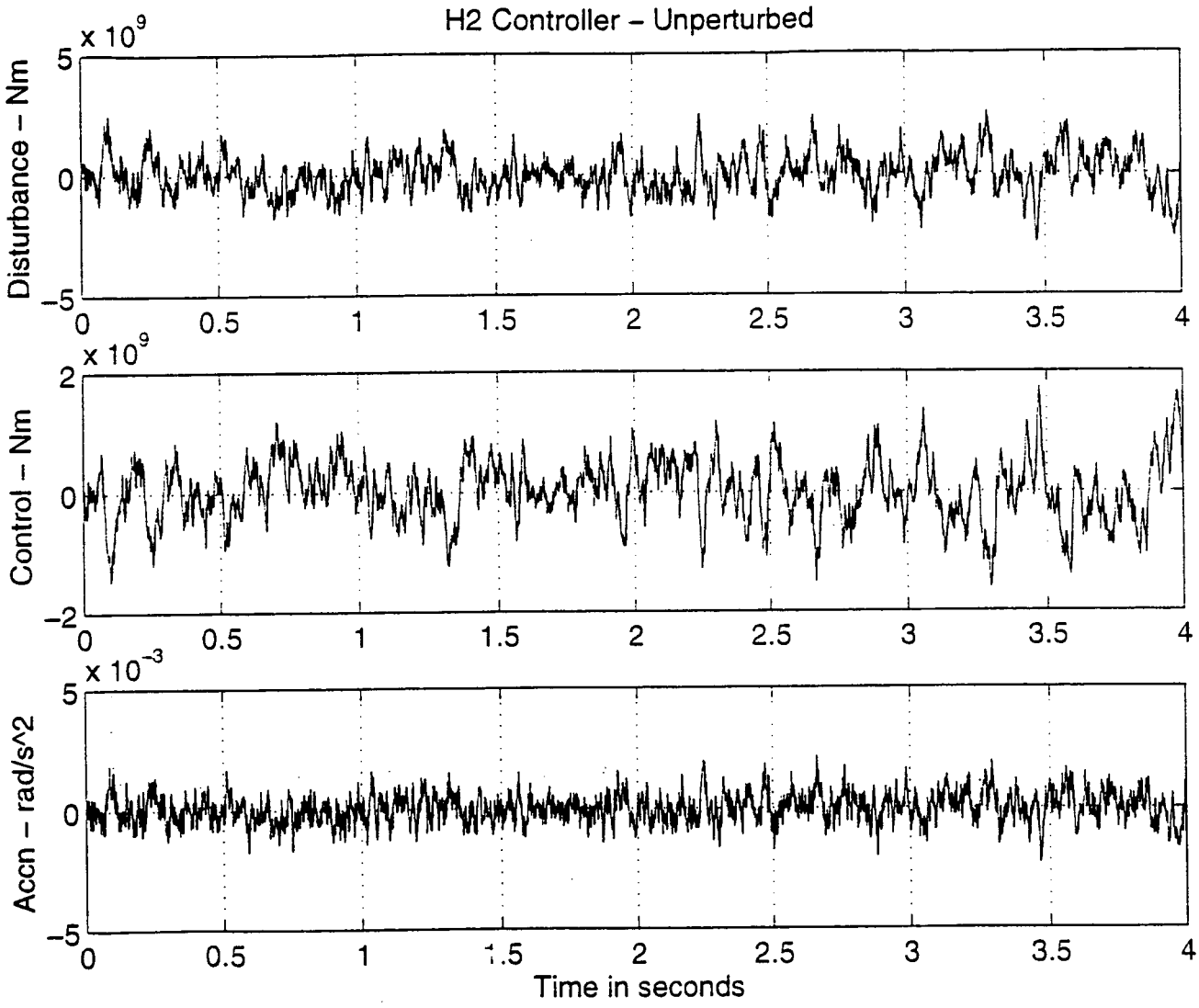


Figure 8. Unperturbed H_2 Control Response

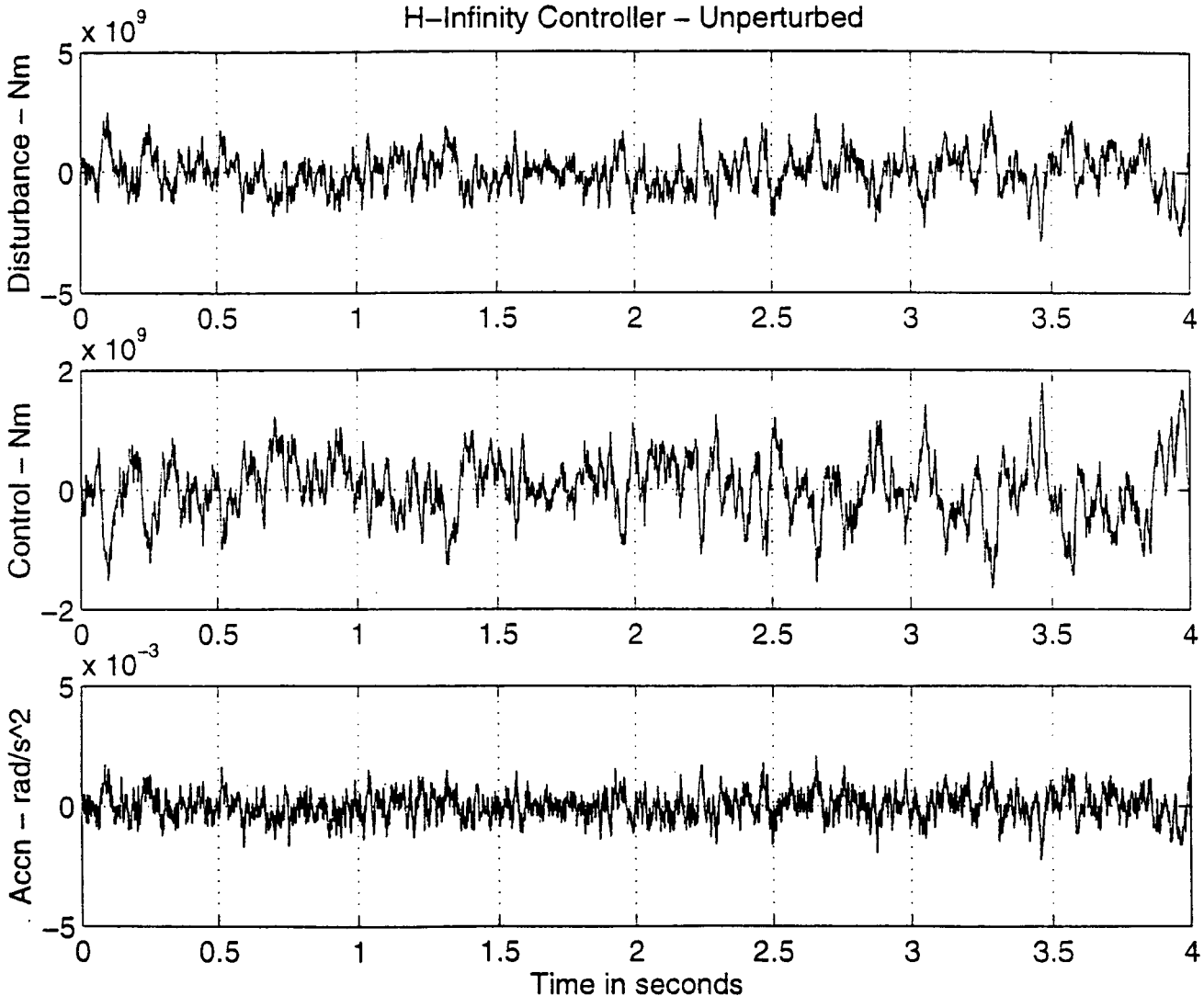


Figure 9. Unperturbed H_∞ Control Response

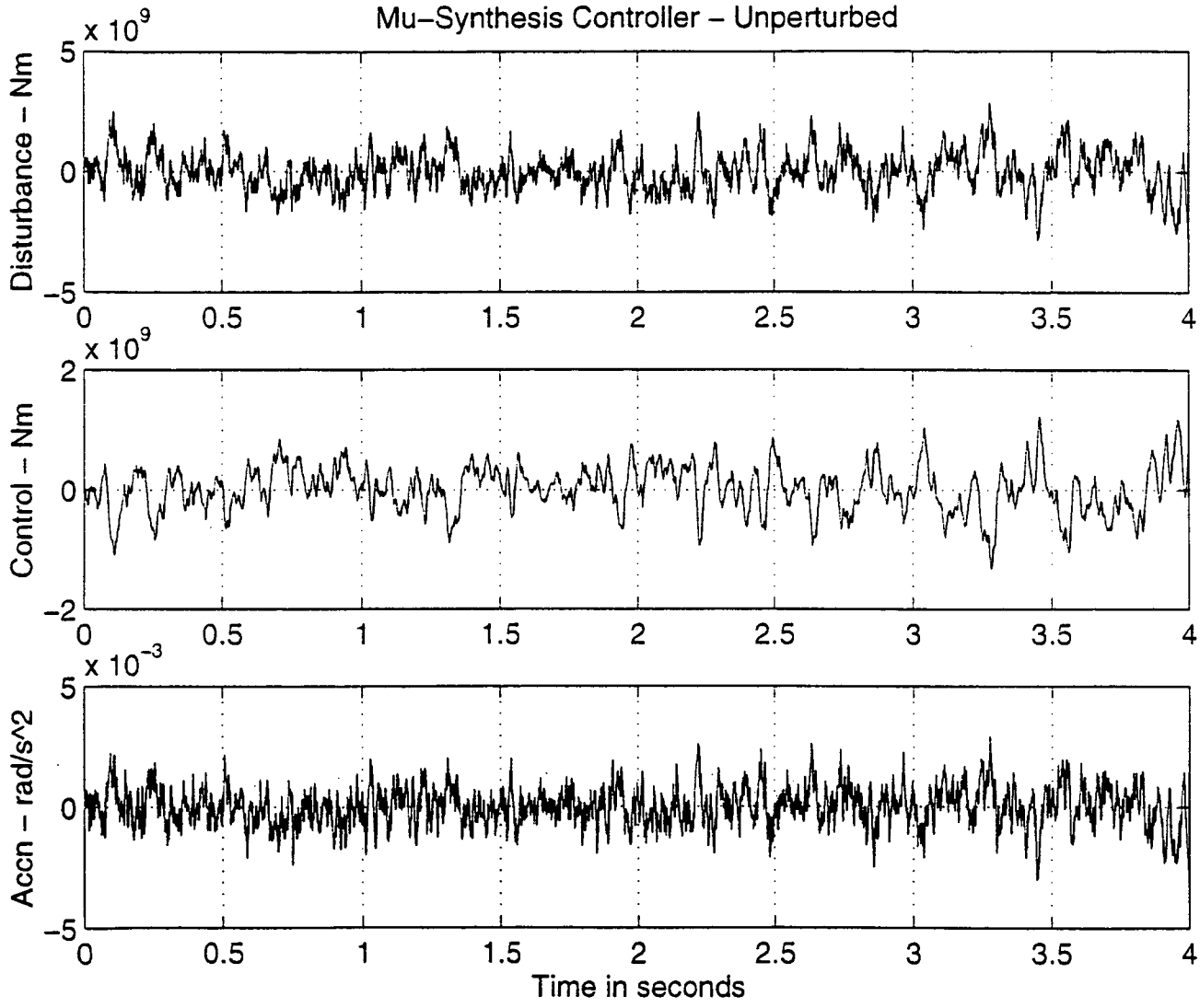


Figure 10. Unperturbed μ-Synthesis Control Response

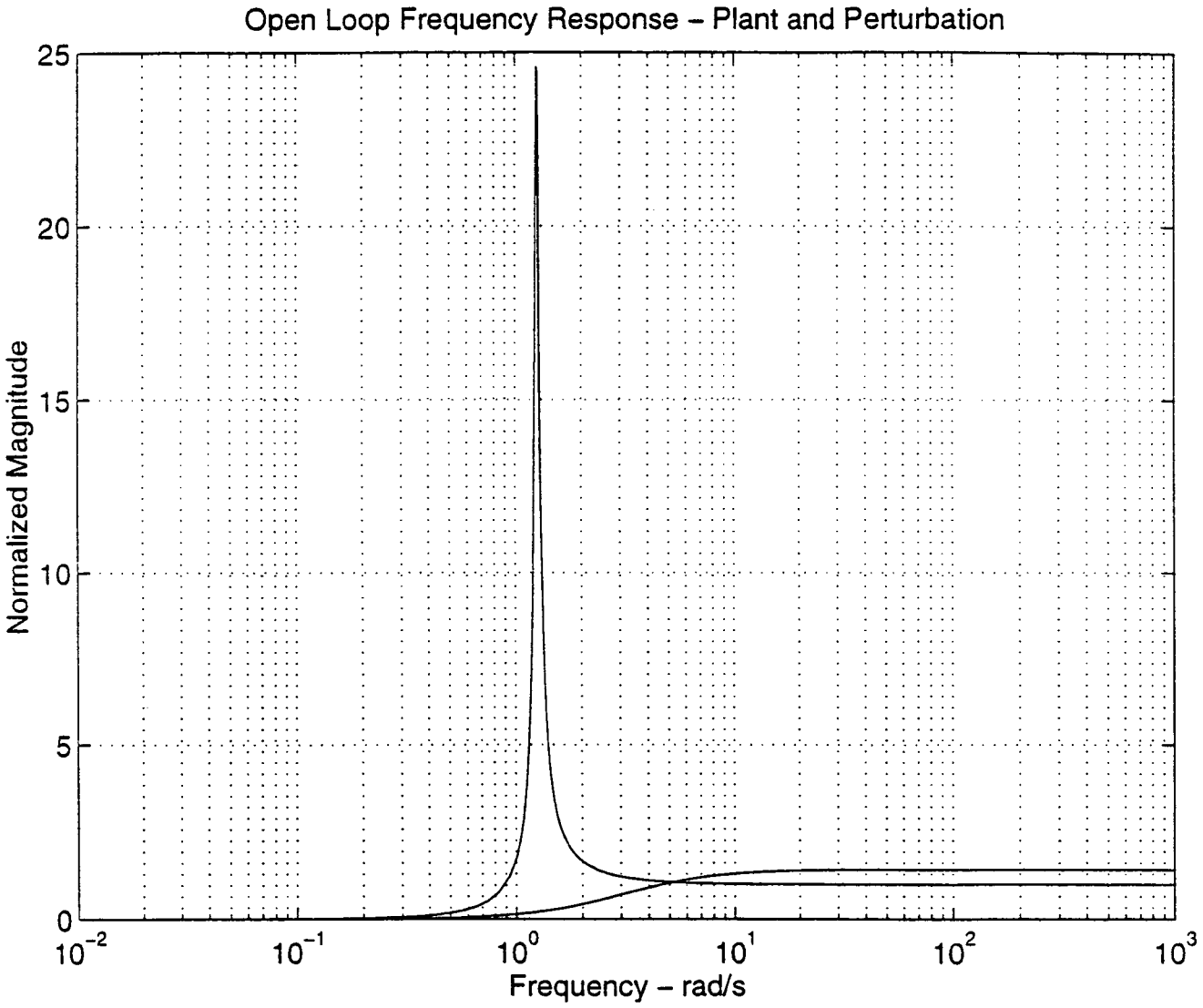


Figure 11. Frequency Response of Open-Loop Plant and Perturbation

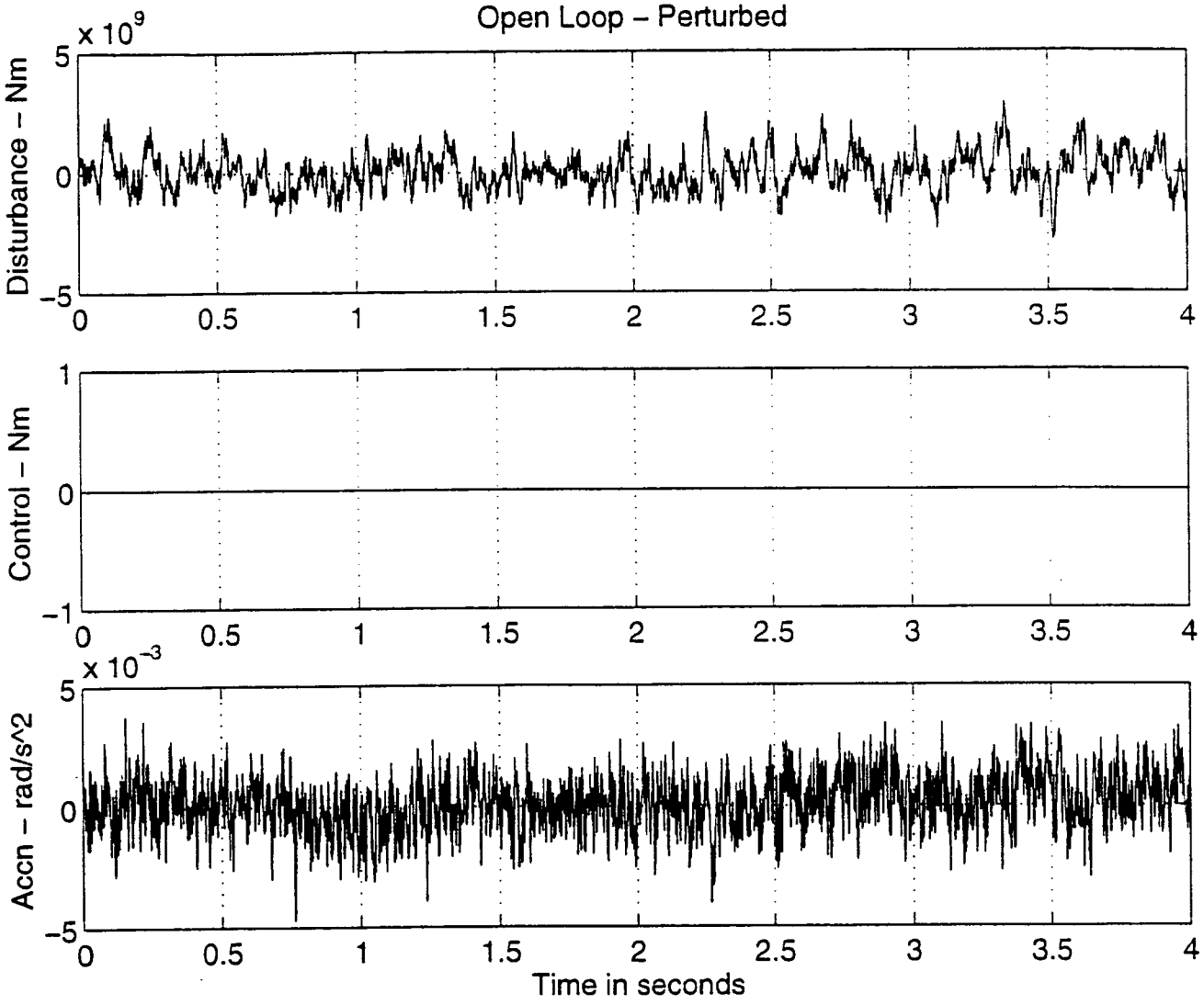


Figure 12. Perturbed Open-Loop Response

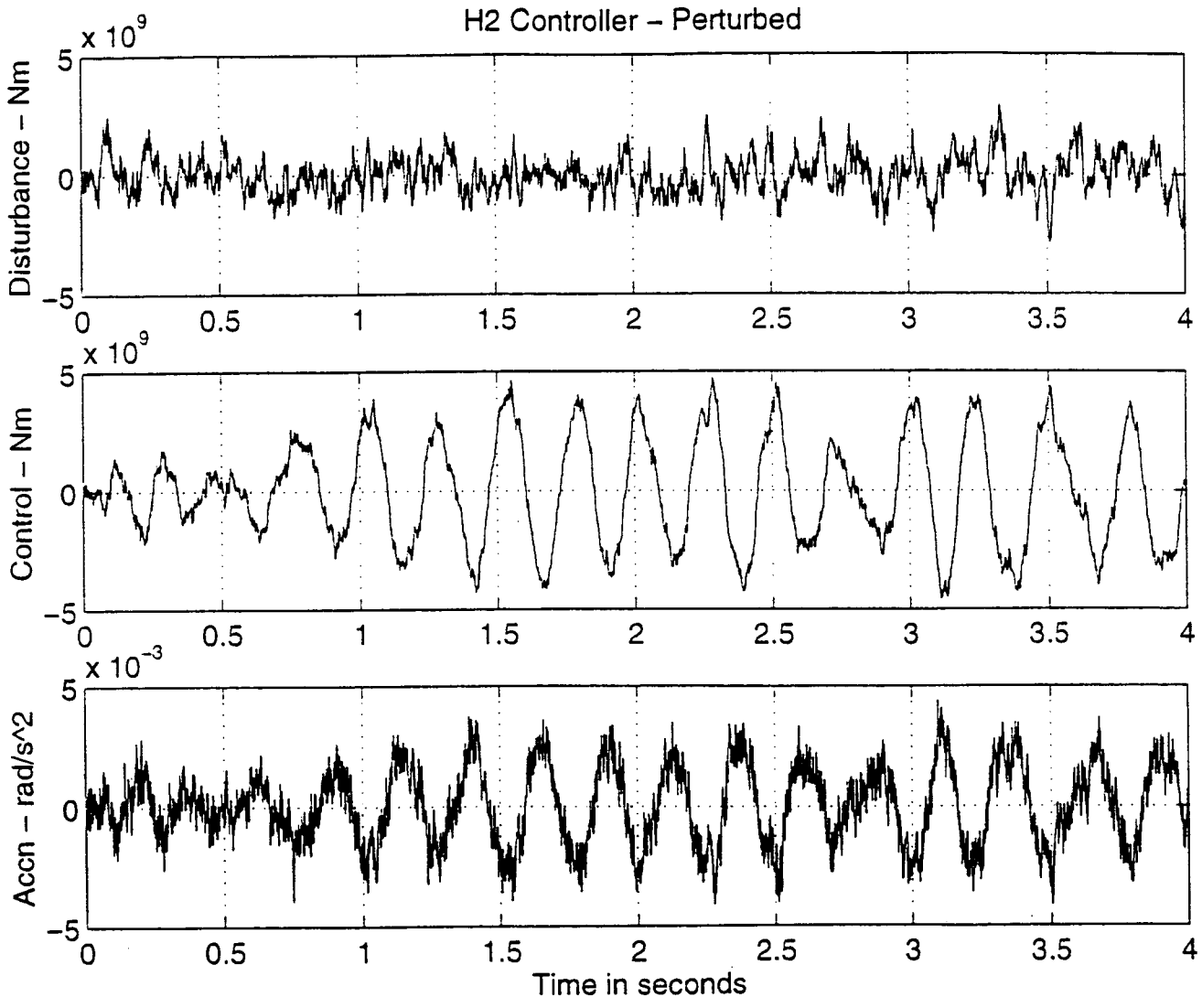


Figure 13. Perturbed H_2 Control Response

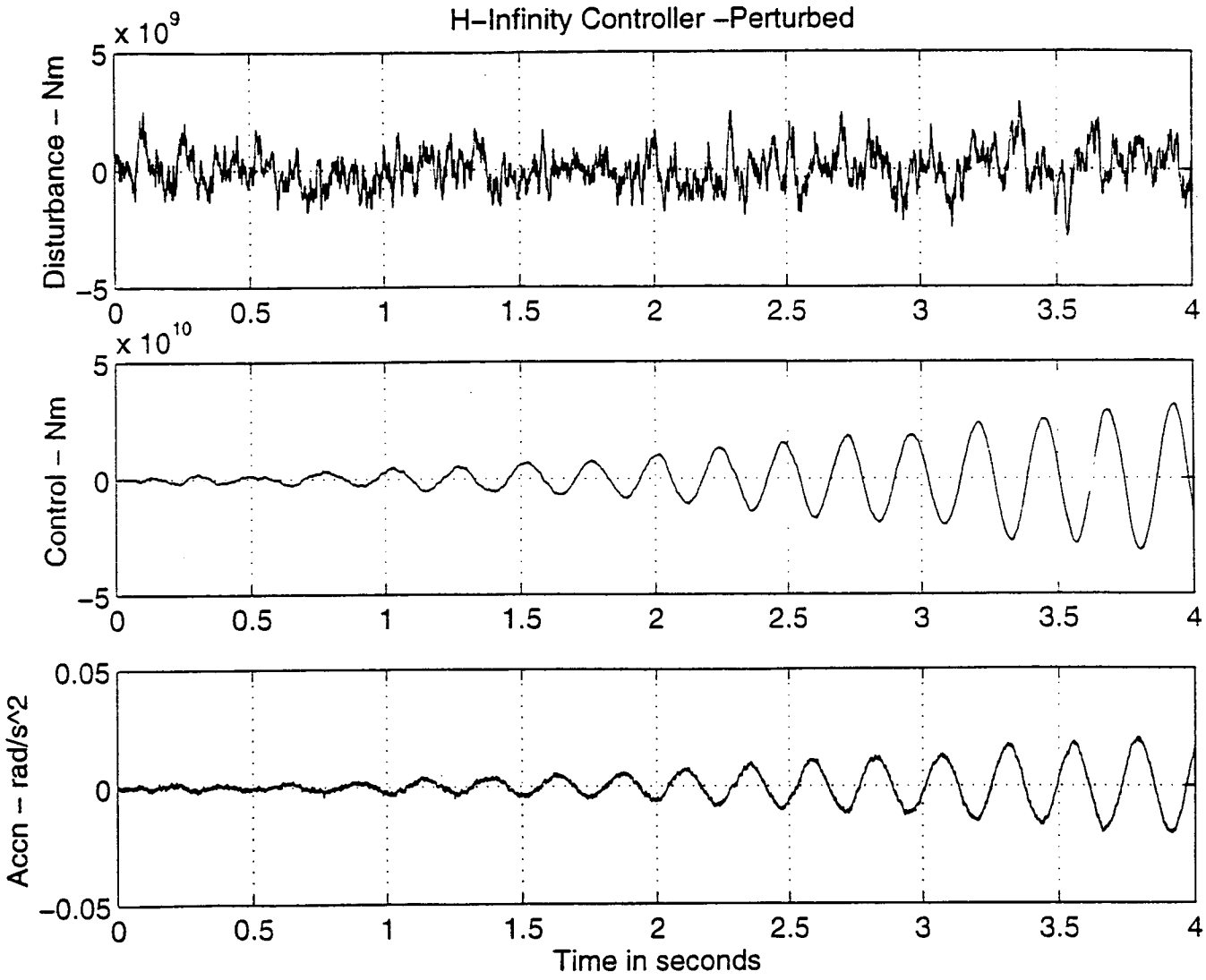


Figure 14. Perturbed H_∞ Control Response

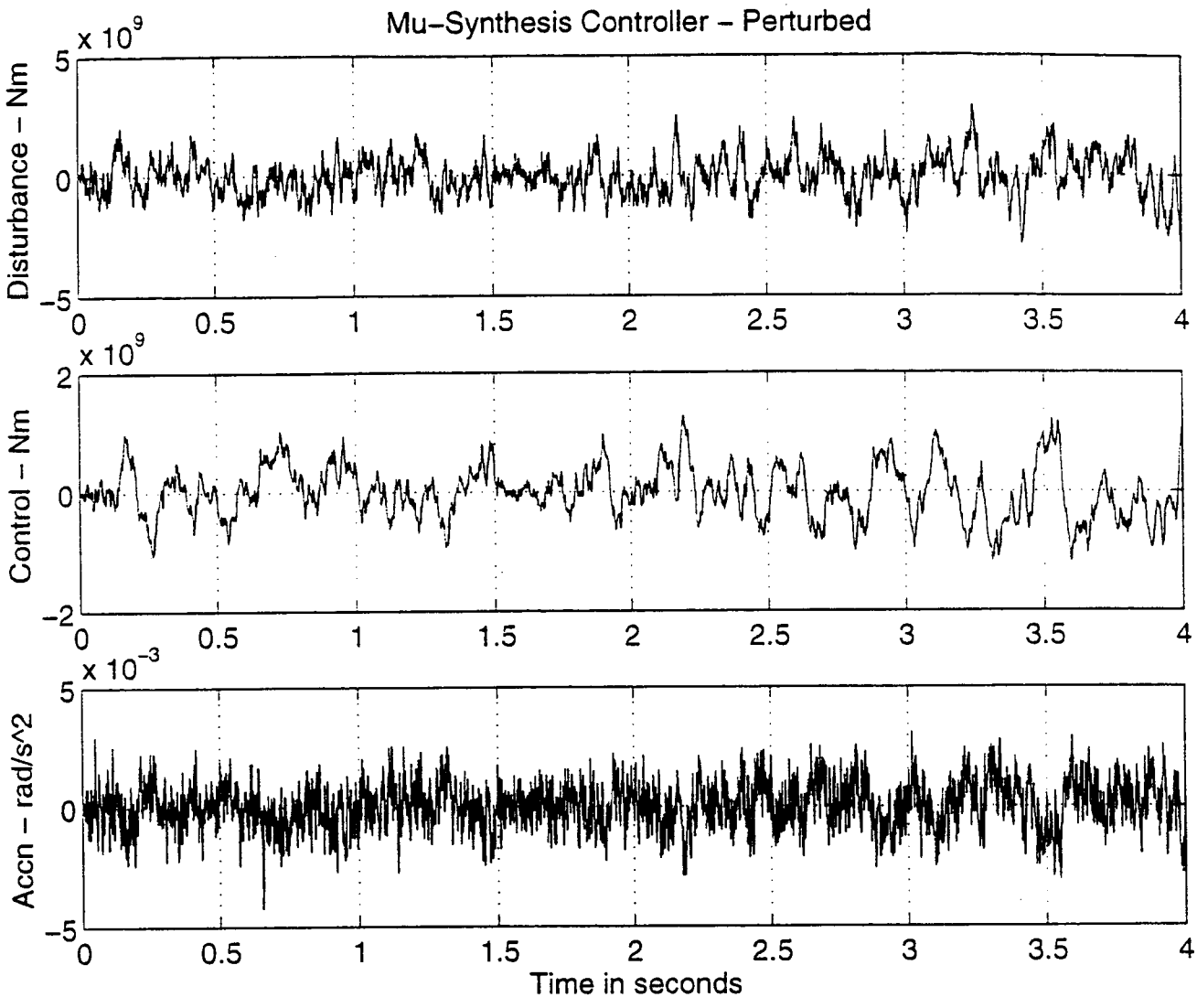


Figure 15. Perturbed μ-Synthesis Control Response

The Shimodate Downbursts on July 15, 1996

by

Hajime Nakamura*

ABSTRACT

On July 15, 1996 strong gust winds accompanied with a severe thunderstorm hit Shimodate city, northwest of Ibaraki Prefecture, resulting in one people dead, 19 injured and 425 houses collapsed. A field survey revealed that the strong winds were caused by at least two downbursts. The intensity of the first one was estimated as F2 by Fujita scale (corresponding to wind speed of 50 - 69 m/s) , which was one of the severest downbursts reported before in Japan.
Doppler weather radar at Narita International Airport caught parent thunderstorm of the downbursts. Echo reflection intensity and Doppler velocity showed precursor events of the downbursts in the thunderstorm cloud such as descent of precipitation core and divergence of winds in the lower level above the surface.

Key Words:

downburst, gust wind, Doppler weather radar, precursor, warning

1. Introduction

In the afternoon of July 15, 1996 a thunderstorm developed in the northern part of the Kanto Plains and moved southeastward passing through Tsukuba. Strong gust winds with hail hit Shimodate city, Ibaraki Prefecture, northwest of Tsukuba, resulting in one people dead, 19 injured, 425 houses collapsed, 2 trains canceled, electric power cut of 8 thousand houses and 3,500 million yen loss to the agriculture etc. Meteorological Research Institute (MRI) performed a field survey of the damages produced by strong winds with Mito Local Meteorological Observatory. It was identified that at least two downbursts occurred successively in 10 minutes, first one being one of the strongest downbursts in Japan reported in the past.

A downburst is a strong descending airflow in cumulus or cumulonimbus clouds which causes a damaging horizontal outflow near the ground surface (Figure 1). Strong downward motion of the airmass in a cloud is accelerated by evaporative cooling of the waterdrops or loading of heavy raindrops or hails onto the air. The speed of outflows of downbursts sometimes reaches 70 m/s but their horizontal scales are almost less than 10 kilometers and their lifetimes are less than 10 minutes. Downbursts with horizontal scale of less than 4 km is especially hazardous to airplane and called microburst. In the United States, during the period 1974 to 1985, microbursts have caused at least 11 civil aviation accidents involving over 500 fatalities and injuries (Proctor, 1988). In Japan 25 events of downbursts have occurred during the period 1981 to 1994 (Ohno et al. 1996).

Japan Meteorological Agency (JMA) have installed 3 Doppler weather radars at Narita, Haneda and Kansai airports and started operation to detect dangerous windshear for aviation which are caused by downbursts and other atmospheric disturbances. These Doppler radars have higher time resolution and greater number of scanning angles than the conventional radars of JMA. Some precursors

* Head, The Second Laboratory, Forecast Research Department, Meteorological Research Institute, Japan Meteorological Agency

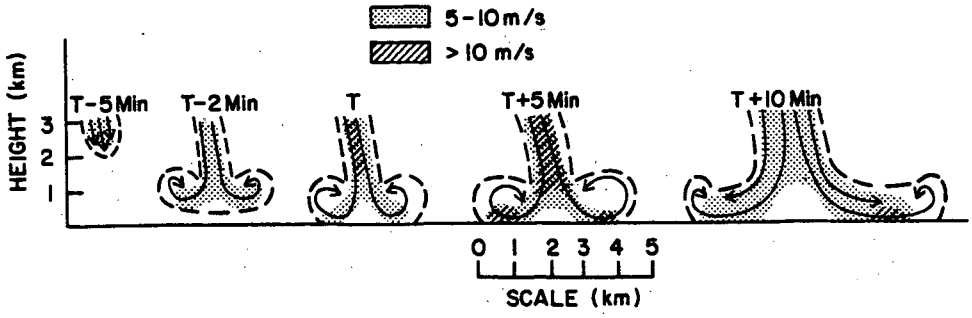


Figure 1 A schematic representation of the evolution and flow within an average downburst obtained by Doppler weather radar from the Joint Airport Weather Studies (JAWS) near Denver (after Wilson et al., 1984). T is the time of initial divergence at the surface. The shading denotes the vector wind speeds.

of the downbursts at Shimodate were observed by Narita Doppler weather radar. The case presented here is the first time in Japan that parent clouds of downbursts and/or the precursors are observed by an operational Doppler weather radar.

This paper will present the results of the field survey, meteorological conditions of the environment air around the thunderstorm, and the precursors of the downbursts identified by Narita Doppler weather radar.

2. Damage characteristics

We investigated mainly the following 3 items in the field survey;
1) degrees of damages to specify strength (speed) of winds,
2) directions in which damaged objects such as trees and constructions fell down or were blown down to determine wind directions, and
3) horizontal extent of damaged area to determine area of the damage-induced wind.
We also made interviews to the residents to get specific features of the event and to specify the time when strong winds occurred.

It was found that there were two areas where damaging winds blew, each 6 km apart. Figures 2 and 3 show the horizontal area and wind directions of the two damage areas.

These figures clearly indicate that
1) shapes of damage areas are ellipse,
2) wind directions distribute radially,
and we also get by interviews the information that
3) hail storm started almost simultaneously with the damage winds.
Therefore, we concluded that the damages

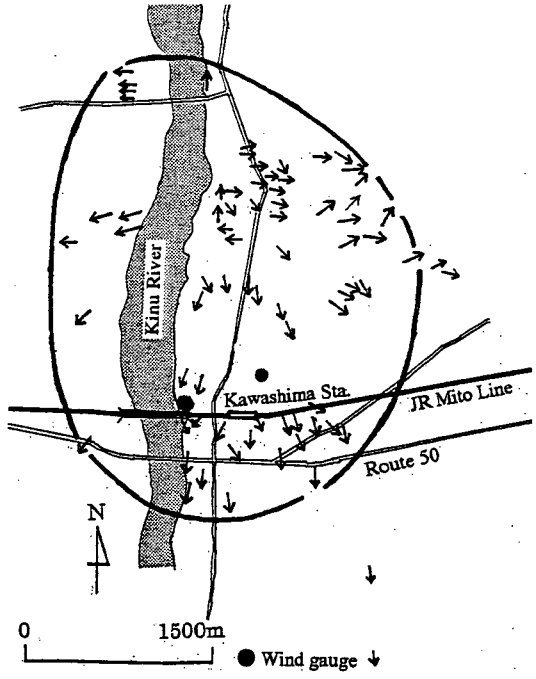


Figure 2 Distribution of damages and directions of winds of the first downburst occurred north of JR Kawashima station, western part of Shimodate City. Dots indicate positions of wind gauges.

were caused by two downbursts.

The first downburst occurred at around 14:51, in the area north of JR Kawashima Station, western part of Shimodate City (Figure 2). The intensity was estimated as F2 by Fujita scale (corresponding to wind speed from 50 to 69 m/s). This is one of the severest downbursts in Japan reported in the past. The damage area was 4 km long and 3 km wide. A wind gauge located in the southern portion of the damaged area recorded 46 m/s maximum instantaneous wind velocity at 14:53:30 and another wind gage located north of JR Kawashima Station observed 47.5 m/s northerly wind.

The second downburst occurred at around 14:59 in the southern part of Shimodate City. The estimated intensity was F1 (wind speed from 33 to 49 m/s) and the area was 2.5 km

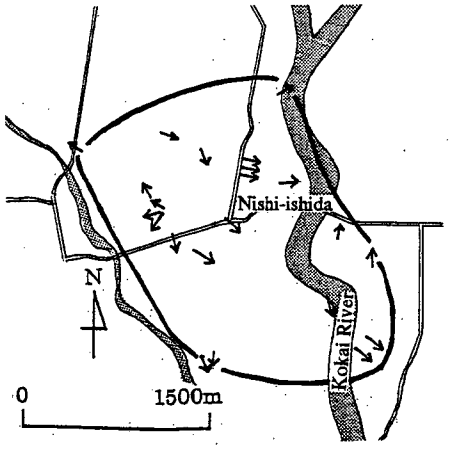


Figure 3 Distribution of damages and directions of winds of the second downburst occurred at southern part of Shimodate City.

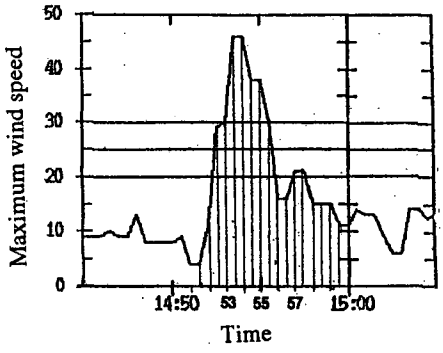


Figure 4 Wind speed record at Kinugawa railroad bridge of JR Mito line.



Photo 1 A completely destroyed house. Intensity of the downburst was estimated from the degree of damage.



Photo 2 Wind directions were estimated from trees blown down and constructions inclined.



Photo 3 Holes made by hails on a pumpkin. Hails as large as a ping-pong ball fell.

long and 1.5 km wide.

Photos 1 to 3 show some examples of the damages.

3. Meteorological Conditions

On July 15, 1996, the Baiu front stayed over northern part of the Japan Island from Niigata to Fukushima Prefecture and the Kanto Plains was covered by the subtropical high pressure extending from the northwest Pacific Ocean. Over the northern part of the Kanto Plains, i.e. Tochigi and Ibaraki Prefectures, weak easterly winds flew in the morning and temperature has risen to over 30℃ at noon. Cumulus clouds were started to form in the center of Tochigi Prefecture in the afternoon and developed to a thunderstorm moving southeastward towards Shimodate city and then Tsukuba city.

Figure 5 shows the distribution of radar echo reflection intensity by the JMA weather radar when the downbursts occurred. A line-shaped echo was extending along the border between Tochigi and Ibaraki Prefectures. There observed the echo reflection intensity over 64 mm/hr and the echo top height as high as 12 km. The downbursts at Shimodate occurred near the southwestern end of the echo.

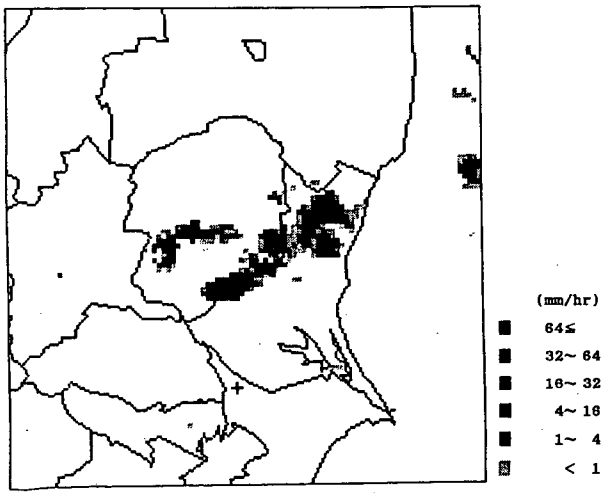


Figure 5 Radar echo reflection intensity at 14:52, July 15, 1966 observed by Tokyo weather radar, JMA.

Pattern of surface winds and temperatures (Figure 6) indicates that cold northerly outflow from the thunderstorm intruded into the warm south-southwesterly air in the western part of the Kanto area and slightly colder easterly flow in Ibaraki Prefecture. The line-shaped echo lay along the border between the cold northerly outflow and the easterly flow. At Shimozuma south of Shimodate temperature decreased from 29℃ to 23℃ and wind direction changed from E to NNE after passage of the thunderstorm.

In order to investigate whether atmospheric vertical stability of the environmental air around the thunderstorm was favorable for formation of cumulus clouds and initiation of downbursts, we calculated the convective available potential energy (CAPE) and $\Delta\theta e$, the difference of the equivalent potential

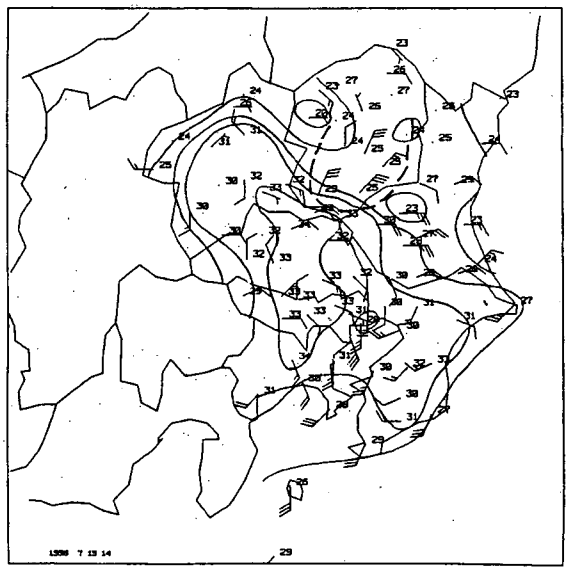


Figure 6 Surface winds and temperature at 14:50, July 15, 1966 obtained by automated weather stations AMEDAS, JMA. Solid lines denote temperature with contour interval of 3 degree and a dashed line denotes boundary of northerly wind.

temperature between its maximum value at the lower level (typically 950 hPa) and its minimum at the middle level (typically 600 hPa) from upper air soundings twice a day at Tateno in Tsukuba city.

Figure 7 indicates that in the afternoon of July 15, CAPE was larger than 1,000 m^2/s^2 which is said to be the threshold value for cumulus clouds to form. $\Delta\theta e$ in the morning of July 15 was 21K. Atkins and Wakimoto (1991) suggested that a wet downburst in the United States often occurs when the criterion $\Delta\theta e >$ 20K is satisfied. Therefore, the conditions of storm environment on July 15 were favorable to cumulus convections and downbursts. However, in many other days in Figure 8, conditions of CAPE and $\Delta\theta e$ were satisfied but there were no reports about thunderstorms and downbursts for most of those days. Thus, it seems to be difficult to forecast thunderstorms and downbursts using only these parameters. One of the reasons is that soundings do not represent conditions of environmental air of a thunderstorm since the storm is of small scale and sounding position is in general far apart from the storm.

4. Precursors observed by Narita Doppler weather radar

Narita Doppler weather radar in operation since April 1996 has a range of 100 km radius and the increment are 150 m in radial direction and 0.7 degree in tangential direction. It takes about 6 minutes to perform one scan mode during which the radar scans 17 elevation angles. Since Shimodate city is about 75 km north of Narita Airport, resolution of the radar near Shimodate is about 900 m in tangential direction and also about 900 m in the vertical. Narita Doppler weather radar has time resolution higher than conventional weather radars and succeeded to catch the details of precursors in the parent thunderstorms of the downbursts presented here.

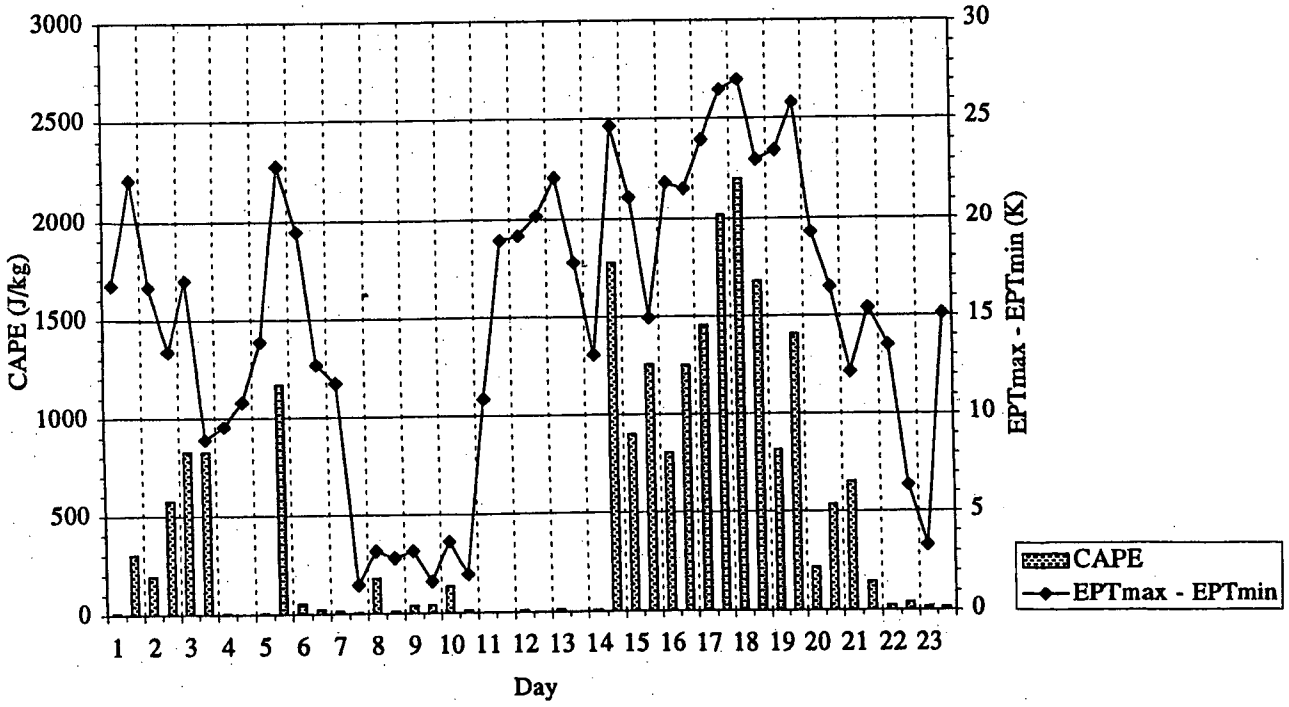


Figure 7 CAPE (convective available potential energy) and $\Delta\theta e$, the difference of the equivalent potential temperature between its maximum in the lower level and its minimum in the middle level in the period from 1 to 23, July 1996 computed from upper air soundings at Tateno.

Figure 8 shows patterns of echo reflection intensity and Doppler wind velocity at the level of about 1 km high, 1.5 minutes before the first downburst. A strong echo reflection intensity is observed above the first downburst area (top figure) and there is a pair of wind towards the radar southeast of the first downburst area (thick hatch) and wind away from the radar northwest of the downburst. The high echo reflection intensity suggests existence of precipitation core or hails and wind pair with opposite direction means divergent wind flows.

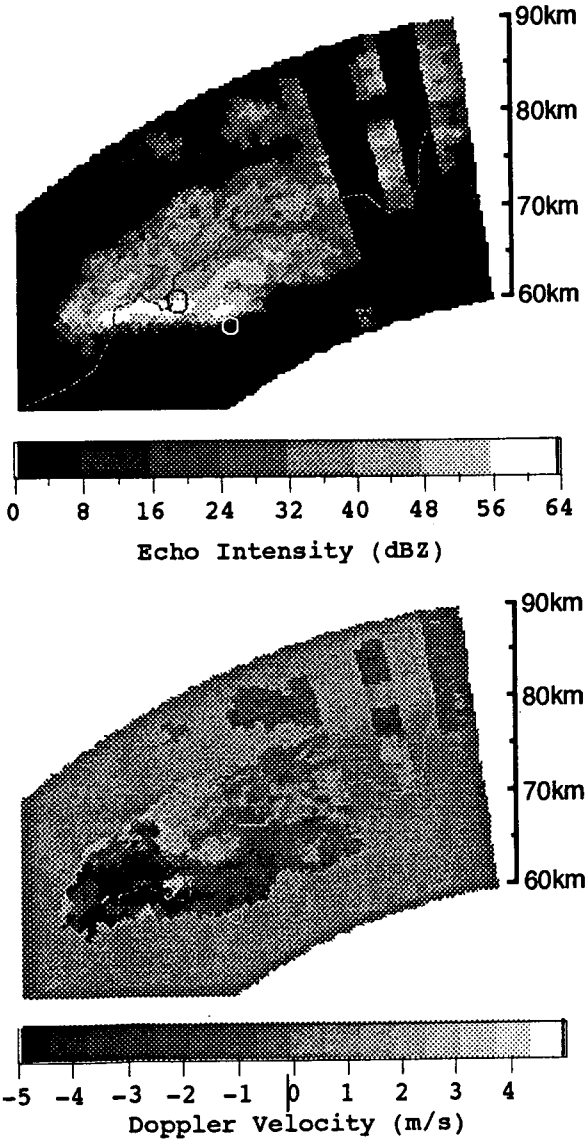


Figure 8 Echo reflection intensity (top) and Doppler velocity (lower) by Narita Doppler weather radar at 14:49:32, July 15,1996. Elevation angle of radar scan is 0.7 degree. Solid line indicates the border between Tochigi and Ibaraki Prefectures and two ellipse damage areas by the downbursts.

Since downbursts are quite dangerous to aviation as well as public, using Doppler radar some attempt have already been performed to detect precursors of downbursts several

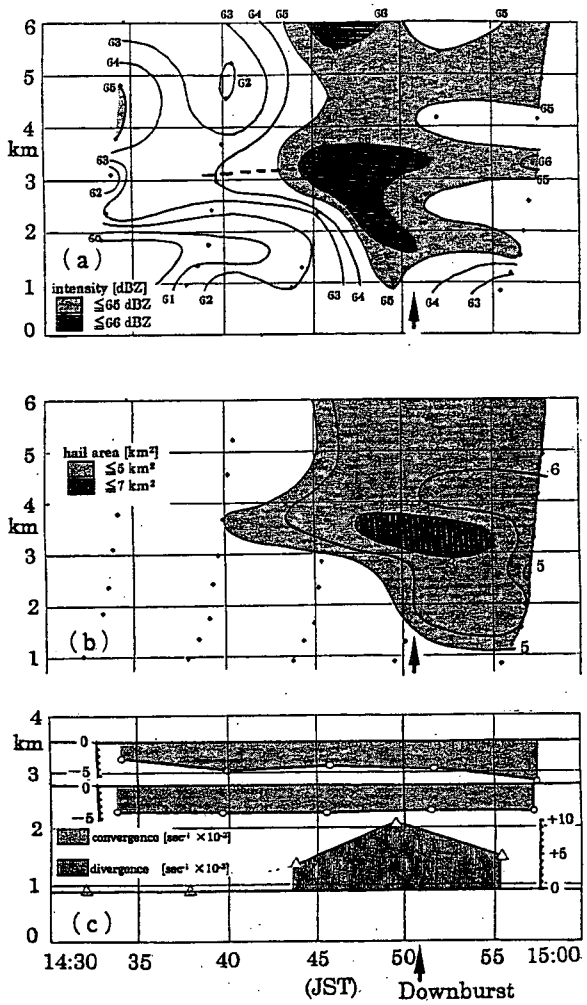


Figure 9 Time-height cross sections composed from Narita Doppler weather radar data (Kusunoki et al., 1996). Top: Echo reflection intensity; middle: hail area, and bottom: convergence in the middle level and divergence near the surface.

minutes before the occurrence of downbursts. As precursors which can be caught by Doppler radar, the followings are for example noted (e.g., wheeler and Roeder, 1995):
(1) divergence in the lower level near the surface
(2) convergence in the middle level
(3) rotation in the middle level
(4) descending precipitation core
(5) notch pattern
(6) extension of hail area

Kusunoki et al. (1996) investigated the precursors of the downbursts using Narita Doppler weather radar. Figure 9 shows time-height cross sections composed from radar beams with different elevation angles which pass through the parent thunderstorm of the first downburst. Figure 9 (top) indicates that the area of high reflectivity at 3 km height level started to descend about 6 minutes before the downburst at the surface and reached 1 km above surface 1 minute before the downburst. Figure 9 (middle) shows that hail area was formed around 3 to 4 km level about 3 minutes before the downburst. Figure 9 (bottom) depicts that divergence area in the lower level existed already 5 to 7 minutes before the downburst.

If we can detect these precursors on real time base by the operational Doppler radar, it will be possible to issue downburst warning to aviation and/or public.

5. Conclusion

We performed a field survey to identify the source of severe winds that brought damages at Shimodate City on July 15, 1996. It was found that the strong winds were caused by at least two downbursts. The intensity of the first one was estimated as F2 by Fujita scale and the second one F1. The meteorological condition of the environment of the parent thunderstorm was examined with upper air soundings at Tateno. A vertical stability index CAPE satisfied the criteria for development of cumulus convection. On of the downburst indices , $\Delta\theta e$, the difference of the equivalent potential temperature was over the criteria for occurrence of downbursts obtained from case studies in the United States. The Doppler weather radar at Narita International Airport caught the precursors of the downbursts such as descending motion of precipitation core, enlargement of hail area in the middle level and divergence in the lower level. It will be expected a rapid progress in developing tools to detect the precursors of downbursts by Doppler radar and we hope that downburst warnings will be issued as operational base in the near future.

Acknowledgments

The author is grateful to the various organizations that helped our field survey: the prefectural offices of Ibaraki and Tochigi; the city offices of Shimodate; the Defence Army; Tokyo Electric Power; Nihon Telegram and Telephone; Japan Railway Higashi-Nihon; Hitachi Shimodate Works; Mito and Utsunomiya Local Meteorological Observatories. The author extends his thanks to Japan Meteorological Agency, High Altitude Observatory and New Tokyo Airport Local Meteorological Observatory for providing data.

References

Atkins, N. T. and R. M. Wakimoto, 1991 : Wet Microburst Activity over the Southeastern United States : Implications for Forecasting. Weather and Forecasting, 6, 470-482.

Kusunoki, K., O. Suzuki, Y. Makihara and Y. Sato, 1996 : The Shimodate downburst on July 15, 1996 II: Precursors of the downburst detected by a gust wind precursor detection tool. Proceedings of

Annual Meeting of Meteor. Soc. of Japan (in Japanese).

Ohno, H., O. Suzuki and K. Kusunoki, 1996 : Climatology of downburst occurrence in Japan. Tenki, 43, 101-112 (in Japanese).

Proctor, F. H., 1988 : Numerical Simulation of an Isolated Microburst, Part I : Sensitivity Experiments, J. Atmos. Sci., 45, 3137-3160.

Wheeler, M. M., and W. P. Roeder, 1995 : Forecasting Wet Microburst on the Central Florida Atlantic Coast in Support of the United States Space Program. 18th Conference on Severe Local Storms, Amer. Meteor. Soc., 654-658.

Wilson, J.W., R.D. Roberts, C. Kessinger and J. MacCarthy, 1984 : Microburst Wind Structure and Evaluation of Doppler Radar for Airport Wind Shear Detection. J. Climate Appl. Meteor., 23, 898-915.

An Investigation of Tuned Liquid Dampers for Structural Control

Dorothy Reed[1], Harry Yeh[1], Jinkyu Yu[2] and Sigurdur Gardarsson[2]

ABSTRACT

Rectangular and circular tuned liquid dampers were investigated through shaking table tests for large amplitude excitation. The experimental results confirm earlier work undertaken for small amplitude excitation and considerably contribute to the body of knowledge describing tank behavior under large amplitude excitation. In addition to the experimental investigation, extensive numerical modeling was undertaken for the rectangular tanks. In particular, the random choice method of solving the fully nonlinear shallow-water-wave equations was found to capture the underlying physical phenomenon adequately, including wave breaking, for most of the frequency range of interest. Regardless of the geometry, the tank behaves as a hardening spring system due to the liquid sloshing motion. This trend is enhanced as excitation amplitude increases.

1. INTRODUCTION

Tuned liquid dampers have performed successfully in passively mitigating undesirable structural motion under a variety of settings, e.g., Fediw, et al., (1993); Fujii, et al., (1990); Tamura, et al., (1988); Wakahara, et al., (1992); (1993). Because the underlying physical phenomenon of the liquid sloshing motion that mitigates the structural vibration is not well understood, particularly for large amplitude excitation, shaking table tests and numerical modeling of the liquid sloshing motion of tuned liquid dampers (TLDs), with an emphasis on its behavior under large amplitude excitation, were undertaken. With the ultimate objective of providing improved design strategies for TLDs, performance measures were defined to provide a context for test evaluation.

Performance is defined as "the capability of a single damping device to effectively reduce undesirable structural motion in a robust manner." In the case of multiple devices, this definition should be extended to incorporate redundancy also. This definition incorporates both effectiveness and robustness. Measures of effectiveness include the following:

- Reduction in peak or RMS structural displacement;
- Reduction in peak or RMS structural acceleration;
- Significant increase in "effective" damping of the structural system as evaluated through a single-degree-of-freedom structural dynamics analysis; or
- Significant increase in energy dissipation per cycle over a system without a damping device.

Although some of these measures are equivalent under certain loading conditions, they provide the designer with metrics. Along with effective mitigation of structural vibration there is a secondary property of robustness to identify the best design. The quality of "robustness" is a less well-defined term in the structural control community, although it has been investigated for multiple tuned mass dampers by Abe and Fujino (1994) and Yamaguchi and Harnpornchai (1993). Abe and Fujino (1994) investigated the influence of errors in predicting the structural natural frequencies upon vibration mitigation by multiple tuned mass dampers (MTMD) and found the MTMDs to be robust under conditions of mistuning. Yamaguchi and Harnpornchai (1993) investigated the influence of offsets in the structural damping ratio and found that MTMDs were less robust

[1] Professor, Dept. of Civil Engineering, University of Washington, Seattle, WA 98195, USA
[2]Graduate Research Assistant, Dept. of Civil Engineering, University of Washington, Seattle, WA 98195, USA.

than a comparable single TMD in this instance. In this paper, a robustly designed tuned liquid damper is defined as one in which effective vibration mitigation occurs when

- slight mistuning of the device occurs;
- damping estimates of the device are slightly inaccurate; and
- energy dissipation by the device is significant over a wide range of amplitudes of excitation.

More specifically, for sinusoidal excitation, these definitions of robustness would be as follows:

- The frequency response curve of the structural system is "flat" over a large region, implying that motion reduction is not very sensitive to slight mistuning of the tuned liquid damper.
- The frequency response curve of the structural system is "flat" over a large region even if the estimate of structural inherent damping parameter is slightly inaccurate.
- Energy dissipation is high over a large frequency range for a wide range of amplitude of motion (i.e., small to large amplitude excitation).

For multiple tuned dampers, redundancy is an important consideration, although it has not received the same attention as effectiveness and robustness. As in any system in which multiple units act together for a common purpose, if one or more fail, then the resulting effectiveness should be investigated to ascertain whether these losses would significantly compromise the vibration mitigation.

In this paper, the results of the investigations are evaluated in the context of how effective and robust the tanks would be in structures subjected to sinusoidal excitation over a wide range of amplitudes.

2. EXPERIMENTAL INVESTIGATIONS

The rectangular tanks of dimensions given in Table 1 were investigated under sinusoidal loading conditions. This investigation was undertaken using the shaking table facility at the University of Southern California. Figure 1 shows the experimental set-up. The data measured included the shaking table displacement, the sloshing forces in the horizontal or along (x) and across (y) directions, F_{wx} and F_{wy}, respectively; the temporal water surface variations η at the end wall and at the middle of the tank, and a videotape of the water wave motion for a half length of the tank. In presenting these results, the following parameters will be used:

a) The fundamental natural frequency of the water sloshing motion predicted by the linear water wave theory

$$f_w = \frac{1}{2\pi}\sqrt{\frac{\pi g}{L}\tanh(\pi\varepsilon)} \qquad (1)$$

where the water depth ratio ε is defined by

$$\varepsilon = \frac{h_0}{L} \qquad (2)$$

g is gravity, L is the tank length, and h_0 is the water depth.

b) Excitation frequency ratio β

$$\beta = \frac{f_e}{f_w} \qquad (3)$$

where f_e is the frequency of the sinusoidal excitation, and f_w is the theoretical natural frequency of the water in the tank calculated using equation (1).

c) Nondimensional water surface elevation η'

$$\eta' = \frac{\eta}{h_0} \qquad (4)$$

where η is the departure of the water surface from the undisturbed water surface depth, h_0.

d) Nondimensional base shear force F_w'

$$F_w' = \frac{F_w}{m_w\omega^2 A} \qquad (5)$$

where F_w is the reaction force of the tank created by sloshing motions induced by the shaking table movement; m_w is the mass of the water in the tank; ω is the excitation angular frequency of the shaking table; A is the shaking table excitation amplitude; and the product

$m_w\omega^2 A$ is the maximum inertia force of the water mass treated as a solid mass. In this analysis, the measured base shear force was obtained by subtracting the inertia force of the mass of the tank from the total force measured by the load cell to identify the force due to sloshing motion only. A low pass filter was also used to eliminate high frequency system noise.

e) Nondimensional phase angle, ϕ'

The phase angle Φ in radians between the shaking table motion and the base shear force has been expressed in units of π, as follows:

$$\phi' = \frac{\phi}{\pi} \tag{6}$$

f) Nondimensional energy dissipation per cycle E_d'

$$E_d' = \frac{E_d}{\frac{1}{2} m_w (\omega A)^2} \tag{7}$$

where the numerator is the energy dissipation per cycle is defined by

$$E_d = \int_{\tau_s} F_{wx} dx \tag{8}$$

with dx referring to integration over the shaking table displacement per cycle, and the denominator of eqn. (8) is the maximum kinetic energy of the water mass treated as a solid mass.

3. ANALYSIS

Although extensive time history analyses were undertaken, the frequency investigation appears to provide more relevant information in the context of design and will be explored in this paper. For the tank of length L=590 mm with water depth of h_0 = 30 mm, the effect of the base excitation amplitude on the wave motion was examined for the excitation amplitudes A = 10, 20 and 40 mm. The results are shown in Figure 2 for maximum wave height, maximum base shear force, phase angle between the fundamental mode of the base shear force F_{wx} and shaking table displacement x, and the energy dissipation per cycle. All quantities have been placed in nondimensional form. It can be seen that the maximum wave height peaks at an excitation frequency much higher than the tank natural frequency evaluated by (1), which demonstrates the nonlinear behavior of the fluid in the tank. After this peak is reached, there is a sudden drop in value. This phenomenon has been labeled by previous researchers for limited small amplitude experiments as the "jump" phenomenon, and the frequency at which it occurs is called the "jump frequency," $f_{jump.}$; e.g., Lepelletier, et al., (1980); Sun, et al., (1991). The existence of the jump frequency at frequency ratios $\beta > 1.0$ indicates that the water sloshing motion displays a "hardening" or "stiffening" spring-type nonlinearity behavior. These results are qualitatively consistent with the data provided by Fujino, et al. (1992) for similar experiments but with much smaller excitation. The maximum excitation amplitude to tank length ratio in their investigation was A/L = 0.0169, whereas the present experiments included the case with A/L = 0.0678.

The curves in the plot of the phase angle (Figure 2(c)) show gentle slopes. The corresponding energy dissipation plot for the three excitation amplitudes shows that as amplitude increases, the energy dissipation over a broader range of frequencies occurs. The effective dissipation over a broad range in this manner illustrates that the tank is a robust energy-dissipating system.

From Figure 2 (a), it can be seen that as the excitation amplitude increases, the value of the jump frequency ratio and the response increases. This increase indicates that the nonlinearity of the water sloshing motion becomes stronger as the excitation amplitude increases. The hardening spring behavior can be explained physically by the fact that the wave propagation speed in shallow water depends on the wave amplitude. Based on the shallow-water wave theory, the propagation speed, S, for a non-breaking wave is $\sqrt{g(h_0 + \eta)}$. For the quasi-steady response of the sloshing motion to the forcing excitation, the excitation frequency, f, and wave propagation speed, S, must be related by

$$f = \frac{S}{2L}, \qquad (9)$$

where L is the tank length. Equation (9) indicates that as the excitation frequency increases, the wave must propagate faster. Consequently, the wave amplitude must increase, and ultimately, greater response results. A similar observation can be made in the case of wave breaking (Reed, et al., 1996).

The relationship between the jump frequency and nondimensional excitation amplitude is shown in Figure 3. This plot includes previous data of Sun, et al., (1991) for small amplitude motion. Although the damper is assumed to no longer be effective at excitation frequencies greater than the jump frequency, the results clearly show that, when the excitation amplitude increases, the frequency range of damper effectiveness widens. Figure 3 further illustrates that when the excitation amplitude goes beyond the value of approximately A/L > 0.025, the slope of the curve increases. This change implies that the rate at which the range of frequencies for which the damper is effective increases. The results clearly demonstrate that the tuned liquid damper performs in a wider frequency range under strong excitation. This behavior also suggests that the nonlinear behavior is responsible for the improved performance and robustness of the rectangular TLD.

4. NUMERICAL ANALYSIS OF THE SLOSHING MOTION IN A RECTANGULAR TANK

A series of numerical simulations were undertaken using the random choice method to solve the shallow-water wave equations (Gardarsson and Yeh, 1994). The results presented here correspond to the simulation for the L = 590 mm tank whose experimental behavior was shown in Figure 2. The length of the tank was meshed with 400 grid points. The hydrodynamic force was limited to the hydrostatic pressure using the wave-heights at the endwalls. Figure 4 contains the frequency analysis comparing the simulations and the measured data. It is seen that the simulated results are in good agreement with the experimental results; however, the jump phenomenon is not captured. The numerical scheme predicts a much gentler, smoother transition over the frequency range for the wave profile and maximum base shear force. The energy dissipation curve compares well for the entire frequency range, with slight discrepancies near the excitation ratio of unity and in the jump region. While the numerical model does not simulate exactly the wave motion over the entire frequency range, it does provide a close approximation of the tuned liquid damper performance through the energy dissipation over the entire range including the conditions under strong excitation motion. This particular result is encouraging, given that the design process may ultimately be formulated upon the maximum performance as defined by the estimated energy dissipation.

5. CONCLUSIONS

Experimental and numerical-modeling investigations of tuned liquid dampers have provided insight into the behavior of these devices in controlling structural vibration, especially under large amplitude excitation. Our conclusions are as follows:

- The TLD exhibits a "hardening" or "stiffening" spring property, i.e. the peak response in wave height and base-shear force occurs at an excitation frequency much higher than the natural frequency f_w based on (1).

- After a gradual build-up of the TLD response, at a certain excitation frequency which is higher than f_w, the response suddenly ceases; this is often termed the "jump" phenomenon. It was found that the TLD's "jump" frequency increases as the excitation amplitude increases.

- In terms of energy dissipation, the greater the excitation amplitude, the wider the range of effectiveness of the TLD.

- The numerical model based on the fully nonlinear, nondispersive, shallow-water wave theory is capable of predicting the observed TLD energy dissipation with satisfactory accuracy. On the other hand, the model failed to predict the "jump" phenomenon in wave amplitude and base shear force.

•Our results indicate that it is the nonlinearity of sloshing motion that makes TLD more effective and robust in structural control under strong motion excitation. In other words, as the excitation increases, the effective frequency range for the TLD becomes wider, hence TLDs are robust in dissipating energy over a broad frequency range.

Acknowledgment: The support of the US National Science Foundation for this project is gratefully acknowledged. The writers would like to thank Dr. Sami Masri for his help and support with the USC shaking table facility.

6. REFERENCES

1. Abe, M. and Y. Fujino (1994), "Dynamic Characterization of Multiple Tuned Mass Dampers and Some Design Formulas," Earthquake Engineering and Structural Dynamics, Vol. 23, pp. 813-835.

2. Fediw, A.A., B. Breukelman, D.P. Morris and N. Isyumov (1993), "Effectiveness of a Tuned Sloshing Water Damper to Reduce the Wind-Induced Response of Tall Buildings," Proc. of the 7th U.S. National Conference of Wind Engineering, Vol. 1, Los Angeles, CA, June 27-20, pp. 233-242.

3. Fujii, K., Y. Tamura, T. Sato and T. Wakahara (1990), "Wind-Induced Vibration of Tower and Practical Applications of Tuned Sloshing Damper," J. Wind Engr. and Ind. Aerodyn., Vol. 33, pp. 263-272.

4. Fujino, Y., L. Sun, B.M. Pacheco and P. Chaiseri (1992), "Tuned Liquid Damper for Suppressing Horizontal Motion of Structures," Journal of Engineering Mechanics, Vol. 118, No. 10, October, pp. 2017-2030.

5. Gardarsson, S, and H. Yeh, (1994), "Numerical Simulations of Bores using the Random-Choice Method," Proc. of the 3rd UJNR Workshop.

6. Lepelletier, T.G. and F. Raichlen (1988), "Nonlinear Oscillations in Rectangular Tanks," Journal of Engineering Mechanics, Vol. 114, No. 1, ASCE, pp. 1-23.

7. Reed, D.A., J. Yu, H. Yeh, and S. Gardarsson (1996), "Experimental and Theoretical Investigations of Tuned Liquid Dampers," to appear in the Journal of Engineering Mechanics, 1997.

8. Sun, L.M., Y. Fujino, B.M. Pacheco, and P. Chaiseri, (1991). "Modeling Tuned Liquid Dampers," Proc. of the 8th International Conference on Wind Engineering.

9. Sun, L. (1991), Semi-analytical modeling of Tuned Liquid Damper (TLD) with Emphasis on Damping of Liquid Sloshing, Ph.D. thesis, University of Tokyo, Tokyo, Japan.

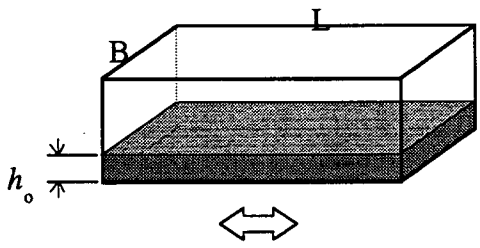
10. Wakahara, T., T. Ohyama and K. Fujii (1992), "Suppression of Wind-Induced Vibration of a Tall Building using the Tuned Liquid Damper," J. Wind Engr. and Ind. Aerodyn., Vol. 41-44, pp. 1895-1906.

11. Wakahara, T. (1993), "Wind-Induced Response of TLD-Structure Coupled System Considering Nonlinearity of Liquid Motion," Shimizu Tech. Res. Bull., No. 12, pp. 41-52.

12. Yamaguchi, H. and N. Harnpornchai (1993), "Fundamental Characteristics of Multiple Tuned Mass Dampers for Suppressing Harmonically Forced Oscillations," Earthquake Engineering and Structural Dynamics, Vol. 22, pp. 51-62.

Table 1: Data for the rectangular tanks.

Case ID	*Tank Size*		*Water Depth* h_0 *(mm)*	*Water Depth Ratio* ε	*Natural Freq.* f_w *(Hz)*	*Excitation Amplitude*	
	Length L (mm)	*Width B (mm)*				*A (mm)*	*A/L*
L335h9.6	335	203	9.6	0.029	0.457	10	0.030
L335h15	335	203	15	0.045	0.571	2.5,5,10,20,30	0.007 - 0.119
L590h15	590	335	15	0.025	0.325	2.5,5,10,20,30,40	0.004 - 0.068
L590h22.5	590	335	22.5	0.038	0.397	2.5,5,10,20,30,40	0.004 - 0.068
L590h30	590	335	30	0.051	0.458	2.5,5,10,20,30,40	0.004 - 0.068
L590h45	590	335	45	0.076	0.558	20	0.034
L900h30	900	335	30	0.033	0.301	2.5,5,10,20,30,40	0.003 - 0.044
L900h40	900	335	40	0.044	0.347	2.5,5,10,20,30,40	0.003 - 0.044
L900h55	900	335	55	0.061	0.406	10,20	0.011 - 0.022
L900h71	900	335	71	0.079	0.459	2.5,5,10	0.003 - 0.011



Excitation direction

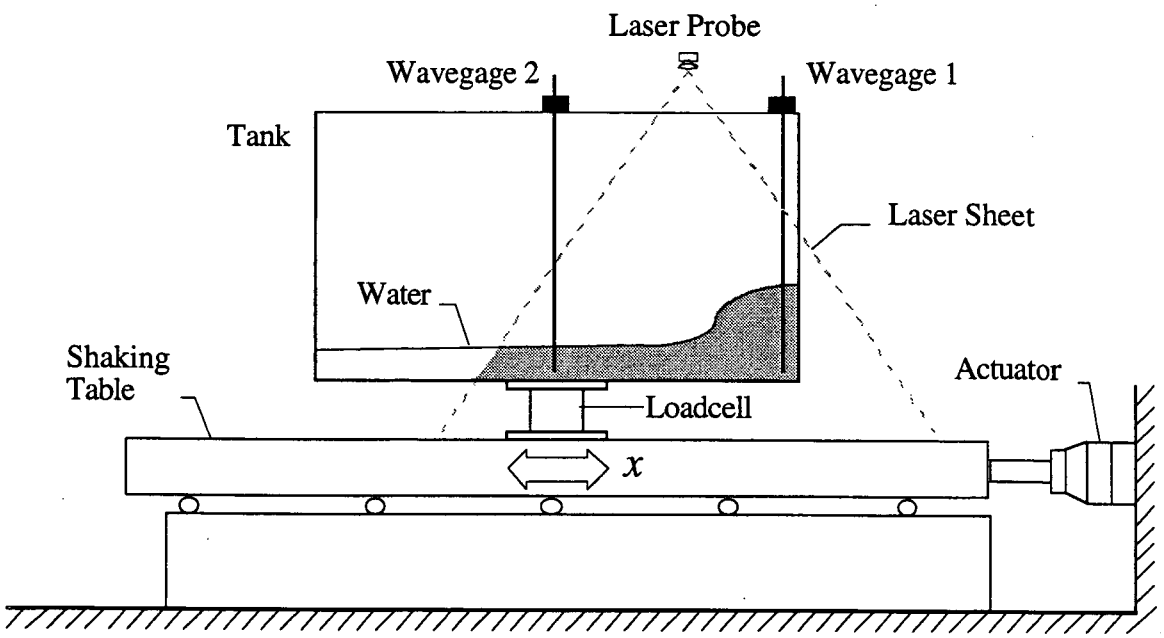


Figure 1: Shaking table experiment set-up

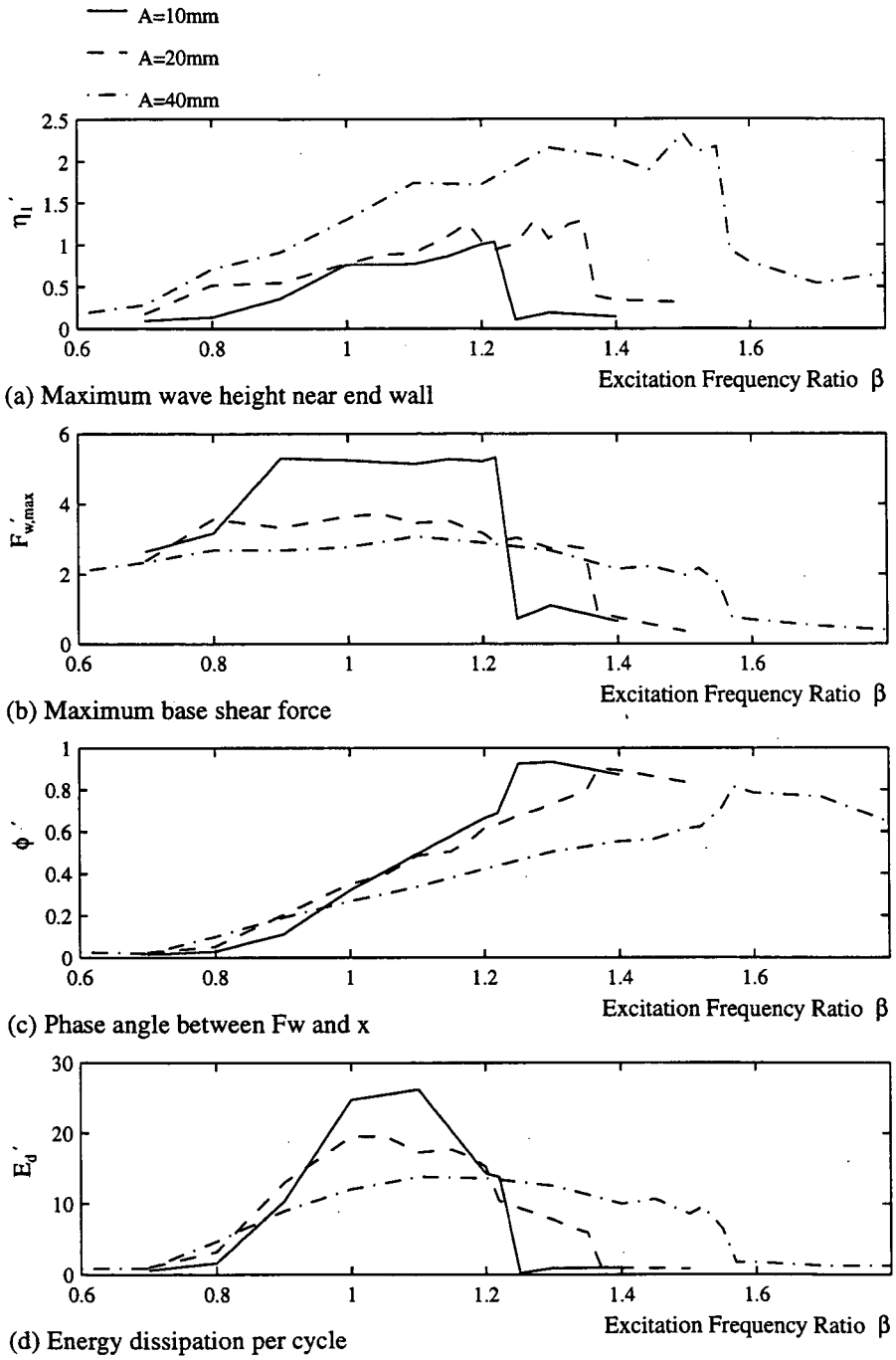


Figure 2: Sample frequency response curves for the water sloshing motion in the shaking table tests of the tank with length L = 590 mm, h_0 = 30 mm and excitation amplitudes A = 10, 20 and 40 mm. β is excitation frequency ratio.

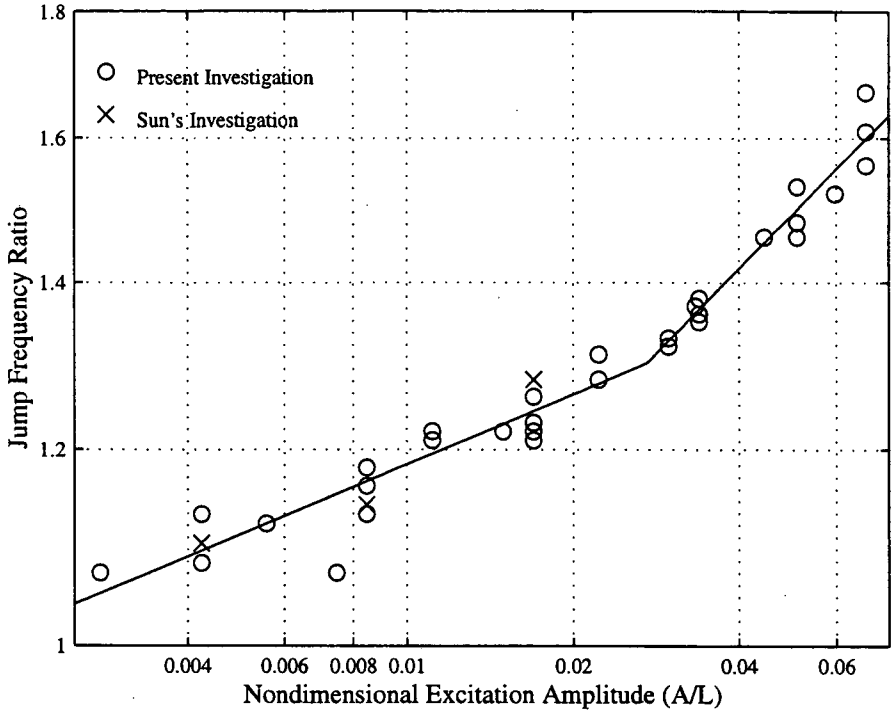


Figure 3: Relationship between the jump frequency ratio and the nondimensional excitation amplitude based on experimental results of Sun, et al. (1991) and the present investigation.

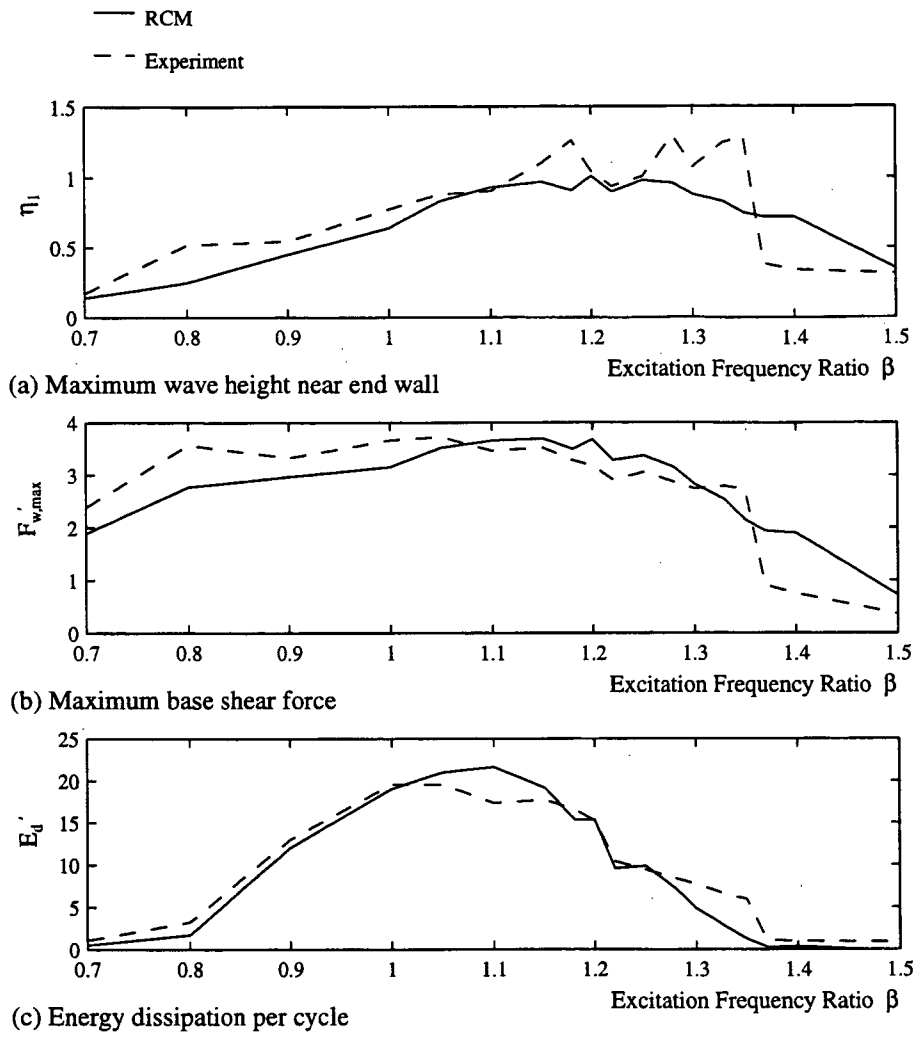


Figure 4: Frequency response comparisons using shaking table data and simulations using the random choice method for the rectangular tank of length $L = 590$ mm, $h_0 = 30$ mm and excitation amplitudes $A = 10$, 20 and 40 mm. β is excitation frequency ratio.

Theme 2

Earthquake engineering

Preparation of Active Fault Maps in Urban Area

Hiroshi MASAHARU[1], Hidetoshi NAKAJIMA[2], Masuo TAGUCHI[3], Tatsuo SEKIGUCHI[4] and Satoko ODAGIRI[5]

ABSTRACT

The Geographical Survey Institute, Japan made "Active Fault Map in Urban Area" which delineates position of active faults around urban area. The scale of these maps is 1:25,000 and they cover major urbanized area and cities in 45 map sheets. They are the most detailed maps on the position of active faults in Japan. The maps show active fault traces and their directions of movement as well as classification of landforms related to judgment of active faults. The specifications and symbols of these maps as well as the process for preparing the maps are explained in this paper. The aim and the role of these maps in earthquake disaster mitigation measures are also discussed.

Keywords:
Active Fault, Earthquake, Landform, Map

1. INTRODUCTION

After 1995 Hyogoken-nanbu earthquake (the Great Hanshin-Awaji Earthquake Disaster) which killed more than six thousand people and was caused by movement of faults just under the ground of urbanized area, the danger of active faults near urbanized area has become widely recognized. An active fault is a fault which is judged to move again in future with intervals of a thousand to several ten thousand years, from landforms showing repeated movements in recent several hundred thousand years. Intensive surveys on active faults are now carried out in Japan as a national project to evaluate risks of earthquakes and thus to mitigate hazards.

Geographic Department of the Geographical Survey Institute (GSI) has carried out geographic surveys and research works about neotectonic landforms. The existence and location of active faults can at first be surveyed by investigating landforms. With this background, the Geographic Department decided to make and publish maps describing the locations of active faults and other neotectonic landforms around urban area at very detailed scale of 1:25,000. As the survey of active faults requires much expert skills and knowledge, the survey work was carried out under collaboration with expert researchers at universities who are regarded as representatives in this research field. The map was named "Active Fault Map in Urban Area."

There already exists a book which shows active faults in whole Japan comprehensively. The book "Active Faults in Japan," first published in 1980 and the revised edition in 1991, uses 1:200,000 topographic maps as base maps. Much detailed information about the location of active faults especially around urban area has been required for disaster mitigation planning and for detailed investigation such as trenching of each active fault. Responding to the requirement, the GSI made "Active Fault Map in Urban Area" and by adopting the scale of 1:25,000, the positional accuracy are greatly improved compared with "Active Faults in Japan."

[1] Head, Third Geographic Division, Geographic Department, Geographical Survey Institute, Ministry of Construction, Kitasato-1, Tsukuba-shi, 305 Japan E-mail: masaharu@gsi-mc.go.jp
[2] Deputy Head, ditto
[3] Assistant Technical Officer, ditto
[4] Chief, Section of Disaster Prevention Geographic Information, Third Geographic Division, ditto
[5] Section of Disaster Prevention Geographic Information, ditto
Titles above written are those in Japanese fiscal year 1996 (April 1996-March 1997).

2. CONTENTS OF THE MAP - MAP SPECIFICATIONS AND SYMBOLS

This map expresses not only neotectonic landforms such as active faults but also other landforms made in Late Quaternary such as terraces or alluvial lowlands.

Active faults are grouped into four classes by their forms and reliability of locations; namely "Active Fault Trace," "Active Fault Trace (site indistinct)," "Active Flexure" and "Active Fault Trace (concealed)." These traces are drawn in red solid, broken or dotted lines respectively with some auxiliary symbols when necessary. But "Active Flexure" needs to be expressed with their width. Therefore we adopted an areal representation with small red dots pattern and arrows showing the downward direction of the flexure. In addition to these classes, the landform features which cannot be specified as active faults clearly under present conditions are grouped as "Presumed Active Fault" and they are expressed in black broken line.

Terraces are grouped into three classes by their formative period; namely "Higher Terrace," "Middle Terrace" and "Lower Terrace." These terraces are painted in orange color using dot screen. Deeper color is used for higher terraces. The newest landforms which were formed in recent thousands years are classified as "Alluvial Lowland," "Fan" and "Filled-up Land or Reclaimed Land." These landforms are painted in green color. Dot pattern is used for "Fan" and line pattern is used for "Filled-up Land or Reclaimed Land."

"Active Fault Map in Urban Area" is printed in five colors. Base topographic map is expressed in one color (gray). Two colors (red and black) are used for active faults etc. and other two colors (orange and green) are used for landform classification. The area expressed in one map sheet is 10 minutes in latitude and 15 minutes in longitude. This corresponds to four map sheets of 1:25,000 Topographic Maps published by the GSI. The Active Fault Map is printed on paper of the size of 788mm×1091mm.

Up to now, 45 map sheets in total of the Active Fault Map in Urban Area are published for the area of three large urban areas in Japan, namely the Metropolitan area, Cyukyo area and Kinki area, and special big cities which are designated by a government ordinance. The maps cover about 15,000 km^2 in total.

3. PROCESS OF PREPARATION OF THE MAP

A committee for preparation of Active Fault Map in Urban Area composed of 16 researchers at universities and staff of the GSI was organized. The committee held several meetings to discuss map specifications including adopting criteria of active faults and representation as map symbols of each feature, areas to be covered by the maps, assignment of survey area to each researcher, and results of survey. Intensive cross-check was done among researchers. Final results of checking were adopted and delineated on the map. As these maps have a characteristic of research result, the names of researchers in charge of respective map sheet is printed on the map.

The maps were made through aerial photo interpretation. Reference materials and research papers are also used. Aerial photos in 1940's and 1960's on a scale of 1:10,000 were used for the survey. The reason of using such old aerial photos is to observe original landforms before development activity. Due to artificial land development, it is becoming hard especially in urban areas of Japan to identify natural landforms created by fault movements. With these large scale photographs, geomorphologic features of active faults were newly discovered in some places.

4. CONCERNS BEFORE PUBLICATION AND RESPONSES TO THE MAPS AFTER PUBLICATION

Because these maps provide information on potential risks of earthquake hazards, cautious consideration was necessary before publishing

them to the open public. In order to avoid misunderstanding on the contents of the maps, brief explanation on the characteristics of the map is printed at lower right corner of each map sheet as "Attention in use." It explains that only the positions of active fault traces are shown in the map and it is not shown when each active fault moved in the past and will move in future. Therefore, the earthquake occurrence risk of each active fault cannot be understood from these maps. More detailed investigations on the activeness, history and other characteristics of each fault are necessary to evaluate the risk of the earthquake occurrence. This evaluation is still very difficult at the present level of science and technology. Furthermore not only information on active faults but also on peripheral ground such as structures are needed to evaluate the strength of ground motion caused by an earthquake.

The Active Fault Maps in Urban Area were published in October, 1996. The maps caught much attention of general public and were sold well as such maps meant for professional use. The responses to these maps were rather positive. Most inquiries on the maps to the GSI were asking where the maps were sold and whether there was an active fault map covering a certain town or city. We hope the maps would contribute to raising awareness of potential earthquake risks among citizens and be useful for disaster mitigation planning.

5. THE ROLE OF "ACTIVE FAULT MAPS IN URBAN AREA" IN EARTHQUAKE DISASTER MITIGATION MEASURES

For earthquake disaster mitigation planning, evaluation of potential risks of earthquake occurrence is required. It is now clear that earthquakes are destruction phenomena of underground rocks at fault planes. Therefore to investigate the existence and the precise positions of active faults is needed first of all for the evaluation of earthquake occurrence.

This can be carried out by geomorphologic study using aerial photo interpretation. This method has advantage that comprehensive survey of active faults is possible although it does not show us underground structures and precise history of previous activities (i.e. earthquakes). The "Active Fault Map in Urban Area" is the result of this effort. It shows the position of active faults around urbanized area in detailed positional accuracy.

It goes without saying that more detailed investigations are necessary for the evaluation of earthquake occurrence. Geophysical prospecting such as seismic prospecting is necessary to clarify underground structures of strata and faults. In some cases, the positions of active faults on the Active Fault Maps were corrected based on the results of seismic prospecting. Trenching of a fault provides detailed information of the activity of the fault including activeness and recent history of its activity. In order to carry out these investigations, information on precise position of active faults is needed. Active faults maps are meant to provide this fundamental information for all the research and survey work relating to active faults.

If potential of earthquake for each active fault were clarified, there still remain problems of evaluation of earthquake vibration at specific position and seismic design of buildings and infrastructures reflecting such knowledge. Preparation of active fault map is one of the efforts for earthquake disaster mitigation which is now carried out as a national project. Active fault map provides information of only the existence and position of active faults as mentioned in the previous section but it is the information that is firstly required for other research and surveys on active faults.

These maps are published to the public because information disclosure of governmental bodies are strongly required nowadays. This would also help to increase awareness on earthquake disaster of citizens who have key role in disaster mitigation.

6. FUTURE WORK AND CONCLUSION

The GSI plans to continue the preparation of the "Active Fault Map in Urban Area" for major urbanized areas such as capitals of prefectures in case that there exist major active faults. To make digital data of active faults and other features from these maps is now under consideration for the use in GIS.

The investigation concerning active fault is now being executed by several governmental organizations in Japan. We hope the Active Fault Maps in Urban Area are used effectively in these active fault investigation projects.

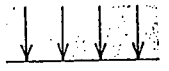
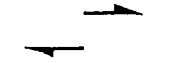
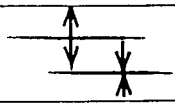
REFERENCES

Sekiguchi, T., Nakajima, H., Tsuzawa, M., Yoshitake, K., Masaharu, H., Taguchi, M. and Odagiri, S.: Preparation of Active Fault Map in Urban Area, Kokudochiri'in Jiho (Report of the GSI) No.86, Geographical Survey Institute, 1996. (in Japanese)

Ikeda, Y., Shimazaki, K. and Yamazaki, H.: A Primer on Active Faults in Japan, University of Tokyo Press, 1996. (in Japanese)

Research Group for Active Faults of Japan: Active Faults in Japan - revised edition, University of Tokyo Press, 1991. (in Japanese)

Table 1 Legend of Active Fault Map in Urban Area (part)

Active Fault Trace		red
Active Fault Trace (site indistinct)		red
Active Flexure		red
Active Fault Trace (concealed)		red
Strike Slip		red
Dip Slip		red
Earthquake Fault		black
Presumed Active Fault		black
Presumed Active Fault (by prospecting data)		black
Active Fold		black
Tilting Surface Direction		black

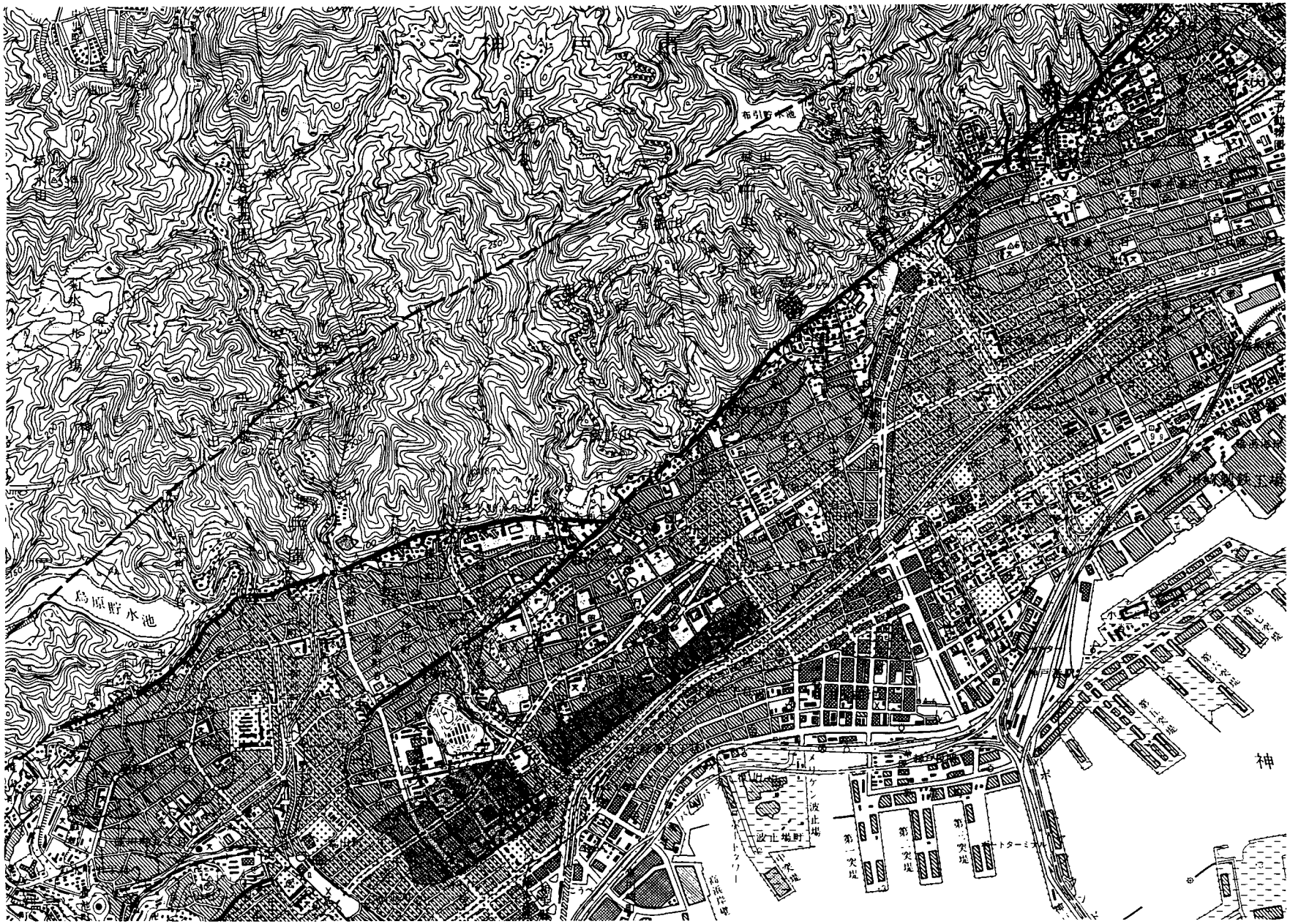


Figure 1 A portion of an Active Fault Map in Urban Area "Kobe" as an example ("Suwayama Fault" can be seen in the middle.)

SIMPLIFIED DESIGN PROVISIONS FOR HYBRID PRECAST CONNECTIONS

by
Geraldine S. Cheok[1] and H. S. Lew[2]

ABSTRACT

A rational design procedure is presented to compute the probable moment, the nominal moment, and the story drift capacities of a hybrid precast moment-resisting beam-to-column connection. The hybrid connections consist of mild steel which is used to dissipate energy by yielding and high strength prestressing steel which is used to provide the shear resistance through friction developed at the beam-column interface by the post-tensioning force. The design procedure is based on 1/3-scale hybrid precast beam-to-column connections tested at the National Institute of Standards and Technology (NIST). The simplified procedure relies on the stress-strain behavior of mild steel up to its ultimate strength and is based on equilibrium considerations at the beam-column joint.

KEYWORDS: Building technology, beam-column, concrete, connection, joint, drift capacity, moment capacity, precast, post-tensioning, seismic design procedure.

1.0 INTRODUCTION

Current building codes (such as the American Concrete Institute and Uniform Building Codes) used in high seismic areas of the United States have evolved toward sets of prescriptive rules which codify design provisions for a few building systems. Seismic resistant reinforced concrete systems have, in effect, been limited to cast-in-place shear walls and special moment resisting frames (SMRF). While these two systems have been shown to perform well during earthquakes, implementation of the details prescribed for a monolithic system into a prefabricated building is difficult.

The current UBC code [ICBO, 1994] allows alternative seismic systems to be used if the following requirements are met:

> "1627.9.2 **Undefined structural systems.** Undefined structural systems shall be shown by technical and test data which establish the dynamic characteristics and demonstrate the lateral-force resistance and energy absorption capacity to be equivalent to systems listed in Table 16-N for equivalent R_W values."

The precast moment frame using hybrid connections, shown in Figure 1, was developed to meet the requirements of an R_W = 12 system. The connection consists of mild steel [f_y = 414 MPa (60 ksi)] located at

[1]Research Structural Engineer, National Institute of Standards and Technology, Gaithersburg, MD.

[2]Chief, Structures Division, National Institute of Standards and Technology, Gaithersburg, MD.

the top and bottom of the beam and high strength prestressing steel [f_{pu} = 1862 MPa (270 ksi)] located at mid-depth of the beam. The mild steel is used to dissipate energy by yielding, and the prestressing steel is used to provide the shear resistance from the friction developed by the post-tensioning (PT) force. The mild steel is fully bonded except for a very short length and the PT steel is unbonded or partially debonded. The purpose of the short unbonded length of the mild steel is to delay fracture of the mild steel bars and the unbonding of the PT steel is intended to delay yielding of the PT steel. The term hybrid refers to the simultaneous use of two types of steel with different roles.

This paper briefly describes design procedures for the hybrid connections that ensure that both the required strength and story drift capacities are achieved. More details on the design procedure may be found in Cheok et al. (1996). The experimental program and connection details may be found in Stone et al. (1995).

2.0 DESIGN CONCEPT

The precast moment frame using the hybrid connection is based upon the following:

1. Multi-story columns are used with single bay beams requiring a connection at the beam column interface, which is also the location of maximum seismic moment.
2. A ductile connection is developed at the beam-column interfaces, causing all yielding at this location and minimal damage to the precast beams.
3. Post-tensioned reinforcement is used to provide a reliable clamping force at the beam-column interface to resist gravity loads.
4. Vertical shear resistance at the beam-column interface is provided by friction created by a combination of the PT clamping force and the compression portion of the moment couple.
5. At the required maximum drift, the PT steel remains elastic.
6. The concrete in the end regions of the beam is confined so that it will not spall at the required maximum drift.
7. Mild steel reinforcement provides a portion of the flexural strength in addition to providing energy dissipation.
8. Sufficient mild steel reinforcement is provided to resist the gravity loads on the beam in the unlikely event of strand anchorage failure. This is provided as a backup collapse prevention mechanism.

3.0 DESIGN FORCES

3.1 General

The drift requirements, strength reduction factors, and base shear may be calculated or obtained as prescribed by the UBC (ICBO, 1994). In a prestressed system, prior to decompression (zero tension stress in concrete), the system will behave in a manner comparable to a cast-in-place system,

except that the beams are not likely to crack. Gross section properties should be used to develop a representation of system stiffness. For the interval between decompression and yield, the section properties are between that of an uncracked section and a cracked section.

3.2 Maximum Drift Demand

The drift demand as used in this section differs from the UBC drift requirement both in purpose and calculation. The UBC drift requirement is a serviceability requirement and is based on drifts of an elastic structure subjected to UBC design forces. The proposed drift demands are estimates of story drifts that a structure may undergo in an earthquake and were computed from non-linear time history analyses of models subjected to a suite of acceleration records obtained from past earthquakes. Drift demands calculated from the non-linear time history analyses are shown in Figures 2 - 4. Based on the dynamic analyses (Figures 2 - 4) the following story drift demands are recommended:

1. 1.5% for UBC soil type 1
2. 3.5% for UBC soil type 2
3. 4.0% for UBC soil type 3

In lieu of the proposed drift demands, non-linear time history analyses using a site specific response spectrum may be used to determine the required drift demand.

4.0 VERTICAL SHEAR RESISTANCE

Vertical shear resistance at the column interface is provided by two mechanisms:

- Friction created by the clamping force provided by the PT force (F_p).
- Friction created by the compression portion of the moment couple induced by gravity, wind, or seismic moments at the beam column interface (C).

The shear demand at the beam column interface is a function of both the applied gravity loads and the induced seismic moments which are limited to the probable moment capacity of the connection (see Notation and Symbols for definitions of variables).

$$V_u \leq \phi V_n \qquad (1)$$

$$V_u \leq 1.4\, V_D + 1.7\, V_L + \frac{M_{pr1} + M_{pr2}}{L_{clear}} \qquad (2)$$

The frictional shear resistance is provided at the interface by the two mechanisms described above.

$$V_n = \mu (F_p + C) \qquad (3)$$

where μ, defined in Notation and Symbols, depends on the surface characteristics of the beam and column at the interface. A roughened surface [6 mm (0.25 in.)] per UBC 1911.7.9 (ACI 11.7.9) is recommended for this connection ($\mu = 1.0$).

4.1 Minimum Clamping Force

Using Eqs. 1, 2, and 3, the minimum required clamping force, after losses, F_p, is

$$\phi \mu F_p = 1.4 V_D + 1.7 V_L$$

$$F_p = \frac{1.4 V_D + 1.7 V_L}{\phi \mu} \quad (4)$$

Losses as defined in ACI 318-95, Section 18.6.1 should be considered.

4.2 Span-to-Depth Ratio

To ensure that no slip occurs between the beam and column, the minimum clear span to overall thickness of member, L/h, ratio shall be

$$\frac{L_{clear}}{h} \geq \frac{1}{\phi \mu} \quad (5)$$

for γ = d/h,

$$\frac{L_{clear}}{d} \geq \frac{1}{\phi \mu \gamma} \quad (6)$$

but not less than the required clear span to effective depth, L/d, ratio of 4 [UBC 1921.3.1.2 (ACI 21.3.1.2)]

5.0 MAXIMUM PRESTRESS

To safeguard against loss of the clamping force during load reversal, the maximum stress in the PT steel must be limited to ensure that no yielding of the PT steel occurs at maximum drift capacity. Lower initial prestress allows for greater strain capacity in the PT steel to accommodate the large story drift demands expected in a major earthquake.

The maximum limit on the concrete prestress is controlled by concrete strength and by the confinement in the compression zones.

6.0 PROBABLE MOMENT CAPACITY

6.1 Limit State Description

The proposed calculation procedure is intended to ensure that the hybrid connection is able to accommodate the story drift demands (See Section 3.2) while retaining at least 80% of its maximum capacity.

The performance requirement for the connection are as follows:

- The PT steel must not yield.
- The mild steel may yield but must not fracture before reaching the required drift demand.
- The compression region of the beam must be able to sustain large strains without degradation of its load carrying capacity.

These requirements are satisfied by limiting the initial stress in the PT steel, providing sufficient unbonded length of both PT and mild steels, and developing appropriate confinement details for the concrete compression zone.

6.2 Calculation Procedure

Assumptions:

1. The Whitney stress block is used for calculation of the concrete compression force.

2. The post-tensioning (PT) steel is located at mid-depth of the beam.

3. The mild steel debonds over a distance equal to 2.75 d_b on either side of the intentionally unbonded length when the beam moment is equal to the probable moment.[3]

4. Neglect the contribution of the compression steel.

The following variables are assumed to be known: A_{ps}, f'_c, $L_{u,ps}$, A_s, f_y, $\epsilon_{ps,ini}$, b, f_u, ϵ_u, d, h, d_b, L_u.

Procedure:

Step 1:

A. Compute the maximum force capacity of the mild steel, T_s.

$$T_s = A_s f_u \qquad (7)$$

The minimum area of bonded steel at the bottom of the connection shall satisfy:

$$A_s \geq \frac{V_D + V_L}{f_y} \qquad (8)$$

B. Determine the value of ϵ_u corresponding to f_u from a σ-ϵ curve for the mild steel.

C. Compute the elongation of the mild steel, Δ_s. The strain is assumed to be equal over the unbonded length.

$$\Delta_s = \epsilon_u (L_u + 5.5 d_b) \qquad (9)$$

Step 2:

A. Assume a neutral axis depth, c. The pivot for the joint rotation is assumed to occur at the neutral axis (see Figure 5).

B. Compute the elongation of the PT steel, Δ_{ps}, due to flexure.

$$\Delta_{ps} = \left[\frac{\frac{h}{2} - c}{d - c}\right] \Delta_s \qquad (10)$$

C. Compute the strain in the PT steel, ϵ_{ps}.

$$\epsilon_{ps} = \frac{\Delta_{ps}}{L_{u,ps}} + \epsilon_{ps,ini} \qquad (11)$$

D. Obtain the stress in the PT steel, f_{ps}, from the σ-ϵ curve for Grade 270 prestressing strands. Check that $f_{ps} < 0.9 f_{pu}$ to prevent yielding.

$$f_{ps} \leq 0.9 f_{pu} \qquad (12)$$

If $f_{ps} > 0.9 f_{pu}$, then:

[3]Tests at NIST have shown that mild steel bars grouted in ducts and subjected to cyclic loading will debond beyond the intentionally unbonded length. This distance varies and can be approximated by assuming the additional debond length will be equal to 2.75 d_b on either side of the intentionally unbonded length.

1. Increase the unbonded length of the PT steel or
2. Increase the amount of PT steel, or
3. Decrease the amount of mild steel.

Return to Step 1 if A_s is changed or to Step 2C if $L_{u,ps}$ is changed.

E. Compute the force in the PT steel, T_{ps}.

$$T_{ps} = A_{ps} f_{ps} \qquad (13)$$

Step 3:

A. Compute the concrete compression force, C_c.

$$C_c = T_s + T_{ps} \qquad (14)$$

B. Compute the neutral axis depth, c.

$$c = \frac{C_c}{0.85 f'_c b \beta_1} \qquad (15)$$

C. Compare the computed value of c from Step 3B with the assumed value of c from Step 2A.

D. If the computed value of c does not agree with the assumed value of c, set c to the value from Step 3B and repeat Steps 2 and 3 until the value of c has converged.

Step 4:

A. Compute the probable moment, M_{pr}, by summing moments about the concrete compressive force.

$$M_{pr} = M_s + M_{ps} \qquad (16)$$

$$M_s = T_s \left(d - \frac{\beta_1 c}{2} \right) \qquad (17)$$

$$M_{ps} = T_{ps} \left(\frac{h}{2} - \frac{\beta_1 c}{2} \right) \qquad (18)$$

Step 5:

A. Check M_s/M_{pr} ratio. To ensure that during load reversal the gap between the beam and the column is closed at zero drift, there has to be sufficient PT force to cause compression yielding of the mild steel. A limit of 0.5 is proposed based on equations developed by Mole [Mole, 1994].

$$\frac{M_s}{M_{pr}} \leq 0.5 \qquad (19)$$

If M_s/M_{pr} is greater than 0.5, reduce A_s and return to Step 1 or increase A_{ps} and return to Step 2E.

6.3 Maximum Drift Capacity

The maximum drift capacity is calculated by setting the mild steel strain equal to the steel strain corresponding to the ultimate tensile strength. This calculated maximum drift capacity is a lower bound.

6.3.1 Computation of Maximum Drift Capacity

The procedure given in Section 6.2, Steps 1 to 3, is used to compute the location of the neutral axis and the following additional procedure is used to obtain the maximum drift capacity.

A. Compute beam rotation, θ (Figure 5).

Using the value of c obtained in the calculation of the probable moment capacity, determine the beam rotation which is taken as the drift capacity.

$$\theta = \frac{\Delta_s}{d - c} \qquad \textbf{(20)}$$

B. The story drift capacity equals the beam rotation, θ, at the probable moment capacity. Since this procedure yields a lower bound for the story drift capacity, no capacity reduction factor is used.

$$\textit{Story drift} = \theta \qquad \textbf{(21)}$$

C. Check that the drift capacity is greater than the drift demand as specified in Section 3.2. If the drift capacity does not meet the drift demand, then increase L_u.

7.0 NOMINAL MOMENT CAPACITY

The nominal moment capacity may be calculated using the two methods presented below. The nominal moment capacity as obtained using Method 2 (Eq. 22) is recommended for its simplicity.

Method 1

The nominal moment capacity is calculated following the procedure outlined in Section 6.2 with the following changes:

- The mild steel stress equal to f_y. Change Equation 7 to read:
$$T_s = A_s f_y.$$
- Set the strain in the mild steel strain equal to the strain at the onset of strain hardening, ϵ_{sh}. $\epsilon_{sh} = 0.01$ typically for Grade 60 bars.
- The total unbonded length is set equal to the intentionally unbonded length, L_u, of the mild steel. Change Equation 9 to read:
$$\Delta_s = \epsilon_{sh} L_u.$$

Method 2

$$M_n = 0.70\, M_{pr} \qquad \textbf{(22)}$$

where M_{pr} is calculated following the procedure outlined in Section 6.2.

8.0 BEAM AND COLUMN DESIGN

The body of the beam away from the connection region shall be designed in accordance with UBC 1994 or ACI 318-95.

Column design for the precast moment frame using the hybrid connections must satisfy capacity design requirements [UBC 1994 and ACI 318-95].

REFERENCES

ACI 318, (1995), "Building Code Requirements for Structural Concrete (ACI 318-95) and Commentary (ACI 318R-95)," American Concrete Institute, Detroit, MI, October.

Cheok, G. S., Stone, W. C., and Nakaki, S. D. (1996), *"Simplified Design Procedure for Hybrid Precast Concrete Connections,"* NISTIR 5765, National Institute of Standards and Technology, Gaithersburg, MD, February, 1996.

International Conference of Building Officials (1994), "Uniform Building Code: Volume. 2, Structural Engineering Design Provisions," Whittier, CA, May.

Mole, A. (1994), "Seismic Response of Hybrid Connections in Precast Concrete Frames," Thesis for degree in Master of Science in Engineering, University of Washington, Seattle, WA, December.

Stone, W. C., Cheok, G. S., Stanton, J. F. (1995), "Performance of Hybrid Moment-Resisting Precast Beam-Column Concrete Connections Subjected to Cyclic Loading," ACI Structural Journal, Vol. 92, No. 2, American Concrete Institute, Detroit, MI, March-April.

NOTATION AND SYMBOLS

A_{ps} = Area of PT steel.
A_s = Area of mild tension steel.
b = Beam width.
C = Total compression force.
C_c = Concrete compression force.
C'_s = Compressive force contribution from the mild compressive steel.
c = Depth from the extreme compression fiber to the neutral axis.
d = Effective depth.
d_b = Diameter of reinforcing bar.
f'_c = Concrete compressive strength.
f_{ps} = Stress in PT steel.
f_{pu} = Ultimate tensile strength of PT steel.
f_u = Ultimate tensile strength of mild steel.
f_y = Yield strength of mild steel.
F_p = Post-tensioning force.
h = Overall member thickness.
L_{clear} = Beam clear span.
L_u = Intentional unbonded length of mild steel.
$L_{u, ps}$ = Unbonded length of the PT steel.
M_n = Nominal moment capacity.
M_{pr} = Probable moment capacity of beam = $M_s + M_{ps}$.
$M_{pr1, pr2}$ = Probable beam end moments as determined in Section 6.
M_{ps} = Beam moment capacity contributed by post-tensioned steel.
M_s = Beam moment capacity contributed by mild steel.

T_{ps} = Tension force in PT steel.

T_s = Tension force in mild tension steel.

V_D = Unfactored shear force due to dead load.

V_L = Unfactored shear force due to live load.

V_n = Nominal shear strength.

V_u = Required shear strength.

β_1 = Factor defined in UBC Section 1910.2.7.3 (ACI 10.2.7.3).

Δ_{ps} = Elongation of the PT steel.

Δ_s = Elongation of the mild steel.

ϵ_{sh} = Strain at onset of strain hardening of mild steel.

ϵ_{ps} = Strain in the PT steel.

$\epsilon_{ps,ini}$ = Initial strain in the PT steel after losses due to post-tensioning force.

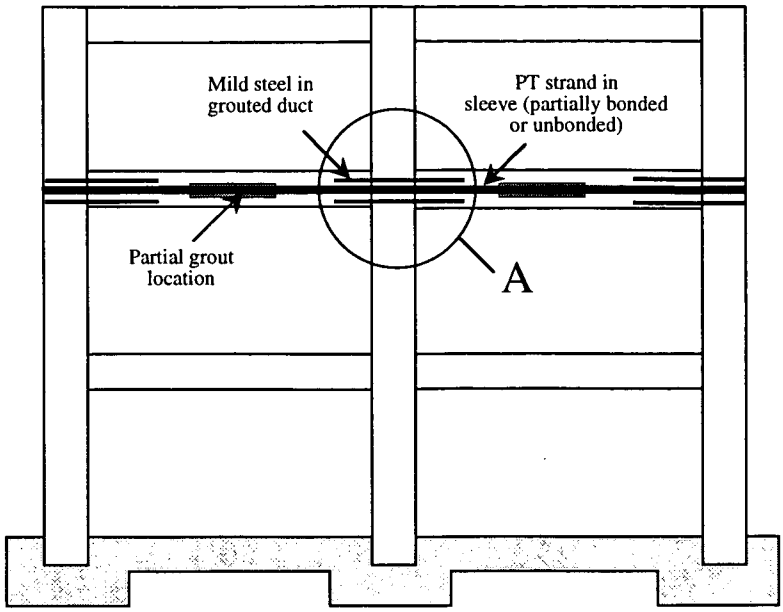
ϵ_u = Mild steel strain at ultimate stress, f_u.

γ = Ratio of d/h.

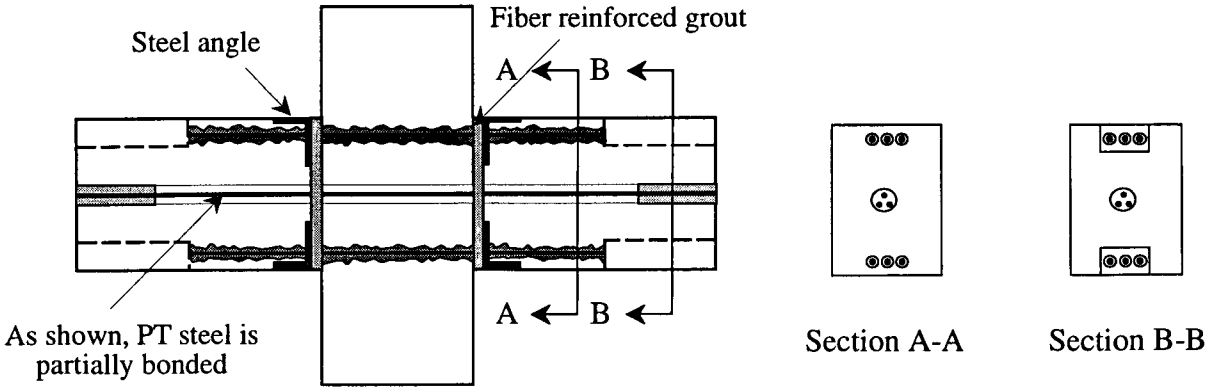
ϕ = Strength reduction factor.

μ = Coefficient of friction as defined in UBC Section 1911.7.4.3 (ACI 11.7.4.3).

θ = Beam rotation.



Elevation



Note: Column bars omitted for clarity

Detail A

Figure 1. Precast Hybrid Moment Connection.

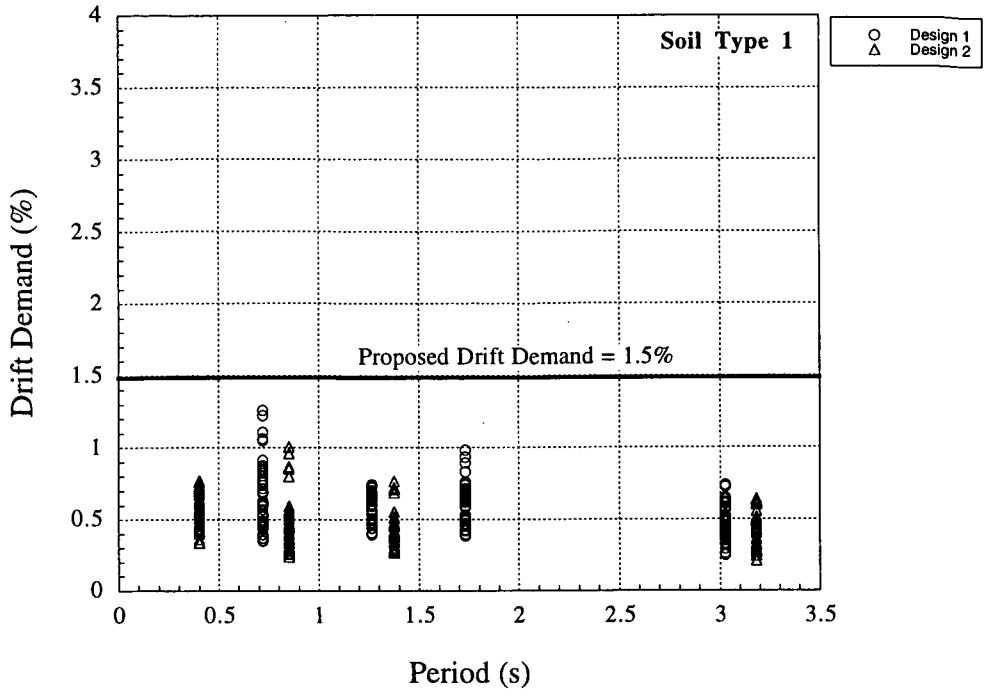


Figure 2. Drift Demand for UBC Soil Type 1.

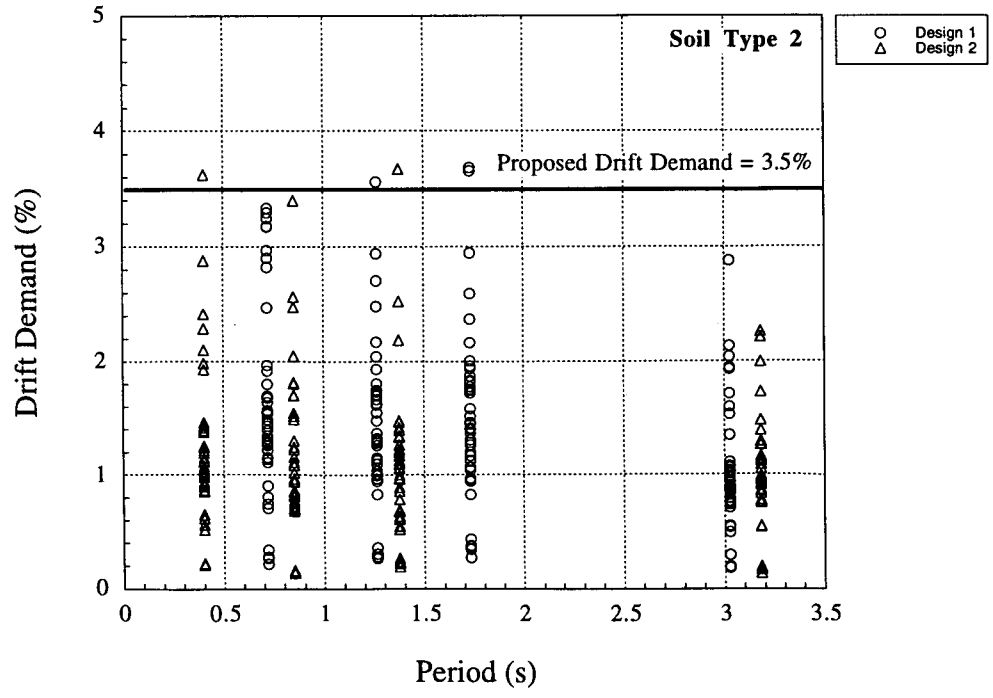


Figure 3. Drift Demand for UBC Soil Type 2.

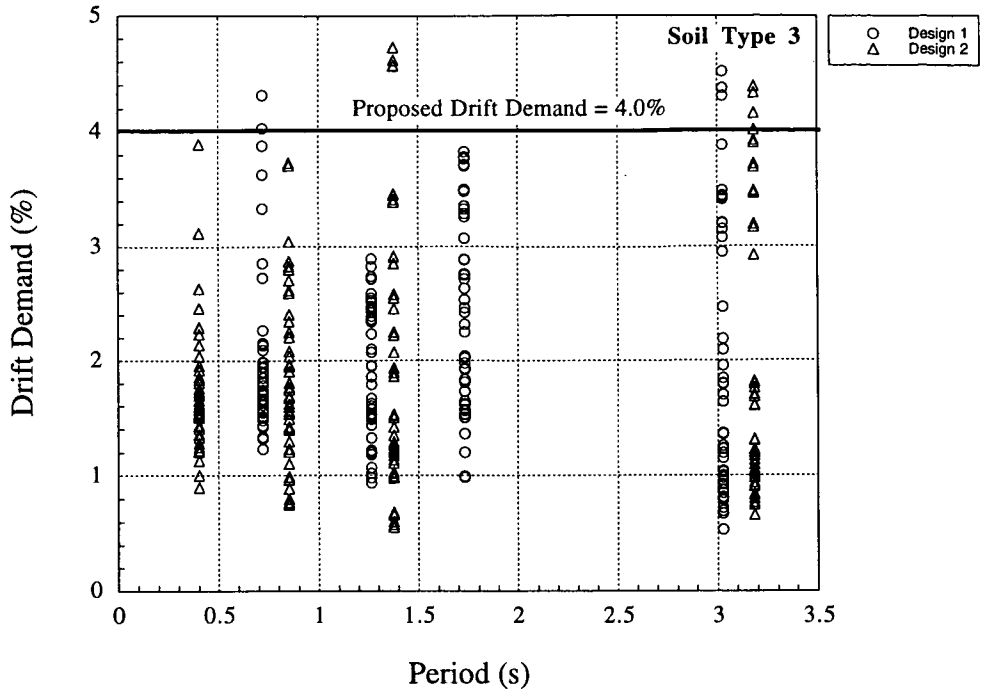


Figure 4. Drift Demand for UBC Soil Type 3.

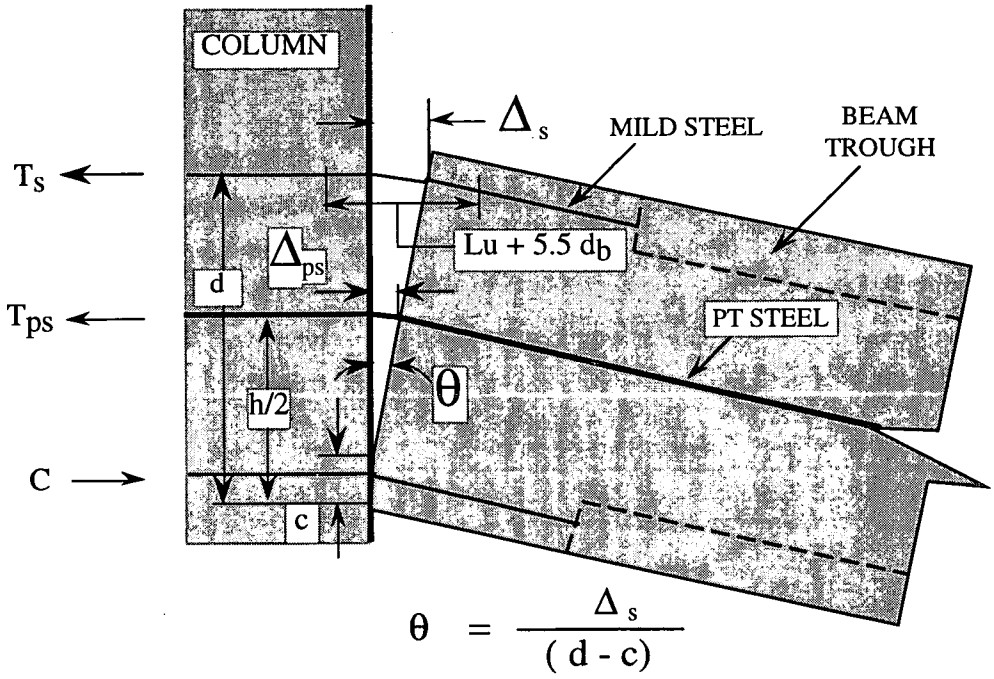


Figure 5. Rotation at the Beam-Column Joint.

SEISMIC RETROFIT OF EXISTING HIGHWAY BRIDGES IN JAPAN

by

Shigeki UNJOH[1], Toru TERAYAMA[2], Yukio ADACHI[2] and Jun-ichi HOSHIKUMA[3]

ABSTRACT

This paper presents current technical developments for seismic retrofit of existing highway bridges in Japan. The histories of the past seismic design codes and past seismic retrofit practices are firstly described. The damage caused by the 1995 Hyogo-ken nanbu Earthquake and the lessons learned from the earthquake are briefly described. The seismic retrofit program after the Hyogo-ken nanbu Earthquake is then described with emphasis on the seismic retrofit of reinforced concrete piers as well as research and development on the seismic retrofit of existing highway bridges.

KEY WORDS : Seismic Retrofit
Highway Bridges
Hyogo-ken nanbu Earthquake
Reinforced Concrete Piers

1. INTRODUCTION

Japan is one of the most seismically disastrous countries in the world and has often suffered significant damage from large earthquakes. More than 3,000 highway bridges suffered damage in the past earthquakes since the 1923 Kanto Earthquake. The earthquake disaster prevention technology for highway bridges had been developed based on the such bitter damage experiences. Various provisions for preventing damage due to instability of soils such as soil liquefaction have been adopted. Furthermore, design detailings including the unseating prevention devices have been implemented. With progress of the improvement of the seismic design provisions, the damage to highway bridges by the earthquakes had been decreasing in recent years.

However, the Hyogo-ken nanbu Earthquake of January 17, 1995, caused destructive damage to highway bridges. Collapse and nearly collapse of superstructures occurred at 9 sites, and other destructive damage occurred at 16 sites (1). The earthquake revealed that there are a number of critical issues to be revised in the seismic design and seismic retrofit of bridges.

After the earthquake the "Committee for Investigation on the Damage of Highway Bridges Caused by the Hyogo-ken nanbu Earthquake" (chairman : Toshio IWASAKI, Executive Director, Civil Engineering Research Laboratory) was formulated in the Ministry of Construction to survey the damage and clarify the factors which contributed to the damage.

On February 27, 1995, the Committee approved the "Guide Specifications for Reconstruction and Repair of Highway Bridges which suffered Damage due to the Hyogo-ken nanbu Earthquake (2)," and the Ministry of Construction noticed on the same day that the reconstruction and repair of the highway bridges which suffered damage during the Hyogo-ken nanbu Earthquake should be made

1) Head, Earthquake Engineering Division, Earthquake Disaster Prevention Research Center, Public Works Research Institute, Ministry of Construction, Tsukuba-shi, Ibaraki-ken, 305 , Japan
2) Senior Research Engineer, ditto
3) Research Engineer, ditto

according to the Guide Specifications. It was decided by the Ministry of Construction on May 25, 1995 that the Guide Specifications should be tentatively used in all sections of Japan as emergency measures for seismic design of new highway bridges and seismic retrofit of existing highway bridges until the Design Specifications of Highway Bridges was revised. The Design Specifications has been revised in November 1996 based on the Guide Specifications and further research and development which were made after the Hyogo-ken nanbu Earthquake.

This paper summarizes the current technical developments for seismic retrofit of existing highway bridges in Japan as well as the past seismic retrofit practices.

2. HISTORIES OF PAST SEISMIC DESIGN CODES AND SEISMIC RETROFIT PRACTICES BEFORE THE HYOGO-KEN NANBU EARTHQUAKE

(1) History of Past Seismic Design Codes for Highway Bridges

One year after the 1923 Kanto Earthquake, it was initiated to consider the seismic effect in the design of highway bridges. The Civil Engineering Bureau of the Ministry of Interior notified "the method of seismic design of abutments and piers" in 1924. The seismic design method has been developed and improved through bitter experiences in a number of past earthquakes and with progress of technical developments in earthquake engineering. **Table 1** summarizes the history of provisions in seismic design for highway bridges.

In particular, the seismic design method was integrated and upgraded by compiling the "Specifications for Seismic Design of Highway Bridges" in 1971, which exclusively provided issues related to seismic design. The design method for soil liquefaction and unseating prevention devices were introduced in the Specifications. It was revised in 1980 and integrated as "Part V : Seismic Design" in "Design Specifications of Highway Bridges." The primitive check method for ductility of reinforced concrete piers were included in the reference of the Specifications. It was further revised in 1990 and ductility check of reinforced concrete piers, soil liquefaction, dynamic response analysis, and design detailings were prescribed. It should noted here that the detailed ductility check method for reinforced concrete piers was firstly introduced in the 1990 Specifications.

(2) History of Seismic Evaluation and Retrofit of Highway Bridges

The Ministry of Construction made seismic evaluation of highway bridges 5 times throughout the country since 1971 as a part of the comprehensive earthquake disaster prevention measures for highway facilities. Seismic retrofit for vulnerable highway bridges had been successively made based on the seismic evaluations. **Table 2** shows the history of past seismic evaluations (4-11).

The first seismic evaluation was made in 1971 to promote earthquake disaster prevention measures for highway facilities. The significant damage of highway bridges caused by the San Fernando Earthquake, U.S.A. in February 1971 triggered the seismic evaluation. Highway bridges with span length longer than or equal to 5m on all sections of national expressways and national highways, and sections of the others were evaluated. Attention was paid to detect deterioration such as cracks of reinforced concrete structures, tilting, sliding, settlement and scouring of foundations. Approximately 18,000 highway bridges in total were evaluated and approximately 3,200 bridges were found to require retrofit.

Following the first seismic evaluation, it had been subsequently made in 1976, 1979, 1986

and 1991 with gradually expanding highways and evaluation items. The seismic evaluation in 1986 was made with the increase of social needs to insure seismic safety of highway traffic after the damage caused by the Urakawa-oki Earthquake in 1982 and the Nihon-kai-chubu Earthquake in 1983. The highway bridges with span length longer than or equal to 15m on all sections of national expressways, national highways and principal local highways, and sections of the others, and overpasses were evaluated. The evaluation items included deterioration, unseating prevention devices, strength of substructures and stability of foundations. Approximately 40,000 bridges in total were evaluated and approximately 11,800 bridges were found to require retrofit. Latest seismic evaluation was made in 1991. The highways to be evaluated was expanding from the evaluation in 1986. Approximately 60,000 bridges in total were evaluated ad approximately 18,000 bridges were found to require retrofit. Through a series of seismic retrofit works, approximately 32,000 bridges were retrofitted by the end of 1994.

In the seismic evaluation in 1986 and 1991, the evaluation was made based on a statistical analysis of bridges damaged and undamaged in the past earthquakes (12). Factors which affect seismic vulnerability were detected as shown in **Table 3. Table 4** shows the inspection sheet proposed to evaluate the seismic vulnerability. Because collapse of bridges tends to be developed due to the excessive relative movement between the superstructure and the substructures, and failure of substructures associated with inadequate strength, the evaluation is made in **Table 4** based on both the relative movement and the strength of substructure.

Emphasis had been placed to install the unseating prevention devices in the past seismic retrofit. Because the installation of the unseating prevention devices was being completed, it had become important to promote the strengthening of substructures with inadequate strength and lateral stiffness.

3. LESSONS LEARNED FROM THE HYOGO-KEN NANBU EARTHQUAKE

Hyogo-ken Nanbu earthquake was the first earthquake which hit an urban area in Japan since the 1948 Fukui Earthquake. Although the magnitude of the earthquake was moderate (M7.2), the ground motion was much larger than anticipated in the codes. It occurred very close to the Kobe City with shallow focal depth.

Damage was developed at highway bridges on Routes 2, 43, 171 and 176 of the National Highway, Route 3 (Kobe Line) and Route 5 (Bay Shore Line) of the Hanshin Expressway, the Meishin and Chugoku Expressway. Damage was surveyed by the "Committee for Investigation on the Damage of Highway Bridges caused by the Hyogo-ken nanbu Earthquake" for all bridges on National Highways, Hanshin Expressways and Expressways in the area where destructive damage occurred. Total number of piers surveyed reached 3,396 (1).

The "Committee for Investigation on the damage of Highway Bridges Caused by the Hyogo-ken nanbu Earthquake" concluded the followings based on the investigations of the damage to highway bridges.

1) Based on the strong motion records and earthquake response analyses of the ground, the effect of the horizontal ground motion by the earthquake on the structures was the largest after the Niigata Earthquake of 1964 when the strong motion observation was initiated. The level of the ground motion was larger than that considered in the practical design. The strong motion was also observed in the vertical direction.

2) There were reinforced concrete piers which were heavily damaged from the bending to

shear at mid-height where some of the longitudinal re-bars were terminated without enough anchorage length. The piers were designed before 1980. These bridges were also damaged to the bottom. Based on the analysis of the relation between the design code and damage piers, 14% in the total piers were heavily damaged on Route 3 (Kobe Line) of Hanshin Expressway which were designed according to 1964 and 1971 Specifications. Heavy damage was not found on Route 5 (Bay Shore Line) of Hanshin Expressway which were design according to 1980 and 1990 Specifications.

3) There were steel bridge piers at which local buckling at the web and flange of rectangular section steel piers was caused by the horizontal earthquake force. Then the fracture at the corner welding occurred and the deck was subsided by the decrease of vertical strength of piers.

4) Most of damage to superstructures were caused by the damage to bearing supports. And there were damage to fixing portion of the restrainers.

5) Some devices to connect adjacent girders were not effective to prevent unseating of superstructures.

6) Many damages such as fracture of set bolts, damage of bearing itself, dislodgement of roller and fracture of anchor bolts, were found at the steel bearings. Damage to rubber bearings were much smaller than that to steel bearings.

7) Further study should be made on the effect of ground flow on bridges. Ground with larger particles, such as gravel sand which is not required to check the liquefaction in the then code, was liquefied. Liquefaction-induced ground flow was also found and some bridge foundations were affected by the ground flow.

4. SEISMIC RETROFIT PROGRAM AFTER THE HYOGO-KEN NANBU EARTHQUAKE

(1) Seismic Design for Reconstruction and Repair

For seismic design of reconstruction of highway bridges that suffered damage due to the Hyogo-ken nanbu Earthquake, the "Guide Specifications for Reconstruction and Repair of Highway Bridges Which Suffered Damage due to the Hyogo-ken Nanbu Earthquake (2)" was issued by the Ministry of Construction on February 27, 1995 upon approval by the "Committee for Investigation on the Damage of Highway Bridges Caused by the Hyogo-ken Nanbu Earthquake." The Guide Specifications was applied only for reconstruction and repair of the highway bridges that suffered damage due to the Hyogo-ken nanbu Earthquake.

The bridges shall be designed so that they can resist with enough structural safety against the earthquake force developed during Hyogo-ken nanbu Earthquake. To achieve this goal, the following basic principles shall be considered.

1) To increase the ductility of whole bridge systems, dynamic strength and ductility shall be assured for whole structural members in which seismic effect is predominant. Although the check of dynamic strength and ductility has been adopted for reinforced concrete piers since 1990, it has not been applied for other structural members such as steel piers and foundations.

2) Seismic safety against the Hyogo-ken nanbu Earthquake shall be verified by dynamic response analysis considering nonlinear behavior of structural members.

3) In design of elevated continuous bridges, it is appropriate to adopt the Menshin Design for distributing lateral force of superstructure to many substructures. The Menshin Design is close to the seismic isolation, but the emphasis is placed to increase energy dissipating capability and to distribute lateral force of deck to substructures.

4) Enough tie reinforcements to assure the ductility shall be provided in reinforced concrete piers, and the termination of main reinforcements at mid-height shall not be made.

5) Concrete shall be filled in steel piers to

assure dynamic strength and ductility. Steel piers designed by the current practice developed local bucking at web and flange plates although they were stiffened by longitudinal stiffeners and diaphragms. This tends to cause sudden decrease of bearing capacity in lateral direction after the peak strength and therefore less energy dissipation is anticipated. This subsequently deteriorates the bearing capacity of steel piers in vertical direction. Because it is now at the stage that technical developments are being made to avoid such behavior, it was decided to tentatively use steel piers with infilled concrete for reconstruction and repair.

6) Foundations shall be designed so that they have enough dynamic strength and deformation capability for lateral force. The dynamic strength and deformation capability of foundations shall be larger than the flexural strength and ductility of piers to prevent damage at foundations.

7) It is suggested to further use rubber bearings because they absorb relative displacement developed between a superstructure and substructures. In design of bearings, correct mechanism of force transfer from a superstructure to substructures shall be considered.

8) The devices to prevent falling-down of a superstructure from substructures shall be designed so that they can assure falling-down of decks. Attention shall be paid so as to dissipate energy and to increase strength and deformation capability.

9) At those sites where potential to cause lateral spreading associated with soil liquefaction is high, its effect shall be considered in design. Because technical information to evaluate earth pressure in laterally spreading soils is limited, it is important to recognize that such evidence exists and that countermeasures shall be taken in any possible ways.

(2) Reference for Applying Guide Specifications to New Highway Bridges and Seismic Retrofit of Existing Highway Bridges

For increasing seismic safety of the highway bridges which suffered damage by the Hyogo-ken nanbu Earthquake, various new drastic changes were tentatively introduced in the Guide Specifications for Reconstruction and Repair of Highway Bridges Which Suffered Damage due to the Hyogo-ken Nanbu Earthquake. Although intensified review of design could be made when it was applied to the bridges only in the Hanshin area, it may not be so easy for field design engineers to following up the new Guide Specifications when the Guide Specifications is used for seismic design of all new highway bridges and seismic strengthening of existing highway bridges. Based on such demand, the Reference for Applying the Guide Specifications to New Bridges and Seismic Strengthening of Existing Bridges was issued on June 30, 1995 by the Sub-Committee for Seismic Countermeasures for Highway Bridges, Japan Road Association.

The Reference classified the application of the Guide Specifications as shown in **Table 5** based on the importance of the roads. All items of the Guide Specifications are applied for bridges on extremely important roads, while some items which prevent brittle failure of structural components are applied for bridges on important roads. For example, for bridges on the important roads, the items for menshin design, tie reinforcements, termination of longitudinal reinforcements, type of bearings, unseating prevention devices and countermeasures for soil liquefaction are applied, while the remaining items such as the design force, concrete infilled steel bridges, and ductility check for foundations are not applied.

Because damage concentrated to single reinforced concrete piers/columns with small concrete section, the seismic retrofit program has initiated for those columns, which were designed by the pre-1980 Design

Specifications, at extremely important bridges such as bridges on expressways, urban expressways, and designated highway bridges, and also double-deckers and overcrossings, etc. which significantly affect highway functions once damaged. The program is 3 years program and approximately 30,000 piers will be evaluated and retrofitted. Unseating devices also should be installed for these extremely important bridges.

Main purpose of the seismic retrofit of reinforced concrete columns is to increase their shear strength, in particular in the piers with termination of longitudinal reinforcements without enough anchoring length. This increases ductility of columns, because premature shear failure could be avoided.

However if only ductility of piers is increased, residual displacement developed at piers after an earthquake may increase. Therefore the flexural strength should also be increased. However the increase of flexural strength of piers tends to increase the seismic force transferred from the piers to the foundations. It was found from an analysis to various types of foundations that failure of the foundations by increasing the seismic force may not be significant if the increasing rate of the flexural strength of piers is less than 2. It is therefore suggested to increase the flexural strength of piers within this limit so that it does not cause serious damage to foundations.

For such requirements, seismic strengthening by Steel Jackets with Controlled Increase of Flexural Strength was suggested. This uses steel jacket surrounding the existing columns as shown in **Fig.1**. Epoxy resin or non shrinkage concrete mortar are injected between the concrete surface ands the steel jacket. A small gap is provided at the bottom of piers between the steel jacket and the top of footing. This prevents to excessively increase the flexural strength.

To increase the flexural strength of columns in a controlled manner, anchor bolts are provided at the bottom of the steel jacket. They are drilled into the footing. By selecting appropriate number and size of the anchor bolts, the degree of increase of the flexural strength of piers may be controlled. The gap is required to trigger the flexural failure at the bottom of columns. A series of loading tests are being conducted at the Public Works Research Institute to check the appropriate gap and number of anchor bolts. **Table 6** shows a tentatively suggested thickness of steel jackets and size and number of anchor bolts. They are for reinforced concrete columns with a/b less than 3, in which a and b represent the width of column in transverse and longitudinal direction, respectively. The size and number of anchor bolts were evaluated so that the increasing rate of flexural strength of columns is less than about 2.

Conventional reinforced concrete jacketing methods is also applied for the retrofit of reinforced concrete piers, especially for the piers which require the increase of strength. It should be noted here that the increase of the strength of the pier should carefully be designed in consideration with the strength of foundations and footings.

5. RESEARCH AND DEVELOPMENT ON SEISMIC EVALUATION AND RETROFIT OF HIGHWAY BRIDGES

(1) Prioritization Concept for Seismic Evaluation

The 3 year retrofit program will be completed in 1997 fiscal year. In the program, the single reinforced concrete piers/columns with small concrete section which were designed by the pre-1980 Design Specifications on important highways have been evaluated and retrofitted and the other bridges with wall-type piers, steel piers, and frame piers and so on as well as the bridges on the other highways should be

evaluated and retrofitted if required in the next retrofit program. Since there are approximately 200,000 piers, it is required to develop the prioritization methods and the evaluation methods of the vulnerability for the intentional retrofit program.

Fig.2 shows the simple flow chart to give the prioritization of the retrofit works to bridges. The importance of highway, structural factor, members vulnerability (reinforced concrete piers, steel piers, unseating prevention devices, foundations) are the factors to be considered for the prioritization.

Priority R of each bridges may be evaluated by Eq.(1).

$$R = I \cdot S \cdot V_T \cdot w_v \cdot (f(V_{RP1}, V_{RP2}, V_{RP3}), V_{MP}, V_{FS}, V_F) \times 100 \quad (1)$$

$$f(V_{RP1}, V_{RP2}, V_{RP3}) = V_{RP1} \cdot V_{RP2} \cdot V_{RP3} \quad (2)$$

in which R = priority, I = importance factor, S = earthquake force, V_T = structural factor, w_v = weighting factor on structural members, V_{RP1} = design specification, V_{RP2} = pier structural factor, V_{RP3} = aspect ratio, V_{MP} = steel pier factor, V_{FS} = unseating device factor, and V_F = foundation factor. The each item and category with a weighting number is tentatively shown in **Table 7**. If applied this prioritization method to the bridges damaged during the Hyogo-ken-nanbu Earthquake, the categorization number is given as shown in **Table 7**.

(2) Seismic Retrofit of Wall-Type Piers

The steel jacketing method as described in the above was applied for reinforced concrete with circular section or rectangular section of a/b <3. It is required to develop the seismic retrofit method for a wall-type pier. The confinement of concrete was provided by a confinement beam such as H-shaped steel beam for rectangular piers. However, since the size of the confinement beam become very large, the confinement may be provided by other measures such as intermediate anchors for a wall-type pier.

The seismic retrofit concept for a wall-type pier is the same as that for rectangular piers. It is important to increase the flexural strength and ductility capacity with the appropriate balance. Generally, the longitudinal reinforcement ratio is smaller than that for the rectangular piers, therefore the flexural strength is smaller. Therefore, it is essential to increase the flexural strength appropriately. Since of the longitudinal reinforcement was generally terminated at mid-height without appropriate anchorage length, it is also important to strengthen both of flexural and shear strength mid-height section.

Fig.3 shows the possible seismic retrofit method for a wall-type piers. To increase the flexural strength, the additional reinforcement by re-bars or anchor bars are fixed to the footing. The number of reinforcement is designed to give necessary flexural strength. It should be noted here that anchoring of additional longitudinal reinforcement is controlled to develop plastic hinge to the bottom of pier rather than the mid-height section with termination of longitudinal reinforcement. And the increase of strength should be carefully designed considering the effect on the foundations and footings. The confinement in the plastic hinge zone is provided by PC bars or re-bars which were installed inside of the column section.

(3) Seismic Retrofit of Two-column Bents

During the Hyogo-ken nanbu Earthquake, some two-column bents were damaged in the longitudinal and transverse directions. The strength and ductility characteristics of the two-column bents have been studied and the analysis and design method was introduced in the 1996 Design Specifications.

The strength and ductility of existing

two-column bents were studied both in the longitudinal and transverse directions. In the longitudinal direction, as the same as a single column, it is required to increase the flexural strength and ductility with appropriate balance. In the transverse direction, the shear strength of the columns or the cap beam is generally not enough in comparison with the flexural strength.

Fig.4 shows the possible seismic retrofit methods for two-column bents. The concept of the retrofit is to increase flexural strength and ductility as well as shear capacity for columns and cap beams. Since axial force in the cap beam is much smaller than that in the columns, to increase the shear capacity is essential for the retrofit of the cap beam. It should be noted here that since the jacketing of cap beam is difficult because of the existing bearing supports and construction space, it is required to develop much effective retrofit measures for cap beam such as application of jacketing by new materials with high elasticity and high strength and out-cable prestressing, etc.

(4) Seismic Retrofit using New Materials

The retrofit work is often restricted because of the limited construction space under the condition to open the public traffic in particular for the seismic retrofit of highway bridges in urban area. Therefore, there are sites that the conventional steel jacketing and reinforced concrete jacketing methods is difficult to be applicable. New materials such as carbon fiber sheets and aramid fiber sheets are attractive to be applied for the seismic retrofit of such bridges with construction restriction as shown in **Fig.5**. Since new materials such as fiber sheets are very light so no needs machines and easy to be construct using glue bond as epoxy resin.

There are various studies on the seismic retrofit methods using fiber sheets. **Fig.6** shows the cooperation effect between the fiber sheets and reinforcement for shear strengthening of a single reinforced concrete column. When carbon fiber sheets, which has the same elasticity and 10 time failure strength as those of reinforcing bar, is assumed to be applied, it is important to design the effect of carbon fiber sheets to achieve the required performance of seismic retrofit. In particular, the strengthening of flexural strength, shear strength and ductility for reinforced concrete column should be carefully evaluated. Based on the experimental studies, it is essential to appropriately evaluate the effect of materials on the strengthening carefully considering the material properties such as the elasticity and strength.

6. CONCLUSIONS

This paper presented seismic retrofit of existing highway bridges with emphasis on the program after the Hyogo-ken nanbu Earthquake. Because most of the substructures designed and constructed before 1971 do not meet with the current seismic requirements, it is urgently needed to study the level of seismic vulnerability requiring the retrofit. Upgrading of the reliability to predict the possible failure modes in the future earthquakes is also very important. Since the seismic retrofit of substructures requires more cost, it is required to develop and implement the effective and inexpensive retrofit measures and the design methods to provide for next event.

REFERENCES

1) Ministry of Construction: Report on the Damage of Highway Bridges by the Hyogo-ken Nanbu Earthquake, Committee for Investigation on the Damage of Highway Bridges Caused by the Hyogo-ken Nanbu Earthquake, 1995
2) Ministry of Construction: Guide Specifications for Reconstruction and Repair of Highway Bridges Which Suffered Damage due to the Hyogo-ken Nanbu

Earthquake, 1995
3) Japan Road Association : Design Specifications of Highway Bridges, Part I Common Part, Part II Steel Bridges, Part III Concrete Bridges, Part IV Foundations, and Part V Seismic Design, 1996
4) Headquarters Office for Earthquake Disaster prevention Countermeasures, Ministry of Construction : Countermeasures against Large-scale Earthquakes, Monthly Journal of Construction, Vol.25, No.1, January, 1972 (in Japanese)
5) Fujii, T. : Road Disaster Prevention Measures, Journal of Road, September, 1978 (in Japanese)
6) Fujii, T. : Road Service and Road Disaster Prevention Measures, Journal of Road, June, 1980 (in Japanese)
7) Yamauchi, Y. : Present Status of Road Disaster Prevention Measures, Journal of Road, December, 1980 (in Japanese)
8) Yoshikoshi, H. : Present Status and Subjects of Road Disaster Prevention Measures, Journal of Road, September, 1982 (in Japanese)
9) Miyaji, A. : Road Disaster Prevention Measures, Journal of Road, September, 1990 (in Japanese)
10) Edited by Road Bureau, Ministry of Construction : Road Traffic and Economy Survey, 1992 Version, December, 1990 (in Japanese)
11) Kawashima, K. : Seismic Design and Earthquake Disaster Countermeasures for Highway Bridges, Journal of Road, September, 1990 (in Japanese)
12) Kawashima, K. and Unjoh, S. : An Inspection Method of Seismically Vulnerable Existing Highway Bridges, Structural Eng./Earthquake Eng., Vol.7, No.7, Proc. JSCE, April 1990
13) Japan Road Association : Reference for Applying Guided Specifications to New Highway Bridge and Seismic Strengthening of Existing Highway Bridges, June, 1995
14) Kawashima, K., Unjoh, S. and Mukai H. : Seismic Strengthening of Highway Bridges, Proceedings of the 2nd US-Japan Workshop on Seismic Retrofit of Bridges, Berekeley, USA, January 1994, Technical Memorandum of PWRI, No.3276
15) Terayama T. and Otsuka, H. : Seismic Evaluation and Retrofit of Existing Multi-Column Bents, Proceedings of the 3rd US-Japan Workshop on Seismic Retrofit of Bridges, Osaka, Japan, December 1996, Technical Memorandum of PWRI, No.3481
16) Hoshikuma. J., Otsuka, H. and Nagaya, K. : Seismic Retrofit of Square RC Column by Steel Jacketing, Proceedings of the 3rd US-Japan Workshop on Seismic Retrofit of Bridges, Osaka, Japan, December 1996, Technical Memorandum of PWRI, No.3481
17) Hosotani, M., Kawashima, K. and Hoshikuma. J. : Seismic Retrofit of Reinforced Concrete Bridge Piers by Carbon Fiber Sheets, Proceedings of the 3rd US-Japan Workshop on Seismic Retrofit of Bridges, Osaka, Japan, December 1996, Technical Memorandum of PWRI, No.3481
18) Public Works Research Center : Research Report by the Committee on Seismic Retrofit Methods using Carbon Fiber Sheet, September 1996 (in Japanese)

Table 1 Past Seismic Design Methods for Highway Bridges

		1926 Details of Road Structure (draft), Road Law, MIA	1939 Design Specifications of Steel Highway Bridges (draft), MIA	1956 Design Specifications of Steel Highway Bridges, MOC	1964 Design Specifications of Substructures (Pile Foundations), MOC	1964 Design Specifications of Steel Highway Bridges, MOC	1966 Design Specifications of Substructures (Survay and Design), MOC	1968 Design Specifications of Substructures (Piers and Direct Foundations), MOC	1970 Design Specifications of Substructures (Caisson Foundations), MOC	1971 Specifications for Seismic Design of Highway Bridges, MOC	1972 Design Specifications of Substructures (Cast-in-Piles), MOC	1975 Design Specifications of Substructures (Pile Foundations), MOC	1980 Design Specifications of Highway Bridges, MOC	1990 Design Specifications of Highway Bridges, MOC
Seismic Loads	Seismic Coefficient	Largest Seismic Loads k_h =0.2	k_h =0.1 ~ 0.35 varied dependent on the site	varied dependent on the site and ground Condition						k_h =0.1 ~ 0.3 Standardization of Seismic Coefficient Provision of Modified Seismic Coefficient Method			Revision of Application range of Modified Seismic Coefficient Method	k_h =0.1 ~ 0.3 Integration of Seismic Coefficient Method and Modified one.
	Dynamic Earth Pressure	Epuations proposed by Mononobe and Okabe were supposed to be used.					Provision of Dynamic Earth Pressure							
	Dynamic Hydraulic Pressure	Less Effect on Piers except High Piers in Deep Water.					Provision of Hydraulic Pressure	Provision of Dynamic Hydraulic Pressure.						
Reinfored Concrete Column	Bending at Bottom	Supposed to be designed in a similar way provided in current Desigin Specifications					Provisions of Definite Design Method							
	Shear	Less Effect on RC Piers except those with Smaller section area such as RC Frame and Hollow Section					Check of Shear Strength						Provision of Definite Design Method, Decreasing of Allowable Shear Stress	
	Termination of Main Reiforement at Mid-Hieght												Elongation of Anchorage Length of Terminated Reinforcement at Mid-Height	
	Bearing Capacity for Lateral Fore							Less Effect on RC Piers with Larger Section Area				Ductility Check	Check of Bearing Capacity for Lateral Force	
Footing							Provisions of Definite Design Method (Designed as a Cantilever Plate)						Provisions of Effective width and Check of Shear Strength	
Pile Foundation			Bearing Capacity in vertical direction was supposed to be checked.				Provisions of Definite Design Method (Bearing Capacity in vertical and horizontal directions)				Special Condition (Foundation on Slope, Consolidation Settlement, Lateral Movement)		Provisions of Design Details for Pile Head	
Direct Foundation			Stability (Overturning and Slip) was supposed to be checked.				Provisions of Definite Design Method (Bearing Capacity, Stability Analysis)							
Caisson Foundation					Supposed to be designed in a similar way provided in Design Specification of Caisson Foundation of 1969				Provisions of Definite Design Method					
Soil Liquefaction									Provisions of Soil Layers of which Bearing Capacity shall be ignored in seismic design				Provisions of Evaluation Method of Soil Liquefaction and the treatment in seismic design	Consideration of effect of fine sand content
Bearing Support	Bearing Support			Provisions of Design Methods for Steel Bearing Supports (Bearing, Roller, Anchor Bolt)						Provision of Transmitting Method of Seismic Load at Bearing				
	Devices Preventing Falling-off of Superstructure							Provision of Bearing Seat Length S		Provisions of Stopper at Movable Bearings, Devices for Preventing Superstructure from Falling (Seat Length S, Connection of Adjacent Decks)			Provisions of Stopper at Movavle Bearings, Devices for Preventing Superstructure from Falling (Seat Longth S_E, Devices)	

Table 2 Past Seismic Evaluations of Highway Bridges

Year	Highways Inspected	Inspection Items	Number of Bridges		
			Inspected	Require Strengthening	Strengthened
1971	All Sections of National Expressways and National Highways, and Sections of the Others (Bridge Length ≧ 5m)	① Deterioration ② Bearing Seat Length S for Bridges supported by Bent Piles	18,000	3,200	1,500
1976	All Sections of National Expressways and National Highways, and Sections of the Others (Bridge Length ≧ 15m or Overpass Bridges)	① Deterioration of Substructures, Bearing Supports and Girders/Slabs ② Bearing Seat Length S and Devices for Preventing Falling-off of Superstructure	25,000	7,000	2,500
1979	All Sections of National Expressways, National Highways and Principal Local Highways, and Sections of the Others (Bridge Length ≧ 15m or Overpass Bridges)	① Deterioration of Substructures and Bearing Supports ② Devices for Preventing Falling-off of Superstructure ③ Effect of Soil Liquefaction ④ Bearing Capacity of Soils and Piles ⑤ Strength of RC Piers ⑥ Vulnerable Foundations (Bent Pile and RC Frame on Two Independent Caisson Foundation)	35,000	16,000	13,000
1986	All Sections of National Expressways, National Highways and Principal Local Highways, and Sections of the Others (Bridge Length ≧ 15m or Overpass Bridges)	① Deterioration of Substructures, Bearing Supports and Concrete Girders ② Devices for Preventing Falling-off of Superstructure ③ Effect of Soil Liquefaction ④ Strength of RC Piers (Bottom of Piers and Termination Zone of Main Reinforcement) ⑤ Bearing Capacity of Piles ⑥ Vulnerable Foundations (Bent Piles and RC Frame on Two Independent Caisson Foundation)	40,000	11,800	8,000
1991	All Sections of National Expressways, National Highways and Principal Local Highways, and Sections of the Others (Bridge Length ≧ 15m or Overpass Bridges)	① Deterioration of Substructures, Bearing Supports and Concrete Girders ② Devices for Preventing Falling-off of Superstructure ③ Effect of Soil Liquefaction ④ Strength of RC Piers (Piers and Termination Zone of Main Reinforcement) ⑤ Vulnerable Foundations (Bent Piles and RC Frame on Two Independent Caisson Foundation)	60,000	18,000	7,000 (As of the End of 1994)

Note) Number of bridges inspected, number of bridges that required strengthening and number of bridges strengthened are approximate numbers.

Table 3 Factors which Affect Seismic Vulnerability of Highway Bridges

Items	Seismic Vulnerability
① Design Specifications	Those designed in accordance with 1926 or 1939 Specifications have higher vulnerability
② Type of Superstructure	• Gerber or simply supported girders with 2 or more spans have higher vulnerability • Arch, frame, continuous girders, cable-stayed bridges or suspension bridges have lower vulnerability
③ Shape of Superstructure	Skewed or curved bridges do not necessarily have higher vulnerability than straight bridges
④ Materials of Superstructure	Reinforced concrete bridges or prestressed concrete bridges have lower vulnerability than steel bridges although the difference is small
⑤ Slope in Bridge Axis	Bridges with slope in bridge axis have higher vulnerability
⑥ Device for Preventing Falling-off of Superstructure	Bridges with devices for preventing falling-off of superstructure have lower vulnerability
⑦ Type of Substructure	Bridges supported by single-line bent piles or by reinforced concrete frame placed on two separate caisson foundations have higher vulnerability
⑧ Height of Piers	Bridges supported by higher piers have higher vulnerability
⑨ Ground Condition	Bridges constructed on soft soil have higher vulnerability
⑩ Effect of Soil Liquefaction	Bridges constructed on sandy soil layers susceptible to liquefaction have higher vulnerability
⑪ Irregularity of Supporting Soil Condition	Bridges constructed on soils with irregularity of supporting conditions have higher vulnerability
⑫ Effect of Scouring	Bridges where the surface soils are scoured have higher vulnerability
⑬ Materials of Substructures	Bridges supported by plane-concrete substructures designed in accordance with 1926 or 1939 specifications have higher vulnerability
⑭ Type of Foundation	Bridges supported by timber, brick, masonry or other old unknown type substructures have higher vulnerability
⑮ Intensity of Ground Motion	Bridges subjected to higher intensity of ground acceleration have higher vulnerability. In particular, vulnerability becomes quite high when the bridges are subjected to peak ground acceleration larger than 400 gal (0.4g)

Table 4 Inspection Sheet to Evaluate Seismic Vulnerability of Highway Bridges

Point of Inspection		Factors of Inspection	Evaluation
Inspection for Vulnerability to Develop Excessive Deformation	Inspection Format (A) Inspection for Deformation of Superstructure	① Design Specifications	4.0: 1926 Specs. or 1939 Specs. 2.0: 1956 Specs. or 1964 Specs. 1.0: 1971 Specs. or 1980 Specs.
		② Superstructure Type	3.0: Gerber Girder or Simply-supported Girders with Two Spans or More 1.5: Simply-supported Girder or Continuous Girders Consisting of Two Spans or More 1.0: Arch, Flame, Continuous Girder (One Span), Cable-stayed Bridge, Suspension Bridge
		③ Shape of Superstructure	1.2: Skewed or Curved Bridge 1.0: Straight Bridge
		④ Materials of Superstructure	1.2: Rc or PC 1.0: Steel
		⑤ Gradient	1.2: 6% or Steeper 1.0: Less Than 6%
		⑥ Falling-off Prevention Device	2.0: None 1.0: One Device
		$P_A = ① \times ② \times ③ \times ④ \times ⑤ \times ⑥$	$P_A =$
	Inspection Format (B) Inspection for Deformation of Substructure	⑦ Type of Substructure	2.0: Single-line Bent Pile Foundation 1.0: Others
		⑧ Height of Pier H	2.0: $H \geq 10m$ 1.5: $5 \leq H < 10m$ 1.0: $H < 5m$
		⑨ Ground Condition	5.0: Extremely Soft in Group 4 2.5: Group 4 2.0: Group 3 1.2: Group 2 1.0: Group 1
		⑩ Effects of Liquefaction	2.0: Liquefiable 1.0: Non-liquefiable
		⑪ Supporting Ground Condition	1.2: Irregular 1.0: Almost Uniform
		⑫ Scouring	1.5: Recognized 1.0: None
		$P_B = ⑦ \times ⑧ \times ⑨ \times ⑩ \times ⑪ \times ⑫$	$P_B =$
Inspection for Vulnerability to Develop Failure Due to Inadequate Strength of Substructure	Inspection Format (C) Inspection for Strength of RC Pier at Termination of Reinforcement	⑬ Shear Span Ratio (h/D)	2.0: $1 < h/D < 4$ 1.0: $h/D \geq 4$ 0.5: $h/D \leq 1$
		⑭ Tension Cracks in Flexure at Terminated Point of Main Reinforcement	2.0: Cracks Wil Occur 1.0: Cracks Will Possibly Occur 0.3: Cracks will Not Occur
		⑮ Safety Factor for Yield Strength at Terminated Section of Main Reinforcement ⑮-1 S_m	3.0: $S_m \leq 1.1$ 2.0: $1.1 < S_m < 1.5$ 0.5: $S_m \geq 1.5$
		⑮-2 S_{mn}	3.0: $S_{mn} \leq 1.1$ 2.0: $1.1 < S_{mn} \leq 1.3$ 1.0: $1.3 < S_{mn} < 1.5$ 0.5: $S \geq 1.5$
		⑯ Shear Stress σ (tf/m^2)	3.0: $\sigma \geq 45$ 2.0: $30 \leq \sigma < 45$ 1.0: $15 \leq \sigma < 30$ 0.5: $\sigma < 15$
		$P_C = ⑬ \times ⑭ \times ⑮\text{-}1 \times ⑮\text{-}2 \times ⑯$	$P_C =$
	Inspection Format (D) Inspection for Strength of Substructure	⑰ Failure of Fixed Supports and Proximity	5.0: Extensive Failure 2.0: Small Failure 1.0: None
		⑱ Extraordinary Damage of Pier	5.0: Extensive Damage 2.0: Small Damage 1.0: None
		⑲ Materials of Substructure	2.0: Plane Concrete Older Than 1926 Excluding Gravity-type Abutment 1.0: Others
		⑳ Construction method of Foundation	2.0: Timer Pile, Masonry, Brick, Other Old Construction Methods 1.5: RC Piles, Pedestal Piles, Pier Supported by Two Independent Caissons 1.0: Foundation Designed by 1971 Specs. and Other Later Specs.
		㉑ Foundation Type	1.5: RC Flame Supported by Two Independent Caisson Foundations 1.0: Others
		㉒ Extraordinary Failure of Foundation	2.0: Recognized 1.0: None
		$P_D = ⑰ \times ⑱ \times ⑲ \times ⑳ \times ㉑ \times ㉒$	$P_D =$
Evaluation of Deformation and Strength			$X = P_A \times P_B =$ and $Y = P_C \times P_D =$

Table 5 Application of the Guide Specifications

Type of Roads and Bridges	Double Deckers, Overcrossings on Roads and Railways, Extremely Important Bridges from Disaster Prevention and Road Network	Others
Expressways, Urban Expressways, Designated Urban Expressway, Honshu-Shikoku Bridges, Designated National Highways	Apply all items, in principle	Apply all items, in principle
Non-designated National Highways, Prefectural Roads, City, Town and Village Roads	Apply all items, in principle	Apply partially, in principle

Table 6 Tentative Retrofit Method by Steel Jacketing

Column/Piers	Steel Jackets	Anchor Bolts
$a/b \leqq 2$	SM400, t=9mm	SD295, D35 ctc 250mm
$2 < a/b \leqq 3$	SM400, t=12mm	
Column supporting Lateral Force of A Continuous Girder through Fixed Bearing and with $a/b \leqq 3$		

Table 7 Example of Prioritization Factors for Seismic Retrofit of Highway Bridges

Item	Category	Evaluation Point
Importance of Highway (I)	1) Emergency Routes 2) Overcrossing with Emergency Routes 3) others	1.0 0.9 0.6
Earthquake Force (S)	1) Ground Condition Type I 2) Ground Condition Type II 3) Ground Condition Type III	1.0 0.9 0.8
Structural Factor (V_T)	1) Viaducts 2) Supported by Abutments at Both Ends	1.0 0.5
Weighting Factor on Structural Members (V_T)	1) Reinforced Concrete Pier 2) Steel Pier 3) Unseating Prevention Devices 4) Foundation	1.0 0.95 0.9 0.8
Reinforced Concrete Pier (1) Design Specification (V_{RP1})	1) Pre-1980 Design Specifications 2) Post-1980 Design Specifications	1.0 0.7
Reinforced Concrete Pier (2) Pier Structure (V_{RP2})	1) Single Column 2) Wall-Type Column 3) Two-Column Bent	1.0 0.8 0.7
Reinforced Concrete Pier (3) Aspect Ratio (V_{RP3})	1) $h/D \leqq 3$ 2) $3 < h/D < 4$ with cut-off Section 3) $H/D \geqq 4$ with cut-off Section 4) $3 < h/D < 4$ without cut-off Section 5) $H/D \geqq 4$ without cut-off Section	1.0 0.9 0.9 0.7 0.7
Steel Pier (V_{MP})	1) Single Column 2) Frame Structure	1.0 0.8
Unseating Prevention Devices (V_{PS})	1) Without Unseating Devices 2) With One Device 3) With Two Devices	1.0 0.9 0.8
Foundations (V_F)	1) Vulnerable to Ground Flow (without unseating devices) 2) Vulnerable to Ground Flow 3) Vulnerable to Liquefaction (without unseating devices) 4) Vulnerable to Liquefaction	1.0 0.9 0.7 0.6
Evaluation of the Priority R	1) $R \geqq 0.8$ 2) $0.7 \leqq R < 0.8$ 3) $R < 0.7$	Priority Rank A Priority Rank B Priority Rank C

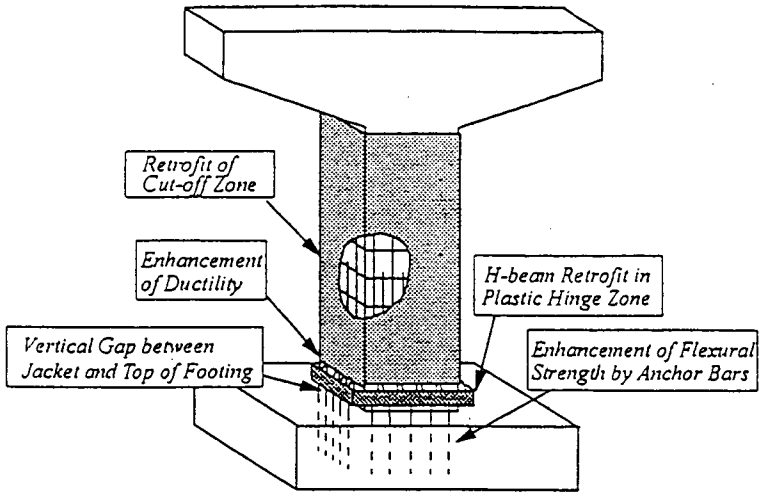
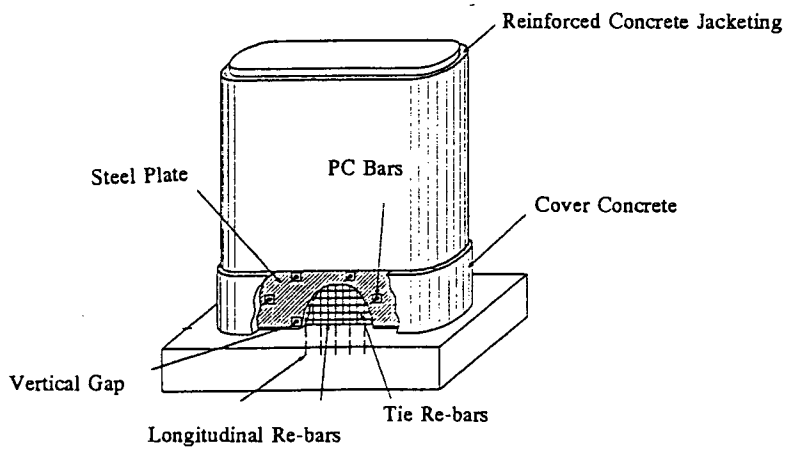
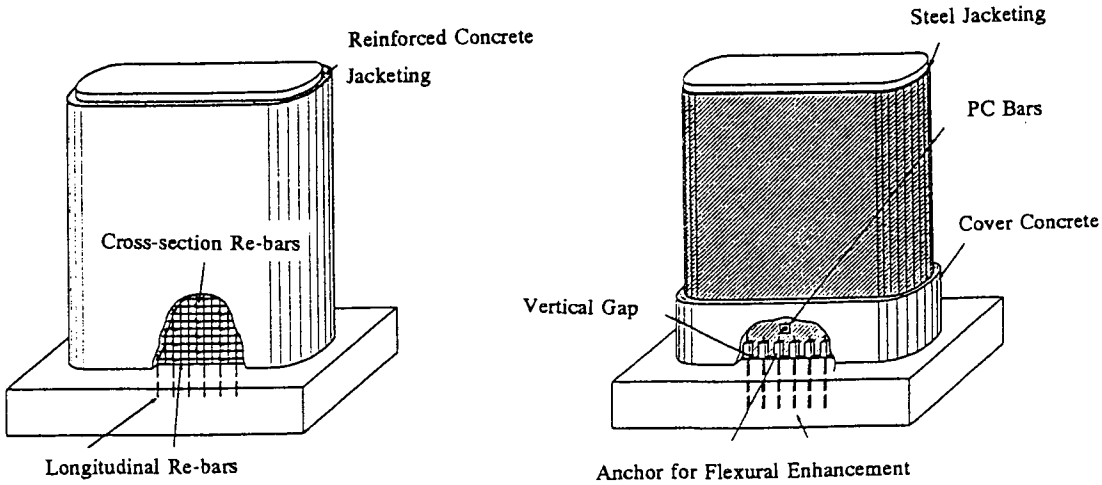


Fig.1 Seismic Retrofit of Reinforced Concrete Piers by Steel Jacket with Controlled Increase of Flexural Strength



(a) Integrated Seismic Retrofit Method with Reinforced Concrete and Steel Jacketing



(b) Reinforced Concrete Jacketing (c) Steel Jacketing

Fig.3 Seismic Retrofit of Wall-Type Piers

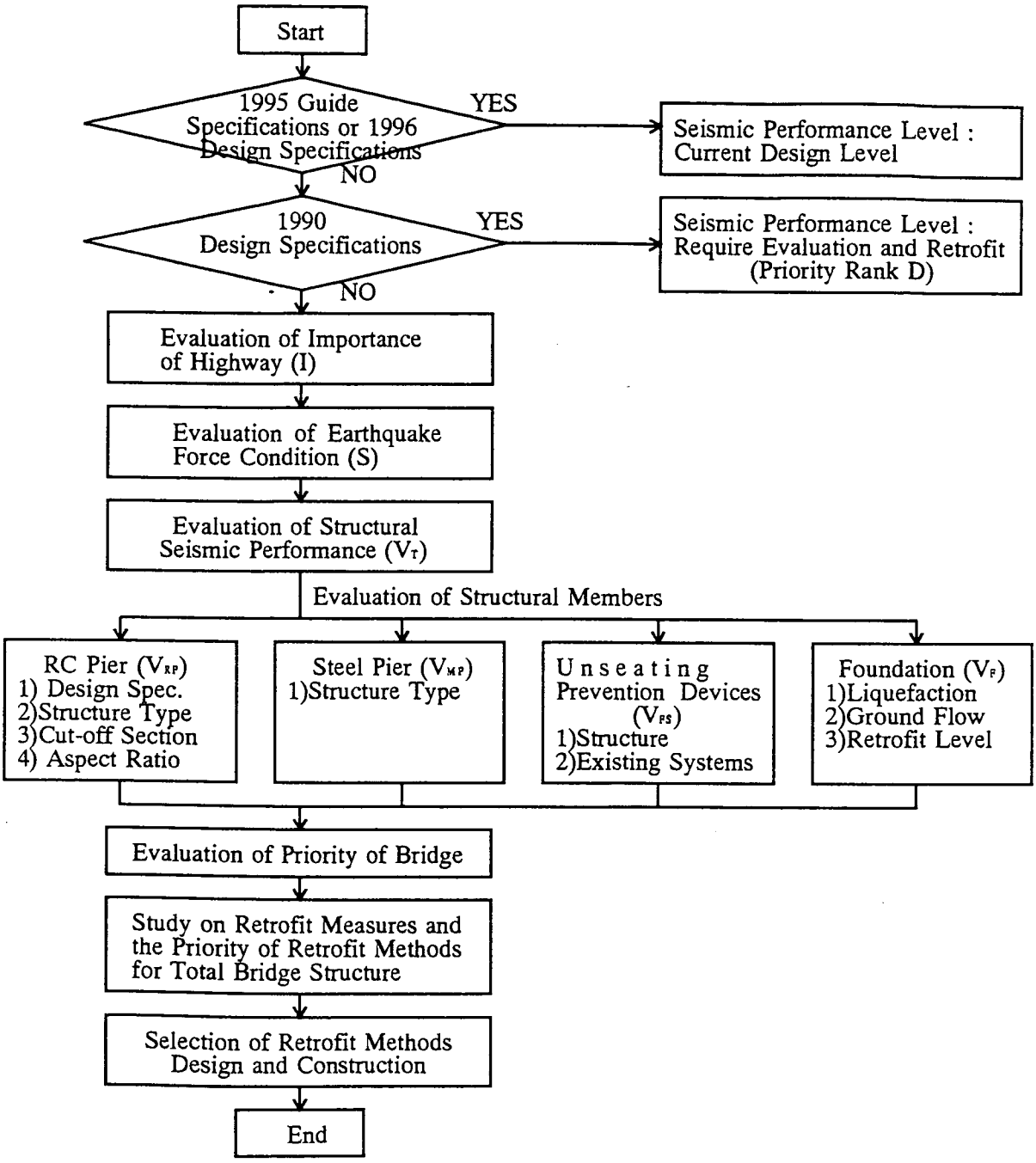
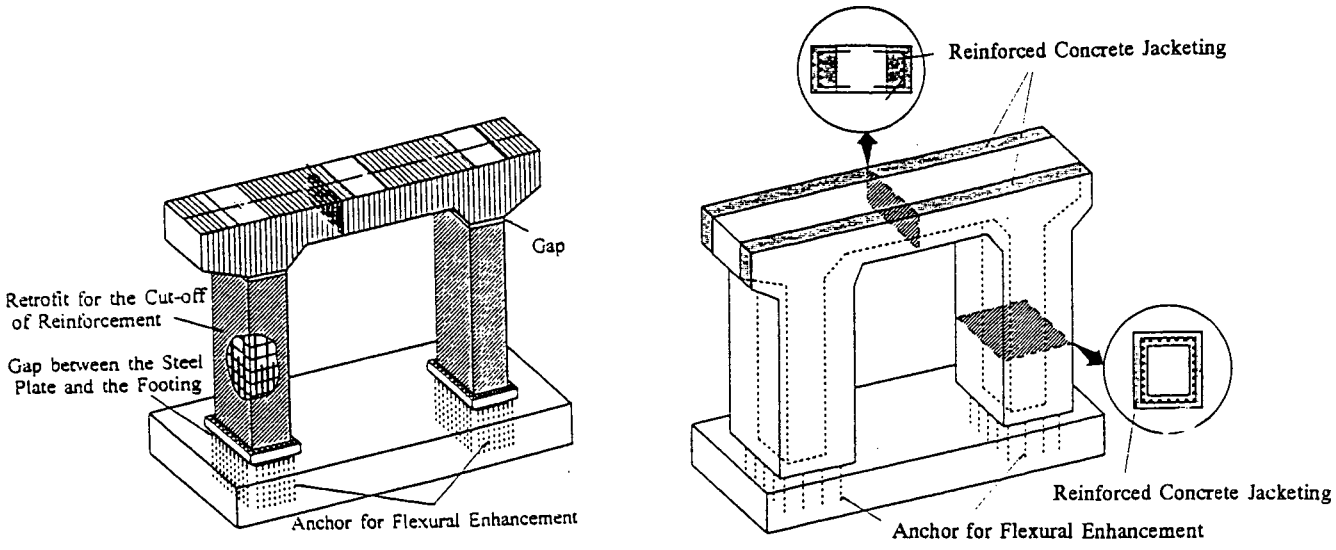


Fig.2 Prioritization Concept of Seismic Retrofit of Highway Bridges



(a) Steel Jacketing (b) Reinforced Concrete Jacketing

Fig.4 Seismic Retrofit of Two-Column Bents

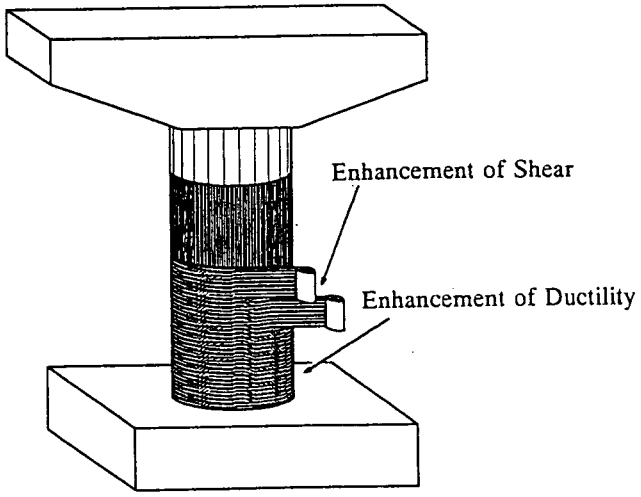
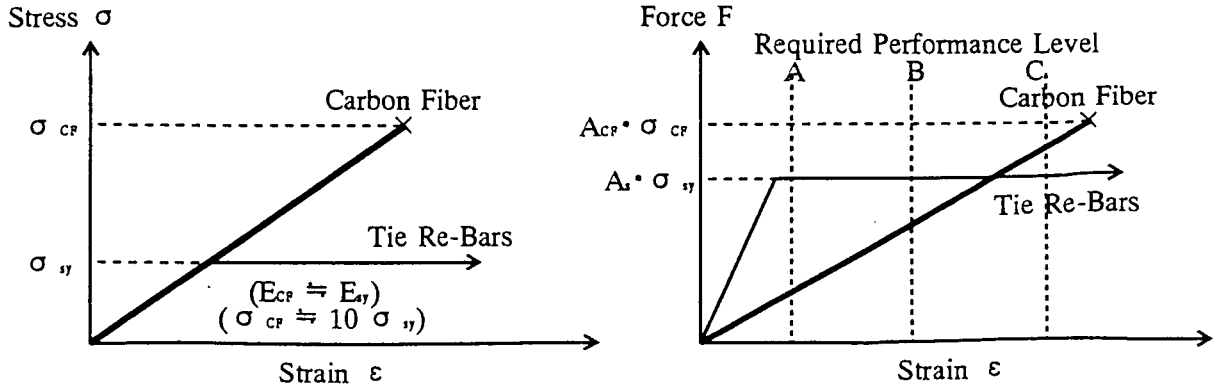


Fig.5 Application to New Materials for Seismic Retrofit of Reinforced Column



(a) Stress-Strain Relation (b) Force-Strain Relation

Fig.6 Cooperative Effect between Tie Reinforcement and Carbon Fiber Sheets

Shake-Table Testing of U.S. and Japanese Bridge Column Design

by

W. Phillip Yen[1], James D. Cooper[2], Toru Terayama[3]and Hisanori Otsuka[4]

ABSTRACT

This paper described a preliminary finding of shake-table tests of three one-sixth scale models that were designed from a U.S. and Japanese cooperative study in comparative seismic design of bridge columns. This study was undertaken by the Federal Highway Administration's (FHWA) Turner-Fairbank Highway Research Center and Japan's Public Works Research Institute (PWRI). Test results reflected the different design approaches, and earthquake patterns (strong ground motion data) occurred in this two countries. Future investigations needed of the test results were discussed.

KEYWORDS: Seismic Design; Comparative Design; Shake Table Test; Bridge Design; Residual Displacement.

1. INTRODUCTION

1.1 Background

Recently, three large destructive earthquakes have occurred in the United States and Japan. These earthquakes, the Loma Prieta earthquake in 1989, the Northridge earthquake in 1994, and the Kobe earthquake in 1995, have severely damaged a number of highway bridges, and have cost many lives and billions of dollars. Although, most of the damaged bridges were designed and constructed prior to the implementation of modern seismic design codes, significant damage also occurred in some bridges built to more recent codes. Column failure due to insufficient ductility and inadequate shear reinforcement was found to be the most important factor causing bridge collapse or failure.

In order to better evaluate the current bridge seismic codes, and to improve bridge performance under earthquakes, a cooperative research study of the highway bridge columns was undertaken by the Federal Highway Administration's (FHWA) Turner-Fairbank Highway Research Center and Japan's Public Works Research Institute (PWRI). Under this cooperative research project, a review of seismic design philosophy and criteria for bridges of both countries was conducted, and a comparative design study for a representative bridge column was performed using the present bridge design

[1] Research Structural Engineer, Structures Division , Turner-Fairbank Highway Research Center, Federal Highway Administration , McLean, Virginia 22101

[2] Chief, Structures Division, Ditto.

[3] Senior Research Engineer, Earthquake Engineering Division, Public Works Research Institute Tsukuba Science City, Japan

[4] Professor, Department of Civil Engineering, Kyushu University, 6-10-1, Hakozaki, Higashi-ku Fukuoka, Japan

specifications (at that time). [Note: Japan has revised the seismic design specifications for bridges due to the Kobe earthquake, and issued in November 1996.]

Seismic design specifications used in this comparative study are: the newly issued (Spring 1995) Division I-A: Seismic Design of the AASHTO Standard Specifications for Highway Bridges and Part V: Seismic Design of the Japan Road Association's (JRA) Specification for Highway Bridges, issued in 1990. As a follow up to this comparative design, three one-sixth scale models were constructed and tested on a shake-table. The preliminary findings of the shake-table test of these three scaled models are presented in this paper. The details of the prototype bridge columns developed by the comparative designs, such as column sizes, main and transverse reinforcement, and the design approaches were compared. Further steps to investigate the results (data) of the shake-table test were discussed.

1.2 Objectives

The objectives of this cooperative research study are (1) to better assess the current seismic design codes in column design, and (2) to improve bridge performance under earthquakes. The shaking-table test results of the scale models will be evaluated to give an indication of the adequacy of current design criteria for bridge piers. .

2. DESIGN COMPARISON

For obtaining an actual comparison of these design codes, a bridge representative of the most common type in both countries was selected and shown in Figure 1. A comparative design based on the same force level were designed. The detailed comparison of the bridge columns seismic designs were compared by Yen et al (1996). The fundament characteristics, such as sizes, reinforced steels were shown in the Table 1. Following by this prototype design comparison, three scaled models were constructed according to these prototype designs.

As part of the comparison of results and exchange of design examples, a parametric study of different sizes was performed by both sides to make the comparison between the two design codes more meaningful. However, during the designing process, a temporary guideline of bridge seismic designs were issued after the Kobe earthquake. This temporary guideline was then included into this competitive design to check two different natural period type designs. In Table 1 the AASHTO bridge column size was 7 ft (2.1 m) in diameter, while the JRA columns were 2.7m (9ft), and 3.2 m (10.5 ft) in diameter.

3 SHAKE-TABLE TESTS

3.1 Test Setup

All scaled models were tested in the shake-table at the Vibration Laboratory of the Public Works Research Institute. These tests were to examine how the bridge columns behaved under a real earthquake-type shaking. Test setup is shown in Figure 2. The bottom of testing specimen (scaled column) was anchored at the center of the shake-table, and the top of the specimen was connected by two simply supported girders. The total length of the model bridge is 17m, and a total dead load weighted 26.8tf of the

superstructure was placed on the girders. The concrete column specimen and girders were connected by pin supports and the other ends of girders were supported by low friction roller bearings on the steel frames. These steel frames were away from the shake table to allow the girders to move in the longitudinal direction. All excitations were given along the longitudinal direction axis of the model bridge. All the inertia forces during the excitation were considered to be carried by the model column. A total of 86 channels of electrically monitoring instrumentation were installed on each test specimen. These included 60 strain gages on the longitudinal and transverse reinforcement, five accelerometers to measure acceleration, nine displacement transducers were used to measure the absolute and relative horizontal displacement, and twelve transducers were used to determine the curvature of the column at six levels.

3.2 Test Specimens Design

Considering the available facilities, the scale factor of model design was determined to one-sixth of the prototype. The height of the column (from the supporting pin to the bottom of the column) is then defined as 2,442mm which is obtained from original height 14,650mm divided by this scale factor. The diameter of each column is then determined as 356mm, 450mm and 533mm, respectively. Dimension analysis was designed to determined the input acceleration so that the scale down of time-axis and the mass of superstructure could be determined. The scale factor of acceleration is 1, but the time axes need to be reduced to $1/\sqrt{6}$ and the mass of superstructure is obtained as 26.8tf. This value is an approximate value of the prototype weight 960tf dividing by $(6)^2$. To simulate the actual conditions as closely as possible, the specimens were designed such that the model columns have the same longitudinal reinforcement ratio and the same volumetric ratio as the prototype columns. The model specimens are given in Table 2.

3.3 Shaking Table Test Program

A series of excitations was applied to test each specimen under different level's ground motions. The revised Kaihoku-bashi record was used as excitation acceleration record. This is because that this record was specified as a standard ground motion for the type-I soil in the Design Specifications for Highway Bridges, Part V- Seismic Design. The maximum response acceleration spectrum with a damping ratio of 0.05 of the specified motion was 0.2g. The time scale of acceleration was compressed to $1/\sqrt{6}$, so that the acceleration of the shake table could simulate as closely as possible to the original conditions.

Each excitation increased in intensity of maximum acceleration response spectrum (ARS) from 0.2g to 1.0g by 0.2g increment. The maximum 1.0g excitation level was determined by the stroke limit of the shake table facility. At the maximum ARS, five excitations were tested. Since tests under the design load, each of specimens did not reach to the ultimate stage after the test sequence indicated, an additional mass was added to the superstructure (from 26.8tf to 40.0tf). With carrying a mass of 40.0tf, another sequence of ground motion was applied from a single cycle of the

maximum ARS of 0.2g to five cycles of the maximum ARS of 1.0g. In the case that the specimen did not reach the ultimate stage after the five cycles of excitation, the excitation would be continuing until the specimen reach the ultimate stage or the maximum excitations of twenty. Ultimate stage was defined as a column specimen loses major bearing capacity.

3.4 Test Results

U.S. Specimen, (D=356mm)

First flexural cracking of concrete was occurred at the bottom of the column when the maximum ARS of 0.4g was applied. Flexural cracks extended up to an approximate height of 0.6m after the fifth excitation of ARS of 1.0g was applied. After adding the mass to 40tf, the spalling-off of cover concrete was recorded when the fifth excitation of ARS of 1.0g was applied. No longitudinal reinforcement fractured at the time of the eighteenth excitation of ARS of 1.0g was applied. The test was completed at this point because of the displacement limitation of the roller supporting was reached.

Japanese Specimen (1), (D=450mm)

First flexural concrete cracking was observed at the bottom of the column when the maximum ARS of 0.4g was applied. Flexural cracks extended up to an approximate height of 0.5m after the fifth excitation of ARS of 1.0g was applied. After adding the mass to 40tf, the spalling-off of cover concrete was recorded when the second excitation of ARS of 1.0g was applied. One of longitudinal reinforcement fractured when the seventh excitation of ARS of 1.0g was applied.

Japanese Specimen (2), (D=533mm)

First flexural cracking was noticed at the bottom of the column when the maximum ARS of 0.2g was applied. Flexural cracks extended up to an approximate height of 0.6m after the fifth excitation of ARS of 1.0g was applied. After adding the mass to 40tf, the spalling-off of cover concrete was recorded when the fourteenth excitation of ARS of 1.0g was applied. One of longitudinal reinforcement fractured when the eighteenth excitation of ARS of 1.0g was applied.

3.5 Load-Deformation Characteristics

The horizontal load-deformation hysterisis at the top of three columns are shown in Figure 3-5 respectively. Each figure implies the load-deformation hysterisis of the maximum ARS of 0.4g and the first and fifth excitation of the maximum ARS of 1.0g. The horizontal loads are calculated by multiplying the measured acceleration by the mass. In all cases, the hysterisis loop of the maximum ARS of 0.4g is almost elastic, while the loops of the first and fifth excitation of the maximum ARS of 1.0g show the behavior of the good energy absorption. Figure 3 shows that the fifth excitation of 1.0g have the residual displacement while the first excitations of 1.0g have almost no residual displacement for the U.S. specimen. Figure 4 and 5 show that the two Japanese specimens have almost no residual displacement.

3.6 Residual Displacement

The recorded residual displacements after each excitation are shown in Figure 6. Three specimens have almost the same residual displacement up to the 11th excitation, which was the first excitation after adding the mass. The residual displacement of U.S. specimen increased largely after the 13th excitation, compared with the two Japanese specimens. However, the U.S. specimen maintained the adequate capacity until the completion of the test while the residual displacement reached 120mm (which is almost 6% of a column height). On the other hand, Japanese specimen (1) could not provide the sufficient capacity at the residual displacement of 40mm which is 1.6% of a column height. The residual displacement of Japanese specimen(2) also gradually increased and reached the ultimate stage at the residual displacement of 60mm that is 2.5% of a column height. The U.S. specimen has a larger residual displacement, but did not reach the ultimate stage until the last excitation.

4. CONCLUSIONS AND RECOMMENDATIONS

This paper presented design comparisons of design principles and results from seismic design of a typical bridge column by both US and Japanese methods. The results here do not seek to show the stronger or weaker design but rather to compare the different design approaches, and to learn from each. From the natural periods compared in Table 1, the AASHTO pier is more flexible than the JRA piers in this case. These designs may also reflect the difference in the strong ground motion, which is affected most by the soil profile type.

From the results of shaking-table test, three 1/6 scale column models performed very well under the design loads. There was no critical damage, such as fracture of longitudinal rebars, in the design level test. After increased to approximate 150% of the design loads, results show US specimen has no critical damage till the limitation of the shake-table's displacement was reached. However, the residual displacement increased more than the other two Japanese specimens. The Japanese specimens experienced fracture of longitudinal rebars at the bottom connections. Major difference in the design detail is the transverse confinement. The U.S. uses spiral type with closer spacing instead of hoop type with relatively larger spacing from Japanese design, and may provide sufficient ductility under large horizontal displacement. Compared with a simple static and dynamic analytical model, shake-table test results agree each other very well. Much more detailed analyses are needed to investigate the differences of dynamic behavior among three specimens.

During the shake-table tests, 86 channels' data sets were recorded for each specimen. These data included curvature displacement of model columns, contain much information of bridge column's performance in a simulated earthquake event, particularly, while bridge column receives much greater earthquake load than design load. Nonlinear finite element model or mathematical modeling would be very helpful to examine the bridge model dynamic characteristic. Thus two analytical modeling are recommended to be used in examining the data.

For Finite Element Modeling, a

nonlinear program such as SAP2000 is expected to model the bridge column in detail dynamic response. In the System Identification Method, a generalized multiple input and multiple out system identification method developed for bridge structures (Yen, et al, 1996) will be used to assess the dynamic parameter of the model bridge. This system identification method uses both excitation forces (input data) and structural dynamic response (output) to estimate the system transfer function.

REFERENCES:

AASHTO, 1995, Interim Revisions to the AASHTO *Standard Specifications for Highway Bridges*, "Division I-A: Seismic Design," American Association of State Highway and Transportation Officials, Washington, DC.

Japan Road Association, 1990, "Specifications for Highway Bridges," Part V: Seismic Design.

Kawashima, K., 1994, "Seismic Design Force of Bridges," Proceedings of the Second International Workshop on Seismic Design of Bridges, Queenstown, New Zealand.

Kawashima, K., and Hasegawa, K., 1994, "New Design Specifications for Highway Bridges in Japan," Earthquake Spectra, Vol. 10, No. 2.

Sultan, M, and Kawashima, K. 1994, "Comparison of the Seismic Design of Highway Bridges in California and in Japan", Recent Selected publications of Earthquake Eng. Div., PWRI, Japan. (Technical Memorandum of PWRI No. 3276)

Terayama, T., Otsuka, H., Yen, W. P. and Cooper, J. D., 1996 "Shaking Table Test of Bridge Columns: Design by Japan and U.S. Codes". Proceedings of 12th Bridge Engineering Workshop, Buffalo, NY.

Yen, W. P., Cooper, J.D., and Friedland, I. M. 1995, " Comparison of the U.S. and Japanese Highway Bridge Seismic Design Criteria", Proceedings of the 27th UJNR Panel Meeting on Winds and Seismic Effects, Tsukuba City, Japan.

Yen, W. P., Cooper, J. D. , Otsuka and H., Terayama, T. , 1996, "Comparison of U.S. and Japanese Highway Bridge Column Seismic Design", Proceedings of the 28th UJNR Panel Meeting on Winds and Seismic Effects, NIST, Gaithersburg, MD

Yen, W. Phillip, Baber, Thomas T., Barton, Furman, "Modal Identification of a Cable-Stayed Bridges" Proceedings of ASCE Engineering Mechanics Conference, Fort Lauderdale, FL, April 1996.

Table 1. Comparison of Design Results

	U.S. (AASHTO) DESIGN	JAPANESE DESIGN (1)	JAPANESE DESIGN (2)
Column Size	Diameter = 7 ft (2.1m)	Diameter = 2.7 m (9 ft)	Diameter = 3.2m (10.5ft)
Main Reinforcement (longitudinal direction)	56-#18 bars (56-D57)	2X54-D51 bars (2X54-#16 Double layer)	2X32 -D32 bars (Double Layer)
Transverse Reinforcement	#7 @ 3"(D22@75) (Spiral type)	D22 @150 (#7@6") (Hoop type)	D19 @150 (#7@6") (Hoop type)
Fundamental Natural Period (longitudinal direction)	1.32 sec	0.93 sec	0.85 sec
Axial Load	698tf	795tf	894tf
Concrete Gross Area	38.48 ft^2 (3.57m^2)	5.73m^2 (61.63 ft^2)	8.04 m^2

Table 2. One-Sixth Model Columns

	U.S. DESIGN	JPAANESE DESIGN (1)	JAPANESE DESIGN (2)
Diameter of Column	D=356mm A=995 cm^2	D=450 A=1590cm^2	D=533 A=2231cm^2
Longitudinal Reinf.	D19 X 14 As= 40.10 cm^2 (ρ=4.03%)	D13 X 24X2 As= 60.82cm^2 (ρ=3.80%)	D10X25X2 As= 35.61cm^2 (ρ=1.60 %)
Transverse Reinf.	D6@40 (spiral) ρ_s = 1.02%	D6@85 (double hoop) ρ_s = 0.84%	D6@110 (double hoop) ρ_s = 0.52%
Axial Load and Stress at Bottom (Dead Load)	Pdead = 14.25tf σdead = 14.3kgf/cm^2	Pdead = 14.46tf σdead = 9.1kgf/cm^2	Pdead = 15.06tf σdead = 6.7kgf/cm^2

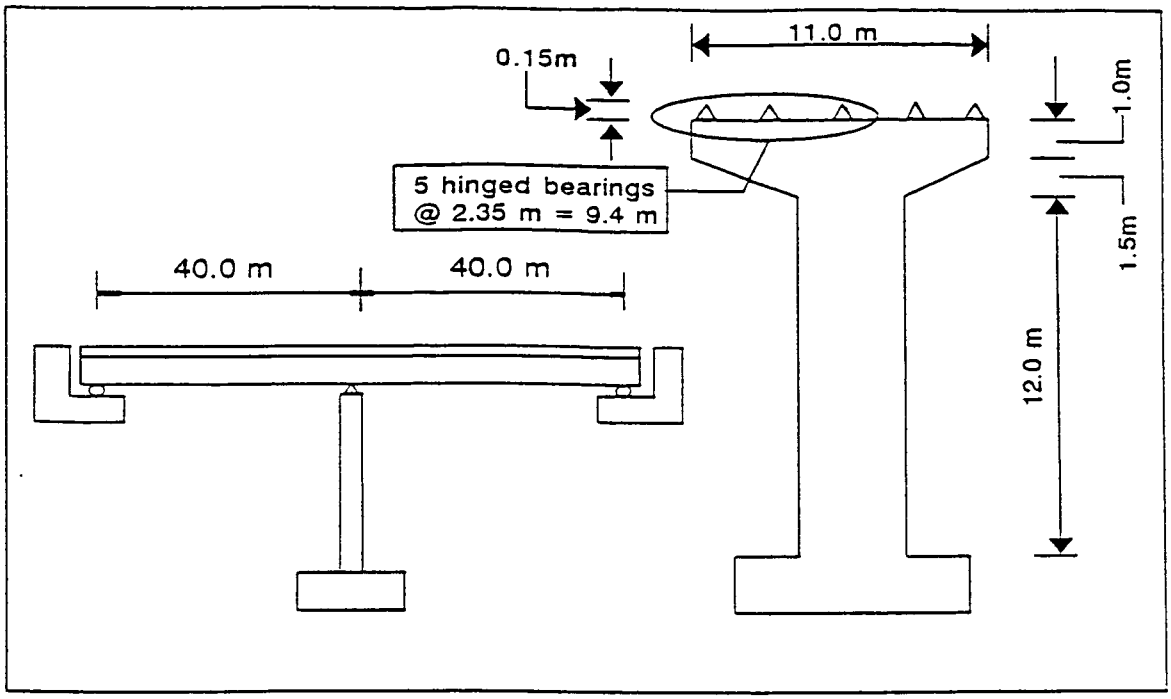


Figure 1. The Selected Bridge Column Design Dimensions

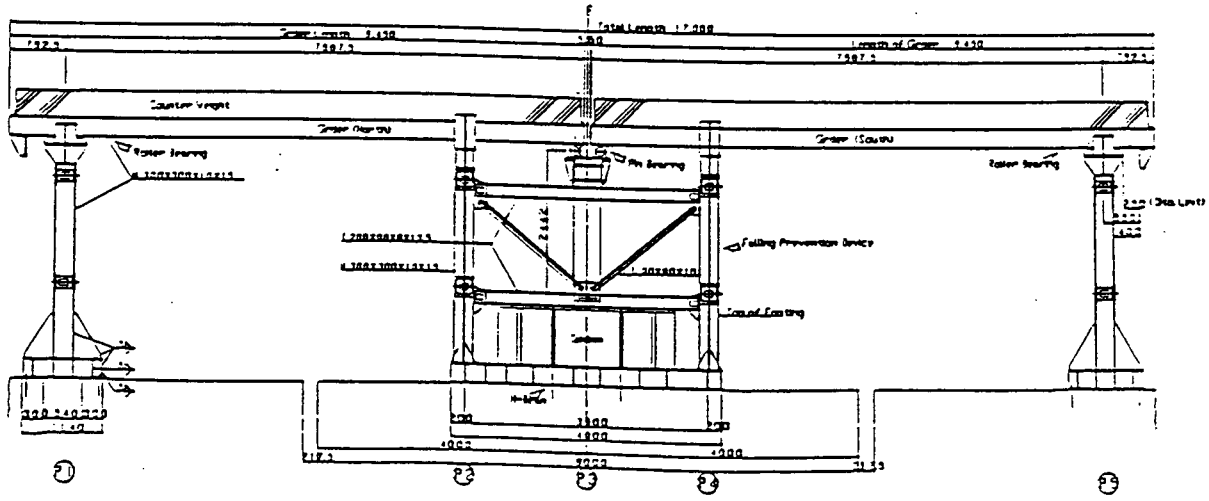


Fig 2 Test Setup

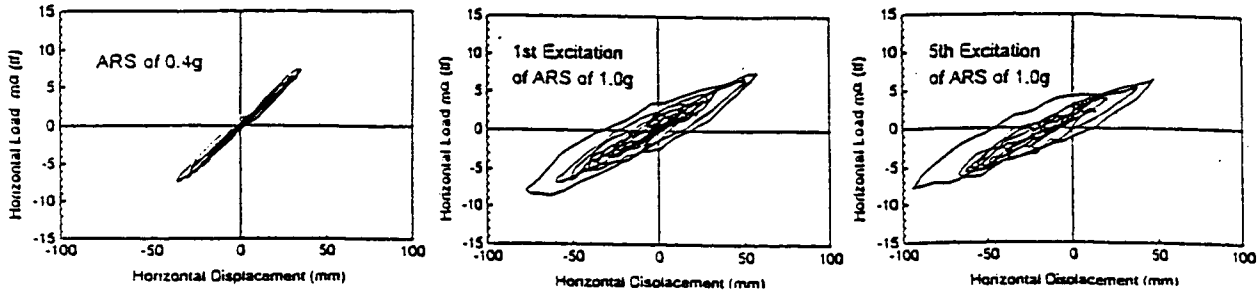


Fig 3 Load -Displacement Hysteresis (ϕ356)

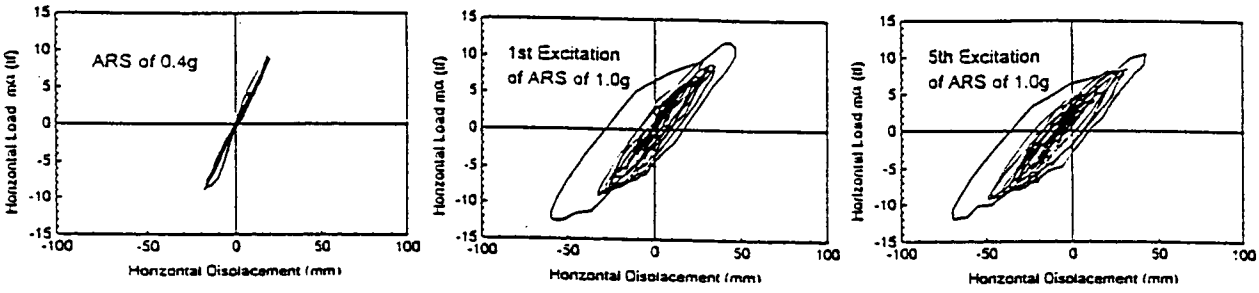


Fig. 4 Load -Displacement Hysteresis (ϕ450)

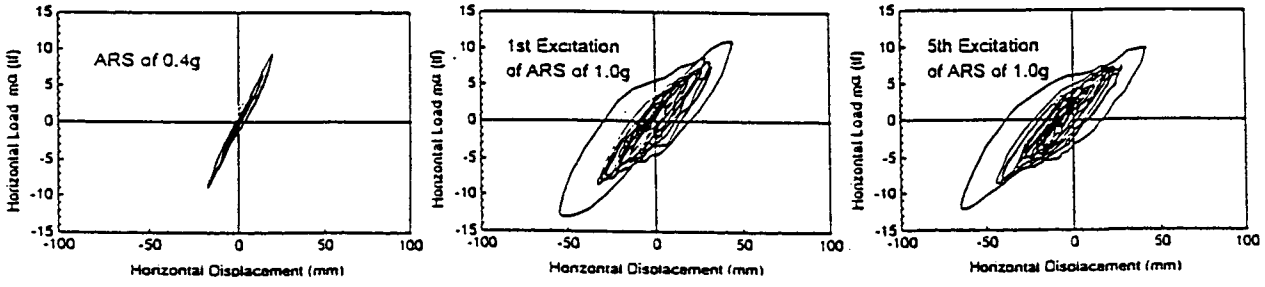


Fig. 5 Load -Displacement Hysteresis (ϕ533)

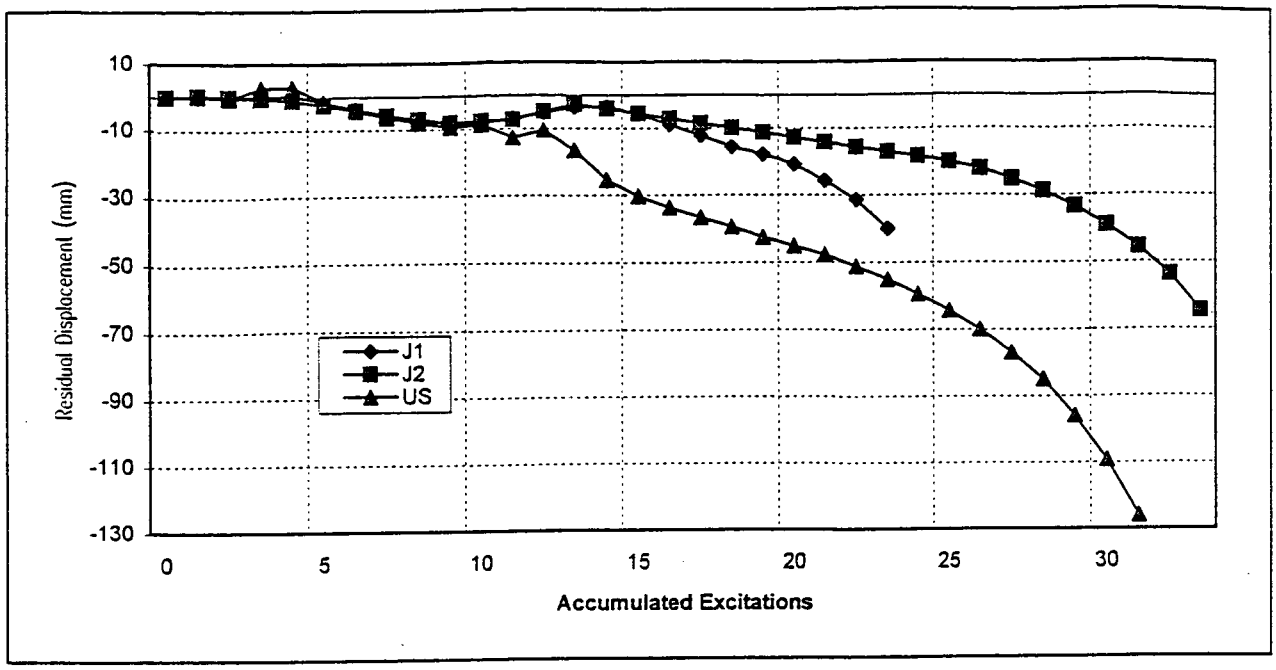


Figure 6 Residual Displacements

Deformation of Kobe Ohashi Bridge Foundation Caused by 1995 Great Hanshin Earthquake, Japan

by

Hanlong Liu[1], Susumu Iai[1], Koji Ichii[1] and Toshikazu Morita[1]

ABSTRACT

During the 1995 Great Hanshin earthquake, there was about 0.6 to 0.8m seaward displacement induced at the pneumatic caissons which were embedded to a depth of 33m. In order to identify the mechanism of deformation, the effective stress analysis was performed to take into account the soil-structural and water-structural interactions. The constitutive model used in this study is a multiply mechanism type defined in strain space and can take into account the effect of rotation of principal stress axis directions. The earthquake acceleration recorded at a depth of 83 meters on the Port Island during the 1995 Great Hanshin earthquake was used as input bedrock motion. The results of analysis show that the seaward residual displacements were 0.46 m at the top of a caisson and 0.48 m at the top of the other caisson, resulting in a total of 0.94m. The order of computed residual displacement was in good agreement with the measured. The results indicate that the excess pore water pressure increasing in the fill soil around the caissons and in the diluvial layers significantly affected the performance of caissons. The performance of pneumatic caisson foundation for soil improvement was also discussed.

Key Words: Kobe Ohashi Bridge,
Pneumatic Caisson Foundation,
Effective Stress Analysis,
Liquefaction,
Residual Deformation

1. INTRODUCTION

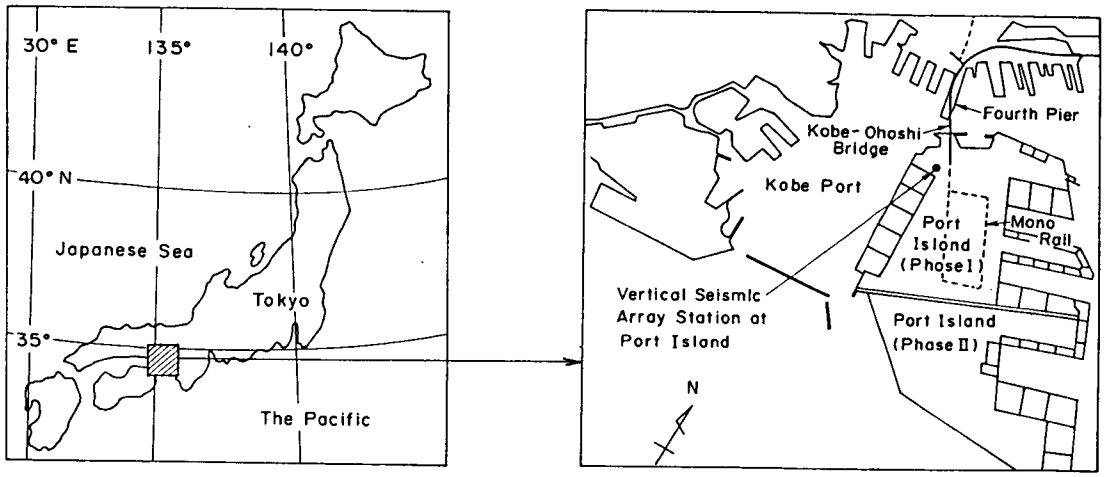
Kobe port is located in the south of Kobe city about 17 km from the epicenter of the 1995 Great Hanshin earthquake. The Kobe Ohashi Bridge, 319 meters long, with a central span 217 meter long and two-side spans 51 meter long, lies on the site between the Fourth Pier and the Port Island in Kobe port area. It is the only bridge connecting Port Island with the Kobe city. There are two pneumatic concrete caissons P2 and P3 used for the foundations to support the main span of the bridge. The location and cross section are shown in Fig.1. During the 1995 Great Hanshin earthquake, the bridge was shaken by a strong earthquake motion having the peak acceleration of 670 Gal and 172 Gal in the N-S horizontal and vertical directions at the bedrock 83m deep from the ground surface. Though the pneumatic caissons were embedded in soil to a depth of 33m and founded on a firm foundation of Holocene origin, there were about 0.60 to 0.80m residual displacements toward sea and 0.36 to 0.93 degrees angle of seaward inclination induced due to earthquake. The bridge and the damage around the bridge after earthquake was shown in Photo.1, and the relative movement between the upper structure of bridge and foundation at P2 was shown in Photo. 2. In order to identify the mechanism of the deformation for the foundation, an effective stress analysis was performed in this study based on the results of the geotechnical investigations and in-situ velocity measurements.

2.EFFECTIVE STRESS ANALYSIS

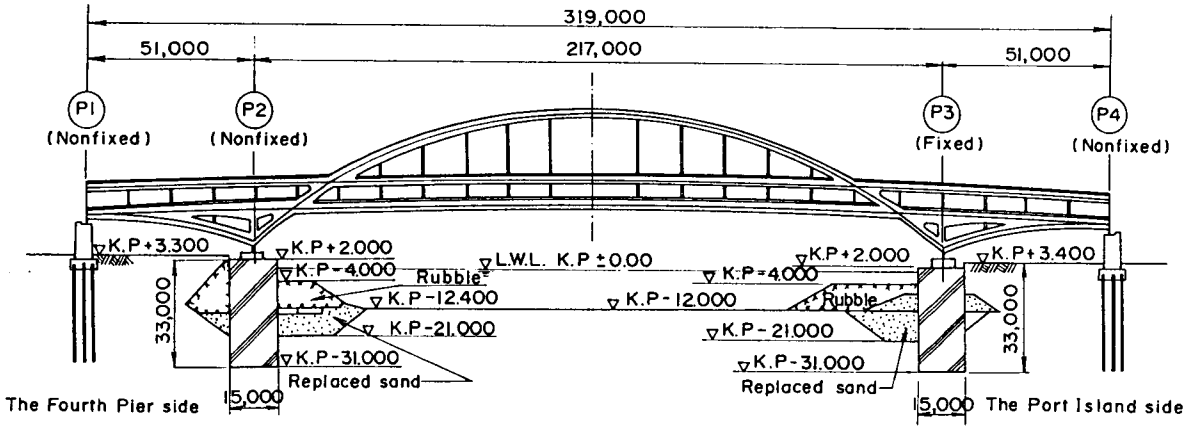
2.1 Constitutive Equations

The constitutive model used in this study is a strain space plasticity type and consists of a multiple shear mechanism in the plane strain

1) Geotechnical Earthquake Engineering Laboratory, Port and Harbour Research Institute, Ministry of Transport, 3-1-1, Nagase, Yokosuka 239, Japan
Tel: 81-468-44-5028, Fax: 81-468-44-4095



(a) Location



(b) Cross section

Fig.1 The location and cross section of Kobe Ohashi Bridge

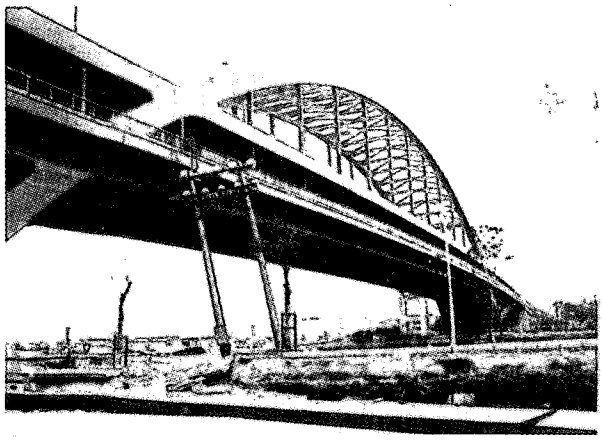


Photo 1 The Kobe Ohashi Bridge

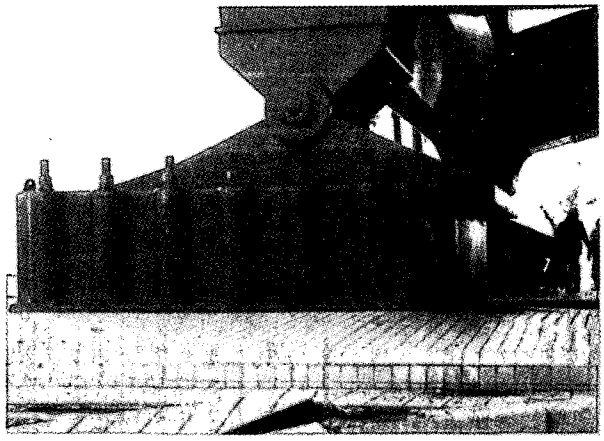


Photo 2 The damage at foundation P2

condition(Iai et al, 1992a). With the effective stress and strain vectors written by

$$\{\sigma'\}^T = \{\sigma'_x, \sigma'_y, \tau_{xy}\} \quad (1)$$

$$\{\varepsilon\}^T = \{\varepsilon_x, \varepsilon_y, \gamma_{xy}\} \quad (2)$$

the basic form of the constitutive relation is given by

$$\{d\sigma'\} = [D](\{d\varepsilon\} - \{d\varepsilon_p\}) \quad (3)$$

in which

$$[D] = K\{n^{(0)}\}\{n^{(0)}\}^T + \sum_{i=1}^{I} R^{(i)}_{L/U}\{n^{(i)}\}\{n^{(i)}\}^T \quad (4)$$

In this relation, the term $\{d\varepsilon_p\}$ in Eq.(3) represents the additional strain incremental vector to take the dilatancy into account and is given from the volumetric strain increment due to the dilatancy as

$$\{d\varepsilon_p\}^T = \{d\varepsilon_p / 2, d\varepsilon_p / 2, 0\} \quad (5)$$

The first term in Eq.(4) represents the volumetric mechanism with rebound modulus K and the direction vector is given by

$$\{n^{(0)}\}^T = \{1,1,0\} \quad (6)$$

The second term in Eq.(4) represents the multiple shear mechanism. Each mechanism i = 1,2,...,I represents a virtual simple shear mechanism, with each simple shear plane oriented at an angle $\theta_i / 2 + \pi / 4$ relative to the x axis. The tangential shear modulus $R^{(i)}_{L/U}$ represents the hyperbolic stress strain relationship with hysteresis characteristics. The direction vectors for the multiple shear mechanism in Eq.(4) are given by

$$\{n^{(i)}\}^T = \{\cos\theta_i, -\cos\theta_i, \sin\theta_i\}$$

(for i=1,2,...,I) (7)

in which

$$\theta_i = (i-1)\Delta\theta \quad \text{(for i=1,2,...,I)} \quad (8)$$

$$\Delta\theta = \pi / I \quad (9)$$

A schematic figure for the multiple simple shear mechanism is shown in Fig. 2. Pairs of circles indicate mobilized virtual shear strain in positive and negative modes of compression shear(solid lines with darker hatching) and simple shear(broken lines with lighter hatching).

The loading and unloading for shear mechanism are separately defined for each virtual simple shear mechanism by the sign of $\{n^{(i)}\}^T\{d\varepsilon\}$. The multiple shear mechanism takes into account the effect of rotation of principal stress axis directions, the effect of which is known to play an important role in the cyclic behavior of anisotropically consolidated sand(Iai et al 1992b). There are ten parameters in the present model, two of which characterize elastic properties of soil; another two specify plastic shear behavior, and the rest characterize dilatancy.

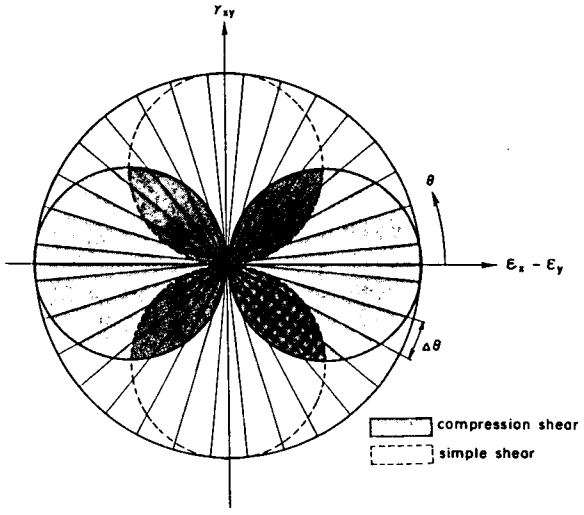


Fig. 2 Schematic figure for multiple simple shear mechanism

2.2 Finite Element Modeling

The finite element mesh shown in Fig.3 was used for the analysis of Kobe Ohashi Bridge under plane strain condition. Total of 2660 nodal points and 4654 elements were used. Five types of elements were used in the analysis, those were linear elements for caisson, nonlinear elements

for sand and clay; beam elements for the upper structure of bridge, liquid elements for water and joint elements for the boundaries between a soil and a structure. The sea water was modeled as incompressible fluid and was formulated as an added mass matrix based on the equilibrium and continuity of fluid at the solid-fluid interface (Zienkiewicz,1977).

2.3 Model Parameters

The model parameters were calibrated by referring to the in-situ velocity measurements and other relevant test results. Shown in Fig.4 were the results of the geotechnical investigations at the Fourth Pier and the Port Island in the vicinity of Kobe Ohashi Bridge.

The dilatancy parameters of fill soil and the sand replacing the original clay layer in Kobe Port were determined referring to Rokko Island data(Inagaki, et al.,1996). The dilatancy parameters for other soils were calibrated based on the SPT N-values and laboratory test results[Ministry of Transport, 1993]. The calibrated liquefaction resistance curves are shown in Fig.5. The computation parameters are shown in Table 1.

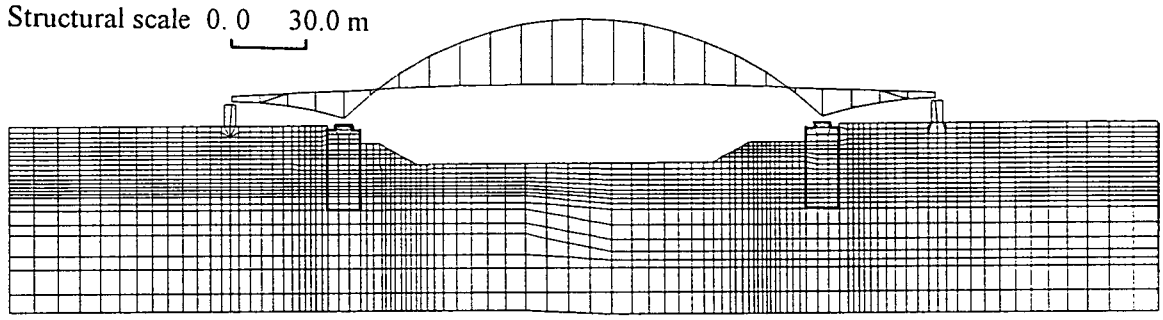
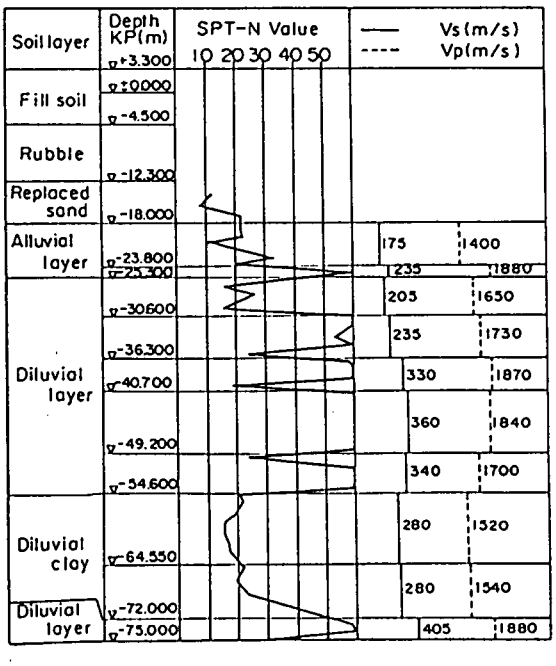
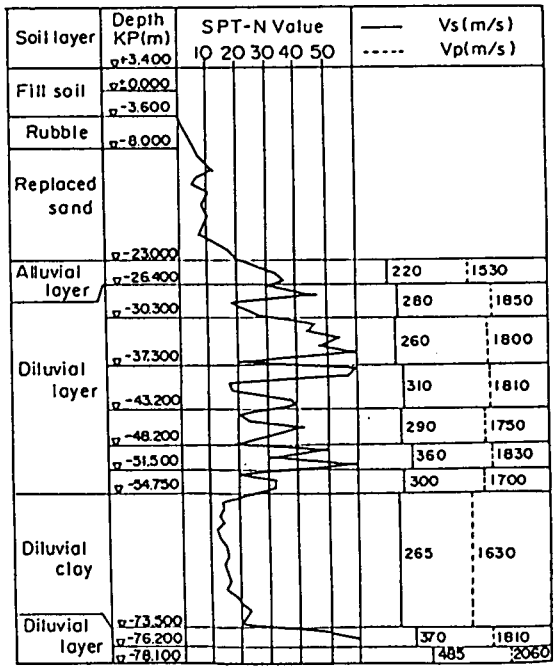


Fig.3 Finite element mesh for Kobe Ohashi Bridge



(a) The Fourth Pier



(b) The Port Island

Fig.4 In-situ investigation results(After Okashita et al. 1996)

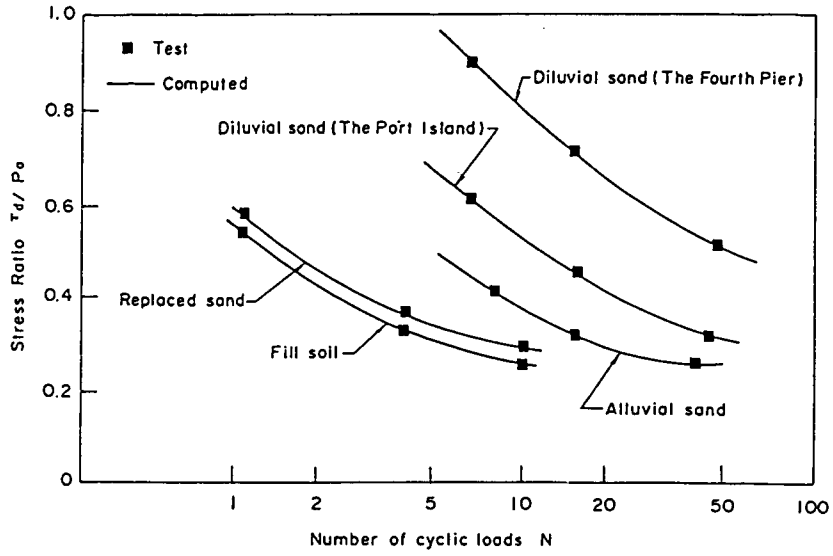


Fig.5 Computed liquefaction resistance curve

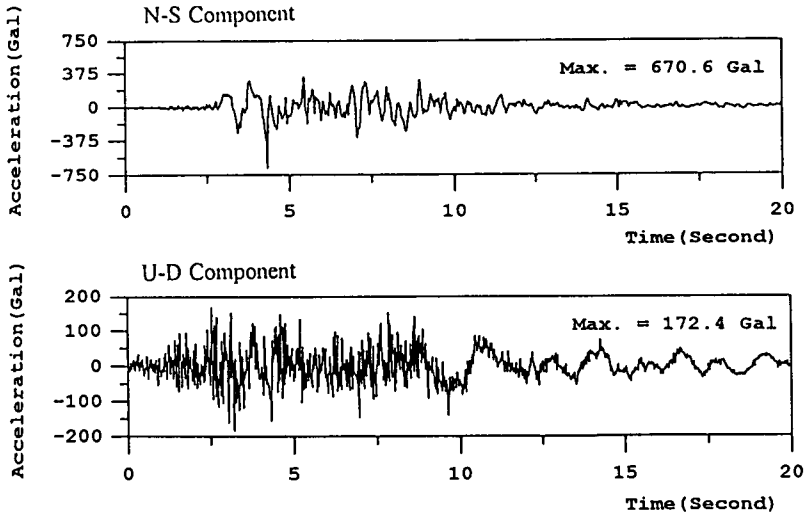


Fig.6 Earthquake motion at 1995 Great Hanshin earthquake recorded at 83 meters depth on Port Island

Table 1 Calculated parameters

Layer No.	γ (tf/m^3)	G_0 (tf/m^2)	K_0 (tf/m^2)	$-\sigma_m$ (tf/m^2)	ϕ'_f (deg.)	ϕ'_p (deg.)	Dilatancy parameters S_1	w_1	p_1	p_2	c_1
Fill soil	1.80	8000	20928	6.300	36	28	0.005	10.5	0.5	0.6	3.40
Replaced sand	1.80	7400	19358	10.60	36	28	0.005	5.50	0.6	0.8	2.30
Alluvial layer	1.96	6100	15958	14.67	36	28	0.005	16.0	0.5	0.8	2.50
Diluvial layer(1)*	1.89	17000	44472	25.00	40	28	0.005	145.	0.5	0.6	25.3
Diluvial layer(2)*	1.87	21000	54936	25.00	40	28	0.005	16.5	0.5	0.8	3.43
Replaced stone	1.92	18000	47088	22.27	40						
Clay layer	1.62	12000	31392	36.30	30						

* Diluvial sand layer(1) is in the Fourth Pier and Diluvial sand layer(2) is in the Port Island.

2.4 Input Accelerations

The earthquake motions were recorded with a vertical seismic array in the Port Island at the ground surface and at depths of 16 m, 32 m and 83m.during January 17,1995 Great Hanshin earthquake. The recording was successfully operated by the Development Bureau of Kobe City.

The site of vertical seismic array is very close to the Kobe Ohashi Bridge with only a distance about 150m. The records at the depth of 83 m shown in Fig. 6 was used as the bedrock motion in the effective stress analysis. The maximum horizontal acceleration in N-S direction is 670.6Gal, while the maximum vertical acceleration is 172.4Gal. It was noted in here that, though the orientation error of seismograph at the depth of 83m was existence(Sugito et al. 1996), the original data was used in this study.

Before the dynamic response analysis, a static analysis was performed to simulate the stress distributions to take the effect of gravity into account. The same constitutive model was used as in the earthquake response analysis but under drained condition. With these initial conditions and the parameters mentioned earlier, an earthquake response analysis was performed on the Kobe Ohashi Bridge. The analysis was conducted with the undrained conditions (Zienkiewicz et al. 1982) in order to simplify the analysis. The numerical time integration was made using of Wilson-θ method (θ=1.4) with the time interval of 0.01 seconds. Rayleigh damping (α=0 and β=0.005) was used to ensure the stability of numerical solution process.

3. RESULTS OF ANALYSIS

The results of the effective stress analysis of the Kobe Ohashi Bridge were shown in Figs. 7 and 10. Shown in Fig. 7 was the displacement and acceleration responses of Nodes 764 and 1658 at the top of caissons P2 and P3 indicated in Fig.8(a).

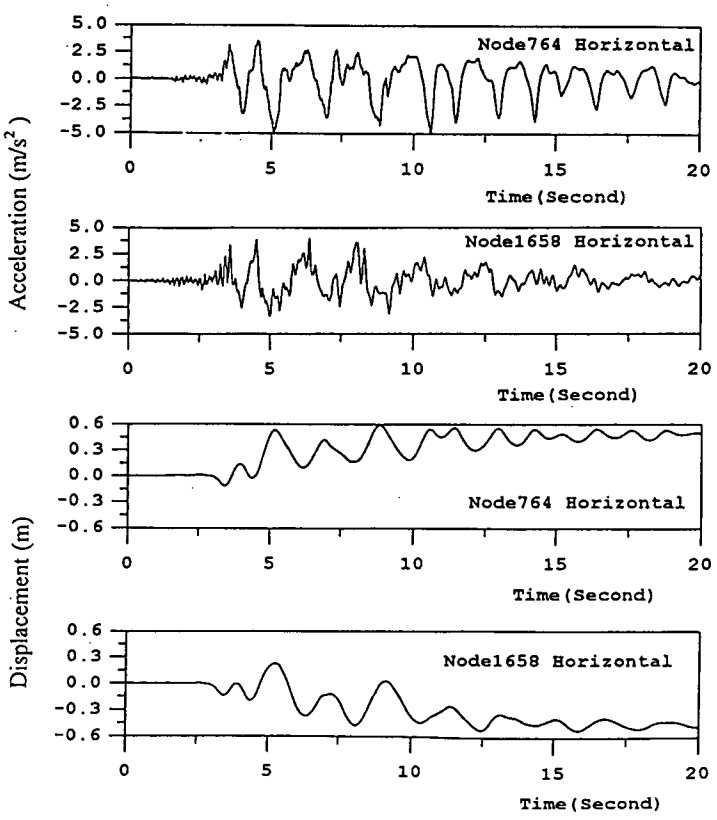
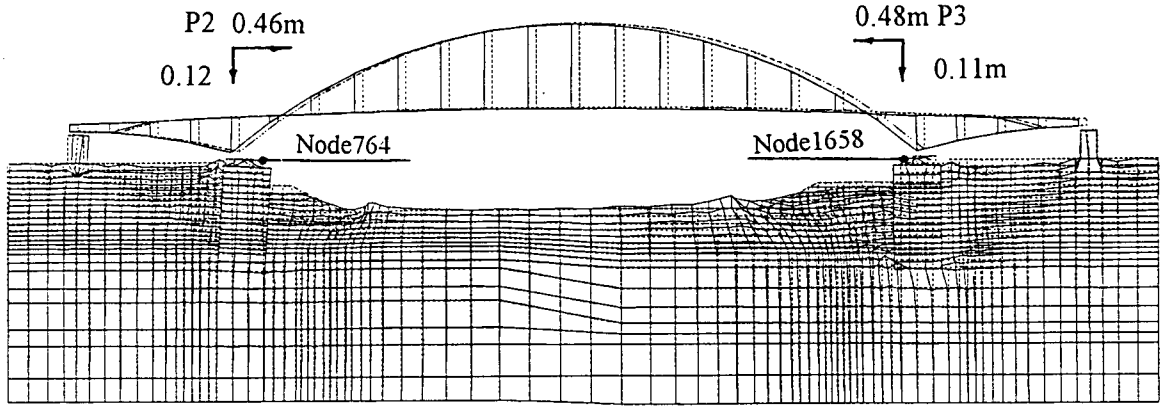


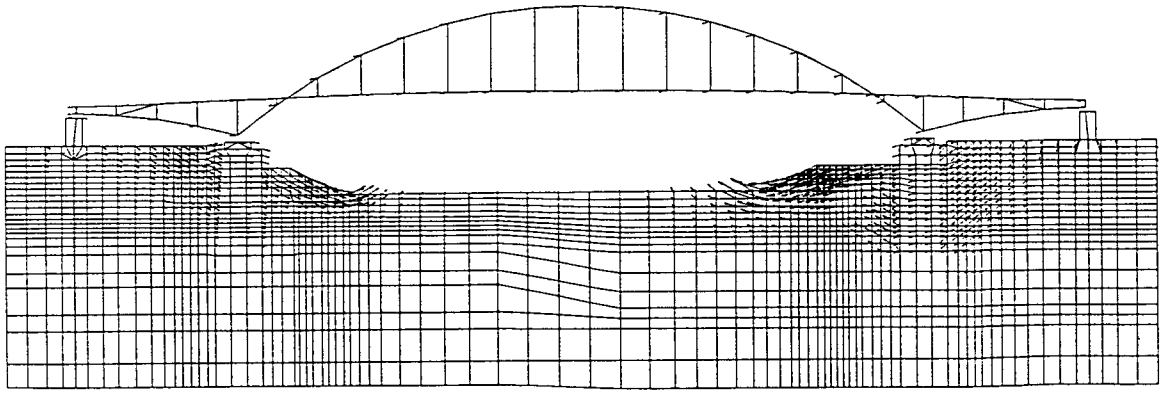
Fig. 7 Time history of deformation and acceleration

The displacements were gradually increased for about 15 seconds and then stayed closed to at the residual values. The shape and vectors of deformation at the end of the earthquake was shown in Fig.8(in figure, the deformation is scaled five as large for the plotting). It was seen that the deformation in the foundation was mainly around the caissons and both of two sides moved toward the sea. The predicted and measured results for the caissons are summerized in Table 2. The computed horizontal displacements were 0.46 m at P2 and 0.48 m at P3 while the settlement were 0.12 m and 0.11 m respectively, the total relative horizontal displacement was 0.94 m. The order of computed deformation was consistent well with the measured after earthquake.

To evaluate the degree of liquefaction of the foundation, the excess pore water pressure ratio specified in terms of $(1-\sigma'_m/\sigma'_{m0})$ was computed, where σ'_m, σ'_{m0} were the current and initial mean effective stresses. The time histories of pore water pressure ratios of elements 384, 1819 in the fill soil and elements 710, 1463 in the replaced sand indicated in Fig.10 were shown in Fig. 9. The pore water pressure were gradually increased to the ratio of 0.85 for about seven seconds and then remained at the high values until the end of earthquake. The residual displacements in Fig.7 were increased with the developement of excess pore water pressure. Distribution of the computed excess pore water pressure ratio contour at the end of the earthquake is shown in Fig. 10. It appeared that liquefaction occurred in the fill soil and replaced sand, these high excess pore water pressures may have affected the performance of the pneumatic caissons for the Kobe Ohashi Bridge.



(a) The shape



(b) The vectors

Fig. 8 The shape and vectors of computed deformation(main part)

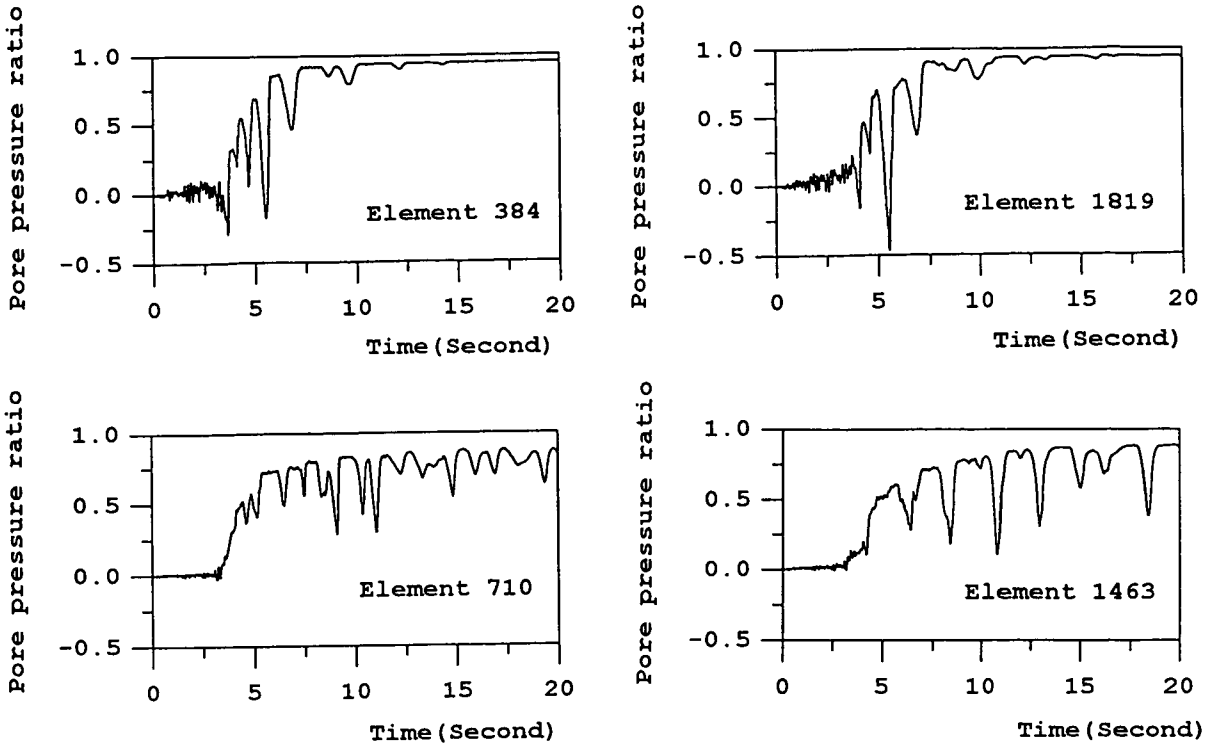


Fig. 9. Time history of excess pore water pressure ratio

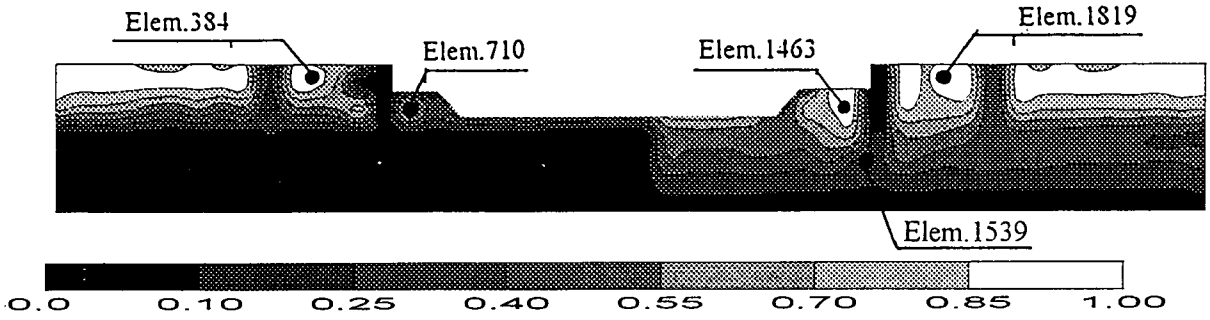


Fig. 10. The computed excess pore water pressure ratio

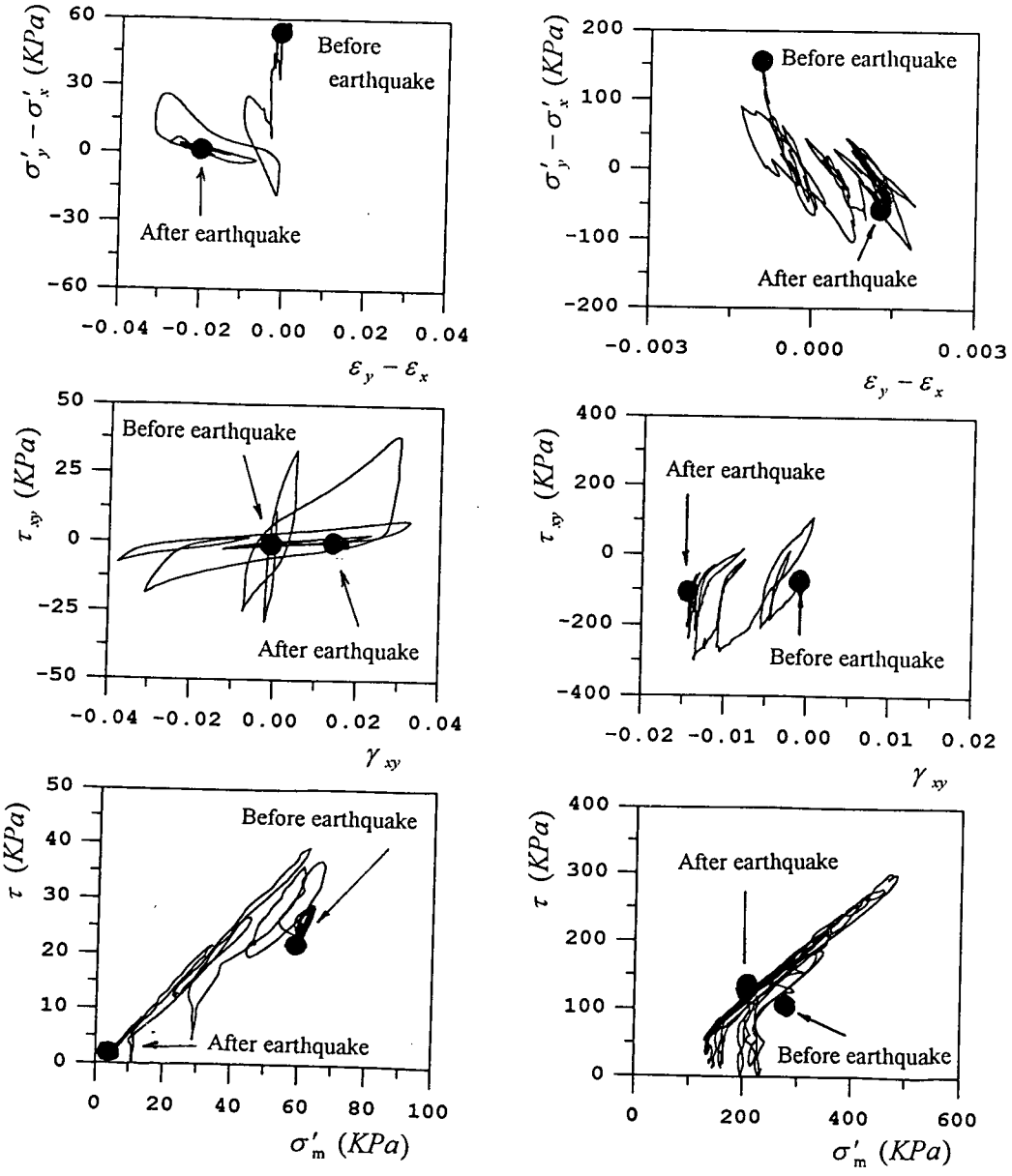
Table 2 The results for caissons

Items	Caisson	P2	P3
Horiz. disp (m)	Compu.	0.46	0.48
	Measu.	Total:	0.60 - 0.80
Incl. angle (deg.)	Compu.	0.68	0.07
	Measur.	0.36 - 0.73	0.78 - 0.93

4. MECHANISM OF DEFORMATION

In order to look into the mechanism of deformation of pneumatic caisson foundations, the stress and strain of soils in the upper fill soil and in the diluvial layer of Port Island indicated by element 384 and 1539 in Fig.10 were plotted in Fig.11. In the fill soil, the effective stress path rapidly decreased and closed to the original as shown at the bottom in Fig.11(a). In accordance with this, the axial strain difference was gradually induced as shown in the upper row of the same figure and the magnitude of the shear strain γ_{xy} in the upper fill was relatively small.

It can also be seen from Fig.11(b) that, in the diluvial layer of Port Island, the effective stress path gradually approached the failure line with fluctuation around the initial deviatoric stress. Even the effective mean stress was once decreased 35 percent, the final value, however, is 220KPa. In accordance with this, the axial strain difference was gradully induced as shown in the middle row of the same figure. The shear strain γ_{xy} was also gradually induced but with a relatively small value. As a result, the deformation of pneumatic caisson foundation was likely to be induced due to the existence initial stress and its release in accordance with overall softening of saturated soil with the mechanism of cyclic mobility.



(a) In fill soil (b) In diluvial layer of Port Island

Fig.11 Predicted stress strain relation and stress path

5. INFLUENCE OF EXCESS PORE WATER PRESSURE

In order to evaluate the effect of the excess pore water pressure increase in the foundation, the following three cases of analyses were performed by introducing an artificial soil model, to be called non-liquefiable soil model which has the same properties as those used in the aforementioned analysis but completely lacks the characteristics of dilatancy. The case which dealt with the actual bridge foundation during the earthquake shown in the previous is designated as Case-1. Case-2 is to idealize both the upper fill and the diluvial layer were the non-liquefiable soils. Case-3 is to idealize only upper fill was non-liquefiable, and Cases-4 is to idealize only diluvial layer was non-liquefiable.

In order to quantify the individual effect of excess pore water pressure increase in the upper fill and diluvial layer, the principal results of the deformation were summarized in Table 3 including those of Case-1. The excess pore water pressure distribution for case-2 to 4 were shown in Fig.12. The results of Case-2 shown that the seaward displacement was 0.31m at the top of a caisson while 0.17m at the top of the other caisson, and resulting in a total of only 0.48m induced purely due to the inertia force of the earthquake. Therefore, it was revealed that the excess pore water pressure increasing in the foundation was to increase the displacement about 2 times as those induced purely by the inretia force due to the earthquake. When there is no effect of excess pore water pressure increase in the foundation, deformation becomes quite localized around the caisson foundation in case-2. The result of Case-3 shown that the excess pore water pressure increase in the upper fill and replaced sand will increase the deformation of caisson about 1.5 times of those induced in Case-2. It is speculated that the soil improvement in the upper soil can restrain the displacement of caisson foundation. The excess pore water pressure increase in the diluvial layers under the caisson P3 as shown in Case-4 was to increase the displacement about 20 percent of those induced in Case-1. It was also noted from Fig.9(a) that the shear deformation under caisson foundation P3 was far larger than that under caisson foundation P2, so the reason was speculated due to the high excess pore water pressure occured in the diluvial layer.

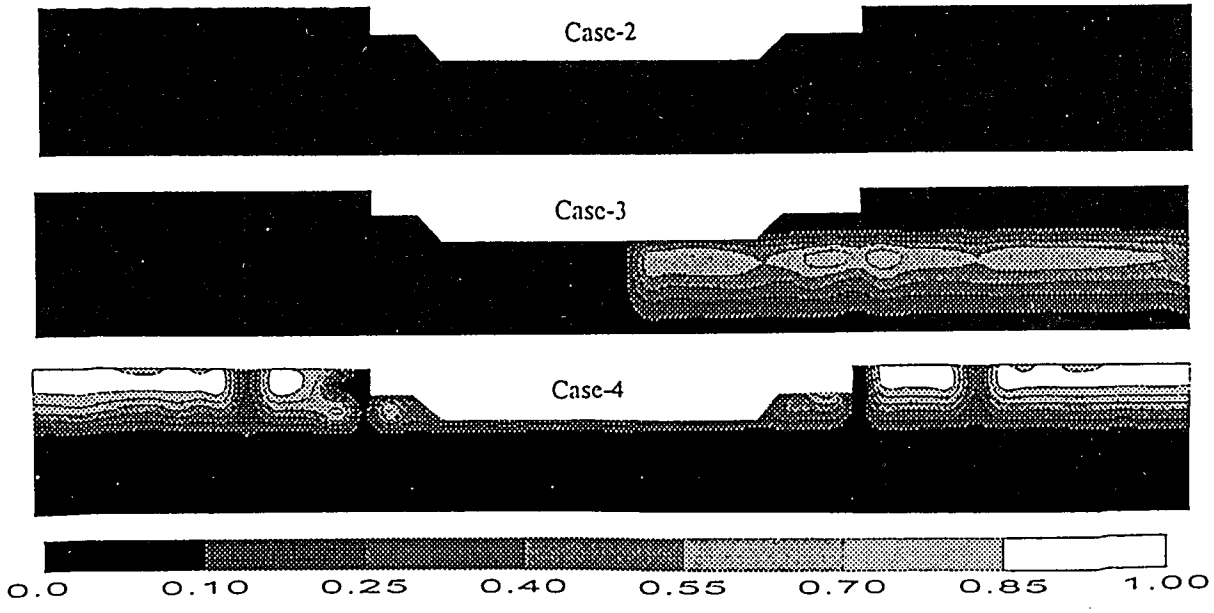


Fig.12 Computed excess pore water pressure for Case-2 to 4

Table 3 Computed residual displacement

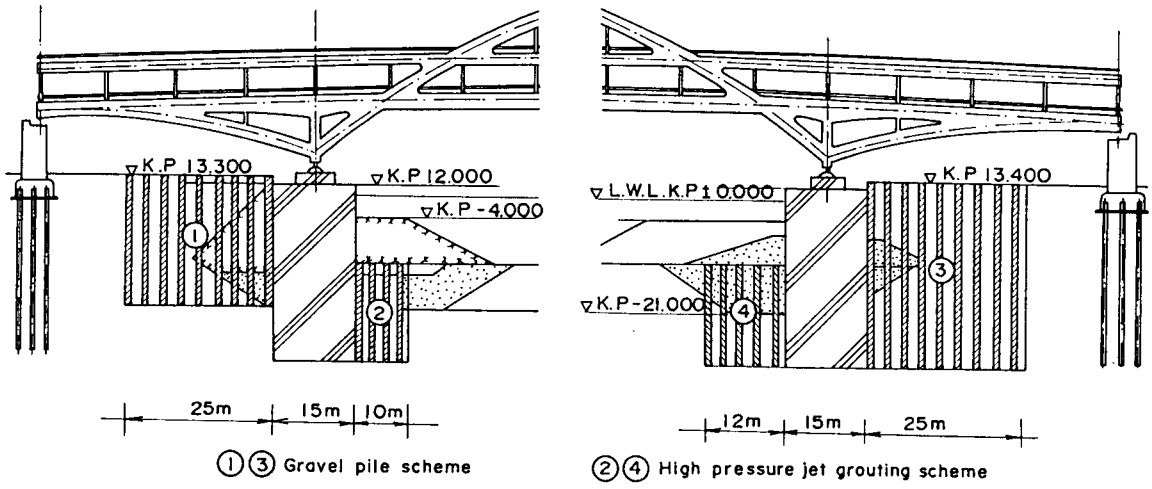
Case	P2(m)	P3(m)	Total(m)
Case-1	0.46	0.48	0.94
Case-2	0.31	0.17	0.48
Case-3	0.28	0.34	0.62
Case-4	0.46	0.16	0.62

6. SOIL IMPROVEMENT ANALYSIS

For the safety operation of bridge, the soil improvement was taken around the caisson by the Kobe city after earthquake. The High Pressure Jet Grouting scheme and Gravel Pile scheme were used to improve the strength and liquefaction resistance of soil. The areas of improvement were shown in Fig.13(Okashita et al. 1996).

In order to evaluate the effectiveness, the analysis for the improved foundation was conducted in here. The same cross section as shown in Fig.1 but partly material parameters changed and the same input motions indicated in Fig. 7 were used for the post improvement analysis. The parameters for improved area was shown in Table 4. Fig.14 was the computed residual displacement. The computed horizontal residual displacement were 0.19m on the top of caisson in the Fourth Pier and 0.39m in the Port Island, respectively resulting in a total of 0.58m total deformation which reduced about 38 percent with the un-improvement case. The settlements at both of two sides reduced to 0.04 m. The comparison of results was shown in Table 5. Fig.15 was the distribution of excess pore water pressure ratio.

Comparing to Fig.10, the excess pore water pressure around the caissons was restrained, and the range of liquefaction was reduced obviously, so the soil improvement after earthquake was effective and reasonable.



(a) In the Fourth Pier side

(b) In the Port Island side

Fig.13 Soil improvement area

Table 4 Parameters for improved areas

Soil No.	γ (tf/m^3)	G_0 (tf/m^2)	K_0 (tf/m^2)	$-\sigma_m$ (tf/m^2)	ϕ'_f (deg.)
①	1.80	8800	23020	6.430	40
②	1.80	10600	27730	14.67	40
③	1.80	8800	23020	6.430	40
④	1.80	10600	27730	14.67	40

Table 5 The computed displacement for improvement

	Improvement	P2	P3
Horiz. disp. (m)	Before	0.46	0.48
	After	0.19	0.39
Vertical disp. (m)	Before	0.12	0.11
	After	0.04	0.04
Prone angle (deg.)	Before	0.68	0.07
	After	0.28	0.07

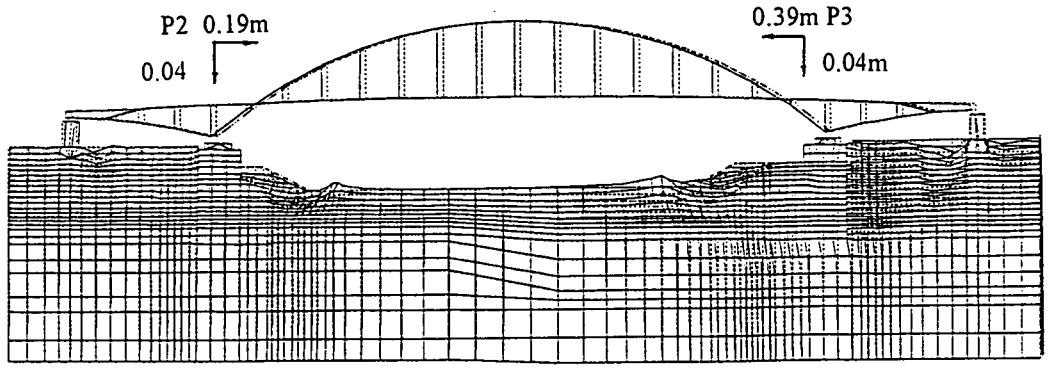


Fig.14 Computed residual deformation after improvement

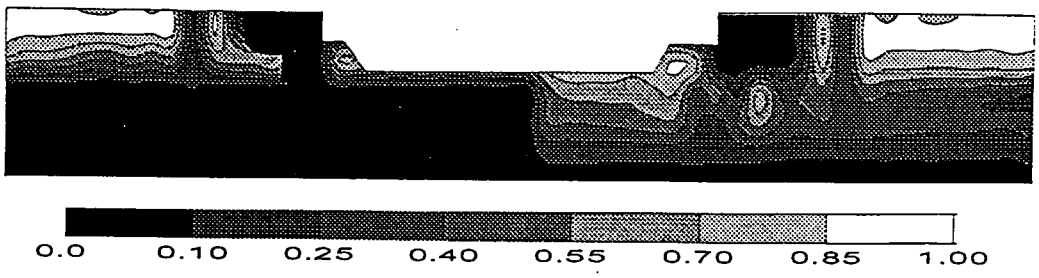


Fig.15 Computed excess pore water pressures after improvement

7. CONCLUSIONS

The effective stress analysis was performed for the Kobe Ohashi bridge during the 1995 great Hanshin earthquake, and led to the following conclusions.

The computed horizontal displacements were 0.46 m on a caisson in the Fourth Pier and 0.48 m on another caisson in the Port Island, the total seaward displacement was 0.94 m. The settlements were 0.12m and 0.11m at P2 and P3 respectively. The order of computed displacement was in good agreement with the measured after earthquake.

Under the earthquake excitation, the pore water pressure increased in the foundation and may have affected the performance of the pneumatic caisson. The excess pore water pressure increasing in the fill soil increased the deformation of pneumatic caissons about two times as large as that purely caused by the seismic inertia force. It was also found that the excess pore water pressure increasing in the diluvial sand layer of Port Island result bigger

shear deformation at the bottom of caisson. The deformation of pneumatic caisson foundation was likely to be induced due to the existence of release in accordance with overall softening of saturated soil with the mechanism of cyclic mobility.

After ground improvement, the computed horizontal residual displacement were 0.19m on the top of caisson in the Fourth Pier and 0.39m in the Port Island, respectively, the total of seaward displacement was 0.58m which was reduced by 38 percent, the excess pore water pressure increasing around the caisson is constrained, so the effect of ground improvement was confirmed.

Based on the above analysis, it was also concluded that, the present model used in the paper has the potential ability to simulate the characteristics of deformations of pneumatic type foundation under strong earthquake motion.

ACKNOWLEDGMENT

The authors gratefully acknowledge the Kobe City for kindly permitting the use of data relevant to the Kobe Bridge. The supports of the STA Fellowship of Japan is also acknowledged.

REFERENCES

1) Editorial Committee for the Report on the Hanshin-Awaji Earthquake Disater, 1996, Damage to Civil Engineering Structures, Bridge Structures. 283-286(in Japanese)
2) Iai, S., Matsunaga, Y and Kameoka, T 1992a, Strain space plasticity model for cyclic mobility, Soils and Foundations, Vol.32, No.2, pp.1-15
3) Iai, S., Matsunaga, Y and Kameoka, T 1992b, Analysis of cyclic behavior of anisotropically consolidated sand, Soils and Foundations, Vol.32, No.2, pp.16-20
4) Inagaki, H., Iai, S., Sugano, T., Yamazaki, H., and Inatomi, T. 1996, Perfor-mance of caisson type quey walls at Kobe port, Soils and Foundations, Special Issue. pp.119-136
5) Inatomi, T., Zen, K., Toyama, S., etc., 1997, Damage to port-related facilities by 1995 Hyogoken-nanbu earthquake, *Technical Note of the Port and Harbour Research Institute*, Ministry of Transport, Japan, 857
6) Japan Architecture Association, 1988, Handbook of Structural design of architecture foundation, pp.163-169
7) Ministry of Transport ed. 1993, Handbook for Liquefaction remediation of reclaimed land, pp.243-245(in Japanese)
8) Okashita, K., Okutani S., Ojima S., and Fujita, C., Numerical study on seismic damage of caisson foundations due to ground liquefaction and examination of countermeasures. Proc. of Civil Engineer Society of Japan on Great Hanshin-Awaji Earthquake, Tokyo, pp.611-618(in Japanese)
9) Sugito, M., Sekiguchi, K., Yashima, A. , Oka, F., Taguchi.Y and Kato, Y. 1996, Correction of orientation error of borehole strong motion array records obtained during the South Hyogo Earthquake of Jan.17, 1995, *Journal of Structural Mechanics and Earthquake Engineering*, JSCE, 12(3 and 4), pp.51-63
10) Yoshimi, Y. 1991, Liquefaction on Sand Foundation, Gihoudo Press, 2nd edition, pp.86(In Japanese)
11) Zienkiewicz, O.C. 1977, The Finite Element Method, 3rd edition, McGraw-Hill Book Co.
12) Zienkiewicz, O.C. and Bettess, P. 1982, Soils and other saturated media under transient, dynamic load conditions, Soil Mechanics-Transient and Cyclic Loads, Pande & Zienkiewicz eds., John Wiley and Sons, pp.1-16

New Strong Motion Array Observation System of the Public Works Research Institute

by
Koichi Yokoyama [1], Keiichi Tamura [2], Hideki Sugita [3], Riki Honda [4] and Akira Chiba [4]

ABSTRACT

Strong motion records obtained by dense instrument array are essential for research of ground motion, including propagation characteristics of seismic wave, effect of the ground condition, etc.

The Public Works Research Institute (PWRI), Ministry of Construction, has been conducting array observation since 1980 in four areas around Suruga Bay: Sagara, Yaizu, Numazu and Matsuzaki. In 1996, these arrays were replaced with a new system and in 1997, new arrays were additionally installed in five areas. Two arrays were deployed in Kobe (Hyogo Prefecture), and one in each of Odawara (Kanagawa Prefecture), Makuhari-Narashino (Chiba Prefecture) and Tateyama (Chiba Prefecture).

In the new system, all accelerographs are connected with the workstation in PWRI by digital telephone (ISDN) line. All accelerographs are under the control of this workstation, and various functions such as acquisition of strong motion data, check of the status of the accelerographs are operable on-line from PWRI.

This paper describes the new array observation system, including major functions of the system, site condition of the arrays, configuration of accelerometer deployments.

Key Words : Strong Motion,
Array Observation

1. INTRODUCTION

Rationalization of seismic design method requires accurate estimation of the earthquake ground motion. Research of the ground motion characteristics has progressed widely in the last several decades. In spite of such achievements, research of earthquake ground motion still has many unsolved topics.

One of such topics is the spatial variation of ground motion, especially that in the space with the order of several kilometers or less. Investigation of the damage of the past earthquakes or analyses of the strong motion records revealed that ground motion is considerably different at different points. In the 1995 Hyogoken Nanbu Earthquake, it was also observed that there were cases in which structures near the severely damaged structure were little damaged and that difference of the ground motion is considered as one of major reasons. Such spatial variation of ground motion is essential for rational seismic design because it determines the difference of the ground motion that should be considered in the seismic design of large scale civil engineering structures, such as long span bridges, tunnels, pipelines, etc.

As is widely recognized, for the research of the ground motion characteristics, strong motion records are indispensable, and for the research of spatial variation of ground motion, strong motion records obtained by instrument arrays are essential.

The importance of the dense array for strong motion monitoring is widely recognized. The Executive Committee of the International Association for Earthquake Engineering decided in 1977, to hold the International Workshop on Strong Motion Earthquake Instrument Arrays, which was

1) Director, Earthquake Disaster Prevention Research Center, Public Works Research Institute, Ministry of Construction, Asahi 1, Tsukuba-shi, Ibaraki-ken, 305 Japan,
2) Head, Ground Vibration Division, ditto.
3) Head, Earthquake Disaster Prevention Technology Division, ditto.
4) Research Engineer, Ground Vibration Division, ditto.

also consented by the International Association of Seismology and Physics of the Earth's Interior (IASPEI). The workshop was held in 1978 in Hawaii[1], and in advance of that workshop, the Steering Committee of Earthquake Engineering of Japan Science Council organized the Workshop on Strong Motion Earthquake Instrument Arrays to prepare the master plan of array observation.

After the 1995 Hyogoken Nanbu Earthquake, importance of array observation of strong motion is reaffirmed. Necessity of array observation is mentioned in the reports such as, Proposal on Earthquake Resistance for Civil Engineering Structures (Vol.1) by the Japan Society of Civil Engineers[2], the first report of the Special Committee for Investigation of Hanshin-Awaji Great Earthquake Disaster, Japan Science Council[3], etc.

Considering such situation, the Public Works Research Institute started the installation program of dense accelerograph array for strong motion observation, and during the period of 1981 to 1985, PWRI deployed four arrays in Shizuoka Prefecture (Sagara, Yaizu, Numazu and Matsuzaki) [4] [5]. Since then PWRI has been conducting the strong motion observation by those dense arrays.

In 1996, PWRI renewed those existing four arrays, and in 1997 it additionally installed five new arrays: two Kobe Arrays (West and East) in Hyogo Prefecture, Odawara array in Kanagawa Prefecture, Makuhari-Narashino Array and Tateyama Array in Chiba Prefecture.

Locations of nine arrays are shown in Fig.1. Each array consists from about ten observation stations and there are 97 stations in total. (Some stations have more than one observation point and, therefore the total number of observation points is 103.) All accelerographs are connected to the workstation installed at PWRI with a digital telephone line and they are under the control of the workstation.

2. NEW ARRAY OBSERVATION SYSTEM

Fig.2 illustrates the typical equipment of an observation station. One station has an observation house, which contains the data transmission controller, and one to six accelerometers (acceleration sensors). The data transmission controller conducts time calibration every second using the information of time received through the GPS antenna. All accelerometers are set underground at various depths and, in general, one of the accelerometers of each observation point is set at the depth of 2m. The data transmission controller is connected to the workstation with the digital telephone (ISDN: Integrated Services Digital Network) line.

When accelerometers detect ground motion, the data transmission controller stores the strong motion data on the non-volatile memory, and sends alarm signal and the data to the workstation at PWRI. On the workstation, addition of the data to the database, plot of distribution of the recorded peak accelerations on the map, and calculation of acceleration response spectra and Fourier spectra, etc. are performed.

Maintenance of the observation system is also automatically conducted, as is scheduled, under the control of the workstation. The workstation can check the status of accelerometers by sending test signals through the data transmission controller. It also can check the condition of the data transmission controller, such as backup battery, available memory capacity, accuracy of clock etc.

3. SITE CONDITION OF ARRAYS

In this section, site condition of each array is described briefly.

3.1 Sagara Array [6]

Sagara Array is located in Shizuoka Prefecture and in the west of the Suruga Bay. The area around the Suruga Bay, which was severely damaged in the 1854 (Ansei era) Tokai Earthquake (Inferred magnitude is 8.4), is alluded to have a high possibility to be hit by a large earthquake. This is because in the Suruga Bay runs the Suruga Trough, which is shown in Fig.1. The Suruga Trough is considered to be seismically active because the

Philippine Sea Plate and the North America Plate collide there.

Configuration of observation points is shown in Fig.3(a) and the cross section of the ground along the line A-A' is shown in Fig.3(b). (In the figure of the ground cross section, the accelerometers installed at the depth of 2m are not explicitly shown to make the figure simple. It is also the same with the following figures of other arrays except Tateyama Array.) The installation depths of the accelerometers are listed in Table1.

Most of the area is covered with soft alluvial layers and the bedrock is Sagara Group. The surface layers consist mainly from the deposits of the Hagima River. They are soft and their shear wave velocity is about 100m/sec. The bedrock has the shear wave velocity of about 400m/sec. Depth of the bedrock varies gradually along the section A-A' and therefore it is expected that the effect of the variation of ground condition is observed.

There are ten observation points and the distance between observation points is less than a few hundred meters. Additional accelerometers (hereinafter, accelerometer installed at the depth deeper than 2m will be referred to "additional accelerometer".) are installed at observation points Nos.4, 5, 8 and 10. The deepest accelerometers at observation points Nos.4, 5, 8 and 10 are all installed in the bedrock layer.

3.2 Yaizu Array [7]

Yaizu Array is located in the northeast of Sagara Array and it also faces the Suruga Bay. Configuration of observation points is shown in Fig.4(a), and the cross section of the ground along the line A-A' is shown in Fig.4(b). The installation depths of the accelerometers are listed in Table 2.

The surface layer consists mainly from deltaic sediment and back-marsh sediment. It is soft and its shear wave velocity ranges from 100 to 200m/sec. The layer deeper than 25m is the alternation of sand and clay. Shear wave velocity increases gradually and reaches 600m/sec at the bedrock, basaltic layer. The bedrock layer is found at the depth of 10m at the observation point No.1, which indicates the variation of the depth of the bedrock layer.

In this array, the accelerometers are mainly installed at the shallow layer and additional accelerometers are installed at observation points Nos.5 and 9. The deepest accelerometer at No.9 is at the depth of 113m and reaches the bedrock. Observation point No.1 has one accelerometer at the depth of 10m, in the bedrock, and not equipped with the accelerometer at 2m deep.

3.3 Numazu Array [8]

Numazu Array also faces the Suruga Bay on its south end. Configuration of observation points and the cross section of the ground along the line A-A' are shown in Figs.5(a) and (b) respectively and the installation depths of the accelerometers are listed in Table 3.

The Numazu array ranges from the foot of Mt. Ashitaka to the coastal line facing the Suruga Bay. The mountainous area is covered with a soft loam layer and a stiff gravelly layer exists underneath. The area between the Tokaido Shinkansen Line and The Tokaido Line is covered with an alluvial layer, which is about 10-15m thick and consists of the organic soil with shear wave velocity of less than 100m/sec. It is underlain by relatively stiff alluvial layers with shear wave velocity of 200m/sec or larger. Under these alluvial layers exists a stiff diluvial gravelly layer whose shear wave velocity is about 500m/sec.

There are 14 observation points in Numazu Array. Observation points Nos.2, 7, 8 and 9, for example, are about only 100m apart. Observation points Nos.3, 10, 11 and 13 are equipped with additional accelerometers and the deepest accelerometers at these observation points are all installed in the diluvial gravel layer. Accelerometer of the observation point No.14, which does not have a accelerometer at the depth of 2m, is set in the gravel layer.

3.4 Matsuzaki Array [9]

Matsuzaki Array is located in the west coastal area of the Izu Peninsula, facing the Suruga Bay. Configuration of observation points and the cross

section of the ground along the line A-A' are shown in Figs.6(a) and (b) respectively and the installation depths of the accelerometers are listed in Table 4.

Matsuzaki Array spreads from the top of Mt. Ushibara to the north end of the plain area. The observation points Nos.1 to 5 are deployed on the steep slope of Mt. Ushibara. The difference of the elevation between points Nos.1 and 5 is about 150m. It is expected the effect of the topographical condition will be observed. The slope is covered with relatively soft alluvial soil, and the accelerometers are installed both at the depth of 2m and in the stiff layer underneath.

The plain area is mainly covered with the alluvial soil, that is, stream deposits of the Naka River and marine deposits. Shear wave velocity of the alluvial soil is about 150m/sec.

There are 11 observation points in this array. The additional accelerometers are installed at observation points except Nos.7, 10 and 11. Most additional accelerometers are mainly in the bedrock or stiff gravel layer. Exception is one of the accelerometers of the observation point No.6, which is installed 10m deep. The other is located at the depth of 40m in the bedrock at this observation point. Point No.6 is located near the foot of Mt. Ushibara where depth of the bedrock layer varies, and therefore it is an important point to observe the effect of the depth variation of a base layer.

3.5 Kobe Arrays (West and East)

Kobe Arrays are both located in the east part of the Kobe City, facing the Osaka Bay. This is part of the area, which suffered severe damage in the 1995 Hyogoken Nanbu Earthquake. The arrays cross the band where the highest seismic intensity 7 was declared by the Japan Meteorological Agency.

It is known that the area including Kobe and Osaka has many active faults and in the array area there are active fault trace and fault scarp, which are presumed to be a part of the Gosukebashi Fault and a part of the Ashiya Fault, respectively[10]. Their locations are shown in Fig.7(a) with the configuration of the observation points.

It is not expected that such a large earthquake will hit this area soon after the 1995 Hyogoken Nanbu Earthquake. But it is meaningful to record the strong motion at the area where once unprecedentedly strong ground motion was observed, because comparison of the ground motion characteristics would lead to various finding.

Figs.7(a) and (b) show the configuration of observation points and the cross section of the ground along the line A-A' respectively, and the installation depths of the accelerometers are listed in Table 5.

The Kobe Arrays range from the mountainous area belonging to the Rokko mountains, to the artificially reclaimed islands in the coastal area. Bedrock is granite and its shear wave velocity is about 2km/sec. The bedrock layer lies at a shallow depth in the northern mountainous area around the observation points Nos.10 and 11 of the West Array. It is said, however, that the bedrock is at more than 1km depth in the coastal area. The area between the south of Hankyu Kobe Line and National Highway Route No.43 is covered with thin alluvial layers. In the southern area of Route No.43 is mainly an artificially reclaimed land covered with about 20m thick soft soil, which is underlain by alluvial and diluvial layers. Some of the strong motion records of the 1995 Hyogoken Nanbu Earthquake showed that the ground motion of the reclaimed land was damped because of the inelastic behavior of the ground and, to the contrary of what was widely admitted, its peak acceleration at the ground surface was smaller than that of underground records. It is expected that strong motion records by Kobe Arrays, whose ground condition varies from the bedrock of granite to the relatively new reclaimed land, may contribute to the research about such phenomena.

Kobe West Array consists of twelve observation points and it has additional accelerometers at observation points Nos.2, 4, 6, 7, 8 and 11. One of the accelerometers of the observation point No.11 is set in the granite bedrock. At the observation points Nos.2 and 4, six and five accelerometers respectively are installed in various layers including the soft surface layer whose shear wave velocity is less than 150m/sec, and the diluvial

layer at the depth of 80 - 100m whose shear wave velocity is about 500m/sec.

In Kobe East Array there are nine observation points and additional accelerometers are installed at observation points Nos.2, 3 and 6-9. The observation point No.2, which is located on the artificially reclaimed soft ground of the Fukae Hama, has five accelerometers and the deepest accelerometer is installed at 100m deep in the silty layer whose shear wave velocity is about 300m/sec. The deepest accelerometers of the observation points Nos.3 and 7 are at the depths of 40m and 32m respectively and both are in the gravelly layer with shear wave velocity of about 400m/sec or more.

3.6 Odawara Array

Odawara Array is located in the east of the center of Odawara City, facing the Sagami Bay. It expands along the coastal line and it crosses the Kozu-Matsuda Fault. Kozu-Matsuda Fault[10], which is shown in Fig.8(a) with the configuration of the observation points, is considered to be a part of the Sagami Trough. The Sagami Trough is the boundary of the Philippine Sea Plate and the North America Plate (or the Okhotsk Plate) and several huge earthquakes occurred on the trough, such as the 1923 Kanto Earthquake (M=7.9) and the 1703 (Genroku era) Kanto Earthquake (M=7.9-8.2). The Kozu-Matsuda Fault is estimated to accumulate dislocation at the ratio of about 3.5mm/year and it is considered seismically active.

The cross section of the ground along the line A-A'(Fig.8(a)) are shown in Fig.8(b) and the installation depths of the accelerometers are listed in Table 6.

Odawara Array expands crossing the Kozu-Matsuda Fault, including the mountainous area (observation point No.4) to the Sakawa River. Discontinuity of the ground condition between the observation points Nos.1 and 2, shown in Fig.8(b), corresponds to the Kozu-Matsuda Fault. In the east area of the fault, bedrock with a shear wave velocity of about 700-1000m/sec exists at a small depth and the deepest accelerographs of Nos.2-4 are installed in this layer. The ground condition changes drastically in the west area of the fault. It consists mainly from the alternation of sandy and clayey layers whose shear wave velocity is about 200-400m/sec, and the diluvial gravelly layer with the shear wave velocity of 600-1000m/sec underlies them. Ground under the observation point No.8 was judged to be diluvial from the boring data, but further investigation is required to confirm it.

Odawara Array consists of 11 observation points. This array is equipped with large number of deeply installed accelerometers and additional seismometers are installed at all observation points except Nos.6 and 11. The deepest accelerometer of the observation point No.9 is installed at the depth of 88m; in the gravel rock layer underling the gravelly diluvial layer. The shear wave velocity of the rock is about 700m/sec.

3.7 Makuhari-Narashino Array

Makuhari-Narashino Array is located on the coastal line facing the Tokyo Bay on its southwest end. Configuration of observation points and the cross section of the ground along the line A-A' are shown in Fig.9(a) and (b) respectively and the installation depths of the accelerometers are listed in Table 7. Northeast part of this array (observation points Nos.1 and 2.) is in Narashino City and the rest is in Makuhari district of Chiba City.

The area around Tokyo Bay is seismically active. Coastal area of Narashino district is newly reclaimed land and therefore it is expected the ground motion of the newly reclaimed soft ground will be recorded.

The Makuhari-Narashino Array consists of 11 observation points and additional accelerometers are installed at observation points Nos. 1, 3, 5, 8, 10 and 11. The array site can be divided into three parts.

The northeast part including observation points Nos.1 and 2 is located on the lowland in the plateau, which is filled with the soft deposit. That deposit is about 13m thick and its shear wave velocity is less than 100m/sec. The soft deposit consists of three layers; superficial sandy filling, organic soil and silty sand. The underlying diluvial sandy layer has shear wave velocity of about

300m/sec. Three of the four accelerometers of observation point No.1 are installed in the three layers of soft deposit and the deepest one is in the diluvial layer.

The area between observation point No.3 and National Highway Route No.14 is a plateau, which is covered with 4-5 meter thick loam layer and the diluvial sandy layer exists under the loam layer. Shear wave velocity of the loam layer is 100-200m/sec and that of the underlying diluvial layer is more than 300m/sec. Additional accelerometers of the observation points Nos.3 and 5 are installed at the shallow depth (at the depth of 10 and 6m respectively) and at the depth of 30m in the diluvial layer.

The area between Route No.43 and the seashore is artificially reclaimed land and it is covered with 10-30m thick soft layer with the shear wave velocity of less than 200m/sec. The sandy diluvial layer underneath has the shear wave velocity of 300m/sec. The deepest accelerometer is installed at the observation point No.8, which has three additional accelerometers at the depths of 8, 30 and 100m.

3.8 Tateyama Array

Tateyama Array is located in the southern part of the Boso Peninsula, facing the Tateyama Bay. Tateyama City, which is located close to the Sagami Trough, suffered severe damage in the 1703 Kanto Earthquake and the 1923 Kanto Earthquake. Many fault models[11] proposed as the causative faults of these earthquakes, lie under Tateyama City. It can be said, therefore, that Tateyama Array is located also seismically active area.

Configuration of observation points, cross section of the ground along the line A-A' and the installation depths of the accelerometers are shown in Fig.10(a), (b) and Table 8, respectively. In Fig.10(b), accelerometers at the depth of 2m are also shown. There are 11 observation points and observation points Nos.4, 6 and 10-12 are equipped with additional accelerometers.

There is a small hill in the Shiroyama Park and observation points Nos.1-3 are installed on its slope. Thin soft clayey soil covers the hill and its thickness is large at the bottom of the hill. Therefore the accelerometer of the observation point No.3 is installed at the depth of 7m while those of observation points Nos.1 and 2 are at the depth of 2m.

The other observation points are deployed in the plain area. The plain area is uniformly covered with an about 10m thick alluvial sand layer and an about 10m thick alluvial clayey layer. Beneath them lies a rock stratum, whose depth varies steeply. Therefore in this array, it is expected that the effect of the spatial variation of the depth of base layer will be observed.

3. CONCLUDING REMARKS

The new strong motion array observation system of the Public Works Research Institute is introduced. The arrays that had been deployed around the Suruga Bay between 1981 and 1984 were renewed and five new arrays were additionally installed; Kobe West Arrays, Kobe East Arrays, Odawara Array, Makuhari-Narashino Array and Tateyama Array. Strong motion observation at these sites are considered important from the view point of earthquake engineering for reasons such as that they are located in seismically active areas or near active faults, and that the ground conditions of these arrays vary spatially.

Authors hope the strong motion records that will be obtained by these arrays attribute to the progress of earthquake engineering technology, earthquake disaster prevention technology and so on.

ACKNOWLEDGMENT

The observation stations of the arrays are installed in the places such as parks, school grounds and other various facilities with the permission of the owners, the administrators, the municipal corporation etc. Installation of these arrays could not have been done without their understanding and cooperation. Authors would like to express their sincere gratitude to everybody and every

organization concerned.

REFERENCES

1) Proceedings of the International Workshop on Strong Motion Earthquake Instrument Arrays, International Association for Earthquake Engineering, May 1978
2) Proposal on Earthquake Resistance for Civil Engineering Structures (Vol.1), Japan Society of Civil Engineers, May 1995. (in Japanese)
3) First Report of the Special Committee for Investigation of Hanshin-Awaji Great Earthquake Disaster, Japan Science Council, October 1995. (in Japanese)
4) T. Okubo, T. Arakawa et al., Dense Instrument Array Program of the Public Works Research Instiute and Preliminary Analysis of the Records, Proceedings of 8th World Conference on Earthquake Engineering, 1984
5) T. Iwasaki, Y. Sasaki, et al., Dense Instrument Array System by PWRI for Observing Strong Earthquake Motion, Proceedings of the 18th Joint Meeting, U.S.-Japan Panel on Wind and Seismic Effects, UJNR, May 1986
6) T. Arakawa, K. Kawashima, et al., Dense Instrument Array Observation by Public Works Research Institute, -(1) Observation System at Sagara Area -, Technical Memorandum of PWRI, No.1847, July 1982. (in Japanese)
7) T. Arakawa, K. Kawashima, et al., Dense Instrument Array Observation by Public Works Research Institute, -(2) Observation System at Yaizu Area -, Technical Memorandum of PWRI, No.1994, March 1983. (in Japanese)
8) T. Arakawa, Y. Sasaki, et al., Dense Instrument Array Observation by Public Works Research Institute, -(3) Observation System at Numazu Area-, Technical Memorandum of PWRI, No.2140, September 1984. (in Japanese)
9) Y. Sasaki, K. Tamura et al., Dense Instrument Array Observation by Public Works Research Institute, -(4) Observation System at Matsuzaki Area -, Technical Memorandum of PWRI, No.2238, May 1985. (in Japanese)
10) Active Fault Map in Urban Area, Geographical Survey Institute, September 1996.
11) R. Sato et al., Japan Earthquake Fault Parameter Handbook, March 1989, Kajima Institute Publishing Co., Ltd. (in Japanese)

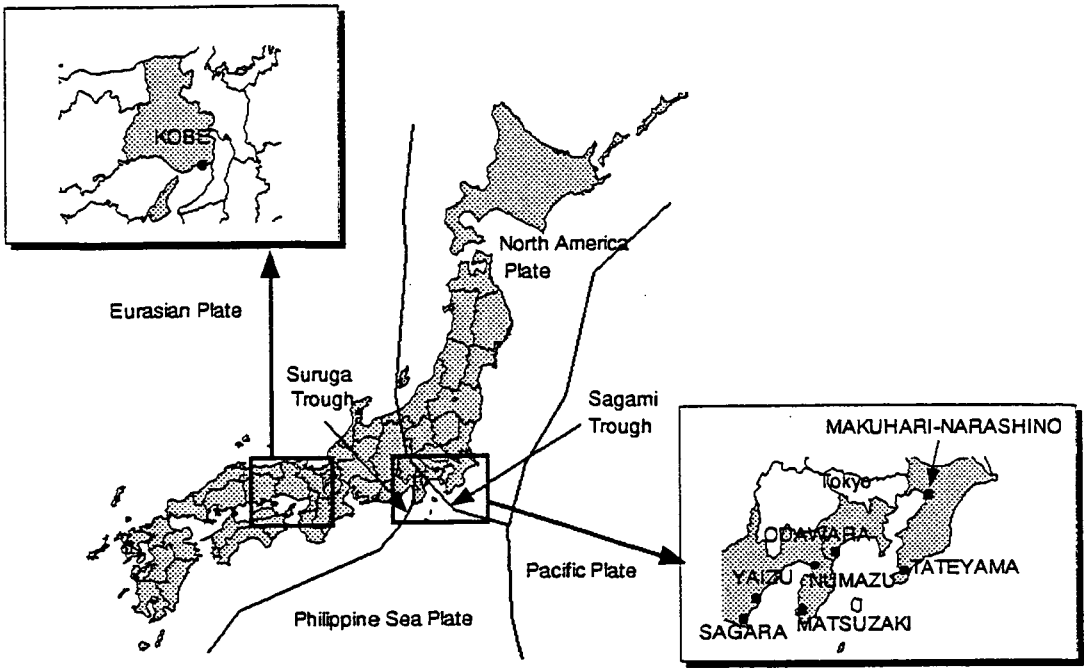


Fig.1 Locations of Arrays

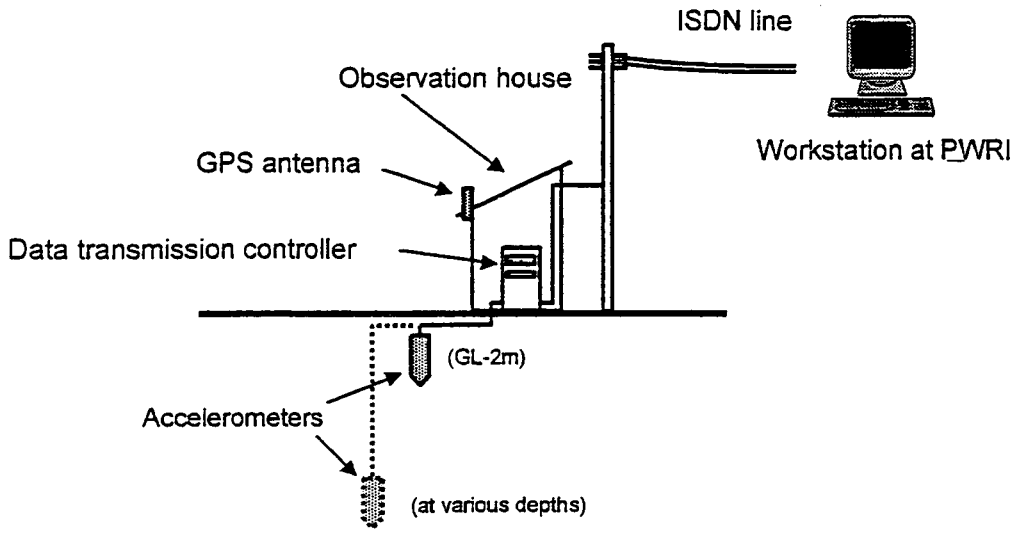


Fig.2 Illustration of devices installed in each observation station

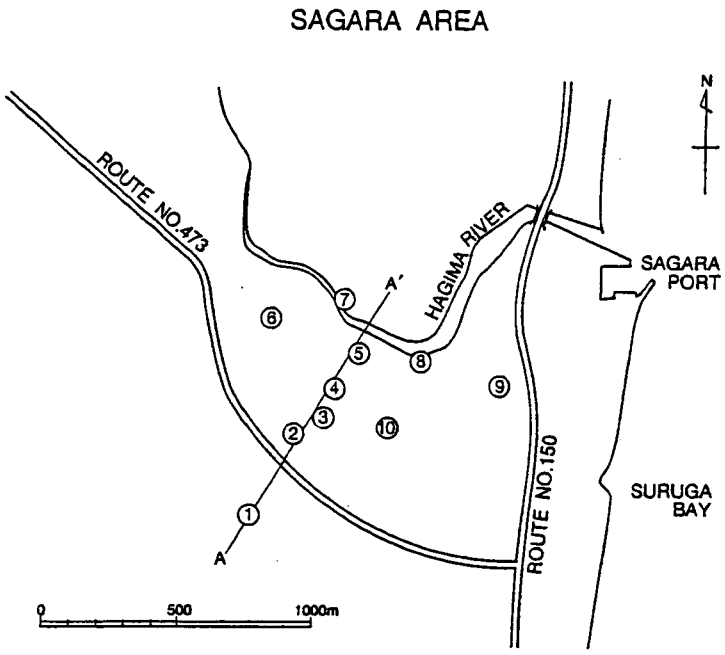
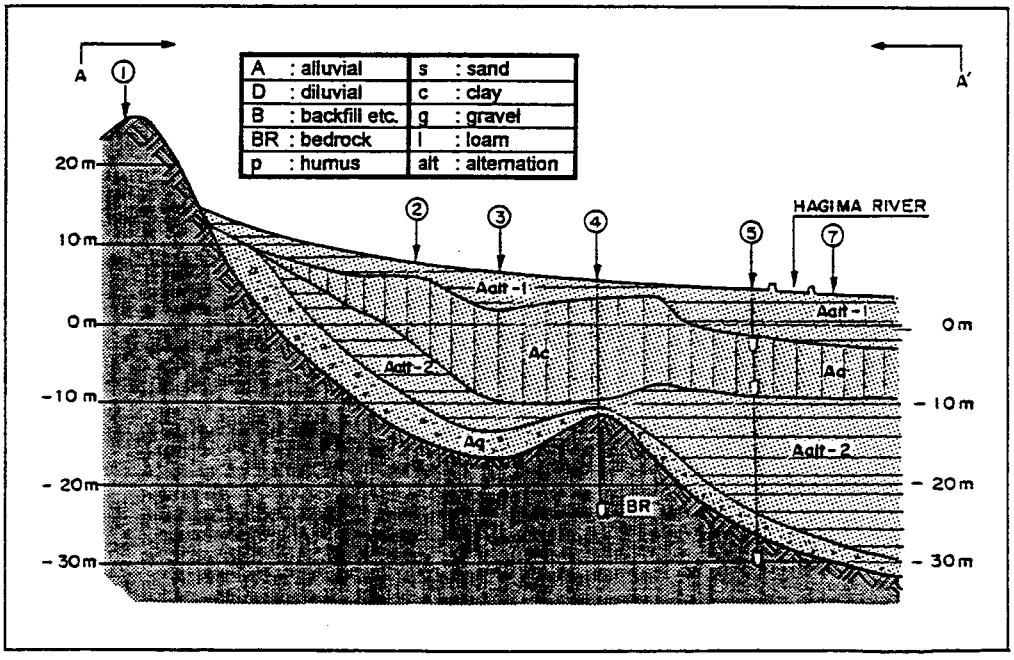


Table 1 Accelerometer Installation Depth of Sagara Array

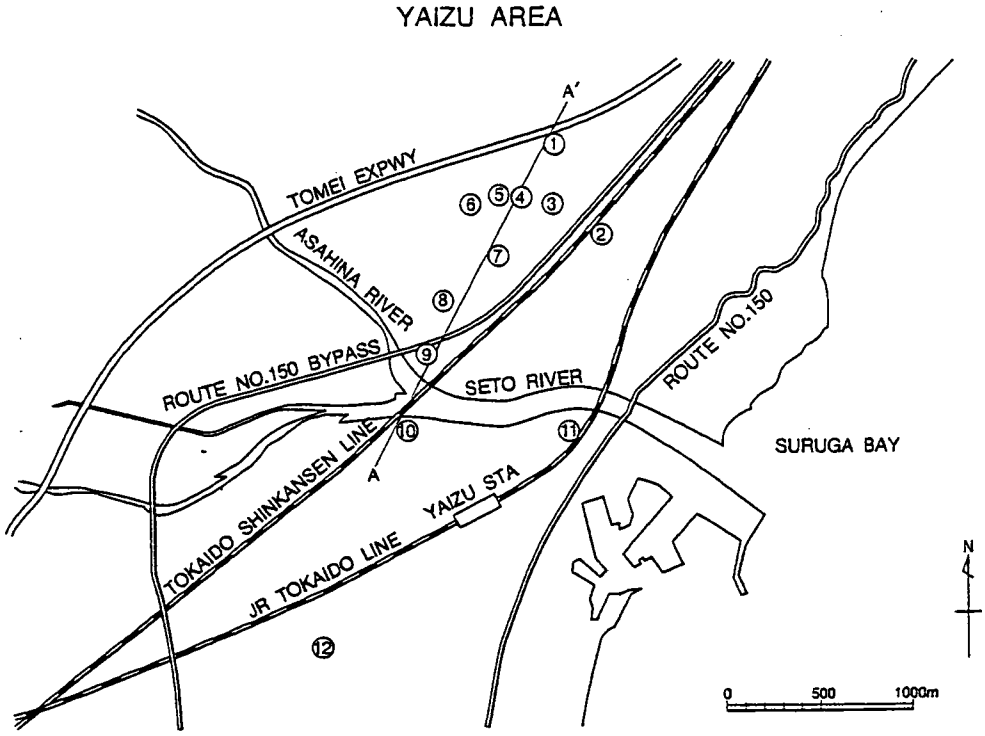
Observation Point No.	Accelerometer Installation Depth [m]
1	2
2	2
3	2
4	2, 30
5	2, 8, 12, 32
6	2
7	2
8	2, 36
9	2
10	2, 30

(a) Configuration of Observation Points

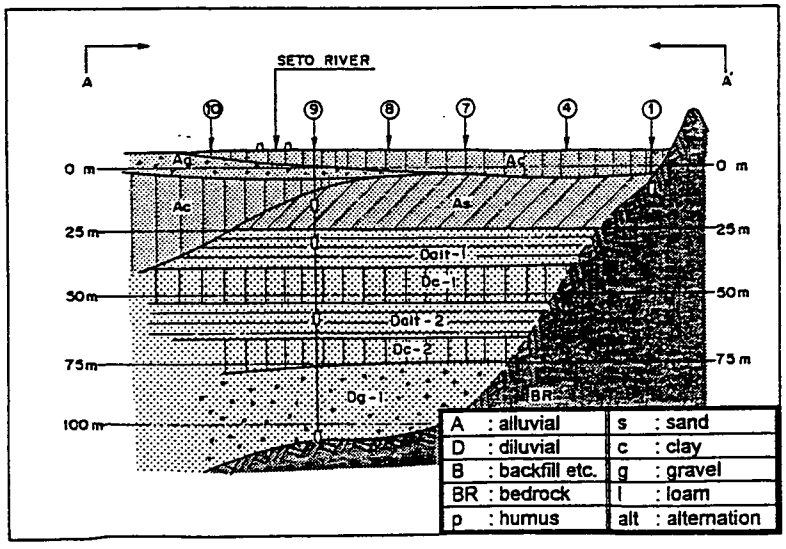


(b) Section of the Ground along A-A' line

Fig.3 Site Condition of Sagara Array



(a) Configuration of Observation Points

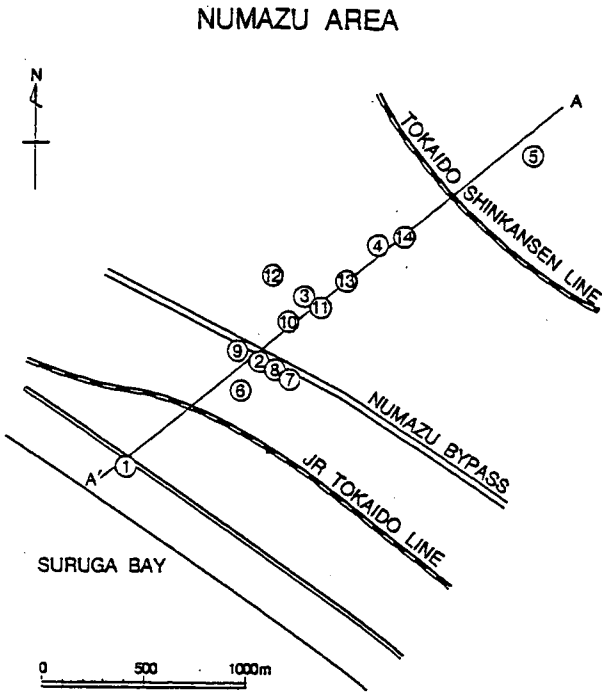


(b) Section of the Ground along A-A' line

Table 2 Accelerometer Installation Depth of Yaizu Array

Observation Point No.	Accelerometer Installation Depth [m]
1	10
2	2
3	2 —
4	2
5	2, 15
6	2
7	2
8	2
9	2, 20, 30, 63, 113
10	2
11	2
12	2

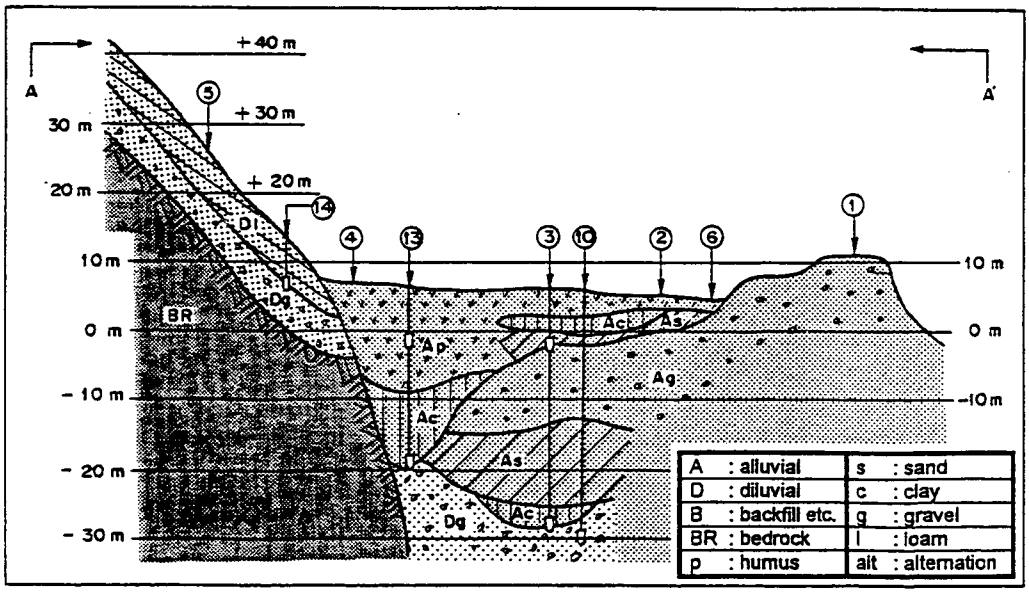
Fig.4 Site Condition of Yaizu Array



(a) Configuration of Observation Points

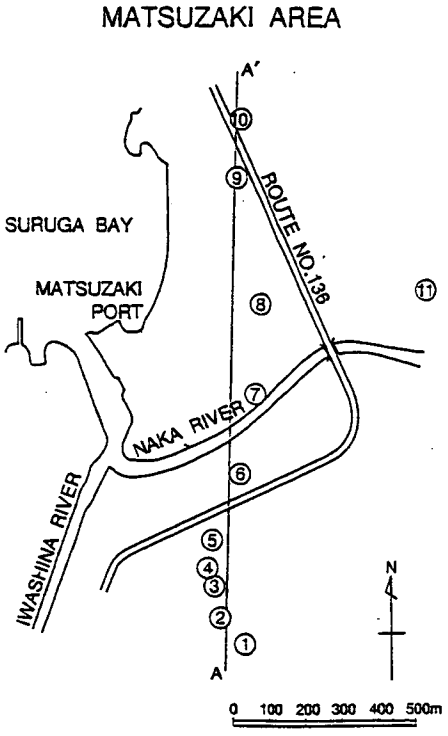
Table 3 Accelerometer Installation Depth of Numazu Array

Observation Point No.	Accelerometer Installation Depth [m]
1	2
2	2
3	2, 10, 32
4	2
5	2
6	2
7	2
8	2
9	2
10	2, 35
11	2, 32
12	2
13	2, 9, 27
14	11



(b) Section of the Ground along A-A' line

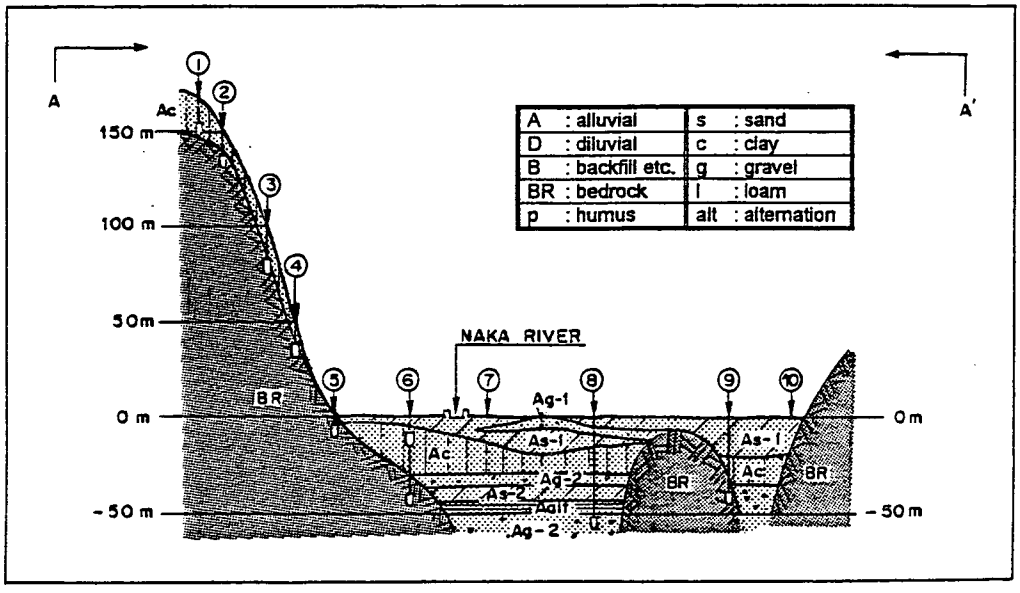
Fig.5 Site Condition of Numazu Array



(a) Configuration of Observation Points

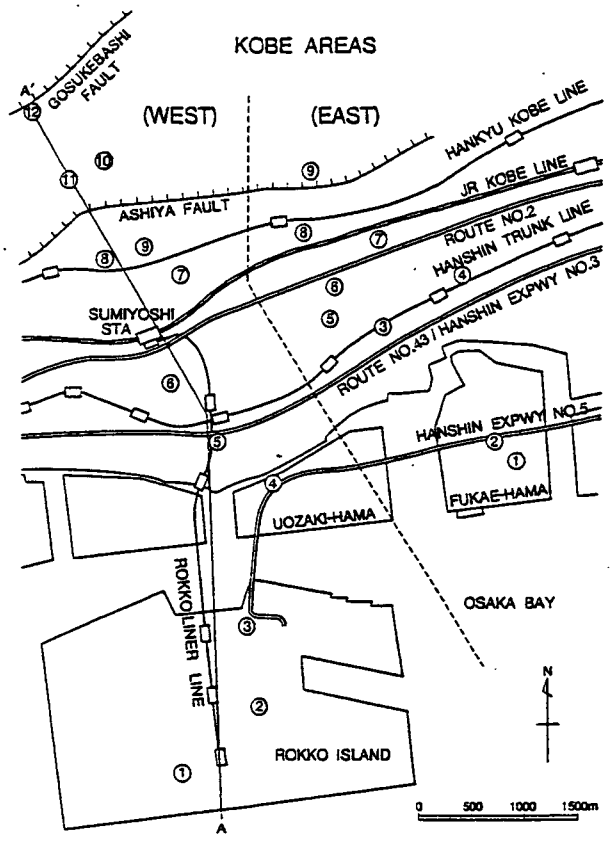
Table 4 Accelerometer Installation Depth of Matsuzaki Array

Observation Point No.	Accelerometer Installation Depth [m]
1	2, 24
2	2, 13
3	2, 11
4	2, 9
5	2, 5
6	2, 10, 40
7	2
8	2, 52
9	2, 38
10	2
11	2

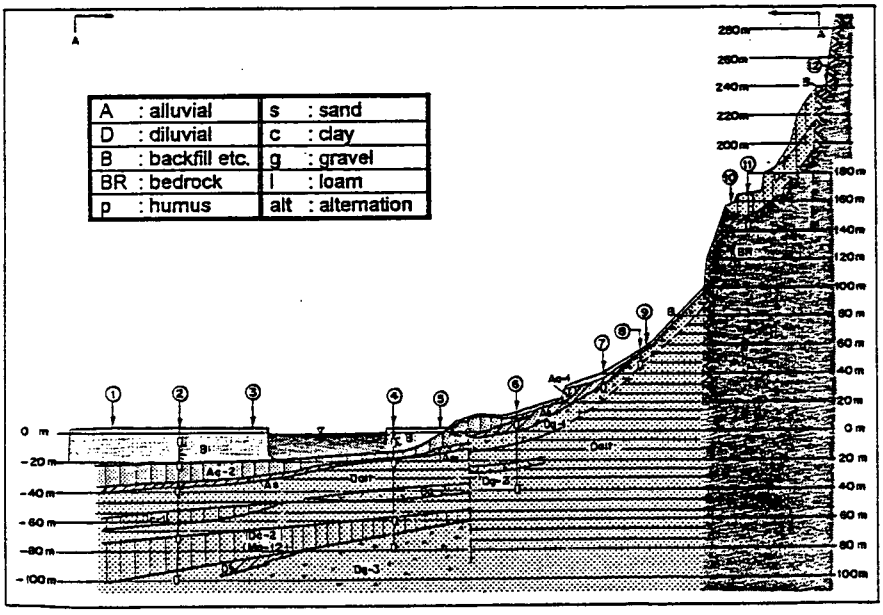


(b) Section of the Ground along A-A' line

Fig.6 Site Condition of Matsuzaki Array



(a) Configuration of Observation Points



(b) Section of the Ground along A-A' line

Fig.7 Site Condition of Kobe Arrays

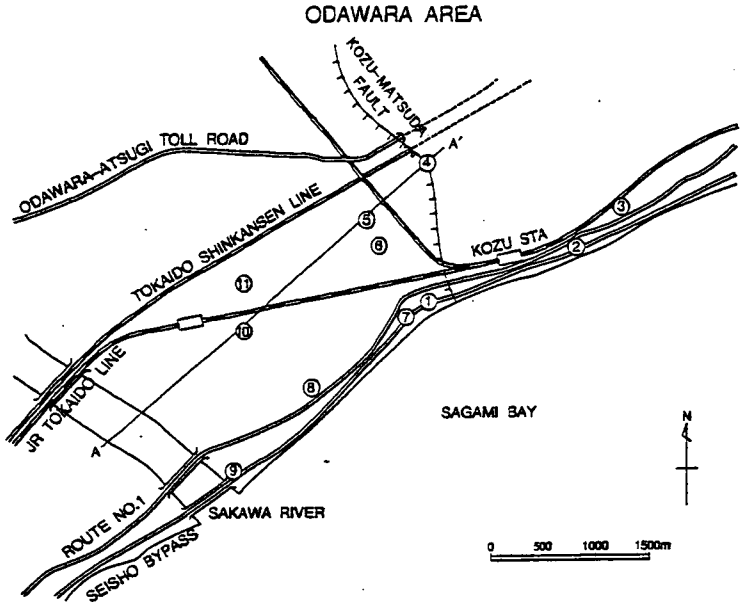
Table 5 Accelerometer Installation Depth of Kobe Arrays

(West)

Observation Point No.	Accelerometer Installation Depth [m]
1	2
2	2, 10, 25, 43, 75, 102
3	2
4	2, 10, 23, 61, 80
5	2
6	2, 7, 50
7	2, 10
8	2, 10
9	2
10	2
11	2, 20
12	2

(East)

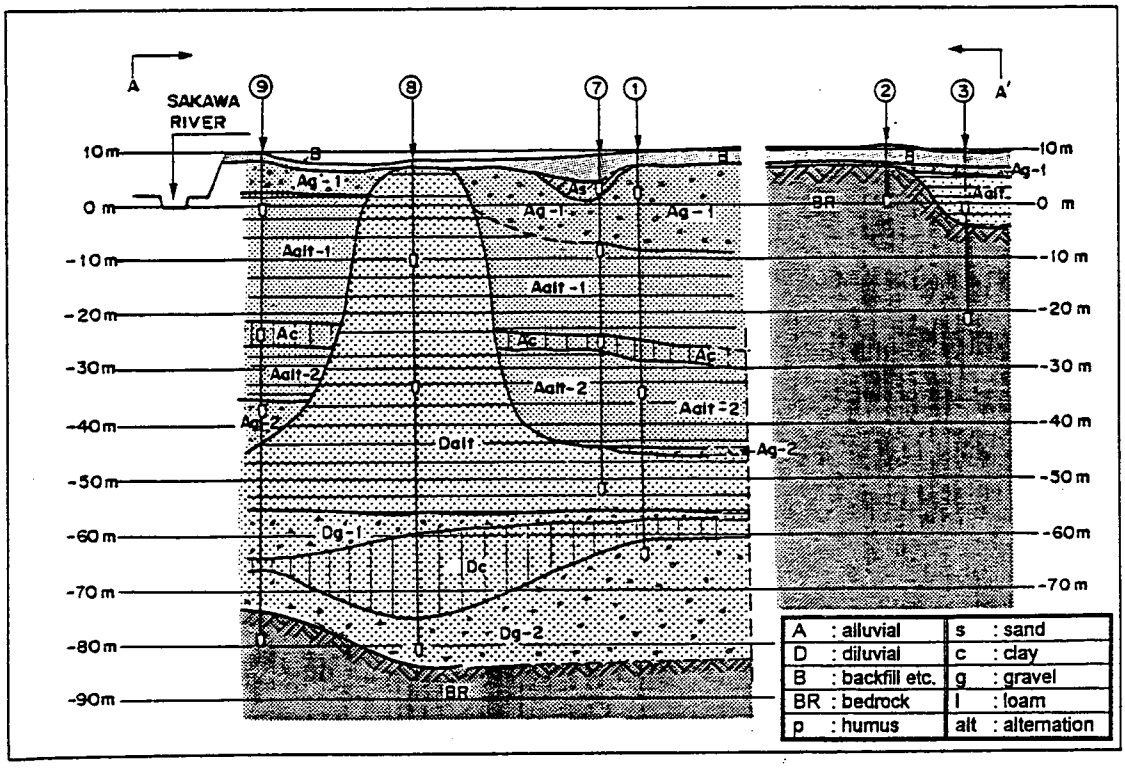
Observation Point No.	Accelerometer Installation Depth [m]
1	2
2	2, 8, 26, 54, 100
3	2, 14, 40
4	2
5	2
6	2, 16
7	2, 13, 32
8	2, 15
9 —	2, 12



(a) Configuration of Observation Points

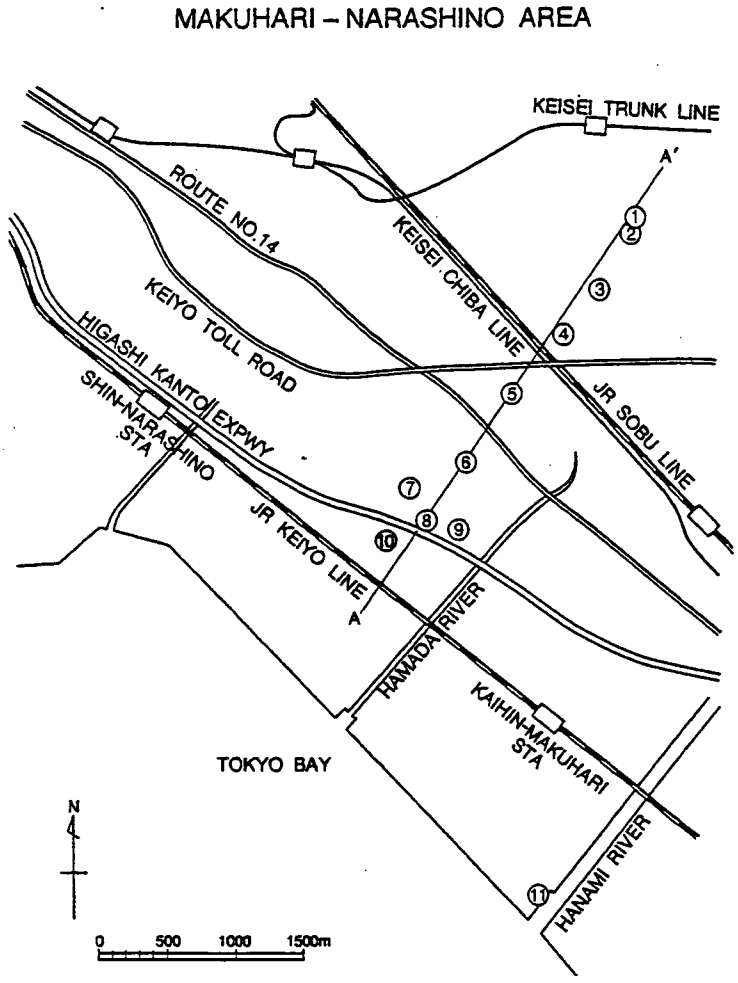
Table 6 Accelerometer Installation Depth of Odawara Array

Observation Point No.	Accelerometer Installation Depth [m]
1	2, 7, 44, 73
2	2, 10
3	2, 10, 30
4	2, 30
5	2, 12, 20, 51
6	2
7	2, 7, 17, 34, 60
8	2, 18, 41, 90
9	2, 10, 34, 46, 88
10	2, 14, 24, 50, 90
11	2



(b) Section of the Ground along A-A' line

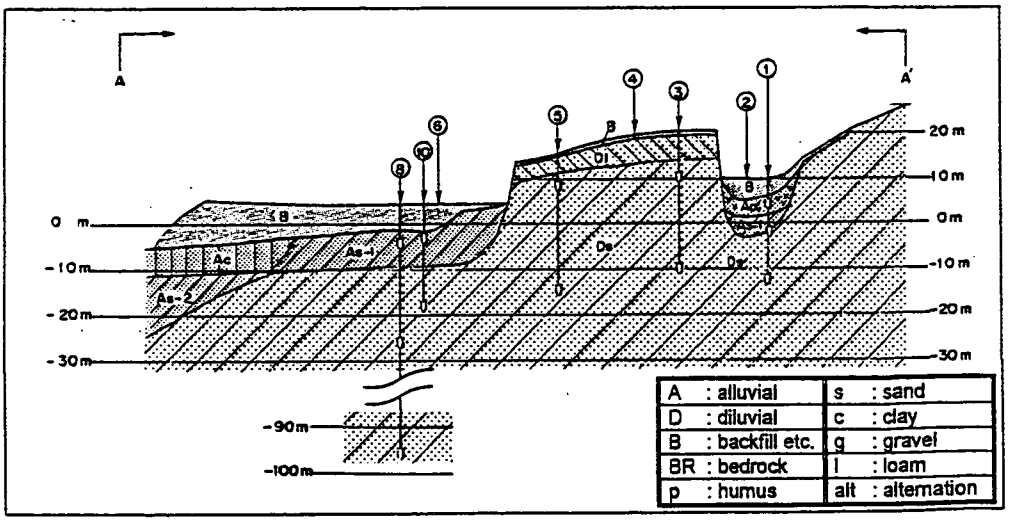
Fig.8 Site Condition of Odawara Array



(a) Configuration of Observation Points

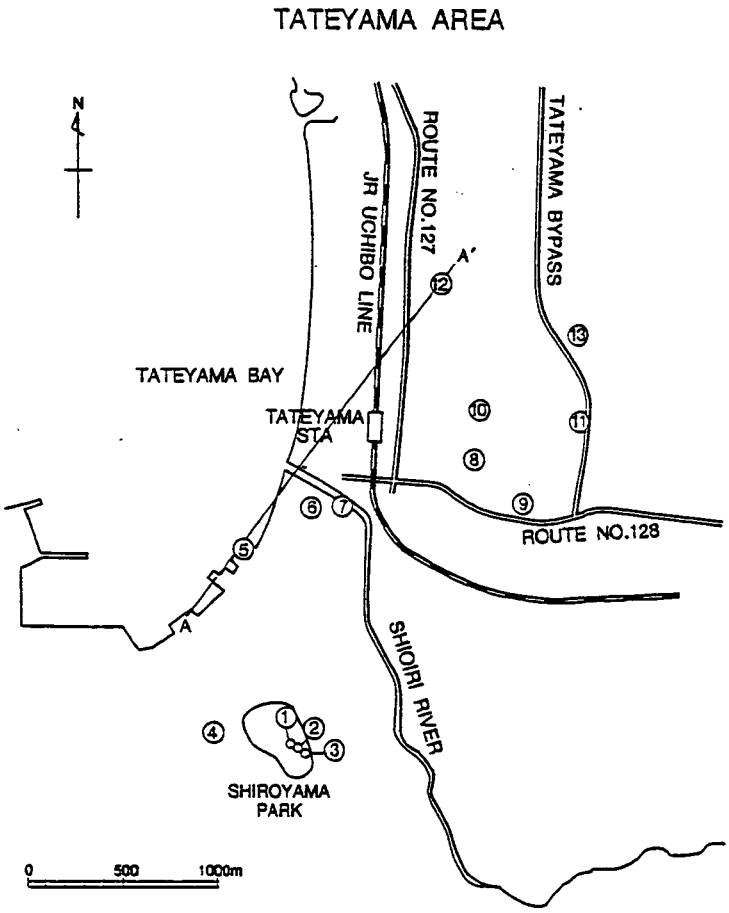
Table 7 Accelerometer Installation Depth of Makuhari-Narashino Array

Observation Point No.	Accelerometer Installation Depth [m]
1	2, 6, 12, 22
2	2
3	2, 10, 30
4	2
5	2, 6, 30
6	2
7	2
8	2, 8, 30, 100
9	2
10	2, 7, 22
11	2, 9, 19, 45



(a) Configuration of Observation Points

Fig.9 Site Condition of Makuhari-Narashino Array

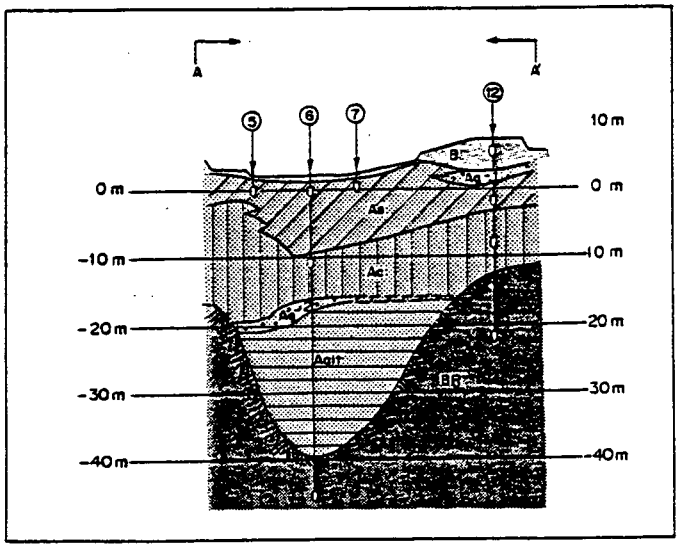


(a) Configuration of Observation Points

Table 8 Accelerometer Installation Depth of Tateyama Array

Observation Point No.	Accelerometer Installation Depth [m]
1	2
2	2
3	7
4	2, 21
5	2
6	2, 13, 47
7	2
8	2
9	2
10	2, 8, 41
11	2, 13
12	2, 9, 15, 29
13	2

A	: alluvial	s	: sand
D	: diluvial	c	: clay
B	: backfill etc.	g	: gravel
BR	: bedrock	l	: loam
p	: humus	alt	: alternation



(b) Section of the Ground along A-A' line

Fig.10 Site Condition of Tateyama Array

Site Amplifications for Generic Rock Sites

by

David M. Boore and William B. Joyner

ABSTRACT

Seismic shear-wave velocity as a function of depth for generic rock sites has been estimated from borehole data and studies of crustal velocities, and this velocity has been used to compute frequency-dependent amplifications for zero attenuation for use in simulations of strong ground motion. We define a generic rock site as one whose velocity at shallow depths equals the average of those from the rock sites sampled by the borehole data. Most of the boreholes are in populated areas and for that reason the rock sites sampled are of particular engineering significance. The amplifications on rock sites sampled by the boreholes can be in excess of 3.5 at high frequencies, in contrast to the amplifications of less than 1.2 expected on very hard rock sites. The consideration of unattenuated amplification alone is computationally convenient, but what matters for ground-motion estimation is the combined effect of amplification and attenuation. For reasonable values of the attenuation parameter κ_0, the combined effect of attenuation and amplification for rock sites peaks between about 2 to 5 Hz with a maximum level of less than 1.8. The combined effect is about a factor of 1.5 at 1 Hz and is less than unity for frequencies in the range of 10 to 20 Hz (depending on κ_0).

The borehole data yield shear-wave velocities ($\overline{V}_{30}$) of 618 and 306 m/s for "rock" and "soil" sites, respectively, when averaged over the upper 30 m. From this, we recommend that $\overline{V}_{30}$ equals 620 and 310 m/s for applications requiring the average velocity for "rock" and "soil" sites in western North America.

By combining the amplifications for rock sites and the site factors obtained from our analysis of strong-motion data, we derive amplifications for sites with $\overline{V}_{30}$ = 520 m/s (NEHRP Class C, corresponding to a mix of rock and soil sites) and $\overline{V}_{30}$ = 310 and 255 m/s (average soil and NEHRP Class D sites, respectively). For the average soil site the combined effect of amplification and attenuation exceeds a factor of 2.0 for frequencies between 0.4 and about 4 Hz, with a peak site effect of 2.4; the peak of the NEHRP Class D site effect is 2.7.

This paper is a shortened version of a recently published paper (Boore and Joyner, 1997).

KEYWORDS: Earthquakes; frequency; seismic shear-wave velocity; site amplification.

1. INTRODUCTION

Simulations of ground motions are often needed on rock sites, e.g., for use in seismic analysis and design of structural systems and in building codes. As is the case for soil sites, not all rock sites are created equal (e.g., Steidl *et al.*, 1996), and for site-specific applications the properties of the local site should be used

in the simulations. In many cases, however, it is sufficient to do the simulations for a representative or generic rock site. The main purpose of this paper is to present average velocity vs. depth and amplification vs. frequency for such sites. The amplifications can be used directly in the stochastic model for simulating earthquake ground motions (e.g., Boore, 1996).

The amplifications are based on shear velocity and density as functions of depth. The first task in the paper is to obtain a profile of shear-wave velocity vs. depth. To do this we use an extensive set of shear-wave travel-time measurements made in boreholes to constrain the shallow velocities, and we use studies of *P*-wave velocities in the crust as a guide for choosing the deeper velocities. The next task is to compute the amplifications; for this we use the quarter-wavelength approximation introduced by Joyner *et al.* (1981). The approximation is checked using wave propagation to calculate the exact response of the velocity structure used in the quarter-wavelength approximation.

2. VELOCITY AND DENSITY STRUCTURE

The travel time of *S* waves (S_{tt}) from the surface to any depth below a site is the fundamental property needed for the determination of the amplification (velocities, of course, can also be determined from S_{tt}). These travel times are available from downhole surveys made in boreholes, and can be used to estimate directly the amplification at high frequencies. We have entered all the S_{tt} from over 210 boreholes logged over the past 20 years by J. Gibbs, T. Fumal, and colleagues (Fumal *et al.*, 1981, 1982a, 1982b, 1984; Gibbs, 1989; Gibbs *et al.*, 1975, 1976, 1977, 1980, 1990, 1992, 1993, 1994a, 1994b; Gibbs and Fumal, 1994); in addition, we have added data from a few other published studies (Fletcher *et al.*, 1990; Thiel and Schneider, 1993) and from several unpublished studies (written communications from J. Gibbs, 1995 and T. Fumal, 1996). We then assigned a "rock" or "soil" classification to each borehole, based on surficial geology, following Joyner and Boore's (1981) scheme that "rock" sites are those described by terms such as "granite", "diorite", "gneiss", "chert", "graywacke", "limestone", "sandstone", or "siltstone", as long as the rock is overlain by less than 4 to 5 meters of soils. The distribution of shear velocity averaged over the upper 30 m (most of the holes were 30 m or shallower) is shown in Figure 1 for the two subsets of the borehole database. In the subsequent analysis we use only the data from 57 "rock" boreholes.

The borehole data are increasingly scarce at depth greater than 30 m, and for this reason our velocity function is constructed by using the borehole results to determine the best average shallow velocity, and then using *P*-wave velocities in the crust based on velocity surveys and earthquake location studies to estimate deeper *S*-wave velocities on the assumption that Poisson's ratio is close to 0.25 at depths in excess of several kilometers. We patch together the shallow and deeper velocity functions in order to obtain a continuous velocity-depth function.

The shallow velocity is obtained by interpolating the observed times in boreholes at 2 m intervals from the surface to the deepest recording in each hole, averaging S_{tt} at each depth for which at least two interpolated values are available, fitting a functional form to the average S_{tt} as a function of depth, and

converting this average travel time into a velocity-depth function. Figure 2 shows the individual travel times, the geometrically averaged travel times, a power-law fit to the averages (determined using unweighted least-squares) between 0 and 30 m, and the number of data points for each depth. Straightforward differentiation of the travel-time function (see Figure 2) yields the following equation for the shear velocity:

$$\beta(z) = 2.206\ z^{0.272} \qquad (1)$$

with the units of β and z being km/s and km, respectively. The power-law functional form was chosen after trials with several other forms. It has the advantage of providing a simple relation between travel time and velocity and a good fit to the observations, but it has the obvious disadvantage of predicting zero velocity at the surface. The value at 1 m depth (337 m/s) is reasonable. We replace the velocity between 0 and 1 m depth with a constant-velocity layer such that the travel time to 1 m equals that given by the power-law fit. The influence of these shallow depths on the amplification is only at very high frequencies (in excess of 30 Hz), however, and, as shown later, attenuation will severely blunt the amplification at these frequencies. We use equation (1) for the shear-wave velocity between 0.001 and 0.03 km.

Because of a lack of data, it is difficult to constrain the shear-wave velocity at greater depths. At depths below 4 km we estimate shear-wave velocity from compressional velocities, assuming a constant Poisson's ratio of 0.25. We chose 4 km because the lithostatic pressure at this depth is about 1 kbar, the pressure at which most cracks should be closed and below which Poisson's ratio should be near 0.25 for the crustal rocks of concern to us (e.g., Clark, 1966; Christensen and Mooney, 1995; Christensen, 1996). There is good evidence that Poisson's ratio is not constant at shallower depths (e.g., Nicholson and Simpson, 1985), and for this reason we cannot directly use the numerous measurements of crustal *P*-wave velocities obtained from refraction experiments and from earthquake location investigations to obtain *S*-wave velocities for depths less than 4 km. Representative *P*-wave velocity profiles are shown in Figure 3. We adjusted the parameters of a power-law functional form to roughly agree with the measured *P*-wave results below 4 km and converted this to a function giving *S*-wave velocity by dividing the *P*-wave velocities by $\sqrt{3}$. Our function is indicated by the heavy line in Figure 3.

We patch together the velocities at depths less than 0.03 km (from boreholes) and greater than 4 km (from *P*-waves) with two power law functions. In doing this we were guided by the *P*-wave velocities near 3.7 km/s at 0.2 km depth for Franciscan rocks on either side of the southern San Francisco Bay (Hazlewood and Joyner, 1973; Hazlewood, 1974). For Poisson's ratio of 0.25, this *P*-wave velocity yields an *S*-wave velocity of 2.1 km/s; we consider this an upper bound and therefore constrained the velocity function to pass through a smaller value at a depth of 0.2 km. Our final velocity model is plotted in Figure 4.

The density is given as a function of shear velocity by the simple relation

$$\rho(z) = 2.5 + (\beta(z) - 0.3) \times \frac{(2.8-2.5)}{(3.5-0.3)}$$

with ρ in gm/cc and β in km/s. Equation (2)

is a simple interpolation of end point values chosen by referring to various reference books and from personal experience of one of the authors (WBJ) in measuring densities; it is only to be used for shear velocities between 0.3 and 3.5 km/s. A density of 2.5 gm/cc was assigned to velocities less than 0.3 km/s.

3. 30 m TIME-AVERAGED VELOCITY FOR "ROCK" AND "SOIL" SITES

A site measure of importance in predicting ground shaking and in building codes (e.g., Boore *et al.*, 1994; Borcherdt, 1994; Midorikawa *et al.*, 1994) is the time-averaged shear-wave velocity from the surface to 30 m depth $\overline{V}_{30} = 30/S_{tt}(30\text{ m})$, where the units of $\overline{V}_{30}$ are m/s). The travel time curve fit to the data in Figure 2 yields an average velocity of 618 m/s; a similar analysis for the "soil" subset of the borehole database yields 306 m/s. Based on these results, we suggest that average "rock" and "soil" sites in western North America correspond to average velocities of 620 and 310 m/s, respectively. These numbers can be used to compare ground-motion attenuation equations base on "rock" and "soil" site classifications with those that use $\overline{V}_{30}$ to characterize the geology at a site.

4. THE QUARTER-WAVELENGTH APPROXIMATION

The quarter-wavelength approximation for computing site amplification was introduced by Joyner *et al.* (1981). For a particular frequency the amplification is given by the square root of the ratio between the seismic impedance (velocity times density) averaged over a depth corresponding to a quarter wavelength and the seismic impedance at the depth of the source (as used here, the averages of the seismic velocity and density are determined separately instead of their product being averaged; this should make little difference in the results). The approximation is relatively insensitive to discontinuities in seismic velocity; the method does not produce the peaks and valleys due to the interference of multiply-reflected waves. We consider this lack of resonant effects to be an advantage if, as in this paper, an amplification function insensitive to the details in the layering is desired.

Comparisons of the approximate and exact theoretical amplifications include those of Boore and Joyner (1991), Boatwright (personal commun., 1987), and Silva and Darragh (1995); we include another comparison in this paper. The available comparisons suggest that the quarter-wavelength approximation provides a good estimate of the mean values of the response.

The algorithm is the following: the S travel time ($S_{tt}(z)$) from the surface to depth z is either taken from downhole surveys or is computed using shear velocity as a function of depth; the average velocity to depth z, $\overline{\beta}(z)$, is $z/S_{tt}(z)$ and the frequency corresponding to the depth, $f(z)$, is 1/(4 times $S_{tt}(z)$); a travel-time-weighted average is taken of the density, $\overline{\rho}(z)$; and the amplification ($A(f)$) is given by

$$A(f(z)) = \sqrt{\rho_s \beta_s / \overline{\rho}(z)\overline{\beta}(z)}, \quad (3)$$

where the subscript s represents values in the vicinity of the source.

When we refer to amplification, we mean the Fourier amplitude spectrum of the surface motion produced for **unattenuated** incident

plane waves divided by the Fourier amplitude spectrum that would have been recorded at the surface of a uniform halfspace by the same incident planewaves (the amplification therefore approaches unity for very long-period waves). Of course, the site response of interest includes attenuation, but we have considered the amplification and attenuation separately because we prefer to parameterize the attenuation by the operator exp ($-\pi \kappa_0 f$). By so doing, it is natural in computer simulations to treat the amplification
and attenuation as separate entities, though this distinction may be somewhat artificial. A careful study of the response of a particular site to seismic waves should include attenuation as a point property with depth. Even then it is important to recognize that using a parameter such as **Q** to represent the attenuation is only a phenomenological description of a complex process involving intrinsic and scattering attenuation mechanisms.

5. AMPLIFICATION FROM VELOCITY AND DENSITY PROFILES

We use the velocity and density functions to compute amplifications, using the quarter-wavelength approximation, and assuming that the velocity near the source is close to the velocity in our model at 8 km depth (the amplifications are only sensitive to variations of several km in this source depth for frequencies less than 0.1 Hz). The computations were made by program *Site_Amp* (Boore, 1996). The results are shown in Figure 5. The amplification for rock sites increases from near 1 at 0.1 Hz to over 3 for frequencies greater than about 12 Hz.

In order to check the quarter-wavelength assumption, the velocity model was replaced with one consisting of a stack of constant-velocity layers (such that the travel time to each interface in the stack was the same as in the continuous velocity model), and the amplification was computed using the propagator-matrix method of Haskell (1960), as implemented by C. Mueller's program *Rattle*for *SH* waves. (A **Q** of 10,000 in each layer was used to simulate no attenuation.) Because the base of the velocity model is at 8 km in high-velocity material, incidence angles of 30 and 45 degrees were used to approximate the range of angles that would exist for events not directly under the site (the incidence angles would be smaller for input at shallower depths because of refraction). The amplifications are shown in Figure 5. The oscillations at high frequencies are due to the finite thickness of the layering (1 m for the first two layers and 2 m to depths of 0.2 km). The quarter-wavelength approximation is a good representation of the overall amplification; it has the advantages of being insensitive to the layering in the system, taking little computation time, and allowing back-of-the-envelope estimates of the amplification and the depths affecting various frequencies of motion.

As discussed earlier, we choose to separate amplification and near-site attenuation for ease in incorporating the two effects in our computer codes for calculating ground motions; what counts for ground motions, of course, is the combined effect of amplification and attenuation. Figure 6 shows this combined effect for a range of values of the attenuation parameter κ_0 found by Silva and Darragh (1995) for rock sites in western North America (the amplification factors of Boore, 1986, were used to obtain these estimates). For reasonable values of κ_0 (i.e., in excess of

0.01 for most rock sites in western North America, although an average value of 0.005 was obtained by Hough *et al.*, 1988, on granitic rocks in the Anza region of southern California), the large amplifications at high frequencies are much reduced by the attenuation. It is important to note, however, that the overall effect of the amplification and attenuation is still larger than unity over a wide range of frequencies of engineering interest.

The quarter-wavelength approximation makes it easy to answer the question of what depth influences what frequency. The relationship between depth and frequency is shown in Figure 7 for our rock model. This figure shows that frequencies as low as 1 Hz are influenced by velocities in the upper few hundred meters of the Earth at rock sites. At soil sites the primary influence on 1 Hz amplification would be at even shallower depths. The velocity models used in the calculation of wave propagation in layered media should have near-surface velocities that are commensurate with the frequencies of the calculated motions. We fear that a number of seismologists use models with near-surface shear-wave velocities that are too high, thinking that the near-surface layers can be neglected without realizing that although the thickness is small, the travel time through the layers is not small.

6. AMPLIFICATIONS FOR OTHER SITE CLASSES

It is useful to obtain amplification functions for sites other than the very hard rock and rock sites. Rather than repeat the analysis of this paper for boreholes falling into other classes, we use a combination of the rock amplification shown in Figure 5 and the empirical results of Boore *et al.* (1994) in which response spectra are given as a function of $\overline{V}_{30}$. Our scheme is simple: we use the ratio of response spectra computed from Boore et al. (1994) for sites with $\overline{V}_{30}$ = 620 m/s and V_{30} equal to the desired velocity as a correction factor applied to the rock amplifications. We used subjective judgment to extend the correction factors to frequencies outside the range used by Boore *et al.* (1994). The procedure assumes that the ratio of Fourier and response spectra are the same. This is not strictly true, particularly at frequencies higher than about 8 Hz. We fine tune the amplifications by generating simulated response spectra for the desired $\overline{V}_{30}$ and comparing them with the empirical response spectra of Boore *et al.* (1994). Ratios of the spectra for various frequencies are used in an iterative procedure to adjust the amplifications. We chose three site classes: the NEHRP building code classes C and D (BSSC, 1994) and the average soil class. $\overline{V}_{30}$ for the two NEHRP classes (520 and 255 m/s) are given by the geometrical means of the velocities defining the boundaries of each class. The velocity for an average soil site (310 m/s) was discussed in the previous section.

We show the combined effect of amplification and attenuation in Figure 8. The site effect for the soil sites exceeds a factor of 2 over a wide range of frequencies of importance in engineering. The attenuation parameter κ_0 was held fixed at 0.035 s in the derivation of the amplifications. Consistent results can also be obtained for other values of κ_0 as long as the amplification is adjusted by the factor exp $(-\pi(\kappa_0 - \kappa_{new})f)$.

7. CONCLUSIONS AND DISCUSSION

Using borehole data and studies of crustal velocities, we have estimated seismic shear-wave velocity and density as a function of depth for rock sites such as are found in many tectonically active regions, with an average $\overline{V}_{30}$ of 620 m/s. From the shear-wave velocity and density vs. depth functions we produce amplifications as a function of frequency for use in simulations of strong ground motion. The amplifications are in excess of 3.5 at high frequencies. Attenuation, however, will reduce these amplifications such that the combined effect for the rock sites might have a maximum of about a factor of 1.8 for $\kappa_0 = 0.02$ s and 1.5 for $\kappa_0 = 0.04$ s. The scatter in the amplifications computed for individual boreholes is considerable, suggesting that the mean amplifications proposed in this paper should be used with caution for site-specific studies. The large variation in site response for rock sites has also been emphasized by Schneider and Silva (1994).

We also find from the analysis of borehole data that average "rock" and "soil" sites are characterized by time-averaged shear-wave velocities in the upper 30 m of 620 and 310 m/s, respectively.

Although we have treated them separately, there may be a correlation between the attenuation parameter κ_0 and $\overline{V}_{30}$. This is certainly the case in going from very hard rock, for which κ_0 is often less than 0.01 s (e.g., Atkinson, 1996), to ordinary rock, for which we and others find representative values near 0.04 s for κ_0. There may also be a tendency within the generic rock category for κ_0 to decrease with increasing $\overline{V}_{30}$ (W. Silva, written commun., 1995). Correlations between κ_0 and $\overline{V}_{30}$, however, might depend on geographic region and class of geologic materials beneath a site. κ_0 is affected by more of the travel path than the part contributing to the amplification (Anderson et al., 1996). For this reason two sites with the same V_{30} could have different values of κ_0 (as has been found by Atkinson, 1996, for very hard rock sites in southeastern and southwestern Canada, with κ_0 being less than 0.004 for sites in the former region and 0.011 for sites in the latter region). In addition, the correlation between κ_0 and $\overline{V}_{30}$ is probably different for rock and for soils. We expect that near-surface velocity gradients in soils would be less than in rocks and that scattering would be less important in soils. For these reasons, the amplification function and κ_0 might be different for two sites with the same $\overline{V}_{30}$.

Although our primary reason for separating the effects of amplification and attenuation is for convenience in providing input parameters for our computer codes for estimating ground shaking, we note that measurements of κ_0 from data also use a similar separation. Any measurement of κ_0 is tied to the amplification. In most cases of measurements of κ_0, however, the amplification is implicitly assumed to be unity, or at least independent of frequency over the range used in determining κ_0, a result that the borehole data suggests is unlikely to be true. The high-frequency dependence of the amplification is critically dependent on the gradient of the velocity with depth near the surface (e.g., less than 10 m for $f > 10$ Hz, according to Figure 7). In order for the rock amplifications to flatten for frequencies greater than 10 Hz, however, the gradient in the upper 10 m would have to be replaced by a constant velocity layer. The borehole data in Figure 2 argues against this,

at least for rock sites. If κ_0 is independent of frequency, then in principle it should be possible to distinguish between a site with constant amplification at high frequency and one with increasing amplification: a plot of the log of the spectrum vs. linear frequency will approach a straight line in the former case, while an increasing amplification will lead to curvature of the high-frequency part of the spectrum. To study this, we replotted Figure 6 using log, linear axes. The curvature was very hard to see, and would be completely obscured for real, noisy data. On the other hand, determinations of κ_0 by fitting a straight line to log spectrum vs. frequency (Anderson and Hough, 1984) yields estimates near 0.034 for the case when κ_0 is 0.040. Therefore, as expected, measurements of κ_0 which do not account for increasing amplification with frequency will be lower than measurements that account for the amplification. Caution must be used in comparing values of κ_0 from various studies; it is necessary to consider what, if any, account has been taken of amplification of the spectrum.

As the example above illustrates, derived parameters are dependent on the assumptions embedded in the underlying model, a point that we fear is often overlooked. Another example is in the estimation of seismic moments of small earthquakes at rock sites, which are usually determined with no regard for the amplifications that can occur due to the decrease in seismic velocities near the Earth's surface; Figure 6 suggests that such determinations might be systematically high by a factor of about 1.4 for many rock sites (those with $\overline{V}_{30}$ considerably less than several km/s) if computed from waves with frequencies of 1 Hz. The factor would be more than 1.4 for soil sites.

The rock amplifications have been modified to obtain amplification factors that are appropriate for sites classified by average shear-wave velocities $\overline{V}_{30}$ equal to 520, 310, and 255 m/s. These site classes correspond to NEHRP class C, average soil, and NEHRP class D, respectively. The combined effect of the amplification and attenuation reaches a factor of 2.7 for $\overline{V}_{30} = 255$ m/s and exceeds a factor of 2 for a wide range of frequencies of engineering interest.

We stress the obvious point that rock sites on which strong motions have been recorded are not underlain by uniform half spaces; our analysis of borehole data finds a strong gradient with depth, presumably due to weathering processes and open fractures. It would be a mistake, however, to assume that the same gradients apply to the rock beneath soil sites. If rock recordings are to be used as input to a soil column, then these rock recordings should first be deconvolved to a depth where the velocity profile is comparable to the rock beneath the soil column (that depth could be 1 km or more), before being convolved with the response of the rock between that depth and the base of the soil column. This is a site-specific matter and requires the determination of shear velocity to sufficient depths, both beneath the rock recording and beneath the soil column.

8. ACKNOWLEDGMENTS

We thank Jim Gibbs for helping enter the borehole data and Charles Mueller for use of his program *Rattle*. Jim Gibbs and Tom Fumal provided unpublished travel-time data for two boreholes, and Joe Fletcher supplied computer files of S_{tt} for several rock sites in southern California (Keenwild and Pinyon Flat). Harold Magistrale provided velocity

and density profiles for a few locations, also in southern California. We also thank Rachel Abercrombie, Peter Malin, and Tom McEvilly for data and information about the Cajon Pass, Parkfield area, and Oroville boreholes. We are grateful to Walt Silva for his discussions and comments and to Mehmet Celebi and Roger Borcherdt for their thoughtful reviews of the manuscript. This work was partially supported by the U.S. Nuclear Regulatory Commission.

9. REFERENCES

Anderson, J. G. and S. E. Hough (1984). A model for the shape of the Fourier amplitude spectrum of acceleration at high frequencies, *Bull. Seism. Soc. Am.* **74**, 1969-1993.

Anderson, J.G., Y. Lee, Y. Zeng, and S. Day (1996). Control of strong motion by the upper 30 meters, *Bull. Seism. Soc. Am.* **86**, 1749-1759.

Atkinson, G.M. (1996). The high-frequency shape of the source spectrum for earthquakes in eastern and western Canada, *Bull. Seism. Soc. Am.* **86**, 106-112.

Boore, D. M. (1986). Short-period *P*- and *S*-wave radiation from large earthquakes: implications for spectral scaling relations, *Bull. Seism. Soc. Am.* **76**, 43-64.

Boore, D.M. (1996). SMSIM -- Fortran programs for simulating ground motions from earthquakes: version 1.0, *U.S. Geol. Survey Open-File Rept. 96-80-A, 96-80-B*, 69 p.

Boore, D.M. and W.B. Joyner (1991). Estimation of ground motion at deep-soil sites in eastern North America, *Bull. Seism. Soc. Am.* **81**, 2167-2185.

Boore, D.M. and W.B. Joyner (1997). Site amplifications for generic rock sites, *Bull. Seism. Soc. Am.* **87**, (in press).

Boore, D.M., W.B. Joyner, and T.E. Fumal (1994). Estimation of response spectra and peak accelerations from western North American earthquakes: An interim report, Part 2 *U.S. Geol. Survey Open-File Rept. 94-127*, 40 pp.

Borcherdt, R.D. (1994). Estimates of site-dependent response spectra for design (methodology and justification), *Earthquake Spectra* **10**, 617-653.

Building Seismic Safety Council (BSSC) (1994). NEHRP recommended provisions for seismic regulations for new buildings, Part 1 - Provisions, FEMA 222A, Federal Emergency Management Agency, 290 p.

Christensen, N.I. (1996). Poisson's ratio and crustal seismology, *J. Geophys. Res.* **101**, 3139-3156.

Christensen, N.I. and W.D. Mooney (1995). Seismic velocity structure and composition of the continental crust: A global view, *J. Geophys. Res.* **100**, 9761-9788.

Clark, S.P., Jr. (Editor) (1966). *Handbook of Physical Constants*, Geological Society of America Memoir 97, 587 p.

Fletcher, J.B., T. Fumal, H.-P. Liu, and L.C. Carroll (1990). Near-surface velocities and attenuation at two boreholes near Anza, California, from logging data, *Bull. Seism. Soc. Am.* **80**, 807-831.

Fumal, T.E. (1978). Correlations between seismic wave velocities and physical

properties of near-surface geologic materials in the southern San Francisco Bay region, California, *U.S. Geol. Survey Open-File Rept. 78-1067*, 114 p.

Fumal, T.E., J.F. Gibbs, and E.F. Roth (1981). In-situ measurements of seismic velocity at 19 locations in the Los Angeles, California region, *U.S. Geol. Survey Open-File Rept. 81-399*, 121 p.

Fumal, T.E., J.F. Gibbs, and E.F. Roth (1982a). In-situ measurements of seismic velocity at 10 strong motion accelerograph stations in central California, *U.S. Geol. Survey Open-File Rept. 82-407*, 76 p.

Fumal, T.E., J.F. Gibbs, and E.F. Roth (1982b). In-situ measurements of seismic velocity at 22 locations in the Los Angeles, California region, *U.S. Geol. Survey Open-File Rept. 82-833*, 138 p.

Fumal, T.E., J.F. Gibbs, and E.F. Roth (1984). In-situ measurements of seismic velocity at 16 locations in the Los Angeles, California region, *U.S. Geol. Survey Open-File Rept. 84-681*, 109 p.

Gibbs, J.F. (1989). Near-surface *P*- and *S*-wave velocities from borehole measurements near Lake Hemet, California, *U.S. Geol. Survey Open-File Rept. 89-630.*

Gibbs, J.F. and T.E. Fumal (1994). Seismic velocities and geologic logs from borehole measurements at seven strong-motion stations that recorded the 1989 Loma Prieta, California, earthquake, Part IV, *U.S. Geol. Survey Open-File Rept. 94-552*, 89 p.

Gibbs, J.F., T.E. Fumal, and R.D. Borcherdt (1975). In-situ measurements of seismic velocities at twelve locations in the San Francisco Bay region, *U.S. Geol. Survey Open-File Rept. 75-564*, 87 p.

Gibbs, J.F., T.E. Fumal, and R.D. Borcherdt (1976). In-situ measurements of seismic velocities in the San Francisco Bay region...Part II, *U.S. Geol. Survey Open-File Rept. 76-731*, 145 p.

Gibbs, J.F., T.E. Fumal, and R.D. Borcherdt (1977). In-situ measurements of seismic velocities in the San Francisco Bay region...Part III, *U.S. Geol. Survey Open-File Rept. 77-850*, 143 p.

Gibbs, J.F., T.E. Fumal, and E.F. Roth (1980). In-situ measurements of seismic velocity at 27 locations in the Los Angeles, California region, *U.S. Geol. Survey Open-File Rept. 80-378*, 167 p.

Gibbs, J.F., E.F. Roth, T.E. Fumal, N.A. Jasek, and M.A. Emslie (1990). Seismic velocities from borehole measurements at four locations along a fifty-kilometer section of the San Andreas fault near Parkfield, California, *U.S. Geol. Survey Open-File Rept. 90-248*, 35 p.

Gibbs, J.F., T.E. Fumal, D.M. Boore, and W.B. Joyner (1992). Seismic velocities and geologic logs from borehole measurements at seven strong-motion stations that recorded the Loma Prieta earthquake, *U.S. Geol. Survey Open-File Rept. 92-287*, 139 p.

Gibbs, J.F., T.E. Fumal, and T.J. Powers (1993). Seismic velocities and geologic logs from borehole measurements at eight strong-motion stations that recorded the 1989 Loma Prieta, California, earthquake, *U.S. Geol. Survey Open-File Rept. 93-376*, 119 p.

Gibbs, J.F., T.E. Fumal, and T.J. Powers (1994a). Seismic velocities and geologic logs from borehole measurements at seven strong-motion stations that recorded the 1989 Loma Prieta, California, earthquake, *U.S. Geol. Survey Open-File Rept. 94-222*, 104 p.

Gibbs, J.F., T.E. Fumal, R.D. Borcherdt, R.E. Warrick, H.-P. Liu, and R.E. Westerlund (1994b). Seismic velocities and geologic logs from boreholes at three downhole arrays in San Francisco, California, *U.S. Geol. Survey Open-File Rept. 94-706*, 40 p.

Hadley, D. and H. Kanamori (1977). Seismic structure of the Transverse Ranges, California, *Geol. Soc. Am. Bull.*, **88**, 1469-1478.

Haskell, N.A. (1960). Crustal reflection of plane *SH* waves, *J. Geophys. Res.* **65**, 4147-4150.

Hauksson, E. (1987). Seismotectonics of the Newport-Inglewood fault zone in the Los Angeles basin, southern California, *Bull. Seism. Soc. Am.* **77**, 539-561.

Hauksson, E. and L.M. Jones (1988). The July 1986 Oceanside (M_L = 5.3) earthquake sequence in the continental borderland, southern California, *Bull. Seism. Soc. Am.* **78**, 1885-1906.

Hazlewood, R.M. (1974). Preliminary report of seismic refraction survey along the east side of the San Francisco Bay, Alameda County, California, *U.S. Geol. Survey Open-File Rept.*, 10p.

Hazlewood, R.M. and W.B. Joyner (1973). Preliminary report of seismic refraction survey, Redwood Shores, San Mateo County, California, *U.S. Geol. Survey Open-File Rept.*, 9p.

Hough, S. E., J. G. Anderson, J. Brune, F. Vernon III, J. Berger, J. Fletcher, L. Haar, T. Hanks, and L. Baker (1988). Attenuation Near Anza, California, *Bull. Seism. Soc. Am.* **78**, 672-691.

Joyner, W.B., R.E. Warrick, and T.E. Fumal (1981). The effect of Quaternary alluvium on strong ground motion in the Coyote Lake, California, earthquake of 1979, *Bull. Seism. Soc. Am.* **71**, 1333-1349.

Magistrale, H., K. McLaughlin, and S. Day (1996). A geology-based 3D velocity model of the Los Angeles basin sediments, *Bull. Seism. Soc. Am.* **86**, 1161-1166.

Midorikawa, S., M. Matsuoka, and K. Sakugawa (1994). Site effects on strong-motion records observed during the 1987 Chiba-Ken-Toho-Oki, Japan earthquake, *Proc. 9th Japan Earthq. Eng. Symp.* **3**, E085-E090.

Nicholson, C. and D.W. Simpson (1985). Changes in V_p/V_s with depth: Implications for appropriate velocity models, improved earthquake locations, and material properties of the upper crust, *Bull. Seism. Soc. Am.* **75**, 1105-1123.

Schneider, J.F. and W.J. Silva (1944). What is rock? Implications for site response estimation (abs.), *Seism. Res. Lett.* **65**, 44.

Silva, W. J., and R. B. Darragh (1995). Engineering Characterization of Strong Ground Motion Recorded at Rock Sites, Electric Power Research Institute, Palo Alto, Calif., Report No. TR-102262.

Steidl, J.H., A.G. Tumarkin, and R.J. Archuleta (1996). What is a reference site?, *Bull. Seism. Soc. Am.* **86**, 1733-1748.

Thiel Jr., C. C. and J. F. Schneider (1993). Investigations of Thirty-Three Loma Prieta Earthquake Strong Motion Recording Sites, final report of project sponsored by the Building Contractors Society of Japan and the Electric Power Research Institute, California Universities for Research in Earthquake Engineering (CUREe), Dept. of Civil Engineering, Stanford Univ., Stanford, Calif.

Wald, D.J., D.V. Helmberger, and T.H. Heaton (1991). Rupture model of the 1989 Loma Prieta earthquake from the inversion of strong-motion and broadband teleseismic data, *Bull. Seism. Soc. Am.* **81**, 1540-1572.

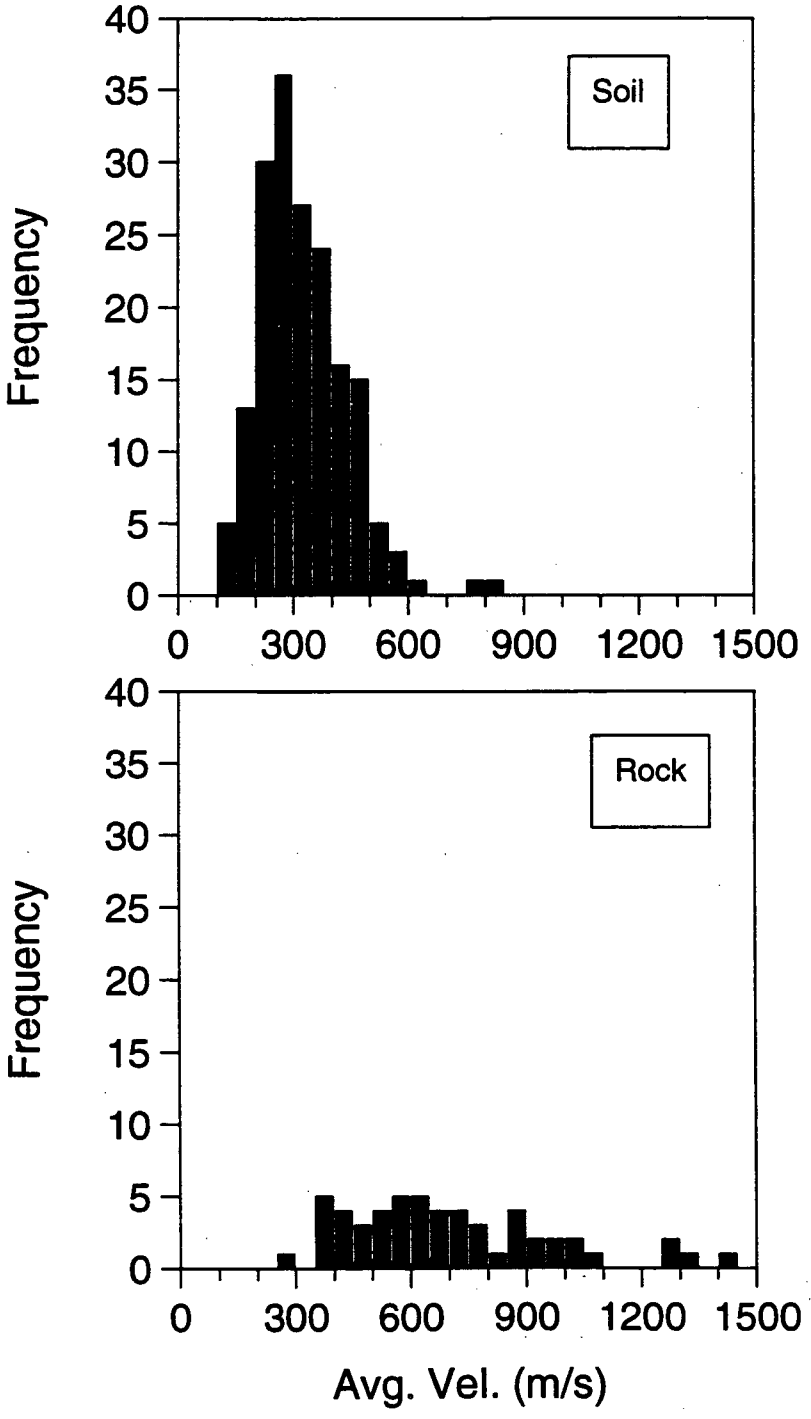


Figure 1. Histograms of shear velocity averaged over the upper 30m, from downhole surveys in boreholes. Many of the boreholes did not quite reach 30m, and for the sake of estimating representative velocity distributions, small extrapolations of the travel time to 30m were used in computing the average velocities. The subsequent analysis of the shallow velocities in this paper make no use of such extrapolations. Fitting travel-time curves to the observed travel times gives average velocities of 618 m/s and 306 m/s for rock and soil boreholes, respectively.

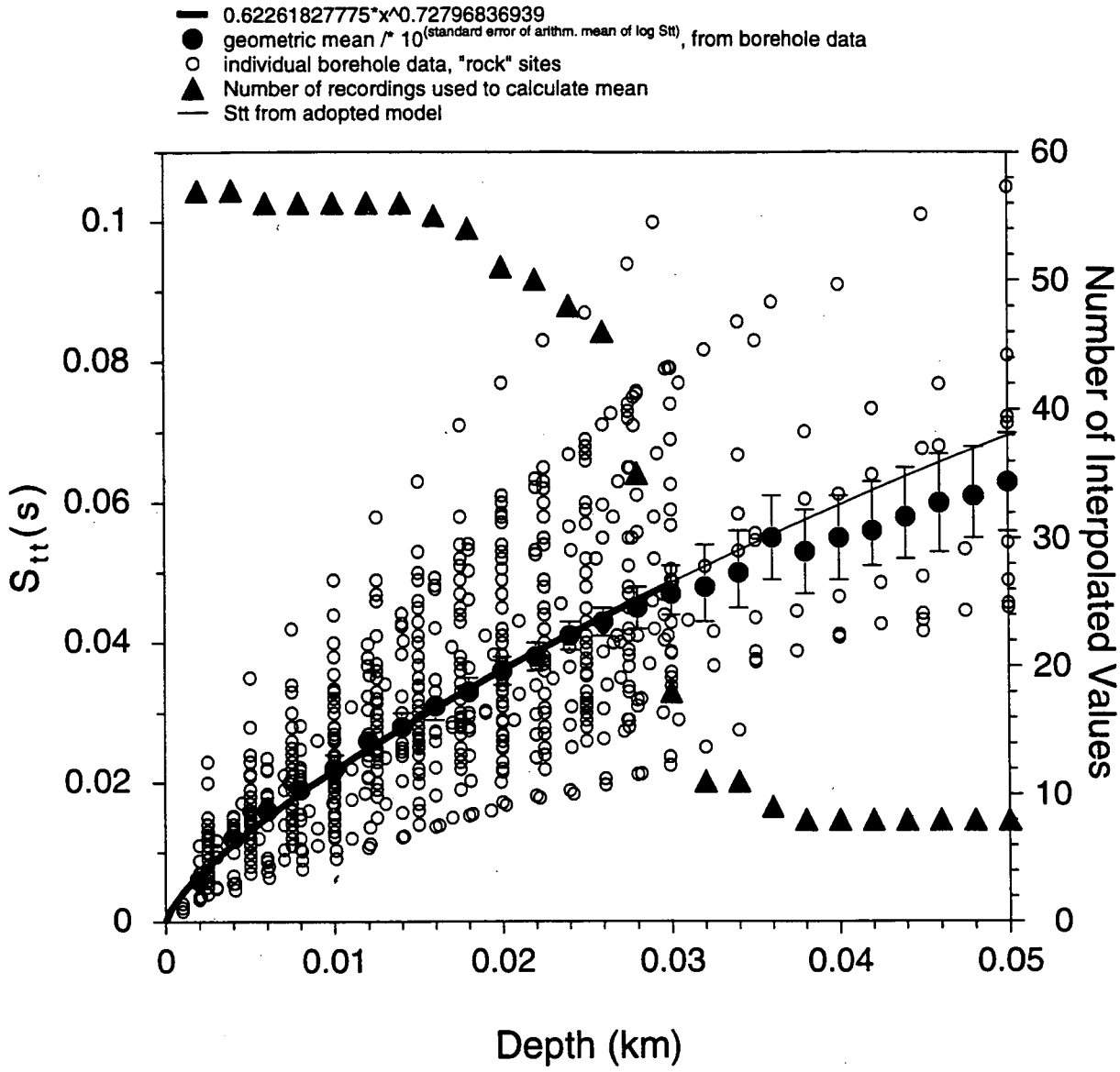


Figure 2. S-wave travel time vs. depth (left axis). The circles are the individual observations, and the solid dots are the geometric means of the interpolated travel times, with standard error of the mean indicated by the error bars. The least-squares fit of a power law is given by the heavy line ($S_{tt} = 0.623z^{0.728}$), and the travel time corresponding to the adopted velocity model is given by the light line. The number of interpolated values at each depth is given by the filled triangles (right axis).

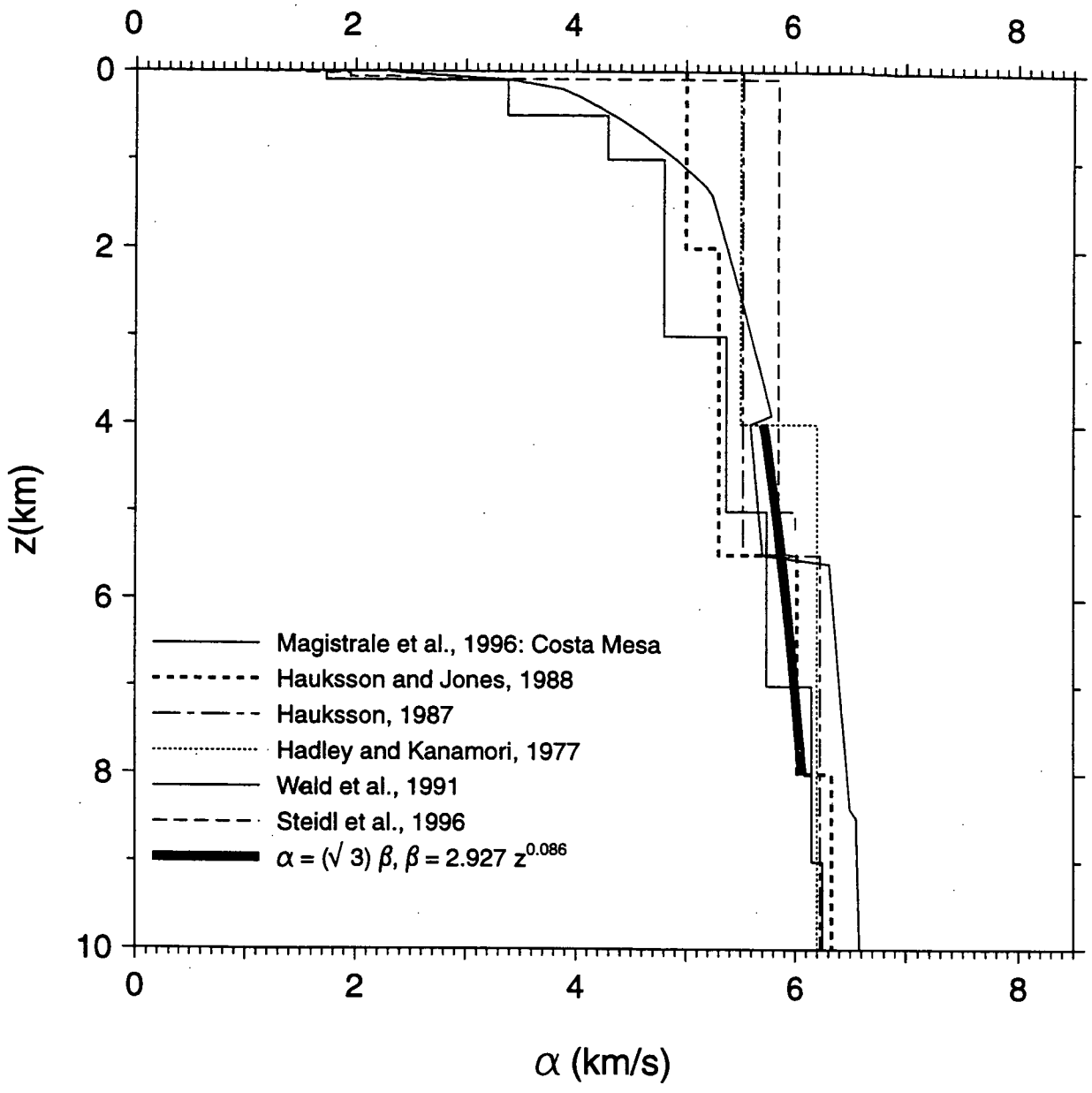


Figure 3. P-velocity vs. depth to 10 km. The heavy line is obtained by multiplying the generic rock shear velocities used in this paper by $\sqrt{3}$; this assumes a Poisson's ratio of 0.25, which we realize is much too small for shallow depths. The intent of this figure is to compare the final velocity profile used in the amplification calculation (heavy line) with various P-velocity profiles at depths greater than several kilometers, where we expect Poisson's ratio to be close to 0.25. The Magistrale *et al.*, 1996, curve is for a point at 33.64° N and 117.93° W.

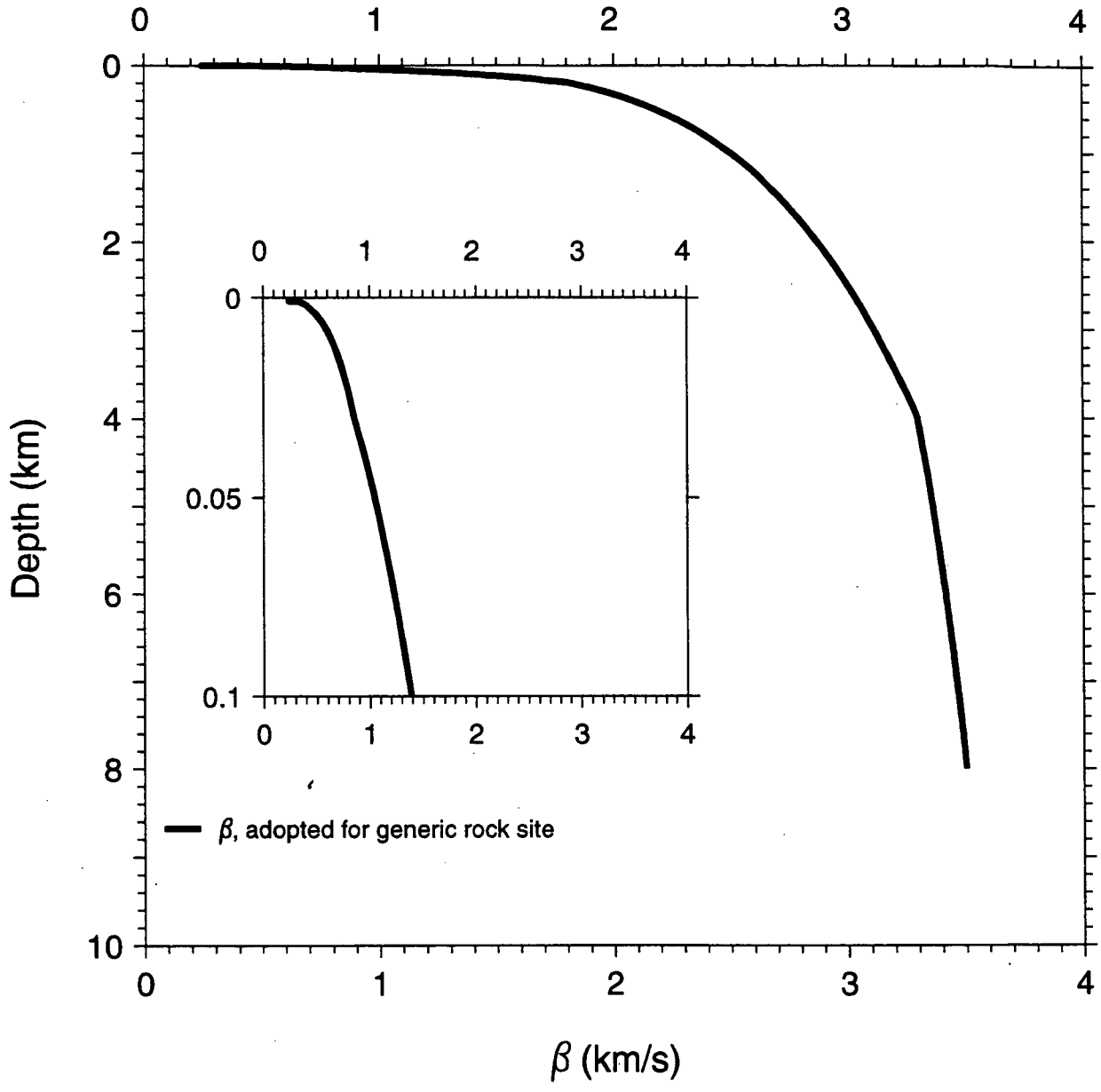


Figure 4. S-velocity vs. depth adopted in this paper for generic rock sites.

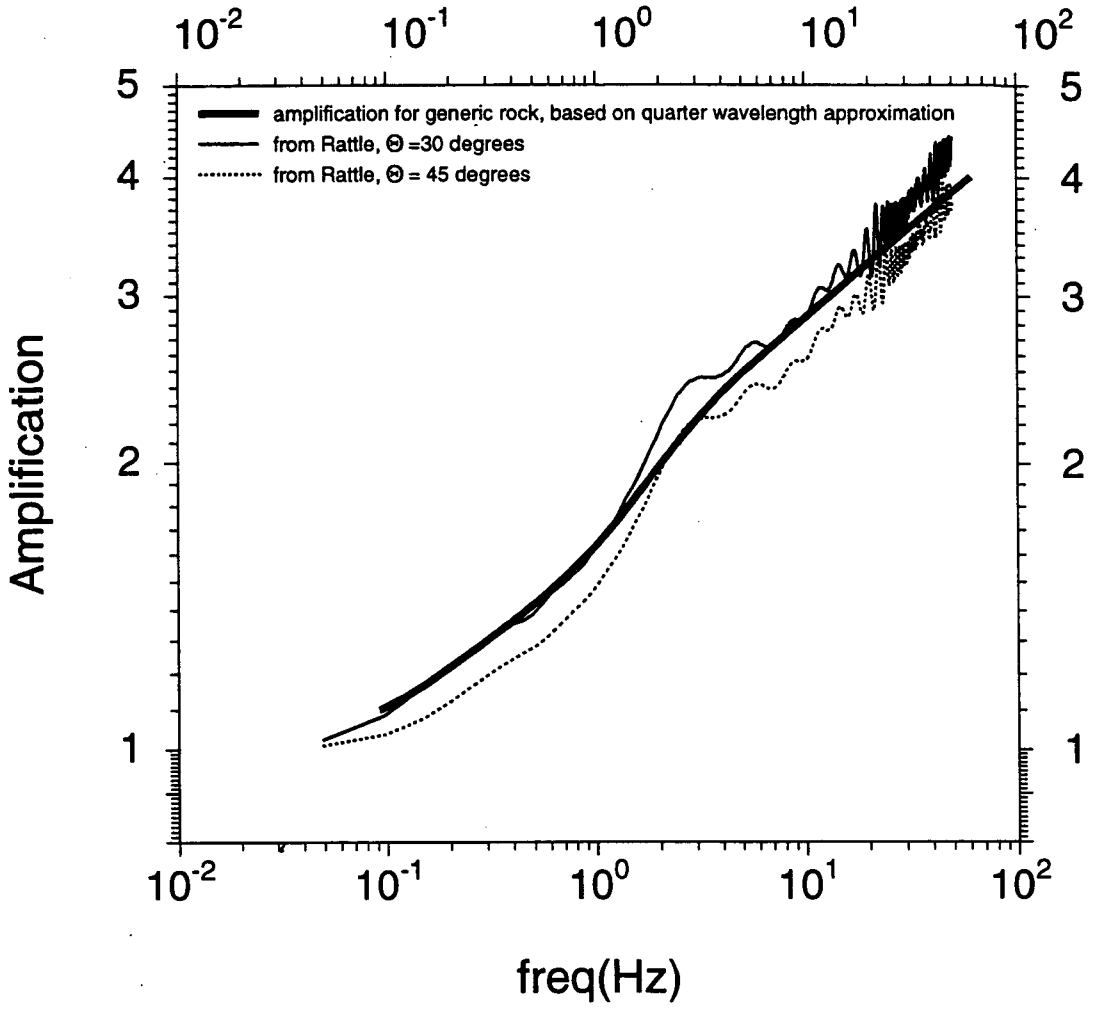


Figure 5. Amplification vs. frequency. The solid line is computed using the quarter-wavelength approximation and the velocity profile shown in Figure 4. The results from plane SH waves incident at the base of a 8-km thick stack of constant-velocity layers (with $Q = 10000$) closely approximating the adopted continuous shear-wave velocity are shown by the light lines for angles of incidence of 30 and 45 degrees; the results were computed from the Haskell matrix method, as implemented by program *Rattle* by C. Mueller.

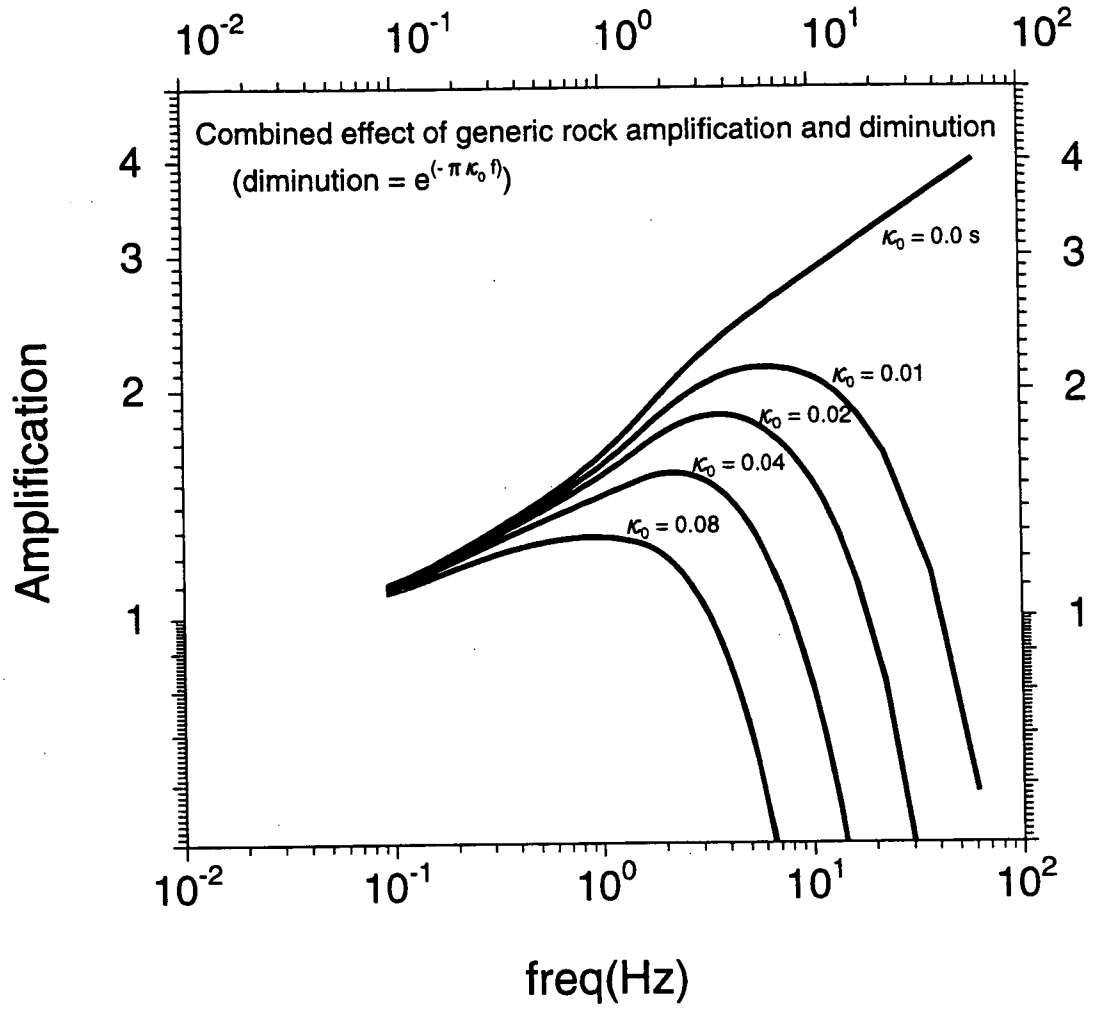


Figure 6. The combined effect of the generic rock amplification given in Figure 5 and the attenuation given by $\exp(-\pi\kappa_0 f)$.

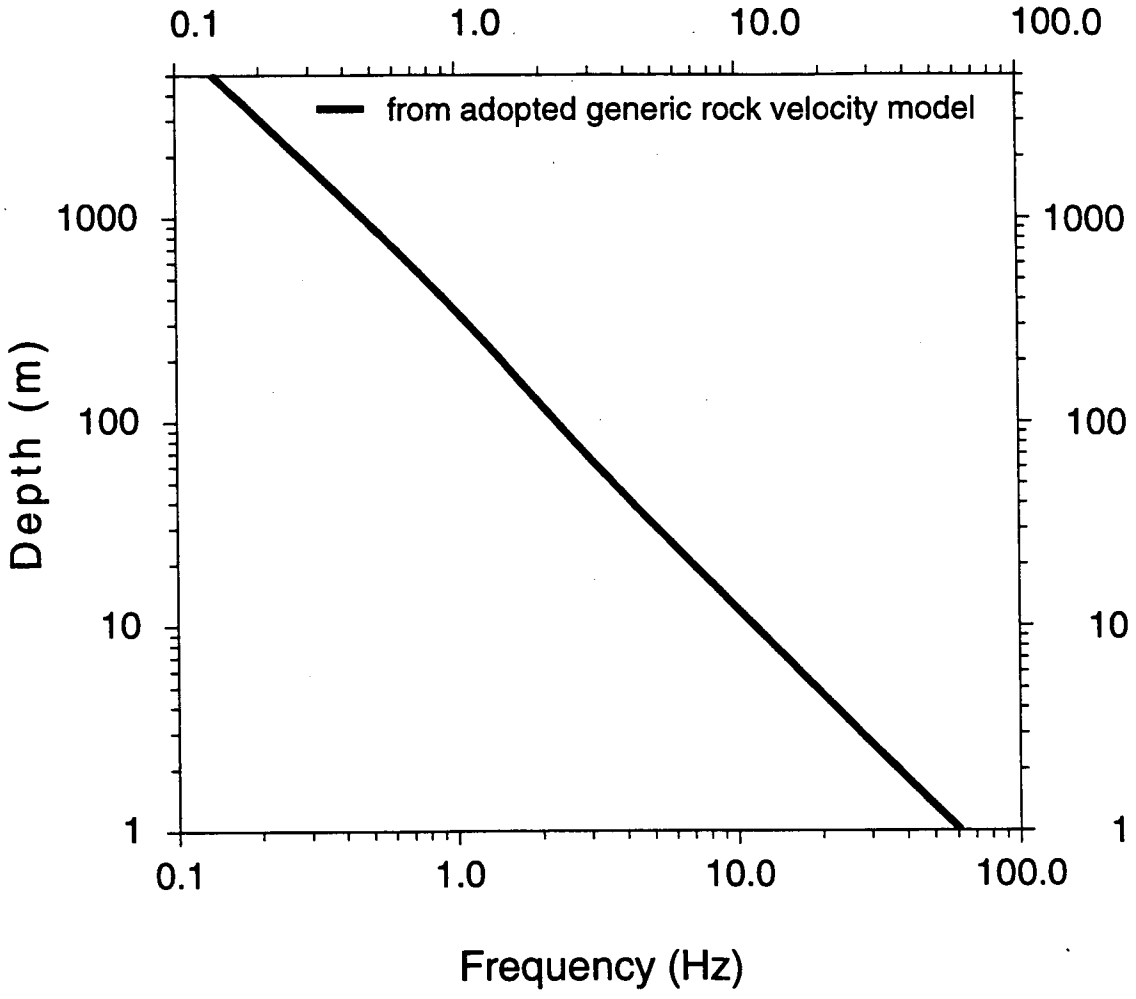


Figure 7. The depth corresponding to a quarter wavelength as a function of frequency for the adopted rock shear-wave velocity model. This figure provides a rough idea of what depths influence what frequencies in the site response.

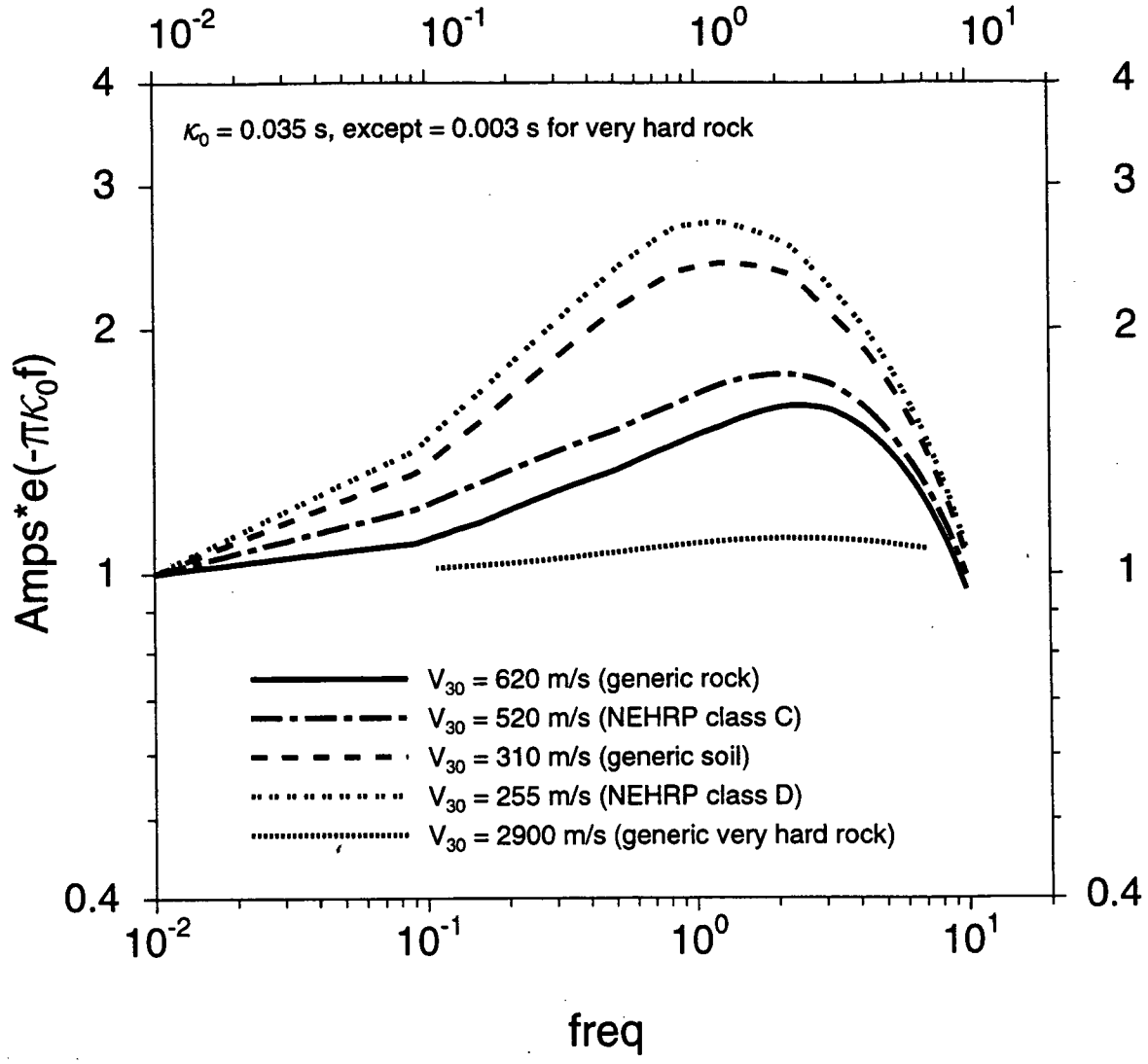


Figure 8. The product of Fourier spectral amplifications and the diminution factor $\exp(-\pi\kappa_0 f)$ for various site conditions, as measured by the average shear-wave velocity in the upper 30 m. The diminution factor used $\kappa = 0.035$ s for all cases except the very hard rock case, for which $\kappa = 0.003$ s.

The K-NET — a year after —

by

Shigeo Kinoshita [1], Keiichi Ohtani [2] and Tsuneo Katayama [3]

ABSTRACT

We started to release the K-NET strong-motion data from June, 1996 and about one year passed. In this article, we report the development of K-NET and some applications using the K-NET information released on the Internet.

Key Words : K-NET, Strong-motion

1. Development of K-NET

1.1 K-NET information on the Internet

We offered the K-NET information through graphical user interface on the World-Wide-Web in 1996. From April, 1997, the text pages of K-NET are available on the Internet for more quick distribution of the K-NET data.

1.1.1 Strong-motion records

We released the strong-motion records obtained by the K-NET on the Internet. However, the Internet capacity in this country is so poor that it becomes impossible to get the K-NET data on the Internet just after moderate earthquakes occurred. For example, in case of the Izu-Hanto-Toho-Oki earthquake swarm occurred in March, 1997, a part of users did not connect to the K-NET Internet site. To settle this problem, we constructed two mirror sites of our control center and started to release the K-NET information from these mirror sites from April, 1997. Now, users can get the K-NET data from the following three Internet sites.

(1) control center:
http://www.k-net.bosia.go.jp/
(2) mirror site #1:
http://www.k-net.ostec.co.jp/
(3) mirror site #2:
http://www.k-net.geophys.tohoku.ac.jp/

The mirror sites #1 and #2 were installed in Osaka and Sendai cities, respectively. Also, from April, 1997, users can download all strong-motion records obtained from a specific event in a lump sum. Such a data retrieve is possible for events selected by users.

1.1.2 Site information

We set up K-NET ftp site at October, 1996. From the ftp site, users can get all the soil data of K-NET stations in a lump sum. Also, the two mirror sites set up the ftp sites and started the service of K-NET data release from April, 1997. The address of these ftp

1) Head of Earthquake and Volcanic Disaster Prevention Laboratory, National Research Institute for Earth Science and Disaster Prevention, Science and Technology Agency, Tsukuba-shi, 305 Japan
2) Director of Disaster Prevention Research Division, ditto
3) Director-General, ditto

sites are obtained by changing the header part of Internet address from http to ftp. The ftp sites are also possible to release the K-NET strong-motion data. In this case, the data set is constructed with data directories which correspond to earthquake origin times.

1.1.3 Maximum acceleration map

Usually, we make a maximum acceleration map when we get more than 50 three-component seismograms for an earthquake. Figure 1 shows an example. This map was obtained from the Hiuganada earthquake of October 19, 1996. The JMA magnitude is 6.6. The contour lines of acceleration are calculated by using Splines interpolation. From these maps, we can interpret the local characteristics of maximum acceleration.

1.1.4 Application software

In 1996, we released a viewer program which plots the K-NET seismograms. In 1997, we are going to revise the viewer program and release the following application programs:

(1)program for the calculation of velocity and displacement seismograms,

(2)program for the calculation of Fourier and Power spectra,

(3)program for the calculation of response spectra, and

(4)program for the calculation of JMA seismic intensity defined by JMA in 1996.

These programs can plot the calculated results.

1.2 Off-line release of the K-NET information

From April, 1997, user can copy the K-NET strong-motion data to user's MO and/or DAT at the control center and mirror site #2. This is a self-servise. Also, we distributed the strong-motion data obtained in 1996 by CD-ROM. Such a service is going to be done every half year. The recording characteristics of accelerograph used in the K-NET was also published.

1.3 Use of K-NET

The K-NET started to release the strong-motion data on the Internet from June 3, 1996. Figure 2 shows the number of accessed pages for every day. Usually, the release of K-NET data on the Internet is made within 24 hours after an earthquake occurred. For example, in case of the earthquake of March 16, 1997(M=5.6), we obtained 209 three-component seismograms and released these data within about 3 hours. In such a case, the number of accessed pages became from 1,000 to 3,000 pages.

2. Applications

Since the K-NET starts, about one year passed. Some application studies using the K-NET data were reported during this period. Representative applications are as follows.

2.1 Monitor for strong quake

The K-NET95, an accerelograph used in the K-NET, has two communication ports. One is directly connected to a modem belong to a local municipal government. Among them, about 600 seismographs were incorporated in the Seismic Intensity

Information Network of the Fire Defence Agency (FDA). This network consists of about 3,400 stations. Just after an earthquake, the FDA may get the seismic intensity information in the hypocentral area within several minutes. The data will help local governments to assess the extent of the affected area and to manage their disaster response efficiently. This network is going to start in 1997.

The students of Tokyo University are opening the seismic intensity information on the Internet by using the K-NET data. The address is http://yagamo.u-tokyo.ac.jp/426/shindo.html. They show seismic intensity map just after the K-NET data are released. They used a formula for calculation of JMA seismic intensity defined by the JMA in 1996.

2.2 Utilization as a buck up network

Many research institutes are performing small-scale array observation on the basis of their original purposes. The K-NET supports these observations as a backbone network. Namely, the K-NET supports the data which can not be covered in their arrays. For example, the K-NET data obtained from the earthquake of December 21, 1996(M=5.4) helped an array observation deployed in Tama area, Tokyo, to interpret the existence of remarkable S-waves totally reflected in the Philippine Sea Plate.

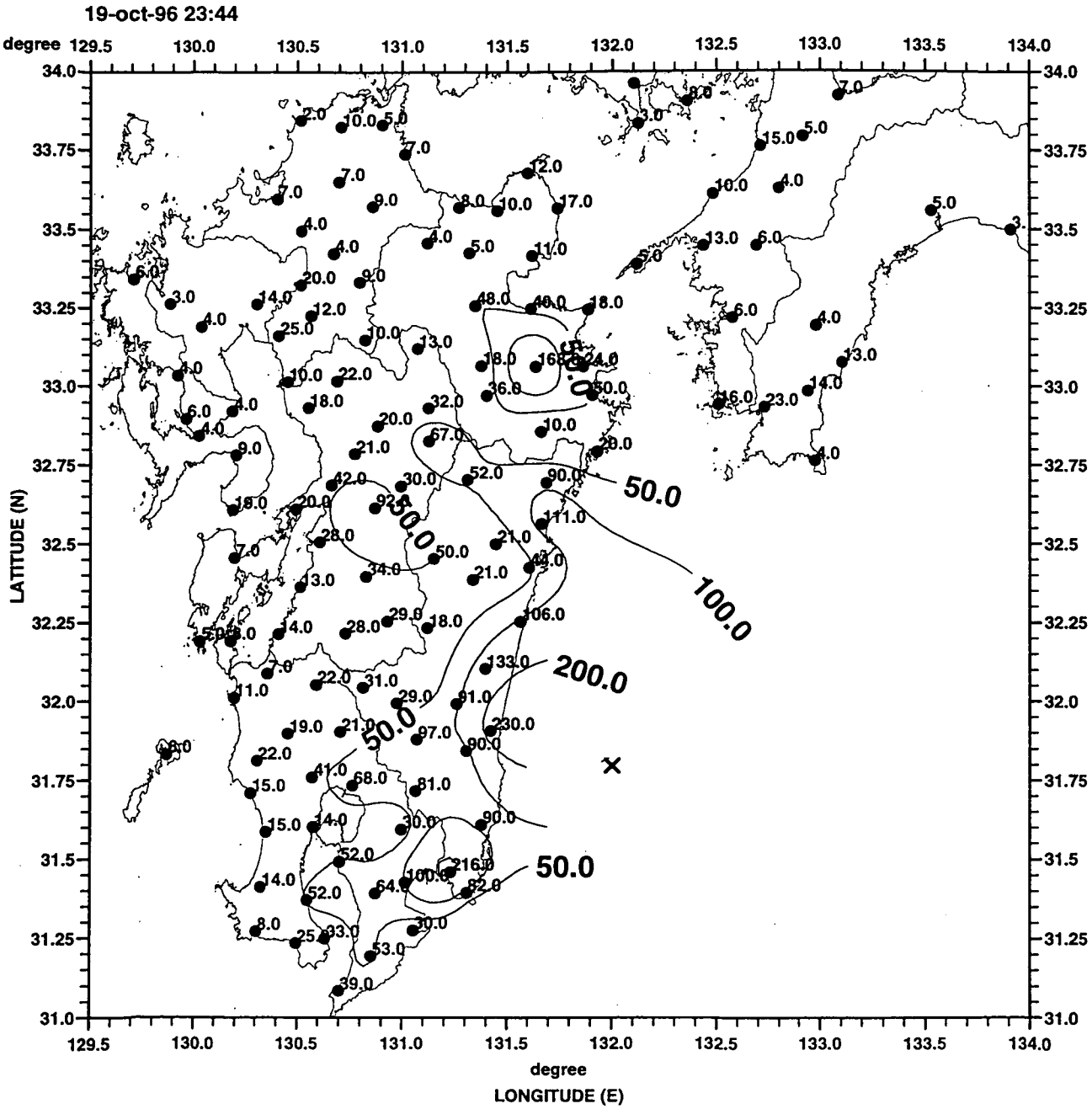
2.3 Studies on seismic wave propagation

The K-NET is suitable on the seismic wave propagation in a hypocentral area with a radius of about several hundred kilometers. Study on the regional attenuation of seismic wave is one of the reasonable research subjects. For example, the K-NET data obtained from earthquake of September 11, 1996(M=6.2) showed that S-waves severely attenuate when they pass through the volcanic front in Kanto area as shown in Figure 3. Solid circles in this figure show the triggered stations during the earthquake.

2.4 Studies on near field seismograms

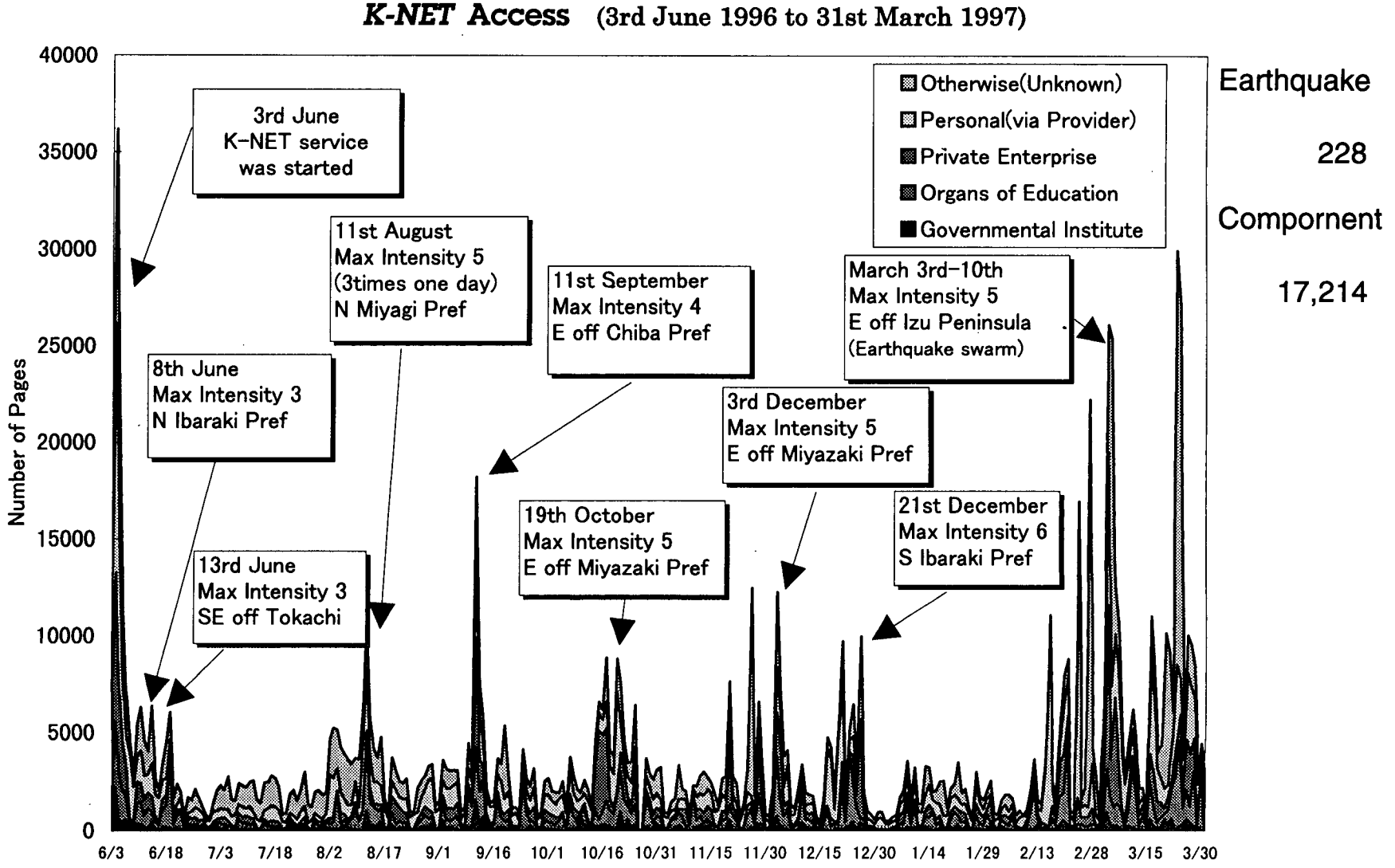
As the K-NET seismographs are distributed all over Japan with a station to distance of about 25 kilometers, they have the opportunity which obtains near field seismograms. In 1996, the K-NET95 installed at the Naruko station recorded the main and after shocks during the Miyagi-ken Hokubu earthquake. The JMA magnitude of main shockis 5.9. The largest acceleration is over 700 Gals at the site. Some research institutes tried to get the after shock records around Naruko site and tried to interpret the main shock seismogram obtained at the Naruko station.

Fig. 1



MAXIMUM ACCELERATION (N-S or E-W or U-D)

Fig.2



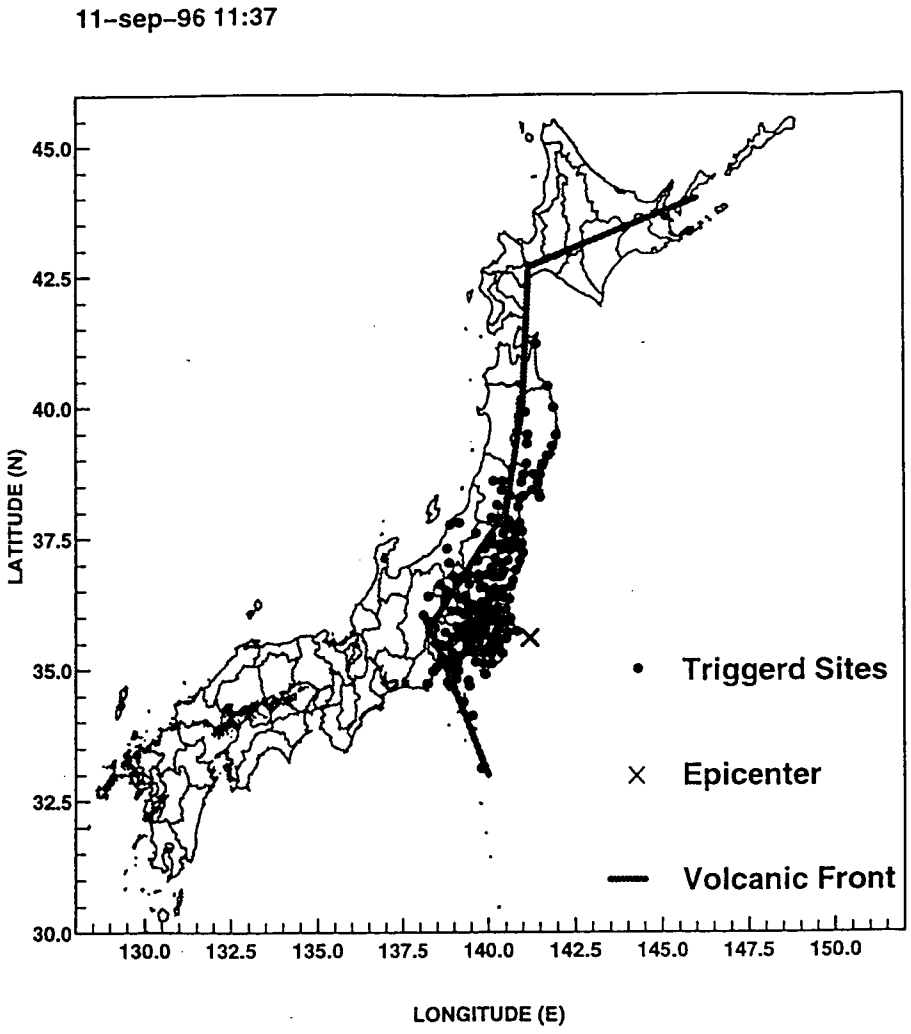
Earthquake

228

Compornent

17,214

Fig.3


11-sep-96 11:37
45.0
42.5
40.0
37.5
35.0
32.5
30.0
LATITUDE (N)
130.0
132.5
135.0
137.5
140.0
142.5
145.0
147.5
150.0
LONGITUDE (E)
Triggerd Sites
Epicenter
Volcanic Front

Seismic Design of Non-Structural Building Components in the United States

by

Andrew W. Taylor[1], and Long T. Phan[2]

ABSTRACT

Seismic design requirements for nonstructural building components of five major building codes, including the 1994 Uniform Building Code, the 1994 Standard Building Code, the 1994 NEHRP Recommended Provisions for Seismic Regulations for New Buildings, the New Zealand Building Code, and nonstructural provisions used in Japan, were reviewed in this study. Comparisons of codes reveal wide variation in seismic force and displacement requirements for nonstructural components, both in terms of levels of stringency and levels of details. The difference in seismic force requirements between the most and least stringent codes can be more than five times.

KEYWORDS: building codes; building technology; earthquake engineering; non-structural components; seismic design suspended ceilings

1. INTRODUCTION

Nonstructural building components are elements within or attached to buildings to provide them with essential services and functions, such as heating and cooling, lighting, escalators, electrical power, etc. These components are not a part of the building structural system, and are not designed to contribute to the resistance of earthquake forces. In most building codes, nonstructural components are commonly grouped into two categories: (1) *architectural*, and (2) *mechanical and electrical*. *Architectural* nonstructural components include, for instance, cladding, suspended ceilings, exterior and interior nonbearing walls and partitions, parapets, penthouses, etc. *Mechanical and electrical* nonstructural components include most building secondary systems such as boilers, furnaces, storage tanks, HVAC systems, piping systems, elevator components, electrical systems, and lighting fixtures, etc.

In several past earthquakes, it has been documented that damage to both *architectural* and *mechanical* nonstructural building components can have a great effect on the safety of occupants, functionality of facilities, and loss of property. While statistical cost data for nonstructural damage are scarce, it is widely agreed and reported that the economic effects of all nonstructural damage combined generally exceed those of structural damage in an earthquake (U.S. Congress 1995; Seismic Safety Commission 1995). In many cases, these "indirect losses" due to damaged equipment, lost inventory and records, and revenue can be two to three times greater than the cost of replacing collapsed buildings or structures, as often reported in the 1971 San Fernando (Ayres and Sun 1973; Meehan 1973), the 1989 Loma Prieta (Shephard et al. 1990), and the 1994 Northridge earthquakes (Hall 1995).

[1,2]Research Structural Engineer, Structures Division, Building and Fire Research Laboratory, National Institute of Standards and Technology, Gaithersburg, Maryland, USA, 20899

Nonetheless, most of the research efforts in seismic engineering to date have focused on improvements of the structural design of buildings to prevent total collapse, rather than on the performance of nonstructural components. This is consistent with the life-safety philosophy inherent in the model building codes in the United States and justifiably so, since the concern for total building collapse, which has more serious life safety implications, is naturally greater than the concern for local failure of nonstructural components. As a result, most newly constructed buildings stand a good chance that they will not collapse during an anticipated earthquake. It is only recently that more research attention has been paid to the performance of nonstructural components and secondary systems. The result is that many of the current model building codes and seismic provisions in use in the U.S., such as the 1994 Uniform Building Code (UBC 1994), the 1994 Standard Building Code (SBC 1994), and the 1994 National Earthquake Hazard Reduction Program (NEHRP) Recommended Provisions for Seismic Regulations for New Buildings (BSSC 1995a, 1995b), now contain revised and more stringent seismic design requirements for various nonstructural building components and equipment. For example, the 1994 NEHRP Recommended Provisions contains a new *Importance Factor* I_p and revised seismic force and displacement equations for nonstructural components based on recent actual earthquake performance data, which were not considered in the preceding NEHRP document (1991). However, most of the new design requirements and recommendations for nonstructural components have only recently been included in the U.S. building codes (1994 editions). The effectiveness of these new requirements or recommendations in limiting damage to nonstructural components is not yet known because implementation of these new provisions has just started, and there has not been a major earthquake in the United States since 1994 to allow a thorough assessment.

Numerous instances of damage to nonstructural components during past earthquakes have been reported (Ayres and Sun 1973; Meehan 1973; Shephard et al. 1990; Hall 1995). Typical damage includes failures of suspended ceilings, lighting fixtures, piping systems, mounting fixtures and anchors for equipment, cladding, partitions, etc. Much of this damage reportedly resulted from two main causes aside from being the direct result of structural failure. One cause is the incompatibility of movement between the building and nonstructural components and also between different nonstructural components which were installed in close proximity to one another. The other cause is the inadequacy of nonstructural components (mainly the support conditions and the mounting fixtures) to sustain seismic lateral load.

Among instances of damage due to displacement incompatibility are damage to suspended ceilings and other components located in or above suspended ceilings in commercial office buildings. These components include the suspended acoustical tile ceiling itself; fire sprinkler systems; light fixtures; and HVAC ducts. Problems arise because these components are co-located in the ceiling area, and their movements during an earthquake are often incompatible due to differences in the component flexibility. For example, fire sprinkler heads usually project through suspended acoustical tile ceilings. During an earthquake, if the movements of the suspended ceiling and the sprinkler pipes are incompatible, either the sprinkler heads or the suspended ceiling, or both, will be damaged. Not only does this decrease the ability of the sprinkler system to suppress post-earthquake fires, but it also may result in broken sprinkler heads and flooding of the building. Another example is distortion of the acoustical tile ceiling grid, which may cause ceiling tiles, lighting fixtures, and ventilation grills resting in the grid to fall.

Examples of damage due to the inadequacy of nonstructural components to sustain seismic lateral force include failures of anchors to hold equipment in place, such as water tanks and boilers. This results in equipment sliding off supports, spilling of contents, and disruption of service. Other nonstructural damage of this type includes failure of light fixtures and suspended ceilings at points of connection, and cracks in partition walls.

The objectives of this paper are to assess the current state of knowledge in seismic design of nonstructural building components, as reflected in various model building codes currently in use in the United States and other countries.

2. CODES FOR SEISMIC DESIGN OF NONSTRUCTURAL COMPONENTS

This section summarizes the seismic requirements for the design of nonstructural components, in terms of lateral force and displacement, of four building codes with earthquake provisions currently in use in three countries; the United States, New Zealand, and Japan. In the U.S., the codes reviewed include two of the national model codes, namely the 1994 Uniform Building Code (UBC 1994) of the International Conference of Building Officials, and the 1994 Standard Building Code (SBC 1994) of the Southern Building Code Congress International. In New Zealand, the 1992 New Zealand Standard (NZS 1992) is reviewed. And in Japan, two seismic building codes are reviewed: (1) the Guideline for Seismic Design of Building Nonstructural Components published by Public Buildings Association in 1987 (see IAEE 1992), and (2) Guideline for Seismic Design of Building Equipment published by Building Center of Japan in 1984 (see Hirosawa et al. 1991). Also reviewed is the 1994 NEHRP Recommended Provisions for Seismic Regulations for New Buildings (BSSC 1995a, 1995b). The NEHRP Recommended Provisions contain seismic design provisions to be considered for adoption in a future version of the national model codes. The following review of codes and recommended provisions is intended to reveal the variation in seismic design requirements for nonstructural components between different codes of practice. Provisions and design information relevant to the design of nonstructural components of each of the above listed documents are summarized below.

2.1 Uniform Building Code (UBC 1994)

2.1.1 Seismic Force Requirement

Permanent nonstructural components and their attachments shall be designed to resist the total design lateral seismic force, F_p, prescribed below:

$$F_p = ZI_pC_pW_p \quad \text{(UBC 1994 equation 30-1)}$$

where:

Z is the seismic zone factor, which ranges between 0.075 (seismic zone 1) to 0.40 (seismic zone 4). Values of Z for different seismic zones and seismic zone designation are given in UBC 1994 Table 16-I and UBC 1994 Figure 16-2.

I_p is the seismic importance factor for nonstructural components and their attachments. Values of I_p corresponding to different UBC occupancy categories are listed in UBC 1994 Table 16-K.

C_p is the horizontal force factor. Values of C_p for nonstructural components are given in UBC 1994 Table 16-O. C_p varies between 0.75 (for most mechanical and electrical equipment) to 2.0 (for exterior and interior ornamentation and appendages, signs and billboards, etc.).

W_p the weight of an element or component.

2.1.2 Seismic Displacement Requirement

UBC 1994 is less specific with requirements for seismic displacements of nonstructural components. In general, UBC 1994 requires that, for Essential and Hazardous Facilities (building categories 1 and 2), the lateral-force design shall consider the effects of relative motion of the points of attachment to the structure.

2.2 Standard Building Code (SBC 1994)

2.2.1 Seismic Force Requirement

The 1994 SBC provides two different sets of seismic force requirement for nonstructural components, one for architectural components and their attachments, and one for mechanical, electrical components and their attachments.

For architectural components and their attachments, the design seismic force F_p is determined as follows:

$$F_p = A_v C_c P W_c$$

For mechanical, electrical components and their attachments, the design seismic force F_p is determined as follows:

$$F_p = A_v C_c P a_c W_C$$

where:

A_v is the effective peak velocity-related acceleration ($0.05 \leq A_v \leq 0.40$), to be selected from 1994 SBC Figure 1607.1.5A, *Contour Map of Effective Peak Velocity-Related Acceleration Coefficient.*

C_c is the Seismic Coefficient from 1994 SBC Tables 1607.6.3 (for architectural components and their attachments) and 1607.6.4A (for mechanical, electrical components and their attachments).

P is the Performance criteria factor, varied with seismic hazard exposure group (I to III) and determined from 1994 SBC Tables 1607.6.3 for architectural components and their attachments and 1607.6.4A for mechanical, electrical components and their attachments. Table 1607.1.6 of the 1994 SBC lists the seismic hazard exposure group for buildings.

a_c is the attachment amplification factor, determined in accordance with 1994 SBC Table 1607.6.4B. The value of a_c is either 1.0 or 2.0.

W_c is the operating weight of the nonstructural component.

2.2.2 Seismic Displacement Requirement

The 1994 SBC provides two sections dealing with seismic displacement requirements for nonstructural building components, one for *architectural* components (1994 SBC section 1607.6.3.2) and the other for the attachment of *mechanical and electrical* (1994 SBC section 1607.6.4.2) components. For *architectural components*, deformation due to design story drift Δ_m, computed as the difference between story-level displacements δ_{xm}, shall be considered. δ_{xm} is computed as follows (1994 SBC section 1607.5.6):

$$\delta_{xm} = C_d \delta_{xem}$$

and,

$$\delta_{xem} = (g/[4\pi^2 I])(T_m^2 F_{xm}/w_x)$$

Where:

δ_{xem} is the deflection of level x in the mth mode at the center of the mass at level x.

C_d is the deflection amplification factor (given in 1994 SBC Table 1607.3.3).

g is the acceleration due to gravity (feet per second^2).

T_m is the modal period of vibration, in seconds, of the mth mode of the building.

F_{xm} is the portion of the seismic base shear in the mth mode, induced at level x.

w_x is the portion of the total gravity load of the building, W, located or assigned to level x.

For *mechanical and electrical* components, the 1994 SBC requires that relative seismic displacements between two points of support (or points of attachment) of these components be considered and accommodated. In calculating the relative seismic displacements between points of support, the difference in elevation between the supports and the out-of-phase displacements across portions of the building that are capable of moving in a differential manner such as at seismic and expansion joints, are to be considered (1994 SBC section 1607.6.4.2). Displacements at points of support shall be computed as described above.

$$\delta_{xem} = (g/[4\pi^2 I])(T_m^2 F_{xm}/W_x)$$

Where:

δ_{xem} is the deflection of level x in the mth mode at the center of the mass at level x.

g is the acceleration due to gravity (feet per second^2).

T_m is the modal period of vibration, in seconds, of the mth mode of the building.

F_{xm} is the portion of the seismic base shear in the m[th] mode, induced at level x.

W_x is the portion of the total gravity load of the building, W, located or assigned to level x.

2.3 New Zealand Standard (NZS 4203: 1992)

2.3.1 Seismic Force Requirement

The horizontal seismic force, F_{ph}, on nonstructural components of a building (referred to as parts of the building) shall be determined from:

$$F_{ph} = C_{ph} W_p R_p \qquad \text{(NZS eqn. 4.12.1)}$$

The vertical seismic force, F_{pv}, on nonstructural components of a building shall be determined from:

$$F_{pv} = C_{pv} W_p R_p \qquad \text{(NZS eqn. 4.12.2)}$$

where:

W_p is the weight of the nonstructural components or their attachments.

R_p is the risk factor for nonstructural components or attachments, NZS Tables 2.3.2 and 4.12.1.

C_{ph} is the seismic coefficient, which shall be taken equal to the basic horizontal coefficient C_{pi} (basic horizontal coefficient for nonstructural components and attachments at level i). C_{pi} shall be computed as follows:

$$C_{pi} = C_b(T_{pe}, \mu_p) C_{fi} / 0.4 \qquad \text{(NZS eqn. 4.12.7)}$$

and,

μ_p is the structural ductility factor for the nonstructural components. Values for μ_p corresponding to various nonstructural component are listed in NZS 4203 Table C4.12.1. μ_p = 1.0 for connections for machinery, switch gear and the like.

$C_b(T_{pe}, \mu_p)$ is the basic seismic acceleration coefficient for intermediate soil and T_{pe} is the equivalent period of the nonstructural components given by = $0.2\ T_p/T_1$ but not to be taken less than 0.4 s. T_1 is the fundamental translational period of vibration of the structure (NZS 4203 Section 4.5.2). Tabulated values of C_b corresponding to different values of T_p and μ_p are given in NZS 4203 Table 4.6.1.

C_{fi} is the floor acceleration coefficient at levels between the building base and the uppermost principal seismic weight. C_{fi} shall be determined by either the equivalent static method (NZS equation 4.12.5) or the modal response spectrum method (NZS equation 4.12.6) listed below:

$$C_{fi} = \frac{C_b(T_1, \mu_0)}{C_b(T_1, 1)} C_{fo}\left(1 - \frac{h_i}{h_n}\right) + C_{fn}\left(\frac{h_i}{h_n}\right)$$

(NZS 4203 equation 4.12.5)

or

$$C_{fi} = \frac{C_b(T_1, \mu_0)}{C_b(T_1, \mu)} \frac{F_1}{W_1}$$

(NZS 4203 equation 4.12.6)

μ_0 is the structural ductility factor calculated using the overstrength values (NZS 4203 Section 4.12.2). C_{fo} is the floor acceleration coefficient at and below the base of the building. C_{fo} may be computed as follows:

$C_{fo} = 0.4\ RZL_s$ for the serviceability limit state (NZS equation 4.12.3(a)), or
$C_{fo} = 0.4\ RZL_u$ for the ultimate limit state (NZS 4.12.3(b)).

C_{fn} is the floor acceleration coefficient at the level of the uppermost principal seismic weight. C_{fn} may be computed as follows:

$$C_{fn} = \frac{C_b(T_1, \mu_0)}{C_b(T_1, \mu)} \frac{F_n}{W_n}$$

R is the building risk factor, listed in NZS Tables 2.3.1 and 4.6.3.

Z is the zone factor ($0.4 \le Z \le 0.8$), shown in NZS Figure 4.6.2.

L_s, L_u are limit state factors for serviceability state (1/6) and ultimate state (1.0), respectively.

F_i is the equivalent static lateral force at level i; or inertial force at level i found from combination of modal inertial force.

F_n is the inertial force at the height of the uppermost principal seismic weight, h_n.

h_i is the height of level i above the level where the ground provides lateral restraint to the structure.

h_n is the height from the base of the building to the level of the uppermost principal seismic weight.

C_{pv} is taken as RZL_s for the serviceability limit state and RZL_u for the ultimate limit state.

An alternate method for obtaining C_{ph} (or C_{pi}) without having to use NZS equation 4.12.7 is to read the normalized values of C_{ph} from NZS Table C4.12.2. These values were calculated for the following assumptions:

- Each structure has equal story heights and weights.
- The fundamental period, T_1, is not less than the greater of 0.6 s and $0.10n$, where n is the number of stories.
- The nonstructural components, with their connections, are stiff ($T_p = 0$, $T_{pe} = 0.45$ s).
- The structures are sited on flexible or deep soil sites.

2.3.2 Seismic Displacement Requirement

The seismic displacement requirement of NZS 4203 is less specific than the seismic force requirement. In general, NZS requires that "*deflections of parts (nonstructural components) under the prescribed seismic forces shall be limited so as not to impair their strength or function, or lead to damage to other building components*" (NZS 4203 Section 4.12.1.7). Connections between nonstructural components and the building structure shall be designed to accommodate the interstory deflections determined by either the equivalent static method (NZS 4203 section 4.8), the modal response spectrum method (NZS 4203 section 4.9), or the numerical integration time history method (NZS 4203 section 4.10).

2.4 1994 NEHRP Recommended Provisions for Seismic Regulations for New Buildings (BSSC 1995a, 1995b)

The seismic force and displacement requirements for nonstructural building components (including architectural, mechanical, and electrical components) prescribed in this document (1994 edition) were completely revised from the previous edition (NEHRP 1991). The changes include introduction of the component importance factor I_p and new force and displacement equations. Specific requirements for relative seismic displacement are recommended and a more rational basis for connection design is provided.

2.4.1 Seismic Force Requirement

All nonstructural components and their attachments shall be designed for the seismic force, F_p, centered at the component's center of gravity and distributed relative to the component's mass distribution, described herein (1994 NEHRP section 3.1.3):

$$F_p = 4.0C_aI_pW_p \quad \text{(NEHRP eqn. 3.1.3-1)}$$

Alternately, F_p may be computed in accordance with the following equations:

$$F_p = a_pA_pI_pW_p/R_p \quad \text{(NEHRP eqn. 3.1.3-2)}$$

and

$$F_{p(min)} = 0.5C_aI_pW_p \quad \text{(NEHRP eqn. 3.1.3-5)}$$

where:

C_a is the seismic coefficient at grade, expressed as a fraction of acceleration of gravity and determined based on Soil Profile type (A to E) and the effective peak ground acceleration coefficient A_a (determined from NEHRP seismic ground acceleration map 1). C_a may be obtained as described in NEHRP section 1.4.2.3 or from NEHRP Table 1.4.2.4a. The maximum value of C_a is 0.44 (for soil type D).

I_p is the component importance factor which represents the greater of the life-safety importance of the component and the hazard exposure importance of the structure. I_p is either 1.0 or 1.5. I_p is 1.0 for all nonstructural components and their

attachments except for those components listed below, in which case I_p is 1.5:

- Life-safety component that is required to function after an earthquake.
- Component contains material that would be significantly hazardous if released.
- Component poses a significant life-safety hazard if separated from primary structure (e.g., parapets, exterior wall panels).
- Component can block a means of egress if damaged (e.g., exit stairs).

W_p is the component operating weight.

a_p is the component amplification factor which represents the dynamic amplification of the component relative to the fundamental period of the structure (T). a_p varies from a minimum value of 1.0 to a maximum of 2.5. NEHRP provides two sets of a_p values, one for architectural components and their attachments as listed in NEHRP Table 3.2.2 and one for mechanical and electrical components and their attachments as listed in NEHRP Table 3.3.2. In both cases, the value of a_p = 1 is for components generally regarded as rigid or rigidly attached. The value of a_p = 2.5 is for components generally regarded as flexible or flexibly attached.

R_p is the component response modification factor, representing the energy absorption capability of the component's structure and attachments. Current R_p values, listed in NEHRP Tables 3.2.2 for architectural components and their attachments and NEHRP Table 3.3.2 for mechanical and electrical components and their attachments, are judgmentally determined based on the experience of the responsible committee and vary from 1.5 to 6.0. In general, a higher value of R_p is associated with more ductile materials and detailing.

A_p is the component acceleration coefficient at point of attachment to the structure, expressed as a fraction of gravity. A_p may be computed using the following equations :

$$A_p = C_a + (A_r - C_a)(x/h)$$

(NEHRP eqn. 3.1.3-3)

where:

A_r is the component acceleration coefficient, expressed as a fraction of gravity, at the structure roof level. A_r may be computed as follows:

$$A_r = 2.0A_s \leq 4.0C_a \quad \text{(NEHRP eqn. 3.1.3-4)}$$

A_s is the structure response acceleration coefficient, expressed as a fraction of gravity. A_s shall be computed for each principle horizontal direction of the structure using the equation listed below. The larger value of A_s shall be used in computing A_r.

$$A_s = 1.2\frac{C_v}{T^{2/3}} \leq 2.5C_a$$

(NEHRP eqn. 3.1.3-7)

C_v is the seismic coefficient, expressed as a fraction of acceleration of gravity and determined based on Soil Profile Type (A to E) and the effective peak velocity-related acceleration A_v (may be obtained from NEHRP map 2). C_v may be obtained in accordance with 1994 NEHRP section 1.4.2.3 or from 1994 NEHRP Table 1.4.2.4b. The maximum value of C_v is 0.96 (for Soil Profile Type E).

T is the effective fundamental period of the structure.

x is the elevation of nonstructural component relative to grade elevation.

h is the average roof elevation of structure relative to grade elevation.

2.4.2 Seismic Displacement Requirement

Seismic relative displacement D_p between two connection points on the same building or structural system shall be designed to accommodate the smaller of the following two equations (1994 NEHRP section 3.1.4):

$$D_p = \delta_{xA} - \delta_{yA}$$

(NEHRP equation 3.1.4-1)

or

$$D_p = (X - Y)\Delta_{aA}/h_{sx}$$

(NEHRP equation 3.1.4-2)

For two connection points on separate buildings or structural systems (e.g.

connection points across an expansion joint), D_p shall be designed to accommodate the smaller of the following equations:

$$D_p = |\delta_{xA}| + |\delta_{yB}|$$

(NEHRP equation 3.1.4-3)

or

$$D_p = X\Delta_{aA}/h_{sx} + Y\Delta_{aB}/h_{sx}$$

(NEHRP equation 3.1.4-4)

where:

δ_{xA} is the deflection at building level x of Building A, determined from elastic analysis and multiplied by the deflection amplification factor C_d. C_d values for different structural systems are listed in 1994 NEHRP Table 2.2.2.

δ_{yA} is the deflection at building level y of Building A, determined from elastic analysis and multiplied by the C_d factor.

δ_{xB} is the deflection at building level x of Building B, determined from elastic analysis and multiplied by the C_d factor.

δ_{yB} is the deflection at building level y of Building B, determined from elastic analysis and multiplied by the C_d factor.

X is the height of upper support attachment at level x as measured from grade.

Y is the height of lower support attachment at level y as measured from grade.

Δ_{aA} is the allowable story drift for Building A as defined in 1994 NEHRP Table 2.2.7.

Δ_{aB} is the allowable story drift for Building B as defined in 1994 NEHRP Table 2.2.7.

h_{sx} is the story height used in the definition of the allowable drift, Δ_a, in 1994 NEHRP Table 2.2.7. Δ_a/h_{sx} is the allowable drift index.

The 1994 NEHRP Recommended Provisions also prescribe required clearances for suspended ceiling and other ceiling components such as fire sprinkler heads and light fixtures.

2.5 Seismic Building Codes of Japan (IAEE 1992 and Hirosawa et al. 1991)

Seismic design requirements for building mechanical equipment and nonstructural components are provided by two documents: (1) *Guideline for Aseismic Design and Construction of Building Equipment*, published by the Building Center of Japan (1984) and (2) *Guideline for Aseismic Design for Architectural Nonstructural Elements*, published by Public Building Association (1987). The coefficients used in determining the design seismic force are similar between these two guidelines when the *Modified Seismic Coefficient Method* is used as the design method. The requirements for nonstructural components and building equipment are described below.

2.5.1 Seismic Force Requirement

Nonstructural components and their attachments shall be designed to resist the total lateral design seismic force, F_H, which was prescribed based on the modified seismic force coefficients method:

$$F_H = K_H W$$

and

$$K_H = ZIK_1K_2k_0$$

where:

K_H is the lateral design seismic force coefficient.

W is the weight of the nonstructural component or equipment (in units of kgf).

Z is the seismic zone factor. Z = 1.0 for Seismic Zone A, 0.85 for Seismic Zone B, and 0.70 for Seismic Zone C.

I is the seismic importance reduction factor. I = 1.0 for important building equipment, and 2/3 for general building equipment. Building owners and structural designers can determine importance and select the appropriate value for I.

K_1 is the floor response amplification factor of a building, which varies between 1.0 and 3.33. K_1 = 1.0 at the basement floor and 3.33 at the roof level.

K_2 is the response amplification factor of the nonstructural component or equipment. Specific values of K_2 are provided for some architectural components. In general, K_2 ranges between 1.0 and 2.0.

k_0 is the standard design seismic force coefficient (0.3).

The value of $I \cdot K_1 \cdot K_2 \cdot k_0$ shall be not less than 0.6 for important nonstructural components and 0.3 for ordinary nonstructural components.

The vertical design seismic force, F_v, shall be determined by the following formula:

$$F_V = K_V W$$

where K_V is the vertical design seismic force coefficient ($K_V = K_H/2$).

2.5.2 Seismic Displacement Requirement

Similar to other codes, seismic displacement requirements are not as specific as the seismic force requirements. The current building codes of Japan require that for pipes, vertical pipes shall be subjected to a maximum story drift of 1/200 radian times the story height. Pipes through expansion joints shall be designed for possible maximum relative displacement between two structures.

2.6 Summary of Codes

Provisions relevant to the seismic design requirements for nonstructural building components of five seismic engineering documents, which include the 1994 Uniform Building Code, the 1994 Standard Building Code, the 1994 NEHRP Recommended Provisions, the 1992 New Zealand Standard (NZS 4203), and the 1982 and 1987 Japanese codes, are reviewed and summarized in sections 2.1 to 2.5. The review shows wide variations in seismic design requirements between codes, both in terms of seismic force and displacement calculations and in listings of nonstructural components and corresponding coefficients.

For the *seismic force requirement*, the building codes use three basic coefficients to account for the following factors in prescribing the design force:

- Seismicity of the region where the building is located (*seismic zone factor*, or *effective peak-velocity acceleration*, or *component acceleration coefficient*).
- Functionality of nonstructural components and buildings in terms of life-safety importance (*seismic importance factor*, or *component risk factor*, or *component performance criteria*).
- Response characteristics of nonstructural components to seismic lateral load (*component seismic coefficient*, or *component horizontal force factor*, or *component response amplification factor*).

The above three factors are considered in the seismic force requirements of the 1994 UBC, 1994 SBC, and in equation 3.1.3-1 of the 1994 NEHRP Recommended Provisions. Other factors not explicitly included in the seismic design requirements of the above three codes, but which are explicitly considered in the 1992 NZS 4203, the 1982 and 1987 Japanese building codes, and in equation 3.1.3-2 of the 1994 NEHRP Recommended Provisions are:

- Response characteristics of the building to seismic lateral load (*building seismic coefficient*).
- Site soil profile (*building seismic coefficient*).
- Component location relative to building height (*floor response amplification factor*).

Table 2.1 summarizes the coefficients affecting the calculation of seismic lateral force of the codes reviewed. In terms of level of detail, the seismic design requirements of the 1994 NEHRP Recommended Provisions (equation 3.1.3-2) and the 1992 NZS 4203 appear to require the most detailed information for the calculation of design lateral force for nonstructural components. Of all five documents reviewed, only the 1994 NEHRP Recommended Provisions provides two alternate methods for computing the seismic lateral force requirement.

For the *seismic displacement requirement*, the 1994 SBC and the 1994 NEHRP Recommended Provisions are more specific

than other building codes in prescribing the required seismic lateral displacement. Both of these documents provide formulas for calculating the displacement at points of support for nonstructural components. The 1994 NEHRP Provisions also specifically prescribe detailed requirements for clearance between co-located ceiling components, such as clearance between suspended ceiling and fire sprinkler heads. The 1994 UBC, New Zealand Standard NZS 4203, and the 1982 and 1987 seismic building codes of Japan are less precise in prescribing seismic displacement requirements for nonstructural building components. In general, all codes require that attention be paid to the relative displacement between connection points of nonstructural components, especially connection points that are located on separate structural systems or buildings (anchors for piping systems crossing expansion joints, for example).

3. COMPARISON OF CODE SEISMIC DESIGN REQUIREMENTS

3.1 Introduction

As was shown in Section 2, there are noticeable variations in code requirements for nonstructural building components, both in terms of level of detail in the requirements and in the calculation procedures. Some codes have more detailed descriptions of nonstructural building components and assign more specific coefficients to various components, while others are less specific in listing the applicable components. In such cases the seismic coefficients necessary for computing seismic lateral force and displacement requirements must be estimated.

In the following sections, comparison of cases where maximum seismic forces are required by the codes reviewed in Section 2 will be conducted. The difference in seismicity in different countries is accounted for by using the maximum local seismic zone factors for the appropriate countries. Comparison of seismic displacement requirement also will be discussed.

3.2 Comparison of Maximum Seismic Force Requirement

Table 3.1 summarizes the seismic lateral force requirements and the conditions which result in maximum seismic force requirements for various nonstructural components by the four building codes and the 1994 NEHRP Recommended Provisions. The components listed in Table 3.1 are selected from the 1994 SBC list of nonstructural components, since this code appears to have the most detailed list and description of the components. For uniformity, different terminologies between codes which refer to the same quantity are made consistent in Table 3.1. For example, W_p is used for all codes in Table 3.1 to refer to the weight of nonstructural components, instead of W_c as used in the 1994 SBC. The 1994 NEHRP Recommended Provisions provide two different methods for computing the seismic lateral force requirement for nonstructural building components. One is given in NEHRP equation 3.1.3-1 which does not consider the component's amplification and response modification factors, while the other, given in NEHRP equation 3.1.3-2, considers these factors. Thus, two columns which list seismic force requirements according to the two methods of 1994 NEHRP Recommended Provisions are provided in Table 3.1.

As seen from Table 3.1, significant variations in maximum lateral force requirements exist between codes. In terms of *maximum seismic force requirements*, the 1994 NEHRP Recommended Provisions equation 3.1.3-1 appears to be most stringent. Next are the 1992 New Zealand Standard NZS 4203 and the Japanese building codes (1982 and 1987). The 1994 SBC is as stringent as NEHRP equation 3.1.3-1 and even more stringent than the NZS 4203 and the Japanese codes when dealing with safety equipment such as fire protection equipment and pipe systems. For other components, the 1994 SBC seismic force requirements are in general less conservative than those of the above codes. The 1994 UBC appears to be the least stringent of all building codes and recommended provisions reviewed. The difference in level of seismic force

requirement between the codes can be more than five times for some components. For example, maximum seismic force requirements for fire protection equipment and system vary from $0.45W_p$ to $2.64W_p$ between the 1994 UBC and equation 3.1.3-1 of the 1994 NEHRP Recommended Provisions.

3.3 Comparison of Seismic Displacement Requirement

Numerical comparison of code-prescribed seismic displacement requirements is not possible since the calculation for displacement of nonstructural building components requires case-specific information such as building mode of vibration, modal period, and base shear, etc. Thus comparisons similar to section 3.2 are not conducted here. Instead, only a general discussion is presented here for comparative purposes.

The 1994 NEHRP Recommended Provisions provide the most detailed seismic displacement requirements compared to other building codes reviewed. Besides formulas prescribing the relative seismic displacement between connection points for nonstructural components on the same building (NEHRP equations 3.1.4-1 and 3.1.4-2) and on separate buildings (NEHRP equations 3.1.4-3 and 3.1.4-4), NEHRP Provisions also prescribe clearances for co-locating systems such as suspended ceiling and fire sprinkler heads.

The 1994 SBC provides specific formulae for computing seismic displacement for nonstructural components. SBC's *architectural components* are required to accommodate design story drift, which is computed as the difference between story-level displacements. In computing story-level displacement, SBC considers *deflection amplification* of different seismic resisting systems.

Seismic displacement requirements of other codes besides the 1994 NEHRP and the 1994 SBC are much less specific. In general, all codes require that differences in elevations and in structural systems between connection points shall be considered in computing seismic displacement of connection points.

4. CONCLUSIONS

Widespread damage sustained by nonstructural components, especially components related to ceilings, during recent earthquakes has illustrated the continuing need for evaluation of existing seismic design requirements and for development of methods to mitigate losses caused by damage to these nonstructural components. Despite the widespread damage reported in post earthquake surveys, only a handful of studies focusing on nonstructural performance has been identified.

There are wide variations in seismic design requirements for nonstructural building components between the two current U.S. national model building codes (the 1994 UBC, which is adopted in part by much of the western U.S., and the 1994 SBC, which is adopted in part by the southeastern U.S.), the 1992 New Zealand Standard NZS 4203, the current building codes of Japan (1982 and 1987), and the 1994 NEHRP Recommended Provisions for Seismic Regulations for New Buildings.

In terms of levels of detail, the 1994 UBC, 1994 SBC and 1994 NEHRP equation 3.1.3-1 appear to be simplest, with three factors considered for calculation of the seismic force requirement: (1) factor to account for *seismicity of regions*, (2) factor to account for *functionality of nonstructural components and buildings*, and (3) factor to account for *response characteristics of nonstructural components*. While the 1994 NEHRP equation 3.1.3-2, the 1992 NZS 4203, and the Japanese building codes require, in addition to the above three factors, more detailed information such as the *seismic response characteristics of the building, site soil profile* information, and *component location* relative to building height. Also, the 1994 SBC and the 1994 NEHRP Provisions are more specific in prescribing the seismic displacement requirements and clearances for nonstructural components than other building codes reviewed in this report.

In terms of levels of stringency, the variation between the most and least stringent seismic force requirement can be more than five times. The most stringent seismic force requirement is that of the 1994 NEHRP

document. Next in stringency is the 1992 New Zealand Standard NZS 4203, and then the Japanese building codes. The least conservative code with respect to seismic force requirements for nonstructural building components is the 1994 UBC. The UBC also appears to lack the flexibility in assigning different levels of importance to different nonstructural components.

5. REFERENCES

Ayres, J.M; and Sun, T-Y. (1973), "*Nonstructural Damage*", The San Fernando, California Earthquake of February 9, 1971, National Oceanic and Atmospheric Administration, Washington, D.C., pp. 735-776, Vol. I, Part B.

BSSC (1995a), Building Seismic Safety Council (BSSC), "*NEHRP Recommended Provisions for Seismic Regulations for New Buildings - Part 1: Provisions*", prepared for the Federal Emergency Management Agency (FEMA), FEMA 222A, May.

BSSC (1995b), Building Seismic Safety Council (BSSC), "*NEHRP Recommended Provisions for Seismic Regulations for New Buildings - Part 2: Commentary*", prepared for the Federal Emergency Management Agency, FEMA 222A, May.

Hall, J.F. (1995), Technical Editor, "*Nonstructural Damage*", Northridge Earthquake of January 17, 1994 Reconnaissance Report, Earthquake Spectra, p.p. 453-513, Vol. 1, Publication 95-03, April.

Hirosawa, M.; Mizuno, H.; and Midorikawa, M. (1991), "*State-of-the-Art Report on Seismic Design of Building Equipment and Nonstructural Component in Japan*", Building Research Institute, Ministry of Construction, Japan, May.

IAEE (1992), International Association for Earthquake Engineering, "*Japan Standards for Aseismic Civil Engineering Construction*", Earthquake Resistant Regulations -- A World List, Tokyo, Japan, 1992.

Meehan, J.F. (1973), "*Public School Buildings*", The San Fernando California Earthquake of February 9, 1981, National Oceanic and Atmospheric Administration, Washington, D.C., pp. 667-884, Vol. I, Part B.

NZS (1992), Standards Association of New Zealand, "*Code of Practice for General Structural Design and Design Loadings for Buildings (New Zealand Standard NZS 4203: 1992)*", Wellington, New Zealand.

Phan, L.T.; and Taylor, A.W. (1996), "State of the Art Report on Seismic Design Requirements for Nonstructural Building Components," NISTIR 5857, National Institute of Standards and Technology, Gaithersburg, Maryland, June.

SBC (1994), Southern Building Code Congress International (SBCCI), "*Standard Building Code*", 1994 Edition, Birmingham, Alabama.

Seismic Safety Commission (1995), State of California, "*Northridge Earthquake - Turning Loss to Gain*", SSC Report No. 95-01, Sacramento, California.

Shephard, R.B.; Wood, P.R.; Berill, J.B.; Gillon, N.R.; North, P.J.; Perry, A.K.; and Bent, D.P. (1990), "*The Loma Prieta, California, Earthquake of October 17, 1989 - Report of the NZNSEE Reconnaissance Team*", Bulletin of the New Zealand National Society for Earthquake Engineering (NZNSEE), Vol. 23, No. 1, March.

UBC (1994), International Conference of Building Officials (ICBO), "*Uniform Building Code - Structural Engineering Design Provisions*", Volume 2, Whittier, California.

U.S. Congress (1995), Office of Technology Assessment, "*Reducing Earthquake Losses*", OTA-ETI-623, U.S. Government Printing Office, Washington, D.C., September.

Table 2.1 **Coefficients Affecting Seismic Force Requirements in Various Building Codes**

Coefficients to account for ↓	**1994 UBC**	**1994 SBC**	**1994 NEHRP Eq. 3.1.3-1**	**1994 NEHRP Eq. 3.1.3-2**	**NZS 4203**	**Japan**
1) Seismicity of Region Where Buildings are Located	• Seismic Zone Factor: Z (0.075 - 0.4)	• Effective Peak-Velocity Acceleration: A_v (0.05 - 0.4)	• Seismic Coefficient: C_a (0.04 - 0.44) (varies with soil type)	• Component Acceleration Coefficient: A_p ($\leq 4.0\ C_a$)	• Seismic Zone Factor: Z (0.4 - 0.8)	• Seismic Zone Factor: Z (0.7 - 1.0)
2) Functionality of Components in Terms of Life-Safety Importance	• Seismic Importance Factor: I_p (1.0 - 1.5) (varies with Occupancy Category)	• Performance Criteria Factor: P (0.5 - 1.5) (varies with Seismic Hazard Exposure Group)	• Component Importance Factor: I_p (1.0 - 1.5) (varies with degree of affect on life-safety)	• Component Importance Factor: I_p (1.0 - 1.5) (varies with degree of affect on life-safety)	• Component Risk Factor: R_p (1.0 - 1.1) (varies with degree of affect on life-safety). • Building Risk Factor: R (0.6 - 1.3)	• Seismic Importance Reduction Factor: I (1.0 or 2/3)

Table 2.1 **(continued)**

Coefficients to account for ⇓	1994 UBC	1994 SBC	1994 NEHRP Eq. 3.1.3-1	1994 NEHRP Eq. 3.1.3-2	NZS 4203	Japan
3) Component Seismic Response Characteristics	• Horizontal Force Factor: C_p (0.75 - 2.0)	• Component Seismic Coefficient: C_c (0.6 - 3.0) • Attachment Amplification Factor: a_c (1.0 - 2.0)	• Implied in constant: 4.0	• Component Amplification Factor: a_p (1.0 - 2.5) • Component Response Modification Factor: R_p (1.5 - 6.0)	• Implied in Seismic Coefficient: C_{ph} (through component ductility factor μ_p)	• Response Amplification Factor: K_2 (1.0 - 2.0)
4) Building Response Characteristics and Soil Site Profile	• Not explicitly considered	• Not explicitly considered	• Not explicitly considered	• Implied in Component Acceleration Coefficient: A_p	• Implied in Seismic Coefficient: C_{ph}	• Not explicitly considered
5) Component Location Relative to Building Height	• Not considered	• Not considered	• Not considered	• Implied in Component Acceleration Coefficient: A_p	• Implied in Seismic Coefficient: C_{ph}	• Floor Response Amplification Factor: K_1 (1.0 - 10/3) (varies with height)

Table 3.1 **Comparison of maximum seismic force requirement of various codes**

CODES	1994 UBC	1994 SBC	NZS 4203 (1992)	1994 NEHRP		1987 JAPAN
CONDITIONS FOR MAXIMUM SEISMIC FORCE REQUIREMENTS	• Structures are located in Seismic Zone 4 (Z=0.4). • Structures are Essential & Hazardous facilities, or Standard Occupancy Structures with anchorage of machinery and equipment for life-safety systems (I_p=1.5).	• Structures are located in regions where Effective Peak Velocity-related Acceleration Coefficient, A_v = 0.4. • Structures are of Seismic Hazard Exposure Group III. • Resilient mounting systems are of the types which cause Attachment Amplification Factor a_c to be 2.0.	• Structures are located in regions of maximum Zone Factor (Z=0.8). • Components and attachments are designated as P.I and P.II (R_p = 1.1).	• Structures are located at sites with Soil Profile Type D and Effective Peak Ground Acceleration Coefficient A_a = 0.4 (C_c = 0.44). • Structures are located in regions where Effective Peak Ground Acceleration Coefficient A_a = 0.4.		• Structures are located in seismic zone A (Z = 1.0). • Equipment/ components are designated as Important Building Equipment. • Equipment/ components are located at top level of building (K_i = 10/3).
1. Exterior nonbearing walls	$0.45W_P$	$0.54W_p$	$0.60W_p$	$1.76W_P$[d]	$0.88W_p$[e]	$1.33W_p$
2. Wall attachments	$1.2W_P$	$1.8W_p$	$2.2W_p$	$1.76W_P$[d]	$0.88W_p$[e]	$1.33W_p$
3. Veneer connections	$1.2W_P$	$1.2W_p$	$2.2W_p$	$1.76W_P$[d]	$1.76W_p$[e]	$1.33W_p$
4. Fire protection equipment and systems	$0.45W_P$	$2.4W_p$	$2.2W_p$[a]	$2.64W_P$[d]	$1.65W_p$[e]	$2.0W_p$
5. Pipe systems	$0.45W_P$	$2.4W_p$[b]	$2.2W_p$[a]	$2.64W_P$[d]	$1.65W_p$[e]	$2.0W_p$
6. Suspended ceilings	$0.45W_p$	$0.54W_p$[c]	$2.0W_p$[a]	$2.64W_p$[d]	$1.76W_p$[e]	$1.33W_p$
7. Lighting fixtures	$0.45W_P$	$0.804W_p$	$2.0W_p$[a]	$1.76W_P$[d]	$1.76W_p$[e]	$1.33W_p$

Notes: [a] Computed with μ_p assumed to equal 1.0 since values of μ_p for these components are not available in the 1992 NZS 4203.
[b] Pipe systems for gas and high hazard piping.
[c] For fire-rated membrane.
[d] Computed using 1994 NEHRP equation 3.1.3-1, $F_p = 4.0C_aI_pW_p$.
[e] Computed using 1994 NEHRP equation 3.1.3-2, $F_p = a_pA_pI_pW_p/R_p$

Micro-Distribution of Peak Ground Acceleration in Hanshin Area Estimated by Seismograph Data and Seismic Intensity obtained by Questionnaires for the 1995 Great Hanshin Earthquake

by

Shiro Takada[1] and Ryuzo Ozaki[2]

ABSTRACT

In this paper the distribution of peak ground acceleration during the 1995 Great Hanshin Earthquake is estimated by the shape interpolation method. In order to grasp the detailed seismic intensity, we distributed questionnaires within the struck area and calculated the seismic intensity from such questionnaires.

As a result, the distribution of the large values of acceleration is coincident with distribution of the damage in struck areas. The distribution of high level of seismic intensity obtained from questionnaires corresponds to the distribution of the level 7 of the JMA intensity.

Key Words: Shape Interpolation Method, Seismic Intensity, Questionnaires, Peak Ground Acceleration, Geographical Information System

1. INTRODUCTION

Urban functions in highly developed cities are greatly dependent upon lifeline systems such as electric power, gas, water and communication networks. In view on decision making of strategies for restoration workings as well as on the prevention of secondary disasters due to earthquake damage, it is indispensable to obtain information of earthquake damage to lifeline systems as quickly and exactly as possible. Several seismographs are generally arranged at the vicinity of important facilities of lifeline systems in order to obtain records for seismic ground motions which are greatly related to the earthquake damage to lifeline systems. Because it is neither economical nor possible to arrange many seismographs for the whole lifeline systems, Takada et al.[1] proposed a method to estimate seismic ground motions at arbitrary locations through the seismograph data observed at limited locations. Such method which uses the shape interpolating function of F.E.M. and B.E.M. is applied to seismograph data observed during the 1995 Great Hanshin Earthquake in order to estimate the distribution of peak ground acceleration in wide range areas.

The scale of ground intensity as considered by the Japan Meteological Agency (hereafter JMA) is one based on index which present the objective ground intensity. However, it is well known that the observatories of JMA are not placed in areas close each other, so the JMA intensity is very macroscopic. By the other hand, there are 2 facts of really concern following the 1995 Great Hanshin Earthquake. One is related with the unpublished boundaries of intensity by the JMA and the other is that the distribution of JMA intensity was not observed and estimated sufficiently to be treated numerically. By taking into account the above-mentioned situations, the ground intensity is evaluated herein by applying the methodology proposed by Ota et al.[2], in which the ground intensity is obtained as the result of questionnaires in order to grasp the distribution of ground intensity.

---

1)Professor, Department of Architecture & Civil Engineering, Kobe University, Rokkodai, Nada, Kobe 657, Japan

2)Graduate Student, Department of Science & Technology, Kobe University, ditto

2. ESTIMATION OF GROUND MOTION BY APPLYING A METHODOLOGY WHICH USES SHAPE INTERPOLATING FUNCTION

2.1 Methods

The method used in this paper to estimate seismic ground motions at arbitrary locations through the seismograph data observed at limited locations considers the shape interpolating function used in F.E.M. and B.E.M.[3]. This shape interpolation functions make the values given by a dispersive function to be treated as a continuous function. In F.E.M., the interpolation function is continue and is used to interpolate values between the nodes.

At first, lets consider that peak ground acceleration is observed at the four points of a square-shape area, the peak ground acceleration at any arbitrary point within this square-shape area is possible to be estimated by using both the Eq.2.1 and the shape interpolating function, which is expressed as follows:

$$A_{max}(\xi,\eta)=N_1(\xi,\eta)A_1+N_2(\xi,\eta)A_2 +N_3(\xi,\eta)A_3+N_4(\xi,\eta)A_4 \quad (2.1)$$

in which

$$N_1(\xi,\eta)=0.25(1-\xi)(1-\eta)$$
$$N_2(\xi,\eta)=0.25(1+\xi)(1-\eta)$$
$$N_3(\xi,\eta)=0.25(1+\xi)(1+\eta)$$
$$N_4(\xi,\eta)=0.25(1-\xi)(1+\eta).$$

Note: $A_i(i=1\text{-}4)$ is the peak ground acceleration at i-th observatory.

However, in practice the seismographs are not arranged at the four corners of a perfect square, but set up at the four corners of a quadrilateral. So it is necessary to modify the estimating equation for an arbitrary quadrangle shape.

For instance, lets consider an array of seismographs located at the corners of a square. On this way, we can estimate easily the peak ground acceleration at the point (x,y) by using Eq.2.2, if the correspondence of the point (x,y) in global coordinates to the point (ξ,η) in local coordinates exists. The relationship between global and local coordinates can be represented as follows:

$$x=\sum_{i=1}^{4}N_i(\xi,\eta)x_i, \quad y=\sum_{i=1}^{4}N_i(\xi,\eta)y_i \quad (2.2)$$

where x_i and y_i are x and y coordinates of i-th observatory, respectively.

On the same way, estimation can be done if the shape is either hexagonal or octagonal one. By considering the fact that the more the observation points, the better the accuracy of estimation, the octagonal shape is used in this research.

The observed acceleration value can be significantly affected by the difference of ground conditions such as soft ground and hard one. As shown in Fig.2.1, we firstly convert the observed value from surface to bedrock. Secondly, the peak ground acceleration is interpolated on bedrock and lastly the interpolated acceleration is converted from bedrock to surface. Thus, the peak ground accelerarion at ground surface can be obtained by multiplying the amplification factor c_G related with ground classification as follows:

$$A_{max}=\sum_{i=1}^{m}N_i(\xi,\eta)A_i\frac{c_G}{c_{Gi}} \quad (2.3)$$

where c_{Gi} is the amplification factor of the i-th observetory.

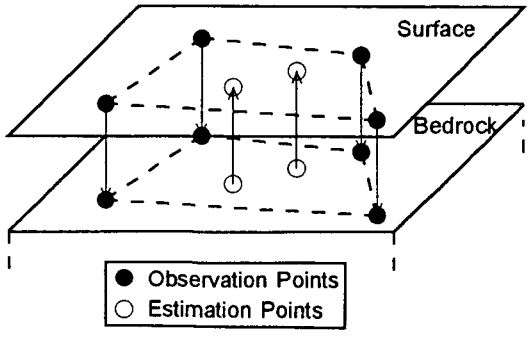


Fig.2.1 Concept of estimation of acceleration taking into account the spatial distribution.

Regarding to the procedure to determine the value of c_G, firstly we established 20 ground

classifications; secondly representative boring log of each classifications is extracted; thirdly, the ground model is made up based on the boring log and lastly we conduct nonlinear response analyses by using the made up model. We evaluate the value of c_G from the maximum acceleration of the input seismic wave and the response one. Fig.2.2 and Fig.2.3 show respectively the extracted boring logs and the relationship between the maximum acceleration of the input seismic wave and the response one.

2.2 Data

After the 1995 Great Hanshin Earthquake, owing to the cooperation of not only some universities and public agencies such as Kobe University and JMA but also to the cooperation of private companies such as *Osaka Gas* and *Kansai Electric Power Company*, we got many valuable ground motion data. We arranged east longitude, north latitude, peak ground accelerations and peak ground velocities of these databases which are obviously in terms of observed positons (east longitude and north latitude).

2.3 Results

2.3.1 Monitoring Network

At first, it was necessary to set up the monitoring network in order to estimate the distribution of ground acceleration. The monitoring network of the horizontal component is shown in Fig.2.4. Monitoring network is arranged for the whole Kobe area which is divided by 7 areas based on Geographcal Information System (hereafter GIS). We use the octagonal shape function in order to avoid the extrapolation and also to improve the accuracy of the estimation.

2.3.2 Results of Estimation

Fig.2.5 shows the distribution of horizontal acceleration estimated by applying the above-mentioned method. Each area is divided into the Cho-moku, the acceleration is presented by the representative value of the Cho-moku. In this figure the blank area is the area of which we have no data in GIS.

From Fig.2.5, in Kobe, Nishinomiya and Ashiya Cities where the earthquake damage was heavy, the estimated acceleration shows more than 600 Gals. In nearby places such as Itami and Takarazuka Cities the estimated acceleration is also large. It is typical that the distribution of large acceleration values has a L-type form. Compared with the distribution of intensity level 7 by JMA, areas such as Suma, Nagata, Chuo, Nada and Higashinada Ward have very large accelerations. In Tarumi Ward, although the estimated acceleration shows a large value, the distribution of the estimated acceleration shows a proper result.

The method used in this paper has the possibility to take into account the set up conditions of the monitoring network. For the case in which the number of observation points is small, the weight of an observation point will be high and the estimated result will be much influenced by the observed value. We set up a monitoring network a long time after the occurrence of the 1995 Great Hanshin Earthquake by using the observation points. Due to that, it took a long time to set up the monitoring network and calculate the (ξ,η) which is used in Eq.2.3, it prompt to the need to be prepared, it implies that the monitoring network should be arranged before the occurrence of an earthquake. If there is a point in which data cannot be obtained, we must set up the monitoring network again after earthquake. In order to grasp the damage information just after eathquake and to help making the reconstruction strategies, the estimation of ground motion needs to be conducted as soon as possible after earthquake. Thus, we should set up as many seismographs as possible in order to be able to arrange multiple networks and to evaluate quickly the seismic response in the unexpected situation.

2.4 Verification of Accuracy

In this section we verify the accuracy of

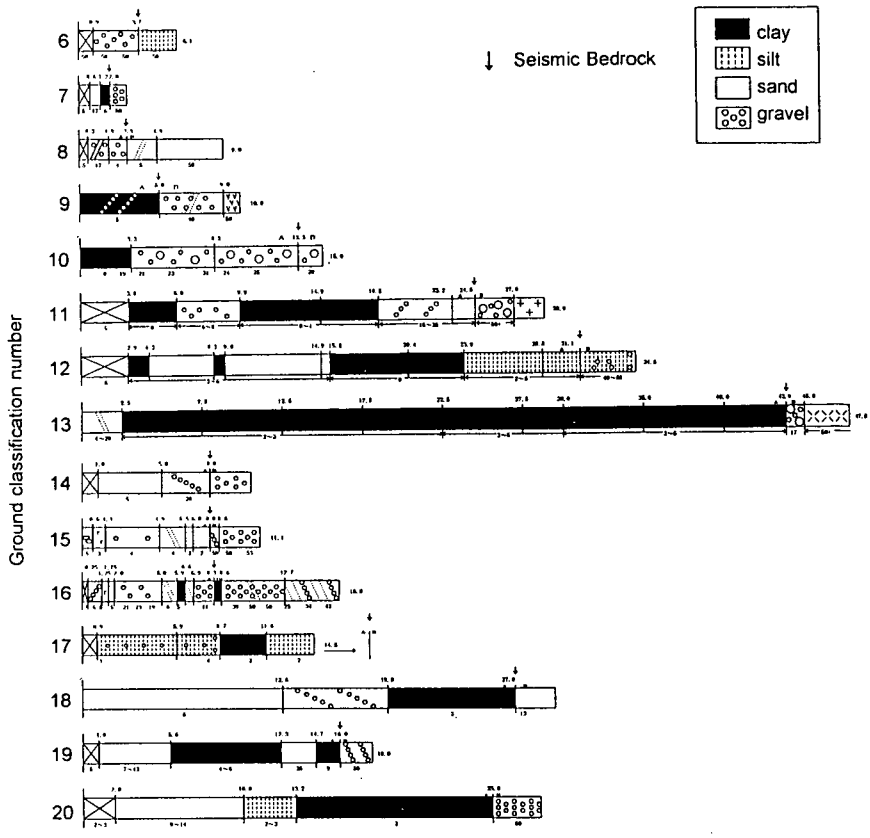


Fig.2.2 Extracted boring logs.

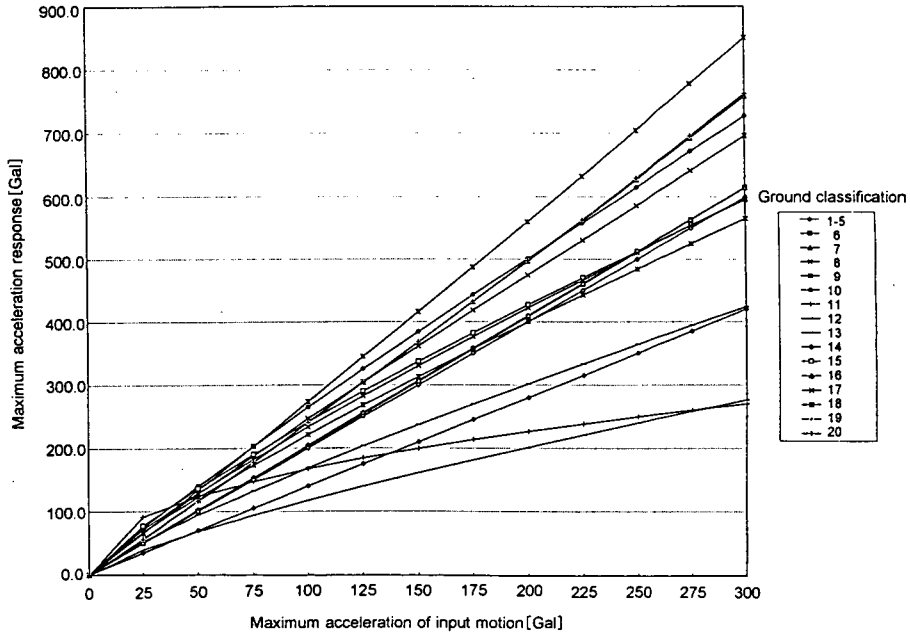


Fig.2.3 Relationship between the maximum acceleration of the input motions and the response.

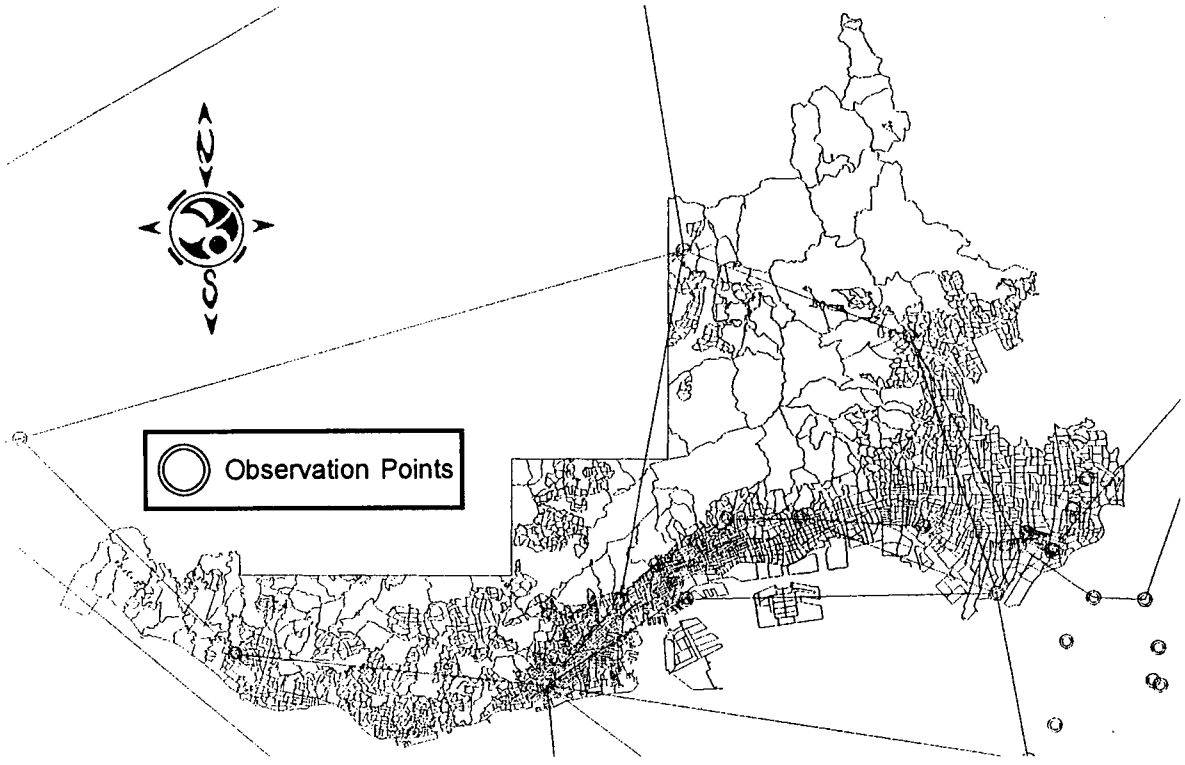


Fig.2.4 Monitoring network of the horizontal component.

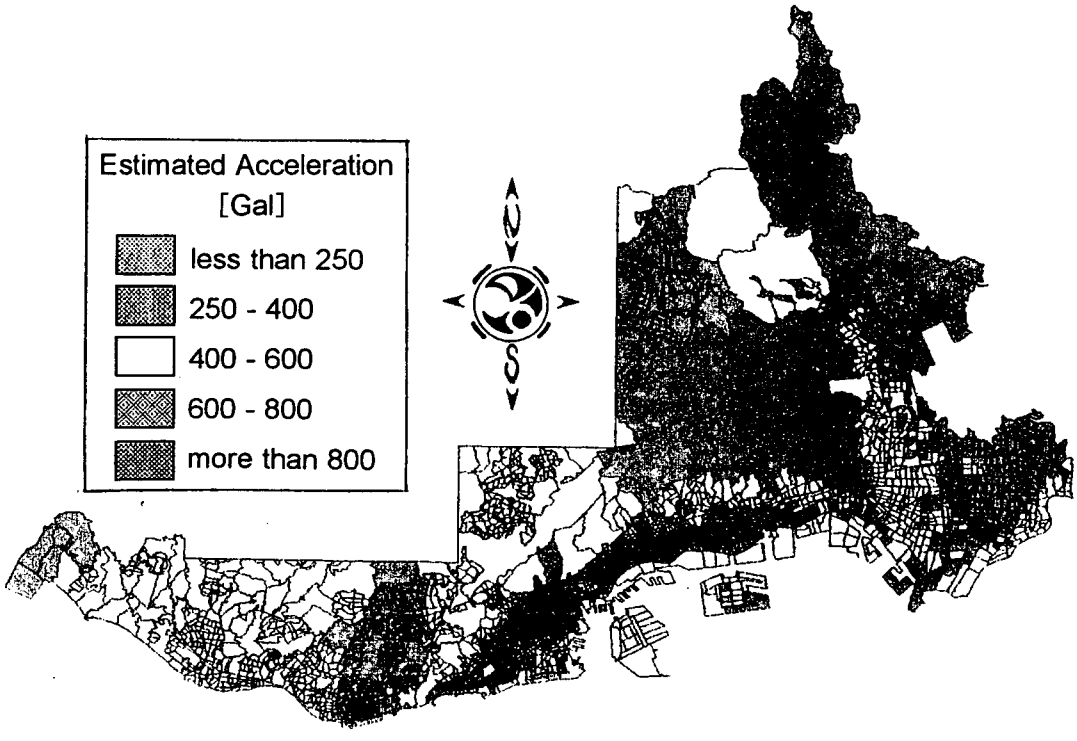


Fig.2.5 Distribution of the maximum acceleration in the horizontal component.

estimation by the shape interpolation method. For the horizontal component which has many records, some observation points are located inside the monitoring network on GIS. Thus, it is possible to estimate the acceleration at the observation points and compare them with the observed values. The result is shown in Fig.2.6.

As is shown in Fig.2.6, the estimated acceleration is coincident with the observed one except at one point. It is considered that the estimated acceleration at the point is much influenced by the low acceleration observed near there. So, if the number of observation points is small and a close-space network is not arranged such as in the case of the 1995 Great Hanshin Earthquake, the shape interpolation method cannot express the local site amplification. However, for the whole area struck by an earthquake, the shape interpolation method is possible to apply.

3. SEISMIC INTENSITY OBTAINED BY QUESTIONNAIRES

3.1 Methods

3.1.1 Distribution of Questionnaires

In order to grasp the detailed distribution of ground intensity obtained by questionnaires, it is necessary to distribute many questionnaires. By this way, thanks to the aid of the Board of Education and the principal committee in the objective area, we distributed the questionnaires directly to 189 public elementary schools and junior high schools. Fig.3.1 shows the distribution area of questionnaires.

The number of distributed questionnaires is more than 20000, and the collection ratio is more than 80%. Table 3.1 shows the collection

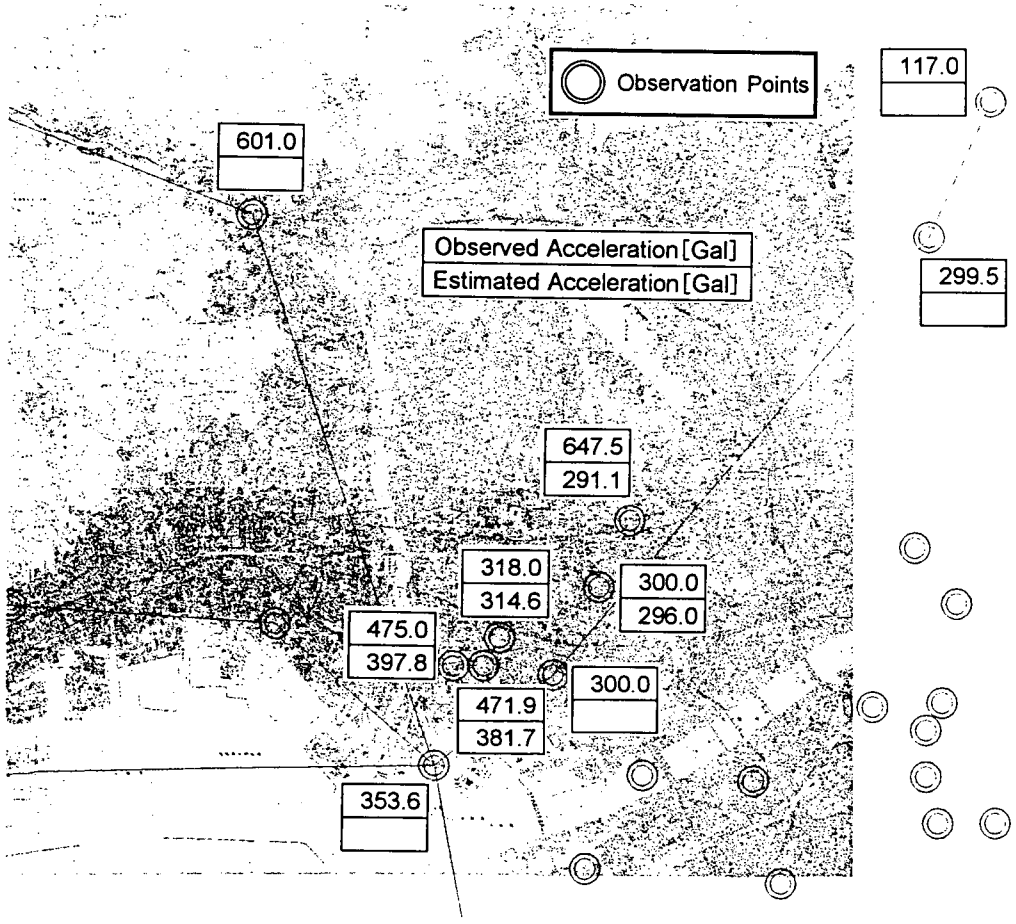


Fig.2.6 Comparison between the estimated acceleration with the observed one.

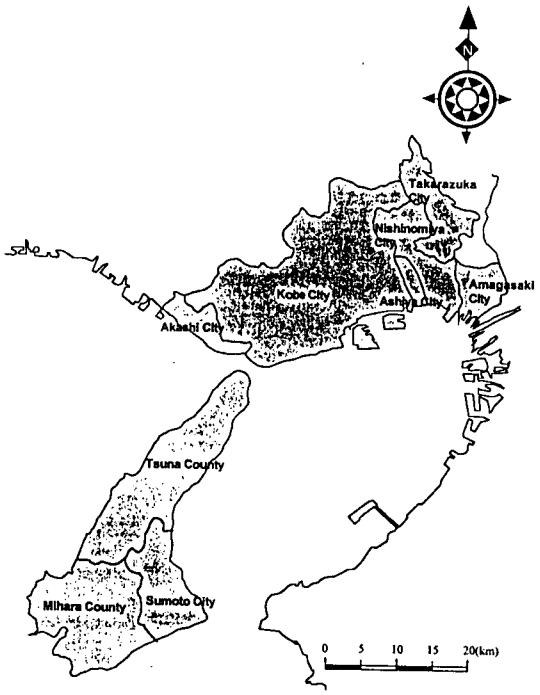


Fig.3.1 Distribution area of questionnaires.

Table 3.1 Collection ratio.

City or County	Number of Junior high school	Collection Ratio(%)	Number of Effective Answers
Takarazuka	12	81.4	1,097
Nishinomiya	11	83.8	1,072
Amagasaki	22	70.5	1,624
Ashiya	3	86.2	255
Itami	0	0	75
Kawanishi	0	0	18
Kobe	82	87.3	8,571
Akashi	12	82.5	1,283
Sumoto	5	90	538
Tsuna	6	90	1,364
Mihara	7	90	500
Subtotal	160		16,397
	Number of Elementary School		
Tsuna	29	90	2,549
Total	189		18,946

ratio and the number of effective answers. The collection ratio is the ratio between the collected questionnaires and the distributed questionnaires, and the "effective" means that the address at the 1995 Great Hanshin Earthquake of the person who answered the questionnaire is able to be specified. Further, the collection ratio in Awaji Island is an estimate, because we could not grasp the exact number of distributed questionnaires.

3.1.2 Evaluation of Ground Intensity

In this paper, the method for evaluation of ground intensity is as follows. The ground intensity is established in order that it can be read from a low level to a high one varying proportionally the selected number for the questioned item becomes greater. As the ground intensity obtained by questionnaires is based on the JMA intensity, the category number has a number from one to seven for each item. But the ground intensity obtained by questionnaires is created for earthquake levels less than 6 in JMA intensity. It implies that the intensity level 7 of JMA is not presented sufficiently.

Two concepts are introduced in the ground intensity obtained by questionnaires, one is a condition factor that takes into account that people who answered the questionnaire are not necessarily under the same situation, and the other is an intensity factor to quantify the answer for the sensuous response. The former is related with the location details of the answering person and accounts the difference in the kind, the floor number and the age of the house where the answering person was during earthquake. It is presented mostly respect to a wooden house of one story. The latter is the factor that presents the relation between each items. The item which answer the seismic response of houses is the basic item. If the frequency distribution of the answer for the i-th item is similar to the one for the basic item, the category number of the i-th item corresponds to the one of the basic item. Thus, the intensity factor is presented by the relative amount to the basic item and is computed statistically based on some earthquakes. The intensity factor I for each answering person based on the questionnaire is presented as follows:

$$I=\frac{\alpha}{N_e}\cdot\sum_{i}^{N_e} m_i\cdot\beta \tag{3.1}$$

where α, m_i and N_e are the condition factor,

the category number for the i-th item and the number of effective answers in the item concerning to the ground intensity obtained by questionnaires respectively. β is the intensity factor for m_i. The summation is conducted about only effective answers. The ground intensity obtained by questionnaires I_Q is calculated by converting the intensity factor given to each person by Eq.3.1 into effective double digits of the JMA intensity. The conversion equation is expressed as follows:

$$I_Q=2.958\cdot(I-1.456)^{0.547} \qquad (3.2).$$

3.2 Results

3.2.1 Preliminary Investigation

As above-mentioned the ground intensity proposed by Ota et al. is established for earthquakes of intensity levels less than 6 in the JMA intensity. Respect to the 1995 Great Hanshin Earthquake, it is possible to state that damage was severe and it was the first time that level 6 of the JMA intensity was surpassed. In order to verify the application to this earthquake, we conducted a preliminary investigation sixth months after the earthquake (July '95) with students of our laboratory. The number of answering persons was 30.

The student's locations at the time the earthquake occurred were Kobe, Ashiya, Nishinomiya, Kakogawa, Sakai and Osaka City. Table 3.2 shows the total amount. The average of intensity factor is 4.843 and the standard deviation is 0.789. As shown in this table, the intensity factor is very high in seriously damaged areas and it becomes lower according the epicentral distance is long. Thus, the evaluation of ground intensity by questionnaires for the 1995 Great Hanshin Earthquake is considered to be appropriated.

3.2.2 Distribution Characteristics

Fig.3.2 and Fig.3.3 show the distribution of

Table 3.2 Total amount of preliminary investigation.

No.	City	Ward	Town	Cho-moku	Seismic Intensity Factor	Seismic Intenisty obtained from Questionnaires	JMA Intensity
1	Kobe	Higashinada	Motoyamanaka	3	5.694	6.5	7
2	Kobe	Higashinada	Mikage	Nishihirano	5.565	6.4	7
3	Kobe	Higashinada	Sumiyoshiyamate	7	4.330	5.3	6
4	Kobe	Higashinada	Uozakikita	1	5.229	6.1	7
5	Kobe	Nada	Shinoharakita	3	4.255	5.2	6
6	Kobe	Nada	Nadakita	6	6.219	7.0	7
7	Kobe	Nada	Rokkodai	1	4.313	5.3	6
8	Kobe	Nada	Jouchi	4	5.258	6.1	7
9	Kobe	Nada	Takaha	5	4.651	5.6	6
10	Kobe	Nada	Shinoharaminami	3	5.859	6.7	7
11	Kobe	Nada	Shinoharadai		4.388	5.3	6
12	Kobe	Nada	Shinoharanaka	5	4.750	5.7	7
13	Kobe	Nada	Yuminogi	2	5.020	5.9	7
14	Kobe	Nada	Ichinosan		4.347	5.3	6
15	Kobe	Nada	Yahata	1	4.760	5.7	7
16	Kobe	Nada	Biwa	1	5.587	6.4	7
17	Kobe	Nada	Yuminogi	2	5.040	5.9	7
18	Kobe	Chuo	Kitamotomachi	4	4.346	5.3	6
19	Kobe	Suma	Yokoo	9	3.687	4.6	6
20	Kobe	Nishi	Ikawadani	Junwa	4.815	5.7	6
21	Kobe	Nishi	Ikawadani	Arise	4.711	5.6	6
22	Kobe	Kita	Seiwadai	2	4.348	5.3	6
23	Ashiya		Kasuga	No.13	5.505	6.4	7
24	Nishinomiya		Nakamaeda	7	5.818	6.6	7
25	Nishinomiya		Koshien	5th Street	4.922	5.8	6
26	Nishinomiya		Takasu	1	4.798	5.7	6
27	Osaka	Minato	Yahataya	1	4.460	5.4	4
28	Osaka	Yodogawa	Higashimikuni	6	4.013	4.9	4
29	Sakai		Nonoi	No.735	4.404	5.3	unknown
30	Kakogawa		Yoneda	Hiratsu	4.187	5.1	unknown

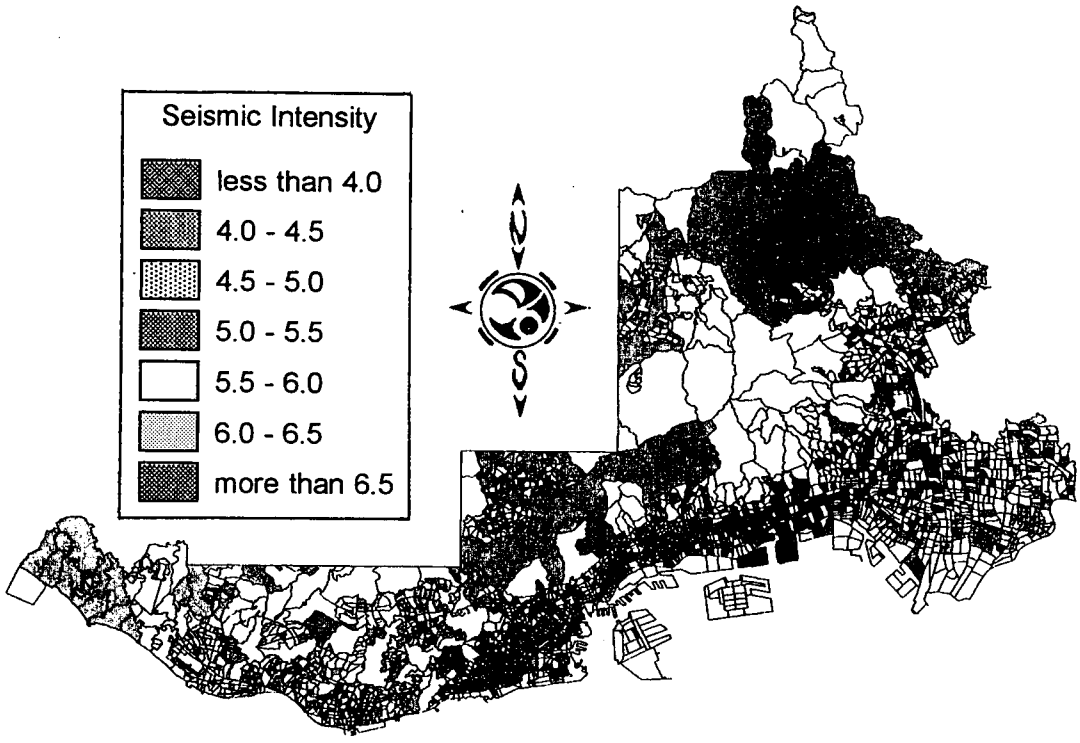


Fig.3.2 Distribution of seismic intensity obtained by questionnaires for each Cho-moku.

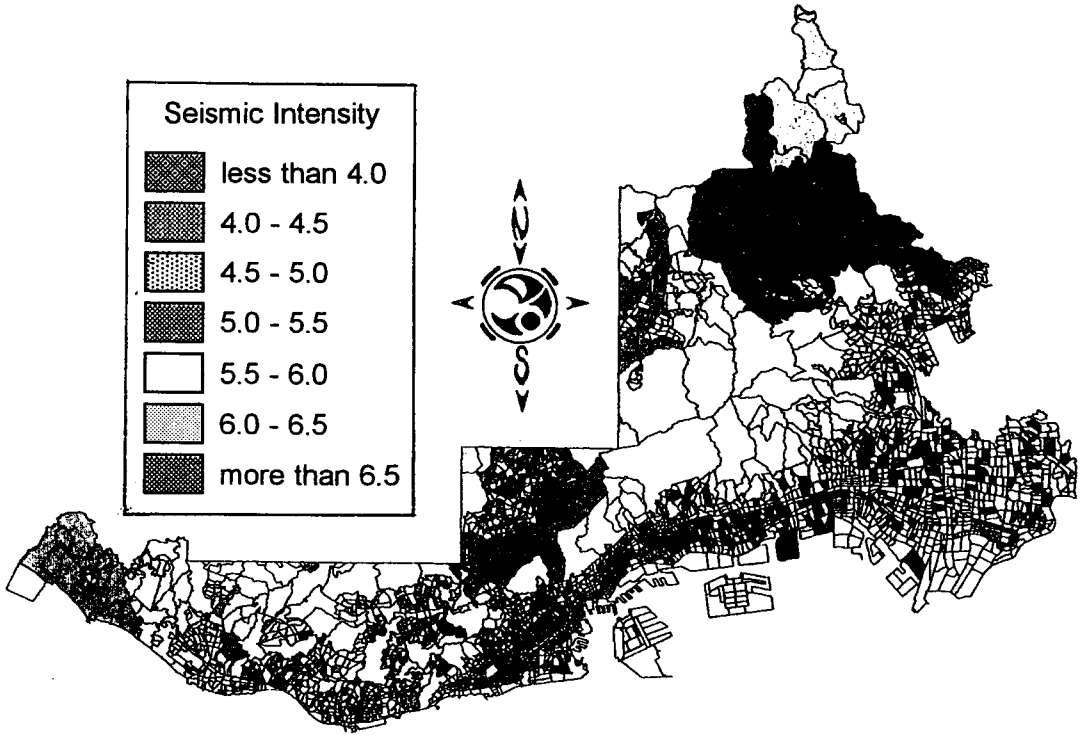


Fig.3.3 Distribution of seismic intensity obtained by questionnaires for each Cho-Cho-moku.

the seismic intensity obtained by questionnaires calculated for each Cho-moku and for each Cho-Cho-moku which has at least three answering persons, except for Awaji Island, north of Kita Ward, and Nishi Ward. The distribution shown in Fig.3.2 corresponds to that of intensity level 7 by JMA. The method considered herein is suspected to be applicable for earthquakes in which the intensity is more than the level 6 of JMA. It means that a detailed study may be possible.

Regarding to the JMA intensity, at south-east areas of Kobe, south area of Nishinomiya, Ashiya and a part of Takarazuka City, the level is 7. The intensity level in other areas was 6. Respect to the seismic intensity obtained by questionnaires, at north areas of Takarazuka City, south-east area of Kita Ward, Suma Ward, north of Tarumi Ward in Kobe City the intensity is lower in the level 5, while for at the north of Mt. Rokko and south-east areas of Akashi City the intensity is higher in the level 5. The distribution of level 7 and higher level 6 is in harmony with distribution of level 7 of JMA intensity except in the south-east area of Akashi City in which the intensity is large part of level 6. Taking into account that ground intensity is constant and the attenuation of distance is negligible within 5 km from the fault, the structural damage in Akashi City is different between the east and west areas. Thus, it is possible to say that the seismic intensity was greatly affected by local conditions in this area.

Fig.3.4 shows the cumulative relative frequency distribution of the seismic intensity obtained by questionnaires at the area where the JMA intensity level is 6 and 7. As shown in Fig.3.4, the boundary intensity between the level 6 and 7 by JMA corresponds to level 6.0 of those obtained by questionnaires.

By the other hand, Fig.3.5 shows the relationship between the fault distance and the seismic intensity obtained by questionnaires. The equation of regression is given by the method of least squares, and is expressed as follows:

$$I_Q = -0.05 \cdot d + 6.02 \qquad (3.3)$$

where I_Q is the seismic intensity obtained by questionnaires and d (km) is the fault distance. The objective faults are Nojima, Suwayama and Ashiya fault. As the seismic intensity by questionnaires is computed for every Cho-moku, the fault distance is calculated as the shortest distance between the fault and the center of gravity of the Cho-moku. According to Eq.3.3, if the distance is longer than about 90 km respect to the above-mentioned faults, the seismic intensity obtained by questionnaires becomes less than 1.4.

As was also aforementioned, the seismic intensity proposed by Ota et al., in which a weight is put on each item for the sensuous response of the answering person, the intensity factor is computed by linear summation of the

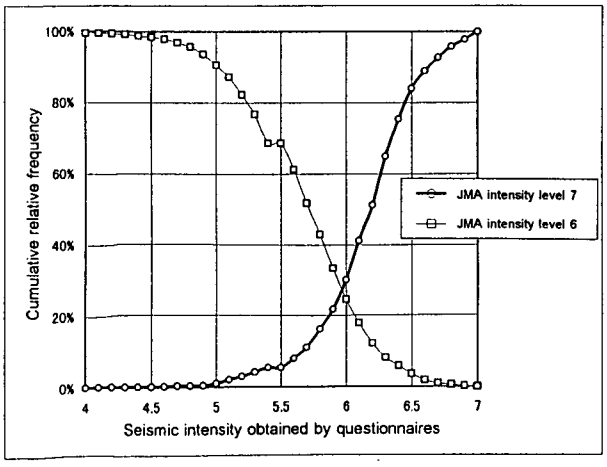


Fig.3.4 Cumulative relative frequency distribution of the seismic intensity obtained by questionnaires.

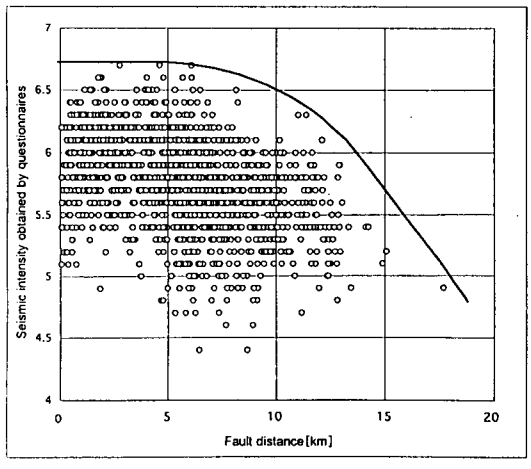


Fig.3.5 Relationship between the fault distance and the seismic intensity obtained by questionnaires.

weight and is converted into the JMA intensity by the equation based on past earthquakes. And in parallel form, the seismic intensity obtained by questionnaires is also calculated. The conversion equation is regressed by 32 data sets, but due to these data sets under level 5 of JMA intensity, the equation is inadequate to be applied to the 1995 Great Hanshin Earthquake. For this purpose, we propose a new conversion equation by using the data of the 1995 Great Hanshin Earthquake for future research. Fig.3.6 shows the relationship between the intensity factor and the JMA intensity, on this way the new conversion equation is as follows:

$$I_Q=2.334\cdot L_n(I)+2.538 \qquad (3.4).$$

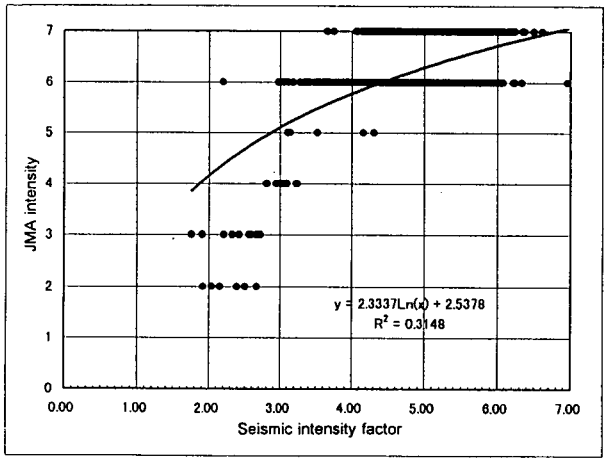


Fig.3.6 Relationship between the JMA intensity and the seismic intensity factor.

By this way, we estimated the relationship by applying the expression proposed by Midorikawa et al.[5]. Fig.3.7 shows the relationship between the seismic intensity obtained by questionnaires with the overturning rate of tombstones, the regression equation is as follows:

$$Y=5.7963\cdot L_n(I_Q)-9.6795 \qquad (3.5).$$

Since both the objective area is concentrated to high level intensity areas and the data of low level is few, the equation which calculate the seismic intensity obtained by questionnaires gives a little high values. In the future, it would be necessary to accumulate the data and to apply the convenient regression equation.

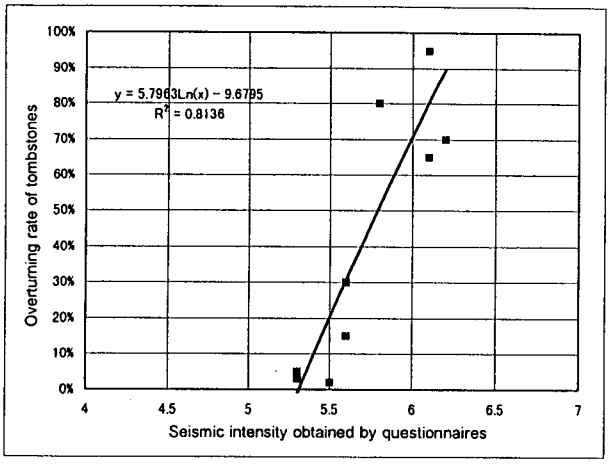


Fig.3.7 Relationship between the seismic intensity obtained by questionnaires and the overturning rate of tombstones.

3.3 Discussion

3.3.1 Relationship to the Overturning Rate of Tombstones

There is a convenient method for evaluation of the seismic intensity which is based on the overturning rate of tombstones[4]. For the grasp of the distribution of the seismic intensity obtained by questionnaires it is necessary to distribute questionnaires as many as possible and also to conducte it before people forget the sensuous response. Thus, in order to measure the seismic intensity in a simple form, it is useful to express the relationship between the seismic intensity obtained by questionnaires to the overturning rate of tombstones.

3.3.2 Relation to Records of Peak Ground Motion

Next, we examine the relationship between records by seismographs and the seismic intensity obtained by questionnaires. Fig.3.8 and Fig.3.9 show relationships for the peak ground acceleration (hereafter PGA[Gal]) and peak ground velocity (hereafter PGV[Kine]) respectively. This PGA data is the observed value. This PGV data is computed by integration of the time history of the acceleration in which a part corresponds to the observed value. As shown in Fig.3.9, the PGV of the 8th pier of Kobe port is very large compared with the

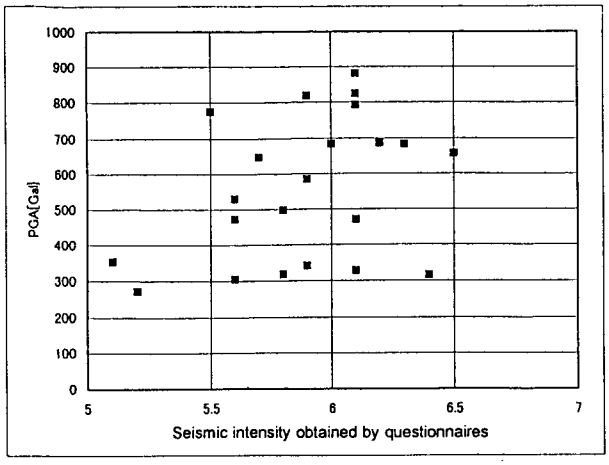


Fig.3.8 Relationship between the PGA and the seismic intensity obtained by questionnaires.

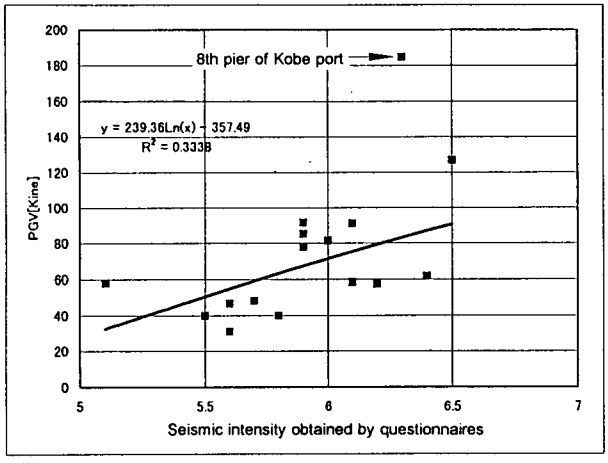


Fig.3.9 Relationship between the PGV and the seismic intensity obtained by questionnaires.

seismic intensity obtained by questionnaires. On this way, it is possible to consider that recorded seismic waves have long periods due to nonlinearities of the ground at the 8th pier of Kobe port. These figures also show that the PGV has more relation to the seismic intensity obtained by questionnaires than the PGA. The reason is that the seismic intenisty obtained by questionnaires is calculated by a medium which is the housings. Further the damage ratio of houses is more related to the PGV than the PGA. The regression equation by the method of least squares permits to relate the PGV and the seismic intensity obtained by questionnaires, which is as follows:

$$PGV=239.36 \cdot L_n(I_Q)-357.49 \qquad (3.6).$$

The regression of data corresponding to the 8th pier of the Kobe port was excluded.

4. CONCLUSIONS

We have estimated the distribution of peak ground acceleration in wide range areas by applying the observed data. The distribution of the estimated acceleration more than 600 Gals is coincident with the distribution of the heavy damaged areas. Further compared with the distribution of the level 7 of JMA intensity, an appropiated result was obtained. Also we have verified the accuracy of the estimation, as result the shape interpolation method is considered to be possible to be applied even if the local site amplification is not given.

Next, we have distributed questionnaires densely and calculated the seismic intensity by the collected questionnaires. As result, the distribution of the high level of seismic intensity obtained by the questionnaires corresponds to the distribution of the level 7 of the JMA intensity.

Also, we estimated the relationship to the ratio of the fallen tombstones and the peak ground motions and proposed the regression equations which express the relationship with the seismic intensity obtained by the questionnaires.

REFERENCES

[1]Takada, S., Takatani, T. Ogawa, Y. & Fukui, S. : An Estimating Method of Seismic Ground Motions for Monitoring System. Journal of Structural Engineering, 1994, Vol.40A, 1151-1160

[2]Ota, H., Goto, N. & Ohashi, H. : A Questionnaire Survey for Estimating Seismic Intensities. Bulletin of the Faculty of Engineering, Hokkaido University, 1979, No.92, 117-129

[3]Washizu, H., Miyamoto, H., Yamada, Y., Yamamoto, Y. & Kawai, T. : Handbook of Finite Element Method I, Baifukan, 1981

[4]Omori, F. : Investigation on the Nobi

Earthquake, Oct. 28 1891. Report by Survey Bureau for Earthquake Disaster Prevention, 1899, Vol.28, 79-95
[5]Midorikawa, S. & Fujisawa, K. : Isoseismal Map of the Hyogo-Ken Nanbu Earthquake In and Around Kobe City Estimated from Overturing of Tombstones. J. Struct. Constr. Eng., AIJ, 1996, No.490, 111-118

THE 1996 SEISMIC DESIGN SPECIFICATIONS OF HIGHWAY BRIDGES

by

Kazuhiko KAWASHIMA[1], Masanori NAKANO[2], Kazuhiro NISHIKAWA[3], Jiro FUKUI[4], Keiichi TAMURA[5] and Shigeki UNJOH[6]

ABSTRACT

This paper presents the revised Seismic Design Specifications of Highway Bridges in 1996 as well as the background of the revision. Damage features of bridges in the 1995 Hyogo-ken nanbu Earthquake is firstly described with emphasis on the lessons learned from the earthquake. Seismic performance levels and design methods as well as the seismic design force introduced in the 1996 Design Specifications are then described. The ductility design methods for reinforced concrete piers, steel piers, foundations, and bearings are also briefly described.

KEY WORDS : Seismic Design
Highway Bridges
Design Codes
Hyogo-ken nanbu Earthquake
Ductility Design Method

1. INTRODUCTION

Highway bridges in Japan had been considered safe even against extreme earthquake such as the Great Kanto Earthquake (M7.9) in 1923, because various past bitter experiences have been accumulated to formulate the seismic design method (Kawashima (1995)). Large seismic lateral force ranging from 0.2g to 0.3g has been adopted in the allowable stress design approach. Various provisions for preventing damage due to instability of soils such as soil liquefaction have been adopted. Furthermore, design detailings including the unseating prevention devices have been implemented.

In fact, reflecting those provisions, number of highway bridges which suffered complete collapse of superstructures was only 15 since 1923 Great Kanto Earthquake. Based on such evidence, it had been regarded that the seismic damage of highway bridges had been decreasing in recent years.

However, the Hyogo-ken nanbu Earthquake of January 17, 1995, exactly one year after the Northridge, California, USA, earthquake, caused destructive damage to highway bridges. Collapse and nearly collapse of superstructures occurred at 9 sites, and other destructive damage occurred at 16 sites (Ministry of Construction, 1995a). The earthquake revealed that there are a number of critical issues to be revised in the seismic design and seismic strengthening of bridges in urban areas.

After the earthquake the "Committee for Investigation on the Damage of Highway Bridges Caused by the Hyogo-ken nanbu Earthquake" (chairman : Toshio IWASAKI, Executive Director, Civil Engineering Research Laboratory) was formulated in the Ministry of Construction to survey the damage and clarify the factors which contributed to the damage.

1) Professor, Department of Civil Engineering, Tokyo Institute of Technology, O-okayama, Meguro-ku, Tokyo, 152, Japan
2) Deputy Director, Research and Information Division, Economic Affairs Bureau, Ministry of Construction, Kasumigaseki, Chiyoda-ku, Tokyo, 100, Japan
3) Head, Bridge Division, Bridge and Structure Department, Public Works Research Institute, Ministry of Construction, Tsukuba-shi, Ibaraki-ken, 305, Japan
4) Head, Foundation Division, Bridge and Structure Department, ditto
5) Head, Ground Vibration Division, Earthquake Disaster Prevention Research Center, ditto
6) Head, Earthquake Engineering Division, Earthquake Disaster Prevention Research Center, ditto

On February 27, 1995, the Committee approved the "Guide Specifications for Reconstruction and Repair of Highway Bridges which suffered Damage due to the Hyogo-ken nanbe Earthquake," (Ministry of Construction 1995b) and the Ministry of Construction noticed on the same day that the reconstruction and repair of the highway bridges which suffered damage in the Hyogo-ken nanbu earthquake should be made by the Guide Specifications. It was decided by the Ministry of Construction on May 25, 1995 that the Guide Specifications should be tentatively used in all sections of Japan as emergency measures for seismic design of new highway bridges and seismic strengthening of existing highway bridges until the Design Specifications of Highway Bridges was revised.

In May, 1995, the "Special Sub-Committee for Seismic Countermeasures for Highway Bridges" (chairman : Kazuhiko KAWASHIMA, Professor of the Tokyo Institute of Technology) was formulated in the "Bridge Committee" (chairman : Nobuyuki NARITA, Professor of the Tokyo Metropolitan University), Japan Road Association, to draft the revision of the Design Specifications of Highway Bridges. The Special Sub-Committee drafted the new Design Specifications of Highway Bridges, and after the approval of the Bridges Committee, the Ministry of Construction released it November 1, 1996.

This paper summarizes the damage feature of highway bridges by the Hyogo-ken Nanbu earthquake and the new Design Specifications of Highway Bridges issued in November 1996.

2. DAMAGE FEATURES OF BRIDGES IN THE HYOGO-KEN NANBU EARTHQUAKE

Hyogo-ken Nanbu earthquake was the first earthquake which hit an urban area in Japan since the 1948 Fukui Earthquake. Although the magnitude of the earthquake was moderate (M7.2), the ground motion was much larger than anticipated in the codes. It occurred very close to the Kobe City with shallow focal depth.

Damage was developed at highway bridges on Routes 2, 43, 171 and 176 of the National Highway, Route 3 (Kobe Line) and Route 5 (Bay Shore Line) of the Hanshin Expressway, the Meishin and Chugoku Expressway. Damage was surveyed for all bridges on National Highways, Hanshin Expressways and Expressways in the area where destructive damage occurred. Total number of piers surveyed reached 3,396 (Ministry of Construction, 1995a). **Fig.1** shows Design Specifications referred to in design of the 3,396 piers. Most of piers (bridges) which suffered damage were designed according to the 1964 Design Specifications or older Design Specifications. Although the seismic design methods have been improved and amended several times since 1926 based on damage experience and progress of bridge earthquake engineering, only a requirement for lateral force coefficient was provided in the 1964 Design Specifications or older Specifications.

Fig.2 compares damage of piers on the Route 3 (Kobe Line) and Route 5 (Bay Shore Line) of the Hanshin Expressway. Damage degree was classified as As (collapse), A (nearly collapse), B (moderate damage), C (damage of secondary members) and D (minor or no damage). Substructures of the Route 3 and Route 5 were designed with the 1964 Design Specifications and 1980 Design Specifications, respectively. It should be noted in this comparison that the intensity of ground shaking in terms of response spectra was smaller at the Bay Area than the narrow rectangular area where JMA Seismic Intensity was VII (equivalent to Modified Mercalli Intensity of X-XI). The Route 3 was located in the narrow rectangular area while the Route 5 was located in the Bay Area. Keeping in mind such difference of ground motion, it is apparent in **Fig.2** that

about 14% of the piers on Route 3 suffered As or A damage while no such damage was developed in the piers on the Route 5.

Although damage concentrated on the bridges designed with the older Design Specifications, it was thought that essential revision was required even in the recent Design Specifications to prevent damage against destructive earthquakes such as the Hyogo-ken nanbu earthquake. The main points requiring modifications were;

(1) it was required to increase lateral capacity and ductility of all structural components in which seismic force is predominant so that ductility of a total bridge system be enhanced. For such purpose, it was required to upgrade the "Check of Ductility of Reinforced Concrete Piers," which has been used since 1990, to a "Ductility Design Method," and to apply the Ductility Design Method to all structural components. It should be noted here that "check" and "design" is different; the check is only to verify the safety of a structural member designed by other design method, and is effective only to increase the size or reinforcements if required, while the design is an essential procedure to determine the size and reinforcements,

(2) it was required to include the ground motion developed at Kobe in the earthquake as a design force in the Ductility Design Method,

(3) it was required to specify input ground motions in terms of acceleration response spectra for dynamic response analysis more actively,

(4) it was required to increase tie reinforcements and to introduce intermediate ties for increasing ductility of piers. It was decided not to terminate main reinforcements at mid-height for preventing premature shear failure, in principle,

(5) it was suggested to adopt multi-span continuous bridge for increasing number of indeterminate of a total bridge system,

(6) it was suggested to adopt rubber bearings for absorbing lateral displacement between a superstructure and substructures. It was important to consider correct mechanism of force transfer from a superstructure to substructures,

(7) it was suggested to include the Menshin design (seismic isolation),

(8) it was required to increase strength, ductility and energy dissipation capacity of unseating prevention devices, and

(9) it was required to consider the effect of lateral spreading associated with soil liquefaction in design of foundations at the site vulnerable to lateral spreading.

3. BASIC PRINCIPLE OF SEISMIC DESIGN

Table 1 shows the seismic performance level provided in the revised Design Specifications in 1996. The bridges are categorized into two groups depending on their importance; standard bridges (Type-A bridges) and important bridges (Type-B bridges). Seismic performance level depends on the importance of bridges. For moderate ground motions induced in the earthquakes with high probability to occur, both A and B bridges should behave in an elastic manner without essential structural damage. For extreme ground motions induced in the earthquakes with low probability to occur, the Type-A bridges should prevent critical failure, while the Type-B bridges should perform with limited damage .

In the Ductility Design Method, two types of ground motions must be considered. The first is the ground motions which could be induced in the plate boundary-type earthquakes with magnitude of about 8. The ground motion at Tokyo in the 1923 Kanto Earthquake is a typical target of this type of ground motion. The second is the ground motion developed in earthquakes with magnitude of about 7-7.2 at very short distance. Obviously the ground motions at Kobe in the Hyogo-ken nanbu earthquake is a typical target of this type of

ground motion. The first and the second ground motions are called as Type-I and Type-II ground motions, respectively. The recurrence time of the Type-II ground motion may be longer than that of the Type-I ground motion, although the estimation is very difficult.

4. DESIGN METHODS

Bridges are designed by both the Seismic Coefficient Method and the Ductility Design Method as shown in **Fig.3**. In the Seismic Coefficient Method, a lateral force coefficient ranging from 0.2 to 0.3 has been used based on the allowable stress design approach. No change was introduced since the 1990 Specifications in the Seismic Coefficient Method.

In the Ductility Design Method, assuming a principle plastic hinge formed at the bottom of pier as shown in **Fig.4(a)** and the equal energy assumption, a bridge is designed so that the following requirement is satisfied.

$$P_a > k_{he} W \quad (1)$$

where

$$k_{he} = \frac{k_{hc}}{\sqrt{2\mu_a - 1}} \quad (2)$$

$$W = W_U + c_P W_P \quad (3)$$

in which, P_a = lateral capacity of a pier, k_{he} = equivalent lateral force coefficient, W = equivalent weight, k_{hc} = lateral force coefficient, μ_a = allowable displacement ductility factor of a pier, W_U = weight of a part of superstructure supported by the pier, W_P = weight of a pier, and c_P = coefficient depending on the type of failure mode. The c_P is 0.5 for a pier in which either flexural failure or shear failure after flexural cracks are developed, and 1.0 for a pier in which shear failure is developed. The lateral capacity of a pier P_a is defined as a lateral force at the gravity center of a superstructure.

In the Type-B bridges, residual displacement developed at a pier after an earthquake must be checked as

$$\delta_R < \delta_{Ra} \quad (4)$$

where

$$\delta_R = c_R(\mu_R - 1)(1-r)\delta_y \quad (5)$$

$$\mu_R = 1/2\{(k_{hc} \cdot W/P_a)^2 + 1\} \quad (6)$$

in which δ_R = residual displacement of a pier after an earthquake, δ_{Ra} = allowable residual displacement of a pier, r = bilinear factor defined as a ratio between the first stiffness (yield stiffness) and the second stiffness (post-yield stiffness) of a pier, c_R = factor depending on the bilinear factor r, μ_R = response ductility factor of a pier, and δ_y = yield displacement of a pier. The δ_{Ra} should be 1/100 of a distance between the bottom of a pier and a gravity center of a superstructure.

In a bridge with complex dynamic response, the dynamic response analysis is required to check the safety of a bridge after it is designed by the Seismic Coefficient Method and the Ductility Design Method. Because this is only for a check of the design, the size and reinforcements of structural members once determined by the Seismic Coefficient Method and the Ductility Design Methods can only be increased if necessary. It should be noted however that under the following conditions in which the Ductility Design Method is not directly applied, the size and reinforcements can be determined based on the results f a dynamic response analysis as shown in **Fig.3**. The conditions when the Ductility Design Method should not be directly used include:

(1) principle mode shapes which contribute to bridge response are different from the ones assumed in the Ductility Design Methods,

(2) more than two modes significantly contribute to bridge response,

(3) principle plastic hinges form at more than two locations, or principle plastic hinges are not known where to be formed, and

(4) response modes for which the equal energy assumption are not applied.

In the seismic design of a foundation, a lateral force equivalent to the ultimate lateral capacity

of a pier P_u is assumed to be a design force as

$$k_{hp} = c_{df} P_u / W \quad (7)$$

in which k_{hp} = lateral force coefficient for a foundation, c_{df} = modification coefficient (=1.1), and W = equivalent weight by Eq.(3). Because the lateral capacity of a wall-type pier is very large in transverse direction, the lateral seismic force evaluated by Eq.(7) becomes in most cases excessive. Therefore if a foundation has sufficiently large lateral capacity compared with the lateral seismic force, the foundation is designed assuming a plastic hinge at the foundation and surrounding soils as shown in **Fig.4(c)**.

5. DESIGN SEISMIC FORCE

Lateral force coefficient k_{hc} in Eq.(2) is given as

$$k_{hc} = c_z \cdot k_{hc0} \quad (8)$$

in which c_z = modification coefficient for zone, and is 0.7, 0.85 and 1.0 depending on zone, and k_{hc0} = standard modification coefficient. **Table 2** and **Fig.5** show the standard lateral force coefficients k_{hc0} for the Type-I and the Type-II ground motions. The Type-I ground motions have been used since 1990 (1990 Specifications), while the Type-II ground motions were newly introduced in the 1996 Specifications. It should be noted here that the k_{hc0} at stiff site (Group I) has been assumed smaller than the k_{hc0} at moderate (Group II) and soft soil (Group III) sites in the Type-I ground motions as well as the seismic coefficients used for the Seismic Coefficient Method. The Type-I ground motions were essentially estimated from an attenuation equation for response spectra that was derived from a statistical analysis of 394 components of strong motion records. Although the response spectral accelerations at short natural period are larger at stiff sites than at soft soil sites, the tendency has not been explicitly included in the past. This was because damage has been more developed at soft sites than at stiff sites. To consider such fact, the design force at stiff sites has been assumed smaller than that at soft sites even at short natural period. However being different from such a traditional consideration, the Type-II ground motions were determined by simply taking envelops of response accelerations of major strong motions recorded at Kobe in the Hyogo-ken nanbu Earthquake. It was considered appropriate to set realistic ground motions.

Although the acceleration response spectral intensity at short natural period is higher in the Type-II ground motions than in the Type-I ground motions, the duration of extreme accelerations excursion is longer in the Type-I ground motions than the Type-II ground motions. As will be described later, such a difference of the duration has been taken into account to evaluate the allowable displacement ductility factor of a pier.

6. EVALUATION OF DISPLACEMENT DUCTILITY FACTOR OF A REINFORCED CONCRETE PIER

(1) Evaluation of Failure Mode

In the ductility design of reinforced concrete piers, the failure mode of the pier is evaluated as the first step. Failure modes is categorized to 3 types based on the bending capacity and shear capacity of the pier as

1) $P_u \leqq P_s$: bending failure
2) $P_s < P_u \leqq P_{s0}$: bending to shear failure
3) $P_{s0} < P_u$: shear failure

in which P_u = bending capacity, P_s = shear capacity in consideration of the effect of cyclic loading, and P_{s0} = shear capacity without consideration of the effect of cyclic loading.

The ductility factor and capacity of the reinforced concrete piers are determined according to the failure mode as described later.

(2) Displacement Ductility Factor

Th allowable displacement ductility factor of a pier μ_a in Eq.(2) is evaluated as

$$\mu_a = 1 + \frac{\delta_u - \delta_y}{\alpha \delta_y} \quad (9)$$

in which α = safety factor, δ_y = yield displacement of a pier, and δ_u = ultimate displacement of a pier. As well as the lateral capacity of a pier P_a in Eq.(1), the δ_y and δ_u are defined at the gravity center of a superstructure. In a reinforced concrete single pier as shown in **Fig.4(a)**, the ultimate displacement δ_u is evaluated as

$$\delta_u = \delta_y + (\phi_u - \phi_y) L_P(h - L_P/2) \quad (10)$$

in which ϕ_y = yield curvature of a pier at bottom, ϕ_u = ultimate curvature of a pier at bottom, h = height of a pier, and L_P = plastic hinge length of a pier. The plastic hinge length is given as

$$L_P = 0.2h - 0.1D \quad (0.1D \leqq L_P \leqq 0.5D) \quad (11)$$

in which D is a width or a diameter of a pier.

The yield curvature ϕ_y and ultimate curvature ϕ_u in Eq.(10) are evaluated assuming a stress-strain relation of reinforcements and concrete as shown in **Fig.6**. The stress σ_c - strain ε_c relation of concrete with lateral confinement is assumed as

$$\sigma_c = \begin{cases} E_c \varepsilon_c \{1 - \frac{1}{n} \frac{\varepsilon_c}{\varepsilon_{cc}})^{n-1}\} \\ \qquad (0 \leqq \varepsilon_c \leqq \varepsilon_{cc}) \\ \sigma_{cc} - E_{des}(\varepsilon_c - \varepsilon_{cc}) \\ \qquad (\varepsilon_{cc} < \varepsilon_c \leqq \varepsilon_{cu}) \end{cases} \quad (12)$$

$$n = \frac{E_c \varepsilon_{cc}}{E_c \varepsilon_{cc} - \sigma_{cc}} \quad (13)$$

in which σ_{cc} = strength of confined concrete, E_c = elastic modules of concrete, ε_{cc} = strain at maximum strength, and E_{des} = gradient at descending branch. In Eq.(12), σ_{cc}, ε_{cc} and E_{des} are determined as

$$\sigma_{cc} = \sigma_{ck} + 3.8 \alpha \rho_s \sigma_{sy} \quad (14)$$

$$\varepsilon_{cc} = 0.002 + 0.033 \beta \frac{\rho_s \sigma_{sy}}{\sigma_{ck}} \quad (15)$$

$$E_{des} = 11.2 \frac{\sigma_{ck}^2}{\rho_s \sigma_{sy}} \quad (16)$$

in which σ_{ck} = design strength of concrete, σ_{sy} = yield strength of reinforcements, α and β = coefficients depending on shape of pier (α =1.0 and β =1.0 for a circular pier, and α = 0.2 and β = 0.4 for a rectangular pier), and ρ_s = tie reinforcement ratio defined as

$$\rho_s = \frac{4A_h}{sd} \leqq 0.018 \quad (17)$$

in which A_h = area of tie reinforcements, s = space of tie reinforcements, and d = effective width of tie reinforcements.

The ultimate curvature ϕ_u is defined as a curvature when concrete strain at longitudinal reinforcing bars in compression reaches an ultimate strain ε_{cu} defined as

$$\varepsilon_{cu} = \begin{cases} \varepsilon_{cc} & \text{for Type I ground motions} \\ \varepsilon_{cc} + \frac{0.2 \sigma_{cc}}{E_{des}} & \text{for Type II ground motions} \end{cases} \quad (18)$$

It is important to note here that the ultimate strain ε_{cu} depends on the types of ground motions; the ε_{cu} for the Type-II ground motions is larger than that for the Type-I ground motions. Based on a loading test, it is known that a certain level of failure in a pier such as a sudden decrease of lateral capacity occurs at smaller lateral displacement in a pier subjected to a loading hysteresis with more number of load reversals. To reflect such a fact, it was decided that the ultimate strain ε_{cu} should be evaluated by Eq.(18), depending on the type of ground motions. Therefore, the allowable ductility factor μ_a depends on the type of ground motions; the μ_a is larger in a pier subjected to the Type-II ground motions than a pier subjected to the Type-I ground motions.

It should be noted that the safety factor α in Eq.(9) depends on the type of bridges as well as the type of ground motions as shown in **Table 3**. This is to preserve higher seismic safety in the important bridges, and to take account of the difference of recurrent time between the Type-I and the Type-II ground motions.

(3) Shear Capacity

Shear capacity of reinforced concrete piers is evaluated by a conventional method as

$$P_s = S_c + S_s \quad (19)$$

$$S_c = 10\, c_c\, c_e\, c_{pt}\, \tau_c\, b\, d \quad (20)$$

$$S_s = \frac{A_w\, \sigma_{sy}\, d\, (\sin\theta + \cos\theta)}{10 \times 1.15a} \quad (21)$$

in which P_s = shear capacity, S_c = shear capacity shared by concrete, S_s = shear capacity shared by tie reinforcements, τ_c = shear stress capacity shared by concrete, c_c = modification factor for cyclic loading (0.6 for Type-I ground motions, 0.8 for Type-II ground motions), c_e = modification factor for scale effect of effective width, c_{pt} = modification factor for longitudinal reinforcement ratio, b, d = width and height of section, A_w = sectional area of tie reinforcement, σ_{sy} = yield strength of tie reinforcement, θ = angle between vertical axis and tie reinforcement, and a = spacing of tie reinforcement.

The modification factor on scale effect of effective width, c_e, was based on the experimental study of loading tests of beams with various effective height and was newly introduced in the 1996 Specifications. **Table 4** shows the modification factor on scale effect.

(4) Arrangement of Reinforcement

Fig.7 shows suggested arrangement of tie reinforcement. Tie reinforcement should be deformed bars with a diameter equal or larger than 13 mm, and it should be placed in most bridges at a distance of no longer than 150mm. In special cases such as the bridges with pier height taller than 30m, the distance of tie reinforcement may be increased at height so that pier strength should not be sharply decreased at the section. Intermediate ties should be also provided with the same distance with the ties to confine the concrete. Space of the intermediate ties should be less than 1m.

(5) Two-Column Bent

To determine the ultimate strength and ductility factor for two-column bents, it is modeled as the frame model with plastic hinges at the both end of lateral cap beam and columns as shown in **Fig.8**. Each elastic frame member has the yield stiffness which is obtained based on the axial load by the dead load of the superstructure and the column. The plastic hinge is assumed to be placed at the end part of a cap beam and the top and bottom part of each column. The plastic hinges are modeled as spring elements with bilinear moment-curvature relation. The location of plastic hinges is half distance of the plastic hinge length off from the end edge of each member, where plastic hinge length L_P is assumed to be Eq.(11).

When the two-column bent is subjected to the lateral force in the transverse direction, axial force developed in the beam and columns is affected by the aoolied lateral force. Therefore, the horizontal force-displacement relation is obtained through the static push-over analysis considering axial force N - moment M interaction relation. The ultimate state of each plastic hinges is obtained by the ultimate plastic angle θ_{pu} as

$$\theta_{pu} = (\phi_u/\phi_y - 1)\, L_P\, \phi_y \quad (22)$$

in which ϕ_u = ultimate curvature and ϕ_y = yield curvature.

The ultimate state of the whole two-bent column is determined so that all 4 plastic hinges developed reach the ultimate plastic angle.

7. EVALUATION OF DISPLACEMENT DUCTILITY OF A STEEL PIER

(1) Basic Concept

To improve seismic performance of a steel piers, it is important to avoid specific brittle failure modes. **Fig.9** shows the typical brittle failure mode for rectangular and circular steel piers. The followings are the countermeasures to avoid such brittle failure modes and to improve seismic performance of steel piers:

1) fill the steel column with concrete

2) improve structural parameters related to buckling strength

- decrease the width/thickness ratio of stiffened palates of rectangular piers or the diameter/thickness ratio of steel pipes
- increase the stiffness of stiffeners
- reduce the diaphragm spacing
- strengthen corners using the corner plates

3) improve welding section at the corners of rectangular section

4) eliminate welding section at the corners by using round corners

(2) Concrete Infilled Steel Pier

In a concrete infilled steel pier, the lateral capacity P_a and the allowable displacement ductility factor μ_a in Eqs.(1) and (2) are evaluated as

$$P_a = P_y + \frac{P_u - P_y}{\alpha} \tag{23}$$

$$\mu_a = \left(1 + \frac{\delta_u - \delta_y}{\alpha \delta_y}\right) \frac{P_u}{P_a} \tag{24}$$

in which P_y and P_u = yield and ultimate lateral capacity of a pier, δ_y and δ_u = yield and ultimate displacement of a pier, and α = safety factor (refer to **Table 3**). The P_a and the μ_a are evaluated idealizing that a concrete infilled steel pier resists flexural moment and shear force as a reinforced concrete pier. It is assumed in this evaluation that the steel section be idealized as reinforcing bars and that only steel section resists axial force. A stress vs. strain relation of steel and concrete as shown in **Fig.10** is assumed. The height of infilled concrete has to be decided so that bucking is not developed above the infilled concrete.

(3) Steel Pier without Infilled Concrete

A steel pier without infilled concrete must be designed with the dynamic response analysis. Properties of the pier need to be decided based on a cyclic loading test. Arrangement of stiffness and welding at corner must be precisely evaluated so that brittle failure should be avoided.

8. DYNAMIC RESPONSE ANALYSYS

Dynamic response analysis is required in the bridges with complex dynamic response to check the safety factor of the static design. Dynamic response analysis is alos required as a "design" tool in the bridges for which the Ductility Design Method is not directly applied. In dynamic response analysis, ground motins which are spectral fitted to the following response spectra are used;

$$S_I = c_Z \cdot c_D \cdot S_{I0} \tag{25}$$

$$S_{II} = c_Z \cdot c_D \cdot S_{II0} \tag{26}$$

in which S_I and S_{II} = acceleration response spectrum for Type-I and Tyoe-II ground motions, S_{I0} and S_{II0} = standard acceleration response spectrum for Type-I and Type-II ground motions, respectively, c_Z = modification coefficient for zone (refer to Eq.(8)), and c_D = modification coefficient for damping ratio given as

$$c_D = \frac{1.5}{40h_i + 1} + 0.5 \tag{27}$$

Table 5 and **Fig.11** show the standard acceleration response spectra (damping ratio h=0.05) for the Type-I and Type-II ground motions.

It is recommended to use at least three ground motions per analysis, and take an average to evaluate the response.

In the dynamic analysis, modal damping ratios have to be carefully evaluated. To determine themodal damping aratios, a bridge may be divided into several sub-strucctures in which energy dissipating mechanism is essentially the same. If one can specify a damping ratio of each sub-structure for a given mode shape, the modal damping ratio for i-th mode, h_i, may be evaluated as

$$h_i = \frac{\sum_{j=1}^{n} \phi_{ij}^T \cdot h_{ij} \cdot K_j \cdot \phi_{ij}}{\Phi_i^T \cdot K \cdot \Phi_i} \tag{28}$$

in which h_{ij} = damping ratio of j-th substructure in i-th mode, ϕ_{ij} = mode vector

of j-th substructure in i-th mode, k_j = stiffness matrix of j-th substructure, K= stiffness matrix of a bridge, and Φ_i = mode vector of a bridge in i-th mode, and is given as

$$\Phi_i^T = \{\phi_{i1}^T, \phi_{i2}^T, \cdots\cdots, \phi_{in}^T\} \quad (29)$$

Table 6 shows recommended damping ratios for major structural components.

9. MENSHIN DESIGN

(1) Basic Principle

Implementation of the Menshin bridges should be carefully decided from not only seismic performance but function for traffic and maintenance point of view, based on the advantage and disadvantage of increasing natural period The Menshin design should not be adopted at the following conditions;

1) sites vulnerable to lose bearing capacity due to the soil liquefaction and the lateral spreading,

2) bridges supported by flexible columns,

3) soft soil sites where potential resonance with surrounding soils could be developed by increasing the fundamental natural period, and

4) bridges with uplift force at bearings.

It is suggested that the design should be made with an emphasis on an increase of energy dissipating capability and a distribution of lateral force to as many substructures as possible. To concentrate the hysteretic deformation at not piers but bearings, the fundamental natural period of a Menshin bridge should be about 2 times or longer than the fundamental natural period of the same bridge supported by the conventional bearings. It should be noted that an elongation of natural period aiming to decrease the lateral force should not be attempted.

(2) Design Procedure

Menshin bridges are designed by both the Seismic Coefficient Method and the Ductility Design Method. In the Seismic Coefficient Method, no reduction of lateral force from the conventional design is mae.

In the Ductility Design Method, the equivalent lateral force coefficient k_{hcm} in the Menshin design is evaluated as

$$k_{hcm} = \frac{k_{hcm}}{\sqrt{2\mu_m - 1}} \quad (30)$$

$$k_{hcm} = c_E \cdot k_{hc} \quad (31)$$

in which k_{hcm} = lateral force coefficient in menshin design, μ_m = allowable ductility factor of a pier, c_E = modification coefficient for energy dissipating capability (refer to **Table 7**), and k_{hc} = lateral force coefficient by Eq.(8). Because the k_{hc} is the lateral force coefficient for a bridge supported by the conventional bearings, Eq.(31) means that the lateral force in the Menshin design can be reduced, as large as 30%, by the modification coefficient c_E depending on the modal damping ratio of a bridge.

Modal damping ratio of a menshin bridge h for the fundamental mode is computed as Eq.(32). In Eq.(32), h_{Bi} = damping ratio of i-th damper, h_{Pi} = damping ratio of i-th pier or abutment, h_{Fui} = damping ratio of i-th foundation associated with translational displacement, $h_{F\theta i}$ = damping ratio of i-th foundation associated with rotational displacement, K_{Pi} = equivalent stiffness of i-th pier or abutment, K_{Fui} = translational stiffness of i-th foundation, $K_{F\theta i}$ = rotational stiffness of i-th foundation, u_{Bi} = design displacement of i-th Menshin device, and H = distance from a bottom of pier to a gravity center of a deck.

In the Menshn design, the allowable displacement ductility factor of a pier μ_m in Eq.(30) is evaluated by

$$h = \frac{\Sigma K_{Bi} \cdot u_{Bi}^2 \left(h_{Bi} + \frac{h_{Pi} \cdot K_{Bi}}{K_{Pi}} + \frac{h_{Fui} \cdot K_{Bi}}{K_{Fui}} + \frac{h_{F\theta i} \cdot K_{Bi} \cdot H^2}{K_{F\theta i}}\right)}{\Sigma K_{Bi} \cdot u_{Bi}^2 \left(1 + \frac{K_{Bi}}{K_{Pi}} + \frac{K_{Bi}}{K_{Fui}} + \frac{K_{Bi} \cdot H^2}{K_{F\theta i}}\right)} \quad (32)$$

$$\mu_m = 1 + \frac{\delta_u - \delta_y}{\alpha_m \delta_y} \quad (33)$$

in which α_m is a safety factor used in Menshin design, and is given as

$$\mu_m = 2\alpha \quad (34)$$

where α is the safety factor in the conventional design (refre to **Table 3**). Eq.(34) means that the allowable displacement ductility factor in the menshin design μ_m should be smaller than the allowable displacemnent ductility factor μ_a by Eq.(2) in the conventional design. The reason for the smaller allowable ductility factor in the menshin design is to limit the hysteretic behavior of a pier at the plastic hinge zone so that principle hysteretic behavior occurs at the menshin devices as shown in **Fig.4(b)**.

(3) Design of Menshin Devices

Simple devices stable against extreme earthquakes have to be used. The bearings have to be anchored to a deck and substructures with bolts, and should be replaceable. The clearance has to be provided between a deck and an abutment or between adjacent decks.

Isolators and dampers must be designed for a desired design displacement u_B. The design displacement u_B is evaluated as

$$u_B = \frac{k_{hem} W_U}{K_B} \quad (35)$$

in which k_{hem} = equivalent lateral force coefficient by Eq.(31), K_B = equivalent stiffness, and W_U = dead weight of a superstructure. It should be noted that because the equivalent lateral force coefficient k_{hem} depends on the type of ground motions, the design displacement u_B also depends on it.

The equivalent stiffness K_B and equivalent damping ratio h_B of a Menshin device are evaluated as

$$K_B = \frac{F(u_{Be}) - F(-u_{Be})}{2u_{Be}} \quad (36)$$

$$h_B = \frac{\Delta W}{2\pi W} \quad (37)$$

$$u_{Be} = c_B \cdot u_B \quad (38)$$

in which F(u) = restoring force of a device at a displacement u , u_{Be} = effective design displacement, ΔW = energy dissipated per cycle, W = elastic strain energy, and c_B = coefficient to evaluate effective displacement (=0.7).

10. DESIGN OF FOUNDATION

Th evaluation methods of ductility and strength of foundations such as pile foundations and caisson foundations was newly introduced in the 1996 Specifications.

In a pile foundation, a foundation is so idealized that a rigid footing is supported by piles which are supported by soils. The flexural strength of a pier defined by Eq.(7) shall be applied as a seismic force to foundations at the bottom of the footing together with the dead weight superstructure, pier and soils on the footing. **Fig.12** shows the idealized nonlinear model of a pile foundation. The nonlinearity of soils and piles is considered in the analysis.

The safety of the foundation shall be checked so that 1) the foundation shall not reach the yield point of a foundation, 2) if the primary nonlinearity is developed in the foundations, the response displacement shall be less than displacement ductility limit, and 3) the displacement developed in the foundation shall be less than allowable limit. The allowable ductility and allowable limit of displacement were commented as 4 in displacement ductility, 40cm in horizontal displacement and 0.025rad in rotation angle.

For a caisson type foundation, the foundation is modeled as a reinforced concrete column which is supported by soil spring model and the safety is checked in the same way as the pile foundations.

11. DESIGN AGAINST SOIL LIQUEFACTION AND LIQUEFACTION-INDUCED GROUND

FLOW

(1) Estimation of Liquefaction Potential

Since the Hyogo-ken nanbu Earthquake of 1995 caused liquefaction even at coarse sand or gravel layers which had been regarded invulnerable to liquefy, a gravel layer was included in the soil layers that require liquefaction potential estimation. Soil layers that satisfies the following conditions is estimated to be potential liquefaction layers:

1) saturated soil layer which is located within 20m deep under the ground surface and in which ground water level is within 10m deep.
2) soil layer in which fine particle content ratio FC is equal or less than 35% or plasticity index I_P is equal or less than 15.
3) soil layer in which mean grain size D_{50} is equal or less than 10mm and 10% grain size D_{10} is equal or less than 1mm.

Liquefaction potential is estimated by the safety factor against liquefaction F_L as

$$F_L = R/L \quad (35)$$

where, F_L = liquefaction resistant ratio, R = dynamic shear strength ratio and L = share stress ratio during an earthquake. The dynamic shear strength ratio R may be expressed as

$$R = c_w R_L \quad (36)$$

where, c_w = corrective coefficient for ground motion characteristics (1.0 for Type-I ground motions, 1.0-2.0 for Type-II ground motions), and R_L = cyclic triaxial strength ratio. The cyclic triaxial strength ratio was estimated by laboratory tests with undisturbed samples by in-situ freezing method.

The shear stress ratio during an earthquake may be expressed as

$$L = r_d k_{hc} \sigma_v / \sigma_v' \quad (37)$$

where, r_d = modification factor shear stress ratio with depth, k_{hc} = design seismic coefficient for the evaluation of liquefaction potential, σ_v = total loading pressure, σ_v' = effective loading pressure.

It should be noted here that the design seismic coefficient for the evaluation of liquefaction potential k_{hc} is ranging from 0.3 to 0.4 for Type-I ground motions, and from 0.6 to 0.8 for Type-II ground motions.

(2) Design Treatment of Liquefaction for Bridge Foundations

When the liqeufaction occurs, the strength and the bearing capacity of a soil decreases. In the seismic design of highway bridges, soil constants of a sandy soil layer which is judged liable to liquefy are reduced according to the F_L value. The reduced soil constants are calculated by multiplying the coefficient D_E in **Table 8** to the soils constants estimated on an assumption that the soil layer does not liquefy.

(3) Design Treatment of Liqeufaction-Induced Ground Flow for Bridge Foundations

When the liquefaction-induced ground flow that may affect bridge seismicity is likely to occur, this influence was included in the revised Design Specifications in 1996. The case in which the ground flow that may affect bridge seismicity is likely to occur is generally that the ground is judged to be liquefiable and is exposed to biased earth pressure, for example, the ground behind a seaside protection wall. The effect of liquefaction-induced ground flow is considered as the static force acting on structure. This method premises that the surface soil is of the non-liqeufiable and liquefiable layers, and the forces equivalent to the passive earth pressure and 30% of the overburden pressure are applied to the structure in the non-liquefiable layer and liquefiable layer, respectively.

The seismic safety of a foundation is checked by confirming the displacement at the top of foundation caused by ground flow does not exceed an allowable value, in which a foundation and the ground are idealized as shown in **Fig.12.** The allowable displacement of a foundation may be taken as two times the yield displacement of a foundation. In this

process, the inertia force of structure is not necessary to be considered simultaneously, because the liquefaction-induced ground flow may take place after the principle ground motion.

12. BEARING SUPPORTS

The bearings are classified into two groups; the first is the bearings which resist the seismic force of Eq.(2), and the second is the bearings which resist the seismic force considered in the Seismic Coefficient Method. The first and the second bearings are called as the Type-B bearings and the Type-A bearings, respectively. Seismic performance of the Type-B bearings is, of course, much higher than the Type-A bearings. In the Type-A bearings, a displacement limiting device, which will be described later, has to be co-installed in both longitudinal and transverse directions, while it is not required in the Type-B bearings. Because of the importance of bearings as one of the main structural components, the Type-B bearings should be used in the menshin bridges.

The uplift force applied to the bearing supports is specified as

$$R_U = R_D - \sqrt{R_{heq}^2 + R_{veq}^2} \quad (38)$$

in which R_U = design uplift force applied to the bearing support, R_D = dead load of superstructure, R_{heq} and R_{veq} are vertical reactions caused by the horizontal seismic force and vertical force, respectively. **Fig.13** shows the design forces for the bearing supports.

13. UNSEATING PREVENTION SYSTEMS

Unseating prevention measures are required for the highway. bridges. The measures required for the highway bridges are as:

1) the unseating prevention systems have to be so designed that unseating of a superstructure from their supports can be prevented even if unpredictable failures of the structural members occur,

2) the unseating prevention systems are consisted of providing enough seat length, a falling-down prevention device, a displacement limiting device, and a settlement prevention device,

3) enough seat length must be provided and a falling-down prevention device must be installed at the ends of a superstructures against longitudinal response. If the Type-A bearings are used, a displacement limiting device has to be further installed at not only the ends of a superstructure but each intermediate support in a continuous bridge, and

4) if the Type-A bearings are used, a displacement limiting device is requested at each support against transverse response. The displacement limiting device is not generally required if the Type-B bearings are used. But, even if the Type-B bearing is adopted, it is required in skewed bridges, curved bridges, bridges supported by columns with narrow crest, bridges supported by few bearings per piers, and bridges constructed at the sites vulnerable to lateral spreading associated with soil liquefaction.

The seat length S_E is evaluated as

$$S_E = u_R + u_G \geqq S_{EM} \quad (39)$$

$$S_{EM} = 70 + 0.5l \quad (40)$$

$$u_G = 100 \cdot \varepsilon_G \cdot L \quad (41)$$

in which u_R = relative displacement (cm) developed between a superstructure and a substructure subjected to a seismic force equivalent to the equivalent lateral force coefficient k_{hc} by Eq.(2), u_G = relative displacement of ground along the bridge axis, S_{EM} = minimum seat length (cm), ε_G = ground strain induced during an earthquake along the bridge axis, and is 0.0025, 0.00375, and 0.005 for Group-I, II and III sites, respectively, L= distance which contributes to the relative displacement of ground (m), and l = span length (m). If two adjacent deck are supported by a pier, the lager span length should be l in evaluating the seat length.

Inthe menshin deisgn, in addition to the above

requirements, the following copnsiderations have to be made.

1) To prevent collisions between a deck and an abutment or between two adjacent decks, enough clearance must be provided. The clearance between those structural components S_B shall be evaluated as

$$S_B = \begin{cases} u_B + L_A \\ \quad \text{between a deck and an abutment} \\ c_B \cdot u_B + L_A \\ \quad \text{between two adjacent decks} \end{cases} \quad (42)$$

in which u_B = design displacement of menshin devices (cm) by Eq.(35), L_A = redundancy of a clearance (generally $\pm$ 1.5cm), and c_B = modification coefficient for clearance (refer to **Table 9**). The modification coefficient c_B was determined based on an analysis of the relative displacement response spectra. It depends on a difference of natural periods $\triangle T = T_1 - T_2$ ($T_1 > T_2$), in which T_1 and T_2 represent the natural period of the two adjacent bridge systems.

2) The clearance at an expansion joint L_E is evaluated as

$$L_E = u_B + L_A \quad (43)$$

in which u_B = design displacement of menshin devices (cm) by Eq.(35), and L_A = redundancy of a clearance (generally $\pm$ 1.5cm).

14. CONCLUDING REMARKS

The preceding pages presented an outline of the new Seismic Design Specifications of Highway Bridges issued in 1996 as well as the damage features of highway bridges in the Hyogo-ken nanbu earthquake. The Hyogo-ken nanbu earthquake was the first earthquake which developed destructive damage in an urban area since the 1948 Fukui Earthquake. Because it had been considered that such destructive damage could be prevented due to the progress of construction technology in recent years, it provided a large impact on the earthquake disaster prevention measures in various fields. The "Part V Seismic Design" of the "Design Specifications of Highway Bridges" (Japan Road Association) was totally revised in 1996, and the design procedure moved from the traditional Seismic Coefficient Method to the Ductility Design Method. The revision was so comprehensive that the past revisions in the last 30 years look minor.

Major point of the revision was the introduction of explicit two-level seismic design consisting of the Seismic Coefficient Method and the Ductility Design Method. Because the Type-I and the Type-II ground motions are considered in the Ductility Design Method, three design seismic forces are totally used in design. Seismic performance for each design force was clearly stated in the Specifications.

The fact that lack of near-filed strong motion records prevented to seriously evaluate the validity of recent seismic design codes is important. The Hyogo-ken nanbu earthquake revealed that history of strong motion recording is very short, and that no near-field records have yet been measured by an earthquake with magnitude on the order of 8. It is therefore essential to have enough redundancy and ductility in a total bridge system. It is hoped that the revised Seismic Design Specifications of Highway Bridges contributes to enhance seismic safety of highway bridges.

ACKNOWLEDGMENTS

Drafting of the revised version of the "Part V Seismic Design" of the "Design Specifications of Highway Bridges" was conducted at the "Special Sub-committee for Seismic Countermeasures for Highway Bridges" and was approved by the Bridge Committee, Japan Road Association. The first and other authors of this paper served as chairman and executive members in the Special Sub-committee. The authors thank all members of the Special Sub-Committee and the Bridge Committee.

REFERENCES

1) Japan Road Association : Design Specifications of Highway Bridges, Part I Common Part, Part II Steel Bridges, Part III Concrete Bridges, Part IV Foundations, and Part V Seismic Design, 1996
2) Kawashima, K.: Impact of Hanshin/Awaji Earthquake on Seismic Design and Seismic Strengthening of Highway Bridges, Report No. TIT/EERG 95-2, Tokyo Institute of Technology., 1995
3) Ministry of Construction: Report on the Damage of Highway Bridges by the Hyogo-ken Nanbu Earthquake, Committee for Investigation on the Damage of Highway Bridges Caused by the Hyogo-ken Nanbu Earthquake, 1995
4) Ministry of Construction: Guide Specifications for Reconstruction and Repair of Highway Bridges Which Suffered Damage due to the Hyogo-ken Nanbu Earthquake, 1995

APPENDIX

TABLE OF CONTENTS OF "Part V : SEISMIC DESIGN" OF "DESIGN SPECIFICATIONS FOR HIGHWAY BRIDGES," JAPAN ROAD ASSOCIATION, 1996

1. General
   1.1 Scope
   1.2 Definition of Terms
2. Basic Principle of Seismic Design
3. Loads and Design Conditions Considered in Seismic Design
   3.1 Loads and Combinations
   3.2 Effects of an Earthquake
   3.3 Inertia Force
   3.4 Importance
   3.5 Modification Factor for Zone
   3.6 Modification Factor for Ground Condition
   3.7 Ground Surface Assumed in Seismic Design
4. Seismic Design by Seismic Coefficient Method
   4.1 Lateral Force Coefficient
   4.2 Dynamic Earth Pressure
   4.3 Dynamic Hydraulic Pressure
5. Seismic Design by Ductility Design Method
   5.1 General
   5.2 Evaluation of Safety
   5.3 Lateral Force Coefficient
6. Check of Safety by Dynamic Response Analysis
   6.1 General
   6.2 Analytical Models and Analytical Procedures
   6.3 Ground Motions
   6.4 Evaluation of Safety
7. Seismic Design of Foundations at the Soils Vulnerable to Instability
   7.1 General
   7.2 Seismic Design of Foundations at the Sites Vulnerable to Failure of Clayey Materials or Soil Liquefaction
   7.3 Seismic Design of Foundations at the Sites Vulnerable to Lateral Spreading
   7.4 Evaluation of Soft Clay or Silty Clay with Potential Failure
   7.5 Evaluation of Sandy Soils with Potential to Develop Soil Liquefaction
   7.6 Soil Layers whose Bearing Capacity Should be Decreased
8. Menshin Design
   8.1 General
   8.2 Menshin Design
   8.3 Seismic Force in Menshin Design
   8.4 Design of Devices
   8.5 Evaluation of Natural Period of a Menshin Bridge
   8.6 Evaluation of Damping Ratio of a Menshin Bridge
   8.7 Design Detailings in Menshin Design
9. Capacity and Ductility of Reinforced Concrete Piers
   9.1 General
   9.2 Lateral Capacity and Ductility
   9.3 Lateral Force and Lateral Displacement at Yield and Ultimate
   9.4 Stress-Strain Relation Assumed in Concrete
   9.5 Shear capacity
   9.6 Design Detailings to Enhance Ductility
   9.7 Termination of Main Reinforcement at Mid-height
   9.8 Lateral Capacity and Ductility of Frame Piers
   9.9 Effect of Eccentricity of Vertical Load in Inverted L-Shaped Piers
10. Lateral Capacity and Ductility of Steel Piers
   10.1 General
   10.2 Steel Piers with Infilled Concrete
   10.3 Steel Piers without Infilled Concrete
   10.4 Seismic Design of Anchor
   10.5 Effect of Eccentricity of Vertical Load in Inverted L-Shaped Steel Piers with Infilled Concrete

11. Lateral Capacity of Foundations
11.1 General
11.2 Evaluation of Seismic Force, Reaction Force and Displacement of Foundations
11.3 Yield of Foundations
11.4 Evaluation of Response of Foundations when Principle Plastic Hinge Occurs at Foundations, and Allowable Maximum Response Displacement
11.5 Check of Safety
12. Bearings and Their Surrounding Structures
12.1 General
12.2 Seismic Design Force for Bearings and Their Surroundings
12.3 Evaluation of Safety
12.4 Structures of Bearings and Their Surroundings
13. Unseating Prevention Systems
13.1 General
13.2 Seat Length
13.3 Unseating Prevention Devices
13.4 Excessive Displacement Limiting Devices
13.5 Devices for Preventing Settlement of a Superstructure
13.6 Joint Protector
13.7 Strengthening of Portion of Superstructure where Unseating Prevention Devices is Connected
13.8 Unseating Prevention Systems in Transverse Direction
14. Structure to Reduce Bridge Response

Table 1 Seismic Performance Levels

Type of Design Ground Motions		Importance of Bridges		Design Methods	
		Type-A (Standard Bridges)	Type-B (Important Bridges)	Equivalent Static Lateral Force Methods	Dynamic Analysis
Ground Motions with High Probability to Occur		Prevent Damage		Seismic Coefficient Method	Step by Step Analysis or Response Spectrum Analysis
Ground Motions with Low Probability to Occur	Type-I (Plate Boundary Earthquakes)	Prevent Critical Damage	Limited Damage	Ductility Design Method	
	Type-II (Inland Earthquakes)				

Table 2 Lateral Force Coefficient k_{hc0} in the Ductility Design Method

(a) Type-I Ground Motions

Soil Condition	Lateral Force Coefficient k_{hc0}		
Group I (stiff)	$k_{hc0}=0.7$ for $T \leqq 1.4$		$k_{hc0}=0.876T^{-2/3}$ for $T > 1.4$
Group II (moderate)	$k_{hc0}=1.51T^{-1/3}$ ($k_{hc0} \geqq 0.7$) for $T < 0.18$	$k_{hc0}=0.85$ for $0.18 \leqq T \leqq 1.6$	$k_{hc0}=1.16T^{-2/3}$ for $T > 1.6$
Group III (soft)	$k_{hc0}=1.51T^{-1/3}$ ($k_{hc0} \geqq 0.7$) for $T < 0.29$	$k_{hc0}=1.0$ for $0.29 \leqq T \leqq 2.0$	$k_{hc0}=1.59T^{-2/3}$ for $T > 2.0$

(b) Type-II Ground Motions

Soil Condition	Lateral Force Coefficient k_{hc0}		
Group I (stiff)	$k_{hc0}=4.46T^{2/3}$ for $T \leqq 0.3$	$k_{hc0}=2.00$ for $0.3 \leqq T \leqq 0.7$	$k_{hc0}=1.24T^{-4/3}$ for $T > 0.7$
Group II (moderate)	$k_{hc0}=3.22T^{2/3}$ for $T < 0.4$	$k_{hc0}=1.75$ for $0.4 \leqq T \leqq 1.2$	$k_{hc0}=2.23T^{-4/3}$ for $T > 1.2$
Group III (soft)	$k_{hc0}=2.38T^{2/3}$ for $T < 0.5$	$k_{hc0}=1.50$ for $0.5 \leqq T \leqq 1.5$	$k_{hc0}=2.57T^{-4/3}$ for $T > 1.5$

Table 3 Safety Factor α in Eq.(9)

Type of Bridges	Type-I Ground Motions	Type-II Ground Motions
Type-B	3.0	1.5
Type-A	2.4	1.2

Table 4 Modification Factor on Scale Effect for Shear Capacity Shared by Concrete

Effective Width of Section d (m)	Coefficient c_e
$d \leqq 1$	1.0
d=3	0.7
d=5	0.6
$d \geqq 10$	0.5

Table 5 Standard Acceleration Response Spectra

(a) Type-I Response Spectra S_{I0}

Soil Condition	Response Acceleration S_{I0} (gal=cm/sec^2)		
Group I	$S_{I0}=700$ for $T_i \leqq 1.4$		$S_{I0}=980/T_i$ for $T_i > 1.4$
Group II	$S_{I0}=1{,}505T_i^{1/3}$ ($S_{I0} \geqq 700$) for $T_i < 0.18$	$S_{I0}=850$ for $0.18 \leqq T_i \leqq 1.6$	$S_{I0}=1{,}360/T_i$ for $T_i > 1.6$
Group III	$S_{I0}=1{,}511T_i^{1/3}$ ($S_{I0} \geqq 700$) for $T_i < 0.29$	$S_{I0}=1{,}000$ for $0.29 \leqq T_i \leqq 2.0$	$S_{I0}=2{,}000/T_i$ for $T_i > 2.0$

(b) Type-II Response Spectra S_{II0}

Soil Condition	Response Acceleration S_{II0} (gal=cm/sec^2)		
Group I	$S_{II0}=4{,}463T_i^{2/3}$ for $T_i \leqq 0.3$	$S_{II0}=2{,}000$ for $0.3 \leqq T_i \leqq 0.7$	$S_{II0}=1{,}104/T_i^{5/3}$ for $T_i > 0.7$
Group II	$S_{II0}=3{,}224T_i^{2/3}$ for $T_i < 0.4$	$S_{II0}=1{,}750$ for $0.4 \leqq T_i \leqq 1.2$	$S_{II0}=2{,}371/T_i^{5/3}$ for $T_i > 1.2$
Group III	$S_{II0}=2{,}381T_i^{2/3}$ for $T_i < 0.5$	$S_{II0}=1{,}500$ for $0.5 \leqq T_i \leqq 1.5$	$S_{II0}=2{,}948/T_i^{5/3}$ for $T_i > 1.5$

Table 6 Recommended Damping Ratios for Major Structural Components

Structural Components	Elastic Response		Nonlinear Response	
	Steel	Concrete	Steel	Concrete
Superstructure	0.02 ~ 0.03	0.03 ~ 0.05	0.02 ~ 0.03	0.03 ~ 0.05
Rubber Bearings	0.02		0.02	
Menshin Bearings	Equivalent Damping Ratio by Eq.(26)		Equivalent Damping Ratio by Eq.(26)	
Substructures	0.03 ~ 0.05	0.05 ~ 0.1	0.1 ~ 0.2	0.12 ~ 0.2
Foundations	0.1 ~ 0.3		0.2 ~ 0.4	

Table 7 Modification Coefficient for Energy Dissipation Capability

Damping Ratio for 1st Mode h	Coefficient c_E
$h < 0.1$	1.0
$0.1 \leqq h < 0.12$	0.9
$0.12 \leqq h < 0.15$	0.8
$h \geqq 0.15$	0.7

Table 8 Reduction Coefficient D_E for Soil Constants due to Soil Liquefaction

Range of F_L	Depth from the Present Ground Surface x (m)	Dynamic Shear Strength Ratio R	
		$R \leqq 0.3$	$0.3<R$
$F_L \leqq 1/3$	$0 \leqq x \leqq 10$	0	1/6
	$10<x \leqq 20$	1/3	1/3
$1/3<F_L \leqq 2/3$	$0 \leqq x \leqq 10$	1/3	2/3
	$10<x \leqq 20$	2/3	2/3
$2/3<F_L \leqq 1$	$0 \leqq x \leqq 10$	2/3	1
	$10<x \leqq 20$	1	1

Table 9 Modification Coefficient for Clearance c_B

$\Delta T/T_1$	c_B
$0 \leqq \Delta T/T_1 < 0.1$	1
$0.1 \leqq \Delta T/T_1 < 0.8$	$\sqrt{2}$
$0.8 \leqq \Delta T/T_1 \leqq 1.0$	1

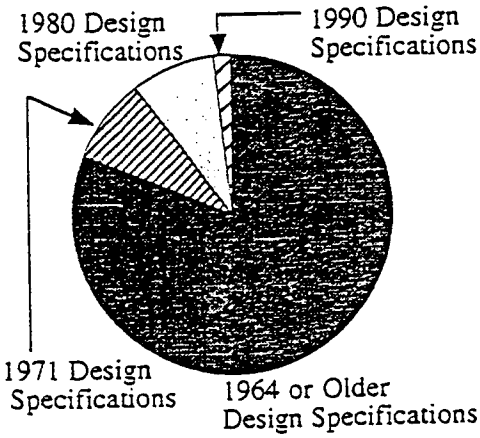
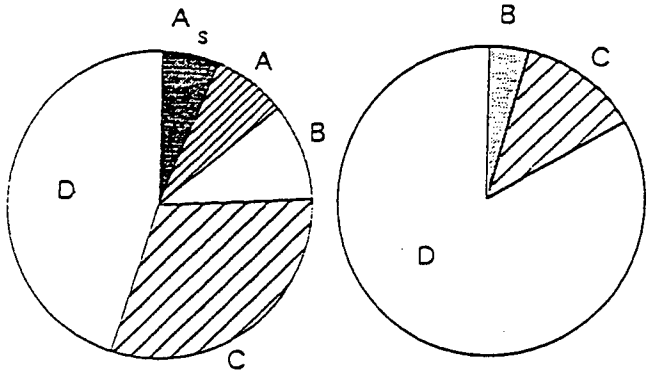


Fig.1 Design Specifications Referred to in Design of Hanshin Expressway



(a) Route 3 (b) Route 5

Fig.2 Comparison of Damage Degree between Route 3 and Route 5 (As : Collapse, A : Nearly Collapse, B : Moderate Damage, C : Damage of Secondary Members, D : Minor or No Damage)

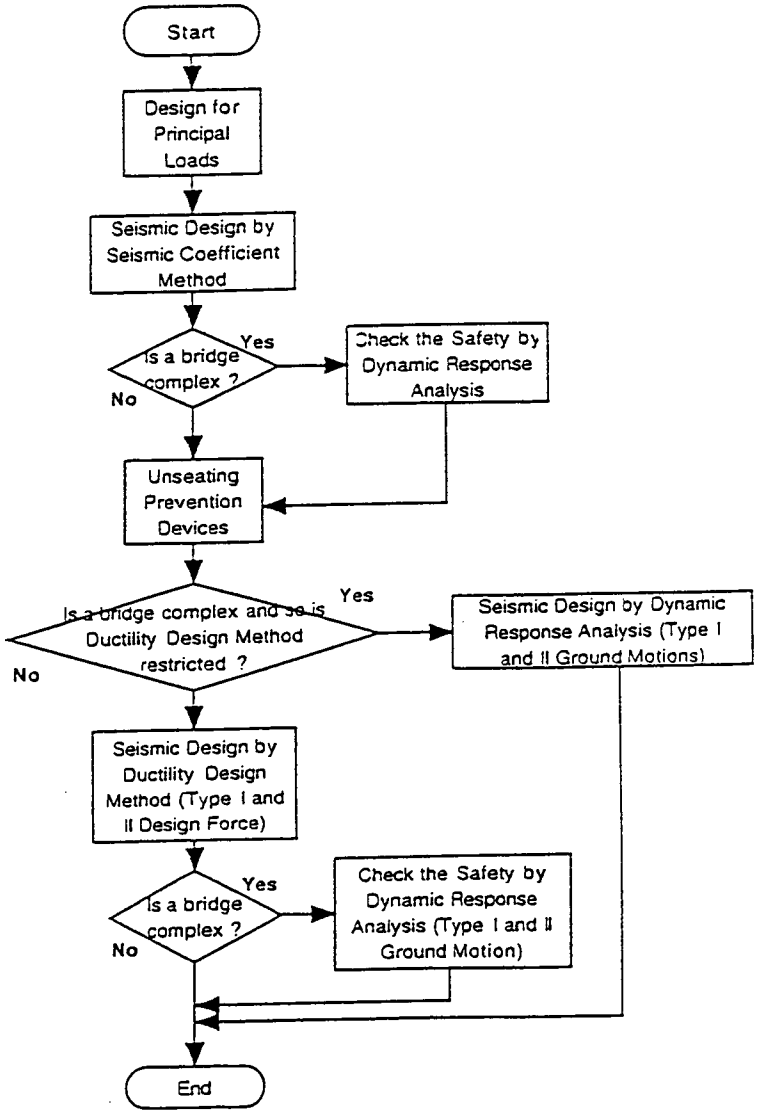
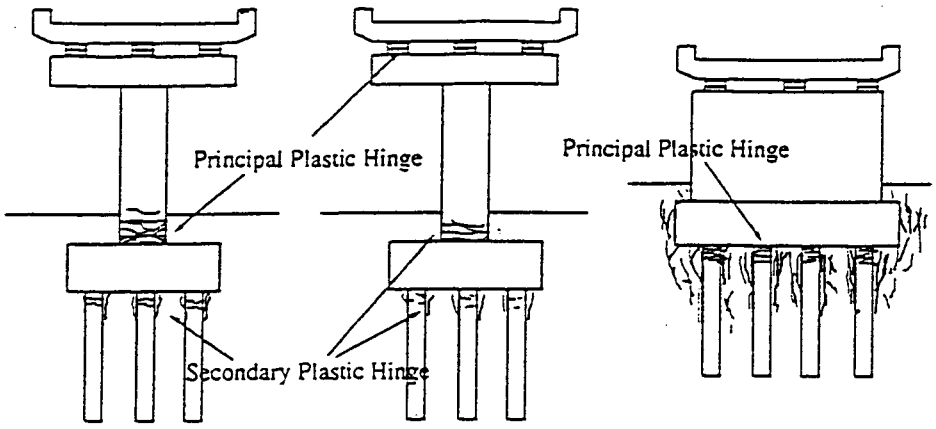


Fig.3 Flowchart of Seismic Design



(a) Conventional Design (b) Menshin Design (c) Bridge Supported by A Wall-type Pier

Fig.4 Location of Primary Plastic Hinge

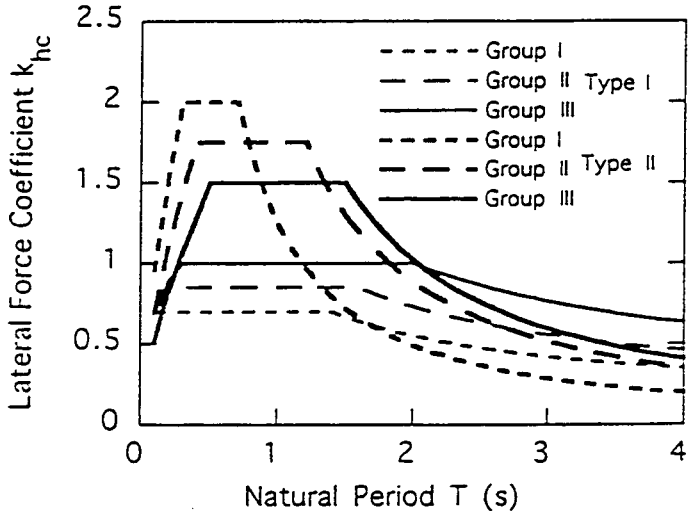
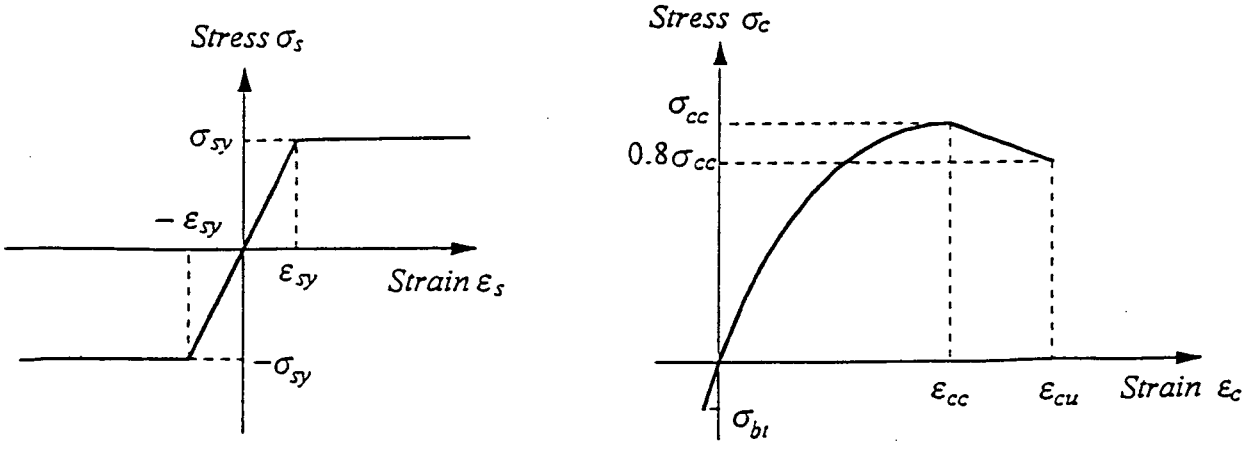
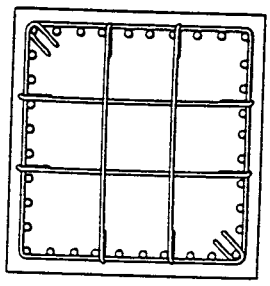


Fig.5 Type I and Type II Lateral Force Coefficients in the Ductility Design Method

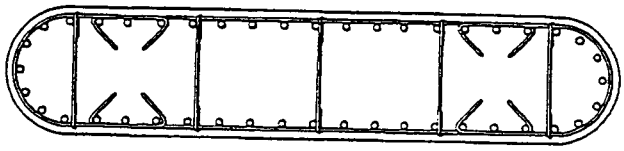


(a) Reinforcing Bars (b) Concrete

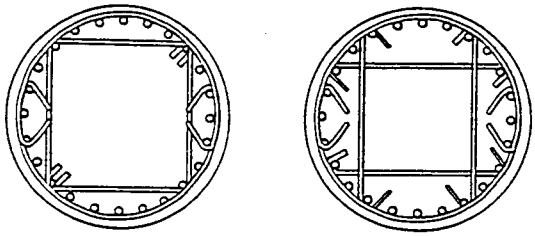
Fig.6 Stress and Strain Relation of Confined Concrete and Reinforcing Bars



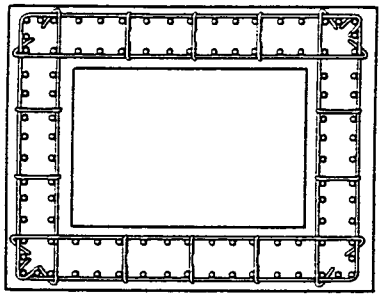
(a) Square Section



(b) Semi-square Section



(c) Circular Section



(d) Hollow Section

Fig.7 Confinement of Core-concrete by Tie Reinforcement

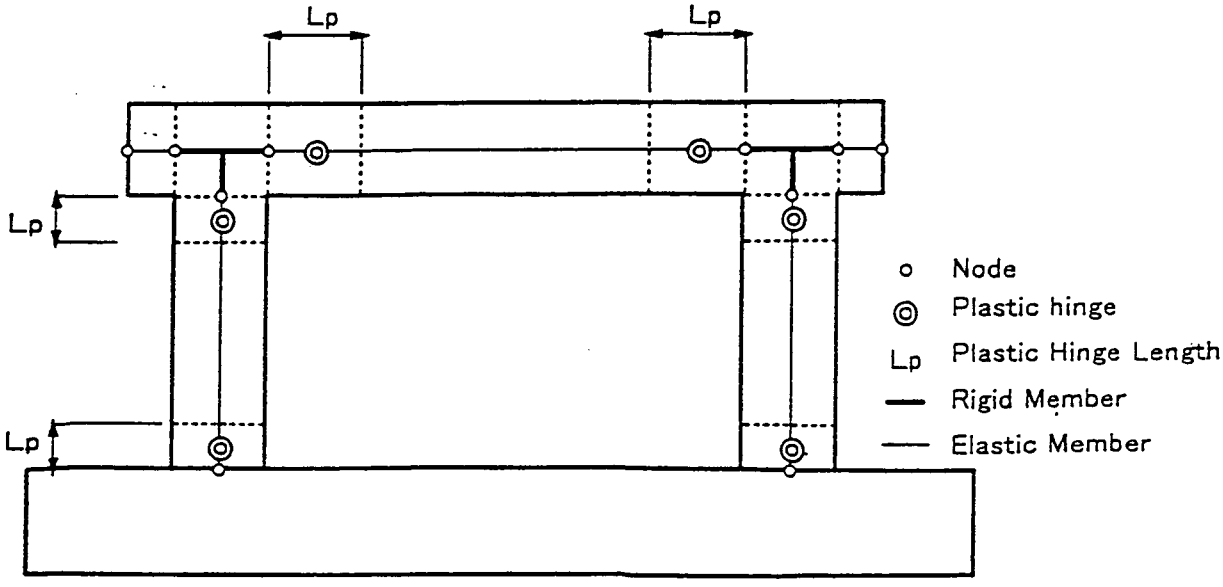
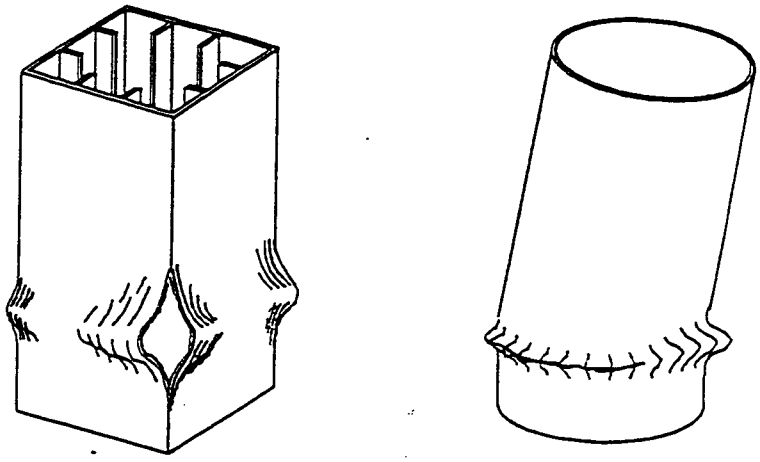
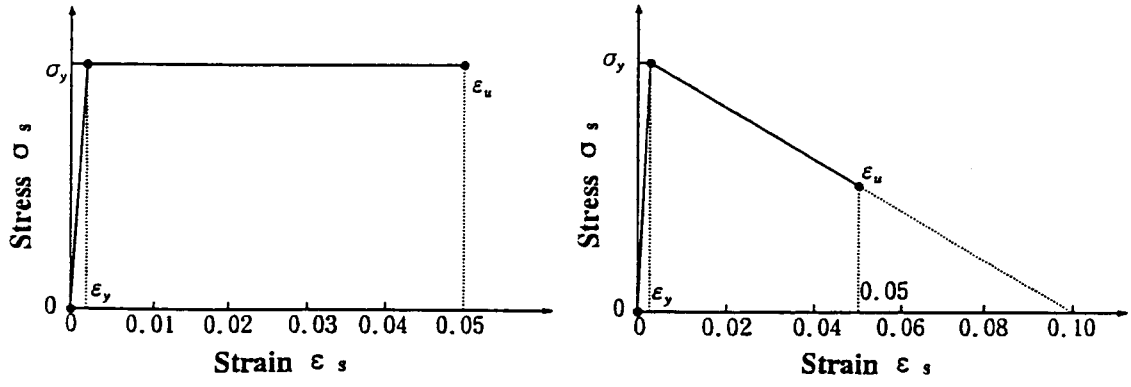


Fig.8 Analytical Idealization of A Two-Column Bent

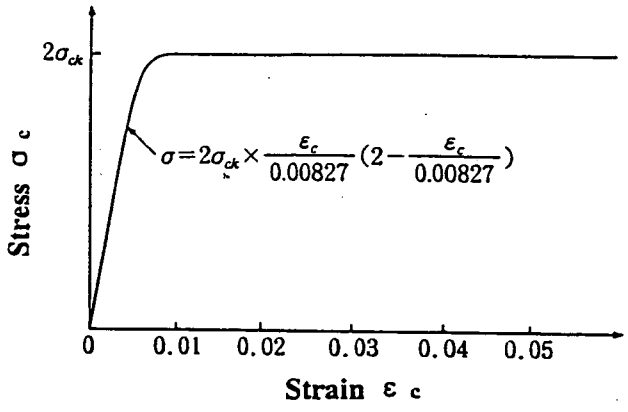


(a) Fracture of Corners (b) Elephant Knee Buckling

Fig.9 Typical Brittle Failure Modes of Steel Piers



(a) Steel (Tension Side) (b) Steel (Compression Side)



(c) Concrete

Fig.10 Stress-Strain Relation of Steel and Concrete

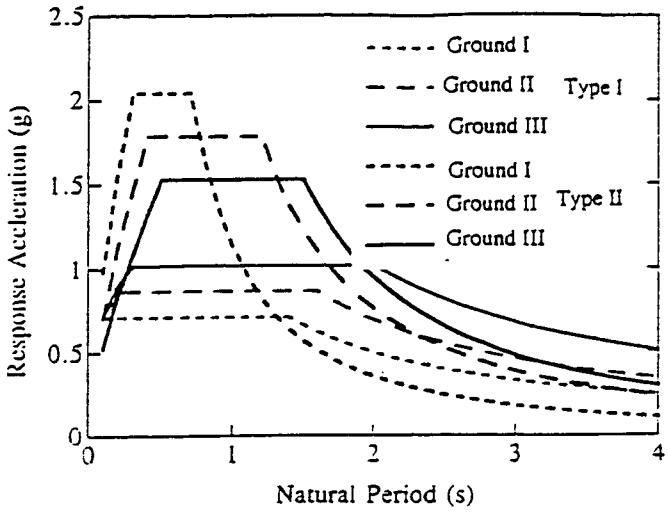
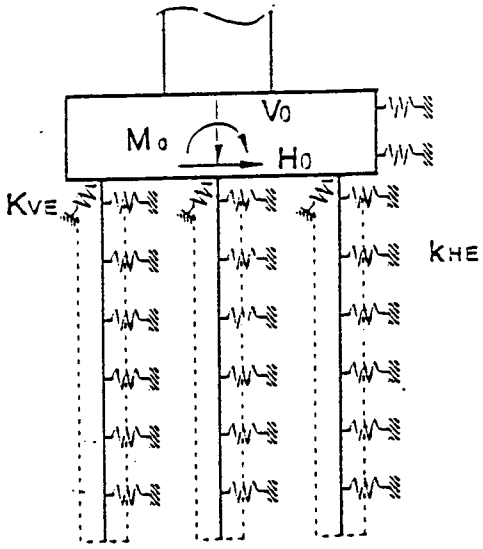
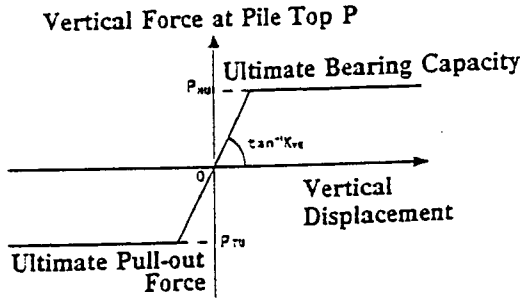


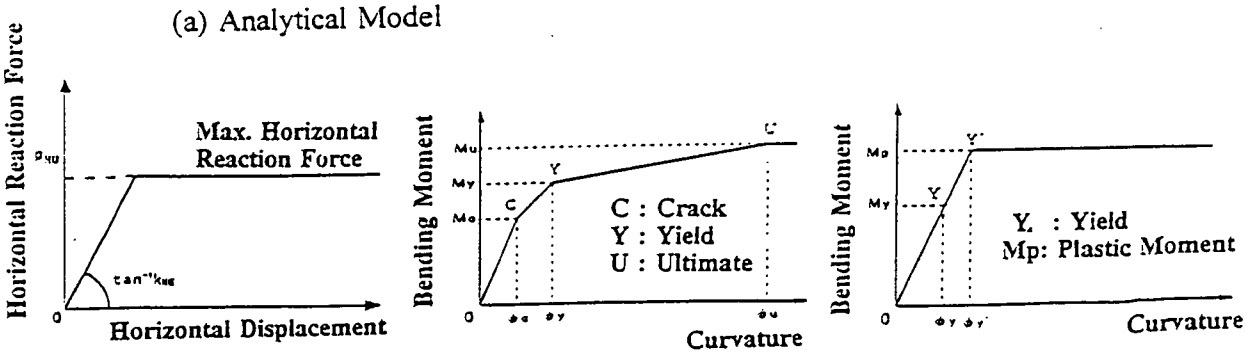
Fig.11 Type I and Type II Standard Acceleration Response Spectra



(a) Analytical Model



(b)Vertical Force vs. Vertical Displacement Relation



(c) Horizontal Force vs. Horizontal Displacement Relation

(d) Moment vs. Curvature Relation of Reinforced Concrete Piles

(e) Moment vs. Curvature Relation of Steel Pipe Piles

Fig.12 Idealized Nonlinear Model of A Pile Foundation

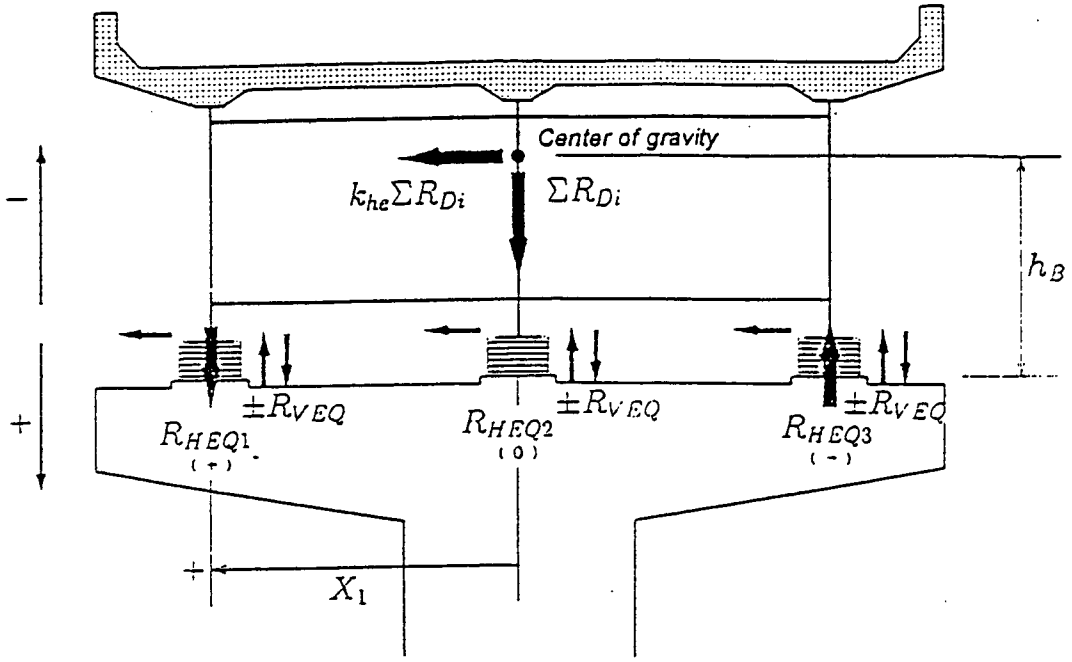


Fig.13 Design Forces for Bearing Supports

Earthquake Strong Ground-Motion Measurement For Public Safety

(Preliminary Procedures for Estimates of the Number and Location of Strong-motion Stations Needed to Significantly Improve Public Earthquake Safety)

by

Roger D Borcherdt*

ABSTRACT

Tragic life and property losses from recent earthquakes dramatically illustrate the need to reduce the impact of future earthquakes to manageable levels. Quantitative measurements of damaging shaking using modern instrument technology provide an important new opportunity for significant progress. Thorough sets of shaking measurements on the ground and in man-made structures are essential for improving earthquake resistant design and for improved emergency response capabilities. A new methodology is based on estimates of the annual exceedance rate and annual population exposure for 0.1g, as inferred from probabilistic seismic hazard calculations. Preliminary estimates derived for the United States and Puerto Rico indicate that as many 7100 ground-motion stations are needed to ensure that the next major earthquake is adequately recorded. The estimates, when considered with corresponding estimates for man-made structures, suggest that major new efforts are needed in some urbanized areas to ensure complete sets of measurements for Public Earthquake Safety.

KEYWORDS

Strong-motion instrumentation, Earthquake hazard reduction, Emergency response, Strong motion, National Seismic Hazard Maps.

1. INTRODUCTION

Staggering losses from recent earthquakes impacting Northridge, California ($15 to $25 billion, 64 lives) and Kobe, Japan (> $100 billion and 5500 lives) clearly demonstrate the potential impact of moderate to large earthquakes on modern urbanized societies. These tremendous potential losses argue strongly for dramatically accelerated programs to improve public earthquake safety as quickly as resources permit. Without such efforts in an ever growing urbanized society the cost and potential impact of a single earthquake disaster can have global consequences.

Reduction of life and property losses to low and manageable levels requires significant improvements in both *Hazard Mitigation* and *Emergency Response*. Quantitative measurements of strong shaking and its effects are the basis for significant progress in both areas. Modern technology offers important new opportunities to acquire and interpret these essential measurements in near real-time for each urbanized area likely to experience earthquake disasters.

This report presents a methodology presented at a workshop concerned with "an action plan for strong-motion programs to mitigate earthquake losses in urbanized areas" organized by the Committee for Advancement of Strong-Motion Programs in Monterey, CA, April 2-4, 1997. The methodology is preliminary and can be improved with more detailed information that might become available in the future such as

* United States Geological Survey
Menlo Park, CA 94025

detailed (1:250,000 scale) geologic maps. The methodology is presented here for evaluation and comment from an international perspective.

2. HAZARD MITIGATION

The collapse of buildings, bridges, and other man-made structures is the major cause of loss of human life and property during earthquakes. The major cause of structural failure and collapse during earthquakes is strong ground shaking. Consequently, reduction of life and property loss requires man-made structures that can resist earthquake-induced shaking levels likely to be experienced during the life of the structure.

Quantitative knowledge of earthquake shaking and its effects on structures can be gained only from instrumental measurements of shaking both on the ground and in the affected structures during the earthquake. Presently, strong motion recordings in the areas of most significant damage from past earthquakes are very limited, with many critical issues concerning the nature of near source motions, soil behavior, and structural response not yet measured for damaging earthquakes. Consequently, billions of dollars are presently being expended to retrofit various public transportation facilities and steel, moment-frame structures for which few actual recordings of strong shaking have yet been measured. Such efforts without complete knowledge of the in-situ shaking performance of the various types of structures are likely to require further improvement and significant additional expenditures in the future.

Comprehensive sets of strong-motion measurements near, on and in structures from the next major earthquake are needed to quantitatively evaluate causes of damage and loss and to develop improved design, construction, and retrofit codes to ensure public safety in subsequent earthquakes. Without instrumentation in place to make such measurements, important opportunities to develop procedures to ensure earthquake resistant structures are missed and costs to rectify the situation in an ever growing urbanized society increase dramatically. Society can not afford to not have the instrumentation in place to accurately measure the next earthquake.

2.1 Instrumentation Estimate on a National Scale for the US

Towards developing an estimate of ground-motion instrumentation required to ensure that adequate sets of measurements are acquired in densely urbanized areas of the United States for purposes of *Hazard Mitigation*, preliminary estimates have been developed for the coterminous US. These estimates, based on recently developed preliminary procedures, have been most thoroughly developed for ground-motion instrumentation. Estimates for structural instrumentation are not yet complete and not provided.

Recent earthquakes emphasize that in order to adequately document ground shaking for purposes of Hazard Mitigation, instrumentation must be located throughout the areas near the earthquake source and the urbanized areas most affected by the earthquake. Rapid variations in the intensity of shaking due to distance and local geologic conditions and in the density of structures and population imply that the density of instrumentation must vary accordingly. In determining the appropriate density for instrumentation, factors considered important were the probability for significant levels of ground shaking and the amount of population exposed to possibly damaging levels of shaking.

Working in conjunction with A. Frankel, probability levels for ground shaking were determined from the calculations for the recent probabilistic seismic ground shaking maps developed for the 1997 NEHRP recommended building code provisions (Frankel, et al., 1996). The probability levels were specified as the annual frequency of exceedance for various levels of peak ground acceleration for the reference ground condition NEHRP site class B/C with shear velocity 750 m/s. The annual frequencies were specified for grid cells of dimension 0.1 degree latitude by 0.1 degree longitude for the entire national map. The

population distribution for the United States was provided by Frankel for the same set of cells.

The first type of area considered important for instrumentation is that for which significant amounts of the population are exposed to possibly damaging shaking levels. These areas are important because they help identify areas for which life and property losses may be concentrated in future earthquakes. More detailed evaluations must await detailed inventories of the built environment.

Estimates of the population exposed to various levels of ground shaking were estimated as the product of the population specified for each cell and the annual frequency of exceedance for a specified level of ground acceleration. One factor considered important in estimating the amount of necessary instrumentation is the amount of population exposed to a specified level of shaking. With the level of shaking chosen at 0.1g, the corresponding amount of instrumentation for each cell was specified as proportional to the amount of exposed population for the cell, with the maximum amount of instrumentation per cell being chosen at 20 for a cell with near maximum exposure. A cell in the San Francisco Bay region for which the maximum amount of exposed population is 5920 was used. Twenty instruments per cell of approximate dimension 100 square km implies an instrument spacing on a grid with elements spaced at about 2.2 km. This spacing corresponds to about 3 wavelengths for horizontally propagating 1 second shear waves in the reference ground condition, "firm to hard rock" and to more than 12 wavelengths for soft soils (NEHRP site class E; Borcherdt, 1994). This spacing does not preclude spatial aliasing, but should permit significant improvements in ground-motion estimation for purposes of earthquake engineering.

The second type of area considered important for instrumentation is that near the source for which ground motions levels might be especially high, but not necessarily densely populated. To ensure that these areas would be adequately instrumented, instrumentation was specified for each cell in proportion to the annual exceedance of peak acceleration at 0.1g, with the amount of instrumentation chosen as 2 per cell for one of the cells with the highest annual frequency of exceedance in the San Francisco Bay region. This specification suggests a instrument spacing on a grid of about 7.1 km or more than 9 wavelengths for 1 second waves in "firm to hard rock" and more than 39 wavelengths in soft soils.

The final estimates of ground shaking were specified for each cell as the maximum of the amount of instrumentation implied by the proportion of exposed population to 0.1 g and the amount per cell proportional to the annual exceedance probability for 0.1 g. The amount of instrumentation implied by this procedure is illustrated for the coterminous US (Figure 1a), and California (Figure 1b). The amounts are summarized by state in Table 1. Instrumentation for cells for which the proportion is less than 0.1 or the grid spacing is about 32 km were not included in the totals. In addition, in order to develop the estimates using Excel 7.0 it was necessary to reduce the number of cells that Frankel used for the entire map (1.5×10^5). This reduction was achieved by using only those cells for which the population exposed annually to 0.1g was greater than 3. This reduction eliminated cells in extremely remote areas such the Sierra Nevada Mountains and some areas in Nevada.

The estimate for the total number of stations in the coterminous United States is 5280 or about 5300 instruments (Figure 1a, Table 1). This number is at best a rough estimate considering the grid element size of about 100 square km. The estimate does not include Alaska, Hawaii, or Puerto Rico. Guesses for these areas are 125, 75, and 75, respectively yielding a total estimate of about 5550 station locations.

The estimate does not account for increased levels of ground shaking caused by amplification effects of local geologic deposits. As a rough guess based on detailed considerations for the San Francisco region, the estimate in areas of soft soils such as San Francisco, Seattle, Boston, New York, Memphis and Saint Louis needs to be

increased by at least 50 percent. A conservative increase of 50 percent to account for soft-soil amplification effects suggests a total number of ground-motion instrumentation stations for the United States of about **7100** (see Table 1). This number though large needs to be considered in the context of population exposed annually, potential losses from future earthquakes, and present retrofit expenditures expected to exceed several billion dollars over the next decade.

For effective evaluations of structural response and failure during earthquakes, thorough and complete sets of measurements are required on a wide variety of man-made structures, including a variety of types of buildings, bridges, and lifelines. Accurate estimates of structures to be instrumented throughout the US can best be derived based on detailed inventories.

One crude estimate for the amount of structural instrumentation might be derived from the number proportional to the population exposed annually to 0.1g. This number for the United States would suggest that about 3500 structures should be instrumented with about 3000 of these being in California. Adjustments to this estimate are easily computed by changing the proportionality constant, derived by assuming that 20 structures per 100 square-km cell with a population of 5920 exposed annually to 0.1g. This number should also be adjusted to account for ground shaking amplification effects.

2.2 Station Estimate on a Regional Scale for the San Francisco Bay Area

Towards a more in-depth evaluation of instrumentation needs, estimates of instrumentation needs based on a specific earthquake scenario. The San Francisco Bay Region provides a good location for such considerations, because of dense urbanization near an earthquake source zone with a large potential for a large earthquake. These estimates are used to evaluate the estimates developed on the basis of the criteria available for national estimates.

2.2.a Station estimate to document ground-shaking variations

To thoroughly document damaging levels of ground shaking, instrumentation must be sufficiently dense to document variations in crustal rupture and source radiation characteristics, variations in shaking due to distance from the source, and amplification effects of near-surface geologic deposits.

Ground motion estimates for a repeat of the California earthquake of April 18, 1906 (Borcherdt, et al., 1995) accounting for variations in local geology are shown for the city and county of San Francisco in Figure 2. These estimates are derived from spectral attenuation relations of Boore et al., (1994, 1995) for an event of M_w =7.7 and the NEHRP site factors specified for the 0.1 g level (Borcherdt, 1994). Superimposed on the map is a grid comprised of square elements of 1.7 km^2 corresponding to 35 stations per 100 square kilometers. This grid spacing corresponds to about a 75 percent increase in the maximum number of 20 stations per 100 square kilometers assigned for site class B/C for the national consierations.

The map illustrates that the station spacing of about 35 stations per 100 km^2 is minimal for providing a thorough record of expected variations in ground shaking in the San Francisco Bay area with its rapid variations in geology. In areas near the margins of the bay with large variations in expected ground motion, the map suggests a more dense spacing is needed. This result suggests that the number of instruments estimated on a national scale also is a minimum estimate. The assumption on which the national estimate is based, implies 42 instruments for the city and county of San Francisco. Figure 2 indicates that a more complete distribution of instruments is needed to thoroughly document expected shaking levels. The distribution shown includes the original 42 stations plus an additional 181 stations.

2.2.b Station estimate to account for geographic distribution of built environment and expected earthquake losses

Instrumentation deployed for hazard mitigation and emergency response purposes must account for the location, nature and magnitude of losses expected to man-made structures. The geographic distribution of residential and commercial losses estimated for a repeat of the 1906 earthquake are shown for the city of San Francisco (Figure 3). The losses as depicted were kindly provided by Risk Management Solutions, Inc. The estimates are based on detailed inventories of the built environment and associated assessed vulnerabilities. The estimated losses are shown in units of $1,000 per approximately ½ city block. Superimposed on the map are two grids with cell size of approximately 1.7x1.7 km^2 and 100 km^2, respectively.

The map shows that the highest expected losses are concentrated in downtown San Francisco. The concentration of especially severe losses in parts of downtown San Francisco suggests that instrumentation in these areas should be relatively dense and not spaced more than several blocks apart. Examination of the spacing implied by the 1.7x1.7 km^2 suggests that this spacing is adequate except for those areas of highest damage expected in downtown San Francisco. The map of expected losses shows that most dense instrumentation assumed for areas of the highest population exposure with soft soils is a minimal estimate. For comparison, this assumption implies about 42 stations for the city and county of San Francisco, while a number considered more appropriate to document ground shaking in areas of high loss for purposes of hazard mitigation is about 110.

3) EMERGENCY RESPONSE

Reduction of loss of life and property immediately following earthquake disasters can be dramatically improved if the location and severity of damages can be rapidly assessed. Modern instrumentation technology now permits such assessments to be made in densely urbanized areas within a few minutes of the occurrence of the event. Such quick assessments can significantly improve emergency response capabilities. Rapid assessments can speed-up treatment of injuries, reduce number of casualties, facilitate evacuations, if flooding or fire are imminent, and permit more rapid and efficient deployment of emergency operations.

Modern instrumentation deployed on the ground permits areas of strongest shaking to be quickly identified. Instruments on structures such as buildings, bridges, freeway overpasses, and dams permit rapid assessment of probable damage state with resultant appropriate dispatch and routing of emergency response resources. Measurements on lifelines such as electric power transmission facilities, gas and oil lines, and rapid transit facilities allow efficient shut down and prevention of additional disaster.

Reducing the time for disaster assessment and resultant emergency response from hours to a few minutes can save untold amounts of life and property. Important examples illustrating the application of modern technology to Disaster Reduction are now being implemented for Yokohama, Japan.

Ground-motion instrumentation deployed for *Hazard Mitigation* purposes, if equipped with rapid communication capabilities, can also serve critical emergency response purposes. The density of station spacing in the Figures 1a and 1b suggests this station density would also be satisfactory in many cases for measuring shaking levels for purposes of emergency response. Equipping selected stations with appropriate telecommunication capabilities could be a cost-effective means of dramatically improving emergency response and thereby reducing the disastrous effects of future earthquakes.

4) ACKNOWLEDGMENTS

Jawhar Bouabid of Risk Management Solutions, Incorporated kindly provided estimates of loss for the City and county of San Francisco California and assisted in the initial display of the ground shaking maps. Arthur Frankel kindly provided calculations of the annual exceedance rates for various levels of ground motion, a corresponding

grid of population values, and considerable discussion and insight with respect to their interpretation. William Joyner graciously provided his valuable insight and thoughts regarding estimation procedures. Gary Glassmoyer helped reduce the size of some very large files to manageable levels for a modern spreadsheet. Each of these efforts are sincerely appreciated. M. Celebi, D. Oppenheimer, and C. Stephens provided helpful review comments.

5) REFERENCES CITED

Borcherdt, R.D., 1994, Estimates of site-dependent response spectra for design (methodology and justification), *Earthquake Spectra*, 10, pp 617-653.

Borcherdt, R.D., Lawson, S., Pessina, V., Bouabid, J., and Shah, H.C., 1995, Applications of geographic information system technology (GIS) to seismic zonation and earthquake loss estimation, *State-of-the-Art Lecture, Fifth International Conference on Seismic Zonation, Procs.*, Nice, France, v. III, *p. 1933-1973.*

Boore, D.M., Joyner, W.B., and Fumal, T.E., 1994a, Estimation of response spectra and peak accelerations from western North American earthquakes: an interim report part 2, U. S. Geological Open-file Report, 94-127, 40 pp.

Boore, D.M., Joyner, W.B., and Fumal, T.E., 1994b, Estimation of response spectra and peak accelerations from western North American earthquakes: an interim report part 2 with insert, U. S. Geological Open-file Report, 94-127, 4 pp.

Frankel, A., Mueller,C., Barnhard, T., Perkins,D., Leyendecker, E.V., Dickman,N., Hanson,S., and Hopper, M., 1996, National Seismic Hazard Maps, June 1996, Documentation, http://gldage.cr.usgs.gov/eq/hazmapsdoc/junecover .shtml.

Table 1. Ground-motion instrumentation estimated for US.

State		Population Ann. Exp. to 0.1g	Instru.~ Ann. Exp. Pop.	Instru.~ Ann. Exc. Rate	Max Instr wrt Pop.Exp. & Ann Exc Rate	Max Instr Incl. Amplif. Effects
Arizona	AZ	190	0.6	6.6	7	7
Arkansas	AR	1,498	5.1	18.0	19	19
California	CA	882,400	2981.1	2528.4	4394	5493
Colorado	CO	56	0.2	0.0	0	0
Connecticut	CT	866	2.9	0.7	3	3
Dist. Columbia	DC	48	0.2	0.0	0	0
Georgia	GA	405	1.4	0.3	1	1
Idaho	ID	786	2.7	24.1	24	24
Illinois	IL	4,447	15.0	31.5	39	58
Indiana	IN	450	1.5	2.1	2	4
Kentucky	KY	977	3.3	16.0	16	24
Maryland	MD	310	1.0	0.1	1	2
Massachusetts	MA	2,133	7.2	1.3	7	11
Missouri	MO	3,579	12.1	24.4	31	47
Montana	MT	937	3.2	62.7	63	63
Nevada	NV	3,534	11.9	100.4	100	100
New Hampshire	NH	250	0.8	0.2	1	1
New Jersey	NJ	8,979	30.3	2.7	30	46
New Mexico	NM	999	3.4	4.3	5	8
New York	NY	9,324	31.5	4.3	33	50
North Carolina	NC	32	0.1	0.0	0	0
Ohio	OH	366	1.2	0.2	1	2
Oklahoma	OK	62	0.2	0.1	0	0
Oregon	OR	10,056	34.0	116.8	123	184
Pennsylvania	PA	2,388	8.1	0.9	8	12
South Carolina	SC	1,871	6.3	14.7	15	22
Tennessee	TN	4,229	14.3	25.3	31	47
Utah	UT	8,385	28.3	38.1	47	71
Virginia	VA	375	1.3	0.1	1	2
Washington	WA	39,348	132.9	245.6	275	412
Subtotal		989,282	3,342	3,270	5,280	6,713
Alaska ~			75.0	75.0	*125*	*188*
Hawaii ~			50.0	50.0	*75*	*113*
Puerto Rico ~			50.0	50.0	*75*	*113*
Total		989,282	3517.2	3445.0	5555	7125

~ Guesses

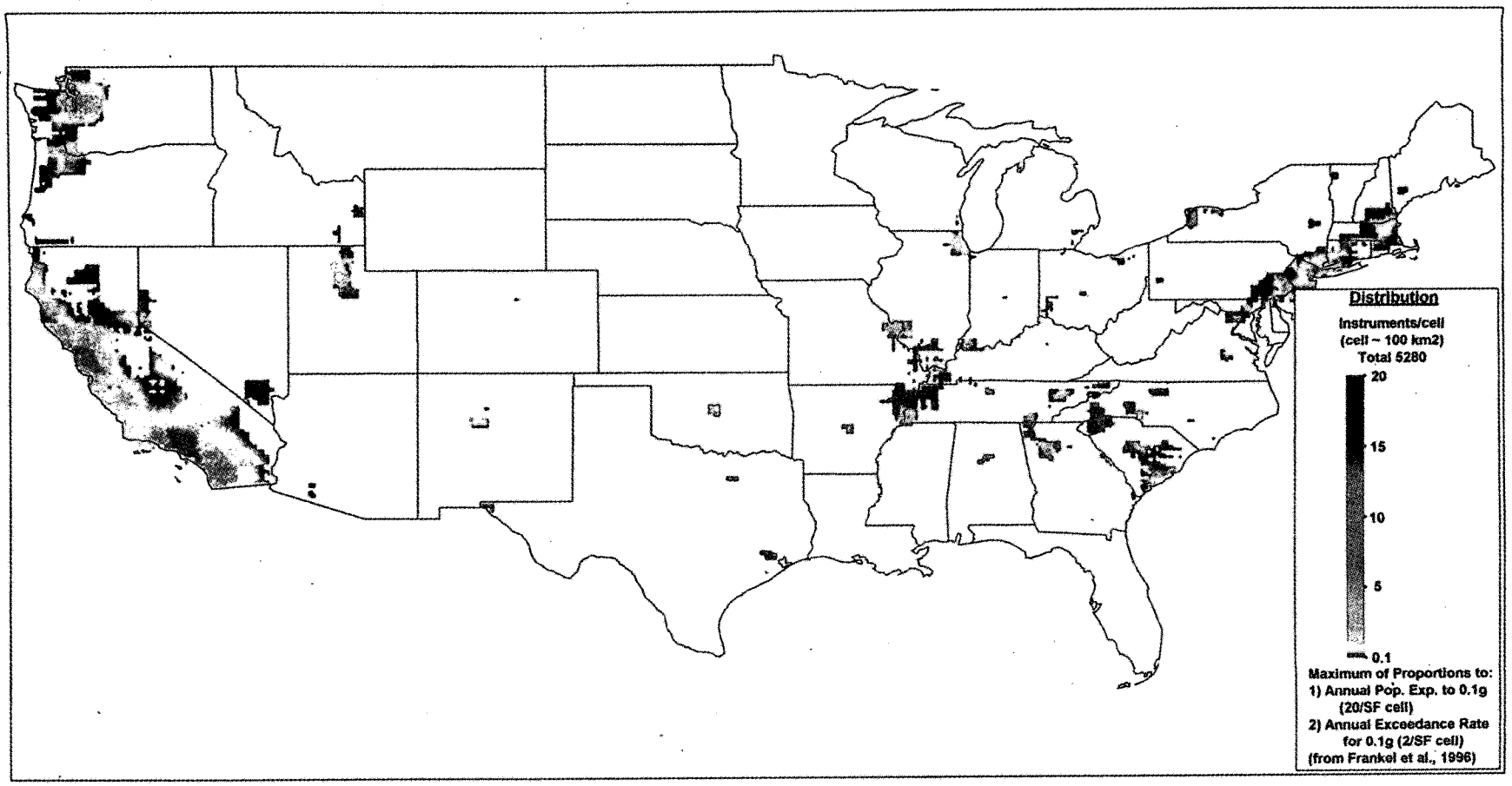


Figure 1. Station distribution for (a) the coterminous US and (b) California and Nevada inferred from the maximum station distribution per 100 square km implied by an estimate of the annual population exposure to 0.1g and annual exceedance rate for 0.1g.

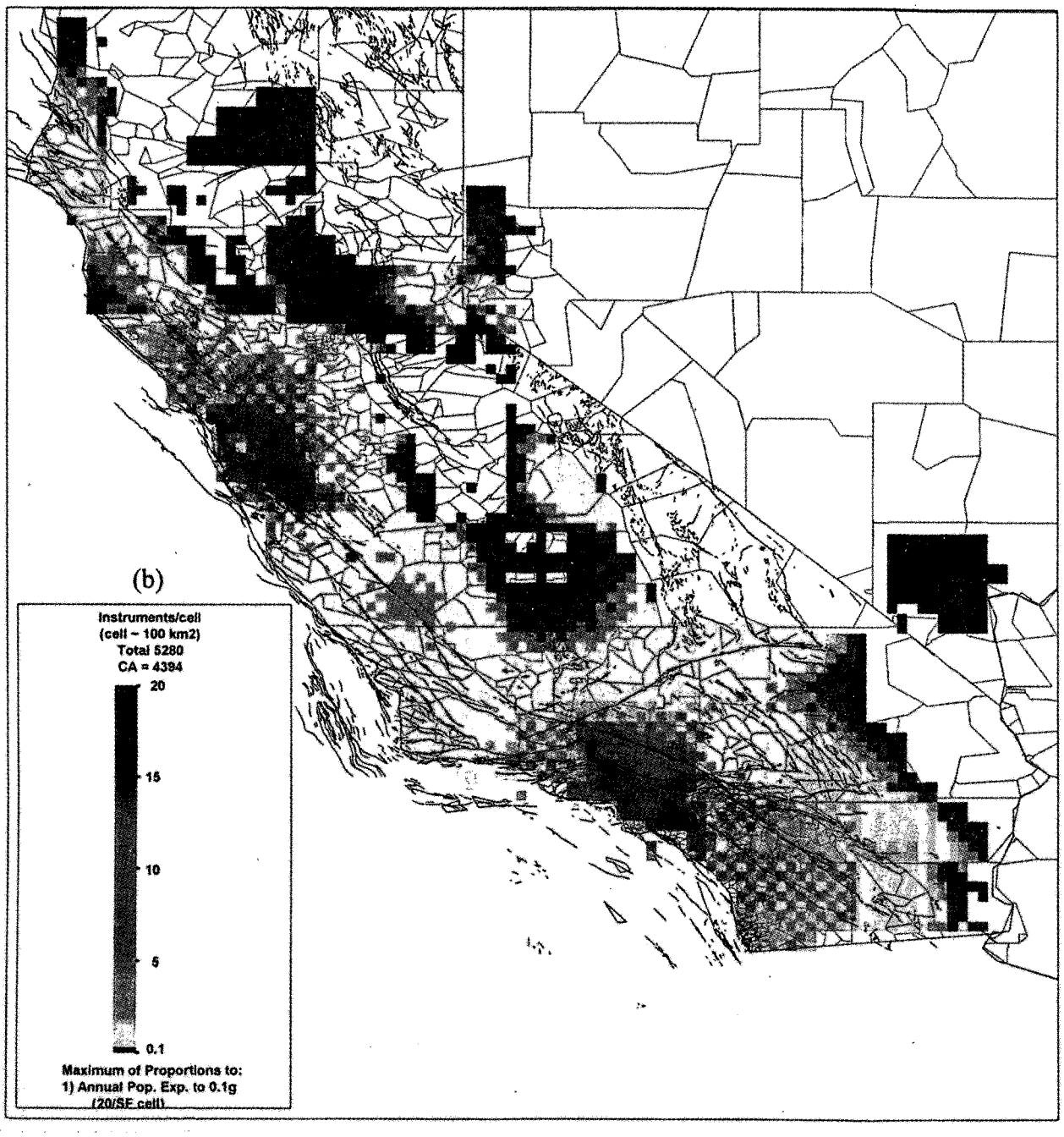
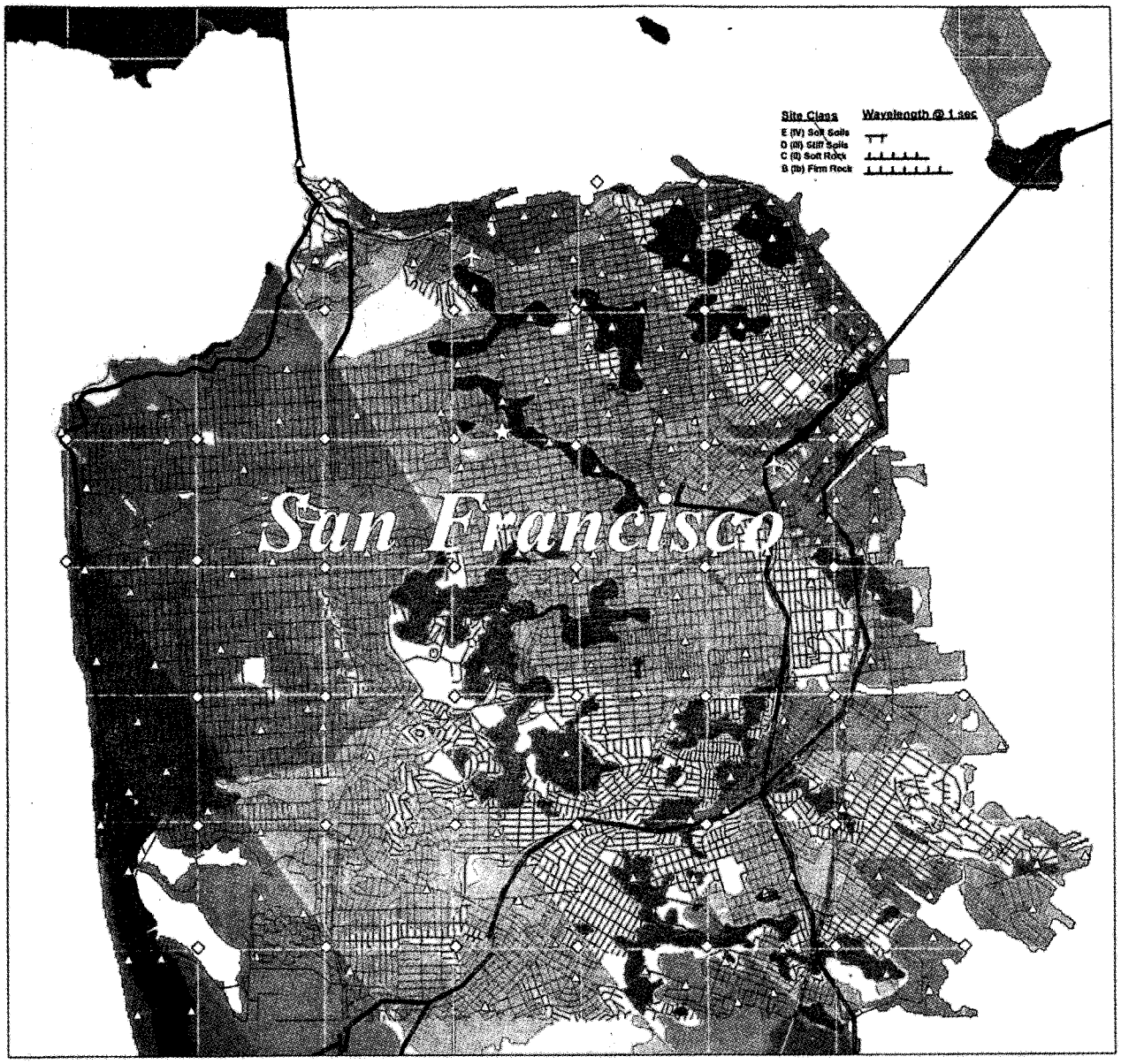


Figure 1b. Station distribution for California and Nevada inferred from the maximum station distribution per 100 square km implied by an estimate of the annual population exposure to 0.1g and annual exceedance rate for 0.1g.



Ground-Motion Measurement for Public Safety (Grid 35 Sm .Sta./100 km2)

Sa 1.0 sec Mw = 7.7 (1906); Census tracts (149), white; Str.mot. sta. (~42+~181), triangle

- 1.39 to 2.6
- 1.19 to 1.39
- 0.99 to 1.19
- 0.79 to 0.99
- 0.59 to 0.79
- 0.39 to 0.59
- 0.19 to 0.39
- 0 to 0.19

Figure 2. Maps showing expected ground shaking for spectral acceleration at 1 second for a repeat of the 1906 earthquake in the city of San Francisco with station distribution of about 35 stations per square 100 km(42 stations) and station distribution

IDNDR ACTIVITIES OF THE WORLD ROAD ASSOCIATION (WRA/PIARC)

by

Toshio Iwasaki[1], Michio Okahara[2], and Kyohei Ito[3]

ABSTRACT

In response to the United Nations proposal on IDNDR, the World Road Association (WRA or PIARC) organized a working group G2 " Natural Disaster Reduction," in 1990. The group conducts various studies on disaster reduction measures for roads in 1990-99. This paper briefly describes the results of its past activities and the future prospect.

Key Words : Emergency Management
Natural Disaster
Repair Methods
Road Disaster
Road Networks

1. INTRODUCTION

Many countries are always facing threat of destruction from natural disaster such as earthquakes and cyclones. In view of this fact, the United Nations declared the period of 1990-99 to be the International Decade for Natural Disaster Reduction (IDNDR), and prosed that special efforts should be made.

In response to the appeal of the United Nations, the World Road Association (WRA or its old nickname PIARC) proposed in 1989 to organize a special working group associated with IDNDR and to make its own action for reducing road-related disasters. Thus, Working Group G2 "Natural Disaster Reduction" started its studies in 1990, with Chairman T. Iwasaki of Japan and some 20 Members from various countries.

In view of the essential roles of road traffic at times of disaster, the Working Group G2 has conducted various investigations including an international survey on road disasters and published a report entitled "Comprehensive Report on Natural Disaster Reduction for Roads," in 1995.

In the Report the results of the international survey, including various natural events causing road disasters in 21 countries, are first introduced, and then pre-event measures for major kinds (landslide, earthquake, flood, and snow avalanche) are described in detail. Pre-event measures here include damage risk assessment, retrofit, and disaster preparedness plans.

Furthermore, repair methods, both temporary and permanent, for severely damaged road structures are illustrated. Disaster preparedness and emergency management such as organization for repair, and emergency survey and emergency operation for avoiding secondary disasters, are also discussed. The Comprehensive Report, consisting of 9 Chapters, are written in English and has a French summary.

2. INTERNATIONAL SURVEY ON ROAD DISASTER

2.1 OUTLINE

The G2 group conducted a questionnaire survey on road disasters in 1991 and 1992,and collected information relating to the likely types of damage to road and road transportion facilities which may cause major socio-economic problems as a result of natural events. The G2 received answers from 21 countries worldwide.

Table 1 shows the numbers of various natural disasters causing major road damage reported from 21 countries, of the 1991-92 survey. From the survey road disasters can be classified into five groups as follows:
1) Landslide, including debris flow, rock fall, and slope failure,
2) Earthquake,

1) President, Civil Engineering Research Laboratory (CRL),4F, Kyodo Bldg, 1-18 Kanda Suda-cho, Chiyoda-ku, Tokyo 101 Japan
2) Director, Structure and Bridge Dept.,P.W.R.I., Tsukuba, 305 Japan
3) Head, Engineering Division, CRL,,1-18 Kanda Suda-cho, Chiyoda-ku, Tokyo 101 Japan

3) Flood,
4) Snow avalanche, and
5)Other hazards: volcanic eruption, tsunami, storm surge, dense fog, heavy snow, strong wind, wildfire, sand accumulation and downburst are examples.

Descriptions of four major disastrous events: Landslide, Earthquake, Flood, Snow Avalanche and related information will be given in Chapters 3 to 6 of this paper. Other Hazards and additional topics will be briefly explained in this Chapter (2.2-2.5).

2.2 EXAMPLES OF OTHER HAZARDS

Volcanoes : Volcanoes erupt molten lava, ash solid (or pyroclastic) fragments, steam and gases when the pressure of dissolved gas becomes high enough to burst the enclosing molten magma. Some eruptions produce mostly lava, which is liquid magma that moves down-hill away from the vent in stream known as lava flows. When lava flows advance and spread over roads, the roads are destroyed and buried by the lava flows. Ash falls also become obstacles to transportation because of deposits of ash on roads and vehicles and darkness caused by ash clouds.

When ashes and other volcanic debris have blocked rivers, major disasters have been caused by the resulting floods and by sudden releases of debris and water that flow rapidly and violently downstream, known as lahars. Mixtures of hot pyroclastic materials and gases erupted from craters sometimes flow very rapidly along steep slopes, known as pyroclastic flows, which may cause damage to road structures as well as casualties.

Table 1 Number of Various Natural Disasters Causing Major Road Damage [1]
(Reported from 21 Countries; 1991-92 Survey)

Country	Landslide	Earthquake	Flood	Avalanche	Other Hazards
Algeria	5	2	4	—	Sand Accumulation
Australia	—	1	9	—	—
Belgium	1	3	5	—	2 Fires, 2 Storms
Canada	5	1	5	—	—
Chile	5	5	5	5	3 Volcanoes, 2 Rainy Seasons
Denmark	—	—	—	—	—
Ecuador	2	2	1	—	—
France	5	—	—	—	—
Finland	1	—	2	—	—
Hungary	—	5	5	—	—
India	5	5	5	—	Cloudburst
Indonesia	3	—	—	—	—
Iran	—	5	5	5	—
Italy	5	7	6	1	2 Dense Fogs, 2 Heavy Snows
Japan	5	5	5	5	Volcano, Tsunami, Storm Surge, Dense Fog, Heavy Snow
New Zealand	4	2	8	1	Volcano
Norway	4	—	4	3	—
Philippines	—	1	1	—	Volcano
Saudi Arabia	1	—	1	—	—
Sweden	3	—	—	—	—
U.S.A.	5	5	5	4	Volcano, 4 Strong Winds
Total	59	48	76	24	7 Volcanoes, 4 Strong Winds, 3 Dense Fogs,3 Heavy Snows,2 Fires,2 Rainy Seasons,2Storms,Cloudburst,Sand Accumulation, Storm Surge, and Tsunami

Tsunamis : A tsunami is caused by seabottom deformation due to a submarine earthquake or landslide along the coastline. A tsunami propagates to the coast like a fast-rising tide, running inland and inundating roads, housing areas or farms. The extent of innundation depends upon the magnitude of the tsunami as well as the topography of the coastal area.

Storm Surges : A severe storm which hits a coast is usually accompanied by a storm surge, i.e., an abnormal rising of water produced by the strong wind pressure and a large decrease in atmospheric pressure. Typhoons and cyclones are generated frequently in the west of North Pacific Ocean and in the Indian Ocean. Coastal areas have suffered an enormous amount of damage, mainly severe inundation of roads, housing and farms, due to storm surges.

Dense Fogs : Fogs appear depending on meteorological and topographical conditions. A heavy fog restricts the visibility of drivers. On expressways, speed restrictions are enforced and sometimes the road is closed to avoid risks of traffic accidents.

Heavy Snows and Blizzards : The visibility of drivers is restricted by blizzards and sometimes stuck in heavy snow. On expressways, speed restrictions are enforced and the road is sometimes closed.

Wildfires : Wildfires such as forest fires sometimes block roads.

Sand Accumulation : In desert areas, sand accumulations may block roads, and drivers may lose their ways.

Downbursts : A mass of air moves down very rapidly and bursts in every direction on the ground surface.

2.3 IDNDR ACTIVITIES IN SELECTED COUNTRIES

IDNDR activities were reported from four countries: Ecuador, France, Japan, and U.S.A. The following summary is as of 1992:

Ecuador : 1) Disaster prevention plan against the phenomenon El Nino.
2) Disaster reduction plan for volcanic eruptions at: Tungu, Guagua, Pichincha, and Cotopaxi.
3) Disaster reduction plan against earthquakes in Esmeraldas and Guayas.

France : France created a national committee for IDNDR that includes three sections:
1) Earthquakes and volcanoes section,
2) Meteorological hazards section,
3) Surface hazards section,
The national projects in these sections are in the process of definition.

Japan : The government headquarters for IDNDR is set up in the National Land Agency headed by the Prime Minister. The Ministry of Construction has established an MOC headquarters for IDNDR, and is now promoting:
1) International cooperation on disaster prevention
2) Disaster countermeasures in Japan, and
3) Information supply and education.

U.S.A. : Aiming at reducing disaster toll, U.S.A. set up the U.S. Advisory Committee on USDNDR. Areas of U.S. activities are:
1) Prediction, 2) Land-use planning, 3) Education, 4) Postdisasater programs, 5) Social science, 6) Intra/Intergovernment issues, 7) Demonstration projects, 8) Basic research, 9) Data handling and Information flow, and 10) International activities

2.4 TECHNICAL ASSISTANCE REQUIRED

Chile, Ecuador, India, Japan, Philippines, and U.S.A. reported technical assistance required.

Chile : Chilean rivers have torrential characteristics and transport a lot of bedload. For the resulting work 14 buldozers are used. The maintenance has been done since 1986, however, the number of bulldozers is too small.

Ecuador : 1) Training of technical staff to manage emergency, referring especially to construction of Bailey type bridges,
2) Geological and technical studies to make maps of risky zones for stability of grounds and road banks, and
3) Study on work for flood control.

India : Exchange of literature on various landslide control techniques, instrumentation, analytical

methods, case histories from other countries.

Japan : Exchange of information and cooperative studies for technical development.

Philippines : 1) Intensive investigation observation of seismic fault activities, earthquakes, and strong ground motions,
2) Reexamination of seismic design standards for bridges, buildings, and dams,
3) Reinforcement of disaster prevention measures,
4) Examination of redevelopment plans for areas where the sinking rate is high,
5) Review of alignment of major roads such as the Kennon road in Baguio city,
6) Establishment of a system for recovery from damage,
7) Countermeasure techniques gainst liquefaction, seismic diagnosis of existing buildings and other structures, and
8) Study of strong vibrations, predictive surveys and the establishment and operation of a strong motion observation network.

U.S.A. : No technical assistance is required as technical resources are already available from a number of public and private sources. A great need is to coordinate these sources in addressing the impact of natural hazards on road development.

2.5 REQUESTS TO PIARC WORKING GROUP G2

Six countries made requests to G2.
Ecuador : Requests are principally about pre-event preventive activities on protection of bridges, coating of riverbeds, work for flood control and slope stability.

France : Collecting information and knowledge on slope stabilization from other countries.

Iran : Presently there is no special request. Any proposals for training courses and workshops, forwarding of information on warning systems and equipment, and any other types of information required for compilation of technical knowledge in the areas of flood, earthquake, avalanche and landslide hazard control would be appreciated.

Japan : 1) To make an arrangement to reserve one or a half page of the bulletin Routes/Roads of PIARC for specific use of the G2 during the IDNDR period, so that the readers can learn large-scale natural disasters related to roads occurred in the world.
2) To hold workshops/seminars on IDNDR by PIARC G2. Those will provide access for members, particularly developing countries, to join in the IDNDR activities of PIARC G2.

Philippines : Earthquake countermeasures are not merely technical issue, but require consideration of economic and social conditions of the particular country. Technical assistance and cooperation plus aid are desired whenever possible. Presently we need help to determine degree of danger to stricken structures brought about by the recent surge of natural disaster (eruption of Mt. Pinatubo), and carry out emergency rehabilitation to minimize the influences of damage to economic activities, since the present situation will be likely to continue for some time.

U.S.A. : 1) To develop, publish and disseminate guidance to mitigate the effects of natural disasters on roads. Typical procedure for prediction, prevention, preparedness and postdisasters assessment are potential study topics.

2) To collect and disseminate the following information from each PIARC member country :
a)National sources of information on natural hazards
b)Past (10 years), present and proposed research efforts pertaining to natural hazard dentification, investigation, and mitigation.
c)Training materials available for courses associated with natural hazard identification, investigation, and mitigation.

3. LANDSLIDES

3.1 GENERAL FEATURES

Landslides include various types of mass movement of rock and soil sliding down a slope, such as slides, flows, failures, and falls. These types are illustrated in Table 2 and Fig. 1. The characteristics and major causes of each type landslide can be described as follows:

Slides are slow movements occurring on slopes with a gradient of 5-30° . They occur mostly in places with particular geology or geological

formations, such as where there is overconsolidated clay or shattered rocks along large tectonic lines. They are also greatly affected by ground water conditions. Most flows are wet and high speed moving masses with a rate of movement more than a few meters per second. Debris flows and mud flows are caused by rainfall or volcanic activities, and occur in valleys steeper than 3° gradient. Slope failures and rockfalls are rapid mass movements where there is a gradient more than 30° . They occur in loose layers such as talus, weathered rock, pyroclastic deposits and well-jointed rocks, and may be triggered by heavy rainfall or earthquake.

Water from rainfall, snow melting, or reservoirs which reduces soil strength is the most general cause of landslides. Cutting slopes or embankments for road construction also reduce slope stability.

Most landslides are caused by heavy rain or earthquake, but in the areas of quick-clay distribution in North Europe and North America, landslides are caused by small changes in slope stability from earthwork or erosion.

3.2 LANDSLIDE EFFECTS ON ROADS

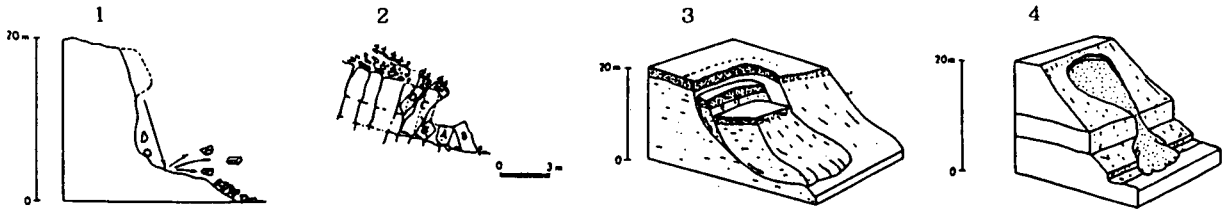
Landslides frequently cause interruption to traffic by collapse of roads or collapsed material from the upper slopes, bridge failures due to debris flows, and direct damage to vehicles from high-speed mass movement such as falls or slope failures.

The effects of landslide-induced road damage on socio-economic activities are village isolation, house relocation, evacuation of persons, increase in prices of commodities, and so on. Well-developed road networks, however, can minimize those effects. The sediment area of a rock fall or small slope collapse is not usually wide, and the damage is mall.

In less developed areas landslides tend to occur many times at the same location in the

Table 2 Classification of Landslide Types [1]

Type of Movement			Type of Material		
			Bedrock	Engineering Soils	
				Mostly Coarse	Mostly Fine
Falls			Rock Fall	Debris Fall	Earth Fall
Slides	Rotational	Few Units	Rock Slump	Debris Slump	Earth Slump
	Translational		Rock Block Slide	Debris Block Slide	Earth Block Slide
		Many Units	Rock Slide	Debris Slide	Earth Slide
Lateral Spreads			Rock Spread	Debris Spread	Earth Spread
Flows			Rock Flow	Debris Flow	Earth Flow
Complex			Combination of two or more Principal Types of Movement		



1) Fall; 2) Topple; 3) Slide; 4) Flow.
Broken lines indicate the original ground surface, arrows show portions of the trajectories of individual particles of the displaced mass.

Fig. 1 Types of Landslides [3]

monsoon or rainy season. Where construction of a temporary road is difficult, long detours have to be used. Continuous movement of a large-scale slide makes restoration and prevention work difficult, and the original route must be changed. A landslide which occurs in an urban area causes damage not only to roads but also to infrastructure along roads, such as water supply and sewer pipes.

4. EARTHQUAKES

4.1 GENERAL FEATURES

When a large earthquake strikes, road networks in the affected area play very important role in providing evacuation routes for victims and transportation routes for staff and materials for repair. This role can be secured by undertaking immediate repair soon after the quake outbreak and making the road networks functional.

The character of damage to roads depends on many factors such as earthquake magnitude, epicentral distance, and geographical and geological conditions. Accordingly, it is difficult to predict every aspect of damage to road structures. Furthermore, for social and economic reasons it is impossible to complete seismic retrofit for all road structures within a short period.

For reducing seismic damage to roads, it is essential to take pre-event measures prior to an event. Pre-event measures include damage risk assessment and seismic retrofit. In conducting retrofit, it is important to consider the social and economic character of the route and the probability of serious disasters due to road damage.

4.2 SEISMIC EFFECTS ON ROADS

Past earthquakes caused varieties of damage to roads. Fig. 2 outlines a classification of seismic damage to roads into three categories: (A) road damage due to ground shaking, (B) effects of damage to auxiliary facilities along roads, and (C) other effects such as those of tsunami and fire which may prevent the use of roads.

Roads are effective when their networks are maintained. Damage to those roads which do not have any detour routes has extensive impacts on social and economic activities of the communities in the vicinity of the damaged sections. When a strong earthquake hits a region and many roads suffer serious damage in a very large area, it is crucial to restore arterial roads going through the region and to make them functional as soon as possible. Until those roads are restored, it is difficult to perform rescue operations smoothly and to repair seriously suffered facilities in the areas.

Duration of repair of damaged roads largely depends on damage type. Table 3 shows a relation between the damage pattern to road sections and the approximate duration to repair and reopen. It is important to notice the following features regarding damage patterns and repair duration:

1) Frequent damage patterns are road surface damage (cracks and bank settling),and slope failures in mountain areas.

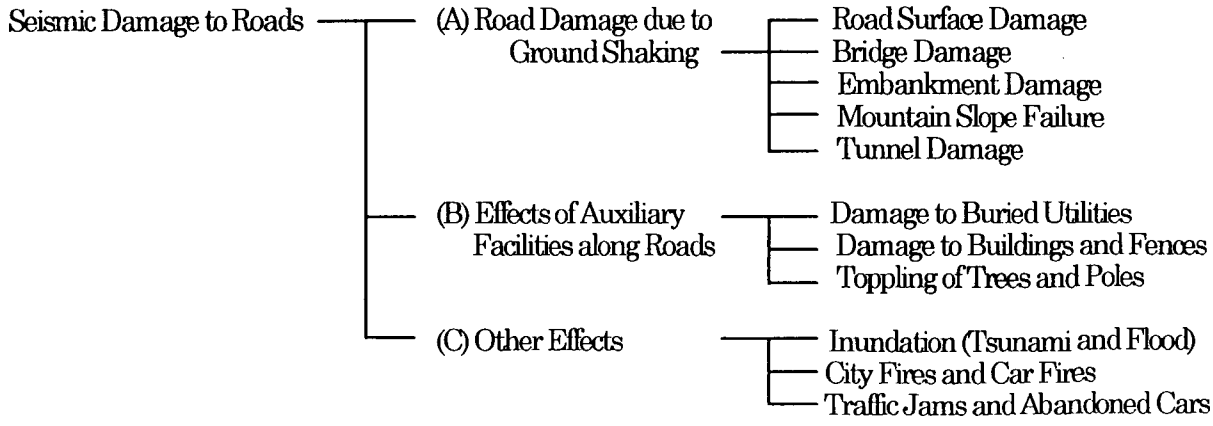


Fig. 2 Classification of Seismic Damage to Roads [1,2]

2) Bridge damage and large slope failure take a fairly long time for repair and reopening.

5. FLOODS

5.1 GENERAL FEATURES

Floods are natural phenomena caused by overflowing of river water due to heavy rain or snow melting. Floods have caused numerous disasters to road facilities such as road embankments and bridge structures in many countries. Besides direct damage to facilities, indirect damage such as disruption of the transportation system has been caused by floods.

Principal types of flood damage to road facilities are catergorized as follows:

1) Interruption of road transportation due to submergence of the road surface.

2) Washout of bridges, road embankments, culverts, and retaining walls.

3) Settlement, inclination or toppling of bridge piers due to scouring. In the worst case, the bridge superstructure may fall.

4) Burying of bridge and road surface by aggrading of the river bed.

5) Break in the road due to diversion of the main river channel.

5.2 LESSONS LEARNED FROM PAST FLOODS

Many countries pointed out the characteristics of damage due to scouring. The following outlines lessons learned from the past flood experiences.

1) Temporary bridge systems, like Bailey bridges, logs and planks, and rolls of wire netting for temporary restoration work with stone sausages or gabions should be kept ready.

2) Existing bridges on pile foundations showed very good stability against floods.

3) Impact from heavy buoyant debris, such as wooden logs, caused more damage to structures than flood water caused.

Table 3 Seismic Damage Patterns to Roads and Time to Repair and Reopen [1,2]

Road Sections	Damage Patterns	Approximate Duration to Repair and Reopen Hours: 1 3 / Days: 1 3 7 / Months: 1 3 / Years: 1 3
Embankment on Flat Plain	Crack, Settling, Bump, Swell	- -
	Collapse (Slide, Flow)	- - - - - - - - - - - - -
Mountainous Road with Steep Slope (Cut and Bank)	Small Slope Failure, Rockfall, Erathfall	- - - - - - - - - - - - -
	Large Slope Failure, Collapse (Slide, Flow)	- - - - - - - - - - -
	Girder Fall	- - - - - - - - - - -
	Superstructure Failure (Movement, Buckling)	- - - - - - - -
Bridge	Failure of Bearing Support	- - - - - - - -
	Crack, Failure of Substructure (Column, Foundation)	- - - - - - - -
	Settling of Approach Bank	- - - - -
Tunnel	Erathfall on Tunnel Entance due to Slope Failure	- - - - -
Lowland Road	Innundation due to Tsunami	- - - - -
Urban Street	City Fire	- - - - -
	Traffic Jam, Abandoned Cars	- - - - -
Auxiliary Systems (Signal, Fence, Pole)	Fall and Toppling onto Roads	- - - - - - - -

4) Until a temporary structure was completed,the additional travelling had a significant effect on the lives of the local population, causing additional travel time and costs.

6. SNOW AVALANCHES

6.1 GENERAL FEATURES

Snow avalanches are phenomena caused by release of snow cover due to meteorological and artificial factors. Avalanches have caused numerous disasters to roads such as traffic blockage, damage to automobiles, and destruction of retaining walls.

6.2 DAMAGE EXAMPLES AND COUTERMEASURES

Typical types of snow avalanche damage to roads can be categorized as follows:

1) Interruption of road transportation due to snow debris on the road.

2) Damage to moving vehicles and to road structures.

The past avalanche damage to roads has indicated the following lessons:

1) Prediction and forecast systems should be established to reduce avalanche damage.

2) Information network systems should be organized to reduce traffic interruption.

The following measures are effective to reduce road damage by snow avalanches:

1) Avalanche-prone slopes should be selected and identified.

2) A study should be made on reasonable criteria for avalanche prevention facilities.

3) Snow cover should be artificially removed from slopes where avalanches tend to occur.
4) Avalanche prevention facilities should be installed.
5) Avalanche forecast systems should be upgraded.

6) Education and training to cope with snow avalanches should be enhanced.

7. REPAIR METHODS

7.1 GENERAL

When roads sustain severe damage from events such as landslides and earthquakes, repair is normally performed in two stages: temporary repair and permanent repair.

Temporary repair implies quick repair on heavily damaged structures to open the particular section for emergency use. Since a primary objective of temporary repair is to restore traffic as soon as possible, various restrictions may be necessary, such as limitations on sections and lanes that can be used, types and weight of vehicles permitted,driving speed, and hours when the road is open to ordinary traffic.

Permanent repair, on the other hand, is reliable repair for which the necessary time and resources can be assigned. In this stage proper methods can be chosen, in view of the kind of damage, future importance, economic considerations, and expected remaining life of structures that need repair.

7.2 ROAD SURFACE REPAIR METHODS

When there are large cracks and major settling of road surfaces, adequate methods for temporary repair should be selected from the following, in order to quickly reopen:
1) Filling with earth and other materials,
2) Filling with asphalt,
3) Filling with mortar 0r concrete
4) Injecting resin,

7.3 BRIDGE REPAIR METHODS

In accordance with the location and type of bridge damage, proper permanent repair methods may be selected from the following examples:

<u>For Foundations</u>:

1) Widening footings and adding piles
2)Construction of underground walls and beams, and steel sheet piles

3) Ground improvement and earth-anchoring
4)Reinforcement with large stones around affected foundations
5) Total replacement

For Reinforced Concrete Structures:

1) Injecting resin, plastics, mortar, or concrete into openings
2) Lining by RC or steel plates around heavy cracks
3) Adding RC shear walls
4) Banding by steel belts
5) Total replacement

For Steel Structures:

1) Concrete pouring into cross section of steel box columns
2) Adding steel plates outside steel piers
3) Lining steel piers by RC
4) Replacing damaged structural members
5) Total replacement

7.4 EMBANKMENT REPAIR METHODS

In accordance with the repair objectives of damaged embankments, appropriate permanent repair methods may be selected from the following:

To Secure Stability against Rainfall:

1) Drain
2) Asphalt curb

To Maintain Traffic Flow:

1) Banking and paving
2) Asphalt seal
3) Asphalt injection into void and opening

To Strengthen Embankments:

1) Banking
2) Construction of retaining walls
3) Construction of frameworks on bank slopes

To Strengthen Supporting Ground:

1) Additional banking on ground near bank feet
2) Soil improvement work such as soil densification
3) Draining underground water
4) Driving steel sheet piles

7.5 SLOPE REPAIR METHODS

In accordance with the principal repair objectives for failed mountain slopes, appropriate permanent repair methods may be selected from the following examples:

To Prevent Erosion, Collapse and Rockfalls at Slopes (Against Rainfall Effects)

1) Draining from surface and underground
2) Spraying mortar and concrete
3) Constructing masonry walls, concrete blocks and concrete walls on slopes
4) Construction of frameworks by precast concrete, cast-in-place concrete and spray concrete
5) Cutting unstable slopes

To Prevent Collapse and Rockfall at Slopes (Against Gravity Effects)

1) Cutting entire slopes
2) Construction of retaining walls by masonry, block or concrete
3) Anchoring slope surface into deeper rock by steel wires, rods, and bolts
4) Construction of frameworks
5) Counterweight fills
6) Preventing movement of unstable rocks by wire ropes and wire nets

To Restrain Movement of Unstable Soil and Rock along Slope Surface

1) Setting railings, of wooden piles and tree branches
2) Driving H-shape steel pile sheets and placing nets
3) Setting wire cages with stones along slopes

To Protect Road Traffic from Collapse and Rockfall

1) Placing wire nets with pocket space for catching falling rocks
2) Setting railings of H-shape steel poles, nets, ropes and expansible metals
3) Retaining walls with catch space
4) Adding covering road with steel or reinforced concrete shelters

8. DISASTER PREPAREDNESS AND EMERGENCY MANAGEMENT

8.1 GENERAL

Disaster reduction measures to prevent or reduce natural disaster to roads and their time phases can be shown as Fig. 3.

Overall measures can be grouped into three phases: regular work, pre-event measures and post-event measures. First, consideration of disaster reduction in the regular work consisting of planning, design, construction, and management is most crucial for mitigating natural hazards to roads.

Pre-event measures include damage potential assessment, retrofit work, and disaster preparedness.

Post-event measures consist of emergency measures (emergency survey and emergency operation) and repair work. Emergency survey is a quick survey to understand the nature and degree of damage to roads and facilities, with objectives of responding to the needs of emergency operation and repair. From the emergency survey the management staff should obtain an outline of all damage concerned.

Emergency operation may consist of disaster-relief aid for rescuing and searching for victims, and also actions for avoiding successive hazards which often follow the original event. Work to close and restrict the use of damaged roads and to install temporary supports for preventing complete collapse or partially damaged structures are typical emergency operations. The emergency survey and emergency operation will often be conducted consecutively as emergency measures.

8.2 PRE-EVENT PREPAREDNESS MEASURES

Vulnerability of Road Network : In addition to damage potential assessment, preevent preparedness measures are also very important.

Road management offices should thoroughly understand the vulnerability of road networks in the region concerned and availability of detours. Future additions of road networks should be considered for areas where most roads, including detours, are likely to seriously suffer from hazards.

Road Management Systems : Road offices should improve management systems with consideration of the following factors:

1) Collection of road damage information
2) Needs for emergency measures and repair
3) Cooperation with construction and materials

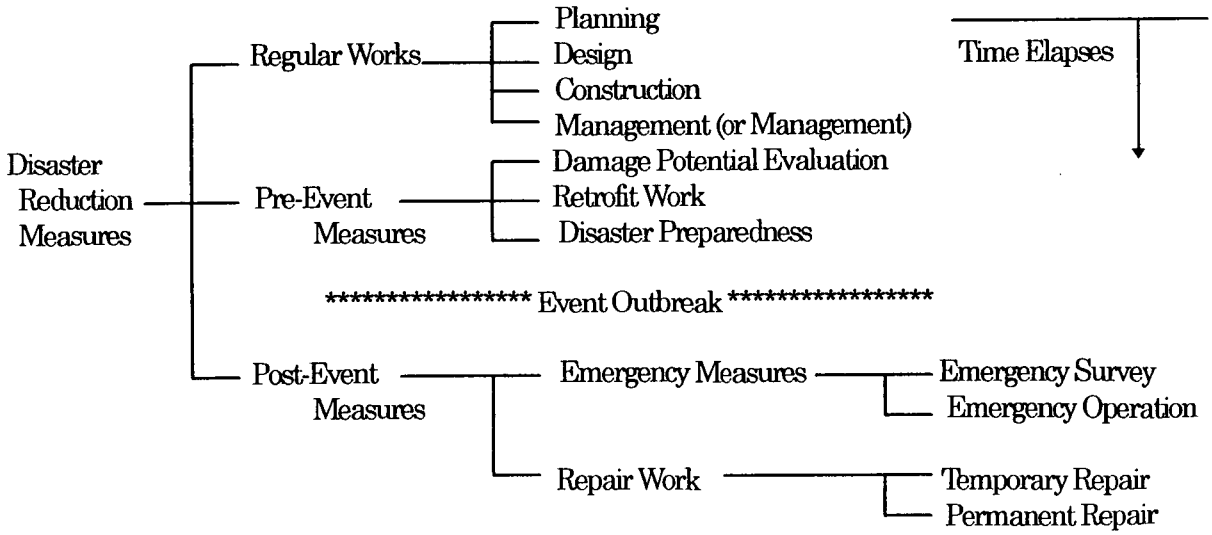


Fig. 3 Disaster Countermeasures and Time Phases [1,2]

delivery industries
4) Consultation with disaster experts
5)Storage of construction materials and equipment for emergency use
6) Call of off-duty staff.

Education, Training and Exercises : Road maintenance staff should be aware of possible results of road damage and the effects on society and on economic activities. Training exercises that assume a hypothetical disaster are effective in getting the staff accustomed to disaster situation. In these exercises an emphasis should be placed on actions to be taken just after road damage, and on procedures for communicating disaster information among the road offices.

8.3 POLICY AND ORGANIZATION FOR REPAIR

Procedures for Repair Work : When a hazardous event causes serious damage to roads and related facilities, some of the following measures should be taken, based on the type and magnitude of the disaster.

1) Call of staff members
2) Setup of emergency organization system
3) Emergency survey and emergency operation
4) Road closures and traffic restrictions
5) Temporary repair
6) Permanent repair

Emergency Organization : For smooth repair of damaged roads, it is effective to set up a special organization which copes exclusively with the repair work. When establishing a special system to cope with a serious road disaster, the following factors should be carefully considered.

1) Assignment of each staff member's role
2) Sufficient staff numbers for field teams
3) System for instruction and information collection
4)Portable communication system between responsible staff members
5) Consultation with experts and supervisors
6) Cooperation with specialized companies
7) Good care of staff health

Repair Plan and Repair Priority : In planning repair of damaged roads, the degree of the entire disaster, characteristics of the affected area, traffic demands, and repair priority should be considered.

Traffic Management : Traffic management should be adequately enforced, taking into account the pattern and degree of road damage. Appropriate control should be selected from different traffic control measures such as (a) complete closure, and (b) partial restriction in kind or weight of vehicles, time of opening, driving speed, lanes to open, or alternating one-way use.

Information Communication and Public Relations : For smooth implementation of repair work it is essential to have a good system for accurate information communication. In communicating with related organization immediately after a serious disaster, public telephones may not be available. In such cases disaster priority telephones, radio phones, or wireless phones may work effectively. Availability and effectiveness of these emergency communication media should be checked during normal times.
It is also important to work on public relations and provide local residents with updated information on road damage and repair prospects. Mass media such as newspaper, radio and television may be effectively employed for this purpose.

8.4 EMERGENCY MEASURES

Emergency Survey : Emergency survey is to obtain an outline of all the damage to road networks. In addition it is crucial to identify damaged portions which have high potential for subsequent complete collapse.

From the emergency survey the necessity to close roads or restrict their use should be judged in view of the relation between degree of road damage and road traffic use. An outline of damage to important structures such as long bridges should also be obtained. It is also essential to transmit the results of the emergency survey to the director at the headquarters office as soon as possible.

Emergency Operation : When serious road damage happens and causes accidents and injuries, the road management office should undertake first aid operations to rescue and search for victims, in cooperation with emergency aid organizations such as police and fire stations.

When damaged portions likely to result in complete collapse are found from the emergency survey, emergency operations such as closure and restrictions of road use, identification of dangerous areas, and warnings to road users should be executed promptly. In this way successive hazards can be avoided.

9. ACTIVITIES FOR THE SECOND TERM (1996-99)

9.1 OUTLINE

In succession to the the above investigations described in Chapters 2 through 8,the G2 Group (with 23 members from 19 countries; Chairman: T. Iwasaki) is now focusing the following 4 topics from 1996 to 1999:

1) Updating the Comprehensive Report
2) Holding G2 Seminars
3) Review of Codes and Guidelines
4) Emergency Planning and Management

9.2 UPDATING THE COMPREHENSIVE REPORT

Leader : H. Aoki (Japan)
Members : G. H. Tsohos (Greece)
R. Medeot (Italy)
T. Iwasaki (Japan)
L. Lefdal (Norway)
V. Cuéllar (Spain)
J. Santamaria (Spain)

Since the international survey done in 1991-92 covered disastrous events up to 1990,the Group is now conducting an updated questionnaire survey on recent road disasters since 1990. The new survey will cover the 1994 Northridge Earthquake and the 1995 Kobe Earthquake, and other major disasters worldwide.

The Group will revise the Comprehensive Report, while referring to the survey results and additional documents to be collect from G2 activities. The new version (to be published in 1999) will include lessons from recent road disasters, hazard potential assessment, new codes and guidelines, emergency planning and management, and so on.

9.3 HOLDING G2 SEMINARS

Leader : G. Pilot (France)
Members : All G2 Members

Several international seminars on natural disaster reduction for roads are organized by G2 Group for selected regions in disaster-prone developing areas. The seminars are devoted to decision makers and engineers working in the field of roads and road transport, who have to deal with natural disasters and their effects on highway infrastructures and road transport.

The seminars also address the effects of natural disasters that occur in many developing countries, such as landslide, earthquake, flood, avalanche, storm, volcano, etc.

One of the objectives of the G2 Seminars is to disseminate and exchange existing knowledge among experts from various disaster-prone countries. Information collected from the Seminars will be used in revising the G2 Comprehensive Report.

The First International Seminar was successfully completed in New Delhi, India, on January 29-31, 1997, with a great support of the Indian Organizing Committee (Chairman: A. K. Gupta, G2 Member). Keynote lectures, invted presentations and discussions were actively made under the following sessions:

1) Inaugural and Plenary,
2) Landslides,
3) Floods,
4) Volcanoes and Cyclones,
5) Earthquakes, and
6) Conclusions.

Some 150 experts participated in the seminar from 14 countries: 8 Asian, 5 European, and Cuba.

Scheduled programs for subsequent international G2 seminars are:
1) 2nd Seminar : For Mediterranean Countries, in May, 1998,
2) 3rd Seminar : For Latin American Countries, in 1998-1999.



Photo 1 PIARC G2 International Seminar in New Delhi, India (January, 1997)

9.4 REVIEW OF CODES AND GUIDELINES

Leader : R. Medeot (Italy)
Members: M. Okahara (Japan)
J. D. Cooper (U.S.A.)

Seismic codes and guidelines of bridges including the following will be reviewed:

1) CEN Eurocode 8, Part 2 (1994, Europe)
2) TNZ Bridge Manual (1994, New Zealand)
3) AASHTO Standards and CALTRANS Bridge Design References (1995, U.S.A.)
4) JRA Specifications for Highway Bridges (Japan, 1995)

The following key aspects will be overviewed and referred in the new G2 Comprehensive Report:

1) Design philosophy and performance criteria
2) Design seismic forces and site conditions
3) Analysis methods and analytical models
4) Design requirements, and
5) Future trends

9.5 STUDY ON EMERGENCY PLANNING AND MANAGEMENT

Leader : V. Cu éllar (Spain)
Members: R. Diaz (Spain)
To be nominated from Africa, Asia, N. America, Oceania, and S. America.

Emergency planning and management is a crucial aspect for mitigating road damage and resulting hazards caused by natural events such as landslide, earthquake, and flood. This group will collect, through the international survey, appropriate information on the following subjects, and compile the results in the G2 Comprehensive Report:

1) Laws and regulations concerning emergency situations
2) Emergency planning and disaster preparedness (pre-event and post-event measures)
3) Emergency management (lessons learned from actual road disasters)

10. CONCLUSIONS

PIARC Working Group G2 " Natural Disaster Reduction," began work in 1990, in response to the United Nations proposal on IDNDR. The G2 conducted various studies including a survey on road disasters, and published the Comprehensive Report [1] in 1995.

From the international survey it becomes apparent that landslide, earthquake, flood and snow avalanche are four major hazards, and that other hazards include volcanic eruption, tsunami, storm surge, strong wind, and wildfire. Road management executives should consider disaster preparedness measures against these effects on road safety.

Road management agencies should take proper disaster reduction measures to protect road networks from natural hazards. Disaster reduction measures can be classified into three categories: regular works, pre-event measures, and post-event measures.

Regular works include planning, design ,construction, and management, which are all important in reducing disaster. Pre-event measures may be:
1) Damage potential assessment,
2) Rretrofit work, and
3) Ddisaster preparedness.

Post-event measures may relate to two different phases: emergency measures (emergency survey and emergency operation) and repair work (temporary repair and permanent repair).

Road planners, designers, engineers, and management staff should take necessary actions regarding disaster countermeasures at each of their work stages. They should have ample knowledge of disaster countermeasures, including laws and regulations, pre-event measures, emergency organization systems, emergency operations, and temporary and per-manet repair methods.

It is also commonly recognized that development of better road networks that can provide detours in case of road blockades, improvement of post-disaster measures for proper repairing of damaged roads, and construction of safer roads are of great importance in promptly reopening traffic and saving communities attacked by disasters.

Exchanges of experiences and technical information on road disasters among various countries should be continued and enhanced, to make contributions to reduction of catastrophic life loss, property damage, and social and economic disruption which can be caused by natural disasters of roads and interruption of road traffic.

It is also recommended that road management agencies in disaster-prone countries consider preparing regulations and guidelines for dealing with natural disaster of roads and related structures, considering their own situations and natural conditions.

Finally the G2 Group will conntinue its work from 1996 to 1999, and publish the new Comprehensive Report in 1999, to distribute at the 21st PIARC World Road Congress to be held in Kuala Lumpur, Malaysia. During this period the G2 will focus on 4 topics:
1) International survey on recent road disasters worldwide, and revising the G2 Comprehensive Report,
2) Holding G2 international seminars,
3) Review of codes and guidelines, and
4) Emergency planning and management .

ACKNOWLEDGMENTS : The authors express their sincere appreciation to G2 members, especially to Messrs G. Pilot, M.Hirano, R.S.Cheney, and H Aoki for their enormous efforts.

REFERENCES :

[1] PIARC G2 (1995): Comprehensive Report on Natural Disaster Reduction for Roads, PIARC Report 72.01.B.
[2] PIARC G2 (1995): Natural Disaster Reduction for Roads, Report of the Working Group, PIARC Report 20.72.B.
[3] Cruden,D..M, Varnes, D.J.(1993), Landslides Analysis and Control Special Report 230, National Academy of Science, U.S.A

PIARC G2 MEMBERS (As of April, 1997) :

Chairman : T. Iwasaki, Japan
Secretaries : G. Pilot, France (Leader)
H. Aoki, Japan (Leader)
Members : Y. Bittencourt, Brasil
N. Sabatakakis, Greece
G. H. Tsohos, Greece
A. K. Gupta, India
K. Zand, Iran
R. Yom-Tov, Israel
R. Medeot, Italy (Leader)
M. Okahara, Japan
A. F. A. Hamid, Malaysia
L. Lefdal, Norway
M. Fierbinteanu, Rumania
V. Cuëllar, Spain (Leader)
J. Santamaria A., Spain
J. D. Cooper, U.S.A.

Corres-ponding Members : R. Plamondon, Quebec-Canada
W . Sanchez G., Cuba
H. Shad, Iran
H. Serim, Turkey
A. J. Burns, United Kingdom
M. Nene, Zaire

Planning and Implementation of a Soil-Structure Interaction Experiment

by

Mehmet Çelebi[1]

ABSTRACT

The significant parameters in developing a soil-structure interaction experiment are reviewed. The parameters were described within five major recommendations determined during a workshop held in 1992. These recommendations of the workshop are presented. The current status of the soil-structure interaction experiment are discussed.

KEYWORDS: soil-structure-interaction, building, shear wave velocity, stiffness, foundation,

1. INTRODUCTION

The objectives of this paper are (a) to introduce the background information in establishing a special purpose array in a seismically active region of the United States to study specifically the effect of soil-structure interaction, (b) to review and define the parameters and details of soil-structure experiment, and (c) to describe the current state of implementation.

In the past, during design/analysis processes of engineered structures, it was assumed that the foundation of a structure was fixed to a rigid underlying medium. In the last four decades, however, it has been recognized that soil-structure interaction (SSI) alters the response characteristics of a structural system. In important engineered structures, detailed numerical and closed-form-solution methods are applied to perform SSI analyses. To date, the strong-motion data from instrumented buildings are insufficient to confirm the validity of the soil-structure interaction analysis methods and procedures as applied to structures other than nuclear power plant structures. Soil-structure interaction procedures are now included in various codes (*e.g.* ATC--3, NEHRP--1985).

Since 1978, during several workshops and technical meetings, specific recommendations have been repeatedly made to instrument a building for soil-structure interaction studies (*e.g.* Lee, 1978; Iwan, 1978; Iwan 1981). As recently as November 4--5, 1991, during the NSF workshop on ``Experimental Needs for Geotechnical Earthquake Engineering," held in Albuquerque, New Mexico, strong-motion instrumentation for soil-structure interaction was given a high priority (Higgins, 1992). U.S. Geological Survey (a) Circular 947 describes a general SSI scheme (Çelebi et al, 1987) and (b) Circular 1079 spells out priority recommendations for special purpose arrays including those that will facilitate soil-foundation interaction studies (Page et al, 1992).

A workshop held in 1992 resulted in a set of recommendations (upon which this paper is

[1] Research Civil Engineer, Earthquake Hazards Team, U.S. Geological Survey, Menlo Park, Ca., USA 94025

based) to define the needs for and the parameters essential for implementation of a soil-structure interaction experiment. During that workshop, beneficial and adverse effects of soil-structure interaction were discussed (Çelebi, Lysmer and Luco, 1992). Prior to this workshop, there have been no meetings that directly addressed the detailing of a soil-structure interaction experiment except the ones related to the critical structures of nuclear power industry [*e.g.* the Lotung Array] (Tang, 1987, Tang et al, 1987a, 1987b, 1990, 1991) .

2. MOTIVATION

Although, currently, there are over 200 instrumented structures in the United States, there is no instrumented structure that will allow detailed calibration and/or confirmation of the validity of the soil-structure interaction analysis methods. The significant sets of data acquired during the 1987 Whittier, 1989 Loma Prieta and 1994 Northridge earthquakes provide insight into structural responses and clearly show that soil-structure interaction took place in several instrumented buildings; however, the data set is insufficient to calibrate soil-structure interaction methods or to quantify the significant parameters related to it. That is, to date, we do not have strong-motion response data from instrumented structures complete enough to carry out detailed studies of the methods and procedures used in soil-structure interaction analyses, and, in turn, assess their impact on design codes and related analysis procedures. Examples of deficiencies in existing instrumented building systems are as follows:

(a) The strong-motion instrumented structures do not have pressure transducers and accelerometers around the periphery of the foundation system (1) to check the horizontal and vertical dynamic pressures and the variation of the forces, and (2) to quantify rocking and uplifting during strong-motion events.

(b) There are no downhole arrays below the foundation or in the vicinity of a building to carry out studies related to vertical spatial variation of motions to calibrate convolution and deconvolution processes and applications. (The only building with a tri-axial downhole instrument is in Norwalk, California. However, the downhole instrument is within a caisson (of a cluster of caissons) only 30 feet below the basement level. Recent data shows that its motion is same as the basement of the building; Çelebi, 1993a and b). The cluster of caissons has altered the soil condition by making it stiffer than it was. Therefore, the foundation and the caissons have very similar motions.

(c) There are no horizontal spatial arrays in the vicinity of a building to specifically study free-field motions and how these motions are altered by interaction with the foundation of a building structure. Specific question as to at what distance from a building the ground motion is unaffected by the interaction of a building has not yet been answered.

3. IDEAL SOIL-STRUCTURE INTERACTION EXPERIMENTAL SCHEME

An ideal layout of arrays that includes soil-structure interaction instrumentation is provided in Figures 1 and 2 (Çelebi etal , 1977; Çelebi and Joyner, 1978). Such a layout should have four main arrays:

1. Superstructure array
2. Soil-structure interaction array
3. Vertical Spatial array
4. Horizontal Spatial array.

These arrays are depicted schematically in both Figures 1 and 2.

4. LOTUNG AND HUALIEN EXPERIMENTS

The most detailed soil-structure interaction (SSI) experiment to date was implemented in 1985 by EPRI at Lotung. The purpose of the Lotung experiment was to facilitate the study of SSI for a 1/4- and 1/12-scale, reinforced-concrete, cylindrically-shaped nuclear power plant containment models under strong ground motion earthquakes (EPRI, 1989; Tang , 1987 and Tang *et al*, 1987a, b 1990). The Lotung experiments provided insight into the SSI response of a very stiff structure (fixed-based frequency on the order of 7--10 Hz and SSI frequency of 2.7 Hz) on an extremely soft soil condition (shear wave velocity of the top layer between 300--1000 ft./sec. (100-330 m/s). The results of the Lotung experiment showed that the response of the structure was mainly in the rocking mode (rigid-body rotation) and that the SSI effect in structural deformation and seismic wave spatial variation under stiffer soil conditions were not addressed. To remedy those shortcomings, another experiment at a stiffer soil site, Hualien, has been implemented (Tang et al, 1991). The shear wave velocity of the top layer at this site is approximately 1200 ft./sec. (~400 m/s). Some of the lessons learned from the Lotung experiment and from the instrumentation schemes of both the Lotung and Hualien arrays can be used in the study of soil-structure interaction for regular building structures. However, the natural frequencies of the containment structures of both the Lotung and Hualien experiments are much higher than those of regular buildings, the subject of the SSI experiment discussed herein.

5. RECOMMENDATIONS OF THE 1992 WORKSHOP

5.1 Recommendation 1: (Needs and Motivation)

A field experiment be implemented to observe the structural behavior of and the soil-structure interaction (SSI) effects for a typical (and regular) building (hereinafter referred to as typical building) during strong-motion earthquakes. This principal recommendation is motivated by the fact that there is still great uncertainty as to the significance of seismic soil-structure interaction (SSI) for typical structures. There may be both beneficial and adverse effects of soil-structure interaction. However, in many cases, SSI is simply ignored in design without establishing whether it will increase or decrease the response of the structure. The additional detailed recommendations to follow provide guidelines for the design of an experiment, which, if activated by a strong earthquake, will remove some of the above uncertainties.

It is necessary to consider what is currently known about SSI effects and what can realistically be observed and analyzed by current methods. For example, it is known that a major manifestation of SSI is a contribution to the rocking motion of the structure and perhaps to local deformations of the foundation of the structure. Thus, the instrumentation should be designed to observe these effects. Observations which can be checked against the results of numerical calculations are much more valuable than observations for which such comparisons cannot be made. Thus, the building, its foundation system, and the site configuration should be relatively simple --- thus the need for a typical and regular building.

The motivations for an SSI experiment can be itemized as:

(a) To improve the state-of-the-art of formulations and procedures for the evaluation of SSI effects.

(b) To provide a clear and useful guidance as to when SSI should be incorporated in the analysis of a building, and, when necessary, how it should be done.

(c) To check the accuracy of numerical prediction of SSI and, in particular, of the rocking of the foundation since there is not yet great confidence in specific numerical predictions of the amount of rocking -- a major contributor to SSI.

5.2 Recommendation 2: (Site Location and Soil Conditions)

The test site should be located in an area with relatively high seismicity, and should be easily accessible for installation and maintenance of the instrumentation.

The following areas are identified by the USGS as having the highest earthquake probabilities (WGCEP, 1988, 1990):

(i) The San Francisco Bay Area [Faults: San Andreas, Hayward and Rogers Creek],

(ii) Southern California (Upland, Redlands, San Bernardino) [Faults: San Jacinto and San Andreas].

In order for the SSI effects to be significant the test site should be a soil site rather than a rock site. Also, the geometry and ground water conditions of the site should be relatively simple such that the incident wave field can be well-defined and analyzed. This leads to the following recommendations:

(a) The site should not be too shallow. Rock should be located at an appreciable depth (*e.g.* more than 50 feet below the foundation level of the candidate structure).

(b) A firm alluvial site is preferable. Such a site would consist of sands and gravels with shear-wave velocities V_s in the range of 500--1000 fps (~150--300 m/s) within the upper 50 feet of the site.

(c) The site should be level and essentially horizontally layered. This is a critical requirement if observations are to be compared with analytical results.

(d) The site should not be liquefiable and should have a stable ground water level.

(e) A detailed site investigation should be performed before the site is selected. The investigation should include several borings to establish stratigraphy, { in situ} shear-wave velocity measurements, laboratory tests on undisturbed samples and ground water observations.

(f) Permanent open space around the building must be ensured for long-term observation of free-field motions. This requirement is a ``must" and the chances of it being satisfied are probably highest if a public building is chosen for the experiment.

5.3 Recommendation 3: (Foundation)

The foundation system of the candidate structure should be as simple as possible and should not inherently minimize SSI effects. Thus:

(a) The preferred foundation type is a stiff box or mat foundation. The contact surface with the underlying soil should be approximately plane.

(b) A 1- or 2-story basement is acceptable. However, the foundation system should not be fully compensated since this will tend to minimize the inertial SSI effects, one of the

effects that is desirable to observe. (A fully compensated foundation system is one for which the weight of the displaced soil is equal to the weight of the entire structure including the basement).

(c) The initial experiment should exclude pile supported structures.

5.4 Recommendation 4: (Superstructure)

It is preferable that a new building (before construction starts) can be identified for instrumentation as part of the SSI experiment rather than using an existing building. It is further recommended that the building (to be instrumented for an SSI experiment) have the following general characteristics:

(a) The geometry and load-carrying system of the structure should be as simple and regular as possible. A building which is symmetric about two axes is preferable. The design of the building should fall within the scope of current seismic design codes. It should also be amenable to accurate analysis.

(b) It is desirable that the structure have different stiffnesses in its two principal directions. However, the aspect ratio of its plan dimensions should not exceed 3 to 1 (preferably 2 to 1). Furthermore, to insure that there is reasonable radiation damping, the building should not be too slender.

(c) The structure should not be too light, since this would minimize SSI effects. A reinforced concrete structure or a steel structure with concrete walls is preferable.

(d) The fixed-base natural period of the superstructure should be of the order 0.5 seconds. This corresponds to a 5- to 10-story building, depending on the building type.

(e) If at all possible, a new, yet-to-be-constructed, building should be chosen. With access to the structure during construction, the load-carrying system of the structure can be clearly defined and instrumentation can be more easily installed. This is especially important if pressure cells or other instruments are to be installed on the external basement walls or in the backfill.

5.5 Recommendation 5: (Instrumentation)

Several types of instrumentation should be employed to record forces, motions and local deformations in the structure and the surrounding soil.

5.5.1. Superstructure Instrumentation:

The main instrumentation in the superstructure should be digital accelerometers with a common time base. Enough instruments should be installed to determine the translational, torsional and rocking motions at least at three levels of the structure, including the base level and the top floor. The exact location of the instruments should be determined only after extensive analytical response studies and ambient and forced vibration tests of the structure. Additional sensors should be installed within the structure to measure story drifts and slab deformations at several levels.

5.5.2. Foundation Instrumentation:

In addition to accelerometers, other sensors (linear variable displacement transducers [LVDT] or other instruments) should be installed to record local deformations of the foundation system. This is especially important if the foundation mat is flexible or if shear walls are founded on independent foundations. It is also desirable to be able to record dynamic contact pressures on basement walls and the foundation slab. Unfortunately, currently

available pressure cells are not reliable for observations that extend over several years. Also, they are virtually impossible to install in an existing backfill. Direct recording of contact pressures may therefore not be practical. It may, however, be possible, and it is certainly desirable, to install rugged instruments that can record wall/soil separation or foundation uplift.

5.5.3. Free-field Instrumentation:

A minimum of three boreholes should be instrumented to record free-field motions. The boreholes should surround the instrumented building and should be located far enough away from all existing and planned structures to ensure that the records obtained are not contaminated by SSI effects. However, the boreholes should not be so far away from each other that incoherency effects destroy the coherency between the motions observed in the different boreholes. At least three triaxial accelerometers should be installed in each borehole: at the surface, at mid-depth, and at a depth deeper than the foundation level of the candidate building. If the bedrock is within a depth of 300 feet (~100 m) an additional instrument should be installed at the soil/rock interface in each boring.

The surface instruments in the three borehole sets will double as a surface array. However, it is recommended that additional surficial instruments be deployed closer to the building to detect any changes in motion due to SSI and/or due to the presence of the backfill.

6. CURRENT STATUS

6.1 Selection of Hardware

In selecting hardware, priority was given to those that will be deployed below and in the periphery of the foundation and basement. These are:

(a) Downhole accelerometers: Triaxial downhole accelerometers have been selected and purchased. The intent is to deploy these immediately below the foundation of the building at least at two but preferably at three vertical locations. In addition, at a distance away from the building, another downhole array containing 2-3 downhole accelerograps will be deployed.

(b) Pressure Transducer Systems: In selecting pressure transducer system, consultations with technical staff of USGS and other institutions led to the concept of combinations of flatjack and differential pressure transducer system (Kilgore, Johnston and Warrick, personal communication, 1996). Figure 3 depicts a conceptual schematic of the deployment of the flatjack and the differential pressure transducer combination system. Several flatjacks will be buried between sand layers below the foundation system and outside of the side walls. Each flatjack will be connected to a valve inside the building. The connection will lead from the valve to a differential pressure transducer (DPT) and a dummy flatjack. Thus differential variation of the pressure below the foundation and on the side walls of the building will be realized. With the use of flatjacks, it will be possible to record the average differential pressure over a larger area than the usually smaller area that pressure transducer covers.

(c) Structural Array Hardware: Currently, we plan to deploy only accelerometers throughout the superstructure. However, laser technology allows deployment of displacement transducers although, at present, these are very costly to acquire

and deploy.

(d) Recording Systems: We intend to use a standard digital recording systems that works on ±2.5 volt signal. The DPT, accelerometers and downhole accelerographs work with this signal.

6.2 Selection of Site

We are in contact with the officials of City and County of San Bernardino. These officials will assist us in identifying a project that is on the drawing table and meets our requisite parameters. We expect this to occur within the next 12 months.

7. MANAGEMENT AND OTHER BENEFITS OF THE EXPERIMENT

When implemented, the experiment will be managed and maintained by the USGS National Strong Motion Program (NSMP). The data acquired through the experiment will be open to all investigators. It is anticipated that the data will be used as key research material related to soil-structure interaction methods. Future workshops may be held to discuss the data and related researches.

8. CONCLUSIONS

This paper present requisite parameters for a soil-structure-interaction experiment. The parameters were established during a 1992 workshop. Current status of the project is described.

9. ACKNOWLEDGEMENTS

This paper is based on input from the participants of the 1992 workshop (USGS – Open File Report No. 92-295 [Çelebi, Lysmer and Luco, 1992]). Guidance and advice provided by J. Lysmer, E. Luco snd J. Roesset and others are appreciated. I designing the pressure transducers systems, B. Kilgore, M. Johnston and R. warrick, all of USGS, provided valuable input. Finally, the author thanks the officials of County ansd City of San Bernardino for their willingness to assist in developing the experiment.

10. REFERENCES

Çelebi, M., Lysmer, J., and Luco, E., *(compilers)*, 1992, Recommendations for a Soil-Structure Interaction Experiment (Report based on a workshop held at San Francisco, Ca on February 7, 1992), USGS, OFR: 92--295, April 1992.

Çelebi, M., and Joyner, W., 1987, Instrumentation for spatially varying ground response integrated with structural response in a seismically active region, PROC., Joint IASPEI/IAEE Working Group on ``Effects of Surface Geology on Seismic Motion," IUGG XIX General Assembly, Vancouver, B.C., August 1987.

Çelebi, M., etal , 1987, Integrated instrumentation plan for assessing the seismic response of structures---a review of the current USGS program, USGS Circular 947.

Çelebi, M., 1993a, Seismic response of two adjacent buildings with downhole and free -field recordings (Part I: Data and Analysis), *Journal of Structural Division*, American Society of Civil Engineers, v. 119, no. 8, pp.2461-2476, August 1993.

Çelebi, M., 1993b, Seismic response of two adjacent buildings with downhole and free -field recordings (Part II: Interaction), *Journal of Structural Division*, American Society of Civil Engineers.v. 119, no. 8, pp. 2477-2492, August 1993.

EPRI, 1989, Proceedings: EPRI/NRC/TPC Workshop on Seismic Soil-Structure Interaction Analysis Techniques Using Data from Lotung, Taiwan, Volumes 1 and 2, EPRI NP--6154.

Higgins, C. J., 1992 (editor), PROC. NSF Workshop---Experimental Needs for Geotechnical Earthquake Engineering, Albuquerque, New Mexico, November 4--5, 1991 (in preparation).

Iwan, W. D., ed., 1978, Proceedings of the International Workshop on Strong Motion Instrument Arrays, May 1978, Honolulu, Hawaii.

Iwan, W. D., ed., 1981, Proceedings of the U.S. National Workshop on Strong-Motion Earthquake Instrumentation, April 1981, Santa Barbara, California.

Lee, K. L., W. F. Marcuson, K. H. Stokoe, and F. Y. Yokel, editors, 1978, Research needs and priorities for geotechnical earthquake engineering applications, Workshop at the University of Texas, Austin, June 1978.

Page, R., Boore, D. M., Bucknam, R. C., and Thatcher, W. R., 1992, Goals, Options, and Priorities for the USGS Earthquake Hazards Reduction Program: 1991--1995, USGS Circular 1079, February 1992.

Tang, H. T., 1987, Large-scale soil-structure interaction, EPRI NP--5513--SR.

Tang, H. T., etal , 1987a, A large-scale soil structure interaction experiment: Part I--Design and construction, SMIRT 9, Vol. K2, 177--182.

Tang, Y. K., etal , 1987b, A large-scale soil-structure interaction experiment: Part II--EPRI/NRC Research Program on Method Validation, SMIRT 9, Vol. K2, 183--188.

Tang, H. T., etal , 1990, Lotung large-scale seismic experiment and soil-structure interaction method validation, Nuclear Engineering and Design, 123, 397--412.

Tang, Y. K., etal , 1991, The Hualien large-scale seismic test for soil-structure interaction research, SMIRT 11, Transactions, Vol. K, August 1991, 69--74.

WGCEP (Working Group on California Earthquake Probabilities), 1990, Probabilities of Large Earthquakes in the San Francisco Bay Region, California, U.S. Geological Survey Circular 1053.

WGCEP (Working Group on California Earthquake Probabilities), 1988, Probabilities of Large Earthquakes Occurring in California on the San Andreas Fault, USGS OFR: 88--398.

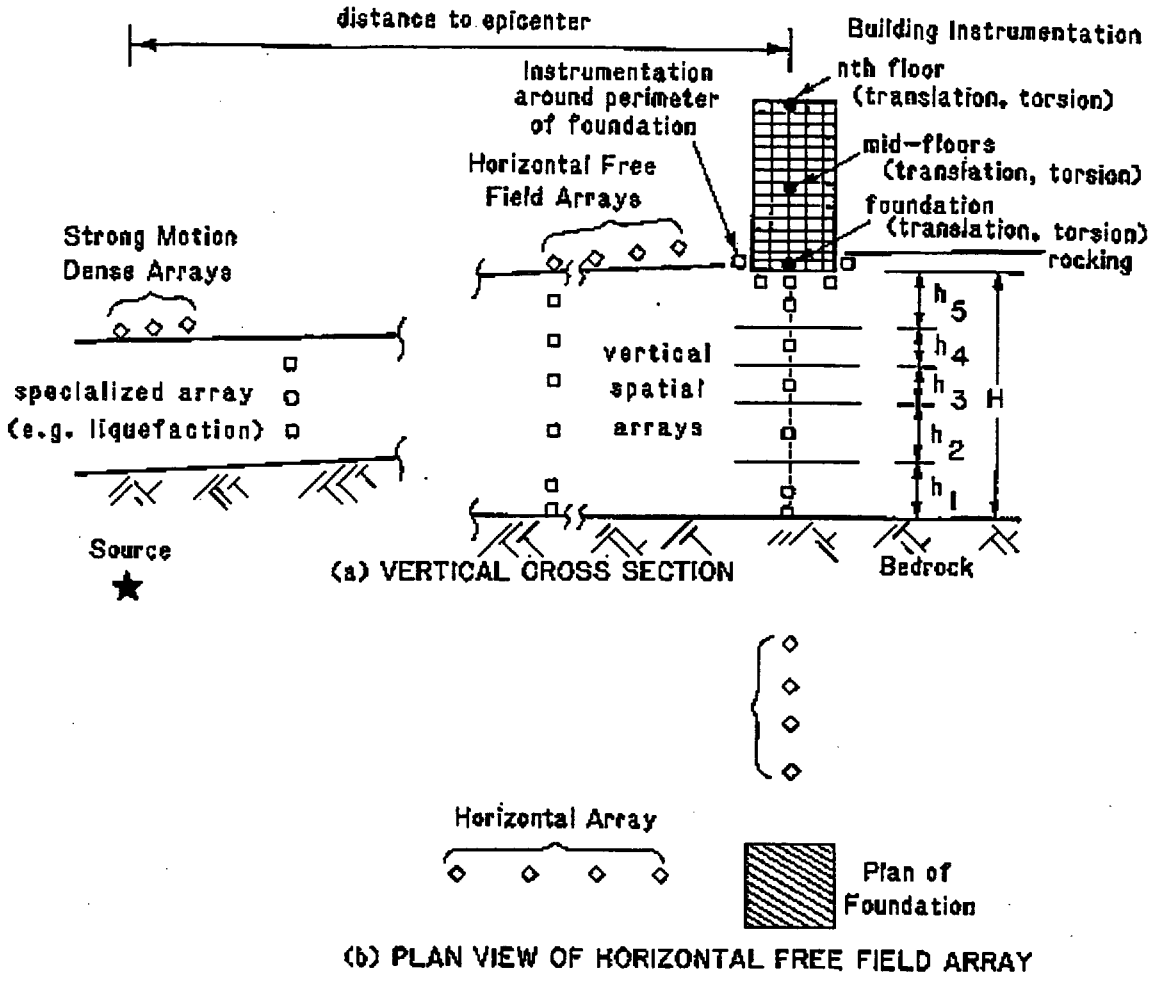


Figure 1. General Description of an Integrated Soil-Structure Interaction Experiment

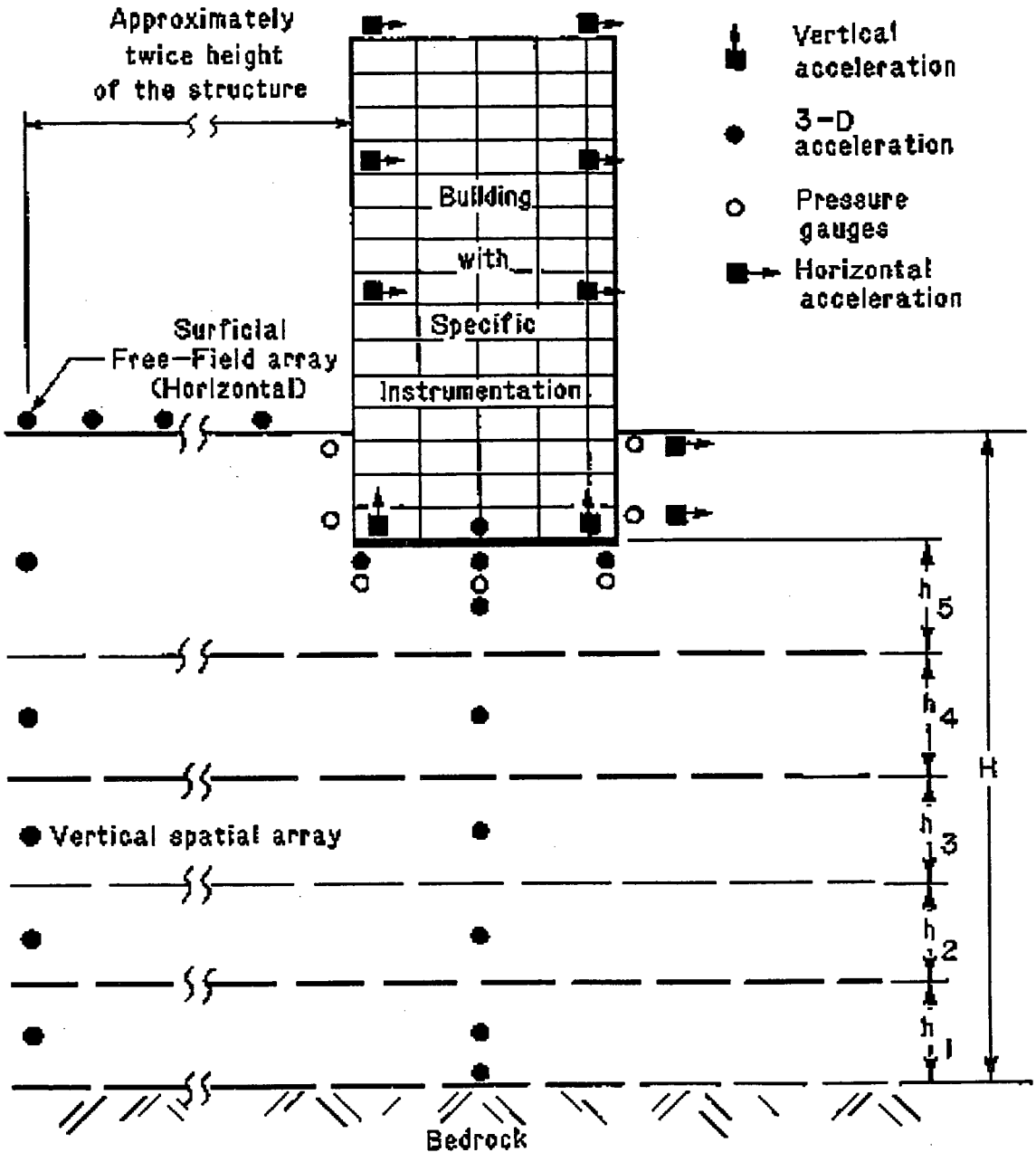
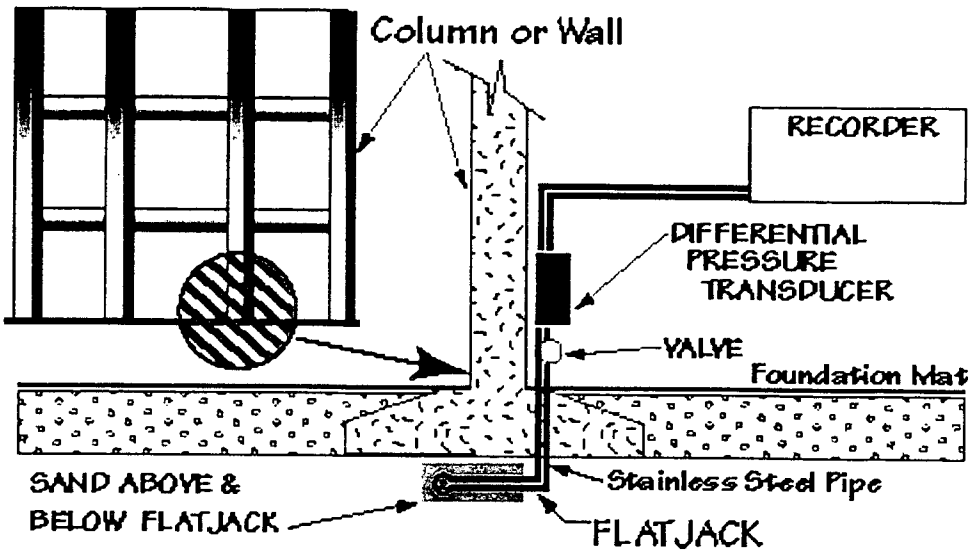


Figure 2. Details of Instrumentation in the Vicinity of the Building, Below and Around the Foundation of Soil-Structure Interaction Experiment



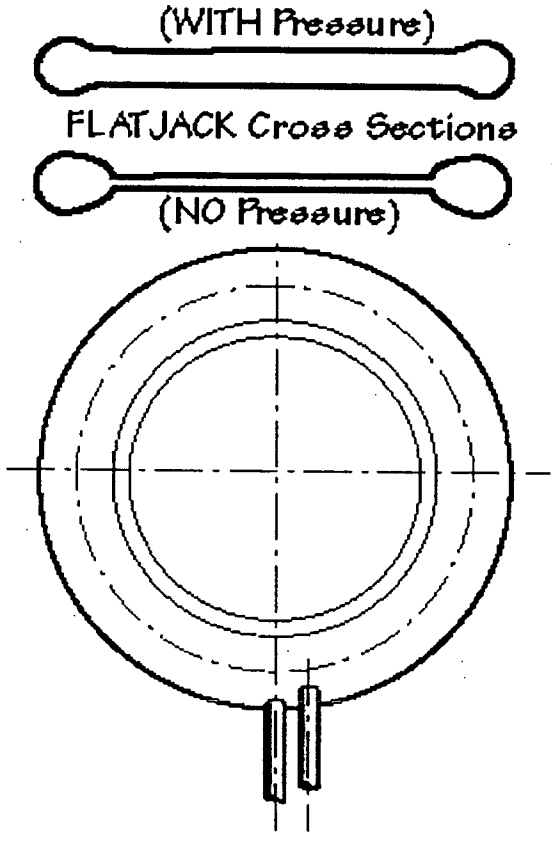


Figure 3. Flatjack and Differential Pressure Transducer Configuration around the Foundation of the Building

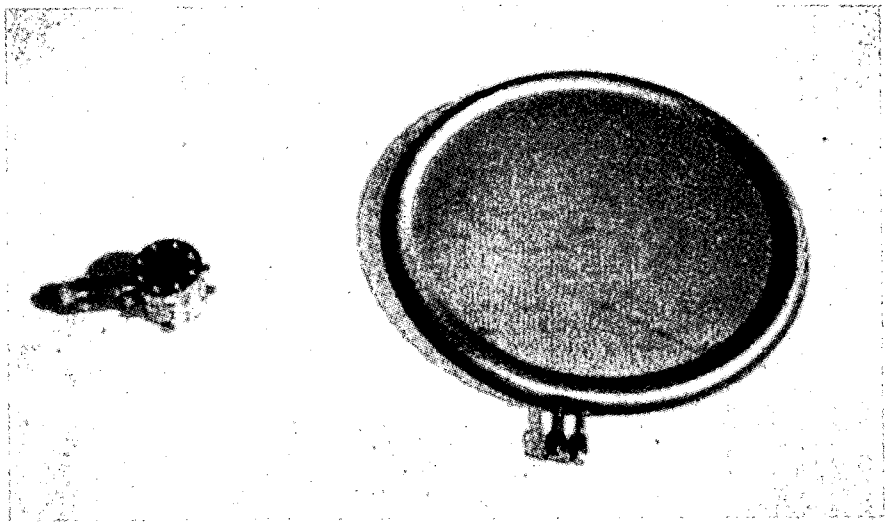


Figure 4. Actual Flatjack (50 cm in diameter) and Differential Pressure Transducer

Deformation Properties of Coarse-grained Materials from Cyclic and Monotonic Loading Triaxial Tests

by

Tsuneo UESAKA[1], Hitoshi YOSHIDA[2] and Tomoya IWASHITA[3]

ABSTRACT

Cyclic and monotonic loading triaxial tests on large-scale specimens of coarse-grained materials with differing relative densities were performed. The effects of bedding errors at the top and bottom ends of specimens were confirmed for coarse-grained materials. As the strain of a soil material is larger, its stiffness decays, which indicates strain-dependency of the stiffness, that is, non-linear properties of the material. The effects of the loading pattern on the testing, the grain shape of materials and the relative density of specimens on the strain-dependency of the Young's modulus of coarse-grained materials were evaluated. The strain-dependency of the Young's modulus of coarse-grained materials was compared with that of a fine sand.

Due to the bedding error, the Young's modulus of coarse-grained materials externally measured from the displacement of a cap was from 5% to 25% smaller than the locally measured ones for this test set. The Young's modulus from cyclic loading (CL) and that from monotonic loading (ML) tests almost agreed for a range of small axial strain less than 10^{-5} (0.001%). The strain-decay of Young's moduli of dense coarse-grained materials from the cyclic loading and monotonic loading tests differed from that of loose ones for a range of axial strain more than about 5×10^{-5} (0.005%). The decay in the Young's modulus of the loose specimens with the increase in axial strain was smaller in the CL tests than in the ML tests. However, the decay in the Young's modulus of the dense specimens with the increase in axial strain was larger in the CL tests than in the ML tests. The strain-decay of Young's modulus of dense coarse-grained materials was different from that of sands.

***Key Words** : bedding error, coarse-grained materials, relative density, triaxial test, Young's modulus*

1. INTRODUCTION

It is important to evaluate the non-linear properties of granular materials such as rockfill and gravel materials during strong quake motions for earthquake response analyses of rockfill dams and structures constructed on a gravel bed. The deformation properties of coarse-grained materials for a range of shear strains less than 0.1% become input material properties for response analyses, and have a

1) Director of Dam Department, Public Works Research Institute, Ministry of Construction Tsukuba Science City, 305 Japan
2) Head of Fill Dam Division, ditto
3) Research Engineer, Fill Dam Division, ditto

significant effect on the dynamic response. As input values, the results by laboratory element tests or in-situ tests have been used. It is essential to improve the precision of the material stiffness measurement from laboratory tests. When axial deformation is measured from the external displacement, the axial strain may be over-estimated due to the bedding error between the ends of the specimen and the cap and pedestal of the triaxial cell. The bedding error occurs due to the looseness at the ends of the specimen and a poor fit between the specimen ends and the cap or the pedestal. The effect of the bedding error is larger for the tests on dense specimens of coarse-grained materials prepared in the laboratory than for tests on fine sands (Tatsuoka et al., 1992). This study confirms the effect of the bedding error for large-scale triaxial tests on coarse-grained materials having angular and round grain shapes. As the strain of a soil material increases, its stiffness decays, which indicates strain-dependency of the stiffness, that is, non-linear properties of the material. The strain-dependency of stiffness is affected by materials, specimen conditions, and testing methods, etc. We evaluate the effect of the loading pattern on the testing, the grain shape of materials and the relative density of specimens on the strain-dependency of Young's modulus of coarse-grained materials. We also compare the strain-dependency of Young's modulus of coarse-grained materials with that of a fine sand.

2. TESTED MATERIALS

The testing was performed with specimens compacted by two kinds (CRR and RBG) of coarse-grained materials. The material CRR consists of crushed gabbro rocks having angular shaped grains and the material RBG is riverbed andesite gravel having round shaped grains. The physical properties of both materials are shown in Table 1.

3. EXPERIMENTAL METHOD

Triaxial tests on large specimens with a diameter of 300 mm and a height of 600 mm were performed. Photograph 1 shows the triaxial testing apparatus used in this study. A load cell installed inside the triaxial cell and combined with the cap of a specimen measured the axial load directly acting on the specimen without including piston friction. The local and external axial strains for a small range were measured. The local axial strains were measured by means of a local deformation transducer (LDT). The LDT is a thin strip of phosphor bronze on which a couple of strain gauges are attached at the central part of each side of the surface. The LDT strip is 500 mm long, 5 mm wide, and 1.2 mm thick, as shown in Photo. 2, and measured the deformation of the central part (approx. 47 cm) of the lateral surface of the specimen excluding the ends of the specimen, as shown in Photo. 3. The external axial strains (EXT) were measured from the displacement of a specimen cap to which a couple of targets were attached, using gap sensors installed on column standings fixed on the base of the triaxial cell, as shown in Photo. 4.

The specimens were prepared by compacting the materials with an electric vibrator in six layers. The specimens were set up in two kinds of relative density Dr of 50% (loose) and 85% (dense) for CRR, only 85% (dense) for RBG. The grain size distribution of the specimens was the same for both materials as shown in Figure 1. The top and bottom ends of the specimens were in contact with a porous stone disk fixed to the cap and pedestal. The

specimens were then saturated until a B-value of at least 0.95 was reached.

Consolidated drained triaxial tests were carried out with two loading patterns of cyclic loading (CL test) and monotonic compression loading (ML test). The cyclic loading triaxial tests (CL test) were performed by staged confining pressure testing in the each stage of which the confining pressure was gradually increased from lower pressure to higher pressure (σ c' = 0.1, 0.2, 0.4, 0.6 MPa). Figure 2 shows a schematic figure of the process of the staged loading. At each loading stage with the constant lateral confining pressure, twelve cycles of symmetric sinusoidal cyclic axial stresses with a constant amplitude of deviator stress were applied at a loading frequency of 0.1 Hz on the specimen. As the stiffness of the specimen, the equivalent Young's modulus Eeq was obtained using the hysteresis loop of the tenth cyclic loading as shown in Figure 3 (a). The data of loads and displacements were filtered for more than 1.0 Hz and less than 0.0001 Hz. In the monotonic loading triaxial compression tests (ML test), a constant axial strain rate of 0.5 %/min was used. At the start of an operation, the loading piston and the triaxial chamber piston were separated to avoid the strain history acting on the specimen during the action of combining the pistons. At the time of the pistons contacting and load acting on a specimen just after the start of operation, the strain was defined as zero. The data of loads and displacements were fed at a sampling frequency of 200 Hz, and were filtered for more than 2.0 Hz. As the stiffness of the specimen, the secant Young's modulus Esec was obtained for each sampling data as shown in Figure 3 (b).

4. RESULTS OF TESTS

(1) Effects of Bedding Error

The effects of the bedding error on strain measurements of gravel obtained from triaxial tests have been reported by several researchers (Tatsuoka et al., 1994, Hamano et al., 1995, and Tanaka et al., 1995). We compared the strain measurements from the LDT and the EXT for the tests on CRR and RBG. Figures 4 show the relationships between Eeq and the single amplitude axial strain (ε a)sa from the CL tests on CRR and RBG, and Figures 5 show the relationships between the deviator stress (σ_1-σ_3) and the axial strain ε a from the ML tests. The Young's modulus Eeq and the deviator stress (σ_1-σ_3) measured by the LDT are greater than those by the EXT for both the CL and ML tests. At an elastic range of (ε a)sa of 10^{-5} or less, the differences of the stiffness are between 5% and 25% for the CL tests on both CRR and RBG.

(2) Comparison of Stiffness from Cyclic Loading and Monotonic Loading Tests

Figures 6 show the strain-decay curves of the Young's moduli Eeq and Esec from the CL and ML tests plotted against ε a for the ML tests and its single amplitude (ε a)sa for the CL tests. For a range of small axial strain less than 10^{-5}, the Young's modulus from the CL test and that from the ML test almost agree for both CRR and RBG. The moduli at the initial small strain are constant, which shows that the deformation behaves elastically.

The rates of decay of the two Young's moduli Eeq and Esec from the CL and ML tests respectively begin to differ for a range of axial strain more than about 5×10^{-5}. On the loose

specimen, whose relative density Dr = 50%, the decay in the Young's modulus with increase in axial strain is smaller in the CL tests than in the ML tests. On the dense specimen, whose Dr = 85%, the decay in the Young's modulus with increase in axial strain is, however, larger in the CL tests than in the ML tests. Figures 7 show hysteresis loops with single amplitude axial strain (ε a)sa of about 2×10^{-4} from the CL tests on specimens with Dr of 50% and 85%. The cyclic strain of the loose specimen moves to the compressive side, so the hysteresis loop is not closed. The equivalent Young's modulus Eeq in Figure 6 (a), thus, is somewhat overestimated, but only by about 3%, and the decay of Eeq is unchanged from the tendency noted above.

Several researchers (Tatsuoka et al., 1994, and Hamano et al., 1994, etc.) have reported the comparisons between the locally measured stiffness of sand from the CL and the ML tests. Figures 8 show the strain decay curves of the Young's moduli, Eeq and Esec, from the CL and the ML tests on loose (Dr = 45%) and dense (Dr = 70%) Toyoura sand which is Japanese fine sand (Tatsuoka et al., 1994). It can be seen from Figures 8 that, on sand also, the Young's modulus Eeq from the CL tests agrees well with the Esec from the ML tests for a range of initial axial strain less than about 10^{-5}. The strain-dependency of Young's moduli Eeq and Esec of sands, however, differs from that of coarse-grained materials shown in Figures 6. Regardless of the relative density of the sand specimens, the strain-dependency of Young's modulus of sand is smaller in the CL tests than in the ML tests for a range of more than about 5×10^{-5}.

Comparing Figures 6 and 8, the strain-dependency of Young's moduli Eeq and Esec of dense coarse-grained materials differs from that of dense sands. The strain-decay of Young's modulus of dense coarse-grained materials is larger in the CL tests than in the ML tests. On the other hand, the strain-decay of dense sands is smaller in the CL tests than in the ML tests. Dong et al. (1994) also reported similar results from the tests on various dense gravels whose Dr is greater than 80%, with the results for this set of tests on both the dense CRR and RBG specimens. Dong et al. explained these phenomena as follows. This difference between the deformation properties of sands in the CL tests and the ML tests is primarily due to the effect of cyclic strain hardening; i.e., the increase in the stiffness due to the change in the structure by drained cyclic loading itself. In the case of CL tests on dense gravels with constant lateral confining pressure, however, due to the high stiffness, as the cyclic strain amplitude becomes large, a reduction in the axial stress (thus the reduction in the mean stress) when loaded in triaxial extension becomes very large. This mechanism overwhelms the effect of cyclic strain hardening. The main reason why the strain-decay of Young's modulus of loose CRR specimens is similar to that of sands is that the effect of cyclic strain hardening overwhelms the effect of a reduction in the mean stress.

5. CONCLUSIONS

The test results of the cyclic and monotonic triaxial tests on loose and dense coarse-grained materials are summarized as follows.

[1] Due to the bedding error, the Young's modulus externally measured from the displacement of a cap was 5% to 25% smaller than the locally measured modulus for this test set on coarse-grained materials.

[2] The Young's modulus from cyclic loading and that from monotonic loading tests almost agreed for a range of initial small axial strain less than 10^{-5}.

[3] The strain-decay of Young's moduli Eeq and Esec of dense coarse-grained materials from cyclic loading and monotonic loading tests differed from that of loose coarse-grained materials. Comparing the results of coarse-grained materials with that of sands, the strain-decay of Young's modulus in cyclic loading and monotonic loading tests on loose coarse-grained materials was similar to those of the sands. The strain-decay of Young's modulus of dense coarse-grained materials, however, was different from that of sands.

REFERENCES

Dong, J., Nakamura, K., Tatsuoka, F., and Kohata, Y. (1994): Deformation Properties of Gravels in Triaxial Compression Tests and Cyclic Triaxial Tests, Pre-failure Deformation of Geomaterials, Balkema, pp.17-23.

Hamano, M., Toriihara, M., Hirama, K. (1994): Comparison Between Static and Dynamic Modulus of Deformation Using Small Strain Gauge, Proc. of the 29th Japan National Conference on Soil Mechanics and Foundation Engineering, The Japanese Society of Soil Mechanics and Foundation Engineering, pp.763-764.

Hamano, M., Toriihara, M., Hirama, K. (1995): Dynamic Deformation Properties of Gravel Changed Grain Size Using Small Strain Gauge, Proc. of the 30th Japan National Conference on Soil Mechanics and Foundation Engineering, The Japanese Society of Soil Mechanics and Foundation Engineering, pp.957-958.

Tanaka, Y., Kokusho, T., Okamoto, T., Kudo, K. (1995): Effect of Non-uniformity on Dynamic Deformation Properties of Gravel, Proc. of the 50th Annual Conference of The Japan Society of Civil Engineers, Vol. Ⅲ, pp.460-461.

Tatsuoka, F., and Shibuya, S. (1992): Deformation Characteristics of Soils and Rocks from Field and Laboratory Tests, Report of the Institute of Industrial Science, The University of Tokyo, Vol.37 No.1.

Tatsuoka, F., Teachavorasinskun, S., Dong, J., Kohata, Y., and Sato, T. (1994): Importance of Measuring Local Strains in Cyclic Triaxial Tests on Granular Materials, Dynamic Geotechnical Testing, Vol. Ⅱ, ASTM STP 1213, pp.288-302.

Table 1 Properties of the tested materials

		CRR	RBG
Density of soil particles	ρ s (g/cm^3)	2.93	2.56
Water content	w (%)	0.54	1.03
Maximum void ratio	emax	0.569	0.432
Minimum void ratio	emin	0.142	0.167
Maximum grain size	Dmax (mm)	63.0	63.0
50% passing grain size	D50 (mm)	10.2	10.2
Uniformity coefficient	Uc	30	30
Grain shape		angular	round

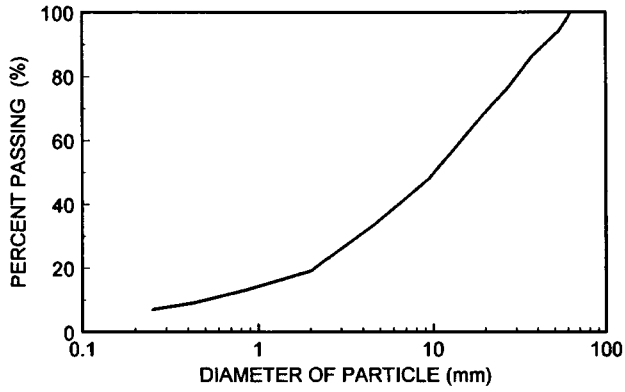


Figure 1 Grain size distribution curve of the tested materials

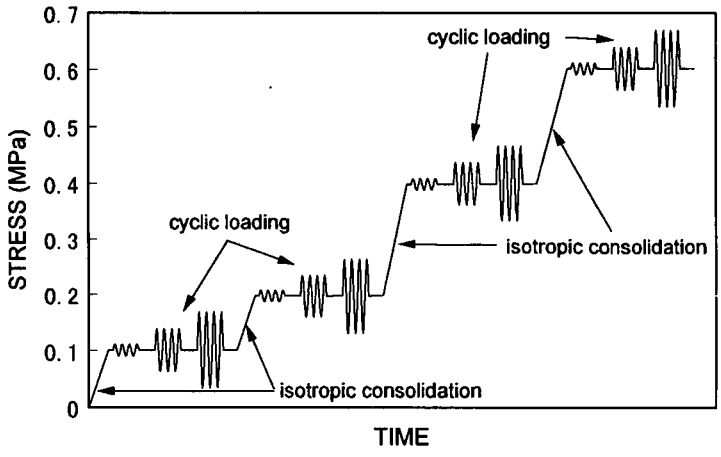
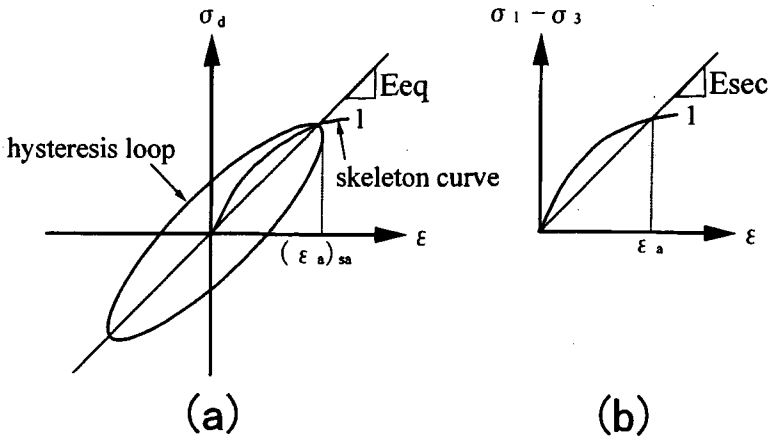
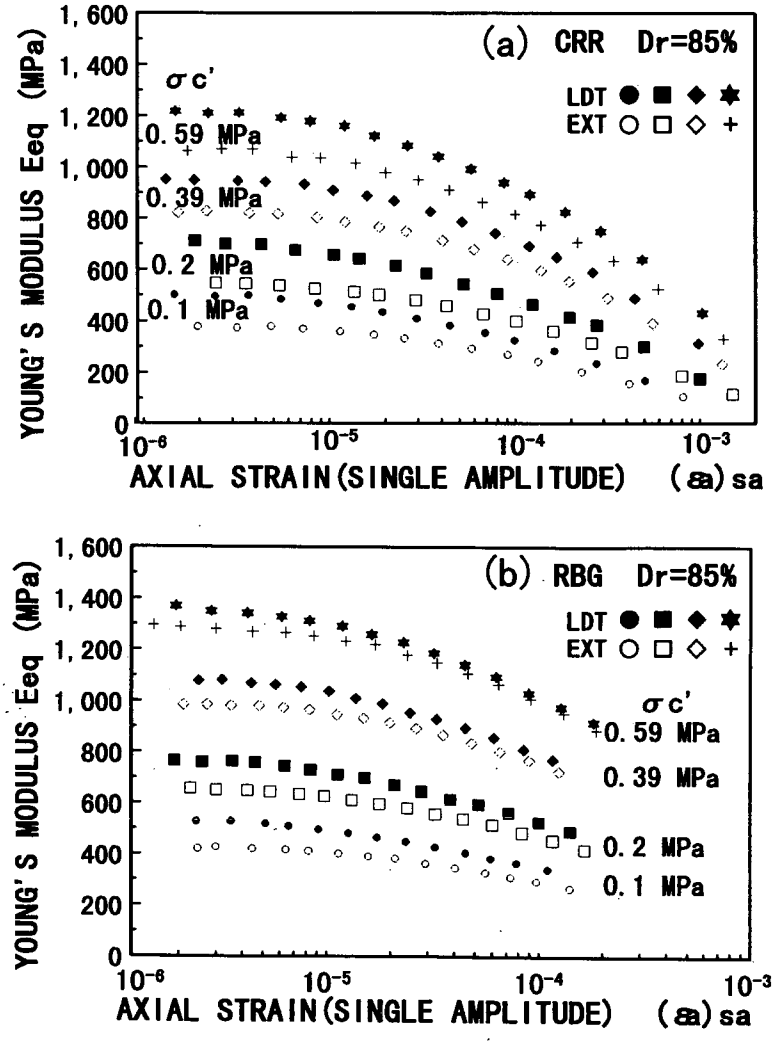


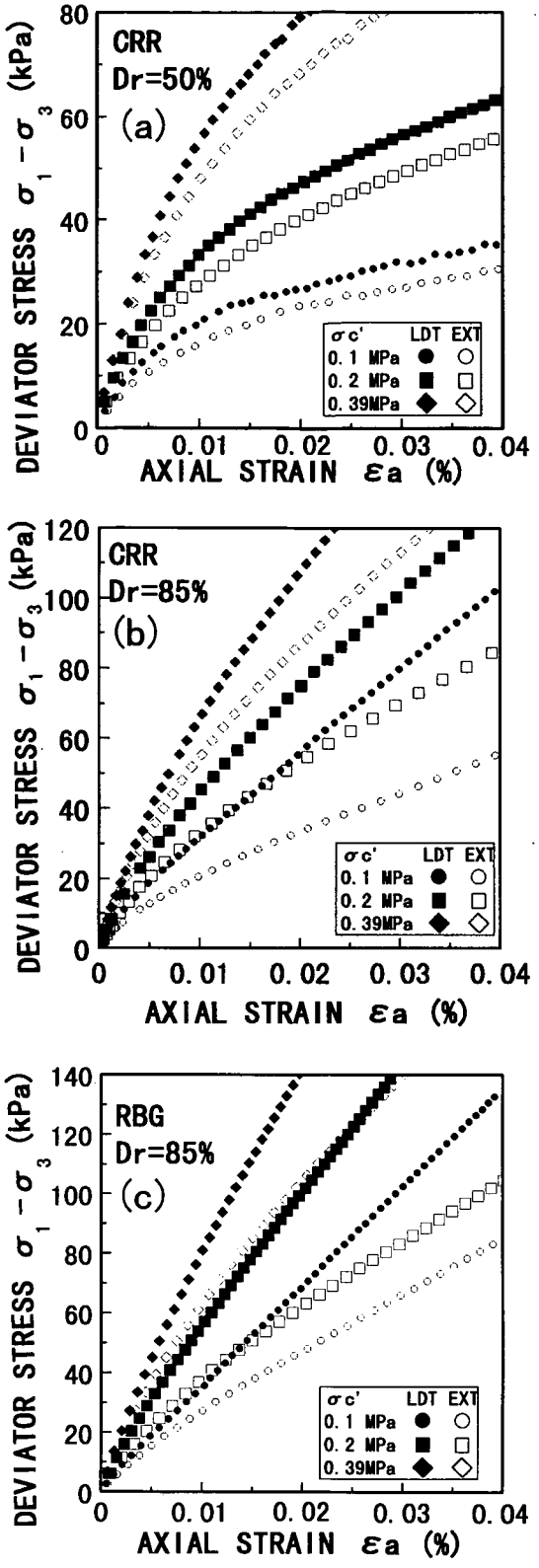
Figure 2 Illustration of process of cyclic loading test



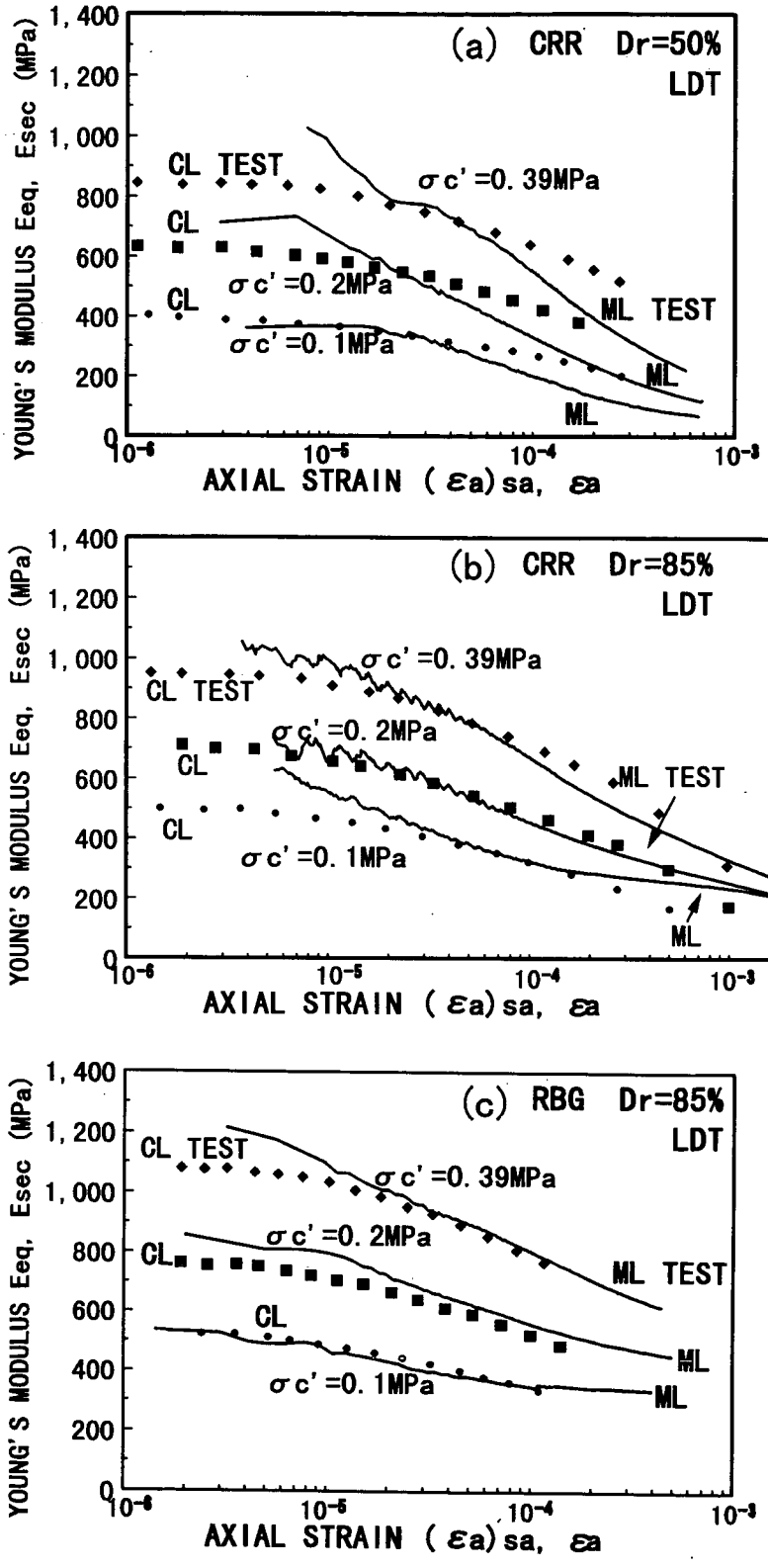
Figures 3 Definitions of Young's moduli from (a) cyclic and (b) monotonic loading



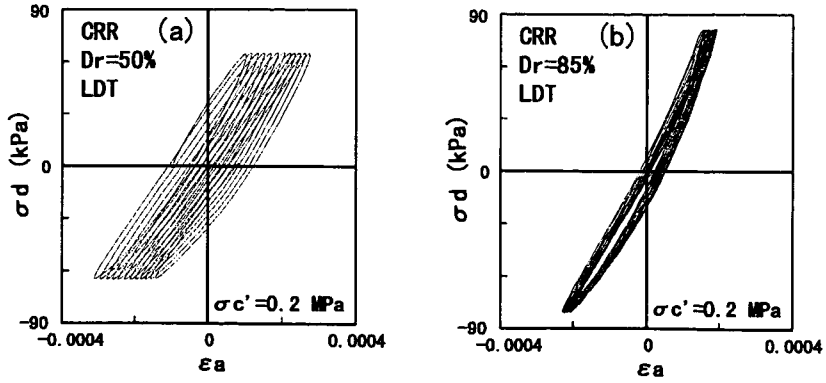
Figures 4 Comparisons of Eeq ～ (ε a)sa measured locally and externally in cyclic loading triaxial tests; (a) CRR and (b) RBG



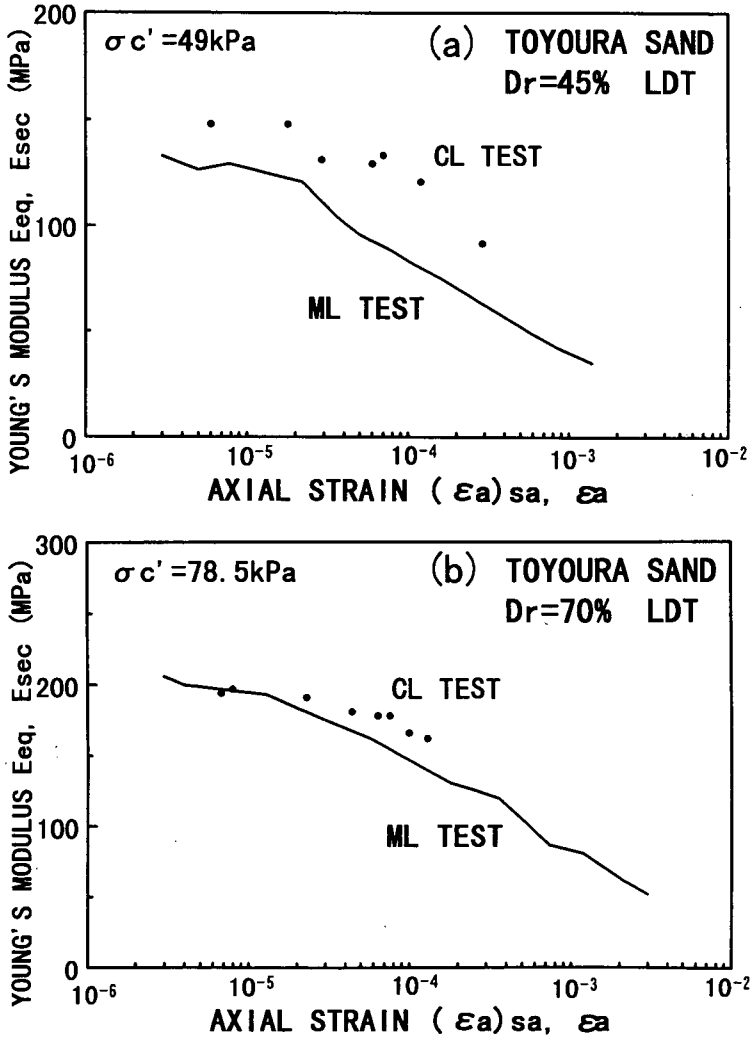
Figures 5 Comparisons of deviator stress ～ ε a measured locally and externally in monotonic loading triaxial tests; (a) loose CRR and (b) dense CRR



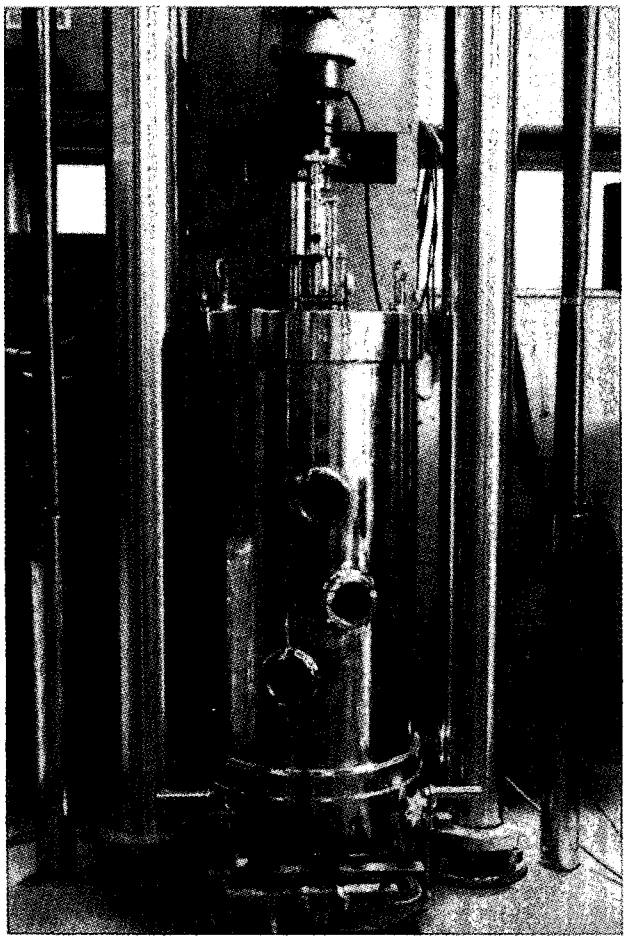
Figures 6 Comparisons of Eeq～(ε a)sa from cyclic loading tests and Esec～ε a from monotonic loading tests; (a) loose CRR, (b) dense CRR, and (c) dense RBG



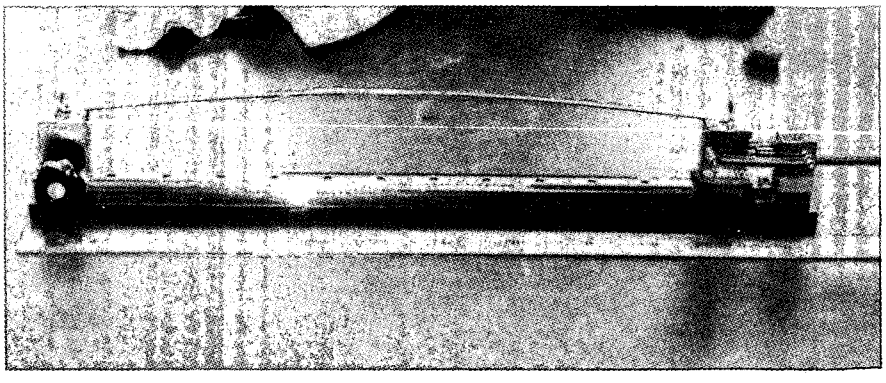
Figures 7 Hysteresis loops from cyclic loading tests at (ε a)sa = 2×10^{-4} ; (a) loose CRR, (b) dense CRR



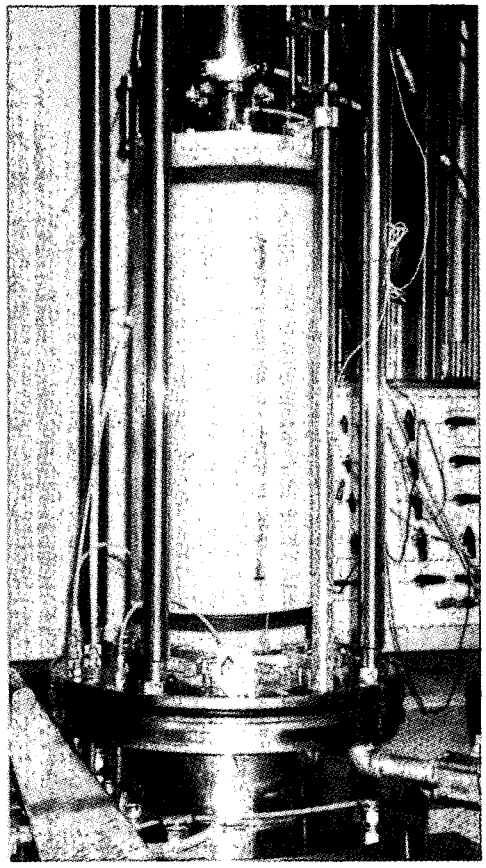
Figures 8 Comparisons of Eeq～(ε a)sa from cyclic loading tests and Esec～ ε a from monotonic loading tests;(a) loose Toyoura sand and (b) dense Toyoura sand (Tatsuoka et al., 1994)



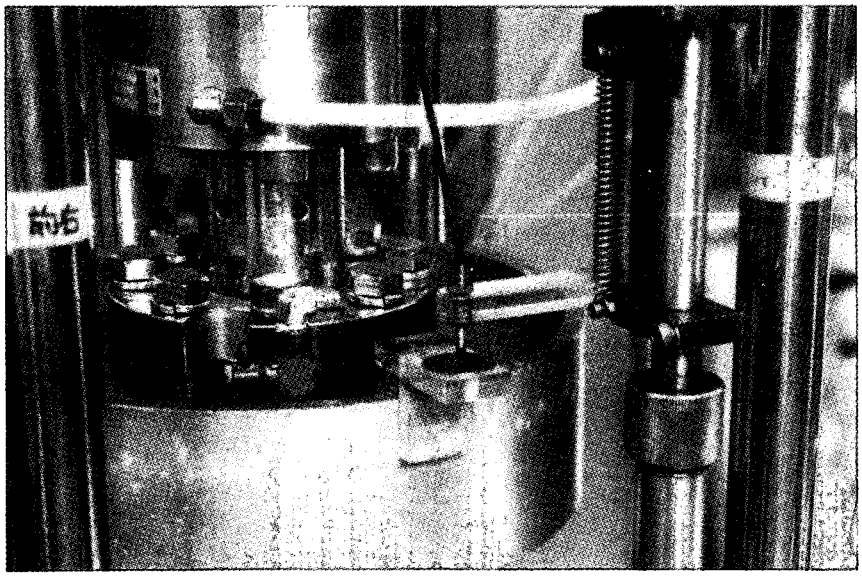
Photograph 1　Large-scale triaxial testing apparatus



Photograph 2　Local deformation transducer (LDT)



Photograph 3 LDT attached on the side of a specimen of coarse-grained materials



Photograph 4 Gap sensor and target attached on the top cap of a specimen

MODELING DYNAMIC FIELD PHENOMENA WITH THE ARMY CENTRIFUGE

by

R.S. Steedman[1], W.F. Marcuson III[2] and R.H. Ledbetter[2]

ABSTRACT

The U.S. Army Engineer Waterways Experiment Station (WES), located in Vicksburg, Mississippi, has recently installed a uniquely powerful and large centrifuge. Although much of the recent world-wide interest in centrifuge modeling has concentrated on geotechnical problems, the new WES centrifuge facility will address research needs in physical modeling across the full range of engineering applications. The purpose of this paper is to describe the WES centrifuge, to discuss current research being conducted in the centrifuge facility and our vision for the future. The research described here will focus on field problems involving dynamics particularly earthquake work and blast loading. However, the WES centrifuge is uniquely broad-based in its research applications; many types of field problems, involving fluid-flow, heat transfer, and cyclic and static loading are being addressed in a wide range of fields: geotechnical, structural, environmental, hydraulics, coastal engineering, and engineering for cold regions. Some initiatives in these areas are also described.

KEYWORDS: centrifuge; physical modeling; dynamic loading; earthquake engineering; blast phenomena; groundwater; cold regions; dredge material; contaminant migration

1. INTRODUCTION

The WES has a long history of physical modeling. Its pioneering research in the early 1930s in areas of hydraulics engineering and flood control used scaled physical models carved in the loess soil. Hydraulic physical modeling experiments which replicated such historic locations as the Los Angeles Harbor, the New York Harbor, Niagara Falls, and the Old River Control Structure on the Mississippi River have been conducted throughout its 65 years of service to the Army and the Nation.

During the past several decades, with the advent of analog and digital computers, WES moved into the numerical modeling arena. With the rapid advance in computer technology leading to PCS and supercomputers, research is now being conducted using numerical modeling techniques including finite difference, finite element, discrete element, and discontinuous deformation analysis. Recent accomplishments include the development of a three-dimensional water quality model for the entire Chesapeake Bay, the use of complex three-dimensional codes to investigate cratering and air-blast effects from explosive events, and the use of two-dimensional effective stress finite element analysis for predicting large deformations occurring in embankment dams as the result of earthquake induced liquefaction in the dam and/or its foundation material.

The WES centrifuge is capable of spinning a payload of up to 8 tonnes and achieving accelerations of up to 350 gravities (g). This centrifuge provides a physical modeling capability which greatly enhances research techniques. Case histories and/or physical model experiments are required to validate numerical computer codes. Physical models have the advantages of being controllable, relatively inexpensive, and provide better known conditions than field cases.

---

[1] Associate, Andrew N. Schofield & Associates, Ltd., 9 Little St. Marys Lane, Cambridge, CB2 1RR, UK

[2] Geotechnical Laboratory, U.S. Army Engineer Waterways Experiment Station, 3909 Halls Ferry Road, Vicksburg, MS, USA 39180-6199

Researchers can better control the material properties and boundary conditions of physical models. The cost of centrifuge experiments is far less than full-scale field experiments which may involve hundreds of thousands or millions of dollars.

2. MODELING FIELD PROBLEMS IN A CENTRIFUGE

Physical modeling of field problems generally involves the construction and experimentation with scale models of a prototype or field structure. The response of the model to a physical perturbation such as cyclic loading, earthquake, ocean waves, explosion or even freezing or groundwater changes can be measured and interpreted in terms of the field problem under consideration. Realistic model behavior data can provide valuable information for designers about failure mechanisms and long term performance.

In many engineering fields, particularly geotechnical engineering, gravitational effects dominate performance. Where the behavior of a material is stress dependent, such as with the engineering properties of soil, then simple scaling of a field problem and experimental investigations on the laboratory floor will give erroneous results. For example, in a slope failure it is common to observe cracking near the ground surface where the confining stresses are low but the shear stresses are high, rupture along a slip surface at greater depth and finally flow at depth as the confining pressure increases still further and the shear stress ratio reduces to a value below the critical state or characteristic threshold value, (Figure 1).

If one were to attempt to model the slope failure in Figure 1 on the laboratory floor at 1/50 scale without the benefit of a centrifuge, the effective confining stresses in the soil would be 50 times less than those same stresses in the field and hence could bring the full depth of soil in the model into a region where tensile fracture (or cracking) dominates.

The use of a centrifuge however, overcomes this modeling error by increasing the weight of each particle in the model by an equivalent number of gravities. Generally the linear scale of the model and the number of gravities are chosen to be identical. Therefore, a 1/50 scale model of a 20 m high earth slope would be 400 mm high. Under a steady acceleration of 50 gravities (approximately 500 m/s^2), it would have identical self-weight stresses at equivalent points in the model and in the prototype. The behavior of the miniature slope will then mimic the behavior of the prototype. Each soil 'element' in the centrifuge model is subject to the same stress path as its equivalent 'element' in the full scale prototype.

Figure 2 shows a silt slope failure in remolded Vicksburg loess, carried out on the WES centrifuge. Details of the failure can be seen, including the cracking near the top of the slope, and rupture along the slip surfaces which run nearly parallel to the slope. The response shown is typical of loess behavior with no deep seated flow movement.

Scaling relationships can be derived from physical principles which interpret the centrifuge model experimental investigation data in prototype terms (Schofield 1980 and 1981, Schofield and Steedman 1988). These are summarised in Table 1.

As a technique for solving engineering problems, the use of the centrifuge was first pioneered in the Soviet Union and in the United States (US) during the 1930s (some references claim the concept of a centrifuge model can be traced to the 19th century or earlier). Although the idea did not fully develop in the US at that time, the Soviets recognized its potential in the area of weapons effects and developed a major program of centrifuge modeling. It is understood that this continued until the recent political changes.

In the west, the development of centrifuges for study of geotechnical problems was led by academic researchers in the United Kingdom (UK) committed to the study of soil as a plastic material. A number of centrifuge centers developed in the UK, US and

in Europe during the 1970s and 1980s, primarily attached to universities or research institutions.

Miniature instrumentation and, recently, the development of affordable advanced data acquisition systems has revolutionized the potential for centrifuge models. Model experiments can now provide detailed quantitative information on the response of a model at many different points for comparison with numerical models or analytical solutions. Miniature instrumentation has already been developed which can measure displacements, pore fluid pressures, accelerations, resistivity, wave height, shear wave velocity, and so on. 'In-flight' site investigation tools can perform cone penetration probes, vane shear experiments or other explorations of the 'site'. Miniature cameras can observe the behavior of the structure in close up. Systems can load the soil and structures, trigger earthquakes, generate water waves, freeze ice sheets, carry out staged construction, release contaminants or detonate explosives.

The wide range of physical phenomena that may be created in a centrifuge and the quality and detail of the data that may be captured from a model in-flight clearly provides substantial opportunities for engineering research studies. The Corps of Engineers has been involved with centrifuge modeling since the 1970s, and the recent development of the WES Centrifuge Research Center in Vicksburg demonstrates the Army's full commitment towards the use of physical modeling as an integral part of engineering analysis.

3. THE WES CENTRIFUGE

The design specification of the centrifuge followed a review of available academic facilities which had shown that none were able to routinely conduct experimental models of the large field structures and problems with which the Corps is principally concerned (Ledbetter, 1991). The facility was therefore designed with a unique operating envelope. It was required that model containers should be easily placed on and off the centrifuge and these requirements led to the design of a beam centrifuge with a swinging platform based on the French designed Acutronic 661, 665, and 680 series of geotechnical centrifuges. Other centrifuges in this Acutronic family include one at Rensselaer Polytechnic Institute, Troy, New York, at the Centre for Cold Oceans Resources Engineering, St. Johns, Newfoundland, and several in Japan and Europe. Figure 3 shows the WES Centrifuge in its containment structure; key parameters are listed in Table 2 and Figure 4 shows the performance envelope relating payload capability to centrifugal acceleration. Prototypes of the order of 300 m in breadth and 300 m deep can be simulated in models subjected to up to 350 gravities (around 3500 m/s^2).

A wide range of modeling capabilities was required and actuators and appurtenances have been designed to fulfill these requirements. Models can be constructed in a range of containers that depend on the geometry of the problem under investigation (plane strain, axi-symmetric, three dimensional, etc.) and the type of phenomenon to be recreated.

Recent world-wide interest in centrifuge modeling has concentrated on geotechnical applications; however, the WES centrifuge facility has a much broader mission. The WES centrifuge will address research needs in physical modeling across the full range of engineering applications. Investigations are possible under climatic conditions ranging from desert to polar to ocean regions. Key capabilities include: (1) force and displacement controlled load systems, (2) earthquake simulation, dynamic vibration loading and water wave generation, (3) blast loading, (4) model package environmental control, (5) in flight manipulation of the model materials and fluids, (6) miniature instrumentation, cameras and in flight site interrogation, and (7) high speed data acquisition and control systems.

The new capabilities that will flow from the centrifuge will depend on the ingenuity of its users and the design of its appurtenances. In this respect the design of the centrifuge itself is merely one component of the development of new capabilities in physical modeling.

4. CENTRIFUGE MODELING OF DYNAMIC PROBLEMS

The use of centrifuges to address field problems involving dynamics dates back many years. As noted above, the Soviets made use of centrifuges as early as the 1930s and 1940s for the study of weapons effects. WES, which first used centrifuge modeling for cratering studies in the 1970s, has now developed the capability for carrying out such explosive investigations on its new centrifuge (as discussed further below).

In the field of earthquake modeling, Professor Mikasa at the University of Osaka pioneered the development of the first centrifuge 'earthquake' actuator by using a tilting mechanism to create a pseudo-static lateral acceleration field on a soil model in flight, (Mikasa et al. 1969). Steedman (1991) provides a review of the application of the centrifuge to dynamic geotechnical studies which highlights some of the important achievements of Japanese researchers in earthquake centrifuge modeling.

Since the 1980s, a variety of actuators have been developed around the world for the simulation of earthquake-like base shaking on centrifuge models. These have ranged from sophisticated units using servo-hydraulic systems to provide broad band shaking input to less mechanically complex systems that can apply a broadly sinusoidal base shaking motion of a given duration and frequency. In general, limitations posed by the high gravitational field in which the equipment must work and the high development cost has restricted the use of servo-hydraulic systems to low g centrifuge applications and small models. At WES, the requirement to conduct experimental models of large field problems has led to the development of a robust mechanical shaker designed to operate at over 200 gravities, significantly higher than any earthquake centrifuge modeling on other beam centrifuges carried out to date. Early indications, using a prototype version of the system developed together with Cambridge University, have provided encouraging results, as seen in Figure 5.

The WES earthquake shaker (Figure 6) uses the angular momentum stored in high speed rotating flywheels to provide the energy source for the shaking motion. Power is transferred from the flywheels to the base plate beneath the model via a continuously oscillating shaft which is briefly 'grabbed' by a high speed clutch for the desired duration of excitation. Figure 7 shows the equivalent-shear-beam laminar model container which is 900 mm in length, 650 mm in height and 355 mm in width. This container incorporates shear sheets on each of the end walls to transfer the complementary shear stresses generated on vertical planes in the specimen by base shaking in the horizontal direction. This improves the uniformity of shear.

From Table 1 it is seen that as the g level is increased it is necessary to increase the frequency of shaking and simultaneously to reduce the amplitude of motion. At high g levels these small displacements may become comparable to the manufacturing tolerances of the moving parts; particular attention has been paid to this issue in the design of the WES shaker. The resulting system is robust and economic, and will provide a pre-programmed duration and frequency of shaking.

In fields such as the seismic design of retaining walls, centrifuge model studies have provided valuable insights into the mechanisms underlying the onset of permanent movement and the ultimate failure of different forms of wall. Conventional approaches to the prediction of permanent movement of monolithic walls have been investigated and refined using centrifuge model behavior data (Steedman and Zeng 1996). Other studies have investigated the point of application of the dynamic force increment and the consequences of the development of excess pore pressures and liquefaction in the backfill behind anchored walls (Steedman and Zeng 1990).

A key area of interest to WES has been the study of liquefaction and the dynamic response of embankments and dams. WES has made extensive use of centrifuge modeling in this field to provide realistic data for the validation of numerical codes and other analyses and a substantial program of research is planned for the new facility (described further below).

The WES involvement and interest in centrifuge earthquake engineering experiments and studies dates back about twenty years to collaboration with the University of Cambridge (Morris 1979). WES conducted experiments in the 1980s of models including dry and saturated embankments with and without surface supported and embedded structures. Figure 8 shows one of these experiments for investigating a nonlinear dynamic effective stress method of analysis.

Shown in Figure 8 is a schematic view of a saturated embankment with an embedded structure for simulating strong soil-structure interaction during earthquake shaking. The foundation sand was Leighton Buzzard Sand with a mean grain size of 0.225 mm at an average relative density of 52%, and the structure was a solid piece of aluminum alloy. Centrifuge experiments were at a nominal centrifugal acceleration of 80 g. Therefore, the model simulated a structure 8.6 m high by 12 m wide embedded 2 m in the foundation sand. Peak acceleration of the input horizontal shaking at the base of the model was 0.13 g.

Accelerometers (ACC), pore pressure transducers (PPT) and a linear variable differential transformers (LVDT) were used to monitor the response of the model as shown in Figure 9. As can be seen, a significant amount of instrumentation was used to obtain good and reliable data. An important advantage of centrifuge earthquake experiments is the wealth of data and information that can be acquired, as evidenced in this figure.

Figure 10 shows computed and measured horizontal accelerations at the top of the structure at the location of ACC 1938 (Figure 9). Vertical accelerations due to rocking of the structure occurred and are shown in Figure 11 along with computed motion. The frequency content is higher than seen in Figure 10 because the foundation soils are stiffer under the compressive stresses due to rocking than under the induced shear stresses from the horizontal acceleration.

Contours of computed residual porewater pressures in the foundation are shown in Figure 12 along with the measured maximum values (indicated by the triangles). Very symmetrical distributions of the residual porewater pressures are seen for the model investigations. The measured responses shown in Figures 10 through 12 cannot be obtained by any other means under the equivalent prototype stress states and provide valuable insight to behavior under earthquake excitation and for numerical model development and verification.

Other fields involving dynamic loading that have been addressed using the centrifuge include dynamic loading of foundations ('machine vibration'), (see Laue and Jessberger 1994), and wave loading on coastal defences and sea bed deposits (Sekiguchi et al. 1994).

The modeling of instability of sand beds caused by water waves at g has been hampered by the need for very large or deep wave tanks. At high g it becomes practical to adopt viscous scaling of the pore fluid because of the small size of the wave tank, and researchers at Kyoto University have shown that using this technique, wave induced liquefaction can be reproduced in a sand bed deposit, (Sekiguchi et al. 1994). This class of problem will also be addressed in future at WES.

5. CURRENT RESEARCH AT WES

A number of research projects using the centrifuge are currently underway at WES. In the following paragraphs, a few of these investigations are described which demonstrate the Corps' interest in a wide range of applications. Some of these fields are entirely new to centrifuge modeling.

In the field of earthquake engineering, a large study has commenced to investigate aspects of the prediction of liquefaction. This has the potential for a major impact on the design of remedial measures for earth dams in seismic areas in the US. To date, the factors which strongly influence the prediction of a soil to liquefy and its residual strength as used for design purposes have been evaluated only on laboratory element test data and fortuitous field performance data. The new research approach is to use the new large earthquake shaker mounted on the WES centrifuge to conduct a series of models experiments, monitoring the development of excess pore fluid pressure in the foundation soils directly as a function of the density, amplitude of shaking and number of load cycles. This approach will not need to extrapolate design factors from small laboratory samples and may lead to significant improvements in design and analysis techniques.

A second research program is concerned with the gravity driven mixing and flow of immiscible fluids as oils seep into the natural groundwater environment. The purpose of the models is to acquire data suitable for the validation of numerical models of DNAPL (denser than water non-aqueous phase liquid) movement in groundwater, the development of which have been hampered by the lack of realistic experimental or field data. In a centrifuge model under high gravity, the time taken for a diffusion event is reduced by the square of the model scale over the equivalent time in the field. This occurs because of the small physical size of the model and the higher hydraulic gradients. This is a strong advantage for any experiments investigating long term diffusion type problems as the centrifuge can achieve in a few hours what would take many years to tens of years of monitoring in the field.

The first centrifuge experiments undertaken by the Corps in the 1970s were in the field of blast crater modeling. More recent work has studied the effects of blast and blast induced liquefaction on structures. Figure 13 shows a crater formed in dry sand in the blast chamber on the WES centrifuge, with a buried charge equivalent to 500 lb of high explosive (PETN). The model, at 45 gravities, has a crater diameter of 300 mm, equivalent to 13.5 m in the field. The WES centrifuge has a substantial capability for modeling the effects of explosions on a wide range of structures, again benefiting from the capability to operate at up to 350 gravities. In the scaling of blast phenomena, energy scales with N^3, Table 1, and hence 1 gm of high explosive at 100 gravities will generate an event equivalent to a 1 tonne explosion in the field. At 350 gravities, large explosions can be replicated. The program of work in blast modeling includes the simulation of field events to demonstrate the internal consistency of the models and the effects of explosions on a range of structures and facilities in different ground conditions.

Engineering for cold regions is another field of interest to the Corps and in this area studies have commenced concerning the effects of ice forces on structures with the growing of an ice sheet under increased gravity in a specially designed insulated container. Earlier studies at Cambridge University have shown that ice grown under increased gravity in the laboratory has an internal structure like that of a multi-year ice sheet in the Arctic, with a profile of snow on the surface, random crystals at shallow depth and vertically oriented crystals below that. If ice sheets of similar form to those found at sea can be formed in a centrifuge model then this pioneering research may provide a new route altogether for the development of engineering solutions for cold regions engineering.

Finally, in the environmental area, a research program has been initiated to investigate the consolidation of dredged material and the consequential damage to capping layers. Initial experiments have addressed the long term settlement of the material. Continuing experiments will investigate the movement of contaminants. As was noted earlier, small volumes of material in a centrifuge can replicate large volumes in the field. For contaminant migration investigations, this means that even small samples, which can be readily managed in the laboratory, can provide a basis for realistic modeling and simulation of the behavior of the full scale prototype. Samples can be used this

way rather than simply used to acquire parameters in a laboratory element test.

6. VISION

The development of the WES Centrifuge Research Center marks the transition of centrifuge modeling from a pure geotechnical engineering research tool to a modeling technique of wide application in engineering work. The Centrifuge Research Center aims to become the world's leading centrifuge modeling facility supporting the Corps of Engineers, the Army, the Department of Defense, other federal agencies and other nations, collaborating with academic and industrial organizations and addressing novel and demanding engineering problems world-wide.

7. CONCLUSIONS

The WES is continuing its tradition of 65 years of physical modeling with the acquisition of the most powerful centrifuge known to date and the development of unique applications and appurtenances for conducting research. Centrifuge investigations are possible across a wide range of engineering fields. Research is being conducted in earthquake engineering, environmental problems concerning groundwater flow, geotechnical engineering, blast phenomena, cold regions and ice formation, dredge material disposal behavior, and contaminant migration. Research is planned in the engineering areas of soil-structure interaction (behavior of large lock structures), hydraulics and coastal (wave loading on beaches and sea beds), and airfield pavements. The Corps is convinced that numerical and physical modeling must progress together to solve today's and future engineering problems. The centrifuge will allow us to investigate phenomena not previously feasible including the performance of large civil engineering structures up to and beyond their design limits and long term prediction of environmental problems.

The WES centrifuge modeling capability marks the transition in centrifuge development from academic research to broad application in engineering research and problem solving. The increase of gravity in a centrifuge and its influences on physical processes provides great benefit for modeling field phenomena. The opportunities for application to physical processes are limited only by imagination.

8. ACKNOWLEDGMENTS

The support of the U.S. Army Engineer Waterways Experiment Station during the preparation of the manuscript is appreciated and acknowledged. Permission to publish this paper was granted by the Chief of Engineers, U.S. Army Corps of Engineers.

9. REFERENCES

Laue J. and Jessberger H. L. (1994), "Behaviour of Foundation Systems In Sand With Dynamic Sinusoidal Loadings", Proc. Centrifuge 94, Leung, Lee and Tan (eds), pp 265-275, Balkema.

Ledbetter R. H. (1991), "Large Centrifuge: A Critical Army Capability For The Future", Misc. Paper GL-91-12, USAE Waterways Experiment Station, Geotechnical Laboratory, May.

Morris D. V. (1979), "The Centrifugal Modelling Of Dynamic Soil-Structure Interaction and Earthquake Behavior", European Research Office, U.S. Army, London, England.

Mikasa M., Takada N. and Yamada K. (1969), "Centrifugal Model Tests of a Rock Fill Dam", Proc. 7th ICSMFE, Mexico, Vol. 2, pp 325-333.

Schofield A. N. (1980), "Cambridge Geotechnical Centrifuge Operations", Geotechnique, Vol.20, pp 227-268.

Schofield A. N. (1981), " Dynamic and Earthquake Geotechnical Centrifuge Modelling", Proc. Int. Conf. Recent Advances in Geotechnical Earthquake Engineering and Soil Dynamics, Vol.3, pp 1081-1100, Univ Missouri Rolla, Rolla, MO.

Schofield A. N. and Steedman R. S. (1988), "Recent Development Of Dynamic Model Testing In Geotechnical Engineering", Proc. 7th World Conf. Earthquake Eng, Vol. VIII, pp 813-824, Tokyo-Kyoto, 2-9 August.

Sekiguchi H., Kita K. and Okamoto O. (1994), "Wave Induced Instability Of Sand Beds", Proc. Centrifuge 94, Leung, Lee and Tan (eds), pp 295-300, Balkema.

Steedman R. S. (1991), "Centrifuge Modeling For Dynamic Geotechnical Studies", Proc. 2nd Int. Conf. Recent Advances in Geotechnical Earthquake Eng. and Soil Dynamics, March 11-15, St Louis, MO, pp 2401-2417.

Steedman R. S. and Zeng X. (1990), "The Influence Of Phase On The Calculation Of Pseudo-Static Earth Pressure On A Retaining Wall", Geotechnique 40, No.1, pp 103-112.

Steedman R. S. and Zeng X. (1996), "Rotation Of Large Gravity Walls On Rigid Foundations Under Seismic Loading", ASCE Geotechnical Special Pub. No. 60, pp 38-56.

Table 1. Scaling Relations

PARAMETER	FIELD	CENTRIFUGE MODEL (Ng)
Stress	σ	σ
Strain	ε	ε
Length, displacement	L	L/N
Area	A	A/N^2
Force	F	F/N^2
Volume	V	V/N^3
Mass	M	M/N^3
Energy	E	E/N^3
Frequency	f	Nf
Velocity	v	v
Acceleration	a	a/N
Time (for inertial events)	t	t/N
Time (for diffusion events)	t	t/N^2

Table 2. Key Characteristics of the Army Centrifuge

Army Centrifuge	
Radius to platform	6.5 m
Payload at 143 g	8000 kg
Payload at 350 g	2000 kg
Capacity	1144 g-tonne

Table 1. Scaling Relations

PARAMETER	FIELD	CENTRIFUGE MODEL (Ng)
Stress	σ	σ
Strain	ε	ε
Length, displacement	L	L/N
Area	A	A/N^2
Force	F	F/N^2
Volume	V	V/N^3
Mass	M	M/N^3
Energy	E	E/N^3
Frequency	f	Nf
Velocity	v	v
Acceleration	a	a/N
Time (for inertial events)	t	t/N
Time (for diffusion events)	t	t/N^2

Table 2. Key Characteristics of the Army Centrifuge

Army Centrifuge	
Radius to platform	6.5 m
Payload at 143 g	8000 kg
Payload at 350 g	2000 kg
Capacity	1144 g-tonne

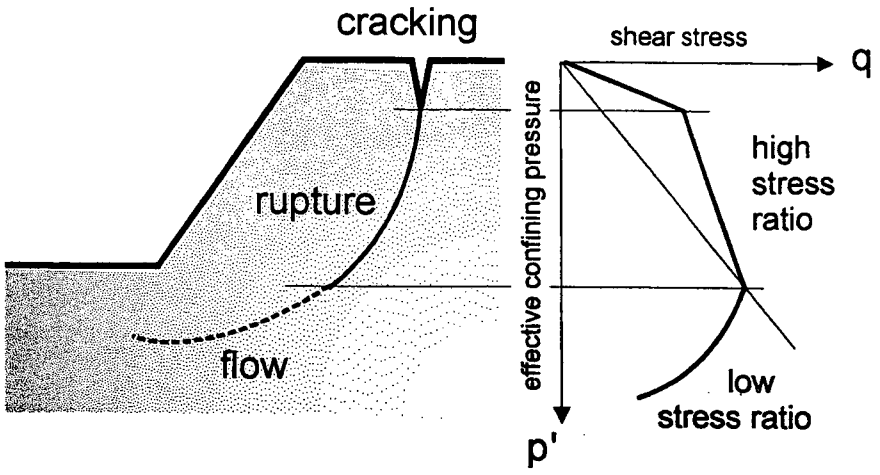


Figure 1: Ratio of shear stress to confining pressure governs soil behavior

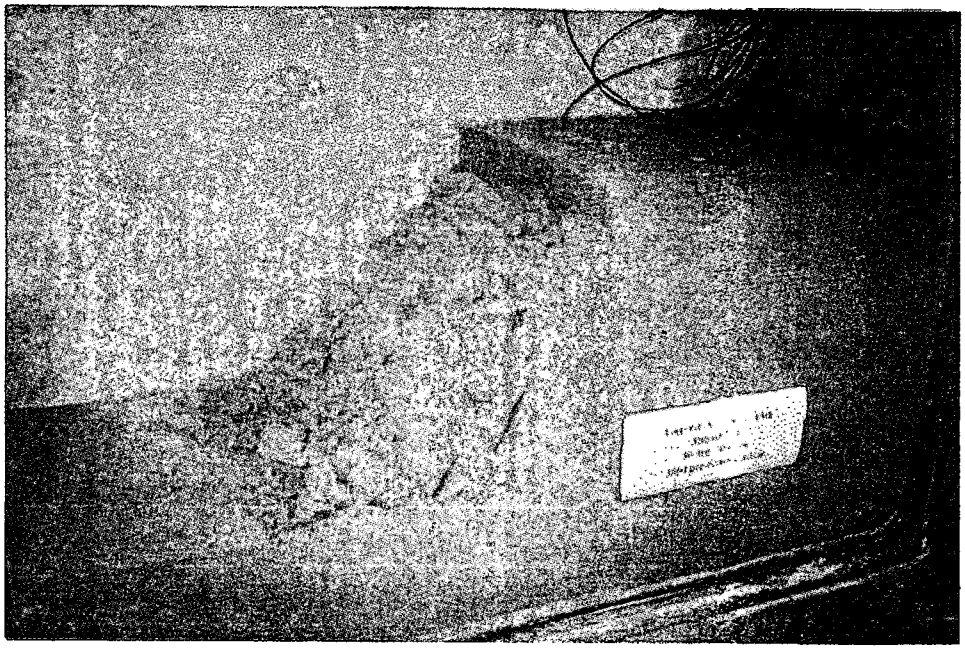


Figure 2: Failure of a silt slope in Vicksburg loess

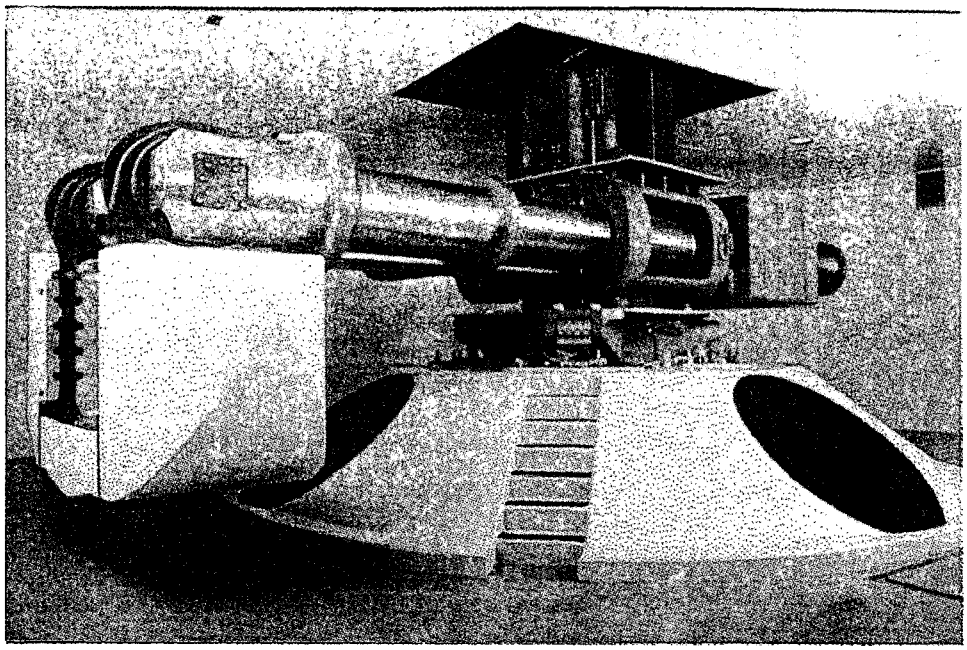


Figure 3: The Army centrifuge at the Waterways Experiment Station

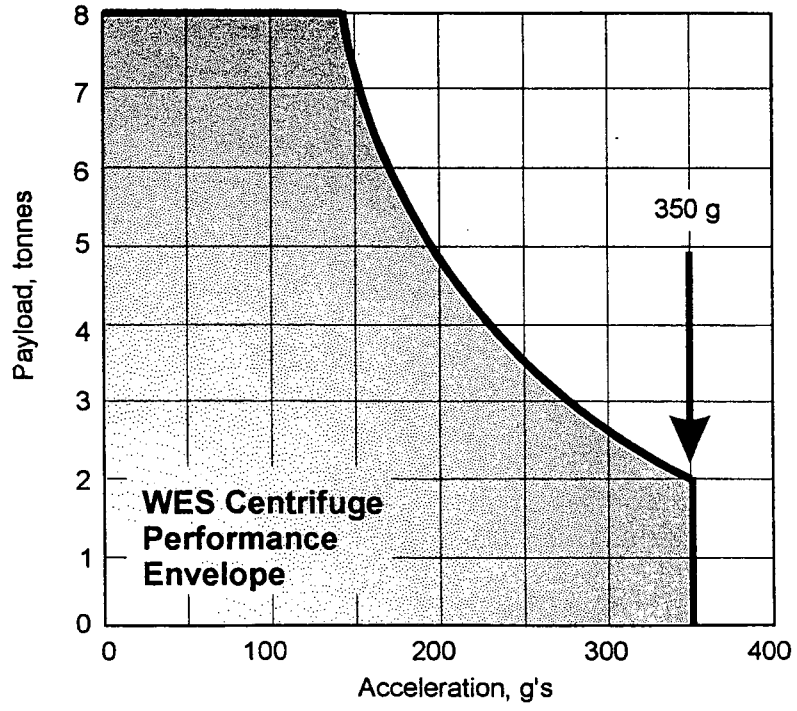


Figure 4: WES Centrifuge performance envelope

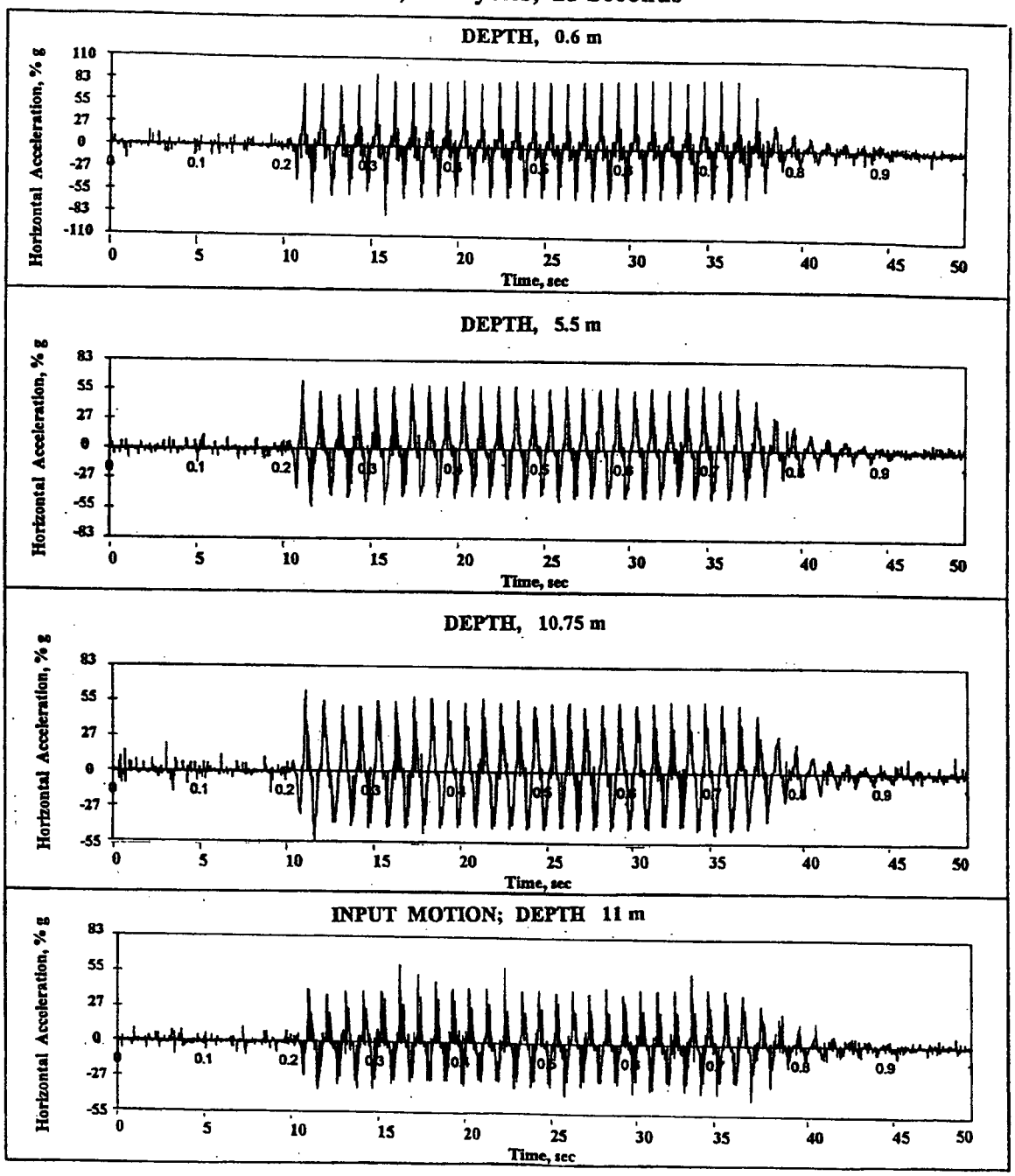


Figure 5: Accelerations recorded at different depths in a dry sand bed (prototype units)

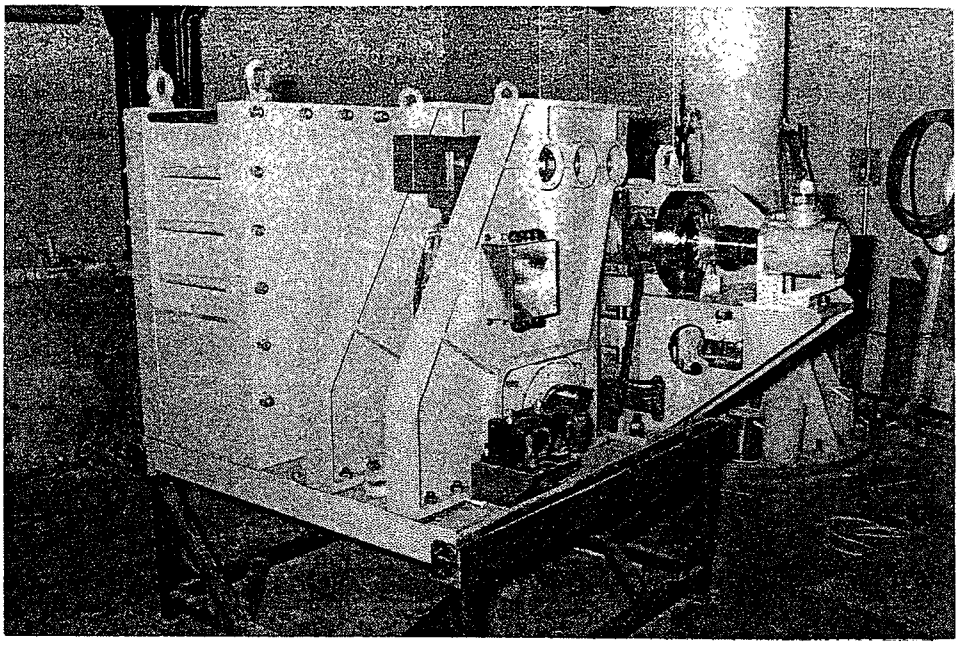


Figure 6: The WES earthquake shaker

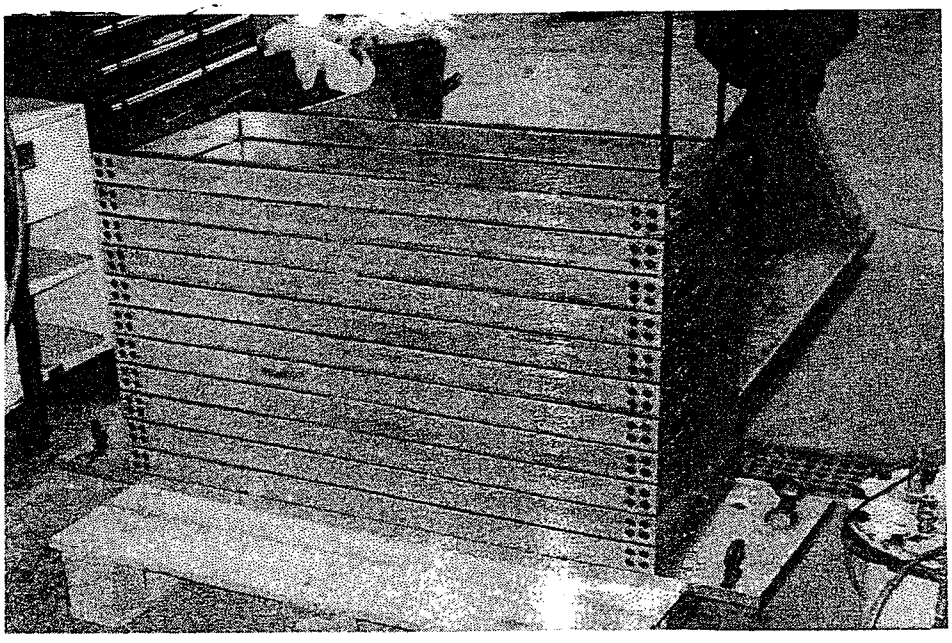


Figure 7: Equivalent-Shear-Beam model container

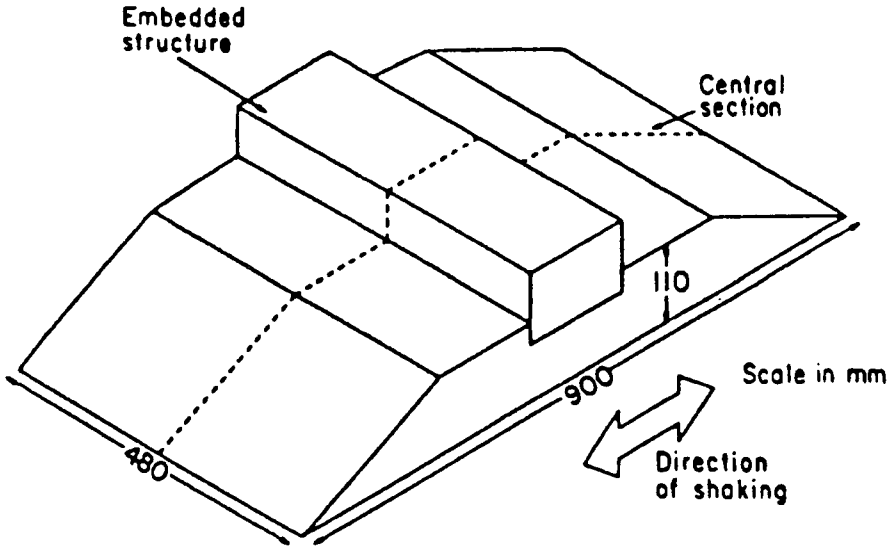


Figure 8: Model of large embedded structure in saturated sand embankment experiments at 80 g

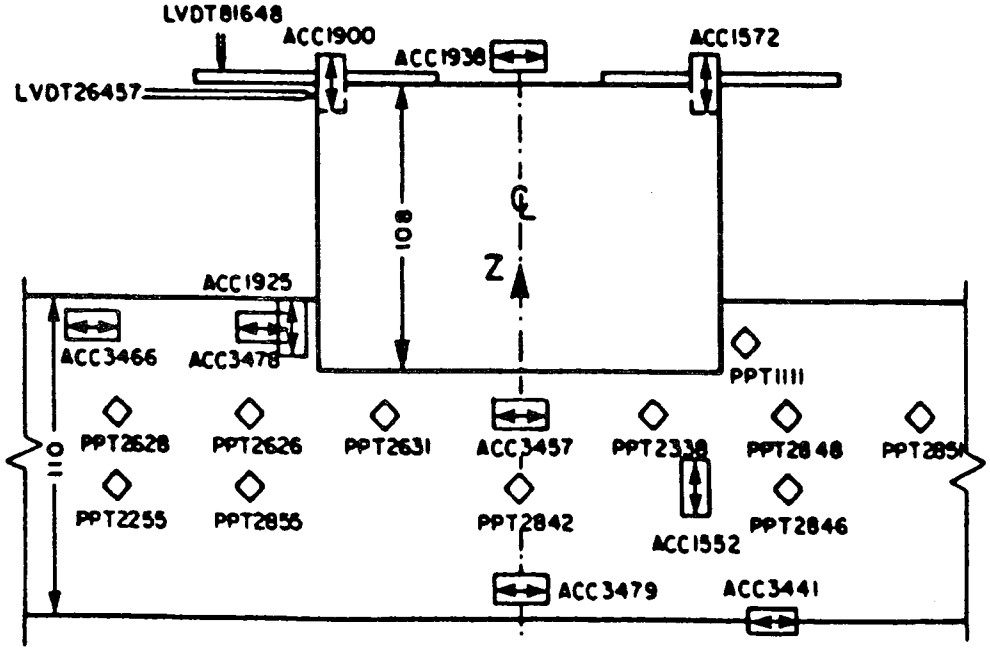


Figure 9: Location of instrumentation in central section of the embedded structure model

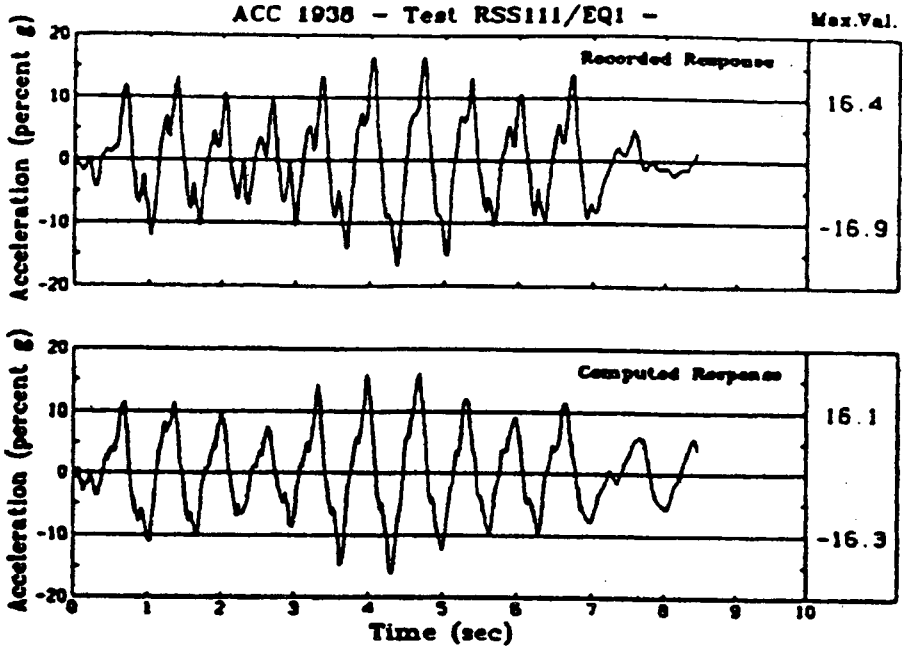


Figure 10: Recorded and computed horizontal accelerations at ACC 1938 (prototype units)

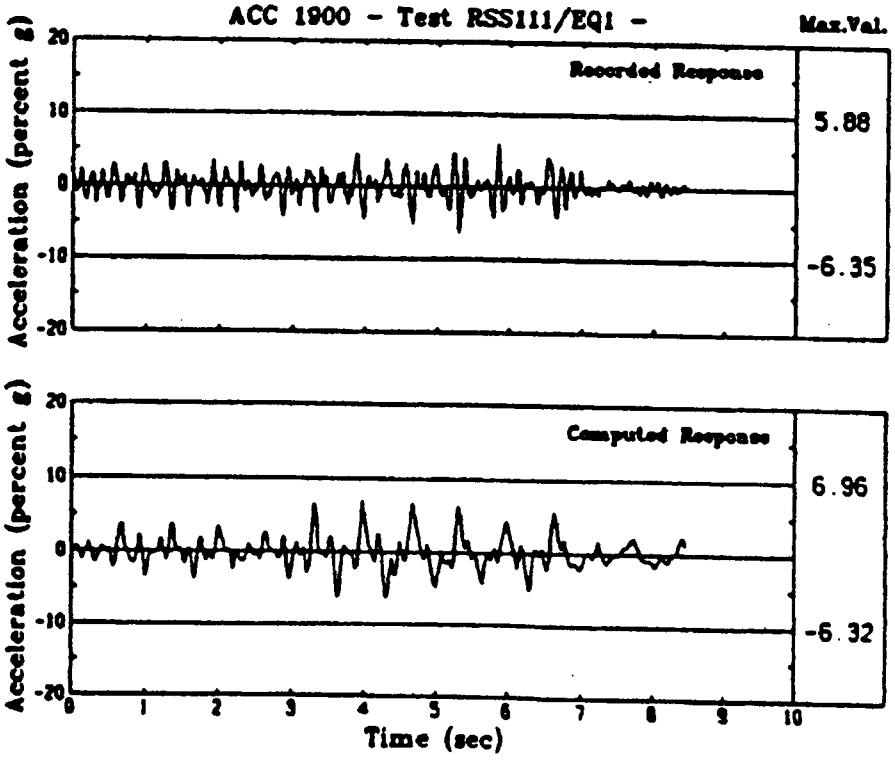


Figure 11: Recorded and computed vertical accelerations at ACC 1900 (prototype units)

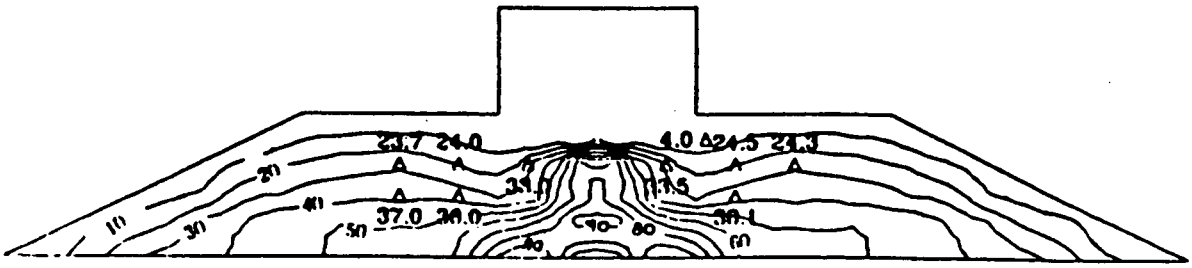


Figure 12: Residual pore water pressures in a saturated embankment model

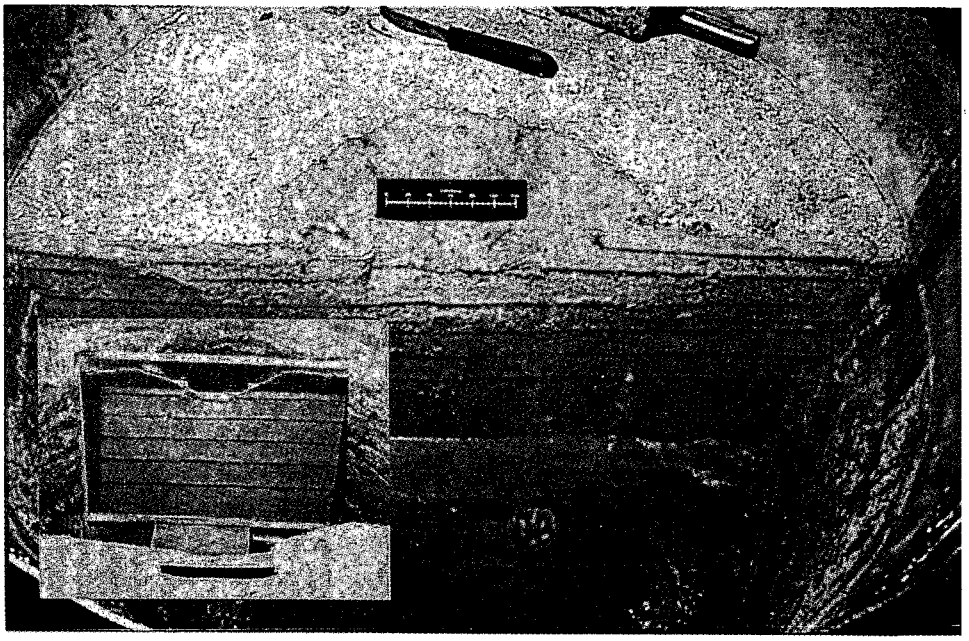


Figure 13: Crater formed in dry sand with buried charge

Long Term Health Consequences of The Great Hanshin-Awaji Earthquake and Strategies for Mitigating Them

by
Naotaka, SHINFUKU[1]

ABSTRACT

The writer had a rare experience as medical doctor to become victim and observer of a major disaster. His office at the Kobe University Medical School was located at the center of the Hanshin-Awaji Earthquake. The writer experienced the Great Hanshin-Awaji Earthquake on January 17,1995 in Kobe. He analyzed the physical and psychological consequence of the earthquake based on his experience. Stress related physical symptoms and psychological symptoms have greatly changed like time factor after the earthquake. Long term health consequences are influenced mostly by socio-environmental conditions of victims. Solitary death, depression, alcohol abuse are reported as major and continuing health problems. These problems are sometimes attributed to inappropriate building structure of temporary houses where more than 40 000 victims live even after two years from the earthquake. The importance of long term and wide range programs for the victims including housing, employment and financial support is stressed.

KEY WORDS: Hanshin-Awaji earthquake, Long term health consequences, Temporary housing, Kobe, PTSD.

1. INTRODUCTION

The earthquake took place at 5 am 46 minutes,January 17.1995.. Many people considered its timing was rather fortunate.
If it had happened in the mid-night,rescue works by neighbors might have been impossible. If the earthquake was one or two hours later.transportations systems would have started.This might surely had caused the death of many more peoples due to traffic accidents. The Japanese scale for the damage was reported at first as 6, but it was revised to 7 afterwards. Richter scale was 7.2.

The earthquake hit just below the major city areas of Hanshin which include Kobe city of approximately 1.5 million population. One year after the earthquake,Kobe city lost almost 100.000 population due to migration to non-damaged areas[1].
The number of the population affected by the earthquake was estimated as 2.4 million. City gas supply was cut to 857 400 households. Every household will have 3 family members in average. This enabled a very rough estimation of the population affected by the earthquake.

The number of the people who lost their housing and had to stay at shelters was over 320 000. In April 1995, the number of the dead was reported 5502. But it was revised in July to 6048 as some of the victims died at private hospitals were not included in the initial counts.

The official number of the dead due to the Earthquake was once again revised to more than 6.500 in August 1995 as some of the delayed death cases , such as pneumonia and suicide,were certified resulting from the Earthquake. [1]

---

[1] Professor of International Health and Epidemiology, ICMR, Kobe University School of Medicine Kobe, Japan

Three quarters of the immediate death was due to asphyxia by house furnitures and roof materials. Other major causes were due to burn, multiple fractures including cervical area, and traumatic shock[1].

Many people were unable to understand what had happened soon after the earthquake. This period is sometimes called as " 6 hour vacuum". When the earthquake struck, the writer was unable to realize that it was the earthquake. He thought that it was some kind of an explosion under his house. Also, it took long time for many people in Kobe to realize that the epicenter of the earthquake was near Kobe. Nobody expected the earthquake in Kobe area. Kobe University was a center of the hard hit area. Many victims in Kobe area could realize the magnitude of the earthquake only after watching the burning scene of Nagata district by television .It is important to know that population affected by the disaster is sometimes the least informed on the magnitude and nature of the disaster.

2.HEALTH PROBLEMS BY TIME

2.1.By Day-soon After the Earthquake

Immediate medical needs were emergency medicine. At Kobe University Medical school.a considerable number of victims brought to emergency services were found as DOA, Dead on Arrival. For medical services, many were for orthopedic surgery. Several cases of crash syndrome were also reported. Forensic department of our medical school was extremely busy for administrative autopsy and certification of death.

Soon after the earthquake, most of victims experienced emotional numbness. A writer's friend who lost his parents told that he felt out of touch with the reality. He said that he could not feel sadness. Shaking feeling of the body continued due to frequent after—shocks. The writer experienced a kind of depersonalization (feeling that everything is unreal). Depersonalization could be a psychological protection from the disaster.

Two or three days after the earthquake, majority of the victim became talkative and joyful. Some people even became hypomaniac and showed signs of psychomotor excitements. These symptoms might be caused from the joy of survival.

Major medical problems at the early stage were recurrence of chronic disease , such as diabetes , hypertension, mental diseases due to the suspension of habitual medication. Loss of memory and disorientation were reported, particularly among the elderly.

2.2. By week

For the first week. everybody was tense to secure food, water and information. Kind of a battle field friendship existed for a certain period. This resulted in the sustainment of mental excitement and friendship among victims. However. fear of aftershock and general anxiety were experienced at the same time.

Survivor's guilt was strong for those who lost family members[2].

The writer had an abnormal sense of time. One day was felt as eternal. But he could not remember the event of the previous day.

After one week, the focus of the health care was shifted from emergency medical care to care for chronic patients. Treatment of the chronic patients including hypertension, diabetes mellitus and mental diseases were resumed. Care for senile demented and mentally handicapped in shelters posed difficult problems for manager of shelters. Insomnia was common at crowded shelters. Acute stress responses such as nightmare were reported. Psychiatric emergency care were established at some shelters[3].

Volunteer including medical professionals flooded Kobe and damaged areas. It is reported that almost 1.5 million volunteers from all over Japan, and some from abroad,came to Hanshin area for assistance after the Earthquake[4].

After 10 days,the life in shelters became very stressful for many victims. Increase of acute stress response including serious stress ulcer was reported. Department of Internal Medicine of Kobe University Medical School was busy for the treatment of many cases of extremely serious stress ulcer. Anxiety reaction and sleep disorder was common.

Increase of pneumonia and bronchitis was reported among the elderly. The earthquake took place in January which was winter in Japan.

After two weeks,victims start facing the reality and the loss including family members,housing and job. Depression became manifest among victims. A few suicide cases were reported. Acute symptoms of Post traumatic symptoms (PTSD) such as flash back continued among victims.

2.3. By Month

After one month,a considerable number of the aged people became unable to meet with the continued stressful events of their lives. Among elderly victims, dementia.disorientation incontinence were often reported. The consumption of alcohol was increased among victims which led to the epidemic of alcohol-related problems in some shelters. Alcohol related violence are sometimes reported. Children showed regression. Burnout syndrome of volunteers become commonplace.

After two months, most of victims were transferred from shelter to temporary housing by lot. Later, this arrangement was criticized. In shelter, neighborhood could stay together.At one time,more than 320,000 people stayed at shelters such as school and public buildings. Government started the building of temporary housing which were similar to military barrack. For victims at temporary housing allocated by lot,neighbors were foreigners. Community was destroyed. Many victims faced the degradation of social status and economic difficulty which , in turn, caused depression. The above psychological consequence is similar to the experiences of victims of other disaster[2].

3. LONG TERM HEALTH CONSEQUENCES

The recovery work from the earthquake has been rapid. Major transportation such as Shinkannsen resumed after three months. However,long term heath and mental health problems among victims continued even after one or two years from the earthquake.

These long term effects will include the following areas.

- psychological effects
- stress related physical symptoms such as hypertension
- lowering of immunity and its effect.allergy.cancer etc..
- effects of nutritional unbalance
- long term effects to children

3.1. Vulnerable Population Group

Among the victims,the most disadvantaged population groups included the followings,

- the elderly who lost kin
- a family of mother and children
- physically and mentally disadvantaged
- foreigners from developing countries

Victims with money, relatives , job, supportive friends were able to leave temporary houses at the early stage. Only the very disadvantaged population was obliged , and still is obliged ,to stay at temporary houses. These population group has high rate of physical and psychological health problems.

3.2.Long Term Psychological Effects

Major problems affecting the victims are psychological difficulties resulting from isolated life at temporary housing. Burnout, apathy and passive attitude,loss of hope are common among victims. Alcohol problems has been reported on the increase among those living

in temporary housings. This isolation and the loss of community sometime have lead many tragedies such as suicides and so called " solitary death". Lack of local health manpower is cited as one of the major contributing factor for this tragedy.

It is well known that strong life threatening experiences cause long-term physical and psychological effects. Some of well known examples of these syndromes are inmates of Nazi concentration camp and Vietnam veterans. Those who experienced disastrous life events suffer from post traumatic stress syndromes(PTSD)characterized by nightmare, insomnia, flash back of the event , various neurotic and depressive symptoms. Victimes of the Hanshin earthquake are no exception. According to our study on school children, psychological effects were high among girls, younger age, those who lost families and friend. Neurotic symptoms reduced after 6 months but depressive symptoms and physical complaints continued even after 12 months. Many reports relatively low frequency of PTSD among victims comparing the data in other countries.

3.3.Long Term Physical Effects

The risk factors of physical impacts of the disaster is not only the experience of the disaster. There are many factors.

The biggest one is housing and nutritional condition of victims. Isolated life style induces alcohol use cigarette smoking thus increasing the risk of hypertension and coronary heart diseases. In addition, lack of intake of fresh vegetable and usual intake of fast food facilitate high cholesterol increasing the risk of coronary heart disease.

Cold temperature and insufficient air conditioning tend to cause common cold, bronchitis and emphysema. Some experts suggest the lowering of immunity among victims and predict the higher prevalence of cancer.

However, the scientific and large scale epidemiologic studies have yet to be completed for the victims of the Great Hanshin Awaji Earthquake. Long term physical and mental consequences of life at shelter and temporary housing should be studied further.

There are relatively few study on the long term physical consequences among victims of the disaster. A four year follow up study about victims of Armenia earthquake in 1988, showed a higher rate of coronary heart diseases. Risk factors were old age, male sex, trapped inside the house, who lost family members and close friends.

4. STRATEGIES TO PREVENT LONG TERM HEALTH PROBLEMS

For health professional living in Hyogo Prefecture, the most important concern is how to promote health among victims of the disaster and especially how to prevent the so-called solitary death at temporary houses. Temporary houses built after the earthquake are now resided mostly by the elderly and socially disadvantaged population. There may exist several strategies to prevent long term health problems among victims of the Hanshin-Awaji Earthquake.

4.1. Building of Housing and Environmental Conditions Favoring Human Contacts and Supports

From psychological points of view, it was a mistake to allocate the victims by lot to temporary houses. At shelter, peoples from the same communities could gather together. This prevented for victims to feel lonely. At temporary houses, neighbor are foreigners gathering from many communities. In the Philippines, I was impressed to find that victims of Pinatubo Mountain eruption was relocated as a community to new resettlement area. At the relocation of victims after the disaster, it would be useful to make efforts to keep community as long and as complete as possible. This arrangement would reduce stress and loneliness among victims.

At the temporary houses in Hyogo, several attempts have been undertaken to increase human contacts among victims. Community centers were open at each temporary house group for resident to come and to chat.

Both private and communal spaces are necessary for temporary houses. Four of five houses could share corridor and gardens. Group home for victims has been discussed as a possible solution for elderly victims needing physical and psychological care.

4.2.Establishment of Human Network Preventing Long Term Health Consequences

Immediately after the earthquake, there was a flooding of volunteers to Kobe area to take care of victims. It is reported that almost 1.5 million volunteers came to Kobe and vicinities after the earthquake. Some groups of house wives in Kobe area were visiting regularly temporary houses just to talk with elderly resident. Local governments mobilized public health nurses to visit temporary houses, However, the number of public health nurse is very limited. In each temporary house communities, autonomous committee have been set up to foster self help among victim residents. These mechanisms have been working to prevent solitary death and long term health problems .

4.3. Giving the Meaning and Hope to Their Life

VIctor Frankle wrote in his famous book based on his experience of Nazi Concentration camp " Those who could find the meaning in life and kept hope could survive."
It is very difficult for those who lost their housing, money, friend and partner at old age to find the meaning and hope .
Surely, human network is important to assist victims to find the meaning of life and to hope for future.

However, the minimum amount of compensation to build the house and to start a small scale business will be indispensable for victims to find the meaning of life. Personal compensation of the amount 30 000 to 40 000 U.S.D to the victims is a hot political issue at present. According to recent news, there may be some possibility for the Government to provide a seed money as long term loan as compensation to the victims of the Great Hanshin Awaji Earthquake.

CONCLUSION

World Health Organization defines health as " Physical, mental, social well being and not merely the lack of diseases or infirmity".
It is important to know that good physical health depend much on good mental health and good mental health depend on sound social environment including housing and community.

Human being is forgetful. However, it is important to remember that a considerable number of victims of the Hanshin Awaji Earthquake are still suffering from variety of psychological and physical problems. We have to continue to promote the awareness of the public on long term health consequences from the disaster and effective measures to reduce these problems. Long term health consequences could not be solved only by health sectors.

Dialogue should be held between health professionals and architect ,city planners, economists and concerned specialists to develop comprehensive and long term programs for victims which include housing,schooling,employment and community activation[6]. Multi-sector cooperation is a prerequisite to reduce long term health problems of victims of disaster.

REFERENCES

1. Shigeaki Baba, Hiroshi Taniguchi ,Seiki Nambu et al, Essay, The Great Hanshin Earthquake, Lancet,1996,347:307-09.
2. Beverley Raphael, When Disaster Strikes,Basic Books, Inc.,Publisher, New York,1986. (Translated into Japanese by T Ishimaru, Misuzu

Publishing Company)
3.N Shinfuku,Hanshin earthquake, my experience and psychological care, Gendai-no-esupuri,Shibundo, 1995 June, No 335,195-205.(In Japanese)
4. N Shinfuku, Psychological care and International Cooperation, Kokorono-kagaku, 1996 Jan, vol. 65,68-77. (In Japanese)
5. T Williams, Post Traumatic Stress Disorders: a handbook for clinicians, Published by Disabled American Veterans, 1987.
6. N Shinfuku, Future task, HANSHIN AWAJI DAI-SHINNSAI-SHI,Asahi Shinnbunn Syuppann-sha,1996,528-532. (In Japanese).

Rapid Needs Assessment and Loss Estimation from Natural Hazards: Lessons Learned from Hurricane Marilyn, U.S. Virgin Islands

by

Joel D. Selanikio[1], Josephine Malilay[1] and W. Dana Flanders[2]

ABSTRACT

Rapid epidemiologic assessment of needs and estimation of losses in areas affected by disasters is becoming recognized as one of the most important first steps in guiding the relief and recovery efforts (1). A cluster sampling technique adapted from one developed for the Expanded Program on Immunizations of the World Health Organization is currently being refined. This technique was used in the United States Virgin Islands after Hurricane Marilyn (and in Florida after Opal). In this paper, the results of that work, and the lessons learned, are summarized. In addition, future directions for further refinement of the technique are discussed.

KEYWORDS: disaster; cluster survey; hurricane; needs assessment; loss estimation

1. INTRODUCTION

On September 15 and 16, 1995, Hurricane Marilyn struck the U.S. Virgin Islands (St. Thomas, St. John and St. Croix). The greatest extent of damage was to St. Thomas, the most populated of the three islands, and the economic center of the islands.

In the aftermath of the hurricane, U.S. Federal relief plans came into effect, and soon approximately 3000 Federal workers were transported to St. Thomas to assist in relief and recovery.

Disaster managers needed to identify health and medical needs of the population on the island, and also to estimate the nature and extent of structural damage. Initially, no reliable information was available. A team of epidemiologists from CDC, began the daunting task of estimating the damage.

2. METHODS

In order to survey the island, a cluster sample survey design was chosen, based on the one used by the Expanded Program on Immunization (EPI) of the World Health Organization for assessing vaccination coverage levels in areas for which lists of inhabitants are not available (2,3) This technique had been used for needs assessment after Hurricane Andrew devastated Florida in 1992 (4).

In addition to the proportional estimates of needs used in previous experiences, we attempted to use a new modification to the sampling technique to enable the estimation of the *number* of people remaining in the affected area, as well as the *number* of housing units damaged and destroyed. This technique had been proposed, (5) but never field-tested.

2.1 Cluster Selection

We obtained an accurate map of St. Thomas from the FEMA Disaster Field Office, and divided the island into 440 clusters (Figure 1).

---

[1]Health Studies Branch, Division of Environmental Hazards and Health Effects, National Center for Environmental Health, U.S. Centers for Disease Control and Prevention, Atlanta, Georgia, USA 30341

[2]Division of Epidemiology, Rollins School of Public Health, Emory University, Atlanta, Georgia, USA 30322

Each cluster was approximately 0.5 miles by 0.5 miles. Based on estimates of population density provided by the U.S.Census (1990 population of St. Thomas 48,166) and the Virgin Islands Department of Health, we stratified the 440 clusters into 4 zones: East, North, Central (encompassing the only city, Charlotte Amalie) and West.

A random sample of clusters from each zone was chosen, with the number chosen in each zone proportional to the population density. A total of thirty clusters was chosen, with replacement.

2.2 Housing Unit Selection

The sampling units within each cluster were housing units, defined as a building, or part of a building, used to house a group of associated individuals such as a family. A total of 7 housing units were chosen from each cluster, by random selection similar to that used in the EPI method.

Our survey was not concerned only with particular attributes of surveyed *individuals* (access to drinking water, for example): we also wanted to assess attributes of included housing units. Housing units that were not occupied, or were destroyed, were therefore included in our survey, unlike the standard EPI method.

2.3 Total Housing Unit Counts Per Cluster

In order to estimate population remaining on the island, and to estimate numbers of damaged and destroyed housing units, according to the method proposed by Malilay *et al* (5), it was necessary to count, if possible, or estimate the total number of housing units per cluster.

2.4 Survey Content

The survey team rated the housing unit as either destroyed/uninhabitable, substantially damaged or undamaged. The survey team interviewed an adult member of every housing unit selected, if there were inhabitants. Adult members of each housing unit were asked about the number and the age of inhabitants, number of sick and injured persons, supply of food and water, access to sanitary facilities, method used for purifying water, access to telephone and motorized transportation, and attentiveness to local radio broadcasts.

2.5 Analysis

Data were analyzed in the Microsoft Excel software program using the cluster sampling methods described by Malilay, *et al* (5).

3. RESULTS

A survey was conducted approximately one week after the hurricane, and again one week later. There were no inhabited housing units without at least one adult. Data were analyzed in the Microsoft Excel software program.

The results of the two surveys are presented below in two categories: proportional estimates and numerical estimates of population (counts).

3.1 Proportional Estimates of Needs

Table 1 shows the results of the proportional estimates for both iterations of the survey.

11% of inhabitants included in the first survey (14% in the second survey) were living in (i.e., camping on the site of) housing units that were completely destroyed, with 67% (78%) in housing units that were damaged but habitable.

The proportions of ill and injured persons were low: 5% (10%) and 2% (4%), respectively. Nearly 100% of inhabitants surveyed were purifying their water in some way, and had access to a flushing toilet.

Most importantly, only 12% (9%) of inhabitants reported access to a working telephone, but 86% (89%) had access to a motorized vehicle, and nearly 100% were monitoring local radio

broadcasts.

3.2 Numerical Estimates of Population

The 1990 U.S. Census for the Virgin Islands reported the St. Thomas population as 48,166 persons.

Our initial estimates of the population remaining on St. Thomas after the hurricane were based on our field estimates of housing units per cluster. In many cases we had to estimate, rather than count, the numbers of housing units per cluster. The resulting population estimates were an improbable 69,082 for the first survey and 112,030 for the second survey.

Suspecting that inaccurate estimates of housing units per cluster were causing the inaccurate estimates of population, we modified the technique to incorporate 1990 U.S. Census housing unit counts. Specifically, we correlated census Block Numbering Areas (BNAs) with the zones of our sampling map. We then divided the total number of housing units given for the BNAs in a particular zone by the total number of clusters in that zone, giving us a figure for housing units per cluster.

The estimates made using this modified method were 53,640 for the first iteration and 55,898 for the second The average for the two iterations was 54,769.

4. DISCUSSION

4.1 Proportional Estimates of Needs

The estimates of needs provided by us to disaster managers were invaluable in shaping mitigation strategies.

An example of this concerned communication with the affected population, and transportation. Initially, disaster managers were issuing informational bulletins on local radio stations, and mentioning a phone number to call for further information, or to report an urgent need for assistance. In addition, initial plans called for house-to-house provision of essential items, a very time- and personnel-intensive endeavor.

As our survey showed, however, only a small proportion of the affected population had access to a telephone. A large proportion, however, had access to a motorized vehicle, and attention to local radio broadcasts was almost universal.

As a result, disaster managers set up centralized distribution points around the island and publicized these locations on local radio stations. This centralized strategy required fewer personnel and less time, thus freeing up much-needed personnel for other tasks.

4.2 Numerical Estimates of Population

Estimates of population incorporating our field estimates of housing units per cluster were unreliable: 69,082 and 112,030. These numbers were especially unlikely since it was felt that few inhabitants had left the island as a result of the hurricane:[3] one would expect the post-hurricane population to be equal to or slightly lower than the pre-hurricane population. The inaccuracy was the result of difficulty in counting housing units per cluster in the field, a task complicated by rough terrain, over-large clusters, limited maps with very little detail and a very large proportion of unmarked roads.

Realizing that our estimates were not reliable, we obtained an alternative means for estimating housing units per cluster, using 1990 U.S. Census data and overlaying it onto our map.

As reported above, this modification produced

---

[3]This may have been partly the result of initial weather forecasts which predicted that Marilyn would not significantly hit St. Thomas, and partly because St. Thomas, as an island, has limited routes for departure.

estimates of 53,640 and 55,898. The difference was therefore 2,258, with an average of 54,769.

We later found that the 1995 Population and Housing Survey of the U.S. Virgin Islands[4] produced a population estimate for St. Thomas of 54,259. This estimate differs from our average estimate by only 510.

This very clearly illustrates the importance of obtaining accurate counts of housing units per cluster in order to obtain valid estimates of population.

5. LESSONS LEARNED

As discussed above, it is of critical importance to obtain accurate counts of housing units per cluster. In situations where census data (or other reliable source) is available, this data should be used.

The matter is more complex in instances when accurate housing unit counts are not known. In these instances a number of strategies can be used to increase the ability to good counts of housing units in the field.

5.1 Maps

For a map to be useful for cluster sampling in a disaster setting it must accurately represent the area being surveyed, and must include the names of major natural and artificial landmarks: rivers, roads, etc.

5.2 Cluster design

It is important to realize that while clusters must be exhaustive (i.e., include the entire area being surveyed) and mutually exclusive, they do not need to be the same size. Far more important than uniform size is "manageability". By this we refer to two factors: size and boundaries.

A cluster must be small enough to enable the team to accurately count housing units. A five-mile-by-five-mile cluster will confound even a conscientious effort on the part of the surveyor.

In addition, a cluster should be designed in such a way that the surveyor in the field with map in hand will be able to locate all the boundaries of the cluster. That is, she should be able to "define" the cluster in the field. Defining clusters on a map without incorporating physical boundaries which can be located in the field will render the team unable to find any particular cluster in the field.

6. CONCLUSIONS

We field-tested the modified cluster sampling method described by Malilay *et al* (4). We were able to use it to describe not only proportions of inhabitants with needs, but also to accurately assess the population remaining in the area.

Accurate counts of housing units in the area being surveyed, we found, were critically important to this method.

7. ACKNOWLEDGMENTS

The authors gratefully acknowledge the support of the Federal Emergency Management Agency (FEMA) and the Health Department of the U.S. Virgin Islands.

8. REFERENCES

1. Anker M. Epidemiological and statistical methods for rapid health assessment: introduction. World health statistics quarterly, 1991; 44: 94-97

[4] Conducted by the Eastern Caribbean Center of the University of the Virgin Islands, with the assistance of the Population Division of the Bureau of the Census

2. Lemeshow S, Robinson D. Surveys to measure programme coverage and impact: A Review of the methodology used by the Expanded Programme on Immunization. *World Health Stat Q* 1985; **38**: 65-75.

3. Henderson RH, Sundaresan T. Cluster sampling to assess immunization coverage: a review of experience with a simplified sampling method. *Bulletin of the World Health Organization* 1982; **60**: 253-260.

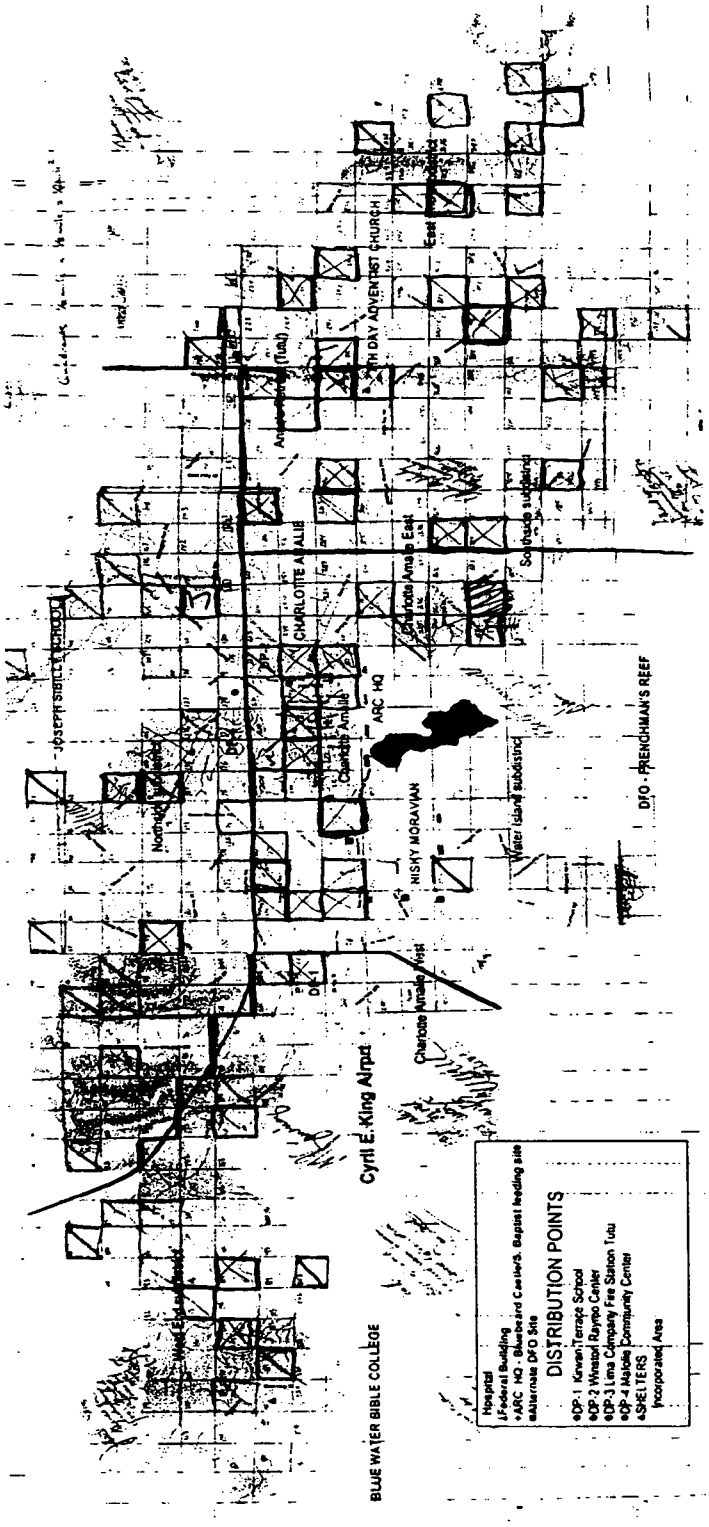
4. Hlady W, Quenemoen L, Armenia-Cope R, et al. Use of a Modified Cluster Sampling Method to Perform Rapid Needs Assessment After Hurricane Andrew. *Annals of Emergency Medicine* 1994: **23**; 719-725.

5. Malilay J, Flanders WD, Brogan D. A modified cluster-sampling method for post-disaster rapid assessment of needs. *Bulletin of the World Health Organization*, 1996; **74** (4): 399-405.

Table 1. Proportional Estimates of Needs after Hurricane Marilyn, St. Thomas, U.S. Virgin Islands, September 1995 (figures are percentages of persons included in the survey)

HOUSING	9/23	9/30
housing unit completely destroyed	11	14
housing unit damaged but habitable	67	78
HEALTH		
ill	5	10
injured	2	4
lacking prescription medicines	3	6
purifying drinking water	99	99
access to a flushing toilet	99	99
NUTRITION		
sufficient food for three days	86	88
drinking water within one mile	65	71
TRANSPORTATION/COMMUNICATION		
listening to local radio station	98	99
working telephone	12	9
working motor vehicle	86	89

Figure 1: Map of St. Thomas, U.S. Virgin Islands, depicting clusters chosen for sampling.



Theme 3

Storm Surge and Tsunamis

Offshore Tsunami Profiles Observed at the Costal Wave Stations

by

Toshihiko Nagai [1], Noriaki Hashimoto [2], Kazuyoshi Shimizu [3] and Fujio Kitamura [4]

ABSTRACT

This paper presents offshore tsunami profiles observed by NOWPHAS (Nationwide Ocean Wave Information Network for Ports and Harbours) wave-measuring instruments installed at various coastal wave stations and tide stations in Japan. Included are wave profiles of damage - inflicting tsunamis generated by the 1993 Hokkaido-Southwest Earthquake, the 1994 Hokkaido - Eastoff Earthquake, the 1996 Iri-Anjaya Earthquake, and other smaller recently occurring tsumamis. Also presented are characteristiscs and phenomena of interest clarifed through various analyses performed on observational data.

Key Words : NOWPHAS, Tsunami, Wave Gauges, Wave Observation

1. INTRODUCTION

Analysis of observed offshore tsunami profiles provides valuable information for clarifying their charactertics, which is essential for preventing disasterous consequences. Here, we present profiles of several damage-inflicting tsunamis which recently struck Japan, i.e., tsunamis generated by the 1993 Hokkaido-Southwest Earthquake on Jul. 12, 1993, the 1994 Hokkaido - Eastoff Earthquake on Oct. 4, 1994, the 1995 Hyogo - South Earthquake on Jan.17, 1995, and the 1996 Irianjaya Earthquake on Feb.17, 1996. Wave data was measured by NOWPHAS (Nationwide Ocean Wave Information Network for Ports and Harbours) wave - measuring instruments installed at various coastal wave stations and tide stations in Japan. Also presented are characteristics and phenomena of interest clarifed through various analyses performed on observational data.

2. WAVE-MEASURING INSTRUMENTION

Figure 1 shows the NOWPHAS wave observation network in Japan (Nagai et al., 1996, 1994a) which is operated under the conspices of the Ports and Harbours Bureau of the Ministry of Transport (MOT) and its associated agencies including the Port and Harbour Research Institute (PHRI). This nationwide network of wave - measuring instrumentaion is the product of long-term intensive efforts directed at obtaining more precise and reliable coastal wave information for disaster prevention purposes and the planning, design, and construction of ports and other coastal structures.

Figure 2 shows three types of wave-measuring instruments employed in the NOWPHAS network: (1) The ultrasonic wave (USW) gauge, a widely employed instrument

1) Chief, Marine Observation Laboratory, Hydraulic Engineering Divison, Port and Harbour Research Institute (PHRI), Ministry of Transport (MOT), 3-1-1 Nagase, Yokosuka, 239, Japan

2) Chief, Hydraulic Laboratory, Marine Environmental Divison, PHRI, MOT

3) Ex-Senior Research Engineer, Hydraulic Engineering Divison, PHRI, MOT

4) Ex-Senior Research Engineer, Coastal Development Institute of Technology, 6F 3-16 Hayabusa-cho, Chiyoda, Tokyo, 102, Japan

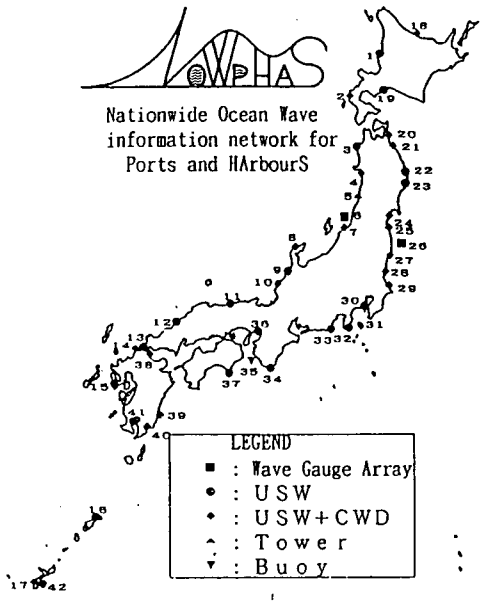


Figure. 1 NOWPHAS Wave Observation Network

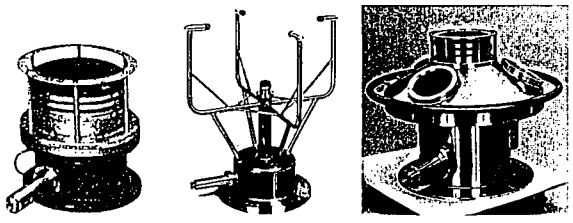


Figure. 2 USW, CWD, and DWDM Wave Gauges Hokkaido – Southwest Earthquake Offshore Tsunami Profile

(jointly developed by the Kaijo Co. and PHRI in the 1960s) which precisely determines wave surface elevation by measuring the time for an ultrasonic wave to travel between the seabed and water surface, (2) The current wave directional (CWD) gauge, a widely employed instrument (developed in the 1970s) which determines wave direction by measuring wave – induced horizontal current fluctuations along the seabed, and (3) The Doppler wave directional meter (DWDM), a newly employed instrument (jointly developed by the Kaijo Co., Marine Surveyors Association, and PHRI in 1995) which uses a single sensor to determine with sufficient accuracy the height, period, and directional spectra of waves. DWDMs have been installed at four coastal stations (**Fig.1**) (Takayama et al., 1995), and in the future are expected to be the main wave – measuring instrument employed under NOWPHAS.

3. HOKKAIDO–SOUTHWEST EARTHRUAKE OFFSHORE TSUNAMI ROFILE

Figure 3 shows 20 min of offshore wave records observed at coastal station No.8 Wajima (Sta. 8) before arrival of the 1993 Hokkaido – Southwest Earthquake tsunami. Shown are water surface elevation, horizontal current at the seabed in vector form, and the corresponding vector components of water velocity U(m/s) and water direction θ . A USW installed at 50 m measures η and a CWD installed at 27 m measures U and θ . **Figure 4** shows corresponding records observed just after the arrival of the tsunami (Nagai et al., 1993, 1994b, 1995a), where it can be seen from the center line determined by low–pass filtering that distinct, long–period oscillations are generated in η . The wave current is also clearly affected as indicated by the long–period oscillations in the horizontal current vectors numerically determined using a triangular low–pass filter of 10s in length.

Shown in **Figure 5** are pair values of USW – measured filtered η and CWD–measured differential change in seabed pressure p observed at Sta. 4 Akita before (left) and after(right) tsunaimi arrival; where for each case, 20 min of data are plotted at a sampling interval of 0.5s. Before arrival, most values are concentrated around the origin (η =p = 0) indicating no long–period oscillations in η or seabed current. In contrast, however, after the tsunami arrives they are concentrated along the line η =p; thereby indicating

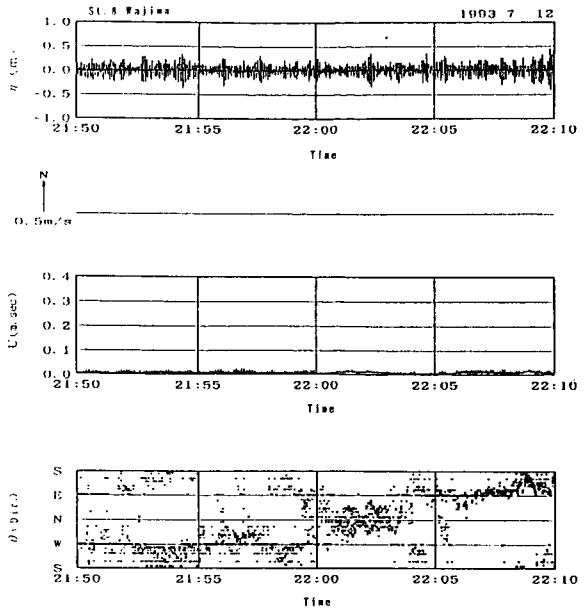


Figure. 3 Offshre Wave Gauge Data before the Tsunami Attack

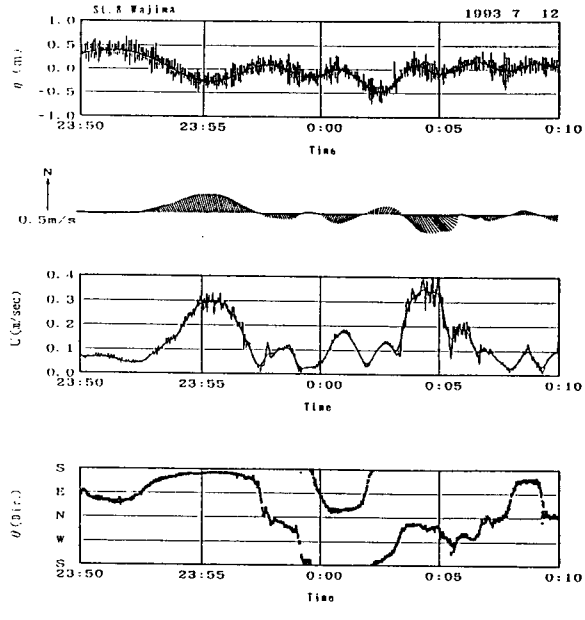


Figure. 4 Offshre Wave Gauge Data after the Tsunami Attack

long-period oscillations occur as expected under linear long wave theory. Taken together, these results confirm the reliability of the observed.

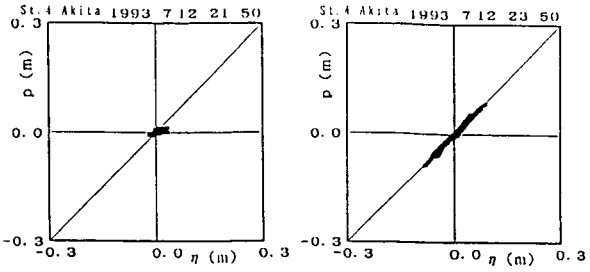


Figure. 5 Comparison of η and p

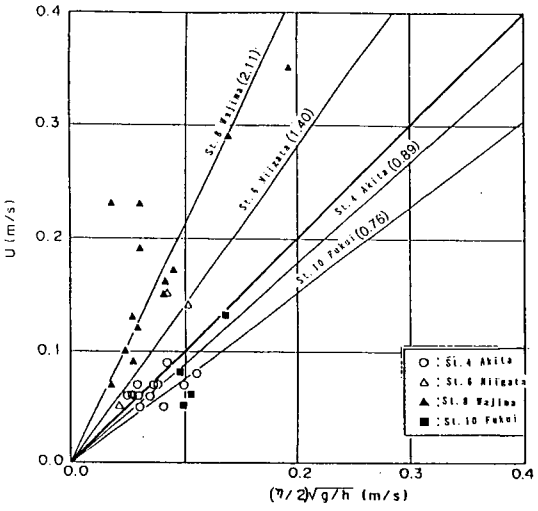


Figure. 6 Comparison of η and U

Under linear progressive long wave theory, the following relationship should hold:

$$U_{Max} = (\eta / 2)(g / h)^{1/2} \quad (1)$$

where U_{Max} is the maximum horizontal water velocity at the seabed, $\eta / 2$ the amplitude of water surface elevation $(\eta_{Max} - \eta_{Min}) / 2$, g the acceleration of gravity, and h the water depth. These parameters are respectively plotted as pair values in **Figure 6** for various wave stations over a 20-min period following the arrival of the tsunami. If eq. (1) is satisfied, then the plotted values should fall on the indicated 45 degree line. For standing waves, $\eta = 0$ at the nodes (y-axis) and U=0 at the antinodes (x-axis). Considering the results, it appears that the observed tsunami is not completely progressive, but rather exhibits characteristics of standing waves due to the effect of wave reflection.

Integration of current velocity over time gives the motion of water particles at the seabed, being shown in **Figure 7** for 20 min before and after the tsunami's arrival at Sta. 8 with and without tide corrections. Motion is shown in the horizontal plane in which the x− and y−axis indicate directions East(+) and West(−) and North(+) and South(−). The

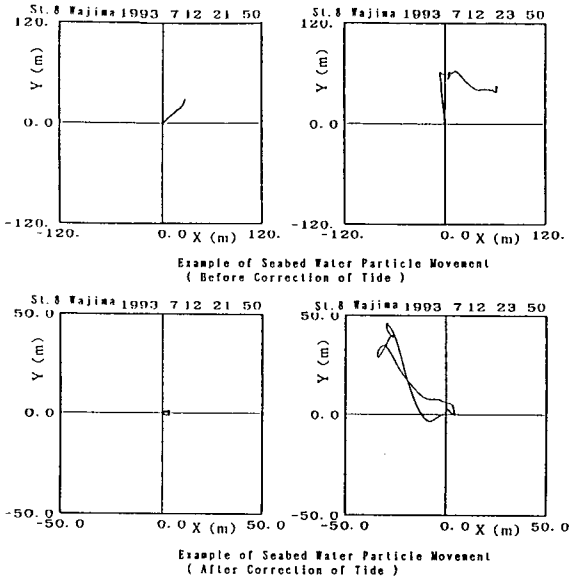


Figure. 7 Seabed Water Particle Movement

effect of the tsunami is quite apparent, especially when considering tide effects. Note that the direction of the constant−velocity tidal current is shown before arrival, and that after correction it is properly accounted for. The amplitude of seabed particle motion due to the tsunami is shown to be about 50m, i.e., a distance much greater than can be explained by even the strongest wind−wave conditions.

Figure 8 shows the low−pass filtered offshore wave profile η and tide record Z, before and until more than 6 hours after tsunami arrival as measured at Sta. 8 (3km offshore), and the Wajima Port tide station, respectively. Upon tsunami arrival just after 0:00LT, both records show a large peak which cannot be accounted for by the effects of wind or tidal motions. In addition, short−period oscillations less than 10 min, i.e., such as those clearly shown in η, cannot be observed in tide records due to the occurrence of low−pass −filter effects in the measuring instrument's seawater drain tube; thereby demonstrating the necessity for deploying offshore wave−measuring instrumentation.

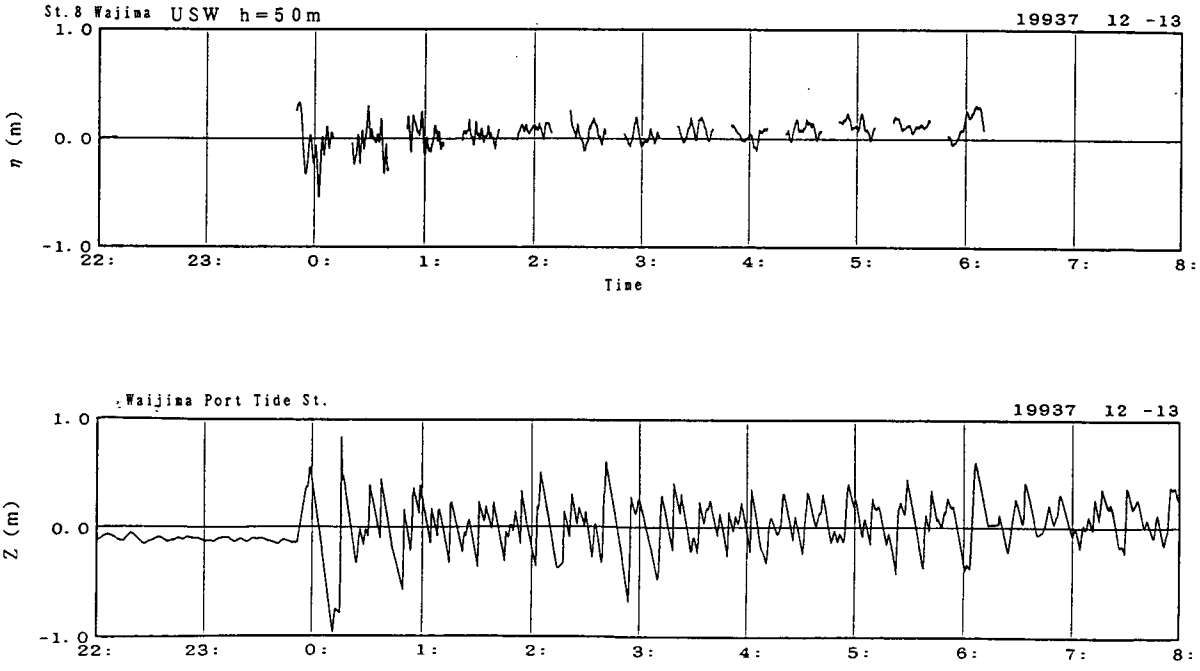


Figure. 8 Comparison of Offshore Wave Profile and Tide Record

4. HOKKAIDO－EASTOFF EARTHQUAKE OFFSHORE TSUNAMI PROFILE

Figure 9 summarizes the heights and periods of the tsunami generated by the 1994 Hokkaido － Eastoff Earthquake as observed along Japan's Pacific Ocean coast by NOWPHAS wave－measuring instrumentation (Nagai et al., 1995b, 1995c). Individual tsunami waves was defined by the zero－up－cross method. A "*" denotes wave station data while all other data is from tide stations. Note that individual tsunami waves show a long period of about 40 min.

Figure 10 shows a continuous offshore profile η of the tsunami as observed at Sta. 19 off Tomakomai Port at a water depth of 18.5 m. This data was obtained as part of a continuous offshore long wave observation project conducted in Oct. 1994 by the Tomakomai Port Construction Office of the Hokkaido Development Agency in order to investigate a port resonance problem caused by long waves. Although η is low－pass filtered, clearly distinguishing the tsunami from wind waves and tides is difficult due to the presence of waves with significant wave heights of more than 2 m and a large range of tidal motion. Nevertheless, when these observations are considered in conjunction with those in **Figure 10**, this confirms the presence of tsunami－generated waves with very long periods of 30 to 80 min.

Figure 11 also shows continuous tsunami wave data observed by tide and offshore wave stations at Sta. 20 Mutsu－Ogawara for the tsunamis generated by the Hokkaido－Eastoff and 1994 Sanriku － Faroff (Dec. 28, 1994) Earthquakes. Also shown are the predicted tides, as well as seabed horizontal current vectors for the Hokkaido － Eastoff tsunami.

The results of applying frequential spectral analysis to the data in **Figure 11** are presented in **Figure 12**, which shows corresponding power spectra and the response

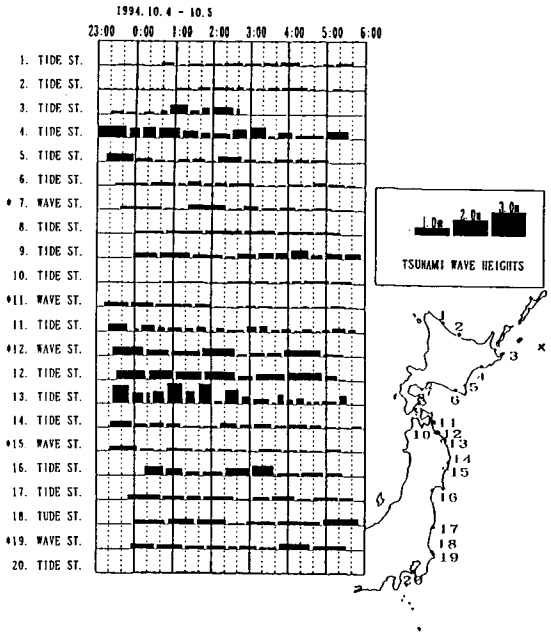


Figure. 9 Tsunami Heights and Periods of the 1994.10 Earthquake

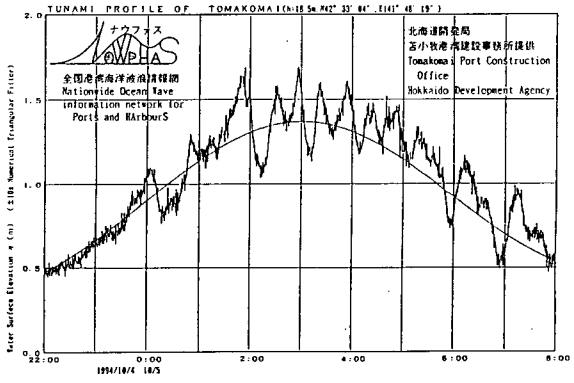


Figure. 10 Tsunami Profile of the No. 7 Tomakomai Port

functions of the wave and tide gauges for each tsunami. Note that both tsunami show the same correlation between their wave and tide spectra; thereby indicating accurate and reliable measurements even under transient, unstable conditions caused by a tsunami.

Figure 13 shows the results of a spectral correlation analysis between η and Z power spectra determined from observation data of the Hokkaido－Eastoff tsunami. Coherence and phase values indicate high stability for measurements at frequencies less than 10^{-3} Hz, which includes the frequency range

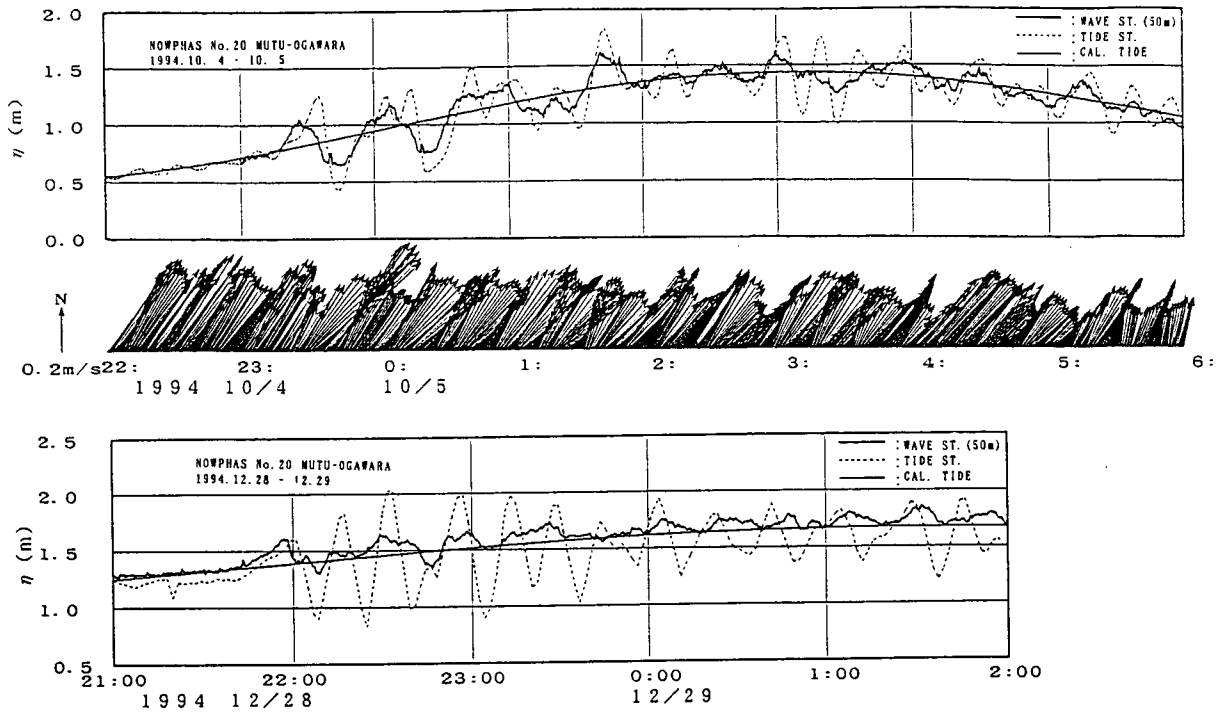


Figure. 11 Tsunami Profile of the No. 20 Mutsu–Ogawara Port

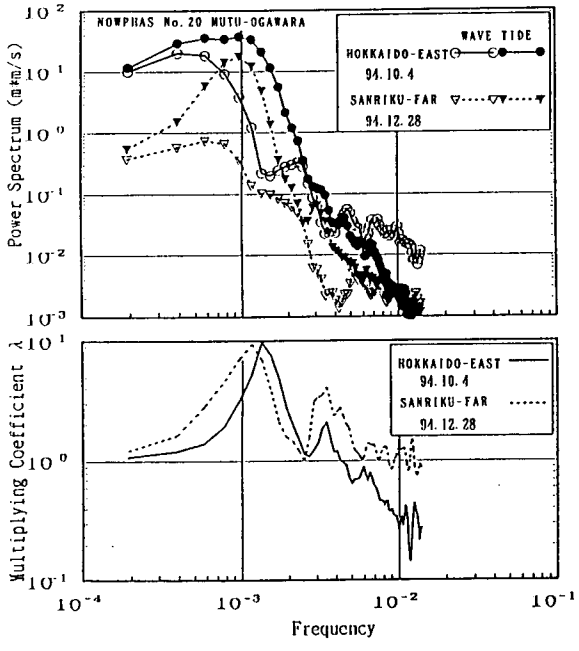


Figure. 12 Frequential Spectra of the No. 20 Mutsu–Ogawara Port

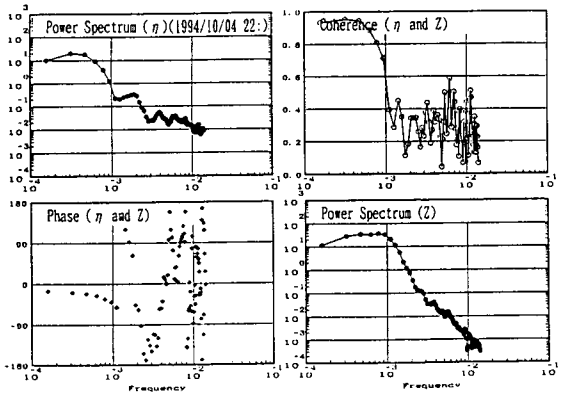


Figure. 13 Spectra Correlation between η and Z

where dominant tsunami energy exists.

Shown in **Figure 14** are corresponding results for spectral correlation analysis between η and the two vector components of seabed horizontal current velocity u and v, where u is the east – west (on – off shore) direction and v the north – south (longshore) direction.

Evaluation of the respective coherence and phase values indicates consistent results with those shown in **Figure 13.**

Figure 15 shows pair values of u and η $(g / h)^{1/2}$ plotted over three 15–min periods in which the first – arriving individual Hokkaido–Eastoff tsunami wave was observed

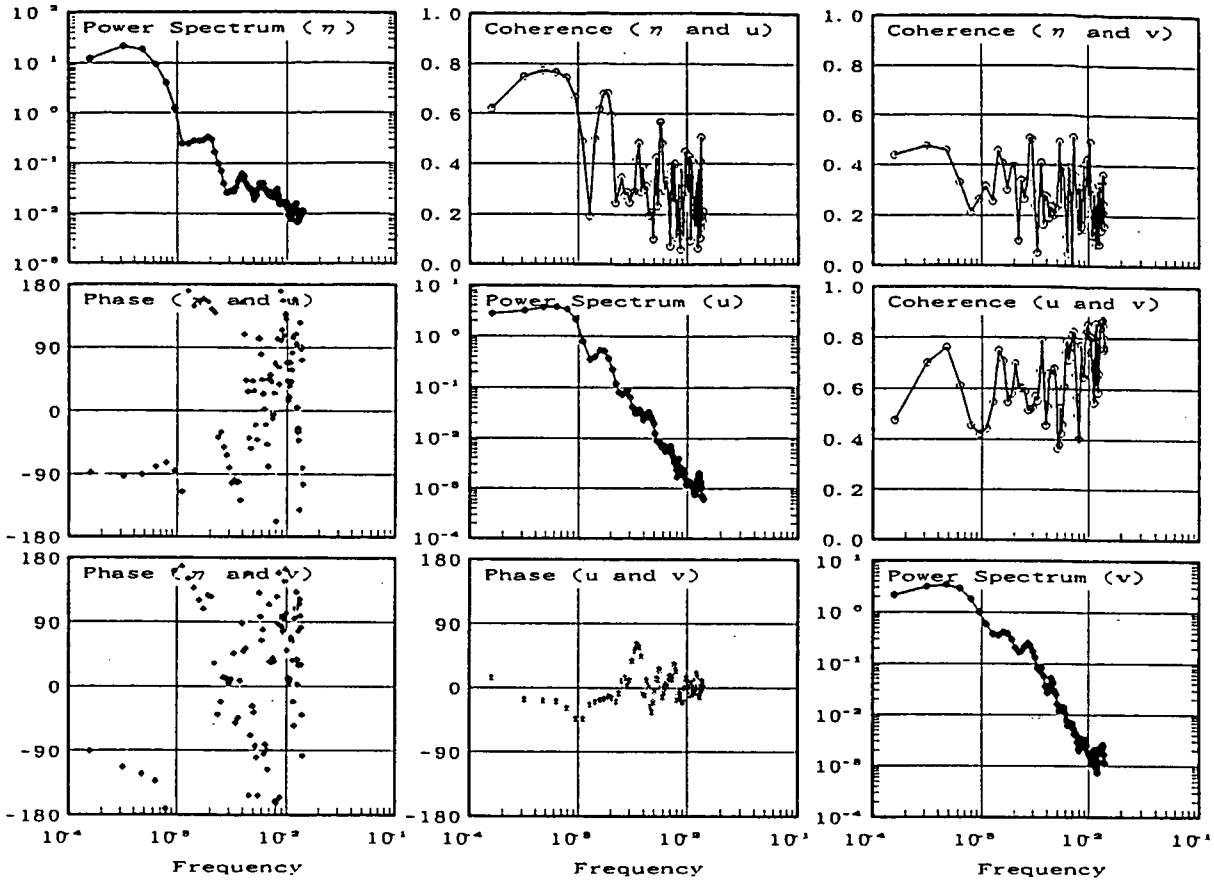


Figure. 14 Spectra Correlation among η , u and v

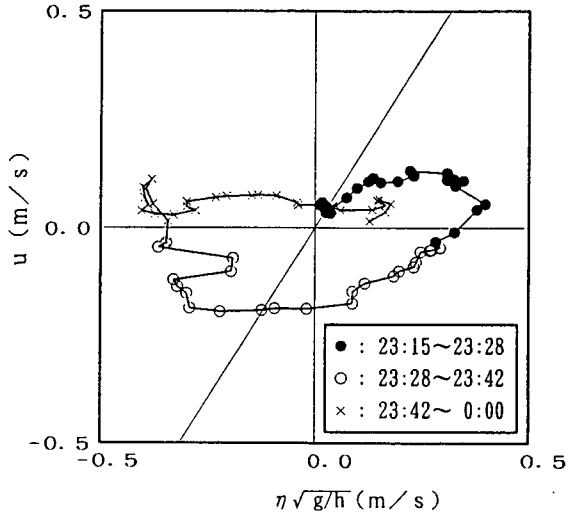


Figure. 15 Relation between η and U for the First Tsunami Wave

by Sta. 20, where the values should fall on the straight line passing through the origin under linear progressive wave theory. In this case, the difference between the observation depth of the USW (50m) and CWD (28m) gauges is accounted for. A comparison of observed values indicates the presence of standing wave characteristics at the early stage of observation due to wave reflections off the coast.

Continuous – observed offshore wave profiles provide a good benchmark from which to evaluate numerical models for simulating tsunami characteristics. **Figure 16** compares observed wave/tide station η / Z and u of the Hokkaido–Eastoff tsunami obtained at Sta. 20 with those calculated by a numerical simulation model of 3 km grid based on linear long wave propagation characteristics(Aida, 1962), and the initial seabed movement determined by the DCRC–3b model (**Table 1**) developed at the University of Tohoku. Good agreement is present for all three measured parameters, possibly being due to employing a grid size that is relatively small compared to tsunami wave length with a 40–min period.

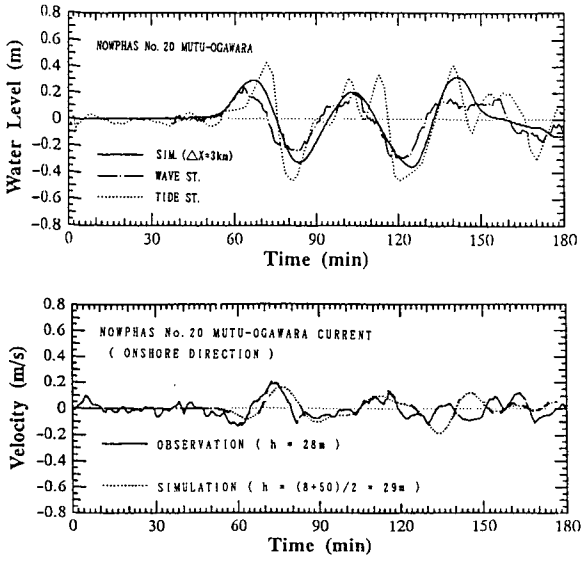


Figure. 16 Comparizon of the Observed and Caluculated Tsunami Profile

Table. 1 The 1994 Tsunami Model (DCRC −3b Model by Univ. of Tohoku)

Origin of Fault	43.210° N, 146.120° E
Length	140 km
Width	70 km
Strike	52°
Dip Angle	77°
Slip Angle	128°
Depth	30 km
Dislocation	7.62 m

5. HYOGO−SOUTH EARTHQUAKE TSUNAMI PROFILE

The city of Kobe and its surrounding region suffered tremendous damage and loss of life when the 1995 Hyogo−South Earthquake stuck during the early morning hours (05:47). **Figure 17** shows USW−measured offshore wave profile before and immediately after striking as observed by Sta. 36 Kobe, where amplitudes of several centimeters and periods of 1 or 2 min are indicated by the low−pass−filtered line, i.e., most of the earthquake's

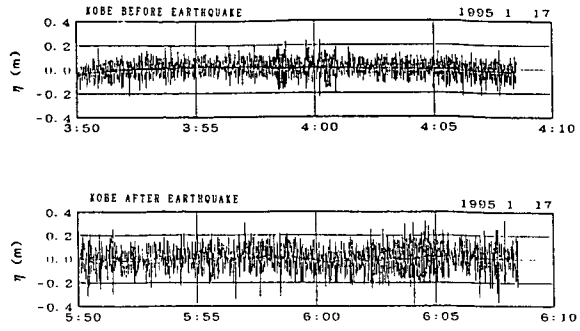


Figure. 17 The 1995 Hygo − South − Earthquake Tsunami Profile Irianjaya Earthquake Tsunami Profile

energy was expended on land areas such that its effect generated only slight movement of the seabed.

6. IRIANJAYA EARTHQUAKE TSUNAMI PROFILE

Figure 18 shows the wave profile of the tsunami generated by the 1996 Irianjaya−Earthquake as observed by Sta. 31 Habu (USW, 50 m) and PHRI (USW and tide station) at the entrance to Tokyo Bay 50 km distant. The tsunami arrived at the bay entrance 20 to 30 min after initial observation at Sta. 31, which indicates that continuous observation and monitoring of offshore waves at this offshore station would allow predicting the strike time and provide an early warning for the Tokyo area. Note that the maximum wave heights are about 10 and 70 cm, respectively, with this amplification in height being due to topographical resonance effects.

The results of applying frequential spectral analysis to the data in **Figure 18** are presented in **Figure 19**, where a distinct resonance peak is apparent and indicates that amplification occurs in the frequency band of 0.9×10^{-3} and 1.5×10^{-3} Hz (T = 18.5 and 11min).

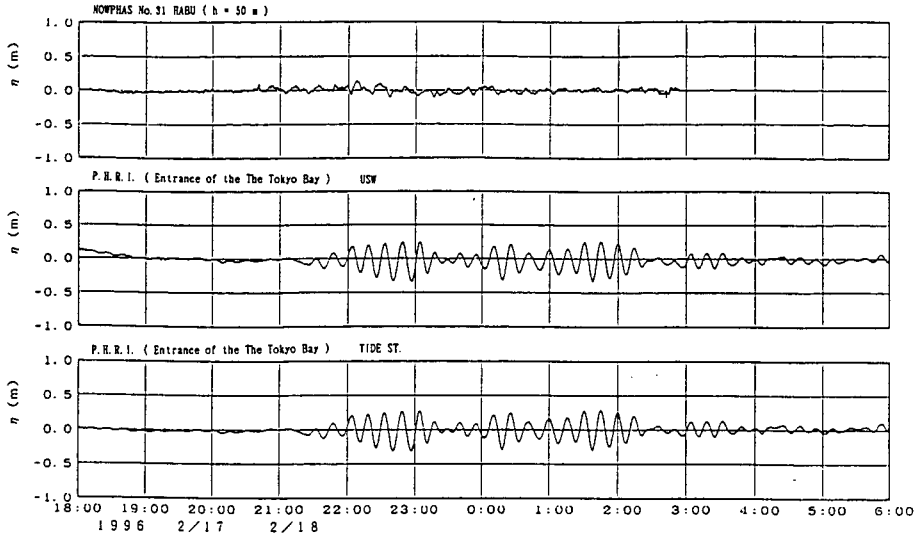


Figure. 18 The 1996 Irianjaya–Earthquake Tsunami Profile

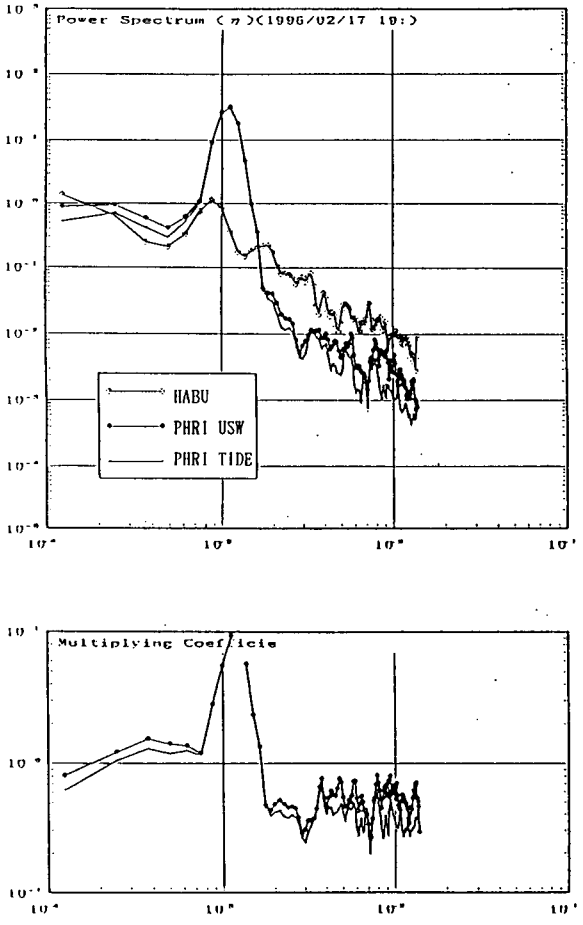


Figure. 19 Frequential Spectra of the 1996 Irianjaya–Earthquake Tsunami Summary

7. SUMMARY

We have analyzed selected wave profiles and associated data of large, recently striking tsunami as observed by NOWPHAS offshore wave–measuring instruments and harbor tide stations throughout Japan. As a result of our analysis, several tsunami characteristics and phenomena of interest have been clarified, and through our better understand we can expect to improve observation capability. To fully understand the characteristics of tsunamis and long waves, however, the data acquisition system of NOWPHAS must be reconfigured to a more continuous observation scheme as wave observations are at the present time only performed for 20min every 2h. Efforts to realize such an observation system are now in progress (Nagai et al., 1995d).

8. ACKNOWLEDGMENTS

For their outstanding cooperation, sincere gratitude is extended to all personnel involved with NOWPHAS, with a special thank you to those from the Ports and Harbours Bureau, District Port Construction Bureaus of MOT, Hokkaido and Okinawa Development Agencies, and PHRI.

REFERECES

Aida,I. (1962), "Numerical Experiments for Tsunami Caused by Moving Deformation of the Sea Bottom, Bull. Earthqu. Res. Inst., vol.47, pp.849–862.

Nagai,T., Sugahara,K, Hashimoto,N., and Asai,T. (1996), "Annual Report on Nationwide Ocean Wave information network for Ports and HArbourS (NOWPHAS 1994)", Technical Note of the PHRI, No.821, 313p. from 1970 to1993 year's versions of the same series of the Annual Reports, See the Technical Notes of the PHRI, No.137, 158, 178, 209, 233, 258, 282, 311, 332, 373, 417, 445, 480, 517, 545, 574, 612, 642, 666, 712, 721, 745, 770, and 796 respectively

Nagai, T., Hashimoto,N., Shimizu,K., and Takayama,T. (1995a), " Tsunami Profiles Observed at the NOWPHAS Offshore Wave Stations ", Second International Workshop on Wind and Earthquake for Offshore and Coastal Structure, UJNR at Berkeley, California

Nagai, T., Hashimoto,N., Hiraishi,T, and Shimzu K.(1995b), " Characteristics of the 1994 Hokkaido–Eastoff–Earthquake Tsunami ", Technical Note of the PHRI, No.802, 97p.

Nagai,T., Hashimoto,N., Hiraishi,T, Shimzu K., Ichikawa, T., Miyabe S.,Kudaka,M., and Kawamata,S .(1995c), " Characteristics of the 1994 Hokkaido–Eastoff–Earthquake Tsunami based on the Field Observation Data", Proceedings of Coastal Engineering, Vol.42, Japan Society of Civil Engineers, pp.351–355.

Nagai,T., Hashimoto,N., Asai,T., Tobiki,I., Ito,K., Toue,T., Kobayashi,A.,and Shibata,I.(1995d), "Relationship of a Moored Vessel in a Harbour and a Long Wave Caused by Wave Groups ", Proceedings of the 24th International Conference on Coastal Engineering (ICCE'94), vol.1, pp.847–860.

Nagai, T ., Sugahara, K. , Hashimoto, N. , Asai, T., Higashiyama,S., and Toda,K.(1994a), "Introduction of Japanese NOWPHAS System and its Recent Topics", Proceedings of HYDRO–PORT'94, PHRI, pp.67–82.

Nagai,T., Sugahara,K, Hashimoto,N., and Asai,T., Higashiyama,S., Toda,K. (1994b) , "Offshore Tsunami Profiles of the 1993 Hokkaido – Southwest – Earthquake Tsunami ", Proceedings of Coastal Engineering, Vol.41, Japan Society of Civil Engineers, pp.221–225.

Nagai, T., Hashimoto, N., and Asai, T.(1993), "The Hokkaido–Southwest–Earthquake Tsunami profiles observed at the NOWPHAS offshore stations",Rept. of PHRI, Vol.32, No.4, pp.51–97.

Takayama, T., Hashimoto, N., Nagai, T., Takahashi, T., Sasaki, H. , and Ito,Y., (1995), " Development of Submerged Doppler–type Directional Wave Meter", Proc. of the 24th International Conference on Coastal Engineering (ICCE'94), vol.1, pp.624–634.

HURRICANE FRAN STORM SURGE ASSESSMENT

by

William E. Roper

ABSTRACT

This paper describes Hurricane Fran as it approached the North Carolina Coast on September 3, 1996, until land fall on September 5th. An overview of the impact in damage and lose of life is presented. The storm surge analysis conducted by the Corps of Engineers for the Federal Emergency Management Agency is summarized. High water marks were identified and recorded at 211 locations. Water level time history is presented at six locations, and water discharge rates at 13 positions along the North Carolina coast. Inundation maps were developed for the surge effected coastal regions.

KEY WORDS: hurricane; storm surge; high water mark; inundation maps; Hurricane Fran.

1. INTRODUCTION

Hurricane Fran after striking the North Carolina coast on September 5, 1996, moved inland effecting Virginia, Maryland, and West Virginia causing over five billion dollars in damage. In the aftermath of this storm a detailed study was taken under the direction of the Federal Emergency Management Agency to evaluate the storm surge and inundation that resulted from Hurricane Fran. A summary of that evaluation is presented here to include high water mark data, time history of the storm surge, inundation maps, and inlet water flows.

2. OVERVIEW OF IMPACT

Hurricane Fran slammed into North Carolina's southern coast with sustained winds of approximately 115 MPH, and gusts as high as Hurricane Fran slammed into North Carolina's southern coast on September 5th with sustained winds of approximately 115 MPH, and gusts as high as 125 MPH. At some point, 1.7 million customers in North Carolina and 400,000 customers in Virginia lost electricity. The death toll was at 36, including 23 in North Carolina. Flooding has also been a severe problem in North Carolina, Virginia, West Virginia, and Maryland. Fran produced rainfall amounts of over 10 inches in parts of eastern North Carolina and western Virginia.

Damages for homes and businesses in North Carolina were approximately $2.3 billion. Damages/costs related to the public (debris removal, roads and bridges, public buildings, utilities, etc.) was about $1.1 billion for NC. Agricultural damage (crops, livestock, buildings) in North Carolina was over $700 million. Wake County (Raleigh and vicinity) alone reported over $900 million in damage to residential and commercial property. Finally, forestry/timber losses for the state exceeded $1 billion.

Taken collectively, total damages/costs for North Carolina was near $5 billion. With the addition of lesser damages for states to the north, the storm's total cost excessed $5 billion, making Fran the third most costly hurricane in U.S. history, moving Opal (1995) into fourth place. However, it's important to note that the figures for earlier storms are not adjusted for inflation. Just prior to landfall of Fran, a small portion of western North Carolina-

[1]Director, Civil Works Research and Development, U.S. Army Corps of Engineers, Washington, DC 20314-1000.

in the Bat Cave, Chimney Rock, Lake Lure areas--received up to 11 inches of rain in a 3 hour period. The rains were the result of nearly stationary, very heavy thunderstorms associated with an upper level low pressure system. Severe damage to property in the immediate area resulted, with about 70 homes and businesses being destroyed or significantly damaged. Figures 1 and 2, are GOES-8 IR images of Hurricane Fran prior to land fall on September 4 and 5. Figure 3 is an image at land fall or September 5th.

3. HURRICANE FRAN HIGH WATER MARKS AND INUNDATION MAPPING

3.1. Purpose

Hurricane Fran made landfall along the North Carolina coast in the vicinity of Carolina Beach, NC on September 5, 1996. As a result of this storm, The Wilmington District of the Corps of Engineers (COE) was tasked by the Federal Emergency Management Agency (FEMA) to locate high water marks along the coastal area impacted by the storm and produce inundation mapping based on these high water marks. The purpose of this report is to present the high water mark data and other information developed during this study.

3.2. High Water Marks

High water mark data was collected following the hurricane at various locations along the coastal areas of North Carolina impacted by the surge from Hurricane Fran. This data was collected by personnel from three organizations. Dewberry and Davis, a consulting engineering firm under contract to FEMA, collected preliminary data on the coastal beaches immediately following the storm. The data they collected was compiled in a report for FEMA titled Hurricane Fran North Carolina High Water Mark Survey and Coastal Inundation Mapping, dated September, 1996. The U.S. Geological Survey (USGS) also collected high water mark data along the beaches following the storm.

The COE was tasked with the mission of collecting additional high water marks where needed and producing inundation maps. Most of the data collected by the COE was in areas which were inaccessible immediately following the storm and along the coastal creeks along the west side of the Atlantic Intracoastal Waterway(AIWW) impacted by the storm surge. Data was collected from Southport, NC north to Beaufort, NC. In collecting the high water marks an attempt was made to collect both inside and outside marks. A total of 211 high water marks were collected.

3.3. Method of Collection High water data was collected based on visual observations by personnel who were familiar with collection of highwater mark data. The high water marks were identified in the field and the location along with other pertinent information was described on data forms. A picture of the high water mark was taken at each location. Figures 4 thru 7 are examples of the pictorial data developed for each high water mark.

3.3.1 Coordinates The geographic location of the HWM's were described using latitude and longitude. The coordinates of the high water marks were determined in the field using the Geographic Positioning System(GPS). The coordinates of the marks taken by Dewberry and Davis were determined based on a dual frequency Differential Geographic Positioning System(DGPS). The procedure is described in their report. The coordinates of the marks taken by the USGS and COE were determined using a hand held GPS unit. The locations were later verified in the office with the use of topographic maps.

3.3.2 Elevations Elevation of high water marks taken by Dewberry and Davis were determined using DGPS as mentioned above and described in their report. The elevation of marks taken by the USGS and COE were determined using conventional survey methods. Bench mark elevation data from USGS and various other sources was obtained and used for vertical control. Elevations were obtained by conventional leveling using two 2- man survey teams. Representatives of the COE were in the field with the survey teams to coordinate the effort.

Table 1 is a sample of the data collected for each of the 211 high water mark sites.

3.4 Inundation Mapping

Storm surge mapping was accomplished using the Arc-Info 7.04 Unix Geographic Information System (GIS) software and constructed GIS datasets. The base GIS datasets were obtained from the State of North Carolina Center for Geographic Information and Analysis (NCCGIA) consisted of the following:

1. NC County Lines
2. NC Roads (primary and secondary)
3. NC Hydrography (water and land)

These datasets were used for the overall base mapping of the inundated areas.

The inundation line for the storm was developed using USGS 1:24000 scale quadrangle sheets. The line was first delineated on the quad sheets utilizing the HWM elevations and locations obtained in the field. The line was then digitized and entered into the Arc-Info data base and overlaid on the base maps. HWM location points collected in the field were also converted to a GIS dataset and overlaid on the maps. The limits of mapping for the inundation line were set at points where the inundation became insignificant.

Listed below are the Quadrangle sheets used to produce the inundation limits.

Southport, NC	Spicer Bay, NC
Kure Beach, NC	Sneads Ferry, NC
Carolina Beach, NC	New River Inlet,
Hubert, NC	Wrightsville Beach, NC
Scotts Hill, NC	Browns Inlet, NC
Tampstead, NC	Swansboro, NC
Topsail, NC	Salter Path, NC
Holly Ridge, NC	

A sample inundation map is shown in figure 8 for the Wrightsville Beach Area. The maps are printed at a scale of 1:24000 and are identified by the same name as the USGS quad sheets used to produce the inundation limits. The HWM numbers shown on the map are referenced to Table 1 as HWM ID numbers.

4. Storm Surge

Tide levels along the North Carolina and South Carolina Coast for the time period during the storm were available at five locations. Location information on the five gages are listed below.

Gage Name	Mean Tide Level (ft)	Peak During Fran (ft)
Myrtle Beach, Springmaid Pier	2.73	7.3
Wilmington, NC	2.20	7.1
Beaufort, Duke Marine Lab	1.60	6.4
Hatteras Ocean Gage	1.90	4.0
Oregon Inlet	1.00	2.9

The tide range for the period at the Wilmington is shown graphically in figure 8.

The storm surge was also recorded at one location along the AIWW by Mr. Spencer Rogers, NC Sea Grant at his residence which is located on the western side of the AIWW between Carolina Beach and Wrightsville Beach, NC. These observations give a very accurate record of the storm surge along the New Hanover County coast line. The plot of the surge is shown on figure 9.

5. Stream Gages

There are no USGS recording stream gages in the

coastal area impacted by the storm which would have recorded the storm surge. There are, however, gages on all of the major inland rivers which recorded stream flow data during the storm which show the effects of the rainfall associated with the storm on the inland rivers and streams. Data was furnished by the USGS at the gages shown in table 2.

6. CONCLUSIONS

The assessment of the storm surge during Hurricane Fran was one of the most comprehensive under taken. The data collection and report format used is expected to become a standard for future events of similar importance by the Federal Emergency Management Agency.

The data collected during this assessment on high water marks, storms surge time history, and inlet discharge rates will be used to validate and refine storm surge predictive models by the U.S. Army Corps of Engineers.

These data will also be used in a study currently underway by the Corps of Engineers to evaluate the performance of beach areas protected by Federal projects versus beaches that are not protected. Beaches in both categories were impacted by Hurricane Fran.

7. ACKNOWLEDGMENTS

The author gratefully acknowledges the assistance of Mr. Linwood Rogers of the U.S. Army Corps of Engineers Wilmington District for the data and report information on the storm surge from Hurricane Fran.

8. REFERENCES

Hurricane Fran High Water Marks and Inundation Mapping Report, U.S. Army Corps of Engineers, Wilmington District, Wilmington, NC, September 1996 .

Hurricane Fran-North Carolina High Water Mark Survey and Coastal Inundation Mapping, Dewberry and Davis Inc., Engineering Consultants, September 1996.

Hurricane Fran Images, National Oceanographic and Atmospheric Administration, Silver Springs, MD, September 1996.

Table 1
Pertinent High Water Mark Data-Coastal North Carolina

HWM ID	HWM Field Number	Inside(I) or Outside(O)	Type Line	Quadrangle Sheet	Latitude	Longitude	Elevation (ft, msl)	Obtained By
SOUTHPORT-KURE BEACH-CAROLINA BEACH AREA								
1	hwm 2010	O	Debris	Southport	33°55'01.38282"	78°01'04.07487"	5.4	Dewberry and Davis
2	hwm 2011	O	Debris	Southport	33°53'59.41651"	78°03'51.12476"	11.2	Dewberry and Davis
3	hwm 2013	O	Debris	Southport	33°53'59.41651"	78°03'51.30939"	12.2	Dewberry and Davis
4	NH-2F	O	Mud	Kure Beach	33°57'51.11887	77°55'17.31822'	8.4	U.S. Geological Survey
5	hwm2014	O	Debris	Kure Beach	33°58'10.66001"	77°55'08.05241"	12.5	Dewberry and Davis
6	NH-60-KB	I	Mud	Kure Beach	33°58'25.92355"	77°54'52.85720"	14.1	U.S. Army Corps of Engineers
7	NP-3P	O	Debris	Kure Beach	33°58'51.55023"	77°54'48.18686"	14.0	U.S. Geological Survey
8	NH-4P	O	Mud	Kure Beach	33°58'54.67583"	77°54'42.74307"	14.8	U.S. Geological Survey
9	NH-61-KB	I	Mud	Kure Beach	33°59'00.65651"	77°54'42.32002"	14.0	U.S. Army Corps of Engineers
10	hmw2018	O	Debris	Kure Beach	33°59'12.64196"	77°54'42.01731"	15.1	Dewberry and Davis
11	NH-5F	O	Mud	Kure Beach	33°59'15.81296"	77°54'37.14494"	14.5	U.S. Geological Survey
12	hwm2017	O	Debris	Kure Beach	33°59'21.23023"	77°54'36.26851"	15.4	Dewberry and Davis
13	hwm2015	O	Debris	Kure Beach	33°59'32.48636"	77°54'33.77071"	15.3	Dewberry and Davis
14	NH-6P-B	O	Debris	Carolina Beach	34°00'19.38965"	77°54'14.67800"	15.2	U.S. Geological Survey
15	NH-6P-C	O	Mud	Carolina Beach	34°00'20.04577"	77°54'13.95665"	14.9	U.S. Geological Survey
16	NH-6P-A	O	Debris	Carolina Beach	34°00'22.04308"	77°54'14.93977"	10.3	U.S. Geological Survey
17	NH-8P	O	Mud	Carolina Beach	34°00'42.57287"	77°54'04.64222"	13.5	U.S. Geological Survey
18	NH-7G	O	Mud	Carolina Beach	34°00'40.51155"	77°54'04.23011"	13.2	U.S. Geological Survey
19	NH-9P	O	Mud	Carolina Beach	34°00'42.34586"	77°54'03.62369"	13.6	U.S. Geological Survey
20	NH-62-CB	I	Mud	Carolina Beach	34°00'58.80906"	77°53'57.52466"	13.5	U.S. Army Corps of Engineers
21	NH-11P	0	Mud	Carolina Beach	34°01'27.76556"	77°53'44.99743"	11.5	U.S. Geological Survey
22	NH-10G	O	Mud	Carolina Beach	34°01'28.76047"	77°53'47.75225"	9.0	U.S. Geological Survey

Gage Location	Drainage Area (sq. mi)	September Discharges (cfs) Mean	Min.	Max.
Tar River near Tar River, NC	167	62.2	.28	671
Neuse River near Falls, NC	771	182	67.8	463
Neuse River near Clayton, NC	1150	339	136	661
Trent River near Trenton, NC	168	122	4.56	1577
New River near Gum Branch, NC	94	86.5	4.25	887
Deep River near Ramseur, NC	349	227	17.7	1934
Deep River at Moncure, NC	1434	740	24.1	10580
Cape Fear River at Fayetteville, NC	4395			
Cape Fear River at William O. Husk L&D	4852	1601	935	2927
Cape Fear River at Lock # 1 nr Kelly, NC	5255	1976	985	3609
Hood Creek near Leland, NC	21.6	27.1	.51	75.1
Black River near Tomahawk, NC	676	544	13.4	3319
Waccamaw River at Freeland, NC	680	621	.31	4825

Table 2. Water Discharge Rates at North Carolina River Inlets

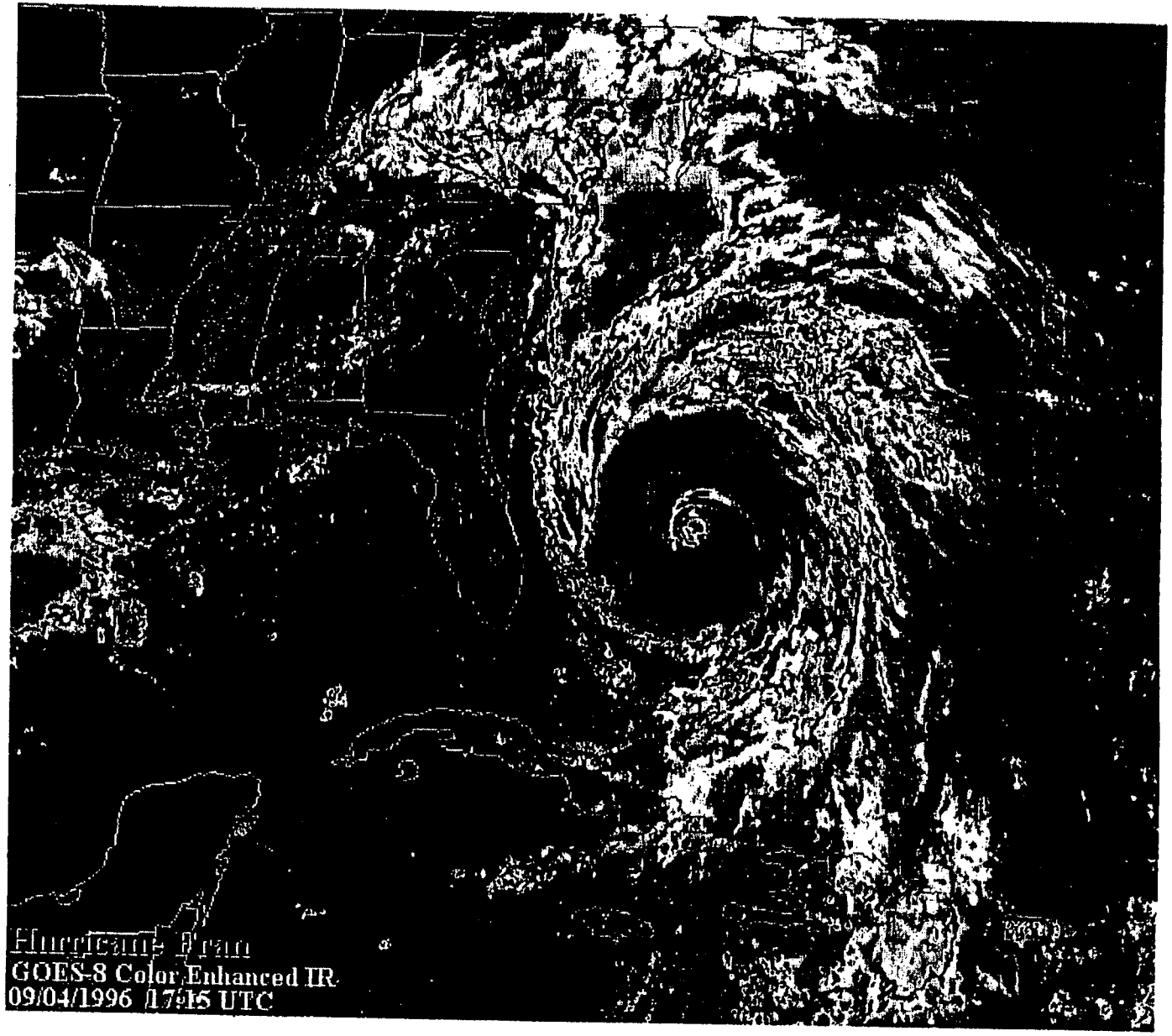


Figure 1. GOES-8 Image of Hurricane Fran on September 4, 1996

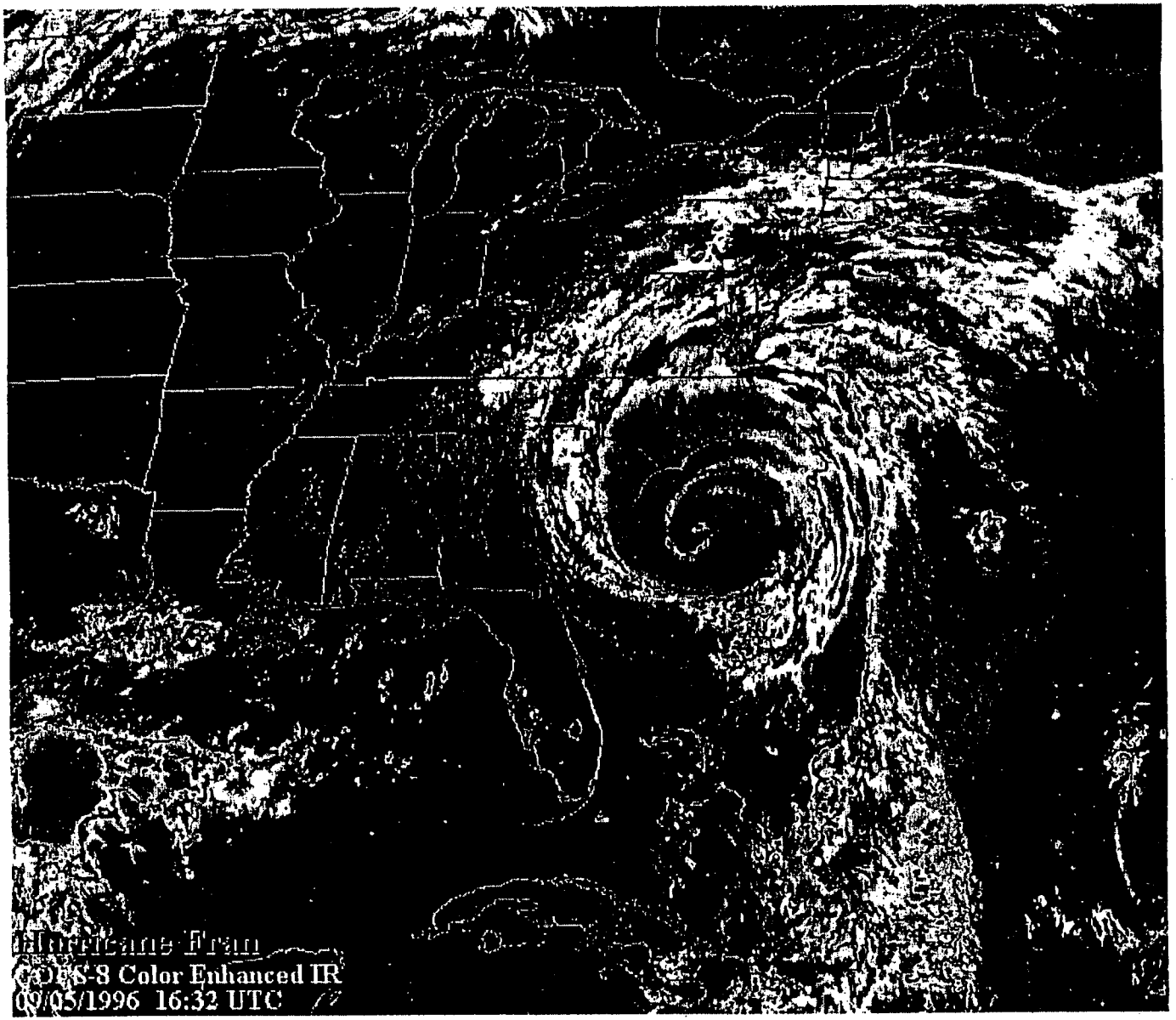


Figure 2. GOES-8 Image of Hurricane Fran on September 5, 1996 Before Landfall

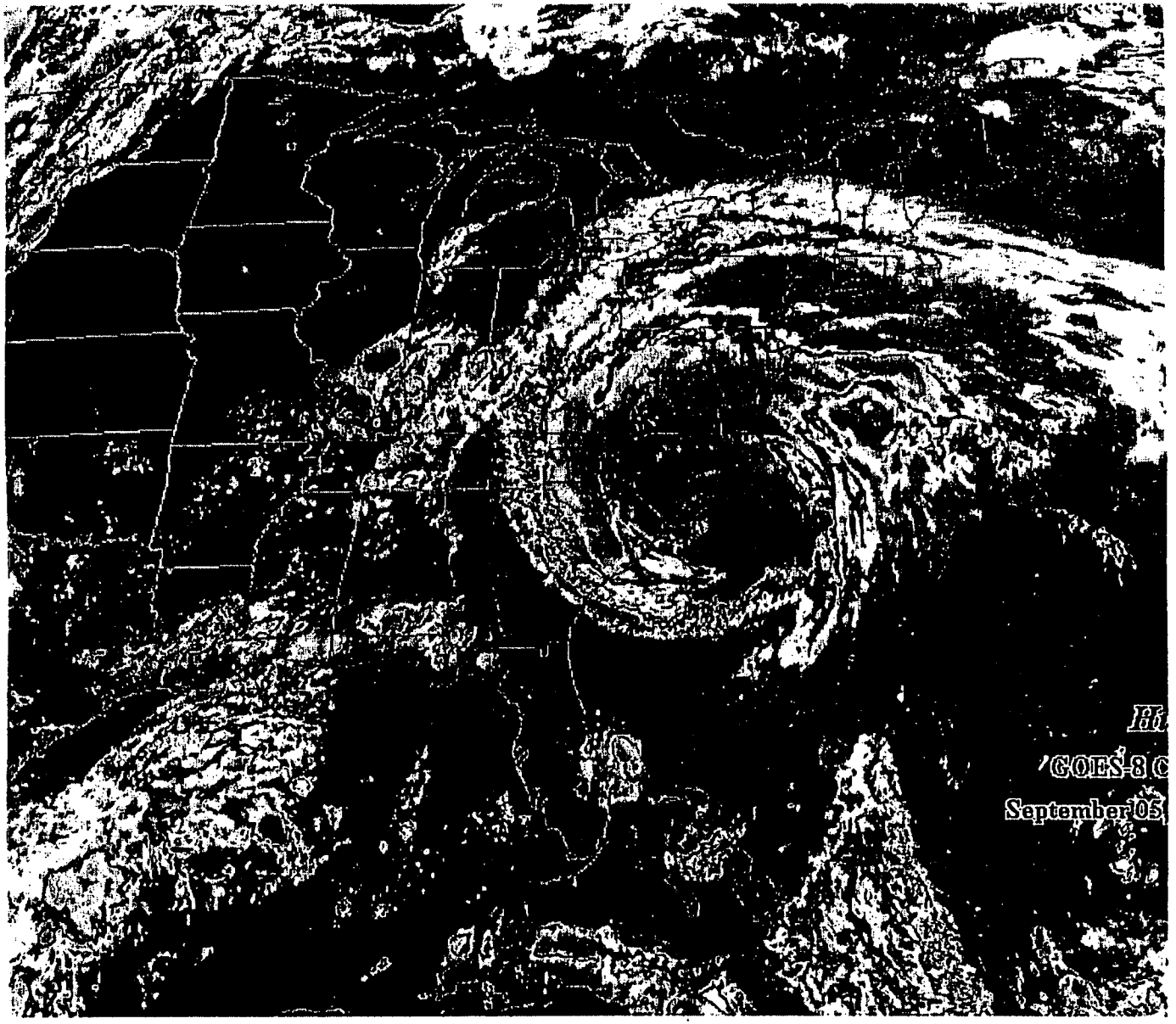


Figure 3. GOES-8 Image of Hurricane Fran on September 5, 1996 at Landfall

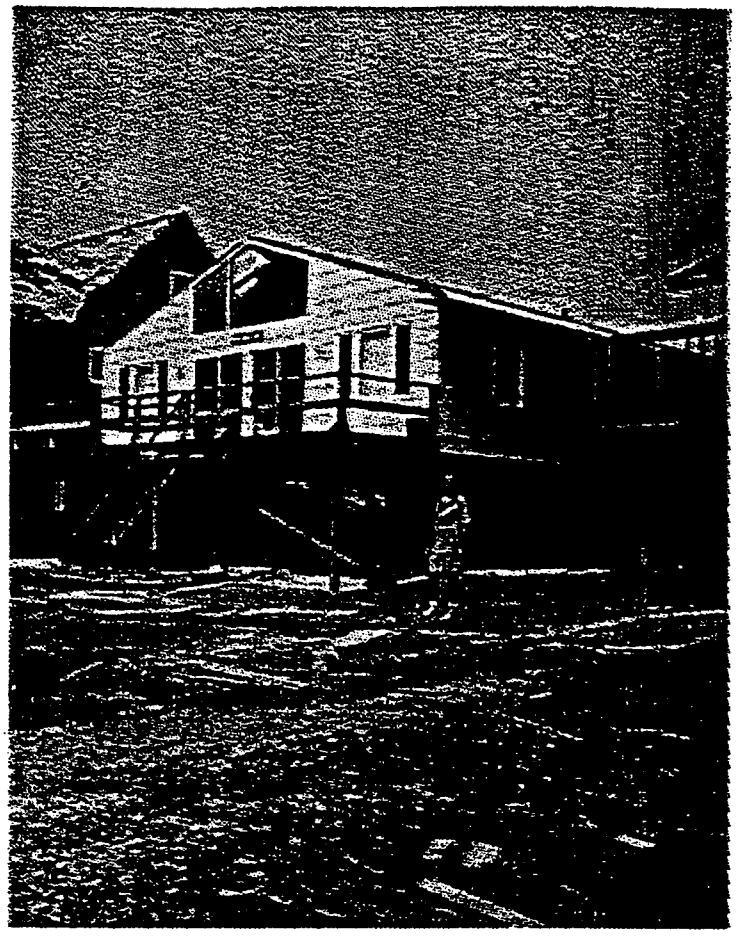


Hurricane Fran, September 1996

HWM Number:	NH-13P	**Taken By:**	US Geological Survey
HWM Elevation (ft, msl):	9.5	**Date Taken:**	08 Sept 1996
Latitude:	34° 02'01.2758"	**Longitude:**	77° 53'32.8701"
HWM Type:	Mud Line	**Outside or Inside:**	Outside
USGS 7.5 minute Quadrangle Sheet:	Carolina Beach, NC		
Nearest Town:	Carolina Beach, NC		
Address:	Intersection of Raleigh Ave. and Woody Hewett Ave.		
Remarks:	High water mark is behind Britts Donut Shop and Honeybears. Mark is on telephone pole 46 inches above parking lot.		

US Army Corps of Engineers
Wilmington District

Figure 4. High Water Mark at Carolina Beach, NC



Hurricane Fran, September 1996

HWM Number:	C-1	**Taken By:**	U.S. Geological Survey
HWM Elevation (ft, msl):	13.9	**Date Taken:**	07 Sept 1996
Latitude:	34° 24'06.06"	**Longitude:**	77° 35'01.32"
HWM Type:	Debris Line	**Outside or Inside:**	Outside
USGS 7.5 minute Quadrangle Sheet:	Holly Ridge, NC		
Nearest Town:	Topsail Beach, NC		
Address:	2319 South Shore Drive		
Remarks:	Debris Line in front yard.		

US Army Corps of Engineers
Wilmington District

Figure 5. High Water Mark at Holly Ridge, NC

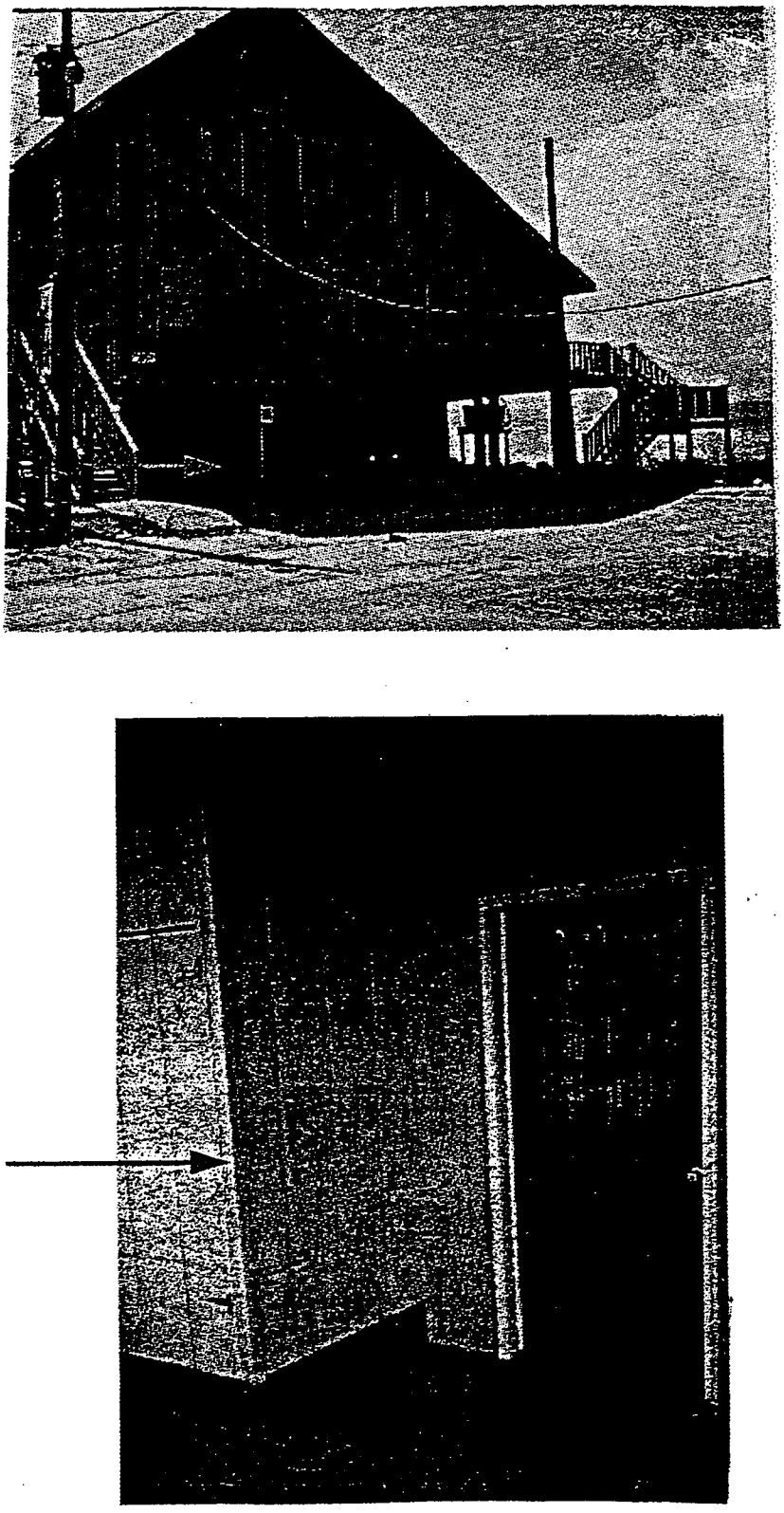


Figure 6. Two High Water Mark Locations Wrightsville Beach, NC

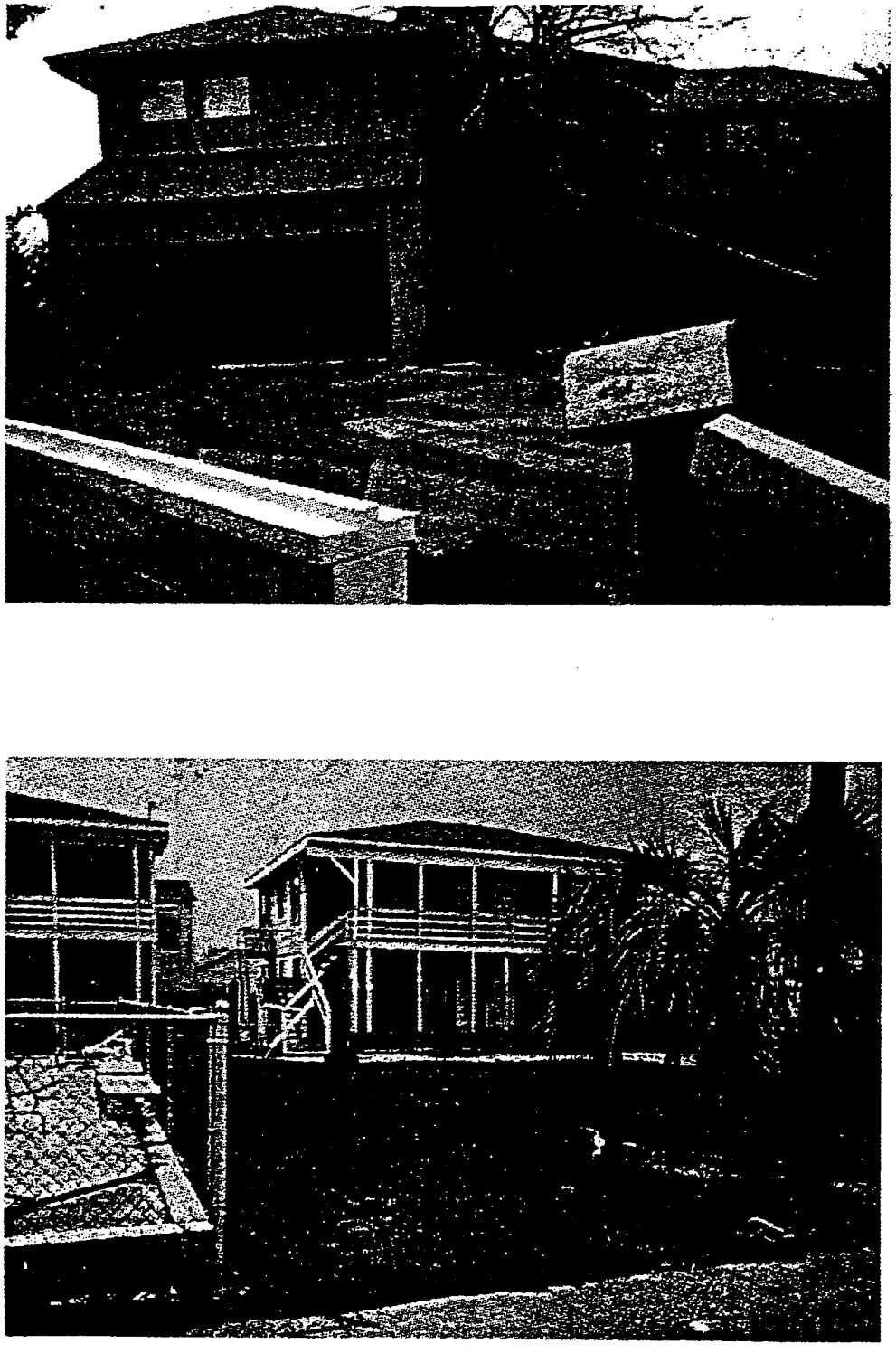


Figure 7. Two High Water Mark Locations Hampstead, NC

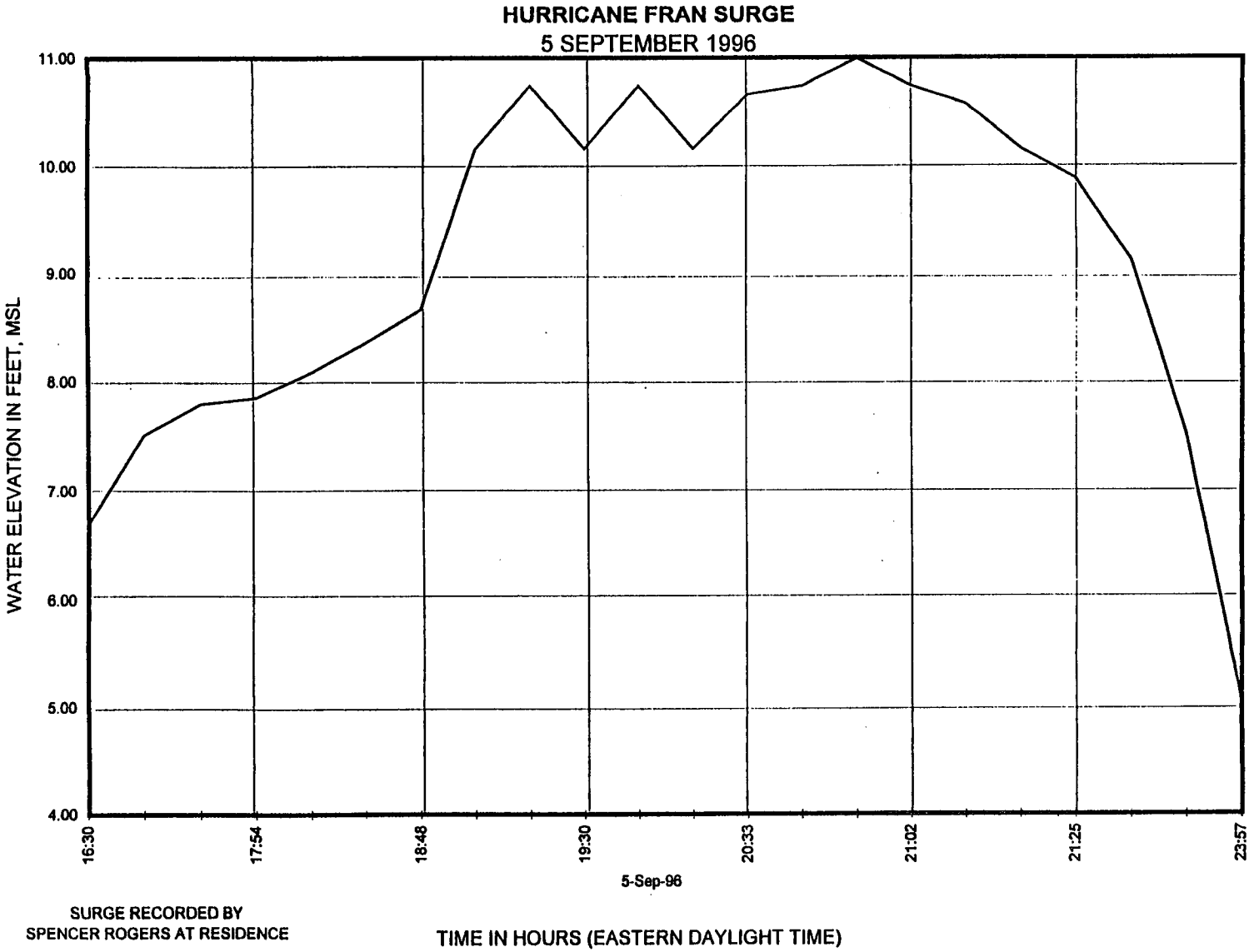


Figure 9. Storm Surge Time History at Spencer Rogers Residence

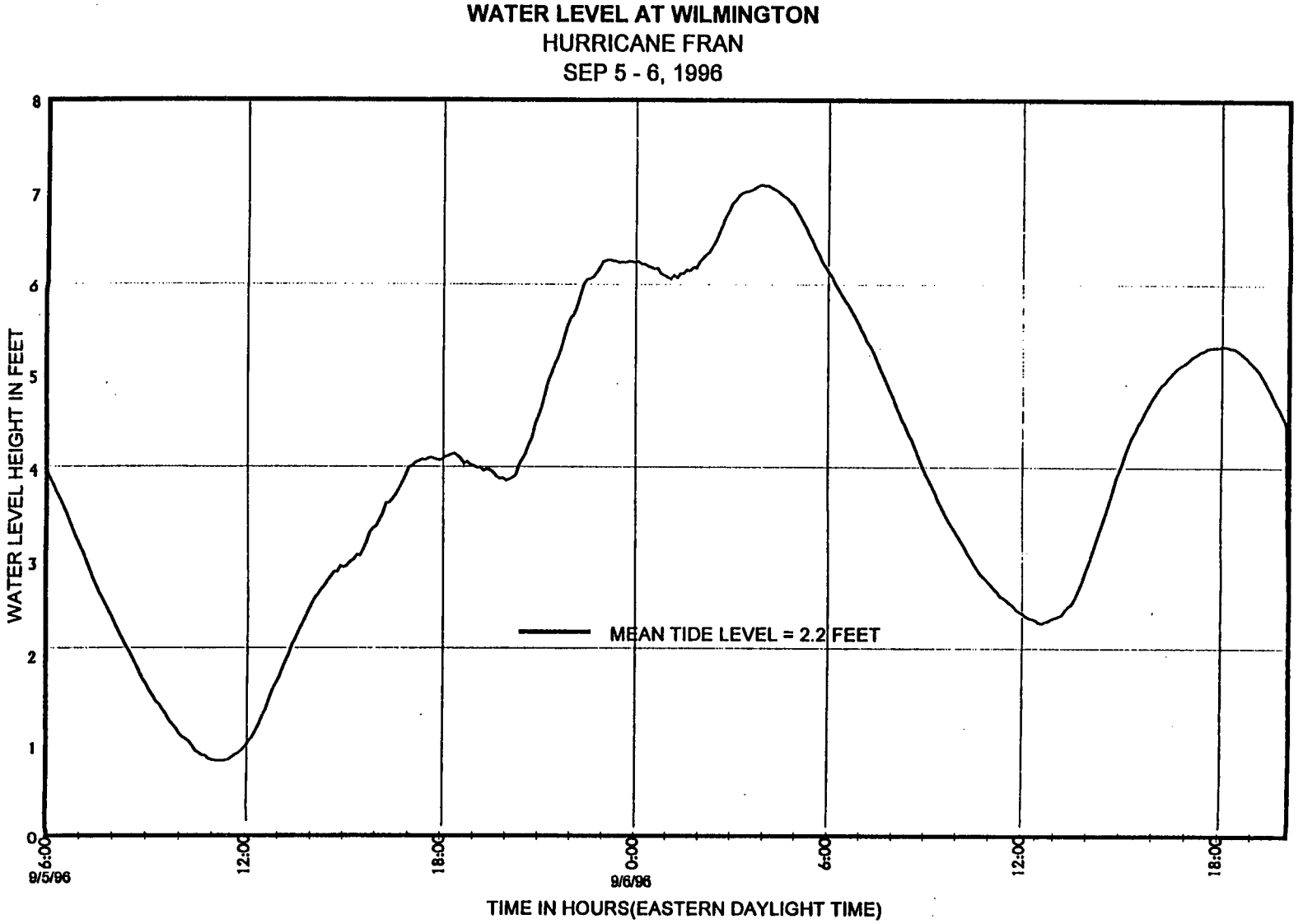


Figure 8. Water Level Time History at Wilmington, NC

Numerical Modeling of Recent Trans-Pacific Tsunami Recorded at Tide Gauges in Japan

by
Yuichiro Tanioka and Masami Okada

ABSTRACT

Numerical simulation of the trans-Pacific tsunami is examined for three large earthquakes (the 1996 Aleutian, 1995 Chile, and 1996 Irian Jaya earthquakes) occurred in the last two years. Overall, the observed and computed maximum tsunami heights at tide gauges in Japan show good agreements.

1. INTRODUCTION

In 1960, the tsunami from the Chilean earthquake propagated across the Pacific ocean and killed about 140 people in Japan. Since then, the trans-Pacific tsunami was studied extensively. In recent years, numerical modeling of trans-Pacific tsunami have been significantly developed (Goto et al, 1988, Imamura et al., 1990, etc.). However, these numerical methods have never examined by recent trans-Pacific tsunamis caused by large earthquakes. The fault parameters for those earthquakes can be reliably estimated using various data, such as seismic, geodetic, or near-field tsunami data..

In last two years, tsunamis from three large earthquakes (the 1995 Chile, 1996 Irian Jaya, and 1996 Aleutian earthquakes) propagated across the Pacific ocean and recorded at tide gauges in Japan. In this paper, we use those three earthquakes as test cases to examine the numerical method to compute the trans-Pacific tsunami. The fault parameters of the earthquakes are carefully estimated from the available data. The observed tsunami heights at tide gauges are compared with the computed heights.

2. METHOD

(1) Generation of Tsunami

The initial condition of tsunami is the water surface displacement caused by ocean bottom deformation due to faulting. The fault motion of the earthquake can be described by the fault parameters: the location of the fault, geometry (strike, dip, and rake), the fault size (length and width) and the slip amount. From these fault parameters, the ocean bottom deformation can be computed using Okada's (1985) equations.

(2) Computation of Tsunami Propagation

Atsunami which is generated by a large earthquake can be treated as a linear long wave because the wavelength is substantially larger than the water depth.

Seismology and Volcanology Department, Meteorological Research Institute, Tsukuba, 305 Japan

For tsunamis propagating a long distance such as across the Pacific ocean, the effects of Earth's sphericity and rotation (Coriolis force) must be also included. The integrated equations for linear long waves with the Coriolis force in the spherical coordinate system (longitude φ and latitude θ) are

$$\frac{\partial Q_\varphi}{\partial t} = -\frac{gd}{R\sin\theta}\frac{\partial h}{\partial \varphi} - fQ_\theta$$

$$\frac{\partial Q_\theta}{\partial t} = -\frac{gd}{R}\frac{\partial h}{\partial \theta} - fQ_\theta$$

$$f = 2\Omega\cos\theta$$

and

$$\frac{\partial h}{\partial t} = -\frac{1}{R\sin\theta}\left[\frac{\partial}{\partial\theta}(Q_\theta \sin\theta) + \frac{\partial Q_\varphi}{\partial\varphi}\right]$$

where R is the radius of the earth, g is the acceleration of gravity, d is water depth, Ω is the rotation vector of the earth, h is the height of the water displaced from equilibrium position, and Q is The flow rate. We solved the above equations using finite-difference calculations on a staggered grid system.

Further, the grid size on the entire Pacific Basin must be carefully chosen to make the effects of numerical and physical dispersion equal. Imamura et al., (1990) showed that the choice of the grid size can be evaluated using the Imamura number, *Im*, defined as

$$\mathrm{Im} = \Delta x \sqrt{1 - \left(C_0 \Delta t / \Delta x\right)^2} \Big/ 2h \qquad (2)$$

where Δx is the grid size, Δt is the time step, and $C_0 = \sqrt{gh}$. The value of *Im* must be about 1 to simulate the linear Boussinesq equation using the finite difference computation for a linear long wave. We chose the grid size (Δx) of 5 minutes and the time step (Δt) of 5 seconds to satisfy the stability condition of numerical computation. Using Equation (2) for the above case, Im is 1.15 in the N-S direction by assuming that the average depth is 4000m. In the E-W direction, Im varies with latitude and Im is 0.73-1.15 within the latitude between 50 and 0 degree. These results show that Im for the above case is about 1, so the 5 mitutes grid system on the Pacific Basin should make the numerical dispersion equal to the physical dispersion.

Near coastal area, the bathymetry changes rapidly and cannot be adequately represented by a 5 minutes grid (~ 10 km). Therefore, in the coastal area (near the west coast of North America, Aleutian, Hawaii, and Japan), 1 minutes grid (~ 2 km) spacing is used. In addition to that, 20 seconds grid (~ 600 m)spacing is used near some of the tide gauge stations in Japan.

3. THE 1996 ALEUTIAN EARTHQUAKE

The Aleutian earthquake of June 10, 1996 (Ms 7.6, Mw 7.9) occurred off the Delarof Islands, Alaska (Figure 1). The NEIS Preliminary Determination of Epicenters (PDE) provides the source parameters: origin time, 04:03:35.48 GMT; epicenter, 51.564°N, 177.588°W; magnitude, Ms 7.6. The focal mechanism of the earthquake from the Havard CMT indicates thrust type faulting with a shallow dip angle (20°) (Figure 1). It

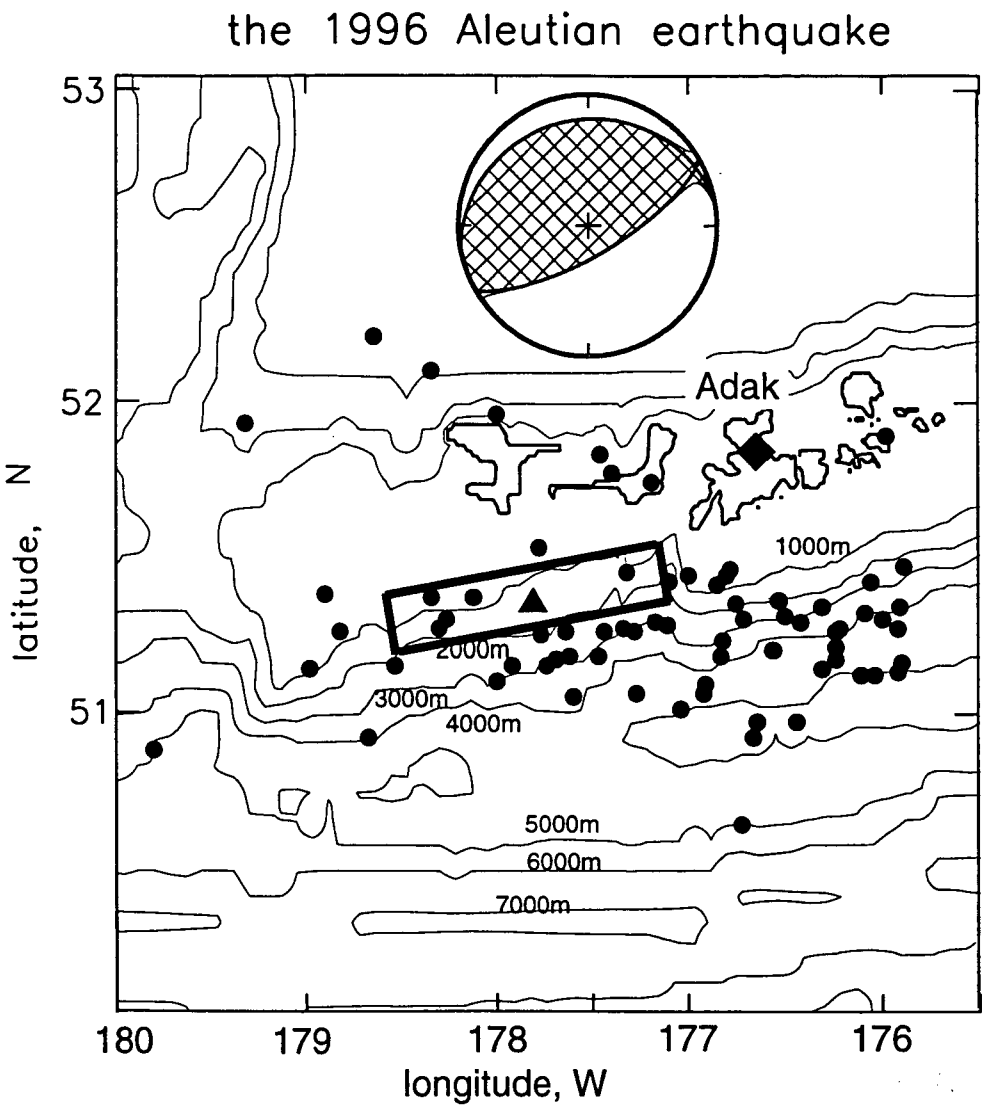


Figure 1. The focal mechanism and the best fault model of the 1996 Aleutian earthquake. A frame shows the best fault model. A triangle is the epicenter of the mainshock. Circles are the epicenter of aftershocks. Diamond shows the tide gauge (Adak).

generated trans-Pacific tsunamis which were recorded at tide gauge stations in the west coast of North America, Hawaii and Japan. The source time function of the earthquake was determined by the Michigan group (Tanioka and Ruff, 1997) using teleseismic body waves. It shows the duration of 54 seconds, the seismic moment of $7.3X10^{20}$ Nm and the depth of 18 km. No significant directivity was also observed.

There is one near-field tsunami waveform recorded at a tide gauge station, Adak, about 100 km away from the epicenter (Figure1). Using a pure thrust type fault (strike=260°, dip=20°, rake=90°) which is consistent with the focal mechanism, we computed the tsunami waveform at Adak for various fault sizes. The best fault model which

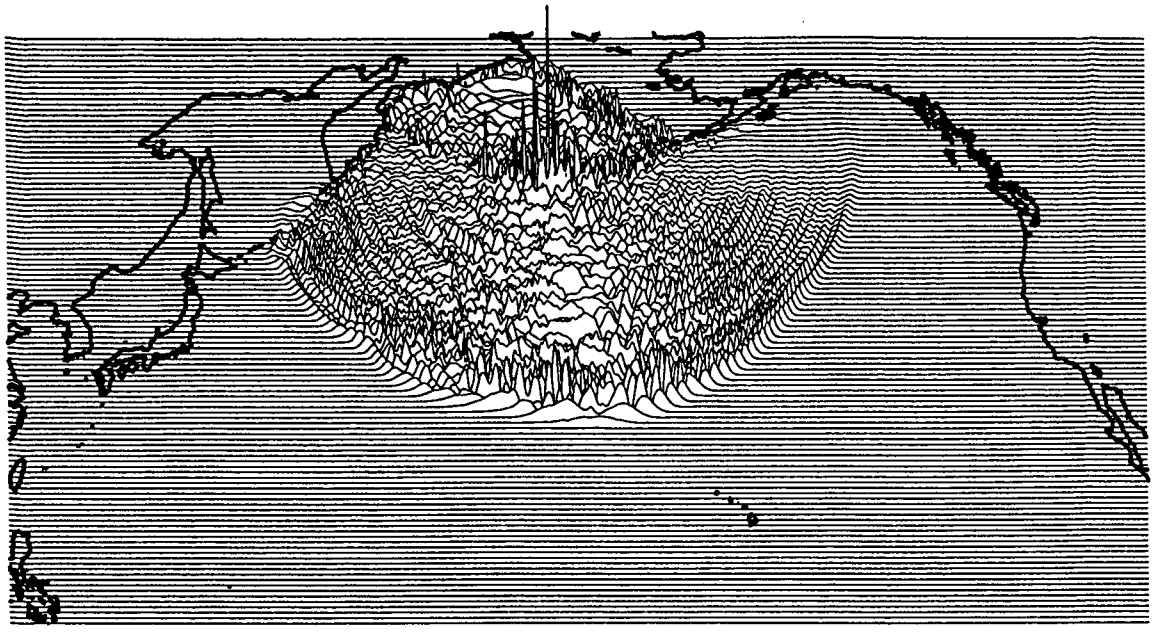


Figure 2. Snapshot of tsunami 3 hours after the 1996 Aleutian earthquake

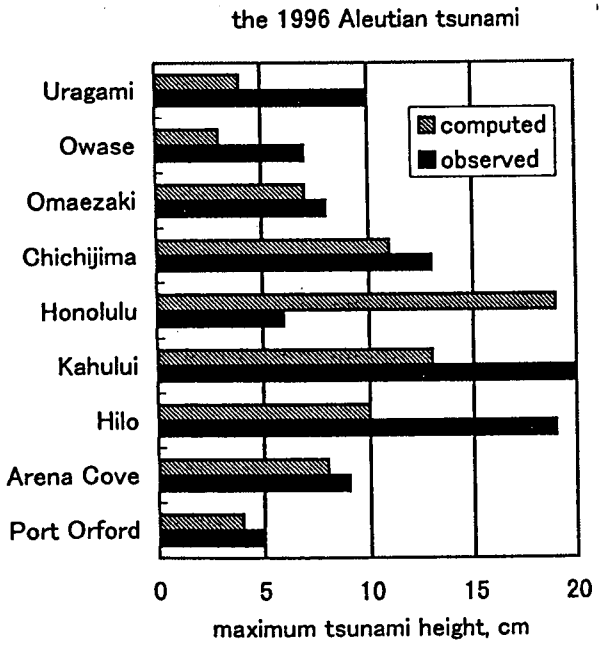


Figure 3. Comparison of observed and computed maximum tsunami heights at tide gauges in Japan, Hawaii, and west coast of North America.

explained the observed waveform well is shown in Figure 1 (length 110 km, width 20 km, slip 4 m). The epicenter is located near the center of the fault. This result and no significant directivity from the body wave analysis may suggest the bilateral rupture process of the 1996 Aleutian earthquake. Also, the rupture area is much smaller than the aftershock area (Figure 1). This may indicate that the moment release of the mainshock was concentrated in the asperity area..

Using this fault model, now we compute the trans-Pacific tsunami. Figure 2 shows the snapshot of tsunami propagation across the Pacific ocean 3 hours after the earthquake. As we can see in Figure2, large tsunamis propagate toward Hawaii, but very small tsunamis propagate toward the west coast of North America. This is due to the directivity effect; tsunami heights are usually smaller in the direction parallel to the orientation

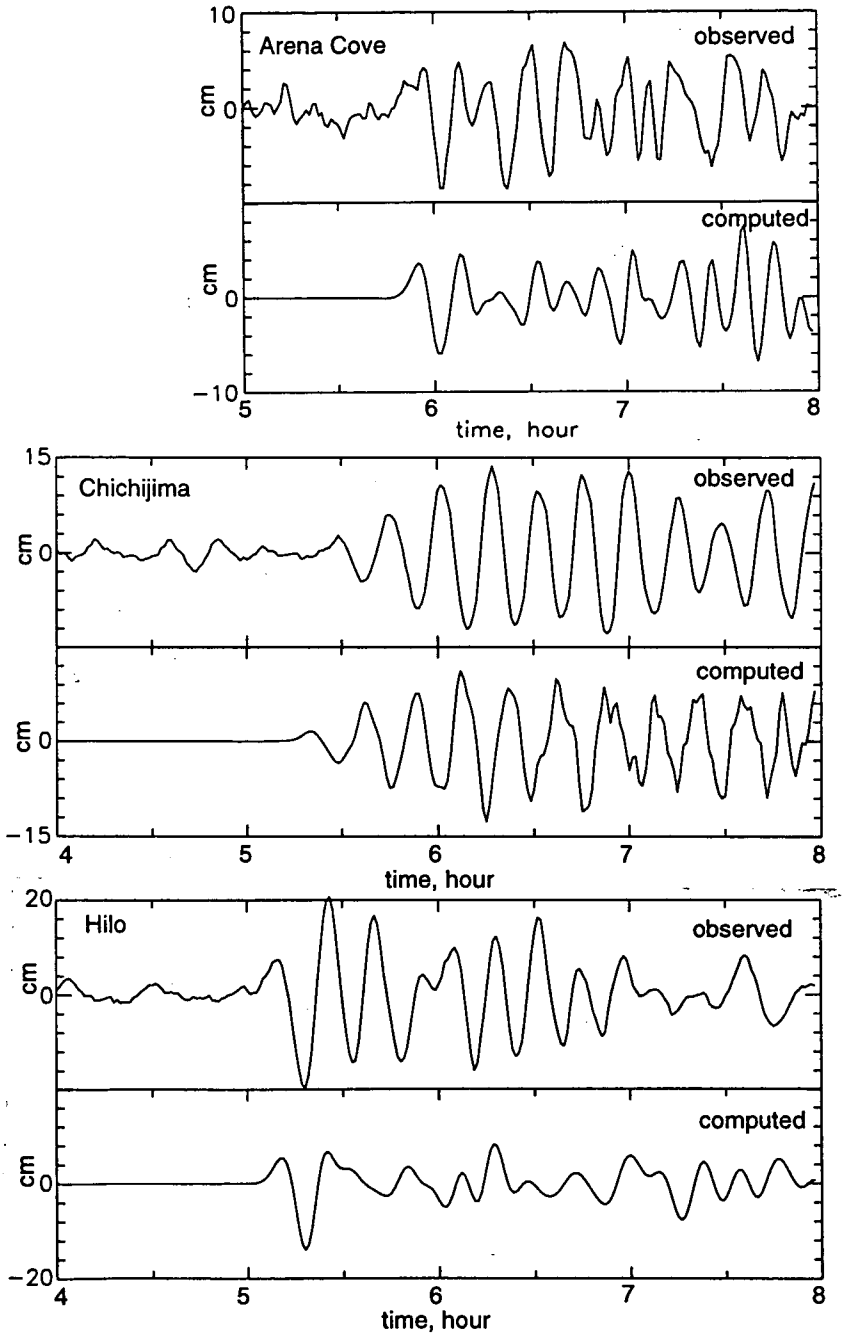


Figure 4. Comparison of observed and computed tsunami waveforms at three tide gauges.

(strike) of the fault (Ben-Menahem and Rosenman, 1977). Figure 3 compare the observed and computed maximum tsunami heights at the tide gauges in Japan (Uragami, Owase, Omaezaki, and Chichijma), Hawaii (Honolulu, Kafului, and Hilo), and the west coast of North America (Arena Cove and Port Orford). The maximum tsunami heights represent the largest tsunami heights during 3 hours from the first peak. The observed and computed maximum tsunami heights

fit well except at the Hawaiian stations. In Figure 4, we compared the observed and computed waveforms at three tide gauges. At Arena Cove and Chichijima, the observed and computed waveforms show the very good agreement, but not at Hilo. This may suggest that finer grid system or more accurate bathymetry near Hawaii is necessary to improve the accuracy of the model.

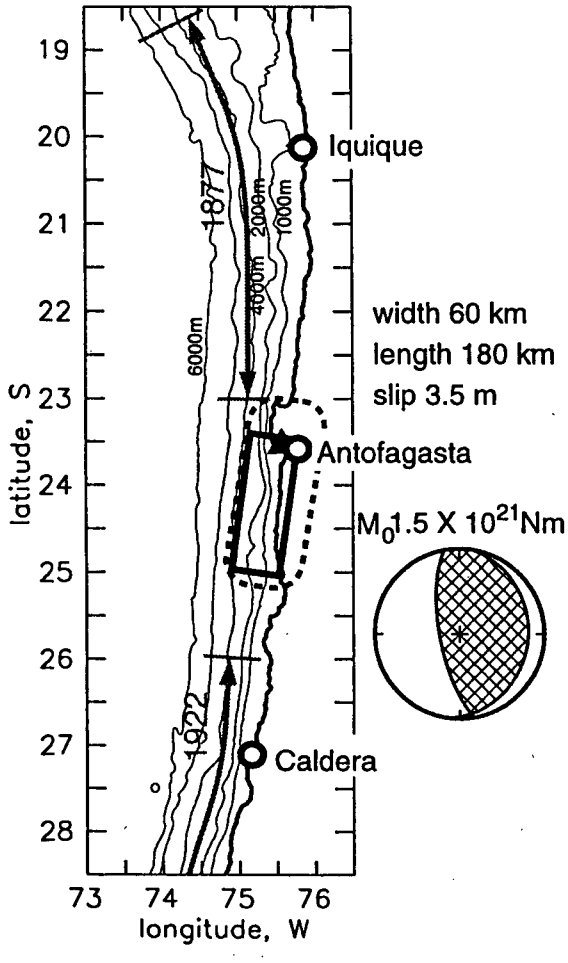


Figure 5. The best fault model and the focal mechanism of the 1995 Chile earthquake. A flame shows the best fault model. A star is the epicenter of the mainshock. Dashed ellipse shows the aftershock area. Circles are tide gauges.

4. THE 1995 CHILE EARTHQUAKE

The Chile earthquake of July 30, 1995 (Mw 8.0) occurred off Antofagasta, Northern Chile (Figure 5). The NEIS Preliminary Determination of Epicenters (PDE) provides the source parameters: origin time, 05:11:23.6 GMT; epicenter, 23.340°N, 70.294°W; magnitude, Ms 7.3. The focal mechanism of the earthquake (Ruegg et al., 1996) indicates thrust type faulting with a shallow dip angle (19°) (Figure 1). Ruegg et al., (1996) also determined three subevents from body wave analysis and suggested that the

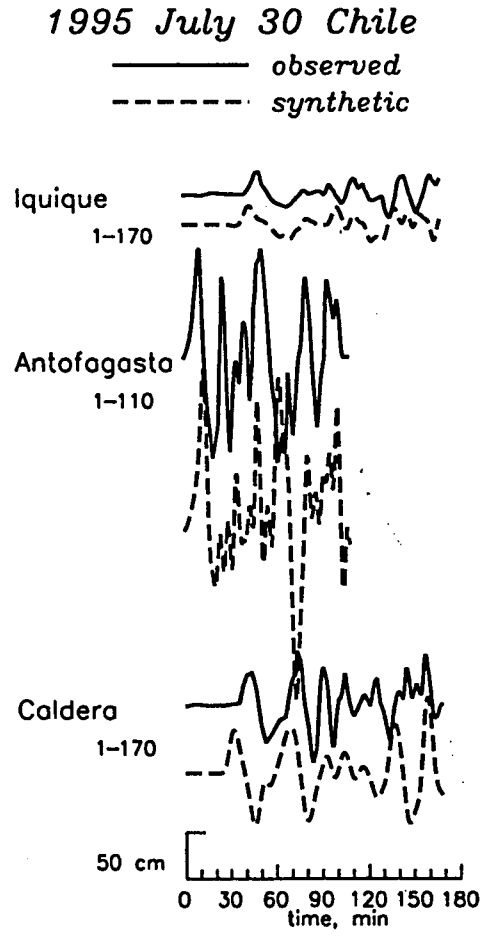


Figure 6. Comparison of the observed and computed tsunami waveforms

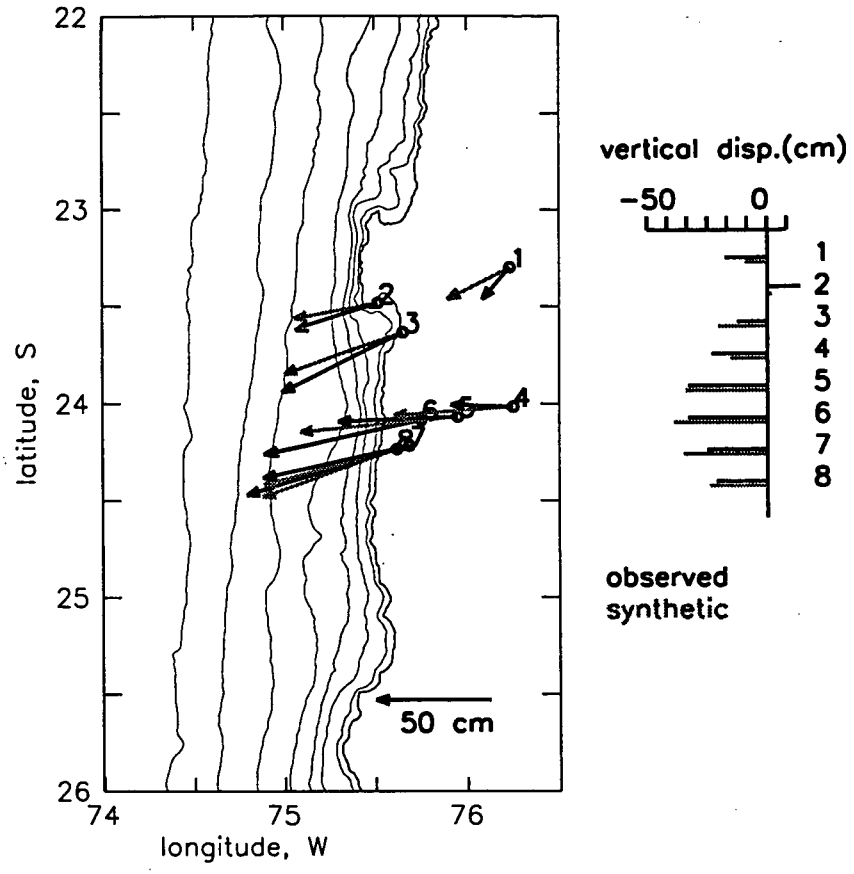


Figure 7. Comparison of the observed and computed coseismic displacement field. (left) Comparison of the horizontal displacements. (right) Comparison of the vertical displacements.

rupture propagated to southward, the fault length is about 180 km. The total seismic moment is estimated as 0.9 X 10^{21} Nm. They also determined the fault width of 60 km and slip of about 5m using the coseismic surface displacement field observed by the GPS network near the source region.

The 1995 Chile earthquake also generated large tsunamis. In addition to the coseismic displacement data (Ruegg et al., 1996), we used the tsunami waveforms recorded at three tide gauges in northern Chile (Figure 5) to determine the fault parameters. Using a thrust type fault (strike=8°, dip=20°, rake=107°), we computed the tsunami waveforms and the surface displacement field for various fault sizes and depths. The best fault model (length 180 km, width 60 km, slip 3.5 m) is shown in Figure 5. The depth of the down-dip edge of the fault is well-estimated as 40 km. Figure 6 shows the computed tsunami waveforms also fit well with the observed waveforms. Figure 7 shows that the computed surface displacement field is consistent with the observed field. The seismic moment is 1.5 X 10^{20} Nm by assuming that the rigidity 4 X 10^{10} N/m^2. This result is consistent with

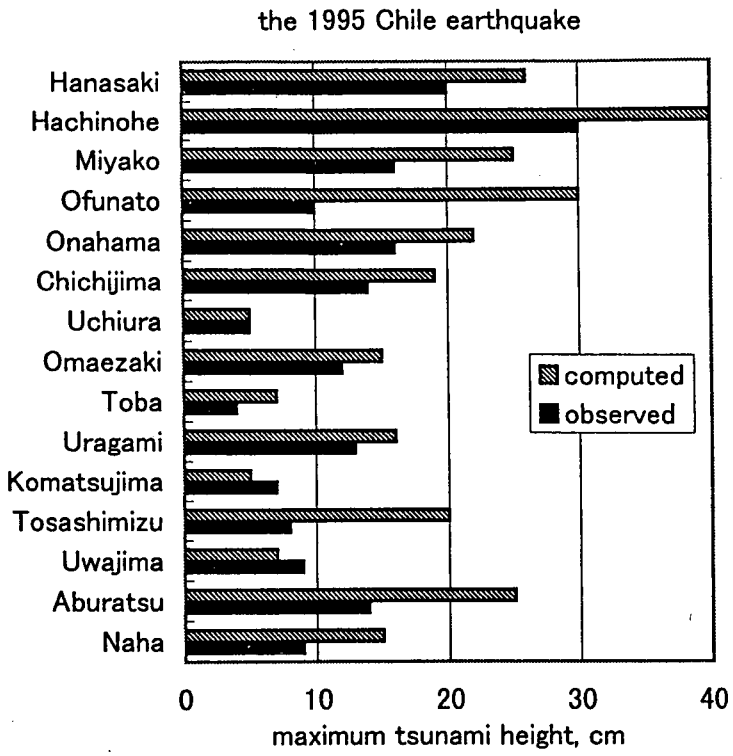


Figure 8. Comparison of the observed and computed maximum tsunami heights at tide gauges in Japan.

the estimate from the body wave analysis.

Tsunamis from the 1995 Chile earthquake propagated across the Pacific ocean and recorded at tide gauge stations in Japan. We computed the trans-Pacific tsunami using the above fault model which is well-determined by seismic, coseismic displacement, and near-filed tsunami data. .Figure 8 shows that the observed and computed maximum tsunami heights during 3 hours after the first arrival of tsunami at tide gauges in Japan. Computed maximum tsunami heights are slightly overestimated the observed maximum tsunami heights. More detail investigation is necessary to investigate this small differences.

5. THE 1996 IRIAN JAYA EARTHQUAKE

The Irian Jaya earthquake of February 17, 1996 (Mw 8.1) occurred off Biak Islands, Indonesia (Figure 10). The NEIS Preliminary Determination of Epicenters (PDE) provides the source parameters: origin time, 05:59:30.55 GMT; epicenter, 0.891°S, 136.952°E; magnitude, Ms 8.1. The focal mechanism of the earthquake from Harvard CMT indicates thrust type faulting with a very shallow dip angle (11°) (Figure 9). The source time function of the earthquake was determined by the Michigan group (Tanioka and Ruff, 1997) using teleseismic body waves. It shows the total duration of 50 seconds with the

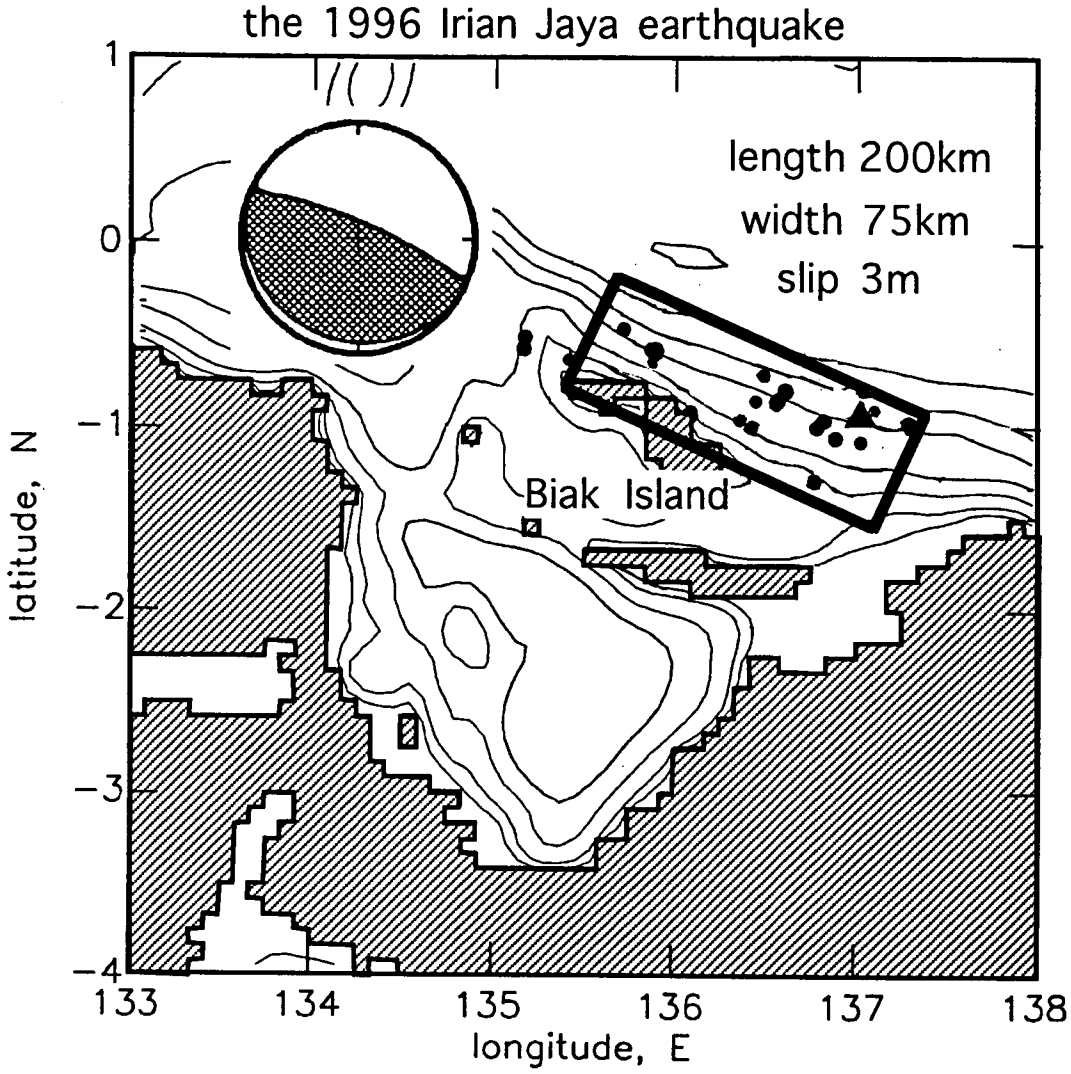


Figure 9. The focal mechanism and the best fault model for the 1996 Irian Jaya earthquake. A flame shows the best fault model. A triangle represents the epicenter of the mainshock. Circles shows the epicenters of the aftershocks.

initial phase of 18 seconds and the seismic moment of 18 X 10^{20} Nm

For this earthquake, we do not have a near-field tsunami waveform recorded at tide gauge. We estimated the fault size (length 200 km, width 75 km) from the aftershock distribution (Figure 10). From the seismic moment of 18 X 10^{20} Nm and a rigidity of 4 X 10^{10} N/m^2, the average slip is calculated to be 3 m.

Tsunamis from the 1996 Irian Jaya earthquake also recorded at tide gauge stations in Japan. We computed the tsunami using a pure thrust type fault (strike=115, dip=10, rake=90) with the above fault size. Figure 10 shows that the observed computed maximum tsunami heights at tide gauge stations in Japan. Overall, the observed and computed maximum tsunami heights shows the good agreements.

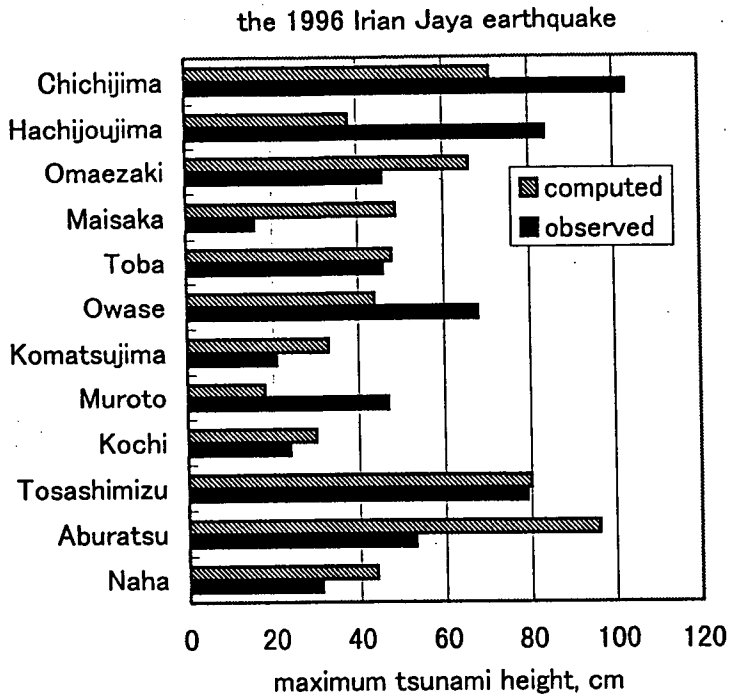


Figure 10. Comparison of the observed and computed maximum tsunami heights at tide gauges in Japan.

6. CONCLUSION

The rupture area of the 1996 Aleutian earthquake is much smaller than the aftershock area. It is located near the epicenter. This indicates that the rupture area of the 1996 Aleutian earthquake did not overlap with the rupture area of the 1986 Andreanov earthquake although the aftershock areas overlaped each other.

Overall, the numerical simulation of the trans-Pacific tsunamis performed well. However, at a few tide gauge station, the difference between the observed and computed maximum tsunami heights was more than factor 2. We still need the improvement of the numerical modeling of trans-Pacific tsunami.

REFERENCE

Ben-Menahem, A. and M. Rosenman, Amplitude pattern of tsunami waves from submarine earthquakes, J. geophy. Res., 77, 3097-3128, 1972

Imamura, F., N.Shuto, and T. Goto, Study of Numerical simulation of the transoceanic propagation; Part 2: Characteristics of tsunami propagating over the Pacific Ocean.

Goto, T., F. Imamura, and N. Shuto, Study of Numerical simulation of the transoceanic propagation of tsunami Part 1, *Jishin 2, 41*, 515-526

Okada, Y., Surface deformation due to shear and tensaile faults in a half space, *Bull. Seism. Soc. Am., 75,*1135-1154, 1985

Ruegg,J.C. et al., The Mw=8.1 Antfagasta (North Chile) earthquake of July 30, 1995: First results from teleseismic and geodetic data, *Geaphys. Res. Lett.*, 1996

Tanioka, Y., and L.J. Ruff, Source time function. Seismo. Res. Lett., (in press).

Use of Relationships between Moment Magnitude and Water Level Measurement Station Amplitudes by the Tsunami Warning System to Forecast Tsunamis in the Far Field

by

Michael E. Blackford

ABSTRACT

The United States Tsunami Warning System uses the surface wave magnitude as its criteria for issuing either a Tsunami Information Bulletin or a Regional Warning/Watch immediately following the occurrance of potentially tsunamigenic earthquakes in the Pacific. Recent developments in seismometry and the characterization of earthquake size by the relatively rapid determination of seismic moment has led the System to consider adopting the moment magnitude, derived from the seismic moment, as the criteria for message issuance in the next few years. Moment magnitude is now used by the System to assist in making decisions about continuance or cancellation of warnings. This is possible because statistically significant relationships have been derived between tsunami source area and impact area pairings, which is in essance a quantification of tsunami history. Using Hawaii as an example, it would take an earthquake with at least a moment magnitude of 8.4 in the Alaska-Aleutian area to generate a tsunami in Hilo that would begin to be considered destructive. Thus, one would certainly lean toward canceling a warning for an earthquake with a moment magnitude around 8.0.

KEY WORDS: surface wave magnitude; moment magnitue; tsunami warning; tsunami amplitude; destructive tsunami

1. INTRODUCTION

Since the establishment of the Tsunami Warning System in the United States the Warning Centers traditionally have not included estimates of the severity of the expected tsunami in warnings they issue. This is primarily due to the fact that tsunamis, which are destructive in the far field, result from earthquakes with surface wave magnitudes that are near, or above, the saturation level for this type of magnitude determination. The Tsunami Warning System bases its initial warning message on the location and surface wave magnitude of the potentially tsunamigenic earthquake without reference to any water level measurements in the near field. This is done in order to disseminate the warning as rapidly as possible following the earthquake's origin time.

Recent advances in the ability to estimate quickly the moment magnitude, Mw, of potentially tsunamigenic earthquakes and the determination of better relationships between Mw and tsunami amplitudes recorded on water level measuring instruments has led to the possibility of including a qualification of the potential far field tsunami in the initial warnings issued. This paper shall describe the advances that have made far field tsunami severity estimation a possibility.

2. MAGNITUDE ESTIMATION

The threshold used by United States Tsunami Warning Centers for the issuance of far field tsunami warnings is a surface wave magnitude of 7.5. For warnings within their areas of regional responsibility the Centers use lower magnitude thresholds: 6.8 for the Hawaii region and 7.0 for Alaska, Washinton, Oregon, California, and the Canadian Province of British Columbia. . It is assumed that other regional tsunami warning systems use similar lower thresholds since a lower magnitude earthquake may generate a locally destructive tsunami that can be barely noticed in the far field. The type of magnitude determined for the regional potentially tsunamigenic earthquake may or may not be the

Pacific Tsunami Warning Center, National Weather Service, Pacific Region, Ewa Beach, Hawaii, USA, 96706

traditional Ms. Nevertheless whatever type of magnitude is used, it is usually related to the Ms by typically considering only a small portion of the spectrum of energy radiating from the earthquake rupture. This is due largely to the prevalent use of seismometers that respond to a relatively narrow frequency band of the radiated seismic energy

Over the last couple of decades or so a new class of seismometers have begun to supplant the narrow band instruments. These seismometers not only have a more uniform response to a much broader band of the seismic energy, but they also are able to accomodate a much larger range of earthquake size than was possible with the earlier instruments. The cost and ease of installation of this new class of seismometers is becoming comparable to the traditional narrow band instruments, thus it can be assumed that in time they will probably become instrument of choice for seismic studies and applications such as the Tsunami Warning System.

As the number of broadband, high dynamic range seismometers increase around the globe, and the means to communicate with them cheaply and reliably in near real time becomes a reality, it becomes possible to determine moment magnitudes in a time frame that allows the Warning Centers to apply these determinations to the forecasting of tsunami amplitudes,as well as their arrival times, which has been possible for some time.

The Pacific Tsunami Warning System is now routinely using TREMORS to process seismic data from the broadband station KIP. TREMORS is an automatic system, developed by the French Laboratorie d'Geophysique in French Polynesia, that provides a rough estimate of an earthquake's location and a determination of the earthquake's seismic moment from a single stations's data following an algorithm developed by Okal and Talandier (1987). The system outputs its determinations, based on very long periond waves, at approximately twelve minutes and fifty minutes after detection. Of course, several minutes may pass before a detection occurs at KIP from a distance source. The possibility of sending the data to the Warning Centers from other TREMORS equipped stations automatically when it becomes available is under consideration.

The Alaska Center makes use of its long period and broad band data to calculate automatically seismic moments based on the body waves recorded at several of its staions. This method of seismic moment determination is based on the work of Tsuboi, et al. (1995). The Center uses the body waves because of the necessity to make very rapid determinations of the seismic moment in the regional environment

3. RELATIONSHIPS BETWEEN MOMENT MAGNITUDE AND WATER LEVEL GAUGE AMPLITUDE

In order to relate the size of great earthquakes of the last century to modern day moment magnitude, Katsuyuki Abe (1979) developed relationships between the tsunami amplitudes recorded on representative water level guages and more modern great earthquakes whose seismic moments could be determined independently. In order to derive statistically significant coefficients, Abe devided his limited data set into three source areas: the northwest Pacific subduction zones including those off the Kamchatka peninsula, the Kuril Islands, and the Pacific shores of northeastern Japan, the Alaska-Aleutian subduction zone, and the Peru-Chile subduction zone of South America. He also identified five "receiver " areas: Japan, Alaska, California, Honolulu, and Hilo Hawaii. Suffient differences exist between the responses of the Honolulu and Hilo to common tsunamis to merit the distinction. In his study the independent variable was the earthquake magnitude, termed Mt, which was equivalent to Mw except that it was derived from tsunami amplitudes recored on water level gauges.

This paper examines the inverse of this relationship and considers the independent variable to be the tsunami amplitude. A base of sixty-five tsunamigenic earthquakes was used to

determine values for variables a and b in the relationship:

$$\log H = -a + bM$$

where H is the tsunami amplitude in meters and M is the moment magnitude. The results of this study are given in Table 1 together with measures of the error of a and statistical parameters bearing on the significance of the relationship. Most of the source-receiver combinations could also be grouped into three sets with similar values for a and b. Reasons for this grouping are not readily apparent.

4. "DESTRUCTIVE" TSUNAMI CRITERIA

The initial issuance of tsunami warnings is based solely on earthquake magnitude without giving consideration to water level gauge measurements. Criteria for canceling a warning, however, can take into account the tsunami amplitude that can be expected based on data presented in Table 1. If some lower limit can be set to define the tsunami amplitude separating "destructive" tsunamis from those doing no significant harm, then a minimum moment magnitude of concern can also be identified.

As an example, for Hawaii a minimum tsunami amplitude of seventy-five centimeters is used to distinguish destructive from non-destructive tsunamis. In this case the mean moment magnitude and worst case moment magnitude can be determined and used as part of the information considered to decide whether to cancel a tsunami warning, continue the warning in borderline cases where additional data is desires before cancellation, or to upgrade the limited warning to include the entire Pacific because the tsunami is expected to be destructive to some degree throughout the Pacific. Table 2 summarizes this example.

5. CONCLUSIONS

Statistically significant relationships can be made between moment magnitude and tsunami gauge amplitude. In order to accomplish this it is necessary to consider the data in terms of source receiver pairs. These relationships can, in turn, be used to provide assistance in making the decision whether or not to cancel a warning before a region would need to initiate a costly evacuation that may not be necessary. This process of establishing relationships between tsunami source areas and impact areas is in essence a quantification of the historical tsunami information known about the area.

6. REFERENCES

Abe, K., (1979), "Size of Great Earthquakes of 1837-1974 Inferred from Tsunami Data," *Journal of Geophysical Research*, Vol. 84, 1979, pp. 1561-1568.

Talandier, J., Reymond, D., and Okal, E.A., (1987), "Mm: Use of a Variable Period Mantle Magnitude for the Rapid One Station Estimation of Teleseismic Moments," *Geophysical Research Letters*, Vol. 14, No. 8, 1987, pp. 840-843.

Tsuboi, S., Abe, K., Takano, K., Yamanaka, Y., (1995), "Rapid Determination of Mw from Broadband P Waveforms," *Bulletin of the Seismological Society of America*, Vol. 85, No. 2, 1995, pp. 606-613.

Table 1: Parameters and statistics for logH = -a + b*M

Data Set	n	Grp	a	Std. est. err.of a	b	corr. coef.	T	p
NWHO	10	A	7.677	0.135	0.822	0.875	5.124	9.030E-4
NWHI	8	B	10.153	0.239	1.169	0.847	3.899	7.991E-3
NWCA	7	B	9.317	0.107	1.013	0.940	6.188	1.607E-3
NWAK	7	A	7.263	0.110	0.804	0.930	5.657	2.399E-3
AKHO	6		5.092	0.194	0.513	0.818	2.840	4.687E-2
AKHI	7	A	7.580	0.223	0.862	0.915	5.069	3.871E-3
AKCA	3	A	7.887	0.134	0.832	0.959	3.378	1.832E-1
AKJA	4		3.772	0.220	0.389	0.641	1.180	3.594E-1
SAHO	8	C	6.302	0.172	0.655	0.880	4.548	3.900E-3
SAHI	7	B	8.745	0.206	1,044	0.933	5.798	2.151E-3
SACA	5	C	6.148	0.075	0.641	0.977	7.868	4.278E-3
SAJA	4		8.198	0.158	0.898	0.963	5.602	3.687E-2
SAAK	3	C	6.331	0.130	0.679	0.965	3.724	1.670E-1
GRPA	27		7.254	0.255	0.791	0.817	7.076	<1.00E-6
GRPB	22		10.148	0.383	1.164	0.764	5.301	3.445E-5
GRPC	16		6.341	0.154	0.655	0.922	8.892	<1.00E-6

Table 2: Mean and worst case Mw for 75cm. tsunami amplitude

NWHO	NWHI	AKHO	AKHI	SAHO	SAHI
9.2 9.0	8.6 8.4	9.7 9.3	8.6 8.4	9.4 9.2	8.3 8.1

Theme 4

Seismic Information Systems

Development of Real-time Seismic Information System for M.O.C.

by

Shun-etsu ODAGIRI[1], Hideki SUGITA[2], Masahiro KANEKO[3], Tomofumi NOZAKI[2] and Tadashi HAMADA[2]

ABSTRACT

This paper presents a research and development of "Real-time Seismic Information Systems for Ministry of Construction (MOC)" to support the emergency responses for civil infrastructure immediately after an earthquake. Emphases are placed on information systems for earthquake ground motion detection, structural damage and ground hazard estimation, structural damage detection and high-speed data communication using seismograph network and innovative multi-media technologies.

Key Words: *Earthquake Disaster, Real-time Information System, Seismograph Network, Damage Estimation, Damage Detection*

1. INTRODUCTION

Damage on civil infrastructures such as highways and river facilities due to an earthquake does not only reduce their functions but also affects the socio-economic activities in and around the damaged area[1]. Therefore, besides improving seismic performance of the civil infrastructures, pre-earthquake risk management to evaluate and mitigate their damage and post-earthquake emergency responses to reduce the effects caused by the destruction must be jointly promoted.

The MOC promoted a five-year comprehensive research project to develop disaster information systems from 1987, and compiled a "Guideline for Disaster Information Systems (Draft)[2]" which supports sectors responsible for the civil infrastructure respond emergency situations in terms of the disaster information. Taking possible techniques of information communication and processing into account, and based on the experiences of several past large natural disasters, the guideline deals with frameworks of the disaster information systems useful for acquisition, communication and analysis of the disaster information. Although seismic information systems at MOC have been developed based on the guideline, they are required to be more sophisticated in consideration of the experiences of serious disaster caused by 1995 Hyogo-ken Nanbu earthquake, progress of information oriented lifestyle and of recent technology innovation, such as remote sensing and multi-media technologies.

1995 Hyogo-ken Nanbu earthquake was the first destructive earthquake occurred right under a highly integrated urban area in Japan. Based on the experiences, the following information systems are pointed out to be urgently required for the real-time emergency activities immediately after an earthquake.

1) Real-time earthquake detection system to

1) Research Coordinator for Information Technology, Planning and Administration Dept., Public Works Research Institute, Ministry of Construction,: Tsukuba Science City, 305 Japan
2) Earthquake Disaster Prevention Technology Div., Earthquake Disaster Prevention Research Center, ditto
3) Ground Vibration Div., ditto

know the earthquake scale

2) Real-time estimation system to give an outline of civil infrastructure damage
3) Earthquake disaster detection system to grasp civil infrastructure damage which spreads over wide area.
4) Multi-media communication systems to transmit various kinds and a large amount of disaster information to sections and organizations concerned.

This paper introduces current state of seismic information systems at MOC, and the required real-time seismic information system for earthquake detection, damage estimation, damage detection and high-speed data communication for the emergency responses on civil infrastructure.

2. CURRENT STATE OF SEISMIC INFORMATION SYSTEMS

2.1 Communication Network for Disaster Prevention at MOC

Based on the experiences of repeated typhoons in 1940s, MOC recognized the importance to secure the communication network during a disaster, and has developed its exclusive communication network for disaster prevention. Since Niigata earthquake in 1964 in Japan when the efficiency of the exclusive communication network for disaster prevention, development of the communication network has been promoted all the more. MOC has now its nationwide communication network with 1,300 stations and 600 million channel-km of communication lines, which is the next largest network to that of Nippon Telephone and Telegram (NTT).

The communication network for disaster prevention is one of the essential parts of the earthquake disaster prevention framework at MOC. It is now being sophisticated based on the experiences of 1995 Hyogo-ken Nanbu earthquake and the revision of the National Disaster Prevention Plan (issued by the National Disaster Prevention Board, January 1996). The efforts includes revising the communication network from analogue to digital and linking it to the seismograph network and the disaster image transmission system.

Besides the communication network for disaster prevention, the optical communication network is under construction utilizing the public space such as highways and rivers. Focusing on the multi-media oriented lifestyle in coming 21 century, it is planned to complete 300 thousands kilometers of the optical communication line until 2010. As it focuses not only on the management of public facilities in usual time but also on the use for regional disaster countermeasures, it will be an essential data communication infrastructure to develop the real-time seismic information system.

2.2 Seismic Information Systems at other Organizations

At national and regional public bodies whose emergency response organizations are designated by laws, various information systems are applied to support the response actions. After Hyogo-ken Nanbu earthquake, "real-time earthquake disaster prevention" to cope with emergency response without conflicts is discussed actively, and information systems to

Table 1 Real-time Information Systems at Other Organizations

ORGANIZATIONS	EQ DETECTION (SEISMOGRAPH etc.)	DAMAGE ESTIMATION
CUBE	ABOUT IN CALIFORNIA	- ALARM
JR (UrEDAS)	EACH 20-80km ALONG MAJOR RAILWAY	- ALARM - EMERGENCY STOP
TOKYO GAS (SIGNAL)	ABOUT 300 IN KANTO AREA	- LIQUEFACTION RISK - DAMAGE DISTRIBUTION
TOKYO	ABOUT 50	- CASUALTY, FIRE SPREAD - DAMAGE DISTRIBUTION
KAWASAKI CITY	ABOUT	- DITTO
YOKOHAMA CITY	ABOUT 150	- DITTO

provide the prompt estimates of the damage on the residents and the facilities are being developed and applied. Table 1 shows examples of the real-time information systems at several organizations.

3. REAL-TIME INFORMATION SYSTEM FLAMEWORK

3.1 Information required for the emergency responses on civil infrastructure

Emergency response activities that is necessary for the management of the civil infrastructures vary depending on the time period after an earthquake. Therefore, it is important to treat necessary information with appropriate accuracy according to the response activities. The response activities can be classified into three restoration stages and the fundamental policies in each stage can be shown in Table 2[3]. The information required in each restoration stage are summarized as follows.

1) In the first stage, the bi-value information if the areas are seriously affected and if the facilities have serious damage that may cause secondary disaster
2) In the second stage, the damaged parts and their damage seriousness to judge the necessity of the restoration.
3) In the third stage, the detailed information of the facilities for the complete restoration accounting the future plans of the region.

Table 2 Fundamental Policies of Restoration Stages

RESTORATION STAGES	TIME PERIOD	FUNDAMENTAL POLICIES
1ST STAGE	EQ OCCURRENCE ~ 1 HOUR	- GRASPING OUTLINE OF DISASTER - EMERGENCY ACTION
2ND STAGE	~ 1 DAY	- GRASPING TOTAL DAMAGE STATUS - TEMPORARY REPAIR
3RD STAGE	~ 1 WEEK	- GRASPING DETAILED DAMAGE STATUS - PERMANENT REPAIR

3.2 Configuration of Real-time Seismic Information System

The entire image of the real-time seismic information system is shown in Fig. 1. The system consists of four subsystems: i.e., an earthquake detection system, a damage estimation system, a damage detection system and a high-speed communication system. Function and configuration of each subsystems are as follows.

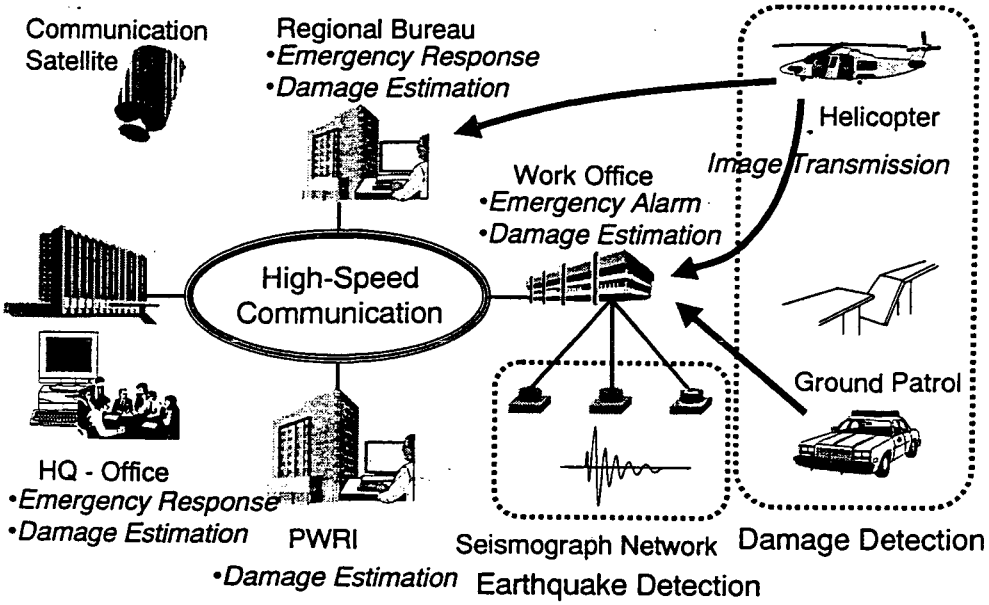


Fig.1 Real-time Seismic Information System

1) The earthquake detection system supports activating the emergency activities of the sectors in charge of the facilities by detecting the ground motion characteristics. The system mainly consists of the seismograph network.
2) The damage estimation system improves the emergency activities by roughly estimating the ground hazard and structural damage on facilities. The seismograph network and information processing devices are combined in this system.
3) The damage detection system improves the understanding of damage by combining images from a helicopter, images and data from the ground patrol.
4) The high-speed communication system transmits the data inside/ outside the organization by combining a optical communication network and innovative multi-media communication devices.

4. EARTHQUAKE DETECTION SYSTEM

It is of great importance to measure the seismic intensity at the facilities by densely placed seismographs for understanding the scale of an earthquake and possible damage on facilities. Also, the initial activities of the sectors concerned can be improved in terms of its quickness if the seismic information can be aggregated to them instantly.

From the above point of view, MOC has started constructing a Seismograph Network in 1995. In the Seismograph Network, about 800 strong-motion seismographs are placed with the interval of 20 to 40km along highways and rivers, and their data are sent to the sectors responsible for the facilities through the communication network for disaster prevention.

Fig. 2 shows the structure of the Seismograph Network. Ground motion characteristics detected at each station is aggregated at each regional construction office, and the data array are sent to the headquarters office and also to PWRI. In order to perform rapid data transmission through the present communication lines with limited capacity, small number of data representing the ground motion characteristics, such as a maximum acceleration, a seismic intensity (SI) value and the equivalent JMA seismic intensity level are to be sent.

The Seismograph Network is a fundamental system for the real-time seismic information system. In combination with a damage estimation system described later, following advantages can be derived.

1) Possible areas seriously affected can be predicted based on the quantitative data such as the maximum acceleration and SI-value.
2) The initial response activities can be more efficient with the prioritized damage seriousness of inspection sites.

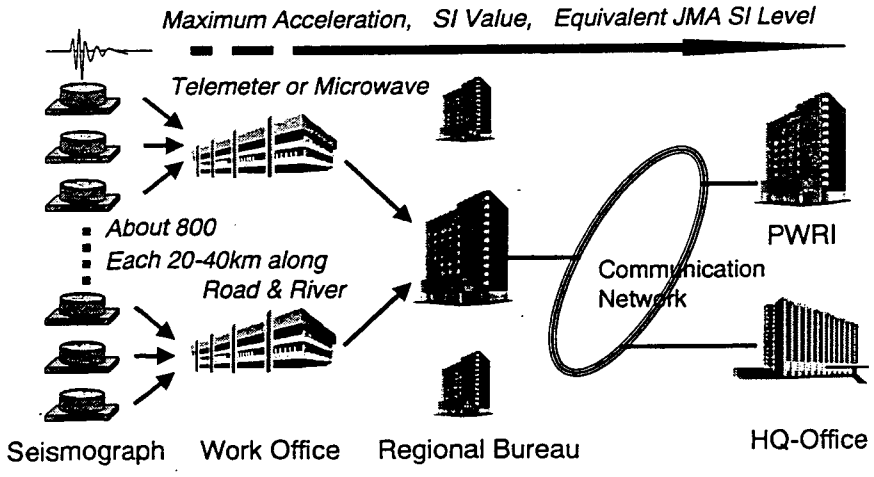


Fig.2 Structure of Seismograph Network

3) Support by the neighboring district without possible serious facility damage can be decided rapidly.

5. DAMAGE ESTIMATION SYSTEM

5.1 Structure of Damage Estimation System

The system can estimate possible ground hazard and possible structural damage on facilities by analyzing a large quantity of information regarding ground motion characteristics, ground conditions and structural conditions. This system will contribute to rationalize the initial response activities, i.e. understanding the outline of disaster and decision making on prioritized inspection area.

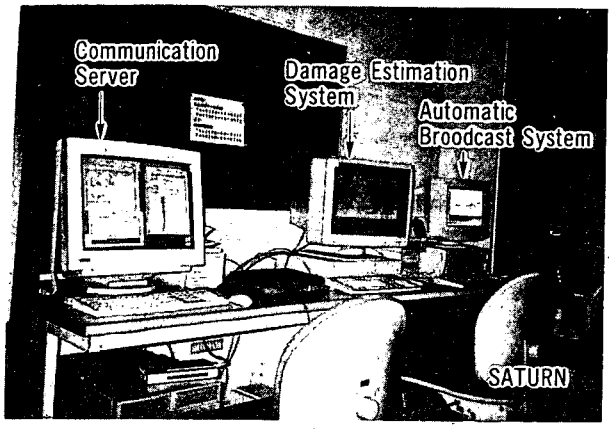


Photo.1 Prototype of Damage Estimation System:SATURN

PWRI and Kanto Regional Construction Bureau has jointly developed a prototype system (SATURN: Seismic Assessment Tool for Urgent Response and Notification) which roughly estimates the liquefaction risk and possible damage on highway bridges using the ground motion characteristics acquired by the Seismograph Network and other databases. At this time, the prototype system can perform the estimation within 15 minutes immediately after an earthquake. As shown in Photo 1, the prototype system works in cooperation with the communication server that receives and stores the seismic information in it.

5.2 Damage Estimation Methodologies

Fig. 3 illustrates the execution flow of damage estimation by the system. The execution proceeds through three steps: i.e., estimation of ground motion characteristics at facility sites, estimation of liquefaction risk, and estimation

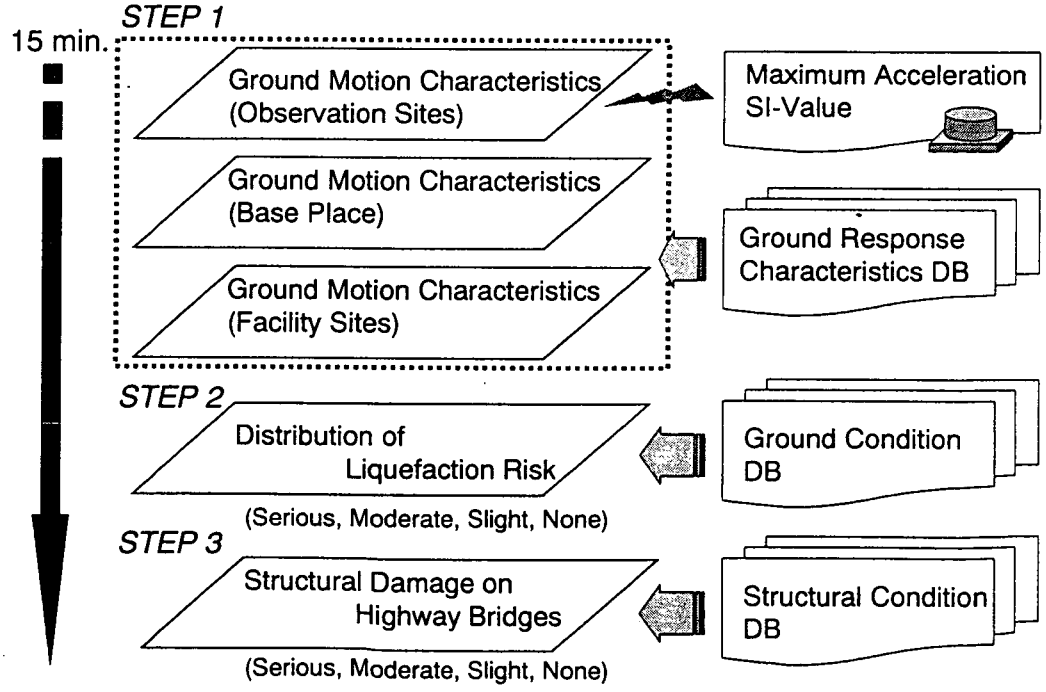


Fig.3 Flowchart of Damage Estimation

of the structural damage on highway bridges. Basic concepts of each steps are as follows.

(1) Ground Motion Characteristics at Facility Sites

Ground motion characteristics such as a maximum acceleration and a SI-value at a certain point can be estimated by interpolating them monitored at plural seismograph stations surrounding the point as shown in Fig 4. To avoid topographical influences on the estimation, ground motion characteristics are interpolated not at the ground surface but at the base place. Although the ground response characteristics must be known to estimate the ground motion characteristics at base place, immediately after an earthquake, it is quite difficult to calculate the response characteristics by the one-dimensional wave propagation method for all the points. Therefore ground response characteristics at station/ facility sites are calculated in advance and are stored in a database. It realizes the rapid information processing right after an earthquake.

(2) Distribution of Liquefaction Risk

The estimation of the liquefaction risk in the affected area is carried out by combining two kinds of estimation, i.e. estimation on a line along highway facilities, and estimation on areas besides highway facilities. Estimation along highway facilities can be carried out with sufficient ground condition data by calculating the "resistance values against liquefaction: F_L" and the "liquefaction index: P_L" regulated in the [Specifications for Highway Bridges] revised in 1996. Estimation on areas besides highway facilities is performed by a simplified method based on the topographical micro-zoning due to the insufficiency of ground condition data.

Fig. 5 shows a example of the distribution

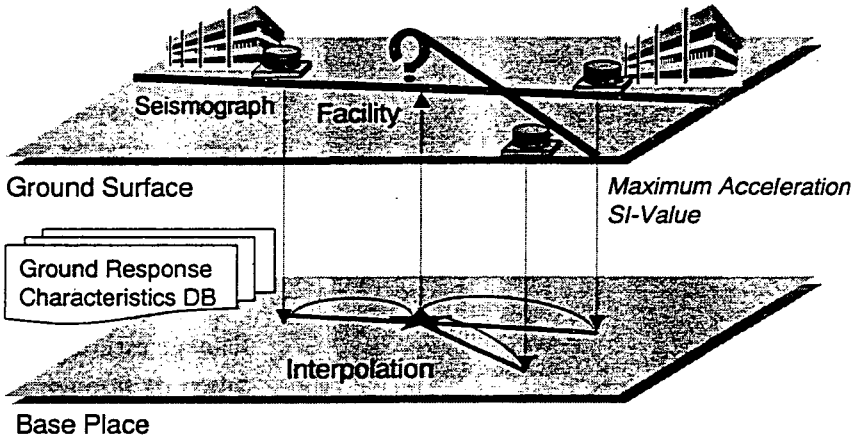


Fig.4 Estimation of Ground Motion Characteristics at Facility Site

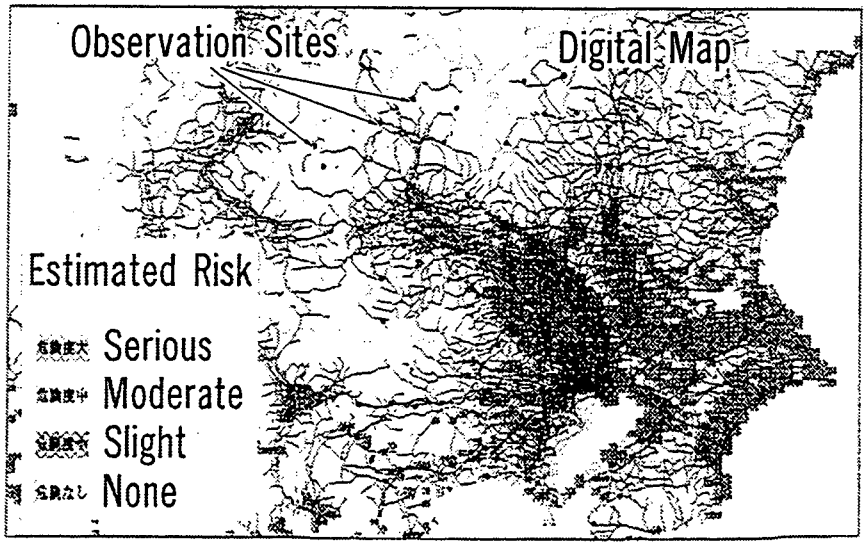


Fig.5 Estimated Liquefaction Risk distribution

of liquefaction risk. The liquefaction risk is displayed in four simplified categories of "serious, moderate, slight and no risk" as it is referred in an emergency situation immediately after the earthquake.

(3) Structural Damage on Highway Bridges

It is general to apply the response analysis methodology with mathematical models to know the behavior of highway bridges during an earthquake. However, it is difficult to complete the calculation by the general methodology urgently after an earthquake. Also at present, the information of the structure condition is not sufficiently prepared for the computation.

From the emergency response's point of view, the most important task is to know if each bridge is passable or not. Therefore, rough estimation on serious damage of bridges gives a effective information to decide the emergency inspection strategies. Fig. 6 shows an example of estimated structural damage in the affected area. Estimated damage is displayed in four simplified categories of "serious, moderate, slight and no damage".

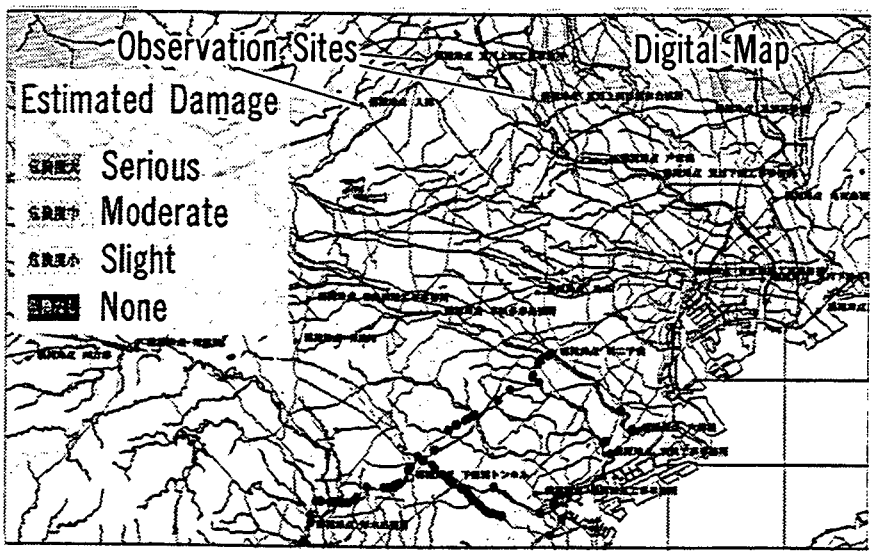


Fig.6 Estimated Structural Damage on Highway Bridges

The structural damage possibility of bridges is estimated by combining damage possibilities of bridge parts, such as columns, foundations and bearings. Damage possibilities of bridge parts are estimated by comparing their strength and ground motion characteristics such as maximum acceleration and SI-value. Here, the relationship between ground motion characteristics and occurrence of damage must be statistically studied in advance based on damage cases due to past

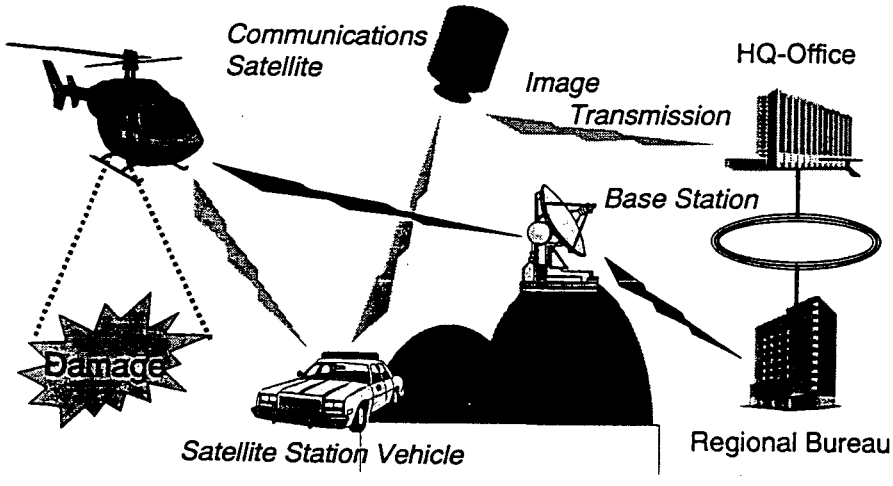


Fig.7 Helicopter Image Transmission System

earthquakes.

6. DAMAGE DETECTION SYSTEM

6.1 Remote Sensing by Image from Helicopter

Inspection by a helicopter from the air is quite efficient in terms of the damage detection after an earthquake[4] because it is not affected by the damage on the road or traffic congestion, and because it can collect the information of wide area in a short time. Also, visual images such as those taken by a video camera can provide desirable information in a short time. The structure of the helicopter image transmission system is shown in Fig. 7.

There are three helicopters administrated by MOC which are disposed at Tokyo, Osaka and Fukuoka. Among them, two of them are introduced after the 1995 Hyogo-ken Nanbu earthquake. They are equipped with various sophisticated information devices. Those include a video camera, a thermal image sensor, a GPS device to determine the position of the helicopter and other communication devices. Also the relay stations and the relay lines for the digital signals from helicopters are being improved.

It should be noted that the proper combination of flight rules of a helicopter and rules of taking images are important. For instance, overall images of the affected area and distribution of seriously damaged facilities, which are required on the first stage of restoration, are inspected by taking the images of panoramic view with much height in the sky. On the second stage, information for the emergency restoration such as damage on columns and cracks on embankments can be obtained by flying along the facilities with large magnification. An example image of a highway bridge taken from a helicopter is shown in Photo. 2.

6.2 Damage Detection by Ground Patrol

Although it takes time to reach the damaged site, the ground patrol can collect more detailed damage information than that by from the air. An efficient way of information collection is to combine the inspection from the

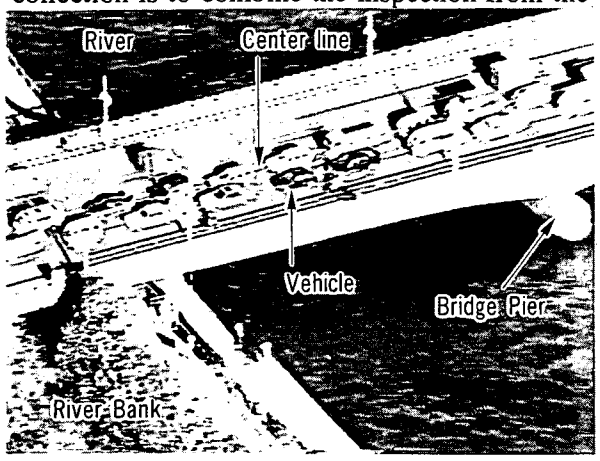


Photo. 2 Image of Highway Bridge Taken From Helicopter



Photo.3 Satellite Communication Vehicle

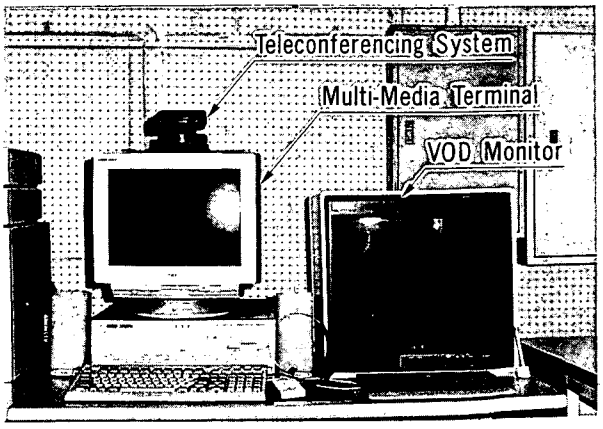


Photo.4 Prototype System for Damage Analysis based on Visual Image

air and that by the ground patrol. For instance, after grasping damage distribution from the air, detailed damage conditions can be inspected smoothly by the ground patrol.

The detected information can be transmitted through a communications satellite by dispatching a satellite communications vehicle or by assembling the small relay station at the site. The transmitted image can be referred at plural sectors and it is easy to hold the information in common among the sectors. In addition, the cellular system exclusive for MOC (K-COSMOS) is being constructed to transmit the information of a handy computer terminal and a digital camera

6.3 Damage Analysis Based on Visual Images

Visual images collected in a damaged area are aggregated at the headquarters office through the communication network for disaster prevention. In the headquarters, therefore, an information system which enables to classify and store a large amount of data systematically and enables to analyze damage conditions promptly is essential. Photo. 4 shows a prototype system for damage analysis based on visual images. Using the system, adding up of damage and remote judging of damage seriousness can be carried out based on visual images.

(1) Adding up of Damage based on Helicopter Images

Based on the transmitted image shown in a VOD monitor, discerning and adding up damage conditions can be carried out by operating engineering workstation. Procedures are as follows.

1) Discerning damage conditions- posing, rewinding and slowly playing of image are available using VOD (video on demand) function of the system.

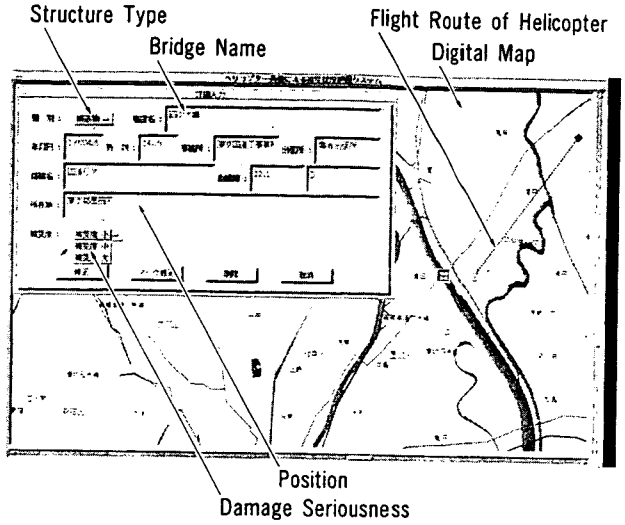


Fig.8 Adding Up Damage Conditions

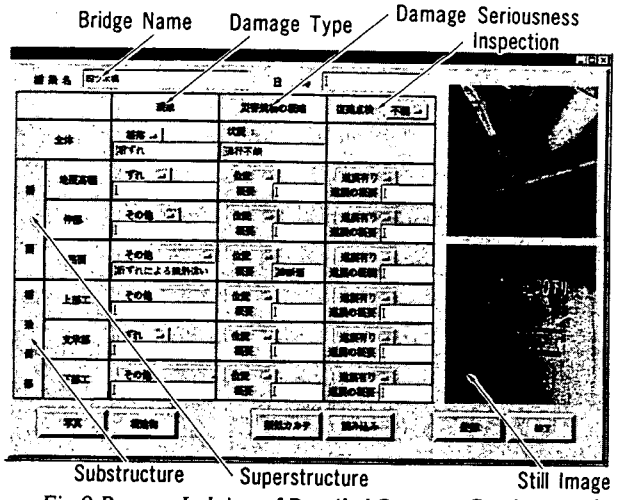


Fig.9 Remote Judging of Detailed Damage Conditions of a Highway Bridge

2) Marking damaged sites on a digital map- this operation is possible by referring the position of the helicopter displayed on the map automatically.

3) Typing structure type, structure name and damage seriousness in a worksheet on the display- attributes of the facility from the database is displayed on the worksheet automatically by cricking the proper position.

4) After completing the inputs of damage information, a damage record map and a table of the damaged sites are created and stored automatically by the system; the created data can be commonly referred by the sectors concerned.

Fig. 8 shows an image to adding up damage

conditions using the system.

(2) Remote Judging of Damage Seriousness based on Visual Image from Surface

Detailed damage records can be created by experts for each facility based on the detected information such as digital camera images and video images by the ground patrol. Based on the detailed damage information which can be referred commonly by the work office, PWRI and other supporting sectors through the disaster prevention communication network, the detailed damage record is created by plural sectors jointly through the TV conference. Fig 9 shows an example of the detailed damage record of a highway bridge.

To judge the damage seriousness of remote sites efficiently, it is desirable to apply the information regarding the ground condition and the structure condition by constructing their database during the usual situation and by linking them to the image data in the emergency situation.

7. HIGH-SPEED COMMUNICATION NETWORK USING MULTI-MEDIA TECHNOLOGIES

7.1 Fundamental Requirements for High-Speed Communication Network

As a major part of the real-time seismic information system, communication network for the disaster prevention is required to be sophisticated by applying innovative multi-media technologies. For activating above described information systems on earthquake detection, damage estimation and damage detection, issues to be required are as follows.

1) Transmission Capability- transmission of various media (numerical data, character data, voice data, still and animating image data) with required preciseness and speed
2) Common Utility- cooperative work (processing, exchanging and reference of data) by several sectors connected to the network
3) Seismic Safety- communication lines, devices and network redundancy

7.2 Experimental Study on High-speed Communication Network

As a high-speed communication network which satisfy several issues described above, communication system with Asynchronous Transfer Mode (ATM) was selected. And its possibility to the emergency response activities was studied through experiments. The structure of the high-speed communication network for the experiment is shown in Fig 10.

PWRI, Tokyo National Highway Work Office and Japan Construction Information Center (JACIC) were connected each other by the optical fiber cable. These three organizations were designated respectively as a supporting sector at remote site, a sector responsible for restoration activities and a headquarters office responsible for decision making. Different kinds of information devices were located in these three organizations corresponding to their roles. Devices are the VOD server to store and provide images, the database server to provide mapping/ structural data and the application server for the damage detection/ analyzing system.

Regarding the efficiency of high-speed communication network to the damage detection, following points were derived.

1) Helicopter images can be transmitted instantly to the HQ Office and the supporting sector. The most recent digital image compressing technology reduces the fail of the quality and enables discerning and aggregating damage information.
2) Judging damage seriousness at remote site can be realized with sufficient preciseness. However, the data transmission speed from

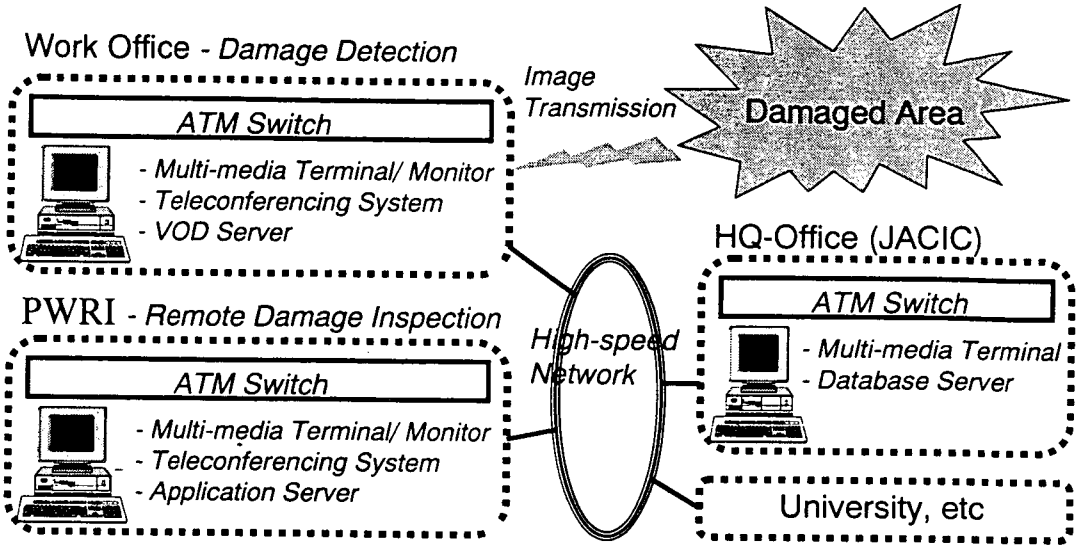


Fig.10 Experimental High-speed Communication Network

database servers and the workability of application shall be improved for smooth execution of cooperative works such as creating the detailed damage records.

8. CONCLUSIONS

Research and development of "Real-time Seismic Information System" was introduced focusing on a earthquake detection, damage estimation, damage detection and high-speed communication. By improving emergency response activities for civil infrastructures immediately after an earthquake, earthquake effects in and around the damaged area caused by structural destruction is anticipated to be much reduced.

For minimizing earthquake effects, pre-earthquake risk management and post-earthquake emergency response must be jointly promoted. Therefore, further study on "Comprehensive Seismic Information System" is required to be made for the pre-earthquake risk management including earthquake loss estimation methodologies and loss reduction strategies.

REFERENCES

1) K. KAWASHIMA, H. SUGITA and T. KANOH: Estimation of Earthquake Induced Economic Damage, Report of Public Works Research Institute, Vol. 186, December 1991
2) Public Works Research Institute, MOC: Guideline of Disaster Information System for Civil Infrastructures, Technical Note of Public Works Research Institute, Vol. 58, March 1992
3) Public Works Research Institute, MOC: Manual For Repair Methods of Civil Engineering Structures Damaged by Earthquakes, Technical Note of Public Works Research Institute, Vol. 45, December 1986
4) K. KAWASHIMA, H. SUGITA, T. KANO, T. NAKAJIMA, S. UNJOH and H. IIDA: Development of Surveying Systems for Detecting Seismic Damage Using Helicopters, Report of Public Works Research Institute, Vol. 192, January 1994

Accessing Natural Hazards Data from CD-ROM and on the Web

by

Allen M. Hittelman[1] and Paula K. Dunbar[1]

ABSTRACT

The National Geophysical Data Center and its collocated World Data Center-A for Solid Earth Geophysics acquires, processes, and analyzes technical data that are useful in natural hazards risk assessment. These data sets include information on earthquakes, tsunamis, topography, and global ecosystems. Personnel at NGDC are continually researching new technologies for disseminating these data. This paper presents several examples of seismicity, earthquake strong motion, hazards images, and ecological characterizations available on CD. Interactive search and retrieval capabilities via the World Wide Web of NGDC hazards data are also described.

KEYWORDS: earthquake; environmental data; geophysical data; GIS; GeoVu; seismicity; strong motion; topography; tsunami; World Wide Web

1. INTRODUCTION

The National Geophysical Data Center (NGDC) and its collocated World Data Center-A (WDC-A) for Solid Earth Geophysics acquires, processes, and analyzes technical data that are useful in natural hazards risk assessment. These data sets include information on earthquakes, tsunamis, topography, and global ecosystems. Personnel at NGDC are continually researching new technologies for disseminating these data. For example, many NGDC hazards data sets have been published on CD-ROM. Although CDs are a convenient distribution media, the data are in a variety of formats and difficult to access. The multiplatform GeoVu software was developed at NGDC to provide a versatile data access system. GeoVu allows users to quickly and easily browse, compare, and make selections from large data sets using intuitive menu files (an ASCII file developed by the data producer). These menu files help navigate through complex directory structures and integrate documentation. As a result of the increasing popularity of the World Wide Web, NGDC has developed tools to use these menu files to provide online access to data and metadata from the CDs. Interactive search and retrieval capabilities via the Web are also available for several natural hazards and digital elevation data sets. The following sections describe examples of NGDC natural hazards data published on CD, and online access to natural hazards data and information via our Internet site (http://www.ngdc.noaa.gov).

2. SEISMOLOGY PROGRAM

NGDC and its predecessors have been archiving earthquake data for the past century and currently hold the largest archive of historical earthquake event and strong motion data in the world. These data have been grouped into subsets by region, date, and theme; and disseminated on CD and via the World Wide Web. Two CD collections of earthquake data were recently released: Seismicity Catalogs and Earthquake Strong Motion.

2.1 Seismicity Catalogs

In June 1996, NGDC published a CD-ROM of earthquake catalogs which is a comprehensive compilation of the collections of the NGDC and National Earthquake Information Center of the U.S. Geological Survey. The CD-ROM set contains data for more than 4 million earthquakes dating from 2100 B.C. to 1996 A.D. The data contain information on epicentral time of origin, location, magnitudes, depth and other earthquake-related parameters. Three types of

[1] National Geophysical Data Center, National Oceanic and Atmospheric Administration (NOAA), E/GC1, 325 Broadway, Boulder, CO 80303

catalogs are included on the CDs: (1) Local (containing data from single stations or local networks), (2) Regional (containing data from regional networks, such as CALNET in central California), and (3) Teleseismic (containing data from around the world). Catalogs have been contributed from various worldwide industrial, academic, governmental, and private sources. The CDs also contain auxiliary data bases which aid in earthquake investigations. These data include: world stress, tsunami, volcanic and fault parameters, digital elevation models, the Summary of Earthquake Data Base, and a bibliography of earthquake-related materials at NGDC. Format information, a data dictionary, and statistical information are also included.

The data on the Seismicity Catalog CDs can be accessed through the GeoVu browse and visualization software included on the CDs. This software allows visualizations such as x-y plots of the data and pre-computed histograms, as well as reformatting of data files to a format specified by the user. Figure 1 shows an example of an x-y plot of latitude vs. longitude for the Beijing, China, State Seismological Bureau earthquake catalog.

In addition to the CD collection, NGDC performs seismic hazard and site analysis upon request. Data retrievals from the earthquake data base may be made according to any number of combinations of parameters such as geographic area, time period, magnitude range, or maximum intensity.

2.2 Significant Earthquake Database and U.S. Earthquake Intensity Database

Two of NGDC's most popular earthquake catalogs are the Significant Earthquake Database and U.S. Earthquake Intensity Database. The Significant Earthquake database that was developed at NGDC. It is a global database containing information on more than 5,000 destructive earthquakes from 2150 B.C. to the present. The events in the file must meet at least one of the following criteria: moderate damage (approximately $1 million or more), 10 or more deaths, magnitude 7.5 or greater, or Modified Mercalli Intensity X or greater (for events lacking magnitude). This database is available as a soft cover book. The U.S. Earthquake Intensity Database is a collection of damage and felt reports for over 22,000 U.S. earthquakes dating from 1638 to 1985. The digital database contains information regarding epicentral coordinates, magnitudes, focal depths, names and coordinates of reporting cities, reported intensities, and the cities' distances from the epicenter. These catalogs are included on the Seismicity Catalogs CD collection and are also available for searching or downloading via the World Wide Web. Users can search on any combination of earthquake and intensity parameters. The results are displayed in a dynamically created HyperText Markup Language (HTML) page based on user-specified criteria.

2.3 Strong Motion Accelerograph Records

The NGDC earthquake strong motion archive, the largest collection of digitized and processed accelerograph records in the world, is available on CD. This CD collection contains more than 15,000 digitized and processed accelerograph records, dating from 1933 to 1994. The data represent a broad range of structural and geologic recording environments. Three types of processed records are included on the CDs: uncorrected (raw), corrected (filtered), and response spectra (includes Fourier spectra). Records were contributed to the archive from various worldwide industrial, academic, and governmental sources. Over 2,000 pages of documentation containing information on the triggering earthquakes, recording stations, record processing procedures, and data format (when available) were digitally scanned (in PCX files) and included on the CDs. These files can be accessed and displayed with the GeoVu software.

Most of the strong motion archive consists of records obtained from various man-made structures. These sites include structures of engineering importance such as dams, bridges, utilities, and large buildings. These records represent a comprehensive collection of

accelerograph data suitable for the analysis of dynamic structural response and soil-structure interaction.

Approximately 5,000 records in the collection are available from ground response sites. Obtained from a wide variety of geologic environments, these records comprise an important subset useful for the study of seismic attenuation in a wide variety of regional geologic media ranging from young alluvium to hard rock. Several near-source records included in the database are useful for source mechanism studies. Also included in the archive are records from several accelerograph instrument arrays which are used to study specific problems in strong ground motion.

2.3.1 Strong Motion Catalog (SMCAT) data inventory software package

The Strong Motion CATalog (SMCAT) data inventory software package for IBM-compatible personal computers is included on the CDs. It contains a comprehensive database which summarizes the characteristics of each accelerogram and facilitates retrieval of records for specific applications from the CDs. The SMCAT database is also available for searching via the World Wide Web. Users can search on any combination of earthquake, station, or accelerograph record parameters; the results are displayed in a dynamically created HTML page. An example of the search parameters page and the search results are shown in Figure 2. The SMCAT database will continue to be updated as additional accelerograph records are added to the NGDC archive.

2.4 Spitak Earthquake CD-ROM

The Spitak Earthquake CD-ROM is another example of natural hazards data distributed on CD. It was a cooperative project between the Russian Academy of Sciences and NGDC. The CD contains a wide variety of information useful in seismic hazard analysis such as information on the geology and geophysics of the area, data for the mainshock and aftershocks, topography data, as well as societal information such as population agriculture, and industry. This CD is also accessible with the GeoVu software. GeoVu allows users to browse data layers using an intuitive menu (an ASCII file developed by the data producer). This menu file is also used in conjunction with Web-based browsers, providing online access to metadata and data from the CD. The online user interface and a data display from the CD is shown in Figure 3.

3. TSUNAMI PROGRAM

NGDC and the WDC-A help to compile, catalog, and synthesize available information on tsunami sources and effects to support modeling, engineering, planning, and educational purposes. These products include historic tsunami data, technical publications, and photographs.

3.1 Pacific Tsunami Database

The Pacific Tsunami Database provides detailed information on the tsunami source and effects. It includes more than 2,000 events since 2,000 B.C. and more than 5,800 tsunami locations. This database is included on the Seismicity Catalogs CD collection and is available via our Internet site.

3.2 Tsunami Publications

Tsunami publications available from NGDC include tsunami catalogs for the United States, the western coast of Mexico, the Pacific, and Peru-Chile. A catalog of submarine volcanoes and hydrological phenomena associated with volcanic events is also available. The latest publication, *Tsunamis Affecting Alaska, 1737-1996*, describes all known tsunamis which have affected Alaska in historic times. In the future, the digital files used in preparing the publications will be converted to HTML pages and accessible on the World Wide Web.

4. HAZARD PHOTOGRAPH COLLECTION

In the interest of hazard education, NGDC routinely collects post-disaster photographs of

geologic hazards for the development of educational slide sets. The goal of the hazard photograph program is to promote a greater understanding of geologic hazards throughout the world and their effects on man and the environment. The sets depict the characteristics and effects of hazards such as earthquakes, volcanoes, landslides, and tsunamis. Of the 35 sets in distribution, 19 relate to earthquake damage, eight to volcanism, three to tsunamis, and five to geologic processes. A recent release is a set on the Great Hanshin-Awaji (Kobe) Earthquake of January 17, 1995. A slide from the Kobe set is shown in Figure 4.

4.1 Geologic Hazards Photos CD-ROM

As part of a data preservation effort, the geologic hazards slide sets were digitally scanned and replicated on a three-volume CD collection. The images (and their companion documentation with credits) are accessible with GeoVu. These images are also available for viewing and downloading via the World Wide Web.

5. TOPOGRAPHY PROGRAM

Topography is an important data layer in many Geographic Information System (GIS) applications for hazards assessment and emergency response. In addition to earthquake and tsunami programs, NGDC also has an active topography program. Numerous national, regional, and global digital elevation models (DEMs) are provided on CD.

5.1 TerrainBase CD-ROM

The TerrainBase CD provides a new global 5-minute mosaic using improved source materials. These data files can be downloaded via the World Wide Web. The data on the CD can be easily imported into any geographic information system and are accessible with the GeoVu software. Using the same technology described in the Spitak Earthquake CD-ROM section 2.5, GeoVu allows users to browse data layers using an intuitive menu file. This menu file also provides online access to metadata and data displays from the CD.

5.2 Global Land One-kilometer Base Elevation Project

NGDC is a participant in the Global Land One-Kilometer Base Elevation (GLOBE) project. GLOBE originated as an ad-hoc international cooperative effort between several organizations interested in creating a global digital elevation model (DEM) on a nominal 1-kilometer grid. GLOBE has been endorsed by the Committee on Earth Observation Satellites (CEOS) subgroup on Auxiliary Data Sets. The Inter-national Geosphere-Biosphere Programme's Committee on Data and Information Systems (IGBP-DIS) is a major participant. NGDC is responsible for dissemination of GLOBE data and thus far has released two prototype data sets (version 0.1, 1995; version 0.5, 1997). By the end of 1997, the GLOBE Project hopes to make available its first complete hybrid global 1-km grid. These data will be distributed on CD-ROM and will be formatted so that the data can be easily imported into a geographic information system. The data and metadata will be accessible with the GeoVu software and eventually available via the Internet.

6. COASTAL RESOURCE MANAGEMENT

The world's coastal areas are particularly vulnerable to natural and manmade hazards. Intelligent management of these resources requires the identification of risks from climate, geophysical events, environmental change, ecological events, and societal pressures to these areas. NGDC and the Cooperative Institute for Research in Environmental Sciences (CIRES) are collaborating with the NOAA Coastal Services Center (CSC) to meet NOAA goals in coastal resource management and information services. Through these collaborative efforts, improved methods for synthesis of ecosystem information and application to current-day problems are being formed.

6.1 Otter Island CD-ROM

As part of its collaboration with CSC, NGDC is pioneering coastal characterization studies to support the needs of regional planners and coastal zone managers. The first CD, an ecological characterization of Otter island, South Carolina, has been produced. The CD contains extensive text and a large bibliography presented in HTML pages accessible with Web browsers. This CD also features an index and a glossary that were created using the tool MetaDex. MetaDex was developed at NGDC to make metadata more accessible by automatically generating indexes and glossaries from HTML, menu, and plain text files. In addition to the large amount of metadata, many GIS data layers are also included. These data are accessible with the ArcView geographic information system software. Videos showing some of the animal species found on the island can also be viewed.

7. CONCLUSION

The future offers many exciting challenges and opportunities for NGDC and the WDC-A. Rapidly changing Web technologies will allow NGDC to provide quick and easy access to data and information in user-specified formats. Users will be able to access information on CDs as well as update data as it becomes available on the Web. New multiplatform programming languages will make data accessible via Web browsers regardless of operating system, network software, or hardware. Multimedia applications will enable data and information to be presented in new and innovative ways. Higher resolution graphics and new higher precision data streams from satellites will provide new insight into many areas of research. Technologies will provide online links to GIS data layers and applications allowing users to not only access data, but to perform online analyses. The future for NGDC definitely holds unprecedented opportunities, limited only by our imaginations.

8. REFERENCES

Brennan A.M., and J.F. Lander, editors, *2nd UJNR Tsunami Workshop, Honolulu, Hawaii, 5-6 November 1990, Proceedings*, 1991, National Geophysical Data Center, Boulder, Colorado, USA, 260 p.

Dunbar, P.K., *Earthquake Strong Motion on CD-ROM, Volume 1: U.S.A., Part A, Volume 2: U.S.A., Part B, Volume 3: Non-U.S.A.*, National Geophysical Data Center, Boulder, Colorado, USA, 1996.

Dunbar, P.K., and D.A. Hastings, *Global Land One-km Base Elevation (GLOBE) Version 0.1 on CD-ROM, Volume 1: Maximum and Minimum 30-Second Elevation Grids, Volume 2: Average 30-Second Elevation Grids*, National Geophysical Data Center, Boulder, Colorado, USA, 1995.

Dunbar, P.K., and D.A. Hastings, *Global Land One-km Base Elevation (GLOBE) Version 0.5 on CD-ROM, Volume 1: Average 30-Second Elevation Grids, Volume 2: Maximum and Minimum 30-Second Elevation Grids, Volume 3: Discrete 30-Second Elevation Grids*, National Geophysical Data Center, Boulder, Colorado, USA, 1997.

Dunbar, P.K., P.A. Lockridge, and L.S. Whiteside, *Catalog of Significant Earthquakes, 2150 B.C.-1991 A.D., Including Quantitative Casualties and Damage*, Report SE-49, National Geophysical Data Center, Boulder, Colorado, USA, 1992, 320 p.

Hedervari, P., *Catalog of Submarine Volcanoes and Hydrological Phenomena Associated with Volcanic Events*, Report SE-42, National Geophysical Data Center, Boulder, Colorado, USA, 1986, 35 p.

Hittelman, A.M., P.A. Lockridge, and P.J. Hayes, *Geologic Hazards CD-ROM, Volume 1: Earthquakes, Volume 2: Volcanoes and Other Phenomena*, National Data Center, Boulder, Colorado, USA, 1993.

Lander, J.F., *Tsunamis Affecting Alaska, 1737-1996*, NGDC Key to Geophysical Research Documentation No. 31, National Geophysical Data Center, Boulder, Colorado, USA, 1996, 195 p.

Lander, J.F., and P.A. Lockridge, *United States Tsunamis 1690-1988*, National Geophysical Data Center, Boulder, Colorado, USA, 1989, 265 p.

Lander, J.F., P.A. Lockridge, and M.J. Kozuch *Tsunamis Affecting the West Coast of the United States, 1806-1992*, NGDC Key to Geophysical Research Documentation No. 29, National Geophysical Data Center, Boulder, Colorado, USA, 1993, 242 p.

Lander J.F., and Harry Yeh, eds., *Report of the International Tsunami Measurements Workshop, 1995*, National Geophysical Data Center, Boulder, Colorado, USA, 102 p.

Lockridge, P.A., *Tsunamis in Peru-Chile, 1985*, Report SE-39, National Geophysical Data Center, Boulder, Colorado, USA, 95 p.

Lockridge, P.A., S.D. Racey, S.J. McLean, *Geologic Hazards CD-ROM, Volume 1: Earthquakes General, Volume 2: Earthquake Events, Volume 3: Tsunamis, Volcanoes, and Other Hazards*, National Geophysical Data Center, Boulder, Colorado, USA, 1997.

National Geophysical Data Center, NOAA, Russian Academy of Sciences, in collaboration with Joint Institute of the Physics of the Earth, Institute of Geophysics and Center of Geophysical Computer Data Study, *Spitak Earthquake 4 Dec. 1988 CD-ROM*, National Geophysical Data Center, Boulder, Colorado, USA, 1994.

Row III, L.W., and D.A. Hastings, *TerrainBase, Worldwide Digital Terrain Data CD-ROM, Release 1.1*, National Geophysical Data Center, Boulder, Colorado, USA, 1995.

Sanchez, A.J., and S.F. Farreras, *Catalog of Tsunamis on the Western Coast of Mexico*, 1993, National Geophysical Data Center, Boulder, Colorado, USA, 79 p.

Soloviev, S.L., Ch.N. Go, and Kh.S. Kim, *Catalog of Tsunamis in the Pacific, 1969-1982*, 1992, Academy of Sciences of the USSR, Soviet Geophysical Committee, Moscow, 207 p.

South Carolina Department of Natural Resources, National Oceanic and Atmospheric Administration Coastal Services Center, and National Geophysical Data Center, *Ecological Characterization of Otter Island, South Carolina CD-ROM: A prototype for interactive access to coastal management information*, U.S. Department of Commerce, National Oceanic and Atmospheric Administration Coastal Services Center, Charleston, South Carolina, USA, 1996.

Whiteside, L.S., D.T. Dater, P.K. Dunbar, S.D. Racey, R.W. Buhmann, and A.M. Hittelman, *Seismicity Catalogs on CD-ROM, Volume 1: North America, Volume 2: Global and Regional*, National Geophysical Data Center, Boulder, Colorado, USA, 1996.

Figure 1: An example of a GeoVu x-y plot of latitude vs. longitude for the Beijing, China, State Seismological Bureau earthquake catalog.

Figure 2: An example of the SMCAT search parameters page and the search results

Figure 3: The online user interface and a data display from the Spitak CD.

Figure 4: A slide from the Kobe slide set.

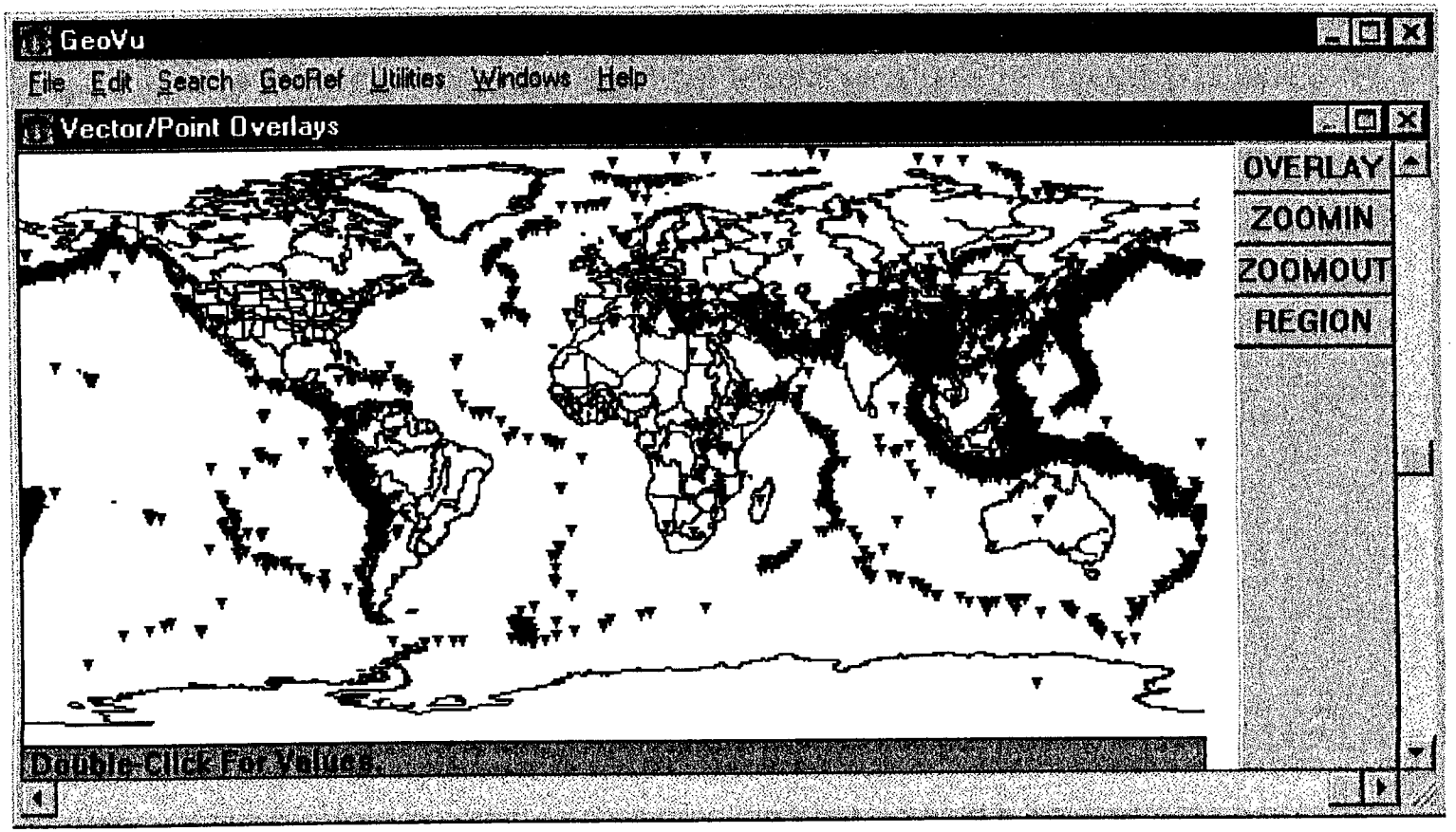


Figure 1: An example of a GeoVu x-y plot of latitude vs. longitude for the Beijing, China, State Seismological Bureau earthquake catalog.

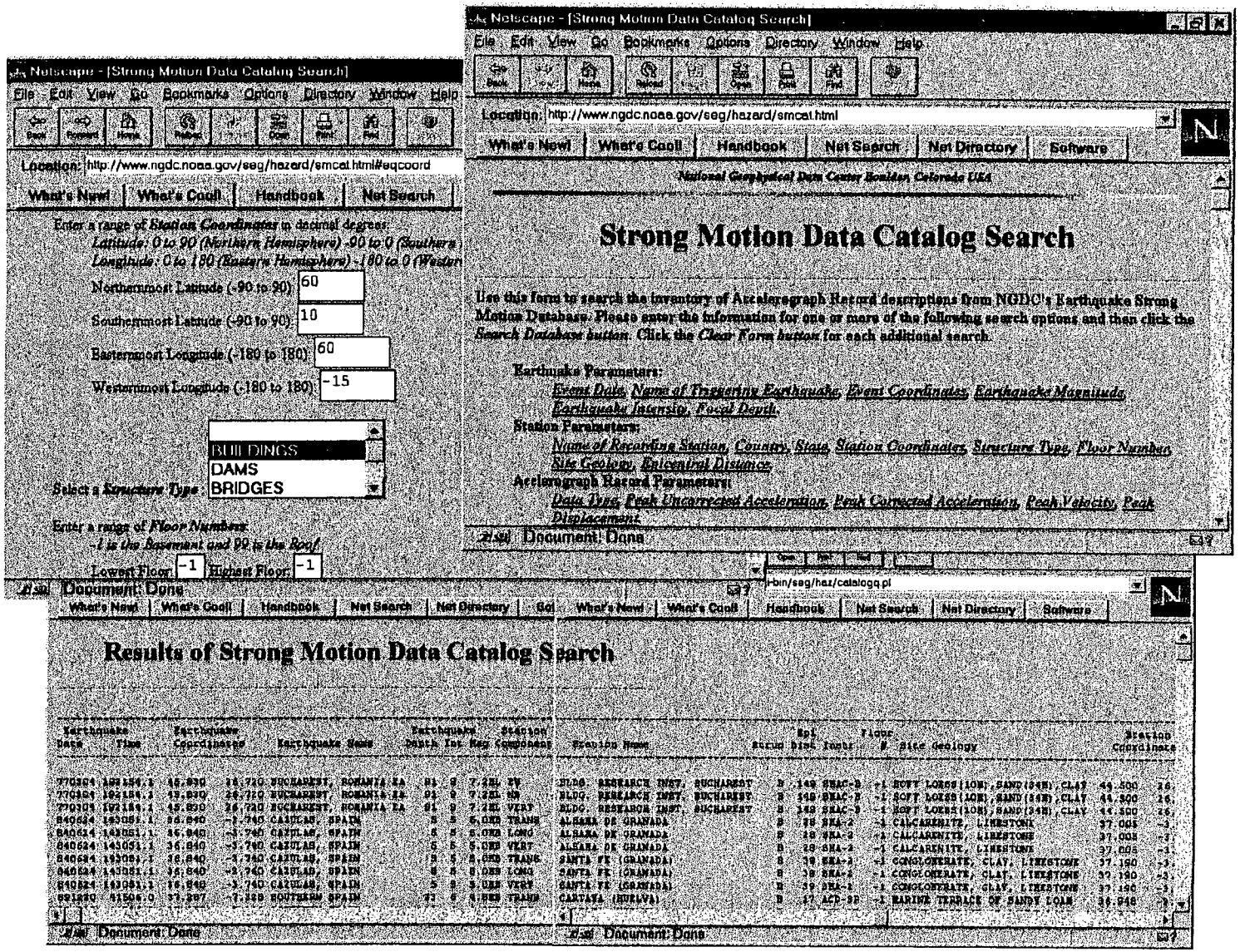


Figure 2: An example of the SMCAT search parameters page and the search results.

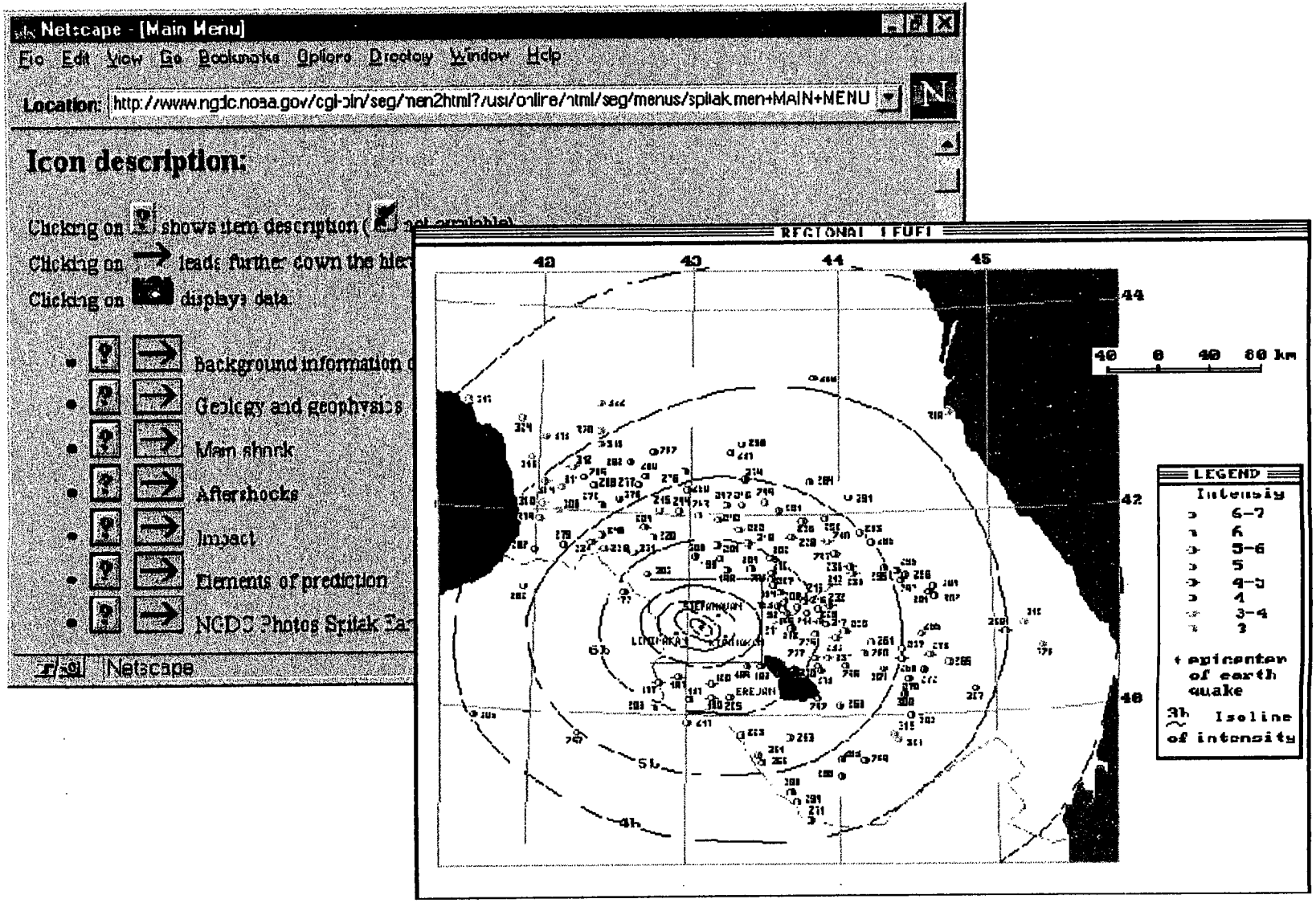


Figure 3: The online user interface and a data display from the Spitak CD.

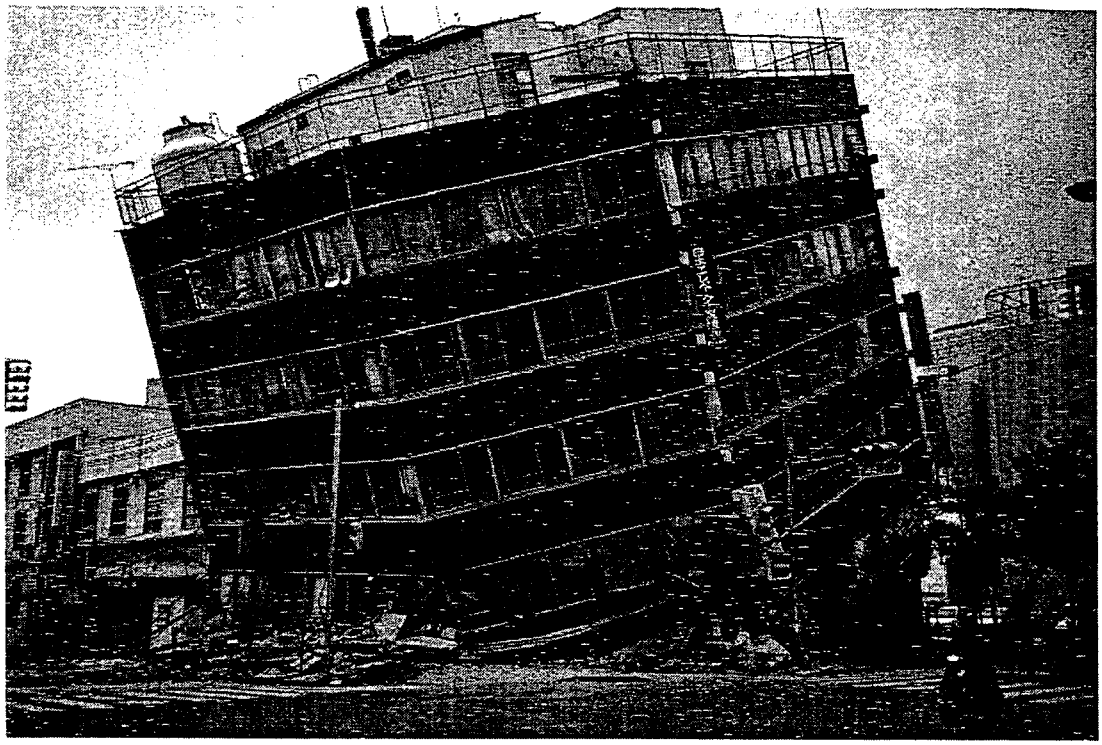


Figure 4: A slide from the Kobe slide set.

Development of the Disaster Information System(DIS/Earthquakes)

by

Kazuo Okayama

ABSTRACT

Utilizing the experiences of the Great Hanshin-Awaji Earthquake, the National Land Agency has been promoting the development of the Disaster Information System/Earthquakes (DIS) which uses the Geographic Information System (GIS). This system is expected to provide quick and appropriate decision making in all three phases, "preparation", "emergency measures" and "recovery/rehabilitation". Since April 1996, the National Land Agency has been operating the Early Estimation System (EES) which automatically estimates the scale of damage caused by an earthquake using the very limited information available immediately after an earthquake occurs. This system began operating in April 1996, and over the period of one year, was activated 41 times by earthquakes of seismic intensity 4 or greater.

Key Words : the Great Hanshin-Awaji Earthquake
the Disaster Information System(DIS),
the Early Estimation System(EES),

I BACKGROUND

I-1 Impact of The Great Hanshin-Awaji Earthquake

The Great Hanshin-Awaji Earthquake, which occurred right under the city of Kobe on January 17, 1995, again showed the importance of rapid response activities by the national government, particularly the importance of estimating damage immediately after an earthquake.

If organizations concerned with disaster prevention have numerical map and geographical location data and a system that combines this data for quick and efficient application, they should be able to quickly determine the state of damage, and support rescue and recovery activities quickly and effectively.

Based on this experience, the National Land Agency has been promoting preparation of a Disaster Information System by utilizing Geographic Information System (GIS) that manages information on topography, ground conditions, population, building stock, disaster response facilities, etc., connected to digital maps on a computer.

I-2 Basic framework of the new disaster prevention

The difficulty encountered in collecting appropriate information after the Great Hanshin-Awaji Earthquake reemphasized the importance of information. How to collect, put in order and analyze information efficiently have become major factors in recognizing the necessity of building a

Director, Earthquake Disaster Countermeasures Division, Disaster Prevention Bureau, National Land Agency, 1-2-2 Kasumigaseki Chiyoda-ward,100 Japan

new system.

The new basic plan which was amended in July 1995 considers the importance of information in the following three stages: prevention, emergency measures and recovery/rehabilitation. It shall promote the construction of geographic information systems to support the realization of disaster-preventive measures.. It also states that the on-line database network shall be construct.

Certain activities are specifically indicated in the new plan. They are utilization and application of geographic information systems, monitoring systems, etc. after the occurrence of a disaster in order to quickly analyze the scale of damage, to collect and comprehend information on primary & general damage and on emergency measures so that it can be passed on to relevant organizations, and to assure that appropriate measures are taken to establish necessary communications.

I-3 Toward the advanced information society

For the past three years or so, there has been a strong trend toward the advanced information society. People are becoming increasingly more aware that something has to be done. There is the personal computer boom. More and more people are beginning to use personal computers, and such computers are increasing their capabilities as well as their kinds day by day.

Maintenance of information on earthquake disasters should be systematically carried out by using geographical information systems which have been making remarkable development in recent years. It is said that 1994, the year before The Great Hanshin-Awaji Earthquake, was the beginning of the advanced information society in Japan, and the people started to discuss the concept of a "Japan Information Super-Highway."

Because of digitalization resulting from sophisticated uses of information, and of technological development epitomized by the downsizing of the calculator the Geographic Information System (GIS) has been making rapid progress in application technology, hardware and software. At present, various kinds of numerical maps are being prepared by concerned organizations.

Handling of a huge amount of information has been made possible by development of data processing technology by computers and communications technology, due to rapid progress in technical innovation, such as optical fiber and communication satellites.

In short, we have reached the stage where we are technically capable of constructing large-scale network systems, such as a disaster information system, that allow us to process a large amount of map data by linking many relevant organizations. Under this situation, the importance of information has been recognized, and the development of the DIS/Earthquakes was initiated.

II DIS/EARTHQUAKES - ITS OUTLINE AND CURRENT STATUS

II-1 Outline of the system

To develop an earthquake disaster information system (DIS/Earthquakes), the National Land Agency established a committee composed of specialists on earthquake disasters and their preventive systems, and persons from related ministries and agencies. References are being made to similar systems, both academic and practical, which have been or are being developed in the U.S.

As shown in Attachment 1, DIS/Earthquakes focuses on three stages of an earthquake disaster. They are emergency period, recovery/rehabilitation period, and preparation period for the next disaster. This system is expected to effectively support quick and appropriate decision making by the organizations concerned.

DIS/Earthquakes is composed of a Disaster Information Control System, which provides a base for analysis, and subsystems that perform actual analysis. The Disaster Information Control System accommodates and manages the information needed for operation of each subsystem in DIS/Earthquakes. As shown in Attachment 2, its data base includes map data on administrative organizations, public facilities, roads, organizations and facilities for disaster prevention, etc.

The National Land Agency places the highest priority to the communications immediately following the occurrence of an earthquake. The Early (Damage) Estimation System (EES) has been in operation since April 1996. This system automatically estimates the scale of damage and indicates the initial activities required within 30 minutes after the occurrence of the earthquake by using very limited information.

The Earthquake Damage Information System continuously collects transient information on damage and recovery concerning public facilities, lifelines, etc. The data base is updated accordingly and the information is shown on maps to assist decision making. The system will also provide information on damage to roads, railways and lifelines to the organizations concerned so that they can effectively utilize it in taking emergency operational measures.

The Emergency Measures Support System utilizes the output from EES and the Earthquake Damage Information System to support search and rescue activities and to help optimize the distribution of relief materials. According to different emergency measures, there will be different systems for transportation, rescue/medical attention, evacuation, and volunteers.

As time passes, recovery/rehabilitation measures become more important, and here comes the Recovery/Rehabilitation Measures Support System, which provides information to support the establishment of recovery and rehabilitation plans at various levels, and to help manage their progress.

The abovementioned systems respond to the activities in the post-earthquake period. However, preparation for the next disaster is also important for the National Land Agency.

The Earthquake Damage Estimation System will forecast the extent of damage due to a future earthquake by map information data base. It will be used to plan and establish various disaster measures before the next one comes.

The Earthquake Disaster Prevention Facilities Preparation Plan Support System will be utilized to select possible sites for emergency facilities. It will also be useful to determine kinds of facilities to be prepared by simulating the effectiveness of different measures for different earthquakes.

III EARLY ESTIMATION SYSTEM (EES)

III-1 Purpose and outline of EES development

Earthquake damage estimation is often used as the initial condition for contingency planning. Such an estimation is based on a compilation of a number of R&D results integrated into a comprehensive system. Such a system may be further integrated to estimate the macroscopic scale of damage and the extent of the affected area by using a very limited amount of input information. EES provides a real-time estimation of the numbers of damaged buildings and casualties. The system has been developed to provide information that contributes to quick and appropriate judgment for making decisions concerning emergency measures when there is only limited information available immediately after the occurrence of an earthquake.

Some of the features of EES are as follows:

- EES covers the entire country,
- EES estimates only damage to buildings and casualties caused by earthquake vibration at the municipality level. It does not estimate damage caused by fires, aftershocks, etc.,
- EES automatically receives seismic information from the Japan Meteorological Agency and is activated when JMA intensity greater than 4 is detected at one or more seismic intensity observation points throughout the country,
- Under the conditions cited above, EES provides the results of estimation with 30 minutes after the occurrence of an earthquake,
- Unlike standard earthquake damage estimation, EES operates with a small computer of the size of work stations.

III-2 System configuration and estimation methods

EES is composed of processing equipment (database server units), terminal equipment for display (clients), printers, etc., all of which are easily available on the market. The equipment in normal service at the main office of the National Land Agency is augmented by stand-by equipment at the Greater Tachikawa Contingency Station. Thus, if there is a problem with one system, the other system

takes over immediately.

The National Land Agency is connected by LAN with simultaneous reporting equipment to receive earthquake information from the Meteorological Agency and to transfer it to the processing equipment. The results of estimation by the processing equipment are automatically outputted to the terminal equipment for display.

The following summarizes the flow for damage estimation:

- EES is automatically activated as described above,
- The seismic data is combined with surface soil and topographical data to estimate the distribution of ground motion severity,
- Based on the estimated distribution of ground motion severity, available building data is utilized to estimate the damage to buildings,
- Available population data is used to estimate causalities caused by building destruction, and
- The results are automatically shown on a display terminal.

Earthquake information from the Meteorological Agency is transmitted within about 10 minutes after it is generated and the estimation of damage is completed in 5 - 20 minutes according to the size of the area affected. Back-up functions are provided for manual input of data when the data cannot be automatically received.

III-3 Outline of the logic for each estimation process

III-3-1 Intensity and estimation grid

For estimation of earthquake damage, JMA seismic intensity is used to represent the severity of ground shaking. It is received in real time from the Meteorological Agency as the initial earthquake information. From seismic intensity observed at the ground surface and consideration of influence of geological features of the earth's crust, it should be possible to estimate the isoplethic curve (contour) for speed distribution of an earthquake. From the estimated contour, intensity distribution on the ground surface is computed taking into account the properties of the surface layers again.(see attachment 4)

The National Land Numeric Information Tertiary Mesh (1km^2 mesh) is used. The properties of the surface layers are classified into 13 types based on geological and topographical data of each grid, from which amplification factors are determined.

By assuming a relationship between the estimated seismic intensity and the building damage, the damage to buildings in each grid is estimated, and the number of damaged houses is integrated for each municipality. Buildings are classified as wooden and non-wooden buildings, and the number of damaged houses is estimated for each of them.

III-3-2 Wooden building damage

The building areas in a municipality was first

obtained for different age groups and they were divided by the average building area per house of the municipality to determine the number of buildings in different age groups in the municipality. These numbers were distributed to each grid in proportion to the night-time population to estimate the number of buildings in each grid.

Buildings were classified into two age groups according to whether or not they were built after 1960, when a major revision of the Building Standards Act was implemented to specify the quantity of framework and walls required.

The whole area of Japan was divided into three groups according to the snow load adopted for structural design. The surface soil properties were regrouped into two, soft and hard, based on the predominant periods computed by using the 13 types previously mentioned.

Therefore, the damage factor for wooden buildings was expressed in terms of seismic intensity, building age, snow load level, and surface soil property. Non-linear response analysis was performed for all the combinations of the four parameters. The number of collapsed buildings was then obtained by multiplying the number of houses in each category by the collapse ratio of the houses in each category.

III-3-3 Non-wooden building damage

Non-wooden buildings were classified by only building age according to whether or not they were built after 1981, when the new Anti-Earthquake Design Act was introduced.

The damage factor for non-wooden buildings was expressed in terms of seismic intensity, building age, and surface soil property. The damage level for non-wooden buildings in each category was estimated by those encountered in the Hanshin-Awaji Earthquake. The collapse ratio for non-wooden buildings built in or after 1982 was assumed to be zero.

III-3-4 Casualties due to building collapse

The number of dead caused by the collapse of wooden and non-wooden buildings was estimated for each municipality. The estimation took into account the time of earthquake occurrence. The change in the numbers of people staying in different "places" was determined from the temporal change of the population during the night-time and the day-time. Population at a certain time of a day was estimated based on the results of personal travel surveys performed in representative cities, with the "places" classified as houses, other facilities, and transient points.

Since it was difficult to develop a logical model to determine the relation between casualties and wooden building, statistical regression of historical earthquake data was made. Data from recent five earthquakes which caused more than 300 dead were used by assuming a linear relation between the two quantities.

The number of dead caused by wooden building collapse was assumed to be proportional to the

number of collapsed wooden buildings and the number of people in them.

It is assumed that dead caused by the collapse of non-wooden building has a linear relation with the number of people in those buildings. This parameter (rate of damage) is estimated based on the data on building collapses during The Great Hanshin-Awaji Earthquake and an accident that recently occurred in Korea.

III-4 Implementation

When emergency measures are taken to respond to damage caused by an earthquake, it is best to try to take proper and efficient measures based on information from the actual site. However, in the case of The 1995 Great Hanshin-Awaji Earthquake, the affected area was in confusion and it was impossible to obtain accurate information from the site. In a large earthquake, the affected area extends over surrounding municipalities, and it is extremely difficult to obtain information at the site. There is also a high probability that the means of information transfer will be destroyed.

EES, however, estimates the scale and the areal extent of damage by only using seismic intensity data immediately following an earthquake. EES places emphasis on the importance of overall damage caused by the earthquake. Thus, although it may not be possible to obtain damage information at the site, the estimated data given within 30 minutes after the earthquake occurrence may be used to prevent delay in initial responses and to help initiate quick and appropriate initial actions and emergency measures.

If EES had been available in the case of The Great Hanshin-Awaji Earthquake, estimation would have been completed within about 15 minutes after the JMA data was received, and estimation results would have been obtained within about 25 minutes after the earthquake occurred. (For a smaller earthquake, time required for estimation would even be shorter.) EES's preliminary estimation was found to give "About 100,000 collapsed buildings and about 4,000 dead". The distribution of seismic intensities is shown in Attachment 5.

A year has passed since the system began operating in April 1996. Over this period, it has been activated by earthquakes above intensity IV 41 times, and has generated results within 15 minutes. Over this period, 13 earthquakes above intensity V occurred. The earthquake in the Satsuma region of Kagoshima Prefecture (southwestern Kyushu) on March 26, 1997 registered a magnitude of 6.2, and had a maximum seismic intensity of "strong 5." The distribution of seismic intensities for this earthquake, as estimated by EES, is shown in Attachment 6. In these instances, the system was able to provide qualitative assessments of the state of damage, and by acting as an early source of information contributed effectively to the start-up phases of the disaster prevention systems. At around seismic intensity V, the graph representing rates of damage has just begun to be expressed. This means that the level of error is greater than the level of data, making it difficult to assess damage quantitatively.

We believe that the reason estimates of damage are higher than actual damage is because verification has been taking place in large urban areas and in regions in northern Japan. There is a need to improve the accuracy of the system by gradually adding more verifications etc. from regional cities in southern Japan.

In any case, the EES has steadily achieved results in the year since it has been in operation.

IV CONCLUSIONS

Regarding the DIS, we are developing GIS maps and carrying out the development of an emergency measures support system for the southern Kanto region, where an earthquake striking directly beneath large urban areas is believed to be imminent. Hereafter, as development of the overall system proceeds, there is a need to respond to the following kinds of issues.

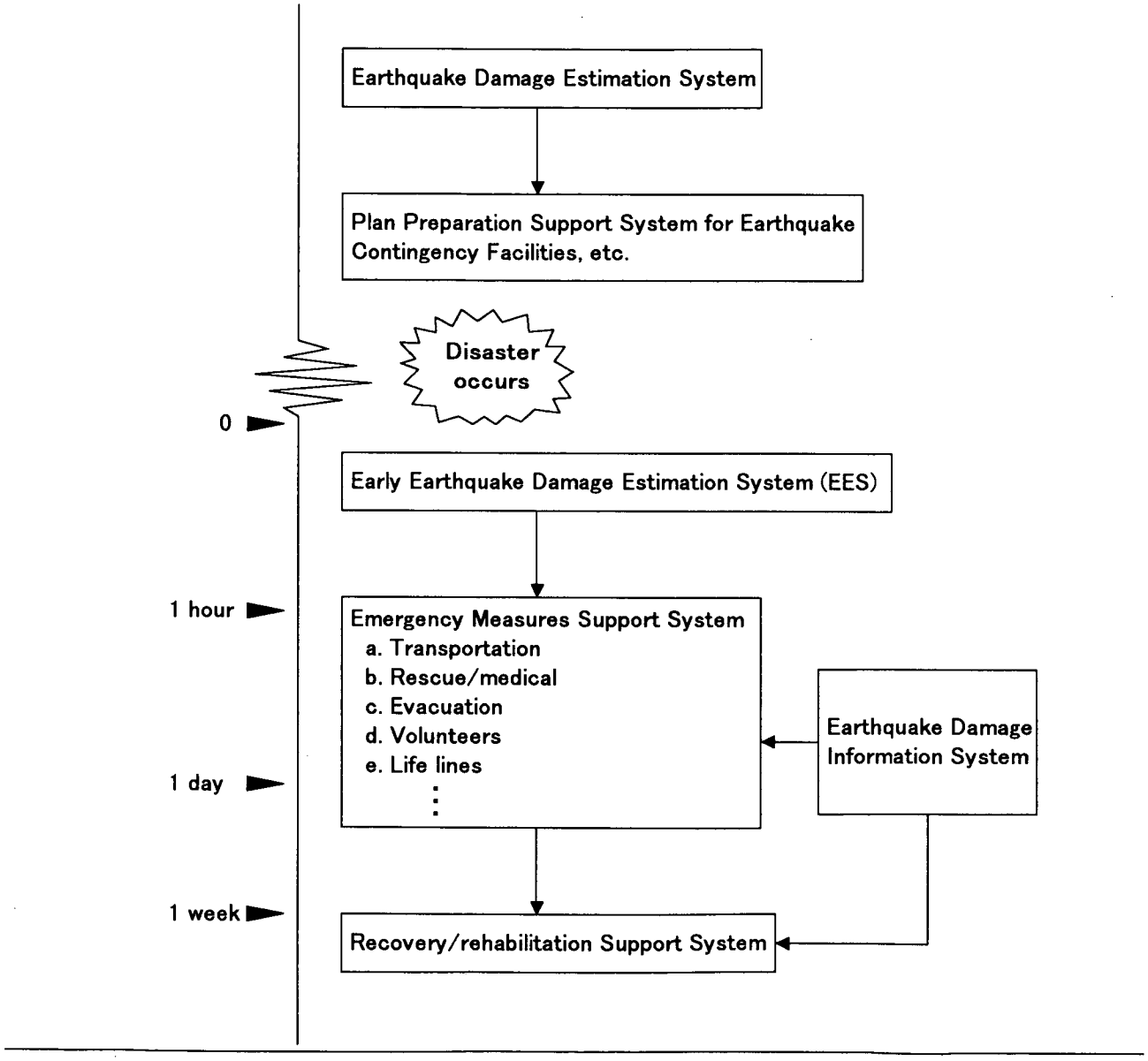
In the case of natural disaster mitigation, it is becoming increasingly important to devise a means of mutual collaboration among related organizations for the effective use of the DIS/Earthquakes. The National Land Agency is willing to advance development of a network with related agencies and local municipalities through LANs using central contingency radios to provide accurate information in real time.

After a disaster, this information will control all countermeasures, so it is necessary to construct an information collection system that responds to expected interruptions and complications of information communication disruption. Therefore, the intent is to strengthen the information collection system by effectively utilizing such communication measures as portable information equipment and the Internet, which has recently been developing remarkably, to enable direct input of damage information sent from the actual site, in addition to information collection utilizing aircraft, etc.

For total preparation of the DIS/Earthquakes, there remain the problems of money and time required to prepare the map data, which is the foundation of the system, and more detailed disaster prevention related data. The National Land Agency is expecting to complete the development of DIS/Earthquakes in five years and hopes that DIS/Earthquakes will become an effective system to be utilized for executing as well as planning contingency measures.

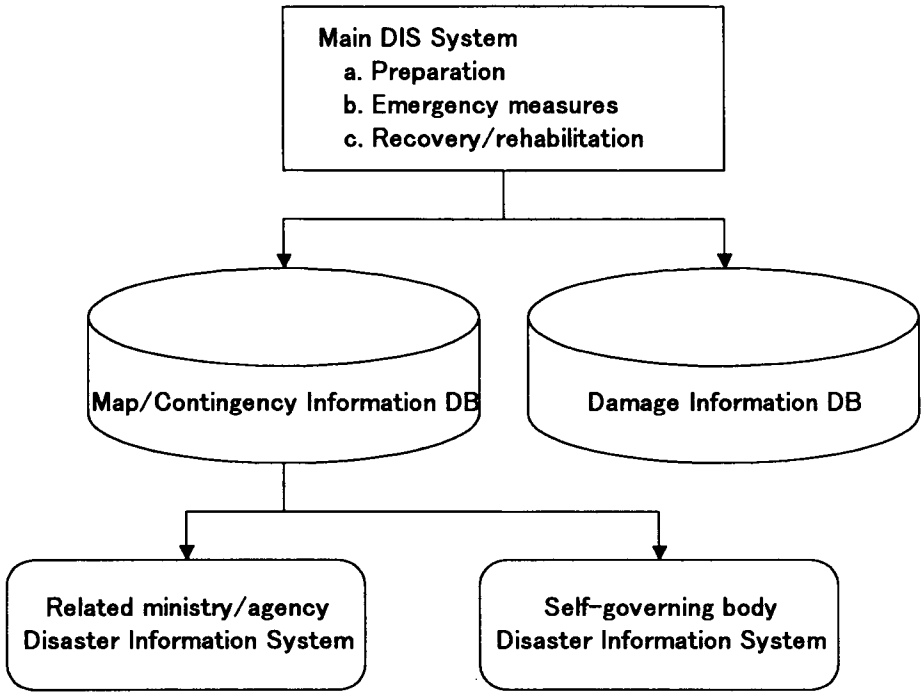
Attachment 1

Composition of DIS (Disaster Information System/Earthquake)



Attachment 2

System Image of DIS (Disaster Information System/Earthquake)



Detailed display functions

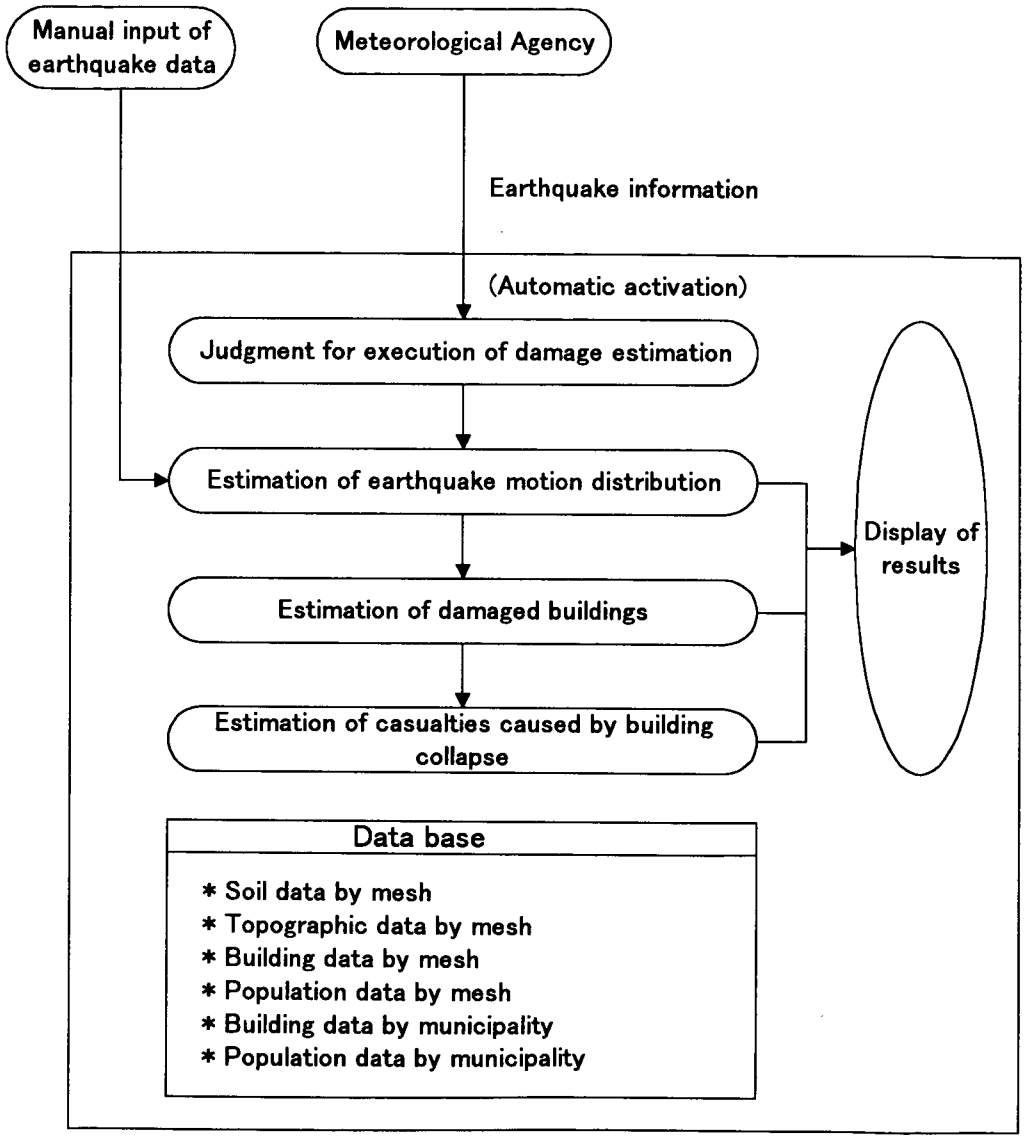
* Accurately displays individual buildings using map data at a maximum scale of 1/2500
* Displays facilities directly involved with disaster prevention, including fire departments, police departments, schools, food storage locations and locations of relief items
* Displays facilities related to emergency transportation, including roads, airports and harbors

Powerful analysis functions

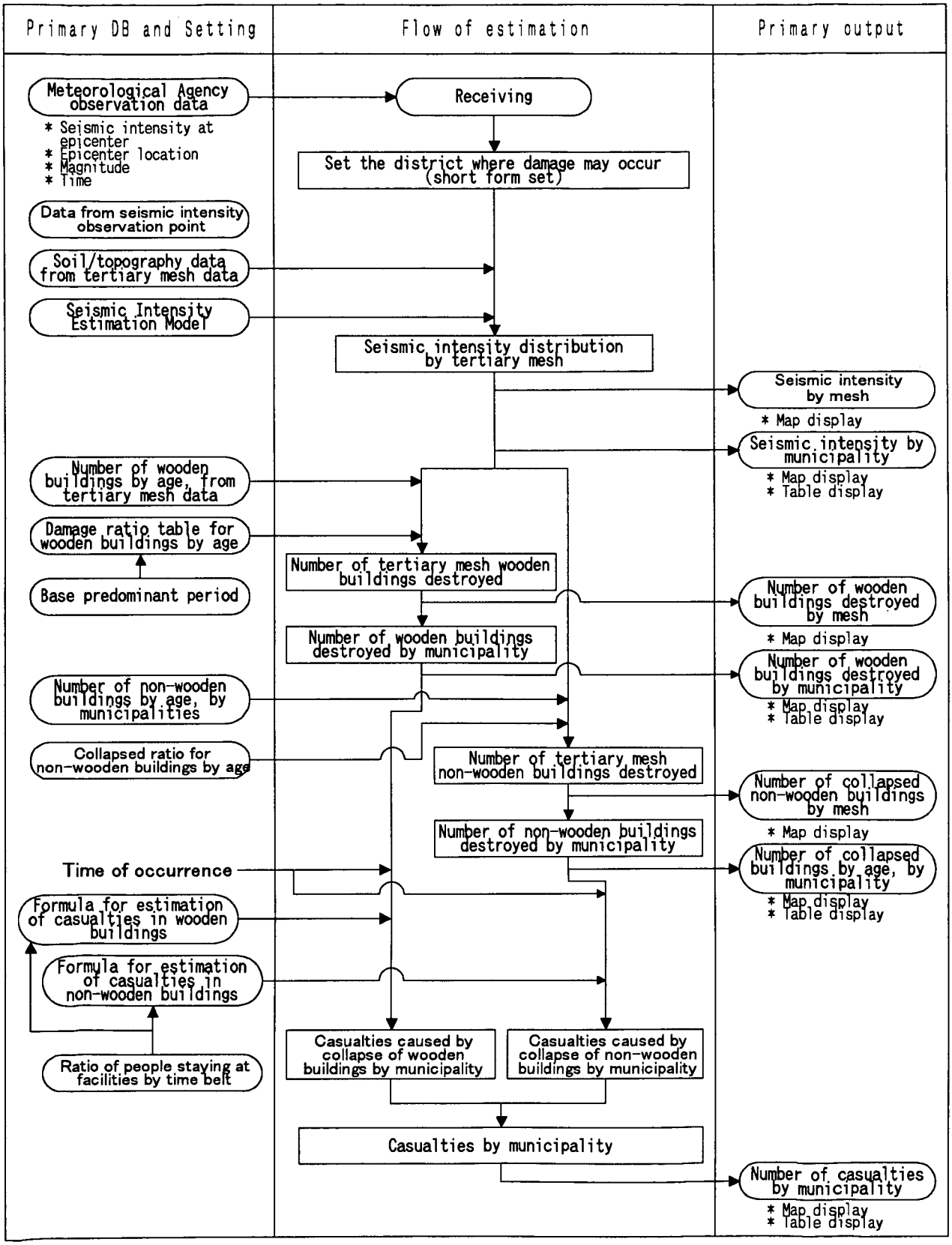
* Sub-systems provide powerful analysis functions
* Sub-systems can be added to respond to new needs as they occur.

Attachment 3

Flow of Earthquake Damage Estimation

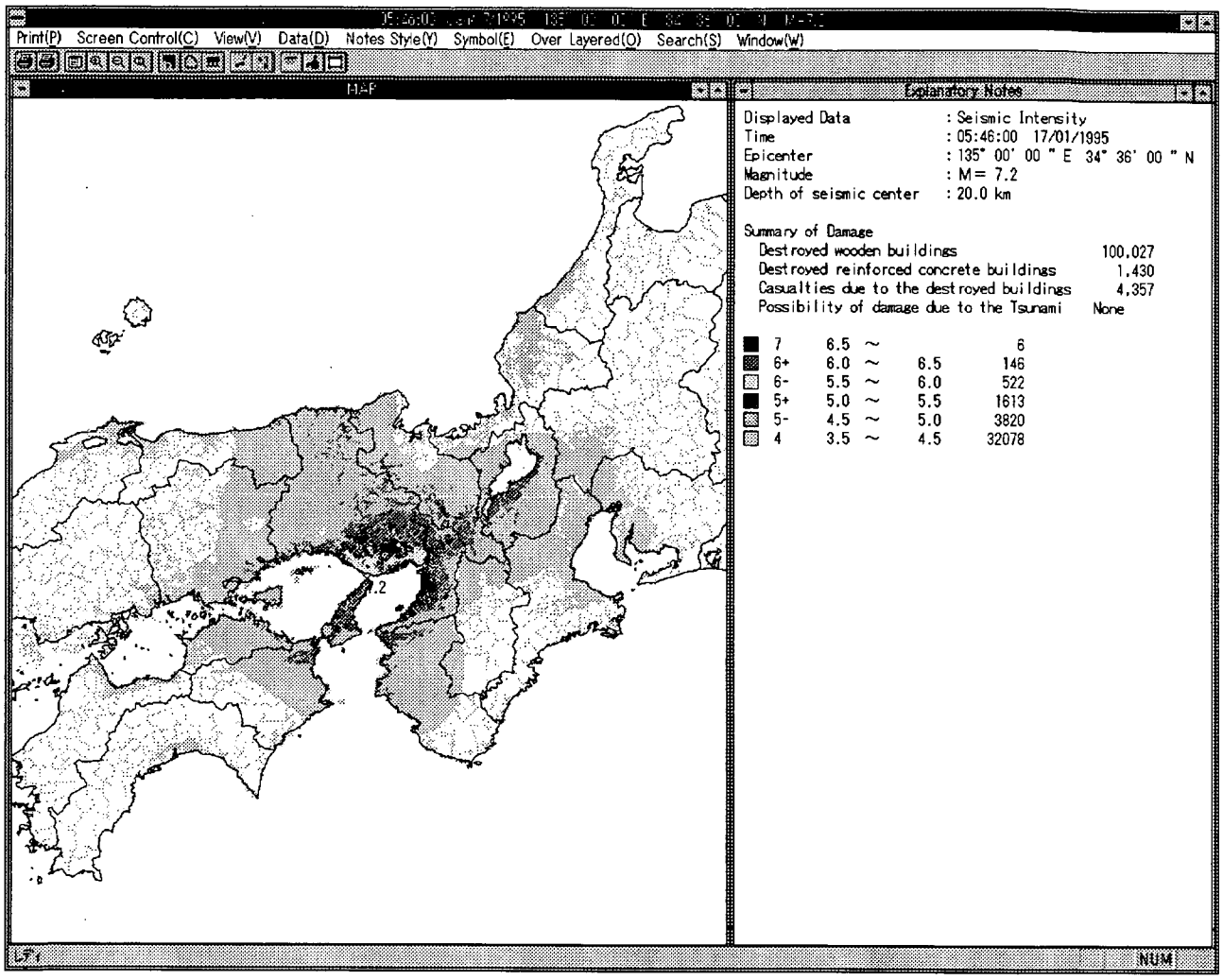


Flow of Earthquake Damage Estimation

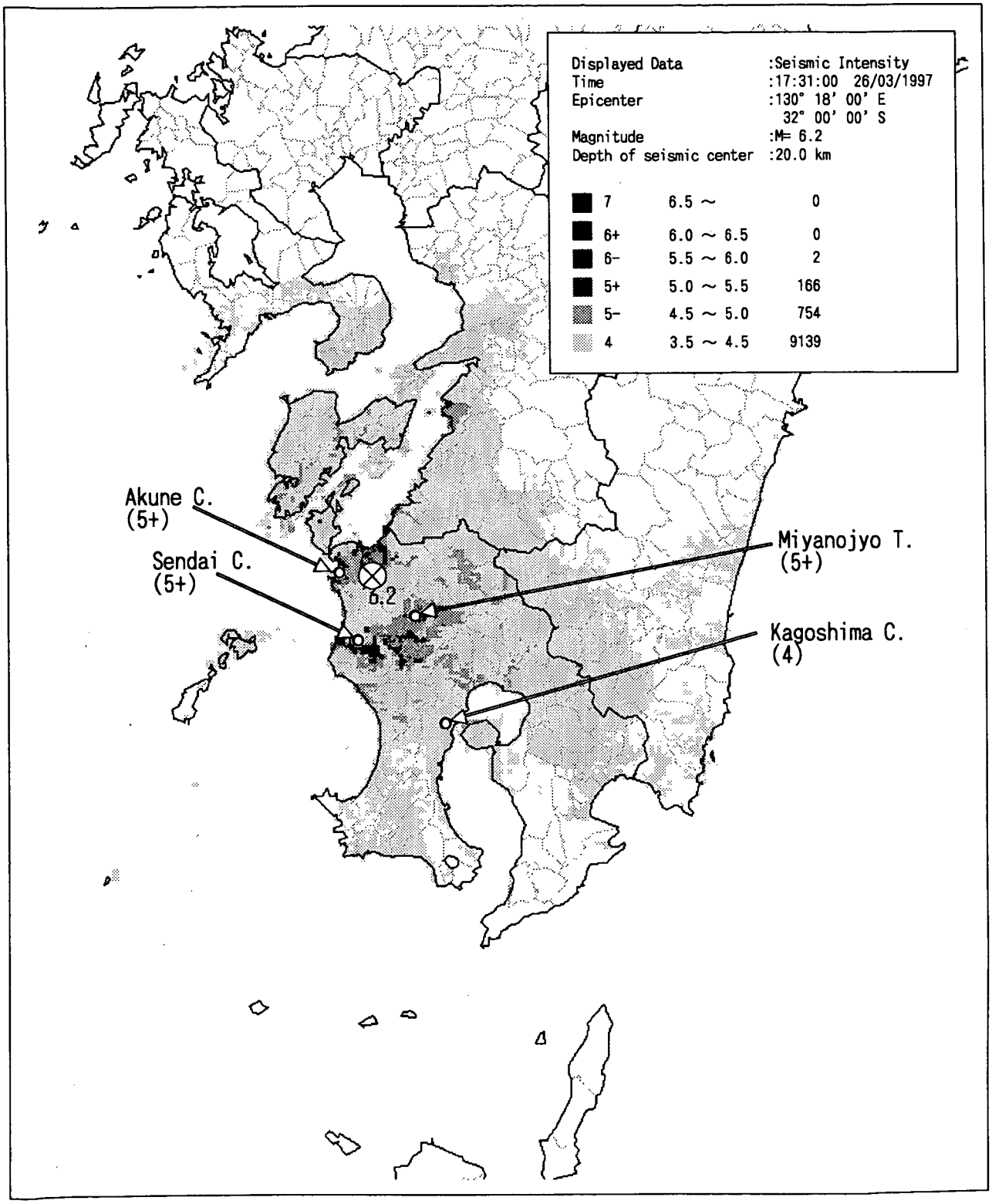


Attachment 5

The estimated result of distribution of seismic intensities in the case of the Great Hanshin-Awaji Earthquake



The estimated result of distribution of seismic intensities in the case of the earthquake in the Satsuma Region of Kagoshima Prefecture on March 26th, 1997



The Use of GIS in Loss Estimation and Risk Assessment

by

Gil Jamieson* and Jeff Milheizler*

ABSTRACT

Recent developments in the technology of Geographic Information Systems (GIS) have facilitated data analysis and display. The power of today's computer systems, in conjunction with state-of-the-art software, gives users the ability to analyze large quantities of data in a relatively short period of time. The Federal Emergency Management Agency (FEMA) is taking advantage of these developments. FEMA has developed a nationally applicable state-of-the-art earthquake loss estimation methodology called HAZUS. This program looks at an earthquake hazard and compares it to the built environment that is affected by the hazard. In addition to providing estimates on the amount of building damage and the cost of replacing and/or repairing these buildings, HAZUS also looks at secondary effects of the quake such as fires that may result due to the event and how many people may require shelter. These results provide emergency managers with a better understanding of potential earthquake losses. Although HAZUS includes a large amount of default data, it is important to understand that improving this information will improve the loss estimate. Loss estimation provides an excellent opportunity for international collaboration and partnership. As HAZUS expands into the multi-hazard realm, these opportunities will increase. Likewise, the benefits of GIS will be more fully realized and HAZUS will become a "multi-hazard loss estimation methodology."

KEYWORDS: earthquake modeling; geographic information systems; HAZUS; loss estimation; mitigation

1. INTRODUCTION

Until fairly recently, it has been difficult to analyze a region's susceptibility to damage from natural hazards. Data on hazards, as well as the built environment and population exposed to these hazards, has only been available in the form of paper maps or tables. Only recently has this information been digitized to the extent that it is valuable in computer modeling. This digital information, when used in conjunction with a geographic information system (GIS), opens up new analysis capabilities.

GIS provides us with the power to get a more explicit view of the risks associated with a community. As technology advances and computers become more powerful, the ability to process data is growing exponentially. Due in large part to this technological advancement, the use of GIS has enjoyed a considerable growth in recent years. The ability of GIS to represent digital data graphically makes it invaluable to a wide range of individuals, ranging from the government planner to the small business owner. Knowing the geographic location of different societal components allows governments to decide where to focus their energy, and small business owners to locate the optimal business site. The use of GIS is expanding and deserves to be recognized for its applicability in the area of risk assessment. The Federal Emergency Management Agency (FEMA) uses GIS technology in a number of programs. One of these programs, "HAZUS," deserves more detailed discussion.

The HAZUS program has been developed under the leadership of the National Institute of

*Hazard Identification and Risk Assessment Division, Mitigation Directorate, Federal Emergency Management Agency, Washington, DC, USA, 20472

Building Sciences and has been overseen by two committees. The first is an eight-member project work group, consisting of earthquake experts, and chaired by Robert Whitman, a professor of Civil Engineering at the Massachusetts Institute of Technology. The second is an eighteen-member project oversight committee, chaired by Henry Lagorio, a professor of architecture at the University of California at Berkeley, that provided input from the viewpoint of potential users. By incorporating recommendations from each of these groups, HAZUS is a loss estimation methodology that is technically sound and user-friendly.

2. A STRATEGY FOR DISASTER LOSS REDUCTION

In 1995, FEMA published the National Mitigation Strategy which establishes goals to substantially increase public awareness of natural hazard risk and to significantly reduce the loss of life, injuries, economic costs, and disruption of families and communities caused by natural hazards. FEMA recognized that to support this goal we needed a consistent means of characterizing risk from the various natural hazards and of estimating the losses that could result. Such a standardized loss estimation / risk assessment tool will allow emergency managers and mitigators to identify opportunities and underscore the need for mitigation measures that reduce those losses.

Results obtained through the HAZUS analysis are not limited to direct physical damage to buildings. Estimates are also made concerning casualties and shelter requirements, the functionality of lifeline systems and essential facilities, direct and indirect losses, and an assessment of the induced hazards of flood, fire, and hazardous material releases. A mitigation module is under development that will also allow HAZUS to be used to calculate how the general building stock will be affected with and without mitigation, thereby further demonstrating the economic benefits of specific mitigation actions.

3. BACKGROUND OF THE HAZUS EARTHQUAKE LOSS ESTIMATION METHODOLOGY

The HAZUS Earthquake Loss Estimation Methodology is a standardized, nationally applicable, PC-based, loss estimation methodology. The methodology overlays earthquake hazards with building inventory, lifeline information, and other data in order to forecast the level of losses occurring during a pre-defined event.

HAZUS runs on an integrated GIS platform. The methodology takes the ease-of-use and functionality that GIS has to offer and adds some features of its own. In addition to the normal GIS functions available, HAZUS has added functions specific to the loss estimation field. These additional capabilities range from defining the hazard, to changing analysis parameters, to viewing the results in a pre-designed report.

HAZUS makes the risk assessment more valuable by providing the results as both a mappable table and as a summary report. Mapping the results provides a powerful visualization of the effect the event has on the community. By seeing where the most damage is predicted to occur, mitigation efforts can be concentrated in these areas. The summary reports that HAZUS produces provide the results in a format that can be easily imbedded in reports and provided to a variety of potential users. It is important not only to perform the risk assessment, but also to present the results in a form that produces action.

HAZUS was designed as a series of "modules," rather than as one continuous program. This modular approach provides flexibility for the addition of future loss estimation models as new models can be directly linked to the already developed product. By designing future models in this same modular format, these models will easily mesh with the program and be able to share modules with similar functions.

HAZUS is designed to allow loss estimates to be performed at different levels of accuracy. The data required for a low-level (Level I) analysis is included with the HAZUS software, and, as a result, this estimate requires minimal effort. At the opposite extreme, the high-level (Level III) analysis is the most precise, and, consequently, requires the most effort. A Level III estimate requires detailed data to be collected and input into the software. From this information, a detailed analysis is conducted that provides a better estimate of the potential damage for a given event. The Level II analysis resides between these two extremes. This analysis uses a combination of detailed data and assumptions. The same basic structure as a Level I analysis is employed, except that certain characteristics have detailed data. For instance, detailed soil mapping may be available for input into the software or the user may have a better hospital database. The HAZUS program can use this improved information while still using the default data in the other modules. This three-level structure provides the user with flexibility depending on the amount of detail required and the amount of data available. Through the use of modules, the program can proceed through its analysis without being dependent on data input.

4. THE IMPORTANCE OF INVENTORY

The development of a sound inventory base is an essential first step in the HAZUS risk assessment / loss estimation process. In a GIS environment, the detail and accuracy of the data impacts the credibility and accuracy of the loss estimates obtained from the analysis. The results produced by any risk assessment performed under GIS are only going to be as valuable as the data that is used in the analysis. As more and more data is included in the estimate, the results will improve. Figure 1 outlines the risk assessment process and the paramount role that inventory plays in the process.

Three data components are necessary in order to perform a loss estimate. These are: the location of ground motion, the different degrees of motion within this location, and the inventory of susceptible items along with their reaction to various strengths and types of ground shaking. Different structures and lifelines react differently. It is important to understand this designation and analyze each type of element separately. Knowing that seismic waves of a certain magnitude cause approximately 25% damage to a steel frame building allows an estimate of seismic damage to be computed. Having a grasp of the inventory, understanding the size and strength of the event, and knowing the various damage states associated with each structure are combined to arrive at the final estimate. GIS makes this analysis possible with a minimum of effort.

HAZUS contains a considerable amount of default inventory for residential, commercial, and industrial buildings, as well as data for lifeline systems and demographics. Additional data, however, as well as more detailed data, can make significant improvements in the results obtained from the analysis.

This issue, the sensitivity of results to high-resolution inventory data in comparison to default information, was examined during the development of HAZUS. While it was found that a more credible forecast can be made with the high-resolution data, a characterization of risk using the default data was a good first step toward reducing a community's vulnerability and risk to the hazard. In fact, pilot tests have shown that while detailed data does provide a better loss estimate, estimates performed using default values were still credible.

FEMA has developed a "Building Inventory Tool" as a component of HAZUS so that users can improve the loss estimates they construct through a HAZUS analysis by incorporating their own building inventory data. This tool maps the building inventory data according to a consistent building classification and occupancy scheme for analysis purposes. Local hazard maps and geotechnical maps depicting soil information can also be imported into HAZUS.

By making data importation simple, we hope that communities will be more willing to gather improved data.

5. RUNNING A HAZUS LOSS ESTIMATE

The first step in running the loss estimation methodology is to select an area for study and provide information about the size and location of the earthquake to be modeled. Also, before the analysis is run, the user should input any improved data that may have been collected. From here, the HAZUS methodology begins to work. Based on the specified size and location of the event, the HAZUS algorithms determine the ground motion associated with the event by looking at local geology and other factors that impact the spread of seismic waves. In addition, HAZUS determines where ground failure may result. The results of these two Potential Earth Science Hazards (PESH) analyses are then carried down through the other modules in order to determine how the event impacts the study region. Figure 2 provides a flowchart of the loss estimation methodology.

The results obtained from the ground shaking and ground failure analyses are compared against the building inventory. Structures in the study region have been classified into 36 different building types (i.e. steel-frames, unreinforced masonry, etc.) and 28 occupancy classes (i.e. residential, commercial, etc.). For each of the 36 model building types, "fragility curves" have been established. These describe how the building will respond to varying levels of ground motion. Structural and non-structural damages are estimated from these curves. Damages are calculated by examining those building components that are sensitive to acceleration and those that are sensitive to inter-story drift.

While essential and high potential loss facilities, and lifelines, are handled on a site-specific basis, the general building stock is handled differently. Analysis is performed on a census tract basis. Buildings for each census tract are aggregated to the centroid of that tract. In the United States, approximately 2500 to 8000 people, on average, reside in each census tract. The census tract level analysis for the general building stock provides a good estimate as to the potential damage in the area of study. An immense amount of time and resources would be required in order to do a site-specific analysis on every building in the study region. Through aggregation to the census tract level, this time commitment is reduced, and the estimate is still found to be credible.

In addition to the data described, the methodology also includes data for high potential loss facilities (e.g. dams, fixed nuclear facilities). While specific estimates are not made on these facilities, GIS allows the user to overlay these structures on a ground motion map or other base layer and see how they are affected (i.e. how much ground motion they experienced).

Similarly, lifelines are examined. Lifelines comprise transportation and utility systems. The transportation systems include roads, bridges, railways, light rail, bus stations, ports, ferries, and airports. The utility systems consist of potable water, wastewater, oil, natural gas, electric power, and communication systems. Each of these is examined in terms of its probability of functionality and the time required for the damaged system to be restored. The functionality is dependent on the damage sustained by the major components of the lifeline system (e.g. electric power switching station). Additionally, HAZUS, through its GIS platform, provides the ability to display these systems on top of a ground motion map. By looking at lifelines in this way, HAZUS produces an estimate as to where damage is likely to occur, the probability that this damage will occur, and how long it will take to repair this damage.

Once the direct physical damage has been determined, induced physical damage is calculated. The induced physical damage module includes inundation, fire following earthquake, hazardous materials, and debris.

Losses associated with this module do not result directly from ground shaking.

The inundation module is capable of examining losses resulting from dam failure, tsunami, seiche, or another source of inundation. In order for these calculations to occur, however, inundation maps must be provided. From these, HAZUS looks at the inventory affected by this inundation and reports back a value that describes the associated losses.

The fire-following earthquake module looks at where fires may occur as a result of the earthquake. HAZUS examines several factors that may affect this. Some of these are the location of fire stations, the number of engines employed by each station, how quickly these engines can respond, and the speed and direction of the wind.

Analysis of hazardous materials releases is not currently available. However, a database of hazardous materials locations is provided in HAZUS. From this, through the GIS interface, the user can look to see which hazardous materials sites may be affected by the earthquake event and the types of chemicals stored at these sites.

The debris component of HAZUS calculates the amount of debris that is generated from the building damage projection. It further divides this into two categories – debris that can be removed using "normal" clean-up machinery and that which requires special equipment. These components affect the speed of emergency response and recovery time.

Social losses are another component of the study region that is examined. Social losses include the number of casualties caused by the earthquake and the number of people that will require temporary housing. HAZUS calculates casualties on four levels. These range from injuries requiring basic medical attention to those that result in death. Each of these is determined based on the level of damage sustained by the structural inventory and the time of day that the event occurred. For instance, if the event occurs at 2:00 am, the majority of the population will be at home. Therefore, the number of casualties will be largely driven by the damage to residential structures.

The temporary housing component is dependent on a couple of factors. First, the methodology looks at the number of households that are displaced due to structural damage or loss of utilities. From this estimate, HAZUS examines the population demographics in order to estimate which of these displaced households are likely to require shelter. Not every displaced household will require shelter. Some of these will opt to stay with relatives or friends. HAZUS takes this fact into consideration and arrives at an estimated shelter demand.

HAZUS also estimates direct and indirect economic losses. These are the dollar losses experienced by the region. The direct economic losses include such things as building loss, building contents loss, relocation cost, wage loss, rental income loss, and the cost of repairing damaged lifelines. The indirect losses are those losses that are felt long after the event. These include such things as the employment rate at different time periods after the event, and how long it will take the region to rebuild. All of these are ramifications that result from the earthquake, and should be included in any loss estimate.

6. CONCLUSIONS

The advent and recent improvements in Geographic Information System (GIS) technology have facilitated the production, grouping, and analysis of various hazard data sets. Information, previously available in a stand alone paper format, can now be compiled and used to convey graphically a better understanding to the public of their exposure and vulnerability to natural hazards.

The HAZUS Loss Estimation Methodology described here uses the technology to conduct

an analysis and produce losses associated with the Earthquake Hazard. It is our belief, that if elected officials and emergency managers develop a better understanding of the potential for losses from future earthquakes, they will be more inclined to take the necessary steps to mitigate and reduce these losses. HAZUS is currently being expanded to demonstrate how specific actions to rehabilitate buildings can reduce loss. Results can be calculated on the mitigated building performance and compared with the results for the existing condition. Similarly the introduction of improved building codes can be modeled to show disaster loss reduction opportunities.

We have emphasized the importance in this article of the need for good building inventory. Good building inventory in this context means an accurate assessment of the building's location in relation to maps depicting high resolution soils data and a good understanding of the age, height, and engineering design that was used in the construction of the building. We believe that equipped with this type of data it is possible to move into the "all hazard" loss estimation / risk assessment field. The GIS technology will permit layering this high resolution building data over various hazard themes. These might include areas of potential flooding, areas subject to high winds, and/or areas subject to tsunami. The new challenge for the engineering profession is to develop building and lifeline "fragility curves" for these new perils consistent with what they have accomplished for earthquake. The United States has formed a team of experts to begin to study and evaluate these possibilities.

The science of loss estimation represents a wide-open opportunity for international collaboration and partnership. Clearly one potential project is to evaluate the applicability and use of HAZUS in studying the potential earthquake hazard in Japan. Opportunities and questions abound over understanding the differences in how the built environment in our two countries will respond to strong ground motion as well as assessing the similarities. We should look for opportunities to further calibrate HAZUS using international earthquake events. Similarly, together we should study how HAZUS might be used as an "international measure" to assess worldwide progress in reducing the earthquake risk.

These questions and many others remain for us to answer. The challenge is significant, but the opportunity afforded us through technology to meet these challenges is more promising than ever before.

7. REFERENCES

Jamieson, and Drury (1996), "Hurricanes and Society: Critical Issues and Future Prospects," Federal Emergency Management Agency, Washington DC.

National Institute of Building Sciences (1997), "HAZUS97 Technical Manual Draft," National Institute of Building Sciences, Washington, DC.

National Institute of Building Sciences (1997), "HAZUS97 User's Manual Draft," National Institute of Building Sciences, Washington, DC.

FEMA RISK ASSESSMENT SYSTEM

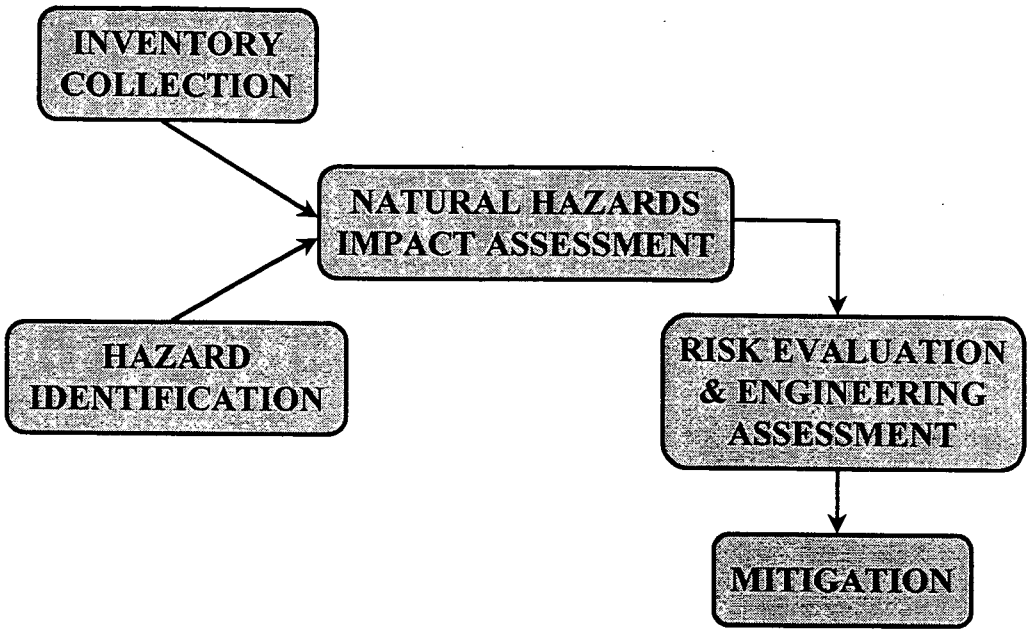


Figure 1: FEMA Risk Assessment System

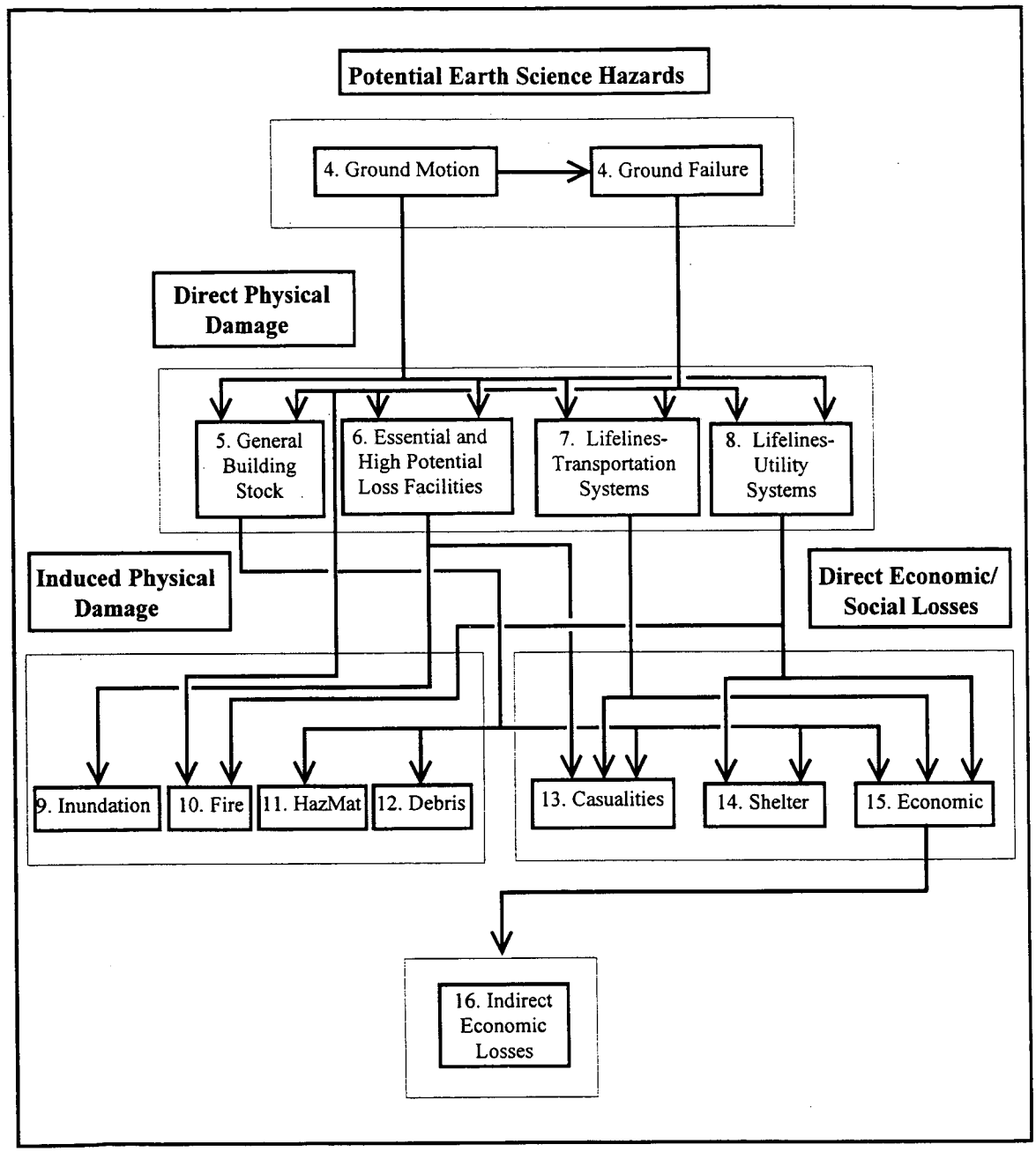


Figure 2: Flowchart of the Earthquake Loss Estimation Methodology

Theme 5

Summary of Joint Cooperative Research Programs

U.S.-Japan Cooperative Earthquake Engineering Research Program on Composite and Hybrid Structures
- Japan side Progress -

by

Isao Nishiyama [1] and Hiroyuki Yamanouchi [2]

ABSTRACT

The composite and hybrid structural research project [1] is being carried out in Japan and the U.S. cooperatively under the UJNR Panel on Wind and Seismic Effects. In Japan, the research started from 1993 fiscal as a five year project under the co-sponsorship of the Ministry of Construction and private sectors such as the Building Contractors Society, the Kozai Club, the Building Center of Japan and the Japan Structural Consultants Association, which constitute domestic cooperative research (Chairman: Prof. H. Aoyama, Nihon Univ.). In this research program, four types of composite and hybrid structure systems are selected and investigated. Three of them are more practical and aimed at developing design guidelines, which are concrete-filled steel tube column system (CFT), reinforced concrete column and steel beam system (RCS) and concrete core wall with exterior steel frame system (HWS). The last one is a research on new materials, elements and systems (RFI) which might be used combined with traditional structural counterparts in composite and hybrid structures in future. This report will summarize the research progress on these four research topics.

Key Words:
Concrete-Filled Steel Tube,
RC Column with Steel Beam,
Core Wall with Exterior Steel Frame,
New Materials, Elements and Systems

1. RESEARCH ON CFT

1.1 Basic Research Plan

There are many experimental and analytical studies on CFT systems which are reported in technical journals. First, the strength and ductility of the CFT systems are predicted by processing these existing data. Secondly, the effectiveness of these predictions will be verified by supplementary experimental studies. As the materials' strengths in use are quickly increasing recently, wide range of structural steel strength and concrete strength are considered to verify the applicability of the predictions.

1.2 Research Items And Its Progress

(1) Experimental and Analytical Study

The objectives of the experimental study are to evaluate the synergistic effects of structural steel tube and filled concrete and to evaluate stress transfer mechanisms in beam-to-column connections. So as to clarify these problems, the following experiments are planned with several study parameters.

a) Experiments
1) stub-column tests
2) stub-column eccentric loading tests
3) beam-column tests
4) beam-to-column connection tests

b) Study Parameters
1) tube shapes (rectangular, circular)
2) tube strengths (400, 600, 800 MPa)
3) width-to-thickness ratio
(FA, FC, FD-rank* 1)
4) concrete strengths (20, 40, 80-90 MPa)
5) connection details (diaphragm, etc.)

---

1) Head, Housing Construction Division, Production Department, Building Research Institute (BRI), Ministry of Construction (MOC), Tachihara-1, Tsukuba, Ibaraki 305, Japan.
2) Director, Research Planning & Information Department, BRI, MOC.

Ninety stub-column tests on rectangular or circular sections were already completed. As the dimensions of the selected specimens are relatively large, and material strengths of structural steel tube and concrete are also large, the maximum test strength reached 1,400 tonf. As for the stub-column eccentric loading tests, sixty specimens have been completed.

From the comparison between these test results with sectional analyses, the stress versus strain models for concrete infill and steel tube are proposed.

As for the beam-column tests, 20 rectangular and 12 circular specimens were tested. Most of the specimens (16 for rectangular and 8 for circular sections) were tested under the constant axial thrust of 40% of yield strength and others (4 specimens each for rectangular and circular sections) were tested under varying axial thrust of 70% of yield strength in compression and 30% in tension. The structural steel strengths (400, 600, 800MPa), concrete strengths (40, 90MPa) and width-to-thickness ratios (FA, FC-rank) were selected as test parameters. As for rectangular sections, 4 specimens were loaded in the direction of the plane which inclined 22.5 or 45 degrees from their principal axes. Fairly good agreements both in restoring force and axial shortening characteristics are obtained between test results and analytical ones, in which the proposed model for stress versus strain relationships for concrete and steel tube are adopted. 3D-FEM analyses were also conducted to see the stress diagram in the CFT beam-columns.

---

* 1 FA-rank of width-to-thickness ratio means that large member ductility is expected thanks to its compact section. FC-rank means that it can at least assure the yield strength of the member without deterioration. The width-to-thickness ratio of FD-rank is chosen as 1.5 times of that of FC-rank.

Ten beam-to-column connection specimens are now under fabrication. Nine of them are one-way frame specimens (seven of them will be tested with constant column axial force and two will be tested with varying axial force) and the rest is the two-way frame specimen.

Ten additional stub-column eccentric loading specimens are also under fabrication, which are planned to evaluate the moment versus axial force diagram of CFT section loaded in the direction of the 45 degrees from the principal axes.

(2) Empirical Study on Ductility

The analytical evaluation of the ductility of beam-columns looks not promising. Therefore, the empirical formulation for the ductility of beam-columns was tried both for rectangular and circular sections using test results in this project and the existing test results. Empirical formula taking into account the factors of axial force, width-to-thickness ratio of steel tube and concrete infill strength were proposed for rectangular and circular sections. The calculated ductilities are compared with test results in good agreement especially with test results completed in this project.

(3) Theme Structure Study

Structural designs of 10, 24 and 40 storied CFT moment frame buildings and CFT dual system buildings were carried out. In these structural design, CFT member strengths were calculated based on the simple (generalized) superposing method proposed in the AIJ-SRC standards [2]. The buildings with the same plan were also designed as pure steel frames. The total amount of structural steel, which is the index for estimating the economy of buildings, used for CFT buildings was compared with that used for pure steel buildings. In this comparison, CFT showed advantages over pure steel especially for higher buildings. The economical difference in CFT buildings with/without bracings was not large. It was because that the weight of bracings and the weight increase in the braced bay frame members compensate with the

weight reduction of other frames which carry less horizontal force.

Above consideration was conducted on the original theme structure which has 32 columns in each story. The modified plans which have 16 or 24 columns in each story, which were expected to show more advantages by CFT columns, were also investigated. The detailed comparison of these plans will be carried out in future.

2. RESEARCH ON RCS

2.1 General

In Japan, a great number of beam-to-column sub-assemblage tests on RCS systems have been conducted. However, most of them are just proof tests to verify the performance of the sub-assemblages which were designed as weak beam systems. Therefore, these test results gives us little information on the shear strength and ductility of the beam-to-column joint panels in the ultimate stage.

Therefore, the experimental study in this research project is planned to obtain the ultimate strength and ductility of the beam-to-column joint panels by making the specimens to be intentionally weak in panels.

2.2 Research Items And Its Progress

(1) Literature Survey - Database

Experimental database was made, in which the information of the load versus displacement relationships is just included as the turning point information such as peak strength and peak displacement etc. but not as a whole curve. The collection of about 400 test data was completed at present and will be maintained (added) in each year.

The following investigation is underway on the collected database: (1) pick up test data which failed in shear of joint panel, (2) classify them in details and geometry, and (3) compare their strengths with existing shear strength formula. Better design formula are expected to be proposed through this study.

(2) Beam-To-Column Connection

a) Stress Transfer Mechanism Study

The shear strength of the joint panel is thought to be the sum of the shear strengths of inner concrete, outer concrete, structural steel and hoops. The contribution of outer concrete is questionable as it is not known how the shear stress is transferred from inner part. So as to make clear the stress transfer mechanism, several sophisticated experiments were carried out. The test results clearly showed the existence of such shear transfer mechanism.

b) Through Column Type Joint Tests

Ten specimens for interior beam-to-column connections were tested. In these tests, the effects of vertical stiffeners and the cover plates were investigated.

c) T- and L-Shaped Joint Tests

Fifteen beam-to-column connection specimens were tested to make clear the effects of the geometries (cruciform, T and L) of the joints. Here, the joint details of the through beam type with FBP, cover plate and band plate are all included. The through column type is also considered. Through these experiments and 3D-FEM analyses, the shape factors for cruciform shaped joint, T-shaped one and L-shaped one are preliminary proposed as 0.30, 0.24 and 0.14, respectively.

d) 3D-FEM Analyses

Elastic and inelastic characteristics of bond and friction between concrete and steel were investigated by basic experiments. The test results were reflected to modify the 3D-FEM program. Eighteen case studies were carried out. The analytically obtained monotonic load versus deflection relationships were compared with the envelops of the cyclic behaviors with good agreement, which verified the effectiveness of 3D-FEM analyses. The 3D-FEM analyses gave us better understanding of the stress distribution in the beam-to-column connection.

e) 3D Joint Tests

So as to see the inelastic behavior of beam-to-column connections under two directional loading, four 3D specimens were constructed. Three of them are through column type and one is through beam type. The test will soon start at BRI and will continue about two months.

(3) Frame Test

So as to understand the overall inelastic behavior and required ductility in each structural elements of RCS frame, a two story (1.35m in story height) and two bay (2.1m in beam span) frame specimen is planned. The frame is designed to be weak panel.

(4) Theme Structure Study

Six- and twelve-storied theme structures were designed, and static and dynamic analyses were conducted. In these theme structure study, the beam-to-column connections were assumed to be elastic. The dynamic analyses were conducted simplifying the frame into lumped mass model. These study gives us the general characteristics of the RCS frames. So as to see the local ductility of RCS frame, the inelastic dynamic frame analyses are planned.

3. RESEARCH ON HWS

3.1 General

The structural system of core wall with exterior steel frame is not common in Japan and its design method is not established yet. So, six, twelve and twenty-four storied theme structures were preliminary designed. According to the preliminary design, six storied model was considered to be designed just depending on the large shear strength of walls. Twenty-four storied model needed hat truss (and belt truss) to reduce large overturning moment induced at the foot of the coupled shear walls, which made the development of general design procedure rather difficult. Therefore, twelve storied theme structure was first selected and the design problem was picked up. Then, the design implication will be expanded into much higher or lower systems. The rationality of the designed system will be verified through the analytical and experimental studies.

3.2 Research Items And Its Progress

(1) Coupled-Shear Wall Test

One-third scale model of 12 storied coupled-shear wall test was carried out. During the test, the forces acting in each member was measured so as to understand the force re-distribution in the coupled-shear walls and boundary beams for design purpose. For this purpose, load cells were installed into all boundary beams. The coupled-shear walls showed very stable hysteresis loops until 1/67 radian in drift index. From the readings of the load cells, it was observed that the boundary beams act like wedges inserted between walls after they crack and expand in length. These test results are under investigation by FEM and MS (multi spring) model analyses.

(2) T- and L-Shape Shear Wall Test

So as to understand the stiffness, strength and deformability of 3D-wall is essential for the design implication to HWS systems. Three one-third scale T-shaped shear wall specimens without boundary columns, which represent the walls of the lowest story of the 12 storied prototype HWS system, were conducted. In these tests, the shear force and flexural moment with different moment-to-shear ratios were applied with varying axial forces.

Large axial force is expected at the corner of the 3D-wall of lowest story when two directional seismic force affects the HWS system. Then, the ductility of the corner part of the wall depends much on its confinement. Therefore, four L-shaped shear walls varying their confinement level were tested with large axial force. These test data are utilized to develop hysteresis model of 3D-walls.

(3) Literature Survey

About eighty papers on boundary beams and thirty papers on RC wall to steel beam connections were surveyed. As for the inelastic

behavior of the boundary beams, the past analytical and experimental information can be considered to be enough for design purpose. On the other hand as for the RC wall to steel beam connections, the isolated joint strength tests can only be found in the reports and no sub-assemblage tests are found. From this viewpoint, some verification test may be necessary for RC wall to steel beam connection. However, as the flexural stiffness of the steel beam with long span is very small and the rotational deformability of the joint itself is not so large, the experiment is not considered.

(4) Theme Structure Study

First, twelve story model building was designed on the basis of the general Japanese design concept. The strength of the designed building was too large to be investigated as the target structure to be developed. Then, the building was revised considering the design concept for the coupled-shear wall in New Zealand [3]. In New Zealand practice, earthquake load is distributed to each wall according to the overturning moment ratio carried by boundary beams. As the building still had large overstrength, the reinforcements in the core walls were intentionally reduced to reach reasonable strength level, 35 percent of the base shear coefficient. The final building is investigated whether it performs well or not under the seismic effects through the dynamic inelastic analyses using fish-bone model or frame model.

4. RESEARCH ON RFI

The following two research groups for " Fiber reinforced plastic (FRP) elements" and " High performance concrete (HPC)" are organized.

4.1 FRP Research

The research program on effective utilization of FRP materials for composite and hybrid structures contains three research items as follows. These items were selected through the feasibility study on effective utilization of FRP.

a) Development of the evaluation method for high-performance FRP-RC panels.

b) Development of the effective repair and/or strengthening method by using FRP for existing RC members.

c) Feasibility study on the effective utilization of FRP to the electrical facilities.

As for the former two items, various types of element tests are underway so as to understand the basic reinforcing characteristics of FRP. As for the last item, electrical problems brought about by using steel reinforcing bars in electrical facilities were identified and the electrical characteristics of FRP were also understood from the literature survey.

4.2 HPC Research Plan

There are few cooperative research between concrete makers and structural designers in Japan. The makers have many technologies but they don't know how to use it. On the other hands, designers have a few information about new technologies of concrete. But they have many hints about the idea of future concrete.

The main objective is to exchange the information of makers and structural designers to discuss about how to use effectively the concrete materials to the structural members and how will be the future concrete. Through the discussions, the following two topics are depicted.

a) Development of ultra light weight and high strength concrete.

b) Development of high tensile strength and high ductility concrete.

As for the light weight concrete, two kinds of concrete which have 1.2 in specific gravity and 30 MPa in strength, and 1.6 in specific gravity and 60 MPa in strength were realized and several fundamental tests on bond strength and compressive strength are on the way.

As for the high tensile strength concrete, various types of fibers with mortal were tested and some of them showed high tensile strength and good compressive ductility. However, it was made clear that the such performance is quite sensitive to the kind of fibers. The investigation will continue.

5. SUMMARY

The Japan side research progress was presented. The five year project is now the final stage in Japan, so the formulation of practical design guidelines are just initiated.

ACKNOWLEDGMENTS

The authors wish to express their great thanks to the members of Japan Technical Coordinating Committee for their useful comments and suggestions.

REFERENCES

[1] " Recommendations for U.S.-Japan Cooperative Research Program - Phase 5 Composite and Hybrid Structures" , Report No. UMCEE 92-29, November 1992.
[2] " AIJ Standards for Structural Calculation of Steel Reinforced Concrete Structures (1987)" , Architectural Institute of Japan.
[3] T. Paulay and M. J. N. Priestley, " Seismic Design of Reinforced Concrete and Masonry Buildings" , John Wiley & Sons, Inc.

U.S.-Japan Cooperative Earthquake Research Program on Composite and Hybrid Structures - U.S.-side Progress

by

Subhash C. Goel[1]

ABSTRACT

A five-year research program on Composite and Hybrid Structures as Phase 5 of the U.S.-Japan Cooperative Earthquake Research Program was recommended to be initiated in 1993 in both countries. The research work in Japan started in fiscal year 1993. However, fuller participation of researchers on both sides started in early summer 1995. The sponsorship of the program is by the National Science Foundation in the U.S. and by the Ministry of Construction along with a number of industry groups in Japan. This paper presents a brief status report of the program and research progress made to date on the U.S. side. Because of diverse and broad scope of the subject area, the research program is organized into the following four groups: Concrete Filled Tube Column Systems (CFT); Reinforced Concrete (RC) and Steel Reinforced Concrete (SRC) Column Systems (RCS); and RC/SRC Wall Systems (HWS); New Materials, Elements and Systems (RFI). A theme structure with well selected layout, geometry and design loads for the research is also presented, which provides a common focus for various systems to be studied, and also a common prototype structure from which the components and sub-assemblages are drawn.

Key Words:
Concrete Filled Steel Tube;
RC Column with Steel Girder;
RCS Core Wall with Exterior Steel Frame;
New Materials Elements and Systems.

1. INTRODUCTION

The U.S.-Japan Cooperative Earthquake Research Program began in 1979 following the recommendations as outlined in the final report of the U.S.-Japan Planning Group for the program (Ref. 1). The overall objective of the total program is to improve seismic safety practices in both countries through cooperative studies to determine the relationship among full-scale tests, small-scale tests, component tests, and related analytical and design implication studies. First four phases of the program have been Reinforced Concrete (RC) Structures, Steel Structures, Masonry Structures, and Precast Concrete Structures. Research on Mixed Steel/RC Structures was identified as an important phase of the program as recommended in the planning group report.

It is widely recognized that innovative uses of two or more different materials in a structure leads to more efficient system for resisting seismic forces. During the past ten years the use of composite and hybrid structures has increased in the U.S. and Japan. In spite of some research and development work by Japanese construction companies, not enough is known at present regarding their seismic behavior or performance. Design procedures and codes for use in typical design offices are not well developed at present.

Considering the importance of developing design guidelines (a unified code development) for typical composite and hybrid structures that are used in current practice, and of developing new and innovative composite structural elements and hybrid systems using advanced new materials and/or devices, a five-year research program on Composite and Hybrid Structures was recommended as the fifth phase of the ongoing U.S.-Japan Cooperative Earthquake Research Program. The recommendations were based on a number of technical meetings of the U.S. and Japan Planning Groups and finally a Joint Planning Group Workshop held in Berkeley on September 10-12, 1992 (Ref. 2).

Because of diverse and broad scope of the subject area, the research program is organized into the following four groups: Concrete Filled

[1] Professor, Dept. of Civil and Environmental Engrg., University of Michigan, Ann Arbor, MI 48109-2125, USA

Tube Column Systems (CFT); RC/Steel Reinforced Concrete Column Systems (RCS); and RC/SRC Wall Systems (HWS); New Materials, Elements and Systems (RFI). A theme structure provides a common focus of the program to facilitate cross comparison between various system types identified and to derive structural elements and sub-assemblages for detailed studies.

2. PROGRAM MANAGEMENT, COORDINATION AND CURRENT STATUS

The research program is planned for a period of five years in both countries, and funding has been provided accordingly. Research work on the Japanese side started in the spring of 1993. However, fuller participation and coordination of research work on both sides started in early summer 1995 when the first group of U.S. research projects were awarded. Cooperation and coordination of work by all participants are most essential to successful completion of this program. Various committees have been formed for this purpose. A Joint Technical Sub-Committee (JTSC) in each of the four components of the research program provides technical advice and coordination. Each JTSC has a co-chairman from each side with membership including all researchers in that area. These groups meet as often as needed. All participants and institutions are also part of the bigger Joint Technical Coordinating Committee (JTCC) to review progress and discuss scientific and technical issues on a common basis. This committee meets once a year. The last (third) JTCC meeting was held in Hong Kong in December 1996. The fourth JTCC meeting is scheduled to be held in fall 1997 soon after the award of third year U.S. research projects which is expected in April-May 1997. A smaller group called Joint Steering Committee (JSC), which consists of key representatives from the JTCC, oversees the entire program and provides guidance on issues that are common to the four components of the program. The overall program has a technical coordinator and a co-chairman from each side.

In addition to sharing of technical information and ideas among researchers, exchange of personnel involved is strongly encouraged. This will occur more now as the research program is getting into its advance stage. Active participation of practitioners and various industry representatives in planning, coordination and execution of the research work is also a strong feature of this program.

3. PROGRAM OBJECTIVES

Since the subject area of the Composite and Hybrid Structures is diverse and broad, the research program was organized into the following four groups: CFT Column Systems; RC/SRC Column Systems; and RC/SRC Wall Systems; New Materials, Elements and Systems. The first three groups aim at developing practical design guidelines (a unified code development) for typical composite and hybrid structures currently used. The last group aims at developing new and innovative composite structural elements and hybrid systems using advanced new materials and/or devices.

4. THEME STRUCTURE

The theme structure provides a common focus and a strong link between various components of the research program, facilitate cross comparisons between various systems to be studied, and also provides a common prototype structure from which the structural elements and sub-assemblages for detailed studies are drawn. The following criteria were used for selection of the theme structure:

- The building plan was selected so as to reflect the benefits that the hybrid structures provide over non-hybrid structures.
- The basic plan is common to various types of hybrid structures. The number of stories and the make-up and combination of structural components and details can be varied.
- Rules to determine dead load, live load and seismic forces to be used in design simulation are common in the U.S. and Japan Groups.

5. RESEARCH ON CFT SYSTEMS

A number of research projects were funded during the first two years. These projects are focusing on the behavior of CFT column-to-WF beam moment connections. The specimens are nearly full size and include circular and square tube sections for columns. The connection details include the use of diaphragms, shear studs, welds, and bolts. The main variables are the connection details to transfer beam forces into the column. The

objectives are:

1) To determine the force transfer mechanism, examine the effects of various connection details on this mechaninsm, and on the connection strength, stiffness and ductility under cyclic loading.

2) Develop and evaluate practical and economical connection details for seismic resistance.

3) Formulate practical design guidelines.

Some testing work also includes study of beam-columns under combined axial force and bending. Analytical studies accompany the experimental work. The analytical models include complex finite element formulations in an effort to develop simpler empirical or mechanics based models for practical design work. Analytical work is also aiming at studying the bond and shrinkage effects, and confinement effects in CFT members subjected to different load conditions.

6. RESEARCH ON RCS SYSTEMS

RCS structures in the U.S. generally consist of columns made of light steel shapes encased in RC. The light steel shape provides ease of erection and connection to the steel beam. Some earlier tests on RCS interior frame connections have been carried out and reported in the literature. In one research project under this program exterior connections are being studied. The joint detail variables are: lateral ties, beam bearing plates, use of FRC in place of stirrups. Effect of floor slab is also included in the study. Analytical studies are also in progress to model the connection and frame behavior.

7. RESEARCH ON HWS SYSTEMS

In one research project on seismic behavior of steel/composite coupling beams and their connections to the RC shear wall has been studied experimentally and analytically. Four one-third scale specimens were tested which represented a portion of the wall and one half length of the coupling beam from a 20 story theme structure. The effect of concrete encasement of the steel beam and details of the connection in the embedded portion have been studied. Two more research projects were initiated last year which deal with studies of composite shear wall-frame systems and steel frames with in-fill RC walls.

8. RESEARCH ON NEW MATERIALS, ELEMENTS AND SYSTEMS (RFI)

The research work in this group aims at developing and application of new and advanced materials in innovative composite structural elements and systems (Research For Innovation - RFI). Thus, the studies in this group are more of feasibility type than those in the previous three groups where the objectives are to develop detailed guidelines for practical design work.

Significant amount of research work has been devoted to advanced cementitious and plastic composite materials. Albeit, the available information needs to be expanded to application in seismic load conditions. In two projects under this program, work is in progress on developing innovative composite systems consisting of steel and fiber reinforced concrete (FRC). The structural elements are made of selective combinations of FRC and steel members. The combinations under study include: FRC-encased open web steel joists, and high performance FRC core encased in slurry infiltrated mat concrete (SIMCON) shells for reinforcement as well as stay-in-place form work. In another project application of fiber reinforced concrete in the joint regions of RCS systems is being studied. Work is also in progress on further development of Engineered Cementitious Composite (ECC) materials and their selective use in structural elements, such as columns with large ductility demands.

9. CONCLUDING REMARKS

A brief overview of the progress of U.S.-Japan Cooperative Earthquake Research Program on Composite and Hybrid Structures has been presented in this paper. This five-year program started in 1993 in Japan and in 1995 in the U.S. The two year time lag is being taken as an opportunity to plan the future research work in a more careful and useful manner in order to derive the most benefit from the work that has already been completed on both sides. The overall coordination efforts, cooperation and exchange of information have been excellent. More active exchange of research personnel during the remaining period of the program will be most beneficial and is being pursued currently in this program.

REFERENCES

1. "Recommendations for a U.S.-Japan Cooperative Research Program Utilizing Large-Scale Testing Facilities," Report No UCB/EERC 79-26, September 1979.

2. "Recommendation for U.S.-Japan Cooperative Research Program - Phase 5 Composite and Hybrid Structures," Report No. UMCEE92-29, November 1992.

Research and Development of Performance-Based Design and Engineering System in Japan

Hiroyuki Yamanouchi[1)]
Hisashi Okada[2)]
and
Masaomi Teshigawara[3)]

Abstract

This paper describes a framework on performance-based structural design and engineering system that should be realized in the future, and introduces a current activity that is underway toward the new structural design/engineering system, at the Building Research Institute (BRI) in cooperation with many professional communities related to building structures.

Introduction

The current structural design methods are based on either strength or ductility, or otherwise the both of a structure. Thus, overall structural performance including others than strength and ductility has not yet become conscious in the mind of not only a structural engineer but also a researcher. Namely, the global structural performance before and after structural design is not always clearly described by a structural engineer. For instance, looking at the structural performance against a specified level of seismic forces, a structural engineer cannot say the expected performance such as remaining inter-story drift, damage degree of non structural elements and lifelines, reparability and so on. This situation is strongly owing to the current prescriptive design codes that bind a structural engineer without design flexibility.

The current design codes do not clearly require target structural performance, whereas design procedures and rules are definitely and prescriptively specified as code provisions. Therefore, under this inflexible system, the performance of a designed structure cannot be clearly predicted and described even by a structural engineer who designed the structure. Furthermore, structural design itself has become "calculation" just to keep restrictively the prescriptive specifications under code provisions.

In the future design system, on the contrary, the target or objective structural performance should firstly be defined as a clear picture, and then in order to attain the performance, a structural engineer may choose an appropriate design method and procedure. Thus, the most important thing toward the future design system is to facilitate a new design system including codes, where a structural engineer can determine target performance and realize it by choosing an appropriate design procedure. It is not until this is realized that a structural engineer can clearly explain the objective and expected performance of a structure designed by him or her to a client.

Structural Performance

The performance of a structure is not limited to structural safety; the word of structural performance has even wider concepts. That is, the concepts includes every structure-related performance; safety, reparability, durability, human comfort, maintainability, constructibility, aesthetics and so on. Furthermore, performance against various actions such as loads and forces should be taken into account. The basic definition and description materials of structural performance have already been proposed by the author elsewhere (1).

---

1) Director, Department of Research Administratiion and Management
2) Associate Director for Composite Structure, Department of Structural Engineering
3) Head of Structure Div., Department of Structural Engineering

Performance-Based Codes and Specification Codes

In recent years, structural technologies of building structures are making a rapid progress. For instance, various technologies such as new structural materials, base isolation and response control devices/systems have been developed.

However, the current codes for building structures in Japan cannot match new structural materials and systems, since they are regulated for conventional structural materials and methods and most of them are of specification types that specify, in detail, materials to be used, sizes and spacing etc., in most cases with numerals.

Therefore, it becomes necessary to convert structural codes from current specification types into performance-based types that prescribe objective performance to be accomplished in designed structures, and to allow structural engineers broad ways in selecting new structural materials and methods for achieving the required performance.

BRI/MOC Action Toward New System

Considering significant needs for a new design and engineering system on the basis of performance, the Building Research Institute, Ministry of Construction, has initiated a three-year National Comprehensive R&D Program entitled " New Structural Engineering System" since the fiscal year of 1995, in coordination with structure-related communities such as those of structural engineers, contractors, industries, academy and so on.

The most critical mission of the Program is to show possible ways to a new structural design and engineering system where a structural engineer can clearly explain the objective and expected performance of a building structure designed by him or her. For this, a lot of issues must be studied, discussed and solved; as a result of preliminary studies for formulating the Program, the major subjects to be dealt with in the Program have been identified, and the committees for the action have been organized, as shown in Table 1.

In this Project, we are examining the following two technical subjects:

1. Develop performance based structural design system. Here, we examine not only seismic performance but also other performances related to building structures,
2. Convert specification codes into performance codes in the Building Standard Law,

and furthermore, social issues related to structural engineering are being dealt with as follows:

3. Propose a menu of social systems which can effectively support performance-based design and engineering in terms of qualification of structural engineers, building confirmation procedures, quality assurance of design and so on.

As shown in Table 1. we have organized a Synthesizing Committee (Chairman is Prof. T. Okada of Shibaura Institute of Technology). This Committee steers and manages this comprehensive project. Under the Committee, we settled three Technical Committees. The tasks of the Technical Committees are as follows:

Technical Committee 1: Evaluation of Performance (Chairman: Prof. H. Akiyama of the University of Tokyo)

The Committee is examining the concepts of performance of structures, definitions of performance, measures of performance, loads and forces and their design levels.

(1)The Structure Performance Evaluation System

The structure Performance Evaluation System is shown in fig.1 . In the frame of (1) in fig.1, " Basic Structure Performances" which are primarily required for the building structure are extracted. In the frame (2), each detailed performance which is limit state for each object of evaluation are

described in general expression. The kinds of loads or external forces in the frame (3), and their sizes in the frame (4), are set along with setting of the frame (1) " Basic Structure Performance " and the frame (2) " Performance Evaluation Items and Basic Required performance ". To this point of the first stage, the condition which the structure should be in, and the loads or the external forces which affects it are set in general expression.

In the second stage, the relation between the loads or the external forces and the basically required performance is set in engineering expression. " Quantitative Definition of the Sizes of Kinds of Loads and External Force " is done in the frame (5). The response value (kind) of performance to evaluate against these loads and external forces , and the limit value which satisfies performance are set in the frame (6) " The Principle of Performance Evaluation".

In the frame (7) " Evaluation or design Method " , the methods to realize " The Principle of Performance Evaluation " are developed with engineering judgment or some design criteria. The response value of performance to evaluate and the limit value to satisfy the performance set in the frame (6) " The principle of Performance Evaluation ", should promote the renewal of the conventional evaluation method, following to the development of social fulfillment and the advancement of evaluation technology. Accordingly, detailed performance evaluation or design methods established by current knowledge are only exemplified in order to renew easily or select practically.

(2)Basic Structure Performance

Safety, Restoration and Serviceability are itemized. Each of them corresponds to security of human lives and properties, and the function and habitability respectively. Table 2 describes the purpose and the contents of these basic structural performance.

(3)Performance Evaluation Items and Basic Required Performance

Required limit states (should-be conditions) for each basic structural performance to each evaluated objects are itemized and described in general expression. They are general definition (explanation) on the performance to evaluate. In table 3, safety limit for safety performance, damage control limit for restoration performance, and serviceability limit for serviceability performance are set. In the left column of table 3 the items to be evaluate are enumerated. These are structural frame, structural member, non-structural member, equipments/machines, fixture, and soil. Structural member and non-structural member might be arrange into one term of part of building. For example safety limit of structural frame states that non-destruction that affects human life should avoid. And in the safety limit of the part of building, a part of building should not drop off, or scatter.

(4)Kinds of Loads and External Force

Normal time (fixed or live loads, force such as buoyancy, negative friction, each pressure, water pressure etc.), abnormal time of snow, wind, earthquake , others (force such as temperature stress, special earth or water pressure etc.) should be considered. Basic structural performance should be kept against these loads and external forces.

(5)Sizes of Loads and External Force

They are fixed corresponding to the basic structure performance. Three level of these and their combination might be set corresponding to the three basic performances; safety, restoration, and serviceability.

(6)Quantitative Definition of the Sizes of Kinds of Loads and External Force

The background and the setting method to define the size are mainly determined in engineering expression.

(7)The Principle of Performance Evaluation

The engineering definition is made for performance to evaluate. In

table 4, not only force, but displacement, energy, and acceleration, velocity, all of response value will be used for evaluating structure performance. In all response values, what kind of response value is used should be determined. It means that structure performance is defined by engineering values. Limit value to satisfy performance are the engineering expression on structure performance.

(8)The Evaluation or the Design method

Practical methods for evaluating the structure performance and designing the performance-based building are necessary to be developed with some engineering judgments (engineering criteria). The response value of performance to evaluate and the limit value to satisfy the performance set in (6) " The principle of Performance Evaluation ", should promote the renewal of the conventional evaluation method, following to the development of social fulfillment and the advancement of evaluation technology. Accordingly, detailed performance evaluation or design methods established by current knowledge are only exemplified in order to renew easily or select practically.

(9)Research items

The following items are considered as necessary research and development subjects.
1) The relation between damage degree and deformation of each member, energy, representative deflection to check.
2) The relation between damage degree and deformation of the whole building, energy and damage distribution along building height.
3) The engineering condition of fracture.
4) The background study to determine the level of loads and external forces.
5) Practical methods for evaluating the structure performance and designing the performance-based building adopting the latest research and developing technology.
6) Monitoring the performance of building, especially after earthquake.

Technical Committee 2: Target Performance Level (Chairman: Prof. Y. Aoki of the Tokyo Institute of Technology)

The main purpose of the Committee is to clarify the recognition and the requirements of owners and users for building structures, and to investigate desirable performance items and levels of building structures from the side of the society. At present (in 1996-1997), as the important subjects, the Committee are collecting and arranging the research data to clarify the performance levels and investigating the methodology to determine the performance levels.

(1) Calibration Working Group
This working group clarifies the performance levels of the building structures according to the present design standards, and examines whether the buildings by the new performance-based structure design standards have equivalent performance levels to the present buildings.
(2) Back Ground Risk Working Group
Safety levels required for building structures are investigated by comparing seismic risks with various kinds of risks existing in human daily lives, considering the characteristics of the risks.
(3) Feasibility Study Group Related to Performance Levels
This study group investigates the recognition and the requirements of owners and users for building structures by questionnaires etc. and their analyses, and the methodology to determine performance levels in a theoretical manner.

Technical Committee 3: Social System (Chairman: Dr. Yano of Nikken Sekkei Inc.)

The purpose of this Committee is to propose a menu of ideal social systems matching the purpose of performance-based design and engineering. Thus, the Committee deals with the problems on design review system, qualification of structural engineers, role of building officials and so on.

In 1995, we began with gathering information on past surveys to gain a better understanding on all elements related to the social system issues, including structural design, construction supervision, building confirmation and inspections, the "kentikushi" system (the qualification system of building engineers in Japan), design codes and regulations. At the next step, we put in order the findings and prioritized problems and issues which must be studied.

On the other hand, in April of 1996 it was officially decided by MOC that the Building Standard Law of Japan should be converted into that based on performance. Considering this change of policy, the Committee has also begun to deal with social systems preferable under the "new performance-based building standard law" that will be realized in a few years, in order that the future law will function smoothly and efficiently. In November of 1996, the Social System Committee established two Working Groups on 1) the survey of the Current Conditions of Social System(WG 1) and 2) the study on desirable Social Structure(WG2).

The contents of the examinations in the Committee and WGs are described below in more detail:

(1) Consideration on the concept of "social system" and its constituent elements(Committee),
(2) Surveys by questionnaire to structure engineers in order to grasp a gist of problems incorporated in the current states and to consider possible solutions toward desirable social systems(WG1),
(3) Identification of issues inherently involved in the "construction process relating to structural performance," which should also be supported by the social systems(WG2), and
(4) Study of ideal social systems compatible with performance-based design and engineering(WG2).

Need For International Coordination/Cooperation

In accomplishing a new structural design world in each country, it is hoped that international harmony and consistency in the conceptual framework on the new system will be attained considering the progressing borderless world. For this aim, an "international committee" is under consideration to be formed in the BRI National Program.

Partly for an initial step of the above action, a Japan-U.S. Workshop on Seismic Building Codes (Performance Based Seismic Engineering of Buildings) was held at the Earthquake Engineering Research Center, University of California, Richmond, CA. The main objectives of the workshop were:

1) to discuss the adequacy and efficiency of present Japanese and U.S. seismic codes in light of the experience derived from recent (1985-1995) significant earthquakes (particularly the 1994 Northridge and the 1995 Kobe earthquakes), and from studies conducted in the last ten years, and to identify problems whose solutions need improvement,
2) to discuss what can be done to improve present seismic code approaches, with particular attention to the interim recommendations for engineering procedures that the Vision 2000 Committee of the SEAOC has recommended for obtaining buildings with predictable and defined performance; and
3) to discuss the development of a work plan and the organization that will be needed to formulate the basic concepts and framework that can be used in Japan and the U.S. to develop practical seismic code regulations whose applications will result in facilities whose seismic performance will be predictable with a reasonable degree of confidence under the different types of earthquake ground motions that can occur during their service life.

The resolutions and recommendations of the Workshop are fully introduced in Appendix. The recommendations of the Workshop should be thought very significant to break through current blocked situations in the structural design/engineering world

and to make progress in international harmony related to a future structural engineering system based on performance.

Just one year after the 1995 Hyogo-Ken-Nanbu Earthquake, and two years after the 1994 Northridge Earthquake, the Seventh U.S.-Japan Workshop on the Improvement of Structural Design and Construction Practice was held. At that time we held a special meeting with some members of SEAOC and ATC to discuss the international coordination and cooperation as the second step. In this meeting, the recommendation was re-affirmed and the following items were recommended.

1) Each side should establish a balanced high level policy/coordination committee with no more than seven members plus ex-officio members from participating governmental agencies.
2) Formal cooperation should be continued between Japan and U.S. Next meeting should be held as soon as possible after formation of the high level committee : preferably within six months from this meeting.

References

(1) H. Yamanouchi, 1992, "An Approach to Performance-Based Design System," the 5 the U.S.-Japan Workshop on the Improvement of Building Structural Design and Construction Practices, ATC-JSCA Joint Workshop, San Diego, Sept. 8-9.

Table 1 R/D Project for Performance Based Design

Development of Performance Based Structural Design System in Japan

Three-year Project from 1995 Fiscal Year

Main Subjects

- Develop Performance Based Structural Design System
  (Not only seismic performance but also other performance)
- Convert specific code to performance code inBuilding Standard Law
- Propose Social System for Performance Based Code

Pre-study of Performance Based Design from 1992 in cooperation with the Kozai Club (Non-profit corporation consisting of steel makers)

Organization of R/D Project on Performance Based Design System in Japan

Technical Committee

Convener: Professor Okada: Tokyo Univ.

Sub Committee 1

Evaluation of Performance

Convener : Professor Akiyama : Tokyo Univ.

Concept of performance of structure
Definition of performance
Measure of performance

Design seismic action, design loads and so on,

Under this sub committee, there are some Working Groups.

Sub Committee 2

Object Performance Level

Convener : Professor Aoki: Tokyo Institute of Tech,

Opinion of clients and users of buildings
Importance category of buildings
Acceptable risk and so on.

Sub Committee 3

Social System

Convener : Dr. Yano: Nikken Sekkei

Construction procedures
Design review
Qualification of engineers
Role of building officials and so on.

An International Committee (under consideration)

Table 2 Basic Structure Performance (required performance)

1) Safety
The purpose to request performance : To avoid hazard which directly affects human lives inside and outside of the buildings. (security o f human lives)

The contents to evaluate performance : To prevent fracture appropriately regarding safety on structure frames, members, interior and exterior finishing materials.

2) Restoration
The purpose to request performance : To secure the repairing ability to the damagecaused by the outer stimuli to the buildings.

The contents to evaluate performance : To control deterioration and damage degrees on structure frames and members, interior and exterior finishing materials, utensils and foundation in he light of repairing ability

3) Serviceability
The purpose to request performance : To secure serviceability (function) and habitability of the buildings

The contents to evaluate performance : To eliminate harmful deformation or vibration on structure frames and members, interior and exterior finishing materials, facilities and foundation in the light of serviceability

Table 3 Evaluated Objects and Fundamental Performance

Perform. / Objects	Safety Limit (keep of Human Life)	Damage Control Limit (keep of Properties)	Serviceability Limit (keep of Function)
Structural Frame	Non-destruction*1 to human life	*within* Assigned Damage	Non-Harmful*2 Def. or Vib. for normal use
(Structural Members)	Non-destruction*1 to human life	*within* Assigned Damage	Non- Harmful*2 Def. or Vib. for normal use
Non-structure Members	Non-Destruction*1, Drop, Scatter to human life	*within* Assigned Damage	Non-Harmful*2 Def. or Vib. for normal use
Equipments / Machines	Non-Overturn, Drop, Movement by deformation or vibration of structural frames or members	*within* Assigned Damage by deformation or vibration of structural frames or members	Non- Harmful*2 Def. or Vib. of structural frames or members for normal use of equipments / machines
Fixture	Non-Overturn, Drop, Movement by deformation or vibration of structural frames or members	*within* Assigned Damage by deformation or vibration of structural frames or members	—
Soil	Non-destruction*1 (decrease of support ability or change*3 of soil)	*within* Assigned Damage (decrease of support ability or change*3 of soil)	Non-Harmful*2 Change*3 for normal use of buildings or traffic

<Supplement>

(*1) destruction : unbalanced state of energy, force or deformation in static or dynamic response

(*2) harmful : available without interferance in the usual usage

(*3) change : landslide, movement, deformation, decrease of stiffness (ex. by liquilifaction), gap, crack of soil

Table 4-1 Basic Structural Performance : Safety

Principal of Performance Evaluation : Failure that affects human life is evaluated in the term of force, deflection and energy.

Performance item \ Action	Permanent (P) D, L. etc	Snow (S)	Wind (W)	Earthquake (E)	Others temp. etc
1) Failure of structural frame	$Qr<Qc$ $\delta r<\delta c$	$Qr<Qc$ $\delta r<\delta c$	$Qr<Qc$ $\delta r<\delta c$ $Er<Ec$ $Ir<Ic$	$Qr<Qc$ $\delta r<\delta c$ $Er<Ec$ $Ir<Ic$	$Qr<Qc$ $\delta r<\delta c$
2) Failure of structural members (column, beam, floor, wall, roof, foundation, pile etc)	$Qr<Qc$ $\delta r<\delta c$	$Qr<Qc$ $\delta r<\delta c$	$Qr<Qc$ $\delta r<\delta c$ $Er<Ec$	$Qr<Qc$ $\delta r<\delta c$ $Er<Ec$	$Qr<Qc$ $\delta r<\delta c$
3) Failure or drop off of non-structural member	$Qr<Qc$	$Qr<Qc$	$\delta r<\delta c$ $Ar<Ac$	$\delta r<\delta c$ $Ar<Ac$	$Qr<Qc$ or $\delta r<\delta c$
4) Drop off, overturn of equipment	$Qr<Qc$	—	$Ar<Ac$ $Vr<Vc$	$Ar<Ac$ $Vr<Vc$	— —
5) Drop off, overturn of contents	$Qr<Qc$	—	$Ar<Ac$ (fix) $Vr<Vc$ (loose)	$Ar<Ac$ (fix) $Vr<Vc$ (loose)	— —
6) Failure of soil	$Qr<Qc$ $\delta r<\delta c$	$Qr<Qc$ $\delta r<\delta c$	$Qr<Qc$ $\delta r<\delta c$	$Qr<Qc$ $\delta r<\delta c$	$Qr<Qc$ $\delta r<\delta c$

Q : force, stress, δ : deflection, E : energy, I : index, A : acceleration, V : velocity
suffix c : criteria(limit value), suffix r : response
[ ] : evaluation method has been temporarily provided.

Table 4-2 Basic Structural Performance : Damage Control

Principal of Performance Evaluation : Damage control limit determined by the economic and technical point of view is evaluated in the term of force, deflection and energy.

Action / Performance item	Permanent (P) D, I. etc	Snow (S)	Wind (W)	Earthquake (E)	Others temp. etc
1) Damage of structural frame	$Qr < Qc$ $\delta r < \delta c$	$Qr < Qc$ $\delta r < \delta c$	$Qr < Qc$ $\delta r < \delta c$ $Er < Ec$ $Ir < Ic$	$Qr < Qc$ $\delta r < \delta c$ $Er < Ec$ $Ir < Ic$	$Qr < Qc$ $\delta r < \delta c$
2) Damage of structural members (column, beam, floor, wall, roof, foundation, pile etc)	$Qr < Qc$ $\delta r < \delta c$	$Qr < Qc$ $\delta r < \delta c$	$Qr < Qc$ $\delta r < \delta c$ $Er < Ec$ $Ir < Ic$	$Qr < Qc$ $\delta r < \delta c$ $Er < Ec$ $Ir < Ic$	$Qr < Qc$ $\delta r < \delta c$
3) Damage of non-structural member	$Qr < Qc$	$Qr < Qc$	$\delta r < \delta c$ $Ar < Ac$	$\delta r < \delta c$ $Ar < Ac$	$Qr < Qc$ oc $\delta r < \delta c$
4) Damage of equipment	$Qr < Qc$	—	$Ar < Ac$ $Vr < Vc$	$Ar < Ac$ $Vr < Vc$	— —
5) Damage of contents	$Qr < Qc$	—	$Ar < Ac$ (fix) $Vr < Vc$ (loose)	$Ar < Ac$ (fix) $Vr < Vc$ (loose)	— —
6) Damage of soil	$Qr < Qc$ $\delta r < \delta c$	$Qr < Qc$ $\delta r < \delta c$	$Qr < Qc$ $\delta r < \delta c$	$Qr < Qc$ $\delta r < \delta c$	$Qr < Qc$ $\delta r < \delta c$

Q : force, stress, δ : deflection, E : energy, I : index, A : acceleration, V : velocity
suffix c : criteria(limit value), suffix r : response

Table 4-3 Basic Structural Performance : Serviceability

Principal of Performance Evaluation : Deflection or vibration that affects normal usage is evaluated in the term of force, deflection, vibration and velocity.

Performance item \ Action	Permanent (P) D, L. etc	Snow (S)	Wind (W)	Earthquake (E)	Others temp. etc
1) Deflection or vibration of structural frame	$\delta r < \delta c$	$\delta r < \delta c$	$\delta r < \delta c$	$\delta r < \delta c$	$\delta r < \delta c$
	$f r < f c$	$f r < f c$	$f r < f c$	$f r < f c$	$f r < f c$
2) Deflection or vibration of structural members (column, beam, floor, wall, roof, foundation, pile etc)	$\delta r < \delta c$ $Qr < Qc$	$\delta r < \delta c$ $Qr < Qc$	$\delta r < \delta c$ $Qr < Qc$	$\delta r < \delta c$ $Qr < Qc$	$\delta r < \delta c$ $Qr < Qc$
	$f r < f c$	$f r < f c$	$f r < f c$	$f r < f c$	$f r < f c$
3) Deflection or vibration of non-structural member	$Qr < Qc$	$Qr < Qc$	$\delta r < \delta c$ $Ar < Ac$	$\delta r < \delta c$ $Ar < Ac$	$Qr < Qc$ or $\delta r < \delta c$
4) Deflection or vibration of equipment	$Qr < Qc$	–	$Ar < Ac$ $Vr < Vc$	$Ar < Ac$ $Vr < Vc$	– –
5) Deflection or vibration of soil	$Qr < Qc$ $\delta r < \delta c$	$Qr < Qc$ $\delta r < \delta c$	$Qr < Qc$ $\delta r < \delta c$	$Qr < Qc$ $\delta r < \delta c$	$Qr < Qc$ $\delta r < \delta c$

Q : force, stress, δ : deflection, f : vibration, A : acceleration, V : velocity
suffix c : criteria(limit value), suffix r : response

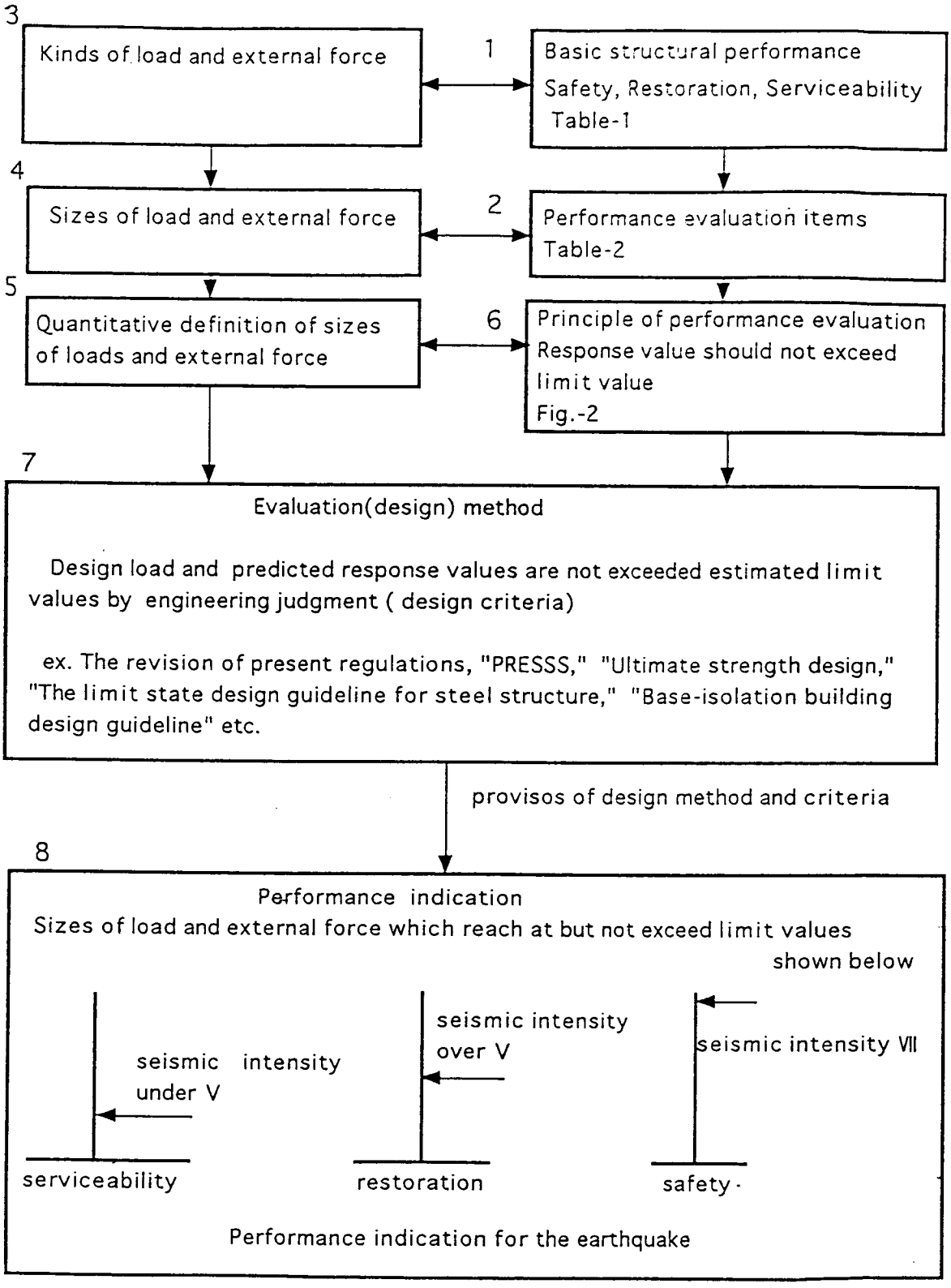


Fig. --1 EVALUATION SYSTEM OF STRUCTURE PERFORMANCE

Manuscripts Authored for Panel Meeting But not Presented Orally

Wind-Induced Response of a Roof Purlin

by

Jianming Yin[1], Douglas A. Smith[2] and Kishor C. Mehta[3]

ABSTRACT

The proper orthogonal decomposition (POD) technique is used to estimate the fluctuating response of a roof purlin on the Texas Tech University full-scale test building. The contribution of the first three eigenvalues to the total energy is calculated and agrees with the wind tunnel results. The accuracy of the reconstruction of the pressure time series is investigated. The static and fluctuating response coefficients for pressure taps are calculated and compared in this paper.

KEYWORDS: full-scale test; proper orthogonal decomposition (pod) technique; purlin; wind-induced response

1. INTRODUCTION

Low-rise buildings are immersed in the near-ground flow field and usually experience higher turbulent flows than high-rise buildings. The turbulence intensity of the approaching flow has significant effects on the peak values of wind pressure, and thus the peak wind loading on the building envelope, especially on the roof area (Cochran et al., 1992). The quasi-steady theory indicates that high turbulence in the approach flow results in high turbulence in wind pressures on a building (Cook, 1990). Therefore, for low-rise buildings, a relatively high fluctuating response of their structural components is expected. In fact, field measurements of purlin deflections on the test building of the Wind Engineering Research Field Laboratory (WERFL), Texas Tech University (TTU) verifies this expectation (Bhavaraju, 1993, Smith et al., 1994).

The static response of the purlin was studied by (Bhavaraju, 1993). In this paper, only the fluctuating response of the purlin is investigated using the Proper Orthogonal Decomposition (POD) technique. The contribution of the first three eigenvalues is obtained. The reconstruction of the pressure time series using the first three eigenvalues is conducted and the accuracy of the reconstruction for pressures at different locations is discussed. The fluctuating response coefficients for pressure taps in the effective area of a purlin are obtained and compared with the static response coefficients.

2. EXPERIMENTAL SETUP

The instrumentation and data acquisition system of the Wind Engineering Research Field Laboratory (WERFL) at TTU have been described in detail by Levitan et al. (1992). A brief description related to this experiment is given here.

The location of the purlin used for this investigation, the designation of pressure taps in the purlin's effective area, (numbered from G10 to G15) and the definition of angle of attack of wind on the building are shown in Figure 1.

---

[1]Research Assistant, Department of Civil Engineering, Texas Tech University, Lubbock, Texas, 79409-1023, USA

[2]Research Assistant Professor, Department of Civil Engineering, Texas Tech University, Lubbock, Texas, 79409-1023, USA

[3]P.W. Horn Professor, Department of Civil Engineering, Texas Tech University, Lubbock, Texas, 79409-1023, USA

This instrumented 25 ft (7.62m) long Z-shaped purlin is simply supported with a 1'-4" (0.41m) overhang adjacent to the wall. Six pressure taps are placed in the effective area of the purlin. Differential pressure transducers are used to measure the pressures at the taps. These transducers are referenced to atmospheric pressure from an underground box (Levitan, 1993). The sampling rate for building surface pressures is 40 Hz.

Two Direct Current Displacement Transducers (DCDT) manufactured by Trans-Tek Incorporated are used for monitoring the midspan deflection of purlin. The DCDTs have a flat frequency response to 20 Hz. The DCDTs are sampled at 10 Hz and filtered at 8 Hz (Smith et al., 1994). The static influence coefficient surface for the purlin was developed experimentally by Bhavaraju (1993) and is shown in Figure 2.

3. PROPER ORTHOGONAL DECOMPOSITION (POD) TECHNIQUE

Wind pressure distribution over the effective area of a structural member is a function of both time and space, say $p(x,y,t)$. The spatio-temporal random characteristics of wind pressure, and thus wind loading, make it difficult to evaluate or predict the fluctuating response of a structure or a member. One technique used to predict the response of structural members to wind loads is the Proper Orthogonal Decomposition (POD). The POD technique decomposes a spatio-temporal random function of wind pressure, $p(x,y,t)$, into several deterministic distributions, $\Phi_i(x,y)$'s, and their associated temporal function or principal coordinates, $a_i(t)$'s. The detailed description of this technique can be found in Loeve (1977). A brief description of the POD technique is given here.

Given simultaneously recorded time series at pressure taps which are uniformly distributed over an area, $p(x_1,y_1,t)$, $p(x_2,y_2,t)$, ..., $p(x_N,y_N,t)$, the covariance, R_{ij}, for each pair of these series at zero time lag can be obtained as:

$$R_{ij}=\int_T p(x_i,y_i,t)p(x_j,y_j,t)dt \qquad (1)$$

where T is the record length.

When $i=j$, the result of the above equation is the autocovariance of $p(x_j,y_j,t)$. Using these covariance values, a real symmetric covariance matrix $[R_{ij}]$ of the order of $N\times N$ can be established. The eigenvectors and eigenvalues of this matrix are determined and the principal coordinate can be computed using:

$$a_i(t)=\frac{\sum_{k=1}^{N} p(x_k,y_k,t)\Phi_i(x_k,y_k)}{\Phi_i^2(x_k,y_k)} \qquad (2)$$

where:
$\Phi_i(x,y)$ is the ith eigenvector; and,
$a_i(t)$ is the ith principal coordinate.

From the definition of $a_i(t)$, it is shown that the principal coordinates are orthogonal. The eigenvectors, which are orthogonal to each other, give the common distributions of wind pressures over an area while the related eigenvalues indicate the relative weighting contributed by their associated eigenvectors.

The original pressure, $p(x,y,t)$, can be decomposed using a set of known eigenvectors and principal coordinates as:

$$p(x_i,y_i,t)=\sum_{k=1}^{N} a_k(t)\Phi_k(x_i,y_i) \qquad (3)$$

For the case under consideration, Eq. 3 can be simplified to:

$$p(x_i,t)=\sum_{k=1}^{N} a_k(t)\Phi_k(x_i) \qquad (4)$$

where:
$a_k(t)$ is k^{th} principal coordinate, and,
$\Phi_k(x_i)$ is i^{th} component of kth eigenvector.

Using the POD technique, Best et al. (1983), Bienkiewicz et al. (1992), Holmes (1990), and Ho (1992) presented, respectively, their results by analyzing pressure data from wind tunnel tests.

3.1 Contribution of eigenvectors

The wind pressure data on the purlin collected at the test building of WERFL are used to construct a covariance matrix. To make the results reasonably comparable with those from wind tunnel tests (Best et al, 1983, Bienkiewicz et al, 1992, Holmes, 1990), only five pressure taps, G10, G11, G12, G14 and G15 are used in order to make the spacing of pressure taps as uniform as possible.

For this work, net pressures across the roof envelope are used. Internal pressure inside the TTU test building is uniform (Yeatts et al., 1993). The external pressure is assumed to be uniformly distributed over the tributary area shown in Figure 3. The net pressure coefficient for the tributary area associated with a specific pressure tap is:

$$C_{PN}(t)=C_{PE}(t)-C_{PI}(t) \quad \text{(downward positive)} \quad (5)$$

where the pressure coefficient, C_p is defined as follows:

$$C_p(t)=\frac{p(t)}{0.5\rho V^2} \quad (6)$$

where:
$p(t)$ is wind pressure;
ρ is air density; and,
V is the mean wind speed averaged over 15 minutes measured at roof height.

Records with the angle of attack approximately equal to 0°, 20°, 315° and 270° are selected for analysis. The calculated results listed in Table 1 show that the first three eigenvalues constitute 80% or more of total energy. The first eigenvalue is typically 50% of the total energy. The results have a good agreement with these from wind tunnel tests by Best et al. (1983). While the contribution of the first eigenvalue in this study is less compared to the results by Bienkiewicz et al. (1992).

3.2 Reconstruction of pressure history

Pressure coefficient time histories can be decomposed using a complete set of orthogonal eigenvectors used as base functions. A limited number of these eigenvectors can be used to reconstruct a new pressure history that approximates the original one. If a complete set of eigenvectors is used, the reconstructed time history will be equal to the original one. In most cases, to ensure the precision of reconstruction and to reduce the calculations, only the first three eigenvectors are used. For this study, the first three eigenvectors account for 80% or more of the total energy, thus the time history is reconstructed using only the first the three eigenvectors.

Fig. 4 shows the original and reconstructed time histories using the first three eigenvalues for record M15N609. The original pressure coefficient histories for G11 and G15 are plotted on the left side and the corresponding reconstructed one on the right side. Pressure taps G11 is, for this angle of attack (23.6°), in the separation bubble and G15 is in the reattachment region.

A comparison of the mean and standard deviation show a good match for tap G11. However there is a significant difference in the couple for tap G15. The cross correlation coefficients of each couple for G11 and G15 are 0.9997 and 0.361 respectively. This implies the accuracy of pressure reconstruction may depend upon the location of a pressure tap.

3.3 Prediction of fluctuating response coefficients of purlin

As mentioned, the purlin deflection was monitored simultaneously along with the surface point pressure in the purlin's effective area. These data can be used to evaluate the fluctuating response characteristics of the purlin to fluctuating wind loads.

The expression for the relationship between the wind pressures acting on a component and the response of the component can be found in Holmes (1990). The static and fluctuating response coefficient for a purlin may not be the same. The equations for static and fluctuating response are:
For static response:

$$\overline{W} = \sum_{k=1}^{N} \eta_k \overline{C}_{pk} A_k q \qquad (7)$$

For fluctuating response:

$$W(t) = \sum_{k=1}^{N} \lambda_k C_{pk}(t) A_k q \qquad (8)$$

where:
$\overline{W}$ and $W(t)$ are the mean and fluctuating component of purlin response;
$\overline{C}_{pk}$ and $C_{Pk}(t)$ are the mean and fluctuating component of a pressure coefficient at tap k;
η_k and λ_k are the static and fluctuating response coefficients of the purlin due to the mean and fluctuating pressure at tap k;
A_k is the tributary area associated with the specific pressure measurement at tap k (under the assumption that $p_k(t)$ is uniformly acting on A_k); and,
q is velocity pressure.
The evaluation method to determine the static purlin response is given by Bhavaraju (1993). The fluctuating response is considered below.

The displacement response of the purlin and the pressure coefficient time histories at taps, numbered G10 through G15, have been measured. For simplicity, the 5 taps are renumbered 1 to 5 instead of G10, G11, G12, G14 and G15, respectively.

Multiplying both sides of Eq. 8 by C_{pj} $(j=1,...5)$ and integrating, we obtain:

$$\int_0^T W(t) C_{pj}(t) dt = \sum_{k=1}^{5} \int_0^T \lambda_k C_{pk}(t) C_{pj}(t) A_k q dt \qquad (9)$$

where T is the record length. In this case T=900 sec.

Introducing the concept of the covariance function, Eq. 9 can be rewritten as:

$$COV(W, C_{pj}) = \sum_{k=1}^{5} \lambda_k A_k q COV(C_{pk}, C_{pj}) \qquad (10)$$

Where $COV(\bullet, \bullet)$ is the value of covariance function at time lag $\tau=0$.

Using these five pressure taps, $j=1,...,5$, five simultaneous equations are established with five unknowns, i.e. fluctuating response coefficients, λ_1 to λ_5. These equations are solved for the λ_i's. The results are shown in Table 2 along with the static influence coefficient.

The fluctuating coefficient, λ_i, usually is not equal to the static coefficient, η_i, and appears to be a function of the angle of attack. For records with similar angles of attack, e.g., 609 and 611($\alpha \approx 20^0$), or 728 and 730($\alpha \approx 4^0$), the fluctuating coefficients have slight difference. This difference may be caused by the differences in longitudinal and lateral turbulence intensities. This difference may also be caused by the response characteristics of the purlin. Figures 5 and 6, taking record M15N609 as an example, demonstrate the comparison of the normalized spectral density functions of the purlin response and local pressures. It is found, from the figures, that the purlin response usually lose some magnitude in the relatively high frequency domain

starting from 0.3 Hz ($\log_{10}0.3 \approx -0.5$) compared to the spectral functions of local pressure. From Table 2, it can be observed that the fluctuating response coefficients are the function of the angle of attack. For example, records 728 and 730, with the angle of attack approximately equal to 0°, the fluctuating response coefficients are higher than those for records 609 and 611 ($a \approx 20°$) which are higher than those of records 795 ($a \approx 315°$, or so-called quartering wind).

Another reason for the difference between static and fluctuating response coefficient is the assumption that the pressure measured at the tap represents the pressure on the whole tributary area. When an oncoming flow is attacking at the direction of 0°, a high-suction bubble enhances the correlation of wind pressure along the width of the purlin. The correlation will decrease as an acting wind skews from normal direction; thus the actual net effect of wind pressure on a tributary area should be lower than the wind pressure measured at a single point because the low correlated pressure components cancel out each other. This so-called area-averaging effect may be one of the factors that cause the fluctuating response coefficient to be lower than the static one.

3.4 Prediction of purlin response using both original and reconstructed pressure histories

Based on the analysis in section 3.2, the reconstructed pressure history, using the first three or more eigenvectors, can be used to approximate the original one. The precision of this reconstruction depends on how many eigenvectors have been used and the location of the pressure tap. The reconstructed histories are used here to predict the purlin response.

In practice, structural response such as support reaction, deflection and bending moment of a member, is of primary concern for engineers for design. Therefore instead of the wind pressures, it is actually the precision of the estimated structural response that determines how many eigenvectors should be used to reconstruct pressures. In this case, since the fluctuating response coefficients, λ_i's ,have been obtained in section 3.3, Eq. 8 can be used to predict purlin response. By substituting original and reconstructed pressure histories into Eq. 8, respectively, two predicted purlin deflection histories for each record are obtained. The standard deviations and ranges of two predicted histories are listed in Table 3 along with the measured response for comparison purposes. The results show a good agreement. Therefore, in this case the first three eigenvectors are sufficient to be used to predict purlin deflection and thus the pressure coefficients.

4. CONCLUSIONS

1) The results obtained from the field measurements at WERFL, Texas Tech show that the first three eigenvalues usually constitute up to 90% of the total energy while the first one alone accounts for 50% or more.

2) The fluctuating response coefficient is different from the static one.

3) Spectral analysis shows that purlin deflection loses some magnitude in the high frequency range.

4) The reconstructed pressures using the first three principal coordinates may be used to estimate the fluctuating response of the purlin.

5. ACKNOWLEDGMENT

The assistance provided by Mr. S.V. Bhavaraju in analysis effort is appreciated. The appreciation also goes to the Wind Engineering Research Field Laboratory team who made available the excellent wind pressure data. The financial support by the National Science Foundation (Grant BCS-8821163) and the Metal Building Manufacturer's Association are gratefully acknowledged by the writers.

6. REFERENCES

Best, R.J. and Holmes, J.D. (1983), "Use of Eigenvalues in the Covariance Integration Method for Determination of Wind Load Effects", Journal of Wind Engineering and Industrial Aerodynamics, Vol. 13, pp 359-370, Elsevier.

Bhavaraju, S.V. (1993), "Wind-Induced Pressures on a Roof Purlin", Master's Thesis, Department of Civil Engineering , Texas Tech University, Lubbock, Texas.

Bienkiewicz, B., Hee-Jung, H., and Sun, Y. (1992), " Proper Orthogonal Decomposition of Roof Pressure", BBAA2, Australia.

Cochran, L.S. and Cermak, J.E. (1992), "Full- and Model-Scale Cladding Pressure on Texas Tech University Experimental Building", Journal of Wind Engineering and Industrial Aerodynamics, Vol 41-44, pp 1589-1600, Elsevier.

Cook, N.J. (1990), "The Designer's Guide to Wind Loading of Building Structures", Part 2, Static Structures, Butterworths, London.

Ho, T.C.E. (1992), "Variability of Low Building Wind Loads", Ph. D. Dissertation, Department of Civil Engineering, Faculty of Engineering Science, The University of Western Ontario, London.

Holmes, J. D. (1990), "Analysis and Synthesis of Pressure Fluctuations on Bluff Bodies Using Eigenvectors", Journal of Wind Engineering and Industrial Aerodynamics, Vol.33, pp 219-230, Elsevier.

Levitan, M.L. (1993), "Analysis of Reference Pressure Systems Used in Field Measurements of Wind Loads", Ph.D. Dissertation, Department of Civil Engineering, Texas Tech University, Lubbock, Texas.

Levitan, M.L. and Mehta, K.C. (1992), "Texas Tech Field Experiments for Wind Loads parts I and II" , Journal of Wind Engineering and Industrial Aerodynamics, Vol.41-44, pp 1565-1588, Elsevier.

Loeve, M. (1977), "Probability Theory I", 4th Edition, Springer-Verlag Inc., New York.

Smith, D.A. (1993), "Stochastic Analysis of Wind Data", Ph. D. Dissertation, Department of Civil Engineering, Texas Tech University, Lubbock, Texas.

Smith, D.A., Mehta, K.C., Yeatts, B.B. and Bhavaraju, S.V. (1994), "Area-Averaged and Internal Pressure Coefficients Measured in the Field", Accepted for publication in the Journal of Wind Engineering and Industrial Aerodynamics.

Yeatts, B.B. and Mehta, K.C. (1993), "Field Experiments for Building Aerodynamics" Journal of Wind Engineering and Industrial Aerodynamics, Vol. 50, pp 213--224, Elsevier

Table 1. Contribution by First Three Eigenvalues

Eigenvalue	Run No. Mode 15						
	609	611	728	730	542	544	795
1st	56%	59%	53%	59%	42%	49%	81%
2nd	17%	16%	20%	23%	20%	20%	10%
3rd	16%	15%	16%	10%	15%	13%	4%
Sum	89%	90%	89%	92%	80%	82%	95%

Table 2. Fluctuating and Static Response Coefficients

Run No.	Angle of attack, θ	I_u	I_v	U	λ_k				
					G10	G11	G12	G14	G15
609	23.6°	0.161	0.139	22.7	0.105	0.084	0.173	0.192	0.046
611	20.1°	0.175	0.151	22.5	0.077	0.079	0.179	0.214	0.064
728	3.9°	0.191	0.180	16.5	0.115	0.148	0.307	0.276	0.080
730	4.9°	0.213	0.153	18.5	0.093	0.146	0.313	0.333	0.035
542	260.2°	0.201	0.150	20.0	0.051	0.087	0.081	0.100	0.064
544	266.5°	0.167	0.201	21.8	0.100	0.100	0.112	0.109	0.068
795	314^0	0.223	0.188	18.1	0.053	0.043	0.114	0.039	0.102
		Static	Coef.	η_k	0.095	0.334	0.555	0.430	0.137

Note: I_u and I_v denote longitudinal, lateral turbulence intensity, respectively; and, U denotes mean wind speed (mph).

Table 3. Comparison of Predicted and Measured Purlin Response ($\times 10^{-3}$ in.)

	609		611		542		544	
	std	range	std	range	std	range	std	range
meas	8.26	51.9	8.95	53.7	6.89	49.6	8.43	69.6
pred1	7.65	56.6	6.95	46.3	6.13	44.5	7.53	50.0
pred2	7.06	50.4	8.70	6.69	5.98	43.5	7.36	59.1

Note: 'meas' denotes the measured purlin response;
'pred1' denotes the predicted purlin response by original pressure histories; and,
'pred2' denotes the predicted purlin deflection by reconstructed pressure histories.

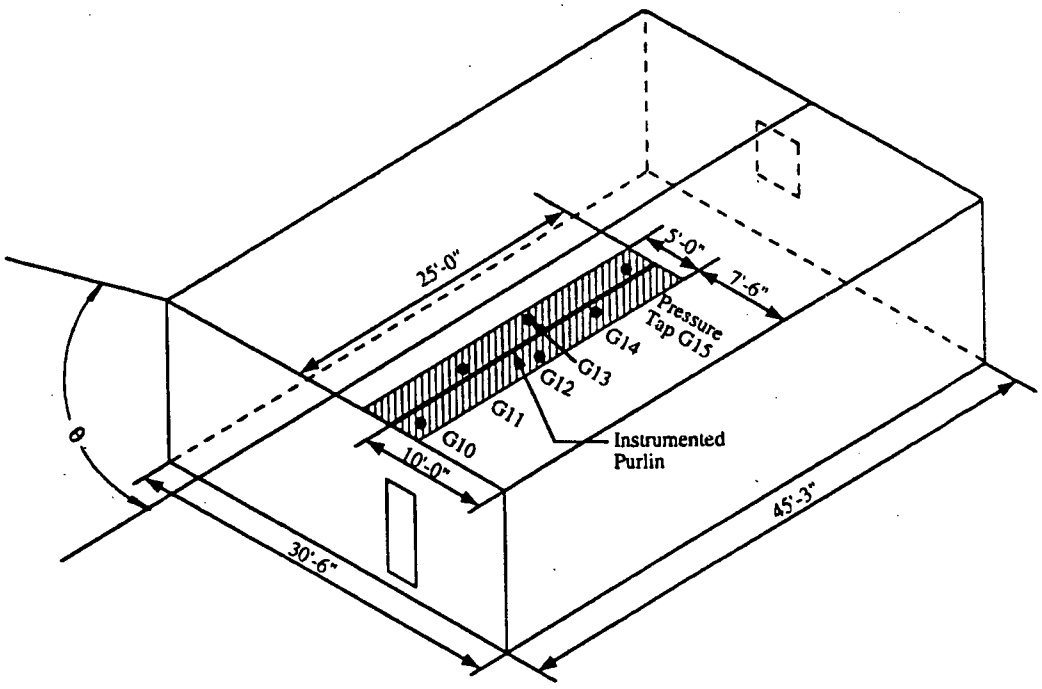


Figure 1. Location of the purlin and the pressure tap designation (Bhavaraju, 1993)

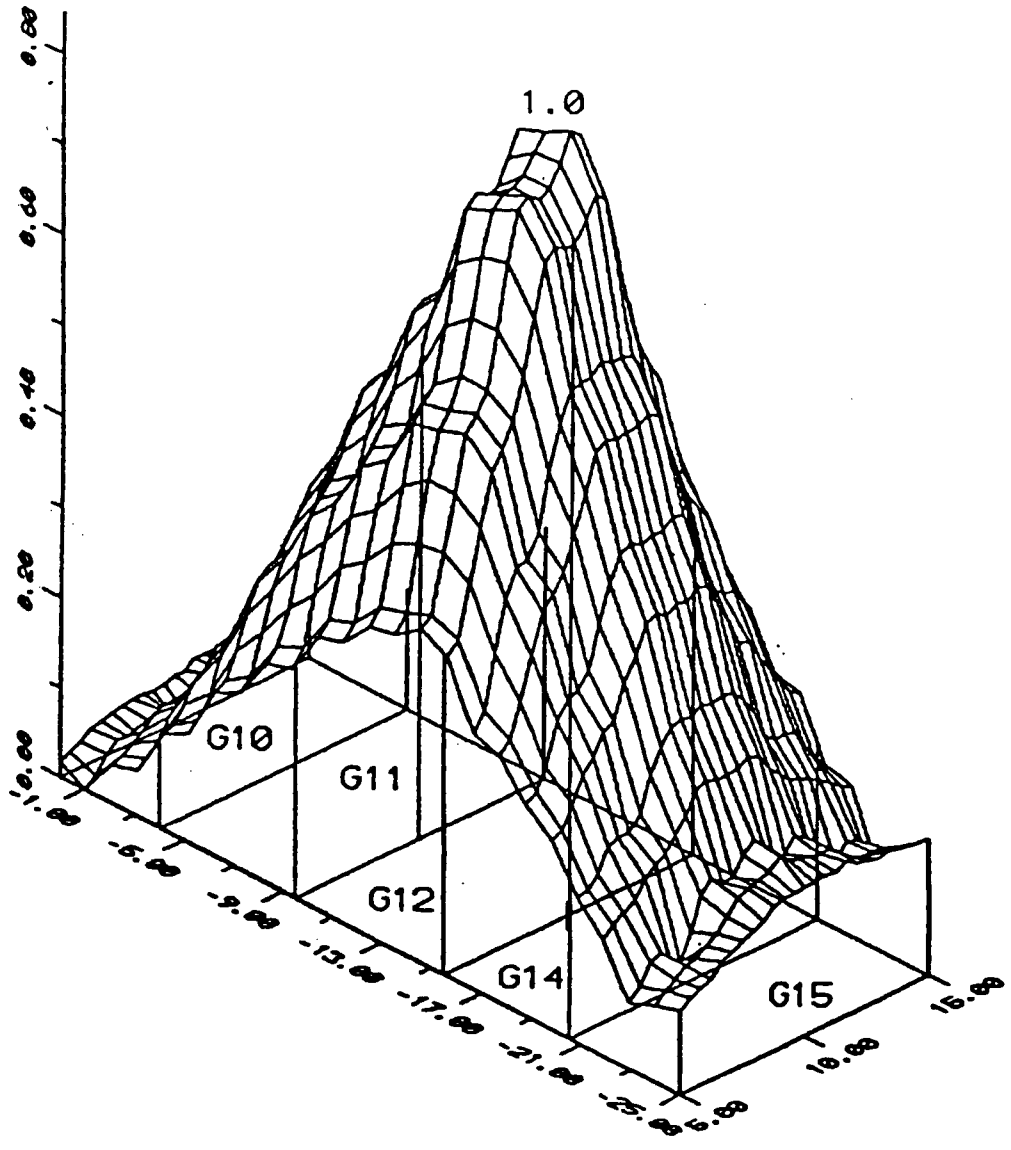


Figure 2. Static influence coefficient surface (Bhavaraju, 1993)

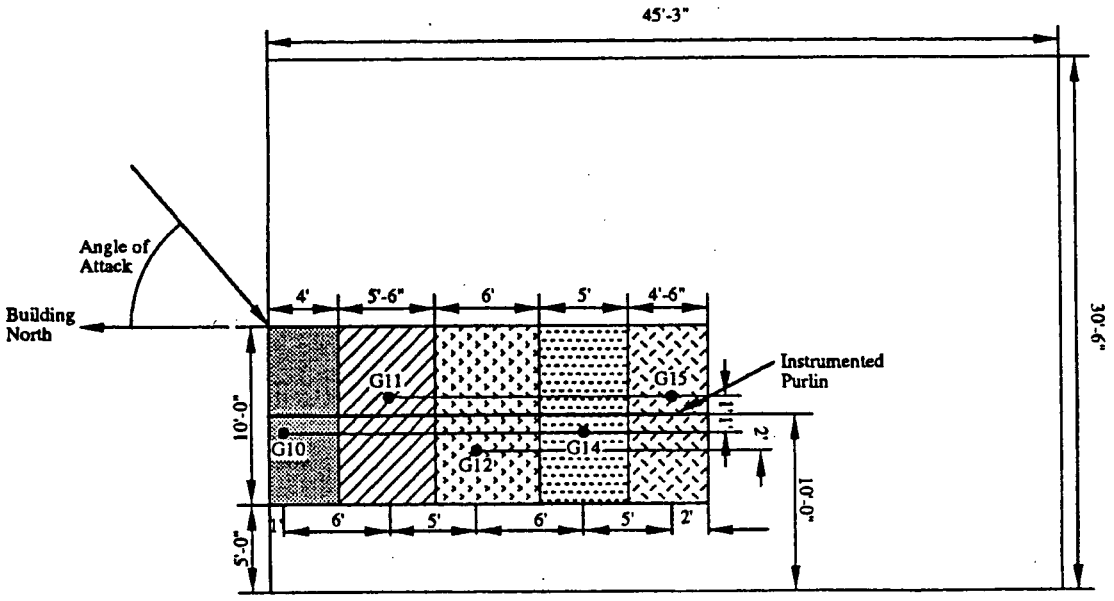


Figure 3. The effective area of pressure taps (Bhavaraju, 1993)

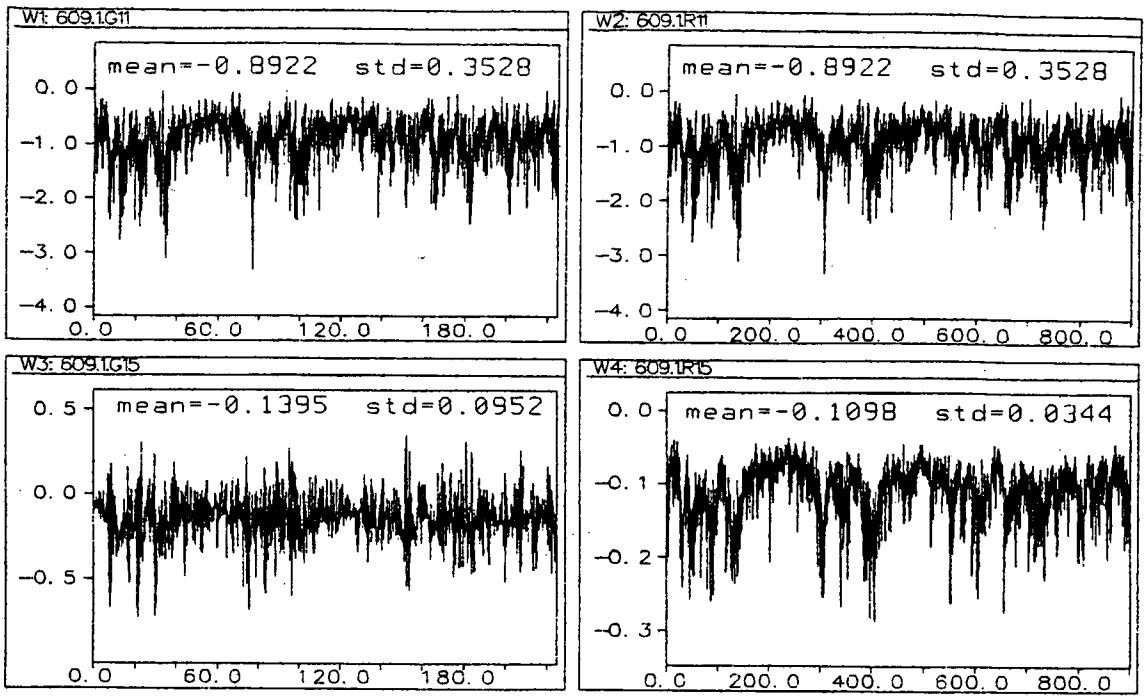


Figure 4. Comparison of original and reconstructed pressure histories

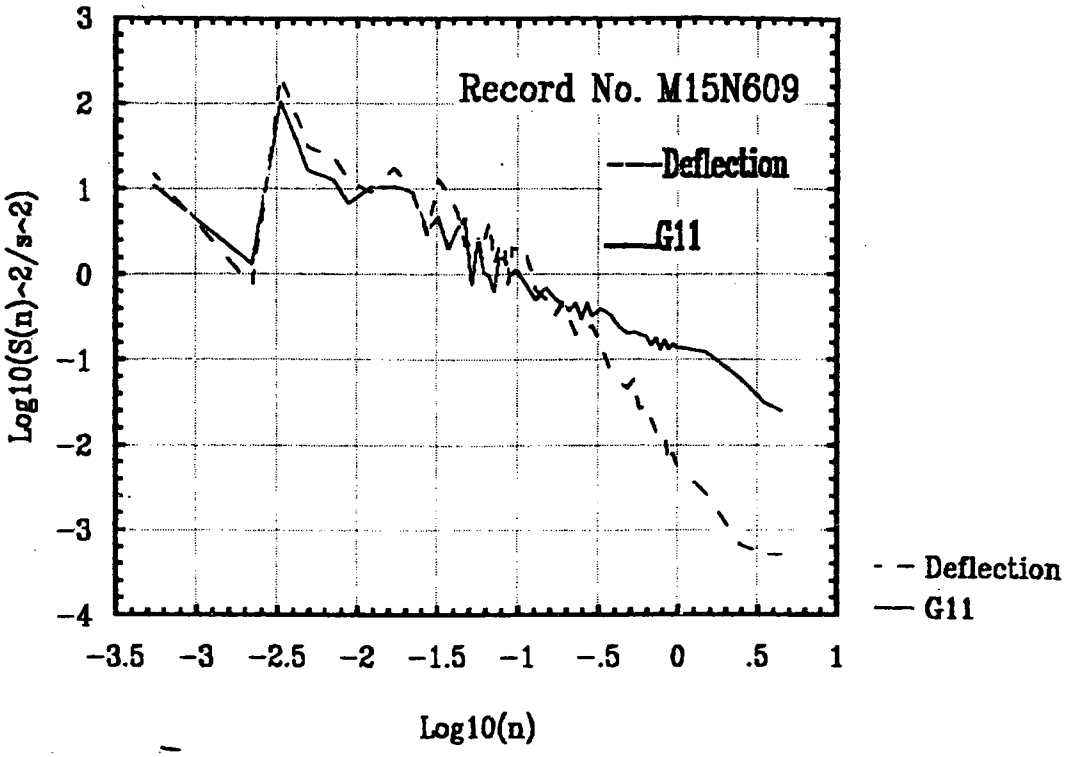


Figure 5. Comparison of normalized spectral density functions (M15N609)

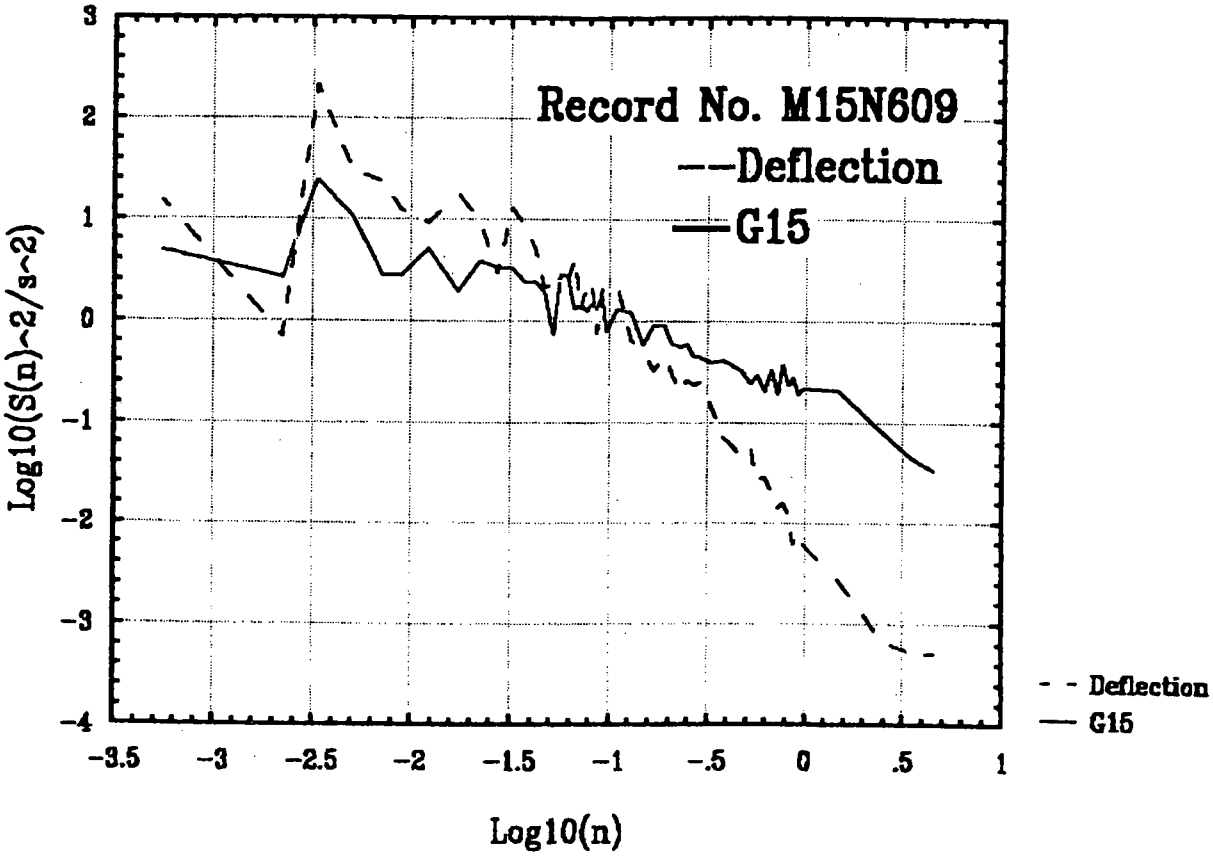


Figure 6. Comparison of normalized spectral density functions (M15N609)

Design of Light-Gauge Steel Shearwalls for Residential Construction in High Wind and Seismic Conditions

by

Jay H. Crandell[1], Shawn McKee[1], William F. Freeborne[2]

ABSTRACT

Light-gauge steel framing has recently become recognized as a viable alternative framing method for residential construction in the U.S. With this recognition, the need to efficiently design for lateral loads produced by wind and seismic forces has prompted research to fill this need. This paper reviews the current status of shearwall design data using light-gauge steel framing and wood-based structural panels. Pilot tests to investigate the applicability of a new design method for shearwalls, known as the "perforated shearwall" method, are presented. Findings from the pilot tests indicate that the method is applicable to light-gauge steel walls and that additional testing is needed to improve the method since it appears conservative.

KEYWORDS: design; light-gauge steel; seismic; shearwall; testing; wind

1. INTRODUCTION

Light-gauge steel framing has recently become a viable alternative construction method in the U.S. residential construction market. However, its competitive use is dependent on efficient methods of design, particularly in the area of wall bracing to provide resistance to lateral loads from wind and seismic forces. Recent research has provided the basic design data for light-gauge steel shearwalls, but an efficient method of design has not been developed, particularly for residential construction applications.

The objective of this paper is to present findings from pilot tests on long shearwalls with openings to investigate the applicability of an efficient shearwall design method known as "perforated shearwalls". This empirical method is believed to be an efficient design approach for residential construction and similar light-frame buildings.

2. BACKGROUND

About 93 percent of the houses in the U.S. are built using traditional wood framing practices, which have performed reasonably well in meeting the large and varied housing needs in the country. However, recent price increases in framing lumber have challenged builders and designers to seek alternative materials and methods for the construction of homes. Light-gauge steel framing has recently grown in its competitive capability as an alternative framing method for homes in the U.S.

While interest in steel framing and other alternative materials for home construction is greater than ever in the U.S., the use of such "non-conventional" materials face many barriers including:

- regulatory
- educational
- economic
- technical

---

[1]Structures and Materials Division, NAHB Research Center, Inc., Upper Marlboro, Maryland, USA, 20774-8731

[2]Department of Policy Development and Research, U.S. Department of Housing and Urban Development, Washington, DC, USA, 20464

The major regulatory barrier is related to the recognition of steel framing in prescriptive building code provisions. Homes in the U.S. are traditionally built using prescriptive building code requirements that specify connections, member sizes, and details for various components of the home. These provisions have historically focused on the application of light-frame wood construction to basic home design conditions. A builder can construct homes following these provisions and a building code official can inspect the construction following the prescriptive requirements in the building code.

This process has been very efficient, largely because builders and code officials are have become very familiar with the materials and methods through decades of use. Also, the prescriptive building code requirements can be applied without the added time and cost of generating an engineered design for every home. Homes and other structures built in this manner are considered "non-engineered" structures.

A recent public-private effort to develop prescriptive construction requirements for light-gauge steel framing in residential construction has resulted in adoption of steel framing in the major residential building code in the U.S. (CABO 1997; HUD 1996). Through time this should result in the removal of barriers to steel framing as local political jurisdictions in the U.S. adopt the newer building code provisions.

With the recent building code success mentioned above, educational barriers are one of the major issues facing use of light gauge steel framing in residential construction. Educational efforts are underway, to help building code officials and builders use light-gauge steel framing appropriately and efficiently. The framing system is very similar to traditional wood frame construction; however, cutting and fastening methods are somewhat different. Also, alignment of vertical and horizontal load bearing members is required for "in-line" framing -- a requirement which is not common or necessary in the traditional wood framing practices.

Economic issues surrounding alternative materials are driven primarily by labor and material costs associated with the final product. These costs also include the "up-front" costs that builders experience when switching to new building systems -- otherwise known as the "learning curve". However, to be competitive with the current home-building process in the U.S., the use of steel framing and other alternatives must be streamlined to allow for its introduction as a site-built or manufactured product with a "pre-approved" regulatory status. This lowers the builder's expenses prior to construction by minimizing design, planning, and approval activities through a straight forward prescriptive or "cook book" approach. The materials must also be readily available with minimal shipping and handling costs. Overall costs in the completed project must finally compare favorably with the builder's current practices to provide an incentive to change. One method to reduce these costs is to eliminate over-design through technological advancement.

Technical barriers have been largely solved through the development of the *Prescriptive Method for Cold-Formed Steel Framing* (HUD 1996) which was used as the basis for the approved building code provisions. However, these provisions are primarily based on conservative engineering specifications and calculations which add unnecessary costs to light-gauge steel framing. In particular, the construction requirements did not include wall bracing requirements in high wind and seismic load conditions because of the lack of an efficient design method for steel shearwalls and because the initial goal was to at least cover lower seismic and wind load conditions. Steel strap bracing was also not included because of the special detailing and anchoring required to achieve good performance with this bracing method, even in lower wind and seismic conditions. Therefore, a recent research goal has been to develop an efficient wall bracing approach for light gauge steel framing to resist lateral loads from wind and seismic forces. Other research has included

system performance of back-to-back C-shape headers and walls under combined axial and bending loads. The objective of this research has been to make steel framing more efficient in the competitive residential construction market.

The traditional design method for shearwalls utilizes hold-down brackets on each wall segment to restrain it from rotating prior to developing the shear capacity of the panel. While this design method is widely used for engineered structures, it is not always the most efficient design method for light residential structures of either wood or steel framing.

Hold-downs require careful placement and pre-planning in the construction phase. In typical residential construction, this level of precision is difficult to control consistently. As a result, the use of many hold-down brackets which must be permanently embedded in the concrete prior to framing often results in construction errors that must be corrected either by changes in the framing layout or replacement of the anchor. These problems may be very costly. Therefore, a more efficient shearwall design method is needed to minimize the number of hold-down brackets, yet still provide adequate performance of shearwalls.

3. LITERATURE REVIEW

Recent racking tests of steel-framed walls with wood-based structural panel sheathing has provided data for use by engineers using traditional shearwall design methods (Serrette 1996). These tests included monotonic and cyclic loading on 4 ft.x 8 ft. (1.2 m x 2.4 m) and 8 ft. x 8 ft. (2.4 m x 2.4 m) wall specimens following the ASTM E 564 test method (ASTM 1995). The specimens included nominal 2x4 and 2x6 steel studs sheathed with two types of wood structural panels -- oriented strand board (OSB) and plywood. Thicknesses of steel studs were 33 mil (0.84 mm) and 43 mil (1.09 mm). Various screw patterns were used and some panels also included ½ in. (12.7 mm) gypsum wall board on the opposite side of the structural panels. Data from these tests has resulted in a recent building code approval giving shear capacities for light gauge steel-framed shearwalls (UBC 1997).

Yasumura and Sugiyama (1984) conducted several small scale tests on wood frame shearwalls with various opening amounts and arrangements. Data from these tests were used to develop an empirical equation for predicting the shear capacity of a wall with openings. The experimenters found that the shear capacity of the scaled walls with openings were related to the wall's capacity without openings by use of a parameter, r, known as the sheathing area ratio. The sheathing area ratio is calculated by the following equation:

$$r = \frac{1}{1 + \frac{A_o}{H \sum L_i}}$$

where,

- r = sheathing area ratio
- A_o = area of openings in the wall
- H = height of the wall
- L_i = length of the wall segment i without openings.

The sheathing area ratio, r, is then used to predict a shear load ratio, F, for the wall which is calculated by the following equation:

$$F = r/(3-2r)$$

The shear load ratio, F, represents the ratio of the wall's capacity with openings to the wall's capacity without openings.

For a given wall with openings, its capacity can be calculated by first determining the sheathing area ratio, r, and then determining the shear load ratio, F. The capacity of the wall is then determined by multiplying the shear capacity of the wall without openings by F. The only restraints (hold-down brackets) necessary are

located at the ends of the walls (see Figure 1). In actual construction this restraint would be placed at the major corners of the structure only. This shearwall design method is known as the "perforated shearwall method". Yasumura and Sugiyama (1984) also developed similar relationships to predict wall capacity at various deflection angles (drifts) up to the ultimate capacity.

Recent full-scale tests of wood frame walls have verified the applicability of the perforated shearwall method using both monotonic and cyclic loading (Dolan 1996). The walls were 8 ft. x 40 ft. (2.4 m x 12.2 m) with various opening amounts and arrangements. Hold-down brackets were placed only at the ends of the walls. A major U.S. building code has recently approved this design approach for wood frame shearwalls (SBC 1996).

In testing that is ongoing, shear capacities of wood frame walls designed using the segmented shearwall approach and the perforated shearwall approach have been compared (Dolan 1997). Conventionally-framed wood walls without any hold-down brackets were also tested with identical opening configurations. Additional testing is planned to quantify the restraint provided by corners so that wood frame shearwalls can be designed without the use of any hold-down brackets in lower lateral load conditions. None of these tests have included walls with steel framing and, therefore, a similar approach to the efficient design of light-gauge steel framing systems has not been found in the literature.

4. EXPERIMENTAL METHOD

To investigate the applicability of the perforated shearwall method to walls framed with light-gauge steel, four pilot tests were conducted using 8 ft. x 40 ft. (2.4 m x 12.2 m) walls with configurations of openings similar to that discussed in the literature search (Dolan 1996; Dolan 1997). The walls were constructed as shown in Figure 1 and Table 1. The construction was nearly identical to tests conducted by Dolan (1996) with the exception of light-gauge steel framing instead of wood framing and screws instead of nails. It should be noted that one of the walls was tested without hold-down brackets to give an indication of a "lower bound" condition.

A monotonic shear load was applied to a steel tube connected to the top of the wall by a hydraulic actuator with a load cell as shown in Figure 2. The load was applied at a rate of 0.6 inches per minute until failure. Deflections were measured using LVDTs. Readings from the load cell and the LVDTs were taken at 0.5 second intervals. The data was reduced to provide load and deflection plots for the tested walls closely following ASTM E 564 procedures (ASTM 1995).

5. TEST RESULTS AND DISCUSSION

Load deflection plots for the three walls are shown in Figure 3. The plots show a high initial stiffness of these walls and considerable shear capacity. However, the ductility appears to be lower than similar wood-frame construction. Ductility is defined as the capability of the wall to continue to deform after peak load without significant loss of capacity. While ductility is not so important for design against wind loads, it is important when designing for seismic loading. The primary failure mode for these walls was tear-out of the screw fasteners from the edges of the oriented strand board sheathing. One wall was tested without any hold-down restraints at the end of the wall (wall '2B'). As expected, the failure mode was bending of the bottom track at the first anchor bolt located about 1 ft. (0.3 m) from the loaded end of the wall. The capacity of this wall was considerably lower than the similar restrained wall (wall '2A'). For this wall, the inclusion of other system effects (i.e. corner framing, gravity loads, etc.) would likely improve the tested performance so that it more accurately represents the shear capacity actual construction.

The detailed data for walls 1, 2A, and 4 are presented in Table 2 along with a comparison of the actual shear load ratio, F, to that predicted by the empirical equation develop by Yasumura and Sugiyama (1984). It is evident from these pilot tests that the perforated shearwall method produces a conservative prediction of the wall shear capacity for the range of openings covered in this study (represented by the sheathing area ratio, r). It also appears that the relationship of F to r is somewhat linear for the range of sheathing area ratios, r, investigated in these tests. Additional testing is needed to adjust the empirical equation for F to better predict the performance of these types steel-framed walls and to provide validation of the empirical equation at lower sheathing area ratios.

6. CONCLUSIONS

The main findings of this study are as follows:

1. Adequate data now exists for the design of light-gauge steel frame walls sheathed with wood-based structural panels.

2. A new shearwall design method, known as the perforated shearwall method, has been pilot tested on long steel framed walls with openings. The test results indicate that this method is a viable design approach for light-gauge steel shearwalls resisting lateral loads from wind and earthquakes.

3. Light-gauge steel walls with wood-based structural sheathing materials are adequately stiff and strong when only the ends of the wall are restrained against uplift, not requiring multiple hold-downs at individual wall segments between openings.

4. Additional testing is needed to finalize and improve the perforated shearwall method when applied to light-gauge steel walls. Also, an appropriate consideration of the ductility of these walls is needed for the purposes of seismic design analysis.

7. ACKNOWLEDGMENTS

The authors gratefully acknowledge the financial support provided by the American Iron and Steel Institute, the National Association of Home Builders, and the U.S. Department of Housing and Urban Development.

8. REFERENCES

ASTM (1995), *Standard Practice for Static Load Test for Shear Resistance of Framed Walls for Buildings*, American Society for Testing and Materials (ASTM), West Conshohocken, Pennsylvania, 1995.

CABO (1997), *One and Two Family Dwelling Code 1996/1997 Amendments*, Council of American Building Officials (CABO), Falls Church, Virginia, 1997.

Dolan, J. Daniel (1996), report unpublished at the time of this writing, Virginia Polytechnic Institute and State University, Blacksburg, Virginia.

Dolan, J. Daniel (1997), report unpublished at the time of this writing, Virginia Polytechnic Institute and State University, Blacksburg, Virginia.

HUD (1996), Prescriptive Method for Residential Cold-Formed Steel Framing - First Edition, prepared for the U.S. Department of Housing and Urban Development (HUD) by the NAHB Research Center, Inc., Upper Marlboro, Maryland, May 1996.

SBC (1996), *Standard Building Code - 1995/1996 Amendments*, Southern Building Code Congress International, Inc., Birmingham, Alabama, 1996.

Serrette, Reynaud (1996), Shear Wall Values for Light Weight Steel Framing, prepared for the American Iron and Steel Institute, Washington, DC, by Santa Clara University, Santa Clara, California, January 1996.

UBC (1997), *Uniform Building Code - Volume 2*, International Conference of Building Officials (ICBO), Whittier, California, 1997.

Yasumura, Motoi and Hideo Sugiyama (1984), "Shear Properties of Plywood-Sheathed Wall Panels with Opening", Trans. of A.I.J. No. 338, April, 1984 (English translations of work first reported in 1976).

Table 1: Wall materials and construction data

Component	Construction and Materials
Framing Members	1-5/8 in x 3-1/2 in. x 33 mil (41.2 mm x 88.9 mm x 0.84 mm) steel studs and 33 mil (0.84 mm) track. Stud connected to track w/one #8 wafer head, self-drilling tapping screw in each flange.
Sheathing	
Exterior	7/16 in. (11.1 mm) oriented strand board (OSB) with #8 bugle head, self-drilling tapping screws spaced at 6 in. (15.2 cm) on edges of panel and 12 in. (30.4 cm) in field of panel, 4 ft. x 8 ft. (1.2 m x 2.4 m) sheets installed vertically on framing.
Interior	1/2 in. (12.7 mm) gypsum wallboard with #6 screws spaced at 7 in. (17.8 mm) on edges and 10 in. (25.4 cm) in the field, 4 ft. x 8 ft. (1.2m x 2.4m) sheets installed vertically, joints spackled and taped.
Structural Base Connections (Bottom of Wall)	
Hold-downs	Simpson HD10 with 9,900 lb (44 kN) allowable load connected to single end studs only
Anchor Bolts	5/8 in. (15.9 mm) diameter tie rods with 6 in. (15.2 cm) stud section reinforcing track at anchor bolt locations.
Loading Tube Connections (Top of Wall)	
Above Openings	Two #10 hex head self-drilling tapping screws attaching headers and track to tube at a spacing of 24 in. (61 cm)[3]
Other Locations	1/2 in. (12.7 mm) diameter bolts with 1-3/8 in. (34.9 mm) washers spaced at 24 in. (61 cm) connecting track to tube

[3]Anchor bolts were not used at header locations because there was no practical method of attachment with 1/2 in. (12.7 mm) diameter bolts. The #10 screws are considered to be a conservative substitution. Light-gauge steel headers were constructed of back-to-back C-shapes.

Table 2: Force-displacement data from monotonic tests

	Wall Specimens		
	1	2A	3
Sheathing Area Ratio, r	1.0	0.76	0.48
Predicted Shear Ratio, F[4]	1.0	0.51	0.24
Actual Shear Ratio, F	1.0	0.62	0.30
Peak Load	42.2 kips (187.7 kN)	26.2 kips (116.5 kN)	12.5 kips (55.6 kN)
Displacement@Peak Load	1.54 in. (3.9 cm)	1.64 in. (4.2 cm)	2.41 in. (6.1 cm)

[4]The predicted shear ratio is based on the empirical formula developed by Yasumura and Sugiyama (1984) for wood-framed shear walls.

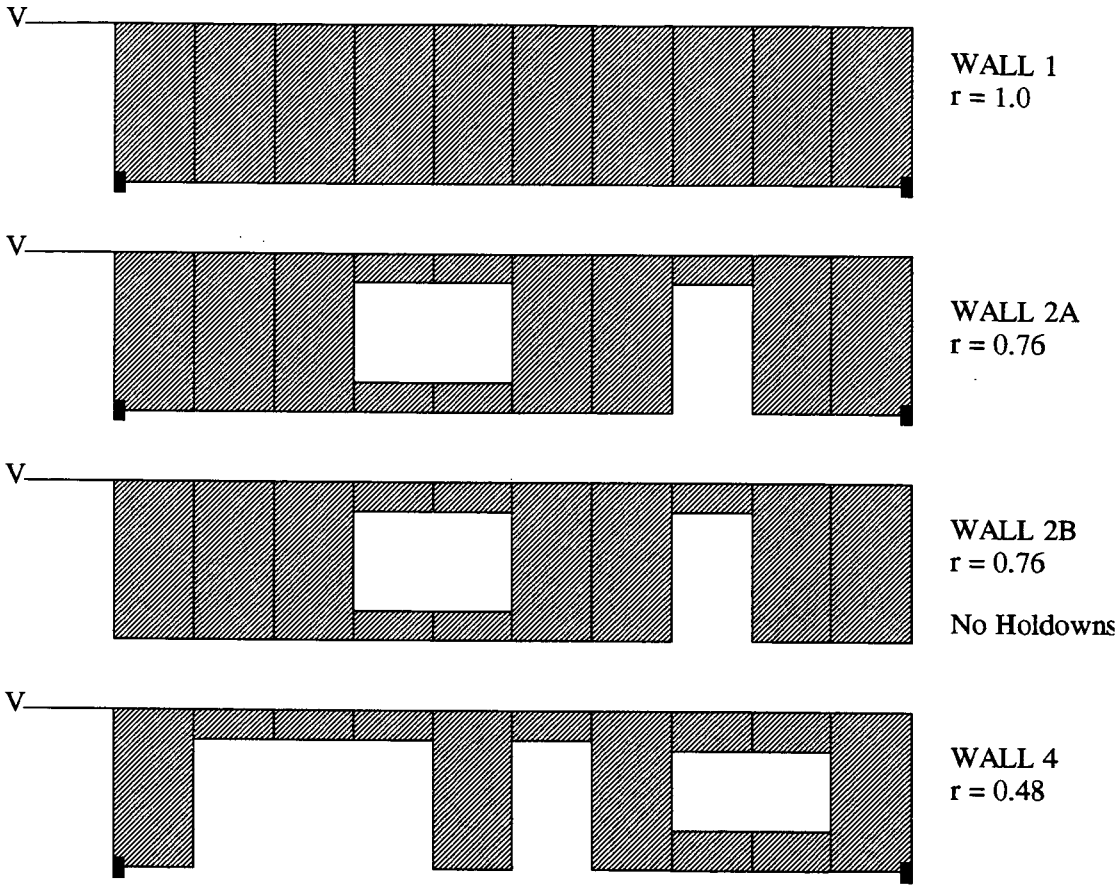


Figure 1: Wall construction

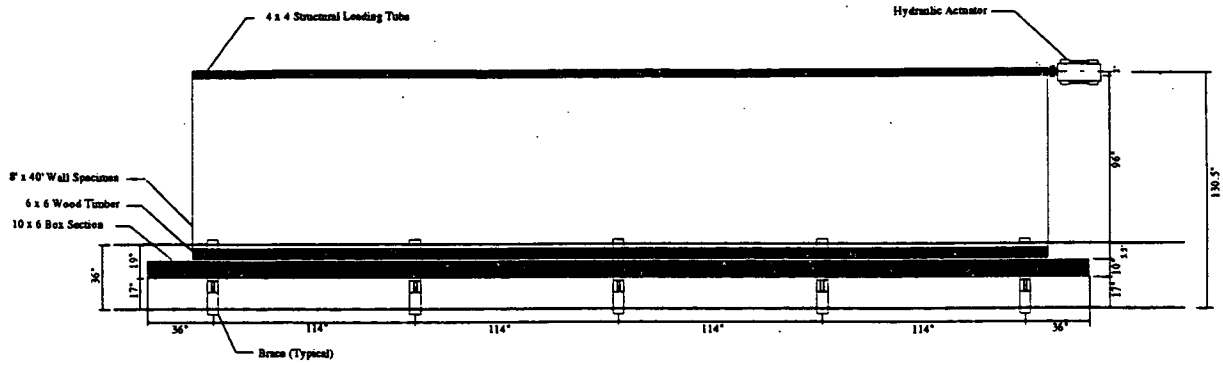


Figure 2: Test apparatus

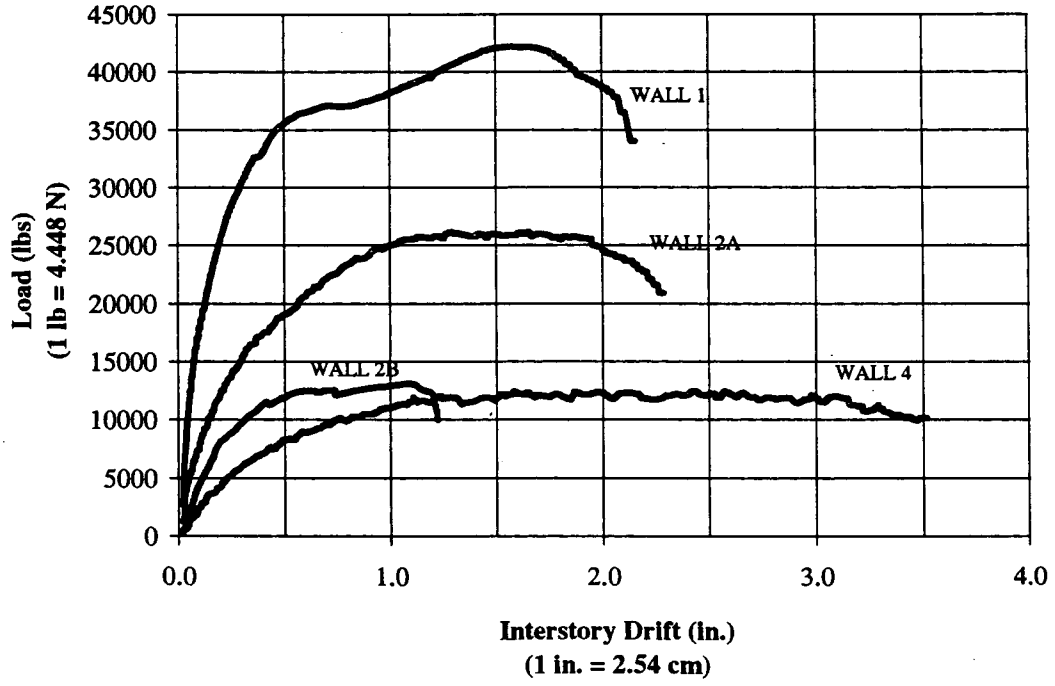


Figure 3: Force-displacement response

CORPS OF ENGINEER EARTHQUAKE ENGINEERING RESEARCH PROGRAM FOR DAMS

by

William E. Roper [1]

ABSTRACT

This paper summarizes the ongoing research work at the Corps of Engineers in the area of earthquake engineering for Dams. This seven year $20 million program involves twenty-one specific work unit efforts and a number of public and private sector partners. The program is managed at the Corps' Waterways Experiment Station. The scope of the program is presented and a selected number of specific work unit areas are reviewed. The program addresses both the geotechnical and structural aspects of dams and related facilities.

KEYWORDS: Earthquake engineering; dams; earthquake; laboratory testing; research; seismic loading; seismic signal

1. INTRODUCTION

The Earthquake Engineering (EQEN) Research Program is the only federally funded program focused on seismic safety of dams and is one of the highest priorities in the Corps R&D program. Most Corps dams were built at a time when earthquake engineering was in its infancy; seismic hazards were not recognized or were poorly understood, and our understanding of them is still changing. The Corps has more than 200 dams and 73 intake towers located in seismic zone 2 or greater (80 percent of the U.S.), most of which would expose downstream populations to mortal hazard in the event of failure to contain their reservoirs (see figure 1). Many of these dams and all of the 73 intake towers would be judged seismically inadequate using current methods of evaluation. Remediation of all of these structures would cost more than a prohibitive $20 billion. Expensive remediation can be avoided in many cases by reevaluating the structures using improved methods of engineering analysis that clearly discriminate between safe and unsafe structures. The cost of remediation of the unsafe structures can be substantially reduced by improved, more cost-effective remediation techniques. A focused, aggressive, coordinated effort of theoretical development, physical modeling, and experiment is required to develop and validate the needed engineering tools.

The program is developing well-verified, practical engineering tools to assess the safety of dams and reservoir control structures (such as intake towers, spillways and gated outlet works), and to remediate dams and control structures found to be unsafe. These tools include advanced field-investigation techniques, physical modeling of the failure processes of the dam-reservoir-foundation systems during earthquakes, cost-effective remediation techniques for dams with deficient seismic stability, and verification of behavior of roller-compacted concrete during earthquakes so that we can use this cost-effective construction process of remediation of seismically susceptible dams and for new construction.

The primary EQEN payoff is avoiding remediation costs for dams that today are judged unsafe only because of the inadequacies in current assessment techniques, and, when remediation is required, avoiding over-construction. Using the tools developed in this research program, the Corps will realize: $100M reduction in remediation costs for each intake tower found to be safe with new methods; a $200M savings for each concrete dam and $50M for each embankment dam found to be safe with more advanced analytical methods. In addition, field

---

[1] Director, Civil Works Research and Development, US Army Corps of Engineers, Washington, DC

investigation costs will be reduced from $500K to $200K per dam (overall projected cost avoidance of more than $50M for the 200+ dams at risk), and there will be reduced uncertainty in seismic damage to dams and increased safety for all Corps dams.

2. RESEARCH PROGRAM PURPOSE

EQEN focuses on the seismic safety of reservoir dams--the Corps' most critical structures from a potential loss of life perspective. Expensive remediation actions are planned for many Corps dams. These actions are necessarily conservative to overcome shortcomings in the current state of the art in earthquake engineering. The EQEN was proposed as a seven-year, $20M R&D effort focused on eliminating inadequacies in present seismic safety evaluation knowledge. Budget restructuring has extended the time length and cost of the program. There is no other national program at this time to develop seismic safety evaluation criteria for our critical Civil Works structures. This program offers the potential for vast cost savings in seismic remediation efforts by performing focused research to ensure that safe dams are not remediated, and dams that are unsafe are remediated as quickly and efficiently as possible.

Even once a logical line of reasoning has been developed to solve the problem, the solution involves a great deal of uncertainty, and may be tentative because of new knowledge provided when earthquakes occur, or because a major state-of-the-art advance may necessitate revisions. To compensate for these shortcomings, we attempt to make design decisions that we hope are sufficiently conservative. The problem is compounded by the fact that most Corps dams were built at a time when earthquake engineering was in its infancy. The problem becomes even more difficult to solve if remediation is required. Examples of these problems were encountered in the seismic safety evaluations for Barkley Dam, Folsom Dam (see figure 2), Sardis Dam, Success Dam, Seven Oaks Dam, and Olmsted Locks and Dams.

The EQEN Program was thus developed to provide a focused research program to improve our ability to assess the seismic safety of our unique Corps Civil Works projects. The cost of partial failure of even one facility will be much greater than the cost of the proposed program. Conversely if even one Corps dam did not need remediation as a result of improved criteria, the cost savings would exceed the program outlay.

2.1 SCOPE OF THE CHALLENGE

At least thirty-nine U.S. States have significant seismic hazard posing a life-safety risk. Consequently, most of our existing dam projects are subject to some degree of seismic hazard and were designed and built at a time when this hazard was not well understood. The Corps has identified at least 200 reservoir dams and 73 intake towers as potentially subject to significant levels of earthquake shaking. With the large levels of uncertainty inherent in present seismic safety evaluation procedures and the consequent need for conservatism, several of these dams and all of the intake towers would be found in need of remediation.

In order to assess the seismic safety of our Corps reservoir dams, we need to be able to reliably predict the ground motions for design, and the amount of damage these ground motions will cause to our projects. Although there have been advancements over the last three decades, the present state-of-the-art in earthquake engineering falls far short of our needs. Consequently, every time the Corps faces a serious seismic safety evaluation, the study turns into a research project that takes a long time and requires experimentation in the laboratory, in the field and on the computer.

Civil Works research in earthquake engineering has led to the ability of the Corps to remediate seismically unsafe dams instead of direct dam replacement. Research activities associated with recently completed remediation at Sardis Dam in Mississippi, for example, results in economic savings of more than $200 million for replacement of a main portion of the dam and

averted more than $600 million for replacement of the entire dam and potentially averted more than $60 billion in losses if the dam failed.

2.2 RESEARCH STRATEGY

The EQEN cooperates with and draws from the basic and applied research elements provided by other Corps R&D efforts, other federal agencies, and academic and professional experts, and extends and integrates these elements with in-house work to address Corps seismic safety issues. EQEN is formulated to contain a balance of short-term work units design to address immediate questions related to currently used methods of analysis, and longer-term efforts to provide better methods with stronger theoretical foundations and greater validation. The program was developed by a combination of input from field offices, OCE Technical Monitors and earthquake engineering researchers.

The program content was formulated through discussions of problems encountered in seismic safety evaluations of Corps projects and an examination of shortcomings in each step of the evaluation process. The program thus forms a matrix with the steps in the solution process applied to the reservoir dam structures of concern. The structures of concern in reservoir dam safety are embankment dams, concrete dams and outlet works. The steps in the solution process are a) defining the earthquake ground motions, b) determining the site characteristics, c) assessing the damage these motions will cause to the site, and d) designing appropriate remediation if needed. Through these efforts, the EQEN Program was established as a multi-year approximately $20M effort. The program will also leverage existing research facilities to push the state-of-the-art in carrying out their research (see figure 4).

As a result of this program, we want to have better estimates of the earthquake ground motions to use in design and we want to be able to predict more accurately and quantitatively the amount of deformation and damage these ground motions will cause to our facilities. If remediation is found necessary, we want to have effective, efficient options to select from and practical tools to design and implement a remedial action.

The elements required to do this are developed from the solution process: 1) evaluation of the seismic hazard, 2) site characterization and conceptualization, 3) modeling the material behavior and computing the expected damage. The development of effective, economical remedial measures puts even greater demands on steps 2 and 3, since the materials are now complex composites, possibly requiring a three dimensional analysis to evaluate. It is the underlying plan of this research program to provide practical products from each work unit that work together to achieve the advancement in the state-of-the-art we seek.

3. GEOTECHNICAL WORK UNITS

The geotechnical work units address the steps involved in solving a seismic problem for embankment dams: earthquake ground motions, site characterization, liquefaction-deformation-damage assessment, and remedial measures.

3.1 EARTHQUAKE GROUND MOTIONS

Knowledge of the behavior of ground motions advances with each new earthquake and breakthroughs in basic research by seismologists. The ground motion work units will maintain cognizance of these advances and translate the aspects important for engineering analysis into usable tools to provide ground motion input for analysis in the form needed as computational ability advances. These work units are thus closely coordinated with the development of structural and geotechnical numerical models.

3.2 SITE CHARACTERIZATION

Present methods of site characterization rely mainly on individual borings to provide key information about stratigraphy, velocities and penetration resistance. The work units in this area propose to 1) develop improved geophysical

techniques to link together borehole information, and to directly measure soil parameters needed for analysis, and 2) resolve the present controversy regarding interpretation of Becker Hammer measurements widely used in liquefaction evaluation of gravelly soils, and possibly develop a new in situ testing tool that is more amenable to direct analysis, so that the translation of field information to inputs needed in numerical analysis is as seamless as possible.

3.3 LIQUEFACTION-DEFORMATION-DAMAGE

The present procedures for assessing liquefaction potential and post earthquake stability rely almost exclusively on empirical correlations between penetration resistance and cyclic and residual strength. These procedures do not provide a basis for quantitatively predicting deformations and assessing damage. Advances have been made in developing more fundamental constitutive models and numerical dynamic analysis codes that can solve large-deformation problems. To advance beyond present procedures it is proposed to perform a combination of physical and numerical modeling research to:

* Critically examine the shortcomings of existing Seed procedures through two focused series of centrifuge experiments which will provide direct observation of underlying mechanisms of behavior of liquefying materials and the deformations that result (Figure 3 Centrifuge Facility). These tests will provide quantitative measurement of residual strength and poorly understood "correction factors": such as K_{sigma} and K_{alpha}; simplified guidance for controlling foundation features necessary to experience large deformations; an improved method of interpreting more traditional laboratory test results; measurement of the actual damage that deformations cause to internal structures such as filter and core zones; and a full-scale performance data base against which various numerical models can be tested.

* Critically examine the present state of development of fundamental constitutive models and large deformation numerical dynamic analysis codes to provide guidance for choosing among them in the short term, and to select the most promising for development, verification, simplification for practical use in the long term. To resolve remediation problems, this effort must work towards a three-dimensional analysis capability.

3.4 REMEDIATION

Efforts to advance remediation guidelines have been slowed by the cost of full scale field testing and the difficulty in generalizing results since remedial actions are very site specific. The centrifuge (Figure 3) gives us the opportunity to perform these full scale tests on a wide variety of remediation geometries to test our ability to compute their effectiveness. It is proposed to perform such a series of centrifuge tests, and later in the program, to design a test to examine the actual state-of-stress and density field that exists in remediated soils, since this stress history plays a major role in the future cyclic behavior of the soil. These efforts, combined with lessons learned from actual remediated sites should provide a basis for improved guidance so that we only remediate as much as actually needed.

4. STRUCTURAL WORK UNITS

The structures work units are designed to develop the necessary analytical tools and corresponding guidance to predict the dynamic response of concrete dams and outlet works from elastic behavior to the development of failure mechanisms. The understanding of the dynamics of the structural response will allow the determination of the ultimate capacity of these critical structures. The work units necessary to develop these products are divided into the areas of concrete dams, outlet works, and earthquake analysis tools.

4.1 CONCRETE DAMS

This work will focus on determining dynamic ultimate capacity of conventionally place and roller-compacted concrete dams. These work

units will address the nonlinear behavior and failure mechanisms of the different types of dams as well as include component tests, scale model tests, and tests of existing structures.

4.2 OUTLET WORKS

This work focuses on determining the ultimate capacity of intake towers and the ductility of other than lightly reinforced concrete members. One major work unit will determine the ductility of lightly reinforced structures. The other work units will focus on other aspects on nonlinear behavior and failure mechanisms of these reinforced concrete structures.

4.3 COMPUTATIONAL TOOLS

These efforts will develop numerical tools to support the dams and outlet works areas. These work units will product time-domain numerical analysis tools compatible with the nonlinear materials models, and postprocessing tools to aid in the interpretation and understanding of output from time-history and response spectrum analyses. Other work units will support the appurtenant structures to the outlet works and dams. These work units will address dynamic earth pressures on walls and the dynamic response of piles.

4.4 INTAKE TOWERS

Existing Corps inake towers of outlet works of dams were designed using the seismic coefficient methods which incorrectly estimates demands placed on an intake tower during a major earthquake. The success of these lightly reinforced concrete towers in resisting failure is dependent upon the magnitude of the earthquake loads and the structural details controlling the nonlinear dynamic response and failure mechanisms of a specific tower (see figure 4). Currently available analysis tools and engineering guidance for intake towers do not properly include these factors.

The research effort will concentrate on evaluating the inherent ductility of existing intake towers. The initial effort will include a survey of existing intake towers to examine their location hazard and the variation of structural parameters. Primarily, the research effort will be a computational and experimental effort to generate a valid structural model representative of those found in the population of existing intake towers. It will include an examination of the performance of reinforcing bar details (lap lengths, development lengths, bond forces, and joint details), substructure experimentation (compression, shear, and moment effects), model tower experimentation (failure mechanisms and bridge/tower interaction), and perhaps nondestructive and destructive testing of a full-scale prototype tower.

5. COORDINATION

Partnering and cooperative research programs are an essential element of the EQEN Program. Current joint efforts include:

* Collaborative studies with NIST, TVA, NSF, DOE, and Japan through UJNR

* International contacts - Japan, China, Turkey, UK, Canada, and Panama

* Corps, FHWA, NCEER - Highway Seismic Research Programs funded by FHWA, executed by NCEER, leverages Corps funding for reinforced concrete and retrofit research.

* Corps, NIST researcher cooperation at NIST Building and Fire Research Laboratory

* Corps, NSF, Quest Structures, Inc. - Full-scale shaking experiments at Donjian Dam (see figure 5) China (1992) for subbottom absorption studies; Planned experiment in 1998 at another concrete arch dam in China.

* Corps, NSF/Quest Structures, Inc./USBR - Geophysical seismic reflection coefficients measured at seven concrete dams in cooperatively funded subbottom absorption study.

6. CONCLUSIONS

The Earthquake Engineering Research Program addresses both the geotechnical and structural aspects of water resources facilities with participation by other federal and state agencies and academic and professional experts. The activities include:

(1) Geotechnical: Development of a) criteria for selecting three-dimensional design earthquake ground motions and characterizing earthquake input required for the design of new and remediation of existing water resource facilities; b) cost-effective, reliable methods to determine site characteristics relevant to seismic performance; to determine, in three dimensions, the extent of potentially liquefiable materials subject to ground failure; and to determine, in three dimensions the adequacy of remedial actions such as ground improvement construction; c) reliable, nonlinear analysis methods to predict the capacity of earth structures to resist damage when subjected to seismic stresses and large, earthquake-induced deformations, and d) development of innovative, least cost, yet reliable remedial measures to strengthen embankment dams and their foundations if necessary.

(2) Structural: Development of a) methods of analysis to predict the extent of damage and ultimate capacity of conventionally placed and roller-compacted concrete dams and reservoir control structures subjected to strong earthquake ground motions, b) least cost remedial measure to strengthen these dams and structures if necessary; c) a material model for predicting nonlinear structural response caused by cracking and large displacements in concrete materials; d) methods for structure-reservoir-foundation interaction analyses that included hydrodynamic effects of the reservoir, uplift pressures beneath the dam, and interaction of the concrete dam with the surrounding rock foundation.

(3) The R&D results from EQEN form the basis for input to Corps guidance documents (ETL, EC, EM), and are put into practice in ongoing seismic safety evaluation projects as results on improved procedures become available. In addition to technical reports and professional papers, the R&D results in improved software, data bases and the aviablity of user manuals to all Corps District offices. In some cases this occures directly and in other cases it is through special projects such as CASE and CAGE. The R&D results form input to workshops seminars, conference presentations and training courses such as PROSPECT courses. For example, more than 100 copies of the Corps shear wave velocity data bases have been distributed to Corps offices, universities, and private industry. This data base provides key input properties for preliminary screening analysis of site response to earthquake ground motions.

7. ACKNOWLEDGMENTS

The author gratefully acknowledges the information and support provided by Dr. Mary E. Hynes, EQEN Program Manager, at the US Army Corps of Engineers Waterways Experiment Station.

8. REFERENCES

Earthquake Engineering Research Program Review Report, US Army Corps of Engineers Waterways Experiment Station, Vicksburg, MS, April 1997

Assessment of Earthquake Engineering for Dams and Related Facilities, Civil Engineering Research Foundation, Washington, DC August 1995

US Army Laboratory of the Year Award Report, Corps of Engineers Waterways Experiment Satation, Vicksburg, MS, January 1996

Seismic Hazard Map

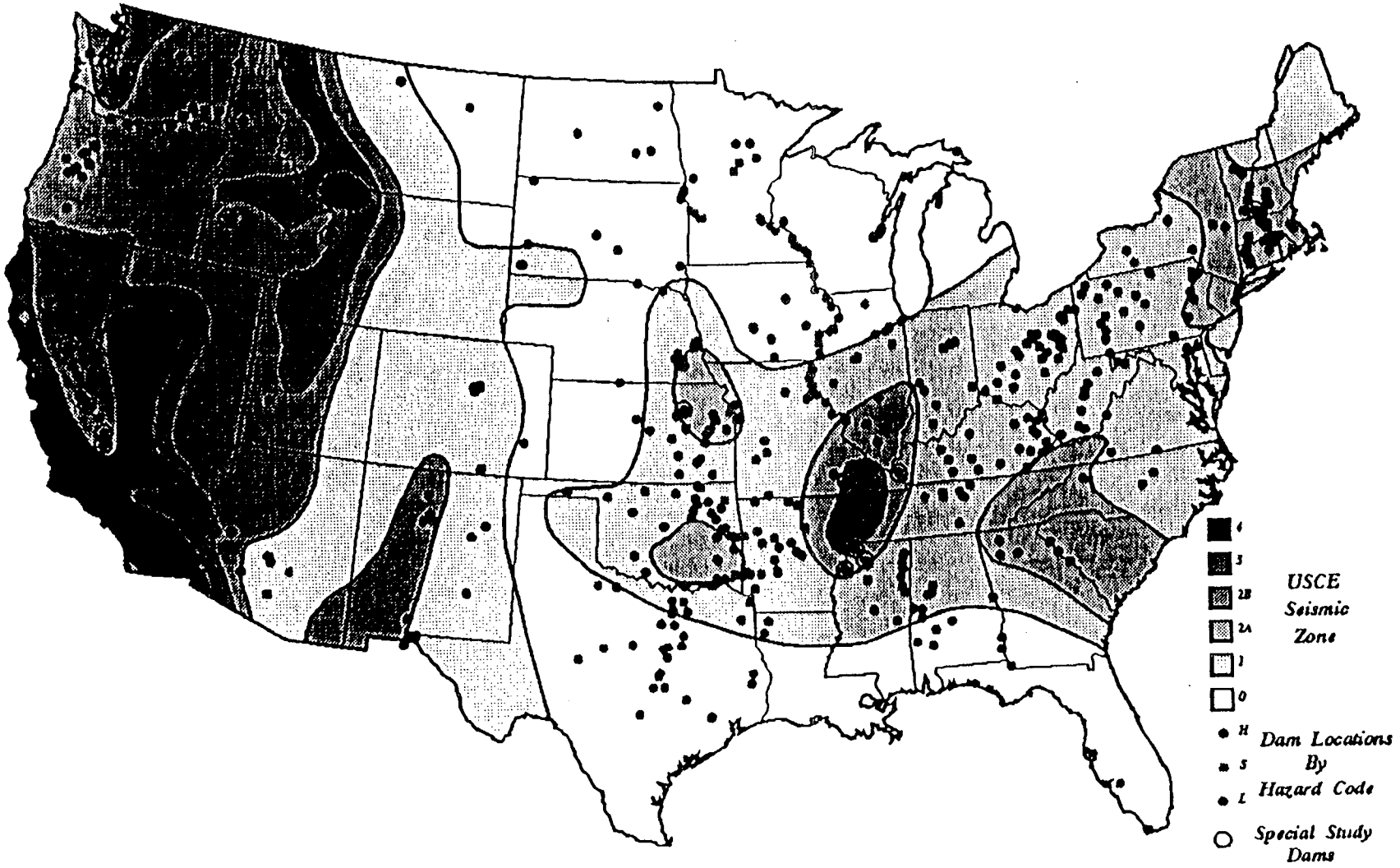
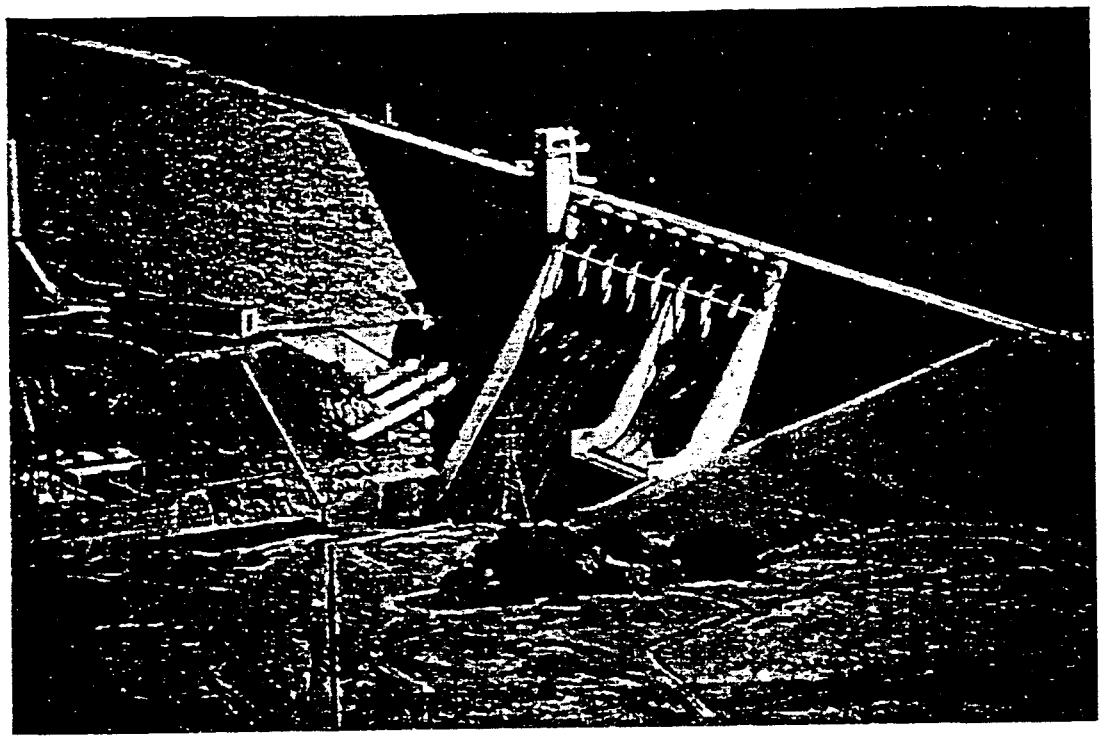


Figure 1. Seismic Risk Zones and Dam Locations



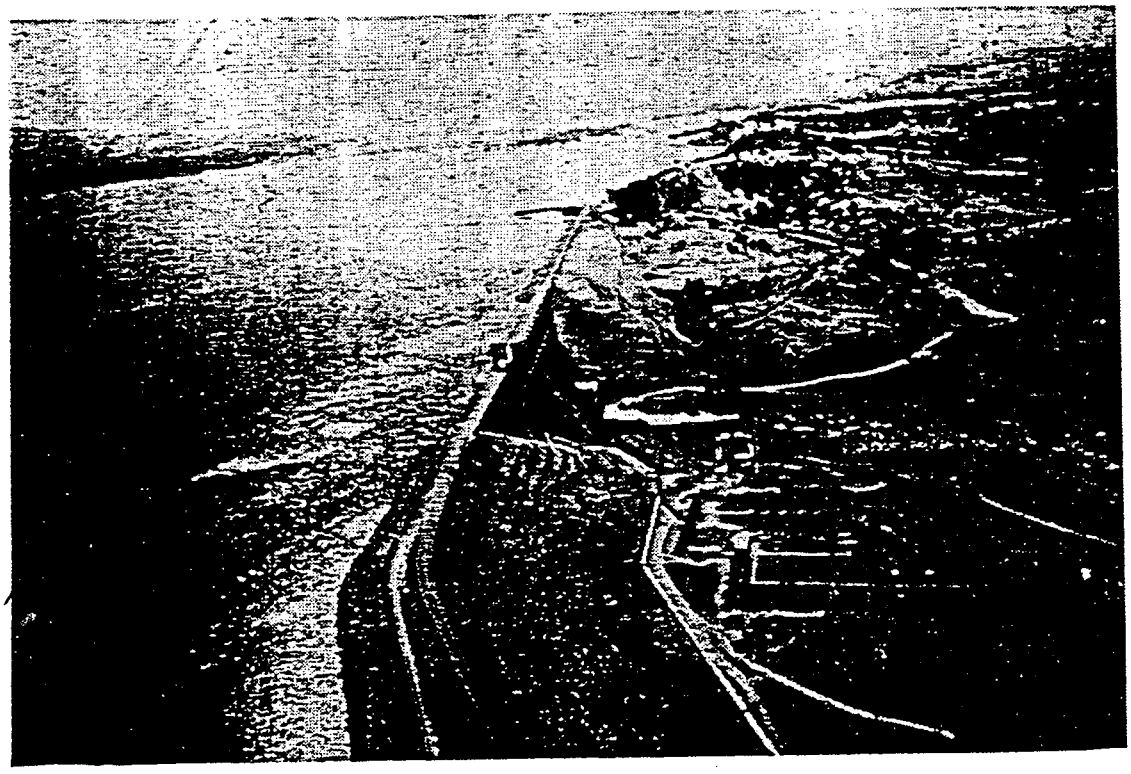
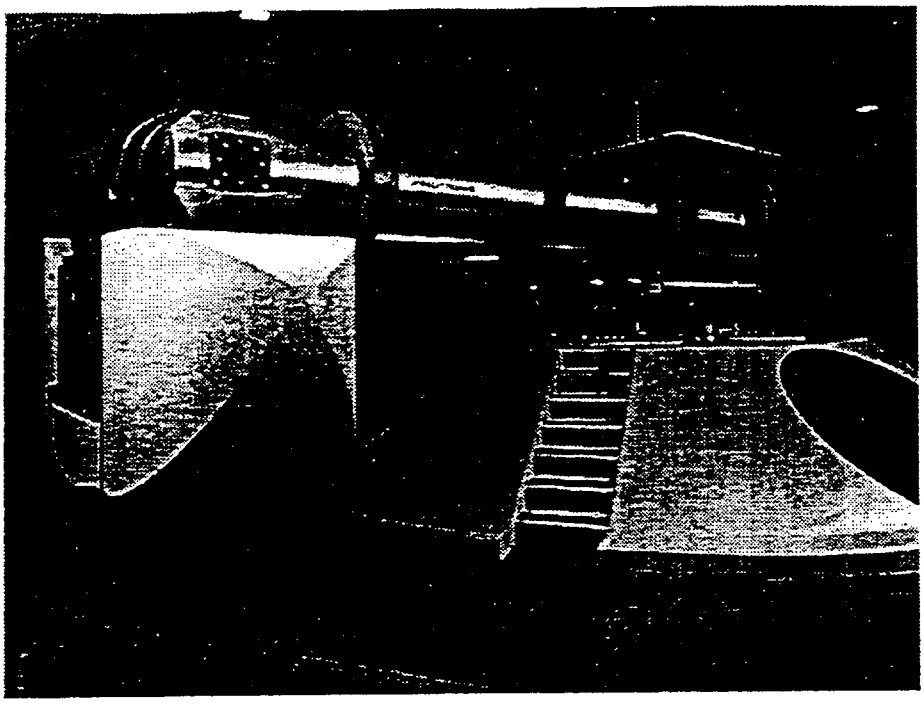


Figure 2. Ariel Views of Folsom Dam and Reservoir



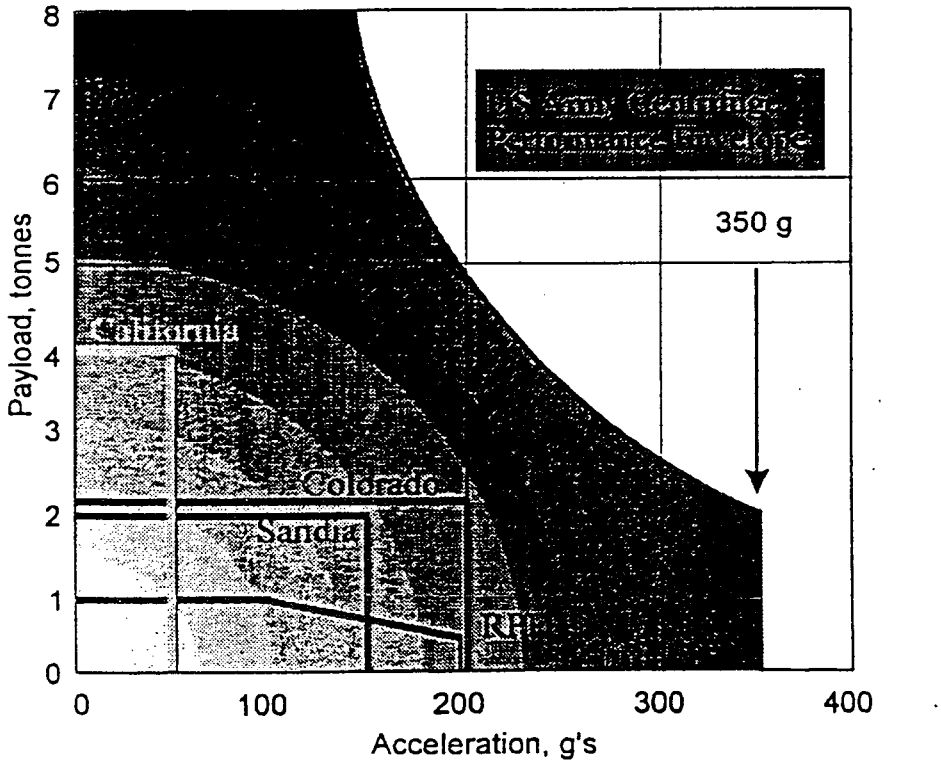


Figure 3. Corps of engineers Geotechnical Centrifuge and Performance Characteristics

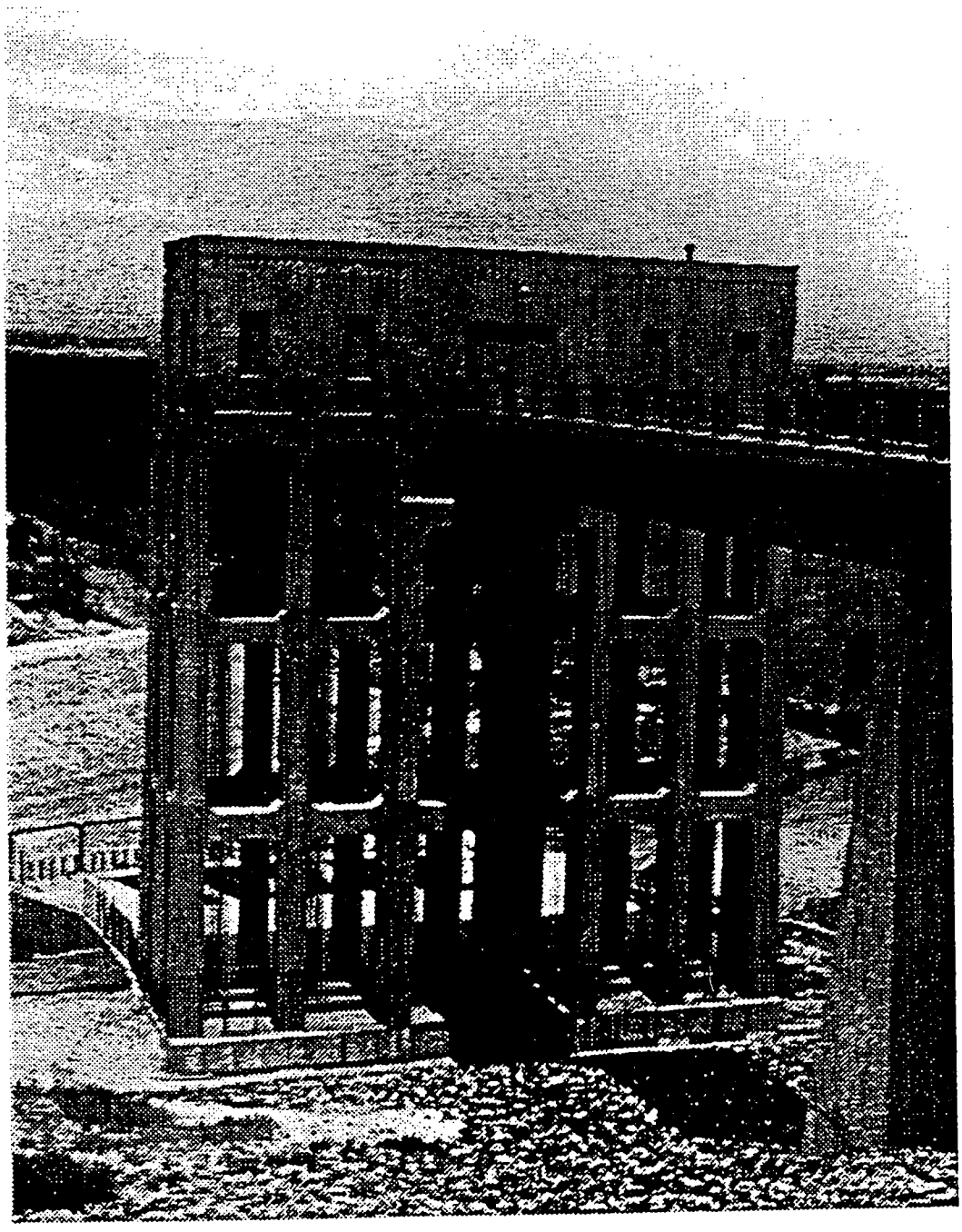


Figure 4. Intake Tower Structure of Prado Dam

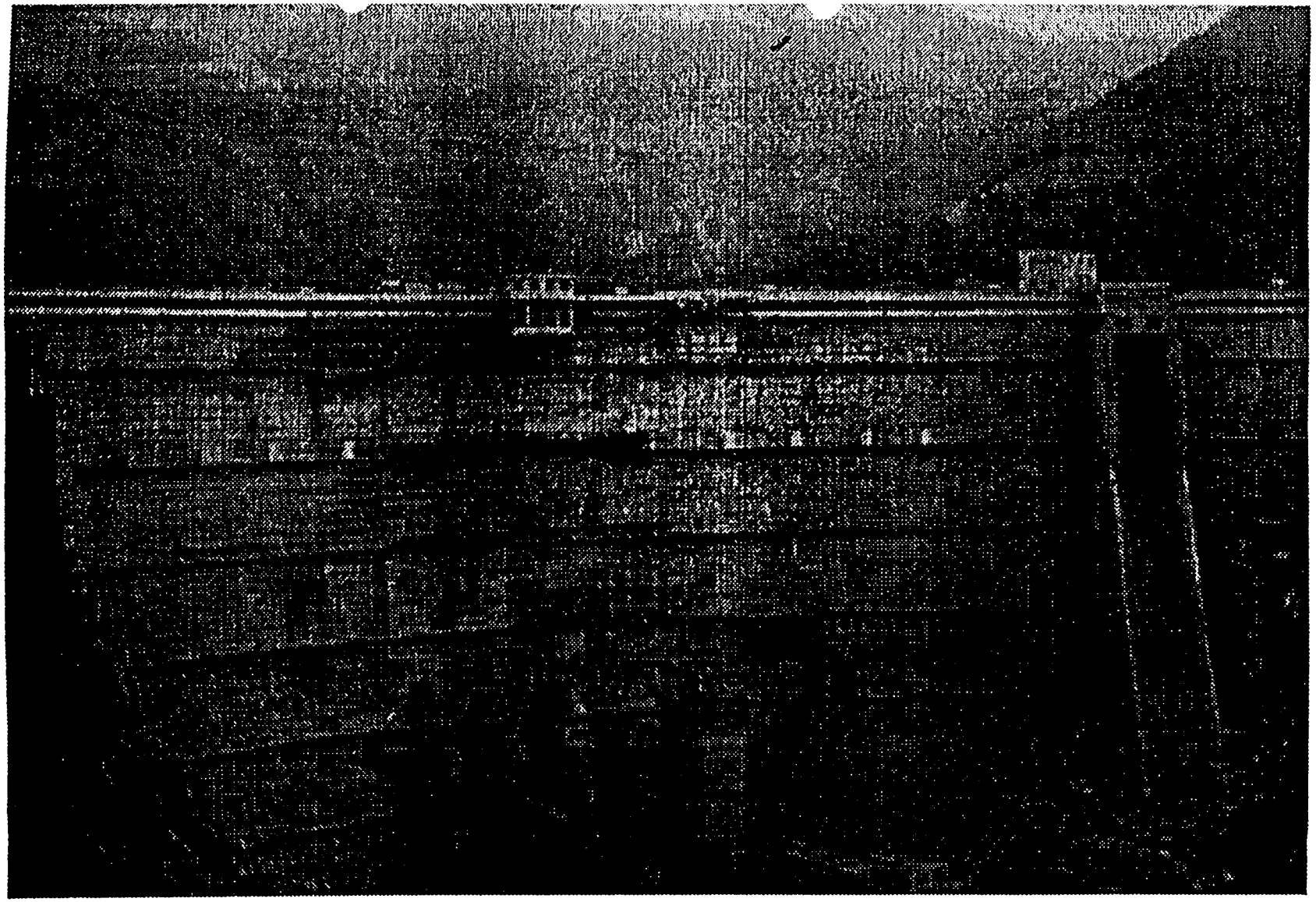


Figure Donjian Dam and Spillway in the Peoples Republic of China

National Strong-Motion Program of the U.S. Geological Survey

by

Mehmet Çelebi[1]

ABSTRACT

The purpose of this paper is to provide current information related to the United States Geological Survey (USGS) National Strong Motion Program (NSMP). The significant part of the information provided can be found on the USGS Web Site: **agram.wr.usgs.gov (Figure 1)**.

KEYWORDS: strong-motion, building, attenuation, spectra, web page, structural response, frequency

1. INTRODUCTION

The occurrence of earthquakes from coast to coast of the conterminous United States as well as in Hawaii, Alaska and Puerto Rico necessitates a well coordinated, cooperative and financially and organizationally stable National Strong Motion Program [NSMP]. The only organization that has the human resources to accomplish the objectives of such a program is the United States Geological Survey (USGS).

The NSMP is dedicated to investigating strong earthquake shaking at soil and rock sites throughout the United States, and its potential impact on engineered structures. These investigations of strong shaking are fundamental and are critically needed for support of seismological studies of source-site effects and, in particular, those engineering efforts aimed at establishment of rational zoning criteria and improvement of seismic design code provisions. The Program's consistency of strong-motion recording and long-term effectiveness are well-illustrated by selected accelerograms (Figure 2), which were recorded during significant U. S. earthquakes that occurred during the past sixty-two years.

The USGS National Strong Motion Program is coordinated in three general components:

A. Operations
B. Data Management
C. Research

The Program is cooperative in the sense that it has agreements with other federal and state agencies and other public and private institutions.

The program has a very significant research component that aims to complement and support mitigation efforts.

The purpose of this paper is to review the background of the USGS National Strong Motion Program (NSMP) and to discuss its current status as well as possible future improvements and developments. Most of

[1] Research Civil Engineer, Earthquake Hazards Team, U.S. Geological Survey, Menlo Park, Ca., USA 94025

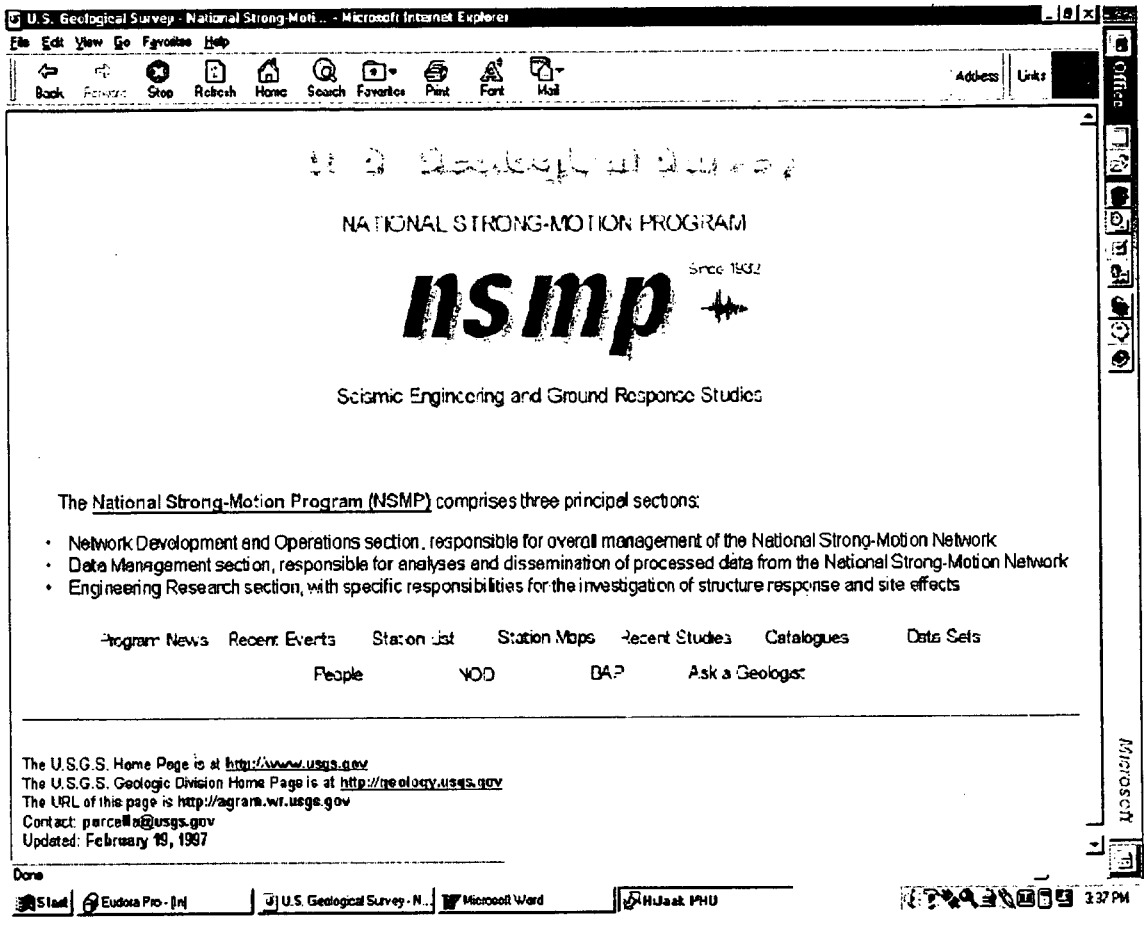


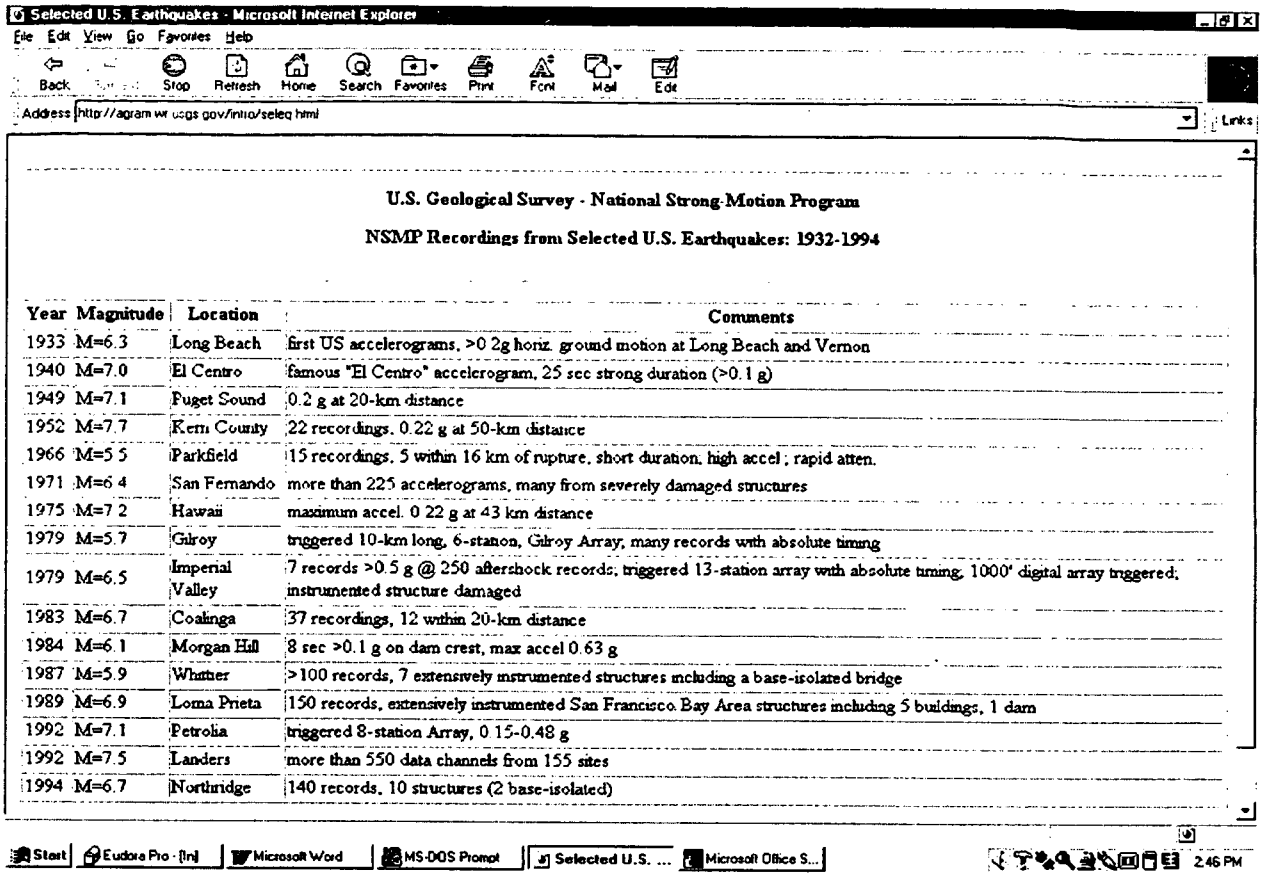
Figure 1. Introduction to the USGS-National Strong Motion Program **[http://agram.wr.usgs.gov] web page.**

the materials presented herein are directly quoted or derived from the web site of the USGS-NSMP **[http://agram.wr.usgs.gov].** The introduction to the web page is shown in Figure 1.

2. HISTORY

The history of strong-motion recording in the United States has roots in the World Engineering Congress that convened in Tokyo in 1929. American engineers returned from these meetings were convinced that there was an immediate need for the United States to develop a rugged seismograph able to record potentially damaging ground motions and to monitor the response of critical structures during strong local earthquakes. In 1931, U. S. Congress allocated additional funds to the Coast and Geodetic Survey for establishment of an engineering seismology program, including the development of a strong-motion seismograph (accelerograph), and the implementation and operation of a national strong-motion network.

The first U. S. accelerographs were installed in southern California in the summer of 1932; by 1972 the network included 575 accelerographs at permanent stations located throughout the United States and in Central and South America. Network responsibilities were transferred to the



U.S. Geological Survey - National Strong-Motion Program

NSMP Recordings from Selected U.S. Earthquakes: 1932-1994

Year	Magnitude	Location	Comments
1933	M=6.3	Long Beach	first US accelerograms, >0.2g horiz. ground motion at Long Beach and Vernon
1940	M=7.0	El Centro	famous "El Centro" accelerogram, 25 sec strong duration (>0.1 g)
1949	M=7.1	Puget Sound	0.2 g at 20-km distance
1952	M=7.7	Kern County	22 recordings, 0.22 g at 50-km distance
1966	M=5.5	Parkfield	15 recordings, 5 within 16 km of rupture, short duration, high accel.; rapid atten.
1971	M=6.4	San Fernando	more than 225 accelerograms, many from severely damaged structures
1975	M=7.2	Hawaii	maximum accel. 0.22 g at 43 km distance
1979	M=5.7	Gilroy	triggered 10-km long, 6-station, Gilroy Array; many records with absolute timing
1979	M=6.5	Imperial Valley	7 records >0.5 g @ 250 aftershock records; triggered 13-station array with absolute timing, 1000' digital array triggered; instrumented structure damaged
1983	M=6.7	Coalinga	37 recordings, 12 within 20-km distance
1984	M=6.1	Morgan Hill	8 sec >0.1 g on dam crest, max accel 0.63 g
1987	M=5.9	Whittier	>100 records, 7 extensively instrumented structures including a base-isolated bridge
1989	M=6.9	Loma Prieta	150 records, extensively instrumented San Francisco Bay Area structures including 5 buildings, 1 dam
1992	M=7.1	Petrolia	triggered 8-station Array, 0.15-0.48 g
1992	M=7.5	Landers	more than 550 data channels from 155 sites
1994	M=6.7	Northridge	140 records, 10 structures (2 base-isolated)

Figure 2. Selected Recordings of USGS-NSMP

National Oceanic and Atmospheric Administration's earthquake program in 1970; in 1973 (with National Science Foundation funding), the entire strong-motion program was absorbed by the Department of the Interior, U.S. Geological Survey, as part of the National Earthquake Hazards Reduction Program. **The National Strong-Motion Program currently operates nearly 900 strong-motion recorders at approximately 550 permanent stations located in 33 States and the Caribbean.**

3. COOPERATIVE PROGRAMS:

The U. S. Geological Survey's National Strong-Motion Program (NSMP) has evolved over more than six decades; the Program is primarily the result of cooperative efforts with many other Federal, state, and local agencies, private companies, and academic institutions. Key participants for whom the NSMP presently maintains instrumentation include the Army Corps of Engineers, the Department of Veterans Affairs, and the Metropolitan Water District of Southern California. Summary of participants in the USGS Cooperative Program is provided in Table 1.

4. MORE ABOUT THE WEB PAGE

4.1 DATA SETS

There is now considerable amount of the USGS data available to the user community

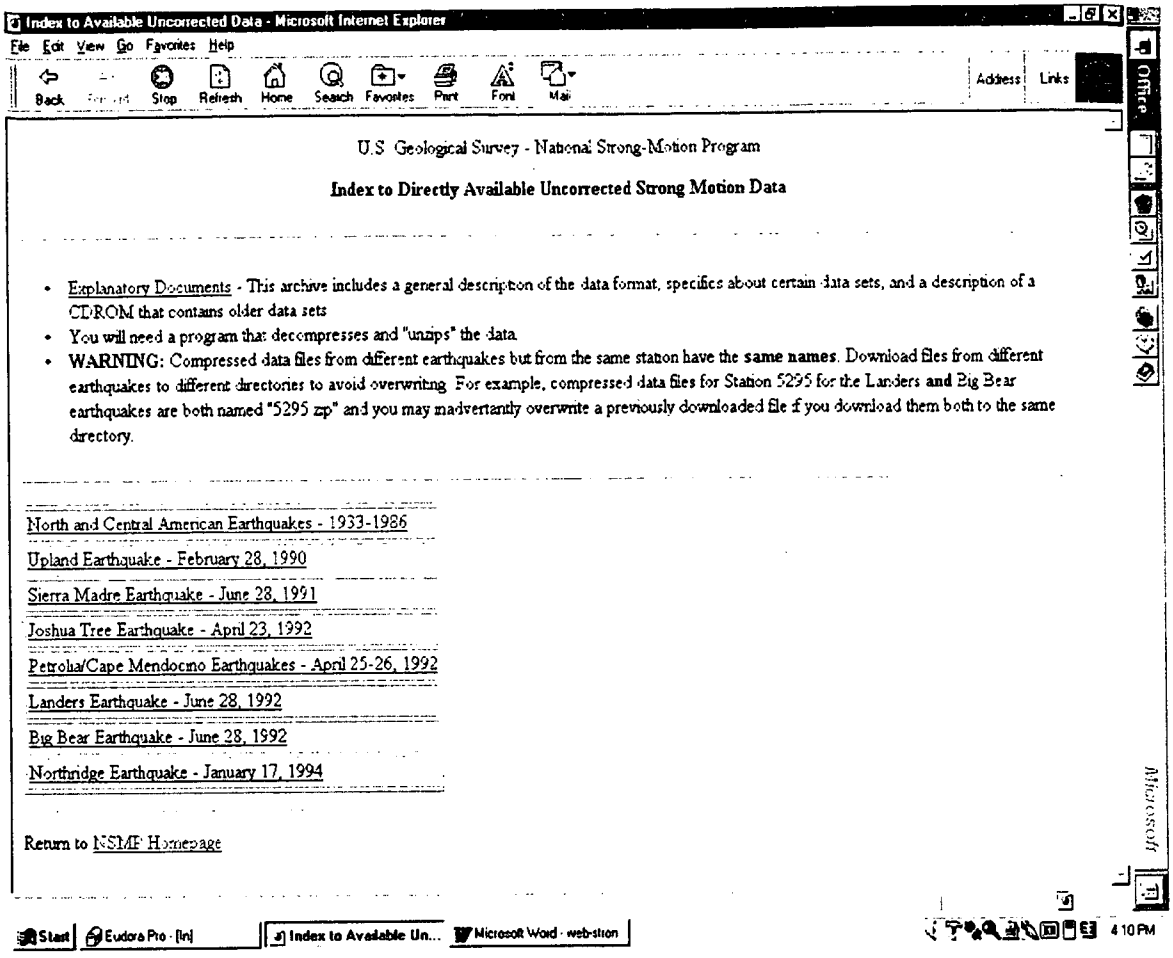


Figure 3. Web page describing the data sets available to user community

through the web. The descriptive information on the data sets is shown in Figure 3. The data can be directly unloaded. Also available on the web is the software BAP used for processing strong-motion data. This software can also be downloaded.

4.2 STATION MAPS AND LISTS

The locations of stations can be found readily on maps and in descriptive lists on the web page. The user has options for maps with faults and highways or 3-dimensional maps or topographical maps with faults for Northern and Southern California. A sample map is shown in Figure 4. A comprehensive descriptive list for all stations of NSMP is included separately. However, for Northern and Southern California, the user can click to any one of the stations and get the descriptive information for that station only. Figure 5 shows what a user can get if he/she clicks the Palo Alto VA Hospital station on the map in Figure 4.

5. RESEARCH COMPONENT

USGS research personnel conduct research using strong-motion data. The research topics encompass a wide variety of topics. Only two of them will be cited herein.

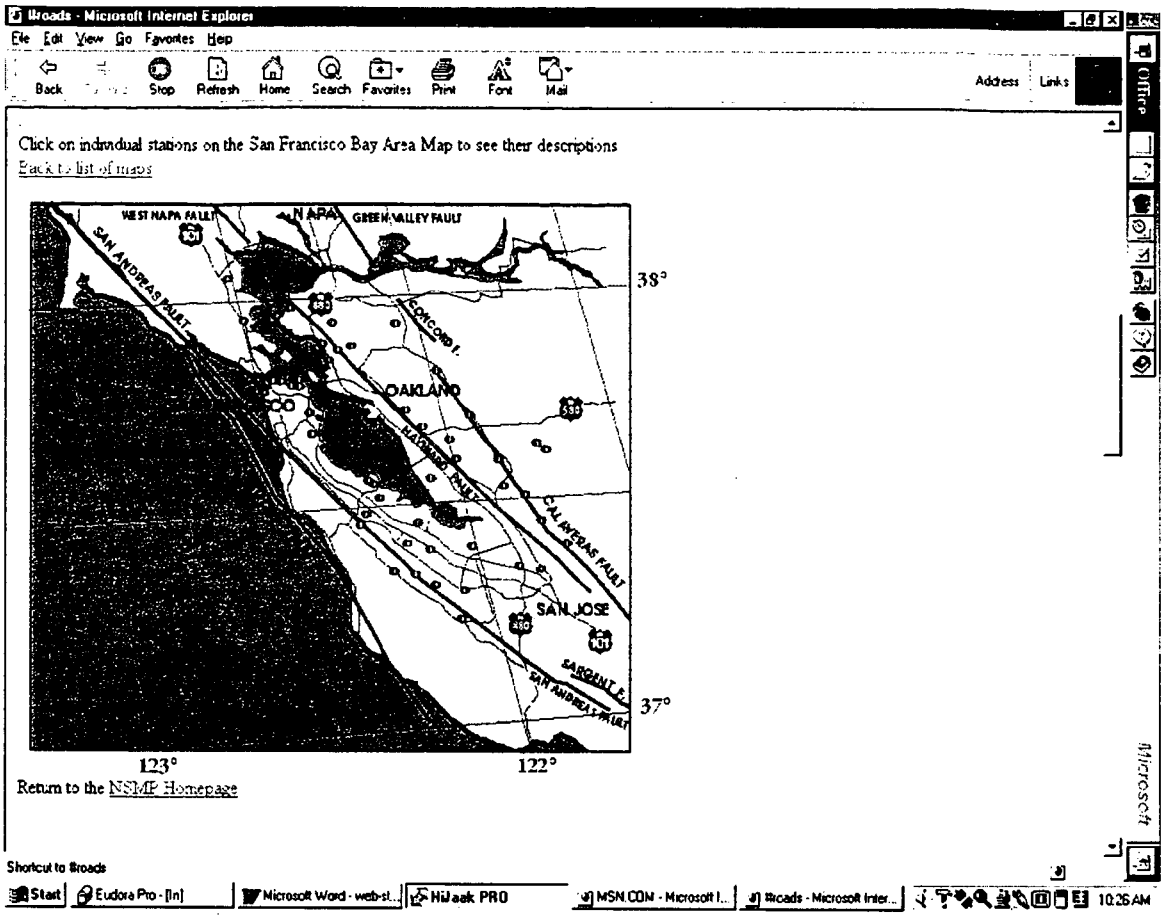


Figure 4. Sample station map on the USGS-NSMP web site.

5.1 Two Sample Research Topics of USGS-NSMP

5.1.1. Development of Attenuation Relationships

The attenuation relationships are developed by regression analyses of strong-motion data collected over many years mainly from Western United States. These relationships are used to predict peak accelerations at a site, for a specified site condition, magnitude and distance from a fault causing an earthquake. There are various definitions of the distance associated with attenuation curves (Joyner and Boore, 1996) . Figure 6 shows a sample attenuation curve (Boore, *personal communication*, 1997). In this particular figure, Boore compares Kobe (M=6.9) and Northridge (M=6.7) peak accelerations, recorded at Site Class C (V_s=180-360 m/s), with the attenuation curve for M=6.95 strike-slip earthquakes. These attenuation curves are used world-wide in various engineering projects for prediction of peak accelerations expected at a site for which a causative fault and associated earthquake magnitude is specified.

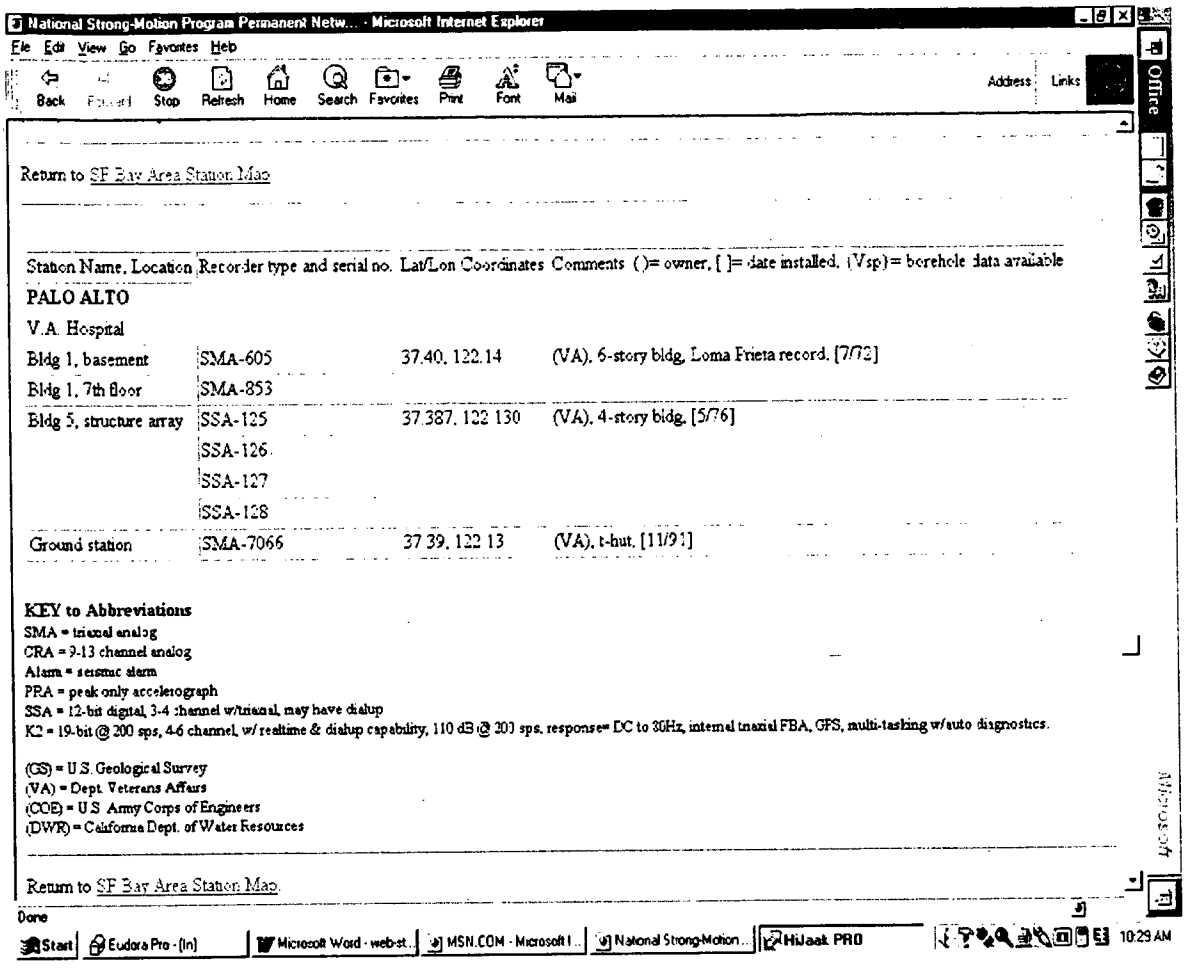


Figure 5. Descriptive information of one station identified by clicking on the map.

5.1.2. Instrumentation of Structures and Structural Response Studies

USGS-NSMP has instrumented structures throughout seismically active regions of the US. Current inventory of instrumented structures is provided in Table 2. One of the unique structures intrumented is the Pacific Park Plaza in Emeryville, Ca. Figure 7 shows Pacific Park Plaza (PPP) Building at Emeryville, Ca. The building was instrumented in 1985 with analog strong-motion recording system. PPP had 21 channels of accelerometers deployed throughout the superstructure. In addition, it had two free-field triaxial accelerographs as shown in the figure. The array recorded response of PPP and its associated free-field sites during the 17 October 1989 earthquake.

These structural response records are probably the most widely studied structural response data from the Loma Prieta earthquake (Aktan, etal., 1992, Anderson, Miranda, Bertero, 1991, Anderson and

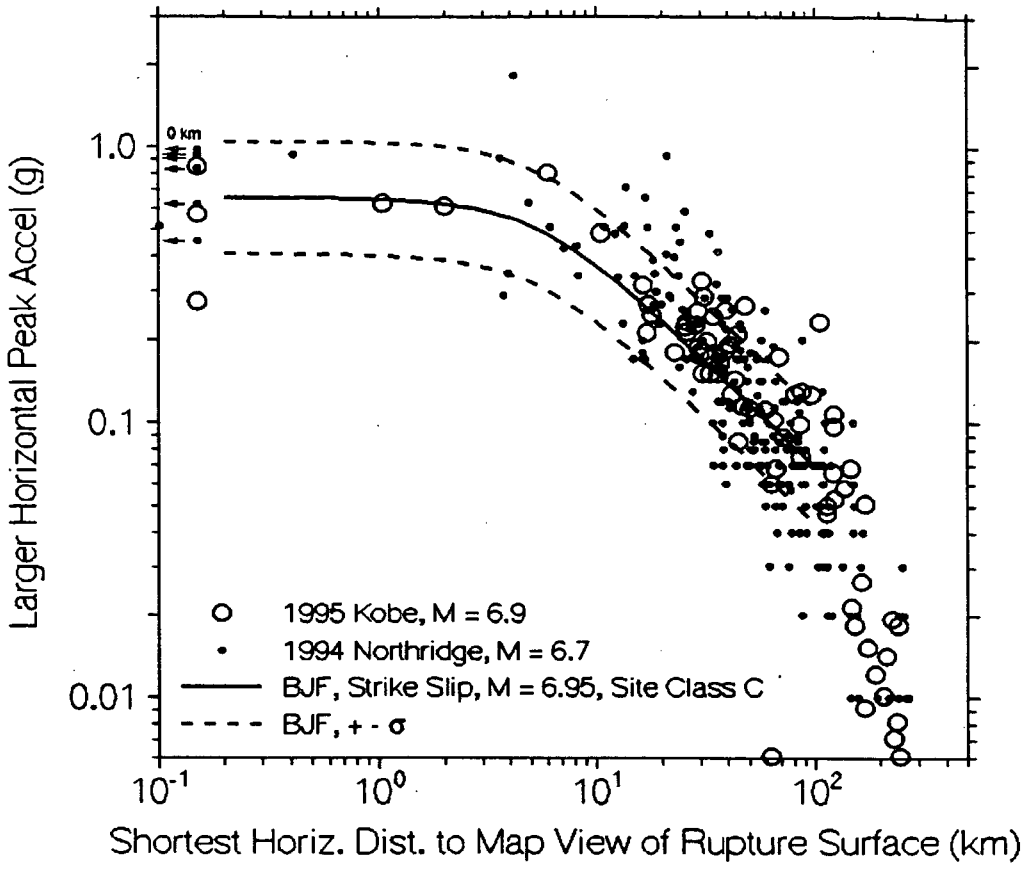


Figure 6. A Sample Attenuation Curve by Boore (*personal communication*, 1997)

Bertero, 1994, Çelebi, 1992, 1996, Çelebi and Safak, 1992, Kagawa etal., 1993,

Kagawa and Al-Khatib, 1993, Kambhatla etal., 1992 and Safak and Çelebi, 1992). Figure 8 shows the time-histories and response spectra of recorded acceleration responses at the roof, ground floor and south free-field (SFF) of the building as well as that at Yerba Buena Island (YBI), a rock site (with largest peak acceleration of 0.06 g). Both sites are approximately 100 km from the epicenter of the Loma Prieta earthquake. Response spectra of amplified motions (largest peak acceleration 0.26 g at the south free-field site [SFF]) are compared to the response spectra of Yerba Buena Island (YBI) in the figure.

Studies conducted using structural response data show that (a) the fundamental mode frequency (period) of the building is 0.38 Hz (2.63 s), (b) there is significant soil-structure interaction, (c) the critical damping percentages (12-15 %) determined using system identification techniques indicates that there is radiation damping, and (d) one wing of the building has significantly larger response as compared to the other two. For structures with wings, such as PPP, or unsymmetrical structures, the response can be significantly affected by the azimuthally variable ground motions from earthquakes with different epicenters. The free-field records have been used in assessing the amplified motions of the East San Francisco Bay and its effects on engineered structures such as the San Francisco Bay Bridge

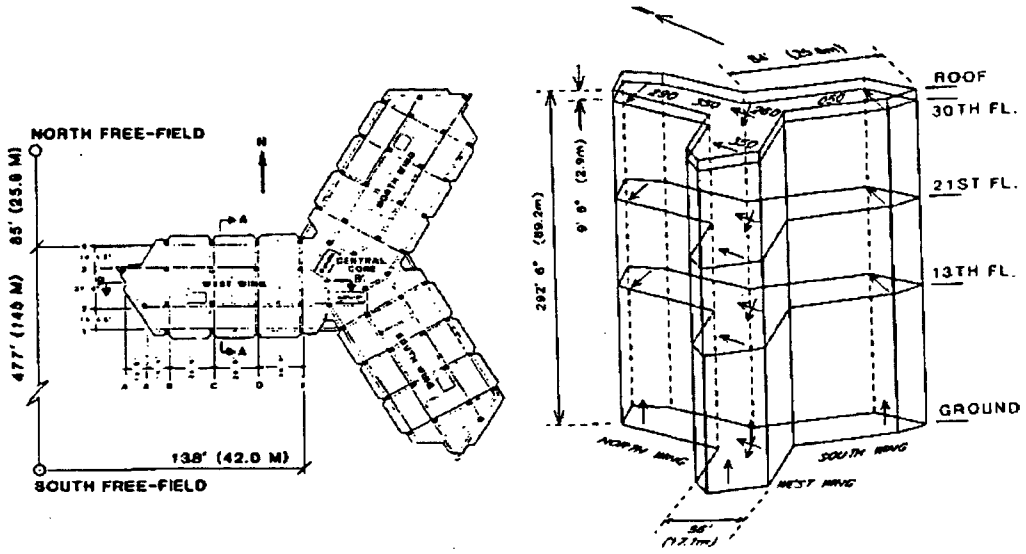


Figure 7. Plan view and three-dimensional schematic of PPP showing the location of accelerometers.

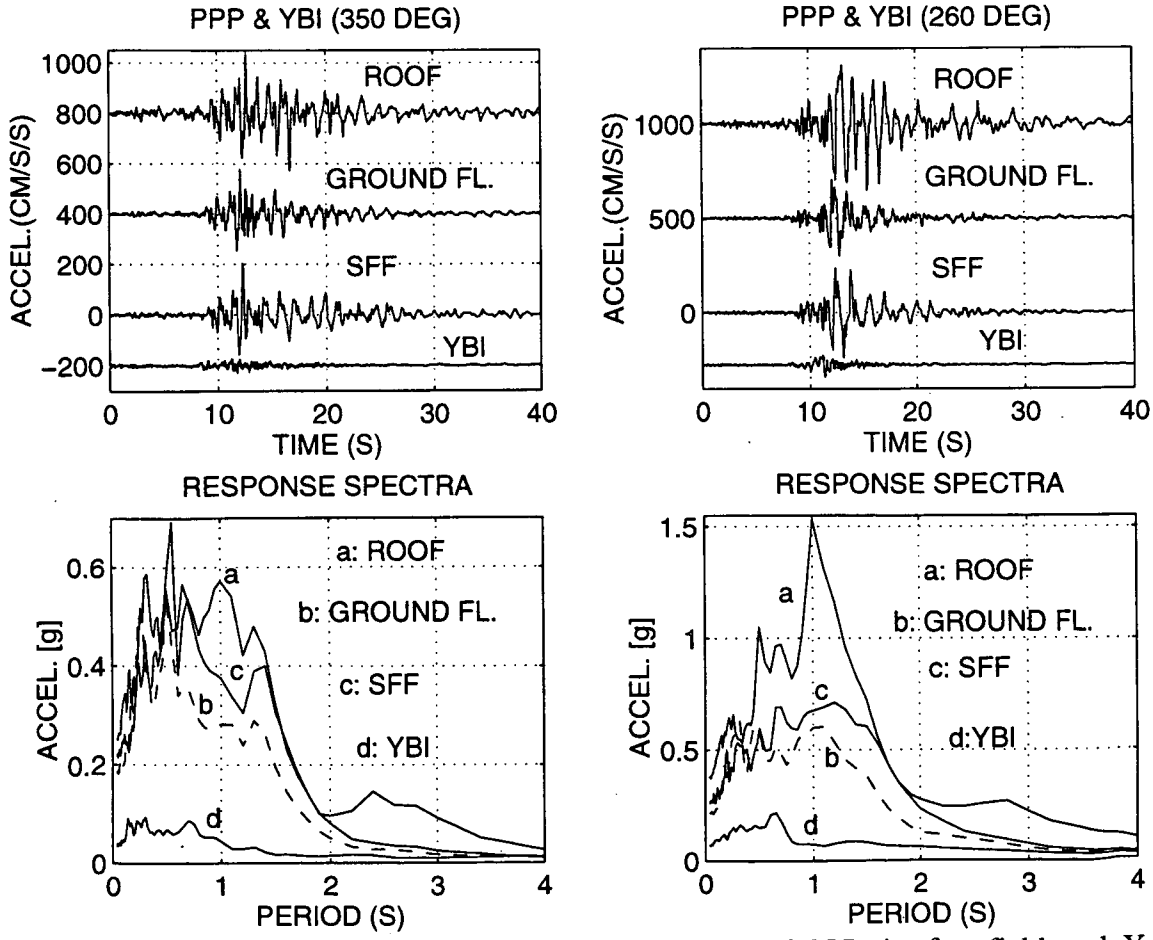


Figure 8. Recorded Ground Motions and Response Spectra of PPP, its free-field and Yerba Buena Island.

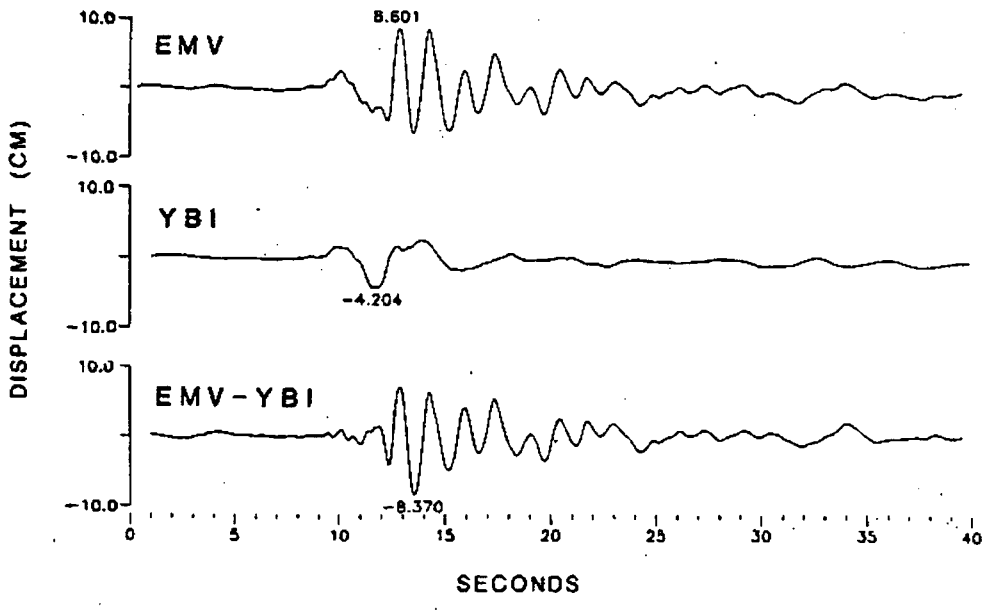


Figure 9. Displacements at Emeryville and Yerba Buena Island and Relative Displacement (from Hanks and Brady, 1991).

(Hanks and Brady, 1991). The south free-field [SFF] station shown in Figure 7 is also known as EMV[2] (designation for Emeryville). Figure 9 shows the displacements at EMV and YBI (Hanks and Brady, 1991). This figure depicts one of the possible reasons as to why one of the Bay Bridge spans between YBI and east end of Bay Bridge collapsed during the LPE. The approximate relative displacement of 8 cm between YBI and east end of Bay Bridge shows how much extension occurred between the two ends and possibly contributed to the collapse of the span.

In January 1997, a downhole accelerograph has been deployed (at 66 meters depth) at the location of the south free-field (SFF). Furthermore, the recording capability has been upgraded to a digital system. In future earthquakes, this site will produce very valuable data that will be available on the web site within a short time following the event.

7. LOOKING TO THE FUTURE

There is intensive effort to upgrade the strong-motion instruments from analog to digital. At the moment, approximately 15 % of the network is digital. In the near future, we expect to upgrade 100 % of the analog systems to digital systems.

Only a few of the special purpose experimental arrays that are in the development stage are cited below:

(a) We are developing a soil-structure interaction experiment for a building structure that will have, in addition to instruments within the building, special purpose instruments in the vicinity of the foundation, below the foundation, and on the surface near a building,

[2] In most studies, the site of south free-field (SFF) is referred to as the Emeryville site [EMV]. The data from this site is one of the most used ground motion records of the LPE strong-motion data set.

(b) Another experiment in the deployment stage is the drift experiment. Selective consecutive floors of two tall buildings are being instrumented in Los Angeles to collect data to specifically measure drift between several pairs of consecutive floors.

(c) Topographical effects have been observed during past earthquakes and their aftershocks. We are attempting to develop a topographical experiment array in an urban environment in the San Francisco Bay Area or Los Angeles.

CONCLUSIONS

The paper presents recent developments and factual information of the National Strong Motion Program of the U. S. Geological Survey. As in the past, plans are for USGS to play a leading national role in establishing and operating strong-motion networks, special purpose arrays, collection and dissemination of data and performing pertinent research for reduction of seismic hazards and improved public safety.

7. ACKNOWLEDGMENTS

This paper was prepared with the intention to provide current information of the USGS-NSMP. Information presented herein has been collected by many dedicated personnel of the NSMP. Ron Porcella is the current chief in charge of operations. Howard Bundock played a key role in initiation and updating the web site.

8. REFERENCES

Aktan, H., Kagawa, T., Kambhatla, A., and Çelebi, M., 1992, Measured and analytical response of a pile supported building, Proceedings of the Tenth World Conference on Earthquake Engineering, A. A. Balkema, Rotterdam, Vol. 3, 1992, 1791-1796.

Anderson, J. C., Miranda, E., Bertero, V. V., and Kajima Project Research Team, 1991, Evaluation of the seismic performance of a thirty-story RC building, Report: UCB/EERC-91/16, Earthquake Engineering Research Center, Univ. of California at Berkeley, July 1991, 254 p.

Anderson, J. C. and Bertero, V. V., 1994, Lessons learned from an instrumented high rise building, Fifth U.S. National Conference on Earthquake Engineering, Proceedings, Earthquake Engineering Research Inst., Oakland, California, Vol. II, 1994, 651-660.

Çelebi, M., 1992, Highlights of Loma Prieta responses for four tall buildings, Proceedings of the Tenth World Conference on Earthquake Engineering, A. A. Balkema, Rotterdam, Vol. 7, 1992, 4039-4044.

Çelebi, M. and Safak, E., 1992, Seismic response of Pacific Park Plaza—I: Data and preliminary analysis, Journal of Structural Engineering, v. 118, Issue 6, June 1992, 1547-1565.

Çelebi, M., 1996, Comparison of damping in buildings under low-amplitude and strong motions, Journal of Wind Engineering and Industrial Aerodynamics, Elsevier Science B. V., 59, 309-323.

Hanks, T. C. and Brady, A. G., 1991, The Loma Prieta Earthquake, Ground Motion, and Damage in Oakland, Treasure Island, and San Francxisco, *Bull. Seism. Soc. of America,* vol. 81, no. 8, pp. 2019-2047.

Joyner, W.,and Boore, D. M., 1996, Recent Developments in Strong-Motion Attenuation Relationships, PROC. 28th Joint Meeting on Wind and Seismic Effects of the U.S.-Japan Cooperative Program in Natural Resources, NIST Report SP 904, August 1966.

Kagawa, T., Aktan, H., Çelebi, M., 1993, Evaluation of soil and structure model using measured building response during the Loma Prieta earthquake, Dept. of Civil and Environmental Engineering, Wayne State Univ., Detroit, Michigan, June 1993, 169 p.

Kagawa, T., Al-Khatib, M. A., 1993, Earthquake response of 30-story building during the Loma Prieta earthquake, Third International Conference on Case Histories in Geotechnical Engineering, June 1-4, 1993, Univ. of Missouri-Rolla, Rolla, Missouri, Vol. I, 547-553.

Kambhatla, A. , Aktan, H. M., Kagawa, T., and Çelebi, M., 1992, Verification of simple soil-pile foundation-structure models, Structures Congress '92 , American Society of Civil Engineers, New York, 721- 724.

Safak, E. and Çelebi, M., 1992, Recorded seismic response of Pacific Park Plaza— II: System identification, Journal of Structural Engineering, v. 18, Issue #6, June 1992, 1566-1589

Table 1. Participants of the USGS-NSMP Cooperative Program

OWNER/AGENCY	STATIONS	ACCELEROGRAPHS
Army Corps of Engineers	67	190
Property Owner (Code mandated)	31	35
California Department of Water Resources	4	7
Department of Veterans Affairs	59	77
General Services Administration	2	8
Hawaii State Civil Defense	5	5
Metropolitan Water District of Southern California	20	35
Oregon Department of Transportation	5	25
University of Puerto Rico	8	8
U.S. Department of Energy	1	6
U.S. Geological Survey	325	421
Utah Geological Survey	7	7
Washington, City of Aberdeen	1	3
Washington, Tacoma Public Utilities	1	3
Washington Dept.of Natural Resources	1	4
Washington Department of Transportation	3	6
TOTALS	540	840

Table 2. Structures Instrumented by USGS-NSMP

		NUMBER OF STRUCTURES	
		Extensively Instrumented (>8 channels)	Moderately Instrumented (4-8 channels)
Buildings			
	Alaska	3	
	California	20	6
	Hawaii	1	1
	Missouri	2	
	Puerto Rico	1	1
	South Carolina	1	1
	Tennessee	2	
	Utah	1	
	Washington	2	
Bridges			
	California	2	
	Oregon	9	
Dams			
	California	19	
	Idaho	2	
	Montana	1	
	New Mexico	1	
	Oregon	13	
	Utah	1	
	Washington	6	

Seismic Hazard Criteria for the U.S. Department of Energy Reservation in Oak Ridge, TN

Karen E. Shaffer and R. Joe Hunt
Lockheed Martin Energy Systems, Inc.
Oak Ridge, TN 37831-8218

Harish Chander, EH-31, and J. K. Kimball, DP-311
U.S. Department of Energy
Germantown, MD 20874

ABSTRACT

Seismic hazard criteria have been in use at the U.S. Department of Energy (DOE) reservation in Oak Ridge, TN since the early 1950s. In response to evolving DOE Orders and technical standards, as well as significant advances in earthquake ground motion engineering, site specific seismic hazard criteria for the Oak Ridge Reservation have been developed based on the Lawrence Livermore National Laboratory and Electric Power Research Institute (EPRI) methodologies. This paper presents the site specific criteria development methodology and provides the Oak Ridge site-specific seismic hazard criteria. A comparison of the Oak Ridge site-specific seismic hazard criteria with the results obtained from 1996 U. S. Geological Survey seismic hazard maps is also provided.

The Oak Ridge National Laboratory, the Oak Ridge Y-12 Plant, and the East Tennessee Technology Park comprise the Oak Ridge Reservation. Plant operations are directed by the DOE-Oak Ridge Operations office. Lockheed Martin Energy Systems, Inc. is the managing and operating contractor for the Oak Ridge Y-12 Plant and the East Tennessee Technology Park. Lockheed Martin Energy Research, Inc. is the managing and operating contractor for the Oak Ridge National Laboratory.

KEYWORDS: criteria; ground motion attenuation; response spectra; seismic hazard

1. INTRODUCTION

The U.S. Department of Energy - Oak Ridge Operations (DOE-ORO), based in Oak Ridge, Tennessee, is rich in history, dating back to World War II when the organization played a major role in the production of materials used in the first atomic weapon. The majority of the DOE-ORO site is situated on Federal land known as the Oak Ridge Reservation. Three primary facility complexes are located on the Reservation: the East Tennessee Technology Park (formerly known as the Oak Ridge K-25 Site and the Oak Ridge Gaseous Diffusion Plant), the Oak Ridge National Laboratory, and the Oak Ridge Y-12 Plant. Administrative facilities and many support facilities necessary for plant operations are also located on the Reservation. Lockheed Martin Energy Systems, Inc. is the managing and operating contractor for the East Tennessee Technology Park and the Oak Ridge Y-12 Plant. Lockheed Martin Energy Research, Inc. is the managing and operating contractor for the Oak Ridge National Laboratory.

Since it's original mission, the DOE-ORO has expanded and today supports more than 60 major DOE activities including energy research and development programs, dismantling and storing nuclear weapons components, environmental management, landlord responsibility for the U.S. Enrichment Corporation, and various educational programs.

Seismic hazard criteria have been applied at the DOE-ORO facilities since the early 1950s. Since that time, the behavior of earthquakes in the central and Eastern U.S. has been better understood and methodologies based on this understanding have been developed. In response to evolving DOE Orders and technical standards and facility safety analysis requirements, the seismic hazard criteria for the Oak Ridge Reservation have been reevaluated using the latest Lawrence Livermore National Laboratory (LLNL) and Electric Power Research Institute (EPRI) methodologies. This paper discusses the site specific criteria development methodology and provides the Oak Ridge site-specific seismic hazard criteria.

2. LOCATION OF THE OAK RIDGE FACILITY COMPLEXES

The Oak Ridge Reservation is located in East Tennessee in the Valley and Ridge physiographic province characterized by a series of long, narrow ridges and slightly broader intervening valleys, with a pronounced northeast-southwest trend extending from Alabama to Newfoundland. Seismic activity in the area is thought to be, primarily, the result of continental compression that is reactivating old faults in the basement at depths of 3 to 12 mi.

The site has relatively shallow soil deposits overlying sound, competent bedrock. The surface bedrock is generally limestone and shales in the valleys and sandstones and siliceous carbonate rocks on the ridges. The thickness of the soil overburden ranges from 10 to 50 ft. For some critical structures, the soil overburden has been excavated and the structures' foundations are supported on bedrock.

Based on the site conditions, site-specific response spectra were developed for rock outcrop motions and are being used as input for modeling soil conditions where needed.

3.SITE-SPECIFIC SEISMIC HAZARD STUDIES

The seismic hazard criteria for the Oak Ridge Reservation are defined in terms of (1) seismic hazard curves of peak ground acceleration (PGA) and peak spectral velocities (PSV) at hard rock outcrop, for varying annual probabilities of exceedance; (2) uniform hazard response spectra (UHRS) for rock outcrop, for specified probabilities of exceedance or return periods; and (3) earthquake time histories representing rock outcrop motions that match the UHRS.

1990 - 1992 Oak Ridge Reservation Study

The seismic hazard curves and site-specific response spectra were first developed during the 1990-1992 time frame using two probabilistic seismic hazard methodologies developed for evaluating nuclear power plant sites in the eastern U. S. These two methodologies were the 1988 version of the LLNL methodology [1], and the EPRI methodology [2]. The results from the EPRI methodology were calculated by Risk Engineering, Inc. while LLNL performed the calculations using the 1988 LLNL methodology. The use of the seismic hazard curves to develop the site-specific response spectra considered the following:

- Seismic hazard results from EPRI and LLNL for PGA (rock) and peak spectral velocities (PSV) at frequencies of 25, 10, 5, 2.5, 1.0, and 0.5 Hz in order to define response spectral values. Figure 1 shows the seismic hazard curves for PGA.

- Determined the pseudo-mean PGA following the guidelines in technical standard DOE-STD-1024-92, *Guidelines for use of Probabilistic Seismic Hazard Curves at Department of Energy Sites* [3]. Examination of Figure 1 shows the LLNL and EPRI methodologies resulted in significantly different estimates of the seismic hazard. To resolve these differences and to allow the results of the two methodologies to be used consistently at all DOE sites, DOE developed the guidelines in DOE-STD-1024-92. The first step in the

guidelines was a combination of the PGA results from LLNL and EPRI to obtain a pseudo-mean PGA which considered the uncertainties from both methodologies.

- Determination of dominant magnitudes and distances for the PGA and the maximum PSV at 2.5 Hz. The second step in the DOE-STD-1024-92 guidelines was to determine the dominant magnitudes and distances. The dominant magnitudes and distances for the earthquakes controlling the hazard were determined for the PGA and the maximum PSV (at 2.5 Hz). These parameters were determined for use in the generation of representative time histories and for subsequent use in deterministic evaluations. The EPRI seismic hazard results were used to determine the dominant magnitudes and distances because their spectral velocity hazard curves gave more weight to direct spectral ordinate ground-motion models than on standard spectral shape ground-motion models. The LLNL results were not used for this purpose because their spectral velocity hazard curves were based more on the use of standard spectral shape models, rather that on direct ordinate models. The dominant magnitudes and distances for the Oak Ridge Reservation are controlled by moderate-size earthquakes (m_b of 5.6 to 6.1) at close distances (25 to 85 km).

- Development of response spectra shapes from deterministically derived spectral shapes based on the dominant magnitudes and distances. The third step in the DOE-STD-1024-92 guidelines was development of median response spectra shapes based on the dominant magnitudes and distances. Actual earthquake records with similar site conditions, magnitude, and distance were examined along with eastern U.S. ground motion attenuation models to determine the response spectra shapes.

- Anchored the median response spectral shapes to the pseudo-mean PGA to define the site-specific response spectra and developed time histories to represent the site-specific spectra. The final step in the DOE-STD-1024-92 guidelines was the definition of the site-specific response spectra obtained by anchoring the median response spectra shapes to the pseudo-mean PGA. Then artificial earthquake time histories were developed to represent the site-specific response spectra. These earthquake time histories were developed to use in the analyses of structures supported on hard rock, and for use in analyses of structures supported on soil considering the behavior of the underlying soil deposit.

After the development of the site-specific response spectra using the guidelines from DOE-STD-1024-92, there were additional concerns raised during an expert peer review about the response spectra shapes in the low frequency range. Because the hazard is dominated by small to moderate magnitude earthquakes at relatively close distances, the spectral shape did not contain any significant energy in the low frequency range. The ratio between PGA and PSV was not consistent with most ground motion attenuation models plus there is much greater uncertainty associated with PSV than with PGA. To address the peer review concerns, the following additional evaluations were performed to supplement the DOE-STD-1024-92 guidelines for determining the PSV for site-specific response spectra:

- Ratios of PSV/PGA using various ground motion attenuation functions for the Eastern U.S. were determined. The attenuation functions used were McGuire et al [4] and Atkinson and Boore [5]. These ratios were used with the pseudo mean PGA to determine the PSV for the Reservation. The differences between Eastern and Western U.S. ratios were examined by comparing the above with the results obtained from the ground motion attenuation by Joyner and Boore [6]. The PSV/PGA ratios ranged from 11 to 20 for the Eastern U.S. attenuation functions for magnitudes and distances associated with annual probabilities of exceedance of 2×10^{-3} and 1×10^{-5}. For Western U.S. attenuation functions, the PSV/PGA ratios ranged from 20 to 38. These comparisons suggest that PSV/PGA ratios for rock sites are smaller in

the Eastern U.S. for moderate magnitude earthquakes at closer distances to the site and about the same for moderate magnitude earthquakes at longer distances for the sites. The main reason the ratios are smaller for the closer distances is that the PGAs are larger for the near-field type Eastern U.S. earthquakes.

- The EPRI 85th percentile peak spectral velocities for 2.5, 1.0, and 0.5 Hz were reviewed. The LLNL 85th percentile peak spectral velocities were not used because, as discussed earlier, their ground motion attenuation models are controlled by standard spectral shapes and therefore do not reflect site-specific conditions.

- The sensitivity of the UHRS obtained as a result of incorporating the DOE-STD-1024-92 guidelines to a range of dominant magnitudes and distances obtained from the hazard analyses for the annual probability of exceedance of 1×10^{-3} was determined. The dominant magnitudes were increased by about one-half magnitude units, and the dominant distances were reduced by about one-half. For the Oak Ridge Reservation, increasing the magnitude controlled the maximum PSV.

- The site-specific response spectra developed for the Perry and Sequoyah Nuclear Power Plants were scaled to the site pseudo mean PGAs. These nuclear plant sites are rock sites and have similar magnitudes and distances as the Oak Ridge Reservation for it's site-specific earthquake. The Perry plant site-specific earthquake was defined as a magnitude 5.3 $\pm$ 0.5 at a distance of 0 - 25 km. The Sequoyah plant earthquake was a magnitude 5.8 $\pm$ 0.5 at a distance of 0 - 25 km. Both plants obtained actual earthquakes with these characteristics for rock sites and determined the 50th and 85th percentile response spectra.

The PSV values obtained from the above evaluations indicated that the PSVs should be increased to account for the larger uncertainties in the low frequency range of the site-specific response spectra. All of the above considerations were factored into the development of the site-specific response spectra shown in Figure 2.

Additional information regarding the development of the seismic hazard curves and the site-specific response spectra may be obtained from *Development of the Site-Specific Earthquake Response Spectra for Eastern U.S. Sites* and it's related references [7].

Updated 1995 Site-Specific Oak Ridge Reservation Study

During the early 1990's, both DOE and the Nuclear Regulatory Commission (NRC) worked with LLNL to determine the reasons for the significant differences between the EPRI and the LLNL seismic hazard methodologies. From this work, it was determined that the main reasons the EPRI and LLNL methodologies gave significantly different results were the uncertainty characteristics assigned by some of the LLNL experts which tended to dominate the hazard and the uncorrelated a and b values assigned to the LLNL recurrence relationships. Based on this, LLNL revised their methodology, and published the results of their revised seismic hazard methodology [8] in late 1993. In addition to changes in the methodology DOE also issued technical standard DOE-STD-1020-94, *Natural Phenomena Hazards Design and Evaluation Criteria for Department of Energy Facilities* [9]. This standard specifies performance categories, target performance goals, and specified probability levels from which natural phenomena hazard loading is developed.

Based on these changes, it was decided to re-evaluate the seismic hazard using the new 1993 LLNL results along with the EPRI results. Figure 3 shows a comparison of the old 1988 LLNL and the new 1993 LLNL seismic hazard results for PGA at the Oak Ridge Reservation. Figure 4 shows a comparison of the EPRI and 1993 LLNL mean seismic hazard curves for PGA. Comparison of Figures 1, 3, and 4 show the new 1993 LLNL results are very similar to the EPRI results. Figure 5 shows a comparison of the EPRI and 1988

LLNL pseudo-mean (DOE-STD-1024-92) and EPRI and the 1993 LLNL geometric mean PGA seismic hazard curve. Examination of these seismic hazard curves show that combining the new 1993 LLNL hazard with the EPRI hazard results in a significant reduction in the seismic hazard at the Oak Ridge Reservation for a specified annual probability of exceedance.

Based on the previous 1990-1992 studies for response spectra shapes, the following ratios were determined for 5% damping:

$$\frac{Max\ PSA}{PGA} = 2.1 - 2.2$$

where PSA is defined as peak spectral acceleration, and

$$\frac{Max\ PSV}{PGA} = 22 - 25$$

Using these spectral shapes, the EPRI and 1993 LLNL geometric mean PGA was used to develop the updated site-specific response spectra for the Oak Ridge Reservation.

To use the new 1993 LLNL results for defining design response spectra at nuclear power plants, the Nuclear Regulatory Commission (NRC) has proposed a target median exceedance probability of exceeding the Safe Shutdown Earthquake of 1×10^{-5} in the 5 to 10 Hz and the 1.0 to 2.5 Hz range. Since the seismic design criteria for the DOE performance category (PC)4 facilities are similar to nuclear power plants, a comparison was made of the PC-4 site-specific response spectra obtained following the NRC guidelines. Based on this comparison, the site-specific response spectra were increased about 10%.

The final seismic hazard curve and site-specific response spectra for rock at the ORR sites are shown in Figures 6 and 7 respectively.

Comparison of the Site-Specific Oak Ridge Seismic Hazard with the 1996 U.S. Geological Survey Seismic Hazard

The U. S. Geological Survey (USGS)[10] has just recently completed an update to their seismic hazard maps. The USGS seismic hazard maps were developed for firm rock conditions, therefore a direct comparison of their seismic maps with the Oak Ridge site-specific hard rock seismic hazard cannot directly be made. The USGS seismic hazard has been converted to hard rock conditions using the approximate conversion factors discussed in the USGS Open-File reports. A comparison of the USGS seismic hazard (converted to hard rock) and the Oak Ridge seismic hazard is shown in Table 1. This comparison shows reasonable agreement for the PGA and the 0.2 second spectral values. The Oak Ridge seismic hazard is slightly lower than the USGS seismic hazard at the 1.0 second spectral value. The primary reason the USGS seismic hazard is higher at the 1.0 second spectral value is one of the conservative ground motion attenuation models which they used to represent the long period ground motions. Additional work is needed to obtain more consensus among the experts concerning ground motion attenuation models in the Eastern U.S.

4. CONCLUSIONS

The seismic hazard criteria has been updated for the Oak Ridge Reservation to provide site-specific response spectra for use in evaluating existing facilities and for the design of new facilities. New methodologies for estimating earthquake ground-motion are continuing to be developed. Evaluation of the new methodologies may be needed to ensure the appropriate site-specific spectra are being used.

5. ACKNOWLEDGMENTS

The authors would like to thank these individuals who contributed to the development of the seismic hazard results and the site-specific response spectra: R. K. McGuire and G. T. Toro of Risk Engineering, Inc., J. B. Savy and B. Davis

of Lawrence Livermore National Laboratory, and R. W. Rucker and E. G. Tourigny of the Department of Energy.

REFERENCES

[1] D. L. Bernreuter, et al., *Seismic Hazard Characterization of 69 Nuclear Plant Sites East of the Rocky Mountains,* NUREG/CR-5250, UCID-21517, USNRC, 1988.

[2] Technical Report NP-4726-A, Electric Power Research Institute, *Seismic Hazard Methodology for Central and Eastern United States,* Vols. 1-11, Rev. 1, 1988.

[3] U.S. Department of Energy, *Guidelines for Use of Probabilistic Seismic Hazard Curves at Department of Energy Sites,* DOE-STD-1024-94, April 1994.

[4] R. K. McGuire et al, *Engineering Model of Earthquake Ground Motion for Eastern North America,* Technical Report NP-6074, EPRI, 1988.

[5] G. M. Atkinson and D. M. Boore, *Stochastic Prediction of Ground Motion and Spectral Response Parameters at Hard-Rock Sites in Eastern North America,* Bulletin of the Seismological Society of America, Vol. 77, 1987.

[6] W. B. Joyner and D. M. Boore, *Measurement, Characterization, and Prediction of Strong Ground Motion,* Proceedings of Earthquake Engineering & Soil Dynamics II, Geotechnical Division, American Society of Civil Engineers, 1988.

[7] J. E. Beavers et al, *Development of Site-Specific Earthquake Response Spectra for Eastern U.S. Sites,* Proceedings of the 4th DOE Natural Phenomena Hazards Mitigation Conference, 1993.

[8] U.S. Nuclear Regulatory Commission, *Revised Livermore Seismic Hazard Estimates for 69 Nuclear Power Plant Sites East of the Rocky Mountains,* NUREG-1488, 1993.

[9] U.S. Department of Energy, *Natural Phenomena Hazards Design and Evaluation Criteria for Department of Energy Facilities,* DOE-STD-1020-94, April 1994.

[10]Frankel, et al., *National Seismic-Hazard Maps: Documentation, June 1996,* U. S. Geological Survey Open-File Report 96-532, 1996.

Table 1. Comparison of the Site-Specific Oak Ridge Seismic Hazard and the 1996 USGS Seismic Hazard

Annual Probability of Exceedance				
		2×10^{-3}	1×10^{-3}	4×10^{-4}
PGA, g's	USGS	0.07	0.10	0.20
	Site-Specific	0.06	0.08	0.15
0.2 sec., g's	USGS	0.11	0.17	0.28
	Site-Specific	0.12	0.16	0.28
1.0 sec., g's	USGS	0.037	0.06	0.10
	Site-Specific	0.025	0.033	0.06

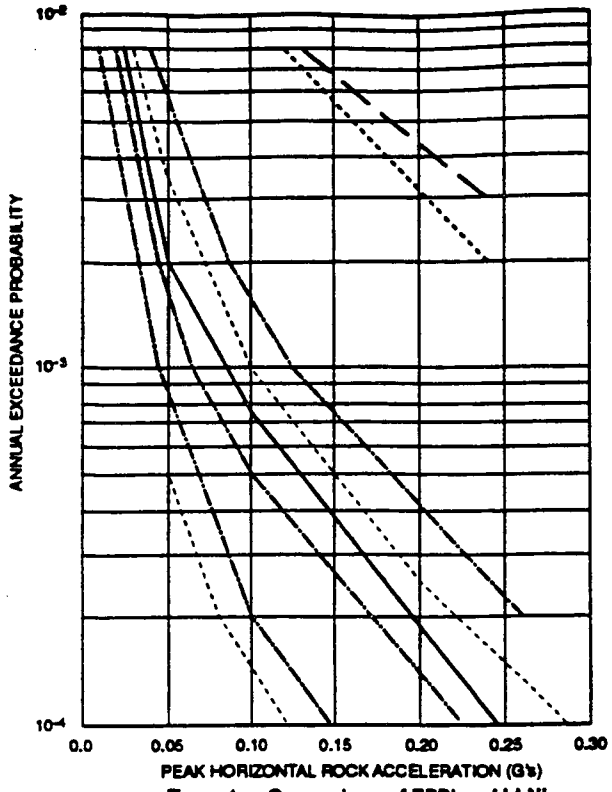


Figure 1 — Comparison of EPRI and LLNL Oak Ridge Seismic Hazard

EPRI MEAN
EPRI 15, 50, AND 85th PERCENTILES
LLNL MEAN
LLNL 15, 50, AND 85th PERCENTILES

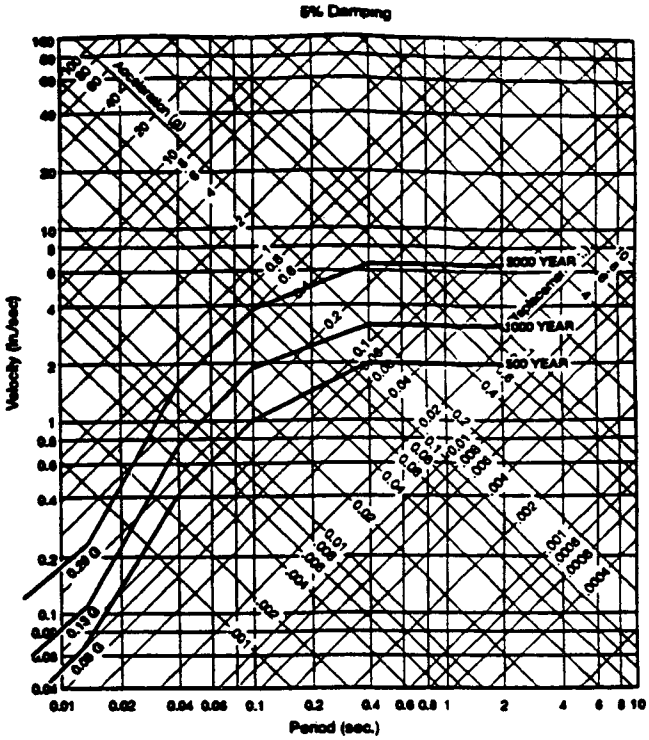


Figure 2 — OAK RIDGE - SITE SPECIFIC UNIFORM HAZARD RESPONSE SPECTRA FOR HORIZONTAL ROCK MOTION

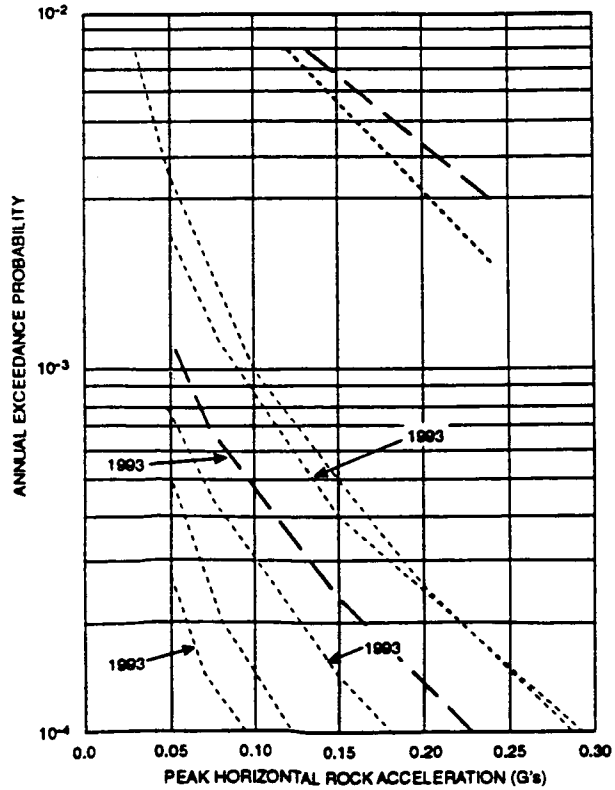


Figure 3 — Comparison of LLNL and 1993 LLNL Oak Ridge Seismic Hazard

LLNL MEAN
LLNL (1993) MEAN
LLNL 15, 50, AND 85th PERCENTILES
LLNL (1993) 15, 50, AND 85th PERCENTILES

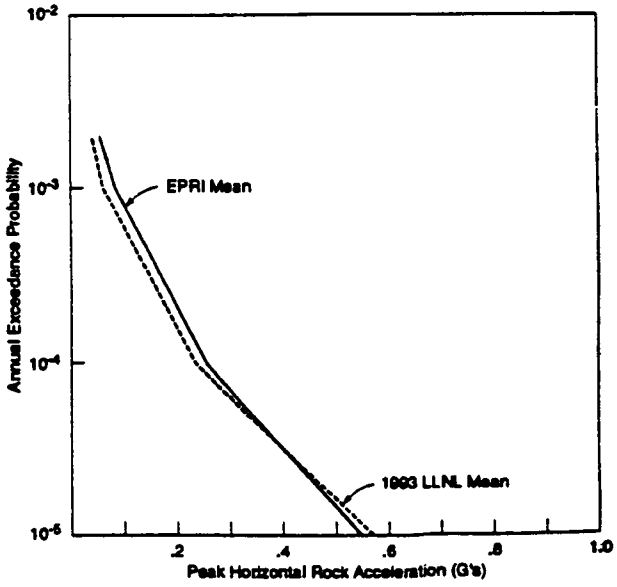


Figure 4 — Comparison of EPRI and 1993 LLNL Oak Ridge Seismic Hazard

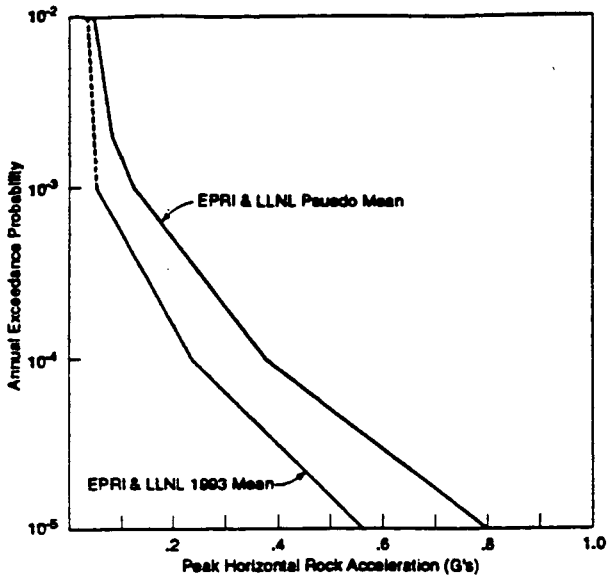


Figure 5 — Comparison of EPRI & LLNL Psuedo Mean and EPRI & 1993 LLNL Mean at Oak Ridge

Y-GA 95-2200

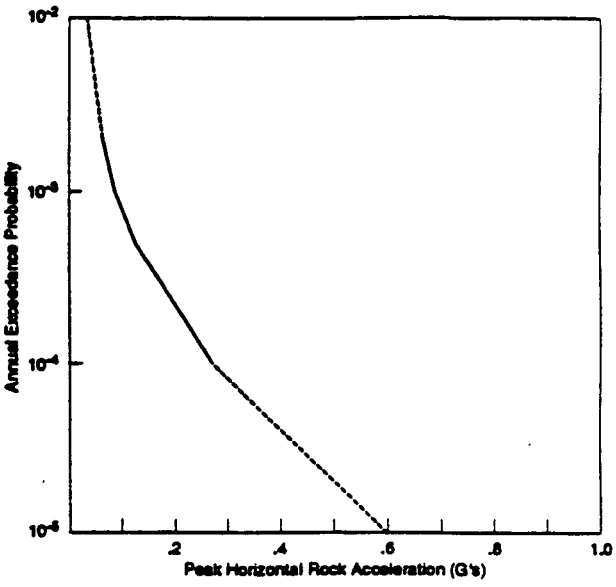


Figure 6 — Oak Ridge Mean Seismic Hazard Curve

Y-GA 95-2201

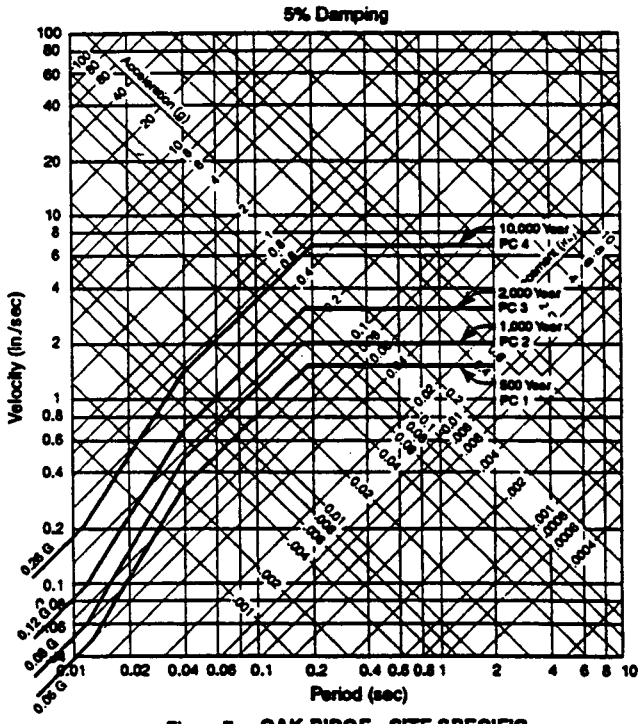


Figure 7 — OAK RIDGE - SITE SPECIFIC RESPONSE SPECTRA FOR HORIZONTAL ROCK MOTION

Y-GA 95-0441R

National Earthquake Loss Reduction Program a New Approach For The United States

by

Robert H. Volland[1]

ABSTRACT

The United States' National Earthquake Hazards Reduction Program has been expanded, based on a study requested by the Congress and completed by the Office of Science and Technology Policy. The study resulted in the establishment of the National Earthquake Loss Reduction Program, which brings twelve or more additional Federal agencies into the Federal government's effort to reduce the Nation's seismic vulnerability.

KEYWORDS: earthquakes; earthquake hazards reduction; NEHRP; seismic design; vulnerabilities

1. INTRODUCTION

The United States has had a national program of earthquake hazards reduction since 1977, when the Congress passed the Earthquake Hazards Reduction Act. The stated purpose of the Act is "...to reduce the risks of life and property from future earthquakes in the United States through establishment and maintenance of an effective earthquake hazards reduction program." The Act's aims include improved understanding, characterization and prediction of seismic hazards and vulnerabilities; improved model building codes and land use practices; development and improvement of seismic design and construction techniques; accelerated application of research results, and reduced risk through post-earthquake investigations and education.

The Act created the National Earthquake Hazards Reduction Program (NEHRP), consisting of the closely coordinated efforts of four Federal agencies – the Federal Emergency Management Agency (FEMA), the United States Geological Survey (USGS), the National Science Foundation (NSF) and the National Institute of Standards and Technology (NIST). The premise of NEHRP is that while earthquakes may be inevitable, earthquake disasters are not. The activities of the NEHRP agencies include basic and applied research, technology development and transfer, training and education, and advocacy for seismic risk reduction measures. In these activities, the NEHRP agencies work collaboratively with each other, with other Federal and state agencies, private companies, universities, and regional, voluntary and professional organizations.

2. THE ROLES OF THE NEHRP AGENCIES

The NSF funds earthquake-related research in the fields of earth science, earthquake engineering, and social science, as well as multi-disciplinary projects. It supports earthquake engineering experimental research facilities and the integration of education and research to develop the next generation of educators, researchers and practitioners.

The USGS monitors seismic activity, identifies and characterizes earthquake hazards, conducts research in support of improved hazard assessment methods, disseminates scientific data and information, and demonstrates the application of earth-science knowledge in effective loss-reduction strategies.

---

[1] National Earthquake Loss Reduction Program, Federal Emergency Management Agency

The NIST conducts problem-focussed research and development to improve standards and practices for buildings and lifelines. It also chairs and provides technical secretariat support to a Federal interagency committee through which 33 agencies develop and incorporate earthquake hazard reduction measures into their respective programs.

The FEMA works to translate the results of research and technology development into effective earthquake hazards reduction measures at state and local levels of government. We administer a program of grants and technical assistance designed to increase the awareness of the earthquake risk and to foster plans and actions to reduce seismic vulnerability. We also support the development and dissemination of improved seismic design and construction techniques for new buildings and rehabilitation guidelines and techniques for existing buildings.

Over the past 20 years, the NEHRP has been successful in developing basic knowledge about seismically vulnerable areas in the United States, about the effects of earthquakes on the built environment, and about measures that can be taken to reduce their impact.

For fiscal year 1998 (October 1, 1997 – September 30, 1998), the Clinton Administration is requesting the Congress to appropriate $96.9 million for NEHRP. Of this total, $28.9 million (30%) is requested for NSF, $47.3 million (49%) is requested for USGS, $18.7 million (19%) is requested for FEMA, and $1.9 million (2%) is requested for NIST.

In recent years, one of the consistent concerns of the Congress and of certain segments of the earthquake hazards community in the United States has been what we call the "implementation gap." By this we mean that, as a society, we in the United States know a lot more about how to reduce our seismic vulnerability than we are putting into practice. In November of 1993, nine Members of our House of Representatives wrote to the President expressing their concerns about the Federal government's efforts to reduce the nation's earthquake losses. Their main concerns focussed on NEHRP and on what they perceived to be a lack of strategic planning, insufficient coordination and implementation of research results, and a lack of emphasis on earthquake loss reduction practices.

3. NATIONAL EARTHQUAKE LOSS REDUCTION PROGRAM

In March of 1994, Dr. John H. Gibbons, the President's Science Advisor and Director of the Office of Science and Technology Policy (OSTP) directed that a study be undertaken to review the research and implementation issues related to earthquake hazards. The results of this effort were formally released in April of 1996 in a document titled *Strategy for National Earthquake Loss Reduction*. The study found that, besides the four agencies that constitute NEHRP, there are a number of other Federal agencies that also have a fundamental interest in, and have significantly investigated, earthquake risk reduction, but that the activities of these agencies lacked an integrating mechanism. The Strategy called for providing an integrating mechanism through the formation of a National Earthquake Loss Reduction Program (NEP). This Program, led by FEMA, is designed to formally associate the earthquake-related activities of twelve or more additional agencies with the ongoing work of the four NEHRP agencies.

Examples of agencies that constitute NEP include:

- The Department of Veterans Affairs, that has been developing seismic standards for hospitals since 1971;
- The Nuclear Regulatory Commission and the Department of Energy, that have been developing seismic standards for nuclear power plants and other critical facilities;
- The Department of Transportation, that has done extensive work on the seismic safety of bridges and elevated roadways;

- The National Aeronautics and Space Administration, that has used space-based platforms to assist in monitoring ground deformation in seismically active areas;
- The General Services Administration, that is responsible for the design, construction or leasing of Federal buildings; and
- The Department of Housing and Urban Development, that administers programs having a major impact on housing and community development.

This brief list suggests two ways in which the formation of NEP will contribute to earthquake loss reduction in the United States. First, it provides a forum in which agencies can share information and experience in developing and applying seismic risk reduction measures. For example, there is increasing interest in performance-based design concepts. Building codes in the United States are based on the life-safety standard. A building built to this standard and subjected to the design seismic event will not collapse or inflict life-threatening injuries on its occupants, even though it may be so severely damaged it is subsequently demolished. Such a standard is clearly inappropriate for structures that the owners would like to have functional – or functional with only minor repairs – immediately after an earthquake, such as hospitals, fire stations and emergency operating facilities. As we proceed to develop performance-based standards, much of the work done by the Departments of Energy and Veterans Affairs and by the Nuclear Regulatory Commission should be of material assistance to the other NEP agencies.

The second opportunity presented by the formation of NEP is the potential for closing the implementation gap by incorporating seismic hazard reduction considerations into the day-to-day conduct of programs administered by the NEP agencies. In the United States, the decision to adopt and enforce building codes rests with the State and local governments, not with the Federal government. However, the Federal government may influence the process by the conditions it attaches to the grant and loan programs it administers. The NEP provides a forum in which such policies and program administration can be discussed. Currently, the NEHRP agencies are developing a strategic plan to guide the Federal seismic loss reduction program into the future. As the planning effort matures, the views of the NEP agencies will be requested and incorporated.

4. CONCLUSIONS

It is important to note that NEP does not replace NEHRP. Rather, NEP will build upon the framework provided by the four NEHRP agencies to improve the linkages in earthquake loss prevention and mitigation between the Federal government, State and local governments and the private sector, where much of the loss reduction measures must be taken.

The Effects of Open Passage on Reducing Wind Response of Tall Buildings

by
H. Okada[1] and L. Kong[2]

ABSTRACT:

An open passage design on tall buildings is investigated to reduce the wind dynamic responses resulted from the periodic vortex shedding of building corners. Initial results of a dynamic balance wind tunnel test for a square section model with sharp edges at an aspect ratio 8:1 and with only a very small opening ratio 1.5% on its 4 walls show a significant reduction of the across-wind dynamic deflection by about 20-25%. The results also indicate that the arrangement with open passages on all its 4 walls is the most effective way comparing to cases with openings either on the side walls or on the back wall being sealed.

Key Words: Wind Response Control
Tall Buildings
Open Passage
Vortex Shedding

1 INTRODUCTION

With the building height increasing rapidly in recent years, the sensitivity to wind excitation has increased dramatically. The need for effective means to control the building dynamic response in the across-wind direction becomes increasingly urgent. In Japan, a plan to build hyper-rise buildings is on the government and construction industries' agenda. One of the most serious challenges associated with this hyper building concept is to reduce the wind induced instability. Apparently, the most effective way to reduce the wind induced instability would be to eliminate the excitation source. It is well known that wind induced vibration of high-rise buildings comes from the periodic vortex shedding at building corners. Therefore, if the vortex shedding process can be somehow disrupted, the periodic loads acted on the building resulted from this vortex shedding process will be reduced and the wind induced motion in the across-wind direction will be controlled. Architectural modification of building configuration would alter the flow pattern around the building, and could lead to the breaking of the vortex shedding system. Open passages at appropriate positions of a building would allow high pressure air to bleed into regions close to the side edges where the vortex shedding is generated, and to the back region of the building which has a strong relation with the across-wind dynamic force as explained by Bearman[1]. Optimisation of this design would possibly be able to eliminate the vortex shedding system completely. Kwok and Bailey[2] have tried various venting slots and corner treatments in an attempt to reduce wind dynamic responses. Dutton and Isyumov[3] conducted a similar investigation by using various gaps. But they used static force balance in their tests. Because it has been considered that results from actual dynamic test and results from static measurement may be quite different regarding to the model dynamic response, the present test used a

1) Associate Director for Composite Structure, Structural Engineering Department, Building Research Institute, Ministry of Construction, Tsukuba City, 305 Japan
2) STA Fellow, Building Research Institute, Ministry of Construction, Tsukuba City, 305 Japan

dynamic balance, designed for this project to measure the actual dynamic deflection of the building model.

2 EXPERIMENT

The preliminary investigation of this research has concentrated on using open passages at centre regions. 3 high-rise building models, respectively with sharp edge corners, round corners and cut corners are tested in the boundary layer wind tunnel in the Building Research Institute of Japan. All models are rigid and have an aspect ratio 8:1 with a square cross section. The width of the 3 models is the same at 70mm. Only the sharp edge model has open passages on its 4 walls, which centred at 80% of the building model height. The size of the opening can be varied if required. The first test was conducted with the sharp edge model for two conditions, without any open passage and with open passage of 30mm×20mm on some walls of the model. This gives an 1.5% opening ratio defined as the opening area of the wall over the total area of the same wall. A dynamic balance is made for this test to allow the model to have two degrees of freedom in both the along-wind and across-wind directions. Two laser displacement sensors are mounted to record the time histories of the model deflections in both directions. Two pairs of springs are selected with one pair at a spring constant $19600\times2kg/s^2$ in the across-wind direction and another pair $68600\times2kg/s^2$ in the along-wind direction. The use of different springs is a consideration of eliminating the beating phenomenon, which otherwise would happen if the two pairs of springs have the same spring constant. The natural frequencies of the model set-up are 13.2Hz in the across-wind direction and 20.0Hz in the along-wind direction. The original damping coefficient of this set-up is 0.38% in the across-wind direction and 0.42% in the along-wind direction. The damping coefficient can be varied by using a liquid damper. The liquid used here is silicone with a density of $10000kg/m^3$, which gives a damping coefficient 2.6% in the across-wind direction and 0.94% in the along-wind direction. During the test, different open passage arrangements are used to see their effects on reducing the dynamic response of the model. The test is carried out in an atmospheric boundary layer flow corresponding to an urban area condition $V= V_o(z/z_o)^{0.25}$, where the boundary layer thickness z_o is about 1000mm, and the free stream wind velocity is varied from 5m/s to 17m/s. The power law boundary layer profile is generated by a spire and roughness system. Based on scale analysis according to a full scale consideration, a data sampling frequency of 500Hz is chosen and a sampling period of 5 seconds is taken. For each test condition, 6 records are made, and this gives a total data length of 15000.

3 RESULT AND DISCUSSION

Some results of the dynamic response for the sharp edge model in the across-wind direction for different open passage arrangements with and without the $10000kg/m^3$ silicone damping are shown in Figure 1 and Figure 2. The y axis is the rms value of the model tip dynamic deflection σ, and the x axis (V/fD) is the wind velocity at the model height position over the product of model natural frequency f in the across-wind direction and the model width D. Figure 1 is the result for the test condition of damping coefficient 0.38% in the across wind direction, and Figure 2 is the result with the $10000kg/m^3$ silicone at a damping coefficient 2.6%.

As expected, the rms value of the model dynamic deflection for the open passage configuration is much smaller than that of without any open passage.

This indicates the effectiveness of the open passage in reducing the dynamic wind response of the building model. Generally, it is seen that all 3 open passage arrangements reduce the model dynamic response significantly considering that the opening ratio is only 1.5% in the present test. Clearly these results show that for both cases with damping ratios 0.38% and 2.6%, open passage on all 4 walls is most effective comparing to either the side walls or back wall having no open passages. On the average, it can be seen that open passage on the side wall is more effective than the open passage on the back wall especially for the 2.6% damping case. This is considered to be due to the reason that open passages on the side walls would allow high pressure air to disturb the vortex generating process directly. Therefore, the authors think that bleeding high pressure air into the edge regions of the side walls where the vortex shedding is actually created should be more effective. In reality, it is always convenient to have open passages on all 4 walls, because first, this is most effective and second, the wind could be from all directions. It is also believed that a larger opening ratio should result in a much bigger reduction of the dynamic response of the building. This will be investigated in the next step.

Apparently, the lock-in phenomenon occurred in the test when the wind speed reaches around 8.5m/s. During the test, for all test conditions in the boundary layer flow, whenever the wind speed gets to this value, the vortex shedding frequency is seen to be controlled by the model natural frequency. However this lock-in phenomenon does not seem to disappear even when the wind speed increases to over 15m/s at the model height. The Strouhal number for this square section model is about 0.91, so based on the model natural frequency 13.2Hz in the across-wind direction and the model width 70mm, the critical wind speed should be about 10m/s where the resonance would occur. But the model dynamic response increases monotonously even when the wind speed reaches over 15m/s and the vortex shedding frequency is still dominated by the model natural frequency. There are two possible explanations. The first is that the lock-in region maybe become wider in a boundary layer flow than that of in a smooth flow. The second explanation is that galloping is happened immediately after the vortex induced vibration or within the lock-in region. Kawai[4] presented some results and analysis which are quite similar to those of the present test. In spite of this, the effectiveness of the open passage arrangement is shown clearly with a reduction of 20-25% of the model dynamic deflection at large wind speeds. It should be mentioned here that the same test is also carried out in a smooth flow condition, and the results do show that in the smooth flow, a clear lock-in region exists between 8m/s and 12m/s.

The power spectra of the model tip dynamic deflection are calculated for some test conditions. A sample is given in Figure 3 for the damping coefficient of 0.38% at two test conditions, without any open passage and with open passages on all 4 walls at a wind speed 10.8m/s at the model height. The y axis is the power spectral density of the model dynamic deflection $S_d(f)$ and the x axis is the frequency f. Apparently, this is inside the lock-in region because only one peak is appeared in the spectra at the model natural frequency of 13.2Hz. From this figure, it can be also seen the effectiveness of the open passage arrangement as the peak value of $S_d(f)$ without any open passage is more than 2 times of the peak with open passages on all its 4 walls and all other $S_d(f)$ values at both lower and higher frequencies are greater as well. For these two particular tests, the difference of their rms value of

the model dynamic deflection σ is about 25%. Another example of the power spectrum is shown in Figure 4 for a wind speed 5m/s at the model height without any open passage and with a damping coefficient 0.38%. Obviously, this test condition is not in the lock-in region yet because there are two peaks appeared on the spectrum. One is the vortex shedding frequency at about 7Hz and the other is the model natural frequency of 13.2Hz.

4 CONCLUSION

Some results of an on-going research project on reducing the dynamic response of high-rise buildings by an open passage design are presented and discussed. The main points from this investigation can be summarised here:

(1) The open passage configuration results in a significant reduction of the dynamic response of the building model in the across-wind direction induced by the periodic vortex shedding on building corners. The model dynamic deflection reduces about 20-25% even for a very small opening ratio 1.5% on all its 4 walls.

(2) The condition with open passages on all its 4 walls tends to be the most effective way in reducing the dynamic response of the building model comparing to the arrangements of either only the front and side walls or front and back walls have open passages.

(3) For the building model used in this test, the Strouhal number is about 0.91. The lock-in phenomenon starts when the wind speed reaches around 8.5m/s. However this lock-in phenomenon does not disappear even when the wind speed gets to over 15m/s at the model height. There are two possible reasons: a longer lock-in region in a boundary layer flow condition, or galloping happened within the lock-in region.

The authors consider that with a combined arrangement of both open passage and cutting corners on the building model, a further reduction of the model dynamic response would be possible. Models with larger opening ratios at different positions and with several open passage arrangements on one model will be used in the continuing investigation. Flow visualisation is also considered to check the flow configuration on the corner regions of the model for these different open passage arrangements. The authors also plan to see if open passages on the corner regions would be able to eliminate the vortex shedding system completely. The same idea is also considered to be applied in an active way by discharging high pressure air into these regions.

REFERENCES

[1] Bearman, P.W., "The effect of base bleed on the flow behind a two-dimensional model with a blunt trailing edge", The aeronautical Quarterly, Vol. XVIII, Aug. 1967.

[2] Kwok, K.C.S. and Bailey, P.A., "Aerodynamic devices for tall buildings and structures", Jnl. of Engrg Mechanics, Vol. 113, No. 3, March 1987.

[3] Dutton, R. and Isyumov, N., "Reduction of tall building motion by aerodynamic treatments", Jnl. of Wind Engrg and Industrial Aerodynamics, Vol. 36, 1990.

[4] Kawai, H., "Vortex induced vibration of a tall building in smooth and turbulent boundary layer flow", Annual Meeting of Japan Institute of Architecture, Sept. 1991.

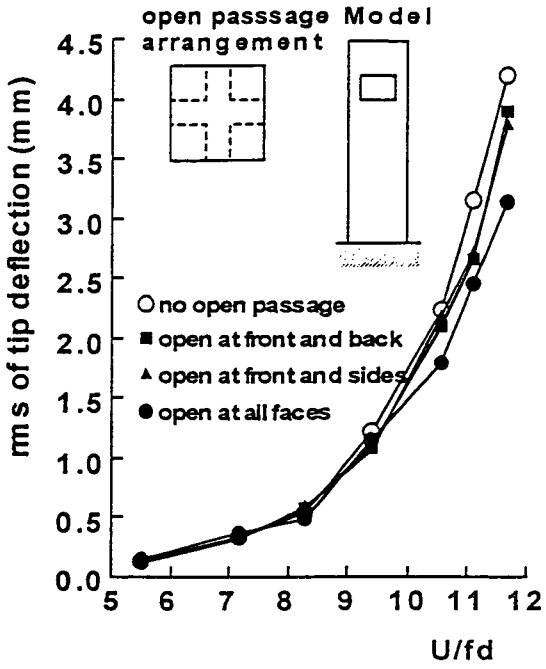


Figure 1 Model dynamic deflection with a damping coefficient 0.38%

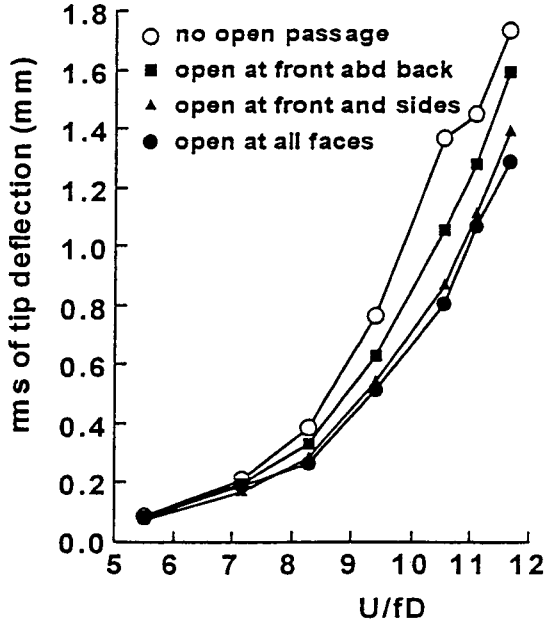


Figure 2 Model dynamic deflection with a damping coefficient 2.6%

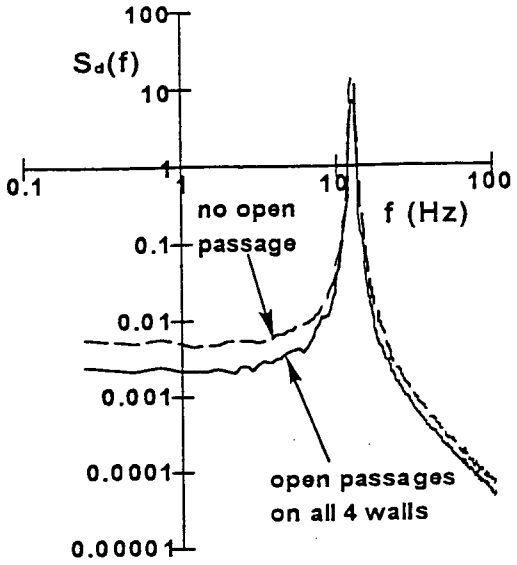


Figure 3 Comparison of the power spectra with and without open passage inside the lock-in region

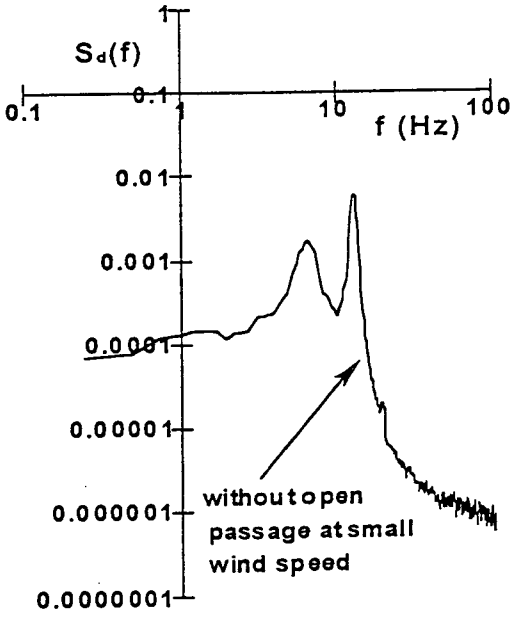


Figure 4 A sample power spectrum outside of the lock-in region

Strength and Ductility Characteristics of Highway Bridge Foundations

by

Jiro Fukui [1], Yoshitomi Kimura [2], Masahiro Ishida [3] and Toshiaki Nanazawa [4]

ABSTRACT

The check of ductility and dynamic strength for highway bridge foundations has been proposed based on the results of research into the behavior of foundations during severe deformation. For seismic design method of foundations, analytical model of pile foundations and caisson foundations were proposed accounting for the non-linear properties of the horizontal ground resistance, vertical ground resistance and the bending stiffness of the foundation body. Horizontal loading tests of pile foundation model were performed to clarify the foundation ductility factor - degree of pile body damage relationship.

Key Words:Seismic Design, Bridges, Strength, Ductility, Pile Foundations, Caisson Foundations, Spread Foundations

1. INTRODUCTION

The Hyogo-ken Nanbu Earthquake of January 17, 1995 caused severe damage to highway bridges, including collapsed bridge piers and bridge falls at many locations. Shortly after the earthquake, the state of this damage was surveyed by visually examining the bridge piers and other above ground structures and emergency restoration work was performed to prevent secondary damage. Because the foundations are underground, it was impossible to directly assess their damage immediately after the earthquake. Surveys of damage to the foundations conducted in conjunction with the restoration work confirmed that little damage was suffered by the foundations(1).

After the earthquake, the "Committee for Investigation on the Damage of Highway Bridges Caused by the Hyogo-ken Nanbu Earthquake" was formulated in the Ministry of Construction to survey the damage and clarify the factors which contributed to the damage. On February 27, 1995, the Committee approve the "Guide Specifications for Reconstruction and Repair of Highway Bridges Which Suffered Damage due to the Hyogo-ken Nanbu Earthquake(2)", and the Ministry of Construction noticed on the same day that the reconstruction and repair of the highway bridges which suffered damage by the Earthquake shall be made by the Guide Specifications. The design method that accounts for the non-linear behavior of foundations based on the results of research at the Public Works Research Institute and elsewhere was included in the Guide Specifications.

This design method, one based on the fact that a foundation provides greater horizontal strength than a bridge pier body, is difficult to apply in a case where the ground around the foundation will liquefy or a case where the bridge pier body has ultimate horizontal strength sufficiently great to withstand the design horizontal seismic coefficient. Thus when the Specifications for Highway Bridges were revised, a model experiment concerning the strength and ductility

1) Head, Foundation Engineering Division, Structure and Bridge Department, Public Works Research Institute, Ministry of Construction, Tsukuba City, 305, Japan
2) Senior Research Engineer, ditto.
3) Research Engineer, ditto.
4) Chief Official, Planning Division, Metropolitan Areas Development Bureau, National Land Agency. (former; Research Engineer, ditto)

of foundations was carried out to propose an seismic design method for foundations.

This paper describes experiments on strength and ductility characteristics of highway bridge foundations conducted by the Public Works Research Institute.

2. FUNDAMENTALS OF SEISMIC DESIGN OF FOUNDATIONS

Damage inflicted on foundations of highway bridges by the Hyogo-ken Nanbu Earthquake was relatively minor. In many cases, the damage was not severe because the horizontal strength of the foundation was greater than that of the bridge pier body or because the foundations provided sufficient ductility to withstand the decline in the horizontal strength of the foundation caused by liquefaction. So judging from the state of the damage, the seismic design method in the present Specifications is a satisfactory design method for foundations.

But during the Hyogo-ken Nanbu Earthquake, load greater than the conventional design seismic force acted on these structures, and the balance of the strengths of the various parts of the bridge and the strength of the foundations have come to differ as, for example, bridge pier bodies designed considering this provide greater strength than in the past. And because it is difficult both to survey the damage to underground foundations and to reinforce these foundations, it is necessary to design foundations so they will not suffer severe damage. So when performing the seismic design of foundations, it should be done in conformity with the following guidelines.

It should be based on the fact that the plastic deformation of the base of a bridge pier body, whose damage can be studied and which can be restored with relative ease, absorbs earthquake energy. For this reason, the horizontal strength of the foundation must be equal to or greater than that of the bridge pier body (See Figure 1 (a)).

In a case where a bridge pier body such as a wall-type bridge pier which has sufficiently great ultimate horizontal strength in the direction at right angles to the bridge axis against the design horizontal seismic coefficient for check of ductility and dynamic strength, it is not necessarily rational to design the horizontal strength of the foundation so that it is equal to or greater than the ultimate horizontal strength of the of the bridge pier. And when liquefaction occurs, the decline in the bearing capacity of the ground around the foundation causes a decline in the strength of the overall foundation, but even in this case, if the horizontal strength of the foundation is greater than the ultimate horizontal strength of the bridge pier body, the structural cross section is excessive, making this an irrational overall bridge design.

Consequently, when designing a foundation in such cases, it is more rational to allow for plasticization at and beyond yield within a range where excessive damage will not be inflicted on the foundation body even when the horizontal strength of the foundation is lower than the ultimate horizontal strength of the bridge pier body. In such cases, the response ductility factor (response horizontal displacement / yield horizontal displacement) of the foundation under the horizontal force corresponding to the design horizontal seismic coefficient for check of ductility and dynamic strength is calculated, and it should be checked to make sure it is below the limiting value (Figure 1(b)).

3. PILE FOUNDATIONS

3.1 Analytical Model of Pile Foundations

In order to check of dynamic strength and ductility for pile foundations, it is necessary to calculate the horizontal strength of pile foundations and its behavior during severe deformation. The displacement method stipulated in the present Specifications handles

the behavior of the foundation as linear behavior by restricting the displacement of the foundation within a range where it is assumed to be elastic behavior. It is impossible to ignore the effects of the non-linear properties of the behavior of the foundation when studying the behavior of the bridge pier during severe deformation. So when check of ductility and dynamic strength for pile foundations, it is necessary to consider the following items as non-linear properties of the behavior of a pile foundation.

[1] Vertical resistance of the piles
[2] Horizontal resistance of the piles
[3] Bending moment - curvature relation of the pile bodies

The horizontal strength of a pile foundation and its behavior during severe deformation can, as shown in Figure 2, be analyzed by replacing the pile foundation with a rigid frame structure supported by a ground spring and considering this to be non-linear.

(1) Vertical Resistance of the Piles

The vertical force at pile top - vertical displacement relationship for a pile generally reveals non-linear behavior. The following method is considered as a method for modelling this kind of non-linear behavior for design purposes.

[1] Approximating the vertical force - vertical displacement curve at the top of the piles with a function (Weibull function curve formula for example).
[2] Modelling the pile tip resistance and the pile surface resistance respectively as elasto-plastic forms.
[3] Modelling the vertical force - vertical displacement curve at the top of the piles with a elasto-plastic form.

At the Public Works Research Institute, the results of vertical loading tests of many piles were organized to propose modelling based on the above methods(3). Considering convenience in actual design work and the precision of the design constant estimation, the following model was used for the design calculations.

The resistance properties in the vertical direction of the pile were considered to be elasto-plastic form, with the pile axial direction spring constant K_{VE} considered to be the initial gradient, and the ultimate bearing capacity P_{NU} and the ultimate pull-out bearing capacity P_{TU} treated as the upper limit values.

In this case, the pile's axial direction spring constant K_{VE} was assumed to be the pile axial direction spring constant K_V calculated as stipulated in the Specifications.

The ultimate bearing capacity P_{NU} and the ultimate pull-out force P_{TU} were considered to be the ultimate bearing capacity of the pile R_U calculated as stipulated in the Specifications and (ultimate pull-out force of the pile P_U) + (effective weight of the pile W). These values did not exceed the ultimate bearing capacity and ultimate pull-out force determined from the stress of the pile body.

(2) Horizontal Ground Resistance

1) Non-linear Properties of the Ground Resistance

The ground reaction force properties should be faithfully modelled so that the horizontal ground reaction force p - horizontal displacement y relationships at varying depths in the ground is the p - y curve used for DNV etc.(4). But when the ground survey precision and the convenience of the calculation in the design task are considered, it is not necessarily appropriate to apply this method to the design of bridge foundations.

Consequently, the horizontal ground resistance was estimated by modelling as a bilinear model of the kind shown in Figure 2 (c). The effectiveness of this analysis method was confirmed and confirming the effectiveness of this analysis method based on an analysis of the results of horizontal loading tests(5).

2) Effects of the Pile Group

Experiments concerning the effects of the pile group have been performed to clarify the horizontal resistance of the pile under various relationships. At the Public Works Research Institute, steel pipe piles with a diameter of 102 mm were arranged as single piles, in straight lines, side by side, and as vertical and batter pile groups in test ground prepared inside a soil tank, then horizontal loading testing was performed on these piles(6). When proposing a design method, the results of horizontal loading tests of pile groups of these kinds are analyzed, and the coefficients η_k of the coefficient of horizontal ground reaction and η_p of maximum value of horizontal ground reaction are introduced.

3) Calculation Method

Based on 1) and 2), the horizontal ground resistance is found as follows.

The horizontal ground resistance properties is considered to be elasto-plastic in form with the coefficient of horizontal ground reaction k_{HE} as the initial gradient, and the maximum value of the horizontal ground reaction force p_{HU} to be the upper limit value (same figure (c)). k_{HE} and p_{HU} can be found from the following formulae.

$$k_{HE} = \eta_k \alpha_k k_H \quad (1)$$

$$p_{HU} = \eta_p \alpha_p p_U \quad (2)$$

Where:

k_{HE} : Coefficient of horizontal ground reaction used for the check of ductility and dynamic strength (kgf/cm^3)

p_{HU} : Maximum value of the horizontal ground reaction force (kgf/cm^2)

k_H : Coefficient of horizontal ground reaction (kgf/cm^2), found as stipulated in the Specifications.

p_U : Passive earth pressure during an earthquake (kgf/cm^2), found as stipulated in the Specifications. It can account for the weight of the soil up to the ground surface which is stable over a long period around a foundation as the overburden load.

α_k : Coefficient for the coefficient of horizontal ground reaction of a single pile.

α_p : Coefficient for the maximum value of the horizontal ground reaction force for a single pile.

η_k : Coefficient for the coefficient of horizontal ground reaction accounting for the pile group effects.

η_p : Coefficient for the maximum value of the horizontal ground reaction force accounting for the pile group effects.

Table 1 presents the values of the coefficient α_k of the coefficient of horizontal ground reaction and the coefficient α_p of the maximum value of the horizontal ground reaction force of a single pile. This was obtained based on an analysis of the results of the horizontal loading test of a single pile shown in 1).

The coefficient η_k for the coefficient of horizontal ground reaction accounting for the pile group effects is the following value.

$$\eta_k = 2/3 \quad (3)$$

The coefficient η_p for the maximum value of the horizontal ground reaction force accounting for the pile group effects is the following value.

Cohesive ground : $\eta_p = 1.0$ (4)

Sandy ground : $\eta_p \cdot \alpha_p =$

Interval between the centers of the piles in the direction at right angles to the loading direction / pile diameter ($\leqq \alpha_p$) (5)

In the case of piles other than those in the front pile in sandy ground, the value is 1/2 of that indicated in (5).

The values of η_k, η_p are found from the results of the analysis of the loading tests of group piles in 2).

(3) The Bending Moment - Curvature Relationship of a Pile Body

When using the displacement method, a pile body is treated as an elastic body in order

to keep the stress of the reinforcing bars etc. of the pile body from exceeding the allowed stress. When calculating the horizontal strength of a pile foundation, it is important to evaluate the behavior of the pile body after yield and the ultimate strength. It is necessary to appropriately model the bending moment - curvature relationship in the pile body.

The points of inflection in the bending moment - curvature relationship when bending moment acts on a concrete pile are usually treated as the cracking time (C), the time when the reinforcing bars begin to yield (Y), and the ultimate time of the section (U). The analytical model was a trilinear model linking these points found for a circular steel reinforced concrete cross section with the axial direction N and subjected to the bending moment M (Figure 2(d)).

Because points of this sort are not clearly revealed on a steel pipe pile, it is modelled as a bilinear model with the point at which the stress of the outermost edge of the steel pipe pile reaches the yield point considered to be the initial gradient, and the plastic moment treated as the maximum value (same figure (e)).

The horizontal load - horizontal displacement curve obtained based on the horizontal loading testing of cast-in-place piles shown in Figure 3 and the results of its analysis are shown in Figure 4. Here, the ground resistance properties are treated as completely elasto-plastic type. An analysis treating the pile body as linear revealed conformity in the area where the amount of deformation is small, but as the amount of deformation rises, the values diverge. This suggests that when the non-linear properties of the bending stiffness of a pile are considered, it is possible to perform a simulation up to the large deformation stage.

3.2 Loading Tests of Limiting Value of Ductility Factor of Pile Foundations

(1) Test Objectives

In the case of a wall type bridge pier at right angles to the bridge axis or a case where liquefaction will occur, it is rational to design the bridge so that the energy is absorbed by the foundation. Even in these cases, it is necessary to design the bridge so that the response ductility factor of the foundation is within a certain value in order to prevent excessive damage to the foundation body.

As a limiting value for this ductility factor, the safety coefficient for the ultimate was used to determine the allowed ductility factor for a reinforced concrete bridge pier. Even when a member which is part of the pile body of a pile foundation reaches the ultimate state, this does not result in an immediate conspicuous horizontal strength decline in the overall foundation system. It is difficult to define the ultimate for an entire pile foundation system. For this reason, loading tests of a model pile foundation is done to clarify the ductility factor of the foundation and the state of damage to the pile body. This information is used as reference data when determining the limiting value of the ductility factor.

Loading tests were performed using PHC, cast-in-place piles, and steel pipe piles which are used for pile foundations of highway bridges. The following section refers to the tests of cast-in-place piles.

(2) Test Method

Figure 5 shows an overview of the loading method. This testing, which is done to clarify the state of damage to a pile body when horizontal force acts upon pile groups, requires that moment and horizontal force act on the model simultaneously. The loading was performed by simultaneously controlling three jacks to hold the vertical load at a constant level and performing alternating positive and negative loading of a horizontal force with the horizontal force H/moment M ratio constant at M/H = 2.5 m.

The pile foundation models used were six reinforced concrete piles with a diameter of

30 cm and a length of 180 cm; three set in the loading direction and two at right angles to the loading direction. The interval between their centers was 75 cm, which was 2.5 times their diameters.

The displacement of the horizontal loading position at the level where the axial direction reinforcing bars at the outer edge of the pile bodies of all piles yielded in the previous analysis was set at 1 δ_y, and positive - negative alternating loading was performed while increasing the displacement in increments of 1 δ_y. Three cycles of loading were done for each δ_y. The vertical load was 84 tf.

(3) Test Results

The models of cast-in-place piles were made using 16 reinforcing bars of type SD295A, D10 as the axial direction reinforcement. The hoop ties were made of SD295A, D4 installed at 4 cm intervals. The distance from the outer surfaces of the piles to the centers of their axial direction reinforcement was 5 cm. The results of material testing show that the compressive strength of the concrete was 323 kgf/cm^2 while the yield point of the steel reinforcing bars was 3,757 kgf/cm^2.

Figure 6 shows the hysteresis curve of the horizontal force and the horizontal displacement of the cast-in-place piles. A description of the state of damage to the piles follows.

At 2 δ_y, signs that the covering concrete would soon collapse appeared at the top and bottom bases of the piles at the ends and in the bottom of the piles in the middle, and maximum load was reached at 3 δ_y. At that time, some of the covering concrete at the bottom of pile 1 separated. At 4 δ_y, covering concrete at the top of pile 1, the top and bottom of pile 3, and the bottom of pile 2 separated, but this did not expose any of the reinforcing steel rods (Photograph 1). At 6 δ_y, steel reinforcing rods were exposed and buckled at the bottom of pile 1 and at the top and bottom of pile 3, and at 7 δ_y, steel reinforcing rods were exposed and buckled even at the top of pile 1. As the cyclic loading continued, the hoop ties and axial direction reinforcement failed reducing the horizontal strength.

While not described in this report, similar loading testing was performed using pile group made up of PHC piles and steel pipe piles. Based on the results of these tests and calculation results, the limit value for the ductility factor of a pile foundation has been set at 4.

4. CAISSON FOUNDATIONS

4.1 Analytical Model of Caisson Foundations

The Hyogo-ken Nanbu Earthquake caused only slight damage to caisson foundations, and it is believed that foundations designed using the seismic coefficient method provide sufficient ductility to guarantee stability. But because caisson foundations are generally used as independent column shaped bodies, it is necessary to verify the strength of caisson foundations. The resistance elements are studied again and the resistance properties are modeled as shown below based on its convenience as a design calculation method and the precision of the ground constant estimation method (Figure 7).

(1) Horizontal Resistance of the Surface of a Foundation

Displacement of a foundation is accompanied by compression of the ground at the front surface of the foundation and a subgrade reaction p_{Hr}. The upper limit value p_{HU} of the horizontal subgrade reaction force at the front surface of the foundation at depth z is found from the following formula.

$$p_{HU} = \alpha_p p_p \qquad (6)$$

Where

p_p: Passive earth pressure strength of the ground (tf/m^2)

α_p: Correction factor of the upper limit value of the horizontal subgrade

reaction force

$$\alpha_p = 1 + \frac{1}{2}\frac{z}{B^*} \quad (\leqq 3.0) \qquad (7)$$

z : Depth from the design ground surface (m)
B : Loading width of the foundation (m)

The correction factor α_p, which accounts for the three-dimensional expansion of the ground resistance at the front surface of a foundation, was set from the analysis and the model experiments. The calculated loading width of the foundation is basically the foundation width, but when the plane shape of the foundation is circular, it is multiplied by 0.8.

The horizontal resistance of the side surface of the foundation has, in the case of a conventional caisson foundation, been considered with the ground resistance of the front surface of the foundation increased by 20%, but the horizontal direction shear subgrade reaction force on the side surface is separated and assessed so that it is possible to deal with various plane shapes. The resistance properties are assumed to be elasto-plasticity type with an upper limit value.

(2) Vertical Resistance of the Side Surfaces of a Foundation

Using a conventional design method, the shear resistance τ_v in the vertical direction of the surfaces of a foundation were ignored, but because according to the shape of the foundation and the execution method, its share of the resistance properties of a foundation is large, it is considered to be the elasto-plasticity type resistance.

(3) Resistance of the Bottom Surface of a Foundation

The resistance of the bottom surface of a foundation accounts for the vertical subgrade reaction force p_{vr} and the horizontal shear subgrade reaction force τ_{sr}. Both subgrade reactions have upper limit values. And in some cases, if rotating displacement occurs on the bottom surface of a foundation, part of it is lifted. For this reason, the resistance of the part which lifts is ignored.

(4) Stiffness of a Foundation Body

Using a conventional design method, a main foundation was treated either as a rigid body or as an elastic body, but it is necessary to also consider behavior following the yield of the foundation body in order to evaluate its strength. For this reason, it is treated as an analysis method which can reduce the bending stiffness according to the bending moment produced in the foundation body. But in order to protect the foundation body from severe damage during an earthquake, the design should limit the stress resultant of the foundation body to less than the yield point of the members.

Under the recent revision of the Specifications for Highway Bridges, the resistance elements of the ground around a foundation are, in principle, considered to be the 6 coefficients of subgrade reaction shown in Figure 8.

[1] Vertical coefficient of subgrade reaction at the bottom surface of a foundation k_v
[2] Horizontal shear coefficient of subgrade reaction at the bottom surface of a foundation k_s
[3] Horizontal coefficient of subgrade reaction at the front surface of a foundation k_H
[4] Horizontal shear coefficient of subgrade reaction at the side surface of a foundation k_{SHD}
[5] Vertical shear coefficient of subgrade reaction at the front surfaces of a foundation k_{SVB}
[6] Vertical shear coefficient of subgrade reaction at the side surface of a foundation k_{SVD}

These ground resistance elements are treated as elasto-plastic bodies with upper limit values.

4.2 Analysis of Loading Tests

Analysis of past horizontal loading tests was performed based on the design calculation

model described in 4.1 in order to verify this design model. Two examples of this analysis are shown below.

(1) Caisson Foundation Model Loading Test

A model caisson foundation with an embedment length of 4.8m and a diameter of 1.4m installed on ground formed from alternating strata of sandy silt and clay was tested by applying static loading up to about 30 cm in one direction. A comparison of the results of this experiment with the results of an analysis performed using the method in 4.1 is shown in Figure 9. The figure reveals that these conform closely up to a horizontal displacement of about 20cm, but over 20cm, the analytical value of the yield strength is evaluated lower than the corresponding experimental value. However, the overall behavior generally coincides.

(2) In-situ Horizontal Loading Test of a Wall Foundation

Figure 10 shows the results of an in-situ horizontal loading test and the results of an analysis using the method described in 4.1 for an actual size wall foundation with an embedment length of 23.8m, a thickness of 1.2m, and a width of 2.4m constructed on ground consisting primarily of alternating strata of clay and silty fine sand. The analytical values conform extremely closely with the experimental results up to the point where the main foundation yields, but are a little smaller after yield.

In addition, identical loading testing was performed on three wall foundations etc., and these experimental values also coincide closely with the analytical results.

5. SPREAD FOUNDATIONS

5.1 Behavior of Spread Foundations During Large Deformation

Under the revised Specifications for Highway Bridges, foundations are designed based on the check of ductility and dynamic strength. But stability calculations for spread foundations continue to be based on the seismic coefficient method as in the past; verification based on the check of ductility and dynamic strength is not necessary. There is a reason for this exception. Because spread foundations are usually supported by a good quality bearing stratum, the ground provides more than enough bearing strength. This means that it is possible to count on the foundation lifting to absorb energy, and that even in a case where a spread foundation displays such non-linear behavior, excessive damage will not be inflicted on the ground.

Figure 11 shows the moment - angle of rotation relationship when horizontal force has acted on a spread foundation along with the subgrade reaction distribution at that time. At the stage where the horizontal force is small, the subgrade reaction force distribution is trapezoidal. Next, the subgrade reaction force distribution becomes triangular because when the active moment exceeds the lift limit moment of the foundation, tensile force does not act between the foundation and the ground. The lift limit moment of the foundation and the lift limit angle of rotation at that time are found with formula (8) and formula (9) shown below.

$$M_o = B V / 6 \quad (8)$$

$$\alpha_o = \frac{12 M_o}{B^3 D k_v} \quad (9)$$

Where:

M_o : Lift limit moment (tf m)

α_o : Lift limit angle of rotation (rad)

V : Vertical force at the foundation bottom surface (tf)

B : Foundation length in the load direction (m)

D : Foundation length in the load right angle direction (m)

k_v : Vertical coefficient of subgrade reaction at the bottom surface of the foundation (tf/m^3)

The subgrade reaction force distribution

is assumed to recover its trapezoidal shape when the subgrade reaction force at the top of the foundation reaches its upper limit.

As a result of trial calculations performed using these methods, a spread foundation design with the seismic coefficient method will, even during a Hyogo-ken Nanbu Earthquake class seismic event, present no problems related to its stability calculations. Therefore, under the revised Specifications, spread foundations are designed based on the seismic coefficient method as in the past.

5.2 Check of Strength of Footing

Turning to the design of footing, the existing design method has been supplemented by a method involving concentrating the actions of the subgrade reactions near the edge of the foundation. This method has been introduced because in the event of action by a powerful earthquake with a low probability of occurring during the years of service of a bridge, the foundation would lift concentrating the subgrade reaction forces near the edge of the footing.

During the revision, the results of trial calculations of the subgrade reaction force distribution based on the method shown in 5.1 were organized, and the design is now done by having the subgrade reaction forces act on a location on the interior side whose distance from the edge of the foundation is only 1/20 of the foundation length (see Figure 12).

6. CONCLUSION

The check of ductility and dynamic strength for highway bridge foundations has been proposed based on the results of research into the behavior of foundations during severe deformation. For seismic design method of foundations, analytical model of pile foundations and caisson foundations were proposed accounting for the non-linear properties of the horizontal ground resistance, vertical ground resistance and the bending stiffness of the foundation body. Horizontal loading tests of pile foundation model were performed to clarify the foundation ductility factor - degree of pile body damage relationship. These tests confirmed that at less than 4 times the yield displacement, the pile bodies are spared serious damage.

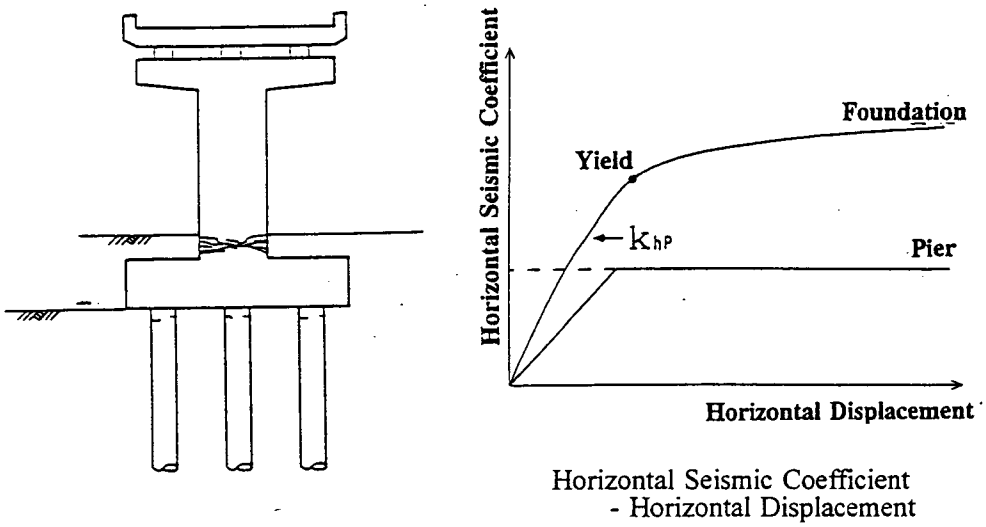
REFERENCES

1) Ministry of Construction : Report on the Damage of Highway Bridges by the Hyogo-ken Nanbu Earthquake, Committee for Investigation on the Damage of Highway Bridges caused by the Hyogo-ken Nanbu Earthquake, 1995.
2) Ministry of Construction : Guide Specifications for Reconstruction and Repair of Highway Bridges Which Suffered Damage due to the Hyogo-ken Nanbu Earthquake, 1995.
3) Okahara et. al.: Research on the Bearing Capacity of Single Piles and Design Methods for Column-shaped Foundations, Technical Memorandum of Public Works Research Institute No. 2919, 1991.
4) Det Norske Veritas : Rule for Design, Construction, and Inspection of Offshore Structure, 1977.
5) Kimura, Tatsuta, Kasuga: Evaluation of the Non-linear Properties of horizontal Resistance of Piles During Severe Deformation, Papers Presented at the Symposium on Limit State Design Methods for Foundation Structures, 1995.
6) Fujiwara, Okahara, Nakatani, Kimura and Takagi: Horizontal Bearing Capacity of Pile Foundations Based on Horizontal Loading Tests, 24th UJNR Joint Panel Meeting,1992.

Table 1 Coefficient

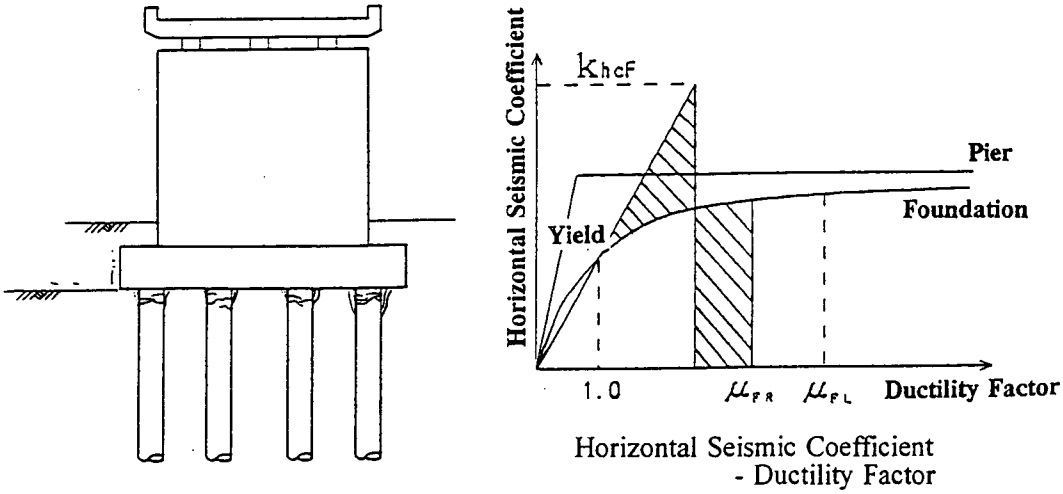
Type of Ground	α_k	α_p
Sandy Ground	1.5	3.0
Cohesive Ground	1.5	1.5

Note: In cohesive ground where $N \leqq 2$, α_p is assumed to equal 1.0.



Horizontal Seismic Coefficient
- Horizontal Displacement

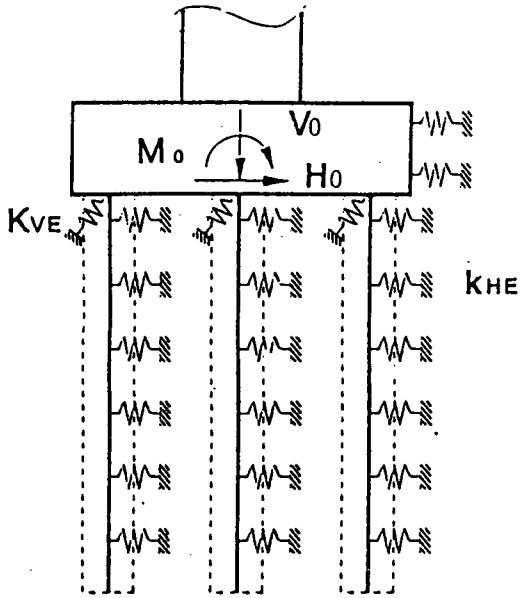
(a) Case of a Principal Plastic Hinge Formed in the Bridge Pier Base



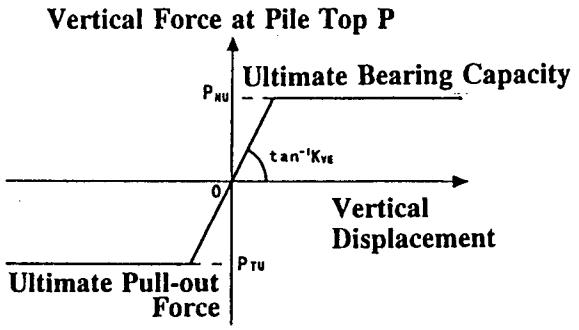
Horizontal Seismic Coefficient
- Ductility Factor

(b) Case of Principal Non-linear Properties in the Foundation - Ground System

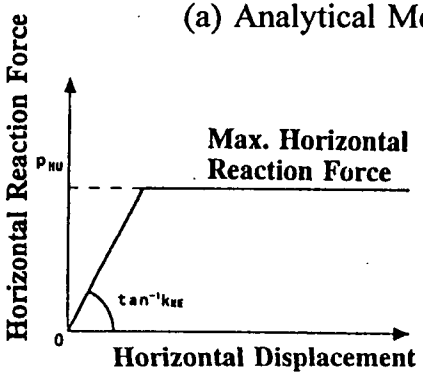
Figure 1. Basic Guidelines for the Design of Foundations Using the Check of Ductility and Dynamic Strength



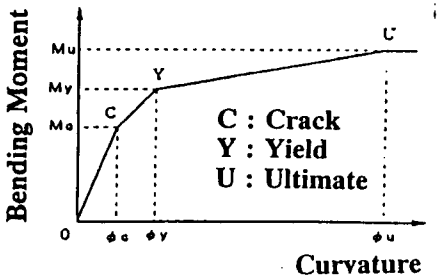
(a) Analytical Model



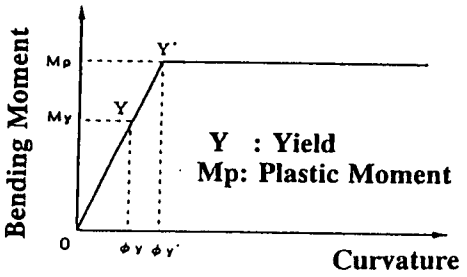
(b)Vertical Force vs. Vertical Displacement Relation



(c) Horizontal Force vs. Horizontal Displacement Relation



(d) Moment vs. Curvature Relation of Reinforced Concrete Piles



(e) Moment vs. Curvature Relation of Steel Pipe Piles

Figure 2. Analytical Models of Pile Foundations

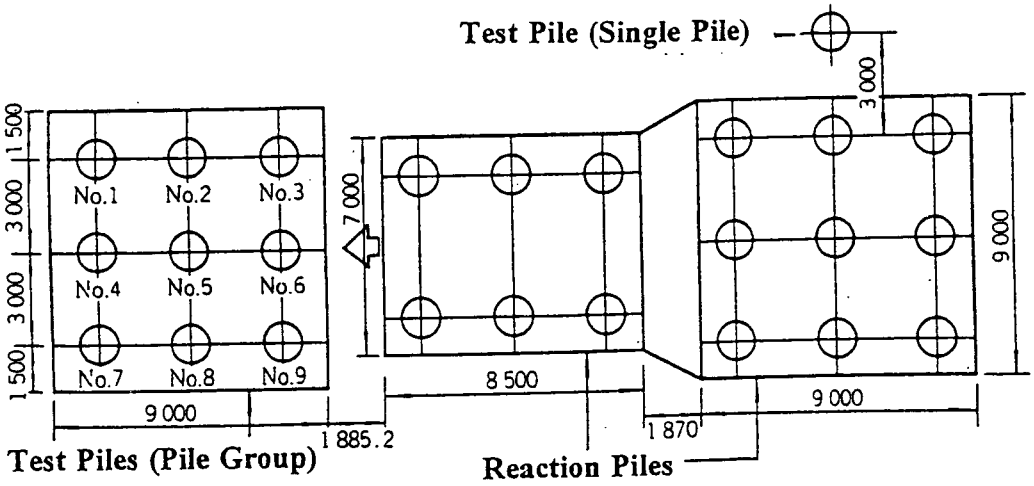


Figure 3. Loading Test of Cast-in-place Pile Foundation

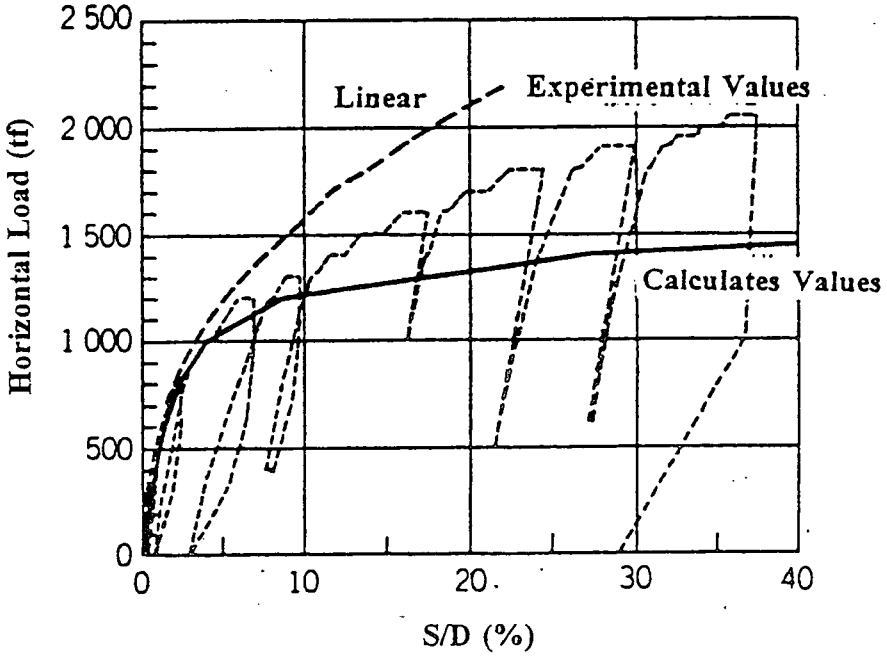


Figure 4. Analysis of the Loading Test of a Cast-in-place Pile Fondation

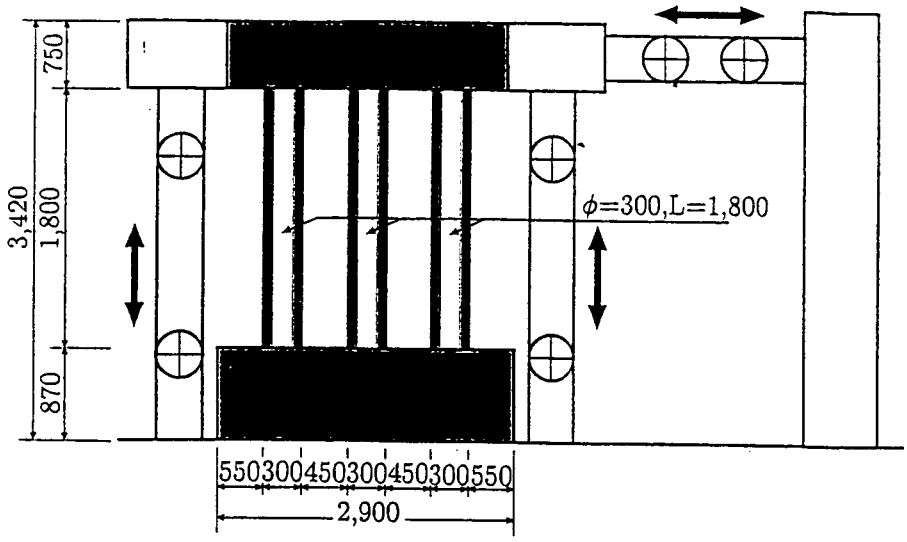


Figure 5. Loading Test

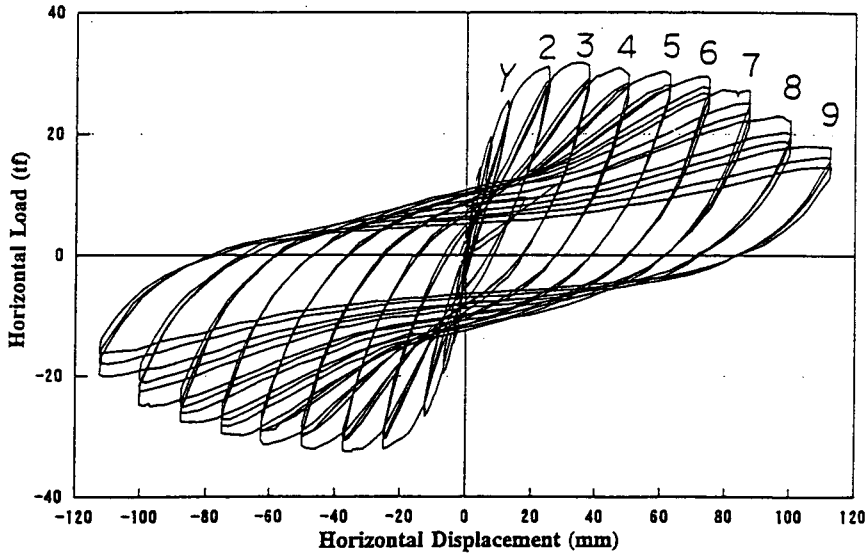
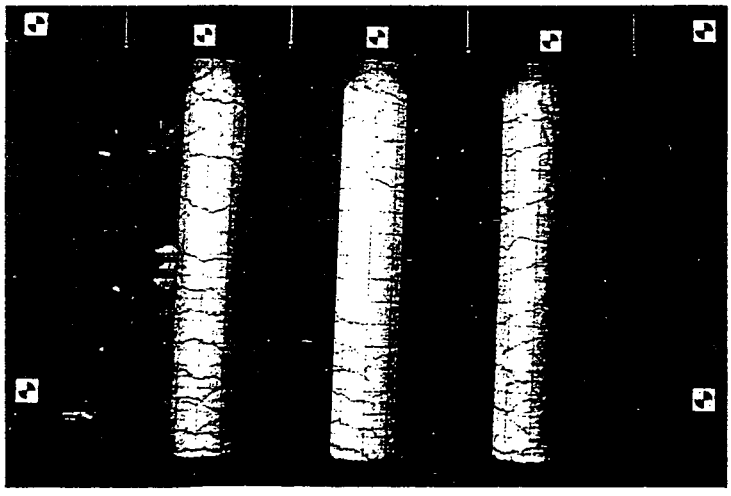


Figure 6. horizontal Load - horizontal Displacement Hysteresis Curve
(Cast- in-Place Piles)



Photograph 1. State of Damage to Pile Bodies
(Cast-in-place Piles, + 4 δ_y)

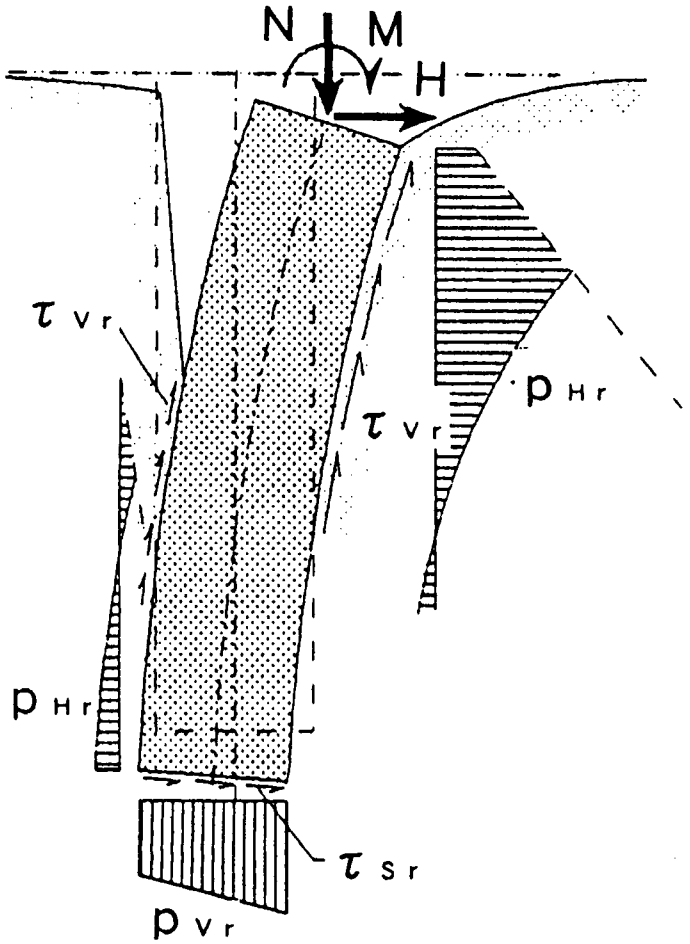


Figure 7. Resistance Elements of Caisson Foundations

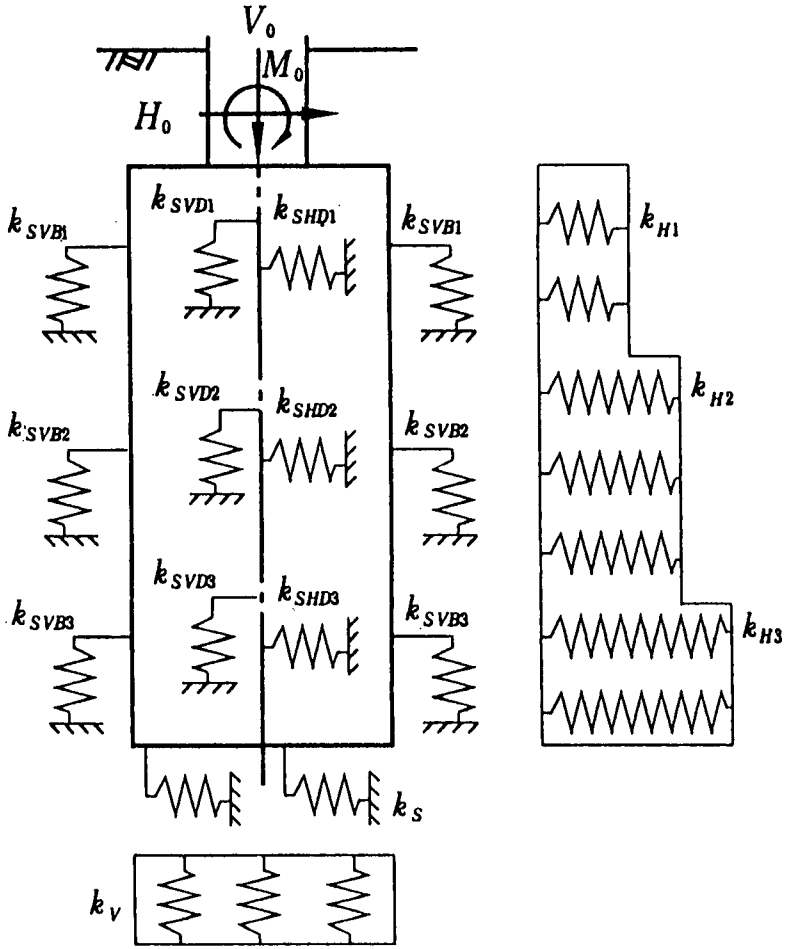


Figure 8. Coefficients of Subgrade Reaction of Caisson Foundations

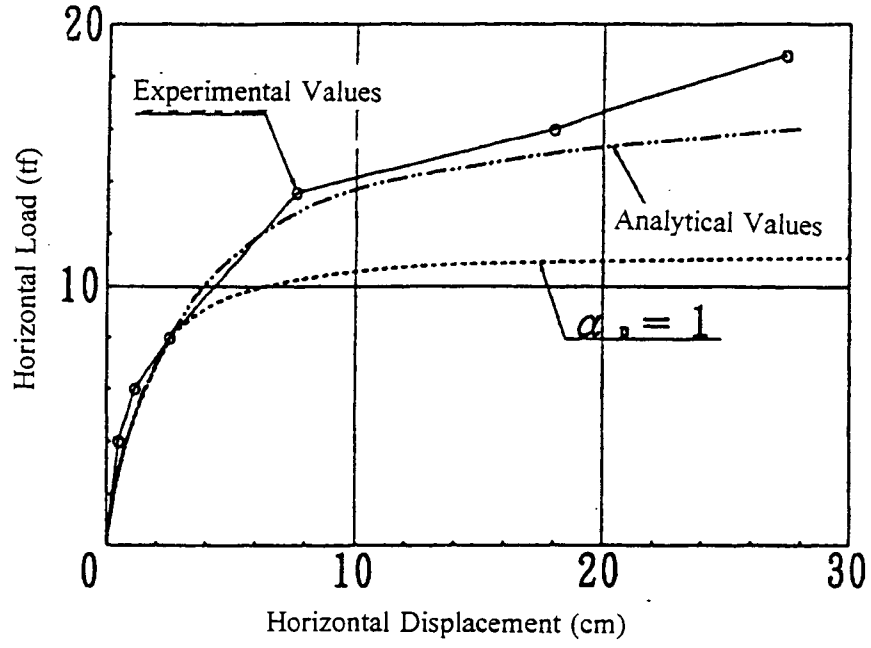


Figure 9. Horizontal Loading Test of a Caisson Foundation

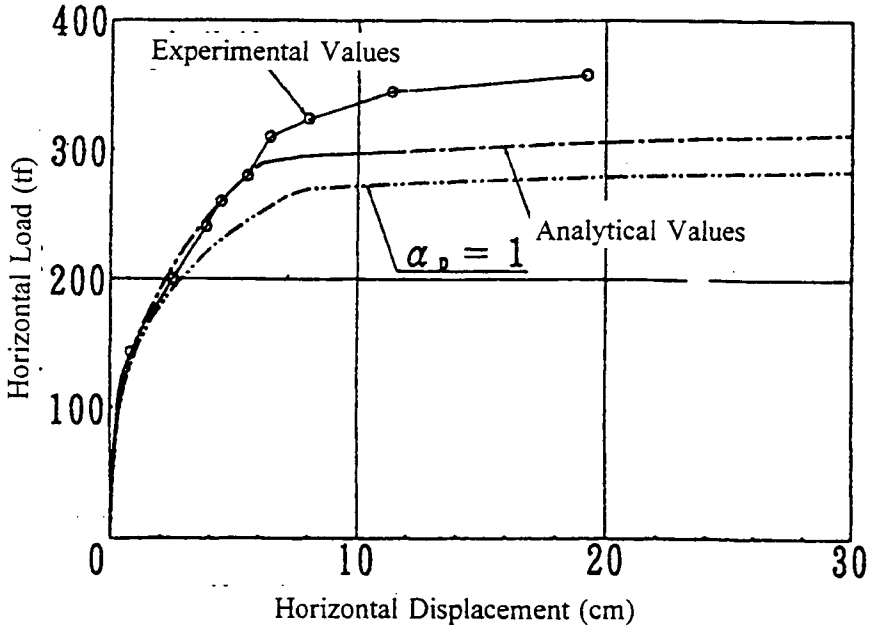


Figure 10. Horizontal Loading Test of a Wall Foundation

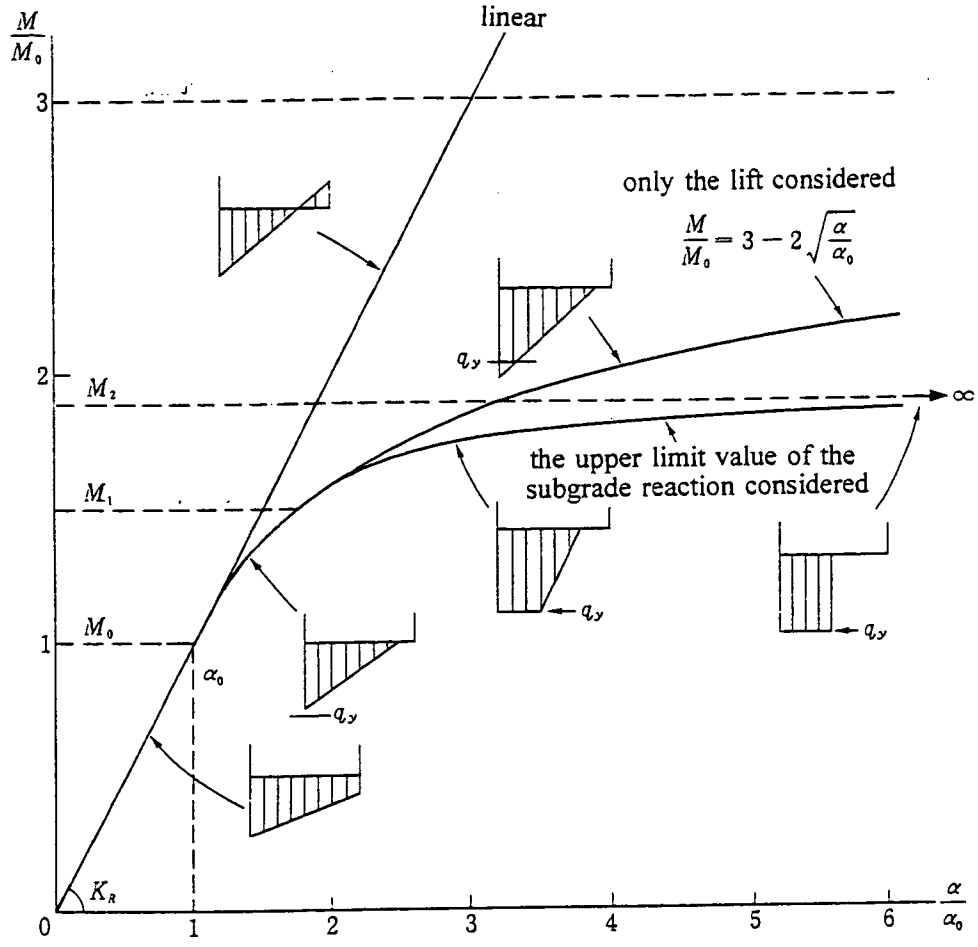


Figure 11. Moment - Angle of Rotation Relationship of Spread Foundation

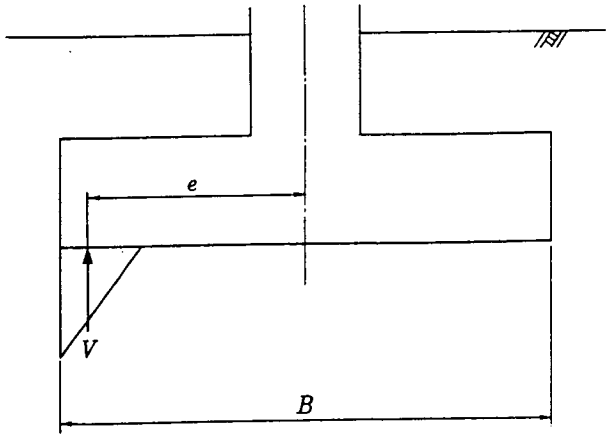


Figure 12. Check of Footing Strength of Spread Foundations

Experimental Study on Tensile Strength of Concrete for Dams

by
Isao NAGAYAMA[1], Kazuo WATANABE[2], Takashi SASAKI[3] and Masahiro HATANO[4]

ABSTRACT

The tensile strength of concrete should be studied comprehensively in order to evaluate the seismic resistance of concrete dams. Direct tensile tests, splitting tensile tests and compressive tests were conducted in order to study the relationship between the compressive strength and the tensile strength of concrete, and the effect of loading rate on the tensile strength of concrete.

The following results were obtained:

1) Compressive strength, splitting tensile strength and direct tensile strength of concrete increase as the cement water ratio increases.
2) The direct tensile strength is smaller than the splitting tensile strength.
3) A higher rate of loading results in a larger tensile strength.

Keywords: *Concrete, Tensile Strength, Rate of Loading*

1. INTRODUCTION

The present Japanese design criteria specifies the middle-third condition in the design of concrete gravity dams and no tensile stress is induced in the dam under the design load combinations. However, large tensile stress is induced in the dams in the dynamic analysis of concrete gravity dams, and a detailed investigation of the tensile strength of concrete is therefore important to secure the seismic resistance of concrete gravity dams.

This paper discusses the results of direct tensile tests of concrete with three different mix proportions under various rates of loading.

2. OUTLINE OF TESTS

2.1. Test Methods

Splitting tensile tests are widely used for evaluating the tensile strength of concrete. However, direct tensile tests are necessary to accurately study the tensile strength of concrete. Direct tensile tests were therefore conducted in this study.

The test equipment is shown in Figure 1. Both ends of the concrete specimen were glued with epoxy resin adhesives to the attachment plates and they were fixed with bolts to the loading plates of universal dynamic test equipment. The bond strength

1) Head, Dam Structure Division, Dam Department, Public Works Research Institute, Ministry of Construction, Tsukuba Science City, 305, Japan
2) Senior Research Engineer, ditto
3) Senior Research Engineer, ditto
4) Assistant Research Engineer, ditto

of the hardened adhesives was approximately 9 N/mm^2 and was much larger than the tensile strength of concrete. The applied load on a concrete specimen was measured with loading cells and the loading rate was controlled at a specified value by the computer. The strain of the concrete specimen was measured using four strain gauges stuck on the specimen surface parallel to loading direction.

Splitting tensile tests and compressive tests were also conducted.

2.2. Mix Proportion of Concrete

The mix proportions of the concrete used in the tests are shown in Table 1. Three types of mix proportions were selected for the tests. They represent the mix proportion of RCD concrete, the conventional concrete used in gravity dams and the conventional concrete used in arch dams and are denoted as "RCD", "GRAVITY" and "ARCH", respectively. The water-cement ratio, which affects the strength of concrete, is 75%, 60% and 45%, respectively.

The concrete specimens were cylinders of 15 cm in diameter and 30 cm in height. To avoid failure at the ends, 3 cm was cut off from both ends of the specimens used for the direct tensile test were.

2.3. Test Conditions

1) Rate of Loading

Five different rates of loading were used in the direct tensile tests in order to investigate the effect of the rate of loading on strength. The rate of loading is as follows:

Compressive test:
0.2 N/mm^2/s
Splitting tensile test:
0.0067 N/mm^2/s
(tensile stress on expected failure plane)
Direct tensile test:
0.0067, 0.2, 2, 20, 60 N/mm^2/s

2) Tested Age of Concrete

All tests were conducted at the age of about 180 days which is selected to avoid the increase in strength by aging. Specimens were cured in water and were dried in a natural room environment for a week before the tests. Three cm was cut off from both ends of the specimens used for

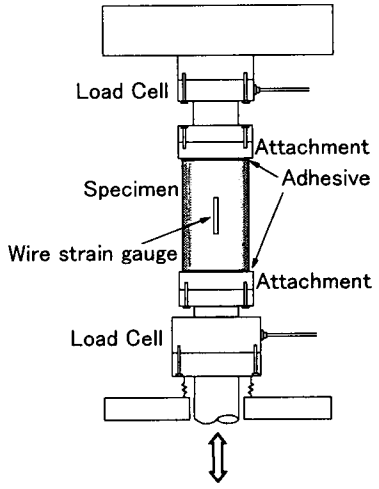


Fig. 1 Test Equipment

Table 1 Mix Proportion of Concrete

Mixture	Gmax (mm)	VC value (sec)	Slump (cm)	Air (%)	W/C (%)	s/a (%)	Unit Weight (kg/m^3)					Admixture (kg)
							W	C	S	G		
										5-20 mm	20-40 mm	
RCD	40	20±10	–	–	75	42	119	159	891	652	612	0.398
GRAVITY	40	–	4±1	4±1	60	40	157	262	760	719	315	0.066
ARCH	40	–	4±1	4±1	45	37	156	347	675	738	433	0.156

the direct tensile tests on the 90th day of water cure.

3. TEST RESULTS

3.1. Comparison of Strengths of Concrete with Different Mix Proportions

The relationship between the cement water ratio and compressive strength is shown in Figure 2, the relationship between the cement water ratio and splitting tensile strength is shown in Figure 3, and the relationship between the cement water ratio and direct tensile strength (loading rate of 0.0067 N/mm^2/s) is shown in Figure 4. All strengths show the larger values for higher cement water ratio. However, the increase is less notable in the splitting tensile strength and the direct tensile strength than in the compressive strength. In addition, the direct tensile strength of RCD is especially low.

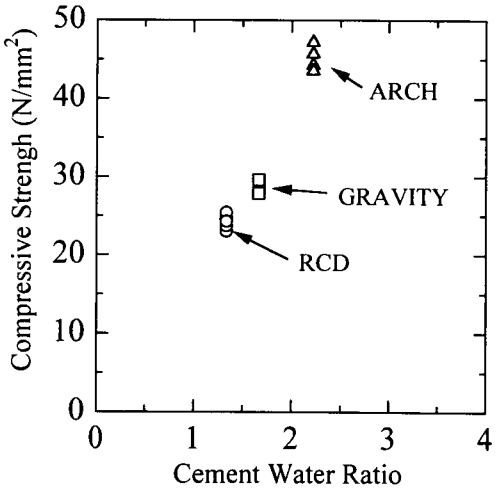


Fig. 2 Relationship between Cement Water Ratio and Compressive Strength

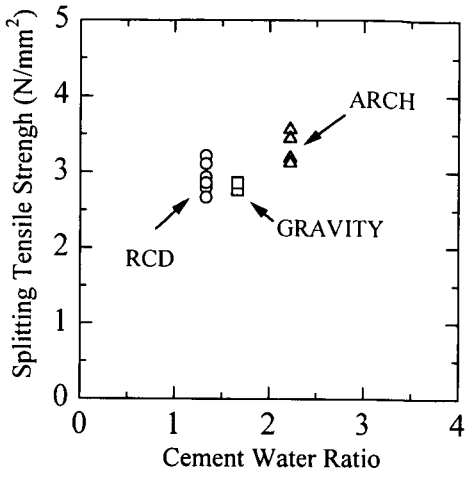


Fig. 3 Relationship between Cement Water Ratio and Splitting Tensile Strength

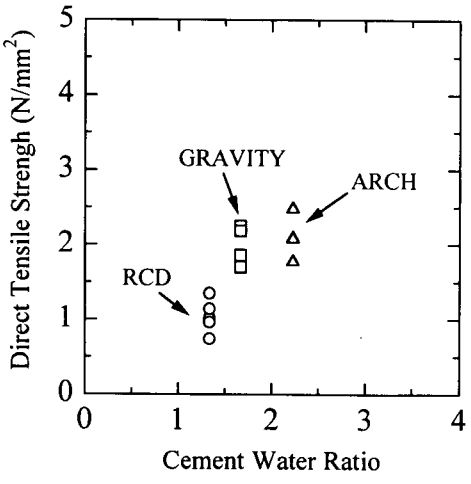


Fig. 4 Relationship between Cement Water Ratio and Direct Tensile Strength

3.2. Relationships between Compressive Strength, Splitting Tensile Strength and Direct Tensile Strength

The relationship between compressive strength and splitting tensile strength is shown in Figure 5 for three mix proportions. The splitting tensile strength increases as compressive strength increases. The ratio of splitting tensile strength to compressive strength is 1/9 to 1/7 for RCD, 1/11 to 1/12

for GRAVITY and 1/9 to 1/10 for ARCH.

The relationship between compressive strength and direct tensile strength (loading rate of 0.0067 N/mm^2/s) is shown in Figure 6 for three mix proportions. The ratio of direct tensile strength to compressive strength is 1/22 to 1/32 for RCD, 1/13 to 1/17 for GRAVITY and 1/18 to 1/25 for ARCH.

The relationship between splitting tensile strength and direct tensile strength (loading rate of 0.0067 N/mm^2/s) is shown in Figure 7 for three mix proportions. The ratio of direct tensile strength to splitting tensile strength is approximately 2/3 for GRAVITY and ARCH, and only 1/3 for RCD, which is significantly smaller than the others.

A smaller direct tensile strength compared to the splitting tensile strength may be attributed to the difference in the failure condition. Failure occurs at the weakest plane in a specimen in the direct tensile test while failure occurs in the prescribed plane in a specimen in the splitting tensile test.

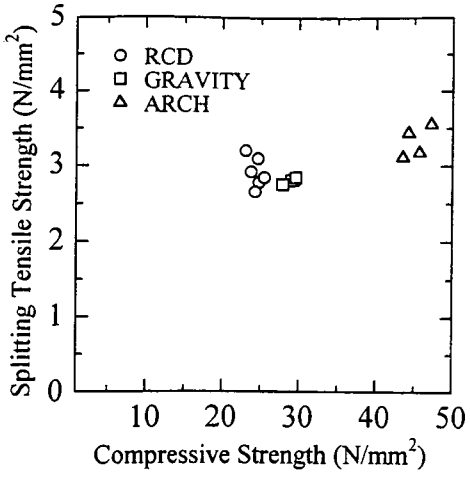


Fig. 5 Relationship between Compressive Strength and Splitting Tensile Strength

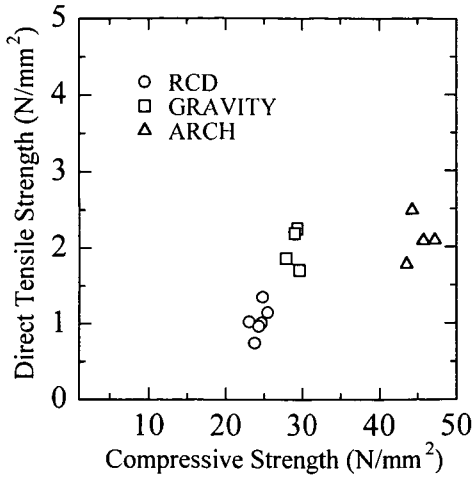


Fig. 6 Relationship between Compressive Strength and Direct Tensile Strength

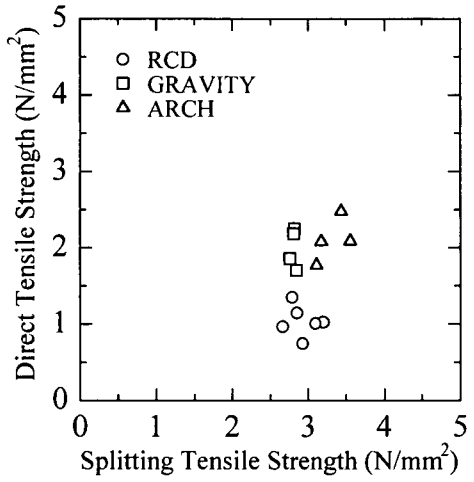


Fig. 7 Relationship between Splitting Tensile Strength and Direct Tensile Strength

3.3. Effects of Rate of Loading on Direct Tensile Strength

The relationship between the rate of loading and direct tensile strength is shown in Figure 8 for RCD, Figure 9 for GRAVITY and Figure 10 for ARCH. These figures are summarized in Figure 11 where the mean values of the test results are plotted. Figure

11 shows that tensile strength of all mix proportions increases, as the rate of loading becomes larger, although the dispersion of test results is large.

Figure 12 shows the normalized direct tensile strength where the tensile strength at a rate of loading of 0.0067 N/mm^2/s is assumed to be unity. The direct tensile strength is about 20% larger at 2 N/mm^2/s than at 0.0067 N/mm^2/s and about 50% larger at 20 N/mm^2/s.

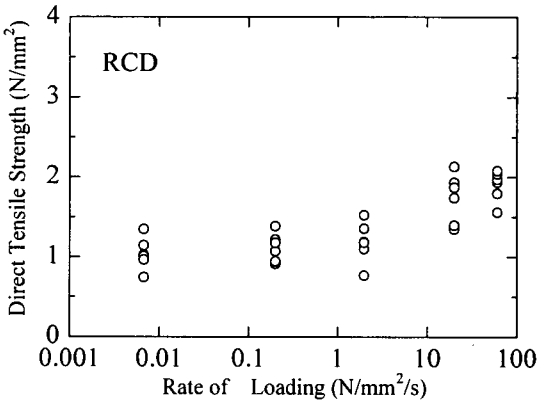


Fig. 8 Rate of Loading and Direct Tensile Strength (RCD Mixture)

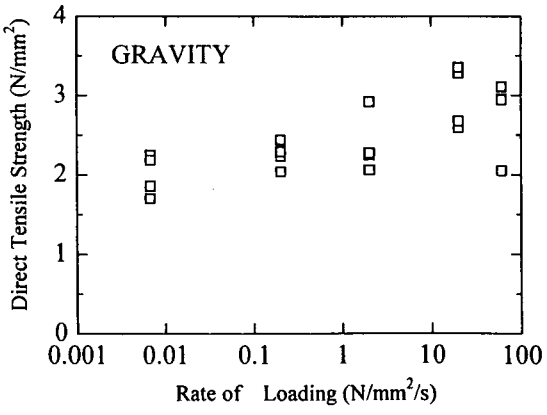


Fig. 9 Rate of Loading and Direct Tensile Strength (GRAVITY Mixture)

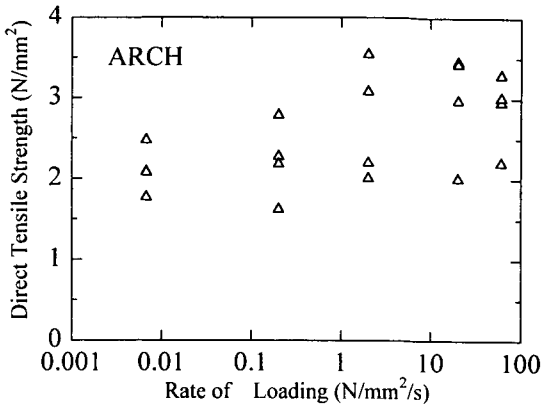


Fig. 10 Rate of Loading and Direct Tensile Strength (ARCH Mixture)

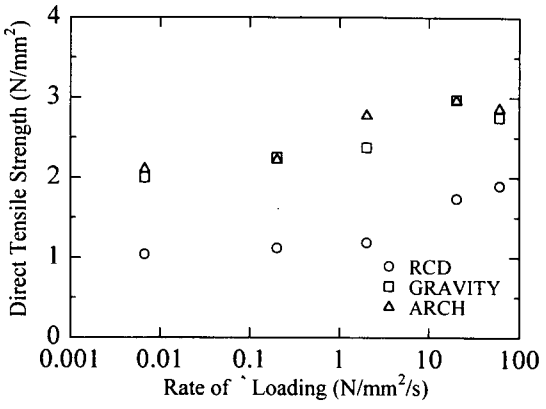


Fig. 11 Rate of Loading and Direct Tensile Strength (All Mixtures)

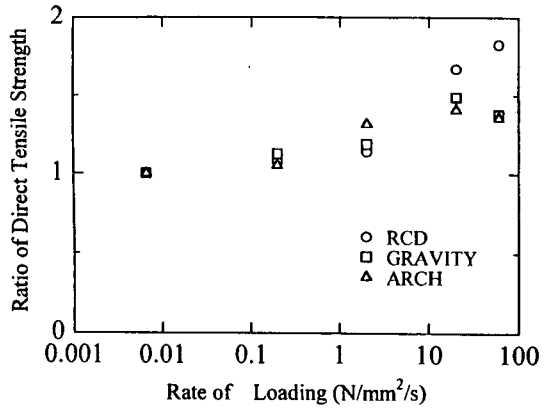


Fig. 12 Rate of Loading and Normalized Direct Tensile Strength

3.4. Effects of Rate of Loading on Elastic Modulus

Elastic modulus is defined here as the secant modulus between 0 μ and 50 μ of strain. The relationship between the rate of loading and the elastic modulus is shown in Figure 13 for RCD, Figure 14 for GRAVITY and Figure 15 for ARCH.

Figure 16 shows the normalized elastic modulus where the elastic modulus at a rate of loading of 0.0067 N/mm^2/s is assumed to be unity. The elastic modulus does not seem to be affected by the rate of loading.

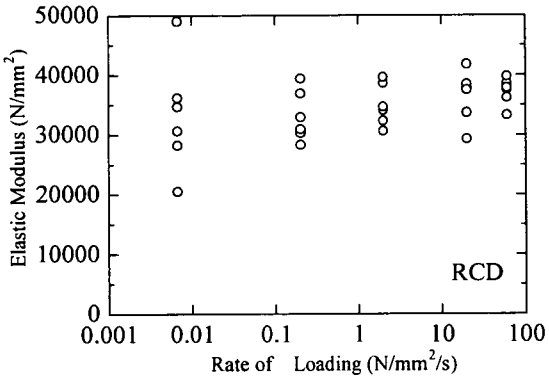


Fig. 13 Rate of Loading and Elastic Modulus (RCD Mixture)

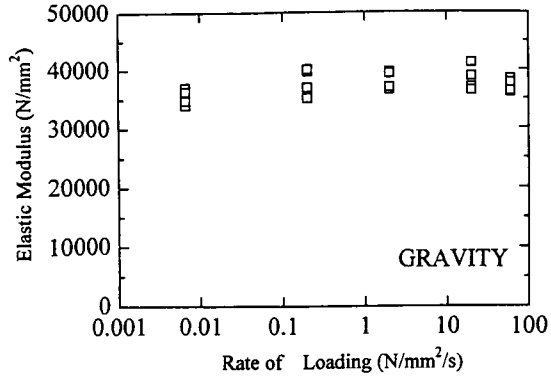


Fig. 14 Rate of Loading and Elastic Modulus (GRAVITY Mixture)

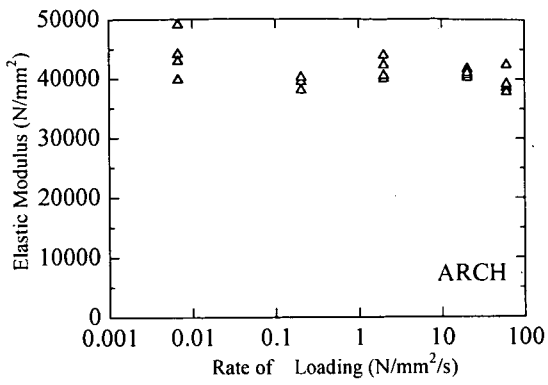


Fig. 15 Rate of Loading and Elastic Modulus (ARCH Mixture)

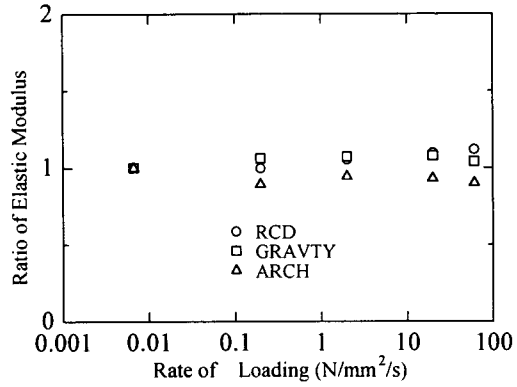


Fig. 16 Rate of Loading and Normalized Elastic Modulus

4. CONCLUSION

The following conclusions are derived from the results of the strength tests.

1) The compressive strength, splitting tensile strength and direct tensile strength of concrete increase as the cement water ratio increases. The increase in the splitting tensile strength and the direct tensile strength, however, is smaller than the increase in the compressive strength.
2) The direct tensile strength of concrete is smaller than the splitting tensile strength of concrete. This tendency is

notable in RCD concrete.

3) The direct tensile strength of concrete increases as the rate of loading increases.
4) The elastic modulus is not affected by the rate of loading.

REFERENCES

1) Isao NAGAYAMA, Kazuo WATANABE and Nobuyuki OBATA: Experimental Study on Direct Tensile Strength of Concrete for Dams, Technical Memorandum No.2914, PWRI, Dec. 1990
2) Isao NAGAYAMA, Kazuo WATANABE, Yoshinobu SYUTO and Nobuyuki OBATA: Experimental Study on Direct Tensile Strength of Concrete for Dams (2), Technical Memorandum No.3193, PWRI, May 1993

Multidisciplinary Cooperative Research to Mitigate Medical Consequences after the Earthquake

by

Keiko Ogawa[1], Ichiro Tsuji[1], Shigeru Hisamichi[1]

ABSTRACT

One important role of the epidemiologists in disaster research is to assess the relationships between possible causal variables and health outcomes. Accordingly, it is essential to evaluate the association between certain factors and health effects in the disaster-affected population. Past studies suggest that post-earthquake "stress" condition could be related with the medical consequences in the immediate, short, and long term periods. The objective of the present study is to design a proposal to evaluate the association between the inconvenience of daily life due to the lifeline disruption and indirect health effects such as the incidence rate of coronary heart disease. Understanding of causal variables enables us to determine the most rational method to allocate resources toward minimizing adverse health outcomes, and to improve the decision-making process at the central (governmental disaster managers) as well as the local (community) levels. More efforts are required to evaluate the relationship between environmental factors and indirect health effects.
Multidisciplinary cooperation is most essential to elucidate causing factors.

KEYWORDS: multidisciplinary research
lifeline disruption
indirect health effects
risk factor

1. INTRODUCTION

The roles of epidemiologists in the disaster research have been discussed (Western, 1972; Noji, 1992) and non-experimental (observational) studies have been performed to identify the risk factors influencing the health outcome (Jones, 1990). Multidisciplinary cooperative researches following earthquakes have evaluated the association between the structural elements and mortality and morbidity directly caused by the structural damages (Jones, 1994). For example, fatalities were examined to estimate the relationship with certain types of the buildings after the Armenian earthquake in 1988 (Noji, 1990). Precast concrete frame was associated with highest mortality per building.

The causal variables related with indirect health effects, however, have not been fully discussed. This "indirect health effect", defined as all health problems not caused directly by the structural damages, are usually reported as long-term health effects. Past studies have suggested that post-disaster stress conditions could be related with indirect health effects.
Some environmental factors or personal experiences such as material loss or death of family members can be indicative of "stressors".

1) Department of Public Health, Tohoku University School of Medicine, Sendai 980 Japan

The disruption of the lifeline, availability of utilities i.e., electricity, water, gas, etc., on which the population depend, is the characteristics of urban disasters. The magnitude of the damage in such disasters has been estimated as the number of the affected population due to the lifeline disruption and the duration required for the reconstruction. These numbers are not sufficient to quantify the total influence on the affected population. The modified indicator should be developed to estimate the overall impact on the population due to lifeline disruption. "The overall impact" should include the stress due to the disruption.

2. OBJECTIVES

The objective of the present study is to establish a proposal which clarifies the causal mechanism and the degree of indirect health effects due to the lifeline disruption after an earthquake.

To achieve this general objective, the specific objective is to assess the association between the inconvenience of daily life due to the lifeline disruption and the incidence of coronary heart disease (CHD) rate and several medical consequences after adjusting the possible confounding factors. The incidence rates of CHD and the other medical consequences should be compiled in a population-based study.

3. BACKGROUND AND IMPORTANCE OF PROJECT

The roles of epidemiologists in the disaster research are three folds;

1. To monitor the health effects on the affected population
2. To investigate the causal relation between environmental factors and the health effects
3. To develop the preparedness strategies in the health sector and to evaluate their effectiveness.

Various studies have investigated the damage of structural elements as risk factors for the health outcomes following earthquakes in Guatemala (Glass, 1977) and in Italy (de Bruycker, 1985) and in Armenia (Noji, 1990). Rescue and medical care were analyzed to determine the effective preparedness strategies to reduce the human casualties (Noji, 1993). De Ville stressed the importance of epidemiologic surveillance to monitor the health effects after the Guatemala earthquake (de Ville, 1976). From the engineering standpoint, there have been investigations on earthquake mortality to define the affecting factors (Coburn, 1987) and to develop the prediction model (Shiono, 1991b).

Most studies after earthquakes, however, were focused on the direct health effects or indirect health effects in rural communities. Investigations on the indirect health effects in urban disasters have been limited.

Indirect health effect refers to all medical health consequences not directly caused by structural damages from the seismic activities during the earthquake. There are a few studies describing indirect health effects (Logue, 1981b). Rapid increase of the mortality from coronary heart disease as reported after the Greece earthquake (Katsouyanni, 1986). Logue emphasized physical and mental disorders among the affected population after a hurricane as indirect health effects (Logue, 1978, 1979, 1980, 1981a). The long-term health effects after the Great Hanshin-Awaji earthquake have also been reported. The importance of long term observations were addressed, and social support such as the provisions and maintenance of daily life was regarded as important elements (Sato, 1997). Considering the duration and the number of

the cases of the indirect health effects, the overall impact on the affected society cannot be overlooked.

4. RESEARCH AND METHODOLOGY

(1) Hypotheses

The indirect health effects after an earthquake in this study is defined as "any kind of health outcomes in both short and long terms after the impact phase which were not caused by structural damages of seismic activities".

The hypotheses to be tested in this investigation is the indirect health problems attributed to the inconveniences of daily life due to lifeline disruption after the Great Hanshin-Awaji earthquake.

(2) Study rationale

After the Great Hanshin-Awaji earthquake, the increased prevalence of hypertension, coronary heart disease and mental disorders has been reported (Sato, 1997). Some studies have suggested that the post-earthquake stress caused adverse medical outcomes after the earthquake. Knowledge of the causal mechanism of indirect health effects enables us to decide the most rational way to allocate resources especially in the early rehabilitation stage. These points are essential to minimize the overall health effects. The cohort study on health-effects after the Armenia earthquake (Melkonian, 1997) showed higher risks of morbidity, especially for CHD in persons exposed to more stressors.
In this report, the stressors included major losses such as financial property or death of family members. The magnitude of mental and physical stress that the people receive during the response and rehabilitation phases should be measured, and causal mechanism should be fully analyzed.

(3) Study design and study subjects

Three different methods are proposed.

a) Case-control study (Proposal 1)

The CHD cases are compared with control cases regarding the inconvenience of daily life due to lifeline disruption. The cases are selected by the hospital record at the major hospitals in the affected area. The controls are selected among the patients who visited the same hospitals for common medical problems on the same day and had lived in the same district as the cases. Both cases and controls should be restricted to persons who remain in the same residence from the onset of the earthquake to the sampling point. We will then compare the strength of the association with the inconveniences of daily life between cases and controls.

b) Retrospective cohort (Proposal 2)

b-1) The inhabitants who had received annual health checks before the earthquake are followed up. We compare the results of both occasions with respect to blood pressure, EKG, blood examinations including liver function.

b-2) The incidence rate of CHD is measured by the claim history file of national health insurance. We will calculate relative risk of inconvenience of daily life for occurrence of indirect health effects, after adjusting for the effects of socio-demographic data and personal damage due to the earthquake.

c) Ecological study (Proposal 3)

The correlation between the inconvenience of daily life and the incidence rate of CHD would be examined across all district which was affected by the earthquake.

(4) Variables to be measured

The following variables are measured in each study.

a) Personal damage due to the earthquake
b) Inconvenience of daily life due to the lifeline disruption
c) Socio-demographic data
d) Possible confounders
e) Indirect health effects

a) Personal damage due to the earthquake

Personal damage due to the earthquake is an important factor in estimating individual stress. The data to be measured include loss of family members and property damage.

b) Inconvenience of daily life due to lifeline disruption

The inconvenience of daily life due to the disruption of lifeline system is measured as possible causal factors for the stressors after the Great Hanshin-Awaji earthquake.

The extent of inconvenience due to post-earthquake suspension of utility service (electric power, water and gas supplies) is calculated in terms of a numerical score consisting of the degree of restriction and the period of restriction. "Degree of restriction" is defined as the extent to which living activities (cooking, toilet use, bathing and washing clothes) is restricted, compared with those of the pre-earthquake condition. "Period of restriction" represents the number of days during which activities are affected. Estimating "degree of restriction" requires detailed information on the suspension pattern of the three utilities and living pattern of the affected people (the level of dependence on the utilities).
The inconvenience of daily life was investigated after the Chiba-Ken-Toho-Oki earthquake in 1987 (Shiono,1989 and 1991a). It was originally aimed at developing a prediction model to estimate the difficulties that people would experience due to the disruption of three utility services: gas, water, and electric power. The study measures more direct impacts on the population than just the number of the affected people and the days required for the recovery.

In the prediction model, the validity was established, based on the comparison of the predicted result and direct observation with a survey method.

In summary, the inconvenience can be estimated on the individual bases from the existing data when the study subjects continue to reside in the same residence before and after the earthquake.

c) Socio-demographic data

The relationship between psychosocial factors and coronary heart diseases has been suggested (Haynes, 1978). All of known risk factors for CHD should also be measured.

d) Possible confounders

In order to avoid confounding bias, we should measure the obesity level and smoking habits.

e) Indirect health effects

Determining a standardized classification and definition of the earthquake-related health effects is required to assess the relationship between health outcomes and causing variables.

In the case-control study (proposal 1), the occurrence of CHD is investigated. In the

retrospective cohort (proposal 2), the results of the annual health checks including blood pressure, EKG and blood examination is compared between before and after the earthquake. The incidence rate of CHD is measured by the claim history file of national health insurance. In the ecological study (proposal 3), the incidence rate of the CHD is measured.

(5) Methodological problems and limitations

The above formula, developed to predict the inconvenience due to lifeline disruption in future disasters, is based on data pertaining to individual households. We, therefore, should restrict the study to subjects who remain living in the same household after the disaster.

5. SUMMARY

The epidemiological approach is very useful in the investigation to identify the risk factors and to elucidate the causal relation. Multidisciplinary cooperation is essential in analyzing the consequences after the disasters.

6.ACKNOWLEDGMENT

We thank Dr. K. Shiono, PhD, Eng , Nagaoka College of Technology, Department of Civil Engineering, for his helpful comments.

7. REFERENCES

Coburn AW, Murakami HO and Ohta Y. (1987) Factors affecting fatalities and injury in earthquakes. Internal report, Engineering seismology and earthquake disaster prevention planning. Hokkaido, Japan, Hokkaido University, 1-80.

de Bruycker, M., Greco,D., and Lechat,M.F. (1985) The 1980 Earthquake in Southern Italy: Morbidity and Mortality. International Journal of Epidemiology 14, 113-117.

de Ville de Goyet C., del Cid E., Romero A., Jeannee E., Lechat M. (1976) Earthquake in Guatemala: Epidemiologic evaluation of the relief effort. Bulletin of the Pan American Health Organization Vol.10, No.2, 95-109.

Glass RI, Urrutia JJ and Sibony S (1977) Earthquake injuries related to housing in a Guatemala village. Science 197, 638-664.

Haynes, SG., Levine S., Scotch N., Feinleib M.,Kannel WB. (1978) The relationship of psychosocial factors to coronary heart disease in the Framingham Study: 1.Methods and risk factors. American Journal of Epidemiology 107:362-383

Jones NP, Krimgold F, Noji EK and Smith GS (1990) Considerations in the epidemiology of earthquake injuries. Earthquake Spectra. Vol 6, No.3, 507-528.
Jones NP, Smith GS and Wagner RM (1994) Risk factors for casualty in earthquake: The application of epidemiologic principles to structural engineering. Structural Safety 13, 177-200.

Katsouyanni K.,Kogevinas M.,Trichopoulos D. (1986) Earthquake-related stress and cardiac mortality : International Journal of. Epidemiology 15,326-330

Logue JN (1978) Long-term effects of a major natural disaster: The Hurricane Agnes flood in the Wyoming Valley of Pennsylvania, June,1972. Doctoral Dissertation, Columbia University Faculty of Medicine, School of Public Health, Division of Epidemiology, New York

Logue JN, Hansen H,and Struening E (1979) Emotional and physical distress following Hurricane Agnes in Wyoming Valley of Pennsylvania. Public Health Reports 94,495-502.

Logue JN and Hansen H (1980) A case-control study of hypertensive women in a post-disaster community. Journal of Human Stress 6 (2), 28-34.

Logue JN, Hansen H,and Struening E (1981a) Some indications of long term health effects of a natural disaster in American Society. Public Health Reports 96 (1), 67-79.

Logue JN, Melick ME, and Hansen H (1981b) Research issues and directions in the Epidemiology of health effects of disasters. Epidemiologic Reviews 3,140-162.

Melkonian, A., Armenian HK., Hovanesian AP(1997) Cohort studies on health-effects from earthquake. Paper presented at the International Symposium on Earthquake and People's Health: Vulnerability reduction, preparedness and rehabilitation; January; Kobe

Noji EK, Kelen GD, Armenian HK, Jones NP and Sivertson KT (1990) The 1988 earthquake in Soviet Armenia: a case study. Annals of Emergency Medicine 19, 891-897.

Noji EK (1992) Disaster epidemiology: Challenges for public health action. Journal of Public Health Policy, 332-340.

Noji EK, Armenian HK, and Oganessian A.(1993) Issues of rescue and medical care following the 1988 Armenian earthquake. International Journal of Epidemiology Vol.22, No.6, 1070-1076.

Sato S. (1997) The long term effects of the Great Hanshin-Awaji earthquake on urban public health. Paper presented at the International Symposium on Earthquake and People's Health: Vulnerability reduction, preparedness and rehabilitation; January; Kobe

Shiono K.(1989) Inconvenience in resident's aily living activities from post-earthquake suspension of utility services. Comprehensive Urban Studies No.38, 149-167.

Shiono K. ,Shumuta Y. (1991a) Inconvenience in resident's daily living activities from post-earthquake suspension of utility services, part 2. Procedure for estimation. Comprehensive Urban Studies No.41, 37-46.

Shiono K., Krimgold F.,Ohta Y. (1991b) Post-event rapid estimation of earthquake fatalities for the management of rescue activity. Comprehensive Urban Studies No.44, 61-106.

Western. KA (1972) The epidemiology of Natural Disasters; The present state of the arts. Dissertation submitted for: The academic diploma in tropical public health, The Department of Tropical Hygiene and Public Health, London School of Hygiene and Tropical Medicine

Large-Scale Physical Model Test on Tsunami Overtopping and Bed Scour Around Coastal Revetment

by

Kenji Noguchi[1] and Shinji Sato[2]

Abstract

A series of hydraulic model tests was performed to investigate tsunami overtopping and bed scour around coastal revetments. The overtopping motion of tsunami and bed scour in front of the revetment were recorded by a video camera. Water surface elevation, flow velocity and overtopped water mass were measured. Sixteen runs of experiments were performed for various combinations of water levels and incident wave heights. The pattern of tsunami overtopping was classified into 6 groups. It is found that the overtopping rate can be estimated from incident tsunami profile. A large-scale scour was produced in front of the revetment by a standing vortex generated by return flow.

Key Words: Tsunami, Overtopping, Scour, Coastal revetment

1. Introduction

The necessity of integrated countermeasure for tsunami disasters has been remarked by Japanese Government since Nihon-Kai Chubu Earthquake tsunami. This countermeasure is structured into three categories, which are coastal structure, regional planning and tsunami evacuation system. In order to plan this countermeasure effectively, it is necessary to study tsunami behavior around coastal structure as a gate of inundation. Tsunami disaster around coastal revetments, one of the coastal structure, will be occurred by tsunami runup and collapse of revetments.

In the numerical simulation of tsunami flooding, inundated tsunami is generally approximated as long wave, even if it overtopped revetments. However, the fluid motion above the revetment has not yet well described. At the same time, the bed in front and back of the revetment would be scoured. In fact some of coastal revetments and sea walls were collapsed by Hokkaido-Nansei Oki earthquake tsunami and Nihon-Kai Chubu earthquake tsunami.

Former laboratory studies about tsunami behavior around coastal structures have been performed under small scale conditions. Therefore, they could not reproduce the size of bed scouring and fluid motion in detail. In this study, a series of large scale hydraulic model tests were performed for

1) Researcher, Coast Division, River Department, Public Works Research Institute, Ministry of Construction, Tsukuba, 305, Japan

2) Head, ditto

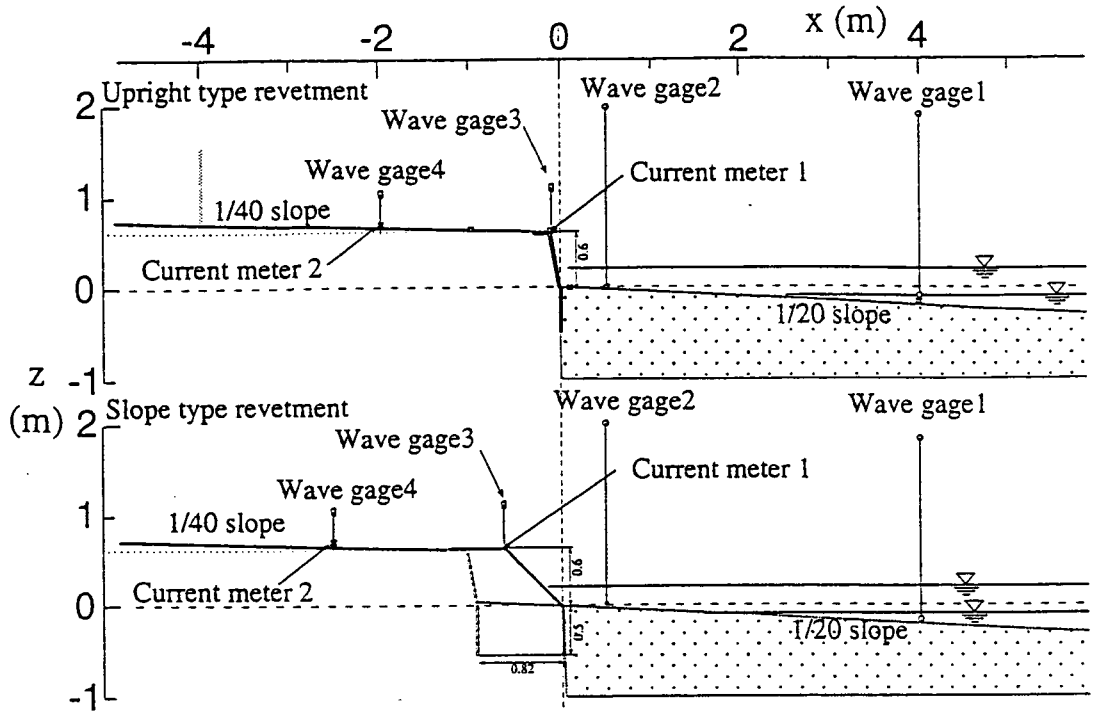


Figure 1 Revetment models and location of instruments

tsunami overtopping and bed scouring in front of a structure.

2. Implementation of hydraulic model tests

Experiments were preformed in a wave channel which is 5m deep, 1.9m wide and 135m long. The channel is equipped with a piston type tsunami wave generator. The wave generator pushes water forward to generate a tsunami with hyperbolic tangential motion within 2m length stroke. The model of sea bottom was filled with fine sand with a 1/20 slope. The wave channel was divided into two channels by a partition wall. A revetment model was installed on one side, in which waves, currents and bed scour patterns were observed. On the other side, in which a trap tank was installed behind the front face of the revetment, the water mass of overtopped tsunami was measured. The coastal revetment

Table 1 Experimental condition and results of overtopping

Case	Incident tsunami height (m)	Initial water level (m)	Overtopping type	Unit width overtopping rate (m^3/m)
1	0.21	0.3	a	0.56
2	0.42	0.3	b	2.67
3	0.21	0.2	a	0.20
4	0.31	0.2	c1	0.88
5	0.20	0.1	a	0.07
6	0.30	0.1	c1	0.44
7	0.18	0	c1	0.06
8	0.40	0	d1	0.60
9	0.40	-0.1	d1	0.35
10	0.41	-0.1	d2	0.41
11	0.20	0	c2	0.03
12	0.30	0.1	c1	0.66
13	0.20	0.1	a	0.06
14	0.40	0	d1	0.65
15	0.41	-0.1	d2	0.58
16	0.21	0.2	a	0.27

model was made of wood. Shoreward floor above the revetment was fixed as a 1/40 slope by cement mortar. The coastal revetment model was 0.6m height and made with 1/10 scale. Revetment types were upright one and sloped one. To protect against the suction of inner material, a cutoff board was settled to 0.5m depth as a fundamental work.

Wave profiles were measured by capacitance type wave gages situated at offshore (x=90m), in front of revetment (x=0.5m and 4m), above revetment (x=-0.1m) and on the shoreward slope (x=-2m). Velocities were measured by propeller current meters situated above revetment and at offshore, which were at the same points with wave gages. Motions of tsunami overtopping and bed scouring in front of revetment were recorded by a video camera.

The physical model tests were performed for 16 cases with incident tsunami wave height ranging from 0.2 to 0.4m. Experimental conditions were arranged for several combinations of among wave height, water level against height of revetment and two revetment types. According to Street and Camfield(1966), the breaker type of tsunami almost depends on the slope of sea bottom. In this study, all the cases were expected to be plunging breaker since offshore slope was 1/20. To produce several phenomenons, initial water level was changed.

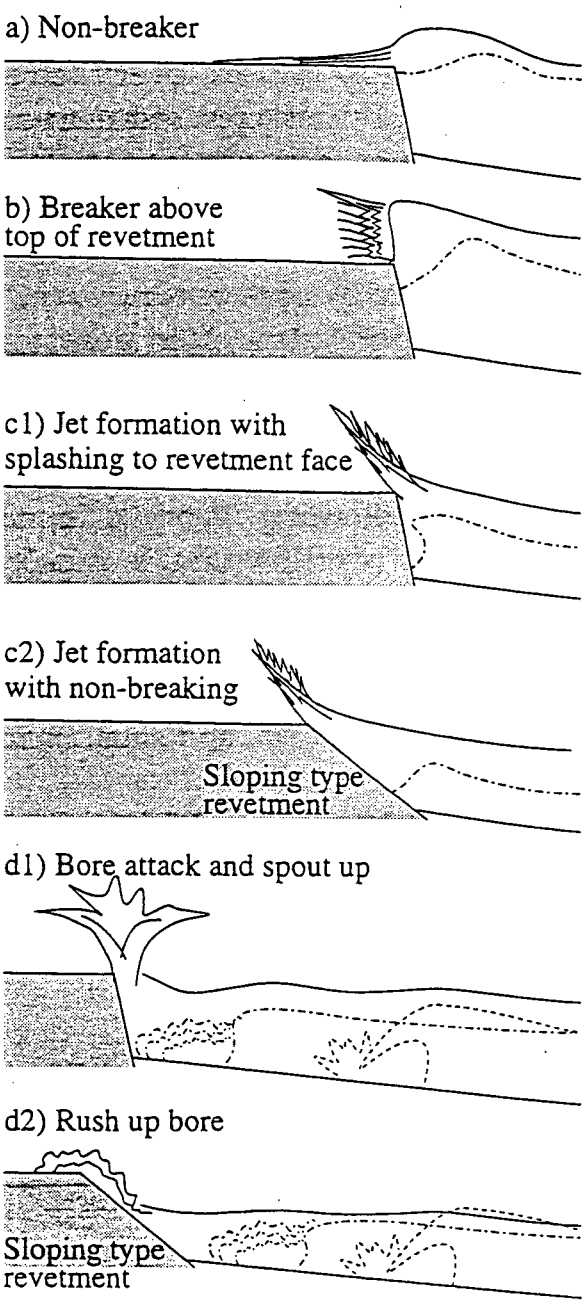


Figure 2 Pattern of overtopping

3. Results of Test

3.1 Patterns of overtopping

Patterns of overtopping were classified into the following 6 patterns

shown in Figure 2 by video capture; "a" overflow without breaking, "b" bursting to forward over the revetment, "c1" wave crest splashing to the revetment face with formation of jet from the top of the revetment face, "c2" formation of jet from the revetment face by non-breaking wave, "d1" strong bore attack after breaking and "d2" rushing up of strong bore after breaking.

Details of patterns are explained in the followings. Type "a" is similar to weir overflow that is usually approximated in tsunami inundation numerical simulation. This pattern occurred under high initial water level from 0.1 to 0.3m, and small incident wave.

In the motion of "b", tsunami arrived at revetment without breaking. When the wave crest reached the top of revetment face, wave front bursts forward.

Though "c1" and "c2" are characterized by jet formation from top of the revetment face, they had different process. Process of "c1" was first plunging breaking in front of revetment, splashing directly to the top of the revetment or via reflected from seabed of front, rushing up along slope and finally to launch jet. Pattern "c2" did not break before the formation of jet which was produced from the loop of partial standing wave formed on the sloping face of the revetment.

Though both "d1" and "d2" occurred by broken bore rushing to the revetment, they showed different motions owing to the difference in the slope angle of revetment face. In case of steep face, bore splashed and breezed up from top of revetment. On the other hand, when the face was more gentle, bore rushed up along the face and directly inundated shoreward of the revetment.

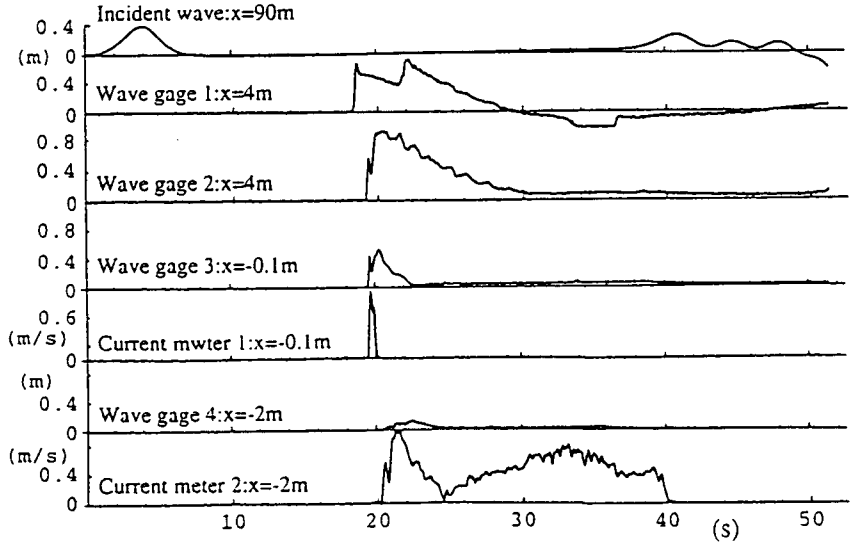


Figure 3 Wave and current profiles (case 8)

3.2 Time series of tsunami profile and flow velocity

Figure 3 shows time series of h and u of case 8 which is discussed in detail later. Pattern of overtopping of case 8 was "d1". The symbol "t" denotes the time from the initiation of data sampling. Tsunami incident wave, which is illustrated on the top, was a single positive wave. At the revetment, a part of tsunami was reflected to offshore and the other overtopped and inundated. The reflected wave was noticed by the second peak at 22s of No.1 wave gage.

No. 2 current meter shows positive value for both directions, since this current meter does not detect the flow direction. Runup velocity reached almost 1m/s. This value is scaled to 3.2 m/s with proto-type scale. The return flow occurred from 24.5s judging from the wave profile. The return flow exceeded 0.6m/s and continued for 15 second.

3.3 Overtopping rate

Overtopping rate and runup height were obtained by two methods. One is known Aida method (1977) similar to formula of discharge for weir. The other is integrated mass flux estimated from water surface elevation and inlet velocity. The unit width mass flux was estimated with the following equations:

The Aida method is expressed by

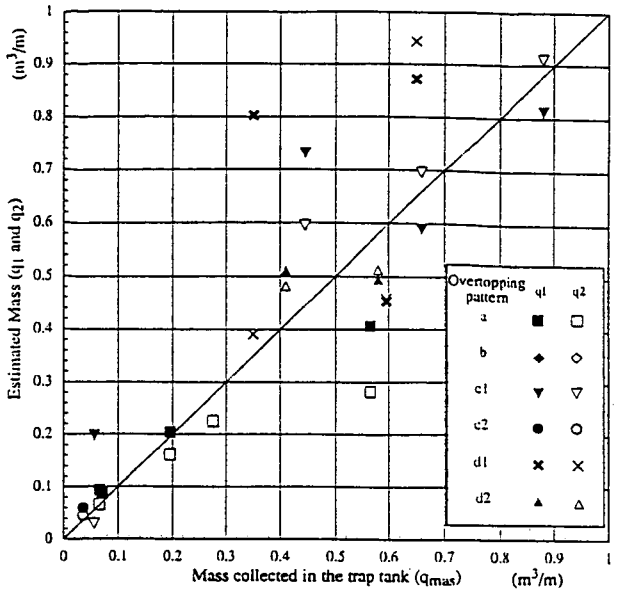


Figure 4 Correlation between overtopped mass and computations by two different methods

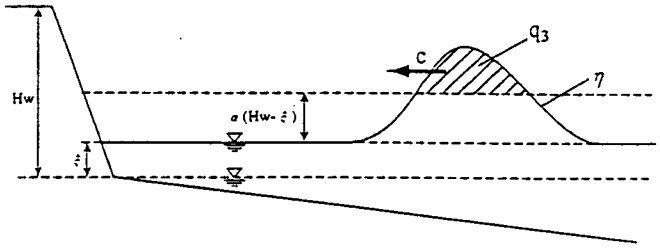


Figure 5 Concept of overtopping mass estimation from incident tsunami profile

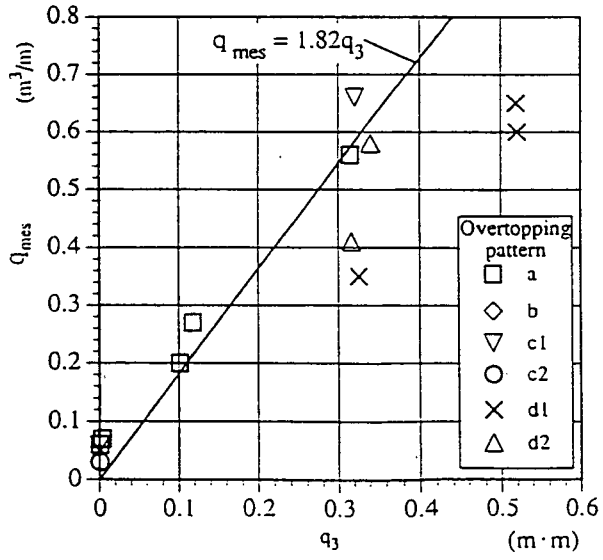


Figure 6 Estimation of mass of overtopped tsunami

$$q_1=\int_{t_s}^{t_e}\frac{1}{2}\eta\sqrt{g\eta}\,dt \quad ---(1)$$

Integrated mass flux is expressed by

$$q_2=\int_{t_s}^{t_e}\eta\cdot u\,dt \quad ---(2)$$

In this test, they could be calculated from water surface elevation (η) and flow velocity (u) above the revetment top. In each equation, "ts" is the start time of inundation and "te" is the start time of backwash. Figure 4 shows correlation between the mass (qmes) of overtopped water collected in the trap tank and estimated mass (q1 and q2). According to this figure, Strong correlation was observed between the mass of overtopped tsunami and the integrated mass flux.

Then, overtopping rate will be estimated from the incident tsunami profile. The concept is illustrated in figure 5. Overtopping rate is supposed to be proportional to the hatched area of tsunami profile that was cut by the broken line. Then it can be written by the following equation.

$$q_3=c\int_{t_{is}}^{t_{ic}}\left\{\eta-\alpha\cdot\left(H_w-\xi\right)\right\}dt \quad ---(3)$$

Where "Hw" is revetment height from origin, "ξ" is initial water, "α" is a parameter obtained from test, "η" is the time series of water surface elevation,

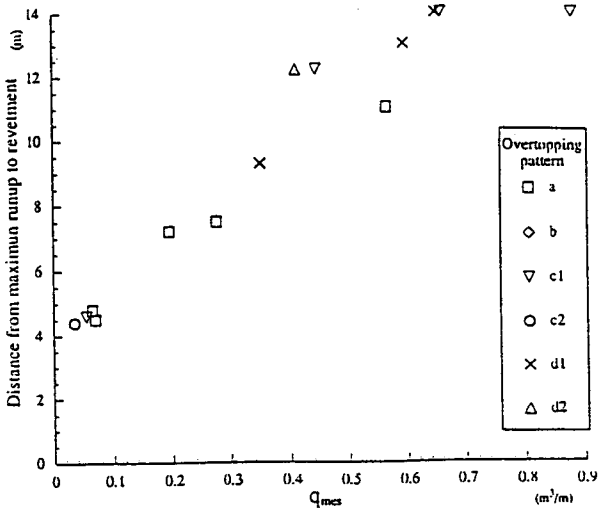


Figure 7 Overtopping rate and runup distance

$c=\sqrt{g\cdot h}$ is wave celerity, g is gravity acceleration and h is water depth.

Figure 6 shows the correlation between q3 and qmes. The line in the figure shows qmes=1.82 q3. The data follow the line well expect for the overtopping pattern of d1 and d2. The reason why d1 and d2 did not match the line was explained from the fact that the energy had decreased significantly by wave breaking for d1 and d2.

Figure 7 shows relation between the overtopping rate and the distance from revetment edge to maximum inundated point. They show strong correlation irrespective of the pattern of overtopping.

3.4 Bed scouring in front of revetment

Bed scouring was analyzed by video. Bed scouring is supposed to be caused by rushing wave and return flow from revetment top. By rushing wave, however, bed scouring was little

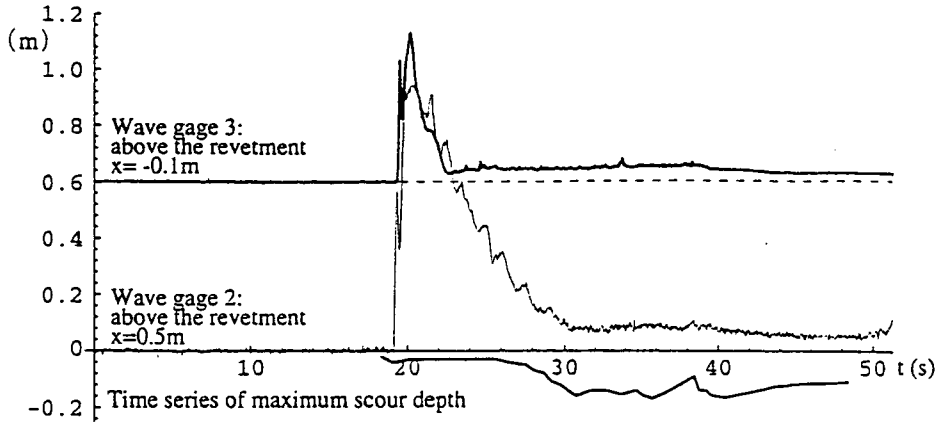


Figure 8 Time series of bed scour depth in front of the revetment (case 8)

and appeared only for low water level and large wave height. By return flow, the bed scour was generated by a standing vortex growing in front of revetment while the return flow continued. The scour depth was almost the same as the vortex diameter. Scoured bed was rapidly recovered by settling sand when the vortex decayed. Significant deposition occurred in 5 cases. The deposited sand, which was captured in vortex, was settled from the vortex area area after the vortex strength became weak.

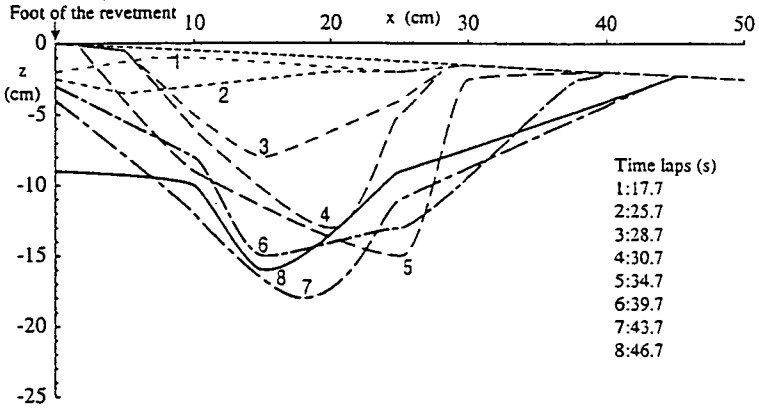


Figure 9 Scoured bed profile change (case 8)

Figure 8 shows time series of scour depth. Scouring in this case was produced firstly by swash, later by return flow and deposition by released sand from vortex. Two sets of time series of water elevation above the revetment and in front of the revetment were illustrated together. For easy to understand, the illustration of revetment top wave elevation was raised 0.6m since the wave gage located 0.6m height from initial water level. Small scouring occurred at the tsunami arrival at the revetment. Main scouring process started after the water level in front of the revetment decreased. Finally, there seems to be equilibrium depth. At last, scoured bed recovered by the released sand along with vortex decay.

Figure 9 shows the profile change of scoured bed in Case 8. Though the bed scour began near the revetment wall, the deep scour areas moved to the area around x=20cm and z=-15cm where the vortex was agitating sand

with a strong scour, This profile is shaped by standing vortex in front of the revetment.

4. Conclusions

Main conclusions are as follows:

1. The pattern of tsunami overtopping was classified into 6 groups.
2. Strong correlation was observed between the mass of overtopped tsunami and the integrated mass flux, which was estimated from water surface elevation and flow velocity above the revetment edge.
3. Overtopping rate was estimated from incident tsunami profile.
4. Scouring by swash was relatively negligible.
5. In front of revetment, a large-scale scour was produced by standing vortex generated by return flow. The scour depth had a strong correlation with overtopping rate.

References

Aida,I.(1977): Numerical Experiments for Inundation of Tsunamis -Susaki and Usa, in Kochi Prefecture-, Bull. Earthq. Res. Inst., Vol.52, pp.441-460.(in Japanese)

Street,R.L. and F.E. Camfield(1966): Observations and experiments on solitary wave deformation, Proc. 10th Int. Conf. Coastal Engineering, pp.284-301.

CORRELATION BETWEEN DAMAGE TO BUILDINGS AND LANDFORM IN THE 1995 HYOGO-KEN NANBU EARTHQUAKE

—An analysis by the application of GIS —

Naohisa Okada, Satoru Kawashima, Yoko Yamada [1)]

1. Abstract

The 1995 Hyogo-ken Nanbu Earthquake occurred in January 1995 brought the biggest damage in the years after the World War II to human beings and tremendous damage to buildings.

The Geographical Survey Institute has implemented landform classification in this earthquake at large scales from the perspective of correlation between damage to buildings by the earthquake and landform (ground) and verified by the analysis using GIS (Geographical Information System.)

Key words:

The 1995 Hyog-ken Nanbu Earthquake
land condition
GIS (Geographical Information System)
Landform classification and damage to buildings

2. Introduction

The Geographical Survey Institute has implemented surveys on land condition since 1960 and has produced land condition maps for the objective of providing basic materials such as natural condition on lands needed as counter-measure for disaster prevention and the planning of land use and development.

In particular, from the damage survey in The 1964 Niigata Earthquake, correlation between land condition and earthquake damage was observed, and usefulness of land condition maps have been evaluated in earthquake disaster.

For instance, depending on the period of sediment of the ground and its materials, there was difference in the value of amplification of seismic movement, and the ground which was newly formed and composed of materials of fine grains was likely to suffer bigger damage.

The objective of this survey was to quantify much data by computer analysis to verify the tendency which had been pointed out to be applicable in this earthquake.

1) First Geographic Division, Geographic Department, Geographical Survey Institute, 1 Kitasato, Tsukuba-shi, Ibaraki-ken, Japan 305

3. Content of the survey

3-1 Extent of the survey

The survey areas were the piedmont of the Rokko mountains which included Takarazuka City, Nishinomiya City, Ashiya City, and Higashi-Nada Ward, Nada Ward, Chuo Ward, Hyogo Ward, Nagata Ward and Suma Ward of Kobe City which were located in the northwest side of the Bay of Osaka. In consideration of topographic characteristics and state of damage, six map sheets at a scale of 1:10,000, such as "Takarazuka," "Ashiya," "Nishinoiya," "Rokko Island," "Sannomiya" and "Nagata" were designated to be the survey areas. The positions of the survey areas are shown in Fig.-1.

3-2 Materials for the survey

In this survey, such materials were used as Damage distribution map of The 1995 Hyogo-ken Nanbu Earthquake (the Second Version) which was produced by the urgent survey implemented after the occurrence of the earthquake, and provisional topographic map at a scale of 1:20,000 in Meiji Period and land condition map at a scale of 1:25,000 and reports made from 1984 to 1986.

The list of materials used in this survey is shown in Table-1.

3-3 Establishment of Survey Committee

For this survey, Survey Committee composed of members from academic societies was established and discussion was made on the contents to be indicated in the land condition map from the perspective of earthquake disaster prevention and details of analysis on landform and damage to buildings. The members of the Survey Committee are shown in Table-2.

3-4 Survey

The major objective of this survey was to study on the composition of land condition map which was applicable to disaster prevention assessment such as earthquake disaster, and to find out causes and effects on correlation between landform and damage to buildings in The 1995 Hyogo-ken Nanbu Earthquake by the application of the methodology of GIS. Flow of the survey is shown in Fig.-2.

4. Composition of land condition map and data digitization

4-1 Composition of land condition map

Composition of land condition map is shown in Table-3. It is composed of "landform classification" which indicates form and characteristic of land, "contour of ground elevation" which describes elevation of lowland from the sea level, "landslide" which indicates slope failure occurred by the earthquake and "disaster status" which indicates the status of collapse and damage to houses and buildings, fire, and liquefaction of ground.

In landform classification, former landform was classified and indicated in order to identify the initial form of artificially deformed area.

In particular, to add value for the application of disaster prevention

assessment such as earthquake disaster prevention, next four items were introduced in the items of expression.

1) Landforms after the change were indicated by additional symbols on the indication of former forms of the artificial change, such as mountain slope, valley plain and terrace.

2) Also in banked up surface in lowland, banked up surface after the change was indicated by additional symbol on the indication of former forms, such as valley plain or flood plain, coastal plain or delta, back marsh, former river bed and sea area.

3) Former shoreline, pond, marsh and drainage system were restored and overlaid on the present landforms.

4) Break lines of slopes (convex break and concave break) were indicated.

4-2 Data digitization

Data collected in 3-2, result of photo interpretation and landform classification made by reconnaissance survey were digitized, and data base was made. GIS which has functions of data analysis, data indication, data retrieval and data output was used for data digitization.

Systems used for data base production are:

EWS: Sun Micro Systems

OS: Solaris ver 2.4

Application: ARC/INFO ver. 7.0.4

Functions with frequent use were studied and selected from the basic functions of ARC/IFO, and programming was made by ARC/INFO micro language AML.

Based on this, all the data which were collected in 3-2 were digitized and stored in each hierarchy as indicated in Fig.-4

4-3 Production of land condition map

Without using traditional production process, land condition maps were produced by the computer by digitizing all the information.

They were produced in the following process. Land condition data and disaster status data, which were the major information for land condition maps, were input by scanning, and ARC/INFO coverage was made. It was stored by Graphics, a standardized file for output of ARC/INFO, as each delineation information, such as color, size and indication system, and various format conversions and ornaments were made, and output was made as land condition map at a scale of 1:10,000.

5. Analysis and result by the application of GIS

On the study of correlation between landform classification and damage to buildings, means of interpretation was changed from traditional visual interpretation to quantitative interpretation by computer processing. Data base of landform classification, land slide, former landform, ground elevation and collected data were analyzed in various forms using ARC/INFO's data retrieval, and data analysis and totaling functions.

Analysis was made in three items shown below.

1) Relation between damage to buildings and land condition (landform classification) and former land use

2) Relation between land slide in the Rokko Mountains district and elevation, slope, slope azimuth and convex break of slope

3) Relation between ground liquefaction

and land condition and former land use
In this survey area, there were remarkable damage to buildings in Ashiya City where analysis of similar items on the damage to wooden buildings was made.

5-1 Damage to buildings and landform

Analysis shown in Table-5 was made to find out the relation between damage to buildings and land condition, and correlation was found out by the quantitative interpretation.
Schematic view of the landform from the mountain side to the sea in the survey area is composed in order of terrace, alluvial fan, gentle frontage of fan, flood plains, valley plain, coastal plain, delta and sea. Landforms of sizable area, such as lowland, relatively higher and well drained and shallow valley on terrace appear as well.
Size of land with damage to buildings in the area was plotted as area of damage to buildings on disaster status map and overlay was made according to land condition and former land use, and total area was summed according to the scale of damage.
Based on this, the area ratio of damage to buildings shown in Fig.-3 was found out.
The ratio of damaged district in each landform classification of land condition was found out by this ratio and that of gentle frontage of fan is the highest and alluvial fan follows. It is observed that there is a peak in gentle frontage of fan and decrease of damage is seen towards both of sea and mountain side. This overlaps for the most part with the arrangement of zone of the earthquake disaster at the southern piedmont of the Rokko Mountains which is indicated as the district hit by a JMA intensity scale of 7.
On the analysis of damage to buildings in Ashiya City, data of respective wooden buildings were extracted from the digital mapping data prepared by the city and their state of damage was read from the distribution map of damage level of buildings (the Building Society) and analysis was carried out. The result is completed in Fig.-4.
Damage was especially concentrated in Ashiya City where 6,937 units were damaged including 270 badly damaged, 1,470 medium damaged and 4,257 slightly damaged, which are 60.5% of wooden buildings out of 11,458 units in the area of object.
In the same way as stated above, the ratio of units of damaged buildings was found out according to landform classification and former land use.
In landform classification, the biggest damage is observed in gentle frontage of fan and decrease of damage is seen towards mountain side in order of alluvial fan and terrace. In lowland, bigger damage is observed in coastal plain or delta and smaller damage is seen in valley plain or flood plain.
In former land use, damaged buildings are distributed equally in each category of use both on all survey areas and Ashiya City.

5-2 Slope failure

Collapse occurred in this earthquake was observed in 248 positions in five sheets (except for "Rokko Island" as it was not observed) in the survey area. Analysis of slope failure was carried out on elevation, slope, slope azimuth, and position between

convex break of slope and slope failure.
In order to compare with the result of the survey area, separate analysis was carried out on the sheet of "Takarazuka," in which mountainous district occupied 65% of the total area and the biggest number of land slides occurred.
On the grid data of elevation, slope and slope azimuth made from 50 grid data of digital map, position information of land slide was overlaid and the density of the occurrence of collapse was summed up. The result is shown in Fig.-5. Position related with convex break of slope is found out in Table-6.
In the category of elevation, it occurs in the elevation more than 50 to 100m, and the density of the occurrence of collapse per 1km is the highest in the elevation between 300 to 400m. In the category of slope, the density of occurrence of collapse in slope category starts to become high at 20 degrees or more, and the highest density per 1km is observed between 40 to 50 degrees. There were no data for 50 degrees or more, therefore analysis has not been carried out.
In slope azimuth, much more collapse is observed in order of NE, N, E, S in all the survey area, and only for Takarazuka Sheet, it is observed in order of the slope of E, S, SE, and NE.
Concerning to collapse and convex break of slope, 80% of the collapse occurred on the valley side below convex break of slope, and approximately 15% of the collapse, which appeared to make convex break slope recessed, were observed on convex break slope.

5-3 Liquefaction

Former land use map and land condition map were overlaid in the limits of occurrence of liquefaction shown on the map of present state of disaster (the second version,) and the size of the area according to each category was summed up. The flow of summing process is shown in Fig.-6.
In the survey area, size of the area where liquefaction occurred totaled 5.48 km^2 including the occurrence of liquefaction of 5.32 km^2 in reclaimed land, which occupied 97% in total area of occurrence. The size of reclaimed area in this survey was 20.62 km^2 and liquefaction occurred in the area of approximately 26% of it. Fig.-7 shows the size ratio of liquefaction in each category in the sheets on which survey was carried out. Overwhelming majority of the area of ground liquefaction is observed in the category of reclaimed land, and some are found only in the specific landforms, such as gentle frontage of fan, natural levee, sand bank or sand bar, coastal plain or delta and valley plain or flood plain. According to former land use, high ratio of the occurrence of liquefaction was observed in the area which was classified as water area in the topographic maps in Meiji Period.

6. Summary

Clear view of correlation between damage to buildings and landform (ground,) which was the primary objective of this survey, was not found out in this survey area.
However, big damage was concentrated in the area classified as gentle frontage of fan, and much smaller damage was observed towards both sea and mountain sides making the peak in this gentle frontage of fan.
Some instances show that areas which have potential for sufferings, such as slope

failure and liquefaction could be predicted by landform information.
It was found out if land classification was digitized, it would be useful for post facto measures and disaster prevention by prompt simulation and analysis.

References

1. Geographical Survey Institute (1966): "Report on the Survey of Land Condition (Kyoto and Harima area) "and attached map.pp.110. 8 sheets.
2. Geographical Survey Institute (1983): "Report on the Survey of Land Condition (Osaka area) " and attached map. Geographical Survey Institute Technical Materials D・2-No.37, pp.182. 4 sheets.
3. Geographical Survey Institute (1965): "Report on the disaster of the Niigata Earthquake" pp.59. 2 sheets.
4. Takashi Okimura (1995): "Survey on the damage to houses and disaster mapping. Report on the urgent survey of damage of the 1995 Hyogo-ken Nanbu Earthquake (Second report) " Department of Engineering, Kobe University, pp.20-41
5. Shingo Tanaka (1995): "Landform classification between Kobe and Hanshin. Report on the 1995 Hyogo-ken Nanbu Earthquake - geology, ground and disaster" Survey Committee of the Hanshin Awaji Earthquake Disaster Japan, Applied Geology Society, pp.23 - 32
6. Geographical Survey Institute (1995): Damage Distribution Map of the 1995 Hyogo-ken Nanbu Earthquake (the Second version.) 21 sheets
7. The City Planning Institute of Japan Kansai Chapter, The Architectural Institute of Japan Kinki Chater. (1995) : Hanshin, Awaji Earthquake disaster's actual situation urgent investigation The distribution map of damage level of buildings (1995) pp.120
8 The Rokko-Sabou Kouji Office (Erosion Control Work Office for the Rokko mountain area) (1995): The distribution map of new and more spread collapse area (1:10000)

Table. 1 Materials

Provisional Topographic Map 1:20,000 in Meiji Period Ikuse-Mura 1886 Kobe 1885 Nishinomiya-machi 1885 Hyougo 1886 Imatsu-mura 1884 Suma-mura 1885 Rokkousan 1186 Material:Geographical Survey Institute
Land Condition Map 1:25,000 「Osaka-seihoku-bu」 「Kobe」 Report 「Kyoto/Harimachiku」 1966 Land Condition Map 1:25,000 「Osaka-seihoku-bu」 Report 「Osakachiku」 1983 Material:Geographical Survey Institute
The distribution map of new and more spread collapse area Material:The Rokko-Sabou Kouji Office Ministry of Construction
Danage distribution map of the 1995 Hyogo-ken Nanbu Earthquake (The second Version) Material:Geographical Survey Institute
Hanshin,Awaji earthquake disaster's actual situation urgent investigate The distribution map of damage level buildings 1995 Material:The committee for reconstruction of earthquake disaster and city planning

Table. 2 Establishment of survey committee

	Name	Authority
Chairperson	Takashi Okimura	Professor,Kobe University
Member	Shingo Tanaka	Professor Emeritus,Kobe University
Member	Masahisa Hayashi	Professor,Shimane University
Member	Kazue Wakamatsu	Visiting Researcher,Waseda University

Table. 3 Contents of Land Condition Map

Landform Classification	Mass-wasting,Unstable slope, Terrace(4 sections), Piedmont aggraded slope(3 sections),Dent or shallow valley Lowland relatively higher and well drained(4 sections), Submersible land surface(2 sections), Water sphere, Artificially deformed area(8 sections), Break lines of slopes(convex,concave), Former drainage system, Former pond,marsh are indicated in all
Contour of ground elevation	Contour at 2m or 4m intervals is indicated in lowland
Land slide	Continuous land slide before the earthquake(2 sections), New land slide by the earthquake, New land slide after the earthquake,Baldness and bare rock
Disaster	Collapse of and damage to houses and buildings(damage leve l,floors 2 sections each), Limits burnt by fire, Area of liquefaction of the ground

Table. 4 A List of Digital Data

Layeres	Data form	Layeres	Data form
Land condition map	polygon	Digital Map (Linear)	line
Deformed area(Additional symbols)	polygon	Digital Map (Altitude)	grid
Former land use	polygon	Land slide by the Rokkou Sabou	polygon
Collapse or seriously damaged	polygon	Contour of ground elevation	line
Slightly damaged	polygon	Convex break of slope	line
Collapse or seriously damaged more than three story building	polygon	Divide	line
		Shaded Map	grid
Slightly damaged more than three story building	polygon	Slope azimuth	grid
		Slope	grid
Fire(burnt area)	polygon	Removed buildings data	point
Liquefaction of ground	polygon	Distribution map of building damage level	point
Digital Map (Rivers)	polygon		

Table. 5 Analysis between Damage to Buildings and Land Condition

		Land Condition		Former land use	
		All survey area	Every Map	All survey area	Every Map
Damaged buildings'area	Collapse	○	○	○	○
	Collapse+Slightly	○	○	○	○
	No damages	○	○	○	○

Relation between Wooden Buildings and Land Condition

		Land Condition		Former land use	
		All survey area	Ashiya City	All survey area	Ashiya City
Number of houses of each damage level	Badly		○		○
	Badly+Medium damage		○		○
	Badly+Medium damage+Slightly		○		○
	No damages		○		○
Rate of each damage level of buildings in each land condition	Badly		○		○
	Badly+Medium damage		○		○
	Badly+Medium damage+Slightly		○		○
Rate of each damage level of buildings in each land condition edge	Badly		○		○
	Badly+Medium damage		○		○
	Badly+Medium damage+Slightly		○		○
Distribution of damaged buildings	Badly		○		○
	Badly+Medium damage		○		○
	Badly+Medium damage+Slightly		○		○

Table. 6 Positions of Convex Break of Slope and Slope Failure

Convex break line	All survey area		Takarazuka sheet	
	Spot	Ratio(%)	Spot	Ratio(%)
Ridge side	9	3.6	0	0.0
On the line	36	14.5	6	8.7
Valley side	203	81.9	63	91.3
Total	248	100.0	69	100.0

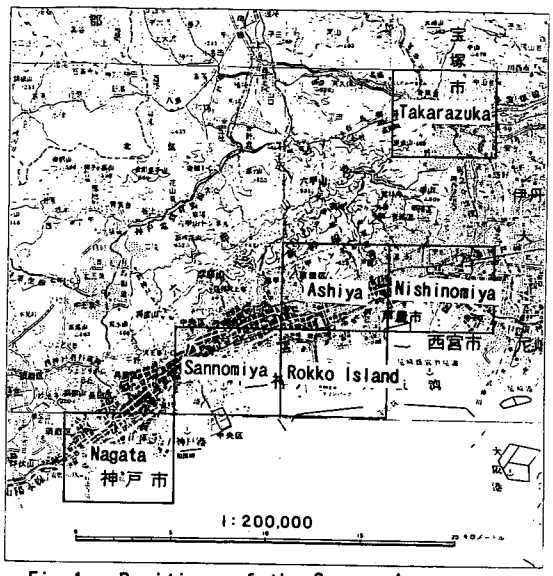


Fig-1 Positions of the Survey Area

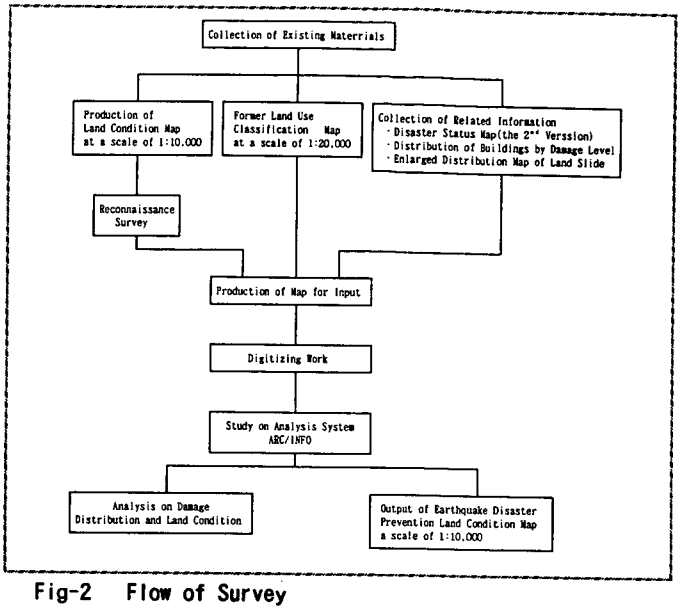


Fig-2 Flow of Survey

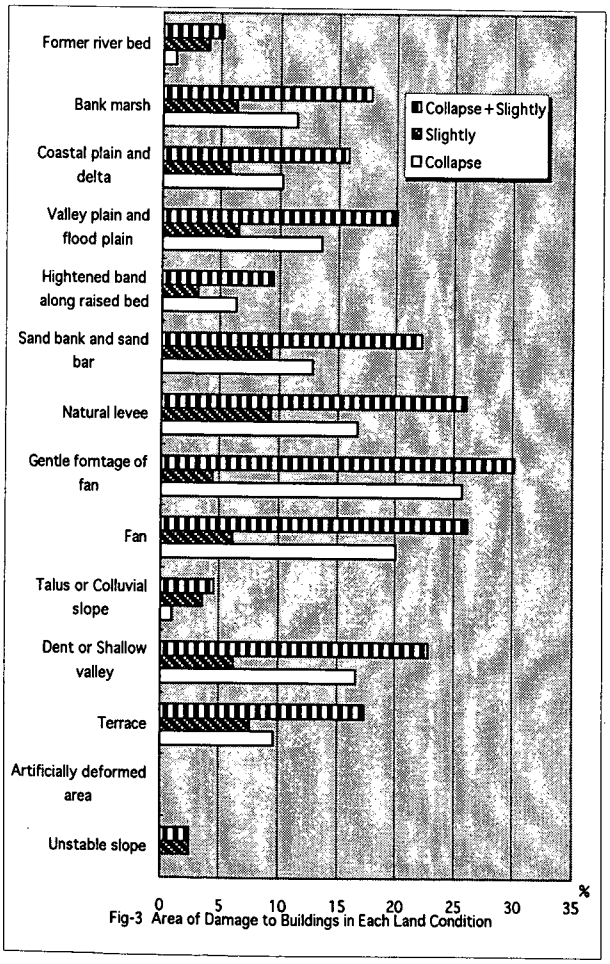
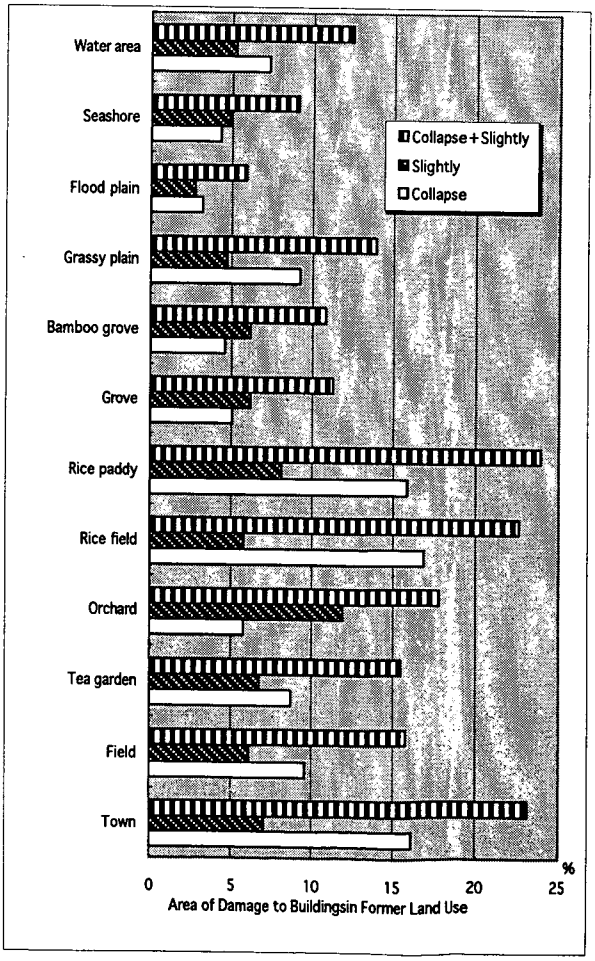


Fig-3 Area of Damage to Buildings in Each Land Condition



Area of Damage to Buildingsin Former Land Use

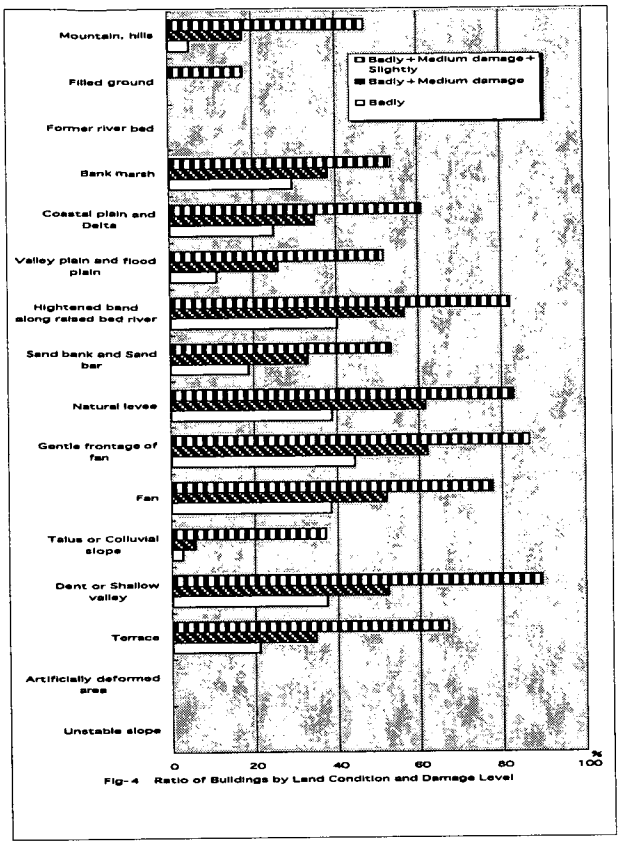
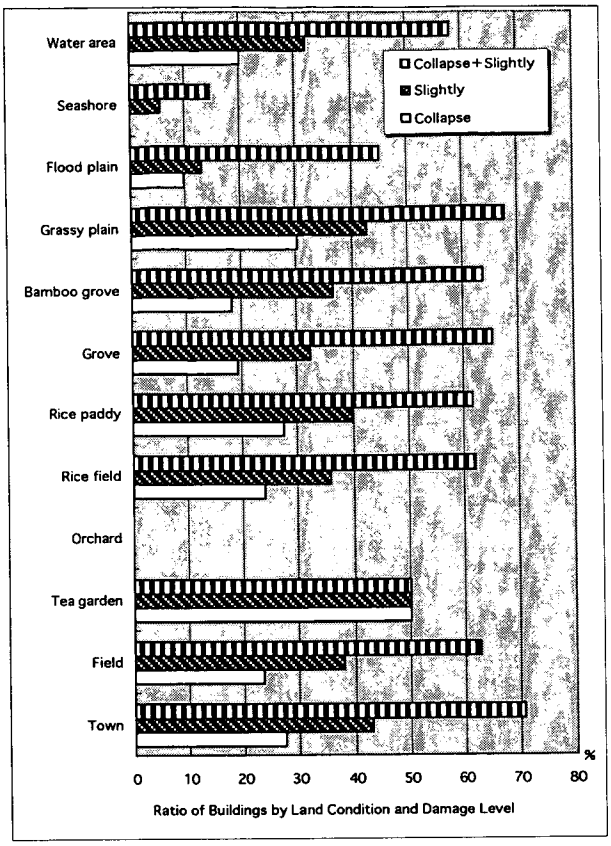


Fig-4 Ratio of Buildings by Land Condition and Damage Level



Ratio of Buildings by Land Condition and Damage Level

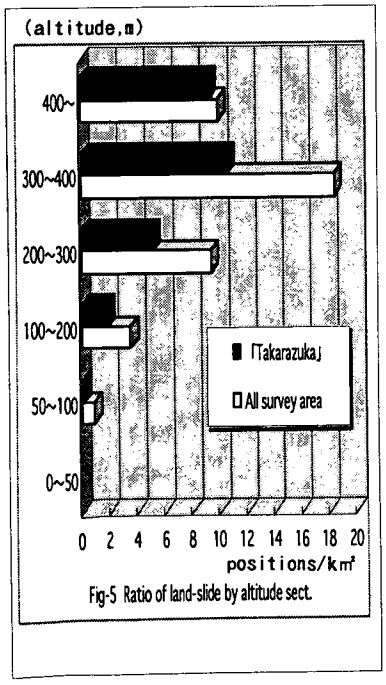
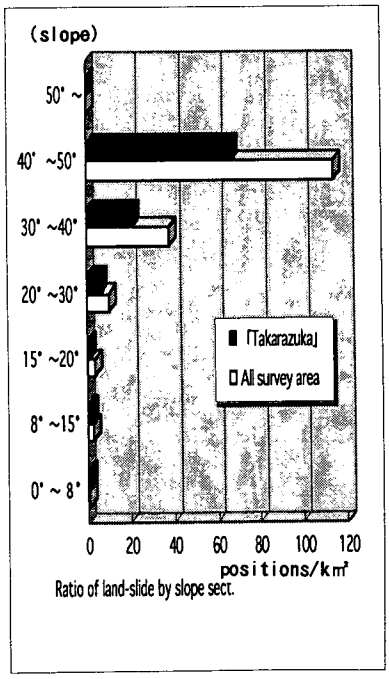
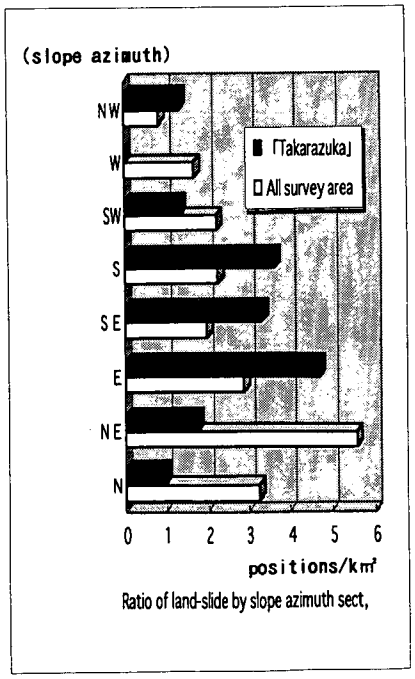


Fig-5 Ratio of land-slide by altitude sect.



Ratio of land-slide by slope sect.



Ratio of land-slide by slope azimuth sect,

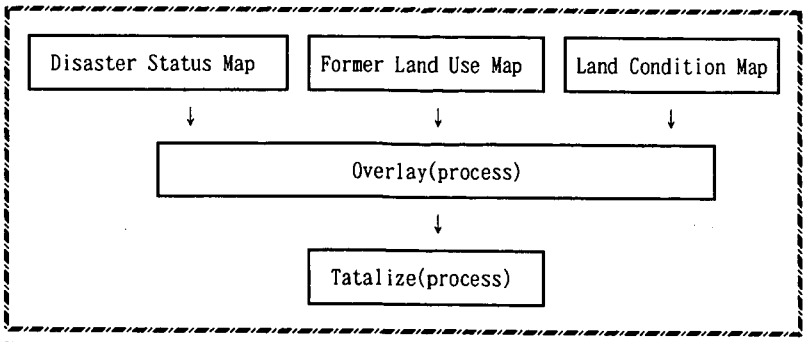


Fig-6 Liquefaction disaster analyzing flowchart

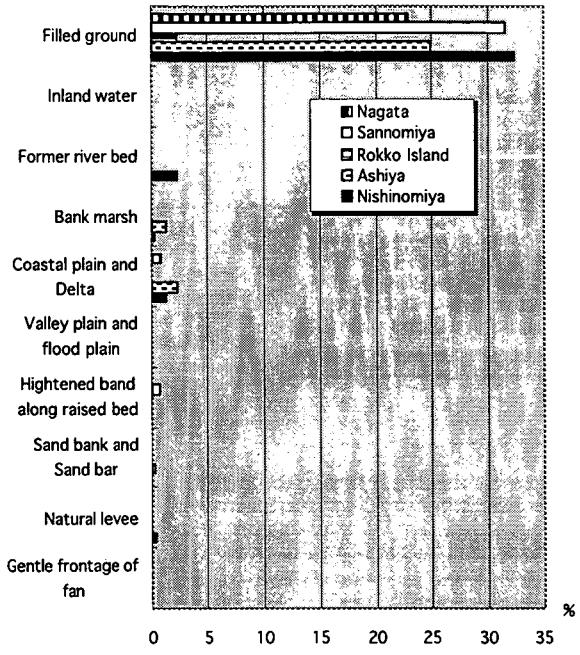
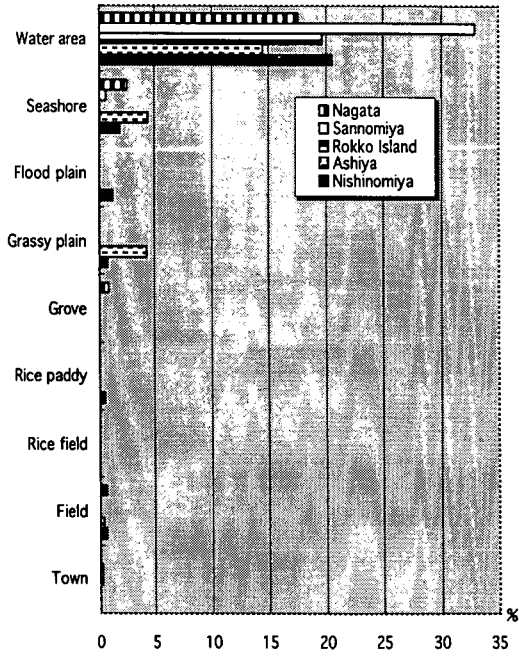


Fig-7 Ratio of liquefaction area in each land condition



Ratio of liquefaction area in each former land use

Appendix

Task Committee Reports

Report of Task Committee A
STRONG MOTION DATA AND APPLICATIONS

Date : 13 May 1997

Place : Public Works Research Institute, Tsukuba, Japan

Attendees:	U. S. side --	William B. Joyner (Acting Chairman)	USGS
		Mehmet K. Celebi	USGS
	Japan side --	Susumu Iai (Chairman)	PHRI
		Riki Honda	PWRI
		Keiko Ogawa	Tohoku University
		Keiichi Ohtani	NIED
		Izuru Okawa	BRI
		Yoshihiro Nakao	PWRI

1. Objective and Scope of Work

To coordinate and promote sharing of strong motion earthquake data among researchers and practicing engineers, and to develop techniques and exchange information for evaluating the destructive effects of earthquake motion.

The scope of work includes:
(1) instrumentation,

(2) recording, processing, and analyzing strong motion data,

(3) engineering characterization of ground motion,

(4) design applications, and

(5) seismic zonation.

The activities of the Task Committee include:
(1) regular exchange of data and publications,

(2) creating procedures for disseminating significant strong motion digital data with regard for the rights and expectations of (a) owner, (b) the users of data and (c) the earthquake engineering community,

(3) planning and conducting T/C workshops and meetings, and

(4) coordinating relevant research activities.

2. Accomplishments

The 1994 Northridge and 1995 Great Hanshin earthquakes had a tremendous impact on

various aspect of the strong motion studies, including characterization of near field motion and site response. Research developments since these earthquakes were very rapid, including proposals for new seismic guidelines, recommendations and codes in both U.S. and Japan as well as a new proposal of world-wide seismic hazard map for International Standards Organization (ISO) seismic guidelines for offshore structures. All these developments happened in 1996 and more are coming in 1997. In view of these developments, the Task Committee A accomplished:

(1) Conducted a workshop on Site Response Subjected to Strong Earthquake Motions on 16 and 17 January 1996, Yokosuka, Japan, one year after the Great Hanshin Earthquake, with the purpose to integrate world wide views on these developments. Distinguished researchers and engineers were invited from all over the world.

(2) Published a proceedings of the workshop to clearly define the current-state-of-the-knowledge based on the results of the workshop.

(3) Sent out a follow-up mission from U. S. to Japan to identify the most updated information on the sources of strong motion data, including those compiled and catalogued by a committee (Chairman: Prof. Kazuo Seo) of the Architectural Institute of Japan.

(4) Closely monitored the on-going changes and new proposals for seismic guidelines and codes, including those of UBC97, NEHRP97, USA and ISO/WG67.

(5) At the suggestion of the Task Committee A members, a call for cooperation between U. S. and Japan in strong motion studies was included in the Earthquake Policy Symposium of the Common Agenda (Clinton and Hashimoto talk).

K-net was completed with the effort of Task Committee A members. Its data availability with ease and timely fashion should be a model to both U. S. and Japan strong motion programs for future development.

3. Future Plans

The future plans include:

(1) Planning a workshop on Soil-structure Interaction (Chairmen: Celebi and Okawa), in the spring 1998 in U. S.

(2) Hosting a new workshop in December 1998 on strong motion studies, which could be held in conjunction with ESG 98 (Effect of Surface Geology), to review and integrate, where possible, the most recent developments since the 1996 workshop.

(3) Coordinate, where appropriate, ongoing developments in strong motion recording programs and data dissemination.

(4) Coordinate, where appropriate, ongoing developments in seismic hazard map and seismic guidelines to be generalized for the world-wide use.

Report of Task Committee B
TESTING AND EVALUATION PROCEDURES FOR BUILDING SYSTEMS

Date: 14 May, 1997

Place: Public Works Research Institute, Tsukuba, Japan

Attendees:	U. S. Side --	H. S. Lew (Chairman)	NIST
		Mehmet K. Celebi	USGS
		Subhash C. Goel	University of Michigan
	Japan Side --	Keiichi Ohtani (Chairman)	NIED
		Takashi Kaminosono	BRI

1. Objective and Scope of Work

The objective of the Task Committee is to develop and recommend rational test procedures and to collect performance data of dynamic response of structures through both laboratory testing of prototype structures and field testing of structures in-situ.

The scope of work includes:

(1) Plans and conducts workshops and joint meetings to identify research topics and develops joint research programs.

(2) Coordinates research projects carried out by various laboratories in the U. S. and Japan. Facilitates publication of research results and implementation of findings in codes and standards.

(3) Facilitates exchange of research personnel, technical information and available testing facilities.

(4) Develops uniform testing procedures including test loading history for case of comparison of results of tests carried out by various researchers, and for establishment of data base.

(5) Develops guidelines for interpretation of test results in consideration for design of structures.

(6) Develops methodology for evaluation and interpretation of physical test results.

2. Accomplishments

(1) The third phase of the U. S. Precast Seismic Structural Systems Program (PRESSS) has been initiated in 1995 with several universities participating in the program. The study is continuing.

(2) In Japan, a 3-year program on the development of design guidelines for

precast/prestressed buildings has been carried out since 1996.

(3) The research program on Composite and Hybrid Structures (CHS) in Japan was initiated in 1993. Experimental and analytical work is being carried out by the Building Research Institute and by several universities and construction companies. The Japan Structural Consultant Association is undertaking an applications study for implementing research results into practice.

(4) The research program on CHS in the U. S. was initiated in 1995 under the sponsorship of the National Science Foundation. Over 16 research projects are in progress.

(5) The third U. S. -Japan Joint Technical Coordinating Committee (JTCC) meeting on CHS was held in December 1996 in Hong Kong. Beyond the current joint program, both sides agreed to continue to coordinate efforts in the development of design guidelines and to transfer technology to the design profession.

3. Future Plans

(1) The forth U. S. -Japan Joint Technical Coordinating Committee meeting on CHS will be held in October 1997 in the U. S.

(2) Several TCC meetings will be scheduled in respective countries in the coming year.

(3) In support of the International Decade for Natural Disaster Reduction (IDNDR) Program, techniques will be explored to disseminate finding of completed Joint Research Projects, such as masonry and precast concrete structures, which were carried out under the auspices of T/C "B" to countries with high seismic risks.

(4) To maximize the usefulness of research data, it is desirable to establish rational test procedures, documentation and retrieval of test data. A joint workshop on Test Procedure, Documentation, and Retrieval of Test Data is proposed to be held before the 30th Joint Panel Meeting to discuss this topic.

Report of Task Committee C
DESIGN, EVALUATION, AND IMPROVEMENT OF STRUCTURES

Date: 13 May 1997

Place: Public Works Research Institute, Tsukuba, Japan

Attendees:	U. S. side --	Noel J. Raufauste (Acting Chairman)	NIST
		Subhash C. Goel	University of Michigan
		W. Phillip Yen	FHWA
	Japan side --	Hisahiro Hiraishi (Chairman)	BRI
		Takashi Kaminosono	BRI

1. Objective and Scope of Work

To develop disaster mitigation guidelines and programs that will improve the performance of new structures and the capacity of existing structures in resisting wind and seismic forces. To establish adequate evaluation of performance, each country will coordinate the development of condition assessment, screening, structural analysis, and design methodologies. Enhance performance can be obtained by the intelligent renewal, repair, and retrofit of existing buildings and other structures. Certain structures will be analyzed and instrumented and then evaluated after disasters. Also, effective use of new advanced materials, smart materials, and structural systems associated with appropriate design methods, will provide structural performance in the life cycle.

The scope of work includes:

(1) Exchanging information, planning, and hosting workshops on new design technologies, evaluation technologies, and repair and retrofit techniques.

(2) Studying new materials and methods for repairing and retrofitting existing structures and for new construction.

(3) Developing a uniform system for screening and analyzing wind and seismic resistance capacity of structures in each country.

(4) Evaluating, composite/hybrid building structures and smart structural systems and providing documentation for post-disaster evaluation of performance.

(5) Developing reliable condition assessment systems for new and existing structures.

(6) Coordinating research projects in the U. S. and Japan to minimize duplication and maximize benefits.

2. Accomplishments

(1) The second workshop on structural control and intelligent material systems was held in the U. S. during 13-15 November 1996 (co-sponsored by NSF and T/C "C" and "G") .

The workshop was held at the University of Maryland, following the ASCE Materials Conference, November 1996.

(2) In order to develop the next U. S. -Japan Cooperative Earthquake Engineering Research Project and a joint initiative, in collaboration with T/C "G", the first meeting was held in conjunction with the U. S. -Japan Workshop on structural control and intelligent material systems in Washington, D.C. in November 1996.

(3) The third U. S. -Japan Technical Coordinating Committee meeting under the U. S. -Japan Cooperative Earthquake Engineering Research Program on Composite and Hybrid Structural Systems was held at Hong Kong during 12-14 December 1996.

(4) In the field of hybrid structural systems, Dr. H. Kuramoto, BRI, started a one-year (October 1996-September 1997) research assignment at Cornell University, and Prof. B. Shahooz, University of Chincinati, performed joint research at BRI for two months (December 1996-January 1997).

3. Future Plans

The following activities are planned for T/C "C"

(1) Develop a reliable methodology for screening and analyzing wind and seismic resistant capacity, and advanced instrumentation technology and expert systems to provide condition assessment of existing structures.

(2) Compile a database of advance materials/systems that have potential for improving structural performance of new construction, and for use in rehabilitating and strengthening existing buildings.

(3) Investigate new design methodologies based on required structural performance using advanced materials and systems.

(4) Develop comprehensive design guidelines for applying advance structural and materials system to be used for composite and hybrid structures under the joint U. S. -Japan Cooperative Earthquake Engineering Research Program. The T/C "C" plans to disseminate the design guidelines through a series of conferences and other media.
The fourth U. S. -Japan Technical Coordinating Committee meeting on Composite and Hybrid Structural Systems will be held in the U. S. in October 1997.

(5) Continue to encourage participation by private industry, consulting engineers, universities, national and local government agencies involved in instrumentation, evaluation, condition assessment, and retrofit and strengthening of existing buildings, for seismic and wind resistance.

(6) Discussions are underway to develop the next U. S. -Japan Cooperative Research Project and to plan a joint initiative on smart structures and materials, in collaboration with T/C "G".

4. Other Activities

The following activities support the work of T/C "C".

(1) U. S. research sponsored by NSF, Corps of Engineers, NIST and FHWA have developed reports on seismic rehabilitation and retrofit strategies, including innovative techniques for strengthening existing buildings and bridges.

(2) An updated report on Civil Infrastructure Systems-Strategic Issues has been published by NSF. Continuing development of NSF's Civil Infrastructure Systems Research Program, including strong emphasis on evaluation and improvement of structures.

(3) NSF is cooperating with Japan Science and Technology Agency (STA/NISTP) on Smart Materials Research proposed by STA.

(4) Continue to encourage conduct of research in the area of retrofit and repair of buildings and structures.

(5) U. S. -Japan Workshop on "Fracture of Steel Buildings in Earthquakes" supported by NSF and STA was held at San Francisco during 2-4 February 1997.

Report of Task Committee D
EARTHQUAKE ENGINEERING FOR DAMS

Date: 13 May 1997

Place: Public Works Research Institute, Tsukuba, Japan

Attendees:	U. S. side--	William E. Roper (Chairman)	COE
		A. G. Franklin	WES
	Japan side--	Hitoshi Yoshida (Chairman)	PWRI
		Tomoya Iwashita	PWRI
		Isao Nagayama	PWRI
		Takashi Sasaki	PWRI
		Syuji Takasu	PWRI
		Tsuneo Uesaka	PWRI
		Yoshikazu Yamaguchi	PWRI

1. Objective and Scope of Work

To develop technical insights into better understanding of the response of dams to seismic effects, the T/C will plan, promote, and develop research initiatives to assist in assuring seismic safety and economical protective countermeasure against earthquake loading for these structures. Its scope of work includes:

(1) Methods of analysis for seismic design of dams including outlet works.
Comparison of design methods and criteria between U. S. and Japan.
Development of "Design Earthquake Ground Motions" for analysis and evaluation of dams.
Assessment of investigation and dynamic analysis methods as tools (modeling, calculation codes).

(2) Dynamic characteristics of dam construction materials and site conditions.
Strength and deformation characteristics during earthquakes(concrete, soil and rock).

(3) Analysis of observed behavior of dams and outlet works during earthquake.
Investigation of the mechanism of damages due to earthquake loading.
Application of the analysis of the observed behavior during earthquake to the earthquake- resistant design.

2. Accomplishments

(1) T/C "D" conducted the First U. S. -Japan Workshop on Advanced Research on Earthquake Engineering for Dams at the Waterways Experiment Station in Vicksburg, Mississippi, USA on 12-14 November, 1996.

(2) Articles related to the first Workshop were printed in the Technical Bulletin of the U. S. -Japan Panel on Wind and Seismic Effects, Issue 4, and in the PWRI Newsletter, No. 68.

3. Future Plans

(1) Exchange of the results of research / investigation and technical information about dam earthquake engineering is encouraged, and feasibility of joint research and investigation is in continuous consideration.

(2) Exchange visits to the institutes concerned, of scientists and engineers between U. S. and Japan, is to be extended for the effective communications

(3) The proceedings of the first Workshop will be published.

(4) T/C "D" will hold the Second Workshop at the Public Works Research Institute, Tsukuba, Japan or at another location in Japan that would enhance field observation opportunities in conjunction with the 31st Joint Panel Meeting in 1999.

Report of Task Committee E
DESIGN FOR WIND AND WIND HAZARD MITIGATION

Date: 13 May 1997

Place: Public Works Research Institute, Tsukuba, Japan

Attendees:			
	U. S. side --	H. S. Lew (Acting Chair)	NIST
		Bogusz Bienkeiewicz	CSU
		Muhammad Hajj	VPI
		Joel D. Selanikio	CDC
	Japan side --	Hisashi Okada (Co-Chair)	BRI
		Hiroshi Sato (Co-Chair)	PWRI
		Nobuyuki Kinoshita	MRI
		Toshiaki Mabuchi	PWRI

1. Objective and Scope of Work

To exchange technical information and to jointly plan, promote and foster research and its dissemination, to improve understanding of wind and its effects on structures, establish more rational wind resistant design methods for structures, and to contribute to wind hazard mitigation.

The scope of work includes:

(1) Characteristics of strong wind, especially boundary layer extreme winds

(2) Wind effects (wind loading on and wind-induced response of structures)

(3) Experimental and analytical methods to predict extreme wind events and their effects

(4) Damage and risk assessment

(5) Wind hazards and wind hazard mitigation

2. Accomplishments

(1) Conducted the planning for the first joint workshop. The main theme of workshop is "The Prediction and Control of Wind-induced Structural Response". The workshop is planned to be held at the East-West Center at the University of Hawaii on October 7-8, 1997. A two day technical site visit will follow.

3. Future Plans

(1) Hold the first joint workshop mentioned above.

(2) Exchange technical information on the following subjects:
a) Topographical effects on wind, and the use of geographic information systems (GIS)

to study these effects
b) Control of wind-induced response of structures
c) Computational fluid dynamics and. wind tunnel tests
d) Prediction of wind-induced response of full-scale structures
e) Investigation of wind hazards, including damage assessment methodologies
f) Wind-resistant design codes, standards, and recommendations

Report of Task Committee F
DISASTER PREVENTION METHODS FOR LIFELINE SYSTEMS

Date : 14 May 1997

Place : Public Works Research Institute, Tsukuba, Japan

Attendees :	U. S. Side --	Noel J. Raufaste (Acting Chairman)	NIST
		Michael E. Blackford	NOAA
	Japan Side--	Koichi Yokoyama (Chairman)	PWRI
		Keiko Ogawa	Tohoku University
		Keiichi Tamura	PWRI
		Tomofumi Nozaki	PWRI
		Michio Osumi	PWRI

1. Objective and Scope of Work

To improve (a) the performance of lifeline systems during earthquakes and (b) engineering and other seismic countermeasures including the capability in damage estimation techniques and inspection procedures.

(1) Planning and conducting workshops on lifeline systems.

(2) Facilitating exchange of technical information.

(3) Promoting development of design guidelines and standards for lifeline systems.

2. Accomplishments

Members of this T/C have been active in the planning of two major efforts between the two countries in earthquake disaster reduction:

(1) The first effort is led by the Science and Technology Agency of Japan and the Office of Science and Technology Policy (OSTP) of U. S. to develop a list of scientific and engineering projects for future collaboration.

(2) The second is the planning and participation in two earthquake policy symposia led by the U. S. Federal Emergency Management Agency and the National Land Agency of Japan, under the U. S. -Japan Natural Disaster Reduction Initiative of the U. S. -Japan Framework for New Economic Partnership (Common Agenda).

3. Future Plans

(1) Encourage collaborative research and development in areas such as: performance prediction and post-measurement through damage assessment of lifeline systems; systems approach to lifeline performance; soil-structure interaction; geographic information systems (GIS) and cost-effective ground improvement techniques and other countermeasures for lifeline facilities.

(2) Encourage and strengthen current efforts in both countries for developing seismic design

guidelines and standards for lifeline systems. Existing UJNR channels should be fully used to facilitate the exchange of relevant information concerning development of guidelines and standards. Possible collaboration of developing of guidelines and standards for lifeline systems should be pursued.

(3) Initiate multidisciplinary cooperative research between lifeline earthquake engineering and public health to assess public health consequences due to the disruption of lifeline systems.

(4) Hold the Seventh Joint Workshop on Disaster Prevention for Lifeline Systems in November 1997 in Seattle, Washington (Seattle is a sister city of Kobe). The workshop will focus on the presentations and discussions of the studies completed after the Northridge and Kobe earthquakes.

Report of Task Committee G
STRUCTURAL CONTROL AND INTELLIGENT MATERIAL SYSTEMS

Date: 13 May 1997

Place: Public Works Research Institute, Tsukuba, Japan

Attendees:	U. S. side--	Noel J. Raufauste (Acting Chairman)	NIST
		W. Phillip Yen	FHWA
		Subhash C. Goel	University of Michigan
	Japan side--	Shigeki Unjoh (Chairman)	PWRI
		Yukio Adachi	PWRI
		Michio Ohsumi	PWRI

1. Objective and Scope of Work

(1) Develop research plans in control of equipment and structures and in high performance structural and material systems.

(2) Implement control techniques for motion reduction or modification.

(3) Implement use of advanced materials in actual design and construction of buildings and other infrastructure systems under seismic or wind environments.

(4) Promote U. S. -Japan cooperation in structural control and intelligent material systems research.

(5) Bring together governmental, academic, and industrial participants in joint pursuit of these efforts.

(6) Contribute to the International Decade for Natural Disaster Reduction (IDNDR) by organizing joint research and other technical activities in structural and intelligent material systems research based on international cooperation.

T/C "G" works closely with other panel task committees and research organizations to provide the leadership in this emerging research by facilitating the exchange data and information through UJNR mechanisms. The scope of work includes:

(1) Providing technical assistance, consultation and coordination of UJNR affiliated research organizations in the initiation, development, and execute their programs in research areas.

(2) Promoting Joint government-university-industry collaborative efforts to facilitate technology transfer and practical implementation.

(3) Sponsoring and conducting interdisciplinary workshops and meetings to identify key area of research and opportunities for cooperation, and to exchange new knowledge and experience in practice.

(4) Developing promotional and demonstrative activities to stimulate public awareness and interest in this field of research.

(5) Providing information useful for the establishment of performance standards, design and also retrofit/rehabilitation of existing structures.

(6) Promoting research in intelligent material systems, sensors, actuators, optimal control system design, and encourage laboratory and field experiments of prototype and full-scale structures.

2. Accomplishments

(1) Under NSF sponsorship, U. S. -Japan Workshop on Smart Structures Technology: Application to Large Civil Structures was held in November 1996 in cooperation with T/C "C". The University of Maryland at College Park hosted the workshop and published the workshop proceedings. At PWRI, a research program on intelligent seismic structure has been conducted since April 1995. This research will develop new technology using self-diagnosis materials and self-repairable materials. A part of the research was presented at the U. S. -Japan Workshop at the University of Maryland in November 1996. Also, members conducted planning for the next U. S. -Japan cooperative research project in the areas of smart materials and smart structures.

(2) In cooperation with T/C "J", the 4th U. S. -Japan Workshop on Earthquake Protective Systems for Bridges was held in December 1996 in Osaka, Japan. The workshop was attended by 20 U. S. and 66 Japanese participants. The proceedings of the workshop were published and distributed by PWRI.

(3) An NSF research initiative on sensors and sensoring systems for power systems and other dispersed civil infrastructure systems was implemented under the joint support of EPRI and NSF.

3. Future Plans

(1) Joint research projects on innovative technologies for active and hybrid control of structures, such as bridges and buildings, particularly work which would advance practical implementation, will be continued by PWRI, BRI, NCEER,CUREE, and other institutions.

(2) NIST will conduct a state-of-the-art review of active control systems and evaluate available technologies for use by designers.

(3) In cooperation with T/C "J", the 5th U. S. -Japan Workshop on Earthquake Protective Systems for Bridges will be held in U. S. at the time mutually convenient to both countries.

(4) In collaboration with T/C "C", a joint planning effort will be made to develop the next U. S. -Japan cooperative research projects in smart materials and smart structural systems.

(5) Task Committee "G" supports the activities of U. S. -Japan Common Agenda and its technical program can serve a technical basis to meet the objectives of the Common Agenda's Initiative on Earthquake Disaster Mitigation Partnership.

4. Other Activities

The following activities support work of T/C "G".

(1) The second International Workshop on Structural Control was held in December 1996 in Hong Kong. The workshop was hosted by the Hong Kong University of Science and Technology.

(2) NSF is cooperating with Japan Science and Technology Agency (STA/NISTP) on Smart Materials Research proposed by STA.

(3) The second world Conference on Structural Control will be held in June 1998 in Kyoto.

(4) NSF in collaboration with Japanese Ministry of Education held a 2nd U. S. -Japan Workshop on Research in Urban Earthquake Hazard Reduction, February 27 to March 1, 1997 in Tokyo. The workshop involved many UJNR agencies from both sides. In addition to discussions pertaining to further fundamental University-based research and those which will advance UJNR objectives, the recent issues and opportunities recommended by U. S. -Japan Common Agenda were also addressed.

Report of Task Committee H
SOIL BEHAVIOR AND STABILITY DURING EARTHQUAKES

Date : 14 May 1997

Place : Public Works Research Institute, Tsukuba, Japan

Attendees :	U. S. side --	A. G. Franklin (Chairman)	WES
	Japan side --	Osamu Matsuo (Chairman)	PWRI
		Susumu Iai	PHRI
		Hiroshi Kobayashi	PWRI
		Hanlong Liu	PHRI
		Chikahiro Minowa	NIED
		Tatsuya Tsutsumi	PWRI

1. Objective and Scope of Work

Government agencies responsible for public works must assure seismic safety and provide economical protection against earthquake hazards.

The objective of the Task Committee (H) is to assist in meeting these needs by enhancing the availability of technology for predicting the dynamic behavior of soils, analyzing dynamic soil-structure interaction, and modifying the earthquake behavior of foundations and earth structures to assure their safe performance during earthquakes.

In accordance with the objective, the scope of work includes:

(1) Exchange information on technological developments and on state-of-the-art and practice related to soil behavior and stability during earthquakes.

(2) Exchange information and technical data relating to field performance, research, and methods of practice.

(3) Plan and conduct programs of cooperative research and/or workshops in coordination with the proposed or ongoing programs.

(4) Make other needed efforts including exchange of researchers between U. S. and Japanese research institutions, and publication of research results and recommended practice.

2. Accomplishments

(1) The Port and Harbour Research Institute (PHRI) has published a Handbook on Liquefaction Remediation of Reclaimed Land. An English translation was produced by the cooperative effort of the Japanese and U. S. sides, and has been published by Balkema & Co.

(2) The National Research Institute for Earth Science and Disaster Prevention (NIED), the

Building Research Institute (BRI), and Wayne State University (WSU), continued work in their cooperative research program "Physical and Numerical Simulation of Structural Damages Due to Liquefaction and Development of Countermeasure Techniques", 1994-1998.

(3) The PHRI, Colorado School of Mines and the Lovelace Institutes (Albuquerque, NM) continued joint research on application of the Nuclear Magnetic Resonance Imaging (NMRI) method to the study of soil behavior and stability during earthquakes.

3. Future Plans

(1) T/C (H) tentatively plans to hold a workshop on the Use of Centrifuge Experiments for Research on Soil Behavior and Stability During Earthquakes in 1998. The committee is studying means of coordinating the workshop with the International Society for Soil Mechanics and Foundation Engineering (ISSMFE) conference "CENTRIFUGE 98" to be held in Tokyo in September 1998.

4. Other Activities

(1) The Japanese Geotechnical Society is preparing to publish in English a book on Liquefaction Remediation. English translation and editing of the draft has been completed with the assistance of Panel members. The English translation is now being prepared for publication.

Report of Task Committee I
STORM SURGES AND TSUNAMI

Date: 13 May 1997

Place: Public Works Research Institute, Tsukuba, Japan

Attendees:	U. S. side--	Michael E. Blackford (Chairman)	NOAA
		Allen M. Hittleman	NOAA
	Japan side--	Shinji Sato (Chairman)	PWRI
		Toshihiko Nagai	PHRI
		Masami Okada	MRI
		Fuminori Kato	PWRI

1. Objective and Scope of Work

The objective of this Task Committee is to mitigate damage from storm surge and tsunami through cooperative research and shared technology and information. The primary cause of storm surge is considered to be tropical cyclones (hurricanes, typhoons). The primary cause of tsunami is considered to be sudden sea floor deformation due to earthquakes, volcanic activity and landslides. Both hazards may cause disasters along coastal regions.

The scope of work of this T/C is as follows:

(1) Exchange results of research on storm surge and tsunami occurrence, generation, propagation, and coastal effects. This includes observations on historical, current, and theoretical tsunamis. Of particular interest is the effort by U. S. and JAPAN to acquire deep ocean tsunami measurements.

(2) Exchange results and status of storm surge and tsunami mitigation activities including analysis of the problem, planning, warning, and engineering approaches.

(3) Exchange information on development of technologies such as computer programs to predict travel times, land-fall locations, inundation and run-up heights, and wave characteristics, improved instrumentation, and use of satellite communication for detection and warning.

(4) Facilitate dissemination through exchanges of literature, technical reports at joint meetings, special workshops, joint projects, and direct interaction among participants.

2. Accomplishments

(1) Task Committee (I) conducted its 4th Workshop on Storm Surge and Tsunamis, Two Great Tsunamis: U. S. -Japan Anniversary Symposium, during 1-3 April 1996, in Hawaii. The proceedings of this Workshop were published by the Tsunami Society for publication in their journal. The proceedings were distributed to Task Committee Members and other interested parties.

(2) Technical information was exchanged on database system for storm surge and tsunami simulation and deep ocean tsunami monitoring system. In support of coastal process research, NOAA is developing coastline digital elevation models blending land and

marine data at a 100-meter resolution. This data will be very useful to storm surge and tsunami modelers. Data will be available on the world wide web, permitting access to 1-degree blocks of data. In March 1997 The Pacific Marine Environmental Laboratory of NOAA deployed its prototype deep ocean pressure sensor at operational depths off of Oahu Island, Hawaii, to test the acoustic communication system between the bottom sensor and a surface communications buoy. The test was successful and PMEL plans to deploy the sensor/buoy system off the Alaska peninsula during the summer of 1997. A similar project is on-going in Japan.

3. Future Plans

The Task Committee will discuss, through mutual communication, plans for a 5th Storm Surge and Tsunami Workshop in the near future. A tentative date and place was proposed for the winter of 1998, Tokyo.

4. Other Activities

(1) The storm surge research community is small and incorporated into related societies and international organizations which define and stimulate work in the field. The Task Committee (I) encourages the conduct of its efforts.

(2) Since tsunamis have been less severe in the U. S. than in Japan, the U. S. has fewer researchers in this specialty. The Task Committee, through its meetings and workshops, encourages exchanges of ideas and joint study by U. S. and Japanese investigators of tsunami events throughout the world.

Report of Task Committee J
WIND AND EARTHQUAKE ENGINEERING FOR TRANSPORTATION SYSTEMS

Date: 14 May 1997

Place: Public Works Research Institute, Tsukuba, Japan

Attendees:	U. S. . side --	W. Phillip Yen (Acting Chairman)	FHWA
		Bogusz Bienkiewicz	Colorado State University
		Ahsan Kareem	University of Notre Dame
		Dorothy A. Reed	University of Washington
	Japan side --	Michio Okahara (Chairman)	PWRI
		Jiro Fukui	PWRI
		Toshio Iwasaki	Civil Engineering Research Laboratory
		Yasushi Josen	PWRI
		Kazuhiro Nishikawa	PWRI
		Toru Terayama	PWRI

1. Objectives and Scope of Work

To:

(1) Plan, promote, and foster research on the behavior of highway bridges when subjected to wind and seismic forces, and

(1) Disseminate research results and provide specifications and guidelines based on the Task Committee's findings. Surface transportation systems play a vital role in the movement of goods and people. Highway bridges are especially influenced by the forces of wind and earthquakes because of their open exposure to those forces.

The scope of work includes:

(1) Focus research on highway bridges without limitation on their size and function.

(1) Investigate existing and new bridge designs and the behavior of whole bridge systems and/or single components of a bridge.

2. Accomplishments

(1) The 12th U. S. -Japan Bridge Engineering Workshop was held during 29-30 October 1996, in Buffalo, New York, U. S. The workshop was attended by 22 U. S. and 21 Japanese participants. The proceedings of the workshop have been published and will be distributed.

(2) The 3rd U. S. -Japan Workshop on Seismic Retrofit of Bridges was held during 10-11 December 1996 in Osaka, Japan. The workshop was attended by 20 U. S. and 66 Japanese participants. The proceedings of the workshop were published and distributed.

(3) In cooperation with T/C "G", the 4th U. S. .-Japan Workshop on Earthquake Protective Systems for Bridges was held during 9-10 December 1996 in Osaka, Japan. The workshop was attended by 20 U. S. and 66 Japanese participants. The proceedings of the workshop were published and distributed.

3. Future Plans

(1) The 13th U. S. -Japan Bridge Engineering Workshop will be held during the fall of 1997, in Tsukuba, Japan.

(2) The 4th U. S. -Japan Workshop on Seismic Retrofit of Bridges will be held in the U. S. at a time mutually convenient to both countries.

(3) In cooperation with T/C "G", the 5th U. S. -Japan Workshop on Earthquake Protective Systems for Bridges will be held in the U. S. at a time mutually convenient to both countries.

(4) Continue to investigate and exchange technical information on improved seismic retrofit and strengthening procedures for highway bridges based on experimental, analytical, and field studies. This exchange should include information on maintenance of existing bridges.

(5) Continue to conduct cooperative research on the seismic performance of bridge piers and columns experimentally and analytically, and encourage research on seismic isolation and hybrid control of bridges in cooperation with T/C "G".

(6) Continue the coordinated research study to compare the seismic design criteria for bridges in Japan and the U. S. and discuss the method and analysis procedures for bridge column design. Continue to exchange information on the application of the limit state design method.

(7) Encourage a research study on seismic, aeroelastic, and aerodynamic response of long span bridges such as cable-supported bridges with emphasis on behavior of composite materials, cable inspection, vibration control, and corrosion protection.

(8) Encourage a coordinated research study on seismic response and control, system identification techniques, nondestructive evaluation of bridge structures, use and performance of structural materials including new materials, and performance of jointless bridges.

(9) Mr. Jun-ichi Hoshikuma, Research Engineer of Earthquake Engineering Division, PWRI is planning a guest researcher assignment on seismic design of bridges in U. S.,during the 1997 fiscal year.

Report of Task Committee K
WIND AND EARTHQUAKE ENGINEERING FOR OFFSHORE AND COASTAL FACILITIES

Date: 14 May 1997

Place: Public Works Research Institute, Tsukuba, Japan

Attendees:	U. S. side ---	William E. Roper(Acting Chairman)	COE
		Ahsan Kareem	University of Notre Dame
	Japan side ---	Tatsuo Uwabe (Chairman)	PHRI
		Masami Okada	MRI

1.Objective and Scope of Work

To develop technical insights necessary to mitigate damage to offshore and coastal facilities due to extreme wind and seismic effects. The Task Committee will plan, promote, and develop research initiatives to meet this objective, and will disseminate the results of their research for incorporation into future specification or design guidelines. Criteria for the design of offshore and coastal facilities may differ greatly from their onshore counterparts. These differences can arise due to their unique design or mass distribution, to the fluid/structure or wind/structure interaction, to the placement of foundation elements in or on soft, fully saturated soils that can be subject to large hydrodynamicpressures, and to the lack of specific environmental data or the engineering experience that has been developed for most onshore sites.

The scope of work includes:

(1) Sponsoring and conducting workshops and meetings to identify key area of research, opportunities for cooperation, and the exchange of knowledge.

(2) Predicting strong ground motions for offshore and coastal sites including assessing the effects of basin geometry, linear, and nonlinear local geological effects using actual seafloor response measurements.

(3) Determining the dynamic response and the interaction of structure/foundation/soil systems to seabed motions and/or extreme wind forces.

(4) Assessing the dynamic response and behavior of various operational facilities mounted on offshore and coastal structures.

(5) Developing assessment methodologies for seismicity and other characteristics of potential seismic sources (e.g. faults) for offshore and coastal sites in regards to how these conditions relate to structural design criteria.

(6) Promoting the implementation of new research results into current design and construction processes.

(7) Developing research efforts to include laboratory and field programs to obtain data on the response of offshore and coastal facilities to extreme wind and seismic forces.

(8) Creating performance standards, design specifications, guidelines, and code recommendations for application to new construction as well as remedial action for existing facilities.

2. Accomplishments

(1) Conducted two workshops on Wind and Earthquake Engineering for Offshore and Coastal Facilities (early and mid 1990s).

(2) Published and distributed the Proceedings of the second workshop to Task Committee members and both sides Secretaries-General.

3. Future Plans

(1) Develop workshop agenda of the third U. S. -Japan Workshop on Wind and Earthquake Engineering for Offshore and Coastal Facilities, June 1998, Japan.

(2) Coordinate, where possible, on-going research on wind and earthquake engineering for offshore and coastal facilities that are of interest to the Task Committee members including sharing research reports.

Technical Site Visits

29TH JOINT MEETING
PANEL ON WIND AND SEISMIC EFFECTS
12-23 May 1997, JAPAN

by
Noel J. Raufaste
Secretary-General, U.S. –side Panel on Wind and Seismic Effects
Building and Fire Research Laboratory
National Institute of Standards and Technology

HIGHLIGHTS OF THE JOINT TECHNICAL MEETINGS 13-16 MAY 1997

- Forty-seven papers were authored; 35 were presented orally. They were organized into five themes: Wind Engineering; Earthquake Engineering; Storm Surge and Tsunamis; Seismic Information Systems; and Joint Cooperative Research. Summaries of Task Committee Workshops conducted during the past year were presented. Sixteen experts represented the U.S.-side in these meetings.

- Technical presentations highlighted important work by the U.S. and Japan Panel. U.S. research in wind engineering is enhanced by links to the extensive research done by Japan's Public Works Research Institute. Panel Task Committee (T/C) activities grow in strength. The T/C structure is an effective vehicle to explore in depth modern seismic and wind technologies being used by both countries. Five T/C workshops/conferences were held in the past year; seven workshops and joint meetings are planned for the coming year. The Panel is expected to create a new T/C on Seismic Information Systems. Interest was evident to pursue joint work in public health issues resulting from natural disasters.

- The UJNR Panels are providing effective collaborations in earth sciences, earthquake and wind engineering, and, newly, disaster response including treatment of casualties. US member agencies should proceed to build up their role in the multi-agency disaster mitigation initiative, the National Earthquake Program, and the US/Japan Earthquake Mitigation Partnership. Higher level attention to the Panel is needed in some US agencies.

- The UJNR Panels on Wind and Seismic Effects, Fire Research and Safety, and Earthquake Research are providing significant activities in the US/Japan Earthquake Partnership. Partnership activities should be focused before the 17-18 September 1997 Earthquake Policy Symposium.

- Japanese laboratories are acquiring and commissioning major new laboratory facilities as a result of post Kobe earthquake appropriations. The U.S. must implement upgrading plans for its wind and seismic experimental research and testing facilities to remain world class.

- Japan has incorporated active control devices in their new buildings to reduce the dynamic response of buildings against high wind and seismic loads. Japan continues to lead in technologies for high performance concrete and steel.

- Japan is leading the world in public works practices as shown by the Trans-Tokyo Bay Highway, and the world's record suspension and cable stayed bridges in the Honshu-Shikoku crossings. These are very expensive structures of high quality design and construction. However, future investments in public works may decline because of Japan's financial problems. Will industry and governmental pressures allow this decline?

- The reconstruction of Kobe has been swift and effective. Port, highway, and rail capabilities appear to have been restored beyond the pre-earthquake status. Industrial and public housing investments are evident. This should be a success story for the Earthquake Policy Symposium and a model for the International Decade for Natural Disaster Reduction.

- Bridge column retrofits observed on the Hanshin Expressway have been carried out expeditiously. The Public Works Research Institute has developed the technical bases for systematic evaluation and strengthening of existing steel and concrete bridges.

- The Panel's newsletter is effective in disseminating its information. The Panel's Web Site is considered useful in deploying information to Japan and US design and construction organizations. NIST will continue to maintain the Web Site during the next year. The site is available at, http://www.bfrl.nist.gov/info/ujnr/ujnr1.html

SUMMARY TECHNICAL SITE VISITS 12 AND 17-23 MAY

Japan is composed of four main islands; Hokkaido, Honshu, Shikoku, and Kyushu and further south the small island of Okinawa. The islands are divided into ten Regions: Hokkaido; Tohoku, Kanto, Hokuriku, Chubu, Kinki, Chugoku, Shikoku, Kyushu, and Okinawa. These regions in turn are divided into 47 Prefectures. Prefectures are analogous to States. Each region except Hokkaido and Okinawa have a Regional Construction Bureau which reports to the Ministry of Construction (MOC) (http://www.moc.go.jp/org/eng/index.html). Within the Hokkaido and Okinawa regions are the Hokkaido Development Agency and the Okinawa Development Agency respectively. These Bureaus are responsible for constructing and maintaining highways, flood control works, dams, and bridges. Prefectures' design and construction work is funded by the National Government and by their own jurisdictions.

In addition, there are several public corporations responsible for specific construction projects such as the Japan Highway Public Corporation, Metropolitan Expressway Public Corporation, Hanshin Expressway Public Corporation, Honshu-Shikoku Bridge Authority, Trans-Tokyo Bay Highway Corporation, and the Housing and Urban Development Corporation. They report to the MOC. Each receives a small percent of funding required for their construction projects as direct funding from the National Government. Loans from the National Government and Prefecture Governments and from private sources make up the remaining 90 to 95 percent of construction monies needed for each project. These loans must be repaid with interest within 30 years.

During the 29th Joint Panel Meeting, 12 technical sites were visited in the greater metropolitan areas of: Tokyo, Yokohama, Hiroshima, Osaka, and Kobe -- all on Honshu.

1. **Trans-Tokyo Bay Highway**. The Trans-Tokyo Bay Highway is a 15-km toll highway that runs across the central portion of Tokyo Bay connecting Kawasaki City located between Tokyo and

Yokohama with Kisarazu City, Chiba Prefecture on the east side of Tokyo Bay. The project consists of a 10 km tunnel starting at Kawasaki City then rising through a manmade island serving as a transition to a 5 km bridge to Kisarazu City. Present construction accommodates two-2 lane highways with space for a future third pair of lanes. This work is under the supervision of the Trans-Tokyo Bay Highway Corporation (TTBHC) (http://www.matsuo-bridge.co.jp/jigyo/bridge/e-br_17.html) and the Japan Highway Public Corporation (JPHC) (http://www.japan-highway.go.jp/index-e.html). The highway system is expected to be open for public traffic in December 1997.

When the highway is completed, the driving distance between Kawasaki and Kisarazu Cities will be reduced from 110 km to 30 km and the travel time will be shortened by 75 percent. Similarly the distance between Tokyo and Kisarazu will be reduced by 45 km.

The delegation visited the Kawasaki manmade island, one of the two such islands, located at the third point from the Tokyo-Yokohama shore line. Since the sea bed is extremely soft to a depth of 30 m, the soil was stabilized by sand compaction. The island was constructed from a 98 m diameter, 2.8 m thick diaphragm wall extending 119 m from the water surface to the sea bottom. A 50 m steel trestle structure protects the island. It was towed to the site by a crane-barge as 14 sections, sunk, and secured to steel piles. This island serves as a ventilation tower. The tower' s unique sail shape design was planned as a monument to civil engineering design and construction. The tower is 80 m high and 250 m at its base. It is divided into seven floors to accommodate tunnel ventilation equipment, tunnel cross overs, and fire fighting equipment.

Tunnel construction was performed by eight pressurized slurry shield tunneling machines each weighing 3200 tons boring a tunnel diameter of 14.1 m. The twin tunnels are 28 m apart and 60 m below the water surface. The project is the longest vehicle traffic tunnel in the world.

The delegation observed and was briefed about the second manmade tunnel -- the Kisarazu Tunnel-bridge Interface Island. It is 650 m long and 100 m wide. The soil at this site was replaced with sand and gravel to accommodate a 750 m ramp from the sea floor connecting the tunnel sections to the bridge system. The island has a protective system of 48 circular steel pile structures 37 m high, filled with sand, and capped with concrete. Fill work is similar to that performed at the Kawasaki manmade island. Steel moles are constructed on either side of the ramps. Armored riprap, rubble stones, and wave dissipating concrete blocks protect the embankment.

Tunneling continued in 1.5 m increments where automated assembly systems install 11 precast wall lining segments for a 1.5 m ring. Each concrete segment measures 4 m by 1.5 m; is 0.65 m thick and weights 10 tons. Reinforcing bars are coated with vinyl. Furnace slag is mixed with the concrete to reduce permeability thereby improving the condition of resisting corrosion of reinforcing bars. Water tight membranes surround the tunnel walls. Both islands are designed for a 4.3 m high wave. TV cameras monitor the structural performance during earthquakes. When the shield tunnel boring machines reached mid points between the two-man-made islands, they were disassembled and removed. The remaining 50 meters of soil was frozen and dug by hand to realize a completed tunnel. Bore alignment was performed using GPS, gyrocompass surveying system, and magnetic resonance. Most construction data have been entered into databases. It is not certain how the information will be used since no other tunnels are planned to be constructed in similar environments. Much attention was given to designing the highway against earthquakes. The elbows at each of the horizontal ends of the

tunnels are potential weak points. Elbows are flexible for about 100 mm at segment joints which experience changes in the roadway slope. Rubber base isolators were installed at these junctions.

The delegation viewed the 4.4 km bridge exiting the Kisarazu manmade island to Kisarazu on Tokyo Bay' s east shore. The bridge experienced 50 cm amplitude vibrations at wind speeds of 15 m/s. PWRI recommended installing 16 tuned mass dampers in the bridge's center four spans. PWRI also recommended adding a 300 mm vertical steel plate to the outside guard rail to change the wind flow on the top rail. Cost of these retrofits was one billion yen, about one percent of the cost of the bridge.

The bridge's superstructure sits on 42 Y-shaped piers; 12 are in deep water. These piers were assembled at fabrication yards and transported to the work site where a floating crane set them in place. The reinforced concrete footings are set on steel pipe piles. The 12 deep water piers are steel and contain a special titanium cladding over a 5 m section in the splash zone to protect against corrosion. A thin layer of copper was placed between the 1 mm titanium sheet and the steel pier. The hot rolling process used squeezes out the molten titanium-copper inter-metallic compound which oxidizes with the residual air forming a bond of 180 MPa or higher. The Nippon Steel Research and Engineering Center played a key role in this innovative development. This was the first use of the cladding process in a construction application. The remaining 30 piers are reinforced concrete with steel sheet pile foundations. Cathodic protection is installed in the reinforced concrete to protect reinforcing steel from corrosion.

The bridge-girder is separated into sections spanning 10 piers with the longest span measuring 240 m. The girder is 22.9 m wide. High damping rubber bearings and other types of rubber bearings were used for the bridge piers. Various concrete strengths were used in the project:

Tunnel segment	48 MPa
Road section	24 MPa
Ventilation Building	24 MPa

Overall this is one of the largest public works projects the Government of Japan has undertaken. TTBH construction costs are about 20% greater than originally planned 10 years ago. The overall construction cost is projected to be 1.5 trillion yen ($18[1] billion). The cost is split 81% from TTBHC and 19% from JHPC. Of the 81% from TTBHC: 6.3% is from capital; 41.1% from government bonds; 25.6% from private loans and loans from the Japan Development Bank; and 26.6% from official loans. It is projected that the project will pay for itself over thirty years. The expected first year traffic volume is 33,000 vehicles per day and is expected to grow to 64,000 vehicles per day after 20 years. One way crossing toll will be 5000 yen ($41.67). In addition, the government will compensate fishermen from the east side of Tokyo Bay for their losses in fishing harvest. Ten year compensations of 50 million yen ($417,000) per year will be paid to their Fishing Association.

A principal reason for the more expensive long tunnel option over a longer bridge system was the vessel traffic. There are over 1,400 ships per day that move through this passage. Although the cost of tunnel construction was estimated by the Government of Japan to be 3 to 4 times more expensive than a series of

[1] Currency conversion 120 yen = $1.00

bridges, considering the potential impact on navigation and the need to reduce environmental impact, the more expensive tunnel option was selected.

2. Nippon Steel Research and Engineering Center (http://www.nsc.co.jp/rd-e.html). The delegation visited the Nippon Steel Corporation's Research and Engineering (R&E) Center at Futtsu, Chiba Prefecture, on the east shore of Tokyo Bay. NSREC is in a six-year-old campus facility. The complex consists of 10 buildings. The delegation was welcomed by Dr. Yukihiko Sumiyoshi, former Director General of the PWRI, and now Executive Counselor with the Nippon Steel Corporation, and Dr. Kato, Director of the Steel Research Laboratory.

Mr. Sato presented a general overview of the R&E Center. The Center's laboratories and offices comprise 100,000 m^2 on a site of 70 ha. The Center employs approximately 1,600 persons, of whom about 650 are researchers (most with Master's Degrees) and the remainder are technical and support staff. Company policy encourages earning a Ph.D. Besides the R&E Center, Nippon Steel operates an Advanced Technology Research Laboratory at Kawasaki City, and seven smaller R&D laboratories at other Nippon steel works sites. During 1995, Nippon Steel noted they were engaged in partnerships with 360 universities and research organizations and have 90 joint research projects.

Nippon Steel's R&D budget is huge by U.S. industry standards: 56 billion yen (about $470 million), or 2.7% of revenues. About one-third of the budget focuses on new business opportunities. After the Hyogo-ken Nanbu Earthquake, Nippon Steel focused much attention to improving the quality of its steel. Fifty percent of steel in Japan is used in building and public works projects. Nippon Steel is the world's largest steel maker. It was noted that the Nippon Steel R&E Center's 650 researchers exceed by a factor of ten the number in the entire American steel industry.

Four of the Center's researchers made presentations on new products. Dr. Kinoshita described research on Earthquake Resistance Research on Buildings and Bridge Piers. Dr. Hagiwara reported on SUF-Steel (a steel with ultra-fine grain structure in the surface layers, giving it the ability to arrest cracks). Here the steel plate's surface layer, composed of super-fine ferrite, has better toughness compared to the composition of the inner layer, and arrests the progress of brittle-crack by absorbing transmitted force through plastic deformation. Testing showed that ultrafine grain (SUF) steel laid on steel sections absorbs shock and eliminated fracture. Nippon Steel developed a production system for this new steel plate for use in ships, marine structures, energy storage tanks, and high-rise buildings. Dr. Sakumoto spoke on Fire Resistant (FR) Steel to increase steel's tensile strength and high temperature yield point by adding molybdenum (MO) and niobium. The FR steel resists a load corresponding to the allowable stress under permanent loading at 600 ^{o}C. The FR steel meets The Ministry of Construction's *Design Specifications for Building Fire Safety* (1988) modification. The FR steel is being incorporated in several Japanese buildings. MO steel has not yet been commercialized. Mr. Tarui summarized work on High Strength Cable Wire for Suspension Bridges such as used on the Akashi-Kaikyo Bridge described later. Dr. Kinoshita described research on beam/column connections; the Center advocates the use of bolted, in preference to welded, connections. He also described experiments using a low yield point steel, with a flat stress-strain curve over a broad strain range, as an energy-absorbing damper in building frames; and the use of concrete-filled hollow steel structural members to provide superior ductility.

A short laboratory tour followed. Its equipment consisted of conventional load testing apparatus of probable 1970's vintage. In evidence were test specimens of bolted beam/column connections, concrete-filled steel members, panels of SUF-Steel, and a segment of steel cable, in various stages of test, untested, mounted in test machines, and post-test. Notable by their omission from the tour were laboratories such as those for metallurgy and process technology, which are implied by the product developments described, but not included in the tour or presentations.

3. Shinjuku Park Tower Building. The Shinjuku Park Tower constructed by Kajima (http://www.kajima.co.jp/), Shimizu (http://www.shimz.co.jp/english/index.html), and Taisai (http://www.taisei.co.jp/) Corporations is an interconnected three building steel frame structure owned by Tokyo Gas Urban Development Company. Located in Nishi-Shinjuku, Tokyo the 264,000 m^2 building complex houses the Park Hyatt Tokyo Hotel, shops, restaurants, offices, and parking facilities. Its southernmost tower is 235 m high (52 stories above ground). Its floor plan is such that the narrow section of the building is in the east-west direction. Strongest winds at this site are in the north-south direction. The first three periods of vibration of the undamped system were estimated to be 5.2 seconds in the transverse direction; 4.5 seconds (longitudinal) and 4.0 seconds (torsional). Because the Park Hyatt Hotel occupies the upper portion of the southern tower, serviceability under wind conditions was an important design consideration. To mitigate the effects of wind-induced vibration, the southern tower is equipped with three-unit V-shaped hybrid tuned mass dampers (TMD), called the Trigon System designed by Kajima Corporation.

The Trigon System combines a passive tuned mass damper with active control operated by a 75 kW capacity electric motor. This compact TMD system has adjustable V-shaped rails which slide on rollers allowing for an easy tuning of the period. The three units were installed on the 39th floor off the southern tower rather than the 52nd floor due to space constraints imposed by the Park Hyatt. The TMD is aligned to control transverse vibrations. The moving mass is placed in the center of the triple nested frame. They are suspended by wire ropes. The height of the TMD is about 3 m, to fit into the floor height.

Each unit of the mass damper system has an auxiliary mass of 110 tons, totaling 330 tons which is 0.25 percent of the total building weight above ground. The range of the adjustable natural period is 3.7 to 5.8 seconds. The active control system becomes operational when accelerometers and sensors for wind or earthquake shows the building motion has exceeded a predetermined threshold value. Sensors are installed at the 39th floor; a seismograph is on the first floor. According to Takenaka, et. al (1994), the units can reduce building acceleration by over 50 percent. The Kajima Corporation literature indicates the Trigon System is one of many hybrid mass damper systems under development.

The building' s damping is related to the Japanese Standard of Comfort. There was discussion about the need to better quantify comfort levels from motion and research needed to develop more precise measurement methods of human comfort.

References: [1] Y. Takenaka, et. al. (1994), *Development and Application of V-Shaped Hybrid Mass Damper for High-Rise Buildings* and *Proceedings of the 2nd International Conference on Motion and Vibration Control, Yokohama*, August 30- September 3, 1994, pp. 563-568. [2] Kajima Corporation Technical Pamphlet 93-80E, *Trigon: Weight Driven Hybrid Seismic Response Control System.*

4. **Kajima Technical Research Laboratory** (http://www.kajima.co.jp/). Dr. Kikuo Koseki, Deputy General Manager KaTRI received the delegation. He provided a general overview of KaTRI's activities, organization, and budget. KaTRI's management is directly under the Kajima Corporation's top management and its steering committee consists of several division heads and chaired by the President of the Kajima Corporation. The Kajima Corporation employs more than 14,000 persons. Its revenue was reported to be $12 billion of which $70 million were allocated to KaTRI. KaTRI has 250 active research projects; 55% of the budget supports 30 projects. KaTRI operates with a staff of 405; 275 are technical and 48 have PhDs. Currently, there are forty-eight Research Associates with assignments at KaTRI. KaTRI is organized into seven departments; 50% of staff work on R&D programs, 20% on outside contracts, and about 25% do consulting engineering work for their branch office. Its research budget is about 1.2% of revenue.

The delegation was shown videos to introduce them to the overall KaTRI activities. The theme of the videos focussed on symbiosis with nature and turning dreams into reality for creation of a pleasant environment. The videos covered construction of buildings, bridges, energy plants, dams, active & passive control devices. Following the videos, the delegation visited six facilities: Active Stiffness Building; Shaking Table Laboratory; Wind Tunnel Laboratory; Geotechnical Centrifuge; Base Isolated Building, and Large Size Structural Testing Laboratory. They all appeared to be high quality facilities.

The Active Variable Stiffness (AVS) Building is an experimental building completed in 1990 that makes instantaneous judgements of seismic tremors, and reduces building motion from tremors by changing its stiffness. This is the first building in the world to which such a system has been applied.

The delegation toured the Shaking Table Laboratory and discussed the six degrees of freedom 5 m by 5 m shake table with a rated load capacity of 30 tons, making it possible to do experiments with large scale specimens. Its displacement is $\pm$ 200 mm (H) and $\pm$ 100 mm (V) and velocity of 1 m/s (H) and 0.5 m/s (V). The system incorporates a floating foundation, which prevents the propagation of vibration to the surrounding environment. Recent experiments using this shaking table have focussed on testing non-structural components of residential structures during earthquakes. Tests concerning the use of base-isolated systems for high aspect ratio residential buildings were being conducted.

The next stop was at the Wind Tunnel Laboratory. This laboratory houses a large boundary layer wind tunnel for investigation the effect of wind on skyscrapers, longspan structures including bridges. This wind tunnel has a test section of cross section of 4.5 m by 2.5 m by 27.7 m in length. Wind speed can be controlled from 0.5 m/sec to 40 m/sec. A future high rise building model with the surrounding urban terrain was being tested in the tunnel. A companion visualization wind tunnel was visited. This tunnel uses laser beams to visualize and analyze air flows inside and around buildings and structures. A proposed stadium model was under study at this time of our visit.

The delegation visited the Geotechnical Centrifuge Laboratory. The Centrifuge has the capacity of 1000 kg payload at 100 G acceleration and 500 kg payload at 200 G. It is fully automated including data acquisition and analysis capabilities. The centrifuge is used to study soil structure interaction, such as tunnel retaining wall, embankment and foundation stability.

The last stop was at the Large-Size Structural Testing Laboratory. On way to this laboratory the delegation reviewed the foundations and base isolators of KaTRI's Base Isolation Building. Using reaction walls and floors in the structural testing laboratory, large scale loading tests are conducted to

examine the strength and earthquake-resisting behavior of nuclear power plants, long-span bridges, marine structures, high-rise buildings. The reaction wall's capacity is rated at 910 ton at 4 m and 450 ton at 12 m and a 2.1 m thick strong floor. Five to ten engineers work at the laboratory; about 50% of their work is supported by in-house funds and 50% by contracted work. The laboratory had several test configurations to test large concrete panels, steel-in-concrete structure testing and reinforcing bar joint structure testing. Many tests concerning hybrid steel & concrete sections of a tunnel were in place during the visit. The delegation returned to the central building and visited several impressive scale demonstration models of recent Kajima projects ranging from actively control buildings to indoor skiing slopes.

Kajima's technology is transferred to subsidiaries, others are sold, and some are transferred to other construction companies. Much technology is transferred to the workforce through training and by special internal committees.

References. [1] *AVS, Active Variable Stiffness System*, Seismic Response Control Series, Tec Pamphlet 91-65E and [2] *New Large Size Structural Testing Laboratory*, KICT Leaflet 85-4.

5. Japan Meteorological Agency (http://www.mri-jma.go.jp/). One of the Japan Meteorological Agency's (JMA) mission is to monitor earthquakes, volcanoes, and tsunamis; predict earthquakes; and distribute advisories and related warnings of natural disasters. JMA prepares and distributes probabilities of earthquake, storm, and volcanic conditions for Japan and surrounding countries. JMA is the official Japanese Agency to issue earthquake information. Dr. Hashida, Deputy Director of JMA met with the US delegation and presented an overview of the JMA organization in their emergency operations control center.

JMA employs about 6,000 persons; 300 staff are responsible for monitoring earthquakes, tsunami and volcanoes throughout Japan. These were the principal topics reviewed during the delegation's visit. The visit was held in offices of the Seismology and Volcanology Research Department. The Department is composed of research laboratories that address earthquake generating mechanism, earthquake and volcanic eruption predictions, earthquake and volcanic observation stations, and generation and propagation of tsunami and estimation of tsunami height at seashore. Discussions centered on new observation techniques of volcanoes and on various phenomena of volcanic activity, such as the estimation of energy releases from nine of eighty six-active volcanoes in Japan by using seismological, geodesic, geomagnetic, and remote sensing techniques. Studies of the growth and collapse of the lava dome and the pyroclastic flow of Unzen Volcano have been studied with seismic, infrasonic, and video image data.

JMA has active work underway to improve earthquake prediction methods. A five-year research project on estimating earthquake and tsunami risks has been done. A prediction model of seismic activity and a method of automatic precursor detection was developed. GPS systems were installed in Marcus Island for the observation of the Pacific plate motion. JMA investigates tsunamis such as the 1993 Hokkaido-nansei-oki Tsunami and improves their tsunami propagation model based on these investigations.

JMA also has an active volcanic airborne ash monitoring program as part of its overall volcano monitoring program. Airborne ash warning information is provided on a 24-hour basis during eruption events to all major aircraft control centers in the Pacific region.

JMA has active collaborations with STA's National Research Institute for Earth Science and Disaster Prevention and regularly exchange seismic information. Other national, academic, city, and regional organizations provide monitoring data to JMA. Since JMA is the only Japan hazard monitoring organization in this area officially operating 24 hours a day, it is the location of choice to compile and process monitoring data on these kinds of events.

6. **Landmark Tower** (http://city.yokohama.jp/bconv/business/ylmtwr-e.html). The Landmark Tower is a 70-story building in the 'Minato-Mirai' (future port area) along the water front in central Yokohama. It is a redeveloped site. The Landmark Tower is 296 m high, the tallest building in Japan. The building features a five-story atrium for shopping, offices, and a hotel. It is constructed of a hybrid steel reinforced concrete frame from the basement to the 8th floor and of a high strength steel frame structure from the 9th to the 70th floor. The foundation consists of 24,000 m^3 of concrete is 24 m below grade. The exterior of the Landmark Tower is a precast concrete panel wall. Its floor area is about 400,000 m^2; 1-1/2 times larger than that of the Empire State Building.

The building incorporates a multi-layer pendulum vibration control system that reduces building sway by about 65 percent. The system includes two tuned active dampers (TAD) of 250,000 kg each at diagonal corners of the Tower. They are the largest in Japan. They are on the first floor of the penthouse, 282 meters above the ground. There are only five other buildings in Japan using TAD. The specifications for the tuned active damper system used in the landmark tower is shown in the table.

Number of Units	2 Units
Dimension	9 m(width) x 9 m(depth) x 5 m(height)
Gross Weight	250,000 kg (one unit)
Moving mass weight	170,000 kg (one unit)
Maximum amplitude	$\pm$ 1.7 m
Maximum control force	400,000 N (each direction)
Adjustable natural period	4.3 to 6.0 seconds

A multi-step pendulum concept was used in the design of the TAD to reduce the height requirement. For the Landmark Tower application a three-step design was used which reduced the total height requirement to less than five meters. This allowed the use of only one floor height to accommodate the TAD system. A single TAD pendulum system required about nine m height.

Because of its height and the severity of winds in the Yokohama area the governing design forces for the Landmark Tower are determined by wind rather than seismic loading. The TAD system is designed to counter vibration conditions by moving mass forces in either a passive or active control operational mode. In the active control mode electric servo motors move the TAD system to achieve maximum structural vibration control. Full-scale free vibration experiments evaluated the effectiveness of the TAD system.

The damping factor ranged from 0.8% with no control, to 2.4% with passive control, to 10.6% with active control.

The Landmark Tower is a fully integrated structural and operation system taking into consideration efficiency, confidence, and safety of the building' s occupants. Each floor is divided into separate fire compartments to direct smoke and gases to wall vents then to the outside. Fire proof shutters are installed in the shopping area to compartment smoke in case of fire. Extensive computer simulations were performed during the design phase to mitigate against wind, earthquakes, and smoke. After completion of the building, full scale smoke tests were performed to verify the design.

The Landmark Tower's facilities include 26 electric substations with back up electricity in case of power failure. Each floor is divided into eight zones to permit fine tuning of the heating and air-conditioning within these spaces. Water is recycled and used for toilets. The elevators are the fastest in the world operating at 750 m per minute. Automatic window washer/wiping systems were installed to provide hotel customers clean windows to admire Yokohama and Tokyo Bay.

7. **Nukui Arch Dam.** The site of the Nukui Dam, a parabolic arch structure, is on the Takiyama River, a branch of the Ohta River System near the town of Kake in the Chugoku Region of Japan, approximately 25 kilometers northwest of Hiroshima. The dam is under construction by the Ministry of Construction (MOC) through their Nukui Dam Construction Office. When completed the dam will rank among the highest of Japan's arch dams. It will be 156 m high, 382 m long, with a concrete volume of 800,000 m^3. The reservoir's capacity is 82 million m^3 with a catchment area of 253 km^2. The total construction cost is 140 billion yen ($1.2 billion). At the time of the delegation' s visit progress toward completion of the project was at about 55%.

The Nukui Dam will play an important role in the flood control of the Ohta River reducing the flood peak of 2,900 m^3/s to 1,000 m^3/s by decreasing water flow by 1,800 m^3/s at the dam site. The dam will ensure a storage of 22 million m^3 to meet the water demand of 300,000 m^3/day for the population with the greater Hiroshima metropolitan area and the surrounding islands. Other purposes of the dam include the maintenance of a relatively steady flow to enhance the natural environment downstream and provide a stable water supply. A power station that is an integral part of the dam project will have a maximum output of 2,300 kilowatts.

The dam is in a narrow stretch of the Takiyama River valley where the abutments may optimally react with the bedrock. The bedrock consists of three units of the Cretaceous Hiroshima granite which range from a relatively medium coarse-grained to a fine grained black mica granite. The upper unit contains conspicuous feldspar phenocrysts and also variegated streaks of the mica. Some minor faulting was observed within the riverbed. The shear parameters of the rock were found adequate by running a series of direct shear tests in the dam foundation area.

Before dam construction started, a diversion tunnel approximately 7 m in diameter and 540 m long and upstream and downstream coffer dams were constructed to divert the Takiyama River around the dam site. These features were seen by the delegation. Excavation of the foundation area was carefully done using a pre splitting procedure to minimize the amount of induced fractures in the bedrock. The material

removed was stored nearby and is now being used for the aggregate making up the concrete of the dam. This application reduced costs and protected the natural surroundings from further mining.

Foundation stability was performed in a two-step process of consolidation grouting and use of curtain grouting. After excavation was completed, a series of grouting procedures were performed to seal coarse cracks found in the foundation area and generally to achieve a relatively uniform foundation surface with improved deformability and permeability. A final curtain grouting procedure was employed to prevent the stored water from permeating the foundation rock and reduce potential uplift of the dam.

Work now underway is focused on the raising the segments making up the body of the dam. When complete the dam will consist of 26 individual segments grouted together to form the dam body. Concrete is mixed in a concrete-mixing plant at the dam crest using automated methods. It is transported to the dam segments by remote control in 6 m^3 buckets using 20 ton cranes. The typical lift for a segment is 2 meters thick. Low heat concrete is used at 430 kg/cm^2 strength. Before a segment is raised a series of stainless steel cooling pipes, forming a grid with 1.5 m spacing and a set of joint-grout pipes are put in place. During and after the concrete pour, about 17 ^oC water is pumped through the cooling pipes to reduce the chance of thermal cracking during the curing of the concrete. In the winter months, when transversal joints between segments are expected to be their widest, grouting is pumped through the joint-grout pipe system to seal the joints between the segments. The proportioning strength of dam body is 430 kg/cm^2, maximum compressive stress is 65 kg/cm^2.

More than 1000 sensors are installed in the dam including optical fiber thermometers to measure temperatures and other instruments to measure seismic loadings and water pressures. To monitor the effects of earthquakes on the dam a set of six accelerometers will be distributed about the dam structure - from near the foundation, at mid-height and at the crest of the dam. In addition, dynamic water pressure will be continuously monitored by a series of six pressure transducers installed on the upstream side of the dam.

The Nukui Dam Project has been under way for 30 years starting with the commencement of the preliminary survey. Compensation was made to families for 27 affected houses and construction of a new school, shrine, and 20 km of new roads. Fifteen years ago work began on the construction of bypass roads around the dam and reservoir site. Work on the dam itself began in 1991 and is expected to be completed during 2001.

8. Kurushima Suspension Bridges, Honshu-Shikoku Bridge Authority
(http://www.webcity.co.jp/mi/tour/hashiE.html). The Onomichi-Imabari highway route connects the main island of Honshu and the southern island of Shikoku. It is the western route of three north-south traffic routes approved in the 1969 comprehensive Japan national development plan to stimulate local commerce and facilitate the industrial development of the region. This route will connect the Hiroshima greater metropolitan area with the Matsuyama area when completed in 1999. The route consists of 10 bridges traversing nine islands. A second central route, which connects Kurasiki on Honshu Island with Sakaide on Shikoku Island was completed in 1988. A third route further to the east, the Kobe-Naruto highway route is described under the summary of the Akashi-Kaikyo Bridge.

The delegation visited Kurushima bridge, located at the south end of the Onomichi-Imabari Highway Route. Kurushima Bridge is a generic name for three consecutive long-span suspension bridges crossing the Kurushima Straits between Ohshima Island and Imabari City. Construction of the three Kurushima bridges began in September 1990; they will be completed in 1999. The three suspension bridges are continuously linked one to the other. The first bridge is 960 m in length with 600 m center span; the second bridge is 1,515 m in length with a 1,020 m center span; and the third bridge is 1,570 m in length with 1,030 m center span.

The structural design is a 3-span, 2-span, and single span with 2-hinged suspension bridge and steel stiffening box girders. Its towers are rigid-framed steel structures. The tower heights are linearly varied; the elevation and the depth of the horizontal members of the towers were decided from engineering design and aesthetics. The latter to complement the surrounding natural land. The anchorages surfaces are precast concrete panels. The anchorages between two connected suspension bridges are gravity-type, which serve two suspension bridges. The bridges' stiffening girders are steel box girders selected for aerodynamic stability and cost consideration.

The construction methods for the underwater foundation of the Kurushima bridges are basically the same as conventional suspension bridges except the first tower of the second bridge. In this tower, the guide pile is employed for the conventional laying-down caisson method to cope with the harsh tidal conditions.

At the time of the delegation' s visit, the substructure and tower constructions of the bridges were completed. Suspension cables and hanger ropes of the first bridge are nearly completed. Erection of catwalk ropes and floor systems are completed in the second bridges. The erection of the suspension cables was recently completed for the third bridge. The cables are made up of 44 strands of wire for the 1st bridge and 102 strands for the other two. Each strand is composed of 5 mm diameter wires.

9. Tatara Cable Stayed Bridge, Honshu-Shikoku Bridge Authority (http://www.webcity.co.jp/mi/tour/hashiE.html). This bridge is the fifth of the 10 bridges crossing the Inland Sea. It is in the middle of the Onomichi-Imabari route. The 890 m center span, 1,480 m, 2-tower and 3-span cable-stayed Tatara bridge, when completed in 1999, will be the worlds longest cable-stayed bridge. The bridge type and location of the towers were influenced by the desire to preserve a natural and environmental look presented by Mt. Kannon of the Seto Island Sea National Park. The bridge construction cost including the approach roads is approximately 100 billion Yen ($800 million).

The center deck span is a steel box girder with fairings; the end spans measuring 270 m and 320 m respectively are PC girder. The girders are on elastomeric bearing base isolators. The design was chosen primarily to compensate for the imbalance of the dead load due to the center length being longer than the sum of the two side spans. While the decks of the side spans and at the location of the towers have been manufactured and erected in large blocks (e.g., 123 m and 163 m steel girders near the towers and 109 m and 102 m pre-stressed concrete girders of the side spans), the center span steel girder in blocks of 20 m was erected from both sides toward the center. The deck width is 30 m; the effective width of the box girder deck is 20 m. The deck is designed for bicyclists and pedestrian traffic on both sides. At the time of the visit, the bridge deck was not completed. Several 10 m long center girder sections were still to be erected.

The reversed Y-shaped towers are 226 m above mean high tide sea level. The tower shape was determined by wind tunnel tests. The design resulted in minimum vibrations. The upper two shafts of

the towers have slits to reduce wind induced vibration from vortex shedding which can damage the structure as demonstrated by wind tunnel model testing. The 168 strand cables are anchored between the deck and the towers in two planes and in a fan-shaped arrangement. Each strand consists of 7 mm diameter galvanized wires. Test dampers are anchored to the cables at deck level to decrease the vibration of the cables. Several tests are underway to evaluate the most effective damping system. The cables are covered with plastic covers designed with prefabricated staggered impressions to reduce the probability of wind and rain induced vibrations and for corrosion protection.

10. Earthquake Restoration Sites (Kobe). Four sites were visited in Kobe: Kobe East Area Redevelopment Project; Kobe City Government (http://www.city.kobe.jp/); the Nadakita-Dainin Public Housing Project; and the Shin Nagata Area Redevelopment Project. The delegation was hosted by the Kinki Regional Construction Bureau of the Ministry of Construction.

The first site, Kobe East Redevelopment Project, is under construction on land formerly occupied by a Kobe Steel Company mill that was seriously damaged in the Hyogo-ken Nanbu Earthquake. The government purchased the land for public housing, now under construction. When completed in April 1998, the project will house 30,000 people in apartments with an average floor space of 70 m^2 for a family of four.

Next, the delegation visited Kobe Government Officials in the new Kobe City Hall building, which survived the earthquake without damage. Next to the new Kobe City Hall is the old City Hall, built in 1957, an eight-story building that suffered collapse of the sixth story. For restoration, the fifth and higher stories were removed, and a new fifth floor, roof, and penthouse were constructed.

A general briefing was made on reconstruction in Kobe after the earthquake. The restoration of port facilities was completed in May 1997. The restoration of highway facilities is nearly complete. Industrial activity has risen to 85 percent of the pre-earthquake level. Forty-three thousand people still are living in temporary housing 2-1/3 years after the earthquake devastated the city. Kobe's population has not yet been restored to the pre-earthquake level of 1.52 million. The four priorities of the reconstruction effort are:

- o resettlement of victims,
- o public aid to the aged,
- o restoration of economic activity, and
- o improve fire fighting technologies.

Kobe authorities now better understand displacement problems that face the elderly following disasters. Older people in temporary housing represent a special problem in the earthquake aftermath, e.g., loneliness and need for special medical assistance. The pre-earthquake communities that provided support were destroyed, and it is difficult for the elderly to adjust. Twenty percent of the victims in temporary housing are over 65. At first, priority was given to the elderly in providing temporary housing, but this policy meant that there were too few temporary housing for young people to help and support. The cost of one unit of temporary housing is about 3 million yen ($25,000). Soon all earthquake victims will be in permanent housing, either public rental housing or houses built with loans available to the victims at very low interest rates.

The Kobe Government enacted new legislation to better fight fires from future earthquakes. All redeveloped sites with plots measuring 250 m by 250 m will have installed 100 tons of water in underground tanks. Large water tanks will be constructed under schools. City zoning now requires increased road width, green spaces are being required for fire breaks and other disaster mitigation efforts, and more redevelopment projects will be created to provide shelter for the underprivileged.

Recent Japanese law requires that public buildings be evaluated for vulnerability to future earthquakes. Owners of buildings cited as vulnerable to earthquakes must develop a strengthening plan. Discussions are underway to require strengthening evaluations for all buildings.

The next stop was the Nadakita-Dainin Public Housing Project, a 5 to 14-story complex of apartments with restrained design are built around a beautifully landscaped central atrium. The project is completed, but not yet occupied. There are 290 dwelling units in the complex, including 90 for senior citizens and 5 for persons confined to wheel chairs. The fraction of units allocated to senior citizens is twice the average of the other new housing projects, because this location, with easy access to city services, is particularly suitable for the elderly. The units contain two to four bedrooms plus a combination kitchen and dining area and bath. Floor areas range from 50 to 70 square meters. The units will be allotted by lottery. The rents are based on income; rents range between 7,000 and 46,000 yen (about $60 to $400) per month.

The final stop was at the Shin Nagata Area Redevelopment Project. Seventy percent of the housing in this area was destroyed by fire in the earthquake. This area was cluttered with old two and three-story buildings. Typically the first story was used for shoe manufacturing and the upper floors for dwelling. Fire leveled these buildings which had large quantities of highly flammable liquid and combustible materials. Redevelopment in this area is being performed by the city government. Before the earthquake, most of the housing was built of wood. The redevelopment will be concrete, there will be more open space, roads will be wider, and water-storage tanks will be installed under building plots. All these features are designed to reduce the fire risk and make fire fighting more effective in future earthquakes. Before the earthquake most of the buildings were small. The redevelopment will be accomplished with taller buildings (up to 30 stories) and will include shopping malls. These changes are in response to land values of one million yen per m^2 ($830 per ft^2). Some new buildings are under construction, and all are expected to be complete within six years. There were 1400 housing units in the area before the earthquake; when redevelopment is complete there will be 3000. The $2.5 billion total cost will be met in part by the national government, in part by the Kobe city government, and in part by sale of apartments to private owners.

Kobe's work in rebuilding its infrastructure and its publications documenting its reconstruction is a success story and case study for those countries facing threats of natural disasters. Its case study would make an important contribution to the closing out of the International Decade for Natural Disaster Reduction (IDNDR) in 1999 and would be an effective contribution to the 2nd Earthquake Policy Symposium of the US-Japan Natural Disaster Reduction Initiative of the US-Japan Framework for New Economic Partnership (Common Agenda) scheduled during 17-19 September 1997, Kobe.

References: [1] *The Great Hanshin-Awaji Earthquake Statistics and Restoration Progress*, April 7, 1997. [2] *Kobe City Restoration Plan* (abridged version), Kobe City Government, June 1995. [3] SRC Construction, "Reconstruction of a Building whose Middle-level Floor Collapsed Due to the Great

Hanshin-Awaji Earthquake, while Lower Floors Remained Intact," Chapter 1. [4] *Nadakita Daini Public Housing Project*, Housing Bureau, Kobe City.

11. Akashi-Kaikyo Bridge, Honshu-Shikoku Bridge Authority

(http://www.hsba.go.jp/bridge/a-route.htm). The Kobe-Naruto highway route will connect Honshu and Shikoku when completed in the Spring of 1998. It is the eastern route of three north-south traffic routes. This about 90 km long Kobe-Naruto Route is marked by the construction of two major suspension bridges including the world' s longest, the Akashi-Kaikyo bridge. This bridge will connect the Kobe area of Honshu with Awaji Island, the sixth largest island in Japan. A second major bridge on this Kobe-Naruto Route, the Ohnaruto Bridge, was completed in 1985 and connects Shikoku Island with the southern end of Awaji island. Construction of the Akashi-Kaikyo Bridge began in 1988 at an estimated cost of 400 billion yen ($3.3 billion). To date, the cost estimate has risen to 470 billion yen ($3.9 billion). More than 100 construction contractors are involved with building the bridge.

This 4 km bridge crosses the Akashi Straits between Honshu and Awaji. A 1500 m wide main shipping lane into the inland sea is traversed by about 1,400 ships per day. The bridge was constructed in 110 m deep water with 4.5 m/sec tidal currents. Design for 67 m/sec wind speeds and a potential 8.5 Richter magnitude earthquake 96 km from the site was considered by the Honshu-Shikoku Bridge Authority (the bridge owner). Geology of the bridge site includes layered alluvium and diluvium deposits over hard "Akashi" or "Kobe" layer. Granite protrudes at the Awaiji anchorage.

The total length of the bridge is 3,910 m from anchorage to anchorage. The main span is 1,990 m with two side spans of 960 m each. The bridge roadway surface has been constructed on top of a 14 m deep by 35.5 m wide truss girder system suspended from main cables passing over two steel towers which rise 297 m above the mean sea level. A 65 m clearance will be maintained over the shipping lane. The 1.12 m diameter main cables were erected by the prefabricated strand method. Approximately 200,000 tons of steel was used in the superstructure and 1.42 million cubic meters of concrete for the substructure.

Anchorages measures 63 m by 84 m in plan, extend into the "Kobe" and granite layers at the site, which required special foundation construction technology. The Honshu anchorage had to be embedded 61 m below sea level and required the anchorage excavation to be performed in open air. Therefore, an 85 m diameter circular slurry wall, 2.2 m thick, was constructed and subsequently used as a retaining wall. Excavation within the slurry wall was followed by the placement of roller compacted concrete to complete anchorage foundation construction. The Awaji anchorage foundation was constructed using steel pipes and earth anchors to support the surrounding soil. The excavated foundation was filled with specially flowing mass concrete. Both anchorages were completed with the construction of a huge steel supporting frame used to anchor the main suspension cable strands.

Main tower piers were constructed in the Akashi Strait. The tower pier foundations were designed to transmit 100,000 tons of vertical force to bedrock, approximately 60 m below the water surface. The foundation was constructed using the newly developed "laying down caisson" method. Steel Caissons, 80 m in diameter and 70 m in height were towed to the tower sites, submerged, and set on the pre-excavated seabed. Pier foundation construction was completed with placement of concrete. Next, the main steel towers were erected on the concrete piers. Each main tower height is 282.8 m and was erected by stacking 30 approximately 10 m high prefabricated steel segments on top of each other. The segments are formed with three separate cells in plan view. Special procedures were used during

fabrication of each segment to assure tight tolerances for proper tower alignment. The tolerances were maintained using laser measuring technologies for controlling all dimensions. The technology resulted in no major erection problems during field bolting and splicing the steel tower segmenting together. An independent, self supporting 160 ton tower crane was used during tower erection. While the tower's cruciform cross section is resistant to wind induced vibration, tuned mass dampers were installed in each tower at varying stages of completion to reduce wind driven tower motion and diminish tower vibration in case of an earthquake.

Before stringing the cable, a pilot hauler rope was attached to each anchorage and placed over the tower tops by helicopter. The pilot rope was used to suspend the catwalk from which work on the main cable erection would proceed. The main cables which have a 1:10 sag ratio were erected using the "prefabricated strand method". Each cable has 290 prefabricated strands and each strand has 127-5.23 mm diameter galvanized wires that were factory fabricated in 4,074 meter lengths. High strength wire with 180 kg/mm^2 tensile strength was used rather than the standard 160 kg/mm^2 wire. Each strand was transported to the construction site where it was pulled from one anchorage over the saddle of each tower and fastened to the opposite anchorage frame. This procedure was repeated 289 times to fabricate each main cable. Each main cable was separated at the anchorage by a splay saddle before attachment to the steel anchorage frame inside the anchorage to distribute cable tension in the foundation equally. A specially designed cable squeezing machine was used to compress the 290 parallel wire strands into the final 1.12 m diameter cable. Cable bands were placed to circumferentially compressed the cable and to maintain the circular shape. Finally, suspender cable hangers were attached to the main cable for supporting the main stiffening truss. Hangar cables were factory fabricated from bundled 7 mm in diameter, 180 kg/mm^2 parallel wire strands. Because the higher strength wire was used, two rather than the usual four hanger ropes were required to support the panel points of the stiffening truss girders.

Steel stiffening truss girder panels were fabricated off site and transported by barge to the bridge tower piers, lifted to roadway elevation, and transported by traveler crane to the proper location for connection to the suspender ropes. This procedure allows for uninterrupted use of the busy shipping lane of Akashi Straights.

Several special technologies were developed to support the design and construction of the Bridge. The aerodynamic stability of long suspension bridges pose major challenges to designers. To verify the design of the bridge, the Honshu-Shikoku Bridge Authority under an agreement with the Public Works Research Institute, designed and constructed the worlds' largest wind tunnel facility and tested full section models in laminar and turbulent wind flow. Other technologies resulting from wind tunnel testing include; installation of vertical plates at bottom center of the highway deck to increase flutter speed. Methods to improved prediction of flutter speed and gust response will be used in future bridge designs. Complete details on the wind tunnel facility and the design, fabrication, and testing of the full section bridge model are contained in past UJNR Panel Proceedings, *Wind and Seismic Effects*.

Another special technology developed for the Akashi-Kaikyo Bridge was use of parallel wire strand for cable fabrication and erection. Rather than using spinning methods for structure cable fabrication, individual parallel wire strands were fabricated off site, transported to the bridge site and strung parallel to each other to form the main cable. The advantage of using this method is the strands are continuous from anchorage to anchorage and eliminate the in place spinning of cables, thus reducing the probability of accidents occurring. To use the parallel wire strand method, a unique cable squeezing machine was

designed to form the parallel strands into the final circular shape. The use of a higher strength wire, 180 kg/mm^2, reduced the number of strands required, thus saving erection time and cost. Use of the higher strength wire also reduced the number of suspender ropes from four to two needed to connect each stiffening truss panel point to each cable hanger attachment on the main cable. This accounts for reduced erection time and cost savings.

Of particular interest was the performance of the bridge in the 17 January 1995 Hyogo-ken Nanbu Earthquake which provided a full scale test of the tower response. The complete bridge structure is designed to resist a 150 km distant, 8.5 Richter magnitude earthquake. Fortunately, erection of the bridge stiffening truss had not begun. The Nojima fault zone passes between the towers of the bridge and caused a permanent lateral and vertical offset of the Awaji tower and anchorage. Ground fault rupture was visible on the northern tip of Awaji Island, approximately 2 km from the Awaji anchorage. The Awaji tower displaced 1.3 m to the west while the Awaji anchorage displaced 1.4 m to the west. The net result was 0.8 m increase in span length between the main towers and a 0.3 m increase in the southern side span length. The Awaji tower pier displaced 0.2 m vertically downward while the Awaji anchorage rose by 0.2 m. The sag in the main cable was reduced by 1.3 m. The increased distance between towers was accommodated by redesigning the two center stiffening panels each of which are now 0.4 m longer than originally designed. Other minor damage was inflicted to the cable squeezing machine which was quickly repaired. Anchorages, piers, and towers were otherwise undamaged.

Discussions are underway to determine tolls for the completed bridge. Estimates range from 3,500 yen ($29.16) to 5,000 yen ($41.67) a seemingly high cost to travel to work daily. Its companion bridge, the Seto Ohashi Bridge completed in 1988 experiences about 2 of the number of expected drivers; will the Akashi-Kaikyo bridge experience the same fate?

12. Hanshin Expressway Public Corporation Retrofit Projects

(http://west.park.or.jp/hanshin-expressway/index-e.html). During the delegation's travels in Kobe, they passed over sections of the Hanshin Expressway that collapsed in the Hyogo-ken Nanbu earthquake and have since been repaired. The Kobe Route Expressway is now supported by both steel-jacketed and concrete piers; the steel-jacketed piers are retrofits, and the concrete piers were completely rebuilt.

The delegation visited the Temposan Junction of the Hanshin elevated highway system in the Osaka area where strengthening of four bridge piers was in progress. In addition, special energy absorbing rubber restrainers (Znaidal), jointly developed by the Hanshin Expressway Public Corporation and Bridgestone Rubber Company, were used to restrain bridge spans from large longitudinal movements during earthquakes. Some non-rubber bearings were replaced with high damping rubber base isolation bearings.

The Hanshin Expressway Public Corporation experienced collapse of many of their bridge piers during the 1995 Hyogo-ken Nanbu earthquake. More than 4,800 piers have been identified to require retrofitting. They are being strengthened by steel jackets, reinforced concrete jackets, or fibre reinforced plastic jackets. Concrete jackets are used primarily for piers in water. Where steel jackets are used, either epoxy resin or high strength non-shrinking mortar is injected between the steel plate and concrete pier. To maintain a constant gap between a steel jacket and the concrete pier, expansion anchors are drilled into the concrete pier; the steel jacket is attached to anchors by means of flat-headed bolts. The pier's pile

foundations were not strengthened. According to the Hanshin Expressway Public Corporation, analysis showed that the foundation was adequate for the new updated design requirements.
The average cost of retrofit for each pier is about $100K; same as an average retrofit cost of piers in the Tokyo area. A typical retrofit cost of similar piers for either concrete or steel jacketing in California is about $15K.

The Hanshin Expressway Public Corporation is funded by the MOC. It was created in 1962 using capital investment funds operating between Osaka-Kobe-Kyoto to construct and manage urban toll road networks. Tolls from the Hanshin Expressway pays for principal and interest on borrowed funds, road construction costs, and operating costs such as road maintenance, salaries, etc. About 90% of borrowed funds are raised by issuing bonds and 10% from loans (6% banks and 4% from National and local governments). In 1985 MOC established provisions for carrying out environmental assessments of urban expressways. Final planning is not started until public opinion has been consulted. Attempts are made to achieve sustainable development such as: designing expressway so they visually harmonize with the urban surroundings; sound barriers and improved highway joints reduce noise and vibration to adjoining property; purchased land beyond 10-20 m from a road edge must be planted with trees and other greenery. In cases where homes still have excessive noise from highways, the National Government provides subsidies to homeowner for sound insulation such as special windows and air conditioners. Residents are compensated for loss of sunlight when an expressway obstructs sunlight. Also, when television reception is affected, residents are provided with antennas.

13. Public Health Impressions Gleaned from the 29th Wind & Seismic Effects Panel Meetings. The following observations from a Panel Member, a medical doctor and public health official from the Center for Disease Control and Prevention (CDC), provided a perspective on multi-displinary planning needed for mitigation of and recovery following natural disasters. The Panel recognizes this need as evident by technical papers presented at the joint meeting on this subject.

At the base of the papers presented and discussions held during the 29th Joint Meeting rest the twin goals of reducing human impact of natural disasters and improving the quality of human life. These goals are shared by the world's public health systems and this confluence of interests can and should lead to greater discussion and productive cooperation between engineers and public health professionals. The following outlines a few topics which show the greatest promise for combined effort.

Field Assessment Systems. During the aftermath of earthquakes and other natural phenomena, it is important to determine the exact mechanisms by which people are injured or killed. Often these mechanisms fall within the field of engineering. An example would be the relative resistance to collapse of structures imparted by their respective material characteristics.

In the past, much of the field data gathered for this purpose has been analogous to the "case series" familiar to physicians. In this type of data-gathering, the doctor describes a number of patients which he or she has encountered. Often the characteristics reported can stimulate discussion and hypothesis-generation about the disease or other phenomenon being studied. It is universally recognized, however, that hypotheses suggested by a case series must then be subjected to testing under conditions in which the data is gathered scientifically and rigorously.

To carry this analogy into the field of engineering, one might imagine a visit to a hurricane-devastated area. Initial attempts to describe damage might include a case series of assessments of the most probable

reason for building and structure failures. Investigations of this case series would reveal plausibly reasons that could account for the damage. For example, it might be noted that homes constructed with overhanging roofs seem to make up a large portion of the roofless homes.

The case series has at this point served an excellent purpose by suggesting a plausible risk factor for the loss of a roof under high winds. Nonetheless, many questions remain to be answered: were there many homes with overhanging roofs that remained intact? How many homes without overhanging roofs lost a roof? What proportion of each group (overhanging or not) remained intact?

The central point addressed by all these questions is: were the homes included in the case series representative of all the homes affected by the high winds? If every home was investigated then we know our results are representative. If not, we must be prepared to convince our colleagues that our sample of homes was not in some way biased (e.g., were all the homes with overhanging roofs that we examined also coincidentally located on higher ground?). This is the purview of statistical sampling.

Work at CDC is underway to develop scientifically and statistically valid methodologies for rapidly gathering information after natural disasters. These methodologies are easily transferrable from the public health professional to the engineer, since the techniques involved (including those which CDC presented at the Panel Meeting) are independent of the particular variable being studied. The technique remains the same whether one is assessing the type of injuries to people after a hurricane, or the type of damage to roofs after the same event.

Human Outcome Studies. Consider the following scenarios presented during the 29th Joint Panel Meeting and at the subsequent technical site visits:

- A construction firm has developed new apartment housing for those made homeless by the Hyogo-ken Nanbu Earthquake. Units have been set aside for elderly residents, and for the handicapped. The arrangement of the space and storage in these units, it is hoped, will allow their occupants to function as fully as possible.
- The owner of a high-rise structure in Yokohama has invested millions of dollars in a TAD (tuned active damper) system to decrease discomfort to building inhabitants that is caused by swaying in high winds.
- The Japanese government has constructed temporary shelter for thousands of persons, many of them elderly, whose homes were rendered uninhabitable by the Hyogo-ken Nanbu Earthquake. The suggestion has been made that certain arrangements of shelter for these refugees (e.g., with space allocated as meeting areas) may more easily allow the refugees to develop mutual support arrangements and thus lessen the psychological burden of their loss.

These three situations, although somewhat unrelated, share one common point: they suggest scientifically testable hypotheses. Will the unique arrangements made for the elderly in the new Kobe apartment buildings indeed make life easier for the inhabitants, as hoped? Does the TAD system actually reduce discomfort in building inhabitants? Can certain arrangements of housing truly reduce psychological morbidity (which has a strong effect on non-psychological health)?

Those involved in each of these projects have good theoretical reasons to believe that their systems will work as planned. Still, theory is a complement, not a substitute, for experimental study, and in each of these cases scientists could actually test the theory as it has been applied, verifying or rejecting it.

CDC has competence in studying human outcomes, particularly those related to morbidity and mortality. The examples above and many other similar scenarios present a unique opportunity for cooperative work between the engineering and the public health communities, and for advancing the Panel' s collective knowledge.

Note: Certain trade names and company products are mentioned in the text to specify the procedure and equipment used. These identifications do not imply recommendation or endorsement by the U.S. or Japan member agencies making up the UJNR Panel on Wind and Seismic Effects.